PROTECTING OUR CROPS - APPROACHES FOR PLANT PARASITIC NEMATODE CONTROL

EDITED BY: Claudia S. L. Vicente, Koichi Hasegawa, Juan Emilio Palomares-Rius and Shahid Siddique

PUBLISHED IN: Frontiers in Plant Science

frontiers Research Topics

ISSN 1664-8714
ISBN 978-2-88971-636-4
DOI 10.3389/978-2-88971-636-4

About Frontiers

Frontiers is more than just an open-access publisher of scholarly articles: it is a pioneering approach to the world of academia, radically improving the way scholarly research is managed. The grand vision of Frontiers is a world where all people have an equal opportunity to seek, share and generate knowledge. Frontiers provides immediate and permanent online open access to all its publications, but this alone is not enough to realize our grand goals.

Frontiers Journal Series

The Frontiers Journal Series is a multi-tier and interdisciplinary set of open-access, online journals, promising a paradigm shift from the current review, selection and dissemination processes in academic publishing. All Frontiers journals are driven by researchers for researchers; therefore, they constitute a service to the scholarly community. At the same time, the Frontiers Journal Series operates on a revolutionary invention, the tiered publishing system, initially addressing specific communities of scholars, and gradually climbing up to broader public understanding, thus serving the interests of the lay society, too.

Dedication to Quality

Each Frontiers article is a landmark of the highest quality, thanks to genuinely collaborative interactions between authors and review editors, who include some of the world's best academicians. Research must be certified by peers before entering a stream of knowledge that may eventually reach the public - and shape society; therefore, Frontiers only applies the most rigorous and unbiased reviews.
Frontiers revolutionizes research publishing by freely delivering the most outstanding research, evaluated with no bias from both the academic and social point of view. By applying the most advanced information technologies, Frontiers is catapulting scholarly publishing into a new generation.

What are Frontiers Research Topics?

Frontiers Research Topics are very popular trademarks of the Frontiers Journals Series: they are collections of at least ten articles, all centered on a particular subject. With their unique mix of varied contributions from Original Research to Review Articles, Frontiers Research Topics unify the most influential researchers, the latest key findings and historical advances in a hot research area! Find out more on how to host your own Frontiers Research Topic or contribute to one as an author by contacting the Frontiers Editorial Office: frontiersin.org/about/contact

PROTECTING OUR CROPS - APPROACHES FOR PLANT PARASITIC NEMATODE CONTROL

Topic Editors:
Claudia S. L. Vicente, University of Évora, Portugal
Koichi Hasegawa, Chubu University, Japan
Juan Emilio Palomares-Rius, Consejo Superior de Investigaciones Científicas (CSIC), Spain
Shahid Siddique, University of California, Davis, United States

Citation: Vicente, C. S. L., Hasegawa, K., Palomares-Rius, J. E., Siddique, S., eds. (2021). Protecting Our Crops - Approaches for Plant Parasitic Nematode Control. Lausanne: Frontiers Media SA. doi: 10.3389/978-2-88971-636-4

Table of Contents

frontiers in Plant Science

EDITORIAL
published: 01 September 2021
doi: 10.3389/fpls.2021.726057

Editorial: Protecting Our Crops - Approaches for Plant Parasitic Nematode Control

Juan E. Palomares-Rius[1]*, *Koichi Hasegawa*[2], *Shahid Siddique*[3] and *Claudia S. L. Vicente*[4,5]

[1] Institute for Sustainable Agriculture-Consejo Superior de Investigaciones Científicas (CSIC), Córdoba, Spain, [2] Department of Environmental Biology, Chubu University, Kasugai, Japan, [3] Department of Entomology and Nematology, University of California, Davis, Davis, CA, United States, [4] MED-Mediterranean Institute for Agriculture, Environment and Development, Institute for Advanced Studies and Research, University of Évora, Évora, Portugal, [5] INIAV, I.P. – Instituto Nacional de Investigação Agrária e Veterinária, Oeiras, Portugal

Keywords: plant-parasitic nematodes, plant-nematode interactions, nematode-microbe interactions, sustainable agriculture, biocontrol, breeding

Editorial on the Research Topic

Protecting Our Crops - Approaches for Plant Parasitic Nematode Control

In agricultural history, the Green Revolution generated by the development of breeding technology, chemical fertilizers, and pesticides has enabled mass production of agricultural crops and solved many (but not all) hunger problems around the world (Pingali, 2012). Plants make up about 80% of the food we consume, while about 40% of food crops are lost by agricultural pests, including plant nematodes (FAO, 2019). The world population in 2021 is ∼7.8 billion and is estimated to reach 10 billion in 2050 (United Nations, 2019). The current proposition imposed on us is to develop methods to increase crop yield and quality while suppressing damage from pests and also reducing the impact on the natural environment. Plant-parasitic nematodes (PPNs) are one of the major constraints in agriculture. Damage caused by PPNs has been estimated from $US80 billion (Nicol et al., 2011) to $US157 billion per year (Abad et al., 2008). However, the full extent of nematode damage is likely underestimated as many growers, particularly in developing countries, are unaware of the presence of PPNs (Jones et al., 2013). This was assumed as nematodes are usually small-body-size, soil-borne pathogens, and the symptoms they cause are often non-specific (Jones et al., 2013). The damage caused by PPNs could be even worse in the future in the context of a growing world population under a Climate Change scenario and the removal or reduction in the use of some nematicides in many parts of the world. Set in the context of the 2020 International Year of Plant Health, this Research Topic "Protecting Our Crops - Approaches for Plant Parasitic Nematode Control" gives new insights into Integrative Approaches for Sustainable PPN Control. Many of the articles are excellent reviews of their specific topic, which could help in pointing out new research directions.

The knowledge of the geographical distribution, prevalence, and diversity of specific PPNs is a keystone point for further development of control measures in a region or country as well to prevent the dispersion of the specific pathogen in unaffected areas. This distribution could be influenced by Climate Change, which forecasts an increase in global temperature with important temperature and precipitation instability and could induce a northward migration/higher altitude shifts and an increase in the damage severity in areas of current distribution (Chakraborty et al., 2000). Climate Change could affect crops (e.g., plant defenses, growth, or period of sowing) as well as the Biological Control Agents (BCAs) associated with a specific nematode. Potato cyst nematodes (*Globodera pallida* and *G. rostochiensis*) are the most economically important

OPEN ACCESS

Edited and reviewed by:
Holger Heuer,
Julius Kühn-Institut, Germany

***Correspondence:**
Juan E. Palomares-Rius
palomaresje@ias.csic.es

Specialty section:
This article was submitted to Plant Pathogen Interactions, a section of the journal Frontiers in Plant Science

Received: *16 June 2021*
Accepted: *24 June 2021*
Published: *01 September 2021*

Citation:
Palomares-Rius JE, Hasegawa K, Siddique S and Vicente CSL (2021) Editorial: Protecting Our Crops - Approaches for Plant Parasitic Nematode Control. Front. Plant Sci. 12:726057. doi: 10.3389/fpls.2021.726057

parasitic nematodes of the potato (*Solanum tuberosum*), in many cases inducing important losses to farmers by reducing production or regulatory restrictions in their trade. These nematodes are challenging due to their survival strategy. Cysts produced by the female's cuticle hardening are highly durable, and viable eggs, protected inside the cysts, can survive for decades in the absence of a host (Turner, 1996). The data revealed about potato cyst nematodes in Kenya (Mburu et al.) and Portugal (Camacho et al.) showed two different scenarios with a widely spread predominant species (*G. rostochiensis*) in Kenya (Mburu et al.) and the wide presence of both species (*G. pallida* and *G. rostochiensis*) in Portugal (Camacho et al.) and differences in the use of resistance cultivars in these two countries. Additionally, the root-knot nematode (RKN) *Meloidogyne enterolobii* (syn. *M. mayaguensis*) has been considered as a global threat for tomato (*Solanum lycopersicum*) production due to the lack of known resistance in commercially accepted tomato varieties (*Mi*-genes does not control *M. enterolobii*) (Moens et al., 2009; Castillo and Castagnone-Sereno, 2020). This species has a broad host range and has been recently found in many countries worldwide in areas with a subtropical to tropical climate (Castillo and Castagnone-Sereno, 2020; Subbotin et al., 2021). Philbrick et al. review the current knowledge on geographic distribution, host range, population biology, control measures, and proposed future strategies to improve *M. enterolobii* control in the tomato. Growing resistant varieties is the most environmentally and economically friendly method to combat RKNs in the field (Seid et al., 2015), but in many cases exerts selection pressure on nematode populations, increasing the number of virulent individuals (Whitehead, 1991; Kaloshian et al., 1996; Hockland et al., 2012) and the need for accurate strategies for sustainable management of the nematode resistance in the field (Barbary et al., 2015). Gartner et al. provide an interesting review of the different resistance genes, their management, and the recent advances in potato genomics to develop molecular markers to aid selection during breeding. Cui et al. characterize the resistance to cereal cyst nematodes (*Heterodera aveane* and *H. filipjevi*), agronomic performance, and end-use quality parameters in four perennial wheat-*Thinopyrum intermedium* lines. Another approach in this research line is the use of alternative crops/cover crops or double-cropping. Double-cropping is defined as producing more than one crop on the same parcel of land in a single growing season, increasing biomass productivity, weed control, and supplying the increased demand for food and feed (Leslie et al., 2017). Rocha et al. studied the use of double-cropping to control one of the major soybean (*Glycine max*) pathogen problems, the soybean cyst nematode (SCN) (*Heterodera glycines*). Double-cropping soybean with wheat (a non-host) has the potential to suppress SCN field populations in comparison to fallow (Rocha et al.). Additionally, this system provides additional farm income. The evidence of these techniques is also evaluated by Rashidifard et al. by studying the crop rotation with sainfoin (*Onobrychis viciifolia*) to reduce *M. enterolobii* infection of maize under greenhouse conditions in a pilot approach. Their results showed that the rotation of sainfoin Esparsette/maize reduced *M. enterolobii* population density by 81 and 60% in the first and repeat experiments, respectively, followed by alfalfa (*Medicago sativa*) 54 and 43%, respectively (Rashidifard et al.).

Novel control methods for PPNs are needed in the context of sustainable agriculture using fewer inputs and being more respectful of the environment and the health of consumers and applicators. Many nematicides are in decline in terms of use or are being banned because of adverse environmental impacts. In this sense, several approaches are pointed for the use of specific plant compounds for the control of PPNs. In this Research Topic, Desmedt et al. have reviewed the metabolites used by plants to defend themselves against PPNs. Metabolites are reviewed by chemical class (e.g., terpenoids, flavonoids, and glucosinolates). Furthermore, the authors discuss strategies for the identification of metabolites and highlight how these anti-nematode metabolites might be of use in crop protection (Desmedt et al.). In this sense, the spray of sugar beet with active enzymes as ascorbate oxidase (an enzyme catalyzing the oxidation of apoplastic ascorbic acid to dehydroascorbic acid) induced plant defenses in a systemic way, resulting in a reduction in the number of *H. schachtii* infecting the plant (Singh et al.). This resistance induced by ascorbate oxidase is partially dependent on the jasmonic acid, ethylene, and salicylic acid pathways (Singh et al.). Another line of research is to induce the plant's defense by using microorganisms as a part of the PPNs management. Wang et al. demonstrated enhanced soybean resistance against SCN by using *Sinorhizobium freedi* strain Sneb183 in an iTRAQ-based proteomic analysis. The results suggested that the *S. fredii* Sneb183 may have a role in inducing isoflavonoid biosynthesis, thereby resulting in enhanced resistance to SCN infection in soybean. In some cases, the plant inoculation by a microorganism or derived compounds produced by microorganisms could induce a priming response by the plant to specific PPNs. Priming of plants by an inducer results in a faster and stronger response of the plant defense upon pathogen attack and could become an environmentally friendly strategy for plant protection (Borges et al., 2014; Conrath et al., 2015). The primed state could be even transgenerationally transmitted (Ramírez-Carrasco et al., 2017). Adss et al. studied the priming induction of soybean cv. Primus by the root application of the compound *N*-3-oxo-tetradecanoyl-*L*-homoserine lactone and the inoculation of the rhizobacterium producer of this compound (*Ensifer meliloti* strain ExpR+) against the root-lesion nematode, *Pratylenchus penetrans*. The results showed reduced root invasion compared to non-primed plants. Primed activated defense upon nematode invasion was indicated by increased production of the phytoalexin glyceollin by the soybean plant, while the preceding root application of the priming agent did not induce a direct defense response (Adss et al.). Compounds derived from microorganisms could also have a detrimental role in nematode infection and could be used for the development of new drugs. Prodoginines are red-colored tripyrrolic compounds produced by many bacterial species (Williamson et al., 2006). Habash et al. studied prodoginines and derivates against nematodes (*C. elegans* and *H. schachtii*) and plant pathogenic fungi (*Phoma lingam* and *Sclerotinia sclerotiorum*). *Caenorhabditis elegans* was affected by prodigiosin and the derivatives in a concentration-dependent manner while

this effect was only detected for prodigiosin only for *H. schachtii* (Habash et al.). All compounds were found to be active against the plant pathogenic fungi studied (Habash et al.). Many of the advances in the development of environmentally benign treatments commented before are also applied in RKNs, and this has been reviewed by Forghani and Hajihassani in this Research Topic.

The ecological knowledge and requirements to activate the infective stage in a plant pathogen are essential points to design strategies for their control. In this sense, the hatching of CNs is finely tuned by the presence of the plant host in the majority of the species (Clarke and Perry, 1977). Ngala et al. studied the *in situ* hatching of encysted eggs of *G. pallida*, *H. carotae*, and *H. schachtii* after the application of root exudates at varying soil depths. The results showed that *G. pallida* hatching depends on soil moisture and effective exposure to root exudates, and to a lesser extent on exudate concentration. *Heterodera carotae* showed over 75% hatching induced by root exudate irrespective of the concentration, with better hatch induction at 20 cm than 10 cm soil depth, while *H. schachtii* mainly depends on the soil moisture level at constant temperature and is not influenced by the type or concentration of root exudates.

How plants and nematodes interact with each other is of great importance. Several systems have been studied in this Research Topic. RKNs infection of roots reactivates the cell cycle with a controlled balance of mitotic and endocycle programs (de Almeida Engler and Gheysen, 2013). Cabral et al. studied the role of the Armadillo BTB Protein ABAP1 in the DNA replication and transcription of nematode-induced galls by *Meloidogyne* spp. This study suggests that *ABAP1* is an essential component for cell cycle regulation throughout gall development and is required for feeding site homeostasis. Using the same group of nematodes, Truong et al. demonstrated that the *M. incognita* nuclear effector MiEFF1 interacts with *Arabidopsis* cytosolic glyceraldehyde-3-phosphate dehydrogenases during nematode parasitism. Plant resistance and susceptibility from RKN is studied using transcriptomics in several plant-nematode systems in this Research Topic as *M. incognita*-sweet potato (*Ipomoea batatas*) (Lee et al.), *M. incognita*-cucumber (*Cucumis sativus* and *C. metuliferus*) (Li et al.), and *M. arenaria-Solanum torvum* (Sato et al.). Zheng et al. reviewed in detail the molecular and cellular mechanisms involved in host-specific resistance to cyst nematodes in crops. This review explains in detail the knowledge of molecular and cellular mechanisms involved in the recognition of cyst nematodes, the activation of defense signaling, and resistance response types mediated by R genes or quantitative trait loci.

Pine wilt disease is caused by the pinewood nematode (PWN), *Bursaphelenchus xylophilus*, and constitutes one of the most important diseases in world forestry. This nematode is native to North America where it is not a pathogen to the endemic pine trees, but it has spread to the far East and some parts of Europe by world trading, causing serious damage to the local susceptive trees (Vicente et al., 2012). In this sense, it is a smart strategy to compare interactions between *Pinus* species with different sensitivities and nematodes with different virulence. Silva et al. studied the comparative analysis of PWN secretome under *P. pinaster* (high-susceptible host) and *P. pinea* (low-susceptible host) stimuli using a proteomic approach. In total, 22 proteins were found to be increased in the PWN secretome under the *P. pinaster* stimulus and 501 proteins increased under the *P. pinea* stimulus, with different protein activities in each host. In addition, the nematode secretome was also conducted by Shinya et al. to identify the virulence determinants of different isolates of PWN with distinct virulence levels. Highly secreted proteins from virulent *B. xylophilus* were selected as candidate virulent factors, and functions of two of them were clearly shown: a glycoside hydrolase family 30 (Bx-GH30) induce plant cell death, and one C1A family cysteine peptidase (Bx-CAT2) was involved in nematode feeding (Shinya et al.).

The editors of this Research Topic thank all authors who contribute and hope that this Research Topic helps the readers to understand and put in a higher view the problems caused by PPNs and their possible solutions in the future.

AUTHOR CONTRIBUTIONS

JEP-R: conceptualization and writing—original draft. JEP-R, KH, SS, and CSLV: writing—review & editing.

FUNDING

Research was supported by the grant RTI2018-095925-A-100 from Ministerio de Ciencia, Innovación y Universidades (Spain) to JEP-R and by the CEECIND/00040/2018 from Science and Technology Foundation (Portugal) to CSLV.

ACKNOWLEDGMENTS

We thank authors who submitted their work for this Research Topic as well as the invaluable help of reviewers during manuscript evaluation.

REFERENCES

Abad, P., Gouzy, J., Aury, J.-M., Castagnone-Sereno, P., Danchin, E. G. J., Deleury, E., et al. (2008). Genome sequence of the metazoan plant-parasitic nematode *Meloidogyne incognita*. *Nat. Biotechnol.* 26, 909–915. doi: 10.1038/nbt.1482

Barbary, A., Djian-Caporalino, C., Palloix, A., and Castagnone-Sereno, P. (2015). Host genetic resistance to root-knot nematodes, *Meloidogyne* spp., in solanaceae: from genes to the field. *Pest Manag. Sci.* 71, 1591–1598. doi: 10.1002/ps.4091

Borges, A. A., Jiménez-Arias, D., Expósito-Rodríguez, M., Sandalio, L. M., and Pérez, J. A. (2014). Priming crops against biotic and abiotic stresses: MSB as a tool for studying mechanisms. *Front. Plant Sci.* 5:642. doi: 10.3389/fpls.2014.00642

Castillo, P., and Castagnone-Sereno, P. (2020). *Meloidogyne enterolobii (Pacara Earpod Tree Root-Knot Nematode). Invasive Species Compendium*. Wallingford: CABI.

Chakraborty, S., Tiedemann, A. V., and Teng, P. S. (2000). Climate change: potential impact on plant diseases. *Environ. Pollut.* 108, 317–326. doi: 10.1016/S0269-7491(99)00210-9

Clarke, A. J., and Perry, R. N. (1977). Hatching of cyst-nematodes. *Nematologica* 23, 350–368. doi: 10.1163/187529277X00075

Conrath, U., Beckers, G. J. M., Langenbach, C. J. G., and Jaskiewicz, M. R. (2015). Priming for enhanced defense. *Annu. Rev. Phytopathol.* 53, 97–119. doi: 10.1146/annurev-phyto-080614-120132

de Almeida Engler, J., and Gheysen, G. (2013). Nematode-induced endoreduplication in plant host cells: why and how? *Mol. Plant Microbe Interact.* 26, 17–24. doi: 10.1094/MPMI-05-12-0128-CR

FAO (2019). *International Year of Plant Health, 2020: Communication Guide*. Rome: International Year of Plant Health 2020: Communication Guide (fao.org).

Hockland, S., Niere, B., Grenier, E., Blok, V., Phillips, M., Nijs, L., et al. (2012). An evaluation of the implications of virulence in non-european populations of *Globodera pallida* and *G. rostochiensis* for potato cultivation in Europe. *Nematology* 14, 1–13. doi: 10.1163/138855411X587112

Jones, J. T., Haegeman, A., Danchin, E. G. J., Gaur, H. S., Helder, J., Jones, M. G. K., et al. (2013). Top 10 plant-parasitic nematodes in molecular plant pathology. *Mol. Plant Pathol.* 14, 946–961. doi: 10.1111/mpp.12057

Kaloshian, I., Williamson, V., Miyao, G., Lawn, D., and Westerdahl, B. (1996). Resistance-breaking nematodes identified in California tomatoes. *Calif. Agric.* 50, 18–19. doi: 10.3733/ca.v050n06p18

Leslie, A. W., Wang, K.-H., Meyer, S. L. F., Marahatta, S., and Hooks, C. R. R. (2017). Influence of cover crops on arthropods, free-living nematodes, and yield in a succeeding no-till soybean crop. *Appl. Ecol.* 117–118, 21–31. doi: 10.1016/j.apsoil.2017.04.003

Moens, M., Perry, R. N., and Starr, J. (2009). "Meloidogyne species: a diverse group of novel and important plant parasites," in *Root-Knot Nematodes*, eds M. Moens, R. N. Perry, and J. Starr (Cambridge, MA: CAB International), 1–13.

Nicol, J. M., Turner, S. J., Coyne, D. L., Nijs, L., den Hockland, S., and Maafi, Z. T. (2011). "Current nematode threats to world agriculture," in *Genomics and Molecular Genetics of Plant-Nematode Interactions*, eds J. Jones, G. Gheysen, and C. Fenoll (Dordrecht: Springer Netherlands), 21–43.

Pingali, P. L. (2012). Green revolution: impacts, limits, and the path ahead. *PNAS* 109, 12302–12308. doi: 10.1073/pnas.0912953109

Ramírez-Carrasco, G., Martínez-Aguilar, K., and Alvarez-Venegas, R. (2017). Transgenerational defense priming for crop protection against plant pathogens: a hypothesis. *Front. Plant Sci.* 8:696. doi: 10.3389/fpls.2017.00696

Seid, A., Fininsa, C., Mengistu, T., Decraemer, W., and Wesemael, W. (2015). Tomato (*Solanum lycopersicum*) and root-knot nematodes (*Meloidogyne* spp.) – a century-old battle. *Nematology* 17, 1–15. doi: 10.1163/15685411-00002935

Subbotin, S. A., Palomares-Rius, J. E., and Castillo, P. (2021). *Systematics of Root-Knot Nematodes (Nematoda: Meloidogynidae), Nematology Monographs and Perspectives*. Leiden: Brill.

Turner, S. J. (1996). Population decline of potato cyst nematodes (*Globodera rostochiensis*, *G. pallida*) in field soils in Northern Ireland. *Ann. Appl. Biol.* 129, 315–322. doi: 10.1111/j.1744-7348.1996.tb05754.x

United Nations (2019). *World Population Prospects 2019*. Available online at: https://population.un.org/wpp/Publications/Files/WPP2019_Highlights.pdf

Vicente, C., Espada, M., Vieira, P., and Mota, M. (2012). Pine wilt disease: a threat to european forestry. *Eur. J. Plant Pathol.* 133, 89–99. doi: 10.1007/s10658-011-9924-x

Whitehead, A. G. (1991). Selection for virulence in the potato cyst-nematode, Globodera pallida. *Ann. Appl. Biol.* 118, 395–402. doi: 10.1111/j.1744-7348. 1991.tb05639.x

Williamson, N. R., Fineran, P. C., Leeper, F. J., and Salmond, G. P. C. (2006). The biosynthesis and regulation of bacterial prodiginines. *Nat. Rev. Microbiol.* 4, 887–899. doi: 10.1038/nrmicro1531

Conflict of Interest: The authors declare that the research was conducted in the absence of any commercial or financial relationships that could be construed as a potential conflict of interest.

Publisher's Note: All claims expressed in this article are solely those of the authors and do not necessarily represent those of their affiliated organizations, or those of the publisher, the editors and the reviewers. Any product that may be evaluated in this article, or claim that may be made by its manufacturer, is not guaranteed or endorsed by the publisher.

frontiers in Plant Science

ORIGINAL RESEARCH
published: 25 May 2020
doi: 10.3389/fpls.2020.00670

Potato Cyst Nematodes: A New Threat to Potato Production in East Africa

*Harrison Mburu[1,2,3], Laura Cortada[2,4], Solveig Haukeland[1,5], Wilson Ronno[6], Moses Nyongesa[7], Zachary Kinyua[7], Joel L. Bargul[1,3] and Danny Coyne[2,4]**

[1] International Centre of Insect Physiology and Ecology (icipe), Nairobi, Kenya, [2] East Africa Hub, International Institute of Tropical Agriculture (IITA), Nairobi, Kenya, [3] Department of Biochemistry, Jomo Kenyatta University of Agriculture and Technology, Juja, Kenya, [4] Nematology Section, Department of Biology, Ghent University, Ghent, Belgium, [5] Biotechnology and Plant Health Division, Norwegian Institute for Bioeconomy Research, Ås, Norway, [6] Food and Agriculture Organization (FAO), Nairobi, Kenya, [7] Kenya Agricultural and Livestock Research Organization (KALRO), Nairobi, Kenya

Potato cyst nematodes (PCN), such as *Globodera rostochiensis* and *Globodera pallida,* are quarantine restricted pests of potato causing major yield and financial losses to farmers. *G. rostochiensis* was first reported from Kenya's key potato growing area in 2015. We sought to determine the diversity, prevalence and distribution of PCN species across the country by conducting a country-wide survey between 2016 and 2018, which included a more focused, follow-up assessment in three key potato growing counties. A total of 1,348 soil samples were collected from 20 potato growing counties. Information regarding local potato farming practices, potato cultivar use, their diversity and availability was also recorded. PCN cysts were obtained from 968 samples (71.8%) in all the counties surveyed, with Nyandarua County recording the highest PCN field-incidence at 47.6%. The majority of PCN populations, 99.9%, were identified as *G. rostochiensis,* while *G. pallida* was recovered from just one field, in a mixed population with *G. rostochiensis.* Inconsistencies in PCR amplification efficiency was observed for *G. rostochiensis* using the recommended EPPO primers, compared with ITS primers AB28/TW81, indicating that this protocol cannot be entirely relied upon to effectively detect PCN. Egg density in Nyandarua County varied between 30.6 and 158.5 viable eggs/g soil, with an average egg viability of 78.9 ± 2.8% (min = 11.6%, max = 99.9%). The PCN-susceptible potato cultivar named Shangi was the most preferred and used by 65% of farmers due to its shorter dormancy and cooking time, while imported cultivars (Destiny, Jelly, Manitou, and Markies) with resistance to *G. rostochiensis* were used by 7.5% of farmers due to unavailability and/or limited access to seeds. Thus, most farmers preferred using their own farm-saved seeds as opposed to purchasing certified seeds. Establishing the distribution and prevalence of PCN and elucidating the local farming practices that could promote the spread of PCN is a necessary precursor to the implementation of any containment or management strategy in the country and ultimately across the region.

Keywords: EPPO, *Globodera rostochiensis*, *Globodera pallida*, Kenya, smallholder farmers, potato seed systems, cv. Shangi

OPEN ACCESS

Edited by:
Christina Cowger, Plant Science Research Unit (USDA-ARS), United States

Reviewed by:
Josselin Montarry, INRA Centre Bretagne-Normandie, France
Louise-Marie Dandurand, University of Idaho, United States

***Correspondence:**
Danny Coyne
D.Coyne@cgiar.org

Specialty section:
This article was submitted to Plant Microbe Interactions, a section of the journal Frontiers in Plant Science

Received: *30 January 2020*
Accepted: *29 April 2020*
Published: *25 May 2020*

Citation:
Mburu H, Cortada L, Haukeland S, Ronno W, Nyongesa M, Kinyua Z, Bargul JL and Coyne D (2020) Potato Cyst Nematodes: A New Threat to Potato Production in East Africa. Front. Plant Sci. 11:670. doi: 10.3389/fpls.2020.00670

INTRODUCTION

Potato is a valuable and nutritious staple crop, driving both food security and Growth Domestic Product (GDP) growth globally (Reader, 2009; Devaux et al., 2014). Approximately half of the world's potato is produced in Asia, especially China, followed by Europe producing about a third (Scott and Suarez, 2012). Only maize is grown in more countries than potato. Africa produces about 7% of global potato output, mainly in Egypt and South Africa (Devaux et al., 2014). Potato production in the East and Central Africa highlands offers great promise despite substantial fluctuations in yields recorded over the last two decades (FAOSTAT, 2018). Potatoes are a popular and valuable crop for both food security and income generation, competing well with maize in the subtropical climates at higher altitudes. Under these conditions, year-round production can be possible, often with at least two seasons per annum. In recent years, however, yields have shown notable declining trends, mainly attributed to major disease outbreaks, inappropriate cropping practices by farmers, substandard seed quality and lack of organized market infrastructure for produce (Janssens et al., 2013; Kaguongo et al., 2014). Emerging markets for processed potatoes (e.g., chips, crisps, starch) furthermore, have increasingly focused attention on potatoes, with rising demand from the fast food industry and processing for added economic value (Abong and Kabira, 2013). Processed potatoes, however, also demand high levels of quality, which can be difficult to sustain in the face of high pest and disease pressures (Janssens et al., 2013; Kaguongo et al., 2014). Thus, any action to improve potato production will have a considerable impact on food security and income in these countries (Scott et al., 2013; Haverkort and Struik, 2015; FAO, 2017b; Okello et al., 2017; Harahagazwe et al., 2018).

In Kenya, potato is the second most important staple food crop after maize and valued at ∼$500 million USD annually (CIP, 2019). About 800,000 Kenyans directly benefit from potato production, while across the whole value chain about 2.5 million people receive income from potato (Abong and Kabira, 2013). However, in Kenya, yields have declined and currently average 9–10 t/ha, much below the potential of 20–40 t/ha (Kiptoo et al., 2016; VIB, 2019), and as reflected across the region attributed to factors listed above. The situation is not helped by the emergence of new pests and diseases, such as the recently detected potato cyst nematodes (PCNs) *Globodera rostochiensis* and *G. pallida* (Mwangi et al., 2015; Mburu et al., 2018). PCNs are subject to strict quarantine regulations in over 100 countries (EPPO, 2017) and are globally considered as the most important pests threatening potato production but are all too often overlooked in less developed countries (Coyne et al., 2018; Niere and Karuri, 2018). The quarantine status of PCNs is, in part, related to their ability to produce quiescent structures known as cysts that consist of the hardened body of the females measuring ∼0.5 mm in diameter enclosing ∼300–500 eggs each. Cysts persist in the soil for long periods of up to 20 years, even in the absence of an appropriate host and can withstand extreme cold temperatures (−15°C) and prolonged desiccation periods (Folkertsma et al., 1997). This diapause cyst stage is broken after the appearance in the rhizosphere of specific root diffusates from a narrow range of hosts, mainly potato, although other solanaceous crops, such as tomato, eggplant or pepper can also stimulate egg hatch (Perry, 2002). The infective juveniles (J2) readily hatch in the presence of a host plant, yet in the absence of a suitable natural host cyst decline has been reported to be ∼0–20% in temperate regions, year-on-year (Devine et al., 1999). PCN decline under subtropical or tropical conditions in Africa is currently unknown. Yield losses associated with PCN will vary according to conditions, and earlier estimates in the EU suggest that for every 20 viable eggs/g soil ∼2.75 t/ha of potatoes are lost (Brown and Sykes, 1983). PCN is mainly spread through cyst-contaminated soil that adheres to the farm machinery, equipment or seeds.

The occurrence of PCN presents a key threat to potato production in Kenya, as well as to the entire East Africa region where potato features prominently as a food security crop or for income generation for millions of smallholder farmers (VIB, 2019). In order to mitigate the PCN threat in potato production, the establishment of the level of infestation, their geographical distribution, and the agronomic and social factors that could be influencing their distribution and spread are essential toward establishing and implementing a national management strategy. This may include exploring alternative sampling strategies, which would contribute to a detailed understanding of the spread of PCNs (Goeminne et al., 2011, 2015; Mimee et al., 2019). Consequently, this study presents the results of a countrywide survey, undertaken to determine the distribution of PCN and the potential damage it is causing in the major potato growing regions of Kenya. We additionally examined farmer potato production practices and how these will need to be taken into consideration for the implementation of future pest management strategies. The information we provide here should further help policy makers and regional stakeholders to make informed decisions related to PCN containment and mitigation.

MATERIALS AND METHODS

Study Sites and Sampling Strategy

In an initial national survey, potato fields in 20 potato growing counties in Kenya were surveyed between 2016 and 2017, selecting approximately 1% of the potato production area per county, in line with the EU directive 2007/33/EC (Official Journal of European Union, 2007). A follow-up in-depth sampling was undertaken in 2018 in the major potato producing counties of Elgeyo Marakwet and Nyandarua as well as Taita Taveta, which presents significant potential for potato production (Jaetzold and Schmidt, 1983). A focused, in-depth study was also undertaken in Nyandarua County in order to estimate yield losses being experienced from PCN. Mean annual temperatures in surveyed counties ranged between 12.9 and 35°C, although lower temperatures of 2°C was recorded in some areas in Nyandarua County where occasional frosting can be experienced. For each sampled field the GPS coordinates were recorded, and a semi-structured questionnaire

administered to capture farmer potato production practices (**Supplementary Material**). A composite soil sample of ∼1.5 kg comprising of 50 sub-samples (cores) was randomly collected from each field using a hand trowel from the top 30 cm of soil following a "zigzag" pattern (Coyne et al., 2018), and placed in a plastic container. When targeting certified potato seed farms (22 sites), ∼2.0 kg of composite soil samples were collected using the same sampling pattern as described above. Each sample was well secured, labeled, placed in a cooler-box and transported to *icipe* laboratories in Nairobi, Kenya, for processing.

Isolation and Identification of Potato Cyst Nematodes

The soil samples were transported to the Kenya Plant Health Inspectorate Services (KEPHIS), where they were air-dried, thoroughly mixed, sieved to remove stones and debris before extraction of cysts from a 200 g sub-sample using the Fenwick can floatation method (EPPO, 2013b). Briefly, using a moderate but constant flow of water, each sample was washed through a 1 mm aperture sieve into the Fenwick can. Organic matter that passed through the 840 μm sieve in the can was collected from the overflow onto a 250 μm sieve. The sieve was backwashed and the final filtrate containing the cysts collected into 200 ml plastic beakers. Extractions were then collected on milk filter papers and air-dried. The cysts were individually handpicked using entomological forceps and counted using a Leica MZ12.5 dissection microscope. Cysts were placed in a 1 ml Eppendorf tube and stored at 4°C; the remaining soil was stored in case of further use.

Cysts recovered from samples were morphologically identified, based on the EPPO (2017) taxonomic guide, under a Leica MZ12.5 dissection microscope. The number of cysts (empty or containing eggs) positively identified as PCN were counted and recorded. About 1–10 cysts recovered from samples were subjected to molecular identification using modified EPPO multiplex-PCR protocols (EPPO, 2017; Mburu et al., 2018) and ITS primers (Joyce et al., 1994) for species identification. DNA amplification was carried out using ProFlex PCR systems^{TM} Base thermocycler (Applied Biosystems Life Technologies) with multiplex primers (PITSr3: 5'-AGC GCA GAC ATG CCG CAA-3', PITSp4: 5'-ACA ACA GCA ATC GTC GAG-3'and ITS5 5'-GGA AGT AAA AGT CGT AAC AAG G-3'), which are species-specific for *G. pallida* (265 bp amplicon) and/or *G. rostochiensis* (434 bp amplicon) targeting the 18S rRNA gene and the internal transcribed spacer ITS1 region and ITS primers (TW81 5'-GTT TCC GTA GGT GAA CCT GC-3' and AB28 5'-ATA TGC TTA AGT TCA GCG GGT-3') targeting the ITS1-5.8S-ITS2 regions (1,100 bp amplicon). Each PCR reaction mixture (One Taq® 2X Master Mix with standard buffer, New England Biolabs® Inc., United States) contained 12.5 μl PCR master mix (One Taq® 2X Master Mix with standard buffer), 1 μl of each primer (forward and reverse), 8.5 μl nuclease-free water and 2 μl of DNA (template) totaling 25 μl volume per reaction. PCR amplicons were electrophoresed through 2% agarose gel at 100V for 1 h to confirm successful amplification and size of the amplicons against a 100 bp ladder (New England Biolabs®, Inc., United States). For sequencing, species-specific PCR reactions were conducted using a singleplex approach with ITS5/PITSp4 primers for *G. pallida* and ITS5/PITSr3 for *G. rostochiensis*; PCR-amplicons were purified using the QIAquick PCR Purification Kit (Qiagen, United States) and sequenced by Sanger sequencing. DNA sequences were manually edited using BioEdit Sequence Alignment Editor (Hall, 1999). The edited sequences were analyzed using NCBI-BLAST tool and compared with previously isolated Kenyan isolates (Mwangi et al., 2015) and other *Globodera* spp. to generate a phylogenetic tree using Seaview software version 4.5.0 (Gouy et al., 2010).

Incidence, Infestation and Yield Loss Assessment

A focused, more in-depth study was undertaken in Nyandarua County, which has the largest area of cultivated potato in Kenya. Data related to incidence and infestation level of PCN across surveyed farms were collected from five sub-counties (Kinangop, Kipipiri, Ol'Kalou, Ol'Joro Orok and Ndaragua). For each sub-county, the average PCN-infestation level was calculated as the mean number of cysts per 200 g soil recovered from all the farms visited. Incidence (%) at the county level was further determined as the number of fields where cysts were isolated from the total number of sampled farms and expressed as a percentage. Based on these results, counties were classified as low PCN-incidence ($50\% \leq X < 70\%$), mid PCN-incidence ($70\% \leq X < 90\%$) and high PCN-incidence ($X \geq 90\%$). Further classification for the in-depth study in Nyandarua County was undertaken at the sub-county level, where infestation levels were classified according to: $1 < X < 25$ cysts, $26 < X < 110$ cysts, $111 < X < 230$ cysts, $231 < X < 495$ cysts, and $496 < X < 985$ cysts per 200 g of soil.

The impact of PCN on potato production was estimated using the Brown and Sykes (1983) regression line, which estimates that for every 20 viable eggs/g soil 2.75 t/ha of potato are lost to PCN. Therefore, PCN egg viability (EV) was assessed using a modified protocol, adapted from Faggian et al. (2012), as described below. Cyst infestation levels varied across the fields within the county, as was the number of fields with different levels of infestation. In order to assess a proportionate number of cysts from fields with different infestation levels, fields were grouped according to infestation level and then cysts were collected from the fields within each cluster group (minimum 10 and a maximum 50 cysts per field). The fields which had over 20 cysts per 200 g soil were grouped into four clusters and a total of 46 fields were included in the assessment: cluster 1 [fields with 200 g soil ($n = 14$)], cluster 2 (between 100 and 200 cysts ($n = 11$)], cluster 3 (between 50 and 100 cysts ($n = 5$)], and cluster 4 (between 20 and 50 cysts ($n = 16$)]. The samples were assessed for egg viability using Nile Blue stain, which stains dead eggs and/or juveniles (J2) (Ogiga and Estey, 1974), allowing the visual differentiation between dead (non-viable) and live (viable) J2s and eggs (non-stained) under the microscope. For the viability tests, cysts were handpicked and placed inside a modified 1.5 ml Eppendorf tube; the end of the tube was cut-off and a nylon mesh glued across the bottom. The tubes were placed inside a 24-well flat-bottomed culture

plate (Falcon®, Thomas Scientific) with 1 ml of 0.01% Nile Blue stain and incubated in the dark at room temperature for 48 h. After incubation, the stain was carefully rinsed and replaced with 1 ml sterile distilled water. Cysts were then individually removed, placed on a glass slide and gently cut open to expose the contents (Faggian et al., 2012). The total number of J2s, viable and non-viable eggs were counted to determine cyst fertility (CF). Subsequently, cyst viability (CV%) was calculated as the total number of live J2s and viable eggs divided by the CF and expressed as a percentage (CV%).

Finally, in each field, soil infectivity (SI) was calculated as the mean number of viable eggs per cyst, multiplied by the total number of cysts extracted in 200 g soil and expressed as viable eggs/g soil. For each sub-county, the mean SI was calculated from all the studied fields. In each sub-county, potato yield losses (t/ha) directly attributable to PCN were estimated based on the SI damage threshold determined by Brown and Sykes (1983).

Detection of Potato Cyst Nematode Resistance *H1* Gene

Molecular analyses was conducted on the most popular potato cultivar grown in Kenya, cv. Shangi (Sinelle, 2018) and four cultivars recently introduced from the EU (cv.s Destiny, Manitou, Markies, and Jelly) (NPCK, 2019) to determine the presence of the *H1* gene, which confers resistance to *G. rostochiensis*. The cv. Jelly, which is resistant to *G. rostochiensis* with *H1* gene (NPCK, 2017), was used as a positive control and cv. Desiree as the susceptible control. DNA was extracted from three leaves of 1-month old potato plants grown in the greenhouse at *icipe*, Nairobi. PCR amplification of the genomic region containing *H1* gene was conducted using 57R, TG689 and BCH markers (Park et al., 2018).

Determining Farmer Practices and Preferences in Potato Production

To understand how current smallholder farming practices could be influencing the incidence and distribution of PCN, farmer interviews were conducted at the household level (HH) during field sampling. A semi-structured questionnaire was used to gather agronomic and socioeconomic data to complement the phytosanitary data obtained from the epidemiological survey. Data on farm size (acres), potato cultivars grown, potato seed source, and crop management strategies, e.g., rotation periods, use of alternate crops, etc. were collected. Enumerators were trained prior to conducting the interviews. Data were collected directly onto tablets and collated using Epicollect® [1] software.

Data Analysis

The data was analyzed using Microsoft® Excel® Version 1911, mean and standard error of the means were calculated using the "psych" package, while the model of significance was detected by analysis of variance with a chi-square test and the pairwise comparison of the treatments undertaken using Tukey's multiple comparison test using the "lsmeans" on R version 3.6.1.

[1] http://www.epicollect.net/

RESULTS

Incidence, Distribution and Identification of Potato Cyst Nematodes

Cysts were detected from farms in all the counties prospected and were recovered from a total of 902 field samples (82.8%) during the initial survey (2016–2017) and in 66 fields (25.6%) in the follow-up survey in 2018. Nyeri County presented the lowest incidence (53%), while counties such as Trans Nzoia, Taita Taveta and West Pokot had 100% incidence (**Figure 1**). Of the 22 certified seed farms sampled, 82% (n = 18/22) farms were infested with PCN.

Detection and Molecular Identification of Potato Cyst Nematodes

Of 968 samples that had sufficient numbers of cysts to enable molecular diagnosis, 170 (17.6%) were identified as *G. rostochiensis* (GenBank accession: MN378644.1, MN378550.1, MN378566.1, 382342.1 – MN382349.1) from a combination of both protocols. A relatively lower PCR amplification efficiency was observed with EPPO primers in PCN-species identification. However, cysts from 61 fields were amplified using ITS primers AB28/TW81 (Joyce et al., 1994), which produced amplicons in samples that previously did not yield any PCR products using the same DNA template with the EPPO primers. Samples amplifying with EPPO primers (ITS5/PITSr3) were recovered from 6 counties, 144 in Nyandarua (46.6%), 13 in Narok (20.3%), 6 in Kiambu (7.0%), 3 in Nakuru (2.2%), 3 in Taita Taveta (27.3%) and 1 in Nyeri (2.2%). PCR products obtained using ITS5/PITSr3 primers were sequenced (MN382342 to MN382345 Kiambu County, MN382346 and MN382347 Nyandarua County, and MN382348 and MN382349 Narok County) and analyzed using the NCBI-BLAST tool. Our findings show high sequence identity (%) ranging from 90 to 95% to *G. rostochiensis* populations from EU, Asia, and Northern and Southern Africa, including those previously described in Kenya (**Figure 2**).

Detection of the *H1* Resistance Gene

The molecular analyses of potato cultivars confirmed the presence of the *H1* gene in cv.s Manitou, Markies, Destiny and Jelly (positive control) but not for cv. Shangi, indicating its susceptibility to *G. rostochiensis* (**Table 1**).

Potato Cyst Nematode Infestation and Yield Loss Assessment

The potential impact of PCN on potato yield from the in-depth survey of 86 fields in Nyandarua County showed that PCN were recovered from 72.1% of sampled fields and prevalent in all sub-counties. The highest incidence was observed in Kinangop (92.9%), followed by Kipipiri (80.0%), Ol'Joro Orok (78.6%), Ol'Kalou (52.9%) and Ndaragua (33.3%). Among these, infestation levels varied: between $1 < X < 25$ cysts (24.4%), $26 < X < 110$ cysts (22.1%), $111 < X < 230$ cysts (14.0%), $231 < X < 495$ cysts (5.8%), and $496 < X < 985$ cysts (5.8%) respectively per 200 g soil. On average, higher infestation levels were found in Kinangop, with the largest number (66.7%)

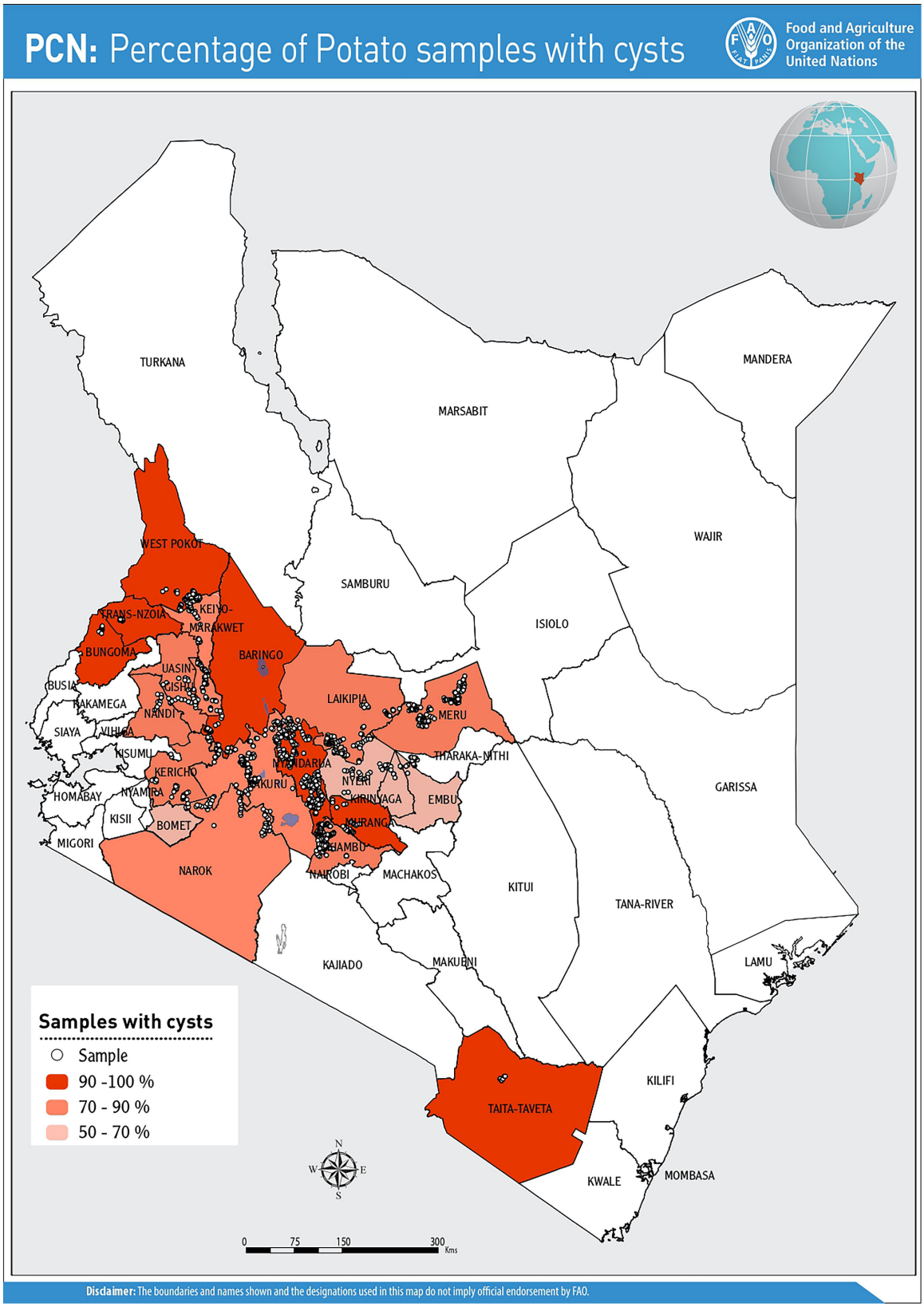

FIGURE 1 | PCN distribution and incidence level classification across the 20 counties in Kenya.

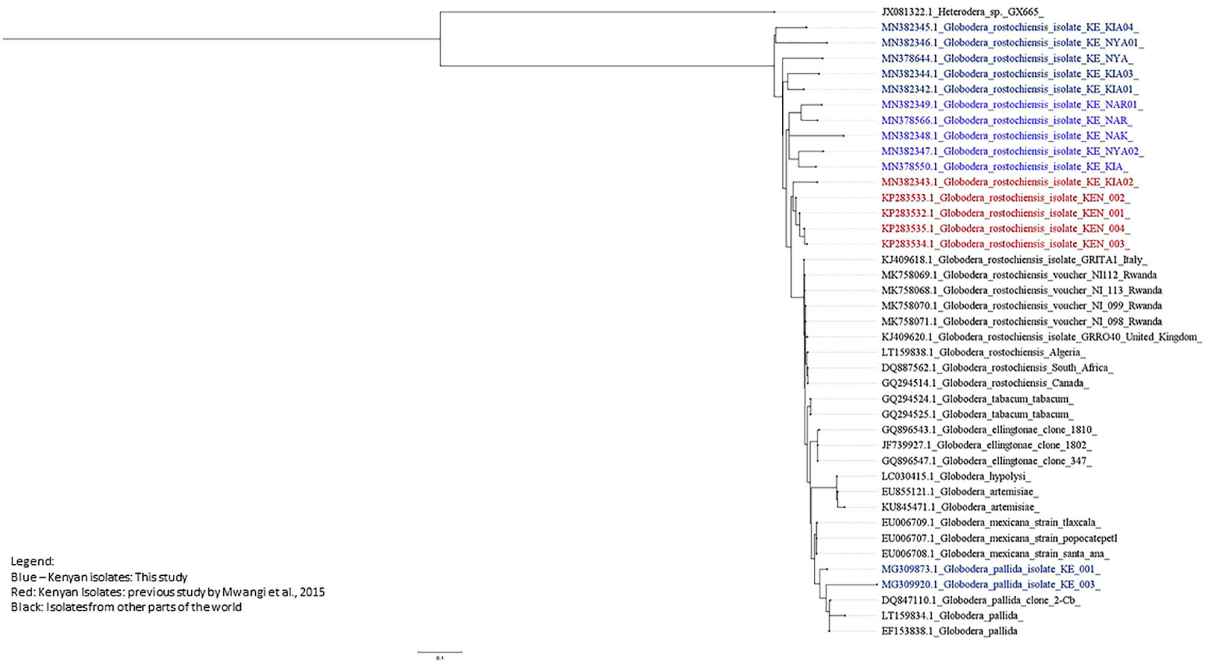

FIGURE 2 | Phylogenetic relation of Kenyan PCN populations compared to those reported in Africa and rest of the world.

TABLE 1 | Detection of *Globodera rostochiensis* (Ro1) *H1 resistance* gene in Kenyan grown potato cultivars.

Cultivars	BCH primers	TG689 primers	57R primers	Classification of PCN resistance[1]
Shangi	+	–	–	Susceptible (This article)
Manitou	+	+	+	Resistant
Markies	+	+	+	Resistant
Destiny	+	+	+	Resistant
Desireé	+	–	–	Susceptible control
Jelly	+	+	+	Resistant control

[1]*As referenced in the National Potato Council of Kenya NPCK (2019).*

of highly infested fields or "hotspots" with cyst counts ≥231 cyst/200 g soil (**Figures 3**, **4**).

The mean CV within Nyandarua County did not differ significantly among sub-counties, although mean CF levels were greater ($p \leq 0.05$) in Kipipiri and Ol'Joro Orok; Kinangop and Kipipiri presented the highest SI levels (viable eggs/g soil) with 158.5 and 90.7 viable eggs/g soil, respectively, while the lowest SI levels were observed in Ol'Kalou (30.6 viable eggs/g soil). Yield losses attributed to PCN, considering the damage threshold of 2.75 t/ha per 20 viable eggs/g soil (Brown and Sykes, 1983), ranged from a minimum of 4.2 t/ha in Ol'Kalou to a maximum of 21.8 t/ha in Kinangop (**Table 2**) based on the SI data per sub-county.

Smallholder Farmer Practices

The average household land size dedicated to potato production was 0.35 ha. Farmers acknowledged the use of up to 34 potato cultivars across Kenya (**Table 3**), among which cv. Shangi was the most preferred (65%, predominant in 13 counties), followed by cv. Arka (10%, predominant in Bungoma and Trans Nzoia Counties). Based on interviews, the overwhelming preference of cv. Shangi is attributed to its short dormancy (∼5–6 weeks) meaning that it does not require refrigeration/cool storage of tubers until the following planting season. It also has a fast cooking time, so it requires less fuel and labor for processing (i.e., boiling). This makes it particularly appealing to women, who are largely responsible for collection of firewood for cooking.

Most farmers (56.0%; n = 752) identified farm-saved seed, which is recycled over several seasons, and ware-potatoes bought from local markets (34.0%; n = 458) as their principal source of planting material. Government and private institutional sources of seed, such as Agricultural Training College-Farms (ATCs) (2.3%), seed aid from the Ministry of Agriculture (2.1%), National Research Organizations (KALRO) (1.7%) or private certified seed multipliers (1.9%) accounted for just 8.9% of seed supply. Noteworthy, the diversity on the sources of potato seed used for planting also varied among counties, although the two informal sources for seed ("Farm-saved" and "Markets") were predominant across counties (**Figure 5**). In counties such as Bungoma, Kirinyaga, Laikipia, Nyeri, and Trans Nzoia only "Farm-saved" and "Markets" seeds were acknowledged to be in use. The lowest diversity of potato seed source was observed in West Pokot, where "Markets" (ware potato) were the sole source of seed. The highest diversity of seed supply (n = 7) was recorded in Nyandarua and Taita Taveta. Only eight counties reported seed multipliers as an accessible source of planting material, and the highest percentage of farmers in Meru County (11.4%) accessed quality declared certified seeds (**Figure 6**). Respondents did not

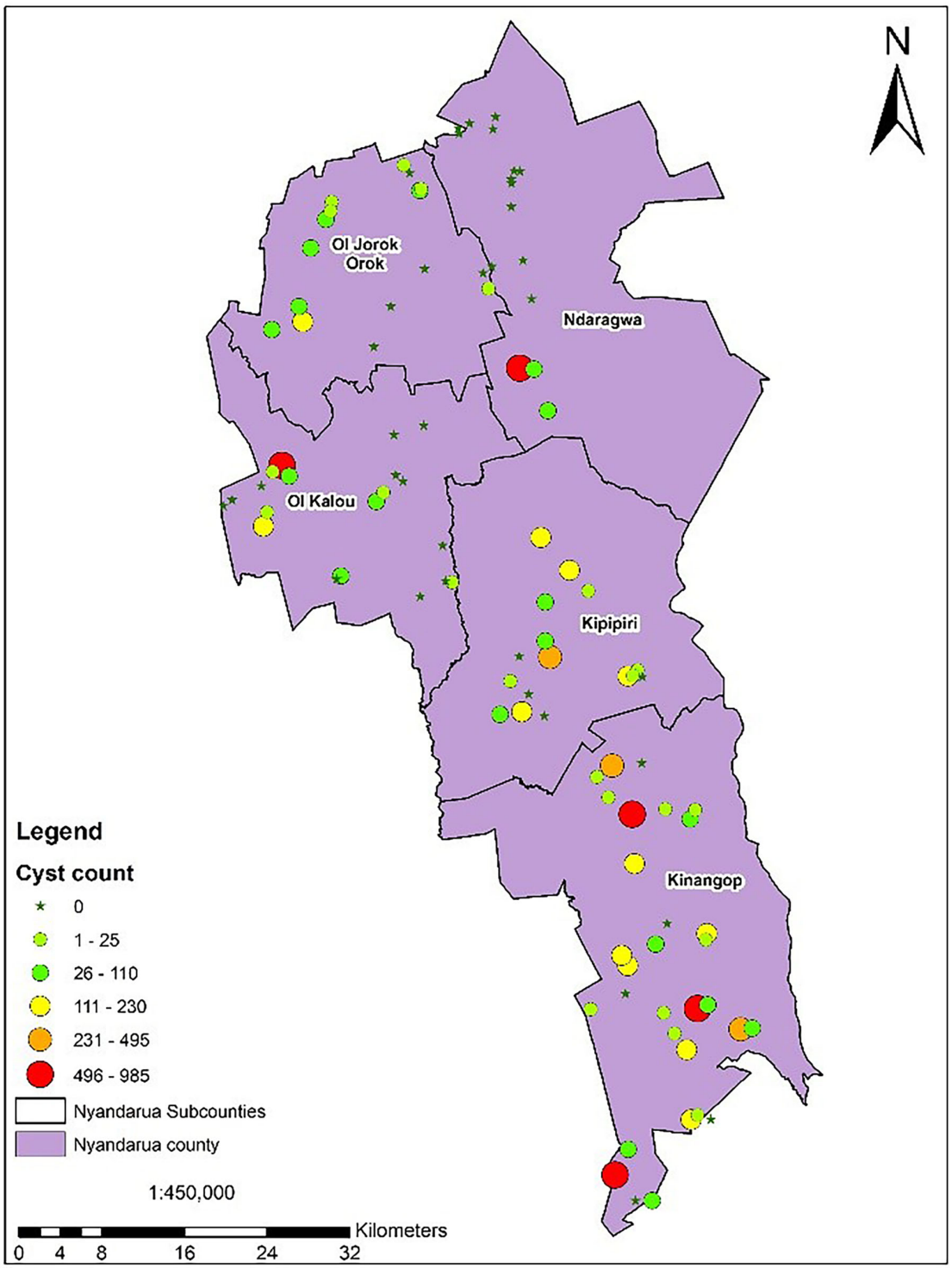

FIGURE 3 | PCN infestation levels across the 5 sub-counties of Nyandarua indicating the "hot-spots" in red.

use certified seeds because of: (i) high cost of potato seeds; (ii) limited impact experienced in terms of increased yields; (iii) scarcity of certified seeds for the most-preferred cultivar (i.e., cv. Shangi) especially at the onset of planting season.

The majority of farmers (89%) indicated that they employed crop rotation to manage potato pests and diseases (**Table 4**). Thus, in six counties surveyed, 100% of farmers practiced rotation, while in the remaining 14 counties crop rotation was

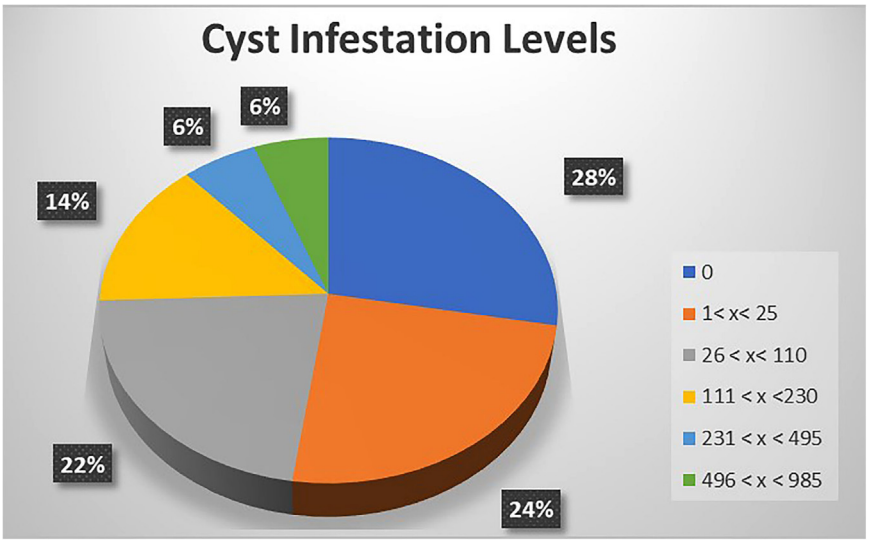

FIGURE 4 | A representation of PCN cyst infestation levels across the 5 Sub-counties of Nyandarua County.

TABLE 2 | Potential yield losses calculated from Brown and Sykes (1983) formula using PCN cyst and egg data.

Sub-county	Mean number of cysts*	Mean cyst fertility (eggs/cyst)*	Mean cyst viability (%)	Mean soil infectivity (viable egg/g soil)	Estimated mean yield loss (t/ha)
Kinangop (*n* = 21)	215 ± 64.9	147.3 ± 7.6	77	158.5	21.8
Kipipiri (*n* = 15)	98 ± 34.9	183.4 ± 13.9	88	90.7	12.5
Ol'Joro Orok (*n* = 15)	48 ± 21.3	180.6 ± 13.1	82	42.3	5.8
Ol'Kalou (*n* = 20)	52 ± 31.6	127.6 ± 13.4	79	30.6	4.2
Ndaragua (*n* = 15)	46 ± 40.0	143.5 ± 22.9	67	37.3	5.1

**Values expressed as mean ± SE; Mean number of cysts recovered from 200 g soil sample.*

practiced by 60.0 to 93.1%. The majority of farmers practiced rotations over a period of >1 year (two cropping seasons) to 7 years (14 cropping seasons) after planting the first crop (72.4%), with one exception where farm-saved potato seeds had been cultivated successively in the same field for over 10 years (or at least 20 successive crops) (**Figure 7**). However, in all rotation schemes described by farmers, only 21.2% included a different crop immediately following the first potato crop.

DISCUSSION

Recent studies reported for the first-time the occurrence of *G. rostochiensis* in Nyandarua County in Kenya (Mwangi et al., 2015). In the present study, we show that this PCN species is widespread and present in particularly high densities across the country, thus causing severe yield losses. The PCN species *G. pallida*, now confirmed in Kenya and sub-Saharan Africa (SSA) from the current study and separately documented as a new disease report (Mburu et al., 2018), is shown to be currently very restricted in its distribution. However, the country-wide distribution of *G. rostochiensis*, including counties bordering Uganda and Tanzania, where potato is also an important staple food source, creates great concern in respect to PCN distribution across the region. The recent report of *G. rostochiensis* in Rwanda (Niragire et al., 2019) demonstrates that the pest is already present and established elsewhere within the region.

During the current study, the inconsistency of positive amplifications to diagnose *G. rostochiensis* between the EPPO protocols (EPPO, 2013a,b) and the Bulman and Marshall (1997) protocol, indicates that false negatives could occur if only EPPO protocols had been used to diagnose Kenyan PCN populations. The Bulman and Marshall (1997) protocol has been commonly used in other parts of the world (Vossenberg et al., 2014), and specifically in detection of *G. rostochiensis* and *G. pallida* samples from Kenya (Mwangi et al., 2015; Mburu et al., 2018). Consequently, it is advised that at least two PCR-based protocols should be used to detect and diagnose PCN populations in the region and, importantly, that the EPPO protocol should not be entirely relied upon. However, the presence of other *Globodera* spp. other than PCN, in the country cannot be discounted either and should also be considered when receiving false positives.

In the East African region potato is a key commodity both for food security and as a cash crop for household income (Thiele et al., 2011). In Kenya, the crop represents a source of income for around 2.5 million people across the value chain (Abong and Kabira, 2013), with between 500,000 to 780,000 people directly involved in potato farming activities (Janssens et al., 2013). PCNs

TABLE 3 | Preferred potato cultivar grown in Kenyan counties and overall percentage uptake.

County	Cultivar	Percentage	Overall%
Bungoma	Arka	72.4	10
Trans Nzoia	Arka	70.0	
Taita Taveta	Asante	43.6	5
Bomet	Dutch Robjin	50.0	5
Laikipia	Humba Thuti	42.9	5
Embu	Kanyoni	30.0	5
Kirinyaga	Mukura Nooke	78.6	5
Baringo	Shangi	75.0	65
Elgeyo Marakwet	Shangi	92.6	
Kericho	Shangi	69.6	
Kiambu	Shangi	71.8	
Meru	Shangi	61.5	
Murang'a	Shangi	66.7	
Nakuru	Shangi	80.9	
Nandi	Shangi	77.8	
Narok	Shangi	89.6	
Nyandarua	Shangi	98.3	
Nyeri	Shangi	57.4	
Uasin Gishu	Shangi	92.9	
West Pokot	Shangi	100.0	

are highly destructive pests of potato, resulting in major losses to production and incurring significant investment toward their management (Niere and Karuri, 2018). They are indigenous to South America but have since become established in various potato growing regions around the world (Brodie et al., 1993; Hodda and Cook, 2009). In SSA, excluding South Africa, PCNs have been detected only in Kenya and Rwanda (Mwangi et al., 2015; Niragire et al., 2019), with a tenuous report from Sierra Leone (EPPO, 2009). The current study, therefore, determines that *G. rostochiensis* is now firmly established in the region and that *G. pallida* is present. The greater proportion of information on the importance of PCN has been established from studies in temperate climates. Kenya has a sub-tropical climate with an absence of prolonged frosting periods and relatively mild minimum temperatures across the year. This provides favorable conditions for 2–3 potato cropping seasons per year, given enough rainfall or irrigation (Gildemacher et al., 2009). The current study provides the first indication of PCN damage potential under such agro-ecological conditions, which provides compelling justification that urgent and serious action is needed. Our current study demonstrates that PCN is seriously threatening potato production in Kenya, where extremely high infestation levels are present. Current data indicate that on average, potato yields are equivalent to 9.9 t/ha, or 24.75% of the potential yield (40 t/ha). This equates to approximately USD $127 million annual potato losses in Kenya, based on two cropping seasons per year of susceptible cultivars, such as cv. Shangi. Even though the damage threshold used to calculate production losses in the current study were based on data from Europe (Brown and Sykes, 1983; EPPO, 2013a), this extrapolation is considered a realistic indication of the magnitude of PCN damage to potato production in Kenya. The

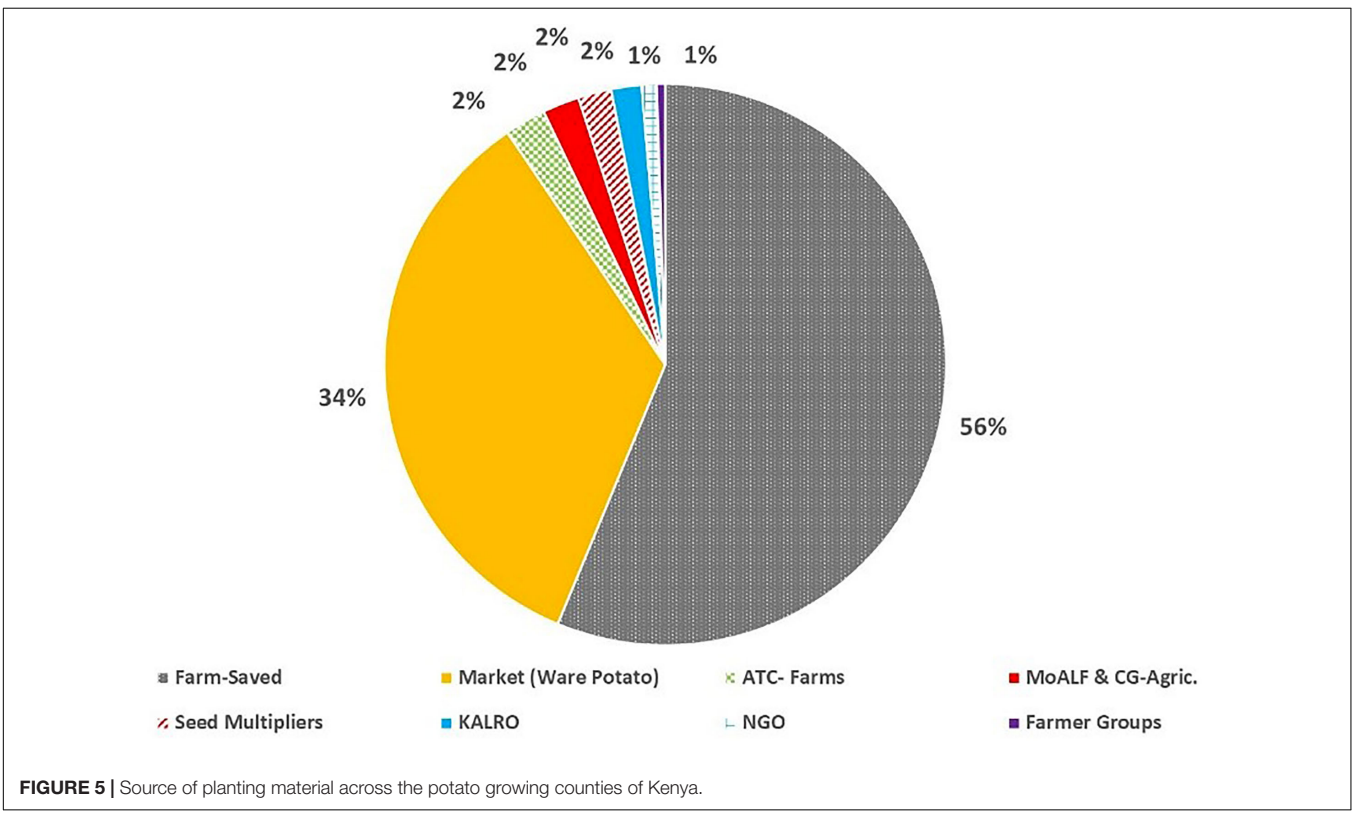

FIGURE 5 | Source of planting material across the potato growing counties of Kenya.

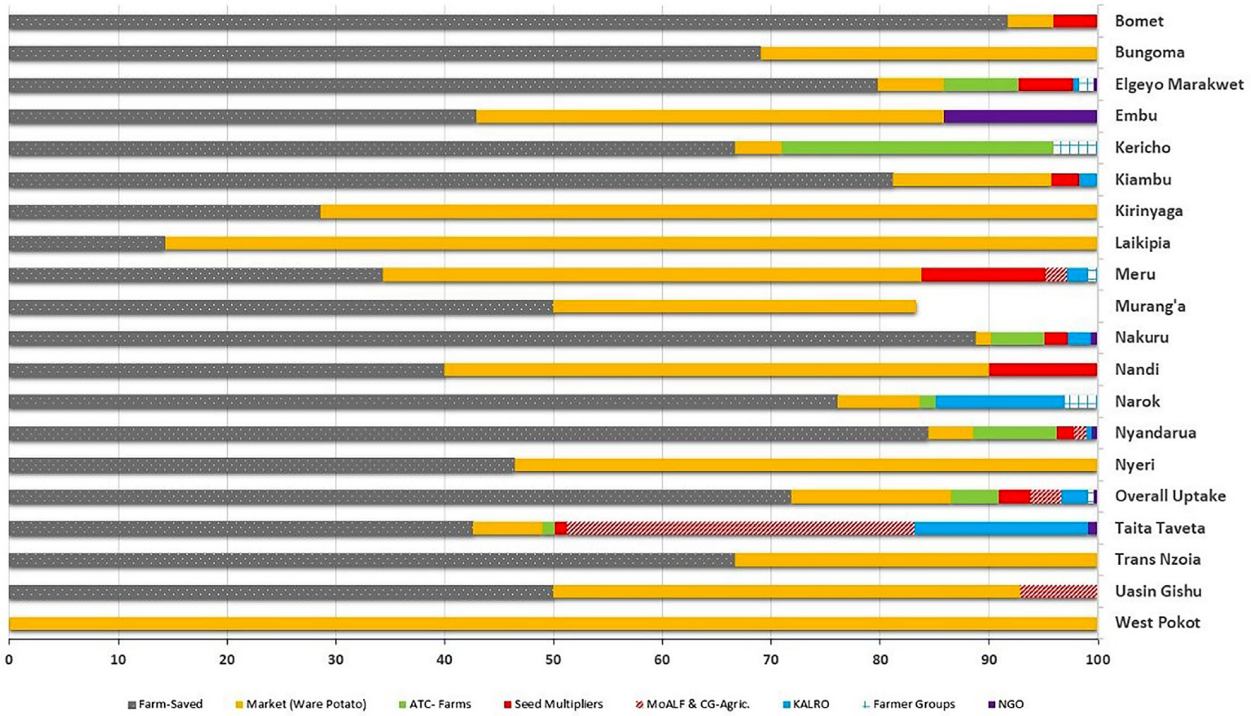

FIGURE 6 | Diversity of seed sources within each county in all potato growing counties in Kenya.

pervasive presence and high densities of PCN across the country undoubtedly helps to explain some of the current potato yield gaps, and why these have been increasing over recent years. Given the persistent shortage of certified seed potatoes and the inherent nature of using farm-saved seed, as highlighted from the current study, potato production gaps are likely to further widen due to low quality of planting material, other pest and diseases, or inefficient post-harvest handling and storage conditions (Muthoni et al., 2013). During the current study, PCN was established in ∼82% of the seed production farms in Kenya. These findings challenge the status of the formal seed system and highlights the urgent need for comprehensive phytosanitary control measures to be implemented in commercial potato seed operations (Cortada, 2018).

Plant parasitic nematodes are, over time, repeatedly overlooked as damaging soil-borne pests in Africa (Coyne et al., 2018). Their subterranean habit and often indistinct damage symptoms contribute to this neglect, and lack of awareness. Given that PCN are readily disseminated through the use of infected potato seed, the routine use of farm-saved tubers for seed in Kenya (Abong and Kabira, 2013) and the region (Gildemacher et al., 2009) undoubtedly encourages and perpetuates the PCN issue. Such inherent lack of awareness across the agricultural spectrum has inevitably played its part in facilitating its spread. How long PCN has been present and how it was introduced remains open to question. Potato was first introduced to Africa in the 17th century by Christian missionaries (VIB, 2019), while evidence of their importation into Kenya dates back over 100 years for agricultural diversification, seed aid (The Kenya Times, 1985) and for research purposes (McArthur, 1989). If we consider the sub-tropical climate, lack of frosting periods, year-round production with multiple cropping seasons per annum of susceptible cultivars, as well as the habitual use of

TABLE 4 | Adoption of crop rotation across the 20 surveyed counties in Kenya.

County	No rotation	Rotation	Percentage
Baringo	2	7	77.8
Bomet	3	23	88.5
Bungoma	2	27	93.1
Elgeyo Marakwet	78	143	64.7
Embu	0	9	100.0
Kericho	0	24	100.0
Kiambu	0	123	100.0
Kirinyaga	0	9	100.0
Laikipia	4	6	60.0
Meru	16	109	87.2
Murang'a	1	8	88.9
Nakuru	13	137	91.3
Nandi	1	9	90.0
Narok	7	62	89.9
Nyandarua	53	313	85.3
Nyeri	9	66	88.0
Taita Taveta	0	94	100.0
Trans Nzoia	1	8	88.9
Uasin Gishu	2	13	86.7
West Pokot	0	4	100.0

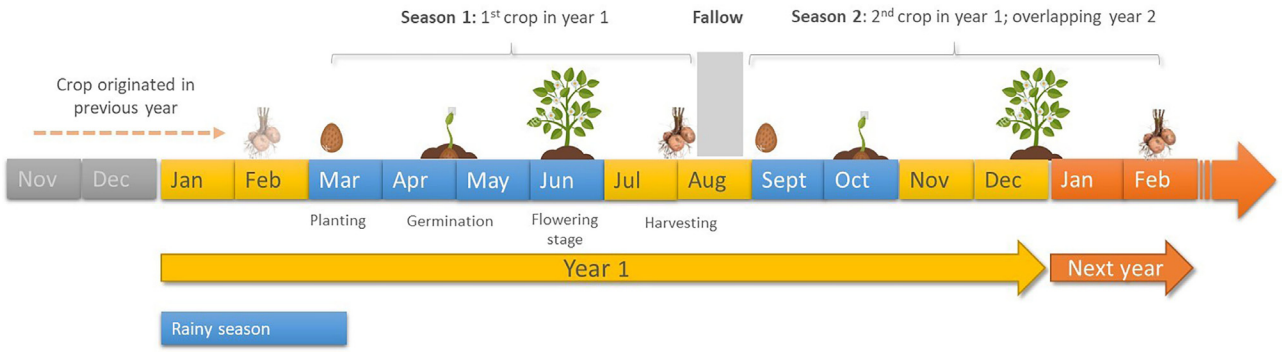

FIGURE 7 | Scheme of potato cropping seasons in 1 year.

farm-saved seed, the introduction of PCN may not have been as long ago as the high infestation levels would suggest (Nyongesa, 2015). The high mean cyst density levels of 98 cysts/200 cc soil (0.49 cysts/cc soil) and up to 985 cysts/200 cc in Kenya, which equate to 980 million cysts/ha, is way above the official detection threshold of 3.8 million cysts/ha in Europe (Spears, 1968; Davie et al., 2017), with mature and female cysts visible to the naked eye attached to roots. The densities encountered are consequently remarkably high and way above European norms. The agroecological factors in Kenya have therefore quite likely supported the "rapid" dispersal of PCN and development of such high densities. It is quite possible that the physiological nature and hatching behavior of these Kenya populations differ from their temperate climate counterparts. For example, the optimum temperature for hatch of the cereal cyst nematode, *Heterodera avenae,* recovered from Egypt was on average 5°C higher than for *H. avenae* populations recovered from Germany (Baklawa et al., 2017). This information is important to determine, as successful management options can be highly dependent on such characteristics.

In line with previous findings (Kaguongo et al., 2014; Sinelle, 2018), farmers interviewed in our study identified cv. Shangi as the most important and preferred potato cultivar. This farmer-selected cultivar was rapidly and informally introduced and distributed in the early 2000s (ISSD Africa, 2016) before its official release (Sinelle, 2018). Its short dormancy and fast sprouting nature makes it appealing and a ready source of recycled seeds that do not require cold storage between planting seasons. It was quickly adopted by Kenyan farmers, thus replacing other potato cultivars due to increasing market demand, early maturity and high yielding, despite its susceptibility to pests and diseases, particularly late blight. To our knowledge, our study is the first report confirming the susceptibility of cv. Shangi to *G. rostochiensis* infection. Following the preliminary results of our study in 2017 (FAO, 2017a; icipe, 2017), PCN testing was made a mandatory procedure for seed certification schemes, with resistance considered necessary for potato cultivars (NPCK, 2019). Consequently, the identification and introduction of cultivars with similar attributes to cv. Shangi, but with resistance against PCN could prove highly beneficial to addressing the PCN problem in Kenya, and the region. In addition, although farmers considered crop rotations as a suitable cultural practice to control pests and diseases, they were unaware of the importance of establishing suitable (non-PCN hosts) and sufficiently long rotation schemes to manage PCN. Smallholder farmers, who represent 98% of potato growers in Kenya, primarily grow potato as a cash crop, and for home consumption. They produce 83% of the national production, with an average farm size dedicated to this crop of less than 0.4 ha/year (Janssens et al., 2013). A lack of suitable land coupled with the prevailing status of potato as an income-generating cash crop deters farmers from practicing fallow or cultivating less lucrative non-host crops. A situation arises therefore with the continued cultivation of potato in infested farms until potato production becomes unprofitable. Awareness campaigns are therefore urgently required to enable farmers to understand the importance of managing this aggressive pest. As per international regulations (IPPC, 2008), countries affected by PCN are required to adopt strict phytosanitary regulations for seed potato production to prevent its further spread within and outside their borders. The results of the current epidemiological study on PCN in Kenya provide a basis upon which to establish suitable management approaches and policies against this destructive nematode pest.

CONCLUSION

Our results show that PCN is widely spread across the main potato growing counties of Kenya. *Globodera rostochiensis* is widely distributed, while *G. pallida* is currently highly restricted but present. More robust sampling techniques will be required to ascertain that fields are free of PCN infestation, rather than having low, below-threshold detection levels. Development of a suitable tool to validate the estimation of yield losses under Kenyan conditions is urgently required. There is need to create awareness with farmers on the importance of using certified seed, adoption of PCN resistant cultivars and practicing crop rotations. Due to inconsistencies in results from established molecular protocols, an in-depth molecular analysis of the PCN from Kenya would be required to fully characterize and understand the genetic complexity of cyst nematode populations present, including PCN pathotypes. Given the sub-tropical

nature prevailing in potato production areas, it will also be important to establish if this has influenced the phenotypic and behavioral nature of PCN in Kenya, which will have significant implications to the development of management options.

DATA AVAILABILITY STATEMENT

Reference sequences used in this study for phylogenetic analysis are freely available at the NCBI database (https://www.ncbi.nlm.nih.gov/) under the following accession numbers: MG309873.1, MG309920.1, MN382342.1 – MN382349.1, MN378550.1, MN378566.1, and MN378644.1.

AUTHOR CONTRIBUTIONS

HM, SH, LC, WR, MN, and ZK designed the study. LC and HM analyzed the data. DC, SH, MN, LC, JB, and HM wrote the manuscript. All authors improved and approved the final manuscript.

FUNDING

This study was funded by the Federal Ministry for Economic Cooperation and Development through the German Federal Enterprise for International Cooperation – GIZ Small grant (2017–2018) Project Number: 16.7860.6-001.00 and FAO (Food and Agricultural Organization of the United Nations) Technical cooperation project (TCP/KEN/3602). Funding is also acknowledged from North Carolina State University under Prime Award No. project OPP1118810; Root, Tubers and Bananas Cluster of the CGIAR. JB was supported by DELTAS Africa Initiative grant # DEL-15-011 to THRiVE-2. The DELTAS Africa Initiative is an independent funding scheme of the African Academy of Sciences (AAS)'s Alliance for Accelerating Excellence in Science in Africa (AESA) and supported by the New Partnership for Africa's Development Planning and Coordinating Agency (NEPAD Agency) with funding from the Wellcome Trust grant # 107742/Z/15/Z and the United Kingdom government. Additional support was obtained from *icipe* institutional funding from the United Kingdom's Department for International Development (DFID), the Swedish International Development Cooperation Agency (SIDA), the Swiss Agency for Development and Cooperation (SDC), Federal Democratic Republic of Ethiopia, and the Kenyan Government. The funders had no role in the design, data collection, interpretation, or decision to submit this publication.

ACKNOWLEDGMENTS

We acknowledge the Laboratory personnel at KEPHIS and *icipe*-IITA nematology lab (*Nem*Africa) for assistance in the laboratory during sample processing and analysis, Richard Bett and Benson Mwangi for the help in generating cyst infestation level maps.

SUPPLEMENTARY MATERIAL

The Supplementary Material for this article can be found online at: https://www.frontiersin.org/articles/10.3389/fpls.2020.00670/full#supplementary-material

REFERENCES

Abong, G. O., and Kabira, J. N. (2013). "The current status of the potato value chain in Kenya," in *Trends and Opportunities in the Production, Processing and Consumption of Staple Foods Crops in Kenya*, eds C. Onyango, G. Unbehend, and M. Lindhauer (Dresden: TUD Press), 56–59.

Baklawa, M., Niere, B., and Massoud, S. (2017). Influence of temperature and storage conditions on the hatching behavior of cereal cyst nematodes *(Heterodera avenae* Wollenweber) from Egypt. *J. Plant Dis.Prot.* 124, 213–225.

Brodie, B. B., Evans, K., and Franco, J. (1993). "Nematode parasites of potatoes," in *Plant Parasitic Nematodes in Temperate Agriculture*, eds K. Evans, D. L. Trudgill, and J. M. Webster (Wallingford: Cab International), 87–132.

Brown, E. B., and Sykes, G. B. (1983). Assessment of the losses caused to potatoes by the potato cyst nematodes, *Globodera rostochiensis* and *G. pallida*. *Ann. Appl. Biol.* 103, 271–276.

Bulman, S. R., and Marshall, J. W. (1997). Differentiation of Australasian potato cyst nematode (PCN) populations using the polymerase chain reaction (PCR). *N. Z. J. Crop Hortic. Sci.* 25, 123–129.

CIP (2019). *Farming Success with Potatoes in Kenya*. Available online at: https://cipotato.org/media/farming-success-potatoes-kenya/2019 (accessed November 5, 2019).

Cortada, L. (2018). *Outcome Case Overview. Roots, Tubers and Bananas (RTB) Report*. 1–4.

Coyne, D. L., Nicol, J. M., and Claudius-Cole, B. (2018). *Practical Plant Nematology: A Field and Laboratory Guide*. Cotonou: SP-IPM Secretariat, International institute of Tropical Agriculture (IITA), 82.

Davie, K., Pickup, J., and Cole, Y. (2017). *Potato Cyst Nematode Management in Scotland*. 1–31.

Devaux, A., Kromann, P., and Ortiz, O. (2014). Potatoes for sustainable global food security. *Potato Res.* 57, 185–199.

Devine, K. J., Dunne, C., O'Gara, F., and Jones, P. W. (1999). The influence of in-egg mortality and spontaneous hatching on the decline of *Globodera rostochiensis* during crop rotation in the absence of the host potato crop in the field. *Nematology* 1, 637–645.

EPPO (2009). PM 7/40(2) *Globodera rostochiensis* and *Globodera pallida*. *Bull. OEPP* 39, 354–368.

EPPO (2013a). PM 7/40(3) Erratum *Globodera rostochiensis* and *Globodera pallida*. *Bull. OEPP* 43, 564–564.

EPPO (2013b). PM 7/40(3) *Globodera rostochiensis* and *Globodera pallida*. *Bull. OEPP* 43, 119–138.

EPPO (2017). PM 7/40(4) *Globodera rostochiensis* and *Globodera pallida*. *Bull. OEPP* 47, 174–197.

Faggian, R., Powell, A., and Slater, A. T. (2012). Screening for resistance to potato cyst nematode in Australian potato cultivars and alternative solanaceous hosts. *Australas. Plant Pathol.* 41, 453–461.

FAO (2017a). *Combating Potato Cyst Nematode (PCN) in Kenya*. Rome: FAO publications, 1–2.

FAO (2017b). *The State of Food and Agriculture. Leveraging Food for Inclusive Rural Transformation*. Rome: FAO publications.

FAOSTAT (2018). *Food and Agricultural Organization of the United Nations. FAO Statistical Database*. Available online at: http://www.fao.org/faostat/en/#data/QC (accessed September 11, 2018).

Folkertsma, R. T., Helder, J., Gommers, F. J., and Bakker, J. (1997). Storage of potato cyst nematode at −80°C. *Fund. App. Nematol.* 20, 299–302.

Gildemacher, P. R., Demo, P., Barker, I., Kaguongo, W., Woldegiorgis, G., Wagoire, W. W., et al. (2009). A description of seed potato systems in Kenya, Uganda and Ethiopia. *Am. J. Potato Res.* 86, 373–382.

Goeminne, M., Demeulemeester, K., Lanterbecq, D., Proft, M. D., and Viaene, N. (2015). Detection of field infestations of potato cyst nematodes (PCN) by sampling soil from harvested potatoes. *Asp. Appl. Biol.* 130, 105–110. doi: 10.1007/978-1-4939-2620-6_11

Goeminne, M., Demeulemeester, K., and Viaene, N. (2011). A method for estimating the contribution of seed potatoes, machinery and soil tare in field infestations with potato cyst nematodes on a national scale. *Commun. Agric. Appl. Biol. Sci.* 76, 311–318.

Gouy, M., Guindon, S., and Gascuel, O. (2010). SeaView version 4: a multiplatform graphical user interface for sequence alignment and phylogenetic tree building. *Mol. Biol. Evol.* 27, 221–224. doi: 10.1093/molbev/msp259

Hall, T. A. (1999). BioEdit: a user-friendly biological sequence alignment editor and analysis program for Windows 95/98/NT. *Nucl. Acids. Symp. Ser.* 41, 95–98.

Harahagazwe, D., Condori, B., Barreda, C., Bararyenya, A., Byarugaba, A. A., Kude, D. A., et al. (2018). How big is the potato (*Solanum tuberosum* L.) yield gap in Sub-Saharan Africa and why? A participatory approach. *Open Agric.* 3, 180–189.

Haverkort, A. J., and Struik, P. C. (2015). Yield levels of potato crops: recent achievements and future prospects. *Field Crops Res.* 182, 76–85.

Hodda, M., and Cook, D. C. (2009). Economic impact from unrestricted spread of potato cyst nematodes in Australia. *Phytopathology* 99, 1387–1393. doi: 10.1094/PHYTO-99-12-1387

icipe (2017). *Training of 20 Government Technicians and Determination of PCN Status in 1,200 Soil Samples. (Icipe Final Narrative. Report., Icipe, Nairobi, Kenya)*. Available online at: http://www.icipe.org/research/plant-health/research-nematodes/projects/fao-emergency-assistance-control-potato-cyst

IPPC (2008). *Extension of Known Potato Cyst Nematode (PCN) in Victoria, Australia.* (IPPC Official Pest Report, Rome, Italy: FAO). No. AU-16/1. Available online at: https://www.ippc.int/IPP/En/default (accessed August 15, 2019).

ISSD Africa (2016). *The Role of Variety User Agreements in Access of Public Potato (Solanum tuberosum) Varieties in Kenya*. Available online at: http://www.issdseed.org/sites/default/files/alp_4_final_report_potato_user_agreements_final.pdf (accessed June 13, 2019).

Jaetzold, R., and Schmidt, H. (1983). *Farm Management Handbook of Kenya RRC-Embu. Vol. II/B*. Nairobi: Ministry of Agriculture.

Janssens, S. R. M., Wiersema, S. G., Goos, H., and Wiersma, W. (2013). *The Value Chain for Seed and Ware Potatoes in Kenya Opportunities for Development*. LEI Memorandum 13-080. LEI Wageningen UR, Den Haag, NL). Den Haag: LEI Wageningen UR, 57.

Joyce, S. A., Burnell, A. M., and Powers, T. O. (1994). Characterization of *Heterorhabditis* isolates by PCR amplification of segments of mtDNA and rDNA genes. *J. Nematol.* 26, 260–270.

Kaguongo, W., Maingi, G., and Giencke, S. (2014). *Post-harvest Losses in Potato Value Chains in Kenya: Analysis and Recommendations for Reduction Strategies*, eds K. Lohr, T. Pickardt, and H. Ostermann (Bonn: Deutsche Gesellschaft für Internationale Zusammenarbeit (GIZ) GmbH), 80.

Kiptoo, K. W., Xia, X., and Kipkemboi, K. K. (2016). Technical efficiency of smallholder potato farmers in Kenya: an analysis of major influencing factors in Koibatek, Baringo County. *Afri. J. Agric.Environ.* 2, 8–15.

Mburu, H., Cortada, L., Mwangi, G., Gitau, K., Kiriga, A., Kinyua, Z., et al. (2018). First report of potato cyst nematode *Globodera pallida* infecting potato (*Solanum tuberosum*) in Kenya. *Plant Dis.* 102, 1671–1671.

McArthur, C. L. (1989). *Evaluation, Choice and use of Potato Varieties in Kenya. Social Science Department, Working Paper 1989-1*. Lima: CIP, 44.

Mimee, B., Dauphinais, N., and Bélair, G. (2019). "Piler Dirt" survey for the sampling and detection of potato cyst nematodes. *Plant Dis.* 103, 2065–2069. doi: 10.1094/PDIS-12-18-2188-RE

Muthoni, J., Shimelis, H., and Melis, R. (2013). Potato production in Kenya: farming systems and production constraints. *J. Agric. Sci.* 5, 182–197.

Mwangi, J., Waceke, J., Kariuki, G., and Grundler, F. (2015). First Report of *Globodera rostochiensis* infesting potatoes in Kenya. *New Dis. Rep.* 31:18.

Niere, B., and Karuri, H. (2018). "Nematode parasites of potato and sweet potato," in *Plant Parasitic Nematodes in Subtropical and Tropical Agriculture*, eds R. Sikora, D. Coyne, J. Hallmann, and P. Timper (Wallingford: CAB International), 222–251.

Niragire, I., Couvreur, M., Karssen, G., Uwumukiza, B., and Bert, W. (2019). First report of potato cyst nematode (*Globodera rostochiensis*) infecting potato (*Solanum tuberosum* L.) in Rwanda. *Plant Dis.* 104:293.

NPCK (2017). *National Potato Council of Kenya. Potato Variety Catalogue*. Available online at: https://npck.org/Catalogues/NPCKCATALOGUE2017bookletK2.pdf (accessed August 20, 2019).

NPCK (2019). *National Potato Council of Kenya. Potato Variety Catalogue*. Available online at: https://npck.org/Catalogues/NPCKOnlineDocument.pdf (accessed August 20, 2019).

Nyongesa, M. (2015). What you need to know about potato cyst nematode (PCN), a new threat to potato farming in Kenya. *HortiNews* 38:44.

Official Journal of European Union (2007). *Council Directive 2007/33/EC of 11 June 2007. L 156, 12–22*. Available online at: https://eur-lex.europa.eu/eli/dir/2007/33/oj (accessed June 11, 2007).

Ogiga, I. R., and Estey, R. H. (1974). The use of meldola blue and nile blue A, for distinguishing dead from living nematodes. *Nematologica* 20, 271–276.

Okello, J. J., Zhou, Y., Kwikiriza, N., Ogutu, S., Barker, I., Shulte-Geldermann, E., et al. (2017). Productivity and food security effects of using of certified seed potato: the case of Kenya's potato farmers. *Agric. Food Secur.* 6, 25–34.

Park, J., Yang, H., De Jong, W. S., and Wang, X. (2018). An evaluation of two *H1*-linked markers and their suitability for selecting *Globodera rostochiensis* resistant potatoes in the New York breeding program. *Am. J. Potato Res.* 95, 170–177.

Perry, R. N. (2002). "Hatching," in *Biology of Nematodes*, ed. D. L. Lee (London: Taylor and Francis), 147–169.

Reader, J. (2009). *The Untold History of the Potato*. London: Vintage, 315.

Scott, G. J., Labarta, R., and Suarez, V. (2013). Booms, busts, and emerging markets for potatoes and potato products in East and Central Africa 1961-2010. *Potato Res.* 56, 205–236.

Scott, G. J., and Suarez, V. (2012). From Mao to McDonald's: emerging markets for potatoes and potato products in China 1961–2007. *Am. J. Potato Res.* 89, 216–231.

Sinelle, S. (2018). *Potato Variety Adoption and Dis-adoption in Kenya*. Nairobi: CIP and Syngenta Foundation.

Spears, J. F. (1968). The golden nematode handbook: survey, laboratory, control, and quarantine procedures. *US Agric. Res. Serv.* 353, 1–86.

The Kenya Times (1985). *Farmers Cry Out: Where is the Rain? Press Article(Monday, March 18, 1985*. Nairobi: The Kenya Times.

Thiele, G., Labarta, R., Schulte−Geldermann, E., and Harrison, G. (2011). *Roadmap for Investment in the Seed Potato Value Chain in Eastern Africa*. Lima: International Potato Center, 27.

VIB (2019). *Potato in Africa. Fact Sheets*. Available online at: http://www.vib.be/VIBDocumentLibrary/VIB_Facts%20Series_Potato%20in%20Africa%20LR.pdf (accessed June 6, 2019).

Vossenberg, B., Voogd, J., Westenberg, M., and Karssen, G. (2014). Comparison of three conventional PCR test (Bulman and Marshall) versions for the molecular identification of *Globodera pallida* and *G. rostochiensis* cysts and juveniles. *EPPO Bull.* 44, 27–33.

Conflict of Interest: The authors declare that the research was conducted in the absence of any commercial or financial relationships that could be construed as a potential conflict of interest.

frontiers in Plant Science

REVIEW
published: 22 July 2020
doi: 10.3389/fpls.2020.01125

Recent Advances in the Development of Environmentally Benign Treatments to Control Root-Knot Nematodes

Fereidoun Forghani and Abolfazl Hajihassani *

Department of Plant Pathology, University of Georgia, Tifton, GA, United States

Root-knot nematodes (RKNs), *Meloidogyne* spp., are sedentary endoparasites that negatively affect almost every crop in the world. Current management practices are not enough to completely control RKN. Application of certain chemicals is also being further limited in recent years. It is therefore crucial to develop additional control strategies through the application of environmentally benign methods. There has been much research performed around the world on the topic, leading to useful outcomes and interesting findings capable of improving farmers' income. It is important to have dependable resources gathering the data produced to facilitate future research. This review discusses recent findings on the application of environmentally benign treatments to control RKN between 2015 and April 2020. A variety of biological control strategies, natural compounds, soil amendments and other emerging strategies have been included, among which, many showed promising results in RKN control *in vitro* and/or *in vivo*. Development of these methods continues to be an area of active research, and new information on their efficacy will continuously become available. We have discussed some of the control mechanisms involved and suggestions were given on maximizing the outcome of the future efforts.

Keywords: root-knot nematodes (RKNs), environmentally benign, biological control, mechanisms, emerging strategies

OPEN ACCESS

Edited by:
Claudia S. L. Vicente,
Instituto Nacional Investigaciao Agraria e Veterinaria (INIAV), Portugal

Reviewed by:
Isabel Conceição,
University of Coimbra, Portugal
Pablo Castillo,
Institute for Sustainable Agriculture, CSIC, Spain
Cleber Furlanetto,
University of Brasilia, Brazil

***Correspondence:**
Abolfazl Hajihassani
abolfazl.hajihassani@uga.edu

Specialty section:
This article was submitted to Plant Pathogen Interactions, a section of the journal Frontiers in Plant Science

Received: *29 April 2020*
Accepted: *08 July 2020*
Published: *22 July 2020*

Citation:
Forghani F and Hajihassani A (2020) Recent Advances in the Development of Environmentally Benign Treatments to Control Root-Knot Nematodes. Front. Plant Sci. 11:1125. doi: 10.3389/fpls.2020.01125

INTRODUCTION

Nematodes are by far the most abundant animals on earth (van den Hoogen et al., 2019) and a dominant component of the soil (Bardgett and Van Der Putten, 2014). Plant-parasitic nematodes (PPNs) are a great threat to agriculture, causing an estimated annual yield loss of over $100 billion worldwide (Abad et al., 2003; Thoden et al., 2011). Among PPNs, the most yield-limiting group are root-knot nematodes (RKNs; *Meloidogyne* spp.). RKNs are obligate sedentary endoparasites which can easily reproduce in roots of over 3,000 plant species (Abad et al., 2003). They are widespread all over the world (Jones et al., 2013), and their population in the soil increases easily under appropriate conditions (Calderón-Urrea et al., 2016; Hajihassani et al., 2018).

Due to their economic importance, there is an ever-increasing need to develop sustainable management strategies and treatments for RKN control. Although cultural controls are commonly used, they are facing more limitations because of the broad host range of *Meloidogyne* spp. and the

presence of mixed populations of different RKN species in the field (Trudgill and Blok, 2001; Xiang et al., 2018). The use of *Meloidogyne*-resistant cultivars has been an effective management tool for RKN; however, not many resistant cultivars are commercially available, and resistance may be overcome by new emerging RKN species such as *M. enterolobii* (Xiang et al., 2018; Hajihassani et al., 2019b).

Application of nematicides has remained the most common short-term management strategy against RKN (Hajihassani et al., 2019a; Medina-Canales et al., 2019); however, in the recent decades several chemicals such as methyl bromide and aldicarb have been withdrawn from the market due to environmental and human health concerns and toxicity to non-target organisms (Kim et al., 2018; Xiang et al., 2018). Although replacement chemicals have been developed, they have not been fully successful in gaining the same levels of efficiency (Desaeger et al., 2017). New products continue to become commercially available and are evaluated for RKN management.

Around the world, researchers have been putting efforts into developing new environmentally benign strategies for RKN management. It is important to note that results from the same treatment may vary *in vivo* and *in vitro* due to other factors in soil such as pH, organic compounds, degradation of nematicide active ingredients, chemicals and biological properties of soil, temperature, *etc.*, affecting the treatment efficiency. Plants themselves are important factors to be considered as they can have different root exudates, causing differences in the properties of their adjacent soil, namely sugars, organic acids, amino acids, microorganisms and their interactions. Root exudates may even directly affect PPN regarding their attraction and/or attachment to the plant (Bell et al., 2019). As different plants may release different chemicals into the soil as attractant/repellent agents (Sikder and Vestergård, 2020), this can be a novel opportunity to control RKN. But little is known about the specific RKN attractants, and research on this topic is at its early stages (Čepulyte et al., 2018).

Biological control such as application of live microbes (bacteria, fungi, *etc.*) and/or their secondary metabolites, essential oils, plant extracts, individual and mixed acids such as organic and amino acids, natural bioactive substances, green manure and industrial wastes are some of the environmentally benign treatments that have been studied for their efficacy against RKN. Other strategies such as ozonated water (Veronico et al., 2017), silicon (Roldi et al., 2017) and steaming and solarization (Kokalis-Burelle et al., 2016) have also been tested. In this review, we discuss the published advances on these treatments since 2015 (as of April 2020) as an all-in-one resource for RKN research.

BIOLOGICAL CONTROL

Modes of Action

The mechanisms involved in biological control fall into two main categories: 1) antagonism against PPN and 2) plant growth promoting factors. These may result directly from the biological agents or from their metabolites (Stirling, 2014). Although other antagonists such as viruses, mites, collembola, turbellarians, oligochaetes, predaceous nematodes, and protozoans have also been tested, they have not yet been proven as efficient as bacterial or fungal organisms, or studied as much. To date, bacteria and fungi remain the prominent antagonists for PPN biocontrol (Xiang et al., 2018).

Biological agents with plant growth promoting factors are another tool considered to replace the chemicals in agriculture. These microorganisms help plants using mechanisms such as directly facilitating resource acquisition and production of cytokinin and gibberellins, and indirectly by production of antibiotics and lytic enzymes (Glick, 2012). All together, these will help the plants mitigate adverse effects of soilborne pathogens including RKN. The interaction between biological control agents with roots primes plants against RKN infection. Some of the mechanisms involved are up-regulation of several endogenous defense genes such as salicylic acid (SA)-dependent pathogenesis related genes of the systemic acquired resistance (SAR), pathogenesis related genes (*PR*-genes), *PR-1b*, *PR-1*, *PR-3*, *PR-5, ACO*, and other genes involved (Molinari and Leonetti, 2019). Enzyme activities, such as glucanase and endochitinase were also enhanced in roots of pre-treated inoculated plants. Hence, the interaction of biocontrol agents with the roots may prime plants against RKN. This topic is recently being explored and could open new doors into novel nematode control tools.

Bacterial Microorganisms

Application of biological control agents and plant growth promotion is not a new concept (Oostendorp et al., 1991) and has already been discussed in several comprehensive reviews (Cross et al., 1999; Khan and Kim, 2007; Timper, 2014; Schouteden et al., 2015; Ntalli and Caboni, 2017; Abd-Elgawad and Askary, 2018; Xiang et al., 2018; Dutta et al., 2019). A number of different bacterial genera, namely *Pasteuria*, *Pseudomonas*, *Burkholderia*, *Arthrobacter*, *Serratia*, *Achromobacter*, and *Rhizobium* are known to have nematicidal potential.

General mechanisms of action involved in biocontrol fit into one of the categories as antibiotic production and/or other antagonism against PPN or induced resistance, which can vary even within a single genus. For example, in the genus *Bacillus*, the anti-RKN mechanism of action is based on enzymatic action for *B. firmus*, toxic antibiotics in *B. cereus* and *B. subtilis*, and toxic protein particles namely cry proteins in *B. thuringiensis* (Abd-Elgawad and Askary, 2018). Application of *B. cereus* strain BCM2 to control *M. incognita* in tomato has shown that it colonized at the root exudates and worked as a second-stage juveniles (J2) repellent, resulting in reduction of the nematode damage (Li et al., 2019). Nematode-infected tomato plants treated with BCM2 showed 67.1% fewer J2 compared with the control. In another pot study using tomato, agrobacteria were reported to enhance plant defense against RKN (Lamovšek et al., 2017). Treating the plants with *Agrobacterium tumefaciens* two days before *M. ethiopica* inoculation resulted in reduced root galling and egg counts 45 and 90 days post-inoculation (DPI). Split-root experiments showed that the observed interaction between *A. tumefaciens* and the plants was systemic.

Co-application of *Chitiniphilus* sp. strain MTN22 and *Streptomyces* sp. MTN14 on Brahmi (*Bacopa monnieri*) has been reported to mitigate the *M. incognita* mediated oxidative stress and augment the bacoside content of the plant (Gupta et al., 2017). In greenhouse studies, fresh and dry biomass were improved by 1.7 and 2.1-fold respectively, upon treatment. Improvements were confirmed using electron microscopy through examination of J2 and eggs, and nematode numbers in the roots. A study has shown that a commercial biocontrol product (NemOut^{TM}) consisted of *B. subtilis*, *B. licheniformis*, and *Trichoderma longibrachiatum* could inhibit *M. incognita* reproduction on tomato (Silva J. de O. et al., 2017). The optimal dose (10 kg/ha) reduced *M. incognita* population density up to 56.5–63.9% compared to the control 65 DPI in the greenhouse. However, application of the fungus *Pochonia chlamydosporia* was still more efficient. None of these microorganisms had negative impacts on tomato growth.

Bacillus amyloliquefaciens strain Y1 was evaluated to control *M. incognita in vitro* and *in vivo* on tomato. Bacterial culture supernatant and crude extract of Y1 significantly inhibited the hatching of RKN eggs and caused J2 mortality (Jamal et al., 2017). The 10–40% supernatant (10–40 µl of bacterial supernatant adjusted to final volume of 100 µl using sterile distilled water) concentrations inhibited egg hatching by 32.5–60.6% after five days of exposure *in vitro*. The J2 mortality increased with increasing treatment concentration and exposure time, reaching the maximum (80%) after three days at 40% concentration. Plant growth parameters were significantly higher in the Y1-treated plants compared to the untreated controls. The researchers were also able to identify a dipeptide cyclo (D-Pro-L-Leu) compound as the anti-RKN compound using chromatographic techniques and nuclear magnetic resonance.

Another study aiming to control *M. incognita* in tomato was performed using *B. cereus* strain Jdm1 (Xiao et al., 2018). Culture supernatant significantly inhibited the egg hatching and reduced J2 numbers *in vivo*. Additionally, Jdm1 treatment decreased the root galling severity (43%) and promoted tomato growth performance. Field studies showed a greater control efficacy of up to 50% for gall index 30 DPI. Bacterial community of the tomato rhizosphere was initially impacted upon treatment, but soon recovered.

A commercial *B. firmus*-based product (Flocter; Bayer CropScience) alone and in combination with synthetic nematicides oxamyl (Vydate; Corteva Agriscience) and fosthiazate (Nemathorin; Syngenta) was examined under greenhouse conditions for the control of *M. incognita* in two independent cropping cycles of tomato (d'Errico et al., 2019). Application of *B. firmus* either alone or in combination with nematicides suppressed nematode population levels in the second crop cycle. However, combined application of *B. firmus* and nematicides resulted in lower galling severity. Root galling index (scale of 0–10) was 7.7 for the control while it was 5.9, 5.5, 5.8, 4.3, and 4.0 for *B. firmus*, oxamyl, fosthiazate, *B. firmus* + oxamyl, and *B. firmus* + fosthiazate, respectively. Thus, the application of *B. firmus* early in the growing season would be effective for the management of *M. incognita* on tomato. Most of these studies were focused on the application of a single strain. It would be promising to test whether co-application of the same bacterial genera members would result in better protection of roots against RKN and to determine if possible synergism exists among the closely related bacteria helping them to better dominate the soil microbiome.

Successful application of *B. subtilis*, *B. pumilus*, and *P. fluorescens* against *M. incognita* on cowpea in a greenhouse study has also been reported (El-Nagdi et al., 2019). The best reduction in nematode numbers was achieved using *P. fluorescens* (89%) followed by combined treatments of *P. fluorescens* and *B. subtilis* (88.50%). The highest yield increase (70.2%) was recorded in combined treatment, followed by 49.3% by *B. pumilus*. Successful application of *Bacillus* for RKN management has also been reported elsewhere, either alone or in combination with *Streptomyces rubrogriseus* and the nematicide Fosthiazate (Yue et al., 2019). These biocontrol agents are promising, but their activity should be evaluated under field conditions.

Another example of *Bacillus* with great anti-RKN potential is *B. pumilus* strain L1. Lee and Kim (2016) reported that this strain produced both protease and chitinase enzymes, which were the main causes for its *M. arenaria* antagonistic characteristics. The 10% bacterial culture caused 88% inhibition of egg hatching and approximately 90% J2 mortality in comparison to the control. Tomato pot experiments revealed significant reduction in the number of galls and egg masses as well as J2 population in soil six weeks after *M. arenaria* infestation. *B. pumilus* L1 not only could be a potential biocontrol agent for RKN but also caused plant growth promotion. Different *Bacillus* may possess different anti-RKN mechanisms, creating numerous paths of research to explore by combining these strains.

Pasteuria penetrans, a widely distributed endospore forming bacterium is well known as a RKN parasite (Liu et al., 2017). Its mechanisms of action are mainly based on affecting the RKN J2. The J2 infected with a few spores of *P. penetrans* will later produce a few or no eggs in host plants, whereas with increasing the number of spores, the J2 becomes less mobile and its ability to penetrate roots can be reduced (Chen and Dickson, 1998; Liu et al., 2017). In a recent work mainly focusing on the physicochemical and biological properties of coffee rhizosphere, the researchers wanted to assess how such properties would influence the *M. exigua* suppression in the field. In the majority of the coffee farms with highest suppressive effects on RKN, *P. penetrans* was a major component of the soil rhizosphere (Botelho et al., 2019). In suppressive soils, approximately 83% of J2s were dead resulting in the highest coffee bean yields.

Soil microbiome was evaluated for *M. hapla* and *M. incognita* suppression (Topalovic et al., 2019). Four soil series with similar texture, organic matter content and pH were collected from different geographical locations. However, only one of the soils was identified as a potential RKN-suppressive soil, and its microbiome was harvested and inoculated into tomato pots infested with *M. hapla* and *M. incognita*. In the case of *M. hapla*, the RKN-suppressive soil had 32% fewer galls per root than the

other soils tested. The suppressive soil was less efficacious in controlling *M. incognita* compared to *M. hapla*. Interestingly, microbial suspensions from the suppressive soil did not affect mortality of any of the nematode species tested *in vitro*, in contrast to the pot studies, highlighting the fact that plant-mediated antagonism and other factors in the soil may play a vital role in the anti-RKN properties of biocontrol strategies.

Rhizobacteria improve soil texture, and the compounds they secrete constitute valuable biostimulants modulating plants' stress responses. These interactions are managed via signal exchanges between plant roots and the microbes (Ma et al., 2011; Backer et al., 2018). It has been proven that biological growth promoting factors may improve plant growth and reduce the negative effect of RKN in seedlings (Khanna et al., 2019). In that study, the effect of plant growth promoting bacteria (*Pseudomonas aeruginosa* and *Burkholderia gladioli*) on growth and antioxidative potential in nematode-infected tomato was assessed, and microorganisms with growth promoting characteristics improved tomato defense to encounter oxidative stress generated under RKN infection. A similar study using tomato infected with *M. incognita* reported that each of *B. cereus*, *B. licheniformis*, and *P. fluorescens* significantly reduced J2 numbers, and plants with *B. cereus* had lower root galling compared to other treatments (Colagiero et al., 2018).

Viljoen et al. (2019) screened 27 plant growth promoting rhizobacteria strains against *M. incognita* on 6-week-old carrot seedlings. Five of the strains, *B. firmus* T11, *B. aryabhattai* A08, *Paenibacillus barcinonensis* A10, *P. alvei* T30, and *B. cereus* N10w caused 86, 85, 85, 81, and 82% reduction in gall numbers, respectively. In the greenhouse, *P. alvei* T30 and *B. aryabhattai* A08 showed potential as biological control agents of *M. incognita* on carrot and tomato, respectively.

Fungal Biocontrol

Application of fungal microorganisms for managing RKN as well as other agricultural pests has been ongoing for decades. Some of the most prominent fungal species for RKN control belong to *Actylellina*, *Arthrobotrys*, *Aspergillus*, *Catenaria*, *Dactylellina*, *Hirsutella*, *Pochonia*, *Purpureocillium*, and *Trichoderma* (Timper, 2014; Abd-Elgawad and Askary, 2018). *Arthrobotrys* and *Dactylellina* can trap RKN J2s in the soil using their hyphal *structures* and decrease the invasion ability of the nematode. However, the extent of RKN mitigation may be influenced by several factors, as soil is a dynamic matrix (Saxena et al., 1987; Hsueh et al., 2013; Wang et al., 2014).

Colonization of plants by particular endophytic fungi can provide plants improved defense against PPN. The mechanisms involved seem to be multifactorial (Schouten, 2016), which are found within a range of genera such as *Acremonium*, *Alternaria*, *Fusarium*, and *Trichoderma* (Qiang et al., 2012). These mechanisms may include repellent activity reducing J2 attraction to roots (Le et al., 2016), attenuated or delayed development of adult females and reduction of their fecundity (Martinuz et al., 2013). Some endophytes such as *Paecilomyces* and *Trichoderma* may also trap and kill RKN in the soil or root systems. These may act at different nematode life stages (*i.e.* eggs, juveniles, or adults) (Bordallo et al., 2002; Rumbos and Kiewnick, 2006; Yao et al., 2015; Schouten, 2016). Competition for resources such as sugars is another mechanism used (Hofmann et al., 2009a; Hofmann et al., 2009b). Production and secretion of nematicidal metabolites have also been confirmed by several *in vitro* and *in vivo* studies (Bush et al., 1993; Kunkel and Grewal, 2003; Goswami et al., 2008; Bacetty et al., 2009; Tian et al., 2014). Finally, production of plant like hormones such as cytokinins and gibberellins and mobilizing and enhancing plant defense are two other mechanisms that some endophytic fungi use (van Loon et al., 1998; Rodriguez et al., 2009; Redman et al., 2011; Sikder and Vestergård, 2020). A novel study recently reported that *P. chlamydosporia* can induce plant-dependent systemic resistance to *M. incognita* (Ghahremani et al., 2019).

Arbuscular mycorrhizal fungi (AMF) are obligate root symbionts that help protect their host plants against biotic stresses such as PPN infection. This is achieved via a number of mechanisms such as higher nutrient uptake, altered root morphology, competing for space and nutrition with PPN, and inducing plant systemic resistance (Schouteden et al., 2015). The host provides photosynthetic carbon for AMF (Gianinazzi et al., 2010) and AMF help with the uptake of water, minerals and even micro-elements (Smith and Smith, 2011; Baum et al., 2015). The symbiosis may also result in increased root growth and branching (Vos et al., 2014). Overexpression of pathogenicity-related genes in plants due to AMF symbiosis has also been reported (Andrade et al., 2010; Hao et al., 2012).

Meloidogyne enterolobii is an emerging and destructive RKN species, and there is ongoing research on the characterization and/or development of biological microorganisms for its control (Silva S. D. et al., 2017). The inhibiting effects of two egg-parasitic fungi, *Pochonia chlamydosporia* (19 strains) and *Purpureocillium lilacinum* (14 strains) against *M. enterolobii* were assessed on agar plates. Reductions of 13 to 84% were observed depending on the fungal strain used. Combining fungal strains, however, did not improve the anti-hatching effect. The most efficacious strains of *P. chlamydosporia* (CG1006, CG1044) and *P. lilacinum* (CG1042, CG1101) were selected for further experiments. Future research should focus on assessing the potential of application timing of biological microorganisms on RKN control and targeting better development of fungal hyphae or conidial structures. Results of the pot studies using tomato and banana revealed that optimal fungal treatments were able to reduce post-harvest egg numbers of RKN in the plants inoculated with 500 eggs. The control effect was mitigated as initial nematode inoculation level increased. In one experiment for banana, the number of eggs after 12 months of *P. chlamydosporia* inoculation was reduced by 34%, and no significant reduction was observed in tomato plants after 3 months. In another experiment with tomato using *P. chlamydosporia* and *P. lilacinum*, the number of eggs was reduced by 34 and 44%, respectively, when initial infestation level was low (500 eggs). It was concluded that the application of *P. chlamydosporia* and *P. lilacinum* could be used as a component of an integrated pest management (IPM) approach in fields with low pressure of the nematode.

In contrast, the effect of three *P. chlamydospora* isolates (Pc-3, Pc-10, and Pc-28) for the control of *M. javanica* on tomato was

not promising (Xavier et al., 2017) as none of the isolates were able to reduce gall severity whether applied individually or in combination. However, the number of eggs was decreased in comparison to the control for isolate Pc-10 and the mixtures Pc-10 + Pc-3 and Pc-10 + Pc28 + Pc-3. In another combined study, suitability of *P. chlamydosporia* for RKN management was further confirmed (Escudero et al., 2017). The novelty of this work was the co-application of chitosan and *P. chlamydosporia* resulting in increased root colonization by the fungi and accordingly higher reductions in RKN damage.

The effect of *P. lilacinum* strain PL251 combined with fluopyram was tested against *M. incognita* (Dahlin et al., 2019). In the greenhouse, the commercial nematicide Velum and strain PL251 were formulated as a wettable granular and applied on tomato. Reductions of 56 and 68% in the number of J2 were achieved after PL251 being used alone and in combination with Velum, respectively. A similar reduction in the root galling was observed for which the index (scale of 0–10) was 3.8 for the control *versus* 1.8 for the plants with the combined treatment. The researchers suggested that Velum would reduce the nematode population at planting and therefore reinforce the biocontrol efficacy of *P. lilacinum* during the growing season.

Kim et al. (2018) screened 500 isolates of endolichenic fungi, *Xylaria* sp., and found that only one strain "KCTC 13121" had strong nematicidal activity. The *in vitro* studies revealed that grammicin at concentrations of 15.9 and 5.87 μg/ml was able to control *M. incognita* with 50% efficiency against J2 and egg hatching after 3 and 14 days, respectively. In addition, the wettable powder-type formulation and fermentation broth filtrate from *X. grammica* KCTC 13121 were able to suppress the development of RKN in tomato and melon. The entomopatogenic fungus *Lecanicillium muscarium*, relatively known as a biocontrol agent against insect pests (Faria and Wraight, 2007), was studied against *M. incognita* in both *in vitro* and *in vivo* conditions (Hussain et al., 2018). Three *L. muscarium* isolates (Lm1, Lm2, Lm3) were effective against *M. incognita* with Lm1 being prominent. Tomato treated with *L. muscarium* was positively affected for plant growth compared with control. Only 5% of the fungus-infected eggs hatched *in vitro* in contrast to 96% in the control. Greenhouse studies also showed that Lm1 decreased the number of galls and eggs by 80 and 90%, respectively.

Another fungus recently studied for its anti-RKN effects was *Metarhizium guizhouense* PSUM02 (Thongkaewyuan and Chairin, 2018). Crude extracts of the fungus grown on a protein-enriched medium contained a protease (33 kDa) which in combination with the fungus spores (1×10^4 spores/ml) completely inhibited hatching of the *M. incognita* eggs within 24 h *in vitro*. The mortality of J2 increased to 100%, 48 h post-treatment. The mycelia invaded immature eggs, while the eggs containing juveniles and the hatched juveniles were resistant. Electron microscopy observations showed extensive damage to eggshell and cuticle upon individual and combined treatments.

Trichoderma longibrachiatum was evaluated *in vitro* for its biocontrol efficacy against *M. incognita* (Zhang et al., 2015). Results showed a strong lethal effect (>88%) on the nematode when J2s were exposed for 14 days to 1×10^5 to 1×10^7 conidia/ml. The same concentrations of the fungus significantly reduced *M. incognita* infection in cucumber and improved plant growth in the greenhouse. *Trichoderma* strains have also been proven effective both as plant growth promoter and *M. incognita* control agent on pepper (Herrera-Parra et al., 2017). Approximately, 22 to 35% reductions in galling index were reported in pots treated with *T. atroviride*, *T. virens*, and *T. harzianum*-C2. In addition, *T. atroviride* reduced the nematode egg production by 63% and the number of females by 14.36%.

Effect of *Trichoderma* spp. and *P. lilacinum* on *M. javanica* in a commercial pineapple production setting has also been studied (Kiriga et al., 2018). Three *Trichoderma* isolates, *T. asperellum* M_2RT_4, *T. atroviride* F_5S_{21}, and *Trichoderma* sp. MK_4 and two *P. lilacinum* (KLF_2 and MR_2) were used. Using individual inocula, *T. asperellum* M_2RT_4 and MK_4 as well as the two *P. lilacinum* isolates reduced *M. javanica* root galling from 61 to 82%. *Trichoderma asperellum* M_2RT_4 was the most effective fungus reducing galling, egg mass and egg numbers by over 82, 78, and 88%, respectively. It also increased root fresh weight by 91%.

Trichoderma spp. may reduce RKN infections through triggering host defense. A group of researchers investigated whether *Trichoderma* modulates the hormone signaling network in the host to induce resistance to nematodes (Martínez-Medina et al., 2017). Using *M. incognita*, they found that root colonization by *Trichoderma* prevented nematode performance both locally and systemically at multiple stages such as invasion, gall formation and reproduction. First, *Trichoderma* primed SA-regulated defenses, limiting nematode root invasion. Then, it enhanced jasmonic acid (JA) regulated defenses, thereby antagonizing the deregulation of JA-dependent immunity by the nematodes, compromising galling and fecundity.

One of the most recent species characterized as anti-RKN is *Mortierella globalpina* (DiLegge et al., 2019). *Caenorhabditis elegans* was infected with a soil slurry containing a microbiome likely to house nematophagous microbes. Infected nematodes were sub-cultured repeatedly to isolate pure cultures of the microbe with nematicidal activity. Pure cultures were confirmed to be antagonistic to *C. elegans* and were identified as *M. globalpina*. *In vitro* studies showed that *M. globalpina* trapped *M. chitwoodi via* hyphal adhesion to its cuticle layer, penetrated it and killed the nematode by digesting its cellular contents. The effectiveness of fungi on both eggs and J2–J4 stages was confirmed using electron microscopy. In the *in vivo* experiments, *M. globalpina* promoted the plant growth. It would be crucial to test this approach on other major RKN species including *M. incognita* and *M. arenaria* to assess its potential broad-spectrum effect. Another path to take would be combining this species with other microbes in search of developing a dynamic multi-dimensional biological control inoculum for agricultural application.

The possibility of using mushrooms as anti-nematode tools has been gaining attraction. In this context, recently the ovicidal, nematicidal, and nematistatic potential of crude extract and metabolites retained from liquid mushroom

cultures was assessed against *M. javanica* (Hahn et al., 2019). The interaction of the mushroom mycelium and *M. javanica* J2 was also examined. A total of 24 mushroom isolates from 15 different species were included. Among them, *Lentinula edodes*, *Macrocybe titans*, and *Pleurotus eryngii* reduced the nematode damage in all experiments. Mushrooms have therefore the potential to control RKN.

Table 1 shows a summary of the biocontrol methods and strategies evaluated since 2015. In comparison to the conventional chemicals, these methods typically need a longer time to show visible results against RKN. Also, their efficacy may drop in the field compared to controlled experimental conditions, which can be due to various external factors in soil impacting the microorganisms. Therefore, it is necessary to put more effort into developing improved biocontrol strategies. One of the possibilities can be the application of targeted/specialized methods. It would be suitable to have the soil properties data such as biological, chemical and texture factors and choose the best biological agent with the highest adjustability to that particular soil.

NATURAL COMPOUNDS

Application of Acids

A variety of different organic acids including amino, acetic, butyric, formic, and propionic acids are known to have toxic effects on certain species of PPN. These are the result of either

TABLE 1 | Summary of biological control strategies tested from 2015 to April 2020 for the control of root-knot nematodes (*Meloidogyne* spp.).

Organism	RKN species	Type of study	Host plant	Reference
Bacteria				
Bacillus cereus	*M. incognita*	*In vitro, in vivo*	Tomato	(Li et al., 2019)
	M. incognita	*In vitro, in vivo*	Tomato	(Xiao et al., 2018)
	M. incognita	*in vitro, in vivo*	Tomato	(Colagiero et al., 2018)
Agrobactrium tumefaciens	*M. ethiopica*	*In vivo*	Tomato	(Lamovšek et al., 2017)
Bacillus amiloliquefaciens	*M. incognita*	*In vitro, in vivo*	Tomato	(Jamal et al., 2017)
Bacillus firmus	*M. incognita*	*In vivo*	Tomato	(d'Errico et al., 2019)
Pseudomonas fluorescens	*M. incognita*	*In vivo*	Cowpea	(El-Nagdi et al., 2019)
	M. incognita	*In vitro, in vivo*	Tomato	(Colagiero et al., 2018)
Bacillus pumilus	*M. arenaria*	*In vitro, in vivo*	Tomato	(Lee and Kim, 2016)
Bacillus licheniformis	*M. incognita*	*In vitro, in vivo*	Tomato	(Colagiero et al., 2018)
Pasteuria penetranse	*M. exigua*	*In vivo*	Coffee	(Botelho et al., 2019)
Fungi				
Pochonia chlamydosporia	*M. incognita*	*In vivo*	Tomato	(Silva J. de O. et al., 2017)
	M. enterolobii	*In vitro, in vivo*	Banana/Tomato	(Silva S. D. et al., 2017)
Purpureocillium lilacinum	*M. enterolobii*	*In vitro, in vivo*	Banana/Tomato	(Silva S. D. et al., 2017)
	M. javanica	*In vivo*	Pineapple	(Kiriga et al., 2018)
Xylaria grammica	*M. incognita*	*In vitro, in vivo*	Melon/Tomato	(Kim et al., 2018)
Lecanicillium muscarium	*M. incognita*	*In vitro, in vivo*	Tomato	(Hussain et al., 2018)
Metarhizium guizhouense	*M. incognita*	*In vitro*	–	(Thongkaewyuan and Chairin, 2018)
Trichoderma longibrachiatum	*M. incognita*	*In vitro, in vivo*	Cucumber	(Zhang et al., 2015)
Trichoderma atroviride	*M. incognita*	*In vivo*	Pepper	(Herrera-Parra et al., 2017)
Virens harzianum				
Trichoderma asperellum	*M. javanica*	*In vivo*	Pineapple	(Kiriga et al., 2018)
Mortierella globalpina	*M. chitwoodi*	*In vitro, in vivo*	Pepper	(DiLegge et al., 2019)
Mushrooms				
Lentinula edodes	*M. javanica*	*In vitro*	–	(Hahn et al., 2019)
Macrocybe titans				
Pleurotus eryngii				
Co-application				
Pochonia chlamydosporia & Chitosan	*M. javanica*	*In vitro, in vivo*	Tomato	(Escudero et al., 2017)
Chitiniphilus sp. & *Streptomyces* sp.	*M. incognita*	*In vivo*	Brahmi	(Gupta et al., 2017)
Pseudomonas fluorescens & *Bacillus subtilis*	*M. incognita*	*In vivo*	Cowpea	(El-Nagdi et al., 2019)
Bacillus subtilis, *Trichoderma longibrachiatum*, & *Bacillus licheniformis*	*M. incognita*	*In vivo*	Tomato	(Silva J. de O. et al., 2017)
Soil microbiome	*M. incognita*, *M. hapla*	*In vivo*	Tomato	(Topalovic et al., 2019)
Purpureocillium lilacinum & Nematicide "Velum"	*M. incognita*	*In vivo*	Tomato	(Dahlin et al., 2019)

microbial decomposition of different compounds in the soil or metabolites produced by microorganisms (Oka, 2010). Several successful applications of acids against nematodes have been reported such as heptalic acid (Abd-Elgawad and Askary, 2018) and hydroxamic acids (Zasada et al., 2005). However, acid's ability against nematodes is heavily influenced by soil conditions (Momma et al., 2006). In a study conducted *in vitro* and in the greenhouse, the nematicidal efficacy of 5-aminolevulinic acid (ALA) on *M. incognita* and other PPN was tested (Cheng et al., 2017) in which ALA exhibited a strong anti-RKN effect and reduced egg hatching of *M. incognita* by 90%. Treatment of the soil with 6.0 mM ALA reduced the galling index (scale of 0–4) from 2.3 in control to approximately 0.3 on tomato. The number of egg masses per root was decreased from about 180 to only 50. It also significantly altered the nematode metabolism including the total protein production, malondialdehyde content, and oxidase activities, suggesting that ALA is a promising biodegradable bionematicide.

In a study on plant secondary metabolites, the anti-RKN capacity of acetic acid and other natural compounds was evaluated against *M. incognita* (Ntalli et al., 2016). The acid treated J2s were examined by electron microscopy, showing that acetic acid harmed the J2 cuticle and degenerated the nuclei of pseudocoel cells and vacuolized the cytoplasm resulting in nematode death. In another work, a total of 237 bacterial strains were screened for their nematicidal activity against RKN. Among those, *Lactobacillus brevis* strain WiKim0069 isolated from kimchi, a Korean fermented food, was found to produce organic acids with nematicidal activity (Seo et al., 2019). The culture filtrate of WiKim0069 had a pH of 4.2 and contained acetic acid (11,190 μg/ml), lactic acid (7,790 μg/ml), malic acid (470 μg/ml), and succinic acid (660 μg/ml). An artificial mixture of the four organic acids produced by WiKim0069 also induced 98% *M. incognita* J2 mortality at a concentration of 1.25%. When the filtrate was tested on *M. incognita* infested plants in pot experiments, it suppressed the formation of galls and egg masses on tomato roots in a dose dependent manner. It was also capable of reducing galls on melon by 62.80% in the field study. We have discussed this study here and not in the biological control section, as such entitlement would be more suitable in case WiKim0069 can produce similar promising results upon application to the soil.

Humic acid was evaluated to control *M. incognita* infecting banana (Seenivasan and Senthilnathan, 2018). *In vitro*, humic acid at 0.08 to 2.0% concentration inhibited egg hatching between 50 and 100%. In parallel, it reduced the mobility of J2 in a concentration affected manner. Pot experiments showed that soil humic acid treatment reduced root galling. Despite the humic acid concentrations used (ranging from 0.04 to 0.4%), the nematode density reduction in soil was 53.5–56.7%, and egg population reduction was 61.9–63.8%. Plant growth improvement was another advantage of humic acid treatment. The positive effect of humic acid on PPN control however, still needs to be confirmed by evaluating other crops under field conditions.

Application of Oils

Scientists and industry have been evaluating the potential of essential oils (EOs) as biopesticides for RKN control. EOs were evaluated as soil biofumigants for the control of *M. incognita* on tomato in greenhouse (Laquale et al., 2015). Three different concentrations (50, 100, and 200 μl/kg soil) of EOs from five different plants were tested. EOs of *Eucalyptus globulus* and *Pelargonium asperum* significantly reduced nematode multiplication and gall formation on roots at all concentrations and increased top and root biomass. In another study, 29 plant-based EOs were evaluated against *M. incognita* both *in vitro* and *in vivo* on tomato (Barros et al., 2019a). Fourteen EOs showed nematicidal activities of 8 to 100% at a concentration of 1,000 μg/ml. The most prominent activity was from Mexican tea (*Dysphania ambrosioides*) EO, which reduced the number of galls and eggs by 99.5 and 100%, respectively. The researchers performed further analysis using chromatography-mass spectrometry and detected (Z)-ascaridole (87.28%), E-ascaridole (8.45%), and *p-cymene* (3.35%), representing 99.08% of the total oil composition from *D. ambrosioides*.

Oils from three Brazilian plants (*Astronium graveolens*, *Hyptis suaveolens*, and *Piptadenia viridiflora*) were evaluated against *M. incognita* both *in vitro* and *in vivo* (Barros et al., 2019b). Only *P. viridiflora* showed toxicity against *M. incognita* and was further studied. *P. viridiflora* major component, benzaldehyde, was identified using the gas chromatography–mass spectrometry and tested against *M. incognita*. It was able to produce up to 65% reduction in the number of eggs while its oxime compound was capable of reducing both galls (up to 84%) and eggs (up to 89%) on tomato. Another work studied the activity of EO extracted from high and low land plants of *Artemisia nilagrica* against *M. incognita* (Kalaiselvi et al., 2019). The altitude at which the plants were grown in affected the nature, quantity, appearance, yield, and chemical composition of the EOs produced. The lethal concentrations (LCs) were also different at 5.75 and 10.23 μg/ml ($LC_{50/48h}$) for EOs extracted from high and low altitude plants, respectively. Both EOs reduced root infection by *M. incognita* on tomato and promoted plant growth under greenhouse conditions. Nematode population (eggs and J2) in the root (10 g) was reduced for about 87 and 68%, following treatment by EOs from high- and low-level plants, respectively. Exposing *C. elegans* as a model organism to *A. nilagrica* oils enhanced its intracellular reactive oxygen species (ROS) production and germline cell apoptosis.

Plant Extracts and Compounds

The nematicidal activity of *Camellia oleifera* and *Paenoia rockii* extracts against *M. incognita* was tested *in vitro* by Wen et al. (2019). The extracts from *C. oleifera* cake and *P. rockii* stems suppressed egg hatching. These extracts also had a nematotoxic

activity on J2, with *P. rockii* being superior. At 5 mg/ml, the *P. rockii* extract caused 100% inactivation of *M. incognita* J2 after seven days. In another study, plant extracts from root and shoot of vetiver (*Vetiveria zizanioides*), a known nonhost grass for certain nematodes, were both toxic on *M. incognita*, resulting in 40 and 70% J2 mortality, respectively (Jindapunnapat et al., 2018). The plant extracts were also repellent to J2 and contained a combination of oil and acid. In a greenhouse study using water extracts from fruits of *Melia azedarach* (Chinaberry), researchers reported success in the control of *M. incognita* and *M. javanica* and increase in soil biological activity (Ntalli et al., 2018). On tomato, *M. incognita* females decreased from about 69 in one gram of roots to only 16 for the extract-treated plants. A similar trend was observed for *M. javanica* with the numbers dropping from 79 to 4.2. In the field studies, the number of J2 were about 3,564 for the untreated control compared to about 1,056 for the water-extract treated plants. Microbial properties of the soils included in the study remained the same, while the frequency of free-living nematodes was increased gradually.

The inhibitory effect of allicin (diallyl thiosulfinate), the key natural antimicrobial compound of garlic was evaluated against *M. incognita* (Ji et al., 2019). *In vitro* studies showed that allicin effectively inhibited the nematode J2. The median LC_{50} was 18.23 mg/L. In the greenhouse experiments, allicin controlled *M. incognita* and improved tomato yield. More interestingly, it increased superoxide dismutase, catalase and peroxidase activity in tomato leaves compared to the untreated control. Thus, allicin could be a potential substitute to synthetic chemical compounds for the control of RKN. For future, it is important to assess if production of an extract would be economically advantageous in large scale for agricultural application. In addition, the activity of these compounds (*e.g.* sorption, movement, or degradation) in the soil under field conditions should be evaluated.

The effect of bioactive saponins extracted from five *Medicago* spp. was evaluated *in vitro* against a number of PPN including *M. incognita* (D'Addabbo et al., 2020). Overall, the efficacy of saponins varied depending on the plant species used. At 500 μg/ml, J2 mortality was over 90% after 8–16 h contact time, while at 1,000 μg/ml, egg hatching ranged from 18 to 39% compared to the water control. Results from this study demonstrate that saponin-rich extracts and plant biomasses from *M. heyniana*, *M. hybrida*, *M. lupulina*, *M. murex*, and *M. truncatula* can be highly suppressive to RKN. Care should be taken in future studies to include toxicity tests assuring the safety of optimal nematicidal dosages of saponin against non-target organisms as they have been reported to be occasionally dangerous to embryonic cells of vertebrates (Hassan et al., 2008).

Plant defense proteins "lectins" are a heterogeneous group of bioactive proteins or glycoproteins which can selectively be recognized and bonded to specific glycans in a reversible manner (Peumans and Van Damme, 1995). *Abelmoschus esculentus* lectin (AEL) was characterized on the basis of structural insights and found to be toxic on *M. incognita* and *M. javanica* (de Lacerda et al., 2017). The AEL (500 μg/ml) reduced J2 hatching with greater effect observed for *M. incognita*. The number of *M. incognita* J2 hatched after 9 days of contact to AEL was about 120 compared to about 220 for the control. In the case of *M. javanica*, the numbers were about 60 and 90 for treated samples and control, respectively. This work expanded the knowledge on application of lectins as part of RKN management strategies, highlighting the importance of their deeper study to identify new suitable lectins and the mechanisms involved.

OTHER STRATEGIES

Soil Modifications

Although using organic soil amendments is a conventional method for managing PPN in different cropping systems (Oka, 2010), there are still emerging amendments being developed. In this context, a green manure derived from *Fumaria parviflora* was evaluated as a soil amendment to control *M. incognita* in tomato under greenhouse and field conditions (Naz et al., 2015). Potted soil was amended with fresh chopped whole plant material of *F. parviflora* at rates of 0 (control), 10, 20, and 30 g/kg, 15 days prior to transplanting, and then 15 and 30 days afterwards. The best control of *M. incognita* resulted when plants were treated with 30 g/kg amendment. The galling index was about 4 (scale of 0–5) for the untreated control in contrast to 1.04 for treated samples. The number of J2s per cm^3 of soil were 414 and 127 for the control and treated plants, respectively. In addition, the root portion of *F. parviflora* showed higher nematicidal activity than the aboveground parts.

The bioactivity of chitin oligosaccharide (COS) dithiocarbamate derivatives against *M. incognita* was evaluated in a study (Fan et al., 2019), in which three different COS derivatives were synthesized and their structures were characterized. Subsequently, nematicidal and egg hatching inhibitory effects, plant growth promotion, toxicity, and phytotoxicity were assessed. As of the mechanism of action, they inferred that nematicidal activity may be correlated with glutathione-binding activity but not heavy metal ion complexation. Two out of three COS derivatives tested were able to reduce egg hatching for over 60% when the concentrations exceeded 0.5 mg/ml. At 2 mg/ml, the 1, 3-dithicyclobutane-N-chitosan oligosaccharide (COSDTB) derivative was able to reduce hatching up to 90%. It also caused 94% J2 mortality at 4 mg/ml. Upon COS treatment, metabolization of tomato plants increased, and photosynthetic pigment contents of leaves were elevated with low phytotoxicity damage. The application of MCF-7 cells in cultures treated with 3 mg/ml COS derivatives resulted in more than 90% viability, demonstrating low cytotoxicity towards mammalian cells. Future studies should be expanded in terms of their inclusiveness for different *Meloidogyne* species, host crops, and soil types.

Silicon's ability to control *M. paranaensis* mediated by coffee plants was evaluated (Roldi et al., 2017). Coffee seedlings were treated with silicate before the inoculation of *M. paranaensis* in contrast to the non-treated control. After transplanting, 2,000 eggs were inoculated to each plant and sampling and data collection

was performed periodically. Root microscopic observations confirmed a reduction in J2 penetration upon silicon treatment. In the two independent experiments performed, silicon was able to reduce the number of *M. paranaensis* per g of root as much as 89%. Treatment in the form of potassium silicate did not affect plant growth.

Soil Treatments

Soil solarization has been used as a pest management technique for decades and was studied against RKN as well (Nico et al., 2003; Melero-Vara et al., 2012). Since 2015, soil solarization and its combination with soil steaming were investigated to develop an affordable, yet efficient approach for the management of RKN in floriculture crops including larkspur, snapdragon, and sunflowers (Kokalis-Burelle et al., 2016). The nematicide methyl bromide was used for comparison. Root galling severity on all three crops was lower in steam treatments than in solarization alone. Steam treatment also resulted in the control of *M. arenaria* comparable to, or greater than that of methyl bromide. In conclusion, it was suggested that steaming followed by solarization would be an efficient method to replace harmful chemicals in floriculture.

Ozonated water (O_3wat) is a well-known treatment in agriculture that inactivates pathogens. It has recently been proven suitable for plant irrigation without causing negative effects (Martínez-Sánchez and Aguayo, 2020). In search of new anti-RKN treatments, the ability of O_3wat to control *M. incognita* was evaluated (Veronico et al., 2017), showing that O_3wat helped protect tomato against *M. incognita* through the modulation of basal defense mechanisms. There was no phytotoxicity damage due to the application of O_3wat on tomato. The root galling index (scale of 0–10) in O_3wat-treated plants was significantly lower than that of untreated control. Untreated control, O_3wat treated samples after nematode inoculation and O_3wat treated samples before nematode inoculation had a root galling index of 3.9, 1.9, and 1.6, respectively. Measuring ROS and H_2O_2 in galls showed their elevated production upon O_3wat treatment. The positive effect would probably be related to the modulated antioxidant systems, which increase the ROS, H_2O_2 and malondialdehyde in nematode feeding sites. Due to its nature, O_3wat will degrade to water within a short time, giving the treatment several advantages for RKN management. For example, O_3wat treatment can be performed as an early treatment in an integrated RKN management approach without affecting soil properties.

Application of Industrial Wastes

With global industrialization and mass production, it is necessary to find new ways of turning industrial wastes into value added products. There have been very few attempts until now to use this concept for RKN management. In one of these studies, agro-industrial wastes, namely rice husk, common bean hull, soybean hull, orange bagasse, poultry litter and a mixture of equal portions of these materials were evaluated against *M. javanica* using pot studies in the greenhouse (Brito et al., 2020). In brief, powdered bean hulls, soybean hulls, orange bagasse and waste mixtures were the most efficient wastes with RKN control ranging from 55 to 100%.

Manipueira is the common name of a liquid residue discharged from cassava (*Manihot esculenta*) starch factories that is rich in nutrients and cyanogenic glycosides. Its nematicidal effect against *M. incognita* was evaluated in a tomato field (Nasu et al., 2015). At 50% concentration, Manipueria showed nematicidal and plant growth promotion activity. Sisal, a native plant of Mexico is becoming more popular in parts of the world as a source of fiber. The effect of sisal liquid residue (fresh and fermented) derived from its industrial processing was evaluated against *M. javanica* (Damasceno et al., 2015). A mortality rate of 100% was obtained for J2 exposed to liquid residue at a concentration of 20% *in vitro*. In the greenhouse it also reduced the number of galls and egg masses per gram of tomato roots, as well as the final population of *M. javanica* in the soil. The fermented liquid residue caused inhibition of the beneficial microorganisms, in contrast to the fresh liquid residue.

CONCLUSIONS AND PROSPECTS

Considering the importance of economic losses caused by RKN and the fact that the restrictions governing the use of chemical nematicides are elevating, it is clear that there is need for the development of new environmentally benign strategies. It is also crucial to continue improving the current green methods in search of making them more efficient. For example, some questions to be addressed for antagonistic fungi/bacteria include what is the optimum rate, timing, frequency and method of application for biocontrol agents especially under field conditions? In addition, agricultural industry and scientists should focus on keeping these developed and/or optimized methods economically advantageous, so that they can be adopted by growers on different farming scales. Biocontrol of RKN has been around for decades, but it is still capable of achieving much more attention and better results as new species are identified, characterized and evaluated for their efficacy against RKN. Currently, targeted sequencing such as 16S and 18S rDNA sequencing has great potential to be applied for detection of new biological agents in RKN management. This will make the biocontrol studies faster, cheaper, and more practical. Furthermore, it would be helpful to focus on the microbiomes of RKN suppressive soils based on the meta data in the future studies, in order to explore possibilities for developing more holistic management strategies with multi-target modes of action.

To date, environmentally benign methods are mostly not fully competent on their own with the traditional chemical practices in terms of protecting plants against RKN. Therefore, it is critical to consider the development and improvement of multidisciplinary management strategies for RKN such as combining microbial strategies using both bacterial and fungal agents with other cultural control practices or host resistance. Both biocontrol and application of soil amendments have been studied to some extent against PPN, but with the recent advances in technology

there is room for deeper studies on how these two strategies can be synergistically used. For example, studies on how the application of certain amendments may influence the soil microbiome in relation to nematodes inhibition. More tools such as O_3wat are also becoming available which may be incorporated into the multi-aspect strategies developed.

In conclusion, future studies should focus on environmentally benign approaches which are based on multidisciplinary strategies that can fill the gaps of single sided management methods. Such approaches will also reduce the chance of resistance as the complexity of different nematicidal components would make resistance highly improbable. Whatever strategy is devised, future attempts should focus on important factors such as synergism between RKN antagonists, environmental conditions, sustainability, studying the effect of new treatments on non-target organisms, and association of individual plants with nematode antagonists of interest.

AUTHOR CONTRIBUTIONS

FF designed the project. Both authors participated in writing and editing the manuscript.

REFERENCES

Abad, P., Favery, B., Rosso, M. N., and Castagnone-Sereno, P. (2003). Root-knot nematode parasitism and host response: Molecular basis of a sophisticated interaction. *Mol. Plant Pathol.* 4, 217–224. doi: 10.1046/j.1364-3703.2003.00170.x

Abd-Elgawad, M. M. M., and Askary, T. H. (2018). Fungal and bacterial nematicides in integrated nematode management strategies. *Egypt. J. Biol. Pest Control* 28, 74. doi: 10.1186/s41938-018-0080-x

Andrade, L. B., da, S., Oliveira, A. S., Ribeiro, J. K. C., Kiyota, S., Vasconcelos, I. M., et al. (2010). Effects of a novel pathogenesis-related class 10 (PR-10) Protein from *Crotalaria pallida* roots with papain inhibitory activity against root-knot nematode *Meloidogyne incognita*. *J. Agric. Food Chem.* 58, 4145–4152. doi: 10.1021/jf9044556

Bacetty, A. A., Snook, M. E., Glenn, A. E., Noe, J. P., Hill, N., Culbreath, A., et al. (2009). Toxicity of endophyte-infected tall fescue alkaloids and grass metabolites on *Pratylenchus scribneri*. *Phytopathology* 99, 1336–1345. doi: 10.1094/PHYTO-99-12-1336

Backer, R., Rokem, J. S., Ilangumaran, G., Lamont, J., Praslickova, D., Ricci, E., et al. (2018). Plant growth-promoting rhizobacteria: Context, mechanisms of action, and roadmap to commercialization of biostimulants for sustainable agriculture. *Front. Plant Sci.* 871:1473. doi: 10.3389/fpls.2018.01473

Bardgett, R. D., and Van Der Putten, W. H. (2014). Belowground biodiversity and ecosystem functioning. *Nature* 515, 505–511. doi: 10.1038/nature13855

Barros, A. F., Campos, V. P., De Oliveira, D. F., De Jesus Silva, F., Jardim, I. N., Costa, V. A., et al. (2019a). Activities of essential oils from three Brazilian plants and benzaldehyde analogues against *Meloidogyne incognita*. *Nematology* 21, 1081–1089. doi: 10.1163/15685411-00003276

Barros, A. F., Campos, V. P., de Paula, L. L., Oliveira, D. F., de Silva, F. J., Terra, W. C., et al. (2019b). Nematicidal screening of essential oils and potent toxicity of *Dysphania ambrosioides* essential oil against *Meloidogyne incognita* in vitro and in vivo. *J. Phytopathol.* 167, 380–389. doi: 10.1111/jph.12803

Baum, C., El-Tohamy, W., and Gruda, N. (2015). Increasing the productivity and product quality of vegetable crops using arbuscular mycorrhizal fungi: A review. *Sci. Hortic. (Amsterdam).* 187, 131–141. doi: 10.1016/j.scienta.2015.03.002

Bell, C. A., Lilley, C. J., McCarthy, J., Atkinson, H. J., and Urwin, P. E. (2019). Plant-parasitic nematodes respond to root exudate signals with host-specific gene expression patterns. *PLoS Pathog.* 15, 1–19. doi: 10.1371/journal.ppat.1007503

Bordallo, J. J., Lopez-Llorca, L. V., Jansson, H.-B., Salinas, J., Persmark, L., and Asensio, L. (2002). Colonization of plant roots by egg-parasitic and nematode-trapping fungi. *New Phytol.* 154, 491–499. doi: 10.1046/j.1469-8137.2002.00399.x

Botelho, A. O., Campos, V. P., da Silva, J. C. P., Freire, E. S., de Pinho, R. S. C., Barros, A. F., et al. (2019). Physicochemical and biological properties of the coffee (*Coffea arabica*) rhizosphere suppress the root-knot nematode *Meloidogyne exigua*. *Biocontrol Sci. Technol.* 29, 1181–1196. doi: 10.1080/09583157.2019.1670781

Brito, O. D. C., Ferreira, J. C. A., Hernandes, I., Silva, E. J., and Dias-Arieira, C. R. (2020). Management of *Meloidogyne javanica* on tomato using agro-industrial wastes. *Nematology* 1–14. doi: 10.1163/15685411-bja10018

Bush, L. P., Fannin, F. F., Siegel, M. R., Dahlman, D. L., and Burton, H. R. (1993). Chemistry, occurrence and biological effects of saturated pyrrolizidine alkaloids associated with endophyte-grass interactions. *Agric. Ecosyst. Environ.* 44, 81–102. doi: 10.1016/0167-8809(93)90040-V

Calderón-Urrea, A., Vanholme, B., Vangestel, S., Kane, S. M., Bahaji, A., Pha, K., et al. (2016). Early development of the root-knot nematode *Meloidogyne incognita*. *BMC Dev. Biol.* 16, 1–14. doi: 10.1186/s12861-016-0109-x

Čepulyte, R., Danquah, W. B., Bruening, G., and Williamson, V. M. (2018). Potent attractant for root-knot nematodes in exudates from seedling root tips of two host species. *Sci. Rep.* 8, 1–10. doi: 10.1038/s41598-018-29165-4

Chen, Z. X., and Dickson, D. W. (1998). Review of *Pasteuria penetrans*: Biology, ecology, and biological control potential. *J. Nematol.* 30, 313–340.

Cheng, F., Wang, J., Song, Z., Cheng, J., Zhang, D., and Liu, Y. (2017). Nematicidal effects of 5-Aminolevulinic acid on plant-parasitic nematodes. *J. Nematol.* 49, 295–303. doi: 10.21307/jofnem-2017-075

Colagiero, M., Rosso, L. C., and Ciancio, A. (2018). Diversity and biocontrol potential of bacterial consortia associated to root-knot nematodes. *Biol. Control* 120, 11–16. doi: 10.1016/j.biocontrol.2017.07.010

Cross, J. V., Solomon, M. G., Chandler, D., Jarrett, P., Rrchardson, P. N., Winstanley, D., et al. (1999). Biocontrol of pests of apples and pears in northern and central Europe: 1. microbial agents and nematodes. *Biocontrol Sci. Technol.* 9, 125–149. doi: 10.1080/09583159929721

Dahlin, P., Eder, R., Consoli, E., Krauss, J., and Kiewnick, S. (2019). Integrated control of *Meloidogyne incognita* in tomatoes using fluopyram and *Purpureocillium lilacinum* strain 251. *Crop Prot.* 124:104874. doi: 10.1016/j.cropro.2019.104874

Damasceno, J. C., Soares, A. C., Jesus, F. N., and Sant'Ana, R. S. (2015). Sisal leaf decortication liquid residue for controlling *Meloidogyne javanica* in tomato plants. *Hortic. Bras.* 33, 155–162. doi: 10.1590/s0102-05362015 0000200004

de Lacerda, J. T. J. G., e Lacerda, R. R., Assunção, N. A., Tashima, A. K., Juliano, M. A., dos Santos, , G. A., et al. (2017). New insights into lectin from *Abelmoschus esculentus* seeds as a Kunitz-type inhibitor and its toxic effects on *Ceratitis capitata* and root-knot nematodes *Meloidogyne* spp. *Process Biochem.* 63, 96–104. doi: 10.1016/j.procbio.2017.09.003

Desaeger, J., Dickson, D. W., and Locascio, S. J. (2017). Methyl bromide alternatives for control of root-knot nematode (*Meloidogyne* spp.) in tomato production in Florida. *J. Nematol.* 49, 140–149. doi: 10.21307/jofnem-2017-058

DiLegge, M. J., Manter, D. K., and Vivanco, J. M. (2019). A novel approach to determine generalist nematophagous microbes reveals *Mortierella globalpina* as a new biocontrol agent against *Meloidogyne* spp. nematodes. *Sci. Rep.* 9, 7521. doi: 10.1038/s41598-019-44010-y

D'Addabbo, T., Argentieri, M. P., Żuchowski, J., Biazzi, E., Tava, A., Oleszek, W., et al. (2020). Activity of saponins from *Medicago* species against phytoparasitic nematodes. *Plants* 9, 1–19. doi: 10.3390/plants9040443

d'Errico, G., Marra, R., Crescenzi, A., Davino, S. W., Fanigliulo, A., Woo, S. L., et al. (2019). Integrated management strategies of *Meloidogyne incognita* and *Pseudopyrenochaeta lycopersici* on tomato using a *Bacillus firmus*-based product and two synthetic nematicides in two consecutive crop cycles in greenhouse. *Crop Prot.* 122, 159–164. doi: 10.1016/j.cropro.2019.05.004

Dutta, T. K., Khan, M. R., and Phani, V. (2019). Plant-parasitic nematode management via biofumigation using brassica and non-brassica plants: Current status and future prospects. *Curr. Plant Biol.* 17, 17–32. doi: 10.1016/j.cpb.2019.02.001

El-Nagdi, W. M. A., Youssefi, M. M. A., Abd-El-Khair, H., Abd Elgawad, M. M. M., and Dawood, M. G. (2019). Effectiveness of *Bacillus subtilis*, *B . pumilus*, *Pseudomonas fluorescens* on *Meloidogyne incognita* infecting cowpea. *Pakistan J. Nematol.* 37, 35–43. doi: 10.18681/pjn.v37.i01.p35-43

Escudero, N., Lopez-Moya, F., Ghahremani, Z., Zavala-Gonzalez, E. A., Alaguero-Cordovilla, A., Ros-Ibañez, C., et al. (2017). Chitosan increases tomato root colonization by *Pochonia chlamydosporia* and their combination reduces root-knot nematode damage. *Front. Plant Sci.* 8:1415. doi: 10.3389/fpls.2017.01415

Fan, Z., Qin, Y., Liu, S., Xing, R., Yu, H., Chen, X., et al. (2019). The bioactivity of new chitin oligosaccharide dithiocarbamate derivatives evaluated against nematode disease (*Meloidogyne incognita*). *Carbohydr. Polym.* 224:115155. doi: 10.1016/j.carbpol.2019.115155

Faria, M., and Wraight, S. P. (2007). Mycoinsecticides and Mycoacaricides: A comprehensive list with worldwide coverage and international classification of formulation types. *Biol. Control* 43, 237–256. doi: 10.1016/j.biocontrol.2007.08.001

Ghahremani, Z., Escudero, N., Saus, E., Gabaldón, T., and Sorribas, F. J. (2019). *Pochonia chlamydosporia* induces plant-dependent systemic resistance to *Meloidogyne incognita*. *Front. Plant Sci.* 10:945, 1–8. doi: 10.3389/fpls.2019.00945

Gianinazzi, S., Gollotte, A., Binet, M.-N., van Tuinen, D., Redecker, D., and Wipf, D. (2010). Agroecology: the key role of arbuscular mycorrhizas in ecosystem services. *Mycorrhiza* 20, 519–530. doi: 10.1007/s00572-010-0333-3

Glick, B. R. (2012). Plant growth-promoting bacteria : Mechanisms and Applications. *ScientifiŁca* 1–15. doi: 10.6064/2012/963401

Goswami, J., Pandey, R. K., Tewari, J. P., and Goswami, B. K. (2008). Management of root knot nematode on tomato through application of fungal antagonists, *Acremonium strictum* and Trichoderma harzianum. *J. Environ. Sci. Health B.* 43, 237–240. doi: 10.1080/03601230701771164

Gupta, R., Singh, A., Ajayakumar, P. V., and Pandey, R. (2017). Microbial interference mitigates *Meloidogyne incognita* mediated oxidative stress and augments bacoside content in *Bacopa monnieri* L. *Microbiol. Res.* 199, 67–78. doi: 10.1016/j.micres.2017.03.005

Hahn, M. H., May De Mio, L. L., Kuhn, O. J., and Da Silva Silveira Duarte, H. (2019). Nematophagous mushrooms can be an alternative to control *Meloidogyne javanica*. *Biol. Control* 138:104024. doi: 10.1016/j.biocontrol.2019.104024

Hajihassani, A., Lawrence, K. S., and Jagdale, G. B. (2018). "Plant parasitic nematodes in Georgia and Alabama," in *Plant Parasitic Nematodes in Sustainable Agriculture of North America*, vol. Vol.2 . Eds. S. A. Subbotin and J. J. Chitambar (Northeastern, Midwestern and Southern USA: Cham: Springer International Publishing), 357–391. doi: 10.1007/978-3-319-99588-5_14

Hajihassani, A., Davis, R. F., and Timper, P. (2019a). Evaluation of selected nonfumigant nematicides on increasing inoculation densities of *Meloidogyne incognita* on cucumber. *Plant Dis.* 103, 3161–3165. doi: 10.1094/PDIS-04-19-0836-RE

Hajihassani, A., Rutter, W. B., Schwarz, T., Woldemeskel, M., Ali, M. E., and Hamidi, N. (2019b). Characterization of resistance to major tropical root-knot nematodes (*Meloidogyne* spp.) in *Solanum sisymbriifolium*. *Phytopathology* 110, 666–673. doi: 10.1094/PHYTO-10-19-0393-R

Hao, Z., Fayolle, L., van Tuinen, D., Chatagnier, O., Li, X., Gianinazzi, S., et al. (2012). Local and systemic mycorrhiza-induced protection against the ectoparasitic nematode *Xiphinema index* involves priming of defence gene responses in grapevine. *J. Exp. Bot.* 63, 3657–3672. doi: 10.1093/jxb/ers046

Hassan, S. M., Moussa, E. A., and Abbott, L. C. (2008). Effects of quillaja saponin (*Quillaja saponaria*) on early embryonic zebrafish (*Danio rerio*) development. *Int. J. Toxicol.* 27, 273–278. doi: 10.1080/10915810802152129

Herrera-Parra, E., Cristóbal-Alejo, J., and Ramos-Zapata, J. A. (2017). *Trichoderma* strains as growth promoters in *Capsicum annuum* and as biocontrol agents in *Meloidogyne incognita*. *Chil. J. Agric. Res.* 77, 318–324. doi: 10.4067/S0718-58392017000400318

Hofmann, J., Hess, P. H., Szakasits, D., Blöchl, A., Wieczorek, K., Daxböck-Horvath, S., et al. (2009a). Diversity and activity of sugar transporters in nematode-induced root syncytia. *J. Exp. Bot.* 60, 3085–3095. doi: 10.1093/jxb/erp138

Hofmann, J., Kolev, P., Kolev, N., Daxböck-Horvath, S., and Grundler, F. M. W. (2009b). The *Arabidopsis thaliana* sucrose transporter gene AtSUC4 is expressed in *Meloidogyne incognita*-induced root galls. *J. Phytopathol.* 157, 256–261. doi: 10.1111/j.1439-0434.2008.01468.x

Hsueh, Y.-P., Mahanti, P., Schroeder, F. C., and Sternberg, P. W. (2013). Nematode-trapping fungi eavesdrop on nematode pheromones. *Curr. Biol.* 23, 83–86. doi: 10.1016/j.cub.2012.11.035

Hussain, M., Zouhar, M., and Ryšánek, P. (2018). Suppression of *Meloidogyne incognita* by the entomopathogenic fungus *Lecanicillium muscarium*. *Plant Dis.* 102, 977–982. doi: 10.1094/PDIS-09-17-1392-RE

Jamal, Q., Cho, J. Y., Moon, J. H., Munir, S., Anees, M., and Kim, K. Y. (2017). Identification for the first time of cyclo (D-Pro-L-Leu) produced by *Bacillus amyloliquefaciens* y1 as a nematocide for control of *Meloidogyne incognita*. *Molecules* 22, 1–16. doi: 10.3390/molecules22111839

Ji, X., Li, J., Meng, Z., Dong, S., Zhang, S., and Qiao, K. (2019). Inhibitory effect of allicin against *Meloidogyne incognita* and *Botrytis cinerea* in tomato. *Sci. Hortic. (Amsterdam).* 253, 203–208. doi: 10.1016/j.scienta.2019.04.046

Jindapunnapat, K., Reetz, N. D., MacDonald, M. H., Bhagavathy, G., Chinnasri, B., Soonthornchareonnon, N., et al. (2018). Activity of vetiver extracts and essential oil against *Meloidogyne incognita*. *J. Nematol.* 50, 147–162. doi: 10.21307/jofnem-2018-008

Jones, J. T., Haegeman, A., Danchin, E. G. J., Gaur, H. S., Helder, J., Jones, M. G. K., et al. (2013). Top 10 plant-parasitic nematodes in molecular plant pathology. *Mol. Plant Pathol.* 14, 946–961. doi: 10.1111/mpp.12057

Kalaiselvi, D., Mohankumar, A., Shanmugam, G., Thiruppathi, G., Nivitha, S., and Sundararaj, P. (2019). Altitude-related changes in the phytochemical profile of essential oils extracted from *Artemisia nilagirica* and their nematicidal activity against *Meloidogyne incognita*. *Ind. Crops Prod.* 139:111472. doi: 10.1016/j.indcrop.2019.111472

Khan, Z., and Kim, Y. H. (2007). A review on the role of predatory soil nematodes in the biological control of plant parasitic nematodes. *Appl. Soil Ecol.* 35, 370–379. doi: 10.1016/J.APSOIL.2006.07.007

Khanna, K., Jamwal, V. L., Kohli, S. K., Gandhi, S. G., Ohri, P., Bhardwaj, R., et al. (2019). Role of plant growth promoting bacteria (PGPRs) as biocontrol agents of *Meloidogyne incognita* through improved plant defense of *Lycopersicon esculentum*. *Plant Soil* 436, 325–345. doi: 10.1007/s11104-019-03932-2

Kim, T. Y., Jang, J. Y., Yu, N. H., Chi, W. J., Bae, C. H., Yeo, J. H., et al. (2018). Nematicidal activity of grammicin produced by *Xylaria grammica* KCTC 13121BP against *Meloidogyne incognita*. *Pest Manage. Sci.* 74, 384–391. doi: 10.1002/ps.4717

Kiriga, A. W., Haukeland, S., Kariuki, G. M., Coyne, D. L., and Beek, N. V. (2018). Effect of *Trichoderma* spp. and *Purpureocillium lilacinum* on *Meloidogyne javanica* in commercial pineapple production in Kenya. *Biol. Control* 119, 27–32. doi: 10.1016/j.biocontrol.2018.01.005

Kokalis-Burelle, N., Rosskopf, E. N., Butler, D. M., Fennimore, S. A., and Holzinger, J. (2016). Evaluation of steam and soil solarization for *Meloidogyne arenaria* control in Florida floriculture crops. *J. Nematol.* 48, 183–192. doi: 10.21307/jofnem-2017-026

Kunkel, B. A., and Grewal, P. S. (2003). Endophyte infection in perennial ryegrass reduces the susceptibility of black cutworm to an entomopathogenic nematode. *Entomol. Exp. Appl.* 107, 95–104. doi: 10.1046/j.1570-7458.2003.00048.x

Lamovšek, J., Stare, B. G., Pleško, I. M., Širca, S., and Urek, G. (2017). Agrobacteria enhance plant defense against root-knot nematodes on tomato. *Phytopathology* 107, 681–691. doi: 10.1094/PHYTO-07-16-0269-R

Laquale, S., Candido, V., Avato, P., Argentieri, M. P., and D'Addabbo, T. (2015). Essential oils as soil biofumigants for the control of the root-knot nematode *Meloidogyne incognita* on tomato. *Ann. Appl. Biol.* 167, 217–224. doi: 10.1111/aab.12221

Le, H. T. T., Padgham, J. L., Hagemann, M. H., Sikora, R. A., and Schouten, A. (2016). Developmental and behavioural effects of the endophytic *Fusarium moniliforme* Fe14 towards *Meloidogyne graminicola* in rice. *Ann. Appl. Biol.* 169, 134–143. doi: 10.1111/aab.12287

Lee, Y. S., and Kim, K. Y. (2016). Antagonistic potential of *Bacillus pumilus* L1 against root-knot nematode, *Meloidogyne arenaria*. *J. Phytopathol.* 164, 29–39. doi: 10.1111/jph.12421

Li, X., Hu, H. J., Li, J. Y., Wang, C., Chen, S. L., and Yan, S. Z. (2019). Effects of the endophytic bacteria *Bacillus cereus* BCM2 on tomato root exudates and *Meloidogyne incognita* infection. *Plant Dis.* 103, 1551–1558. doi: 10.1094/PDIS-11-18-2016-RE

Liu, C., Timper, P., Ji, P., Mekete, T., and Joseph, S. (2017). Influence of root exudates & soil on attachment of *Pasteuria penetrans* to *Meloidogyne arenaria*. *J. Nematol.* 49, 304–310. doi: 10.21307/jofnem-2017-076

Ma, Y., Prasad, M. N. V., Rajkumar, M., and Freitas, H. (2011). Plant growth promoting rhizobacteria and endophytes accelerate phytoremediation of metalliferous soils. *Biotechnol. Adv.* 29, 248–258. doi: 10.1016/j.biotechadv.2010.12.001

Martínez-Medina, A., Fernandez, I., Lok, G. B., Pozo, M. J., Pieterse, C. M. J., and Van Wees, S. C. M. (2017). Shifting from priming of salicylic acid- to jasmonic acid-regulated defences by Trichoderma protects tomato against the root knot nematode *Meloidogyne incognita*. *New Phytol.* 213, 1363–1377. doi: 10.1111/nph.14251

Martínez-Sánchez, A., and Aguayo, E. (2020). Effects of ozonated water irrigation on the quality of grafted watermelon seedlings. *Sci. Hortic. (Amsterdam).* 261:109047. doi: 10.1016/j.scienta.2019.109047

Martinuz, A., Schouten, A., and Sikora, R. A. (2013). Post-infection development of *Meloidogyne incognita* on tomato treated with the endophytes *Fusarium oxysporum* strain Fo162 and Rhizobium etli strain G12. *BioControl* 58, 95–104. doi: 10.1007/s10526-012-9471-1

Medina-Canales, M. G., Terroba-Escalante, P., Manzanilla-López, R. H., and Tovar-Soto, A. (2019). Assessment of three strategies for the management of *Meloidogyne arenaria* on carrot in Mexico using *Pochonia chlamydosporia* var. *mexicana* under greenhouse conditions. *Biocontrol Sci. Technol.* 29, 671–685. doi: 10.1080/09583157.2019.1582267

Melero-Vara, J. M., López-Herrera, C. J., Basallote-Ureba, M. J., Prados, A. M., Vela, M. D., Macias, F. J., et al. (2012). Use of poultry manure combined with Soil Solarization as a control method for *meloidogyne incognita* in carnation. *Plant Dis.* 96, 990–996. doi: 10.1094/PDIS-01-12-0080-RE

Molinari, S., and Leonetti, P. (2019). Bio-control agents activate plant immune response and prime susceptible tomato against root-knot nematodes. *PLoS One* 14, e0213230. doi: 10.1371/journal.pone.0213230

Momma, N., Yamamoto, K., Simandi, P., and Shishido, M. (2006). Role of organic acids in the mechanisms of biological soil disinfestation (BSD). *J. Gen. Plant Pathol.* 72, 247–252. doi: 10.1007/s10327-006-0274-z

Nasu, É., das, G. C., Formentini, H. M., and Furlanetto, C. (2015). Effect of manipueira on tomato plants infected by the nematode *Meloidogyne incognita*. *Crop Prot.* 78, 193–197. doi: 10.1016/j.cropro.2015.08.005

Naz, I., Saifullah,, Palomares-Rius, J. E., Khan, S. M., Ali, S., Ahmad, M., et al. (2015). Control of southern root knot nematode *Meloidogyne incognita* (Kofoid and White) Chitwood on tomato using green manure of *Fumaria parviflora* Lam (Fumariaceae). *Crop Prot.* 67, 121–129. doi: 10.1016/j.cropro.2014.10.005

Nico, A.II, Jiménez-Díaz, R. M., and Castillo, P. (2003). Solarization of soil in piles for the control of *Meloidogyne incognita* in olive nurseries in southern Spain. *Plant Pathol.* 52, 770–778. doi: 10.1111/j.1365-3059.2003.00927.x

Ntalli, N., and Caboni, P. (2017). A review of isothiocyanates biofumigation activity on plant parasitic nematodes. *Phytochem. Rev.* 16, 827–834. doi: 10.1007/s11101-017-9491-7

Ntalli, N., Ratajczak, M., Oplos, C., Menkissoglu-Spiroudi, U., and Adamski, Z. (2016). Acetic acid, 2-undecanone, and (E)-2-decenal ultrastructural malformations on *Meloidogyne incognita*. *J. Nematol.* 48, 248–260. doi: 10.21307/jofnem-2017-033

Ntalli, N., Monokrousos, N., Rumbos, C., Kontea, D., Zioga, D., Argyropoulou, M. D., et al. (2018). Greenhouse biofumigation with *Melia azedarach* controls *Meloidogyne* spp. and enhances soil biological activity. *J. Pest Sci.* 91, 29–40. doi: 10.1007/s10340-017-0909-1

Oka, Y. (2010). Mechanisms of nematode suppression by organic soil amendments-A review. *Appl. Soil Ecol.* 44, 101–115. doi: 10.1016/j.apsoil.2009.11.003

Oostendorp, M., Dickson, D. W., and Mitchell, D. J. (1991). Population development of *Pasteuria penetrans* on *Meloidogyne arenaria*. *J. Nematol.* 23, 58–64.

Peumans, W. J., and Van Damme, E. J. (1995). Lectins as plant defense proteins. *Plant Physiol.* 109, 347–352. doi: 10.1104/pp.109.2.347

Qiang, X., Weiss, M., Kogel, K. H., and Schäfer, P. (2012). *Piriformospora indica*-a mutualistic basidiomycete with an exceptionally large plant host range. *Mol. Plant Pathol.* 13, 508–518. doi: 10.1111/j.1364-3703.2011.00764.x

Redman, R. S., Kim, Y. O., Woodward, C. J. D. A., Greer, C., Espino, L., Doty, S. L., et al. (2011). Increased fitness of rice plants to abiotic stress via habitat adapted symbiosis: A strategy for mitigating impacts of climate change. *PLoS One* 6, 1–10. doi: 10.1371/journal.pone.0014823

Rodriguez, R. J., White, J. F., Arnold, A. E., and Redman, R. S. (2009). Fungal endophytes: Diversity and functional roles: Tansley review. *New Phytol.* 182, 314–330. doi: 10.1111/j.1469-8137.2009.02773.x

Roldi, M., Dias-Arieira, C. R., Da Silva, S. A., Dorigo, O. F., and Machado, A. C. Z. (2017). Control of *Meloidogyne paranaensis* in coffee plants mediated by silicon. *Nematology* 19, 245–250. doi: 10.1163/15685411-00003044

Rumbos, C. II, and Kiewnick, S. (2006). Effect of Plant Species on persistence of *Paecilomyces lilacinus* Strain 251 in soil and on root colonization by the Fungus. *Plant Soil* 283, 25–31. doi: 10.1007/s11104-005-6804-1

Saxena, G., Dayal, R., and Mukerji, K. G. (1987). Interaction of nematodes with nematophagus fungi: induction of trap formation, attraction and detection of attractants. *FEMS Microbiol. Lett.* 45, 319–327. doi: 10.1016/0378-1097(87)90018-8

Schouteden, N., Waele, D. D., Panis, B., and Vos, C. M. (2015). Arbuscular mycorrhizal fungi for the biocontrol of plant-parasitic nematodes: A review of the mechanisms involved. *Front. Microbiol.* 6:1280. doi: 10.3389/fmicb.2015.01280

Schouten, A. (2016). Mechanisms involved in nematode control by endophytic fungi. *Annu. Rev. Phytopathol.* 54, 121–142. doi: 10.1146/annurev-phyto-080615-100114

Seenivasan, N., and Senthilnathan, S. (2018). Effect of humic acid on *Meloidogyne incognita* (Kofoid & White) Chitwood infecting banana (*Musa* spp.). *Int. J. Pest Manage.* 64, 110–118. doi: 10.1080/09670874.2017.1344743

Seo, H. J., Park, A. R., Kim, S., Yeon, J., Yu, N. H., Ha, S., et al. (2019). Biological control of root-knot nematodes by organic acid-producing *Lactobacillus brevis* wikim0069 isolated from kimchi. *Plant Pathol. J.* 35, 662–673. doi: 10.5423/PPJ.OA.08.2019.0225

Sikder, M. M., and Vestergård, M. (2020). Impacts of Root Metabolites on Soil Nematodes. *Front. Plant Sci.* 10:1792. doi: 10.3389/fpls.2019.01792

Silva, J. de O., Santana, M. V., Freire, L. L., Ferreira, B. da S., and Rocha, M. R. da (2017). Biocontrol agents in the management of *Meloidogyne incognita* in tomato. *Ciêc. Rural* 47, 1–7. doi: 10.1590/0103-8478cr20161053

Silva, S. D., Carneiro, R. M. D. G., Faria, M., Souza, D. A., Monnerat, R. G., and Lopes, R. B. (2017). Evaluation of *Pochonia chlamydosporia* and *Purpureocillium lilacinum* for suppression of *meloidogyne enterolobii* on tomato and banana. *J. Nematol.* 49, 77–85. doi: 10.21307/jofnem-2017-047

Smith, S. E., and Smith, F. A. (2011). Roles of Arbuscular mycorrhizas in plant nutrition and growth: New paradigms from cellular to ecosystem scales. *Annu. Rev. Plant Biol.* 62, 227–250. doi: 10.1146/annurev-arplant-042110-103846

Stirling, G. R. (2014). *Biological control of plant-parasitic nematodes. 2nd ed* (Wallingford, Oxfordshire, UK: CAB International). doi: 10.1146/annurev.py.24.090186.002321

Thoden, T. C., Korthals, G. W., and Termorshuizen, A. J. (2011). Organic amendments and their influences on plant-parasitic and free-living nematodes: A promising method for nematode management? *Nematology* 13, 133–153. doi: 10.1163/138855410X541834

Thongkaewyuan, A., and Chairin, T. (2018). Biocontrol of *Meloidogyne incognita* by *Metarhizium guizhouense* and its protease. *Biol. Control* 126, 142–146. doi: 10.1016/j.biocontrol.2018.08.005

Tian, X., Yao, Y., Chen, G., Mao, Z., Wang, X., and Xie, B. (2014). Suppression of *Meloidogyne incognita* by the endophytic fungus *Acremonium implicatum* from tomato root galls. *Int. J. Pest Manage.* 60, 239–245. doi: 10.1080/09670874.2014.958604

Timper, P. (2014). Conserving and enhancing biological control of nematodes. *J. Nematol.* 46, 75–89.

Topalovic, O., Heuer, H., Reineke, A., Zinkernagel, J., and Hallmann, J. (2019). Antagonistic role of the microbiome from a *Meloidogyne hapla*-suppressive soil against species of plant-parasitic nematodes with different life strategies. *Nematology* 22, 75–86. doi: 10.1163/15685411-00003285

Trudgill, D. L., and Blok, V. C. (2001). Apomictic, polyphagous root-knot nematodes: exceptionally successful and damaging biotrophic root pathogens. *Annu. Rev. Phytopathol.* 39, 53–77. doi: 10.1146/annurev.phyto.39.1.53

van den Hoogen, J., Geisen, S., Routh, D., Ferris, H., Traunspurger, W., Wardle, D. A., et al. (2019). Soil nematode abundance and functional group composition at a global scale. *Nature* 572, 194–198. doi: 10.1038/s41586-019-1418-6

van Loon, L. C., Bakker, P. A. H. M., and Pieterse, C. M. J. (1998). Systemic resistance induced By rhizosphere bacteria. *Annu. Rev. Phytopathol.* 36, 453–483. doi: 10.1146/annurev.phyto.36.1.453

Veronico, P., Paciolla, C., Sasanelli, N., De Leonardis, S., and Melillo, M. T. (2017). Ozonated water reduces susceptibility in tomato plants to *Meloidogyne incognita* by the modulation of the antioxidant system. *Mol. Plant Pathol.* 18, 529–539. doi: 10.1111/mpp.12413

Viljoen, J. J. F., Labuschagne, N., Fourie, H., and Sikora, R. A. (2019). Biological control of the root-knot nematode *Meloidogyne incognita* on tomatoes and carrots by plant growth-promoting rhizobacteria. *Trop. Plant Pathol.* 44, 284–291. doi: 10.1007/s40858-019-00283-2

Vos, C. M., Yang, Y., De Coninck, B., and Cammue, B. P. A. (2014). Fungal (-like) biocontrol organisms in tomato disease control. *Biol. Control* 74, 65–81. doi: 10.1016/j.biocontrol.2014.04.004

Wang, X., Li, G. H., Zou, C. G., Ji, X. L., Liu, T., Zhao, P. J., et al. (2014). Bacteria can mobilize nematode-trapping fungi to kill nematodes. *Nat. Commun.* 5, 1–9. doi: 10.1038/ncomms6776

Wen, Y., Meyer, S. L. F., MacDonald, M. H., Zheng, L., Jing, C., and Chitwood, D. J. (2019). Nematotoxicity of *Paeonia* spp. extracts and *Camellia oleifera* tea seed cake and extracts to *Heterodera glycines* and *Meloidogyne incognita*. *Plant Dis.* 103, 2191–2198. doi: 10.1094/PDIS-09-18-1663-RE

Xavier, D. M., Dallemole-Giaretta, R., De Freitas, L. G., Lopes, E. A., Gardiano, C. G., and Ferraz, S. (2017). Combination of isolates of *Pochonia chlamydosporia* for the control of *Meloidogyne javanica* in tomato. *Chil. J. Agric. Anim. Sci.* 33, 24–27. doi: 10.4067/s0719-38902017005000103

Xiang, N., Lawrence, K. S., and Donald, P. A. (2018). Biological control potential of plant growth-promoting rhizobacteria suppression of *Meloidogyne incognita* on cotton and *Heterodera glycines* on soybean: A review. *J. Phytopathol.* 166, 449–458. doi: 10.1111/jph.12712

Xiao, L., Wan, J. W., Yao, J. H., Feng, H., and Wei, L. H. (2018). Effects of *Bacillus cereus* strain Jdm1 on *Meloidogyne incognita* and the bacterial community in tomato rhizosphere soil. *3 Biotech.* 8, 1–8. doi: 10.1007/s13205-018-1348-2

Yao, Y.-R., Tian, X.-L., Shen, B.-M., Mao, Z.-C., Chen, G., and Xie, B.-Y. (2015). Transformation of the endophytic fungus *Acremonium implicatum* with GFP and evaluation of its biocontrol effect against *Meloidogyne incognita*. *World J. Microbiol. Biotechnol.* 31, 549–556. doi: 10.1007/s11274-014-1781-2

Yue, L., Ahmed, S., Liu, Q., and Jian, H. (2019). Management of *Meloidogyne incognita* on tomato with different biocontrol organisms. *Pakistan J. Nematol.* 37, 161–170. doi: 10.18681/pjn.v37.i02.p161-170

Zasada, I. A., Meyer, S. L. F., Halbrendt, J. M., and Rice, C. (2005). Activity of hydroxamic acids from *Secale cereale* against the plant-parasitic nematodes *Meloidogyne incognita* and *Xiphinema americanum*. *Phytopathology* 95, 1116–1121. doi: 10.1094/PHYTO-95-1116

Zhang, S., Gan, Y., and Xu, B. (2015). Biocontrol potential of a native species of *Trichoderma longibrachiatum* against *Meloidogyne incognita*. *Appl. Soil Ecol.* 94, 21–29. doi: 10.1016/j.apsoil.2015.04.010

Conflict of Interest: The authors declare that the research was conducted in the absence of any commercial or financial relationships that could be construed as a potential conflict of interest.

frontiers in Plant Science

ORIGINAL RESEARCH
published: 16 October 2020
doi: 10.3389/fpls.2020.579807

Novel Prodiginine Derivatives Demonstrate Bioactivities on Plants, Nematodes, and Fungi

Samer S. Habash[1], Hannah U. C. Brass[2], Andreas S. Klein[2], David P. Klebl[2], Tim Moritz Weber[2], Thomas Classen[3], Jörg Pietruszka[2,3], Florian M. W. Grundler[1] and A. Sylvia S. Schleker[1]**

[1] INRES Molecular Phytomedicine, University of Bonn, Bonn, Germany, [2] Institute of Bioorganic Chemistry, Heinrich Heine University Düsseldorf, Forschungszentrum Jülich, Stetternicher Forst, Jülich, Germany, [3] IBG-1: Bioorganic Chemistry, Forschungszentrum Jülich GmbH, Jülich, Germany

Bacterial metabolites represent an invaluable source of bioactive molecules which can be used as such or serve as chemical frameworks for developing new antimicrobial compounds for various applications including crop protection against pathogens. Prodiginines are tripyrrolic, red-colored compounds produced by many bacterial species. Recently, due to the use of chemical-, bio-, or mutasynthesis, a novel group of prodiginines was generated. In our study, we perform different assays to evaluate the effects of prodigiosin and five derivatives on nematodes and plant pathogenic fungi as well as on plant development. Our results showed that prodigiosin and the derivatives were active against the bacterial feeding nematode *Caenorhabditis elegans* in a concentration- and derivative-dependent manner while a direct effect on infective juveniles of the plant parasitic nematode *Heterodera schachtii* was observed for prodigiosin only. All compounds were found to be active against the plant pathogenic fungi *Phoma lingam* and *Sclerotinia sclerotiorum.* Efficacy varied depending on compound concentration and chemical structure. We observed that prodigiosin (**1**), the 12 ring- **9**, and hexenol **10** derivatives are neutral or even positive for growth of *Arabidopsis thaliana* depending on the applied compound concentration, whereas other derivatives appear to be suppressive. Our infection assays revealed that the total number of developed *H. schachtii* individuals on *A. thaliana* was decreased to 50% in the presence of compounds **1** or **9**. Furthermore, female nematodes and their associated syncytia were smaller in size. Prodiginines seem to indirectly inhibit *H. schachtii* parasitism of the plant. Further research is needed to elucidate their mode of action. Our results indicate that prodiginines are promising metabolites that have the potential to be developed into novel antinematodal and antifungal agents.

Keywords: prodiginines, natural product, plant pathogens, plant protection, nematode

OPEN ACCESS

Edited by:
Juan Emilio Palomares-Rius, Institute for Sustainable Agriculture (IAS) (CSIC), Spain

Reviewed by:
Paola Leonetti, National Research Council (CNR), Italy
Catherine Lilley, University of Leeds, United Kingdom

****Correspondence:***
Samer S. Habash
samer@uni-bonn.de
orcid.org/0000-0002-4493-1451
A. Sylvia S. Schleker
sylvia.schleker@uni-bonn.de

Specialty section:
This article was submitted to Plant Pathogen Interactions, a section of the journal Frontiers in Plant Science

Received: *03 July 2020*
Accepted: *18 September 2020*
Published: *16 October 2020*

Citation:
Habash SS, Brass HUC, Klein AS, Klebl DP, Weber TM, Classen T, Pietruszka J, Grundler FMW and Schleker ASS (2020) Novel Prodiginine Derivatives Demonstrate Bioactivities on Plants, Nematodes, and Fungi. Front. Plant Sci. 11:579807. doi: 10.3389/fpls.2020.579807

INTRODUCTION

Plant pests (including insects, mites, plant parasitic nematodes), pathogens (e.g., viruses, bacteria, fungi), and weeds are major problems in crop production causing a share of the total global yield losses of up to 18%, 16%, and 34%, respectively (Oerke, 2006). In order to minimize crop losses, chemical, biological, and cultural means side by side with the use of resistant plants are

management strategies in use (Bridge, 1996; Heydari and Pessarakli, 2010; Habash and Al-Banna, 2011; Timper, 2014). Each of these control means has its own challenges, but so far, pesticides are the fastest and the most effective combat means utilized. However, due to environmental hazards and toxicity to humans many pesticides are being banned. Therefore, effective and sustainable alternatives are needed.

Microbial metabolites represent a valuable source of compounds that can be used for development of new drugs and plant protection agents. The bacterial prodiginines are nice examples with a wide range of bioactivities and intensively used in drug discovery research (Darshan and Manonmani, 2015). Prodiginines are tripyrrolic dark red compounds produced as secondary metabolites by many bacterial species within *Serratia* (Williams et al., 1956), *Streptomyces* (Gerber, 1975; Kawasaki et al., 2008), *Hahella* (Kim et al., 2007), and *Vibrio* (Starič et al., 2010), for instance. The family of prodiginines comprises diverse members (as shown in **Figure 1**), some having linear alkyl side chains such as prodigiosin (**1**) and undecylprodigiosin (**2**) while others have cyclic moieties such as cycloprodigiosin (**3**), *meta*cycloprodigiosin (**4**), or streptorubin B (**5**) (Williamson et al., 2006; Stankovic et al., 2014; Hu et al., 2016). In pharmaceutical studies, prodiginines were often used for their antimalarial and antitumor activities (Pérez-Tomás et al., 2003; Papireddy et al., 2011). They also exhibit inhibitory activities on various microbes. For example, *Escherichia coli* exhibited a leaky outer membrane and cells had severely decreased respiration activity upon exposure to prodigiosin (**1**) (Danevčič et al., 2016b). Likewise, treating *Pseudomonas aeruginosa* with prodigiosin (**1**), isolated from *Serratia marcescens,* altered the cell surface hydrophobicity, and biofilm integrity significantly. The treatment also caused nucleic acid degradation of *P. aeruginosa* (Kimyon et al., 2016). Recent research has shown potential applications of prodiginines in food industry as coloring agents, antioxidants, and antimicrobial additives to increase product shelf life (Arivizhivendhan et al., 2018).

In agricultural research, activities of prodigiosin (**1**) against several plant pathogens are described. It was shown that prodigiosin (**1**) totally inhibited spore germination of *Botrytis cinerea,* the causal agent of gray mold (Someya et al., 2001). The purified red pigment of *Serratia marcescens* was found to be effective against juvenile stages of the plant parasitic nematodes *Radopholus similis* and *Meloidogyne javanica* at low concentrations of 83 and 79 μg/mL, respectively, and inhibited nematode egg-hatching ability. After deep analysis of the bioactive red supernatant, prodigiosin (**1**) was detected in the supernatant (Rahul et al., 2014). This evidence supports the potential of the red pigment prodigiosin (**1**) to be applied in several fields.

The bio- and chemical-based derivatization of prodiginines introduces new compounds. These compounds could contribute to an improved microbe resistance management or having stronger bioactivities. Recently, nature inspired prodiginines were produced by combining organic syntheses with a mutasynthesis approach using the HV1-certified bacterium *Pseudomonas putida* KT2440 as host strain (Weist and Süssmuth, 2005; Kennedy, 2008; Kirschning and Hahn, 2012; Klein et al., 2017, 2018; Classen and Pietruszka, 2018). The previously constructed mutasynthesis strain harbors the prodigiosin (**1**) gene cluster from *S. marcescens*, but the bifurcated biosynthetic pathway is blocked upon gene deletion, thus, only one out of two prodiginine building blocks, namely 4-methoxy-2,2'-bipyrrole-5-carbaldehyde (MBC), is produced biosynthetically (Domröse et al., 2015; Klein et al., 2017). The other precursor and especially derivatives thereof are chemically synthesized and fed during cultivation, enabling the production of new and non-natural prodiginines (Klein et al., 2017, 2018). The obtained compounds possessed antibacterial activities against several species with minimum inhibitory concentrations (MIC) ranging from 0.1 to 12 μMM. In the same studies, they demonstrated that the produced prodiginines exhibit modulating activities of autophagy in human breast cancer cells. The novel compounds with such bioactivities could be good candidates to be used against plant pathogens. Their attraction is increased by the fact that prodiginines act on microorganisms in a mode different compared to conventional pesticides.

In our study we present the bioactivities of prodigiosin (**1**), several cyclic derivatives **6**–**9** and a hydroxylated prodiginine **10** against different organisms, particularly focusing on the plant parasitic nematode *Heterodera schachtii*. First, we examined the bioactivities of prodiginines on two nematode species belonging to bacterial feeding and plant parasitic nematodes. We further investigated the effect of the compounds on plant growth using the model plant *A. thaliana* and subsequently evaluated the efficacy of selected compounds in combating nematode parasitism in the pathosystem *A. thaliana*–*H. schachtii*. Finally, we tested the bioactivities of prodiginines on other pathogens by using two species of plant pathogenic fungi.

MATERIALS AND METHODS

Prodiginine Production

Production of Prodiginines 1, 6–9 *via* Biosynthesis or Mutasynthesis

Prodigiosin (**1**) was produced by using the strain *P. putida* pig-r2 as previously described (Domröse et al., 2015). The prodiginine derivatives **6**–**9** (**Figure 2**) were produced *via* mutasynthesis as previously described (Klein et al., 2017, 2018). For details, see **Supplementary Material**.

Chemical Synthesis of Prodiginines

Synthesis of **10** is described in detail in **Supplementary Material**.

Nematode Culture

The wild type of the bacterial feeding nematode *C. elegans*, used in this work, was maintained on nematode growth medium (NGM) and was fed with *E. coli* strain OP50. In the toxicity assay the synchronized first stage nematodes were used (Al Banna et al., 2018). The plant parasitic nematode *H. schachtii* Schmidt used in the experiments was reared on white mustard (*Sinapis alba* L. cv. Albatros) plants which were grown aseptically on 0.2% Knop agar medium. Mature cysts were collected in funnels and hatched

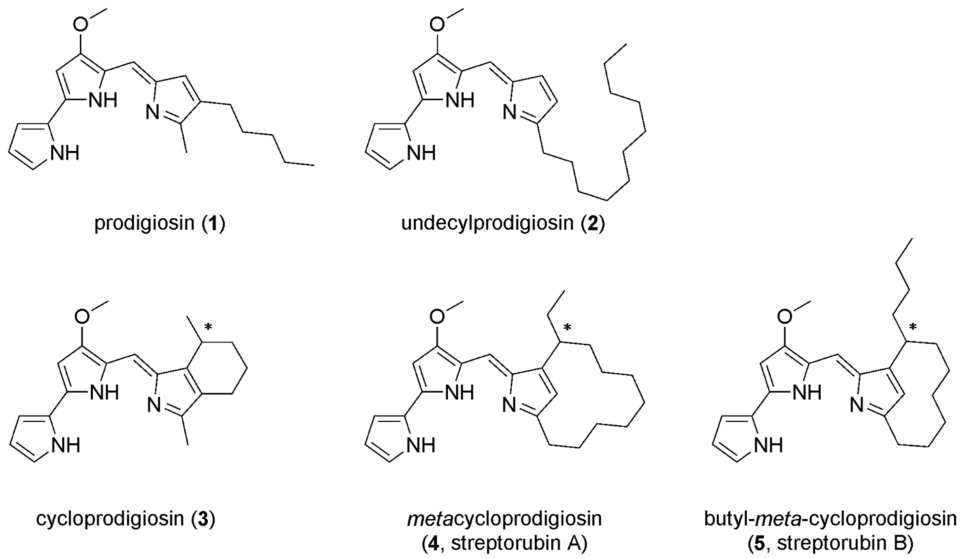

FIGURE 1 | Examples of natural prodiginines: prodigiosin (**1**), undecylprodigiosin (**2**), cycloprodigiosin (**3**), *meta*cycloprodigiosin (**4**), and butyl-*meta*-cycloprodigiosin (**5**).

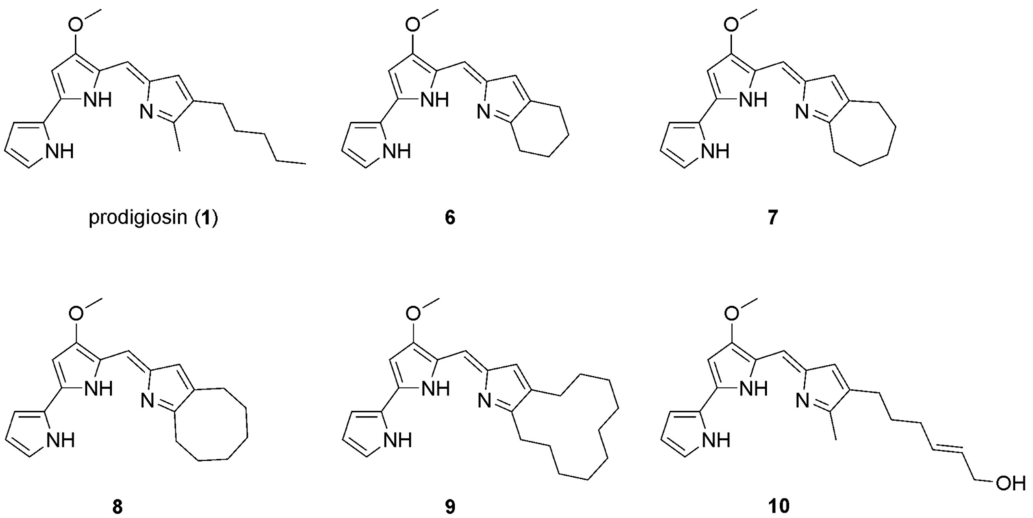

FIGURE 2 | Chemical structure of prodigiosin (**1**) and the derivatives **6–10** that were investigated in this study.

in 3 mM $ZnCl_2$ (Sijmons et al., 1991). The hatched pre-parasitic J2s were collected and used in the experiments.

Effect of Prodigiosin Derivatives on Nematodes

To investigate the effect of prodigiosin derivatives on nematode motility, two nematode species were used. Both nematodes, *C. elegans* and *H. schachtii,* were challenged with the selected compounds **1**, **6–10**. The activity experiment was conducted in 96-well plates (Greiner Bio-One) under aseptic conditions. Each well contained 90–100 nematodes incubated in 60 µL of the compound-containing test solution. The used dilutions were 100, 50, 25, 12.5, and 6.25 µM dissolved in 0.5% (v/v) dimethyl sulfoxide (DMSO) diluted in ddH_2O. Nematodes soaked in 0.5% (v/v) DMSO served as control. Plates were incubated for two days at 24°C in the dark. Numbers of active (moving) and inactive (not moving) nematodes were evaluated using a dissecting microscope. Nematode movement was provoked by adding 2 µL of 1 M sodium hydroxide (NaOH). Those nematodes that remained immobile after challenging with NaOH were regarded as dead. The percentages of nematode motility were calculated. The experiment was set up in three biological replications (each contains three wells per concentration). To decide whether *H. schachtii* J2s were really killed or just paralyzed by prodigiosin (**1**), J2s were washed free of the compound after a

48 h incubation period and subsequently left in water for another 48 h. This was necessary as some *H. schachtii* J2s incubated in **1** showed a slight movement of the tail region after adding NaOH what made a reliable decision difficult. Data were collected and statistically analyzed by one-way analysis of variance (ANOVA) followed by Dunnett's post-hoc test to determine significant differences to the control (SigmaPlot 12.5).

Plant Growth Test

In order to investigate the effect of prodiginines on plants, *A. thaliana* ecotype Col-0 was grown aseptically on agar medium supplemented with modified 0.2% Knop solutions at 16 h light and 8 h dark at 25°C as described previously (Sijmons et al., 1991). Five-days-old plants were transferred to 6-well plates containing 2 mL liquid Murashige and Skoog medium (MS) supplemented with the prodiginines **1**, **6**–**10** at different concentrations (50, 25, 12.5 μM), MS medium supplemented with 1 μM bacterial flagellin (flg22) or with 0.5% (v/v) DMSO were used as controls. Fresh weight of the roots and the shoots were measured after 15 days of incubation. The experiments were performed in five technical replicates and independently repeated three times. Data were statistically analyzed using one-way ANOVA followed by Dunnett's post-hoc test.

Infection Assay

In order to investigate the impact of prodigiosin derivatives on nematode parasitism, prodigiosin (**1**) and prodiginine **9** were selected to be tested. The compounds and the used concentration were chosen based on the previous results of the plant development assay. Compounds were added to the 0.2% Knop agar medium to yield a final concentration of 14 μM. *A. thaliana* Col-0 plants were grown aseptically on the medium with 16 h light and 8 h dark at 25°C as described previously (Sijmons et al., 1991). The infection assay with *A. thaliana* plants was performed as described previously (Habash et al., 2017). Briefly, roots of 10 days old seedlings were inoculated with 60–70 *H. schachtii* J2s per plant. Twelve days after inoculation (DAI), numbers of adult males and females were counted per plant. Furthermore, sizes of females and associated syncytia were measured after 13 DAI using Leica M165C Binocular (Leica Microsystems, Wetzlar, Germany) and Leica Application Suite software. *A. thaliana* plants grown on 0.2% Knop agar medium supplemented with 0.5% (v/v) DMSO were used as control. Experiments were repeated three times and statistically analyzed using one-way ANOVA followed by Dunn's post-hoc test. Each experiment consisted of 12 plants per treatment.

Effect of Prodigiosin Derivatives on Plant Pathogenic Fungi

The plant pathogenic fungi *Phoma lingam* and *Sclerotinia sclerotiorum* were used in this study to evaluate the bioactivity of the compounds on hyphal growth. Both isolates were obtained from the Leibniz-Institut DSMZ (Deutsche Sammlung von Mikroorganismen und Zellkulturen GmbH, Germany) and subcultured on potato dextrose agar (PDA) at 24°C. To test prodiginine bioactivities, PDA was supplemented with the chemicals to several final dilutions. The used concentrations were 50, 25 and 12.5 μM. Fungal discs were cut from the culture media and placed in the middle of PDA plates containing the chemicals. PDA plates with 0.5% (v/v) DMSO alone were used as control. All plates were incubated for 7 days at 24°C. Subsequently, the diameter of the fungal colony was measured, and inhibition percentage was calculated. Experiments were repeated four times, each experiment consisted of 3 technical replicates. Differences between the treatments were statistically analyzed by using one-way ANOVA followed by Dunnett's post-hoc.

RESULTS

Activity of Prodiginines Against Nematodes Is Dependent on Compound Structure and Concentration as Well as Nematode Species

The bioactivity of prodigiosin (**1**) and the derivatives **6**–**10** was determined using two representative soil nematodes with different feeding behavior, the bacterial feeding model nematode *C. elegans* and the plant parasitic nematode *H. schachtii*. The two tested nematode species responded differently to exposure to prodiginines. Results revealed that the impact of the tested compounds on *C. elegans* depends on prodiginine structure and concentration (**Figure 3**). Prodigiosin (**1**) showed the highest nematicidal activity against *C. elegans* juveniles with 0.127 μM being the effective concentration that killed half of the treated nematodes (EC_{50}). This was followed by **7** (35.9 μM), **8** (79.1 μM), and then the other three derivatives. For compounds **10**, **6**, and **9** a reliable EC_{50} could not be determined as only 26, 27, and 33% effectivity, respectively, could be observed at the highest test concentration.

The compounds were much less effective against *H. schachtii* J2s and rather had a static effect. In fact, prodigiosin (**1**) was the only derivative able to cause considerable paralysis of the second stage juveniles. The calculated 48 h EC_{50} value was 13.3 μM and the J2s were able to recover even from the 100 μM treatment as only 27% of the J2s were observed to be dead after a 48 h recovery phase. The impact of a 48 h exposure of the J2s to any other derivative only had a very low neglectable effect with a maximum of about 10% immobile nematodes (100 μM) thus not enabling us to calculate the EC_{50} (**Table 1** and **Figure 4**).

Effect of Prodigiosin (1) and Derivatives 6–10 on Plant Growth

The effect of prodiginines on plant growth was tested in order to obtain a suitable concentration for the subsequent infection assay and to get an indication which compound could be best suited for a possible use as plant protection agent in agricultural applications. Therefore, shoot weight and root weight were determined. The applied concentrations between 12.5 and 50 μM of the derivatives **6** and **8** inhibited plant growth as shoot weight was decreased by more than 70% compared to the DMSO control. Compound **7** was also detrimental for the plant but less severe.

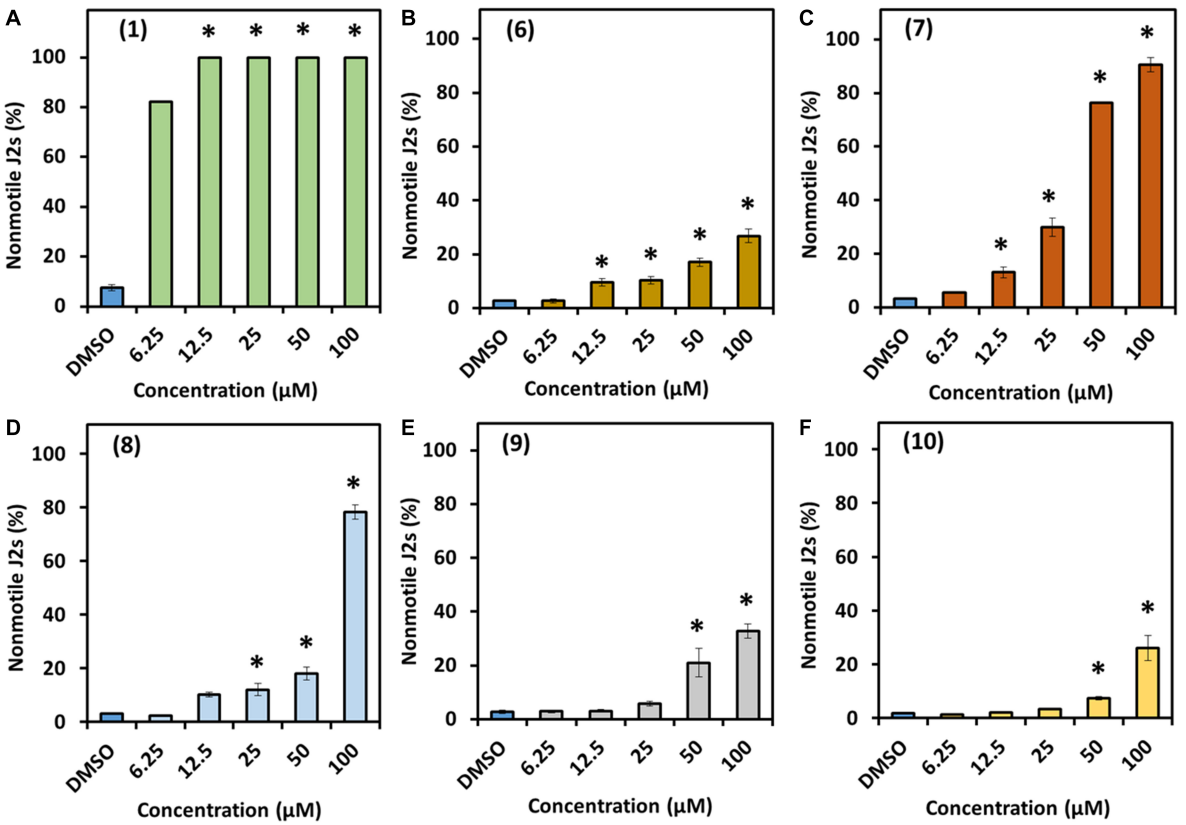

FIGURE 3 | Direct effect of prodigiosin (**1**) and derivatives **6–10** on *C. elegans* first-stage juveniles. **(A)** Compound 1, **(B)** compound 6, **(C)** compound 7, **(D)** compound 8, **(E)** compound 9, and **(F)** compound 10. Values are means ± standard error of three biological replicates ($n = 9$). Asterisks indicate significant differences to the control based on one-way ANOVA followed by Dunnett's post-hoc test ($P < 0.05$).

Cultivating the plants in 25 and 50 μM significantly decreased plant shoot weight, whereas the impact of 12.5 μM was not significant compared to the DMSO control. On the other hand, incubating plants in prodigiosin (**1**, 12.5 μM) and derivative **10** (12.5 and 25 μM) increased shoot weight by up to 70%. Higher concentrations of both derivatives had no significant effect. All concentrations of **9** had no significant effect on shoot weight compared with the control (**Figure 5**).

Comparable effects of the compounds on root weight could be observed. Compound **10** was highly promoting root growth at concentrations of 25 or 12.5 μM. Prodigiosin (**1**) treatment was neutral except for the 50 μM concentration were root weight was significantly reduced. Root weight was decreased significantly when plants were incubated in 50 μM of all other derivatives. The effect was less severe when the concentration was decreased to 25 or 12.5 μM but still root weight was significantly decreased compared to the control with the exception of **9**, where this inhibitory effect was demolished when plants were incubated in 12.5 μM.

Prodiginines Inhibit Nematode Parasitism

Due to the observed neutral to positive effect of prodiginines on plant growth and compound availability, **1** and **9** were selected to investigate their effect on *H. schachtii* parasitism of *A. thaliana*. A final concentration of 14 μM of each molecule was incorporated into the plant growth medium. Medium mixed with DMSO in a final concentration of 0.5% was used as control. Results showed that the number of developed females and males was significantly decreased on the plant roots in presence of compound **1** or **9** compared with the control (**Figure 6**). The number of females was decreased by up to 60%, while the males were up to 42% less in the treatments compared to the control. In total, a reduction of up to 50% in total infection was observed when plant roots are exposed to prodigiosin (**1**) or the derivative **9**.

Furthermore, the size of developed females and their associated syncytia were measured in order to investigate nematode development. Both, developed females and their associated syncytia were smaller in size compared with the control in the presence of compound **1** or **9** in the medium. The female size reached 77 and 80% of that of the females of the control in presence of prodigiosin (**1**) and **9**, respectively. The inhibitory effect on syncytium development was higher as the average size determined was 60 and 75% of the size in the control in presence of prodigiosin (**1**) and **9**, respectively (**Figure 6**).

TABLE 1 | Direct effect of prodigiosin (**1**) and derivatives **6–10** on *H. schachtii* second-stage juveniles.

Compound	Concentration (μm)	Average nonmotile J2s (%)	SE
(**1**)	DMSO	4.4	0.7
	6.25	29.9*	2.4
	12.5	52.0*	2.8
	25	67.2*	3.4
	50	87.2*	1.6
	100	93.3*	1.5
(**6**)	DMSO	1.0	0.7
	6.25	2.8	0.8
	12.5	2.8	0.1
	25	1.4	0.2
	50	1.3	0.1
	100	9.3*	1.3
(**7**)	DMSO	2.2	1.0
	6.25	2.7	0.6
	12.5	2.0	0.7
	25	2.0	0.3
	50	2.3	0.4
	100	10.4*	1.3
(**8**)	DMSO	1.2	1.0
	6.25	2.1	0.6
	12.5	1.8	0.9
	25	1.8	0.5
	50	1.4	0.3
	100	6.0*	1.9
(**9**)	DMSO	1.4	0.4
	6.25	1.9	0.4
	12.5	1.8	0.7
	25	1.7	0.8
	50	2.2	1.1
	100	5.4*	0.5
(**10**)	DMSO	1.0	0.9
	6.25	1.3	0.3
	12.5	1.6	0.8
	25	2.0	1.2
	50	5.2*	2.8
	100	10.0*	4.7

*Values are means ± standard error of three biological replicates (n = 9). *Indicates significant differences to the control based on one-way ANOVA followed by Dunnett's post-hoc test (P < 0.05).*

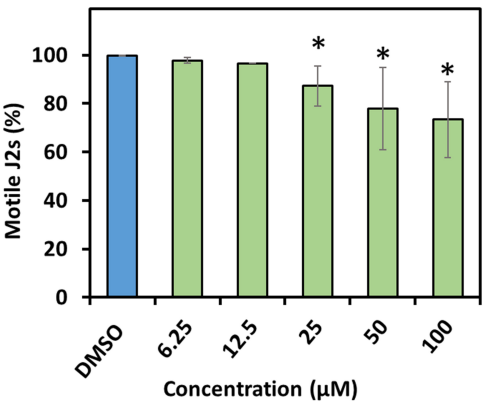

FIGURE 4 | Recovery of second stage juveniles of *H. schachtii* after exposure to prodigiosin (**1**). Percentage of recovered nematodes after 48 h incubation in prodigiosin (**1**) followed by washing and incubation for 48 h in water. Values are means ± standard error of three biological replicates ($n = 9$). Asterisks indicate significant differences to the control based on one-way ANOVA followed by Dunnett's post-hoc test ($P < 0.05$).

Bioactivities Against Plant Pathogenic Fungi

We further investigated the bioactivity of prodiginines against the two plant pathogenic fungi *P. lingam* and *S. sclerotiorum*. Both fungi share host plants with *H. schachtii*. Besides observing a possible antifungal activity, we aimed at getting an indication whether the changes in bioactivity documented for the structurally different prodiginines against nematodes follow a similar pattern in their activity against fungi. The two fungi responded differently to direct compound exposure and the degree of inhibition of hyphal growth varied with the prodiginine and concentration used (**Figure 7**). All tested derivatives except **10** significantly inhibited the hyphal growth of *P. lingam* at 50 μm. When the fungus was cultured on medium containing 25 μM of the compounds, prodigiosin (**1**), **6** and **8** showed significant inhibition. While none of the used compound showed inhibitory activity on hyphal growth at 12.5 μM.

S. sclerotiorum was less sensitive toward the used prodiginines. All compounds inhibited hyphal growth except derivatives **6** and **10,** even when 50 μM was used (**Figure 7B**). Fungal growth varied depending on the tripyrrol applied and ranged from 44% (**8**) to 100% (**10**) compared to the control (**Figure 6B**).

DISCUSSION

Management of plant pathogens in agricultural crop production is indispensable, no matter whether organic, integrated or conventional farming practices are applied. In particular, control of plant parasitic nematodes is extremely challenging. Rising public health concerns about pesticides harmful for the environment led to several effective compounds being banned from the market. This in return, limited the pathogen management options of the farmer during production processes. These reasons urge to find environmentally safe and sustainable alternatives to control pathogens and ensure yield and food quality.

Naturally occurring bacterial metabolites represent a valuable source of active compounds that can be used in different applications including pathogen control. In the last decade, several studies investigated these potential compounds (Schrader et al., 2010; Pathma et al., 2011; Zhai et al., 2018). Prodigiosin (**1**) which is a tripyrrolic red-colored pigment produced by many bacterial species got attention due to its bioactivities and was intensively studied (Darshan and Manonmani, 2015; Yip et al., 2019). Derivatization of compounds is one of the important tools to increase the availability as well as the activity of compounds. Various structure activity studies have already

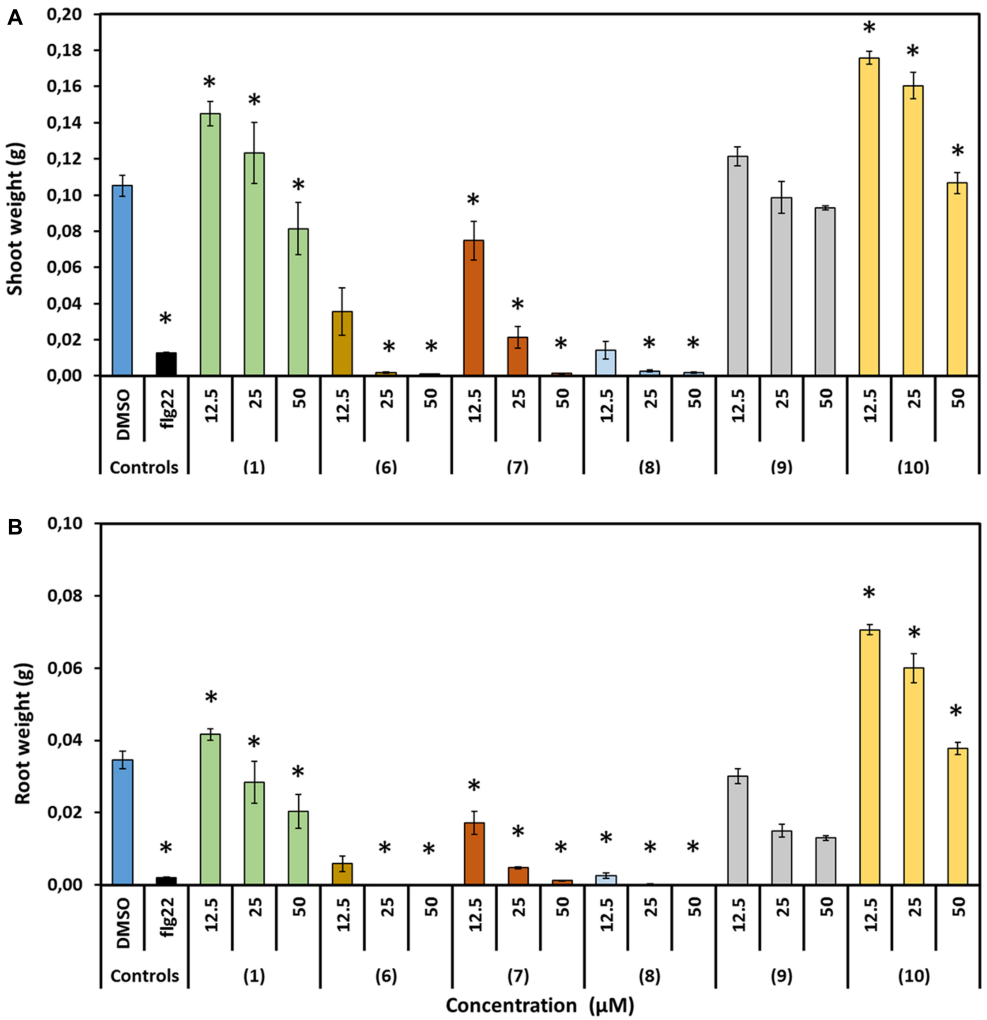

FIGURE 5 | Effect of prodigiosin (**1**) and derivatives **6–10** on *A. thaliana* growth. Figures show growth parameters representing development of *A. thaliana* cultivated on media mixed with prodigiosin (**1**) or different derivatives (**6**–**10**) in three concentrations compared with those growing on medium mixed with DMSO as control. Flg22 (1 µM) treated plants served as controls for successful growth inhibition. **(A)** Average fresh shoot weight (g). **(B)** Average fresh root weight (g). Data are based on three independent experiments. Each bar represents the mean ± standard error of $n = 15$. Asterisks indicate significant differences to the control based on one-way ANOVA followed by Dunnett's post-hoc test ($P < 0.05$).

proven that variation of the prodiginine structure leads to different biological activities (D'Alessio et al., 2000; Papireddy et al., 2011; Marchal et al., 2014a,b; Kancharla et al., 2015). Synthetic biology is one of the approaches that helps this process and provides the tools necessary for applying mutasynthesis or biotransformation concepts for a controlled production of prodiginines in a safe heterologous bacterial host (Klein et al., 2017, 2018). Also biocatalysis approaches employing only the final enzyme of the prodigiosin (**1**) gene cluster and chemically synthesized precursors can lead to new prodiginine structures (Brass et al., 2019).

In our current study, we introduce several lines of results showing the potential of prodigiosin (**1**) and several derivatives including a new prodiginine with a terminal hydroxy group adjacent to an allylic double bond and their bioactivities toward several organisms including nematodes, fungi and plant. We first tested all compounds against the model nematode *C. elegans* and the plant parasitic nematode *H. schachtii* in direct exposure assays. The nematode *C. elegans* is frequently used in studies involved in investigating compounds' bioactivities against multicellular organisms (Sun et al., 2017; Al Banna et al., 2018; Liao, 2018). The nematode *H. schachtii* is one of the devastating pathogens of several economically valuable crops (Steele, 1965; Muller, 1999). We observed that all derivatives are nematicidal for *C. elegans* while basically only the lead structure prodigiosin (**1**) is static for *H. schachtii* J2s. The nematicidal activity of the compounds toward *C. elegans* is clearly dependent on the molecule structure and the concentration with compounds **6**, **9**, and **10** having the lowest efficacy. The difference in compound activity toward the two nematode species could be due to differences in feeding habit. *C. elegance* has a wider mouth part which is an open canal that allows to

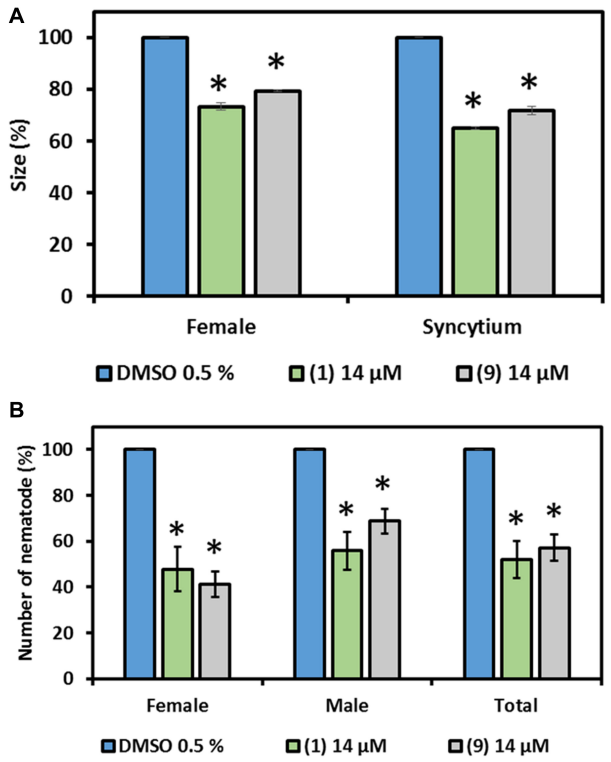

FIGURE 6 | Effect of prodigiosin (**1**) and derivative **9** on *H. schachtii* parasitism of *A. thaliana*. Plants were grown on Knop's agar mixed with prodigiosin (**1**) and derivative **9** and were infected with J2s of *H. schachtii*. Susceptibility parameters were **(A)** average percentage of females, males and total nematodes per plant compared with control and **(B)** average percentage of sizes of females and syncytia at 13 DAI. Plants grown on medium mixed with DMSO (0.5% final concentration) were used as control. Data are based on three independent experiments. Each bar represents the mean ± standard error of $n > 35$. Asterisks indicate significant differences to the control based on one-way ANOVA followed by Dunnett's post-hoc test ($P < 0.05$).

uptake compounds from the environment while in *H. schachtii* the uptake through the mouth is controlled by the spear-like stylet and feeding exclusively occurs at the host plant during the sedentary phase. Thus, the mobile infective juvenile stage of *H. schachtii* used here is not feeding at all consequently limiting uptake of compounds from the environment to passive processes. Same results were demonstrated when both, *C. elegans* and *Meloidogyne incognita,* were exposed to the nanoparticles of silicon carbide. *C. elegans* was much more sensitive and exhibited high mortality as well as accumulation of the nanoparticles in the body after the exposure, while very low mortality and particle accumulation were observed in case of *M. incognita* (Al Banna et al., 2018). Furthermore, the two related nematodes, *H. schachtii* and *Globodera rostochiensis,* behaved differently upon exposure to exogenous application of several amino acids. In these studies, *G. rostochiensis* was shown to be sensitive to the application of methionine while no effect was observed in case of *H. schachtii* (Evans and Trudgill, 1971; Blümel et al., 2018). Both evidences support the hypothesis that different nematode anatomy and biology affect the nematodes' sensitivity toward compounds. The nematicidal activities of prodigiosin (**1**) itself was also observed previously. It was shown that the survival of juvenile stages of *Radopholus similis* and *Meloidogyne javanica* was affected after treatment with the red pigment extracted from *S. marcescens* with LC_{50} (lethal concentration) value of 83 and 79 µg/mL, for *R. similis* and *M. javanica*, respectively. After deep analysis of the pigment using several liquid chromatography approaches and spectroscopic analysis, they confirmed the presence of prodigiosin as a bioactive metabolite (Rahul et al., 2014). All these findings support our results and show that different nematode species could behave differently due to exposer to compounds.

In order to introduce such compounds as agrochemicals, the effect on the plant has to be tested. No previous work was done studying the effect of prodiginines on plant development. Here, we report the effect of prodigiosin (**1**) and derivatives on plant growth of the model plant *A. thaliana* for the first time. *Arabidopsis* growth was different between treatments and was depending on concentration and prodiginine structure. We observed that prodigiosin (**1**) and the 12-ring derivative **9** are neutral for plant growth when low concentrations are applied. In case of the prodiginine **10**, plant growth was even highly promoted at low concentrations.

Based on the plant growth experiment results and compound availability, prodigiosin (**1**) and the 12-ring derivative (**9**) were chosen and a proper concentration was defined to be used to test the effect of the molecules on nematode parasitism on *A. thaliana*. The presence of 14 µM of both compounds in the plant growth medium affected *H. schachtii* parasitism and decreased the total number of adult nematodes per plant up to 50%. Furthermore, the compounds affected nematode development which is reflected by the smaller developed females and associated syncytia. Interestingly, although prodigiosin (**1**) paralyzes the J2s in liquid medium, we could not observe an impact of prodigiosin-supplemented agar on J2 motility. Therefore, we suggest that the observed effect of the two compounds on *H. schachtii* parasitism could be explained by compound-triggered plant defense responses. Similar observations were reported when no direct effect was detected after incubating J2s of *H. schachtii* in amino acids but still decreased parasitism when amino acids were integrated in the growth medium (Blümel et al., 2018). The logical explanation of such an outcome is that the presence of the compounds in the growth medium is activating plant defense responses against the nematode. These tests should be complemented by soil-based experiments in the future to confirm the observed control potential under field conditions. Particularly because in natural environments, factors like compound leaching, soil properties and compound stability affect efficacy.

We tested the bioactivities of the prodiginines against two plant pathogenic fungi. Both fungi can infect the same host plants as *H. schachtii*, thus a double impact of the compounds would increase their value. Our results showed that the direct effect of the prodiginines against the fungi *P. lingam* and *S. sclerotiorum* was even stronger compared to nematodes. The hyphal growth of both tested fungi was affected by the presence of prodigiosin (**1**) and derivatives **6**–**10** in the growth medium. Earlier, it was

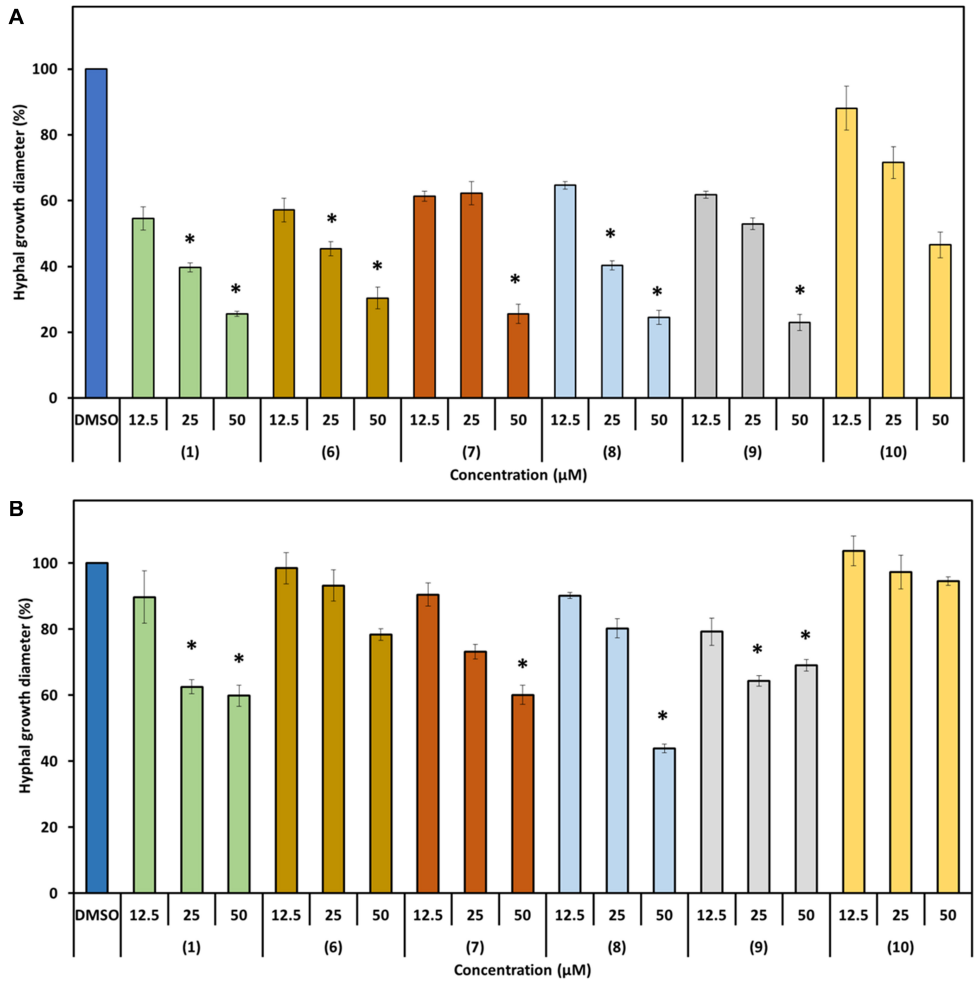

FIGURE 7 | Effect of prodigiosin (**1**) and derivatives **6–10** on fungal hyphal growth. Figures show percentage of hyphal growth of the plant pathogenic fungi cultivated on media mixed with prodigiosin (**1**) or the derivatives **6**–**10** in three concentrations compared with those cultivated on medium mixed with DMSO as control. **(A)** *P. lingam*. **(B)** *S. sclerotiorum*. Values are means ± standard error of four biological replicates (n = 12). Asterisks indicate significant differences to the control based on one-way ANOVA followed by Dunnett's post-hoc test ($P < 0.05$).

shown that prodigiosin (**1**) is active against several fungi and oomycetes. The purified prodigiosin (**1**) from *S. marcescens* F-1-1 inhibited the germination of cystospores and the growth of hyphae of *Phytophthora capsici*. It also appeared to be active against the plant pathogenic fungi *Cochliobolus miyabeanus*, *Pythium spinosum* and *P. ultimum* (Okamoto et al., 1998). According to our results, hyphal growth of *P. lingam* was affected more than that of *S. sclerotiorum*. Such a difference is dependent on fungal species and also demonstrated by previous studies. Chen et al. (2014) presented that the novel fungicide 3-[5-(4-chlorophenyl)-2,3-dimethyl-3-isoxazolidinyl] pyridine (SYP-Z048) affected several pathogenic fungi and the effect was variable between the tested fungi.

Comparing the results of the assays, we show that prodigiosin (**1**) is the most effective and derivative **10** is the least effective obviously reflecting the variability in compound sensitivity between different organisms. Particularly, *P. lingam* appears to be very sensitive to all compounds whereas *H. schachtii* only responded to prodigiosin (**1**). Interestingly, the compounds' impact on plant development does not completely follow the same trend as seen for nematodes and fungi. Although plant growth promotion is highest for the prodiginine with the overall lowest activity against nematodes and fungi (compound **10**), prodigiosin (**1**) is neutral for plant growth depending on the concentration applied.

Compound **9** is a very good example that structural modification of a bioactive lead structure can guide compound activity toward desired properties. The lead structure **1** and derivative **9** have a comparable impact on plant development (neutral) and on parasitism of *H. schachtii* on *A. thaliana* (inhibition). Intriguingly, **1** is highly toxic for *C. elegans*, which is a representative of non-target organisms, whereas **9** does not affect this nematode's vitality at concentrations suitable to control *H. schachtii* and *P. lingam*, which are two important pathogens on sugar beet.

Further detailed investigations are needed to unravel the mode of action against nematodes. Although studies with

nematodes are missing so far, mechanistic insights of the effect of prodigiosin in other organisms were reported. For example, it was shown that the motility of the bacteria *Bacillus cereus*, *Staphylococcus aureus*, *Pseudomonas aeruginosa*, and *Escherichia coli* was inhibited upon exposure to prodigiosin. The inhibition was combined with activation of several features of programmed cell death (Darshan and Manonmani, 2015). In another study, the exposure of *B. subtilis* to prodigiosin was associated with growth inhibition and cell membrane leakage. The authors suggested that prodigiosin affects the bacterial cell by inducing cell lysis activities (Danevčič et al., 2016a). Similarly, *E. coli* exhibited a leaky outer membrane and cells had severely decreased respiration activity upon exposure to prodigiosin (Danevčič et al., 2016b).

Our current results demonstrate the bioactivities of prodigiosin (**1**) and its derivatives (**6**–**10**) against plant pathogenic fungi and parasitic nematodes and thereby introduce new natural compounds that have the potential to be developed into novel plant protection agents.

DATA AVAILABILITY STATEMENT

All datasets presented in this study are included in the article/**Supplementary Material**.

AUTHOR CONTRIBUTIONS

AS, FG, JP, TC, and SH conceived the research concept and designed the experiments. SH performed the assays on plants, nematodes, and fungi. HB, AK, DK, and TW produced and synthesized the used prodiginines. SH drafted the manuscript with input from all authors. All authors reviewed and approved the final manuscript.

FUNDING

This research and the scientific activities of the Bioeconomy Science Center were financially supported by the Ministry of Culture and Science within the framework of the NRW Strategieprojekt BioSC (No. 313/323-400-00213). The funding body had no role in the design of the study and collection, analysis, and interpretation of data or in writing the manuscript.

ACKNOWLEDGMENTS

The authors gratefully acknowledge the Bioeconomy Science Center and the Ministry of Culture and Science of the German State of North Rhine-Westphalia (MKW) for funding the work.

SUPPLEMENTARY MATERIAL

The Supplementary Material for this article can be found online at: https://www.frontiersin.org/articles/10.3389/fpls.2020.579807/full#supplementary-material

REFERENCES

Al Banna, L., Salem, N., Ghrair, A. M., and Habash, S. S. (2018). Impact of silicon carbide nanoparticles on hatching and survival of soil nematodes *Caenorhabditis elegans* and *Meloidogyne incognita*. *Appl. Ecol. Environ. Res.* 16, 2651–2662. doi: 10.15666/aeer/1603_26512662

Arivizhivendhan, K. V., Mahesh, M., Boopathy, R., Swarnalatha, S., Regina Mary, R., and Sekaran, G. (2018). Antioxidant and antimicrobial activity of bioactive prodigiosin produces from *Serratia marcescens* using agricultural waste as a substrate. *J. Food Sci. Technol.* 55, 2672–2681. doi: 10.1007/s13197-018-3188-9

Blümel, R. C., Fischer, D. F., and Grundler, F. M. W. (2018). Effects of exogenous amino acid applications on the plant-parasitic nematode *Heterodera schachtii*. *Nematology* 20, 713–727. doi: 10.1163/15685411-00003169

Brass, H. U. C., Klein, A. S., Nyholt, S., Classen, T., and Pietruszka, J. (2019). Condensing enzymes from *pseudoalteromonadaceae* for prodiginine synthesis. *Adv. Synth. Catal.* 361:adsc.201900183. doi: 10.1002/adsc.201900183

Bridge, J. (1996). Nematode management in sustainable and subsistence agriculture. *Annu. Rev. Phytopathol.* 34, 201–225. doi: 10.1146/annurev.phyto.34.1.201

Chen, F., Han, P., Liu, P., Si, N., Liu, J., and Liu, X. (2014). Activity of the novel fungicide SYP-Z048 against plant pathogens. *Sci. Rep.* 4:6473. doi: 10.1038/srep06473

Classen, T., and Pietruszka, J. (2018). Complex molecules, clever solutions – Enzymatic approaches towards natural product and active agent syntheses. *Bioorg. Med. Chem.* 26, 1285-1303. doi: 10.1016/j.bmc.2017.06.045

D'Alessio, R., Bargiotti, A., Carlini, O., Colotta, F., Ferrari, M., Gnocchi, P., et al. (2000). Synthesis and immunosuppressive activity of novel prodigiosin derivatives. *J. Med. Chem.* 43, 2557–2565. doi: 10.1021/jm001003p

Danevčič, T., Vezjak, M. B., Tabor, M., Zorec, M., and Stopar, D. (2016a). Prodigiosin induces autolysins in actively grown *Bacillus subtilis* cells. *Front. Microbiol.* 7:27. doi: 10.3389/fmicb.2016.00027

Danevčič, T., Vezjak, M. B., Zorec, M., and Stopar, D. (2016b). Prodigiosin - A multifaceted *Escherichia coli* antimicrobial agent. *PLoS One* 11:e0162412. doi: 10.1371/journal.pone.0162412

Darshan, N., and Manonmani, H. K. (2015). Prodigiosin and its potential applications. *J. Food Sci. Technol.* 52, 5393–5407. doi: 10.1007/s13197-015-1740-4

Domröse, A., Klein, A. S., Hage-Hülsmann, J., Thies, S., Svensson, V., Classen, T., et al. (2015). Efficient recombinant production of prodigiosin in *Pseudomonas putida*. *Front. Microbiol* 6:972. doi: 10.3389/fmicb.2015.00972

Evans, K., and Trudgill, D. L. (1971). Effects of amino acids on the reproduction of *Heterodera rostochiensis*. *Nematologica* 17, 495–500. doi: 10.1163/187529271X00215

Gerber, N. N. (1975). A new prodiginne (prodigiosin-like) pigment from Streptomyces. Antimalarial activity of several prodiginnes. *J. Antibiot.* 28, 194–199. doi: 10.7164/antibiotics.28.194

Habash, S., and Al-Banna, L. (2011). Phosphonate fertilizers suppressed root knot nematodes *Meloidogyne javanica* and *M. incognita*. *J. Nematol.* 43, 95–100.

Habash, S. S., Sobczak, M., Siddique, S., Voigt, B., Elashry, A., and Grundler, F. M. W. (2017). Identification and characterization of a putative protein disulfide isomerase (HsPDI) as an alleged effector of *Heterodera schachtii*. *Sci. Rep* 7:13536. doi: 10.1038/s41598-017-13418-9

Heydari, A., and Pessarakli, M. (2010). A review on biological control of fungal plant pathogens using microbial antagonists. *J. Biol. Sci.* 10, 273–290. doi: 10.3923/jbs.2010.273.290

Hu, D. X., Withall, D. M., Challis, G. L., and Thomson, R. J. (2016). Structure, chemical synthesis, and biosynthesis of prodiginine natural products. *Chem. Rev.* 116, 7818–7853. doi: 10.1021/acs.chemrev.6b00024

Kancharla, P., Kelly, J. X., and Reynolds, K. A. (2015). Synthesis and structure-activity relationships of tambjamines and b-ring functionalized prodiginines as potent antimalarials. *J. Med. Chem.* 58, 7286–7309. doi: 10.1021/acs.jmedchem.5b00560

Kawasaki, T., Sakurai, F., and Hayakawa, Y. (2008). A Prodigiosin from the Roseophilin Producer *Streptomyces griseoviridis*. *J. Nat. Prod.* 71, 1265–1267. doi: 10.1021/np7007494

Kennedy, J. (2008). Mutasynthesis, chemobiosynthesis, and back to semi-synthesis: Combining synthetic chemistry and biosynthetic engineering for diversifying natural products. *Nat. Prod. Rep.* 25, 25-34. doi: 10.1039/b707678a

Kim, D., Lee, J. S., Park, Y. K., Kim, J. F., Jeong, H., Oh, T. K., et al. (2007). Biosynthesis of antibiotic prodiginines in the marine bacterium *Hahella chejuensis* KCTC 2396. *J. Appl. Microbiol.* 102, 937–944. doi: 10.1111/j.1365-2672.2006.03172.x

Kimyon, Ö, Das, T., Ibugo, A. I., Kutty, S. K., Ho, K. K., Tebben, J., et al. (2016). Serratia secondary metabolite prodigiosin inhibits *Pseudomonas aeruginosa* biofilm development by producing reactive oxygen species that damage biological molecules. *Front. Microbiol* 7:972. doi: 10.3389/fmicb.2016.00972

Kirschning, A., and Hahn, F. (2012). Merging chemical synthesis and biosynthesis: A new chapter in the total synthesis of natural products and natural product libraries. *Angew. Chem. Int. Ed.* 51, 4012-4022. doi: 10.1002/anie.201107386

Klein, A. S., Brass, H. U. C., Klebl, D. P., Classen, T., Loeschcke, A., Drepper, T., et al. (2018). Preparation of cyclic prodiginines by mutasynthesis in *Pseudomonas putida* kt2440. *Chembiochem* 19, 1545–1552. doi: 10.1002/cbic.201800154

Klein, A. S., Domröse, A., Bongen, P., Brass, H. U. C., Classen, T., Loeschcke, A., et al. (2017). New prodigiosin derivatives obtained by mutasynthesis in *Pseudomonas putida*. *ACS Synth. Biol.* 6, 1757–1765. doi: 10.1021/acssynbio.7b00099

Liao, V. H. C. (2018). Use of *Caenorhabditis elegans* to study the potential bioactivity of natural compounds. *J. Agric. Food Chem.* 66, 1737–1742. doi: 10.1021/acs.jafc.7b05700

Marchal, E., Rastogi, S., Thompson, A., and Davis, J. T. (2014a). Influence of B-ring modifications on proton affinity, transmembrane anion transport and anti-cancer properties of synthetic prodigiosenes. *Org. Biomol. Chem.* 12, 7515–7522. doi: 10.1039/c4ob01399a

Marchal, E., Smithen, D. A., Uddin, M. I., Robertson, A. W., Jakeman, D. L., Mollard, V., et al. (2014b). Synthesis and antimalarial activity of prodigiosenes. *Org. Biomol. Chem.* 12, 4132–4142. doi: 10.1039/c3ob42548g

Muller, J. (1999). The economic importance of *Heterodera schachtii* in Europe. *Helminthologia* 36, 205–213.

Oerke, E. C. (2006). Crop losses to pests. *J. Agric. Sci.* 144, 31–43. doi: 10.1017/S0021859605005708

Okamoto, H., Sato, Z., Sato, M., Koiso, Y., Iwasaki, S., and Isaka, M. (1998). Identification of antibiotic red pigments of *Serratia marcescens* F-1-1, a biocontrol agent of damping-off of cucumber, and antimicrobial activity against other plant pathogens. *Jap. J. Phytopathol.* 64, 294–298. doi: 10.3186/jjphytopath.64.294

Papireddy, K., Smilkstein, M., Kelly, J. X., Shweta, S., Salem, S. M., Alhamadsheh, M., et al. (2011). Antimalarial activity of natural and synthetic prodiginines. *J. Med. Chem.* 54, 5296–5306. doi: 10.1021/jm200543y

Pathma, J., Rahul, G. R., Kamaraj, K. R., Subashri, R., and Sakthivel, N. (2011). Secondary metabolite production by bacterial antagonists. *J. Biol. Control.* 25, 165–181. doi: 10.18641/JBC/25/3/39985

Pérez-Tomás, R., Montaner, B., Llagostera, E., and Soto-Cerrato, V. (2003). The prodigiosins, proapoptotic drugs with anticancer properties. *Biochem. Pharmacol.* 66, 1447–1452. doi: 10.1016/S0006-2952(03)00496-9

Rahul, S., Chandrashekhar, P., Hemant, B., Chandrakant, N., Laxmikant, S., and Satish, P. (2014). Nematicidal activity of microbial pigment from *Serratia marcescens*. *Nat. Prod. Res.* 28, 1399–1404. doi: 10.1080/14786419.2014.904310

Schrader, K. K., Andolfi, A., Cantrell, C. L., Cimmino, A., Duke, S. O., Osbrink, W., et al. (2010). A survey of phytotoxic microbial and plant metabolites as potential natural products for pest management. *Chem. Biodivers.* 7, 2261–2280. doi: 10.1002/cbdv.201000041

Sijmons, P. C., Grundler, F. M. W., von Mende, N., Burrows, P. R., and Wyss, U. (1991). *Arabidopsis thaliana* as a new model host for plant-parasitic nematodes. *Plant J.* 1, 245–254. doi: 10.1111/j.1365-313X.1991.00245.x

Someya, N., Nakajima, M., Hirayae, K., Hibi, T., and Akutsu, K. (2001). Synergistic antifungal activity of chitinolytic enzymes and prodigiosin produced by biocontrol bacterium, *Serratia marcescens* strain B2 against gray mold pathogen, *Botrytis cinerea*. *J. Gen. Plant Pathol.* 67, 312–317. doi: 10.1007/PL00013038

Stankovic, N., Senerovic, L., Ilic-Tomic, T., Vasiljevic, B., and Nikodinovic-Runic, J. (2014). Properties and applications of undecylprodigiosin and other bacterial prodigiosins. *Appl. Microbiol. Biotechnol.* 98, 3841–3858. doi: 10.1007/s00253-014-5590-1

Starič, N., Danevčič, T., and Stopar, D. (2010). *Vibrio sp. DSM* 14379 pigment production-A competitive advantage in the environment. *Microb. Ecol.* 60, 592–598. doi: 10.1007/s00248-010-9671-0

Steele, A. E. (1965). The host range of the sugar beet nematode, *Heterodera schachtii* Schmidt. *J. Sugarb. Res.* 13, 574–603.

Sun, C. L., Zhang, H., Liu, M., Wang, W., and Crowder, C. M. (2017). A screen for protective drugs against delayed hypoxic injury. *PLoS One* 12:e0176061. doi: 10.1371/journal.pone.0176061

Timper, P. (2014). Conserving and enhancing biological control of nematodes. *J. Nematol.* 46, 75–89.

Weist, S., and Süssmuth, R. D. (2005). Mutational biosynthesis - A tool for the generation of structural diversity in the biosynthesis of antibiotics. *Appl. Microbiol. Biotechnol* 68, 141–150. doi: 10.1007/s00253-005-1891-8

Williams, R. P., Green, J. A., and Rappo-Port, D. A. (1956). Studies on pigmentation of *Serratia marcescens*, I. Spectral and paper chromatographic properties of prodigiosin. *J. Bacteriol.* 71, 115–120.

Williamson, N. R., Fineran, P. C., Leeper, F. J., and Salmond, G. P. C. (2006). The biosynthesis and regulation of bacterial prodiginines. *Nat. Rev. Microbiol.* 4, 887–899. doi: 10.1038/nrmicro1531

Yip, C. H., Yarkoni, O., Ajioka, J., Wan, K. L., and Nathan, S. (2019). Recent advancements in high-level synthesis of the promising clinical drug, prodigiosin. *Appl. Microbiol. Biotechnol.* 103, 1667–1680. doi: 10.1007/s00253-018-09611-z

Zhai, Y., Shao, Z., Cai, M., Zheng, L., Li, G., Huang, D., et al. (2018). Multiple modes of nematode control by volatiles of *Pseudomonas putida* 1A00316 from Antarctic soil against *Meloidogyne incognita*. *Front. Microbiol.* 9:253. doi: 10.3389/fmicb.2018.00253

Conflict of Interest: The study was the basis for a patent application. Patent applicant: Forschungszentrum Juelich GmbH; inventors: SH, HB, AK, DK, TW, TC, JP, FG, and AS application number: 10 2020 116 516; status: examination phase.

frontiers in Plant Science

ORIGINAL RESEARCH
published: 22 October 2020
doi: 10.3389/fpls.2020.591715

Ascorbate Oxidase Induces Systemic Resistance in Sugar Beet Against Cyst Nematode *Heterodera schachtii*

*Richard R. Singh[1], Neriza Nobleza[1], Kristof Demeestere[2] and Tina Kyndt[1]**

[1] Department of Biotechnology, Faculty of Bioscience Engineering, Ghent University, Ghent, Belgium, [2] Research Group Environmental Organic Chemistry and Technology (EnVOC), Department of Green Chemistry and Technology, Ghent University, Ghent, Belgium

Ascorbate oxidase (AO) is an enzyme involved in catalyzing the oxidation of apoplastic ascorbic acid (AA) to dehydroascorbic acid (DHA). In this research, the potential of AO spraying to induce systemic resistance was demonstrated in the interaction between sugar beet root and cyst nematode *Heterodera schachtii* and the mechanism was elucidated. Plant bioassays showed that roots of AO-sprayed plants were infested by a significantly lower number of females and cysts when compared with mock-sprayed control plants. Hormone measurements showed an elevated level of jasmonic acid (JA) salicylic acid (SA) and ethylene (ET) in the roots of AO-sprayed plants, with a dynamic temporal pattern of activation. Experiments with chemical inhibitors showed that AO-induced systemic resistance is partially dependent on the JA, ET and SA pathways. Biochemical analyses revealed a primed accumulation of hydrogen peroxide (H_2O_2), and phenylalanine ammonia lyase (PAL) activity in the roots of AO-sprayed plants upon infection by cyst nematodes. In conclusion, our data shows that AO works as an effective systemic defense priming agent in sugar beet against cyst nematode infection, through activation of multiple basal plant defense pathways.

Keywords: ascorbate oxidation, phenylpropanoid, hydrogen peroxide, systemic defense response, cyst nematodes (*Heterodera* spp.)

OPEN ACCESS

Edited by:
Koichi Hasegawa, Chubu University, Japan

Reviewed by:
Muhammad Amjad Ali, University of Agriculture, Faisalabad, Pakistan
Krzysztof Wieczorek, University of Natural Resources and Life Sciences Vienna, Austria

****Correspondence:***
Tina Kyndt
Tina.Kyndt@Ugent.be

Specialty section:
This article was submitted to Plant Pathogen Interactions, a section of the journal Frontiers in Plant Science

Received: *05 August 2020*
Accepted: *28 September 2020*
Published: *22 October 2020*

Citation:
Singh RR, Nobleza N, Demeestere K and Kyndt T (2020) Ascorbate Oxidase Induces Systemic Resistance in Sugar Beet Against Cyst Nematode Heterodera schachtii. Front. Plant Sci. 11:591715. doi: 10.3389/fpls.2020.591715

INTRODUCTION

Sugar beet (*Beta vulgaris* L.) is the primary source of sugar in the temperate zone, and it accounts for 20% of the world's total sugar production. The EU is the world's leading sugar beet producer with 16.84 million tons of sugar production in 2019 (FAOSTAT, 2019). While fungal diseases such as Cercospora leaf spot, rust, powdery mildew and Ramularia leaf spot are the most common aboveground diseases negatively affecting sugar beet yield (Heick et al., 2020; Rangel et al., 2020), belowground plant-parasitic-nematodes (PPN) equally contribute to damage in sugar beet production (Cooke, 1987, 1993). Generally, crop losses caused by PPN have been estimated at $US80 billion per year globally (Nicol et al., 2011). *Heterodera schachtii* [beet cyst nematode (BCN)] is responsible for 90% of all nematode-related sugar beet infestations worldwide (Robb et al., 1992; Agrios, 2005). In addition to direct damage caused by BCN, penetration of nematodes in the roots cause an entry point for infection by other pathogens such as *Rhizoctonia*, viruses, and *Cercospora* spp. (Back et al., 2002; Agrios, 2005). BCN are sedentary endoparasites feeding within the roots of their host (Moens et al., 2018). The root exudates provides a cue for infective second-stage juveniles (J2) to hatch which then invade the roots in the elongation zone behind the root tips

(Wyss and Grundler, 1992; Moens et al., 2018). Upon invasion, the J2 migrate into the cortex after which they initiate a feeding structure (syncytium) in the root vascular tissue (Sobczak and Golinowski, 2009). The syncytium is formed by the breakdown of plant cell walls and subsequent fusion of adjacent protoplasts, resulting in a large multinucleate cell, and provides nutrients for the developing nematodes (Grundler et al., 1998; Kyndt et al., 2013; Anjam et al., 2020). After fertilization, around 200–300 eggs are laid, and once fully developed, the female dies, and its cuticle hardens to form a brown cyst (Khan et al., 2016). Cysts have the ability to survive in the soil for many years in the absence of a suitable host plant, making it difficult to control (Perry et al., 2018).

Protection of sugar beet against BCN is currently based on agronomic measures such as growing tolerant varieties or application of nematicides. Crop tolerance is a useful and necessary adjunct to resistance (Trudgill, 1991) as tolerance reduces the negative effects of pathogens, simultaneously improving plant growth after infections has occurred (Koch et al., 2016). For example, Eberlein et al. (2020) showed control of *H. schachtii* by growing the tolerant Pauletta cultivar. As another possible alternative for nematicides, so-called "induced resistance (IR)" of the plant provides a more sustainable solution, potentially addressing the EU regulations to protect our environment. The most efficient way of IR works through defense priming. Defense priming has two key phases whereby (1) a priming stimulus (also known as priming agent or elicitor) slightly awakens or activates defense responses when applied to plants, and (2) when challenged with a triggering stimulus (a stress factor), defense responses work in much faster and stronger manner than in naïve plants (Martinez-Medina et al., 2016). Priming hence puts a plant in a state of increased alertness with no or minimal gene induction, and no energy and yield loss (Conrath et al., 2015). Plant defense priming has a low fitness cost, activates robust defense responses with broad spectrum activity, and has a low ecological cost (Martinez-Medina et al., 2016). One such defense elicitor is β-aminobutyric acid (BABA), a non-protein amino acid that can activate plant defense to defeat a variety of subsequent stress factors (Conrath et al., 2006, 2015). For example, BABA induces resistance in potato against *Phytophthora infestans* (Bengtsson et al., 2014). Reduced numbers of cyst nematodes *H. avenae* and *H. latipons* were observed on wheat and barley upon foliar sprays with BABA (Oka and Cohen, 2001). However, a major drawback of this defense elicitor is that there have been records of phytotoxic effects on some crop plants (van Hulten et al., 2006; Koen et al., 2014; Luna et al., 2016). Recently, a novel registered defense elicitor—combining chitosan oligomers (COS) and pectin-derived oligogalacturonides (OGA), called COS-OGA—was shown to control mildew attack in grapes, cucumbers, tomatoes (van Aubel et al., 2014; Van Aubel et al., 2016), and *P. infestans* in potato (Van Aubel et al., 2018) and very recently a COS fluorinated derivative chitosan-thiadiazole-trifluorobutene (COSSZFB) was shown to control root knot nematode (RKN) *Meloidogyne incognita* in cucumber seedlings (Fan et al., 2020). In our previous research, this mixture has also been demonstrated to control RKN *M. graminicola* in rice, through systemic activation of the plant phenylpropanoid pathway (Singh et al., 2019). Additionally, silicon (Zhan et al., 2018) and thiamine (Huang et al., 2016) were shown to activate rice defense against *M. graminicola.* In sugar beet, thiamine (Vitamin B6) has been shown effective to activate plant defense against the fungal pathogen *Rhizoctonia solani* (Taheri and Tarighi, 2011), via jasmonate-mediated priming of the phenylpropanoid pathway. However, the use of these or other IR compounds to control BCN in sugar beets has not yet been evaluated.

Naturally, plants express a wide array of defense responses against numerous groups of abiotic and biotic stressors. Plant hormones such as salicylic acid (SA), jasmonic acid (JA) and ethylene (ET) are the central hubs of plant basal immunity (Spoel and Dong, 2008; De Vleesschauwer et al., 2013). ET is known to play a role against RKN infection through activation of JA (Nahar et al., 2011; Mantelin et al., 2017). The JA and SA pathways are known to play a pivotal role for example in Arabidopsis against infection of BCN (Kammerhofer et al., 2015), and in rice defense against *M. graminicola* infection (Nahar et al., 2011; Kyndt et al., 2017). Nematodes have been shown to suppress hormones during a compatible interaction with their host, to attain plant susceptibility. For example, RKNs suppress the SA and ET pathways in infected rice plants (Kyndt et al., 2012), and recent transcriptome data from our lab (Ghaemi et al., in press) provided evidence for ET suppression by BCN in sugar beet. While some hormonal pathways are suppressed by nematodes, others are important for feeding site and nematode development—for example auxin and cytokinin are required for feeding site formation (Gheysen and Mitchum, 2011; Kyndt et al., 2016; Gheysen and Mitchum, 2019). SA biosynthesis in plants follows two pathways namely isochorismate (IC) or the phenylalanine ammonia-lyase (PAL) pathways. The first step of the phenylpropanoid metabolism is the conversion of L-phenylalanine into trans-cinnamate, catalyzed by PAL (MacDonald and D'Cunha, 2007). Increases in PAL activity are often detected in the early response of plants upon pathogen attack (Giberti et al., 2012). In a recent study, JA was shown to protect tomato from RKN infection via a systemic signaling pathway, whereby root infection by nematodes causes signal transmission to the shoots, to induce biosynthesis of JA which is then transported to the root to induce defense against RKN *M. incognita* (Wang et al., 2019). This indicates that communication between tissues (shoot to root and vice versa) are vital for systemic defense signaling.

Reactive oxygen species (ROS) accumulate upon plant encounters with pathogens in a process called the oxidative burst. The most stable ROS, H_2O_2, also has the capacity to act as a signaling molecule (Smirnoff and Arnaud, 2019), playing positive roles in the plant cell (Foyer and Noctor, 2005; Foyer, 2018). At high concentrations this molecule is cytotoxic, and hence antioxidants are needed to protect cells from oxidative damage. Ascorbic acid (AA) also known as Vitamin C, is such a non-enzymatic antioxidant contributing to ROS-scavenging (Foyer and Noctor, 2011). This molecule is known to play a role in plant defense against many pathogens (Mittler et al., 2004), for example in resistance against several PPN. Arrigoni et al. (1979) showed that the application of AA increased tomato resistance

against *M. incognita*. Likewise, Zacheo et al. (1981) showed an increased level of AA in resistant pea plants when challenged by the cyst nematode *H. goettingiana*. In our recent transcriptome analysis of sugar beet upon infection with BCN, we similarly observed strong induction of AA-related genes in resistant plants (Ghaemi et al., in press).

AA is a water-soluble antioxidant that is universally distributed in higher plants, where it acts as a cofactor of many enzymes, and is known to be present in all compartments of plant cells in mM concentrations (Anjum et al., 2014; Foyer et al., 2020). In the apoplast, AA becomes oxidized during the oxidative burst. The reduction/oxidation (redox) state of the apoplastic AA pool is known to be regulated by ascorbate oxidase (AO) (Pignocchi et al., 2003; Foyer et al., 2020), a glycoprotein and a member of the blue copper oxidase family. In the apoplast, reduced AA concentration is lower while the oxidized form of AA, dehydroascorbate (DHA), is more predominant than in the symplast (Smirnoff and Arnaud, 2019). The breakdown of DHA results in the formation of derivatives, such as oxalic, threonic acid and 2,3-L-diketogulonate in the apoplast (Dewhirst and Fry, 2018), which leads to generation of H_2O_2 that could play a role in defense signaling (Smirnoff, 2018). AO was shown to play a role in cell growth (De Tullio et al., 2013) and work on transgenic AO overexpression lines demonstrated that AO plays a role in stress tolerance (Yamamoto et al., 2005; Pignocchi et al., 2006; Garchery et al., 2013; Karpinska et al., 2018). Recently, we elucidated the role of AA oxidation in rice defense responses against RKN, and we discovered that foliar AO application can activate systemic plant defense in the rice roots without any negative effects on plant growth (Singh et al., 2020). The aim of this research was to investigate the potential of AO to also enhance defense responses in the evolutionary diverged dicot plants and against cyst nematodes, which have a rather different infection strategy than RKN. While RKN migrate in-between the cells when they enter the root tissue, CN move intracellularly toward the vascular tissue, causing more damage and hence activating plant defense responses. Next to that, feeding site formation by RKN involves giant cell formation, while CN induce a syncytium through cell wall dissolution (Kyndt et al., 2013). As dicot plant, we worked with the agronomically important sugar beet crop, which production is threatened by BCN infestation.

First, we investigated the susceptibility of AO-sprayed sugar beet plants to BCN. We quantified the alterations in AA and hormone concentrations in sugar beet roots at different time points upon foliar application of AO. Further, we evaluated the functional role of plant defense hormones SA, JA and ET in AO-induced defense, by using hormone inhibitors and gene expression analysis. Finally, we investigated changes in H_2O_2 and PAL activity during the migratory and early sedentary stage of nematode infection in AO-treated vs. naïve plants.

MATERIALS AND METHODS

Plant Material and Growth Conditions

Sugar beet cv. Amarok seeds were germinated in moist potting soil for 4–5 days at 25°C. For short-term infection assays (to determine the number of penetrating juveniles) and for biochemical assays, seedlings were transplanted to PVC tubes containing a mixture of fine sand and synthetic absorbent polymer (SAP) substrate, as a growth medium (Reversat et al., 1999). For long-term infection assays (to determine the number of females and cysts) the seedlings were transplanted to polyvinyl-chloride (PVC) tubes containing fine soil particles. All experiments were conducted in a plant growth room at 25°C, with a 16:8 hours (h) light-regime. The plants were fertilized by supplying Hoagland solution (Hoagland, 1937) as a source of nutrients three times a week.

Nematode Inoculation and Infection Assessment

Beet cyst nematode (BCN), *Heterodera schachtii* Schmidt (cysts originally obtained from Razieh Ghaemi, Iran) was cultured on sugar beet (cv. Amarok) plants. Cysts were obtained from stock cultures, by washing the infected soil, letting the cysts to float in water and subsequent hand-picking with a small paint brush. Full cysts with eggs were selected and allowed to dry before setting up for hatching. For second-stage juveniles (J2) to hatch, cysts were placed in 3 mM of $ZnCl_3$ and transferred to an incubator/shaker at a temperature of 25.5°C at 70 rpm for 4 days (Ghaemi et al., in press). J2 were re-suspended in water and counted under a stereomicroscope. Around 300 J2 nematodes were inoculated per plant 3 weeks after transplanting. One day before and after inoculation, plants were not supplied with any nutrients or water.

To count the number of J2/J3, a subset of plants (n = 8) were collected at 4-days post inoculation (dpi). To visualize the J2/3 nematodes inside the roots, the nematode-infected roots were washed and boiled for 3 min in 0.8% acetic acid and 0.013% acid fuchsin solution, followed by destaining in acidified glycerol. To count the number of females, a second subset of plants (n = 8) were collected at 24 dpi; and to count the number of cysts, a third subset of plants (n = 8) were harvested at 6 weeks post inoculation (wpi). Cysts, collected as described above, were categorized either as empty (no eggs) or full cysts (with eggs) using a stereomicroscope (Leica microsystem). J2/J3 were counted under a stereomicroscope, while females and cysts were counted visually. For all infection experiments, plant shoot height (SH), root length (RL), fresh shoot weight (FSW) and fresh root weight (FRW) were measured, and the plants were visually observed to rule out any negative effects of spraying with AO on plant growth. All experiments were independently repeated at least three times, except for the penetration count at 4 dpi, which was only done twice, each time with eight plants per treatment.

Spraying With Chemicals and Hormone Biosynthesis Inhibitors

The following chemicals and hormone biosynthesis inhibitors with respective concentrations were used: Ascorbate oxidase (AO; Sigma-Aldrich, Merck, Darmstadt, Germany) at 5, 10, and 20 U/mL (Singh et al., 2020), aminooxyacetic acid, a potent inhibitor of ET biosynthesis (AOA; Sigma-Aldrich, Merck, Darmstadt, Germany) at 30 mM (Nahar et al., 2011; Kammerhofer et al., 2015), L-2-aminooxy 3-phenylpropanoic

acid, a potential inhibitor of PAL activity (PAL-Inh; Wako-chemicals, Osaka, Japan) at 10 mM (Kammerhofer et al., 2015) and lipoxygenase-inhibitor diethyldithiocarbamic acid (DIECA; Sigma-Aldrich, Darmstadt, Germany) at 100 μM (Nahar et al., 2011). All chemicals were dissolved in water except for PAL-Inh which was dissolved in 1 mL of EtOH before diluting further in water. All chemicals were foliar sprayed and a surfactant, 0.02% (v/v) of Tween20 was added to all spraying solutions to allow efficient uptake (Nahar et al., 2011). Control plants were mock-sprayed with distilled water containing 0.02% (v/v) of Tween20. In each experiment, 3-weeks-old plants were sprayed until run-off with 6.25 mL of solution. This was done at 24 h prior to nematode inoculation in case where infected plants were used. All chemicals have been optimized in previous publications (see above) with chemical concentrations tested for bio-efficacy and lack of phytotoxicity.

Hormone Measurements

Whole root material was sampled from four biological replicates, each consisting of a pool of four individual plants. Root material was collected 12 and 24 h after foliar applications.

Measurement of IAA, ABA, SA, and JA

A cold extraction of 100 mg of homogenized root material was performed using the modified Bieleski solvent, followed by filtration and evaporation (Haeck et al., 2018). Chromatographic separation of the extracted phytohormones was achieved on an ultra-high-performance liquid chromatography (U-HPLC) system (Thermo Fisher Scientific, San Jose, CA, United States), equipped with a Nucleodur C18 column (5092.1 mm, 1.8 lm) and using a mobile phase gradient consisting of acidified methanol and water. High-resolution mass spectrometric analysis (HRMS) was carried out in a full-scan mode using a Q-Exactive^{TM} Orbitrap mass spectrometer (Thermo Fisher Scientific), applying heated electrospray ionization in polarity switching mode and operating at a mass resolving power of 70 000 full width at half-maximum (Haeck et al., 2018).

Measurement of ET

ET content was determined according to López-Gálvez et al. (2015). A gas chromatograph with flame ionization detector was used (GC-FID) (Finnigan Trace GC Ultra, Thermo Fisher Scientific, Waltham, United States) equipped with the columns15 m/0.53 mm/RT-MSieve 5A (Restek, Bellefonte, United States), 30 m/RTU-Piot (Restek), and 25 m/0.53 mm/CP-PoraBOND Q Fused Silica (Varian, PaloAlto, United States). After calibration of the equipment, samples (∼1 mL) of headspace from weighed chopped material were injected into the column using a gas syringe. The GC oven was set at a constant temperature of 35°C, the carrier gas was helium and the FID used pressurized hydrogen and air. The software Thermo Finnigan Chrom Card32-bit was used to interpret the results.

Evaluation of Priming of Defense Responses

To evaluate a possible primed defense response, we set up a multifactorial experiment including four groups: (1) naïve plants uninfected (2) AO-sprayed uninfected, (3) naïve plants infected, and (4) AO-sprayed infected plants. Three-weeks-old plants were sprayed with AO (20 U/mL), naïve plants were mock-sprayed. Plants were either uninfected or infected with nematodes 24 h after spraying with AO or mock-sprayed. Roots and shoots of all plants were collected at 4 and 24 dpi. A total of four biological replicates per treatment were used, and each biological replicate contained a pool of roots or shoots from 4 to 5 plants. The samples were immediately frozen in liquid nitrogen (N_2) and ground to fine powder using a mortar and pestle.

H_2O_2 Measurement

Hydrogen peroxide level was determined according to Velikova et al. (2000). For each sample, about 100 mg of powder was dissolved in 800 μL of 0.1% (w/v) trichloroacetic acid. The homogenate was centrifuged at 14,000 rpm, at 4°C for 15 min. 60 μL of the supernatant was added to 60 μL of 10 mM potassium phosphate buffer (pH 7.0) and 60 μL of 1 M KI. The absorbance of the supernatant was read at λ_{max} = 390 nm. Hydrogen peroxide content was calculated based on a standard curve made by measuring known hydrogen peroxide concentrations in the same assay.

PAL Activity Measurement

PAL activity was measured according to Camacho-Cristóbal et al. (2002). Hundred mg of each sample was dissolved in 800 μL of 50 mM sodium phosphate as assay buffer containing 2% (w/v) poly vinylpolypyrrolidone (PVPP), 2 mM ethylenediaminetetraacetic acid (EDTA), 18 mM-mercaptoethanol and 0.1% (v/v) Triton X-100. The homogenate was centrifuged at 8,000 rpm, at 4°C for 10 min. In different 2 mL tubes, 135 μL of reaction buffer, 50 μL of 5 mM of L-phenlyalanine, and 20 μL of supernatant were mixed. Absorbance measurement was done using a spectrophotometer at 290 nm. The sample was then incubated in the water bath for 30 min at 40°C, after which 10 μL of hydrochloric acid was added and mixed for 10 min. PAL was assayed by measuring the formation of trans-cinnamic acid at 290 nm. One unit (U) of PAL-activity was defined as the amount of the enzyme that produced 1 nmol trans-cinnamic acid per hour. Negative control reactions had no L-phenylalanine as substrate.

Ascorbic Acid Measurement

Plant root and shoot samples were collected from a pool of 4–5 plants per treatment and crushed in liquid nitrogen. In each assay, 100 mg of crushed material was used per sample. For each measurement, at least 5 biological replicates were analyzed per treatment. Reduced and oxidized AA were measured according to Ueda et al. (2013) and Wu et al. (2017) with slight modifications. Samples were extracted using 6% (w/v) metaphosphoric acid containing 1 mM EDTA. Reduced AA concentration was measured in presence of 100 mM potassium phosphate buffer (PPB) (pH 7.0) and 0.1 units AO. Oxidized AA was measured with sample

containing PPB (pH 7.8) and dithiothreitol. Absorbance was monitored in a microplate reader (TECAN- Spectrophotometer) at 265 nm in the UV-transparent 96-well microplates for 8 mins ($\varepsilon = 14.3\ mM^{-1}\ cm^{-1}$).

Quantitative Reverse Transcriptase PCR (qRT-PCR)

For qRT-PCR, 3 weeks old plants were sprayed with AO and water. Root and shoot tissues were collected at 24 h after spraying for RNA-extraction. A total of four biological replicates and two technical replicates were used. RNA was extracted using Qiagen RNeasy Plant Mini Kit (Hilden, Germany). The RNA concentration and purity were evaluated using the NanoDrop 2000 spectrophotometer. A total of 1 μg of each RNA sample was treated with 1 U of DNaseI enzyme (Thermo Fisher Scientific). The cDNA synthesis was performed using 200 U of Tetro Reverse Transcriptase enzyme and Oligo $(dT)_{18}$ primer (Tetro cDNA Synthesis kit, Bioline, Germany) according to the manufacturer's protocol. Quantitative PCR was performed using SensiMix^{TM} SYBR NO-ROX (Bioline, Germany) on a CFX connect real-time PCR machine (Biorad, United States) as following: 10 min of initial denaturation at 95°C and 40 amplification cycles (25 s at 95°C, 25 s at 58°C, and 20 s at 72°C). After the last step, specificity was tested using a melting curve by gradually increasing the temperature to 95°C. Data were analyzed using Rest 2009 (Pfaffl et al., 2002). The investigated genes included sugar beet orthologs of Arabidopsis markers for the salicylic acid (SA) pathway (*PATHOGENESIS-RELATED1; PR1*), and genes associated with the ET (*RELATED TO AP2–3; RAP2–3*), JA (*LIPOXYGENASE2; LOX2*) pathways, as developed by Schmidt et al. (2020). Expression levels were normalized using two reference genes, *glyceraldehyde-3-phosphate dehydrogenase (GAPDH)* and *Isocitrate dehydrogenase (ICDH)*. All primers used in this study are listed in Schmidt et al. (2020).

Nematicidal Assay

To evaluate if AO has any direct effect on the nematodes, a nematicidal assay was performed. One hundred J2's was placed in eight counting wells (n = 8) with 20 U/mL AO or with water (control). The plates were kept in the dark at room temperature. The number of dead (inactive) and alive (active and moving) nematodes (J2) were counted at a 1-day interval for 4 days. Results were presented as total number of living nematodes out of the total number of nematodes (%).

Data Collection and Statistical Analysis

All statistical analyses were performed using the software SPSS (version 21). The normality of data was checked by the Kolmogorov-Smirnov test of composite normality (α = 0.05). Homogeneity of variance was checked by the Levene test (α = 0.05). Analysis of variance (one-way ANOVA) and multiple comparisons of differences between treatments were then performed by Duncan's multiple range test (α = 0.05). Comparisons between two means were conducted using a two-tailed Student's t-test.

RESULTS

Foliar Application of AO on Sugar Beet Reduces *Heterodera schachtii* Infection in the Roots

Foliar application of AO (20 U/mL) has previously been found to reduce the susceptibility of rice plants to *M. graminicola* infection (Singh et al., 2020), and the transcriptional response provided evidence for a primed ET/JA-dependent defense response. Here, we investigated the potential of AO application on dicot sugar beet to protect this crop plant from BCN infection. In the first preliminary experiment, the dose response effects of AO on sugar beet against *H. schachtii* infection were evaluated. In comparison with control, plants sprayed with 10 U/mL, and 20 U/mL of AO had significantly reduced number of cysts (38% and 60% reduction respectively) (**Supplementary Figure S1A**). No significant changes in plant growth were observed in the treated plants when compared with control (**Supplementary Figures S1B–E**). At a concentration of 20 U/mL, a significant increase in FRW was observed in AO-treated plants when compared with control plants (**Supplementary Figure S1E**). Thus, in further experiments we choose to work with a concentration of 20 U/mL, because of the strongest negative effect on BCN infection and positive effect on root growth.

In the second experiment, plant susceptibility was evaluated by counting the number of J2 and J3 at 4 dpi, the total number of females at 24 dpi, and the total number of cysts (empty or full) at 6 wpi. Foliar application of 20 U/mL AO did not significantly affect the total number of penetrated juveniles (J2 + J3) when compared with mock-sprayed plants (Ctrl) (**Figure 1A**). However, a significantly higher number of J2 in AO-sprayed plants were observed when compared with mock-sprayed plants, and a concomitant decrease of J3 in AO vs. mock- sprayed plants (**Figure 1A**). This suggests that although an equal number of nematodes could penetrate the roots, their development is delayed in AO-sprayed plants compared with control plants already at this early time point.

At later time points, AO-sprayed sugar beet plants contain a significantly reduced number of females (60% reduction at 24 dpi) (**Figure 1B**) and a significantly reduced number of cysts (70% reduction) at 6 wpi (**Figure 1C**). The total number of cysts is not a conclusive indicator for successful control of BCN. Estimating the viable cysts, filled with eggs, is crucial for evaluating effective control measures (Christoforou et al., 2014). Therefore, we counted the number of full cysts, in AO-sprayed vs. mock-sprayed plants. Our result shows a significantly reduced number of full cysts (86% reduction) in AO-sprayed plants when compared with control plants (**Figure 1D**), confirming that AO spraying compromises nematode reproduction on the sugar beet host.

To further investigate whether application of AO has any effects on plant growth, we evaluated RL, SH, FSW and FRW

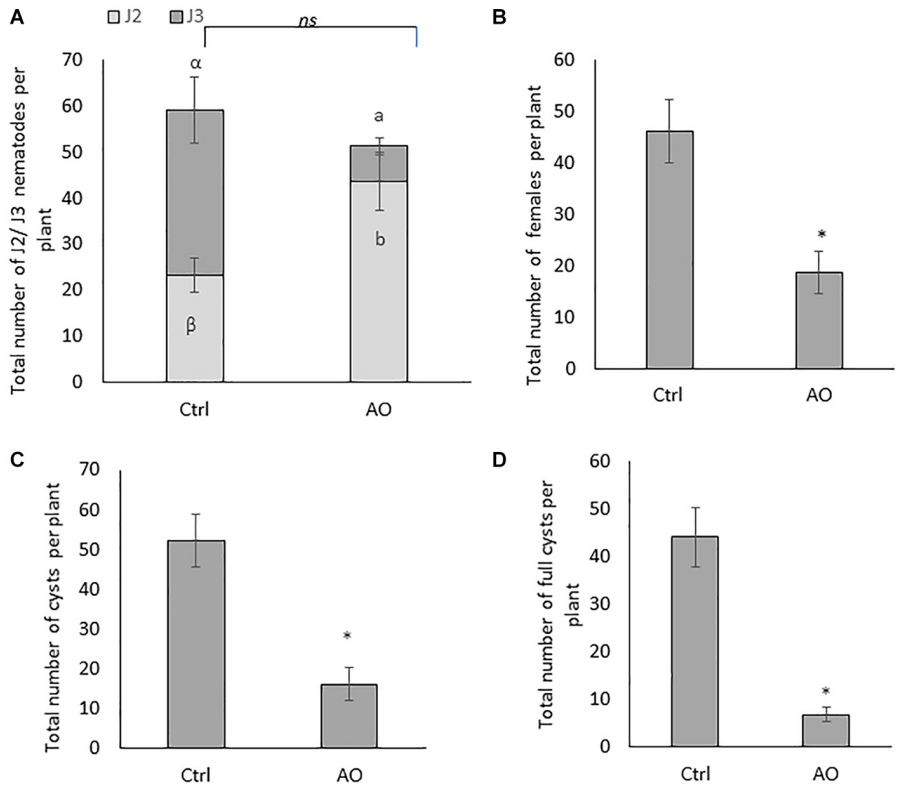

FIGURE 1 | Effect of foliar spraying of AO on *Heterodera schachtii* infection in sugar beet roots. Three-weeks-old plants were sprayed with 20 U/mL AO, while control plants were mock sprayed. One day later, plants were inoculated with 300 second-stage juveniles (J2). Plant responses were analyzed at different time points for different stages of the nematode infection cycle. Total number of **(A)** penetrated juveniles at 4 dpi (J2 and J3), **(B)** females at 21 dpi, **(C)** cysts, and **(D)** full cysts at 6 wpi. Data for **(A)** was analyzed by one-way ANOVA and Duncan's multiple range test ($\alpha = 0.05$). Data for **(B–D)** were analyzed using a two-tailed Student's *t*-test. Different letters and asterisks indicate statistically different means. Bars represent means ± SD of a total of 8 individual plants ($n = 8$).

in plants at 4 dpi, 24 dpi, and 6 wpi. No differences in the phenotype between the mock-sprayed and AO-sprayed plants were observed at 4 dpi (**Supplementary Figure S2**). Also, no negative effects of AO were observed at 24 dpi (**Supplementary Figure S3**) and 6 wpi (**Supplementary Figure S4**). Interestingly, a significant increase in SH (**Supplementary Figures S3A,E**) and root weight (**Supplementary Figures S3D,E**) was observed in AO-sprayed plants at 24 dpi and a significant increase in FRW (**Supplementary Figures S4D,E**) was observed in AO-sprayed plants at 6 wpi. To determine if AO has any direct effect on nematode mortality, we set up a nematicidal assay whereby J2 were incubated in AO or water, and their viability was counted at a 1-day interval for 4 days. We did not observe any significant differences in J2 viability between the AO incubated and water incubated groups, consistently up to 4 days of exposure (**Supplementary Figure S5**). Taken together, these data indicate that AO activates systemic induced resistance against BCN in sugar beet.

AO Shoot Spraying Causes Accumulation of DHA in Roots

To investigate if AO application causes changes in the levels of reduced and oxidized AA (DHA), we measured their levels at 24 h after AO foliar application. Basal level of total ascorbic acid (mostly reduced form of AA) was higher in shoots than in roots (**Supplementary Figure S6**). Significantly higher levels of DHA were observed in roots of AO-sprayed plants (**Supplementary Figure S6**) suggesting that AO has a systemic signaling effect, causing accumulation of DHA in roots. The observation that AA levels are depleted upon AO application in the shoots suggests systemic transport from shoot to root.

AO-Induced Defense in Sugar Beet Is Partially Mediated by Defense Hormone Pathways

To evaluate if foliar AO application on sugar beet plants induces systemic changes in phytohormone levels, roots of AO-sprayed, and mock-sprayed plants were collected 12 and 24 h after spraying. Our results show that the concentrations of IAA and JA were significantly elevated at 12 h after spraying, while the concentrations of ABA, SA and ET were not changed in the roots of AO-sprayed plants at this time point (**Figure 2A**). At 24 h after spraying, the concentration of SA and ET were significantly elevated (∼2 and ∼4 times higher), while the concentrations of ABA, IAA and JA were not changed in the roots

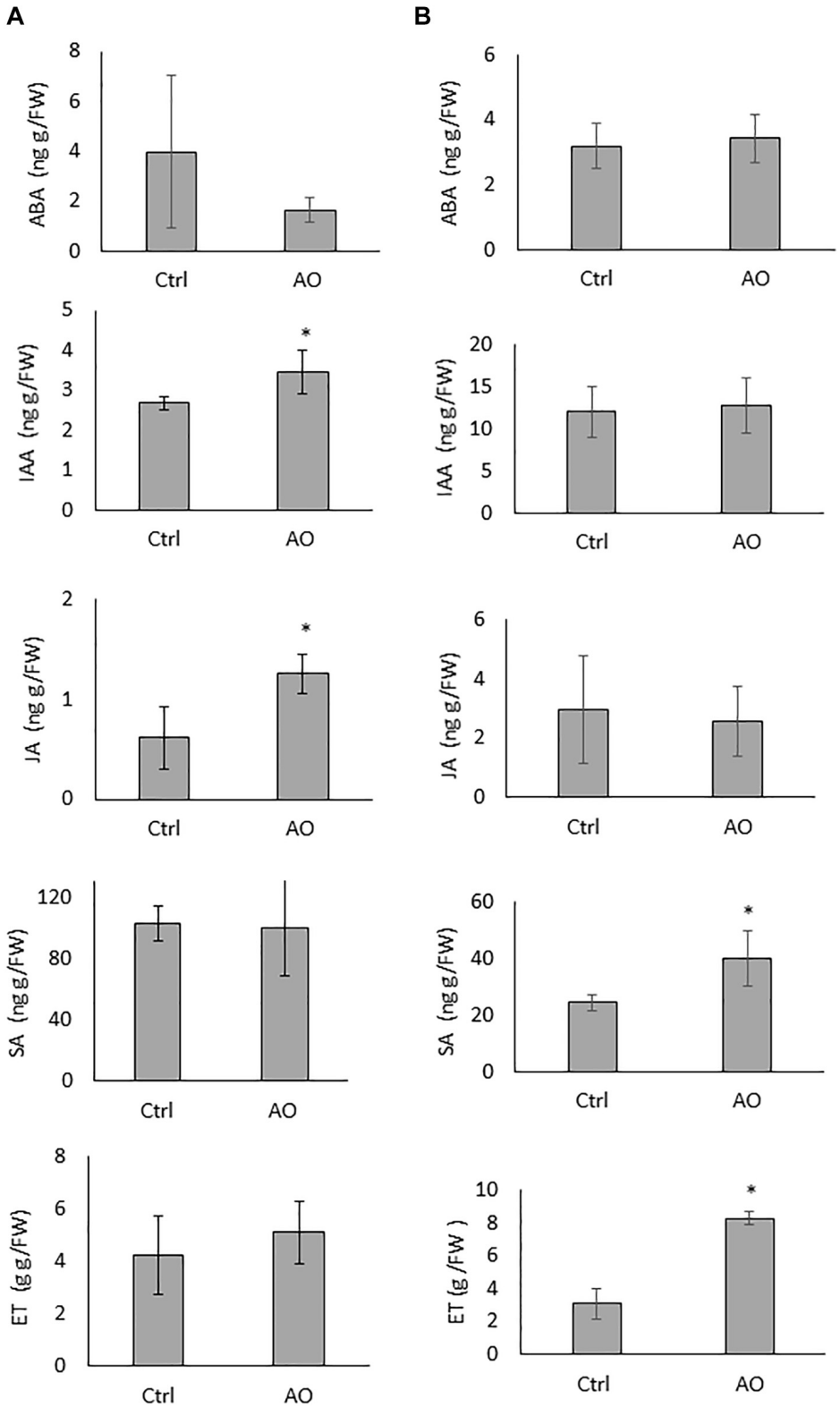

FIGURE 2 | Effect of foliar AO spraying on phytohormone accumulation in sugar beet roots. Hormone ABA, IAA, JA, SA, and ET content in the roots of plants sprayed with (AO, 20 U/mL) or mock sprayed (Ctrl) at **(A)** 12 h and **(B)** 24 h after treatment. Data was analyzed using a two-tailed Student's *t*-test ($\alpha = 0.05$). Asterisks indicate statistically different means. Values presented are the average ± SD of five biological replicates each consisting of at least four individual plants. ABA, abscisic acid; IAA, indole-3-acetic acid; JA, jasmonic acid; SA, salicylic acid, ET, ethylene.

of AO-sprayed plants in comparison with mock-sprayed control plants (**Figure 2B**).

To investigate if AO-induced systemic defense is dependent on increases in the three typical plant defense hormones, SA, JA and ET, we set up infection experiments with inhibitors of these pathways. Plants were foliar sprayed with hormone biosynthesis inhibitors separately and in combination with AO. In a first experiment, we inhibited SA and ET, because they were accumulating in roots upon AO spraying at 24 h (**Figure 2B**). AOA, an ET biosynthesis inhibitor and PAL-Inh, an inhibitor for phenylalanine ammonia lyase were used. To investigate infection severity, the number of cysts was counted at 6 wpi. Our results show a reduced number (64% reduction) of cysts in AO-sprayed plants (**Figure 3A**) which confirms our earlier data see (**Figure 1C** and **Supplementary Figure S1A**). A significant increase in the number of cysts was observed in plants sprayed with AOA when compared with the control plants, showing that ethylene plays a role in the basal defense of sugar beet against BCN. When plants were sprayed with PAL-Inh, there were no significant changes in the number of cysts compared with control plants. However, when AO was combined with AOA or with PAL-Inh, a lower but still significant decrease in number of cysts was observed when compared with plants sprayed with AOA or PAL-Inh alone (**Figure 3A**), showing that AO is still partially active. Based on the observation of JA accumulation at 12 h after AO spraying, we decided to execute a second experiment, to evaluate the role of JA biosynthesis in AO-induced defense against BCN. Upon foliar application of JA biosynthesis inhibitor DIECA a significant increase in number of cysts was observed, showing that LOX-mediated JA production plays a role in sugar beet defense against BCN (**Figure 3B**). Plants sprayed with DIECA + AO showed no significant difference in cyst numbers when compared with control plants. This suggests that AO-induced defense is dependent on LOX-mediated JA production.

To investigate this further, gene expression levels of sugar beet orthologs of three well-known Arabidopsis SA, JA and ET marker genes (developed by Schmidt et al., 2020) were monitored by qRT-PCR on AO-treated and control plants. The results revealed significantly higher expression levels of *LOX2* (JA biosynthesis) and *RAP2-3* (ET responsive transcription factor) in the shoot tissues of AO-treated plants at 24 h after spraying (**Figure 3C**). In the root tissue, a slight induction of the *LOX2* gene was observed in the roots of AO sprayed plants (**Figure 3D**). This observation of a predominant *LOX2* gene induction in shoots correlates well with the recent study of Wang et al. (2019) who demonstrated that the JA needed for tomato defense against root-knot nematodes is produced in aboveground tissues. This suggests that the JA necessary for AO-induced resistance against BCN is also produced in sugar beet shoots.

AO Application Primes Sugar Beet for Enhanced H_2O_2 and PAL Activity Upon BCN Infection

ROS such as H_2O_2 are known to play various roles in basal plant defense responses (Mittler et al., 2004). In this study, we investigated if AO-induced defense is correlated with primed accumulation of H_2O_2 upon BCN infection in sugar beet. H_2O_2 was measured at 4 and 24 dpi both in root and shoot tissues. When comparing the naïve, infected plants with naïve, uninfected plants a significant higher H_2O_2 content was observed in roots and shoots of infected plants at 4 dpi, but not at 24 dpi, showing that BCN infection causes an oxidative burst at early time points (**Figures 4A,B**). In AO-sprayed uninfected plants, no significant differences in H_2O_2 levels were seen, when compared with naïve uninfected plants. However, AO-sprayed infected plants contained significantly higher amounts of H_2O_2 in the roots at both 4 dpi (**Figure 4A**) and 24 dpi (**Figure 4C**), when compared to roots of naïve infected plants. This phenomenon was not observed in the shoots (**Figure 4D**). These results imply that AO-defense activation is correlated with a primed accumulation of H_2O_2 at the site of infection at both early (4 dpi) and at later time point (24 dpi).

To investigate if AO-induced defense is correlated with primed activation of PAL, PAL-activity was measured at 4 and 24 dpi for root and shoot tissues of AO-sprayed uninfected and infected plants and compared with naïve uninfected and infected plants. Our results show no significant changes in PAL-activity at the earliest time point (4 dpi) (**Figures 5A,B**). However, at the later time point (24 dpi), in comparison with naïve plants, we observed a significant increase in PAL-activity in AO-sprayed infected plants, in both roots (∼3× more) (**Figure 5C**) and shoots (∼4× more) (**Figure 5D**). This result suggests that PAL activity is primed for activation at later time points upon BCN infection in AO-sprayed sugar beet plants.

DISCUSSION

Defense priming is known to be induced by different chemical compounds. Primed plants display faster and/or stronger activation of the various defense responses that plants deploy to fight attack by pathogens or pests (Martinez-Medina et al., 2016). For example, the best-known defense priming compound BABA has been shown to induce resistance against PPN in rice, tomato, cucumber, mungbean, and cereals (Oka et al., 1999; Oka and Cohen, 2001; Ahmed et al., 2009; Sahebani et al., 2011; Ji et al., 2015). However, BABA treatment in many plant species results in a stress phenotype that manifests negative effects on growth and development (van Hulten et al., 2006; Koen et al., 2014; Luna et al., 2016) restricting its commercial use. In this research we evaluated the use of another compound that induces plant resistance and defense priming in rice against RKN (Singh et al., 2020)—ascorbate oxidase (AO)—to protect sugar beet plants against BCN *H. schachtii*. Noteworthy, AO does not have negative effects on rice growth. The data reported in this manuscript shows that foliar application of AO results in delayed development of BCN, fewer females and fewer full cysts on the sugar beet host and the treatment even had some positive effects on sugar beet growth. While root-knot nematodes move intercellularly through the roots during their migratory phase, cyst nematodes move intracellularly, creating slightly more damage. On the other hand, while syncytia and giant cells—the feeding sites formed by root-knot nematodes—show functional

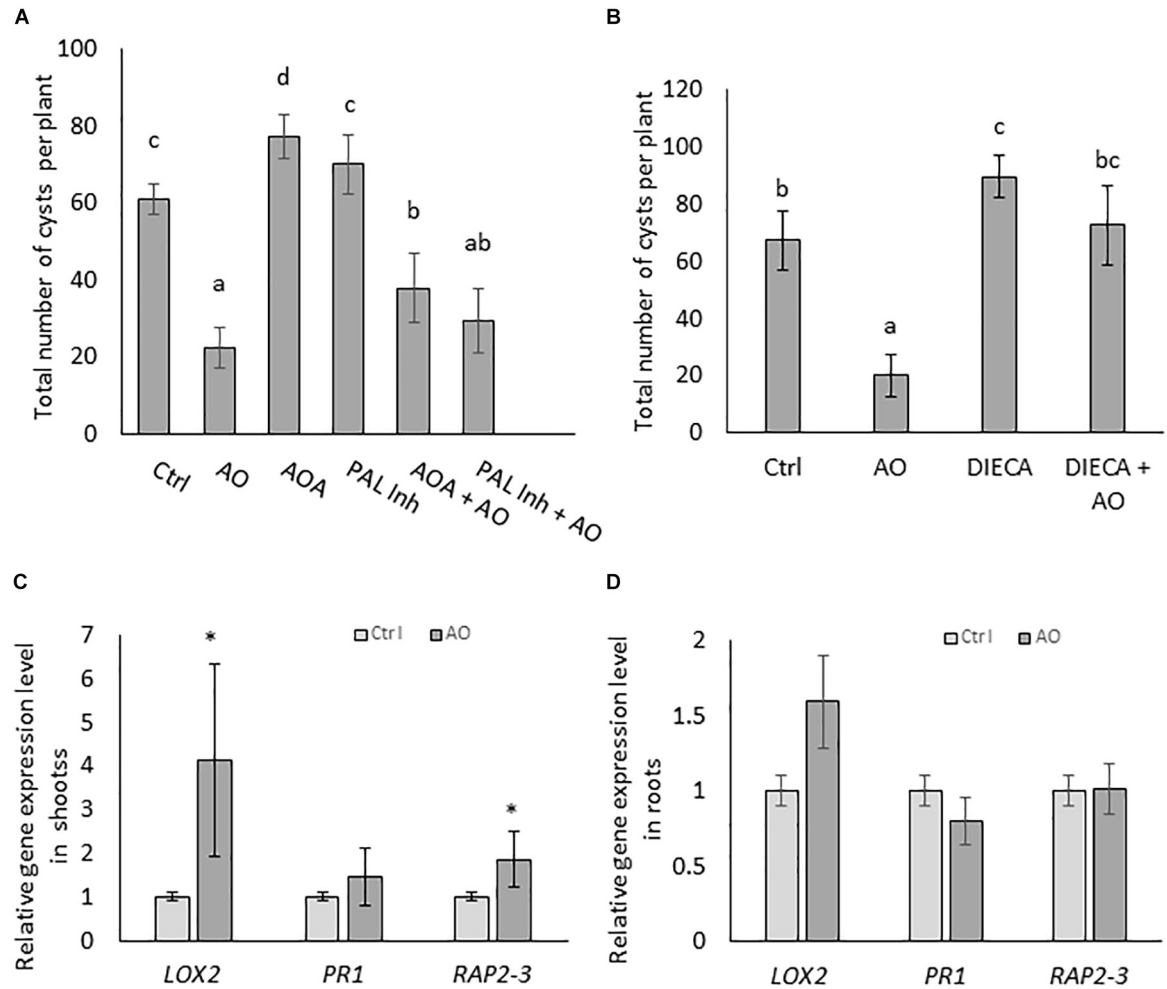

FIGURE 3 | AO-induced defense against cyst nematodes is partially dependent on SA ET, and JA biosynthesis in sugar beet. Three-weeks-old sugar beet plants were sprayed with AO and chemical inhibitors. Plants were sprayed with **(A)** AO, AOA, AOPP (PAL-Inh) either alone or in combination and **(B)** AO, DIECA, and DIECA combined with AO. Water with Tween20 was sprayed as negative control (Ctrl). Plant roots were inoculated with 300 nematodes, 24 h after spraying with respective chemicals. The total number of cysts were counted at 6 wpi. Bars represent means ± SD of the number of cysts of eight plants. For **(A,B)** different letters indicate statistically significant differences (Duncan's multiple range test with $\alpha = 0.05$). Gene expression analysis with qRT-PCR on **(C)** shoots and **(D)** roots of AO treated sugar beet plants. The relative expression levels of JA-biosynthesis gene *LOX2*, SA-response gene *PR1*, and ET-responsive transcription factor *RAP2-3* were analyzed at 24 h after foliar treatment. Values presented are means ± SE of four biological replicates (each a pool of five individual plants) per treatment. Gene expression levels were normalized using two internal reference genes, *GAPDH* and *ICDH*. Data are shown as relative transcript levels in comparison with the control plants (expression level set at 1). In c and d asterisks indicate significant differential expression between AO-treated and control plants (REST-analysis; $\alpha = 0.05$). AO, Ascorbate oxidase; AOA, aminooxyacetic acid; PAL-Inh, AOPP, L-2-aminooxy 3-phenylpropanoic acid.

similarities their ontology is slightly different (Kyndt et al., 2013). Taken together, our results reveal that AO-treatment can protect both dicot sugar beet and monocot rice (Singh et al., 2020) against infection by two groups of nematodes with varying infection strategies without growth penalty effects. Whether this can be extrapolated to other crops and agronomic applications in nematode-infested fields will be an interesting route for further applied research.

It has been shown before that exogenous ascorbic acid (AA) application reduces root infection by the RKN *Meloidogyne incognita* in tomato, and that increased AA levels are present in the roots of *M. incognita* resistant lines (Arrigoni et al., 1979). The authors proposed that AA is utilized for mitochondrial hydroxyproline proteins synthesis to permit development of the cyanide resistant respiration, which is the metabolic process initiated by the cell to potentially counteract the effects of the nematode. Similarly, Fujiwara et al. (2016) showed high accumulation of AA in *Brassica rapa*, a cultivar known to be resistant against *Turnip mosaic virus* (*TMV)*. More recently, we have observed in our own research (Ghaemi et al., in press) that transcripts involved in AA biosynthesis are upregulated in BCN infected roots of resistant plants, but not in susceptible plants, indicating a potential role for AA in sugar beet resistance to *H. schachtii.* In the experiments described in the current

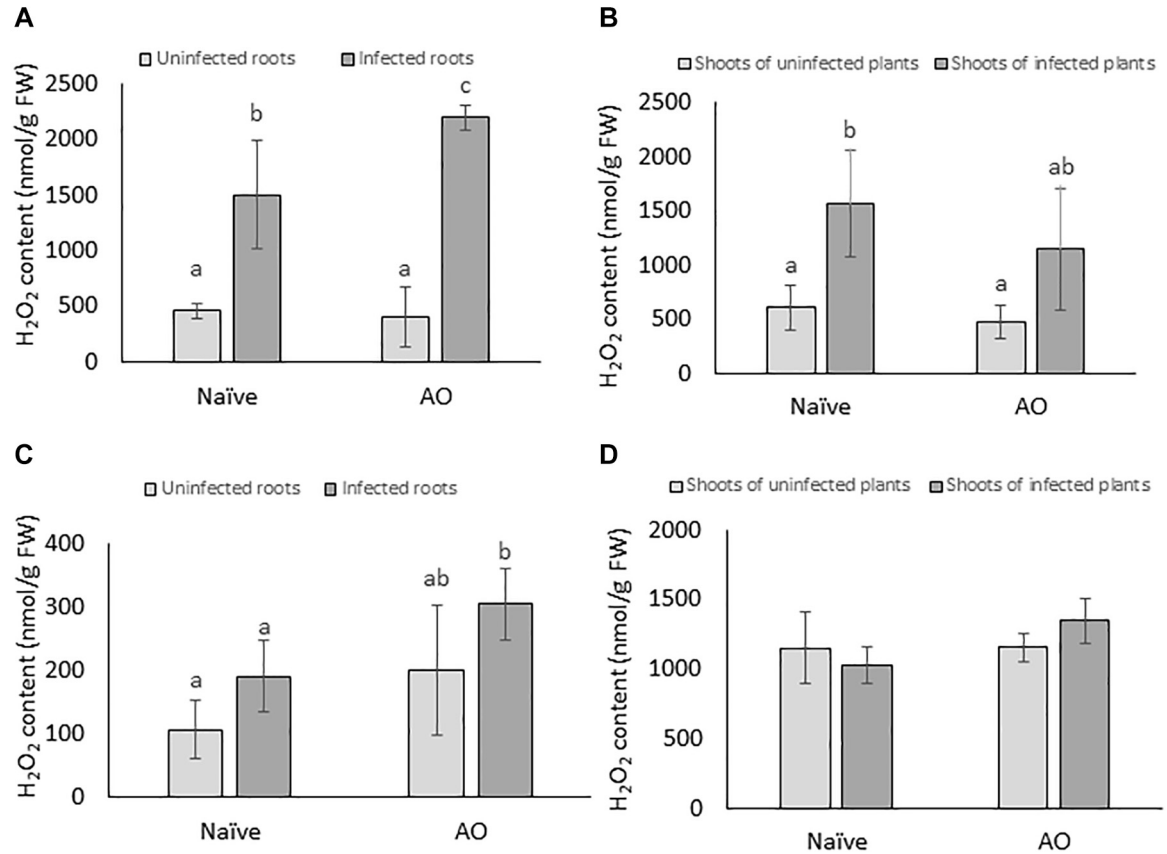

FIGURE 4 | AO induced defense is correlated with primed accumulation of H_2O_2 in sugar beet roots. The H_2O_2 content per gram of fresh tissue at 4 dpi in **(A)** roots and **(B)** shoots; and at 21 dpi in **(C)** roots and **(D)** shoots. Three-weeks-old plants were sprayed with AO or mock sprayed and 24 h later, plant roots were inoculated with nematodes or mock inoculated. Samples were collected at 4 and 21 dpi. Bars represent the average and SD of four biological replicates, each containing a pool of 4–5 plants. Different letters represent statistically significant differences, while graphs without letters **(D)** had no significant differences between the treatments (Duncan's multiple range test with $\alpha = 0.05$).

manuscript, we showed that foliar application of AO is leading to a primed activation of ROS and PAL enzyme activity in roots infected by BCN. AO regulates the redox status of the apoplastic AA pool (Sanmartin et al., 2002; Pignocchi et al., 2003). It has been postulated that oxidation of apoplastic AA via AO could have the same effect on the apoplastic redox state as an oxidative burst (Foyer and Noctor, 2005). In this work we show that AO-induced defense in sugar beet against BCN, is correlated with a temporal pattern of accumulation of JA, ET and SA in the roots, while the concentrations of ABA were unchanged. IAA was slightly accumulating at 12 h after spraying. This could explain why positive effects on shoot and root growth were observed in AO-treated plants.

Our results with hormone inhibitors showed that AO-induced defense is partially dependent on JA, ET, and PAL activity. Kammerhofer et al. (2015) showed that JA triggers early defense responses in Arabidopsis against *H. schachtii* with significant upregulation of JA/ET marker genes at 24 h after inoculation. Here, we confirmed that JA is also important for defense against *H. schachtii* in sugar beet. Transcriptome analysis and hormone measurement of AO-sprayed rice plants revealed that JA biosynthesis pathway and ET-responsive genes were activated in the rice roots (Singh et al., 2020). Here, we extended and confirmed those observations by revealing JA accumulation at 12 h after AO spraying in sugar beet roots. Interestingly, DIECA application precluded AO-induced defense, confirming an important role for LOX-dependent JA production. Indeed, the gene expression analysis confirmed the aboveground induction of *LOX2* (JA biosynthesis gene) and *RAP2.3* (ET response gene) in AO-treated plants, although these genes were not very strongly induced in root tissues. A significant increase in number of cysts in DIECA treated plants confirms that LOX-mediated JA production plays an important role in sugar beet defense against BCN. However, it is possible that DIECA is not only inhibiting JA production and that *LOX2* is involved in production of other compounds than only JA. For example, Farmer et al. (1994) showed that DIECA inhibits the whole octadecanoid signaling pathway in tomato. JA metabolite cis-(+)-12-oxo-phytodienoic acid (cis-OPDA) was noted as the key signaling molecule in the regulation of Arabidopsis defense against the root-knot nematode *M. hapla* (Gleason et al., 2016). Whether other LOX-derived metabolites are involved in AO-induced defense in

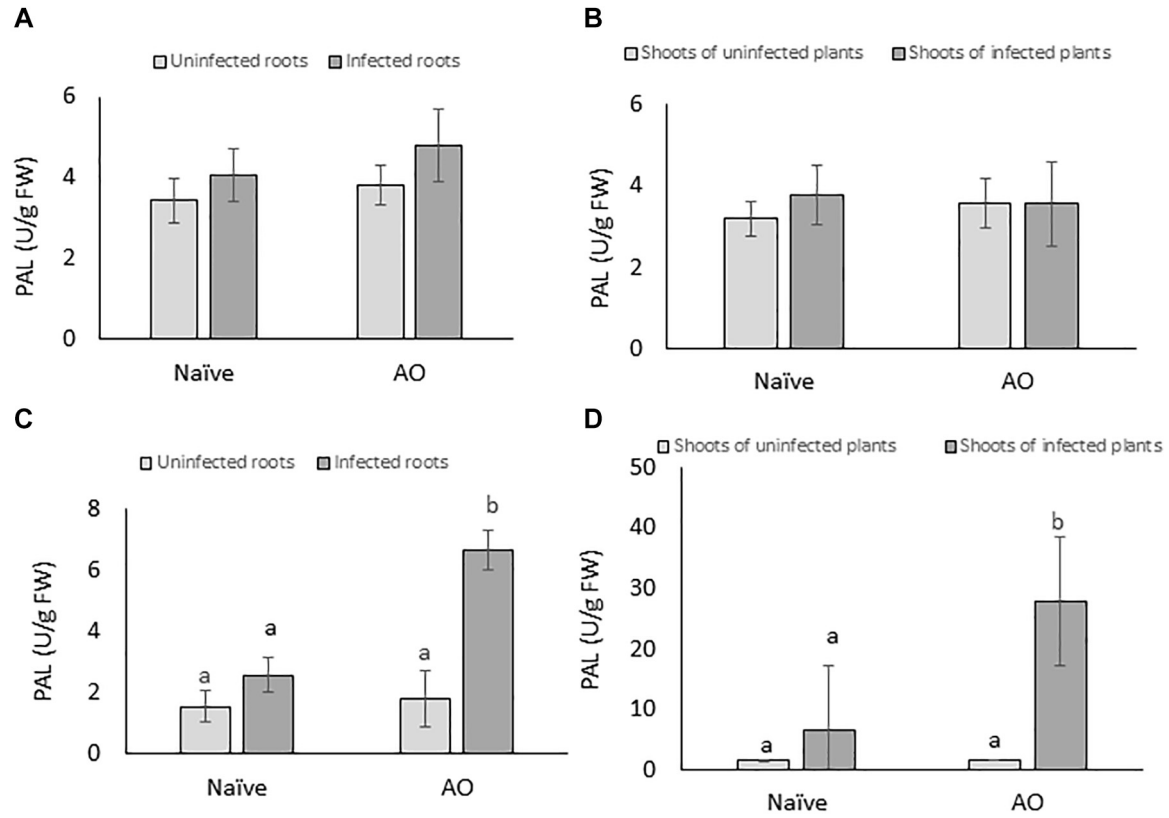

FIGURE 5 | AO induced defense is correlated with phenylpropanoid pathway activation in sugar beet. The PAL enzyme activity per gram of fresh tissue at 4 dpi in **(A)** roots and **(B)** shoots; and at 21 dpi in **(C)** roots and **(D)** shoots. Three-weeks-old plants were sprayed with AO or mock sprayed, and roots were inoculated with nematodes or mock inoculated 24 h after spraying. Samples were collected at 4 and 21 dpi. Bars represent the average and SD of four biological replicates, each containing a pool of 4–5 plants. Different letters represent statistically significant differences, while graphs without letters **(A,B)** had no significant differences between the treatments (Duncan's multiple range test with $\alpha = 0.05$).

sugar beet remains to be elucidated. A full transcriptome and metabolome analysis with multiple time points and tissues, including uninfected and BCN infected sugar beet plants is advised in order to further unravel how AO-induced systemic resistance works. However, the lack of a well-annotated sugar beet genome and detailed functional genetic details of genes and pathways in this understudied crop plant is currently hampering such analyses.

In our experiments we observed that root ET levels are increased at 24 h after AO spraying, the exact moment when we normally execute inoculation. AA is a well-known cofactor for 1-aminocyclopropane-1-carboxylate (ACC) oxidase, the rate-limiting enzyme for ET biosynthesis. Ghaemi et al. (in press) showed that sugar beet plants sprayed with MeJA or with the ET-generator Ethephon (ETH) were significantly less susceptible to BCN when compared to control plants. While our results with the ET-inhibitor confirm a positive role of ET in defense against BCN in sugar beet, ET has been suggested to be critical for syncytium formation during cyst-nematode infection in Arabidopsis (Goverse et al., 2000) and ET levels or signaling were observed to play an important positive role in attraction of *Heterodera glycines* to soybean roots (Hu et al., 2017) and in *H. glycines* development (Tucker et al., 2009). Moreover, the role of ET in parasitism was evidenced by the significant reduction of cyst nematodes inside the roots of ET-insensitive Arabidopsis mutants or wild type plants treated with ET inhibitors (Goverse et al., 2000), an observation which is not confirmed by the results provided in the current manuscript. However, Kammerhofer et al. (2015) demonstrated that BCN are able to interfere with hormone-based defense and signal transduction. ET seems to play different roles at different stages of nematode infection (also reviewed in Kyndt et al., 2013). Indeed, Kammerhofer et al. (2015) showed that ET is only having a role in plant defense at early stages of parasitism, but not in BCN development. In future the levels of ET at other time points after AO treatment, and upon subsequent infection could also be investigated to provide a better time-dependent view on the role of ET in AO-treated plants and in the context of BCN infection.

We also observed an increased concentration of salicylic acid (SA) in AO-sprayed plants at 24 h. Kammerhofer et al. (2015) showed that BCN establishment requires local suppression of the SA pathway. Whereas SA does not play a major role during early *H. schachtii* attraction and infection, it rather acts as a negative regulator during later phases of parasitism. Wubben et al. (2001)

also confirmed a role for SA, mediated by NPR1 and negatively regulated by SNI1, in limiting cyst nematode parasitism during a compatible interaction. By applying the Pal-Inh, which specifically blocks the phenylpropanoid pathway responsible for one branch of SA biosynthesis, we were expecting an increase in plant susceptibility for BCN. However, we did not observe significant changes in the number of cysts when compared with control. Two different biosynthetic pathways of SA exist, with one engaging isochorismate synthases (ICSs) and the other PAL, and hence the other pathway could still produce sufficient SA levels. Importantly, the PAL inhibitor AOPP is also known to inhibit auxin biosynthesis (Soeno et al., 2010) and this could have also influenced nematode infection levels. Auxin is required for cyst nematode feeding site development (Grunewald et al., 2009), and thus inhibiting auxin could perhaps lower the number of cysts, complicating the interpretation of this result.

However, when AO is combined with the PAL-Inh, AO is only partially able to protect the plants compared to control plants, indicating that AO-induced defense is partially dependent on PAL. Indeed, we observed a primed increase in PAL-activity in shoots and roots of AO- sprayed plants upon nematode infection, although only at a later time point. Similarly, our previous research (Singh et al., 2019) showed the importance of the phenylpropanoid pathway in activation of systemic defense against RKN in COS-OGA sprayed rice plants. Which specific phenylpropanoid-derived molecule is important for this systemic signaling remains to be elucidated.

One of the earliest defense responses in plants is ROS production in the apoplast (Coll et al., 2011). Our results show a primed accumulation of H_2O_2 in roots of AO-sprayed plants at both 4 and 24 dpi with BCN. Similarly, Melillo et al. (2006) and Huang et al. (2016) showed an increased H_2O_2 during *M. graminicola* infection in rice and *M. incognita* infection in tomato respectively. In contrast, Siddique et al. (2014) proposed that H_2O_2 is needed for successful syncytium formation in Arabidopsis. Increases in H_2O_2 were observed in Arabidopsis shoots upon BCN infection at 3 dpi (Siddique et al., 2014). Labudda et al. (2018) showed that the development of *H. schachtii*-induced syncytia in roots alters ROS homeostasis in the shoots of infected plants. Similarly, an increased H_2O_2 level was observed in the shoots of nematode-infected sugar beet plants at 4 dpi. The fact that this was not observed in the shoots of these plants at 4 dpi, suggests that in AO-primed plants ROS production is mostly confined to the site of infection (i.e., roots). This local oxidative burst in plant roots is correlated with strongly reduced nematode development in AO-treated plants. ROS act as secondary messengers in the systemic long distance signaling network (Shetty et al., 2008) and in root-shoot communication upon nematode infection (Wang et al., 2019). Communication between aboveground and belowground plant tissues in plant defense against parasitic RKN in tomato was shown to be dependent on an integration between oxidative burst (ROS production), electrical signals and JA synthesis (Wang et al., 2019). The observations reported here indicate that aboveground AO application on shoots is activating DHA accumulation in roots and reveal that this pathway can also protect plants from cyst nematode infection. Application of DIECA, an inhibitor of LOX-dependent JA production, could have inhibited this systemic signaling pathway and hence precluded AO priming activity against BCN. The observation that LOX2 is mainly activated in aboveground tissues, correlates well with the study of Wang et al. (2019) who demonstrated that the JA needed for tomato defense against root-knot nematodes is produced in aboveground tissues. This observation suggests that the JA required for sugar beet defense against BCN is predominantly produced in shoots.

Collectively it can be concluded that AO-induced systemic resistance against BCN is dependent on a time-dependent dynamic pattern of activation of plant defense hormone pathways, with a major role for LOX-dependent JA production. This study shows that AO-induced resistance in sugar beet leads to a primed activation of PAL and H_2O_2 levels upon BCN infection. This treatment protects the plant from cyst nematode infection and could potentially provide an extra tool for farmers to control this parasitic nematode in the field.

DATA AVAILABILITY STATEMENT

All datasets generated for this study are included in the article/**Supplementary Material**.

AUTHOR CONTRIBUTIONS

TK and RS planned and designed the research and wrote the manuscript. RS and NN conducted infection experiments and biochemical analyses. KD and RS did hormone measurements. All authors contributed to the article and approved the submitted version.

FUNDING

This work was financially supported by the Special Research Fund (Bijzonder Onderzoeksfonds) of the Ghent University through BOF13/GOA/030 and BOFSTA/2016/00070. The authors also acknowledge the financial support (AUGE/11/016) from the Hercules Foundation of the Flemish Government for the UHPLC-Q-Exactive™ mass spectrometry equipment available at the EnVOC research group and used for hormone analysis.

ACKNOWLEDGMENTS

We would like to thank Razieh Ghaemi, Department of Plant Pathology, Faculty of Agriculture, Tarbiat Modares University, Tehran, Iran, for providing us with cyst nematodes.

SUPPLEMENTARY MATERIAL

The Supplementary Material for this article can be found online at: https://www.frontiersin.org/articles/10.3389/fpls.2020.591715/full#supplementary-material

REFERENCES

Agrios, G. N. (2005). Plant diseases caused by nematodes. *Plant Pathol.* 4, 565–597.

Ahmed, N., Abbasi, M., Shaukat, S., and Zaki, M. (2009). Induced systemic resistance in mung bean plant against root-knot nematode *Meloidogyne javanica* by DL-β-amino butyric acid. *Nematol. Medit.* 37, 67–72.

Anjam, M. S., Shah, S. J., Matera, C., Różańska, E., Sobczak, M., Siddique, S., et al. (2020). Host factors influence the sex of nematodes parasitizing roots of *Arabidopsis thaliana*. *Plant Cell Environ.* 43, 1160–1174. doi: 10.1111/pce.13728

Anjum, N. A., Gill, S. S., Gill, R., Hasanuzzaman, M., Duarte, A. C., Pereira, E., et al. (2014). Metal/metalloid stress tolerance in plants: role of ascorbate, its redox couple, and associated enzymes. *Protoplasma* 251, 1265–1283. doi: 10.1007/s00709-014-0636-x

Arrigoni, O., Zacheo, G., Arrigoni-Liso, R., Bleve-Zacheo, T., and Lamberti, F. (1979). Relationship between ascorbic acid and resistance in tomato plants to *Meloidogyne incognita*. *Phytopathology* 69, 579–581. doi: 10.1094/phyto-69-579

Back, M., Haydock, P., and Jenkinson, P. (2002). Disease complexes involving plant parasitic nematodes and soilborne pathogens. *Plant Pathol.* 51, 683–697. doi: 10.1046/j.1365-3059.2002.00785.x

Bengtsson, T., Holefors, A., Witzell, J., Andreasson, E., and Liljeroth, E. (2014). Activation of defence responses to *Phytophthora infestans* in potato by BABA. *Plant Pathol.* 63, 193–202.

Camacho-Cristóbal, J. J., Anzellotti, D., and González-Fontes, A. (2002). Changes in phenolic metabolism of tobacco plants during short-term boron deficiency. *Plant Physiol. Biochem.* 40, 997–1002. doi: 10.1016/s0981-9428(02)01463-8

Christoforou, M, Pantelides, I., Kanetis, L., Ioannou, N., and Tsaltas, D. (2014). Rapid detection and quantification of viable potato cyst nematodes using qPCR in combination with propidium monoazide. *Plant Pathol.* 63, 1185–1192. doi: 10.1111/ppa.12193

Coll, N., Epple, P., and Dangl, J. (2011). Programmed cell death in the plant immune system. *Cell Death Differ.* 18, 1247–1256. doi: 10.1038/cdd.2011.37

Conrath, U., Beckers, G. J., Flors, V., García-Agustín, P., Jakab, G., Mauch, F., et al. (2006). Priming: getting ready for battle. *Mol. Plant Microbe Interact.* 19, 1062–1071. doi: 10.1094/mpmi-19-1062

Conrath, U., Beckers, G. J., Langenbach, C. J., and Jaskiewicz, M. R. (2015). Priming for enhanced defense. *Annu. Rev. Phytopathol.* 53, 97–119. doi: 10.1146/annurev-phyto-080614-120132

Cooke, D. (1987). Beet cyst nematode (*Heterodera schachtii* Schmidt) and its control on sugar beet. *Agric. Zool. Rev.* 2, 135–183.

Cooke, D. (1993). "Nematode parasites of sugarbeet," in *Plant Parasitic Nematodes in Temperate Agriculture*, eds K. Evans, D. L. Trudgill and J. M. Webster (Wallingford: CAB International), 133–169.

De Tullio, M., Guether, M., and Balestrini, R. (2013). Ascorbate oxidase is the potential conductor of a symphony of signaling pathways. *Plant Signal. Behav.* 8:e23213. doi: 10.4161/psb.23213

De Vleesschauwer, D., Gheysen, G., and Höfte, M. (2013). Hormone defense networking in rice: tales from a different world. *Trends Plant Sci.* 18, 555–565. doi: 10.1016/j.tplants.2013.07.002

Dewhirst, R. A., and Fry, S. C. (2018). The oxidation of dehydroascorbic acid and 2, 3-diketogulonate by distinct reactive oxygen species. *Biochem. J.* 475, 3451–3470. doi: 10.1042/bcj20180688

Eberlein, C., Heuer, H., and Westphal, A. (2020). Biological suppression of populations of *Heterodera schachtii* adapted to different host genotypes of sugar beet. *Front. Plant Sci.* 11:812. doi: 10.3389/fpls.2020.00812

Fan, Z., Qin, Y., Liu, S., Xing, R., Yu, H., and Li, P. (2020). Chitosan oligosaccharide fluorinated derivative control root-knot nematode (*Meloidogyne incognita*) disease based on the multi-efficacy strategy. *Mar. Drugs* 18:273. doi: 10.3390/md18050273

FAOSTAT (2019). *Food and Agriculture Data, 2019*. Rome: FAO.

Farmer, E. E., Caldelari, D., Pearce, G., Walker-Simmons, M., and Ryan, C. A. (1994). Diethyldithiocarbamic acid inhibits the octadecanoid signaling pathway for the wound induction of proteinase inhibitors in tomato leaves. *Plant Physiol.* 106, 337–342. doi: 10.1104/pp.106.1.337

Foyer, C. H. (2018). Reactive oxygen species, oxidative signaling and the regulation of photosynthesis. *Environ. Exp. Bot.* 154, 134–142. doi: 10.1016/j.envexpbot.2018.05.003

Foyer, C. H., Kyndt, T., and Hancock, R. D. (2020). Vitamin C in plants: novel concepts, new perspectives, and outstanding issues. *Antioxid. Redox Signal.* 32, 463–485. doi: 10.1089/ars.2019.7819

Foyer, C. H., and Noctor, G. (2005). Oxidant and antioxidant signaling in plants: a re-evaluation of the concept of oxidative stress in a physiological context. *Plant Cell Environ.* 29, 1056–1107. doi: 10.1111/j.1365-3040.2005.01327.x

Foyer, C. H., and Noctor, G. (2011). Ascorbate and glutathione: the heart of the redox hub. *Plant Physiol.* 155, 2–18. doi: 10.1104/pp.110.167569

Fujiwara, A., Togawa, S., Hikawa, T., Matsuura, H., Masuta, C., and Inukai, T. (2016). Ascorbic acid accumulates as a defense response to Turnip mosaic virus in resistant Brassica rapa cultivars. *J. Exp. Bot.* 67, 4391–4402. doi: 10.1093/jxb/erw223

Garchery, C., Gest, N., Do, P. T., Alhagdow, M., Baldet, P., Menard, G., et al. (2013). A diminution in ascorbate oxidase activity affects carbon allocation and improves yield in tomato under water deficit. *Plant Cell Environ.* 36, 159–175. doi: 10.1111/j.1365-3040.2012.02564.x

Ghaemi, R., Pourjam, E., Safaie, N., Verstraeten, B., Mahmoudi, S. B., Mehrabi, R., et al. (in press). Molecular insights into the compatible and incompatible interaction between sugar beet and the beet cyst nematode. *BMC Plant Biol.*

Gheysen, G., and Mitchum, M. G. (2011). How nematodes manipulate plant development pathways for infection. *Curr. Opin. Plant Biol.* 14, 415–421. doi: 10.1016/j.pbi.2011.03.012

Gheysen, G., and Mitchum, M. G. (2019). Phytoparasitic nematode control of plant hormone pathways. *Plant Physiol.* 179, 1212–1226. doi: 10.1104/pp.18.01067

Giberti, S., Bertea, C. M., Narayana, R., Maffei, M. E., and Forlani, G. (2012). Two phenylalanine ammonia lyase isoforms are involved in the elicitor-induced response of rice to the fungal pathogen *Magnaporthe oryzae*. *J. Plant Physiol.* 169, 249–254. doi: 10.1016/j.jplph.2011.10.008

Gleason, C., Leelarasamee, N., Meldau, D., and Feussner, I. (2016). OPDA has key role in regulating plant susceptibility to the root-knot nematode *Meloidogyne hapla* in *Arabidopsis*. *Front. Plant Sci.* 7:1565. doi: 10.3389/fpls.2016.01565

Goverse, A., Overmars, H., Engelbertink, J., Schots, A., Bakker, J., and Helder, J. (2000). Both induction and morphogenesis of cyst nematode feeding cells are mediated by auxin. *Mol. Plant Microbe Interact.* 13, 1121–1129. doi: 10.1094/mpmi.2000.13.10.1121

Grundler, F. M., Sobczak, M., and Golinowski, W. (1998). Formation of wall openings in root cells of *Arabidopsis thaliana* following infection by the plant-parasitic nematode *Heterodera schachtii*. *Eur. J.of Plant Pathol.* 104, 545–551.

Grunewald, W., Van Noorden, G., Van Isterdael, G., Beeckman, T., Gheysen, G., and Mathesius, U. (2009). Manipulation of auxin transport in plant roots during Rhizobium symbiosis and nematode parasitism. *Plant Cell* 21, 2553–2562. doi: 10.1105/tpc.109.069617

Haeck, A., Van Langenhove, H., Harinck, L., Kyndt, T., Gheysen, G., Höfte, M., et al. (2018). Trace analysis of multi-class phytohormones in *Oryza sativa* using different scan modes in high-resolution Orbitrap mass spectrometry: method validation, concentration levels, and screening in multiple accessions. *Anal. Bioanal. Chem.* 410, 4527–4539. doi: 10.1007/s00216-018-1112-9

Heick, T. M., Hansen, A. L., Munk, L., Labouriau, R., Wu, K., and Jørgensen, L. N. (2020). The effect of fungicide sprays on powdery mildew and rust and yield of sugar beet in Denmark. *Crop Protect.* 135:105199. doi: 10.1016/j.cropro.2020.105199

Hoagland, D. (1937). Some aspects of the salt nutrition of higher plants. *Bot. Rev.* 3, 307–334. doi: 10.1007/bf02872346

Hu, Y., You, J., Li, C., Williamson, V. M., and Wang, C. (2017). Ethylene response pathway modulates attractiveness of plant roots to soybean cyst nematode *Heterodera glycines*. *Sci. Rep.* 7:41282.

Huang, W. K., Ji, H. L., Gheysen, G., and Kyndt, T. (2016). Thiamine-induced priming against root-knot nematode infection in rice involves lignification and hydrogen peroxide generation. *Mol. Plant Pathol.* 17, 614–624. doi: 10.1111/mpp.12316

Ji, H., Kyndt, T., He, W., Vanholme, B., and Gheysen, G. (2015). β-Aminobutyric acid–induced resistance against root-knot nematodes in rice is based on increased basal defense. *Mol. Plant Microbe Interact.* 28, 519–533. doi: 10.1094/mpmi-09-14-0260-r

Kammerhofer, N., Radakovic, Z., Regis, J. M., Dobrev, P., Vankova, R., Grundler, F. M., et al. (2015). Role of stress-related hormones in plant defence during early infection of the cyst nematode *Heterodera schachtii* in *Arabidopsis*. *New Phytol.* 207, 778–789. doi: 10.1111/nph.13395

Karpinska, B., Zhang, K., Rasool, B., Pastok, D., Morris, J., Verrall, S. R., et al. (2018). The redox state of the apoplast influences the acclimation of photosynthesis and leaf metabolism to changing irradiance. *Plant Cell Environ.* 41, 1083–1097. doi: 10.1111/pce.12960

Khan, M., Arabiat, S., Chanda, A., and Yan, G. (2016). *Sugar Beet Cyst Nematode*. Fargo, ND: North Dakota State University.

Koch, K. G., Chapman, K., Louis, J., Heng-Moss, T., and Sarath, G. (2016). Plant tolerance: a unique approach to control hemipteran pests. *Front. Plant Sci.* 7:1363. doi: 10.3389/fpls.2016.01363

Koen, E., Trapet, P., Brulé, D., Kulik, A., Klinguer, A., Atauri-Miranda, L., et al. (2014). β-Aminobutyric acid (BABA)-induced resistance in *Arabidopsis thaliana*: link with iron homeostasis. *Mol. Plant Microbe Interact.* 27, 1226–1240. doi: 10.1094/mpmi-05-14-0142-r

Kyndt, T., Goverse, A., Haegeman, A., Warmerdam, S., Wanjau, C., Jahani, M., et al. (2016). Redirection of auxin flow in *Arabidopsis thaliana* roots after infection by root-knot nematodes. *J. Exp. Bot.* 67, 4559–4570. doi: 10.1093/jxb/erw230

Kyndt, T., Nahar, K., Haeck, A., Verbeek, R., Demeestere, K., and Gheysen, G. (2017). Interplay between carotenoids, abscisic acid and jasmonate guides the compatible rice-*Meloidogyne graminicola* interaction. *Front. Plant Sci.* 8:951. doi: 10.3389/fpls.2017.00951

Kyndt, T., Nahar, K., Haegeman, A., De Vleesschauwer, D., Höfte, M., and Gheysen, G. (2012). Comparing systemic defence-related gene expression changes upon migratory and sedentary nematode attack in rice. *Plant Biol.* 14, 73–82. doi: 10.1111/j.1438-8677.2011.00524.x

Kyndt, T., Vieira, P., Gheysen, G., and de Almeida-Engler, J. (2013). Nematode feeding sites: unique organs in plant roots. *Planta* 238, 807–818. doi: 10.1007/s00425-013-1923-z

Labudda, M., Różańska, E., Czarnocka, W., Sobczak, M., and Dzik, J. M. (2018). Systemic changes in photosynthesis and reactive oxygen species homeostasis in shoots of *Arabidopsis thaliana* infected with the beet cyst nematode *Heterodera schachtii*. *Mol. Plant Pathol.* 19, 1690–1704. doi: 10.1111/mpp.12652

López-Gálvez, F., Ragaert, P., Haque, M. A., Eriksson, M., van Labeke, M. C., and Devlieghere, F. (2015). High oxygen atmospheres can induce russet spotting development in minimally processed iceberg lettuce. *Postharvest Biol. Technol.* 100, 168–175. doi: 10.1016/j.postharvbio.2014.10.001

Luna, E., Beardon, E., Ravnskov, S., Scholes, J., and Ton, J. (2016). Optimizing chemically induced resistance in tomato against Botrytis cinerea. *Plant Dis.* 100, 704–710. doi: 10.1094/pdis-03-15-0347-re

MacDonald, M. J., and D'Cunha, G. B. (2007). A modern view of phenylalanine ammonia lyase. *Biochem. Cell Biol.* 85, 273–282. doi: 10.1139/o07-018

Mantelin, S., Bellafiore, S., and Kyndt, T. (2017). Meloidogyne graminicola: a major threat to rice agriculture. *Mol. Plant Pathol.* 18, 3–15. doi: 10.1111/mpp.12394

Martinez-Medina, A., Flors, V., Heil, M., Mauch-Mani, B., Pieterse, C. M., Pozo, M. J., et al. (2016). Recognizing plant defense priming. *Trends Plant Sci.* 21, 818–822. doi: 10.1016/j.tplants.2016.07.009

Melillo, M. T., Leonetti, P., Bongiovanni, M., Castagnone-Sereno, P., and Bleve-Zacheo, T. (2006). Modulation of reactive oxygen species activities and H2O2 accumulation during compatible and incompatible tomato–root-knot nematode interactions. *New Phytol.* 170, 501–512. doi: 10.1111/j.1469-8137.2006.01724.x

Mittler, R., Vanderauwera, S., Gollery, M., and Van Breusegem, F. (2004). Reactive oxygen gene network of plants. *Trends Plant Sci.* 9, 490–498. doi: 10.1016/j.tplants.2004.08.009

Moens, M., Perry, R. N., and Jones, J. T. (2018). *Cyst Nematodes-Life Cycle and Economic Importance*. Wallingford: CABI, 1–26.

Nahar, K., Kyndt, T., De Vleesschauwer, D., Höfte, M., and Gheysen, G. (2011). The jasmonate pathway is a key player in systemically induced defense against root knot nematodes in rice. *Plant Physiol.* 157, 305–316. doi: 10.1104/pp.111.177576

Nicol, J., Turner, S., Coyne, D., Den Nijs, L., Hockland, S., and Maafi, Z. T. (2011). "Current nematode threats to world agriculture," in *Genomics and Molecular Genetics of Plant-Nematode Interactions*, eds J. Jones, G. Gheysen, and C. Fenoll (Heidelberg: Springer), 21–43. doi: 10.1007/978-94-007-0434-3_2

Oka, Y., and Cohen, Y. (2001). Induced resistance to cyst and root-knot nematodes in cereals by DL-β-amino-n-butyric acid. *Eur. J. Plant Pathol.* 107, 219–227.

Oka, Y., Cohen, Y., and Spiegel, Y. (1999). Local and systemic induced resistance to the root-knot nematode in tomato by DL-β-amino-n-butyric acid. *Phytopathology* 89, 1138–1143. doi: 10.1094/phyto.1999.89.12.1138

Perry, R. N., Moens, M., and Jones, J. T. (2018). *Cyst Nematodes*. Wallingford: CABI.

Pfaffl, M. W., Horgan, G. W., and Dempfle, L. (2002). Relative expression software tool (REST©) for group-wise comparison and statistical analysis of relative expression results in real-time PCR. *Nucleic Acids Res.* 30:e36.

Pignocchi, C., Fletcher, J., Wilkinson, J., Barnes, J., and Foyer, C. H. (2003). The function of ascorbate oxidase in Tobacco. *Plant Physiol.* 132, 1631–1641. doi: 10.1104/pp.103.022798

Pignocchi, C., Kiddle, G., Hernández, I., Foster, S. J., Asensi, A., Taybi, T., et al. (2006). Ascorbate oxidase-dependent changes in the redox state of the apoplast modulate gene transcript accumulation leading to modified hormone signaling and orchestration of defense processes in tobacco. *Plant Physiol.* 141, 423–435. doi: 10.1104/pp.106.078469

Rangel, L. I., Spanner, R. E., Ebert, M. K., Pethybridge, S. J., Stukenbrock, E. H., de Jonge, R., et al. (2020). *Cercospora beticola*: the intoxicating lifestyle of the leaf spot pathogen of sugar beet. *Mol. Plant Pathol.* 21, 1020–1041. doi: 10.1111/mpp.12962

Reversat, G., Boyer, J., Sannier, C., and Pando-Bahuon, A. (1999). Use of a mixture of sand and water-absorbent synthetic polymer as substrate for the xenic culturing of plant-parasitic nematodes in the laboratory. *Nematology* 1, 209–212. doi: 10.1163/156854199508027

Robb, J. G., Kerr, E. D., and Ellis, D. E. (1992). Factors affecting the economic threshold for *Heterodera schachtii* control in sugar beet. *J. Sugar Beet Res.* 29, 31–43. doi: 10.5274/jsbr.29.1.31

Sahebani, N., Hadavi, N. S., and Zade, F. O. (2011). The effects of β-amino-butyric acid on resistance of cucumber against root-knot nematode, *Meloidogyne javanica*. *Acta Physiol. Plant.* 33, 443–450. doi: 10.1007/s11738-010-0564-0

Sanmartin, M., Drogoudi, P. A., Lyons, T., Pateraki, I., Barnes, J., and Kanellis, A. K. (2002). Over-expression of ascorbate oxidase in the apoplast of transgenic tobacco results in altered ascorbate and glutathione redox states and increased sensitivity to ozone. *Planta* 216, 918–928. doi: 10.1007/s00425-002-0944-9

Schmidt, J., Dotson, B. R., Schmiderer, L., van Tour, A., Kumar, B., Marttila, S., et al. (2020). Substrate and plant genotype strongly influence the growth and gene expression response to *Trichoderma afroharzianum* T22 in Sugar Beet. *Plants* 9:1005. doi: 10.3390/plants9081005

Shetty, N. P., Jørgensen, H. J. L., Jensen, J. D., Collinge, D. B., and Shetty, H. S. (2008). Roles of reactive oxygen species in interactions between plants and pathogens. *Eur. J. Plant Pathol.* 121, 267–280. doi: 10.1007/978-1-4020-8780-6_6

Siddique, S., Matera, C., Radakovic, Z. S., Hasan, M. S., Gutbrod, P., Rozanska, E., et al. (2014). Parasitic worms stimulate host NADPH oxidases to produce reactive oxygen species that limit plant cell death and promote infection. *Sci. Signal.* 7:ra33. doi: 10.1126/scisignal.2004777

Singh, R. R., Chinnasri, B., De Smet, L., Haeck, A., Demeestere, K., Van Cutsem, P., et al. (2019). Systemic defense activation by COS-OGA in rice against root-knot nematodes depends on stimulation of the phenylpropanoid pathway. *Plant Physiol. Biochem.* 142, 202–210. doi: 10.1016/j.plaphy.2019.07.003

Singh, R. R., Verstraeten, B., Siddique, S., Tegene, A. M., Tenhaken, R., Frei, M., et al. (2020). Ascorbate oxidation activates systemic defence against root-knot nematode *Meloidogyne graminicola* in rice. *J. Exp. Bot.* 71, 4271–4284. doi: 10.1093/jxb/eraa171

Smirnoff, N. (2018). Ascorbic acid metabolism and functions: a comparison of plants and mammals. *Free Radic. Biol. Med.* 122, 116–129. doi: 10.1016/j.freeradbiomed.2018.03.033

Smirnoff, N., and Arnaud, D. (2019). Hydrogen peroxide metabolism and functions in plants. *New Phytol.* 221, 1197–1214. doi: 10.1111/nph.15488

Sobczak, M., and Golinowski, W. (2009). "Structure of cyst nematode feeding sites," in *Cell Biology of Plant Nematode Parasitism*, eds R. H. Berg and C. G. Taylor (Heidelberg: Springer), 153–187. doi: 10.1007/978-3-540-85215-5_6

Soeno, K., Goda, H., Ishii, T., Ogura, T., Tachikawa, T., Sasaki, E., et al. (2010). Auxin biosynthesis inhibitors, identified by a genomics-based approach, provide insights into auxin biosynthesis. *Plant Cell Physiol.* 51, 524–536. doi: 10.1093/pcp/pcq032

Spoel, S. H., and Dong, X. (2008). Making sense of hormone crosstalk during plant immune responses. *Cell Host Microbe* 3, 348–351. doi: 10.1016/j.chom.2008.05.009

Taheri, P., and Tarighi, S. (2011). A survey on basal resistance and riboflavin-induced defense responses of sugar beet against *Rhizoctonia solani*. *J. Plant Physiol.* 168, 1114–1122. doi: 10.1016/j.jplph.2011.01.001

Trudgill, D. (1991). Resistance to and tolerance of plant parasitic nematodes in plants. *Annu. Rev. Phytopathol.* 29, 167–192. doi: 10.1146/annurev.py.29.090191.001123

Tucker, M. L., Xue, P., and Yang, R. (2009). 1-Aminocyclopropane-1-carboxylic acid (ACC) concentration and ACC synthase expression in soybean roots, root tips, and soybean cyst nematode (*Heterodera glycines*)-infected roots. *J. Exp. Bot.* 61, 463–472. doi: 10.1093/jxb/erp317

Ueda, Y., Wu, L., and Frei, M. (2013). A critical comparison of two high-throughput ascorbate analyses methods for plant samples. *Plant Physiol. Biochem.* 70, 418–423. doi: 10.1016/j.plaphy.2013.06.006

van Aubel, G., Buonatesta, R., and Van Cutsem, P. (2014). COS-OGA: a novel oligosaccharidic elicitor that protects grapes and cucumbers against powdery mildew. *Crop Protect.* 65, 129–137. doi: 10.1016/j.cropro.2014.07.015

Van Aubel, G., Cambier, P., Dieu, M., and Van Cutsem, P. (2016). Plant immunity induced by COS-OGA elicitor is a cumulative process that involves salicylic acid. *Plant Sci.* 247, 60–70. doi: 10.1016/j.plantsci.2016.03.005

Van Aubel, G., Serderidis, S., Ivens, J., Clinckemaillie, A., Legrève, A., Hause, B., et al. (2018). Oligosaccharides successfully thwart hijacking of the salicylic acid pathway by *Phytophthora infestans* in potato leaves. *Plant Pathol.* 67, 1901–1911. doi: 10.1111/ppa.12908

van Hulten, M., Pelser, M., Van Loon, L., Pieterse, C. M., and Ton, J. (2006). Costs and benefits of priming for defense in Arabidopsis. *Proc. Natl. Acad. Sci. U.S.A.* 103, 5602–5607. doi: 10.1073/pnas.0510213103

Velikova, V., Yordanov, I., and Edreva, A. (2000). Oxidative stress and some antioxidant systems in acid rain-treated bean plants: protective role of exogenous polyamines. *Plant Sci.* 151, 59–66. doi: 10.1016/s0168-9452(99)00197-1

Wang, G., Hu, C., Zhou, J., Liu, Y., Cai, J., Pan, C., et al. (2019). Systemic root-shoot signaling drives jasmonate-based root defense against nematodes. *Curr. Biol.* 29:3430. doi: 10.1016/j.cub.2019.08.049

Wu, L. B., Ueda, Y., Lai, S. K., and Frei, M. (2017). Shoot tolerance mechanisms to iron toxicity in rice (*Oryza sativa* L.). *Plant Cell Environ.* 40, 570–584. doi: 10.1111/pce.12733

Wubben, M. J., Su, H., Rodermel, S. R., and Baum, T. J. (2001). Susceptibility to the sugar beet cyst nematode is modulated by ethylene signal transduction in *Arabidopsis thaliana*. *Mol. Plant Microbe Interact.* 14, 1206–1212. doi: 10.1094/mpmi.2001.14.10.1206

Wyss, U., and Grundler, F. (1992). Feeding behavior of sedentary plant parasitic nematodes. *Neth. J. Plant Pathol.* 98, 165–173. doi: 10.1007/bf01974483

Yamamoto, A., Bhuiyan, M. N. H., Waditee, R., Tanaka, Y., Esaka, M., Oba, K., et al. (2005). Suppressed expression of the apoplastic ascorbate oxidase gene increases salt tolerance in tobacco and Arabidopsis plants. *J. Exp. Bot.* 56, 1785–1796. doi: 10.1093/jxb/eri167

Zacheo, G., Arrigont-Liso, R., Blevo-Sacheo, T., Arrigoni-Liso, R., and Lamberti, F. (1981). Changes of ascorbate free radical reductase in pea roots infested by *Heterodera goettingiana*. *Nematol. Medit.* 9, 181–187.

Zhan, L.-P., Peng, D.-L., Wang, X.-L., Kong, L.-A., Peng, H., Liu, S.-M., et al. (2018). Priming effect of root-applied silicon on the enhancement of induced resistance to the root-knot nematode *Meloidogyne graminicola* in rice. *BMC Plant Biol.* 18:50. doi: 10.1186/s12870-018-1266-9

Conflict of Interest: The authors declare that the research was conducted in the absence of any commercial or financial relationships that could be construed as a potential conflict of interest.

frontiers in Plant Science

ORIGINAL RESEARCH
published: 10 November 2020
doi: 10.3389/fpls.2020.594197

Characterization of Resistance to Cereal Cyst Nematode, Agronomic Performance, and End-Use Quality Parameters in Four Perennial Wheat-*Thinopyrum intermedium* Lines

Lei Cui[1,2], Yongkang Ren[1], Yanming Zhang[3], Zhaohui Tang[1], Qing Guo[1], Yuqi Niu[1], Wenze Yan[1], Yu Sun[1] and Hongjie Li[2]**

[1] College of Agriculture, Shanxi Agricultural University, Taiyuan, China, [2] The National Engineering Laboratory of Crop Molecular Breeding, Institute of Crop Sciences, Chinese Academy of Agricultural Sciences, Beijing, China, [3] Key Laboratory of Molecular Cytogenetics and Genetic Breeding of Heilongjiang Province, College of Life Science and Technology, Harbin Normal University, Harbin, China

OPEN ACCESS

Edited by:
Shahid Siddique, University of California, Davis, United States

Reviewed by:
Shree Pariyar, Julich Research Centre, Helmholtz Association of German Research Centre (HZ), Germany
Abolfazl Hajihassani, University of Georgia, United States

***Correspondence:**
Yu Sun
sunyu203@126.com
Hongjie Li
lihongjie@caas.cn

Specialty section:
This article was submitted to Plant Pathogen Interactions, a section of the journal Frontiers in Plant Science

Received: *31 August 2020*
Accepted: *20 October 2020*
Published: *10 November 2020*

Citation:
Cui L, Ren Y, Zhang Y, Tang Z, Guo Q, Niu Y, Yan W, Sun Y and Li H (2020) Characterization of Resistance to Cereal Cyst Nematode, Agronomic Performance, and End-Use Quality Parameters in Four Perennial Wheat-Thinopyrum intermedium Lines. Front. Plant Sci. 11:594197. doi: 10.3389/fpls.2020.594197

Perennial wheat is considered to be a practical way to increase the flexibility and profitability of sustainable agricultural system, as it can be either a forage grass or a grain crop. Four perennial wheat lines SX12-480, SX12-787, SX12-1150, and SX12-1269 were developed from a series of interspecific crosses between common wheat (*Triticum aestivum*, 2n = 42) or durum wheat (*T. turgidum* var. *durum*, 2n = 28) and the intermediate wheatgrass (*Thinopyrum intermedium*, 2n = 42). These lines were characterized by the vigorous regrowth for at least 3 years. The one- and 2-year-old plants had higher grain yield potential than the 3-year-old perennial plants. The decline of grain yield was associated with plant age-related effects on yield components. The perennial wheat lines were all resistant to both *Heterodera avenae* and *H. filipjevi*, the two distinct cereal cyst nematode species that occur in China, except that line SX12-787 exhibited moderate resistance only to *H. avenae*. The dual-purpose perennial wheat lines were evaluated for quality values of both defoliated grass and harvested grains in the form of amino acid profile, mineral concentration, and contents of protein and fiber. Difference in the quality profile was observed between the perennial lines. These perennial lines had an overall improved quality levels over those of the perennial wheat control Montana-2 (*T. turgidum* × *Th. intermedium*) and the annual wheat cultivar Jinchun 9. The amplification profiles of the molecular markers provided molecular evidence for the introgression of alien chromatin. Genomic *in situ* hybridization detected 16, 14, 14, and 12 *Th. intermedium* chromosomes in lines SX12-480 (2n = 48), SX12-787 (2n = 56), SX12-1150 (2n = 56), and SX12-1269 (2n = 54), respectively, in addition to either 32 or the complete set of wheat chromosomes. The four perennial wheat-*Th. intermedium* lines described here provide valuable sources of perennial wheat for the dual-purpose application of both grain and forage.

Keywords: perennial wheat, *Thinopyrum intermedium*, cereal cyst nematode, agronomic performance, end-use quality parameters, molecular cytogenetic analysis

INTRODUCTION

Recent increase in the global attention has been paid to the development of perennial crop alternatives to annual crops (Jaikumar et al., 2012; Kantar et al., 2016; Cui et al., 2018). Enrichment of genetic diversity, soil conservation, improvement of water quality, and reduction in environmental pollution from fertilizers and pesticides are some of the benefits of perennial crops over annual cereals, especially on certain erodible and marginal lands (Bell et al., 2010). An obvious advantage of perennial wheat over annual cereal crops is its ability to produce forage for livestock and harvestable grain, similar to the way that other annual wheat is used to (Larkin et al., 2014). On the other hand, challenges exist in breeding perennial crops. One of the main issues is the potential buildup of disease pressure due to the persistence of perennial growth habit. Diseases, especially those caused by the soil-borne pathogens, could accumulate over years.

Perennial wheat is one of the promising perennial cereals for cold-temperate regions. It is developed by either direct domestication of wild perennial species or distant hybridization between annual wheat cultivars and perennial wild wheat relatives including *Thinopyrum* spp. (Murphy et al., 2009; Bell et al., 2010; Kantar et al., 2016; Cui et al., 2018). Because wild perennial species have beneficial characteristics, such as perennial growth habit, resistance to several pests and diseases, and nutritional benefits, they are useful in development of perennial wheat and improvement of the nutritional values of annual wheat through wide hybridization (Li and Wang, 2009; Mujoriya and Bodla, 2011; Hayes et al., 2012; Marti et al., 2015). Early attempts to develop perennial wheat can be dated back to the 1920s by Dr. N. V. Tsitin, former Soviet Union (Armstrong, 1936). Significant progress has been made in domesticating the perennial wheatgrass *Th. intermedium* (Host) Barkworth and D. R. Dewey leading to the development of cultivar Kernza as a dual-purpose forage and grain crop (Culman et al., 2013). Montana-2 (PI 505802) is the first commercial winter-hardy perennial wheat cultivar released in 1986; it was developed by crossing durum wheat [*T. turgidum* L. var. *durum* (Desf.); 2n = 28] with *Agrotriticum intermediodurum* Khizhnyak (syn. *Th. intermedium*) (Schulz-Schaeffer and Haller, 1987; Schulz-Schaeffer and Friebe, 1992).

Perennial wheat is desired to grow several years, so resistance to diseases, particularly those caused by certain soil-borne pathogens, is of particular importance. It has been shown that the wheat-*Thinopyrum* derivatives are highly resistant to various fungal and viral diseases, such as the rusts (caused by *Puccinia striiformis* Westend., *P. graminis* Pers.:Pers., and *P. triticina* Eriks.), Fusarium head blight (caused by *Fusarium graminearum* Schw.), powdery mildew (caused by *Blumeria graminis* DC. f. sp. *tritici* Marchal), eyespot (caused by *Tapesia yallundae* Wallwork & Spooner, syn. *Oculimacula yallundae* Wallwork & Spooner), *Barley Yellow Dwarf Virus* (BYDV), *Wheat Streak Mosaic Virus* (WSMV) and its vector wheat curl mite *Aceria tosichella* (Keifer) (Cox et al., 2002, 2005; Fedak and Han, 2005; Li et al., 2005; Jauhar et al., 2009; Li and Wang, 2009). However, little information is available on the potential of perennial wheatgrass as source of resistance against the soil-borne pathogens. Cereal cyst nematode (CCN, *Heterodera* spp.) is one of such parasites that causes significant yield losses in cereal crops and has become an important constraint on wheat production in many parts of the world (Peng et al., 2015; Smiley et al., 2017). This root parasitic nematode comprises several species (Nicol et al., 2011). *Heterodera avenae* Wollenweber is a dominant CCN species in China, which has been identified in the majority of wheat production regions, while *H. filipjevi* (Madzhidov) Stelter is an emerging threat to wheat production (Yuan et al., 2010; Peng et al., 2015). The nematode is able to complete a life cycle in one wheat cropping season. The eggs within the cysts can be viable in the soil for years until proper hatching conditions (Banyer and Fisher, 1971). Monoculture of susceptible wheat cultivars facilitates CCN reproduction in the soil, which ultimately results in outbreaks of the nematode. On the contrary, growing resistant cultivars not only suppresses the development and reproduction of CCN, but also limits the initial nematode density below the economic damage threshold for the next cropping seasons (Nicol et al., 2011; Cui et al., 2016). Extensive screenings in cultivated wheat germplasm have identified limited number of resistant cultivars and breeding lines (Xing et al., 2014; Peng et al., 2015; Cui et al., 2016). Many of the studies have focused on single CCN species only. Under natural field condition, mixed infestation can occur with the coexistence of *H. avenae* and *H. filipjevi*. Some of the known CCN resistant genes are not effective against both nematode species (Cui et al., 2020). Very recent evidence shows that resistance is mediated by distinct quantitative trait loci (QTL) depending on *Heterodera* species. Thus, sources conferring resistance to *H. filipjevi* can be susceptible upon *H. avenae* infestation and vice versa (Cui et al., 2020). Taken together, all of these complicate breeding efforts to develop CCN resistant wheat cultivars. Wild species *Thinopyrum* spp. has shown to be resistant to CCN. Wheat-*Thinopyrum* hybrids were reported to confer resistance to *H. filipjevi* (Li et al., 2012).

Another important challenge for developing perennial wheat is selection of cultivars with consistent grain production and equivalent grain yield to annual wheats since the hybrids with perennial parents have age-related decrease in grain yield and can produce 40–60% yield level relative to the annual counterpart (Bell et al., 2010; Jaikumar et al., 2012). In a perennial wheat breeding program conducted in Australia, several wheat-*Th. intermedium* lines were able to achieve approximately 75% of the grain yield of the annual wheat cultivar in the first year; however, these lines were hardly able to regrowth beyond the first harvest (Larkin et al., 2014). Perennial wheat lines showed persistent longevity for four consecutive years, but grain yield decreased dramatically. During the third and fourth years, these lines barely yielded harvestable grains. Modest grain production and yield decreases over ages might be due to competing sources in a perennial plant between grain yield and persistence, as well as the buildup of pathogens in the soil. For a dual-purpose perennial wheat cultivar, grain yield merely 40% relative to

the annual wheat is considered to be profitable as perennial wheat provides forage for livestock (Bell et al., 2010). To understand the trade-off between plant longevity, forage biomass, and grain yield potential, it requires in-depth studies over multiple ages and years.

We developed four wheat-*Th. intermedium* lines that displayed strong perennial growth habit. These perennial lines were assessed for their field responses to CCN and their agronomical performances on consistency of yield components over multiple years. We measured the parameters relating to the nutritional components of one-year old defoliated grass and grains in comparison with the commercial annual wheat cultivar. The objectives of this study were to characterize their phenotypic responses to the two CCN species, agronomic performances, and quality properties in these perennial wheat lines. The chromosome compositions of these perennial wheat lines were analyzed by genome-specific markers and genomic *in situ* hybridization (GISH). To breed for the dual-purpose perennial wheat, emphasizes on consistent grain yield potential and improved forage biomass can offset inherent physiological constraints on grain production to a profitable and sustainable extent. Simultaneously, constantly high degree of resistance to soil-borne diseases is foremost objective to breed for superior perennial wheat.

MATERIALS AND METHODS

Plant Materials

The pedigrees of the four perennial wheat-*Th. intermedium* lines are shown in **Figure 1**. Line SX12-787 was produced by crossing hexaploid partial amphiploid Xiaoyan 503 (2n = 42, pedigree DR1022/*Th. intermedium*//DR116) with a *Th. intermedium* accession. Lines SX12-480, SX12-1150, and SX12-1269 were developed from the same cross between an octoploid partial amphiploid line (2n = 56, pedigree 91C-9/Yuan 16-3//*Th. intermedium*) and a hexaploid partial amphiploid Xiaoyan 505 (2n = 42, pedigree DR1022/*Th. intermedium*//DR46). The *Th. intermedium* accession and the durum wheat DR46, DR116, and DR1022 were provided by the Institute of Crop Sciences, Chinese Academy of Agricultural Sciences, Beijing, China. The Chinese wheat cultivars Wenmai 19 (Lankao 4/Wen 2540) and Jinchun 9 (Taigu male sterile line/Jinyan 163-12), and perennial wheat cultivar Montana-2 (MT-2, PI 505802) from the United States were used as the controls in the assessments of CCN resistance and quality parameters, respectively. An accession of *Th. intermedium* (2n = 42, JJJ^sJ^sStSt) and common wheat cultivar Chinese Spring (2n = 42, AABBDD) were used to extract DNA for preparation of the probe or the blocker in the GISH analysis.

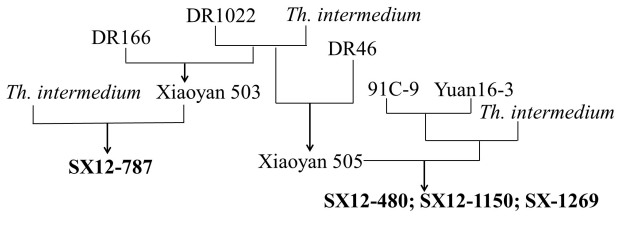

FIGURE 1 | Pedigrees of the four perennial wheat lines SX12-480, SX12-787, SX12-1150, and SX12-1269.

The perennial wheat lines were developed and assessed on the sandy loam soil at Dongyang Agricultural Experimental Station, Shanxi Agricultural University, Jinzhong, Shanxi province (37.56°N, 112.68°E, 801 m als). The local weather condition belongs to the temperate continental arid climate with an annual precipitation of 418 – 483 mm. The long-term annual mean temperature is 9.8°C, the mean frost-free period is 158 days, and the average temperature in winter ranges from −12°C to 12°C (China Meteorological Data Service Center, 2020)[1].

Field Evaluation of CCN Resistance

During the 2013–2014 and 2014–2015 growing seasons, reactions to *H. avenae* (pathotype Ha43) (Yuan et al., 2010) and *H. filipjevi* (pathotype Hfc-1) (Fu et al., 2011) were evaluated at Zhengzhou (ZZ, 34.44°N, 113.24°E, 171 m als) and Xuchang (XC, 34.04°N, 113.74°E, 98 m als), Henan province, respectively. A randomized complete block design with three replicates was used to arrange each line. In each year 20 selfing seeds of the second-year-old perennial plants from the growing season of 2012–2013 were sown in 2 m rows, 0.3 m apart. Eight to ten plants per line were randomly sampled with soil cylinders from each plot at the Zadoks growth stage (GS) 77 (late grain-filling stage) (Zadoks et al., 1974). The roots were carefully raised with tap water in order to visually count the white females (cysts). The phenotype of each line was determined by averaging number of white females (cysts) on the roots per plant and separated into five categories: resistant (<5), moderately resistant (5–10), moderately susceptible (11–14), and susceptible (15–25), and highly susceptible (>25) (Nicol et al., 2009).

Evaluation of Agronomic Traits

Perennial wheat lines were grown in plots consisting of 3 m-long row and spaced 0.4 m that were arranged in a randomized complete block design with three replicates. Twenty-five seeds were sown in a row in early October 2011. Defoliation was performed twice during June (both grain and forage harvest) and November (forage cut preparing for over-wintering) each year, afterwards regrow ability was observed. The agronomic performances were investigated in three consecutive years. Depending on the agronomic traits, evaluation was performed before the first grain and forage harvest at June, or immediately after harvesting. The "first-year plant" refers to individuals during their first growing season (2011–2012), the "second-year plant" denotes plants that show persistent regrowth during the second growing season (2012–2013), and the "third-year plant" represents plants displaying post-harvest regrowth habit for three consecutive years during the third growing season (2013–2014). From each line, plant height (cm), spike length (cm), and number of spikelets per spike were recorded in ten randomly sampled individuals from each plot during the

[1]https://data.cma.cn/en

growing seasons of 2011–2012, 2012–2013, and 2013–2014. Plant height was determined from the ground level to the top of the spike, and spike length was measured from the base of rachis to the top of the spike. In addition, number of spikelets per spike was enumerated and the spikes were threshed in a bench micro-thresher to determine thousand-kernel weight (g). The common practices of irrigation (twice, one before over-winter stage immediately after defoliation, and the other after grain and forage harvesting at June), fertilizers (nitrogen, phosphorus and potassium), and pesticides were conducted following the local farm system.

Analysis of End-Use Quality

The end-use quality of the perennial wheat lines, including 16 amino acids, crude fat, crude protein, crude fiber, ash, phosphorus, iron, selenium and carotene were analyzed by the Inspection and Testing Center for Quality of Cereals and Their Products (Harbin), Ministry of Agriculture and Rural Affairs, China. Forage of the one-year old plants for each line was defoliated and samples were dried at 70°C for 48 h. Forage dry matter (300 g per sample) was taken for quality analysis. Grains (300 g, dry weight) from the first-year plants and common wheat cultivar Jinmai 9 were collected for quality measurements. Method for determination of amino acid profile in forage dry matter was described in the National Standard (GB/T) 18246-2000 (Standardization Administration of the People's Republic of China, 2000). Measurements of crude protein, crude fat, and crude fiber in forage dry matter were based on the National Standards (GB/T) 6432-1994, 6433-2006, 6434-2006, respectively (Standardization Administration of the People's Republic of China, 1994, 2006a,b). Measurements of phosphorus, iron, carotene, and selenium concentrations were performed as described in the National Standards (GB, GB/T) GB/T 6437-2002, GB/T 13885-2003, GB/T 5009.83-2003, and GB 5009.93-2010, respectively (Standardization Administration of the People's Republic of China, 2002, 2003a,b, 2010). To determine the quality levels in the dried grains, methods used to assess the amino acid composition, crude protein, and ash contents were described in the National Standards (GB/T) GB/T 5009. 124-2003 (Standardization Administration of the People's Republic of China, 2003c), the Agricultural Industry Standard (NY/T) 3-1982 (Ministry of Agriculture and Rural Affairs of the People's Republic of China, 1982), and GB/T 5505-2008 (Standardization Administration of the People's Republic of China, 2008), respectively.

Molecular Marker Analysis

Primer pairs for the three simple sequence repeat (SSR) markers (*Xedm 28*, *Xedm16*, and *Xedm105*), one sequence characterized amplified region (SCAR) marker (*SCAR1248*), and one marker obtained from repetitive DNA sequence from *Th. elongatum* (*2P1/2P2*) were used to characterize alien chromatin in perennial wheat lines (**Table 1**) (Wang and Wei, 1995; You et al., 2002; Li et al., 2005; Mullan et al., 2005; Hu et al., 2012). Leaves of four perennial wheat lines, *Th. intermedium*, wheat cultivar Chinese Spring were harvested for DNA isolation using a cetyltrimethyl ammonium bromide (CTAB) based protocol (Fulton et al., 1995). Amplification of the SSR and the SCAR markers was conducted in a 25 μL reaction including 2 μL genomic DNA (10–30 ng/μL), 2.5 μL of PCR buffer (10×), 2.5 μL of dNTP, 1 μL of forward primer and reverse primer each, 15.7 μL deionized water, and 0.3 μL of RT-*Taq*. Cycling conditions consisted of incubation at 94°C for 5 min, 40 cycles of 94°C for 30 s, annealing temperature varied depending on different primers for 45 s, and 72°C for 1 min, and 72°C for 10 min (Yan et al., 2020). DNA amplification was carried out in an Eppendorf 9700 thermocycler (Eppendorf, Hamburg, Germany). The amplification of DNA using the primer pair 2P1/2P2 was conducted in a 20 μL reaction mixture that contained 2 μL 100 ng/μL genomic DNA, 1 μL 10 μmol/L of each primer, 10 μL 2 × *Taq* PCR Master Mix (Taingen Biotech, Beijing, China), and 6 μL sterilized ddH_2O. The profile of DNA amplification was initial denaturation at 94°C for 3 min, followed by 35 cycles of 1 min at 94°C, 47–52°C ramp annealing for 45 s, 1 min for extension at 72°C, and a final extension step at 72°C for 10 min (Li et al., 2005). Separation and visualization of PCR products for SSR markers were completed as described by Zhao et al. (2013). Amplified products of markers SCAR1248 and 2P1/2P2 were electrophoretically separated on a 1.5% agarose gel, stained with ethidium bromide and observed under an ultraviolet (UV) light.

TABLE 1 | Molecular markers used for characterization of the alien chromatin in the perennial wheat lines.

Marker	Genome/chromosome target	Primer (5′-3′)	Annealing temperature	PCR product size	Source of primers
SSR-*Xedm28*	*Thinopyrum elongatum* chromosomes 2ES and 3EL	F-GCTCACTCACGCATCATAGC R-GTTGGCGGAATCCTTCTTC	53.7	151 bp	You et al., 2002; Mullan et al., 2005
SSR-*Xedm105*	*Th. elongatum* chromosome 7EL	F-ACCGCCAGGGAGCTCTGC R-GATGTCCTTCTGGCCGTACT	57	237 bp	You et al., 2002; Mullan et al., 2005
SSR-*Xedm16*	*Th. elongatum* chromosome 7ES	F-TCACCTAACAGCACCACGAG R-GCCGAGTACCAGCAGTACCA	55.8	165 bp	Mullan et al., 2005
SCAR1248	*Pseudoroegneria strigosa* St genome	F-TTAGACATCATGAGCACACC R-ATGATGCAGCAGCAAATTACA	55	850 bp	Hu et al., 2012
2P1/2P2	*Thinopyrum* genus	F-ACAATCTGAAAATCTGGACA R-TCATATTGAGACTCCTATAA	47–52 ramp annealing	277 bp	Wang and Wei, 1995; Li et al., 2005

Genomic *in situ* Hybridization (GISH)

Seeds of the perennial wheat lines were germinated in Petri dishes at 23°C for 24 h, 4°C for 48 h and 23°C for 27.5 h. Root tips 1–1.5 cm in length were pretreated in ice water (0–4°C) for 24 h, and then fixed in ethanol-acetic acid (3:1) for 24 h at room temperature. The fixed root tips were squashed in 45% acetic acid after staining with 1% acetocarmine for 2 h. Chromosome numbers were enumerated under a light microscope (Leica DM LS2, Mannheim, Germany). Genomic DNA of *Th. intermedium* extracted using a CTAB method was labeled with DIG-Nick-Translation mix (Roche, Mannheim, Germany) as a probe, and sheared genomic DNA of Chinese Spring was used as a blocker. Antidigoxin Rhodamine and 4,6-diamidino-2-phenylindole (Roche, Mannheim, Germany) were loaded on slides prior to dark incubation. Hybridization signals were visualized under a Leica fluorescence microscope (Leica DM6000B, Mannheim, Germany). Photos were taken by a Leica digital camera (Model DFC480). The detailed GISH protocol was described by Yan et al. (2020).

Statistical Analysis

Analysis of variance (ANOVA) for the phenotypic responses to two CCN species was performed considering genotype, year, CCN species, genotype by CCN species, genotype by year, year by CCN species, and genotype by year by CCN species interactions as the main factors. The ANOVA for the agronomic traits was performed comprising genotype, year, and genotype by year interaction as the main factors. The ANOVA for forage and grain quality characteristics was performed considering genotype as the main factor. The Fisher's Least Significance Difference (LSD) was used to perform multiple comparisons for differentiating the significant difference among genotypes and among plant ages (i.e., the first, second, and third-year plants) on the means of each parameters examined. Statistical analysis was performed in the IBM SPSS Statistics for Windows, Version 26.0 (IBM Corp., Armonk, NY, United States).

RESULTS

Development of the Perennial Wheats

In order to develop perennial wheats for feed and food consumption, hundreds of interspecific crosses were made in the early 2000. During the early generations from F_1 to F_3, the targets of selection focused on the traits associated with perennial growth habit, such as non-shattering heads, high fertility, and ability of regrowth in the fields. The F_1 hybrids showed a vigorous regrowth habit and were often sterile. Some F_1 plants were able to persist adequately even for more than 7 years in the field and developed numerous tillers, but only a few tillers produced viable seeds. Then, the F_2 and F_3 plants were obtained by either self-pollination or backcrossing to common wheat. However, the persisting life cycle was converted into annual growth habit in some F_2 and F_3 plants. In parallel, the F_2 plants with perennial growth habit were obtained via backcrossing to hexaploid partial amphiploid lines or *Th. intermedium*. Importantly, the fertility of the perennial plants was restored. A wide range of variation in the major agronomic traits, such as spike and seed morphology, was observed at the early generations (**Figures 2A,B**). Both spike and seed morphology in the F_2 and F_3 plants segregated for the wheat, intermediate, and wheatgrass types (**Figures 2A,B**). The intermediate and/or wheatgrass types of F_2 and F_3 plants, which exhibited regrow habit with high seed-setting rates, were selected for further selection for flowering time, plant height and agronomic performances in later generations. A total of 78 lines were obtained at the F_6 generation. Some of these lines showed perennial habit under favorable greenhouse conditions, but did not regrow when transplanted to the field, possibly due to winter killing. Whereas, a number of hybrid plants survived after experience of the hot and dry summer and harsh cold winter at the farm in Shanxi province (37.56°N, 112.68°E, 801 m als). Among them, lines SX12-480, SX12-787, SX12-1150, and SX12-1269 were able to regrow from the crowns of plants after forage removal (**Figures 2C,D**) and remained their productivity for at least 3 years (**Figure 2E**). They were selected as the perennial wheat lines for further characterization of the agronomic performances, quality characteristics, and disease resilience.

Field Resistance to CCN

The ANOVA based on the general linear (GLM) model was carried out for the number of cysts on roots of the perennial lines and the control wheat cultivar Wenmai 19 challenged by *H. avenae* and *H. filipjevi* under natural field infestation during the two growing seasons 2013–2014 and 2014–2015 (**Table 2**). The results indicated that phenotypic responses were independent of year but depended on the genotype and CCN species. The interaction effects were absent, suggesting the high heritability and consistency of the resistance.

At the field of Zhengzhou (ZZ), *H. avenae* is the main CCN species. In the growing season 2013–2014, the perennial wheat lines were highly resistant (line SX12-1269) or moderately resistant (lines SX12-480 and SX12-1150) to *H. avenae*. Although line SX12-787 displayed moderate level of susceptibility, the number of cysts (11.1 ± 3.6) was significantly lower than the susceptible control, an annual wheat cultivar Wenmai 19 (32.3 ± 5.8) ($P < 0.05$) (**Figure 3**). The field trial was repeated using the new seeds during the growing season 2014–2015 and line SX12-480 was excluded due to the very low germination rate. Lines SX12-1269 and SX12-1150 conferred moderate resistance to *H. avenae*, whereas line SX12-787 supported comparable number of cysts (23 ± 8.7) relative to that of susceptible control (23 ± 5.2) (**Figure 3**).

Upon natural infestation with *H. filipjevi* in the field of Xuchang (XC) in 2013–2014, lines SX12-480, SX12-1150, and SX12-1269 were able to mediate high levels of resistance and had significantly large impact on reducing the number of female cysts. Line SX12–787 also conferred resistance to *H. filipjevi*, but to a smaller extent (**Figure 3**). In the following year, the whole experiment was repeated using new seeds, and all the tested perennial lines were able to combat against *H. filipjevi*. In this case, SX12-1269 was highly resistant, and lines SX12-787 and SX12-1150 conferred a moderate level of resistance (**Figure 3**). Taken together, line SX12-1269 conferred high level of resistance

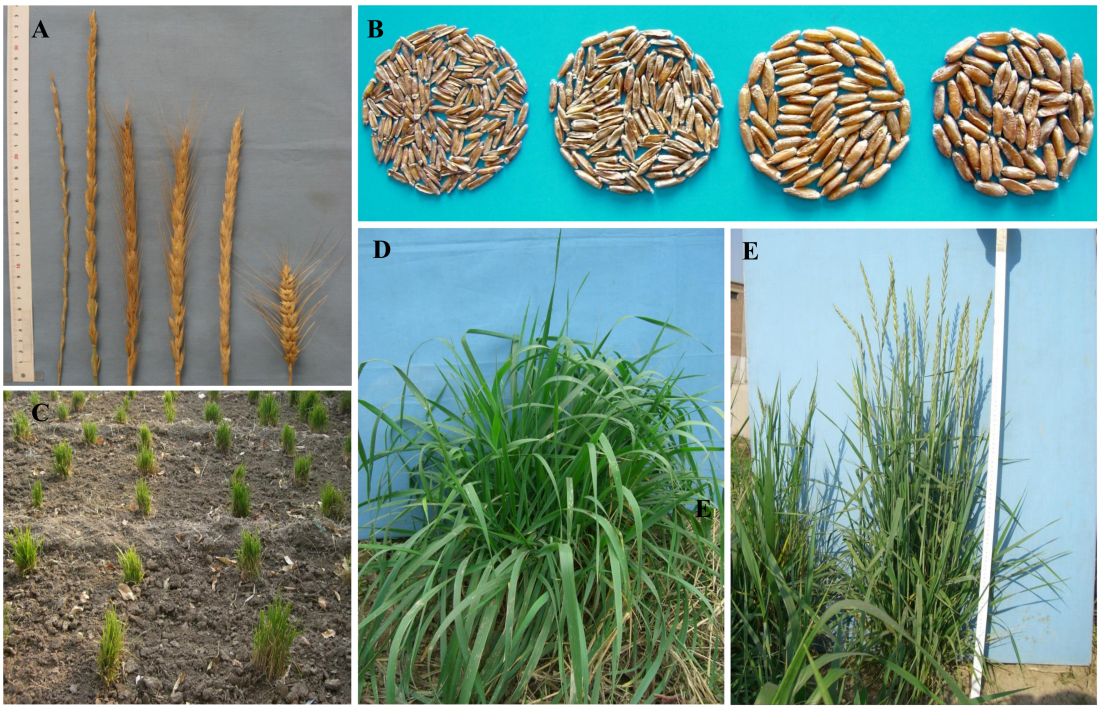

FIGURE 2 | Agro-morphological traits of the perennial lines. **(A)** Morphology segregation in spikes, from left to right *Th. intermedium* spike, four distinct progeny spikes in the F_2 and F_3 generations (wheatgrass type and three different intermediate types), and spike of common wheat cultivar. **(B)** Morphology segregation of seeds in the F_2 and F_3 generations, *Th. intermedium* (first-left) and three different types of progeny seeds (wheatgrass type and followed by two intermediate types). **(C)** Vegetative growth state after winter in April. **(D)** Regenerated vegetative growth after defoliation. **(E)** Performance at the maturity in the field.

TABLE 2 | Mean squares of the analysis of variance for the phenotypic responses to *Heterodera avenae* and *H. filipjevi* of the perennial wheat lines and the control common wheat cultivar Wenmai 19 during the growing seasons of 2013–2014 and 2014–2015.

Source of variation	df	Number of cysts
Genotype	4	633.95***
Year	1	10.24
CCN species	1	221.78**
Genotype × Year	3	40.59
Genotype × CCN species	4	29.83
Year × CCN species	1	2.94
Genotype × Year × CCN species	3	33.89

$^{**}P < 0.01$; $^{***}P < 0.001$.

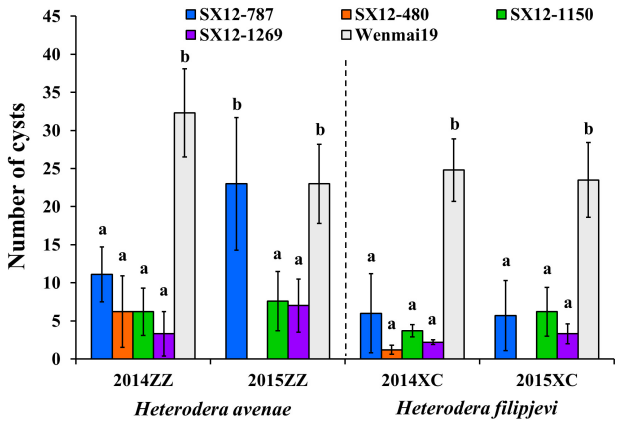

FIGURE 3 | Phenotypic responses of perennial wheat lines SX12-480, SX12-787, SX12-1150, and SX12-1269 and the annual wheat cultivar Wenmai 19 to *Heterodera avenae* (ZZ) and *H. filipjevi* (XC) in the field of Zhengzhou (ZZ) and Xuchang (XC), respectively, based on the number of white females (cysts) during the two growing seasons 2013–2014 and 2014–2015. Bars with the same letters are not significantly different at $P < 0.05$.

against the two distinct CCN species in the field infestations, and the other lines were also able to produce significantly fewer white females on the roots than the susceptible wheat control Wenmai 19 ($P < 0.05$).

Evaluation of Agronomic Traits and Grain Yield Components

The ANOVA based on the GLM was carried out for plant height, spike length, number of spikelets per spike, and thousand-kernel weight of the perennial lines and the control perennial wheat cultivar MT-2 during the three consecutive years from 2011 to 2014 (**Table 3** and **Figure 4**). Genotype and year were the determining factors of the differences in the four agronomic traits. The interaction effect of genotype by year was absent in plant height, spike length, and number of spikelets per spike,

TABLE 3 | Mean squares of the analysis of variance for agronomic traits and grain yield components of perennial wheat lines and the control perennial wheat cultivar Montana-2 during three growing seasons of 2011–2012, 2012–2013, and 2013–2014 representing the one-year-old, 2-year-old, and 3-year-old plants.

Source of variation	df	Plant height	Spike length	Number of spikelets per spike	Thousand-kernel weight
		cm	cm		g
Genotype	4	474.47***	28.81**	68.26***	99.29***
Year	2	556.63***	29.91*	82.47***	43.69***
Genotype × Year	8	24.7	1.82	7.02	9.62**

*$P < 0.05$; **$P < 0.01$; ***$P < 0.001$.

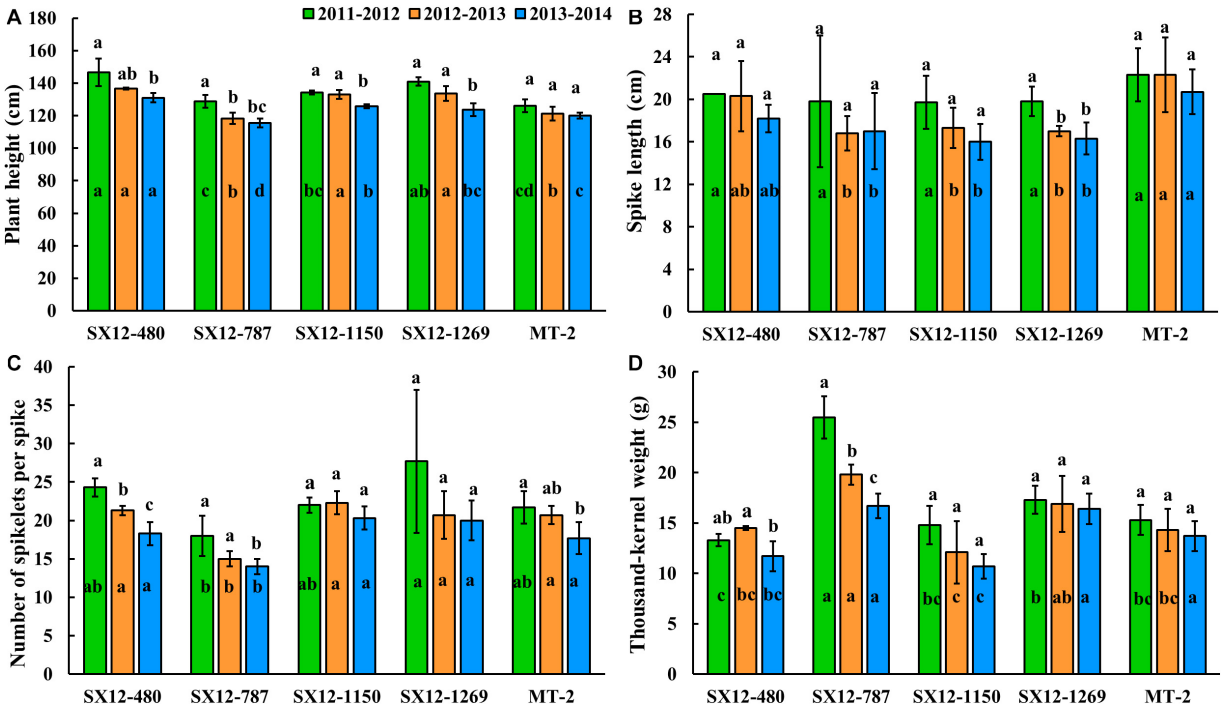

FIGURE 4 | Assessment of agronomic traits including **(A)** plant height and **(B)** spike length and yield components including **(C)** number of spikes per spike and **(D)** thousand-kernel weight of perennial wheat lines developed from present study and the control perennial cultivar Montana-2 over the three growing seasons 2011–2012, 2012–2013, and 2013–2014 in Shanxi province, China. For each factor per growing season, different letters inside bars indicate a significant different among lines using the Fisher's LSD ($P < 0.05$). For the tested variables of each line, different letters above bars represent difference among growing seasons ($P < 0.05$).

highlighting the high heritability of these traits. However, the significant difference in thousand-kernel weight was due to the factor of genotype by year interaction (**Table 3**). Lines SX12-480 and SX12-1269 (133.7–146.7 cm for plant height) were significantly taller than the other lines and the control MT-2 ($P < 0.05$) (**Figure 4A**). There was no significant difference on spike length among the four lines and MT-2 in their first growing season. In the second and third years, MT-2 and SX12-480 bore longer spikes (**Figure 4B**). Compared to MT-2, the four perennial lines produced comparable number of spikelets per spike across all the three growing seasons. Although not significant, improved number of spikelets per spike were found in lines SX12-1269, SX12-480, and SX12-1150 (**Figure 4C**). Furthermore, line SX12-787 stood out at all the growing seasons for the significantly higher thousand-kernel weight than those of the other lines ($P < 0.05$) (**Figure 4D**).

In parallel, to understand the grain yield consistency of perennial lines, a multi-year field study was conducted to compare the agronomic performance of the one-year old plants to the 2- and 3-year old ones (**Figure 4**). Comparing to the first-year plants, the 2-year old plants generally showed congruous plant height. However, the 3-year old plants of four perennial lines reduced their height to a significant extent except MT-2 (**Figure 4A**). Such a trend was also observed for number of spikelets per spike and thousand-kernel weight. Spikelet number and thousand-kernel weight were comparable over 2 years in all the lines tested. When plant life span extended, spikelet number and thousand-kernel weight declined remarkably. It is noteworthy that lines SX12-1150 and SX12-1269 maintained their productivity over plant age by producing comparable number of spikelets and thousand-kernel weight (**Figures 4C,D**). Generally, the perennial wheat lines displayed a reduction in yield

potential with an effect of plant age. Climate variability over years might also have consequences on yield potential. It was difficult to separate the effects of weather fluctuations over years from the age of the plants.

Assessments of Forage and Grain Quality-Related Characteristics of the Perennial Wheat Lines

The first-year perennial lines, intermediate wheatgrass and an annual wheat cultivar Jinchun 9 were evaluated in the form of crude protein, crude fat, crude fiber content, the amino acid profile and the micronutrient contents (**Tables 4**, **5** and **Figure 5**).

Forage harvested from the perennial lines had comparable concentrations of crude protein (96.9–99%), crude fat (75.1–101.6%), and crude fiber (95.4–96.4%) with those obtained from the commercial perennial wheat cultivar MT-2 (**Table 4**). The levels of crude protein and crude fat in grains varied tremendously between the perennial plants and those produced from the annual wheat cultivar Jinchun 9. These values in the perennial grains were 168–196% and 181–198% higher than those in Jinchun 9. Variability was found within the perennial genotypes. Although not significant, improved levels of both crude protein and crude fat comparing with MT-2 were found in all four perennial wheat lines.

Micronutrient concentrations for phosphorus (P) and carotene were found to be higher in the defoliated grass of perennial wheat lines SX12-1150 and SX12-787 than those produced from MT-2. Iron (Fe) level was enormously improved in the perennial lines compared to their perennial donor, *Th. intermedium*. Oppositely, forage obtained from *Th. intermedium* was a better source of selenium (Se). The concentrations of P and Se in the perennial grains were significantly richer than in the annual grains ($P < 0.05$). Among the perennial lines, SX12-480 was particularly intriguing due to high P and Se concentrations in grains and was significantly more than those in MT-2 (**Table 4**). Variation in Fe content was found among the perennial lines. Although not significant, high Fe concentration was observed in lines SX12-787 and SX12-480.

The essential amino acid contents of forage remained generally consistent among the perennial genotypes and wheatgrass, with only a few detectable differences (**Figure 5A**). Line SX12-1150 was characterized by significantly higher levels in histidine, but lower in lysine than that of the other tested lines ($P < 0.05$). Line SX12-787 was slightly lower in histidine and had significantly higher level in lysine. Wheatgrass was a great source of valine, phenylalanine and leucine (**Figure 5A**). When it came to the amino acid profile in grains, the perennial wheat lines were generally richer in comparison with those in MT-2. The increase in amino acid content ranged from 115.9 to 143.2% in histidine, 129.7 to 135.1% in isoleucine, 128.1 to 135.6% in leucine, 133.9 to 321.4% in lysine, 126.9 to 131.6% in methionine, 104.3 to 126.7% in phenylalanine, 132.3 to 193.5% in threonine, and 96.6 to 135.9% in valine (**Figure 5B**). There was a great variation found among the lines examined. Line SX12-1150 stood out for the highest contents in six out of eight tested essential amino acids including histidine, isoleucine, leucine, methionine,

TABLE 4 | Nutritive and quality characteristics of forage and grain from perennial wheat lines, *Thinopyrum intermedium* and annual wheat cultivar Jinchun 9 during the growing season 2011–2012.

Quality trait	Forage				Grain				
	Th. intermedium	MT-2	SX12-1150	SX12-787	Jinchun 9	MT-2	SX12-1150	SX12-787	SX12-480	SX12-1269
Crude protein (%)	–	19.53^{a}	18.93^{a}	19.34^{a}	12.90^{b}	21.03^{a}	25.21^{a}	21.73^{a}	25.22^{a}	22.37^{a}
Crude fat (%)	–	3.70^{ab}	3.76^{b}	2.78^{a}	1.60^{b}	2.81^{a}	3.17^{a}	3.03^{a}	3.06^{a}	2.90^{a}
Crude fiber (%)	–	21.88^{a}	20.88^{a}	21.09^{a}	–	–	–	–	–	–
Phosphorus	–	0.18%^{a}	0.2%^{ab}	0.24%^{b}	2410.00 mg/kg^{c}	–	3037.5 mg/kg a	3063.2 mg/kg a	3211.8 mg/kg b	3102.00 mg/kg^{a}
Iron (mg/kg)	137.00^{a}	223.00^{b}	241.00^{b}	151.00^{a}	–	59.00^{ab}	59.00^{ab}	63.00^{ab}	64.00^{b}	48.00^{a}
Selenium (mg/kg)	0.71^{b}	0.34^{a}	0.37^{a}	0.40^{a}	0.26^{a}	0.27^{a}	0.33^{ab}	0.36^{ab}	0.38^{b}	0.31^{ab}
Carotene (mg/100 g)	–	8.98^{a}	16.85^{b}	9.85^{a}	–	–	–	–	–	–

–, *missing value. Different letters in a row within each factor (forage and grain) indicate a significant difference using the Fisher's LSD ($P < 0.05$).*

TABLE 5 | Non-essential amino acid profile of forage and grains derived from the perennial wheat lines, the control MT-2, and *Thinopyrum intermedium*.

Amino acid (%)	Forage				Grain				
	Th. intermedium	MT-2	SX12-1150	SX12-787	MT-2	SX12-1150	SX12-787	SX12-480	SX12-1269
Alanine	0.75^{a}	1.11^{b}	1.19^{b}	1.24^{b}	0.70^{a}	0.98^{b}	0.8^{ab}	0.94^{b}	0.85^{ab}
Arginine	0.95^{a}	0.98^{a}	1.33^{b}	1.03^{a}	0.84^{a}	1.30^{b}	1.11^{a}	1.28^{b}	1.22^{b}
Aspartic acid	0.92^{a}	1.77^{b}	1.66^{b}	1.85^{b}	0.91^{a}	1.37^{b}	1.22^{ab}	1.30^{b}	1.09^{ab}
Cystine	0.54^{d}	0.00^{a}	0.27^{c}	0.21^{b}	0.44^{a}	0.52^{a}	0.50^{a}	0.55^{a}	0.45^{a}
Glutamic acid	6.94 b	2.58^{a}	2.41^{a}	2.43^{a}	6.22^{a}	8.76^{b}	7.39^{ab}	8.25^{ab}	8.29^{ab}
Glycine	0.79^{a}	0.92^{a}	0.92^{a}	0.96^{a}	0.73^{a}	1.06^{b}	0.91^{ab}	1.00^{b}	0.88^{ab}
Proline	2.47 c	1.65^{b}	1.21^{a}	1.78^{b}	2.49^{a}	2.94^{a}	2.23^{a}	2.79^{a}	2.73^{a}
Serine	1.05^{b}	0.75^{a}	0.82^{a}	0.85^{a}	0.98^{b}	1.37^{c}	0.74^{ab}	1.30^{c}	0.67^{a}
Tyrosine	0.42^{a}	0.39^{a}	0.37^{a}	0.42^{a}	0.56^{a}	0.50^{a}	0.58^{a}	0.54^{a}	0.62^{a}

Different letters in a row within each factor (forage and grain) indicate a significant difference using the Fisher's LSD ($P < 0.05$).

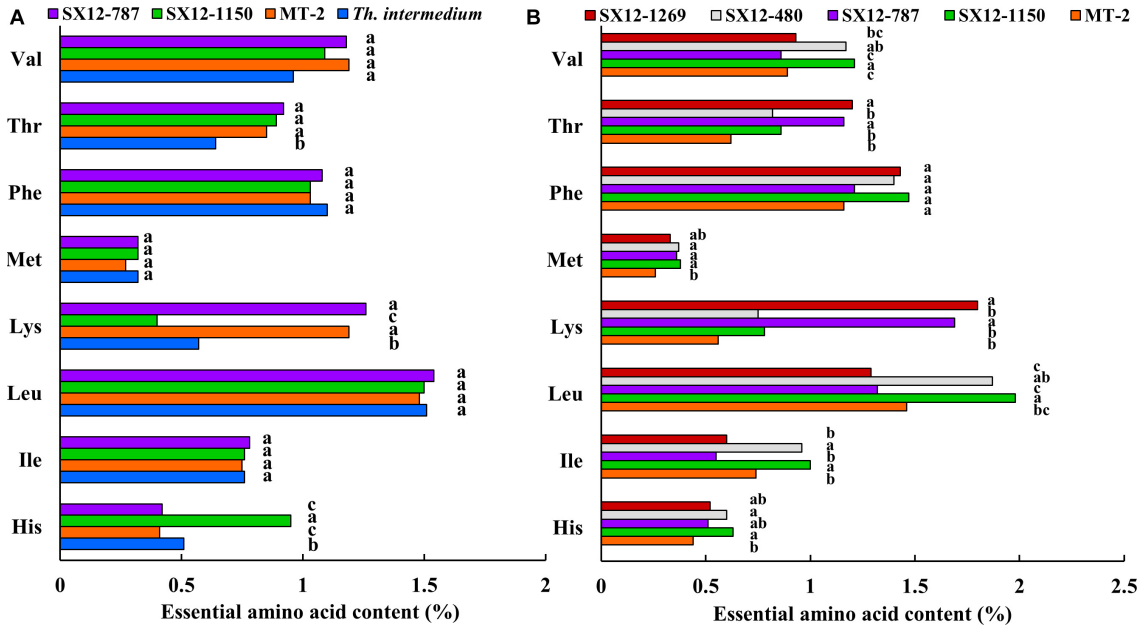

FIGURE 5 | Essential amino acid content of forage and grain from perennial wheat lines and wheatgrass *Th. intermedium* during the growing season 2011–2012. Different letters next to the bars indicate a significant difference using the Fisher's LSD ($P < 0.05$). Amino acid 3-letter codes, Val, valine; Leu, leucine; Ile, isoleucine; Phe, phenylalanine; His, histidine; Lys, lysine; Met, methionine; Thr, threonine. **(A)** Essential amino acid content of forage. **(B)** Essential amino acid content of grain.

phenylalanine, and valine. Line SX12-787 was significantly higher in lysine and threonine than the control MT-2 ($P < 0.05$), whereas isoleucine content was the lowest. Line SX12-1269 had the highest level of lysine and threonine, but leucine level was found to be the lowest. Line SX12-480 ranked in the middle grades in the essential amino acid profile among the perennial lines (**Figure 5B**).

Furthermore, the non-essential amino acid profile was determined in both forage and grains obtained from the perennial lines and compared with the control MT-2 and *Th. intermedium* (**Table 5**). The intermediate wheatgrass had a great potential to the improvement of nutritional values, particularly the concentrations of cystine, glutamic acid, proline, and serine in the forage (**Table 5**). Line SX12-1150 had significantly higher amounts of arginine and cystine in the defoliated grass than those produced from the control MT-2 ($P < 0.05$). Moreover, grains harvested from SX12-1150 were the best sources of alanine, arginine, aspartic acid, glutamic acid, glycine, proline, and serine, which covers majority, if not all, of the non-essential amino acids (**Table 5**).

Molecular and Cytogenetic and Characterization of the Perennial Wheat Lines

The parental genotype *Th. intermedium*, common wheat cultivar Chinese Spring, and the four perennial wheat lines SX12-480, SX12-787, SX12-1150, and SX12-1269 were genotyped using the E and St genome-specific molecular markers. The perennial wheat lines produced the similar diagnostic band of 277-bp

in size with universal E genome marker 2P1/2P2 as their *Th. intermedium* parent, confirming the presence of the wheatgrass chromatin in their genomes. The common wheat cultivar Jinchun 9 did not amplify any of the fragments, indicating the absence of wheatgrass chromatin (**Figure 6A**). All the four perennial wheat lines produced an E genome–specific amplicon of 151-bp in size with marker *Xedm28* (located on 2ES and 3EL) (**Figure 6B**). Besides, all the four lines had chromosome 7E identified by 7ES and 7EL genome–specific amplification of markers *Xedm16* and *Xedm105*, which amplified the expected 165- and 237-bp bands, respectively (**Figures 6C,D**). Marker *SCAR-1248* produced an St genome–specific amplicon of 850-bp in the four lines, indicating that these materials contained the St-genome chromatins (**Figure 6E**).

GISH analysis was applied using the *Th. intermedium* total genomic DNA as a probe and the Chinese Spring total genomic DNA as a blocker to detect the *Th. intermedium* chromosomes in the perennial wheat lines. Lines SX12-787 and SX12-1150 had a mitotic chromosome number of 2n = 56. Fourteen chromosomes showed lilac-pink fluorescence signals, and 42 chromosomes were counterstained with blue fluorescence signals, indicating that both SX12-787 and SX12-1150 contained 14 *Th. intermedium* chromosomes and 42 wheat chromosomes (**Figures 7A,B**). Lines SX12-480 and SX12-1269 contained 48 and 54 chromosomes, respectively. Based on the fluorescence patterns on chromosomes, line SX12-480 (2n = 48) had 16 chromosomes originated from *Th. intermedium* and the other 32 chromosomes belonged to wheat (**Figure 7C**). In line SX12-1269 (2n = 54), there were 12 *Th. intermedium* chromosomes and 42 wheat chromosomes (**Figure 7D**).

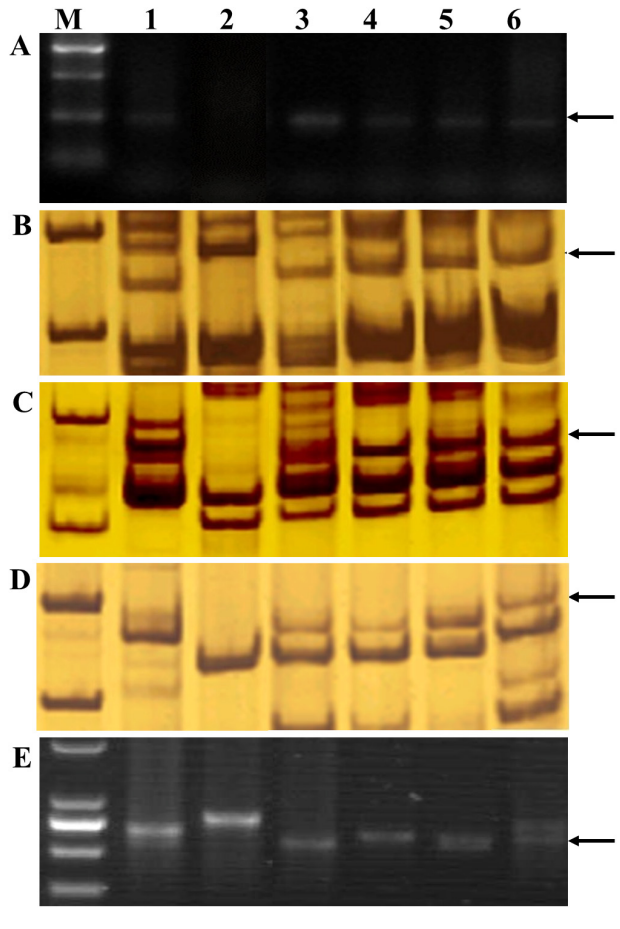

FIGURE 6 | PCR amplification of alien chromosome specific markers **(A)** 2P1/2P2 (repetitive DNA sequence from *Th. elongatum*), **(B)** SSR-*Xedm28* (chromosomes 2ES and 3EL), **(C)** SSR-*Xedm16* (chromosome 7ES), **(D)** SSR-*Xedm105* (chromosome 7EL), and **(E)** *SCAR-1248* (St-genome specific marker). Lanes M, DNA size ladder; 1, *Th. intermedium*; 2, wheat cultivar Chinese Spring; 3, SX12-1150; 4, SX12-480; 5, SX12-1269; 6, SX12-787. Arrows indicate the diagnostic amplification products.

DISCUSSION

Four dual-use perennial lines were developed, which displayed persistent regrowth capability for at least 3 years. Post-harvest regrowth habit allowed to test the hypothesis that perennial grain yield potential declines with increase of plant age. The perennial wheat lines exhibited promising resistance against the parasite cyst nematode *H. avenae* and *H. filipjevi*. These lines were characterized by their superior amino acid contents, and other nutrient compositions such as crude protein, crude fat, P, and Se for both forage and grain over the common wheat control.

The agronomic potential of perennial wheat lines was studied over 3 years, as grain yield may decrease over plant age. Plant height and the grain yield components (i.e., number of spikelets per spike for line SX12-480 and thousand-kernel weight for line SX12-787) for the 3-year-old perennial genotypes relative to one- or 2-year-old genotypes were lower in general. However, spike length and the yield components (i.e., number of spikelets per spike and thousand-kernel weight) remained consistent over time in the perennial wheat lines SX12-1150 and SX12-1169. In many cases, yield declines have been observed in perennial cereals (Tautges et al., 2018), although a number of perennial genotypes showed the consistency in yield components over several years (Jaikumar et al., 2012), or even increases in grain yield (Hayes et al., 2012). The decline of grain yields in 2-year-old plants reflected plant age effect on yield components (Jaikumar et al., 2012). Fundamentally, grain yield penalty over plant ages in perennial plants is associated with trade-off between reproduction and post-harvest regrowth. Perennial plants allocate more resources below ground for extending life span even under harsh environmental conditions and less to seed/grain production (Jaikumar et al., 2012; Vico et al., 2016). Combining consistent grain yield potential with persistent post-harvest regrowth habit may be challenging in perennial wheat breeding programs. Instead, breeding efforts could focus on increasing forage biomass production in order to offset the age-related decline in grain yield.

The generally lower yield potential of the 3-year-old plants was not surprising given the other important fact as the accumulation of (root) pathogens, such as foot rot [caused by *F. culmorum* (W.G. Smith) Sacc.], crown rot (caused by *F. pseudograminearum*

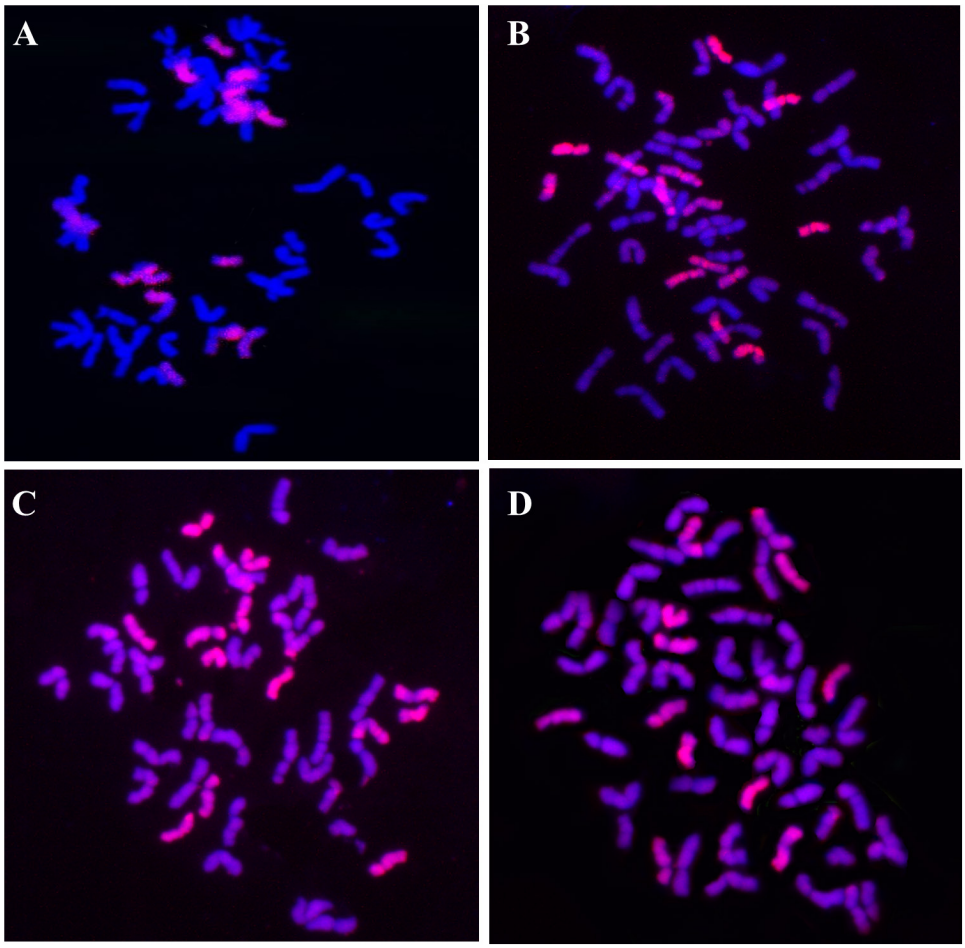

FIGURE 7 | GISH patterns of root-tip cells of the four perennial wheat lines probed with the *Th. intermedium* genomic DNA and blocked with the Chinese Spring genomic DNA. The *Th. intermedium* and wheat chromosomes showed lilac-pink color and blue color, respectively. **(A)** SX12-787, 2n = 56, 14 *Th. intermedium* chromosomes and 42 wheat chromosomes. **(B)** SX12-1150, 2n = 56, 14 *Th. intermedium* chromosomes and 42 wheat chromosomes. **(C)** SX12-480, 2n = 48, 16 *Th. intermedium* chromosomes and 32 wheat chromosomes. **(D)** SX12-1269, 2n = 54, 12 *Th. intermedium* chromosomes and 42 wheat chromosomes.

O'Donnell & T. Aoki), common root rot [caused by *Cochliobolus sativus* (Ito & Kuribayashi) Drechs. ex Dastur], and damping-off/root rot (caused by *Pythium* spp.) (Bell et al., 2010; Jaikumar et al., 2012). The epidemic of plant disease in annual crops always dies out after a few months, till host plant harvest/die; however, this is not the case for the perennial plants. After harvest, plant residues left on the soil surface may result in increase of soil moisture and decrease of soil temperatures, which promote growth of soilborne pathogens (Bockus and Shroyer, 1998). Cox et al. (2005) found that perennial wheat lines were highly susceptible to take-all (caused by *Gaeumannomyces graminis* var. *tritici* J. Walker), resulting in large amount of biomass loss. Little information has been available on the resistance to common root pathogens and pests in perennial donors, as well as their derivatives. So far, only few screening has been publicly available on the phenotypic responses of wheat-*Thinopyrum* hybrids to CCN (Li et al., 2012). The wheat-*T. intermedium* derivatives were found to be the most resistant group of lines against *H. filipjevi* among the germplasm tested in that study including wheat-*Th. ponticum* derivatives and common wheat cultivars. It should be noted that the perennial wheat-*Th. intermedium* lines in our study displayed consistent resistance to both CCN species *H. avenae* and *H. filipjevi*, which could suppress the multiplication of CCN in the soil.

During the last decades, the mineral and protein concentrations of annual wheat cultivars have shown a continuous decline coinciding with the significantly increased grain yield (Fan et al., 2008). Common wheat cultivars are known to be low in content of some essential amino acids, especially lysine and threonine, the two most deficient amino acids (Abdel-Aal and Sosulski, 2001; Horvatić and Ereš, 2002). An effective method to counteract micronutrient malnutrition is to exploit the genetic variation of overall micronutrient availability in the wild wheat relatives and develop cultivars with enhanced nutritional values (Monasterio and Graham, 2000; Murphy et al., 2009). Wild relatives of wheat, such as *Th. intermedium* and *Th. elongatum* (Host) D. R. Dewey, are well-known for their beneficial characteristics including improved nutritional values

(Murphy et al., 2009; Tyl and Ismail, 2019). The wide adaptation of *Th. intermedium* and *Th. elongatum* in hybrid breeding was contributed by their superior end-use quality and nutritional profile. Partial amphiploids derived from different *Thinopyrum* species were found to have higher levels of carotenoids, soluble polyphenols, alkilresorcinols, and better gluten digestibility than common wheat (Gazza et al., 2016). *Thinopyrum intermedium* seed was reported to have a higher concentration of protein and almost all essential amino acids than wheat (Marti et al., 2015). The superiority of *Th. intermedium* over common wheat was highlighted in terms of protein and fiber contents (Marti et al., 2015). Notably, mineral nutrient concentrations and chemical compositions in the newly developed perennial wheat lines were better than the annual cultivar Jinchun 9 for crude protein, crude fat, P, and Se. The perennial wheat lines, in particular, SX12-787 and SX12-1269, were superior in the improvement of wheat nutritive level.

Perennial growth habit is a quantitative trait and is mediated by multiple genes on different alien chromosomes (Cox et al., 2006; Dehaan et al., 2014). The genetic control is not fully exploited yet and one of the loci involved in this post-harvest regrowth capacity is mapped on chromosome 4E of *Th. elongatum* (Lammer et al., 2004). It is particularly worthy of mention that lines SX12-480, SX12-1150, and SX12-1269 persisted to post-harvest regrowth over three to five successive years in the field (unpublished data). GISH patterns showed the presence of 12-16 intact alien chromosomes in the perennial lines. The amplification profiles of the markers specified alien introgression of chromosomes 2ES, 3EL, 7ES, and 7EL in the four perennial wheat lines. Although speculating, whether the perennial regrowth habit is linked to these alien introgression remains to be determined. The first consensus genetic map of *Th. intermedium* has already been available (Kantarski et al., 2017), which provides a valuable tool for wheat breeders to map CCN-resistant gene(s) and the key players involved in the post-harvest regrowth trait.

The perennial wheat generally has unique morphological traits that are quite divergent from annual wheat. Usually, the wild perennial species have performed poorly for some domestication traits, such as small spike and seed size, which need to be rectified in perennial wheat varieties (Davies and Hillman, 1992; Kantar et al., 2016). Common wheat cultivars have a range of thousand-kernel weight from 35.2 to 40.3 g, while approximate 5.9–7.8 g is found for the *Th. intermedium* entries (Larkin et al., 2014). Thousand-kernel weight of the perennial wheat line SX12-787 was as high as 25.5 g in the first year and the other perennial wheat lines yielded a range from 12.1 to 17.3 g (**Figure 4**). The increase in grain weight is probably attributed to the selection criteria in the early generations in which intermediate type of the F_2 and F_3 derivatives were selected for advancing to next generations (**Figures 2A,B**). However, the second year thousand-kernel weight varied from that of the first year, which was consistent with previous research by Hayes et al. (2018). Further research is needed to investigate the relationship of grain yields among the 3 years of harvest and develop better adapted perennial wheat that combined the grain yield and perennial habit. Besides, the four perennial wheat lines were tall in plant height (118.3–146.7 cm). This trait is known to closely relate to forage biomass (Trotter and Frazier, 2008).

CONCLUSION

We have developed four perennial wheat-*Th. intermedium* lines, which showed the remarkable capability to regenerate and persist at least 3 years in the field. Promising resistance was identified to both species of *H. avenae* and *H. filipjevi* that are prevalent in China in these lines. They had superior amino acids and other nutrient compositions for forage and grain over the common wheat control. Analyses of *Thinopyrum* genome-specific molecular marker and GISH indicated that these lines had 12–16 *Thinopyrum* chromosomes. Currently, these perennial wheat lines have been evaluating at multiple geographic locations to test their adaptability to different harsh environments. Meanwhile, new perennial wheat lines are being made using these lines as parents. The development of perennial species has been proposed as an approach to improve the sustainability of agriculture, conserving natural resources while producing food and forage.

DATA AVAILABILITY STATEMENT

The datasets generated for this study are included in the article or are available on request to the corresponding authors.

AUTHOR CONTRIBUTIONS

LC and YS conceived and designed the research. LC, YR, YZ, QG, ZT, YN, WY, and YS conducted the experiments and analyzed the data. LC and HL wrote the manuscript. All authors contributed to the article and approved the submitted version.

FUNDING

This work was supported by the Doctoral Science Foundation of Shanxi Agricultural University (YBSJJ1808), the Agricultural Sci-Tech Innovation Research Program of Shanxi Agricultural University (YGJPY2002), the Key Research and Development Projects of Shanxi Province (201903D221094, 201903D211003, and 201903D211004-2), National Key Research and Development Project (2017YFD0101002), and the Agricultural Science and Technology Innovation Program of CAAS.

ACKNOWLEDGMENTS

The authors thank Prof. Honglian Li, College of Plant Protection, Henan Agricultural University, for his support with CCN disease assay.

REFERENCES

Abdel-Aal, E. S. M., and Sosulski, F. W. (2001). Bleaching and fractionation of dietary fiber and protein from wheat-based stillage. *LWT-Food Sci. Technol.* 34, 159–167. doi: 10.1006/fstl.2000.0741

Armstrong, J. M. (1936). Hybridization of triticum and Agropyron: I. Crossing results and description of the first generation hybrids. *Can. J. Res.* 14, 190–202. doi: 10.1139/cjr36c-016

Banyer, R. J., and Fisher, J. M. (1971). Seasonal variation in hatching of eggs of Heterodera avenae. *Nematologica* 17, 225–236. doi: 10.1163/187529271X00071

Bell, L. W., Wade, L. J., and Ewing, M. A. (2010). Perennial wheat: a review of environmental and agronomic prospects for development in Australia. *Crop Pasture Sci.* 61, 679–690. doi: 10.1071/CP10064

Bockus, W. W., and Shroyer, J. P. (1998). The impact of reduced tillage on soilborne plant pathogens. *Annu. Rev. Phytopathol.* 36, 485–500. doi: 10.1146/annurev.phyto.36.1.485

Cox, C. M., Garrett, K. A., Cox, T. S., Bockus, W. W., and Peters, T. (2005). Reactions of perennial grain accessions to four major cereal pathogens of the Great Plains. *Plant Dis.* 89, 1235–1240. doi: 10.1094/PD-89-1235

Cox, C. M., Murray, T. D., and Jones, S. S. (2002). Perennial wheat germplasm lines resistant to eyespot, Cephalosporium stripe, and wheat streak mosaic. *Plant Dis.* 86, 1043–1048. doi: 10.1094/PDIS.2002.86.9.1043

Cox, T. S., Glover, J. D., David, L., Cox, C. M., and DeHaan, L. R. (2006).). Prospects for developing perennial grain crop. *Bioscience* 56, 649–658. doi: 10.1641/0006-3568(2006)56[649:pfdpgc]2.0.co;2

Cui, L., Qiu, D., Sun, L., Sun, Y., Ren, Y. K., Zhang, H. J., et al. (2020). Resistance to *Heterodera filipjevi* and *H. avenae* in winter wheat is conferred by different QTL. *Phytopathology* 110, 472–482. doi: 10.1094/PHYTO-04-19-0135-R

Cui, L., Ren, Y. K., Murray, T. D., Yan, W. Z., Guo, Q., Niu, Y., et al. (2018). Development of perennial wheat through hybridization between wheat and wheatgrasses: a review. *Engineering* 4, 507–513. doi: 10.1016/j.eng.2018.07.003

Cui, L., Sun, L., Gao, X., Song, W., Wang, X. M., Li, H. L., et al. (2016). The impact of resistant and susceptible wheat cultivars on the multiplication of *Heterodera filipjevi* and *H. avenae* in parasite-infested soil. *Plant Pathol.* 65, 1192–1199. doi: 10.1111/ppa.12495

Culman, S. W., Snapp, S. S., Ollenburger, M., Basso, B., and DeHaan, L. R. (2013). Soil and water quality rapidly responds to the perennial grain Kernza wheatgrass. *Agron. J.* 105, 735–744. doi: 10.2134/agronj2012.0273

Davies, M. S., and Hillman, G. C. (1992). "Domestication of cereals," in *Grass Evolution and Domestication*, ed. G. P. Chapman (Cambridge: Cambridge University Press), 199–244.

Dehaan, L. R., Van Tassel, D. L., and Cox, T. S. (2014). Perennial grain crops: a synthesis of ecology and plant breeding. *Renew. Agric. Food Syst.* 20, 5–14. doi: 10.1079/RAF200496

Fan, M. S., Zhao, F. J., Fairweather-Tait, S. J., Poulton, P. R., Dunham, S. J., and McGrath, S. P. (2008). Evidence of decreasing mineral density in wheat grain over the last 160 years. *J. Trace Elem. Med. Biol.* 22, 315–324. doi: 10.1016/j.jtemb.2008.07.002

Fedak, G., and Han, F. P. (2005). Characterization of derivatives from wheat-Thinopyrum wide crosses. *Cytogenet. Genome Res.* 109, 360–367. doi: 10.1159/000082420

Fu, B., Yuan, H. X., Zhang, Y., Hou, X. S., Nian, G. L., Zhang, P., et al. (2011). Molecular characterisation of cereal cyst nematodes in winter wheat on the Huang-Huai floodplain of China using RFLP and rDNA-ITS sequence analyses. *Australas. Plant Pathol.* 40, 277–285. doi: 10.1007/s13313-011-0043-0

Fulton, T. M., Chunwongse, J., and Tanksley, S. D. (1995). Microprep protocol for extraction of DNA from tomato and other herbaceous plants. *Plant Mol. Biol. Rep.* 13, 207–209. doi: 10.1007/BF02670897

Gazza, L., Galassi, E., Ciccoritti, R., Cacciatori, P., and Pogna, N. E. (2016). Qualitative traits of perennial wheat lines derived from different *Thinopyrum* species. *Genet. Resour. Crop Evol.* 63, 209–219. doi: 10.1007/s10722-015-0240-8

Hayes, R. C., Newell, M. T., DeHaan, L. R., Murphy, K. M., Crane, S., Norton, M. R., et al. (2012). Perennial cereal crops: an initial evaluation of wheat derivatives. *Field Crops Res.* 133, 68–89. doi: 10.1016/j.fcr.2012.03.014

Hayes, R. C., Wang, S., Newll, M. T., Turner, K., Larsen, J., Gazza, L., et al. (2018). The performance of early-generation perennial winter cereals at 21 sites across four continents. *Sustainability* 10:1124. doi: 10.3390/su10041124

Horvatić, M., and Ereš, M. (2002). Protein nutritive quality during production and storage of dietetic biscuits. *J. Sci. Food Agric.* 82, 1617–1620. doi: 10.1002/jsfa.1204

Hu, L. J., Li, G. R., Zhan, H. X., Liu, C., and Yang, Z. J. (2012). New St-chromosome-specific molecular markers for identifying wheat–*Thinopyrum intermedium* derivative lines. *J. Genet.* 91, e69–e74. doi: 10.1007/s12041-012-0158-2

Jaikumar, N. S., Snapp, S. S., Murphy, K., and Jones, S. S. (2012). Agronomic assessment of perennial wheat and perennial rye as cereal crops. *Agron. J.* 104, 1716–1726. doi: 10.2134/agronj2012.0291

Jauhar, P. P., Peterson, T. S., and Xu, S. S. (2009). Cytogenetic and molecular characterization of a durum alien disomic addition line with enhanced tolerance to Fusarium head blight. *Genome* 52, 467–483. doi: 10.1139/G09-014

Kantar, M. B., Tyl, C. E., Dorn, K. M., Zhang, X., Jungers, J. M., Kaser, J. M., et al. (2016). Perennial grain and oilseed crops. *Annu. Rev. Plant Biol.* 67, 703–729. doi: 10.1146/annurev-arplant-043015-112311

Kantarski, T., Larson, S., Zhang, X., DeHaan, L., Borevitz, J., Anderson, J., et al. (2017). Development of the first consensus genetic map of intermediate wheatgrass (*Thinopyrum intermedium*) using genotyping-by-sequencing. *Theor. Appl. Genet.* 130, 137–150. doi: 10.1007/s00122-016-2799-7

Lammer, D., Cai, X. W., Arterburn, M., Chatelain, J., Murray, T., and Jones, S. (2004). A single chromosome addition from *Thinopyrum elongatum* confers a polycarpic, perennial habit to annual wheat. *J. Exp. Bot.* 55, 1715–1720. doi: 10.1093/jxb/erh209

Larkin, P. J., Newell, M. T., Hayes, R. C., Aktar, J., Norton, M. R., Moroni, S. J., et al. (2014). Progress in developing perennial wheats for grain and grazing. *Crop Pasture Sci.* 65, 1147–1164. doi: 10.1071/CP13330

Li, H. J., Arterburn, M., Jones, S. S., and Murray, T. D. (2005). Resistance to eyespot of wheat, caused by Tapesia yallundae, derived from *Thinopyrum intermedium* homoeologous group 4 chromosome. *Theor. Appl. Genet.* 111, 932–940. doi: 10.1007/s00122-005-0025-0

Li, H. J., Cui, L., Li, H. L., Wang, X. M., Murray, T. D., Conner, R. L., et al. (2012). Effective resources in wheat and wheat-Thinopyrum derivatives for resistance to *Heterodera filipjevi* in China. *Crop Sci.* 52, 1209–1217. doi: 10.2135/cropsci2011.11.0591

Li, H. J., and Wang, X. M. (2009). *Thinopyrum ponticum* and *T. intermedium*: the promising source of resistance to fungal and viral diseases of wheat. *J. Genet. Genomics* 36, 557–565. doi: 10.1016/S1673-8527(08)60147-2

Marti, A., Qiu, X., Schoenfuss, T. C., and Seetharaman, K. (2015). Characteristics of perennial wheatgrass (*Thinopyrum intermedium*) and refined wheat flour blends: impact on rheological properties. *Cereal Chem.* 92, 434–440. doi: 10.1094/CCHEM-01-15-0017-R

Ministry of Agriculture and Rural Affairs of the People's Republic of China (1982). *Agricultural Industry Standard (NY/T)3-1982 Method for Determination of Crude Protein in Cereals and Beans Seeds (semi-micro Kjeldahl method)*. Avaliable at: http://english.agri.gov.cn/ (accessed January 14, 2013).

Monasterio, I., and Graham, R. D. (2000). Breeding for trace minerals in wheat. *Food Nutr. Bull.* 21, 392–396. doi: 10.1177/156482650002100409

Mujoriya, R., and Bodla, R. B. (2011). A study on wheat grass and its nutritional value. *Food Sci. and Qual. Manag.* 2, 1–8. doi: 10.7176/FSQM

Mullan, D. J., Platteter, A., Teakle, N. L., Appels, R., Colmer, T. D., Anderson, J. M., et al. (2005). EST-derived SSR markers from defined regions of the wheat genome to identify Lophopyrum elongatum specific loci. *Genome* 48, 811–822. doi: 10.1139/g05-040

Murphy, K. M., Hoagland, L. A., Reeves, P. G., Baik, B. K., and Jones, S. S. (2009). Nutritional and quality characteristics expressed in 31 perennial wheat breeding lines. *Renew. Agric. Food Syst.* 24, 285–292. doi: 10.1017/S1742170509990159

Nicol, J. M., Ogbonnaya, F., Singh, A. K., Bishnoi, S. P., Kanwar, R. S., Li, H. L., et al. (2009). "Current global knowledge of the usability of cereal cyst nematode resistant bread wheat germplasm through international germplasm exchange and evaluation," in *Cereal Cyst Nematodes: Status, Research and Outlook. Proceedings of the First Workshop of the International Cereal Cyst Nematode Initiative*, eds I. T. Riley, J. M. Nicol, and A. A. Dababat (Addis Ababa: International Maize and Wheat Improvement Centre, CIMMYT), 149–153.

Nicol, J. M., Turner, S. J., Coyne, D. L., Den Nijs, L., Hockland, S., and Maafi, Z. T. (2011). "Current nematode threats to world agriculture," in *Genomics and Molecular Genetics of Plant-Nematode Interactions*, eds J. Jones, G. Gheysen, and C. Fenoll (Dordrecht: Springer), 21–43. doi: 10.1007/978-94-007-0434-3_2

Peng, D. L., Peng, H., and Huang, W. K. (2015). "Occurrence, distribution and integrated management of the cereal cyst nematodes (*Heterodera avenae* & *H. filipjevi*) in China," in *Nematodes of Small Grain Cereals: Current Status and Research*, eds A. A. Dababat, H. Muminjanov, and R. W. Smiley (Rome: Food and Agriculture Organization of the United Nations), 17–24.

Schulz-Schaeffer, J., and Friebe, B. (1992). Karyological characterization of a partial amphiploid, *Triticum turgidum* L. var. durum × *Agropyron intermedium* (Host) P. B. *Euphytica* 62, 83–88. doi: 10.1007/BF00037932

Schulz-Schaeffer, J., and Haller, S. E. (1987). Registration of Montana-2 perennial × Agrotriticum intermediodurum Khizhnyak. *Crop Sci.* 27, 822–823. doi: 10.2135/cropsci1987.0011183X002700040058x

Smiley, R. W., Dababat, A. A., Iqbal, S., Jones, M. G. K., Maafi, Z. T., Peng, D. L., et al. (2017). Cereal cyst nematodes: a complex and destructive group of Heterodera species. *Plant Dis.* 101, 1692–1720. doi: 10.1094/PDIS-03-17-0355-FE

Standardization Administration of the People's Republic of China (1994). *National Standard GB/T 6432-1994. Method for the Determination of Crude Protein in Feedstuffs*. Avaliable at: http://openstd.samr.gov.cn/bzgk/gb/newGbInfo?hcno = C3773F65C3F40EE21147390B76DB7C4C (accessed January 14, 2013).

Standardization Administration of the People's Republic of China (2000). *National Standard GB/T 18246-2000. Determination of Amino Acids in Feeds*. Avaliable at: http://openstd.samr.gov.cn/bzgk/gb/newGbInfo?hcno=A9F6869872EE9E44754B11D488EE8E4C (accessed January 14, 2013).

Standardization Administration of the People's Republic of China (2002). *National Standard GB/T 6437-2002. Determination of Phosphorus in Feed-Spectphoto-Metry*. Avaliable at: http://openstd.samr.gov.cn/bzgk/gb/newGbInfo?hcno=3BD37F6598A15947CA047820C8AC605A (accessed January 14, 2013).

Standardization Administration of the People's Republic of China (2003a). *National Standard GB/T 13885-2003. Animal Feeding Stuffs-Determination of the Contents of Calcium, Copper, Iron, Magnesium, Manganese, potAssium, Sodium and Zinc–Method Using Atomic Absorption Spectrometry*. Avaliable at: http://openstd.samr.gov.cn/bzgk/gb/newGbInfo?hcno=DCD3189451F19485837D1F92088CD99E (accessed January 14, 2013).

Standardization Administration of the People's Republic of China (2003b). *National Standard GB/T 5009.83-2003. Determination of Carotene in Foods*. Avaliable at: http://openstd.samr.gov.cn/bzgk/gb/newGbInfo?hcno=2A01DCB90A46CF4AB3B2FB52B4BD8041 (accessed January 14, 2013).

Standardization Administration of the People's Republic of China (2003c). *National Standard GB/T 5009.124-2003. Determination of Amino Acids in Foods*. Avaliable at: http://openstd.samr.gov.cn/bzgk/gb/newGbInfo?hcno=443953BBE177D610A48484A75E4B01E4 (Accessed January 14, 2013).

Standardization Administration of the People's Republic of China (2006a). *National Standard GB/T 6433-2006. Determination of Crude Fat in Feeds*. Avaliable at: http://openstd.samr.gov.cn/bzgk/gb/newGbInfo?hcno=F266E746188C0114B47094E586B35FAA (accessed January 14, 2013).

Standardization Administration of the People's Republic of China (2006b). *National Standard GB/T 6434-2006. Feeding stuffs. Determination of Crude Fiber Content Method With Intermediate Filtration*. Avaliable at: http://openstd.samr.gov.cn/bzgk/gb/newGbInfo?hcno=D8D947F554C1C51DB3D821A17FD48850 (accessed January 14, 2013).

Standardization Administration of the People's Republic of China (2008). *National Standard GB/T 5505-2008. Inspection of grain and oils. Determination of the ash Content by Incineration*. Avaliable at: http://www.cssn.net.cn/cssn/front/gbdetail.jsp?A001=NTgwMzI2Nw== (accessed January 14, 2013).

Standardization Administration of the People's Republic of China (2010). *National Standard GB 5009.93-2010. National food safety standard. Determination of Selenium in Foods*. Avaliable at: http://www.cssn.net.cn/cssn/front/gbdetail.jsp?A001=NTk3ODgwMQ== (accessed January 14, 2013).

Tautges, N. E., Jungers, J. M., DeHaan, L. R., Wyse, D. L., and Sheaffer, C. C. (2018). Maintaining grain yields of the perennial cereal intermediate wheatgrass in monoculture v. bi-culture with alfalfa in the Upper Midwestern USA. *J. Agric. Sci.* 156, 758–773. doi: 10.1017/S0021859618000680

Trotter, T. F., and Frazier, P. F. (2008). "Objective biomass assessment using an active plant sensor (Crop Circle), preliminary experiences on a variety of agricultural landscapes," in *Ninth International Conference on Precision Agriculture*, ed. R. Khosla (Fort Collins: Colorado State University).

Tyl, C., and Ismail, B. P. (2019). Compositional evaluation of perennial wheatgrass (*Thinopyrum intermedium*) breeding populations. *Int. J. Food Sci. Tech.* 54, 660–669. doi: 10.1111/ijfs.13925

Vico, G., Manzoni, S., Nkurunziza, L., Murphy, K., and Weih, M. (2016). Trade-offs between seed output and life span–a quantitative comparison of traits between annual and perennial congeneric species. *New Phytol.* 209, 104–114. doi: 10.1111/nph.13574

Wang, R. R. C., and Wei, J. Z. (1995). Variations of two repetitive DNA sequences in several Triticeae genomes revealed by polymerase chain reaction and sequencing. *Genome* 38, 1221–1229. doi: 10.1139/g95-160

Xing, X. P., Yuan, H. X., Sun, J. W., Zhang, J., Sun, B. J., and Li, H. L. (2014). Resistance to two species of cereal cyst nematode and evaluation methods in major wheat cultivars from Henan Province. *China. Acta Agron. Sin.* 40, 805–815. doi: 10.3724/sp.j.1006.2014.00805

Yan, W., Jin, X., Jiang, B., Qi, X., Chen, Y., Li, X., et al. (2020). Development and molecular cytogenetic characterization of cold-Hardy perennial wheatgrass adapted to northeastern China. *Front. Plant Sci.* 11:582. doi: 10.3389/fpls.2020.00582

You, M. S., Li, B. Y., Tang, Z. H., Liu, S. B., Song, J. M., and Mao, S. F. (2002). Establishment of E-genome-specific RAPD and SCAR markers for *Thinopyrum* spp. *J. China Agric. Univ.* 7, 1–6. doi: 10.1006/jfls.2001.0409

Yuan, H. X., Sun, J. W., Yang, W. X., Xing, X. P., Wang, Z. Y., Riley, I. T., et al. (2010). New pathotypes of Heterodera avenae (cereal cyst nematode) from winter wheat in Zhengzhou. Henan, China. *Australas. Plant Pathol.* 39, 107–111. doi: 10.1071/AP09050

Zadoks, J. C., Chang, T. T., and Konzak, C. F. (1974). A decimal code for the growth stages of cereals. *Weed Res.* 14, 415–421. doi: 10.1111/j.1365-3180.1974.tb01084.x

Zhao, Z. H., Sun, H. G., Song, W., Lu, M., Huang, J., Wu, L. F., et al. (2013). Genetic analysis and detection of the gene MlLX99 on chromosome 2BL conferring resistance to powdery mildew in the wheat cultivar Liangxing 99. *Theor. Appl. Genet.* 126, 3081–3089. doi: 10.1007/s00122-013-2194-6

Conflict of Interest: The authors declare that the research was conducted in the absence of any commercial or financial relationships that could be construed as a potential conflict of interest.

frontiers in Plant Science

REVIEW
published: 13 November 2020
doi: 10.3389/fpls.2020.602079

A Phytochemical Perspective on Plant Defense Against Nematodes

Willem Desmedt[1,2,3], Sven Mangelinckx[4], Tina Kyndt[1] and Bartel Vanholme[2,3]*

[1]Research Group Epigenetics and Defense, Department of Biotechnology, Ghent University, Ghent, Belgium, [2]Department of Plant Biotechnology and Bioinformatics, Ghent University, Ghent, Belgium, [3]VIB Center for Plant Systems Biology, Ghent, Belgium, [4]Research Group Synthesis, Bioresources and Bioorganic Chemistry (SynBioC), Department of Green Chemistry and Technology, Ghent University, Ghent, Belgium

Given the large yield losses attributed to plant-parasitic nematodes and the limited availability of sustainable control strategies, new plant-parasitic nematode control strategies are urgently needed. To defend themselves against nematode attack, plants possess sophisticated multi-layered immune systems. One element of plant immunity against nematodes is the production of small molecules with anti-nematode activity, either constitutively or after nematode infection. This review provides an overview of such metabolites that have been identified to date and groups them by chemical class (e.g., terpenoids, flavonoids, glucosinolates, etc.). Furthermore, this review discusses strategies that have been used to identify such metabolites and highlights the ways in which studying anti-nematode metabolites might be of use to agriculture and crop protection. Particular attention is given to emerging, high-throughput approaches for the identification of anti-nematode metabolites, in particular the use of untargeted metabolomics techniques based on nuclear magnetic resonance (NMR) and mass spectrometry (MS).

Keywords: plant-parasitic nematodes, metabolomics, secondary metabolites, nematode resistance, plant immunity, phytoalexins

OPEN ACCESS

Edited by:
Juan Emilio Palomares-Rius, Consejo Superior de Investigaciones Científicas (CSIC), Spain

Reviewed by:
Ulrike Mathesius, Australian National University, Australia
Trifone D'Addabbo, Italian National Research Council, Italy

****Correspondence:***
Tina Kyndt
tina.kyndt@ugent.be

Specialty section:
This article was submitted to Plant Pathogen Interactions, a section of the journal Frontiers in Plant Science

Received: *02 September 2020*
Accepted: *21 October 2020*
Published: *13 November 2020*

Citation:
Desmedt W, Mangelinckx S, Kyndt T and Vanholme B (2020) A Phytochemical Perspective on Plant Defense Against Nematodes. Front. Plant Sci. 11:602079. doi: 10.3389/fpls.2020.602079

INTRODUCTION

Plant-parasitic nematodes (PPN) are important agricultural pests. Although nematode parasitism is rarely fatal, PPN cause substantial yield losses by diverting nutrients, disrupting water transport, increasing susceptibility to secondary infections, and by acting as vectors for viruses (Bird and Kaloshian, 2003; Nicol et al., 2011). Although quantifying their impact is difficult, estimates suggest that PPN reduce global yields by 10–25% (Nicol et al., 2011). A single nematode species, the soybean cyst nematode *Heterodera glycines*, reduces soybean yield by nearly 10% in the United States (Savary et al., 2019).

Over four thousand PPN species have been identified (Wyss, 1997; Decraemer and Hunt, 2006; Nicol et al., 2011); the majority feed on roots, but some also feed on aerial parts (Fuller et al., 2008). Despite their diversity, most economic losses are caused by a handful of sedentary PPN genera – especially the root-knot nematodes (*Meloidogyne* spp.) and the cyst nematodes (*Heterodera* spp. and *Globodera* spp.; Fuller et al., 2008; Nicol et al., 2011). Effective nematode control is exceptionally difficult and requires an integrated approach that combines chemicals, cultural practices, biocontrol and, where available, resistant varieties (Fuller et al., 2008).

To facilitate the development of novel nematode control strategies, plant nematologists have spent considerable time and effort on studying the mechanisms of plant defense against PPN. One defense mechanism is the production of metabolites with anti-nematode activity, which

in this review we will call *anti-nematode phytochemicals* (ANPs). This review provides an overview of known ANPs, discusses strategies for their identification (with particular focus on metabolomics approaches), and comments on the potential of ANPs in PPN control.

NOTES ON TERMINOLOGY

Secondary Metabolite: plant metabolites can be broadly divided into two groups, primary and secondary metabolites. Primary metabolites are directly involved in the formation of new cells, whereas secondary metabolites are not required for plant growth but instead contribute to processes such as resistance to pests and diseases, attraction of pollinators, and abiotic stress tolerance (Seigler, 1998; Hartmann, 2007). This distinction is not absolute: plant hormones, lignin monomers, and various other metabolites have properties of both primary and secondary metabolites (Seigler, 1998). Furthermore, the classification of metabolites may change as plant science advances: shikimic acid and squalene were long seen as secondary metabolites but are now known to be precursors involved in the biosynthesis of primary metabolites (aromatic amino acids and sterols, respectively; Seigler, 1998). Also, "secondary" metabolites should not be seen as "non-essential": particularly under stressful conditions, impairments in secondary metabolism are often lethal (Seigler, 1998; Hartmann, 2007). Interested readers are referred to an excellent review article (Erb and Kliebenstein, 2020) for an in-depth discussion of plant secondary metabolites and their relation to primary metabolites.

Phytoanticipins and Phytoalexins: Biocidal secondary metabolites produced by plants as protection against pests and pathogens have been divided into *phytoanticipins* and *phytoalexins*. Phytoanticipins are defined as defense compounds which are constitutively present, i.e., regardless of the presence of pests or diseases (VanEtten et al., 1994). By contrast, phytoalexins accumulate only upon perception of pests or pathogens (VanEtten et al., 1994). However, like most distinctions in plant science, the difference between phytoanticipins and phytoalexins is not absolute. Defense compounds may be constitutively present but show a further increase in abundance after pathogen attack. They may also be constitutively present in some organs but produced only upon pest or disease induction in others. In both of those cases, the same compound is both a phytoanticipin and a phytoalexin (VanEtten et al., 1994). Furthermore, phytoalexins may be present constitutively in an inactive storage form (e.g., a glycoside) from which they are released upon pest or pathogen perception (VanEtten et al., 1994).

Nematistatic and Nematicidal Compounds: To study the anti-nematode activity of a metabolite, researchers often expose nematodes to this metabolite in an *in vitro* assay to test whether it is directly toxic to the nematode. The most common assay involves dissolving the compound(s) of interest in water at biologically relevant concentrations and then incubating nematodes in this solution for several hours or days. If most or all nematodes become rigid and immobile, the compound is said to be *nematistatic*. At this point, the nematode may be either reversibly paralyzed or dead. To distinguish between these two possibilities, the nematodes are transferred to clean water. If nematode motility recovers, the compound is only nematistatic (paralyzing). If no recovery is seen, the nematode is dead or irreversibly paralyzed and the compound is said to be *nematicidal*. For many compounds, nematicidal and nematistatic activities are part of a spectrum: low doses and/or brief exposures might be nematistatic, whereas longer exposures or higher doses are nematicidal.

Plant Resistance: Resistance refers to a reduced ability of a pest or pathogen to grow and reproduce on a host plant. Resistance may be qualitative, in which case disease is absent (i.e., the pest or pathogen cannot reproduce), or quantitative, in which case disease severity is reduced (i.e., the pest or pathogen can reproduce, but at a substantially lower rate than is typical for that host; St.Clair, 2010).

Pre- and Post-penetration Resistance: Plant-parasitic nematodes resistance can be classified as *pre-penetration* or *post-penetration* resistance. Pre-penetration resistance refers to a situation in which a nematode is unable to enter the host plant due to e.g., the absence of metabolites needed for host recognition, repellent host exudates or the presence of a physical barrier the nematode is unable to penetrate (Lee et al., 2017). In post-penetration resistance, the PPN enters the host but is then unable to survive or reproduce due to e.g., the presence of toxic metabolites or an inability to feed. For sedentary PPN, this resistance can be further divided into *early* and *late* resistance; early resistance occurs during migration or early feeding site formation, whereas late resistance occurs after the nematode has established a feeding site (Fuller et al., 2008).

Nematode Life Cycles: Plant-parasitic nematodes can be classified according to their lifestyles and modes of parasitism. *Ectoparasitic* nematodes remain outside the plant and penetrate it only with their stylet, whereas *endoparasitic* nematodes enter the host. PPN may also be classified as *sedentary* or *migratory*: migratory PPN remain motile throughout their life (e.g., *Pratylenchus* spp. and *Radophulus* spp.), whereas in sedentary PPN, only second-stage juveniles (J2s) are motile. The migratory J2 finds and penetrates a host and then forms a permanent *feeding site*, in which the nematode completes the remainder of its life cycle in a sedentary form. The principal sedentary nematodes are the *cyst*

nematodes (*Heterodera* spp. and *Globodera* spp.) and the *root-knot nematodes* (*Meloidogyne* spp.). Interested readers can find a brief introduction to the life cycles of the most economically significant PPN in Jones et al. (2013), and more comprehensive discussions of the evolution, diversity, and infection mechanisms of PPN in Perry and Moens (2011) and Smant et al. (2018).

ANPs: A BRICK IN THE WALL OF PLANT IMMUNITY

Plants possess a sophisticated system of defenses against pests and pathogens that consists of both constitutive, pre-formed mechanisms and inducible immune responses which occur upon perception of intruders.

A detailed overview of plant inducible immune responses falls outside the scope of this review (interested readers are referred to e.g., Jones and Dangl, 2006; Andolfo and Ercolano, 2015; Wang et al., 2019), but it is relevant to note that plants are capable of perceiving molecular patterns characteristic for PPN infection and display an induced immune response upon their perception. Such patterns include the pheromone ascaroside (Manosalva et al., 2015; Manohar et al., 2020) and oligogalacturonides released by the intracellular migration of certain PPN species (Sato et al., 2019). Some plants also possess dedicated resistance genes (R-genes), which encode receptors able to recognize specific PPN effectors; some of these R-genes induce a rapid, intense immune response characterized by a hypersensitive response upon PPN perception. Examples of well-characterized anti-nematode R-genes include the *Mi* genes in tomato (against several root-knot nematode species) and *Hero*, *Gpa*, and *Gro* in potato (against potato cyst nematodes; Sato et al., 2019).

In addition to induced immune responses, plants possess constitutive forms of resistance that do not necessitate pest or pathogen perception. Two examples of such resistance are *pre-penetration resistance* and *metabolic resistance*. The former refers to a situation in which a pest or pathogen cannot find or penetrate a suitable host because a molecular pattern required for host recognition is absent, or because the plant possesses an impenetrable barrier (Lee et al., 2017). Metabolic resistance occurs when a pest or pathogen attempts to penetrate a host but encounters a constitutively present metabolite that is sufficiently toxic to prevent colonization (Lee et al., 2017).

Both inducible and constitutive defenses against nematodes rely at least in part on the presence of secondary plant metabolites with anti-nematode activity (as shown in **Figure 1**), which we call ANPs in this review. The remainder of this review will focus entirely on these ANPs; for a broader overview of the various defense mechanisms plants employ against nematodes, readers are referred to other reviews (e.g., Holbein et al., 2016; Sato et al., 2019).

AN OVERVIEW OF KNOWN ANPs

Plants possess an extensive secondary metabolism capable of producing a vast diversity of metabolites; approximately 200,000 plant secondary metabolites are believed to exist

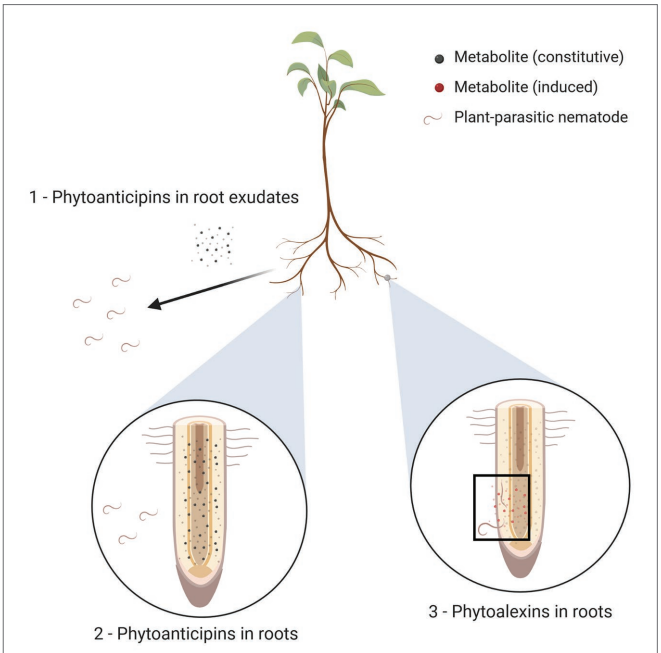

FIGURE 1 | Three types of plant *anti-nematode phytochemicals* (ANPs). (1) Plant roots exude metabolites into their environments (represented here as black dots); these exudates may function as phytoanticipins by exerting repellent or nematicidal activities. (2) Plant tissues (depicted here as roots, but other plant tissues may equally be affected by nematode parasitism) may contain constitutively formed metabolites with anti-nematode activity, irrespective of actual nematode presence; these metabolites are called phytoanticipins and are represented by small black dots. (3) Upon nematode penetration, the plant may respond by locally producing additional anti-nematode compounds; these induced metabolites are called phytoalexins and are shown here as red dots present near the site of nematode penetration and migration (highlighted with black rectangle).

(Viant et al., 2017). In this review, we have chosen to group ANPs in several classes of secondary metabolites: phenolic compounds, terpenoids, saponins, benzoxazinoids, organosulfur compounds, alkaloids, and glucosinolates. This classification is of course not the only possible one, and some compounds could be placed in more than one category.

Grouping ANP studies by chemical class also leads, to some extent, to grouping by plant family. Although all plant species produce multiple classes of secondary metabolites, each has evolved a bias toward specific classes of defensive metabolites. For example, Fabaceae defense compounds are often (iso)flavonoids, Malvaceae and Solanaceae phytoalexins are often terpenoids, and glucosinolates are unique to the order Brassicales (Veech, 1982).

This review limits itself to secondary metabolites for which there is at least tentative evidence that they are involved in plant defense against nematodes, i.e., compounds which are present in tissues affected by nematode parasitism (either constitutively or induced upon nematode infection) and whose presence could be correlated to nematode resistance. Many other nematicidal compounds have been identified in plant extracts, but without an apparent role in plant-nematode interactions; an overview of several such compounds can be found in e.g., Chitwood (2002).

Phenolic Compounds

A major class of ANPs are those derived from the *phenylpropanoid pathway* (PPP), which are frequently lumped together under the umbrella term *phenolic compounds*. Phenolic compounds play a major role in resistance to various plant pests and diseases (Nicholson and Hammerschmidt, 1992; Lattanzio et al., 2006), and a role for phenolic compounds in nematode resistance has been suggested since at least the early 1960s. In general, higher basal and/or induced amounts of phenolic compounds have been found to correlate with nematode resistance in a wide variety of plant-nematode combinations (Wallace, 1961; Giebel, 1970, 1982; Hung and Rohde, 1973; Bajaj and Mahajan, 1977; Pegard et al., 2005; Dhakshinamoorthy et al., 2014; Hölscher et al., 2014).

Plant phenolic compounds are generally derived from the aromatic amino acids L-phenylalanine and (less commonly) L-tyrosine. L-phenylalanine is deaminated by PHENYLALANINE AMMONIA LYASE to form (*E*)-cinnamic acid, which can be *para*-hydroxylated by CINNAMIC ACID-4-HYDROXYLASE to form *para*-coumaric acid. Alternatively, *para*-coumaric acid can be formed directly through deamination of L-tyrosine by TYROSINE AMMONIA LYASE. *para*-Coumaric acid is then activated through the thioester coupling of acetyl-coenzyme A by 4-COUMARATE-CoA LIGASE to form the reactive metabolic intermediate *para*-coumaroyl-CoA. From this point onward, the PPP branches in various directions to form a dazzling array of secondary metabolites that includes hydroxycinnamic acids, flavonoids, tannins, diarylheptanoids, stilbenoids, and many others (Vogt, 2010).

Although most phenolic compounds are produced *via* the PPP, some less common phenolic metabolites, such as alkylresorcinols (Baerson et al., 2010), are produced through polyketide metabolism. These phenolic metabolites are not discussed in this review, as to the best of our knowledge they have not been studied in plant-nematode interactions.

Hydroxycinnamic Acids

Hydroxycinnamic acids (HAs) are hydroxy derivatives of (*E*)-cinnamic acid. The HA *para*-coumaric acid is a core intermediate in the PPP and other HAs (e.g., ferulic acid, caffeic acid, or sinapic acid) are abundant in many plants either as pure compounds or as conjugate forms (Vogt, 2010).

One of the first individual phenolic compounds to be implicated in defense against nematodes was chlorogenic acid (**Figure 2A**). This ester of caffeic acid (**Figure 2B**) and (-)-quinic acid accumulates in several dicot (Wallace, 1961; Hung and Rohde, 1973; Pegard et al., 2005) and monocot (Gill et al., 1996) plants in sites of PPN infection, and induced chlorogenic acid levels appear correlated to nematode resistance in various plant species (Hung and Rohde, 1973; Gill et al., 1996; Pegard et al., 2005; Meher et al., 2015). Furthermore, it was recently shown that chlorogenic acid accumulation was strongly repressed in *Meloidogyne incognita* galls in a susceptible poplar clone (*Populus tremula* × *Populus alba*), which suggests that suppression of chlorogenic acid biosynthesis might be a pathogenesis strategy employed by *M. incognita* (Baldacci-Cresp et al., 2020).

However, chlorogenic acid is only weakly nematicidal (Mnviajan et al., 1992; D'Addabbo et al., 2013). A plausible, but unproven, explanation for this discrepancy is that chlorogenic acid could be a precursor to an unstable, elusive nematicidal compound. One candidate is caffeic acid quinone (**Figure 2C**), a compound that is toxic to nematodes (Mnviajan et al., 1992) and which can be formed from chlorogenic acid: hydrolysis of chlorogenic acid affords quinic acid and caffeic acid, the latter of which can be oxidized to caffeic acid quinone (Hapiot et al., 1996). In further support of this idea, caffeic acid itself has been shown to accumulate after *M. incognita* infection in a resistant tomato cultivar but not in three susceptible ones (Afifah et al., 2019). However, since caffeic acid is also involved in lignification (Boerjan et al., 2003), another defense response against nematodes (Sato et al., 2019), this is circumstantial evidence at best. Furthermore, the involvement of chlorogenic acid in nematode resistance is not universal: in the interaction between coffee and *Meloidogyne exigua*, chlorogenic acid accumulated to a similar degree in a susceptible and a resistant cultivar (Machado et al., 2012).

The phenolic plant hormone salicylic acid (SA) could also be included in this section. Although SA shows some nematistatic and nematicidal activity *in vitro* (Wuyts et al., 2006b), it is present in plant roots at concentrations far below those reported to be nematistatic. Instead, SA appears to be involved in nematode resistance *via* its role as a plant hormone. SA signaling is involved in the regulation of various immune responses against nematodes and is involved in genetic (Branch et al., 2004) and induced resistance to root-knot nematodes (Martínez-Medina et al., 2017). Pre-inoculation treatment with SA or chemical analogs thereof enhances plant resistance to subsequent nematode infection, whereas SA-deficient mutants show increased susceptibility (Wubben et al., 2008; Uehara et al., 2010; Martínez-Medina et al., 2017).

Stilbenoids and Diarylheptanoids

Stilbenoids and diarylheptanoids are two relatively small classes of plant secondary metabolites derived from the PPP.

The biosynthesis of stilbenoids involves the coupling of a phenylpropanoyl-CoA (e.g., cinnamoyl-CoA or *para*-coumaroyl-CoA) to three malonyl-CoA units through repeated condensation reactions catalyzed by STILBENE SYNTHASE. This gives rise to the basic C6-C2-C6 stilbene skeleton (*trans*-resveratrol if derived from *para*-coumaroyl-CoA; pinosylvin if derived from cinnamoyl-CoA). These basic structures can be further modified to form the various derivatives known as stilbenoids (Jeandet et al., 2010).

The biosynthesis of diarylheptanoids is less well-understood, but is similar to that of stilbenoids in its initial steps. A POLYKETIDE SYNTHASE catalyzes a condensation reaction between a phenylpropanoyl-CoA (e.g., *para*-coumaroyl-CoA) and malonyl-CoA to form a diketide intermediate. After a second condensation reaction between this diketide and another phenylpropanoyl-CoA molecule, a linear diarylheptanoid (C6-C7-C6) is formed. Cyclization of this compound gives rise to the phenylphenalenone backbone. Linear and cyclic diarylheptanoids

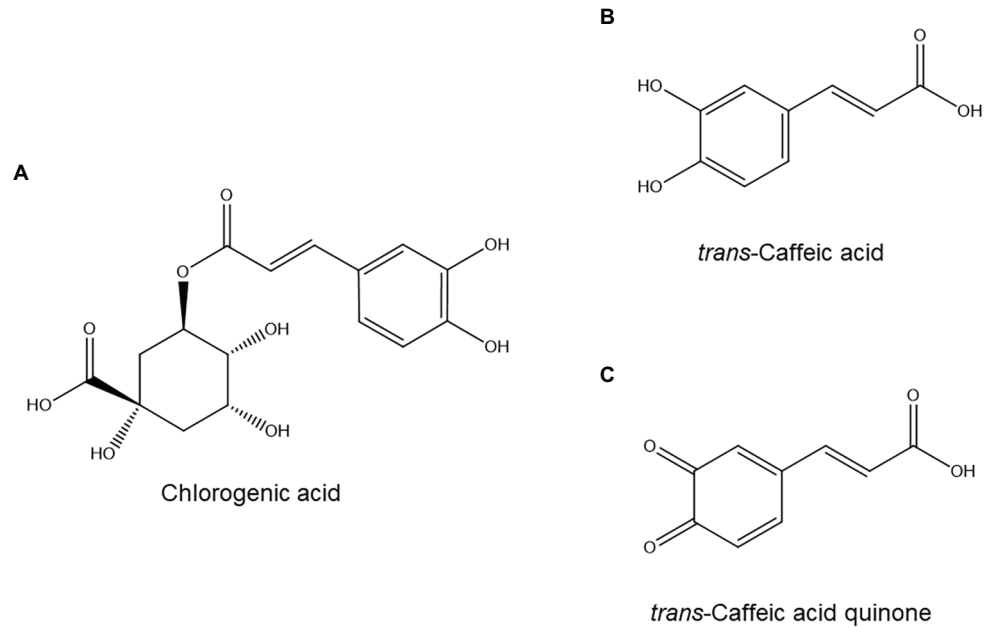

FIGURE 2 | Hydroxycinnamic acids with possible roles in plant resistance to nematodes: chlorogenic acid **(A)**, caffeic acid **(B)**, and caffeic acid quinone **(C)**.

may undergo further processing, notably through hydroxylation (Brand et al., 2006; Munde et al., 2013).

Although few studies have examined the role of stilbenoids and diarylheptanoids in plant disease resistance, the available evidence suggests that they are key defense compounds in plants that produce them (Luis, 1998; Echeverri et al., 2012; Akinwumi et al., 2018). Similarly, their role in PPN resistance also appears to be highly significant. Stilbenoids have been implicated in nematode resistance in pine trees and grape vines. The stilbenoid 3-*O*-methyldihydropinosylvin (**Figure 3B**) accumulated in bark and wood of *Pinus strobus* after infection with the pinewood nematode *Bursaphelenchus xylophilus* and showed significant nematicidal activity *in vitro* (Hanawa et al., 2001). Furthermore, the accumulation of 3-*O*-methyldihydropinosylvin in bark and wood of *P. strobus* coincides temporally with resistance to *B. xylophilus*: the nematode can initially successfully penetrate, but its movement and reproduction stop after approximately 1 week, which is the same time point at which 3-*O*-methyldihydropinosylvin reaches concentrations in bark and wood above those required for nematicidal activity *in vitro*. *In vitro* tests showed that 24 h of exposure to 250 μg/ml of 3-*O*-methyldihydropinosylvin killed 100% of nematodes, while bark and wood of infected *P. strobus* plants accumulated approximately 1,000 and 400 μg/g of this compound. These results, thus, indicate that 3-*O*-methyldihydropinosylvin is a phytoalexin with a major role in *P. strobus* resistance to *B. xylophilus* (Hanawa et al., 2001).

A comparison of two grapevine (*Vitis vinifera*) rootstocks, one of which was susceptible to *M. incognita* and one of which was resistant, also hinted at a possible role for stilbenoids in nematode resistance (Wallis, 2020). The two rootstocks (both with Cabernet Sauvignon as the scion) were inoculated with *M. incognita* and sampled 6 and 12 weeks postinoculation. Throughout the experiment, the resistant and susceptible rootstock showed similar total stilbenoid levels. Furthermore, total stilbenoid content was unaffected by nematode infection in both rootstocks. However, the stilbenoid profile varied significantly between the two rootstocks: the stilbenoid trimer miyabenol C (**Figure 3C**) and the stilbenoid tetramer hopeaphenol (**Figure 3D**) were 4–10 times more abundant in the resistant rootstock. These compounds might act as phytoanticipins against PPN, but their anti-nematode activity was unfortunately not assessed *in vitro*.

Phenylphenalenone phytoalexins have been shown to be key players in banana resistance to the burrowing nematode *Radopholus similis*. When banana roots were collected 12 weeks after nematode inoculation, these cyclic diarylheptanoids were found to be significantly more abundant near *R. similis* infection sites in resistant banana varieties than in the susceptible reference cultivar (Hölscher et al., 2014). Out of 13 phenylphenalenones that could be identified in extracts from the resistant banana cultivars, three showed significant nematistatic activity in an *in vitro* assay (Hölscher et al., 2014). Further investigation on the most abundant of those, anigorufone (**Figure 3A**), showed that its IC_{50} on *R. similis* motility was 59 and 23 μg/ml after 24 and 72 h, respectively (Hölscher et al., 2014). The researchers showed that anigorufone forms complexes with lipids inside the nematode, leading to the formation of large lipid-anigorufone droplets and eventual nematode death (Hölscher et al., 2014). Attempts to quantify anigorufone *in planta* found concentrations of approximately 39 mg/g root tissue in and around *R. similis* infection sites,

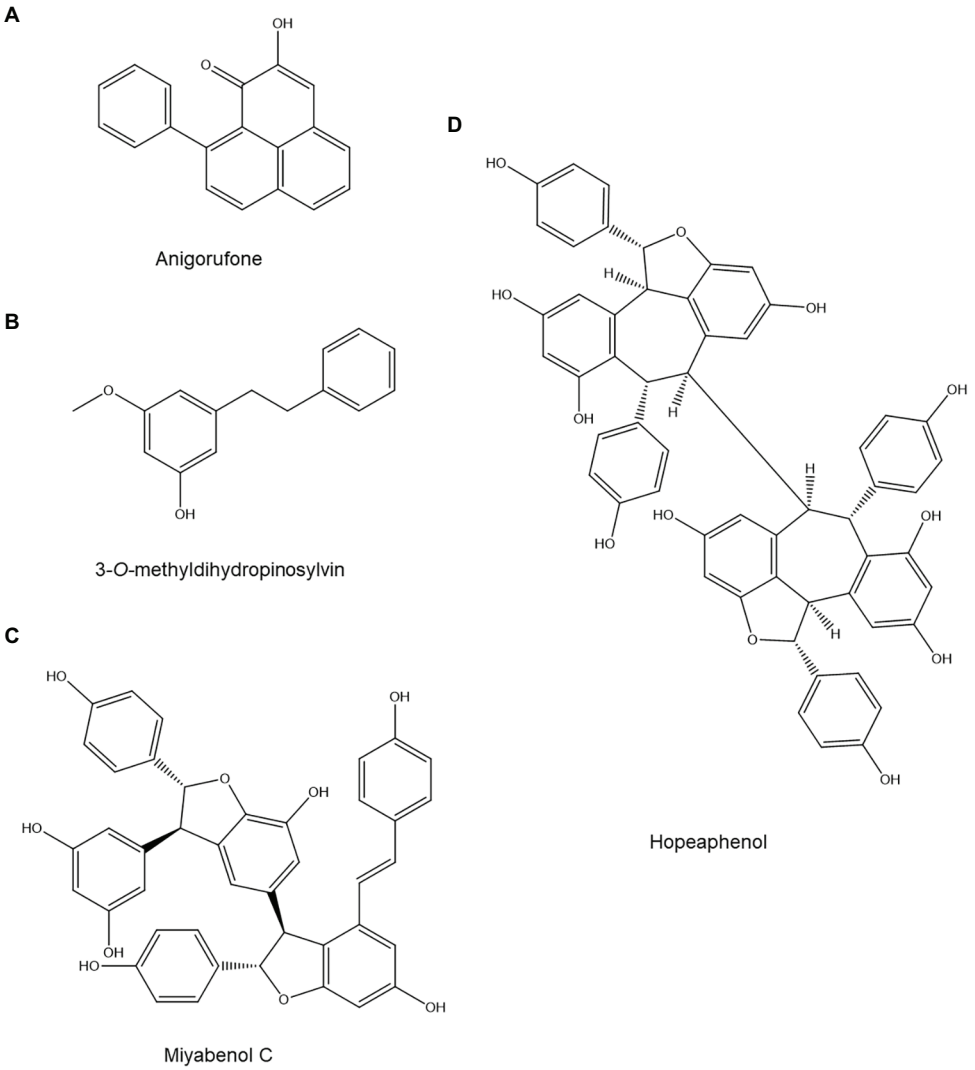

FIGURE 3 | Stilbenoids and diarylheptanoids with possible anti-nematode activity: The phenylphenalenone (cyclic diarylheptanoid) anigorufone **(A)**, the stilbenoid 3-*O*-methyldihydropinosylvin **(B)**, the stilbenoid oligomers miyabenol C **(C)**, and hopeaphenol **(D)**.

which shows that banana roots accumulate biologically relevant anigorufone concentrations (Hölscher et al., 2014).

Flavonoids

Flavonoids are the largest family of phenolic secondary metabolites, with more than 10,000 identified members (Mathesius, 2018). Flavonoids have long been implicated in plant resistance to pests and diseases other than PPN (Treutter, 2005, 2006) and are also among the most widely studied plant secondary metabolites in relation to PPN resistance. This extensive body of research is reflected in the length of this section, which significantly exceeds those on other metabolite classes.

Flavonoid biosynthesis starts similarly to that of stilbenoids, but the first committed step is catalyzed by CHALCONE SYNTHASE rather than STILBENE SYNTHASE. Both enzymes share high sequence homology, and STILBENE SYNTHASE is believed to have evolved from CHALCONE SYNTHASE (Tropf et al., 1994). CHALCONE SYNTHASE condenses *para*-coumaroyl-CoA with three malonyl-CoA units to form a chalcone skeleton, which then undergoes isomerization to form the corresponding flavonoid. Flavonoids may then be further processed through e.g., hydroxylation, methylation, prenylation, and glycosylation (Naoumkina et al., 2010; Falcone Ferreyra et al., 2012). Depending on the flavonoid backbone, flavonoids are subdivided into bioflavonoids (2-phenylchromen-4-one skeleton), isoflavonoids (3-phenylchromen-4-one skeleton), and neoflavonoids (4-phenylcoumarin skeleton; McNaught and Wilkinson, 1999).

In vitro experiments have shown that several common flavonoids show (limited) anti-nematode activity: kaempferol is inhibitory to the hatching of *R. similis* eggs while kaempferol,

quercetin, and myricetin are both repellent and somewhat nematistatic (but not nematicidal) to *M. incognita* juveniles (Wuyts et al., 2006b). The effect of flavonoids on nematode behavior, however, is complex: they can either attract or repel *M. incognita* juveniles depending on their molecular structure and concentration (Kirwa et al., 2018). Flavonoids have been most extensively studied in relation to plant-nematode interactions in the Fabaceae family, whose members produce various isoflavonoids and pterocarpans (phytoalexins derived from isoflavonoids *via* coupling of the isoflavonoid B ring and 4-one position) in response to infection.

A well-studied pterocarpan in relation to nematode resistance is the phytoalexin glyceollin I (**Figure 4E**), produced by soybeans (*Glycine max*). Glyceollin I accumulated near the head region of soybean cyst nematodes (*H. glycines*) as soon as 8 h post penetration in a resistant soybean cultivar but not in a susceptible one (Huang and Barker, 1991). It was undetectable in roots prior to nematode infection but gradually accumulated afterward. Glyceollin I levels peaked 4–6 days post penetration and declined afterward; in the resistant cultivar root, Glyceollin I levels reached 23 μg/g of fresh root, whereas the susceptible cultivar accumulated three times less and showed no preferential accumulation near the nematode head (Huang and Barker, 1991). The authors argue that the preferential deposition near the head of the nematode is indicative of an elicited response (Huang and Barker, 1991); the molecular pattern(s) in the head region of *H. glycines* that are responsible for this remain unidentified.

Similarly, glyceollin I may also play a role in soybean resistance to *M. incognita* (Kaplan et al., 1980a). While the concentration of glyceollin I in roots of a resistant cultivar reached 80 μg/g of fresh root 7 days postinoculation, a susceptible variety accumulated five times less. Furthermore, there was a clear spatiotemporal correlation between glyceollin I accumulation and the occurrence of a hypersensitive response (HR) in the resistant cultivar: both glyceollin accumulation and HR began around 3 days postinoculation and glyceollin I concentrations were highest in the root stele, the only root tissue where HR was observed. Whether HR and glyceollin I accumulation are independent resistance mechanisms or interact in some way remains unclear. The authors also reported that when the *M. incognita*-resistant cultivar was instead inoculated with *Meloidogyne javanica*, a related nematode species to which it is not resistant, glyceollin I did not accumulate, which further supports the hypothesis that glyceollin I deposition is a specific, induced resistance response.

The mechanism of action of glyceollin I against nematodes has been partially elucidated: *in vitro* motility assays showed that biologically relevant concentrations of glyceollin I are strongly nematistatic to J2 juveniles of *M. incognita* and inhibit their respiration (Kaplan et al., 1980a,b) but had no effect on *M. javanica* juveniles (Kaplan et al., 1980a). The precise target(s) of glyceollin I within the nematode remains unknown.

In contrast to glyceollin, the isoflavonoids daidzein (**Figure 4A**) and genistein (**Figure 4B**) – the most abundant flavonoids in soybean roots and their exudates – appear to play no significant role in soybean resistance to *H. glycines*, as both flavonoids accumulated to a similar degree in a susceptible and a resistant cultivar after nematode infection (Kennedy et al., 1999). This observation is supported by the absence of *in vitro* nematicidal activity of these isoflavonoids toward *R. similis* (although a repellent effect was observed; Wuyts et al., 2006b).

Accumulation of the pterocarpan phaseolin (**Figure 4G**) has been reported in the roots of susceptible common bean (*Phaseolus vulgaris*) seedlings 5 days after penetration by *Pratylenchus penetrans*, reaching an estimated concentration of 59 μg/g of fresh root. However, *in vitro* exposure to a similar phaseolin concentration had no effect on PPN motility or survival, which makes it unlikely that phaseolin accumulation is a major contributor toward defense against *P. penetrans* (Abawi and Vanetten, 1971).

By contrast, the pterocarpan medicarpin (**Figure 4F**) did show nematistatic effects against *P. penetrans*, with an IC_{50} just below 20 μg/ml (Baldridge et al., 1998). Resistant alfalfa (*Medicago sativa*) accessions showed significantly higher constitutive expression of several genes involved in isoflavonoid biosynthesis compared to susceptible cultivars, but high-performance liquid chromatography (HPLC) analysis revealed that all varieties contained similar total isoflavonoid levels both before nematode inoculation and for at least the 2 subsequent days. Furthermore, there was no correlation between basal medicarpin concentration and nematode resistance among the tested cultivars (Baldridge et al., 1998). Based on these results, medicarpin and other isoflavonoids appear to be at most minor contributors to alfalfa resistance to nematodes.

The roles of medicarpin and the isoflavonoid formononetin (**Figure 4C**) as well as their malonated glycosides medicarpin-3-*O*-glucoside-6"-*O*-malonate (**Figure 4J**) and formononetin-7-*O*-glucoside-6"-*O*-malonate (**Figure 4K**) in resistance to the stem nematode *Ditylenchus dipsaci* has been studied in white clover (*Trifolium repens*; Cook et al., 1995). A resistant and susceptible white clover variety contained similar basal levels of all four metabolites in roots, leaves, and meristems, but after *D. dipsaci* inoculation, the resistant variety began to accumulate more medicarpin and formononetin in the inoculated meristems. This accumulation began relatively late in the infection process: it was not yet visible 3 days postinoculation but was significant 7 and 10 days postinoculation. The glycosylated forms accumulated to similar degrees in susceptible and resistant plants. Neither the resistant nor the susceptible variety showed systemic flavonoid accumulation: increased flavonoid levels were only observed in the meristem. The direct effects of medicarpin and formononetin on *D. dipsaci* were not examined, so to what extent – if any – these flavonoids contribute to resistance remains unclear (Cook et al., 1995).

Work by the same group on alfalfa showed that neither resistant nor susceptible alfalfa accumulates additional isoflavonoids in aerial tissues after *D. dipsaci* infection, but that the resistant cultivar showed a two- to three-fold increase in root isoflavonoid content (Edwards et al., 1995). The reason for this phenomenon is unclear, but the authors note that *D. dipsaci* predisposes alfalfa to root infection by *Fusarium* wilt and bacterial wilt. Based on

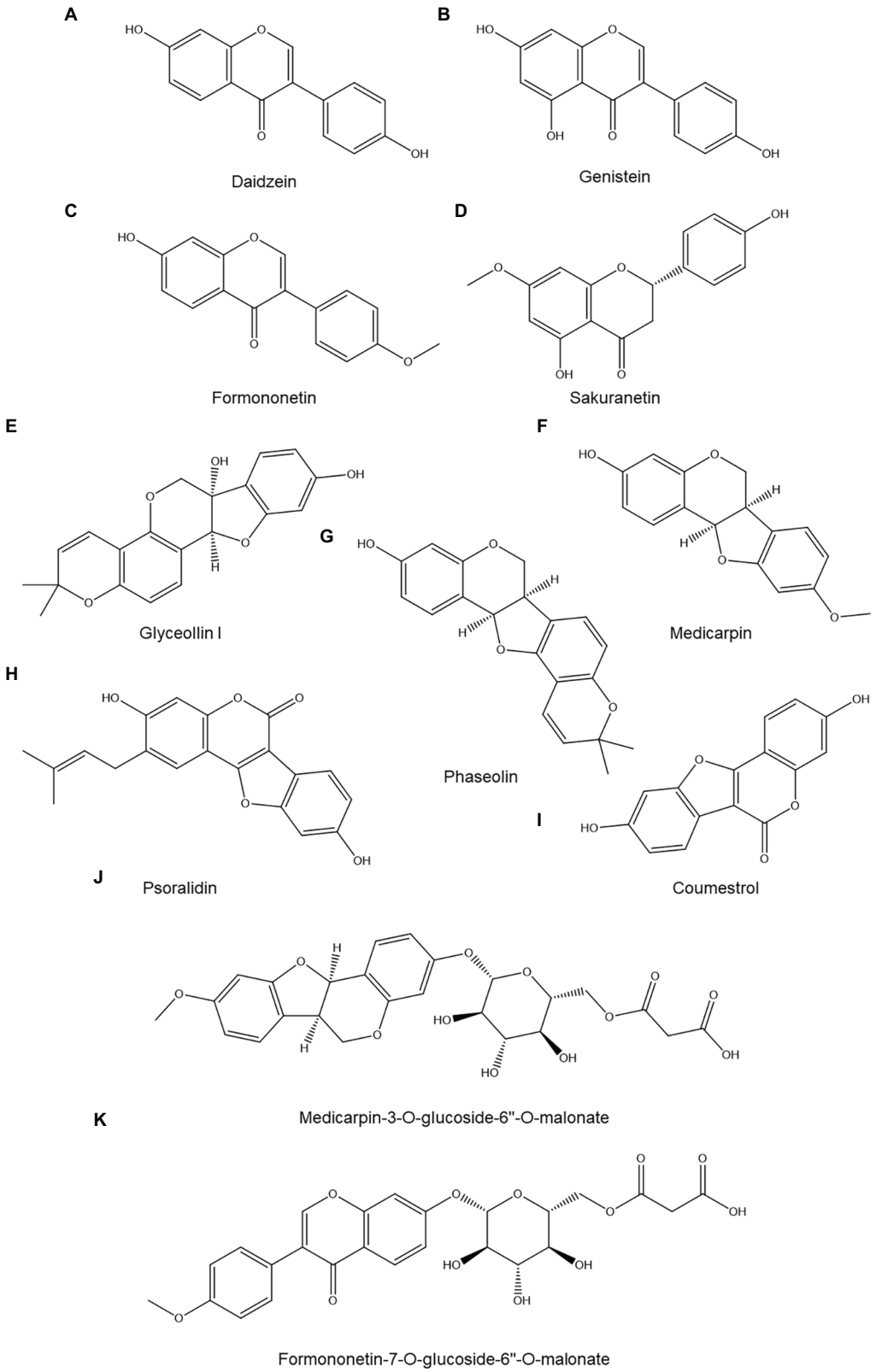

FIGURE 4 | Overview of identified flavonoids discussed in this review: daidzein **(A)**, genistein **(B)**, formononetin **(C)**, sakuranetin **(D)**, glyceollin I **(E)**, medicarpin **(F)**, phaseolin **(G)**, psoralidin **(H)**, coumestrol **(I)**, medicarpin-3-*O*-glucoside-6''-*O*-malonate **(J)**, and formononetin-7-*O*-glucoside-6''-*O*-malonate **(K)**.

this, they speculate that accumulation of defense metabolites in roots might be an adaptive response to prevent secondary infections (Edwards et al., 1995).

Coumestans, oxidized pterocarpans, appear to be significant phytoalexins in plant-nematode interactions. When Lima beans (*Phaseolus lunatus*) and common beans were exposed to the nematode *Pratylenchus scriberni*, to which Lima beans are resistant whereas common beans are susceptible, it was found that Lima beans accumulated substantial quantities of two coumestans tentatively identified as coumestrol (**Figure 4I**) and psoralidin (**Figure 4H**; Rich et al., 1977). Basal levels of coumestrol were similar between Lima and common beans, whereas basal psoralidin levels were two times higher in Lima beans. Two days after infection, coumestrol levels in common beans remained nearly unchanged, whereas those in Lima bean roots had increased more than three-fold. Similarly, psoralidin concentrations were unresponsive to inoculation in common bean but increased over two-fold in Lima bean. Both coumestrol and psoralidin primarily accumulated in Lima bean in and around sites of HR, where these compounds reached concentrations 7–32 times above their *in vitro* IC_{50} toward *P. scriberni* motility (10–15 μg/ml; Rich et al., 1977).

A handful of studies have examined the role of flavonoids in interactions between cereals and nematodes. When shoots of various rice (*Oryza sativa*) varieties were sampled 5 days after inoculation with the stem nematode *Ditylenchus angustus*, a resistant rice variety was found to contain 13 μg/g of fresh weight of the flavonoid phytoalexin sakuranetin (**Figure 4D**), whereas this compound was not found in any of the susceptible varieties that were analyzed (Gill et al., 1996). This result is entirely correlative, since the effects of sakuranetin on *D. angustus* were not investigated.

In oat (*Avena sativa*), Soriano et al. (2004) observed a two- to three-fold increase in the shoot and root concentration of three methanol-soluble compounds with UV-absorbance spectra reminiscent of flavonoids upon infection by *Heterodera avenae* or *Pratylenchus neglectus*, as well as upon foliar treatment with the defense hormone methyl jasmonate. A crude methanol extract of methyl jasmonate-induced oat was highly nematicidal toward *H. avenae*. Two of the three inducible flavonoid phytoalexins could be purified, and one of them was strongly nematicidal. The inducible flavonoids were eventually partially identified as three flavone-*C*-glycosides: an apigenin-*C*-hexoside-*O*-pentoside (not nematicidal), an *O*-methyl-apigenin-*C*-deoxyhexoside-*O*-hexoside (nematicidal), and a luteolin-*C*-hexoside-*O*-pentoside (could not be purified).

Induction of these flavonoids by treating plants with methyl jasmonate 3 days prior to inoculation significantly reduced the total nematode population 10 days postinoculation for both *H. avenae* and *P. neglectus* and increased the percentage of nematodes present outside the root rather than inside. A similar effect was seen when susceptible wheat plants were treated with a flavonoid-rich extract from induced oats plants. Taken together, these results indicate that inducible flavonoids from oat are both repellent and nematicidal. However, these flavonoids appear to be only effective *in planta* against *H. avenae* and *P. neglectus* when they are present prior to or shortly after penetration (e.g., *via* methyl jasmonate pre-treatment). In untreated susceptible plants, infection by *H. avenae* or *P. neglectus* eventually caused the concentration of inducible flavonoids to increase to the level seen in methyl jasmonate-induced plants, and yet the nematodes could reproduce normally (Soriano et al., 2004).

By contrast, HPLC-MS analysis of root extracts from several lines of a single-seed descent population derived from a cross between two oats cultivars different to the one used by Soriano et al. (2004) found no correlation between susceptibility to *H. avenae* and the basal concentration of the three flavonoids mentioned previously. Flavonoid accumulation is thus at most one of several resistance mechanisms against *H. avenae* present in oat germplasm (Bahraminejad et al., 2008).

Arabidopsis thaliana transparent testa (tt) mutants, which are impaired in the biosynthesis of flavonoids, have been used to study the role of flavonoids in PPN resistance. One study reported that none of the tested *tt* mutants differed from their wild type in susceptibility to *M. incognita* (Wuyts et al., 2006a), while another study found that against *Heterodera schachtii* most *tt* mutants show either unchanged or slightly increased susceptibility compared to their wild types (Jones et al., 2007). These results suggest that flavonoids play at most a minor role in PPN resistance in *A. thaliana*.

Several authors have proposed that sedentary nematodes may exploit flavonoids as part of their pathogenesis process (Chin et al., 2018), based on the observations that PPN alter plant auxin homeostasis during feeding site formation (Grunewald et al., 2009a,b) and that several flavonoids have been described as inhibitors of auxin transport (Ng et al., 2015). However, evidence for this hypothesis is circumstantial at best. If PPN extensively manipulated flavonoids as a pathogenesis strategy, it would be expected that *A. thaliana tt* mutants show increased susceptibility. As mentioned in the previous paragraph, this is not generally the case. In support of the idea that PPN exploit flavonoids, it has been reported that the expression of *CHALCONE SYNTHASE*, a key gene in flavonoid biosynthesis, coincides spatiotemporally with an increased auxin response in developing *M. incognita* feeding sites in white clover (Hutangura et al., 1999) and that a flavonoid-deficient *Medicago truncatula* transgenic line hosts smaller *M. incognita* galls than its wild type (Wasson et al., 2009). Both results are, however, entirely correlative and do not prove that PPN manipulate auxin *via* flavonoids.

The results in this section collectively indicate that the role of flavonoids in PPN resistance depends on the specific flavonoids and nematodes involved, and possibly also on the timing of accumulation in the infection process. That the flavonoid glyceollin I plays a role in soybean resistance toward *H. glycines* and *M. incognita* appears convincingly established, but evidence in other pathosystems remains mixed.

Tannins

Tannins are a heterogeneous group of polyphenolic compounds. They are usually divided in two subgroups, the hydrolysable and the condensed tannins. Hydrolysable tannins possess a polyol core to which galloyl groups are esterified, while condensed

tannins are oligomers of two or more flavan-3-ols. Both types show an enormous diversity in degree of polymerization, monomer composition and in decoration with other phenolic compounds (Barbehenn and Peter Constabel, 2011; Salminen and Karonen, 2011). They are involved in plant resistance to insect herbivory (Barbehenn and Peter Constabel, 2011; Salminen and Karonen, 2011) and a handful of studies have also found a correlation between tannin accumulation and nematode resistance. However, no causal evidence has been presented, perhaps because obtaining pure and representative tannin standards remains difficult (Barbehenn and Peter Constabel, 2011). Tannins were historically believed to hinder herbivores by inducing protein precipitation and, thus, depriving them of nutrition (Barbehenn and Peter Constabel, 2011; Salminen and Karonen, 2011). However, more recent evidence has shown that this effect may be negligible *in vivo* and that tannins instead derive their activity from cytotoxic and antinutritive products formed when tannins are oxidized by plant POLYPHENOL OXIDASES or by the alkaline gut environment present in many insect herbivores (Barbehenn and Peter Constabel, 2011; Salminen and Karonen, 2011).

In banana, a cultivar resistant to *R. similis* contained a higher basal condensed tannin concentration than susceptible cultivars when analyzed 12 weeks after inoculation (Collingborn et al., 2000). Although condensed tannin levels increased significantly upon nematode infection in all cultivars, their concentration in the susceptible cultivars remained far below that of the resistant variety. The same trend was observed for flavan-3,4-diols, the main precursors of condensed tannins in banana (Collingborn et al., 2000). The resistant banana cultivar also incorporated propelargonidins alongside the usual procyanidin in its condensed tannins (Collingborn et al., 2000); whether the resistance of the banana cultivar can be attributed to its higher tannin concentration and/or its different tannin composition remains unclear, as the direct effects of banana tannins on *R. similis* were not evaluated.

A putative role for tannins in resistance to the pinewood nematode *B. xylophilus* has also been proposed. When *B. xylophilus* was cultured on the phloem sap of eight pine species, its growth rate was negatively correlated to the concentration of condensed tannins in the sap of each species (Pimentel et al., 2017). However, negative correlations were also observed between nematode growth rate and total flavonoid concentration as well as total phenolic compound concentration. This makes it difficult to assess the relative contribution of condensed tannins, flavonoids, and other phenolic metabolites to the inhibitory effect on *B. xylophilus* (Pimentel et al., 2017).

Terpenoids

Terpenoids, an umbrella term for terpenes and their derivatives, are likely the most diverse class of plant secondary metabolites, with more than 60,000 compounds already identified (Pazouki and Niinemetst, 2016). Terpenes are formed by condensation of two or more activated isoprene units (C5 building blocks), either isopentenyl pyrophosphate or its isomer dimethylallyl pyrophosphate (Cheng et al., 2007). Depending on the number of C5 building blocks involved, this condensation can lead to the formation of a C10 (monoterpene), C15 (sesquiterpene), or C20 (diterpene) terpene. Sesqui- and diterpene units can in turn undergo head-to-head condensation to form C30 (triterpenes, e.g., sterols) or C40 units (tetraterpenes, e.g., carotenoids; Pichersky and Raguso, 2018). All terpenes can be further substituted, e.g., through hydroxylation or acetylation, to form *terpenoids*. Since enzymes acting on terpenoids are both numerous and often highly promiscuous, terpenoids are an exceptionally diverse class of secondary metabolites (Pichersky and Raguso, 2018). Many terpenoids are active against pests and pathogens, and an evolutionary arms race with these attackers may have been a major driver behind the increasing terpenoid diversity seen throughout plant evolution (Pichersky and Raguso, 2018).

The most widely studied group of terpenoids in plant-nematode interactions are the terpenoid aldehydes (TAs) of cotton (*Gossypium* sp.), which include gossypol (**Figure 5A**) and its derivatives. Gossypol is a polyphenolic compound but is included under terpenoids owing to its biosynthesis: it is formed by oxidative coupling of two repeatedly oxidized sesquiterpene units (Heinstein et al., 1979).

The role of TAs in cotton resistance to *M. incognita* has been extensively studied but remains unclear. One article reported that a resistant upland cotton (*Gossypium hirsitum*) cultivar produced higher basal and induced gossypol levels than a susceptible one, and also exuded gossypol and other TAs to its rhizosphere (Hedin et al., 1984). Histological analysis of TAs in *G. hirsitum* demonstrated that TAs accumulated in root tissues traversed by migrating *M. incognita* juveniles and around their developing feeding sites (Veech, 1979). Although this accumulation occurred both in a susceptible and in two resistant cultivars, the resistant varieties showed significantly earlier accumulation (4 days postinoculation rather than 12–14 days). Furthermore, resistant cultivars showed TA accumulation throughout the entire root, whereas in the susceptible variety, TAs accumulated only in the endodermis and cortex (Veech, 1979).

However, a later study examined three different resistant *G. hirsitum* cultivars and found that two of them had lower basal and induced TA concentrations than two susceptible reference cultivars (Khoshkhoo et al., 1994a). Three possible explanations for this observation were hinted at by the authors: (a) TA accumulation might be one of several resistance mechanisms present in cotton, (b) TAs might play no major role in resistance to *M. incognita*, or (c) the ratio of different TAs rather than total TA concentrations might determine resistance.

In tentative support of the third hypothesis, another study on five *G. hirsitum* cultivars found no correlation between *M. incognita* resistance and total basal or induced TA concentrations but did find a correlation between resistance and the abundance of one TA sub-class: methylated TAs (Veech, 1978). The author found that the concentration of methylated TAs decreased in two susceptible cultivars 7 days after nematode inoculation, while it rose in three resistant ones (Veech, 1978). The precise structures of the methylated TAs were not provided, but other studies have shown that methylated TAs in cotton

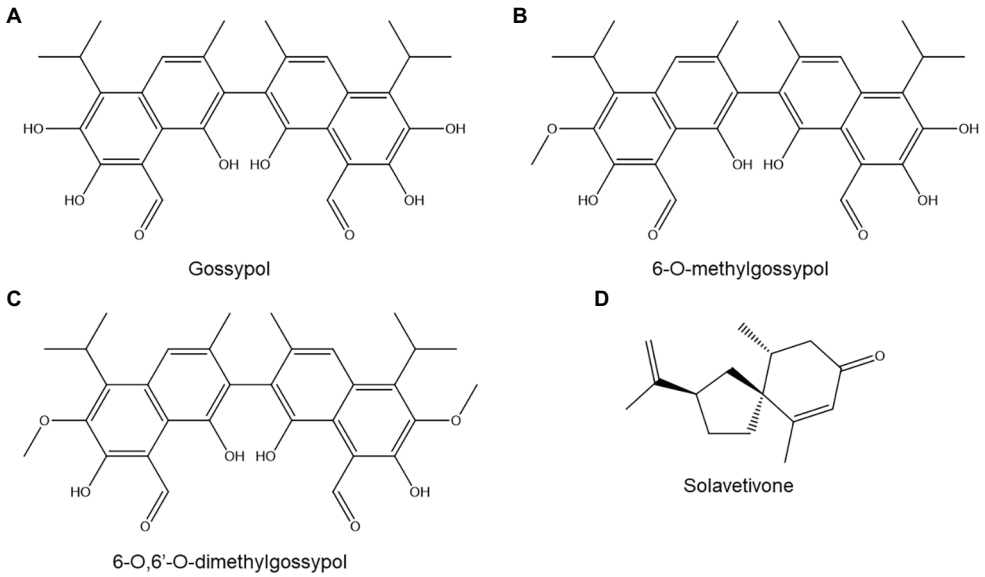

FIGURE 5 | Terpenoids discussed in this review: gossypol **(A)**, 6-*O*-methylgossypol **(B)**, 6-*O*,6'-*O*-dimethylgossypol **(C)**, and solavetivone **(D)**.

root include 6-*O*-methylgossypol (**Figure 5B**) and 6-*O*,6'-*O*-dimethylgossypol (**Figure 5C**; Frankfater et al., 2009).

A crude TA mixture, obtained *via* extraction of *G. hirsitum* roots followed by partial purification, showed strong nematistatic activity toward *M. incognita* juveniles with an IC_{50} of 10–50 µg/ml; concentrations upward of 125 µg/ml were also nematicidal (Veech, 1979). Interestingly, an extract from *Gossypium arboreum*, which is believed to produce only unmethylated TAs, showed significantly lower anti-nematode activity than the *G. hirsitum* extract. In turn, a pure gossypol acetate standard was even less nematicidal than the *G. arboreum* extract (Veech, 1979).

Cotton transgenic lines expressing *A. thaliana NPR1*, a gene involved in SA-mediated immunity, showed enhanced resistance to the reniform nematode *Rotylenchulus reniformis* as well as to various fungal pathogens (Parkhi et al., 2010). The *NPR1* lines showed identical basal root TA levels compared to the control but showed enhanced TA accumulation upon infection with the fungal pathogen *Verticillium dahliae*. The authors did not investigate whether this also occurs upon *R. reniformis* infection, and it was also found that *NPR1* expression triggers other defense responses besides TA accumulation (e.g., higher chitinase and glucanase activity). As such, it is hard to attribute a specific role for TAs in resistance to *R. reniformis*.

In pepper (*Capsicum annuum*), the relative concentrations of various terpenes in root exudates in several varieties were correlated with their susceptibility to *M. incognita* (Kihika et al., 2017). Olfactometer tests confirmed that several terpenes exuded by *C. annuum* had repellent or attractive effects on *M. incognita* J2s, which indicates that exuded terpenes may play a role in PPN susceptibility by enhancing or inhibiting host-finding (Kihika et al., 2017).

Solanaceae produce various sesquiterpene phytoalexins, whose role in PPN resistance remains unclear. One study found that potato varieties in which the sesquiterpene solavetivone (**Figure 5D**) forms a greater than average fraction of total sesquiterpene levels show higher levels of resistance to *Globodera rostochiensis* (Desjardins et al., 1995). However, cultivars with high solavetivone production all shared a common *Solanum tuberosum ssp. andigena* ancestor line (Desjardins et al., 1995), so the resistance of these lines may be caused by another trait inherited from this ancestor line rather than by solavetivone accumulation.

Several plant species produce terpenoid phytoalexins that have not yet been evaluated for a role in nematode resistance. For example, among cereals, maize (*Zea mays*) produces both diterpenoid (kauralexins and dolabralexins) and sesquiterpenoid (zealexins) phytoalexins (Block et al., 2019), while rice produces three different classes of diterpenoid phytoalexins: momilactones, phytocassanes, and oryzalexins (Yamane, 2013). All these terpenoids are involved in defense against fungal, bacterial, and/or insect pests and pathogens (Dillon et al., 1997; Lu et al., 2018; Pichersky and Raguso, 2018; Block et al., 2019), and they are inducible by treatment with resistance inducers that reduce susceptibility to nematodes (Yamane, 2013; Verbeek et al., 2019); it may thus prove fruitful to investigate their role in PPN resistance.

Apart from having direct anti-nematode effects, terpenoids are also involved indirectly in plant-nematode interactions by acting as plant hormones. Abscisic acid is derived from a tetraterpenoid (Nambara and Marion-Poll, 2005), the brassinosteroids from a triterpenoid (Choe, 2006), and the various gibberellins are diterpenoids (Hedden and Thomas, 2012). All of these hormones are known to play varying (often antagonistic) roles in plant resistance to PPN (Nahar et al., 2012, 2013; Kyndt et al., 2017; Bauters et al., 2018; Song et al., 2018; Yimer et al., 2018).

Saponins

Saponins are plant secondary metabolites defined as glycosides of a C30 terpenoid (Moses et al., 2014). Owing to their terpenoid aglycone, they could have been included in the previous section, but due to their diversity and unique properties (e.g., surfactant activity (Osbourn, 1996)), we opted to place them in a separate subcategory. A major example of saponins with roles in plant defense are the toxic glycoalkaloids produced by various Solanaceae, including α-tomatine (**Figure 6A**) from tomato and α-solanine (**Figure 6B**) and α-chaconine (**Figure 6C**) from potato (Osbourn, 1996).

α-Tomatine, which plays a role in tomato resistance to fungal pathogens and insect pests (Elliger et al., 1988), has been evaluated for a role in resistance to *M. incognita* (Elliger et al., 1988). Twelve tomato cultivars with varying resistance levels were assayed for basal root α-tomatine concentrations, and no correlation between α-tomatine production and resistance could be discerned. Furthermore, root α-tomatine concentrations were unchanged by *M. incognita* infection at all examined time points (between 3 and 14 days postinoculation) in both a resistant and a susceptible cultivar. Although it cannot be ruled out that α-tomatine might accumulate selectively near infection sites, which might be missed by bulk root analysis, these data indicate that α-tomatine is unlikely to be a major ANP (Elliger et al., 1988).

One study speculatively linked the resistance of the wild potato species *Solanum canasense* to *Globodera pallida* to its high glycoalkaloid content but provided no evidence for this hypothesis (Castelli et al., 2006). Moreover, in cultivated potato, no correlation was found between tuber glycoalkaloid content (α-solanine and α-chaconine) and resistance to *G. pallida* or *G. rostochiensis* in a breeding population of potato lines with glycoalkaloid contents ranging from 50 to 1,680 mg/kg (Grassert and Lellbach, 1987).

The absence of a role for glycoalkaloids in resistance to potato cyst nematodes is supported by another study, which compared *G. pallida* resistance and root glycoalkaloid content in four potato lines (two cultivated potato varieties and two progenies from a cross between cultivated potato and the *G. pallida*-resistant wild potato *Solanum vernei*; Forrest and Coxon, 1980). There was no correlation between resistance and either basal glycoalkaloid content or glycoalkaloid content 1 month after nematode inoculation. In fact, the most resistant accession had the lowest glycoalkaloid content (Forrest and Coxon, 1980).

In line with these results, alfalfa saponins also do not appear to play a role in nematode resistance: no correlation was found between resistance to *Meloidogyne hapla* and *D. dipsaci* and basal saponin concentration in six alfalfa cultivars (Pedersen et al., 1976).

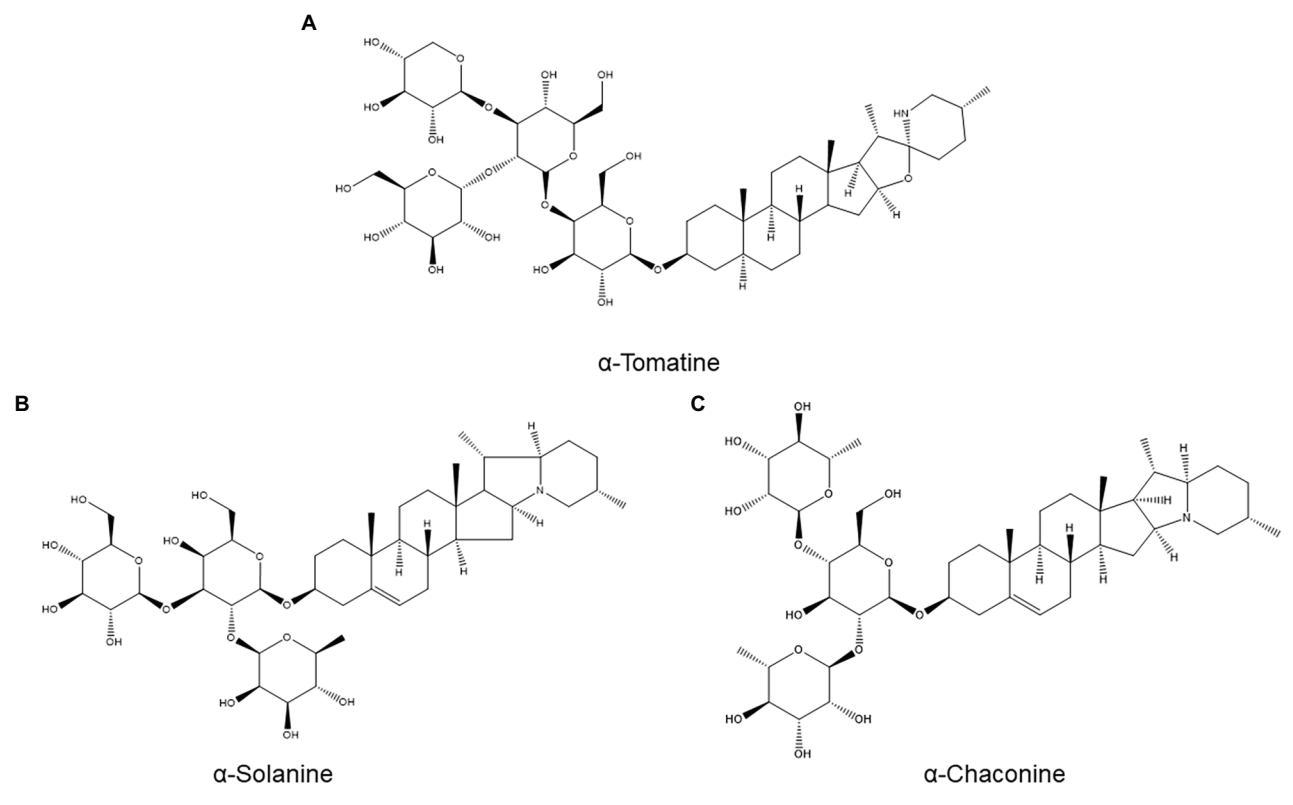

FIGURE 6 | Structures of three saponins investigated for a possible role in nematode resistance: the tomato saponin α-tomatine **(A)** and the potato saponins α-solanine **(B)** and α-chaconine **(C)**.

In oats, however, saponins have been tentatively linked to *H. avenae* resistance. HPLC-MS analysis of fractionated extracts from root tips of single-seed descent lines with varying levels of resistance to *H. avenae* found three peaks whose abundance was highly correlated to *H. avenae* resistance (Bahraminejad et al., 2008). Two of these subfractions contained compounds partially characterized as avenacins, a class of saponins common in oats. The third fraction contained an unstable metabolite that could not be characterized further (Bahraminejad et al., 2008). Although this result is correlative, it suggests that these avenacins might be anti-nematode phytoanticipins.

Overall, there is currently little evidence to suggest that saponins play a major role in plant resistance to nematodes. However, based on the limited range of host plants in which saponins were studied and on the known nematicidal effects of several saponin-rich plant extracts (Chitwood, 2002; Ntalli and Caboni, 2012), it seems premature to draw firm conclusions on the importance of saponins in PPN resistance.

Alkaloids

Alkaloids are an extremely heterogenous group of plant secondary metabolites whose only commonality is that they contain at least one nitrogen atom, often in a heterocyclic ring. Most, but not all, alkaloids are ultimately derived from amino acids. Some authors have proposed the idea that true alkaloids are defined by a common biosynthesis mechanism involving the formation of a Schiff base followed by a Mannich condensation, rather than by a common precursor or structure (Waterman, 1998).

While the taxonomy of alkaloids is complicated and ambiguous, their importance in the plant kingdom is clear. True alkaloids have been found in over one-fifth of all plant species, and over 12,000 unique alkaloids have been identified (Ziegler and Facchini, 2008; Schläger and Dräger, 2016). Many are highly toxic and play important roles in plant defense against pests and pathogens (Mithöfer and Boland, 2012).

Camalexin (**Figure 7A**) is the primary phytoalexin of the model plant *A. thaliana*. This small tryptophan-derived indole alkaloid has been extensively studied and is implicated in *A. thaliana* resistance to a broad spectrum of pests and diseases (Zook and Hammerschmidt, 1998). The *cyp79b2/b3* double mutant, which is severely impaired in camalexin production, showed a statistically significant increase in *H. schachtii* reproduction compared to its wild type (Shah et al., 2015). Similarly, the *pad3* mutant, which is also impaired in camalexin biosynthesis, was significantly more susceptible to *M. incognita* (Teixeira et al., 2016).

The role of nicotine, the principal alkaloid of tobacco (*Nicotiana tabacum*), in resistance to *M. incognita* has been investigated (Davis and Rich, 1987). A resistant tobacco cultivar accumulated significantly more nicotine 4 days after inoculation, whereas the concentration of nicotine in the susceptible cultivar remained unchanged. Whether this plays a causal role in *M. incognita* resistance is unclear: even the susceptible cultivar reportedly contained basal nicotine concentrations that were nematicidal *in vitro* (Davis and Rich, 1987).

Pyrrolizidine alkaloids, a widespread alkaloid family, also play a role in PPN resistance. The available literature on this

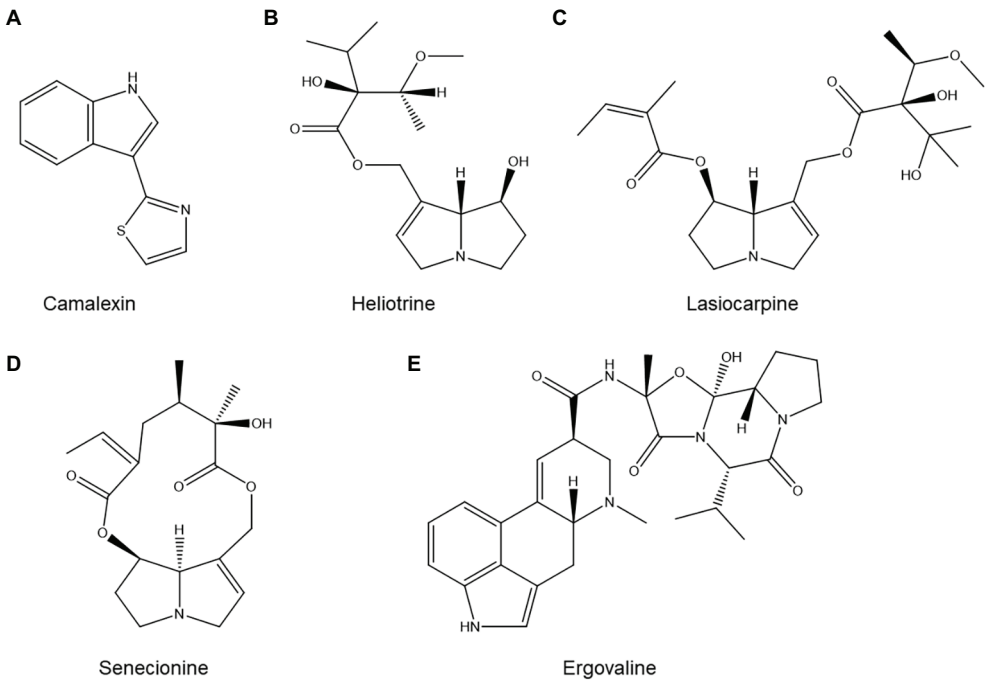

FIGURE 7 | Structures of several alkaloids with possible roles in nematode resistance: **(A)** the *Arabidopsis thaliana* alkaloid camalexin; **(B–D)** three common pyrrolizidine alkaloids with nematicidal activity; and **(E)** ergovaline, one of the ergot alkaloids produced by endophytic fungi of *Pratylenchus*-suppressive grasses.

topic has already been thoroughly reviewed by Thoden and Boppré (2010), so we will not attempt to duplicate this excellent work. Briefly, the authors observe that plants which accumulate substantial amounts of pyrrolizidine alkaloids in their roots are generally very poor hosts for PPN. Moreover, both pure pyrrolizidine alkaloid standards and extracts from pyrrolizidine alkaloid-rich plants tend to be nematicidal *in vitro*, and soil amendments composed of pyrrolizidine alkaloid-rich plants suppress PPN. For illustrative purposes, three common pyrrolizidine alkaloids with known nematicidal activity (Thoden et al., 2009) are shown in **Figures 7B–D**.

Interestingly, not all alkaloids found in plants are produced by the plant themselves. Notably, grasses often contain ergot alkaloids produced by endophytic fungi (e.g., ergovaline, shown in **Figure 7E**). Ergot alkaloids may play a role in resistance to *Pratylenchus* sp., based on the observations that grasses colonized by endophytic fungi such as *Epichloë* spp. suppress *Pratylenchus* in field conditions and that ergot alkaloids are nematicidal *in vitro* (Bush et al., 1997; Bacetty et al., 2009). However, one study showed that in at least one grass-endophyte system, knocking out alkaloid biosynthesis in the fungus did not eliminate its ability to induce resistance to *P. scriberni* in perennial ryegrass (*Lolium perenne*; Panaccione et al., 2006). Alkaloid production is thus at most one of several mechanisms by which fungal endophytes enhance the nematode resistance of their hosts.

Benzoxazinoids

Benzoxazinoids are secondary metabolites with a key role in defense against various insect pests (Niemeyer, 2009; de Bruijn et al., 2018) that are most commonly – but not exclusively – found in grasses, including in cereals such as wheat (*Triticum aestivum*), rye (*Secale cereale*), and maize (Niemeyer, 2009; de Bruijn et al., 2018). All benzoxazinoids are derived from indole, which undergoes a series of steps involving hydroxylation, ring expansion, methoxylation, and glycosylation to yield the various benzoxazinoids (Gierl and Frey, 2001).

The importance of benzoxazinoids in PPN resistance has not been extensively studied but appears to be modest at most. No correlation was found between benzoxazinoid content and resistance to the stubby-root nematode *Paratrichodorus minor* in 12 maize hybrids (Timper et al., 2007), nor between levels of the principal maize benzoxazinoid DIMBOA (**Figure 8A**) and resistance to *P. penetrans* (Friebe, 2001). Furthermore, DIMBOA at the concentration present in maize root exudates was an attractant for *P. penetrans* (Friebe, 2001). Although several rye benzoxazinoids show nematistatic activity *in vitro* (Zasada et al., 2005), their concentration in roots and root exudates is too low to have ANP activity (Meyer et al., 2009).

In contrast to these negative results, another study reported that inoculating wheat with an arbuscular mycorrhizal fungus that repressed benzoxazinoid production significantly increased susceptibility to *P. neglectus* (Frew et al., 2018). Furthermore, a wheat cultivar with higher susceptibility to *P. neglectus* showed lower basal and induced benzoxazinoid concentrations (Frew et al., 2018). Individual benzoxazinoids showed contrasting accumulation patterns between treatments: HMBOA-glucoside (**Figure 8B**) and HDMBOA-glucoside (**Figure 8C**) appeared positively correlated to resistance to *P. neglectus*, whereas this was not observed for DIBOA-glucoside (**Figure 8D**; Frew et al., 2018).

Glucosinolates

Plants in the order Brassicales produce varying levels of glucosinolates, metabolites derived from glucose and an amino

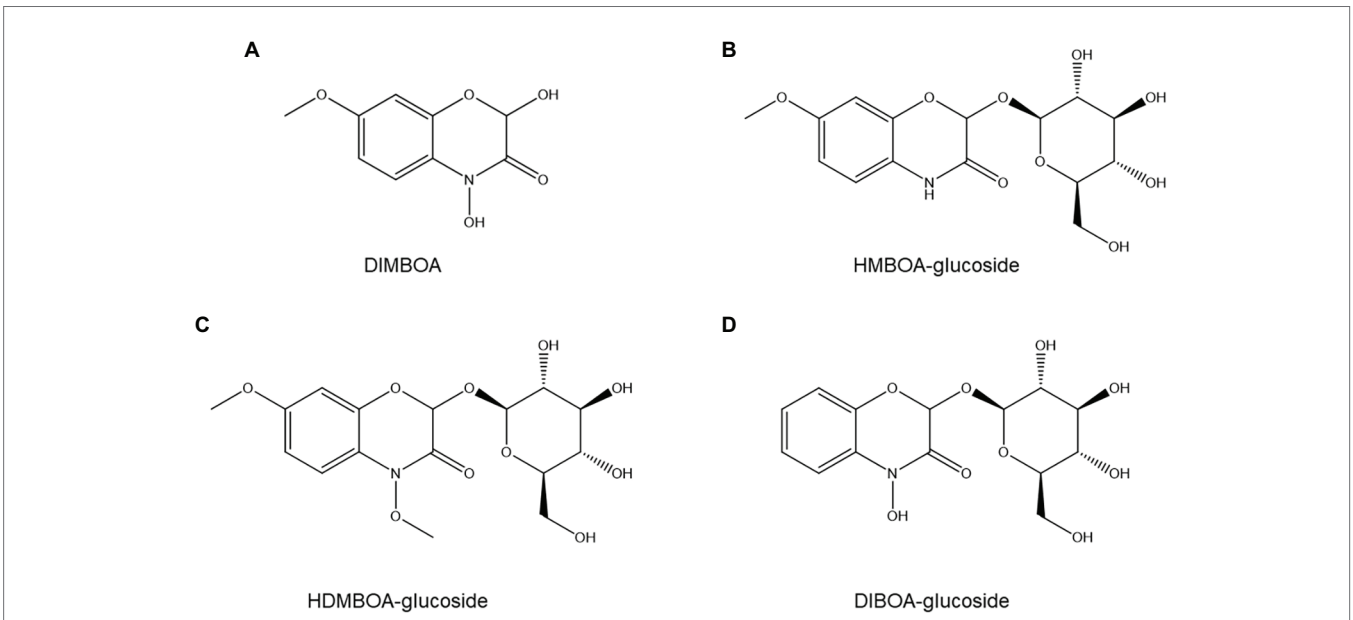

FIGURE 8 | Structures of four common benzoxazinoids evaluated for possible roles in nematode resistance: DIMBOA **(A)**, HMBOA-glucoside **(B)**, HDMBOA-glucoside **(C)**, and DIBOA-glucoside **(D)**.

acid which are characterized by the presence of both sulfur and nitrogen atoms. Enzymatic hydrolysis of glucosinolates by MYROSINASE releases unstable, biocidal isothiocyanates with a major role in resistance to insects and plant pathogens (Rask et al., 2000; van Dam et al., 2009).

In vitro data suggest that glucosinolates have strong nematicidal activity and biofumigation, the use of Brassica seed meal or green manures as soil amendments, can be an effective alternative to chemical fumigation (van Dam et al., 2009). However, the evidence available on their *in vivo* role in resistance to nematodes remains limited.

In a survey of *Brassica napus* accessions, susceptibility to *P. neglectus* proved uncorrelated to total glucosinolate content (Potter et al., 1999). However, a clear relationship was found between susceptibility to *P. neglectus* and the concentration of one specific glucosinolate, 2-phenylethyl glucosinolate (**Figure 9C**). All cultivars producing more than a critical threshold estimated to be between 8 and 12 µmol/g fresh root tissue showed low susceptibility to *P. neglectus*. However, other resistance mechanisms must also exist in *B. napus*, as several accessions with low 2-phenylethyl glucosinolate content also showed low susceptibility (Potter et al., 1999). The efficacy of various *Brassica* species as biofumigants against *P. neglectus* was also correlated with their 2-phenylethyl glucosinolate content but not with their total glucosinolate concentration (Potter et al., 1998).

By contrast, a comparison of the susceptibility of 11 Brassicaceae species toward *M. javanica* found no correlation between resistance and either total glucosinolate content or glucosinolate composition (McLeod et al., 2001).

In *Arabidopsis thaliana*, the *myb34/51* double mutant, which is impaired in the biosynthesis of indolic glucosinolates such as 4-methoxy-3-indolylmethyl glucosinolate (**Figure 9A**) and 1-methoxy-3-indolylmethyl glucosinolate (**Figure 9B**), showed significantly higher susceptibility to *M. incognita* than its wild type (Teixeira et al., 2016). *MYB34* expression is also significantly downregulated in giant cells of *M. incognita*-infected *A. thaliana*, which provides further support for a role for glucosinolates in PPN resistance (Portillo et al., 2013).

Organosulfur Compounds

The resistance of several marigolds (*Tagetes* sp.) toward PPN and the suppressive effect of *Tagetes* cultivation on nematode populations have been attributed to strongly nematicidal polythienyl compounds present in *Tagetes* roots and their exudates, such as *α*-terthienyl (**Figure 10A**; Uhlenbroek and Bijloo, 1958; Chitwood, 2002). A meta-analysis of 175 Asteraceae species found that their suppressive effect on *P. penetrans* populations was highly correlated with their polythienyl content: out of 16 Asteraceae species known to produce α-terthienyl, 15 were suppressive to *P. penetrans* (Gommers and Voorin'tholt, 1976).

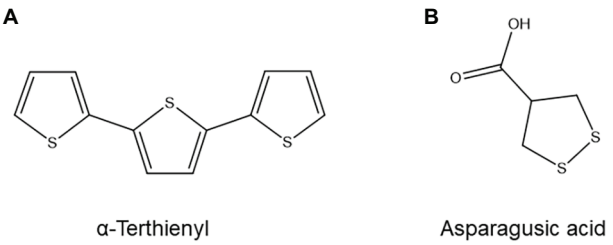

FIGURE 10 | Structure of two nematicidal organosulfur compounds: **(A)** α-Terthienyl, one of several nematicidal polythienyl compounds produced by marigolds. **(B)** Asparagusic acid, a nematicidal asparagus metabolite.

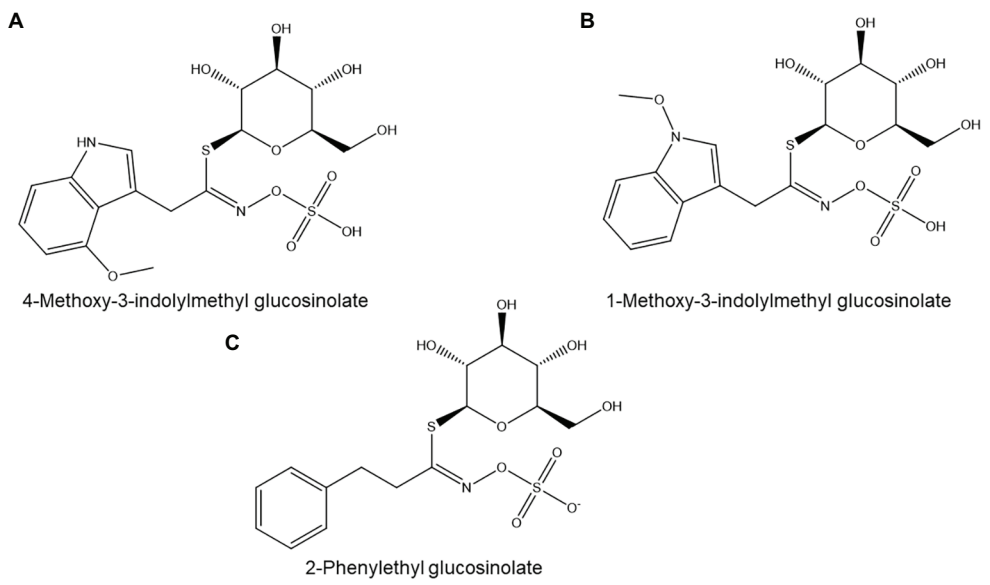

FIGURE 9 | Glucosinolates with possible nematicidal activity: **(A,B)** Two major indolic glucosinolates from *A. thaliana*. **(C)** 2-Phenylethyl glucosinolate, a major glucosinolate from *Brassica napus*.

An unidentified acetylenic dithio compound with a bright red coloration was also correlated with anti-PPN activity: 11 out of 12 evaluated Asteraceae species known to exude this compound were suppressive to *P. penetrans* (Gommers and Voorin'tholt, 1976).

The biosynthesis of α-terthienyl and related compounds remains to be fully elucidated, although several mechanisms have been suggested (Arroo et al., 1995). The nematicidal mechanism of action of α-terthienyl, by contrast, has been studied in more detail than that of most other ANPs. It has been demonstrated that α-terthienyl generates reactive oxygen species upon activation by light and/or peroxidase enzymes (Chitwood, 2002; Hamaguchi et al., 2019). In *Caenorhabditis elegans*, RNAi-lines with suppressed or induced accumulation of SUPEROXIDE DISMUTASE and GLUTATHIONE PEROXIDASE respectively showed increased and reduced susceptibility to α-terthienyl. Furthermore, α-terthienyl readily penetrated the nematode hypodermis (Hamaguchi et al., 2019). These results indicate that α-terthienyl owes its nematicidal effect to its ability to induce oxidative stress inside the nematode (Hamaguchi et al., 2019).

Asparagus (*Asparagus officinalis*), another plant with nematode-suppressive properties, was shown to produce a highly nematicidal compound in its roots that could be identified as the organosulfur compound asparagusic acid (**Figure 10B**; Takasugi et al., 1975). Asparagusic acid at a concentration of 50 ppm has strong nematicidal properties against several PPN species and inhibits *Heterodera* egg hatching (Takasugi et al., 1975). Since asparagus roots were found to contain at least 35 ppm of asparagusic acid, it is likely that this compound is a phytoanticipin with a major role in the anti-nematode activity of asparagus plants (Takasugi et al., 1975). Asparagusic acid biosynthesis is believed to be unique to asparagus and is poorly understood, but likely involves isobutyric acid and methacrylic acid as precursors and the amino acid cysteine as the donor of at least one of the sulfur atoms (Mitchell and Waring, 2014).

IDENTIFYING ANPs: METHODS, CHALLENGES, AND RECENT ADVANCES

Identification of ANPs remains a challenging task, despite technological advances. Historically, most ANPs were identified by preparing crude extracts from nematode-suppressive or resistant plants, either with or without elicitation by nematode inoculation, and then laboriously (sub)-fractionating these extracts until pure compounds, or more frequently mixes of a few related compounds, were obtained. By assaying these (sub-)fractions for anti-nematode efficacy, an active (sub)-fraction could be identified. This fraction was then subjected to a range of analytical methods such as elemental analysis, ultraviolet/visible light (UV/VIS) and infrared spectroscopy, color reagents, and, in more recent studies, mass spectrometry (MS) or nuclear magnetic resonance (NMR). These techniques often allowed the researcher(s) to propose candidate compounds, which were then synthesized chemically and used as analytical standards. This approach is extremely laborious and requires large quantities of input material, often upward of 20 kg (Uhlenbroek and Bijloo, 1958; Takasugi et al., 1975).

Not all researchers who identified ANPs had to start from scratch. In some cases, plant metabolites that had previously been identified as being involved in plant resistance to other plant pests or pathogens were deliberately investigated for a role in PPN resistance. Because these potential ANPs were known in advance, extraction, and quantification could proceed in a targeted, more rapid manner. This "shortcut" facilitated e.g., the identification of glyceollin I as a key player in soybean PPN resistance (Kaplan et al., 1980b).

Further evidence for a causal role occasionally came from histopathological methods, which can show whether metabolites of interest preferentially accumulate at or near PPN infection sites. This approach was used to demonstrate that glyceollin I accumulated near the head of *H. glycines* in resistant soybean (Huang and Barker, 1991) and that terpenoid aldehydes accumulate more rapidly and widely in RKN-affected root areas in resistant cotton cultivars (Veech, 1979).

A more modern, hitherto relatively uncommon approach, for evaluating the role of metabolites in nematode resistance involves infection experiments in mutants impaired in the biosynthesis of these metabolites. If the mutant in question is thoroughly characterized and free of interfering pleiotropic effects (e.g., because the biosynthesis of related products of the same pathway is also eliminated), this method can yield strong evidence for a causal role in resistance. Unfortunately, generating mutants requires either thorough knowledge of the biosynthetic pathways involved in the production of a metabolite (in which case targeted mutagenesis can be used), or an extremely laborious process of random mutagenesis followed by metabolic or phenotypic screening. Furthermore, transformation protocols remain unavailable for many non-model plant species. By consequence, extensive libraries of mutants exist only in a limited number of model plants and pathways. Despite these drawbacks, mutant analysis has been successfully employed to study e.g., the role of *A. thaliana* secondary metabolites in nematode resistance (Shah et al., 2015; Teixeira et al., 2016).

Another method for putative ANP identification involves assembling a panel of different cultivars or closely related species with varying susceptibility to a certain PPN and then trying to correlate this variation in resistance to basal or induced levels of a specific metabolite (Giebel, 1970; Hung and Rohde, 1973; Veech, 1978; Hedin et al., 1984; Grassert and Lellbach, 1987; Elliger et al., 1988; Gill et al., 1996; Baldridge et al., 1998; Potter et al., 1999). This approach has three major downsides: it depends on the proper selection of a sufficiently diverse and representative panel to avoid false positives, it cannot prove causality and it requires a possible ANP to be known in advance. However, the latter downside can be avoided by the emergence of a novel analytical approach: untargeted metabolomics.

Untargeted metabolomics is a collective term for methods that seek to provide an unbiased, comprehensive picture of

the metabolite composition of a biological sample. Through untargeted profiling of plant varieties or species with varying degrees of resistance to a PPN, metabolites with possible roles in nematode resistance may be identified and studied further. As well as requiring little prior knowledge, modern metabolomics methods also require only small quantities of input material (often just 100 mg of fresh plant material). However, much larger quantities of material may still be required later on to allow the extraction and purification of sufficient quantities of putative ANP for bioassays.

Untargeted metabolomic analysis of plant-nematode interactions remains uncommon but has been more widely used to study plant interactions with bacteria, fungi, and insects (Heuberger et al., 2014; Feussner and Polle, 2015; Maag et al., 2015; Tenenboim and Brotman, 2016; van Dam and Bouwmeester, 2016). In relation to the study of ANPs, the objective of untargeted metabolomics is to identify metabolites which discriminate resistant and susceptible plants, either basally or after nematode infection. Such metabolites can then be evaluated for their possible role as ANPs using the various techniques described previously, such as testing their *in vitro* anti-nematode activity or examining the effect of knock-out mutants in their biosynthesis on nematode resistance.

The handful of metabolomics studies performed on plant-nematode interactions are discussed in the remainder of this review.

Gas chromatography-mass spectrometry (GC-MS) based profiling has been used to study the interaction between the sting nematode *Belonolaimus longicaudatus* and three bermudagrass (*Cynodon transvaalensis*) lines with varying levels of susceptibility (Willett et al., 2020). All lines showed extensive metabolomic reprogramming due to nematode parasitism when they were analyzed 3 months after inoculation, but there were substantial differences between lines and between individuals within each line. Nematode-mediated suppression of amino acid levels in the host plants was found to be highly correlated with higher susceptibility, whereas accumulation of L-pipecolic acid, D-glucuronic acid, glycolate, and phenylalanine correlated with lower susceptibility (Willett et al., 2020). The *in vivo* effect of these metabolites was not investigated, so their ANP status remains putative. However, L-pipecolic acid is a known inducer of systemic immunity in plants (Shan and He, 2018; Wang et al., 2018), while phenylalanine is the principal precursor of the phenylpropanoid pathway, which has an important role in plant immunity *via* the biosynthesis of phenolic phytoalexins and lignin (Vogt, 2010).

Another study combined untargeted GC-MS based metabolomics and transcriptomics on soybean roots inoculated either with *H. glycines*, a plant-growth promoting bacterium (PGPB) known to induce partial resistance to *H. glycines* or both (Kang et al., 2018). The authors identified four metabolites which were suppressed in plants 5 days after inoculation with *H. glycines* alone but not in plants co-inoculated with the PGPB and *H. glycines*. These metabolites were the phenolic compound 4-vinylphenol, the alkaloid piperine, the amino acid L-methionine, and the fatty acid palmitic acid. All four showed *in vitro* nematicidal effects at concentrations upward of 500 μg/ml, but no indication was given of the concentration of these metabolites *in planta* (Kang et al., 2018). As such, it is impossible to judge their importance to *H. glycines* resistance.

GC-MS based metabolic profiling of 5, 10, and 15 days-old syncytia in a compatible interaction between *H. schachtii* and *A. thaliana* showed that *H. schachtii* parasitism induces extensive reprogramming of primary metabolism, notably of amino acid and oligosaccharide metabolism (Hofmann et al., 2010). Since the study examined only a single, susceptible cultivar, no candidate ANPs could be identified; however, the oligosaccharides and amino acids identified as being affected by nematode parasitism might be targets for further research.

Combined transcriptome and metabolome (using HPLC-MS/MS) profiling of mature *M. incognita* galls (21 days postinoculation) in poplar roots showed that, compared to uninfected root tissue of the same age, *M. incognita* galls show severe disruption of genes and metabolites involved in cell wall biosynthesis and phenolic metabolism. Interestingly, although galls generally appeared to accumulate greater amounts of phenolic compounds than uninfected roots, chlorogenic acid was among the most strongly repressed metabolites in galls (Baldacci-Cresp et al., 2020).

Untargeted HPLC-MS analysis has been used to identify possible biomarkers for oat resistance to *H. avenae* (Bahraminejad et al., 2008). From a population of 170 single-seed descent lines originating from a cross between two oat cultivars, 15 highly resistant, and 15 highly susceptible lines were selected and grown in a misting chamber (without nematode inoculation). Extracts from the root tips of these lines were subjected to HPLC-MS analysis; for each observed peak, the correlation coefficient between its abundance in each line and that line's resistance to *H. avenae* was calculated. This led to the identification of three peaks whose abundance in uninoculated seedlings was highly correlated to resistance. Attempts to elucidate the structures of the compounds corresponding to these peaks led to the identification of two saponins with sterol cores corresponding to avenacin A-1 and avenacin B-1 but with different (unidentified) glycosides. The third peak contained a compound too unstable for purification. The authors note that HPLC-MS screening is significantly faster and less laborious than resistance trials, and that at least in this breeding population, the three peaks might, after further validation, serve as biomarkers for resistance (Bahraminejad et al., 2008).

HPLC-UV and NMR-based profiling of root extracts from cotton varieties that were either resistant or susceptible to *M. incognita* found only minor differences in the total abundance of flavonoids, gossypol, and gossypol derivatives between the two cultivars when they were sampled at 8, 24, and 35 days after inoculation. However, the resistant cultivar showed significantly higher basal contents of several minor flavonoids and gossypol derivatives that could not be conclusively identified (Alves et al., 2016).

Although MS is best known as a technique for identifying and quantifying metabolites in extracts, MS can also be used as an imaging technique to localize metabolites in plant tissues (a process known as MS imaging, or MSI). An elegant application of this method to study plant-nematode interactions can be found

in Hölscher et al. (2014). The authors took NMR spectra of four subfractions derived from a crude ethanol extract made from *R. similis* lesions in a resistant and susceptible banana variety. Based on these spectra, it was found that the resistant cultivar accumulated significantly larger amounts of several identifiable phenylphenalenone compounds. Sections of root areas showing *R. similis* lesions from a susceptible and resistant banana variety were then subjected to UV-laser desorption/ionization MSI, which revealed that metabolites with *m*/*z*-values corresponding to several of the identified phenylphenalenones accumulated in and near lesions – especially in the resistant cultivar. Several phenylphenalenones were isolated from banana root extracts and were found to be strongly nematicidal. Finally, MSI and Raman microspectroscopy revealed that phenylphenalenone anigorufone exerted nematicidal activity by inducing the formation of large lipid-anigorufone complexes inside the nematode's body. This study demonstrates how metabolomics technologies such as NMR and MS can be used to facilitate all stages of ANP discovery: NMR allowed identification and quantification of possible ANPs, while MS imaging could prove that the localization of the ANP correlated with nematode infection sites and provided information on the ANP's mechanism of action.

NMR has also been used as a standalone metabolomics technique in several studies on plant-nematode interactions, as will be shown in the following paragraphs.

A combination of NMR and UV/VIS-spectrophotometric assays was used to metabolically profile the roots of a *Meloidogyne exigua*-susceptible and resistant coffee cultivar in the presence or absence of nematode infection at 1, 2, and 4 days after inoculation (Machado et al., 2012). The analysis identified the accumulation of phenolic compounds, sucrose, and fumaric acid as being possibly involved in *M. exigua* resistance. Among phenolic compounds, the abundance of chlorogenic acid was unchanged; however, one of its constituent parts, quinic acid, was significantly more abundant in the resistant cultivar. Amino acids levels, total carbohydrate concentration, and total alkaloid concentration appeared uninvolved in resistance (Machado et al., 2012).

Untargeted NMR-based metabolomics has also been applied to the tomato-*M. incognita* interaction. Root tissue from four cultivars (two highly susceptible and two highly resistant) was collected 38 days after inoculation and analyzed; the researchers found several metabolites that accumulated significantly more after infection in the resistant accessions but not in the susceptible ones. Two of these compounds were conclusively identified as caffeic acid and glucose respectively (Afifah et al., 2019). However, no causal evidence for a role for caffeic acid or glucose in resistance was presented.

NMR metabolomics has also been used to study nematode interactions in seedlings of the soursop tree (*Annona muricata*), which is highly resistant to nematode infection (Machado et al., 2019). Extracts of root systems of soursop seedlings with or without *M. javanica* inoculation were harvested at various time points between 1 and 30 days after inoculation, analyzed through NMR and then used for bio-assay guided fractionation. The experiments revealed that soursop root extracts were nematistatic, and that after fractionation, this activity was concentrated in the chloroform fraction. Further NMR analysis of this fraction showed that it contained several acetogenins, a class of secondary metabolites common among the Annonaceae that have known insecticidal activity. No major metabolome shift was seen in nematode-inoculated plants compared to uninoculated plants at time points later than 2 days postinoculation, which supports the notion that the soursop seedlings were highly resistant and that nematodes could not successfully invade (Machado et al., 2019).

Although untargeted metabolomics is a powerful tool for the identification of novel putative ANPs, progress is hindered by the difficulty of high-throughput metabolite identification. A browse through the PlantCyc metabolite database (Schläpfer et al., 2017) shows that even for relatively well-annotated plant species such as tomato, rice, and *A. thaliana*, between 2,500 and 3,000 metabolites are present and the PlantCyc database as a whole contains fewer than 5,000 unique, characterized metabolites. These values can be compared to the estimated 200,000 distinct secondary metabolites believed to be present in higher plants (Viant et al., 2017).

Another challenge in metabolomics studies is the difficulty of obtaining truly representative, unbiased metabolome profiles. Depending on the choice of sample preparation method and/or analytical technique, different parts of the metabolome will be captured in more detail than others (Ernst et al., 2014; Sumner et al., 2015). Although fully discussing the relative merits of different metabolomics methods is beyond the scope of this review, it is worth mentioning that each of the analytical methods described in this review has biases.

NMR provides the most comprehensive structural information about metabolites (including stereochemistry), is highly reproducible, and is not biased toward metabolites of certain sizes or polarities (Moco et al., 2007; Kim et al., 2010, 2011; Schripsema, 2010). However, it is less sensitive than MS and the absence of a separation step prior to analysis often leads to spectra with strong signal overlap in which few metabolites can be identified (Moco et al., 2007; Kim et al., 2010, 2011; Schripsema, 2010). The sensitivity of NMR has improved over the years, but the problem of spectral overlap remains (Moco et al., 2007; Kim et al., 2010, 2011; Schripsema, 2010). Three main solutions exist for this problem: using 2D-NMR methods (Moco et al., 2007; Kim et al., 2010, 2011; Schripsema, 2010), coupling NMR to LC (Moco et al., 2007; Sumner et al., 2015), or fractionating the extract prior to NMR analysis (Moco et al., 2007; Kim et al., 2010). LC-NMR has not yet been used in studies of PPN, whereas fractionation and 2D NMR have been used with some success by e.g., Machado et al. (2019).

GC-MS and HPLC-MS are widely used metabolomics techniques. Both methods share high sensitivity and excellent separation but differ in other important respects. GC-MS uses high-energy ionization, which leads to detailed, reproducible MS spectra that allow straightforward matching to biological databases (Ernst et al., 2014). However, GC-MS can only detect metabolites which are sufficiently volatile, either natively or after chemical derivatization (Moco et al., 2007; Ernst et al., 2014). This limitation restricts its usefulness to

smaller metabolites, whereas ANPs are often relatively large. HPLC-MS, by contrast, is not restricted to volatile compounds but has drawbacks of its own: a single LC column cannot be used to separate metabolites of widely different polarity, and metabolite identification in HPLC-MS may be complicated owing to the relatively poor reproducibility of mass spectra and matrix effects such as the formation of adducts (Ernst et al., 2014). The former disadvantage, however, is usually manageable as most classes of plant secondary metabolites believed to be involved in plant-nematode interactions are semipolar and thus amenable to analysis on a common reversed-phase C18 column (Moco et al., 2007).

Given the differing strengths and weaknesses of NMR, GC-MS and LC-MS, choosing an appropriate technique in advance is important. A common strategy to aid in method selection is to use transcriptome analysis to identify pathways possibly involved in nematode resistance prior to metabolome analysis. Based on the expected size and polarity of the metabolites of pathways identified through transcriptomic analysis, the most appropriate metabolome technique can be chosen. A good example of this approach is found in Baldacci-Cresp et al. (2020): after RNA-seq had shown that the expression of genes involved in phenolic metabolism was severely affected by *M. incognita* parasitism, the authors chose HPLC-MS/MS as the technique best suited to analyzing these metabolites (Baldacci-Cresp et al., 2020).

Despite the challenges involved in choosing an appropriate sample preparation method and analytical technique, metabolomics approaches show clear potential in elucidating the role of secondary metabolites in nematode resistance. As exemplified by the studies mentioned in this review, untargeted metabolomics can identify novel candidate-ANPs in plants, even in non-model species such as *A. muricata* or *C. transvaalensis*.

POSSIBLE APPLICATIONS OF ANPs IN PPN CONTROL

Although the identification of novel ANPs has scientific value in itself, ANP discovery also has practical applications. Perhaps the most obvious is to facilitate the discovery of novel botanical nematicides. The nematicidal properties of isothiocyanates have been exploited for decades, either through chemical methyl isothiocyanate precursors such as metam sodium or dazomet (Chitwood, 2003) or *via* biofumigation (van Dam et al., 2009). Various phytochemical-based nematicides, obtained either through extraction or chemical synthesis, are commercially available (Chitwood, 2003; Ladurner et al., 2014; Medico et al., 2018). Novel ANPs, identified through untargeted metabolomics, may be good lead compounds for the development of novel phytochemical-based nematicides.

Identifying ANPs could also provide targets for crop improvement through genetic engineering, either by increasing the biosynthesis of ANPs already present in a species or by enabling the biosynthesis of novel ANPs through transgenic constructs. Although attractive in theory, no such genetically modified crops have been reported to the best of our knowledge.

Finally, ANPs could act as biomarkers in nematode resistance breeding, where high-throughput targeted metabolomics could be used for screening breeding lines instead of laborious nematode resistance assays. Several articles cited in this review have raised the idea of using metabolic markers in resistance breeding.

Terpenoid aldehyde levels in roots, leaves, and seeds have all been evaluated as biomarkers for cotton resistance to *M. incognita* but with limited success: as discussed previously, the correlation between root TA levels and *M. incognita* is imperfect (Khoshkhoo et al., 1994a) and seed and leaf TA content appear to have no predictive value at all (Khoshkhoo et al., 1994b). High root 2-phenylethyl glucosinolate content has been suggested as a possible biomarker for *Pratylenchus* resistance in canola, although here too some highly resistant genotypes were found to contain low root 2-phenylethyl glucosinolate concentrations (Potter et al., 1999). Tannins have been proposed as biomarkers for *R. similis* resistance in banana (Collingborn et al., 2000). Finally, concentrations of flavonoids (Soriano et al., 2004) and saponins (Bahraminejad et al., 2008) in oat roots have been suggested as biomarkers for *H. avenae* resistance, but once again this approach is complicated by the existence of resistance mechanisms independent of flavonoids against *H. avenae* (Bahraminejad et al., 2008). Since multiple resistance mechanisms appear to exist in most breeding pools, metabolic markers must be thoroughly evaluated for each breeding population to avoid an excessively high false negative rate. However, this may be worthwhile in certain cases due to the laborious and time-consuming nature of conventional nematode resistance screening.

Metabolic markers could also be used to screen for induced resistance. Resistance inducers are exogenously applied chemicals or microbes which stimulate the plant immune response against pests or pathogens (Heil, 2001; Eyles et al., 2010; Pieterse et al., 2014; Mauch-Mani et al., 2017), including PPN (Oka et al., 1999; Oka and Cohen, 2001; Molinari and Baser, 2010; Vos et al., 2013; Fujimoto et al., 2015; Ji et al., 2015; Huang et al., 2016; Zhan et al., 2018; Singh et al., 2019). If metabolic markers can be reliably correlated to induced resistance in a given plant-PPN system, they can be used to screen for novel resistance inducers and to study the longevity of induced resistance in a more high-throughput manner than possible through conventional inoculation experiments.

The emergence of untargeted metabolomics paired with high-dimensional statistical methods may enable selection based on *metabolic profiles* rather than based on specific metabolic markers. In this approach, multiple features, each representing a (possibly unidentified) metabolite associated with PPN resistance, are assessed simultaneously to predict PPN resistance. This approach has been successfully demonstrated in breeding for traits such as resistance to fungal pathogens (Hamzehzarghani et al., 2005; Fernie and Schauer, 2009; Saito and Matsuda, 2010; Tomita et al., 2017) but has not yet been applied to plant-nematode interactions. However, the oat-*H. avenae* cases mentioned in this review hint at the possible utility of this

approach: since resistance mechanisms involving flavonoids (Soriano et al., 2004) and saponins (Bahraminejad et al., 2008) have been identified, metabolic profiling for both classes of metabolites – and possibly others – will be required for reliable screening.

CONCLUSION AND FUTURE PERSPECTIVES

Since the middle of the twentieth century, a substantial number of studies have proven that plants make extensive use of small molecules to defend against PPN. Although the enormous diversity of metabolites, plants, and nematode species studied to date makes generalization difficult, several conclusions can be drawn from the available literature.

First and foremost, the number of ANPs for which a causal role in resistance to nematodes has been conclusively determined remains highly limited. This may, at least, partially be explained by the difficulty of proving causality in ANP studies. In our opinion, conclusively proving a causal role for an ANP in PPN resistance requires four lines of evidence. First, it must be demonstrated that the abundance of a compound or class of compounds is *correlated* with resistance – e.g., by demonstrating that its abundance is higher in resistant varieties. Second, purified or chemically synthesized candidate-ANPs should show anti-nematode activity *in vitro*. Third, the suspected ANP should accumulate *in planta* to a biologically relevant concentration in or near a site of interaction with the nematode. Finally, reducing or abolishing the production of the ANP in a resistant plant (e.g., through gene silencing or chemical inhibition) should diminish resistance. No single study cited in this review presents all four lines of evidence, although several provide the first three. The rarity of the fourth step may be explained by the fact that many studies cited in this review pre-date the -omics era.

This brings us neatly to a second observation: many of the studies cited in this review are relatively old. Indeed, the average age of original research articles on ANPs cited in this review is nearly 25 years. The apparently declining attention given to ANPs in recent decades is also reflected in reviews on plant immunity to nematodes: whereas reviews on plant resistance to nematodes from the 1980s (Giebel, 1982; Veech, 1982) had ANPs as their primary focus, more recent reviews address them briefly (Sato et al., 2019) or do not mention them at all (Holbein et al., 2016). We believe that revisiting ANPs using the novel research methods that have emerged over the last two decades, such as targeted mutagenesis, transcriptomics, and metabolomics, may be a fruitful way to advance plant nematology.

A third conclusion is that several studies cited in this review report that the total concentration of a certain class of secondary metabolites is uncorrelated to PPN resistance, whereas the concentration of one or more specific, often low-abundance, metabolites within that class does show a strong correlation with resistance. Examples of this phenomenon in this review are found among terpenoid aldehydes in cotton (Veech, 1978, 1979; Hedin et al., 1984; Khoshkhoo et al., 1994a; Alves et al., 2016), flavonoids in soybean (Kaplan et al., 1980a,b; Huang and Barker, 1991; Kennedy et al., 1999; Carpentieri-Pipolo et al., 2005; Kang et al., 2018), stilbenoids in grapevine (Wallis, 2020), benzoxazinoids in wheat (Frew et al., 2018), and glucosinolates in canola (Potter et al., 1998, 1999). This observation stresses the importance of using analytical approaches that identify individual metabolites (e.g., HPLC- or GC-MS) instead of relying on less discriminatory techniques such as colorimetric assays.

Finally, a methodological shift in the study of ANPs can be discerned over time. When the study of ANPs began in the 1950s, researchers tended to work in a targeted manner: ANPs were sought in a low-throughput manner in extracts from plants that were known to have nematode-suppressive properties, or by studying metabolites whose role in resistance to other pests or diseases had already been established. As the performance and accessibility of GC/LC-MS and NMR increased, it became possible to work in a less targeted manner. Although untargeted studies of plant-nematode interactions remain uncommon, they have already enabled the identification of a handful of putative novel ANPs.

Taken together, these last two observations point to the importance of metabolomics approaches – which can be untargeted and independent of prior knowledge, and which examine individual metabolites – in identifying novel ANPs. The recent publication of a handful of metabolomics studies on plant-nematode interactions suggests that researchers are indeed beginning to harness the power of metabolomics. Despite their limited number, these studies have already hinted at novel ANPs in several plant species. This early success may lead to a revival of interest in ANP research, a trend that will doubtlessly be enhanced by the rapid growth of biological databases and the development of more user-friendly data analysis tools (e.g., MetaboAnalyst; Chong et al., 2019). Together with other -omics era research techniques, metabolomics may facilitate the arrival of a "golden age" in ANP research in the coming decade.

AUTHOR CONTRIBUTIONS

WD wrote this review with substantial input from SM, TK, and BV. All authors read and approved the final manuscript.

FUNDING

WD is supported by a Baekeland grant (project HBC.2017.0574).

ACKNOWLEDGMENTS

WD acknowledges the financial support of the Flemish government (Agency for Innovation and Entrepreneurship/ VLAIO) and Eastman, who co-sponsored Baekeland, grant HBC.2017.0574.

REFERENCES

Abawi, G. S., and Vanetten, H. D. (1971). "Phaseollin production induced by *Pratylenchus penetrans* in *Phaseolus vulgaris*" in *Abstracts of Papers Presented at the Tenth Annual Meeting of the Society of Nematologists*; August 22–25, 1971. Ottawa: Society of Nematologists, 301.

Afifah, E. N., Murti, R. H., and Nuringtyas, T. R. (2019). Metabolomics approach for the analysis of resistance of four tomato genotypes (*Solanum lycopersicum* L.) to root-knot nematodes (*Meloidogyne incognita*). *Open Life Sci.* 14, 141–149. doi: 10.1515/biol-2019-0016

Akinwumi, B. C., Bordun, K. A. M., and Anderson, H. D. (2018). Biological activities of stilbenoids. *Int. J. Mol. Sci.* 19:792. doi: 10.3390/ijms19030792

Alves, G. C. S., Ferri, P. H., Seraphin, J. C., Fortes, G. A. C., Rocha, M. R., and Santos, S. C. (2016). Principal Response Curves analysis of polyphenol variation in resistant and susceptible cotton after infection by a root-knot nematode (RKN). *Physiol. Mol. Plant Pathol.* 96, 19–28. doi: 10.1016/j.pmpp.2016.06.006

Andolfo, G., and Ercolano, M. R. (2015). Plant innate immunity multicomponent model. *Front. Plant Sci.* 6:987. doi: 10.3389/fpls.2015.00987

Arroo, R. R. J., Jacobs, J. J. M. R., de Koning, E. A. H., de Waard, M., van de Westerlo, E., van Galen, P. M., et al. (1995). Thiophene interconversions in *Tagetes patula* hairy-root cultures. *Phytochemistry* 38, 1193–1197. doi: 10.1016/0031-9422(94)00763-J

Bacetty, A. A., Snook, M. E., Glenn, A. E., Noe, J. P., Hill, N., Culbreath, A., et al. (2009). Toxicity of endophyte-infected tall fescue alkaloids and grass metabolites on *Pratylenchus scribneri*. *Phytopathology* 99, 1336–1345. doi: 10.1094/PHYTO-99-12-1336

Baerson, S. R., Schröder, J., Cook, D., Rimando, A. M., Pan, Z., Dayan, F. E., et al. (2010). Alkylresorcinol biosynthesis in plants: new insights from an ancient enzyme family? *Plant Signal. Behav.* 5, 1286–1289. doi: 10.4161/psb.5.10.13062

Bahraminejad, S., Asenstorfer, R. E., Williams, K. J., Hayasaka, Y., Zwer, P. K., Riley, I. T., et al. (2008). Metabolites correlated with cereal cyst nematode resistance in oats (*Avena sativa*) identified using single seed descent lines. *Nematol. Mediterr.* 36, 145–152.

Bajaj, K. L., and Mahajan, R. (1977). Phenolic compounds in tomato susceptible and resistant to Meloidogyne incognita (Kofoid et White) Chitwood. *Nematol. Mediterr.* 5, 329–333.

Baldacci-Cresp, F., Behr, M., Kohler, A., Badalato, N., Morreel, K., Goeminne, G., et al. (2020). Molecular changes concomitant with vascular system development in mature galls induced by root-knot nematodes in the model tree host *Populus tremula* × *P. alba*. *Int. J. Mol. Sci. Artic.* 21:406. doi: 10.3390/ijms21020406

Baldridge, G. D., O'Neill, N. R., and Samac, D. A. (1998). Alfalfa (*Medicago sativa* L.) resistance to the root-lesion nematode, *Pratylenchus penetrans*: defense-response gene mRNA and isoflavonoid phytoalexin levels in roots. *Plant Mol. Biol.* 38, 999–1010. doi: 10.1023/a:1006182908528

Barbehenn, R. V., and Peter Constabel, C. (2011). Tannins in plant-herbivore interactions. *Phytochemistry* 72, 1551–1565. doi: 10.1016/j.phytochem.2011.01.040

Bauters, L., Hossain, M., Nahar, K., and Gheysen, G. (2018). Gibberellin reduces the susceptibility of rice, Oryza sativa, to the migratory nematode Hirschmanniella oryzae. *Nematology* 20, 703–709. doi: 10.1163/15685411-00003198

Bird, D. M. K., and Kaloshian, I. (2003). Are roots special? Nematodes have their say. *Physiol. Mol. Plant Pathol.* 62, 115–123. doi: 10.1016/S0885-5765(03)00045-6

Block, A. K., Vaughan, M. M., Schmelz, E. A., and Christensen, S. A. (2019). Biosynthesis and function of terpenoid defense compounds in maize (*Zea mays*). *Planta* 249, 21–30. doi: 10.1007/s00425-018-2999-2

Boerjan, W., Ralph, J., and Baucher, M. (2003). Lignin biosynthesis. *Annu. Rev. Plant Biol.* 54, 519–546. doi: 10.1146/annurev.arplant.54.031902.134938

Branch, C., Hwang, C. F., Navarre, D. A., and Williamson, V. M. (2004). Salicylic acid is part of the Mi-1-mediated defense response to root-knot nematode in tomato. *Mol. Plant Microbe Interact.* 17, 351–356. doi: 10.1094/MPMI.2004.17.4.351

Brand, S., Hölscher, D., Schierhorn, A., Svatoš, A., Schröder, J., and Schneider, B. (2006). A type III polyketide synthase from *Wachendorfia thyrsiflora* and its role in diarylheptanoid and phenylphenalenone biosynthesis. *Planta* 224, 413–428. doi: 10.1007/s00425-006-0228-x

Bush, L. P., Wilkinson, H. H., and Schardl, C. L. (1997). Bioprotective alkaloids of grass-gungal endophyte symbioses. *Plant Physiol.* 114, 1–7. doi: 10.1104/pp.114.1.1

Carpentieri-Pipolo, V., Mandarino, J. M. G., Carrao-Panizzi, M. C., Souza, A., and Kikuchi, A. (2005). Association of isoflavonoids with the incompatible response of soybean roots to *Meloidogyne Incognita* Race 3. *Nematropica* 35, 103–110.

Castelli, L., Bryan, G., Blok, V. G., Ramsay, G., Sobczak, M., Gillespie, T., et al. (2006). Investigations of Globodera pallida invasion and syncytia formation within roots of the susceptible potato cultivar Désirée and resistant species *Solanum canasense*. *Nematology* 8, 103–110. doi: 10.1163/156854106776180005

Cheng, A. -X., Lou, Y. -G., Mao, Y. -B., Lu, S., Wang, L. -J., and Chen, X. -Y. (2007). Plant terpenoids: biosynthesis and ecological functions. *J. Integr. Plant Biol.* 49, 179–186. doi: 10.1111/j.1744-7909.2007.00395.x

Chin, S., Behm, C. A., and Mathesius, U. (2018). Functions of flavonoids in plant-nematode interactions. *Plants* 7:85. doi: 10.3390/plants7040085

Chitwood, D. J. (2002). Phytochemical based strategies for nematode control. *Annu. Rev. Phytopathol.* 40, 221–249. doi: 10.1146/annurev.phyto.40.032602.130045

Chitwood, D. J. (2003). "Nematicides" in *Encyclopedia of agrochemicals*. eds. J. R. Plimmer, D. W. Gammon and N. R. Ragsdale (New York, NY: John Wiley & Sons, Inc.).

Choe, S. (2006). Brassinosteroid biosynthesis and inactivation. *Physiol. Plant.* 126, 539–548. doi: 10.1111/j.1399-3054.2006.00681.x

Chong, J., Wishart, D. S., and Xia, J. (2019). Using MetaboAnalyst 4.0 for comprehensive and integrative metabolomics data analysis. *Curr. Protoc. Bioinformatics* 68:e86. doi: 10.1002/cpbi.86

Collingborn, F. M. B., Gowen, S. R., and Mueller-Harvey, I. (2000). Investigations into the biochemical basis for nematode resistance in roots of three Musa cultivars in response to *Radopholus similis* infection. *J. Agric. Food Chem.* 48, 5297–5301. doi: 10.1021/jf000492z

Cook, R., Tiller, S. A., Mizen, K. A., and Edwards, R. (1995). Isoflavonoid metabolism in resistant and susceptible cultivars of white clover infected with the stem nematode *Ditylenchus dipsaci*. *J. Plant Physiol.* 146, 348–354. doi: 10.1016/S0176-1617(11)82067-5

D'Addabbo, T., Carbonara, T., Argentieri, M. P., Radicci, V., Leonetti, P., Villanova, L., et al. (2013). Nematicidal potential of *Artemisia annua* and its main metabolites. *Eur. J. Plant Pathol.* 137, 295–304. doi: 10.1007/s10658-013-0240-5

Davis, E. L., and Rich, J. R. (1987). Nicotine content of tobacco roots and toxicity to *Meloidogyne incognita*. *J. Nematol.* 19, 23–29.

de Bruijn, W. J. C., Gruppen, H., and Vincken, J. P. (2018). Structure and biosynthesis of benzoxazinoids: plant defence metabolites with potential as antimicrobial scaffolds. *Phytochemistry* 155, 233–243. doi: 10.1016/j.phytochem.2018.07.005

Decraemer, W., and Hunt, D. J. (2006). "Structure and classification" in *Plant nematology*. eds. R. N. Perry and M. Moens (Wallingford, UK: CABI Publishing), 3–32.

Desjardins, A. E., McCormick, S. P., and Corsini, D. L. (1995). Diversity of sesquiterpenes in 46 potato cultivars and breeding selections. *J. Agric. Food Chem.* 43, 2267–2272. doi: 10.1021/jf00056a056

Dhakshinamoorthy, S., Mariama, K., Elsen, A., and De Waele, D. (2014). Phenols and lignin are involved in the defence response of banana (Musa) plants to *Radopholus similis* infection. *Nematology* 16, 565–576. doi: 10.1163/15685411-00002788

Dillon, V. M., Overton, J., Grayer, R. J., and Harborne, J. B. (1997). Differences in phytoalexin response among rice cultivars of different resistance to blast. *Phytochemistry* 44, 599–603. doi: 10.1016/S0031-9422(96)00619-X

Echeverri, F., Torres, F., Quiñones, W., Escobar, G., and Archbold, R. (2012). Phenylphenalenone phytoalexins, will they be a new type of fungicide? *Phytochem. Rev.* 11, 1–12. doi: 10.1007/s11101-010-9205-x

Edwards, R., Cook, R., and Mizen, T. (1995). Isoflavonoid conjugate accumulation in the roots of lucerne (*Medicago sativa*) seedlings following infection by the stem nematode *Ditylenchus dipsaci*. *Nematologica* 41, 51–66. doi: 10.1163/003925995X00044

Elliger, C. A., Waiss, A. C., Dutton, H. L., and Rose, M. F. (1988). α-Tomatine and resistance of tomato cultivars toward the nematode, *Meloidogyne incognita*. *J. Chem. Ecol.* 14, 1253–1259. doi: 10.1007/BF01019350

Erb, M., and Kliebenstein, D. J. (2020). Plant secondary metabolites as defenses, regulators, and primary metabolites: the blurred functional trichotomy. *Plant Physiol.* 184, 39–52. doi: 10.1104/pp.20.00433

Ernst, M., Silva, D. B., Silva, R. R., Vêncio, R. Z. N., and Lopes, N. P. (2014). Mass spectrometry in plant metabolomics strategies: from analytical platforms to data acquisition and processing. *Nat. Prod. Rep.* 31, 784–806. doi: 10.1039/c3np70086k

Eyles, A., Bonello, P., Ganley, R., and Mohammed, C. (2010). Induced resistance to pests and pathogens in trees. *New Phytol.* 185, 893–908. doi: 10.1111/j.1469-8137.2009.03127.x

Falcone Ferreyra, M. L., Rius, S. P., and Casati, P. (2012). Flavonoids: biosynthesis, biological functions, and biotechnological applications. *Front. Plant Sci.* 3:222. doi: 10.3389/fpls.2012.00222

Fernie, A. R., and Schauer, N. (2009). Metabolomics-assisted breeding: a viable option for crop improvement? *Trends Genet.* 25, 39–48. doi: 10.1016/j.tig.2008.10.010

Feussner, I., and Polle, A. (2015). What the transcriptome does not tell—proteomics and metabolomics are closer to the plants' patho-phenotype. *Curr. Opin. Plant Biol.* 26, 26–31. doi: 10.1016/j.pbi.2015.05.023

Forrest, J. M. S., and Coxon, D. T. (1980). The relationship between glycoalkaloids and resistance to the white potato cyst nematode, *Globodera pallida* in potato clones derived from *Solanum vernei*. *Ann. Appl. Biol.* 94, 265–268. doi: 10.1111/j.1744-7348.1980.tb03918.x

Frankfater, C. R., Dowd, M. K., and Triplett, B. A. (2009). Effect of elicitors on the production of gossypol and methylated gossypol in cotton hairy roots. *Plant Cell Tissue Organ Cult.* 98, 341–349. doi: 10.1007/s11240-009-9568-0

Frew, A., Powell, J. R., Glauser, G., Bennett, A. E., and Johnson, S. N. (2018). Mycorrhizal fungi enhance nutrient uptake but disarm defences in plant roots, promoting plant-parasitic nematode populations. *Soil Biol. Biochem.* 126, 123–132. doi: 10.1016/j.soilbio.2018.08.019

Friebe, A. (2001). Role of benzoxazinones in cereals. *J. Crop Prod.* 4, 379–400. doi: 10.1300/J144v04n02_18

Fujimoto, T., Mizukubo, T., Abe, H., and Seo, S. (2015). Sclareol induces plant resistance to root-knot nematode partially through ethylene-dependent enhancement of lignin accumulation. *Mol. Plant Microbe Interact.* 28, 398–407. doi: 10.1094/MPMI-10-14-0320-R

Fuller, V. L., Lilley, C. J., and Urwin, P. E. (2008). Nematode resistance. *New Phytol.* 180, 27–44. doi: 10.1111/j.1469-8137.2008.02508.x

Giebel, J. (1970). Phenolic content in roots of some Solanaceae and its influence on IAA-oxidase activity as an indicator of resistance to *Heterodera rostochiensis*. *Nematologica* 16, 22–32. doi: 10.1163/187529270X00423

Giebel, J. (1982). Mechanism of resistance to plant nematodes. *Annu. Rev. Phytopathol.* 20, 257–279. doi: 10.1146/annurev.py.20.090182.001353

Gierl, A., and Frey, M. (2001). Evolution of benzoxazinone biosynthesis and indole production in maize. *Planta* 213, 493–498. doi: 10.1007/s004250100594

Gill, J. R., Harbornez, J. B., Plowright, R. A., Grayer, R. J., and Rahman, M. L. (1996). The induction of phenolic compounds in rice after infection by the stem nematode *Ditylenchus angustus*. *Nematologica* 42, 564–578. doi: 10.1163/004625996X00063

Gommers, F. J., and Voorin'tholt, D. J. M. (1976). Chemotaxonomy of Compositae related to their host suitability for *Pratylenchus penetrans*. *Neth. J. Plant Pathol.* 82, 1–8. doi: 10.1007/BF01977341

Grassert, V., and Lellbach, H. (1987). Untersuchungen des Glykoalkaloidgehalts von Kartoffelhybriden mit Resistenz gegen die Kartoffelnematoden *Globodera rostochiensis* und *Globodera pallida*. *Biochem. Physiol. Pflanz.* 182, 473–479. doi: 10.1016/S0015-3796(87)80076-8

Grunewald, W., Cannoot, B., Friml, J., and Gheysen, G. (2009a). Parasitic nematodes modulate PIN-mediated auxin transport to facilitate infection. *PLoS Pathog.* 5:e1000266. doi: 10.1371/journal.ppat.1000266

Grunewald, W., van Noorden, G., Van Isterdael, G., Beeckman, T., Gheysen, G., Mathesius, U., et al. (2009b). Manipulation of auxin transport in plant roots during rhizobium symbiosis and nematode parasitism. *Plant Cell* 21, 2553–2562. doi: 10.1105/tpc.109.069617

Hamaguchi, T., Sato, K., Vicente, C. S. L., and Hasegawa, K. (2019). Nematicidal actions of the marigold exudate α-terthienyl: oxidative stress-inducing compound penetrates nematode hypodermis. *Biol. Open* 8:bio038646. doi: 10.1242/bio.038646

Hamzehzarghani, H., Kushalappa, A. C., Dion, Y., Rioux, S., Comeau, A., Yaylayan, V., et al. (2005). Metabolic profiling and factor analysis to discriminate quantitative resistance in wheat cultivars against Fusarium head blight. *Physiol. Mol. Plant Pathol.* 66, 119–133. doi: 10.1016/j.pmpp.2005.05.005

Hanawa, F., Yamada, T., and Nakashima, T. (2001). Phytoalexins from *Pinus strobus* bark infected with pinewood nematode, *Bursaphelenchus xylophilus*. *Phytochemistry* 57, 223–228. doi: 10.1016/s0031-9422(00)00514-8

Hapiot, P., Neudeck, A., Pinson, J., Fulcrand, H., Neta, P., and Rolando, C. (1996). Oxidation of caffeic acid and related hydroxycinnamic acids. *J. Electroanal. Chem.* 405, 169–176. doi: 10.1016/0022-0728(95)04412-4

Hartmann, T. (2007). From waste products to ecochemicals: fifty years research of plant secondary metabolism. *Phytochemistry* 68, 2831–2846. doi: 10.1016/j.phytochem.2007.09.017

Hedden, P., and Thomas, S. G. (2012). Gibberellin biosynthesis and its regulation. *Biochem. J.* 444, 11–25. doi: 10.1042/BJ20120245

Hedin, P. A., Shepherd, R. L., and Kappelman, A. J. (1984). Evaluation of cotton polyphenols as factors of resistance to root-knot nematode and Fusarium wilt. *J. Agric. Food Chem.* 32, 633–638. doi: 10.1021/jf00123a052

Heil, M. (2001). Induced systemic resistance (ISR) against pathogens—a promising field for ecological research. *Perspect. Plant Ecol. Evol. Syst.* 4, 65–79. doi: 10.1078/1433-8319-00015

Heinstein, P., Widmaier, R., Wegner, P., and Howe, J. (1979). "Biosynthesis of gossypol" in *Biochemistry of plant phenolics*. eds. T. Swain, J. B. Harbone and C. F. Van Sumere (US: Springer), 313–337.

Heuberger, A. L., Robison, F. M., Lyons, S. M. A., Broeckling, C. D., and Prenni, J. E. (2014). Evaluating plant immunity using mass spectrometry-based metabolomics workflows. *Front. Plant Sci.* 5:291. doi: 10.3389/fpls.2014.00291

Hofmann, J., El Ashry, A. E. N., Anwar, S., Erban, A., Kopka, J., and Grundler, F. (2010). Metabolic profiling reveals local and systemic responses of host plants to nematode parasitism. *Plant J.* 62, 1058–1071. doi: 10.1111/j.1365-313X.2010.04217.x

Holbein, J., Grundler, F. M. W., and Siddique, S. (2016). Plant basal resistance to nematodes: an update. *J. Exp. Bot.* 67, 2049–2061. doi: 10.1093/jxb/erw005

Hölscher, D., Dhakshinamoorthy, S., Alexandrov, T., Becker, M., Bretschneider, T., Buerkert, A., et al. (2014). Phenalenone-type phytoalexins mediate resistance of banana plants (Musa spp.) to the burrowing nematode *Radopholus similis*. *Proc. Natl. Acad. Sci. U. S. A.* 111, 105–110. doi: 10.1073/pnas.1314168110

Huang, J. S., and Barker, K. R. (1991). Glyceollin I in soybean-cyst nematode interactions: spatial and temporal distribution in roots of resistant and susceptible soybeans. *Plant Physiol.* 96, 1302–1307. doi: 10.1104/pp.96.4.1302

Huang, W. -K., Ji, H. -L., Gheysen, G., and Kyndt, T. (2016). Thiamine-induced priming against root-knot nematode infection in rice involves lignification and hydrogen peroxide generation. *Mol. Plant Pathol.* 17, 614–624. doi: 10.1111/mpp.12316

Hung, C., and Rohde, R. A. (1973). Phenol accumulation related to resistance in tomato to infection by root-knot and lesion nematodes. *J. Nematol.* 5, 253–258.

Hutangura, P., Mathesius, U., Jones, M. G. K., and Rolfe, B. G. (1999). Auxin induction is a trigger for root gall formation caused by root-knot nematodes in white clover and is associated with the activation of the flavonoid pathway. *Aust. J. Plant Physiol.* 26, 221–231. doi: 10.1071/PP98157

Jeandet, P., Delaunois, B., Conreux, A., Donnez, D., Nuzzo, V., Cordelier, S., et al. (2010). Biosynthesis, metabolism, molecular engineering, and biological functions of stilbene phytoalexins in plants. *BioFactors* 36, 331–341. doi: 10.1002/biof.108

Ji, H., Kyndt, T., He, W., Vanholme, B., and Gheysen, G. (2015). B-Aminobutyric acid–induced resistance against root-knot nematodes in rice is based on increased basal defence. *Mol. Plant Microbe Interact.* 28, 519–533. doi: 10.1094/MPMI-09-14-0260-R

Jones, J. D. G., and Dangl, J. L. (2006). The plant immune system. *Nature* 444, 323–329. doi: 10.1038/nature05286

Jones, J. T., Furlanetto, C., and Phillips, M. S. (2007). The role of flavonoids produced in response to cyst nematode infection of *Arabidopsis thaliana*. *Nematology* 9, 671–677. doi: 10.3390/plants9020253

Jones, J. T., Haegeman, A., Danchin, E. G. J., Gaur, H. S., Helder, J., Jones, M. G. K., et al. (2013). Top 10 plant-parasitic nematodes in molecular plant pathology. *Mol. Plant Pathol.* 14, 946–961. doi: 10.1111/mpp.12057

Kang, W., Zhu, X., Wang, Y., Chen, L., and Duan, Y. (2018). Transcriptomic and metabolomic analyses reveal that bacteria promote plant defense during infection of soybean cyst nematode in soybean. *BMC Plant Biol.* 18:86. doi: 10.1186/s12870-018-1302-9

Kaplan, D. T., Keen, N. T., and Thomason, I. J. (1980a). Association of glyceollin with the incompatible response of soybean roots to *Meloidogyne incognita*. *Physiol. Plant Pathol.* 16, 309–318. doi: 10.1016/S0048-4059(80)80002-6

Kaplan, D. T., Keen, N. T., and Thomason, I. J. (1980b). Studies on the mode of action of glyceollin in soybean incompatibility to the root knot nematode, *Meloidogyne incognita*. *Physiol. Plant Pathol.* 16, 319–325. doi: 10.1016/S0048-4059(80)80003-8

Kennedy, M. J., Niblack, T. L., and Krishnan, H. B. (1999). Infection by *Heterodera glycines* elevates isoflavonoid production and influences soybean nodulation. *J. Nematol.* 31, 341–347.

Khoshkhoo, N., Hedin, P. A., and McCarty, J. C. (1994a). Terpenoid aldehydes in root-knot nematode susceptible and resistant cotton plants. *J. Agric. Food Chem.* 42, 204–208. doi: 10.1021/jf00037a037

Khoshkhoo, N., Hedin, P. A., and McCarty, J. C. (1994b). Terpenoid aldehydes in root-knot nematode susceptible and resistant cottonseeds as determined by HPLC and aniline methods. *J. Agric. Food Chem.* 42, 804–806. doi: 10.1021/jf00039a041

Kihika, R., Murungi, L. K., Coyne, D., Ng'ang'a, M., Hassanali, A., Teal, P. E. A., et al. (2017). Parasitic nematode *Meloidogyne incognita* interactions with different *Capsicum annum* cultivars reveal the chemical constituents modulating root herbivory. *Sci. Rep.* 7:2903. doi: 10.1038/s41598-017-02379-8

Kim, H. K., Choi, Y. H., and Verpoorte, R. (2010). NMR-based metabolomic analysis of plants. *Nat. Protoc.* 5, 536–549. doi: 10.1038/nprot.2009.237

Kim, H. K., Choi, Y. H., and Verpoorte, R. (2011). NMR-based plant metabolomics: where do we stand, where do we go? *Trends Biotechnol.* 29, 267–275. doi: 10.1016/j.tibtech.2011.02.001

Kirwa, H. K., Murungi, L. K., Beck, J. J., and Torto, B. (2018). Elicitation of differential responses in the root-knot nematode *Meloidogyne incognita* to tomato root exudate cytokinin, flavonoids, and alkaloids. *J. Agric. Food Chem.* 66, 11291–11300. doi: 10.1021/acs.jafc.8b05101

Kyndt, T., Nahar, K., Haeck, A., Verbeek, R., Demeestere, K., and Gheysen, G. (2017). Interplay between carotenoids, abscisic acid and jasmonate guides the compatible rice-*Meloidogyne graminicola* interaction. *Front. Plant Sci.* 8:951. doi: 10.3389/fpls.2017.00951

Ladurner, E., Benuzzi, M., Fiorentini, F., and Lucchi, A. (2014). "Efficacy of NemGuard® Granules, a new nematicide based on garlic extract for the control of root-knot nematodes on horticultural crops" in *Atti Giornate Fitopatologiche*; March 18–21, 2014. Universitá di Bologna, 301–308.

Lattanzio, V., Lattanzio, V. M. T., and Cardinali, A. (2006). "Role of phenolics in the resistance mechanisms of plants against fungal pathogens and insects" in *Phytochemistry: Advances in research*. ed. F. Imperato (Thiruvananthapuram, India: Research Signpost), 23–67.

Lee, H. A., Lee, H. Y., Seo, E., Lee, J., Kim, S. B., Oh, S., et al. (2017). Current understandings of plant nonhost resistance. *Mol. Plant Microbe Interact.* 30, 5–15. doi: 10.1094/MPMI-10-16-0213-CR

Lu, X., Zhang, J., Brown, B., Li, R., Rodríguez-Romero, J., Berasategui, A., et al. (2018). Inferring roles in defense from metabolic allocation of rice diterpenoids. *Plant Cell* 30, 1119–1131. doi: 10.1105/tpc.18.00205

Luis, J. G. (1998). Phenylphenalenone-type phytoalexins and phytoanticipins from susceptible and resistant cultivars of Musa species. Its potencial for engineering resistance to fungi and nematodes into banana. *Acta Hortic.* 490, 425–431. doi: 10.17660/ActaHortic.1998.490.43

Maag, D., Erb, M., and Glauser, G. (2015). Metabolomics in plant-herbivore interactions: challenges and applications. *Entomol. Exp. Appl.* 157, 18–29. doi: 10.1111/eea.12336

Machado, A. R. T., Campos, V. P. V. A. C., da Silva, W. J. R., Campos, V. P. V. A. C., Zeri, A. C. d. M., and Oliveira, D. F. (2012). Metabolic profiling in the roots of coffee plants exposed to the coffee root-knot nematode, *Meloidogyne exigua*. *Eur. J. Plant Pathol.* 134, 431–441. doi: 10.1007/s10658-012-0008-3

Machado, A. R. T., Medeiros, F. S., De Souza Filho, J. D., Sena, M. M., Terra, W. C., and Pimenta, L. P. S. (2019). NMR-based metabolomic screening for metabolites associated with resistance to *Meloidogyne javanica* in *Annona muricata* roots. *J. Braz. Chem. Soc.* 30, 1276–1283. doi: 10.21577/0103-5053.20190022

Manohar, M., Tenjo-Castano, F., Chen, S., Zhang, Y. K., Kumari, A., Williamson, V. M., et al. (2020). Plant metabolism of nematode pheromones mediates plant-nematode interactions. *Nat. Commun.* 11, 1–11. doi: 10.1038/s41467-019-14104-2

Manosalva, P., Manohar, M., von Reuss, S. H., Chen, S., Koch, A., Kaplan, F., et al. (2015). Conserved nematode signalling molecules elicit plant defenses and pathogen resistance. *Nat. Commun.* 6, 1–8. doi: 10.1038/ncomms8795

Martínez-Medina, A., Fernandez, I., Lok, G. B., Pozo, M. J., Pieterse, C. M. J., and Van Wees, S. C. M. (2017). Shifting from priming of salicylic acid- to jasmonic acid-regulated defences by Trichoderma protects tomato against the root knot nematode *Meloidogyne incognita*. *New Phytol.* 213, 1363–1377. doi: 10.1111/nph.14251

Mathesius, U. (2018). Flavonoid functions in plants and their interactions with other organisms. *Plants* 7:30. doi: 10.3390/plants7020030

Mauch-Mani, B., Baccelli, I., Luna, E., and Flors, V. (2017). Defense priming: an adaptive part of induced resistance. *Annu. Rev. Plant Biol.* 68, 485–512. doi: 10.1146/annurev-arplant-042916-041132

McLeod, R. W., Kirkegaard, J. A., and Steel, C. C. (2001). Invasion, development, growth and egg laying by *Meloidogyne javanica* in Brassicaceae crops. *Nematology* 3, 463–472. doi: 10.1163/156854101753250791

McNaught, A. D., and Wilkinson, A. (1999). "Flavonoids (isoflavonoids and neoflavonoids)" in *IUPAC compendium of chemical terminology*. eds. A. D. McNaught and A. Wilkinson (Oxford: Blackwell Scientific Publications).

Medico, E., van Hende, E., El-Ouadi, K., and Villagra, M. M. (2018). "A new terpene nematicide against root knot nematodes on solanaceous and cucurbits." in *Atti Giornate Fitopatologiche*; March 6–9, 2018. Universitá di Bologna, 13–19.

Meher, H. C., Gajbhiye, V. T., Singh, G., and Chawla, G. (2015). Altered metabolomic profile of selected metabolites and improved resistance of *Cicer arietinum* (L.) against *Meloidogyne incognita* (Kofoid & White) Chitwood following seed soaking with salicylic acid, benzothiadiazole or nicotinic acid. *Acta Physiol. Plant.* 37, 1–12. doi: 10.1007/s11738-015-1888-6

Meyer, S. L. F., Rice, C. P., and Zasada, I. A. (2009). DIBOA: fate in soil and effects on root-knot nematode egg numbers. *Soil Biol. Biochem.* 41, 1555–1560. doi: 10.1016/j.soilbio.2009.04.016

Mitchell, S. C., and Waring, R. H. (2014). Asparagusic acid. *Phytochemistry* 97, 5–10. doi: 10.1016/j.phytochem.2013.09.014

Mithöfer, A., and Boland, W. (2012). Plant defense against herbivores: chemical aspects. *Annu. Rev. Plant Biol.* 63, 431–450. doi: 10.1146/annurev-arplant-042110-103854

Mnviajan, R., Singh, P., and Bajaj, K. L. (1992). Nematicidal activity of some phenolic compounds against *Meloidogyne incognita*. *Nematol. Mediterr.* 20, 217–219.

Moco, S., Vervoort, J., Moco, S., Bino, R. J., De Vos, R. C. H., and Bino, R. (2007). Metabolomics technologies and metabolite identification. *Trends Anal. Chem.* 26, 855–866. doi: 10.1016/j.trac.2007.08.003

Molinari, S., and Baser, N. (2010). Induction of resistance to root-knot nematodes by SAR elicitors in tomato. *Crop Prot.* 29, 1354–1362. doi: 10.1016/j.cropro.2010.07.012

Moses, T., Papadopoulou, K. K., and Osbourn, A. (2014). Metabolic and functional diversity of saponins, biosynthetic intermediates and semi-synthetic derivatives. *Crit. Rev. Biochem. Mol. Biol.* 49, 439–462. doi: 10.3109/10409238.2014.953628

Munde, T., Brand, S., Hidalgo, W., Maddula, R. K., Svatoš, A., and Schneider, B. (2013). Biosynthesis of tetraoxygenated phenylphenalenones in *Wachendorfia thyrsiflora*. *Phytochemistry* 91, 165–176. doi: 10.1016/j.phytochem.2012.02.020

Nahar, K., Kyndt, T., Hause, B., Höfte, M., and Gheysen, G. (2013). Brassinosteroids suppress rice defense against root-knot nematodes through antagonism with the jasmonate pathway. *Mol. Plant Microbe Interact.* 26, 106–115. doi: 10.1094/MPMI-05-12-0108-FI

Nahar, K., Kyndt, T., Nzogela, Y. B., and Gheysen, G. (2012). Abscisic acid interacts antagonistically with classical defense pathways in rice-migratory nematode interaction. *New Phytol.* 196, 901–913. doi: 10.1111/j.1469-8137.2012.04310.x

Nambara, E., and Marion-Poll, A. (2005). Abscisic acid biosynthesis and catabolism. *Annu. Rev. Plant Biol.* 56, 165–185. doi: 10.1146/annurev.arplant.56.032604.144046

Naoumkina, M. A., Zhao, Q., Gallego-Giraldo, L., Dai, X., Zhao, P. X., and Dixon, R. A. (2010). Genome-wide analysis of phenylpropanoid defence pathways. *Mol. Plant Pathol.* 11, 829–846. doi: 10.1111/j.1364-3703.2010.00648.x

Ng, J. L. P., Perrine-Walker, F., Wasson, A. P., and Mathesius, U. (2015). The control of auxin transport in parasitic and symbiotic root–microbe interactions. *Plants* 4, 606–643. doi: 10.3390/plants4030606

Nicholson, R. L., and Hammerschmidt, R. (1992). Phenolic compounds and their role in disease resistance. *Annu. Rev. Phytopathol.* 30, 369–389. doi: 10.1146/annurev.py.30.090192.002101

Nicol, J. M., Turner, S. J., Coyne, D. L., den Nijis, L., Hockland, S., and Maafi, Z. T. (2011). "Current nematode threats to world agriculture" in *Genomics and molecular genetics of plant-nematode interactions*. eds. J. Jones, G. Gheysen and C. Fenoll (Dordrecht: Springer), 21–43.

Niemeyer, H. M. (2009). Hydroxamic acids derived from 2-hydroxy-2h-1,4-benzoxazin-3(4h)-one: key defense chemicals of cereals. *J. Agric. Food Chem.* 57, 1677–1695. doi: 10.1021/jf8034034

Ntalli, N. G., and Caboni, P. (2012). Botanical nematicides: a review. *J. Agric. Food Chem.* 60, 9929–9940. doi: 10.1021/jf303107j

Oka, Y., and Cohen, Y. (2001). Induced resistance to cyst and root-knot nematodes in cereals by DL-β-amino-n-butyric acid. *Eur. J. Plant Pathol.* 107, 219–227. doi: 10.1023/A:1011278717976

Oka, Y., Cohen, Y., and Spiegel, Y. (1999). Local and systemic induced resistance to the root-knot nematode in tomato by DL-β-amino-n-butyric acid. *Phytopathology* 89, 1138–1143. doi: 10.1094/PHYTO.1999.89.12.1138

Osbourn, A. (1996). Saponins and plant defence—a soap story. *Trends Plant Sci.* 1, 4–9. doi: 10.1016/S1360-1385(96)80016-1

Panaccione, D., Kotcon, J., Schardl, C., Johnson, R., and Morton, J. (2006). Ergot alkaloids are not essential for endophytic fungus-associated population suppression of the lesion nematode, *Pratylenchus scribneri*, on perennial ryegrass. *Nematology* 8, 583–590. doi: 10.1163/156854106778614074

Parkhi, V., Kumar, V., Campbell, L. A. M., Bell, A. A., Shah, J., and Rathore, K. S. (2010). Resistance against various fungal pathogens and reniform nematode in transgenic cotton plants expressing *Arabidopsis* NPR1. *Transgenic Res.* 19, 959–975. doi: 10.1007/s11248-010-9374-9

Pazouki, L., and Niinemetst, U. (2016). Multi-substrate terpene synthases: their occurrence and physiological significance. *Front. Plant Sci.* 7:1019. doi: 10.3389/fpls.2016.01019

Pedersen, M. W., Barnes, D. K., Sorensen, E. L., Griffin, G. D., Nielson, M. W., Hill, R. R., et al. (1976). Effects of low and high saponin selection in alfalfa on agronomic and pest resistance traits and the interrelationship of these traits. *Crop Sci.* 16, 193–199. doi: 10.2135/cropsci1976.0011183X001600020007x

Pegard, A., Brizzard, G., Fazari, A., Soucaze, O., Abad, P., and Djian-Caporalino, C. (2005). Histological characterization of resistance to different root-knot nematode species related to phenolics accumulation in *Capsicum annuum*. *Phytopathology* 95, 158–165. doi: 10.1094/PHYTO-95-0158

Perry, R. N., and Moens, M. (2011). "Introduction to plant-parasitic nematodes: modes of parasitism" in *Genomics and molecular genetics of plant-nematode interactions*. eds. J. Jones, G. Gheysen and C. Fenoll (Dordrecht, Netherlands: Springer), 3–20.

Pichersky, E., and Raguso, R. A. (2018). Why do plants produce so many terpenoid compounds? *New Phytol.* 220, 692–702. doi: 10.1111/nph.14178

Pieterse, C. M. J., Zamioudis, C., Berendsen, R. L., Weller, D. M., Van Wees, S. C. M., and Bakker, P. A. H. M. (2014). Induced systemic resistance by beneficial microbes. *Annu. Rev. Phytopathol.* 52, 347–375. doi: 10.1146/annurev-phyto-082712-102340

Pimentel, C. S., Firmino, P. N., Calvão, T., Ayres, M. P., Miranda, I., and Pereira, H. (2017). Pinewood nematode population growth in relation to pine phloem chemical composition. *Plant Pathol.* 66, 856–864. doi: 10.1111/ppa.12638

Portillo, M., Cabrera, J., Lindsey, K., Topping, J., Andrés, M. F., Emiliozzi, M., et al. (2013). Distinct and conserved transcriptomic changes during nematode-induced giant cell development in tomato compared with *Arabidopsis*: a functional role for gene repression. *New Phytol.* 197, 1276–1290. doi: 10.1111/nph.12121

Potter, M. J., Davies, K., and Rathjen, A. J. (1998). Suppressive impact of glucosinolates in *Brassica* vegetative tissues on root lesion nematode *Pratylenchus neglectus*. *J. Chem. Ecol.* 24, 67–80. doi: 10.1023/A:1022336812240

Potter, M. J., Vanstone, V. A., Davies, K. A., Kirkegaard, J. A., and Rathjen, A. J. (1999). Reduced susceptibility of *Brassica napus* to *Pratylenchus neglectus* in plants with elevated root levels of 2-phenylethyl glucosinolate. *J. Nematol.* 31, 291–298.

Rask, L., Andréasson, E., Ekbom, B., Eriksson, S., Pontoppidan, B., and Meijer, J. (2000). Myrosinase: gene family evolution and herbivore defense in Brassicaceae. *Plant Mol. Biol.* 42, 93–114.

Rich, J. R., Keen, N. T., and Thomason, I. J. (1977). Association of coumestans with the hypersensitivity of Lima bean roots to *Pratylenchus scribneri*. *Physiol. Plant Pathol.* 10, 105–116. doi: 10.1016/0048-4059(77)90014-5

Saito, K., and Matsuda, F. (2010). Metabolomics for functional genomics, systems biology, and biotechnology. *Annu. Rev. Plant Biol.* 61, 463–489. doi: 10.1146/annurev.arplant.043008.092035

Salminen, J. P., and Karonen, M. (2011). Chemical ecology of tannins and other phenolics: we need a change in approach. *Funct. Ecol.* 25, 325–338. doi: 10.1111/j.1365-2435.2010.01826.x

Sato, K., Kadota, Y., and Shirasu, K. (2019). Plant immune responses to parasitic nematodes. *Front. Plant Sci.* 10:1165. doi: 10.3389/fpls.2019.01165

Savary, S., Willocquet, L., Pethybridge, S. J., Esker, P., McRoberts, N., and Nelson, A. (2019). The global burden of pathogens and pests on major food crops. *Nat. Ecol. Evol.* 3, 430–439. doi: 10.1038/s41559-018-0793-y

Schläger, S., and Dräger, B. (2016). Exploiting plant alkaloids. *Curr. Opin. Biotechnol.* 37, 155–164. doi: 10.1016/j.copbio.2015.12.003

Schläpfer, P., Zhang, P., Wang, C., Kim, T., Banf, M., Chae, L., et al. (2017). Genome-wide prediction of metabolic enzymes, pathways, and gene clusters in plants. *Plant Physiol.* 173, 2041–2059. doi: 10.1104/pp.16.01942

Schripsema, J. (2010). Application of NMR in plant metabolomics: techniques, problems and prospects. *Phytochem. Anal.* 21, 14–21. doi: 10.1002/pca.1185

Seigler, D. S. (1998). *Plant secondary metabolism*. *1st Edn*. New York: Springer Science+Business Media.

Shah, S., Anjam, M., Mendy, B., Anwer, M., Habash, S. S., Lozano-Torres, J., et al. (2015). Damage-associated responses of the host contribute to defence against cyst nematodes but not root-knot nematodes. *J. Exp. Bot.* 68, 5949–5960. doi: 10.1093/jxb/erx374

Shan, L., and He, P. (2018). Pipped at the post: pipecolic acid derivative identified as SAR regulator. *Cell* 173, 286–287. doi: 10.1016/j.cell.2018.03.045

Singh, R. R., Chinnasri, B., De Smet, L., Haeck, A., Demeestere, K., Van Cutsem, P., et al. (2019). Systemic defense activation by COS-OGA in rice against root-knot nematodes depends on stimulation of the phenylpropanoid pathway. *Plant Physiol. Biochem.* 142, 202–210. doi: 10.1016/j.plaphy.2019.07.003

Smant, G., Helder, J., and Goverse, A. (2018). Parallel adaptations and common host cell responses enabling feeding of obligate and facultative plant parasitic nematodes. *Plant J.* 93, 686–702. doi: 10.1111/tpj.13811

Song, L. X., Xu, X. C., Wang, F. N., Wang, Y., Xia, X. J., Shi, K., et al. (2018). Brassinosteroids act as a positive regulator for resistance against root-knot nematode involving RESPIRATORY BURST OXIDASE HOMOLOG-dependent activation of MAPKs in tomato. *Plant Cell Environ.* 41, 1113–1125. doi: 10.1111/pce.12952

Soriano, I. R., Asenstorfer, R. E., Schmidt, O., and Riley, I. T. (2004). Inducible flavone in oats (*Avena sativa*) is a novel defense against plant-parasitic nematodes. *Phytopathology* 94, 1207–1214. doi: 10.1094/PHYTO.2004.94.11.1207

St.Clair, D. A. (2010). Quantitative disease resistance and quantitative resistance loci in breeding. *Annu. Rev. Phytopathol.* 48, 247–268. doi: 10.1146/annurev-phyto-080508-081904

Sumner, L. W., Lei, Z., Nikolau, B. J., and Saito, K. (2015). Modern plant metabolomics: advanced natural product gene discoveries, improved technologies, and future prospects. *Nat. Prod. Rep.* 32, 212–229. doi: 10.1039/c4np00072b

Takasugi, M., Yachida, Y., Anetai, M., Masamune, T., and Kegasawa, K. (1975). Identification of asparagusic acid as a nematicide occuring naturally in the roots of asparagus. *Chem. Lett.* 4, 43–44. doi: 10.1246/cl.1975.43

Teixeira, M. A., Wei, L., and Kaloshian, I. (2016). Root-knot nematodes induce pattern-triggered immunity in *Arabidopsis thaliana* roots. *New Phytol.* 211, 276–287. doi: 10.1111/nph.13893

Tenenboim, H., and Brotman, Y. (2016). Omic relief for the biotically stressed: metabolomics of plant biotic interactions. *Trends Plant Sci.* 21, 781–791. doi: 10.1016/j.tplants.2016.04.009

Thoden, T. C., and Boppré, M. (2010). Plants producing pyrrolizidine alkaloids: sustainable tools for nematode management? *Nematology* 12, 1–24. doi: 10.1163/138855409X12549869072248

Thoden, T. C., Boppré, M., and Hallmann, J. (2009). Effects of pyrrolizidine alkaloids on the performance of plant-parasitic and free-living nematodes. *Pest Manag. Sci.* 65, 823–830. doi: 10.1002/ps.1764

Timper, P., Krakowsky, M. D., and Snook, M. E. (2007). Resistance in maize to *Paratrichodorus minor*. *Nematropica* 37, 9–20.

Tomita, S., Ikeda, S., Tsuda, S., Someya, N., Asano, K., Kikuchi, J., et al. (2017). A survey of metabolic changes in potato leaves by NMR-based metabolic profiling in relation to resistance to late blight disease under field conditions. *Magn. Reson. Chem.* 55, 120–127. doi: 10.1002/mrc.4506

Treutter, D. (2005). Significance of flavonoids in plant resistance and enhancement of their biosynthesis. *Plant Biol.* 7, 581–591. doi: 10.1055/s-2005-873009

Treutter, D. (2006). Significance of flavonoids in plant resistance: a review. *Environ. Chem. Lett.* 4, 147–157. doi: 10.1007/s10311-006-0068-8

Tropf, S., Lanz, T., Rensing, S. A., Schröder, J., and Schröder, G. (1994). Evidence that stilbene synthases have developed from chalcone synthases several times in the course of evolution. *J. Mol. Evol.* 38, 610–618. doi: 10.1007/BF00175881

Uehara, T., Sugiyama, S., Matsuura, H., Arie, T., and Masuta, C. (2010). Resistant and susceptible responses in tomato to cyst nematode are differentially regulated by salicylic acid. *Plant Cell Physiol.* 51, 1524–1536. doi: 10.1093/pcp/pcq109

Uhlenbroek, J. H., and Bijloo, J. D. (1958). Investigations on nematicides: I. Isolation and structure of a nematicidal principe occurring in *Tagetes* roots. *Recl. des Trav. Chim. des Pays-Bas* 77, 1004–1009. doi: 10.1002/recl.19580771103

van Dam, N. M., and Bouwmeester, H. J. (2016). Metabolomics in the rhizosphere: tapping into belowground chemical communication. *Trends Plant Sci.* 21, 256–265. doi: 10.1016/j.tplants.2016.01.008

van Dam, N. M., Tytgat, T. O. G., and Kirkegaard, J. A. (2009). Root and shoot glucosinolates: a comparison of their diversity, function and interactions in natural and managed ecosystems. *Phytochem. Rev.* 8, 171–186. doi: 10.1007/s11101-008-9101-9

VanEtten, H. D., Mansfield, J. W., Bailey, J. A., and Farmer, E. E. (1994). Two classes of plant antibiotics: phytoalexins versus "phytoanticipins". *Plant Cell* 6, 1191–1192. doi: 10.1105/tpc.6.9.1191

Veech, J. A. (1978). An apparent relationship between methoxy-substituted terpenoid aldehydes and the resistance of cotton to *Meloidogyne incognita*. *Nematologica* 24, 81–87. doi: 10.1163/187529278X00092

Veech, J. A. (1979). Histochemical localization and nematoxicity of terpenoid aldehydes in cotton. *J. Nematol.* 11, 240–246.

Veech, J. A. (1982). Phytoalexins and their role in the resistance of plants to nematodes. *J. Nematol.* 14, 2–9.

Verbeek, R. E. M., Van Buyten, E., Alam, M. Z., De Vleesschauwer, D., Van Bockhaven, J., Asano, T., et al. (2019). Jasmonate-induced defense mechanisms in the belowground antagonistic interaction between *Pythium arrhenomanes* and *Meloidogyne graminicola* in rice. *Front. Plant Sci.* 10:1515. doi: 10.3389/fpls.2019.01515

Viant, M. R., Kurland, I. J., Jones, M. R., and Dunn, W. B. (2017). How close are we to complete annotation of metabolomes? *Curr. Opin. Chem. Biol.* 36, 64–69. doi: 10.1016/j.cbpa.2017.01.001

Vogt, T. (2010). Phenylpropanoid biosynthesis. *Mol. Plant* 3, 2–20. doi: 10.1093/mp/ssp106

Vos, C., Schouteden, N., van Tuinen, D., Chatagnier, O., Elsen, A., De Waele, D., et al. (2013). Mycorrhiza-induced resistance against the root–knot nematode *Meloidogyne incognita* involves priming of defense gene responses in tomato. *Soil Biol. Biochem.* 60, 45–54. doi: 10.1016/j.soilbio.2013.01.013

Wallace, H. R. (1961). The nature of resistance in Chrysanthemum varieties to *Aphelenchoides ritzemabosi*. *Nematologica* 6, 49–58. doi: 10.1163/187529261X00270

Wallis, C. M. (2020). Grapevine (Vitis spp.) rootstock stilbenoid associations with host resistance to and induction by root knot nematodes, *Meloidogyne incognita*. *BMC. Res. Notes* 13:360. doi: 10.1186/s13104-020-05201-3

Wang, C., Liu, R., Lim, G. -H., de Lorenzo, L., Yu, K., Zhang, K., et al. (2018). Pipecolic acid confers systemic immunity by regulating free radicals. *Sci. Adv.* 4:eaar4509. doi:10.1126/sciadv.aar4509

Wang, Y., Tyler, B. M., and Wang, Y. (2019). Defense and counterdefense during plant-pathogenic oomycete infection. *Annu. Rev. Microbiol.* 73, 667–696. doi: 10.1146/annurev-micro-020518-120022

Wasson, A. P., Ramsay, K., Jones, M. G. K., and Mathesius, U. (2009). Differing requirements for flavonoids during the formation of lateral roots, nodules and root knot nematode galls in *Medicago truncatula*. *New Phytol.* 183, 167–179. doi: 10.1111/j.1469-8137.2009.02850.x

Waterman, P. G. (1998). "Chemical taxonomy of alkaloids" in *Alkaloids*. eds. M. F. Roberts and M. Wink (US: Springer), 87–107.

Willett, D. S., Filgueiras, C. C., Benda, N. D., Zhang, J., and Kenworthy, K. E. (2020). Sting nematodes modify metabolomic profiles of host plants. *Sci. Rep.* 10:2212. doi: 10.1038/s41598-020-59062-8

Wubben, M. J. E., Jin, J., and Baum, T. J. (2008). Cyst nematode parasitism of *Arabidopsis thaliana* is inhibited by salicylic acid (SA) and elicits uncoupled SA-independent pathogenesis-related gene expression in roots. *Mol. Plant Microbe Interact.* 21, 424–432. doi: 10.1094/MPMI-21-4-0424

Wuyts, N., Lognay, G., Swennen, R., and De Waele, D. (2006a). Nematode infection and reproduction in transgenic and mutant *Arabidopsis* and tobacco with an altered phenylpropanoid metabolism. *J. Exp. Bot.* 57, 2825–2835. doi: 10.1093/jxb/erl044

Wuyts, N., Swennen, R., and De Waele, D. (2006b). Effects of plant phenylpropanoid pathway products and selected terpenoids and alkaloids on the behaviour of the plant-parasitic nematodes *Radopholus similis*, *Pratylenchus penetrans* and *Meloidogyne incognita*. *Nematology* 8, 89–101. doi: 10.1163/156854106776179953

Wyss, U. (1997). "Root parasitic nematodes: an overview" in *Cellular and molecular aspects of plant-nematode interactions*. eds. C. Fenoll, F. M. W. Grundler and S. A. Ohl (Dordrecht: Springer), 5–22.

Yamane, H. (2013). Biosynthesis of phytoalexins and regulatory mechanisms of it in rice. *Biosci. Biotechnol. Biochem.* 77, 1141–1148. doi: 10.1271/bbb.130109

Yimer, H. Z., Nahar, K., Kyndt, T., Haeck, A., Van Meulebroek, L., Vanhaecke, L., et al. (2018). Gibberellin antagonizes jasmonate-induced defense against *Meloidogyne graminicola* in rice. *New Phytol.* 218, 646–660. doi: 10.1111/nph.15046

Zasada, I. A., Meyer, S. L. F., Halbrendt, J. M., and Rice, C. (2005). Activity of hydroxamic acids from *Secale cereale* against the plant-parasitic nematodes *Meloidogyne incognita* and *Xiphinema americanum*. *Phytopathology* 95, 1116–1121. doi: 10.1094/PHYTO-95-1116

Zhan, L. P., Peng, D. L., Wang, X. L., Kong, L. A., Peng, H., Liu, S. M., et al. (2018). Priming effect of root-applied silicon on the enhancement of induced resistance to the root-knot nematode *Meloidogyne graminicola* in rice. *BMC Plant Biol.* 18:50. doi: 10.1186/s12870-018-1266-9

Ziegler, J., and Facchini, P. J. (2008). Alkaloid biosynthesis: metabolism and trafficking. *Annu. Rev. Plant Biol.* 59, 735–769. doi: 10.1146/annurev.arplant.59.032607.092730

Zook, M., and Hammerschmidt, R. (1998). Biosynthesis of camalexin from tryptophan pathway intermediates in cell-suspension cultures of arabidopsis. *Plant Physiol.* 118, 1389–1393. doi: 10.1104/pp.118.4.1389

Conflict of Interest: The authors declare that the research was conducted in the absence of conflicts of interest. Although WD's PhD grant is co-funded by a private sector partner, Eastman, this review does not touch on subjects of commercial relevance to Eastman, and Eastman and its employees were not involved in this review.

frontiers in Plant Science

REVIEW
published: 16 November 2020
doi: 10.3389/fpls.2020.606395

Meloidogyne enterolobii, a Major Threat to Tomato Production: Current Status and Future Prospects for Its Management

Ashley N. Philbrick[1], Tika B. Adhikari[1], Frank J. Louws[1,2] and Adrienne M. Gorny[1]**

[1] Department of Entomology and Plant Pathology, North Carolina State University, Raleigh, NC, United States, [2] Department of Horticultural Science, North Carolina State University, Raleigh, NC, United States

The guava root-knot nematode, *Meloidogyne enterolobii* (Syn. *M. mayaguensis*), is an emerging pathogen to many crops in the world. This nematode can cause chlorosis, stunting, and reduce yields associated with the induction of many root galls on host plants. Recently, this pathogen has been considered as a global threat for tomato (*Solanum lycopersicum* L.) production due to the lack of known resistance in commercially accepted varieties and the aggressiveness of *M. enterolobii*. Both conventional morphological and molecular approaches have been used to identify *M. enterolobii*, an important first step in an integrated management. To combat root-knot nematodes, integrated disease management strategies such as crop rotation, field sanitation, biocontrol agents, fumigants, and resistant cultivars have been developed and successfully used in the past. However, the resistance in tomato varieties mediated by known *Mi*-genes does not control *M. enterolobii*. Here, we review the current knowledge on geographic distribution, host range, population biology, control measures, and proposed future strategies to improve *M. enterolobii* control in tomato.

Keywords: root-knot nematode, population biology, disease management, RNA interference, gene editing

OPEN ACCESS

Edited by:
Koichi Hasegawa, Chubu University, Japan

Reviewed by:
Philippe Castagnone-Sereno, INRA Centre Provence-Alpes-Côte d'Azur, France
Hiromichi Sakai, National Agriculture and Food Research Organization, Japan

****Correspondence:***
Tika B. Adhikari
tbadhika@ncsu.edu
Adrienne M. Gorny
agorny@ncsu.edu

Specialty section:
This article was submitted to Plant Pathogen Interactions, a section of the journal Frontiers in Plant Science

Received: *14 September 2020*
Accepted: *22 October 2020*
Published: *16 November 2020*

Citation:
Philbrick AN, Adhikari TB, Louws FJ and Gorny AM (2020) Meloidogyne enterolobii, a Major Threat to Tomato Production: Current Status and Future Prospects for Its Management. Front. Plant Sci. 11:606395. doi: 10.3389/fpls.2020.606395

INTRODUCTION

Root-knot nematodes are the most widespread soilborne plant pathogen (Agrios, 2005; Perry et al., 2009) and can cause several billion dollars of losses annually (Nicol et al., 2011; Elling, 2013). *Meloidogyne enterolobii* Yang and Eisenback, 1983, known colloquially as the guava root-knot nematode or the pacara earpod tree root-knot nematode (Yang and Eisenback, 1983), is an emerging threat due to its global distribution, wide host range, and the ability to reproduce on tomato genotypes carrying *Mi* resistance genes (Moens et al., 2009; Castagnone-Sereno, 2012). *Meloidogyne enterolobii* alone can cause up to 65% loss, which was higher than any of the other root-knot nematode species examined to date (Castagnone-Sereno, 2012; Castagnone-Sereno and Castillo, 2014). Many farmers may not even realize their fields are infected until the end of the season when crops are harvested, and they observe heavily galled root systems (Schwarz, 2019). Diagnosis of *M. enterolobii* infestation can be challenging due to morphological similarities between it and other root-knot nematode species (Blok and Powers, 2009; Castagnone-Sereno, 2012; Min et al., 2012). In the past, extensive research has been conducted under the International *Meloidogyne* Project (IMP), coordinated by leaders at North Carolina State University to assist developing

countries decrease crop loss attributed to root-knot nematodes. This effort has subsequently generated identification methods and disease management strategies (Sasser et al., 1983). Recently, major research was focused on identifying new sources of genetic resistance to *M. enterolobii* due to the ability of the species to successfully reproduce on crop varieties possessing currently available resistance genes (Hunt and Handoo, 2009; Castagnone-Sereno and Castillo, 2014). Sources of potential genetic and non-host resistance have been identified in tomato (Da Silva et al., 2019), peanut, garlic, grapefruit (Rodriguez et al., 2003), guava (Castagnone-Sereno and Castillo, 2014; Chiamolera et al., 2018), plum, peach (Castagnone-Sereno and Castillo, 2014), and sweetpotato (Schwarz, 2019). Here, we review recent advances in understanding the tomato – *M. enterolobii* pathosystem conducted throughout the world. We will discuss how this progress should facilitate *M. enterolobii* management in tomato production systems. This review will also provide species information and some directions for further research on this aggressive pathogen in tomato production systems.

TAXONOMIC COMPLEXITY

The genus *Meloidogyne* is comprised of approximately 100 species (Hunt and Handoo, 2009; Elling, 2013; Jones et al., 2013). The name "root-knot" refers to the large galls that these nematodes induce on their hosts (Jones et al., 2013). Worldwide, there are four 'major' species of root-knot nematode: *M. arenaria, M. incognita, M. javanica,* and *M. hapla* (Min et al., 2012; Elling, 2013; Jones et al., 2013; Suresh et al., 2019). *M. enterolobii,* initially identified as *M. incognita,* was first discovered in the Chinese pacara earpod tree (*Enterolobium contortisiliquum*) in 1983 (Yang and Eisenback, 1983; Castagnone-Sereno, 2012). In 1988, a species identified as *Meloidogyne mayaguensis* in Puerto Rico was thought to be a new species of root-knot nematode. However, based on morphological and molecular data it was reclassified as *M. enterolobii* in 2004 (Yang and Eisenback, 1983; Castagnone-Sereno, 2012; Elling, 2013; Da Silva and Santos, 2016). The common name, guava root-knot nematode (**Figure 1**), was given because of the significant damage this nematode has caused to guava fruit trees (*Psidium guajava*) in South America (Carneiro et al., 2001; Schwarz et al., 2020).

HOST RANGE AND GEOGRAPHIC DISTRIBUTION

Meloidogyne enterolobii has a broad host range (**Supplementary Table S1**). Only a few crop species (e.g., cabbage, corn, garlic, peanut) and several fruits (e.g., grapefruit, avocado, cashew, citrus, mango, strawberry) have been reported as non-hosts or poor hosts for *M. enterolobii* (Rodriguez et al., 2003; Brito et al., 2010; Freitas et al., 2017). This nematode has been reported worldwide (**Figure 2**) and established mainly in areas with a subtropical to tropical climate (Castagnone-Sereno, 2012; Elling, 2013; de Brita et al., 2018; Kirkpatrick et al., 2018; Da Silva et al., 2019; Overstreet et al., 2019; Schwarz et al., 2020). Although this nematode was originally detected in China, it has now been recorded in several African countries and South America (Elling, 2013; Da Silva et al., 2019). This nematode was also detected in commercial greenhouses in temperate regions in Switzerland (Kiewnick et al., 2009; Castagnone-Sereno and Castillo, 2014; Braun-Kiewnick et al., 2016). In the United States, *M. enterolobii* was first reported in Puerto Rico in 1988 and Florida in 2001 (Brito et al., 2004; Da Silva and Santos, 2016). It has since spread and has been reported in North and South Carolina (Rutter et al., 2019). In North Carolina, samples were originally collected and *M. enterolobii* was identified in 2011, but was not reported until 2013 (Ye et al., 2013). More recently, *M. enterolobii* was found in eight North Carolina counties: Johnston, Harnett, Sampson, Wayne, Greene, Wilson, Nash, and Columbus (Ye et al., 2013; Thiessen, 2018b; Schwarz et al., 2020). This nematode was also recently identified in sweetpotato in Louisiana.

BIOLOGY AND LIFE CYCLE OF *Meloidogyne enterolobii*

Meloidogyne enterolobii is an obligate biotrophic parasite and is not able to complete its life cycle without a living host (Eisenback and Triantaphyllou, 1991; Agrios, 2005; Elling, 2013). As with other root-knot nematodes, this species is an endoparasite, which feeds and matures to the adult stage of the life cycle fully inside host plant tissue (Elling, 2013; Suresh et al., 2019). *Meloidogyne enterolobii* can be distinguished from other *Meloidogyne* spp. based on the morphometrics of females, males, and juvenile stages. The most important diagnostic features are the form of a perineal pattern shape, stylet morphology of males and females, and position of the excretory pore in females; morphology of the head in the male; and the morphometrics of the head and hyaline tail in the second-stage juvenile (J2) (Yang and Eisenback, 1983).

The adult females have a white body and are pear or globe-shaped (Yang and Eisenback, 1983; Castagnone-Sereno and Castillo, 2014). Unlike adult males and J2s, the head of adult females is not distinctly set off from the neck (Yang and Eisenback, 1983; Castagnone-Sereno and Castillo, 2014). The morphometrics of *M. enterolobii* females recorded was average body length including neck 667.2 μm; body width 414.6 μm; neck length 264.8 μm; stylet length 13.4 μm; stylet knob height 2.7 μm; stylet knob width 4.3 μm; dorsal esophageal gland orifice to stylet base 3.7 μm; excretory pore not visible, and the distance from excretory pore to the head end was 178.2 μm (Yang and Eisenback, 1983; Rammah and Hirschmann, 1988). The adult males have a translucent white body and are vermiform, tapering at both ends (Yang and Eisenback, 1983; Castagnone-Sereno and Castillo, 2014). The morphometrics of males was average body length 1,496.4 μm; body width 37.0 μm; stylet length 23.6 μm; stylet knob height 2.6 μm; stylet knob width 4.6 μm; dorsal esophageal gland orifice to stylet base 4.9 μm; excretory pore to head end 165.4 μm; tail length 14.2 μm; and spicule length 28.3 μm (Yang and Eisenback, 1983; Rammah and Hirschmann, 1988). The chief features of the J2s bodies were translucent white and vermiform; truncate head region rounded; slender, and

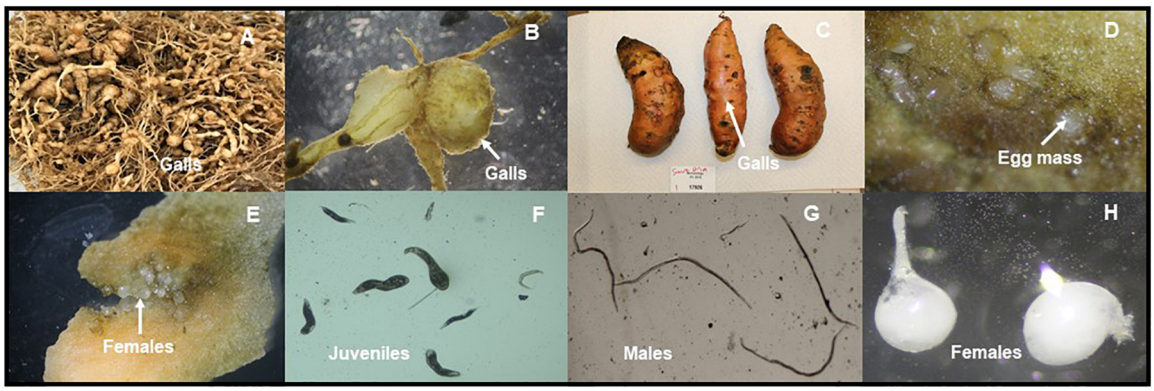

FIGURE 1 | *Meloidogyne enterolobii* individuals and symptoms on different crops in North Carolina, United States (Photos provided by Dr. W. Ye). Large galls and massive root swellings of tomato cv. 'Rutger' in the greenhouse. The nematode was originally collected from Greene County in NC **(A)**. Galls on soybean from Johnston County, NC **(B)**. Galls on sweetpotato from Nash County, NC **(C)**. Egg masses on sweetpotato from Nash County, NC **(D)**. Adult females on sweetpotato from Nash County, NC **(E)**. Infective late second-stage juveniles (J2) from soybean in Johnston County, NC **(F)**. Males from soybean from in Wilson County, NC **(G)**. Females from sweetpotato in Johnston County, NC **(H)**.

FIGURE 2 | Geographic distribution of *Meloidogyne enterolobii* across the world. Numbers in parenthesis in each country indicate the year in which the nematode was reported.

narrow tails with pointed tips, and distinct hyaline tail termini (Rammah and Hirschmann, 1988; Brito et al., 2004).

Although variability in the morphometrics characters of J2 among of *M. enterolobii* isolates from different regions and countries were reported (Brito et al., 2004), the average measurements of J2s were body length 436.6 μm; body width 15.3 μm; tail length 56.4 μm; stylet length 13.0 μm; and excretory pore to head end 11.7 μm (Yang and Eisenback, 1983; Rammah and Hirschmann, 1988). Morphometrics obtained from juvenile specimens, and of the relative lengths of body, tail, and functional and replacement odontostylet (Yang and Eisenback, 1983; Rammah and Hirschmann, 1988), suggest the presence of four juvenile stages of *M. enterolobii* (**Figure 3**).

The life cycle of *M. enterolobii* is similar to that of other *Meloidogyne* spp. (Castagnone-Sereno and Castillo, 2014; Kirkpatrick et al., 2018; Overstreet et al., 2019). Adult females lay eggs in a protective gelatinous matrix which is usually expelled out of the root and into the soil (Moens et al., 2009; Perry and Moens, 2011; Elling, 2013; Jones et al., 2013; Castagnone-Sereno and Castillo, 2014; Overstreet et al., 2019). This matrix keeps the eggs together, protecting them from predation and extreme environmental conditions (Moens et al., 2009). After embryogenesis, the nematode develops into a first stage juvenile (J1), then undergoes a first molt to an infective J2, which hatches from the egg and is vermiform (Eisenback and Triantaphyllou, 1991; Chitwood and Perry, 2009; Moens et al., 2009; Elling, 2013; Jones et al., 2013). Hatching is dependent on both the

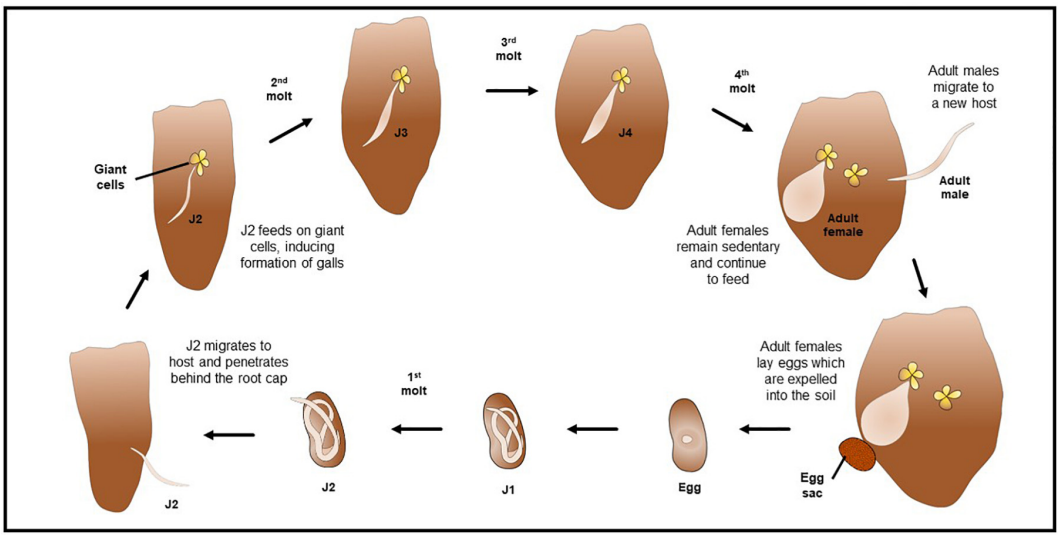

FIGURE 3 | Illustration of the life cycle and root galling of *Meloidogyne enterolobii*.

temperature and moisture conditions of the soil (Moens et al., 2009; Perry and Moens, 2011; Elling, 2013). J2s migrate to a new host's root system and penetrate the root epidermal tissues, usually behind the root cap (Eisenback and Triantaphyllou, 1991; Chitwood and Perry, 2009; Moens et al., 2009; Jones et al., 2013; Kirkpatrick et al., 2018; Overstreet et al., 2019). With a combination of physical damage by propelling their stylets as well as releasing cellulolytic and pectolytic enzymes, these nematodes migrate to the vascular cylinder where they establish permanent feeding sites (Eisenback and Triantaphyllou, 1991; Perry and Moens, 2011; Elling, 2013; Jones et al., 2013; Castagnone-Sereno and Castillo, 2014; Kirkpatrick et al., 2018). These feeding sites are comprised of 'giant cells,' which are responsible for the characteristic galls found on infected root systems (Moens et al., 2009; Elling, 2013; Jones et al., 2013; Castagnone-Sereno and Castillo, 2014; Overstreet et al., 2019). Giant cells are enlarged, multinucleated cells typically arising from plant vascular tissues that provide nutrition to nematodes by reallocating plant metabolites (Eisenback and Triantaphyllou, 1991; Moens et al., 2009; Mitchum et al., 2012). The J2 nematodes molt three more times, to the third (J3), fourth (J4) stages, and then to reproductive adults (**Figure 3**) (Eisenback and Triantaphyllou, 1991; Chitwood and Perry, 2009; Moens et al., 2009; Elling, 2013; Jones et al., 2013; Castagnone-Sereno and Castillo, 2014). The J3 and J4 stages do not feed as they lack a functional stylet (Chitwood and Perry, 2009; Moens et al., 2009; Jones et al., 2013).

Male *M. enterolobii* nematodes are vermiform and leave the root system, and do not feed as adults. However, males of many *Meloidogyne* spp. are only formed in unfavorable conditions, such as extreme soil temperatures, lack of sufficient soil moisture, or situations of overcrowding (Eisenback and Triantaphyllou, 1991; Chitwood and Perry, 2009; Elling, 2013; Jones et al., 2013). Females remain sedentary and continue to feed as they swell and become pear-shaped (Elling, 2013; Jones et al., 2013; Schwarz, 2019). Under favorable conditions, the life cycle of most *Meloidogyne* spp., including *M. enterolobii*, takes about 30 to 35 days to complete and each female can lay up to 600 eggs (Castagnone-Sereno and Castillo, 2014; Da Silva et al., 2019; Overstreet et al., 2019). Several generations of the life cycle may occur throughout the growing season (Chitwood and Perry, 2009).

Meloidogyne spp. can reproduce via amphimixis, facultative meiotic parthenogenesis, and obligate mitotic parthenogenesis (Chitwood and Perry, 2009). *Meloidogyne enterolobii* reproduces via obligate mitotic parthenogenesis or obligatory asexual reproduction (Chitwood and Perry, 2009; Castagnone-Sereno and Castillo, 2014), by which the nucleus separates into two daughter nuclei, having the same genetic material as the original (Chitwood and Perry, 2009). Males are not required for reproduction, but extreme environmental conditions may promote their development from individuals genetically disposed to become female (Eisenback and Triantaphyllou, 1991; Chitwood and Perry, 2009).

IDENTIFICATION METHODS AND POPULATION BIOLOGY

Traditionally, *Meloidogyne* spp. have been characterized through the morphology of adult females and males, including analysis of perineal patterns, which is the shape of cuticle folding around the vulva and anus of adult females. These methods of identification require considerable skill and experience and may otherwise lead to misidentification (Hunt and Handoo, 2009; Min et al., 2012; Elling, 2013). Some of the features of the perineal patterns were useful to separate *M. enterolobii* from other *Meloidogyne* species. In general, the perineal patterns of *M. enterolobii* are oval shape; the dorsal arch is high and round; phasmids are large, and weak lateral lines occasionally present (Karssen and van Aelst, 2001;

Brito et al., 2004). However, perineal patterns within the same species may also vary in individuals from the same population, making identification difficult (Humphreys et al., 2012; Da Silva and Santos, 2016; Suresh et al., 2019). Additionally, *M. incognita* and *M. enterolobii* can have very similar perineal patterns (Humphreys et al., 2012; Schwarz, 2019; Suresh et al., 2019) and *M. enterolobii* was originally thought to be *M. incognita* based on perineal pattern analysis. The perineal pattern of *M. enterolobii* females is an oval shape, dorsal arch usually high and round, weak lateral lines sometimes present, large phasmids and has occasional breaks of striation laterally, and a circular tail tip area lacking striae (Yang and Eisenback, 1983). In addition to their perineal pattern, female root-knot nematodes can be identified to greater taxonomic groups or species by stylet morphology, body shape, or neck length. Males and J2s can be distinguished through body morphometrics or by the morphology of the head and tail (Yang and Eisenback, 1983; Eisenback and Triantaphyllou, 1991; Hunt and Handoo, 2009). However, many *Meloidogyne* species share overlapping measurements and characteristics, making discrimination at the species level difficult (Eisenback and Triantaphyllou, 1991).

Isozyme analysis is a biochemical-based diagnostic method of staining and visualizing esterase, cellulose acetate, and malate dehydrogenase (*Mdh*) isozyme profiles after separation and migration with electrophoresis (Eisenback and Triantaphyllou, 1991; Blok and Powers, 2009). Inter-species variability gives rise to these isozymes, which provide similar catalytic function but diverge in their chemical properties, such as mobility during electrophoresis (Williamson, 1991). *Meloidogyne enterolobii* can be distinguished by the unique pattern of two distinct esterase bands and one malate dehydrogenase band (Brito et al., 2004; Hunt and Handoo, 2009; Pinheiro et al., 2015; Da Silva and Santos, 2016). This method was effective to differentiate and identify young adult females to species, but not for J2s, which are most predominantly found in soil samples (Castagnone-Sereno, 2012; Elling, 2013). Also, it is highly sensitive and can be performed with extracted protein from a single adult female (Eisenback and Triantaphyllou, 1991; Brito et al., 2004; Blok and Powers, 2009). Although isozyme analysis was widely used to identify *Meloidogyne* species (Eisenback and Triantaphyllou, 1991; Blok and Powers, 2009; Hunt and Handoo, 2009; Moens et al., 2009; Castagnone-Sereno, 2012; Elling, 2013; Da Silva and Santos, 2016), this technique requires more than one polymorphic enzyme to confirm the identity of some isolates and the signal of enzyme presence or absence can vary within and across samples.

Species-specific polymerase chain reaction (PCR) assays have been developed and used to differentiate *Meloidogyne* spp. (**Supplementary Table S2**) (Nunn, 1992; Blok et al., 1997, 2002; Zijlstra, 2000; Long et al., 2006; Kiewnick et al., 2013). A sequence characterized amplified region (SCAR) primer set, MK7/F and MK7/R, was used to identify *M. enterolobii* (Ye et al., 2013; Villar-Luna et al., 2015; Schwarz et al., 2020). However, Schwarz et al. (2020) found that the IGS2 primers, MeF/MeR were more specific than the MK7F/MK7R primers. In another study, internal transcribed spacer (ITS) region primers, TW81F/AB28R were used to detect *M. enterolobii* (Suresh et al., 2019). Multiplex PCR has been developed to identify and detect *M. enterolobii, M. incognita,* and *M. javanica* simultaneously using DNA extracted directly from individual galls at various stages of their life cycle (Hu et al., 2011; Elling, 2013). A new quantitative real-time PCR (qPCR) assay that quantifies the amount of nucleic acid present, was developed for the specific detection, identification, and potential quantification of *M. enterolobii* in soil and plant roots (**Supplementary Table S2**) (Toyota et al., 2008; Kiewnick et al., 2015; Sapkota et al., 2016). Additionally, the qPCR assay showed high specificity, sensitivity, and reproducibility (Braun-Kiewnick et al., 2016). A novel satellite DNA family, pMmPet, was discovered in *M. enterolobii*, allowing species-specific identification by PCR, as well as by Southern blot and dot blot analysis (Randig et al., 2009; Elling, 2013). It was shown the satellite repeat was stable among many populations of *M. enterolobii* and high abundancy, allowing for identification of a single individual, thus making it a strong diagnostic tool (Randig et al., 2009).

Loop-mediated isothermal amplification (LAMP) technique that amplifies DNA with high specificity, sensitivity, efficiency, and rapidity under isothermal conditions has been developed (Notomi et al., 2000). Furthermore, LAMP can amplify DNA under isothermal conditions within 1 h using either two or three sets of primers. LAMP assay has been developed and used to identify *M. enterolobii, M. arenaria, M. hapla, M. incognita,* and *M. javanica* (Niu et al., 2011, 2012; Elling, 2013) and has the potential to be used as a simple screening assay in the field (Elling, 2013). High resolution melting curve (HRMC) analysis is a new, post-PCR analysis method, which is simple, fast, and use a single-tube assay method-based on PCR melting (dissociation) curve technique and can discriminate DNA sequences based on their composition, length, and GC content (Reed et al., 2007). HRMC analysis was useful to differentiate different tropical species of *Meloidogyne* (Holterman et al., 2012; Elling, 2013). HRMC technique was also applied to *M. enterolobii* in 2-step nested PCR and single-tube assay and the results showed *M. enterolobii* isolates had different melting peak patterns, with one or two peaks with different heights centered on different melting temperatures, suggesting that the risk of using a fragment that produced multiple amplicons of different length in one species (Holterman et al., 2012). However, evaluating new single copy genes and gene regions in multiplex HRMC assays might be effective to differentiate among isolates of *M. enterolobii* or *M. enterolobii* from other *Meloidogyne* spp. (Holterman et al., 2012; Elling, 2013). Analysis of single nucleotide polymorphisms (SNPs) could be a beneficial low cost and high-throughput tool for *M. enterolobii* diagnosis (Davis et al., 2005; Holterman et al., 2012). Genotyping-by-sequencing (GBS) technique discovers SNPs to whole-genome profiling of association panels (Elshire et al., 2011) and has been used successfully to investigate the phylogenetic genetic relationships of *M. enterolobii*, *M. incognita,* and *M. javanica* populations in South Africa and identify 34 SNPs that were useful to discriminate between the three *Meloidogyne* species investigated (Rashidifard et al., 2018). The complete genomes of the root-knot species *M. incognita*, *M. hapla*, and *M. enterolobii* have been sequenced and reported (Abad et al., 2008; Opperman et al., 2008; Koutsovoulos et al., 2019).

Little genetic variation has been observed within the species of *M. enterolobii*, which is likely due to the mode of reproduction through mitotic parthenogenesis (Perry and Moens, 2011). DNA markers were used to test *M. enterolobii* isolates from different geographic regions and hosts and found this species was genetically homogenous (Tigano et al., 2010).

INTEGRATED DISEASE MANAGEMENT (IDM) STRATEGIES

Integrated disease management (IDM) is the simultaneous use of multiple disease management strategies to suppress disease severity or incidence and reduce the pathogen population below the economic threshold level (Ciancio and Mukerji, 2007). Although IDM is an economically and ecologically sound approach, once *M. enterolobii* populations become established, the pathogen can be difficult to manage (Schwarz, 2019; Schwarz et al., 2020). Thus, identifying effective measures and integrating these into disease management plans can delay disease epidemics, reduce disease intensity, and enhance yields. Several management strategies through soil solarization, biological soil disinfestation, biological control, soil amendments, soil flooding, fumigant and non-fumigant nematicide, and host plant resistance have been employed to minimize the effects of this pathogen in crop production worldwide (Zasada et al., 2010; Noling, 2015). Further, a robust and specific diagnostic method to detect *M. enterolobii* would increase food security and improve quarantine measures to support epidemiological studies and the decision-making process of management tactics on tomato worldwide.

In the United States, particularly in North Carolina, *M. enterolobii* is under an internal quarantine, and infected material, or the nematode in any life stage, cannot be moved out of the state. *Meloidogyne enterolobii* is not transferred by tomato seed but it can be spread through sweetpotato and potato "seed" as the seed pieces (parts of the roots or tuber stems) are in contact with the soil and may become infected (Thiessen, 2018b). Thus, growers need to avoid moving infected plant material, infested soil, and contaminated farm-equipment from infested fields with *M. enterolobii* to non-infested areas (Thiessen, 2018b; Schwarz et al., 2020). However, this may be difficult to accomplish due to the high level of agricultural trade between North Carolina and the surrounding states and even international locations. It is important not to plant infected tomato transplants, but planting non-infected clean transplants is essential to avoid infesting new planting fields.

Cultural Control

Cultural practices are non-chemical management tactics such as crop rotation with non-host crops or resistant cultivars, and these tactics are an economical method for nematode management. Crop rotation to non-host crops has a suppressive effect on *M. enterolobii* populations by inhibiting the reproduction and increase of populations through the absence of a favorable host. Rotation to non-hosts for at least 1 year can help reduce nematode populations (Schwarz, 2019). However, the rotation to non-hosts for a minimum of 3 years is recommended for tomato (Seid et al., 2015). Unfortunately, crop rotation has limits due to the broad host range of *M. enterolobii* (Thiessen, 2018a). Peanut, corn, and wheat have shown to be poor hosts for this nematode and can be utilized as rotation crops (Rodriguez et al., 2003; Brito et al., 2004; Elling, 2013; Castagnone-Sereno and Castillo, 2014; de Brita et al., 2018; Thiessen, 2018b; Schwarz et al., 2020). Weed management is another important prevention strategy because many weed species may serve as hosts to *M. enterolobii* (Rich et al., 2008; Thiessen, 2018b). Since nematodes can be easily transferred by water, farm equipment, and plant material, sanitation can prevent moving the pathogen to non-infested fields (Thiessen, 2018b). Other cultural methods such as fallowing soil, soil solarization, steaming, and flooding can be used under conducive circumstances (Seid et al., 2015; Schwarz, 2019). Additional targeted research in cultural control methods such at tillage, crop rotational plans, and soil amendments are needed to support optimal management of *M. enterolobii* in tomato. In addition, rotating tomato with non-hosts such as peanut (*Arachis hypogaea*), sour orange (*Citrus aurantium*), grapefruit (*Citrus paradise*), garlic (*Allium sativum*) (Rodriguez et al., 2003), and maize (*Zea mays*) (Guimaraes et al., 2003) could reduce *M. enterolobii* populations in soil.

Biological Control

Biological control or biopesticide is defined as an application of live microbes (bacteria and fungi) and their gene products, essential oils, plant extracts, individual and mixed acids such as organic and amino acids, natural bioactive substances, and industrial wastes (Seid et al., 2015; Forghani and Hajihassani, 2020). Some bacterial biocontrol agents that are commercially available include *Bacillus firmus* (Bio-Nem-WP/BioSafe, Agrogreen, Ashdod, Israel), *B. firmus* GB-126 (VOTIVO^{TM}, Bayer CropScience, Raleigh, NC, United States), *B. amyloliquefaciens* strain IN937a, *B. subtilis* strain GB03 (BioYield, Gustafson LLC, Plano, TX, United States), *Bacillus* spp. (Pathway Consortia, Pathway Holdings, NY, United States), and heat-killed *Burkholderia* spp. strain A396 (BioST^{TM}, Albaugh, LLC, IA, United States). These biopesticides have shown a bionematicide activity against eggs, juveniles, and adults and played an important role to manage *Meloidogyne* spp. (Stirling, 2014; Seid et al., 2015; Forghani and Hajihassani, 2020). The most prominent beneficial fungi for managing *Meloidogyne* spp. are *Arthrobotrys* spp. and *Monacrosporium* spp. (Cayrol et al., 1992; Bordallo et al., 2002). These beneficial microorganisms are hematophagous fungi that use sticky mycelia to capture nematodes (Nordbring-Hertz et al., 2006). Some endophytic fungi such as *Paecilomyces* and *Trichoderma* may also trap and kill *Meloidogyne* spp. in the soil or root systems. These beneficial fungi may act at different nematode life stages such as eggs, juveniles, or adults (Schouten, 2016). *Paenibacillus* spp., is one of the growth-promoting rhizobacteria (PGPR) which strongly caused J2 mortality and reduced hatching of several *Meloidogyne* spp. including *M. enterolobii* in tomato (Bakengesa, 2016). Recently, the effects of two egg-parasitic fungi, *Pochonia chlamydosporia* and *Purpureocillium lilacinum* against *M. enterolobii* were assessed *in vitro*. Two strains CG1006

and CG1044 of *P. chlamydosporia* and CG1042 and CG1101 of *P. lilacinum* were found to be the most effective and could be potential biocontrol candidates to manage *M. enterolobii* (Forghani and Hajihassani, 2020). Thus, future research on optimizing growth conditions, efficacy and broad-spectrum action, safety, and stability of beneficial endophytic bacteria or PGPR for commercialization and utilization in IDM need to be researched for ability to control *M. enterolobii*.

Arbuscular mycorrhizal fungi (AMF) are soil fungi that form a mutualistic symbiosis with the roots of plants (Baum et al., 2015; Schouteden et al., 2015). Importantly, AMF-mediated biocontrol mechanisms include altered root morphology, enhanced plant tolerance, competition for space and nutrition with plant-parasitic nematodes, induced systemic resistance (ISR), and altered rhizosphere interactions caused by abiotic and biotic factors, including plant pathogenic nematodes (Cayrol et al., 1992; Gianinazzi et al., 2010; Smith et al., 2010; Baum et al., 2015; Schouteden et al., 2015). In the past, research has been conducted on AMF-mediated biocontrol and their potential involvement in reducing *Meloidogyne* spp. populations (Schouteden et al., 2015). With the increase in microbiome research, the development of beneficial microbial agents for field application to *M. enterolobii* is imperative in the years to come. Also, some consideration should be given toward understanding the plant root interactions with beneficial microorganisms, their symbiotic relationships, and more detailed insights into the complex mechanisms underlying biocontrol agents-mediated effects on *M. enterolobii*. Direct effects of AMF on plant-parasitic nematodes and multiple benefits (Schouteden et al., 2015) suggested that AMF could be used as a biocontrol agent for managing *M. enterolobii* and to enhance nutrient bioavailability for superior tomato fruit quality and yield.

Chemical Control

Chemical nematicides have been used to combat *Meloidogyne* spp.; however, many of these products are being phased out due to environmental and health concerns (Elling, 2013). Two broad categories of nematicides to manage *Meloidogyne* spp., including *M. enterolobii*, are fumigants and non-fumigants. Soil fumigants are formulated as gases or liquids that quickly vaporize into gases and move through open-air spaces in the soil as a gas. Some common soil fumigants that are currently available are 1,3-dichloropropene (e.g., Telone II), metam sodium (e.g., Vapam, Sectagon-42) and metam potassium (e.g., K-Pam) (Zasada et al., 2010; Noling, 2019). Although fumigants are useful for managing *Meloidogyne* spp., they can be expensive, are subject to increased regulatory scrutiny, and do not eradicate an infested field (Zasada et al., 2010). Further, many fumigants are non-selective, also having activity on bacteria, fungi, and weed seeds in the soil. Non-fumigant nematicides are generally formulated as either granules or liquids and incorporated physically or when dissolved in water. These nematicides are either contact or systemic nematicides depending on whether they kill nematodes in soil by contact or are taken up by the plant first and then affect nematodes. Some common chemical non-fumigant nematicides used to control *Meloidogyne* spp. in the United States are fluensulfone (e.g., Nimitz, ADAMA, Raleigh, NC, United States), fluopyram (e.g., Velum Prime and Velum Total, Bayer CropScience, St. Louis, MO, United States), oxamyl (e.g., Vydate, DuPont, Wilmington, DE, United States), ethoprop (e.g., Mocap, AMVAC), and terbufos (e.g., Counter, AMVAC) (Noling, 2015; Watson and Desaeger, 2019). In the European Union and other countries in the world, fumigants metam sodium (AMVAC), and dazomet (e.g., Basamid G Certis, Columbia, MD, United States) were effective to control *M. enterolobii* populations in soil (Anonymous, 1987; Zasada et al., 2010). However, because of negative environmental side effects of these fumigants, metam sodium was recommended only be used with a minimum interval of 5 years[1].

Host Plant Resistance

Planting resistant varieties is the most environmentally and economically friendly method to combat root-knot nematodes in tomato (Seid et al., 2015). Plant resistance genes restrict or prevent nematode reproduction in a host. At least 10 plant resistance genes (*R*-genes; *Mi-1*, *Mi-2*, *Mi-3*, *Mi-4*, *Mi-5*, *Mi-6*, *Mi-7*, *Mi-8*, *Mi-9*, and *Mi-HT*) that confer resistance to *Meloidogyne* spp. in tomato have been identified (El-Sappah et al., 2019). Among them, only five genes (*Mi-1, Mi-3, Mi-5, Mi-9*, and *Mi-HT*) have been mapped. Compared with other *Meloidogyne* spp., *M. enterolobii* is pathogenic on crop genotypes possessing several sources of resistance genes. For example, *M. enterolobii* develops on crop genotypes carrying resistance to the major species of *Meloidogyne*, including resistant cotton, sweetpotato, tomatoes (*Mi-1* gene), potato (*Mh* gene), soybean (*Mir1* gene), bell pepper (*N* gene), sweet pepper (*Tabasco* gene) and cowpea (*Rk* gene) (Fery et al., 1998; Thies and Fery, 2000; Williamson and Roberts, 2009; Castagnone-Sereno, 2012; Quenouille et al., 2013).

The most common deployed gene, *Mi-1,* was originally identified in *Solanum peruvianum* and introgressed into *S. lycopersicum* (Da Silva et al., 2019). This gene is effective in providing resistance to *M. incognita, M. javanica,* and *M. arenaria* (Seid et al., 2015; Da Silva et al., 2019). One of the major concerns of *M. enterolobii* is that the *Mi-1* gene is not effective in controlling this species (Kiewnick et al., 2009; Seid et al., 2015; Da Silva et al., 2019). The resistance spectrum of the *Mi-1.2* gene was assessed against 15 populations of *Meloidogyne* spp. employing two contrasting tomato varieties, 'Santa Clara' (homozygous recessive *mi-1.2/mi-1.2*, susceptible) and 'Debora Plus' (heterozygous *Mi-1.2/mi-1.2*, resistant) (Gabriel et al., 2020). They found that the 'Debora Plus' hybrid possessing the *Mi-1.2* gene was susceptible only to *M. enterolobii* and *M. hapla* but exhibited resistance to the other 13 *Meloidogyne* spp. A great deal of effort has been put into finding new sources of resistance or tolerance to *M. enterolobii* in tomato. Da Silva et al. (2019) evaluated commercial and wild tomatoes and identified three varieties (*Solanum lycopersicum* 'Yoshimatsu' and 'CNPH 1246,' and *S. pimpinellifolium* 'CGO 7650' (= 'CNPH 1195') with tolerance to *M. enterolobii*.

Deployment of a new tomato variety by conventional breeding may take over 10 years. However, this process has been accelerated using PCR-based molecular markers linked to the

[1]http://www.ctb.agro.nl

R gene of interest, and marker-assisted selection (MAS) has been routinely used in tomato breeding programs (Foolad and Panthee, 2012; El-Sappah et al., 2019). In the absence of *M. enterolobii* resistant varieties, grafting tomatoes with resistant rootstocks could be an alternative strategy for this disease management (Louws et al., 2010; Schwarz et al., 2010; Baidya et al., 2017). Two tomato rootstocks, 'Brigeor' and 'Efialto,' showed lower reproduction for one isolate of *M. enterolobii*, but not for a second distinct isolate, indicating some differences in virulence of the isolates of *M. enterolobii* (Kiewnick et al., 2009). Yet within these breeding efforts (whether conventional or marker-assisted), special attention should be paid to genotype resistant or tolerant status to *M. enterolobii*. Plants tolerant to *M. enterolobii* are identified by minimal to no yield loss when infected, even under heavy infestation (Boerma and Hussey, 1992). However, they may still allow populations of the nematode to reproduce and increase, posing significant risk to subsequent susceptible crops and long-term *M. enterolobii* management. Although providing a robust option for avoiding short-term yield and economic losses, use of tolerant varieties should be assessed in the framework of holistic *M. enterolobii* management.

NOVEL APPROACHES TO ENHANCE DISEASE RESISTANCE TO *M. enterolobii* IN TOMATO

Management of *M. enterolobii* is challenging due to its broad host range, high reproductive rates, and its seemingly low economic threshold level. Recent advancements in genetic engineering have made it possible to incorporate and express indigenous and heterologous proteins from one organism to another and develop enhanced nematode resistance in plants. Strategies to engineer one or more natural resistance genes with synthetic resistance may be promising tools to suppress nematode infection and populations in tomato production systems (Gheysen et al., 1996; Jung et al., 1998; Opperman et al., 1998). However, lack of public acceptance of genetically modified organisms (GMO) tomatoes has a restricted deployment of this strategy into the market.

Harnessing Host Plant Resistance Through Marker-Assisted Selection (MAS) in Tomato Breeding Programs

A conventional breeding program involves successive crossing and extensive phenotyping, which make this procedure labor-intensive and time-consuming. Traditionally, bi-parental mapping populations have been used to detect and identify genes or quantitative trait loci (QTL) in tomato for resistance to *Meloidogyne* spp. including *M. incognita, M. javanica, M. hapla,* and *M. enterolobii* (Kiewnick et al., 2009; Foolad and Panthee, 2012; El-Sappah et al., 2019). Genome-wide association studies (GWAS) is a powerful technique to identify SNP markers associated with QTL in cultivated and wild tomato (Hirakawa et al., 2013). The integration of biotechnology techniques into a breeding program can greatly reduce this time to incorporate new resistance genes. Genomics-assisted breeding contributes to advance MAS for evaluating tomato germplasm collections, characterizing populations, finding markers linked to specific alleles of important genes, and stacking disease resistance genes for multiple pathogens including for root-knot nematode management (Arens et al., 2010). For example, the *Mi* region contains two *Mi1-1* and *Mi1-2* genes (Milligan et al., 1998). The *Mi1-2* gene, but not *Mi1-1*, has been suggested to confer resistance to *M. incognita, M. javanica,* and *M. arenaria* (Milligan et al., 1998). The PCR markers tightly linked to *Mi1-2* (Goggin et al., 2004) and *Mi-3* (Yaghoobi et al., 2005) were reported; however, the practical use of these resistance loci (*Mi-2* to *Mi-9*) has not yet been investigated thoroughly. These resistance genes should be assessed to different isolates of *M. enterolobii* and molecular markers linked to these *Mi*-genes as well as other disease resistance genes that are needed to evaluate for their stability in tomato (Arens et al., 2010). Recent advances in whole-genome sequencing have identified large numbers of SNPs and can facilitate the use of MAS more effectively in breeding programs. KASP (Kompetitive Allele Specific PCR), is a novel competitive allele specific PCR for SNP genotyping assay based on dual FRET (Fluorescent Resonance Energy Transfer) (Broccanello et al., 2018). Recently, sequences of SNP markers for the *Mi-1* gene for resistance to root-knot nematodes have been converted using KASP assay and used in tomato breeding (Devran et al., 2016). KASP assays are less expensive, highly reproducible, and flexible compared to other marker systems (Semagn et al., 2014). Thus, characterization of a large set of tomato varieties with SNP markers would be useful for the identification of markers linked to genes for resistance to *M. enterolobii* in tomato. Also, SNPs can be converted to KASP markers and used for the MAS gene pyramiding (Devran et al., 2016).

Developing Transgenic Plants Harboring Previously Cloned Resistance Genes

Genetic engineering offers an alternative to conventional breeding and is mainly focused on two strategies: (i) the transfer of the cloned resistance gene from other plants to tomato, and (ii) the transfer of the *Mi* resistance gene from resistant varieties to susceptible ones with highly desirable production qualities (El-Sappah et al., 2019). The *Ma* locus, which has been mapped to chromosome 7 of Myrobalan plum (*Prunus cerasifera*), has been cloned by a positional cloning approach (Claverie et al., 2011; Khallouk et al., 2011). The subsequent *Agrobacterium rhizogenes*-mediated hairy-root transgenic *Prunus* plants corroborated that the *Ma* locus conferred resistance to *M. arenaria, M. incognita*, *M. javanica, M. floridensis,* and *M. enterolobii* (Bosselut et al., 2011; Claverie et al., 2011). The *Ma* toll/interleukin-1 receptor-like nucleotide binding-leucine-rich repeat (TNL) gene confers high-level and wide-spectrum resistance to *M. incognita*, *M. arenaria*, and *M. javanica* and *M. enterolobii*, and TNL is possibly a candidate gene for the *Ma* locus (Bosselut et al., 2011; Claverie et al., 2011). Furthermore, the *Ma – M. enterolobii* interaction may provide a great opportunity

to decipher nematode effector recognition and TNL signaling (Claverie et al., 2011).

Proteinase inhibitors (PIs) are protein molecules secreted by pathogens, which inhibit the function of proteinases and proteases released by the pathogens (Ali et al., 2017). In *Meloidogyne* spp., PIs become active against all the four classes of proteinases from nematodes such as serine, cysteine, metalloproteinases, and aspartic. Transgenic expression of PIs is a method for managing *Meloidogyne* spp. (Hepher and Atkinson, 1992; Ali et al., 2017). For example, a modified rice cystatin gene (a cysteine proteinase inhibitor) in transgenic *Arabidopsis*, reduced nematode feeding, and fecundity of *M. incognita* females (Urwin et al., 1997). The pyramiding expression system produced synergistic effects by utilizing the two defense responsive genes: a plant *cysteine proteinase inhibitor* (*CeCPI*) and a fungal *chitinase* (*PjCHI-1*) in transgenic tomato and protected all growth stages of *M. incognita* infections (Chan et al., 2015). Future research to investigate interactions between these proteinases and *M. enterolobii* could be a novel approach to manage this nematode in tomato. However, concerns about the durability of such a transgenic resistance and the consumer's acceptance of transgenic tomato will need to be investigated.

Utilizing Host Generated RNA Interference (RNAi) to Silence Nematode Specific Effector Genes

RNA interference (RNAi) has emerged as a powerful strategy to downregulate gene activity and has also proven effective as a control tactic against *Meloidogyne* spp. (Elling, 2013). First described for *Caenorhabditis elegans*, RNAi has been used for silencing genes by suppressing their expression in a wide variety of organisms including plant-parasitic nematodes (Huang et al., 2006b; Ali et al., 2017). In this novel strategy, genes expressed in a range of cell types are silenced when nematodes take up double-stranded RNA (dsRNA) or short interfering RNAs (siRNAs) that elicit a systemic RNAi response (Lilley et al., 2012). These dsRNA molecules ranged from 42 to 1300 bp and were effective in inducing RNAi in both cyst and root-knot nematodes (Lilley et al., 2012). *Meloidogyne* spp. synthesizes effector proteins encoded by parasitism genes, and these effectors represent the molecular interface between the nematode and host (Elling, 2013). The nematode-secreted effectors produced within the esophageal glands play critical roles in parasitism (Davis et al., 2004; Baum et al., 2007; Haegeman et al., 2012). Such developments need to be coupled with an investigation of the mechanisms by which nematodes circumvent resistance (Williamson and Kumar, 2006). The feasibility of silencing nematode genes in the host plants using RNAi has been demonstrated in *Meloidogyne* spp. (Huang et al., 2006a; Yadav et al., 2006). For example, a secreted parasitism protein called 16D10, which is expressed in the subventral esophageal gland cells of multiple *Meloidogyne* spp. and interact directly with a host intracellular transcription regulator (Huang et al., 2006b). Furthermore, the silencing of the *16D10* gene by expressing dsRNA in transgenic *Arabidopsis* enabled the development of transgenic plants that were constitutively resistant to *M. arenaria*, *M. hapla*, *M. incognita,* and *M. javanica* (Huang et al., 2006a,b).

The translationally controlled tumor protein (TCTP) was first identified in mice (Yenofsky et al., 1982). A novel *M. enterolobii* TCTP effector, named *MeTCTP* was able to promote parasitism, probably by suppressing programmed cell death in the host (Zhuo et al., 2017). The silencing of the effector *MeTCTP* resulted in a reduction in parasitism and reproductive potential of *M. enterolobii*, providing evidence of the nematode effector gene as a target for host generated RNAi to achieve disease resistance (Zhuo et al., 2017). Recently, both genome sequence data and new bioinformatics tools have emerged for developing effective dsRNA constructs and stacking of dsRNA sequences to target multiple genes for nematode control (Banerjee et al., 2017). Identification and functional analysis of nematode effector targets using RNAi technology may hold great promise for enhancing plant resistance to *M. enterolobii* in tomato.

Exploiting Efficient Genome Editing Using the CRISPR-Cas9 Technique

The development of the clustered regularly interspaced short palindromic repeats (CRISPR) technology has become a powerful alternative to RNAi for gene silencing (Ali et al., 2019). The CRISPR/Cas9 technique incorporates foreign DNA sequences into host CRISPR loci to generate short CRISPR RNAs (crRNAs) that direct sequence-specific cleavage of homologous target double-stranded DNA by Cas endonucleases (Jinek et al., 2012). The CRISPR-Cas9 genome editing protocols have been established in the free-living nematode, *Caenorhabditis elegans* (Friedland et al., 2013; Dickinson and Goldstein, 2016) which creates DNA modification at specific loci and selects the T-DNA-free mutant (Banerjee et al., 2017). The recent availability of genome sequences for tomato (Sato et al., 2012) and *M. enterolobii* (Szitenberg et al., 2017; Koutsovoulos et al., 2019) could lead to the identification of both host and pathogen novel genes involved in the infection stage and help develop the CRISPR-Cas9 technique for enhancing the resistance to *M. enterolobii* in tomato.

CONCLUSION AND PERSPECTIVES

We have highlighted the progress made by several research groups in the biology and management of *M. enterolobii* in tomato using both conventional and modern technologies. Even with successes in managing other *Meloidogyne* spp. through host resistance, cultural, chemical, and biological control, the recent identification of highly virulent and aggressive nematode, *M. enterolobii*, poses a threat to tomato production globally. To manage this emerging pathogen, substantial investments are necessary to lead fundamental research focused on assessing the pathogen virulence and understanding the species identity, genetic diversity, population genetic structure, evolution, and parasitism mechanisms at a more detailed scale. Whole-genome sequences of *Meloidogyne* spp. will provide opportunities to identify the widespread occurrence of horizontally transferred genes encoding for unique effectors, contributing to successful plant parasitism in nematodes and in the modulation of the plant's defense system, the establishment of a nematode feeding

site, and the synthesis or processing of nutrients (Haegeman et al., 2011). Comparative genomic analyses across *Meloidogyne* spp. need to be exploited to advance understanding of the evolutionary relationships and population genetic structure of *M. enterolobii*. More importantly, the development of robust and specific diagnostic molecular markers is necessary to correctly identify *M. enterolobii* and prevent further spread of this highly destructive nematode. To ensure global food security, modern technologies in conjunction with classical methods should be a key priority for income generation, and sustainability to tomato growers and stakeholders (Barker, 2003). New insights into the current and future risks, supported by a more robust understanding of the interactions between tomato and *M. enterolobii* will enhance the opportunities for developing novel management tools as the ability to use chemical pesticides decrease and the need for food production continues to increase. Strengthening research collaborations and combining multidisciplinary experts working on *M. enterolobii* is required to combat this economically devastating nematode in tomato production systems.

AUTHOR CONTRIBUTIONS

TA and FL discussed and conceived ideas. TA designed the scope of the study. AP and TA wrote the manuscript. AG helped to revise the manuscript and offer additional discussion. All authors have read, edited, and approved it for publication.

FUNDING

Funding for this research was provided by a USDA-NIFA Specialty Crop Research Initiative (SCRI) under award number 2016-51181-25404. Additional funding and resources for this project were supplied by the NC Agricultural Foundation, Inc., the North Carolina Tomato Growers Association, and a USDA-NIFA SCRI award number 2019-51181-30018.

ACKNOWLEDGMENTS

We acknowledge Dr. Weimin Ye, NCDA & CS, Raleigh, NC, United States for providing photos in **Figure 1**.

SUPPLEMENTARY MATERIAL

The Supplementary Material for this article can be found online at: https://www.frontiersin.org/articles/10.3389/fpls.2020.606395/full#supplementary-material

REFERENCES

Abad, P., Gouzy, J., Aury, J.-M., Castagnone-Sereno, P., Danchin, E. G. J., Deleury, E., et al. (2008). Genome sequence of the metazoan plant parasitic nematode *Meloidogyne incognita*. *Nat. Biotechnol.* 26, 909–915.

Agrios, G. N. (2005). *Plant Pathology*, Vol. 5. (San Diego, CA: Academic Press), 845.

Ali, M. A., Azeem, F., Abbas, A., Joyia, F. A., Li, H., and Dababat, A. A. (2017). Transgenic strategies for enhancement of nematode resistance in plants. *Front. Plant Sci.* 8:750. doi: 10.3389/fpls.2017.00750

Ali, M. A., Shahzadi, M., Zahoor, A., Dababat, A. A., Toktay, H., Bakhsh, A., et al. (2019). Resistance to cereal cyst nematodes in wheat and barley: an emphasis on classical and modern approaches. *Int. J. Mol. Sci.* 20:432. doi: 10.3390/ijms20020432

Anonymous (1987). *Gids voor Grondontsmetting in de Praktijk*. Moerdijk: Shell Nederland Chemie B.V.

Arens, P., Mansilla, C., Deinum, D., Cavellini, L., Moretti, A., Rolland, S., et al. (2010). Development and evaluation of robust molecular markers linked to disease resistance in tomato for distinctness, uniformity, and stability testing. *Theor. Appl. Genet.* 120, 655–664. doi: 10.1007/s00122-009-1183-2

Baidya, S., Timila, R. D., Bahadur, K. C. R., Manandhar, H. K., and Manandhar, C. (2017). Management of root-knot nematode on tomato through grafting rootstock of *Solanum sisymbriifolium*. *J. Nepal Agric. Res. Counc.* 3, 27–31. doi: 10.3126/jnarc.v3i1.17272

Bakengesa, J. A. (2016). *Potential of Paenibacillus spp. as a Biocontrol Agent for Root-Knot Nematodes (Meloidogyne spp.)*. Master's thesis, University of Gent, Gent.

Banerjee, S., Banerjee, A., Gill, S. S., Gupta, O. P., Dahuja, A., Jain, P. K., et al. (2017). RNA Interference: a novel source of resistance to combat plant-parasitic nematodes. *Front. Plant Sci.* 8:834. doi: 10.3389/fpls.2017.00834

Barker, K. (2003). Perspectives on plant and soil nematology. *Annu. Rev. Phytopathol.* 41, 1–25. doi: 10.1079/9780851996455.0001

Baum, C., El-Tohamy, W., and Gruda, N. (2015). Increasing the productivity and product quality of vegetable crops using arbuscular mycorrhizal fungi: a review. *Sci. Hortic.* 187, 131–141. doi: 10.1016/j.scienta.2015.03.002

Baum, T. J., Hussey, R. S., and Davis, E. L. (2007). "Root-knot and cyst nematode parasitism genes: the molecular basis of plant parasitism," in *Genetic Engineering*, Vol. 28, ed. J. K. Setlow (Boston, MA: Springer), 17–34. doi: 10.1007/978-0-387-34504-8_2

Blok, V. C., Phillips, M. S., and Fargette, M. (1997). Comparison of sequences from the ribosomal DNA intergenic region of *Meloidogyne mayaguensis* and other major tropical root-knot nematodes. *J. Nematol.* 29, 16–22.

Blok, V. C., and Powers, T. O. (2009). "Biochemical and Molecular Identification," in *Root-Knot Nematodes*, eds R. N. Perry, M. Moens, and J. Starr (Cambridge, MA: CAB International), 98–111. doi: 10.1079/9781845934927.0098

Blok, V. C., Wishart, J., Fargette, M., Berthier, K., and Phillips, M. S. (2002). Mitochondrial DNA differences distinguishing *Meloidogyne mayaguensis* from the major species of tropical root-knot nematodes. *Nematology* 4, 773–781. doi: 10.1163/156854102760402559

Boerma, H. R., and Hussey, R. S. (1992). Breeding plant for resistance to nematodes. *J. Nematol.* 24, 242–252.

Bordallo, J. J., Lopez-Llorca, L. V., Jansson, H.-B., Salinas, J., Persmark, L., and Asensio, L. (2002). Colonization of plant roots by egg-parasitic and nematode-trapping fungi. *New Phytol.* 154, 491–499. doi: 10.1046/j.1469-8137.2002.00399.x

Bosselut, N., Van Ghelder, C., Claverie, M., Voisin, R., Onesto, J. P., Rosso, M. N., et al. (2011). Agrobacterium rhizogenes-mediated transformation of Prunus as an alternative for gene functional analysis in hairy-roots and composite plants. *Plant Cell Rep.* 30, 1313–1326. doi: 10.1007/s00299-011-1043-9

Braun-Kiewnick, A., Viaene, N., Folcher, L., Ollivier, F., Anthoine, G., Niere, B., et al. (2016). Assessment of a new qPCR tool for the detection and identification of the root-knot nematode *Meloidogyne enterolobii* by an international test performance study. *Eur. J. Plant Pathol.* 144, 97–108. doi: 10.1007/s10658-015-0754-0

Brito, J., Powers, T. O., Mullin, P. G., Inserra, R. N., and Dickson, D. W. (2004). Morphological and molecular characterization of *Meloidogyne mayaguensis* isolates from Florida. *J. Nematol.* 36, 232–240.

Brito, J. A., Kaur, R., Cetintas, R., Stanley, J. D., Mendes, M. L., Powers, T. O., et al. (2010). Meloidogyne spp. *infecting ornamental plants in Florida*. *Nematropica* 40, 87–103.

Broccanello, C., Chiodi, C., Funk, A., McGrath, J. M., Panella, L., and Stevanato, P. (2018). Comparison of three PCR-based assays for SNP genotyping in plants. *Plant Methods* 14:28.

Carneiro, R. M. D. G., Moreira, W. A., Almeida, M. R. A., and Gomes, A. C. M. M. (2001). Primeiro registro de *Meloidogyne mayaguensis* em goiabeira no Brasil. *Nematol. Bras.* 25, 223–228.

Castagnone-Sereno, P. (2012). *Meloidogyne enterolobii* (= *M. mayaguensis*): profile of an emerging, highly pathogenic, root-knot nematode species. Nematology 14, 133–138.

Castagnone-Sereno, P., and Castillo, P. (2014). *Meloidogyne enterolobii (Pacara earpod tree root-knot nematode)*. Available online at: https://www.cabi.org/isc/datasheet/33238 (accessed August 20, 2020).

Cayrol, J. C., Dijan-Caporalino, C., and Panchaud-Mattei, E. (1992). La lutte biologique contre les Nématodes phytoparasites. *Courr. Cell. Environ. l'INRA* 17, 31–44.

Chan, Y. L., Yong, H., Hsiao, T. T., Wang, C. J., Tian, Z., and Yeh, K. W. (2015). Pyramiding taro cystatin and fungal chitinase genes driven by a synthetic promoter enhances resistance in tomato to root-knot nematode *Meloidogyne incognita*. *Plant Sci.* 231, 74–81. doi: 10.1016/j.plantsci.2014.11.010

Chiamolera, F. M., Martins, A. B. G., Soares, P. L. M., and Loeiro da Cunha-Chiamolera, T. P. (2018). Reaction of potential guava rootstocks to *Meloidogyne enterolobii*. *Rev. Ceres* 65, 291–295. doi: 10.1590/0034-737x201865030010

Chitwood, D. J., and Perry, R. N. (2009). "Reproduction, physiology, and biochemistry," in *Root-Knot Nematodes*, eds R. N. Perry, M. Moens, and J. Starr (Cambridge, MA: CAB International), 182–194. doi: 10.1079/9781845934927.0182

Ciancio, A., and Mukerji, K. G. (eds) (2007). *General Concepts in Integrated Pest and Disease Management*. (Dordrecht: Springer), 81–130.

Claverie, M., Dirlewanger, E., Bosselut, N., Van Ghelder, C., Voisin, R., Kleinhentz, M., et al. (2011). The *Ma* gene for complete-spectrum resistance to *Meloidogyne* species in Prunus is a TNL with a huge repeated C-terminal post-LRR region. *Plant Physiol.* 156, 779–792. doi: 10.1104/pp.111.176230

Da Silva, A. J., de Oliveira, G. H. F., Pastoriza, R. J. G., Maranhao, E. H. A., Pedrosa, E. M. R., Maranhao, S. R. V. L., et al. (2019). Search for sources of resistance to *Meloidogyne enterolobii* in commercial and wild tomatoes. *Hortic. Bras.* 37, 188–198. doi: 10.1590/s0102-053620190209

Da Silva, M. C. L., and Santos, C. D. G. (2016). Distribution of *Meloidogyne enterolobii* in guava orchards in the state of Ceara, Brazil. *Rev. Caatinga* 30, 335–342.

Davis, E. L., Hussey, R. S., and Baum, T. J. (2004). Getting to the roots of parasitism by nematodes. *Trends Parasitol.* 20, 134–141. doi: 10.1016/j.pt.2004.01.005

Davis, M. W., Hammarlund, M., Harrach, T., Hullett, P., Olsen, S., and Jorgensen, E. M. (2005). Rapid single nucleotide polymorphism mapping in *C. elegans*. *BMC Genomics* 6:118. doi: 10.1186/1471-2164-6-118

de Brita, A. L., de Castrro, B. M., Zanuncio, J. C., Serrao, J. E., and Wilcken, S. R. S. (2018). Oat, wheat and sorghum cultivars for the management of *Meloidogyne enterolobii*. *Nematology* 20, 169–173. doi: 10.1163/15685411-00003131

Devran, Z., Göknur, A., and Mesci, L. (2016). Development of molecular markers for the *Mi-1* gene in tomato using the KASP genotyping assay. *Hortic. Environ. Biotechnol.* 57, 156–160. doi: 10.1007/s13580-016-0028-6

Dickinson, D. J., and Goldstein, B. (2016). CRISPR-based methods for *Caenorhabditis elegans* genome engineering. *Genetics* 202, 885–901. doi: 10.1534/genetics.115.182162

Eisenback, J. D., and Triantaphyllou, H. H. (1991). "Root-knot nematodes: *Meloidogyne* species and races," in *Manual of Agriculture Nematology*, ed. W. R. Nickle (New York, NY: Marcell Dekker), 191–274.

Elling, A. A. (2013). Major emerging problems with minor *Meloidogyne* Species. *Phytopathology* 103, 1092–1102. doi: 10.1094/phyto-01-13-0019-rvw

El-Sappah, A. H., M. M, I., El-Awady, H. H., Yan, S., Qi, S., Liu, J., et al. (2019). Tomato natural resistance genes in controlling the root-knot nematode. *Genes* 10:925. doi: 10.3390/genes10110925

Elshire, R. J., Glaubitz, J. C., Sun, Q., Poland, J. A., Kawamoto, K., Buckler, E. S., et al. (2011). A Robust, Simple Genotyping-by-Sequencing (GBS) Approach for High Diversity Species. *PLoS One* 6:e19379. doi: 10.1371/journal.pone.0019379

Fery, R. L., Dukes, P. D., and Thies, J. A. (1998). 'Carolina Wonder' and 'Charleston Belle: southern root-knot nematode-resistant bell peppers. *Hortscience* 33, 900–902. doi: 10.21273/hortsci.33.5.900

Foolad, M. R., and Panthee, D. R. (2012). Marker-assisted selection in tomato breeding. *Crit. Rev. Plant Sci.* 31, 93–123.

Forghani, F., and Hajihassani, A. (2020). Recent advances in the development of environmentally benign treatments to control root-knot nematodes. *Front. Plant Sci.* 11:1125. doi: 10.3389/fpls.2020.01125

Freitas, V. M., Silva, J. G. P., Gomes, C. B., Castro, J. M. C., Correa, V. R., and Carneiro, R. M. D. G. (2017). Host status of selected cultivated fruit crops to *Meloidogyne enterolobii*. *Eur. J. Plant Pathol* 148, 307–319. doi: 10.1007/s10658-016-1090-8

Friedland, A. E., Tzur, Y. B., Esvelt, K. M., Colaiácovo, M. P., Church, G. M., and Calarco, J. A. (2013). Heritable genome editing in *C. elegans* via a CRISPR-Cas9 system. *Nat. Methods* 10, 741–743.

Gabriel, M., Kulczynski, S. M., Muniz, M. F. B., Boiteux, L. S., and Carneiro, R. M. D. G. (2020). Resistance of 'Debora Plus' tomato bearing Mi-1.2 gene/locus against fifteen *Meloidogyne* species. *Plant Pathol.* 69, 944–952. doi: 10.1111/ppa.13179

Gheysen, G., van der Eycken, W., Barthels, N., Karimi, M., and Van Montagu, M. (1996). The exploitation of nematode-responsive plant genes in novel nematode control methods. *Pestic. Sci.* 47, 95–101. doi: 10.1002/(sici)1096-9063(199605)47:1<95::aid-ps390>3.0.co;2-i

Gianinazzi, S., Gollotte, A., Binet, M.-N., van Tuinen, D., Redecker, D., and Wipf, D. (2010). Agroecology: the key role of arbuscular mycorrhizas in ecosystem services. *Mycorrhiza* 20, 519–530. doi: 10.1007/s00572-010-0333-3

Goggin, F. L., Shah, G., Williamson, V. W., and Ullman, D. E. (2004). Instability of *Mi*-mediated resistance in transgenic tomato plants. *Mol. Breed.* 13, 357–364. doi: 10.1023/b:molb.0000034090.73857.b1

Guimaraes, L. M. P., de Moura, R. M., and Pedrosa, E. M. R. (2003). *Meloidogyne mayaguensis* parasitism on different plant species. *Nematol. Bras.* 27, 139–145.

Haegeman, A., Jones, J. T., and Danchin, E. G. J. (2011). Horizontal gene transfer in nematodes: a catalyst for plant parasitism? *Mol. Plant Microbe Interact.* 24, 879–887. doi: 10.1094/mpmi-03-11-0055

Haegeman, A., Mantelin, S., Jones, J. T., and Gheysen, G. (2012). Functional roles of effectors of plant-parasitic nematodes. *Gene* 492, 19–31. doi: 10.1016/j.gene.2011.10.040

Hepher, A., and Atkinson, H. J. (1992). Nematode Control with Proteinase Inhibitors. European Patent No. EP0502730B1. Munich: European Patent Office.

Hirakawa, H., Shirasawa, K., Ohyama, A., Fukuoka, H., Aoki, K., Rothan, C., et al. (2013). Genome-wide SNP genotyping to infer the effects on gene functions in tomato. *DNA Res.* 20, 221–233. doi: 10.1093/dnares/dst005

Holterman, M. H., Oggenfuss, M., Frey, J. E., and Kiewnick, S. (2012). Evaluation of high-resolution melting curve analysis as a new tool for root-knot nematode diagnostics. *J. Phytopathol.* 160, 59–66. doi: 10.1111/j.1439-0434.2011.01859.x

Hu, M. X., Zhou, K., and Liao, J. L. (2011). Multiplex PCR for the simultaneous identification and detection of *Meloidogyne incognita, M. enterolobii, and M. javanica* using DNA extracted directly from individual galls. *Phytopathology* 101, 1270–1277. doi: 10.1094/phyto-04-11-0095

Huang, G., Allen, R., Davis, E. L., Baum, T. J., and Hussey, R. S. (2006a). Engineering broad root-knot resistance in transgenic plants by RNAi silencing of a conserved and essential root-knot nematode parasitism gene. *Proc. Natl. Acad. Sci. U.S.A.* 103, 14302–14306. doi: 10.1073/pnas.0604698103

Huang, G., Dong, R., Allen, R., Davis, E. L., Baum, T. J., and Hussey, R. S. (2006b). A root-knot nematode secretory peptide functions as a ligand for a plant transcription factor. *Mol. Plant Microbe Interact.* 19, 463–470. doi: 10.1094/mpmi-19-0463

Humphreys, D. A., Williamson, V. M., Salazar, L., Flores-Chaves, L., and Gomez-Alpizar, L. (2012). Presence of *Meloidogyne enterolobii* Yang and Eisenback (= *Mayaguensis*) in guava and acerola from Costa Rica. *Nematology* 14, 199–207. doi: 10.1163/138855411x584151

Hunt, D. J., and Handoo, Z. A. (2009). "Taxonomy, Identification, and Principal Species," in *Root-knot Nematodes*, eds R. N. Perry, M. Moens, and J. Starr (Cambridge, MA: CAB International), 55–88. doi: 10.1079/9781845934927.0055

Jinek, M., Chylinski, K., Fonfara, I., Hauer, M., Doudna, J. A., and Charpentier, E. (2012). A programmable dual-RNA-guided DNA endonuclease in adaptive bacterial immunity. *Science* 337, 816–821. doi: 10.1126/science.1225829

Jones, J. T., Haegeman, A., Danchin, E. G. J., Gaur, H. S., Helder, J., Jones, M. G. K., et al. (2013). Top 10 plant-parasitic nematodes in molecular plant pathology. *Mol. Plant Pathol.* 14, 946–948. doi: 10.1111/mpp.12057

Jung, C., Cai, D., and Kleine, M. (1998). Engineering nematode resistance in crop species. *Trends Plant Sci.* 3, 266–271. doi: 10.1016/s1360-1385(98)01247-3

Karssen, G., and van Aelst, A. (2001). Root-knot nematode perineal pattern development: a reconsideration. *Nematology* 3, 95–111. doi: 10.1163/156854101750236231

Khallouk, S., Voisin, R., Ghelder, C. V., Engle, R. G., Amiri, S., and Esmenjaud, D. (2011). Histological mechanisms of the resistance conferred by the *Ma* gene against *Meloidogyne incognita* in *Prunus* spp. *Am. Phytopathol. Soc. Nematol.* 101, 945–951. doi: 10.1094/phyto-01-11-0004

Kiewnick, S., Dessimoz, M., and Franck, L. (2009). Effects of the *Mi-1* and the *N* root-knot, nematode-resistance gene on infection and reproduction of *Meloidogyne enterolobii* on tomato and pepper cultivars. *J. Nematol.* 41, 134–139.

Kiewnick, S., Frey, J. E., and Braun-Kiewnick, A. (2015). Development and validation of LNA-based quantitative real-time PCR assays for detection and identification of the root-knot nematode *Meloidogyne enterolobii* in complex DNA backgrounds. *Phytopathology* 105, 1245–1249. doi: 10.1094/phyto-12-14-0364-r

Kiewnick, S., Wolf, S., Willareth, M., and Frey, J.-E. (2013). Identification of the tropical root-knot nematode species *Meloidogyne incognita*, *M. javanica and M. arenaria* using a multiplex PCR assay. *Nematology* 15, 891–894. doi: 10.1163/15685411-00002751

Kirkpatrick, T., Lee, J., and Faske, T. (2018). *The Guava Root-Knot Nematode (Meloidogyne enterolobii), a Potential Threat to Arkansas Sweet Potatoes and Other Crops*. Available online at: https://www.uaex.edu/publications/pdf/FSA-7581.pdf (accessed August 20, 2020).

Koutsovoulos, G. D., Poullet, M., Ashry, A. E., Kozlowski, D. K., Sallet, E., Da Rocha, M., et al. (2019). The polyploid genome of the mitotic parthenogenetic root-knot nematode *Meloidogyne enterolobii*. *bioRxiv* [Preprint]. doi: 10.1101/586818

Lilley, C. J., Davies, L. J., and Urwin, P. E. (2012). RNA interference in plant parasitic nematodes: a summary of the current status. *Parasitology* 139, 630–640. doi: 10.1017/s0031182011002071

Long, H., Liu, H., and Xu, J. H. (2006). Development of a PCR Diagnostic for the Root-knot Nematode *Meloidogyne enterolobii*. *Acta Phytopathol. Sin.* 2, 109–115.

Louws, F. J., Rivard, C. L., and Kubota, C. (2010). Grafting fruiting vegetables to manage soilborne pathogens, foliar pathogens, arthropods, and weeds. *Sci. Hortic.* 127, 127–146. doi: 10.1016/j.scienta.2010.09.023

Milligan, S. B., Bodeau, J., Yaghoobi, J., Kaloshian, I., Zabel, P., and Williamson, V. M. (1998). The root-knot nematode resistance gene *Mi* from tomato is a member of the leucine zipper, nucleotide-binding, leucine-rich repeat family of plant genes. *Plant Cell* 10, 307–1319.

Min, Y. Y., Toyota, K., and Sato, E. (2012). A novel nematode diagnostic method using the direct quantification of major plant-parasitic nematodes in soil by real-time PCR. *Nematology* 14, 265–276. doi: 10.1163/156854111x601678

Mitchum, M. G., Wang, X., Wang, J., and Davis, E. L. (2012). Role of nematode peptides and other small molecules in plant parasitism. *Annu. Rev. Phytopathol.* 50, 175–195. doi: 10.1146/annurev-phyto-081211-173008

Moens, M., Perry, R. N., and Starr, J. L. (2009). "*Meloidogyne* species - a Diverse Group of Novel and Important Plant Parasites," in *Root-knot Nematodes*, eds R. N. Perry, M. Moens, and J. Starr (Cambridge, MA: CAB International), 1–13. doi: 10.1079/9781845934927.0001

Nicol, J. M., Turner, S. J., Coyne, D. L., den Nijs, L., Hockland, S., and Tahna Maafi, Z. (2011). "Current nematode threats to world agriculture," in *Genomics and Molecular Genetics of Plant-Nematode Interactions*, eds J. Jones, G. Gheysen, and C. Fenoll (New York, NY: Springer), 3–20.

Niu, J., Jian, H., Guo, Q. X., Chen, C. L., Wang, X. Y., Liu, Q., et al. (2012). Evaluation of loop-mediated isothermal amplification (LAMP) assays based on 5S rDNA-IGS2 regions for detecting *Meloidogyne enterolobii*. *Plant Pathol.* 61, 809–819. doi: 10.1111/j.1365-3059.2011.02562.x

Niu, J. H., Guo, Q. X., Jian, H., Chen, C. L., Yang, D., Liu, Q., et al. (2011). Rapid detection of *Meloidogyne* spp. by LAMP assay in soil and roots. *Crop Protect.* 30, 1063–1069. doi: 10.1016/j.cropro.2011.03.028

Noling, J. W. (2015). *Fumigants Registered for Vegetable Crop Use in Florida. ENY-064*. Gainesville, FL: University of Florida Institute of Food and Agricultural Sciences.

Noling, J. W. (2019). *Movement and Toxicity of Nematicides in the Plant Root Zone*. Gainesville, FL: University of Florida Institute of Food and Agricultural Sciences.

Nordbring-Hertz, B., Jansson, H., and Tunlid, A. (2006). "Nematophagous fungi," in *Encyclopedia of Life Sciences* (Macmillan Publishers Ltd; Nature Publishing Group), 1–11. doi: 10.1038/npg.els.0004293

Notomi, T., Okayama, H., Masubuchi, H., Yonekawa, T., Watanabe, K., Amino, N., et al. (2000). Loop-mediated isothermal amplification of DNA. *Nucleic Acids Res.* 28:E63.

Nunn, G. (1992). *Nematode Molecular Evolution. An Investigation of Evolutionary Patterns Among Nematodes Based Upon DNA Sequences*. Ph.D. dissertation, University of Nottingham, Nottingham.

Opperman, C. H., Acedo, G. N., Saravitz, D. M., Skantar, A. M., Song, W., Taylor, C. G., et al. (1998). "Bioengineering resistance to sedentary endoparasitic nematodes," in *Advances in Molecular Plant Nematology*, eds F. Lamberti, C. de Giorgi, and D. M. Bird (New York, NY: Plenum Press), 221–232. doi: 10.1007/978-1-4757-9080-1_19

Opperman, C. H., Bird, D. M., Williamson, V. M., Rokhsar, D. S., Burke, M., Cohn, J., et al. (2008). Sequence and genetic map of *Meloidogyne hapla*: a compact nematode genome for plant parasitism. *Proc. Natl. Acad. Sci. U.S.A.* 105, 14802–14807. doi: 10.1073/pnas.0805946105

Overstreet, C., McGowley, E. C., Clark, C., Rezende, J., Smith, T., and Sistrunk, M. (2019). *Guava Root-Knot Nematode: A Potentially Serious New Pest in Louisiana*. Available online at: https://www.lsuagcenter.com/articles/page1548428489554 (accessed August 20, 2020).

Perry, R. N., and Moens, M. (2011). "Introduction to plant-parasitic nematodes; modes of parasitism," in *Genomics and Molecular Genetics of Plant-Nematode Interactions*, eds R. N. Perry, M. Moens, and J. Starr (New York, NY: Springer), 3–20.

Perry, R. N., Moens, M., and Starr, J. (2009). *Root-Knot Nematodes*. (Cambridge, MA: CAB International), 520.

Pinheiro, J. B., Boiteux, L. S., Almeida, M. R. A., Pereira, R. B., Galhardo, L. C. S., and Carneiro, R. M. D. G. (2015). First report of *Meloidogyne enterolobii* in capsicum rootstocks carrying the *Me1* and *Me3/Me7* genes in central Brazil. *Nematropica* 45, 184–188.

Quenouille, J., Montarry, J., Palloix, A., and Moury, B. (2013). Farther, slower, stronger: how the plant genetic background protects a major resistance gene from breakdown. *Mol. Plant Pathol.* 14, 109–118. doi: 10.1111/j.1364-3703.2012.00834.x

Rammah, A., and Hirschmann, H. (1988). *Meloidogyne mayaguensis* n. sp. (*Meloidogynidae*), a root-knot nematode from Puerto Rico. J. Nematol. 20, 58–69.

Randig, O., Deau, F., dos Santos, M. F. A., Tigano, M. S., Careiro, R. M. D. G., and Castagnone-Sereno, P. (2009). A novel species-specific satellite DNA family in the invasive root-knot nematode *Meloidogyne mayaguensis* and its potential use for diagnostics. *Eur. J. Plant Pathol.* 125, 485–495. doi: 10.1007/s10658-009-9497-0

Rashidifard, M., Fourie, H., Véronneau, P. Y., Marais, M., Daneel, M. K., and Mimee, B. (2018). Genetic diversity and phylogeny of South African *Meloidogyne* populations using genotyping by sequencing. *Sci. Rep.* 8:13816.

Reed, G. H., Kent, J. O., and Wittwer, C. T. (2007). High-resolution DNA melting analysis for simple and efficient molecular diagnostics. *Pharmacogenomics* 8, 597–608. doi: 10.2217/14622416.8.6.597

Rich, J. R., Brito, J. A., Kaur, R., and Ferrell, J. A. (2008). Weed species as hosts of *Meloidogyne*: a review. *Nematropica* 39, 157–185.

Rodriguez, M. G., Sanchez, L., and Rowe, J. (2003). Host status of agriculturally important plant families to the root-knot nematode *Meloidogyne mayaguensis* in Cuba. *Nematropica* 33, 125–130.

Rutter, W. B., Skantar, A. M., Handoo, Z. A., Mueller, J. D., Aultman, S. P., and Agudelo, P. (2019). *Meloidogyne enterolobii* found infecting root-knot nematode-resistant sweet-potato in South Carolina, United States. *Plant Dis.* 103:775. doi: 10.1094/pdis-08-18-1388-pdn

Sapkota, R., Skantar, A. M., and Nicolaisen, M. (2016). A TaqMan real-time PCR assay for detection of *Meloidogyne hapla* in root galls and in soil. *Nematology* 18, 147–154. doi: 10.1163/15685411-00002950

Sasser, J. N., Eisenback, J. D., Carter, C. C., and Triantaphyllou, A. C. (1983). The International *Meloidogyne* Project - Its goals and accomplishments. *Annu. Rev. Phytopathol.* 21, 271–288. doi: 10.1146/annurev.py.21.090183.001415

Sato, S., Tabata, S., Hirakawa, H., Klein Lankhorst, R. M., de Jong, H., van Ham, R. C. H. J., et al. (2012). The tomato genome sequence provides insights into fleshy fruit evolution. *Nature* 485, 635–641. doi: 10.1038/nature11119

Schouteden, N., Waele, D. D., Panis, B., and Vos, C. M. (2015). Arbuscular mycorrhizal fungi for the biocontrol of plant-parasitic nematodes: a review of the mechanisms involved. *Front. Microbiol.* 6:1280. doi: 10.3389/fmicb.2015.01280

Schouten, A. (2016). Mechanisms involved in nematode control by endophytic fungi. *Annu. Rev. Phytopathol.* 54, 121–142. doi: 10.1146/annurev-phyto-080615-100114

Schwarz, D., Rouphael, Y., Colla, G., and Venema, J. H. (2010). Grafting as a tool to improve tolerance of vegetables to abiotic stresses: thermal stress, water stress and organic pollutants. *Sci. Hortic.* 127, 162–171. doi: 10.1016/j.scienta.2010.09.016

Schwarz, T. (2019). *Distribution, virulence, and Sweetpotato Resistance to Meloidogyne enterolobii in North Carolina*. Master's thesis, Graduate Faculty of North Carolina State University, Raleigh, NC 84.

Schwarz, T., Li, C., Ye, W., and Davis, E. (2020). Distribution of *Meloidogyne enterolobii* in eastern North Carolina and comparison of four isolates. *Plant Health Prog.* 21, 91–96. doi: 10.1094/php-12-19-0093-rs

Seid, A., Fininsa, C., Mekete, T., Decraemer, W., and Wesemael, W. M. L. (2015). Tomato (*Solanum lycopersicum*) and root-knot nematodes *(Meloidogyne* spp.) - a century-old battle. *Nematology* 17, 995–1009. doi: 10.1163/15685411-00002935

Semagn, K., Babu, R., Hearne, S., and Michael Olsen, M. (2014). Single nucleotide polymorphism genotyping using Kompetitive Allele Specific PCR (KASP): overview of the technology and its application in crop improvement. *Mol. Breed.* 33, 1–14. doi: 10.1007/s11032-013-9917-x

Smith, S. E., Facelli, E., Pope, S., and Smith, F. A. (2010). Plant performance in stressful environments: interpreting new and established knowledge of the roles of arbuscular mycorrhizas. *Plant Soil* 326, 3–20. doi: 10.1007/s11104-009-9981-5

Stirling, G. R. (2014). *Biological Control of Plant-Parasitic Nematodes*, 2nd Edn. Wallingford: CAB International.

Suresh, P., Poornima, K., Kalaiarsan, P., Nakkeeran, S., and Vijayakumar, R. M. (2019). Characterization of guava root-knot nematode, *Meloidogyne enterolobii* occurring in Tamil Nadu, India. *Int. J. Curr. Microbiol. Appl. Sci* 8, 1987–1998. doi: 10.20546/ijcmas.2019.809.230

Szitenberg, A., Salazar-Jaramillo, L., Blok, V. C., Laetsch, D. R., Joseph, S., Williamson, V. M., et al. (2017). Comparative genomics of apomictic root-knot nematodes: hybridization, ploidy, and dynamic genome change. *Genome Biol. Evol.* 9, 2844–2861. doi: 10.1093/gbe/evx201

Thies, J. A., and Fery, R. L. (2000). Characterization of resistance conferred by the N gene to *Meloidogyne arenaria* races 1 and 2, *M. hapla, and M. javanica* in two sets of isogenic lines of *Capsicum annuum*. *J. Am. Soc. Hortic. Sci.* 125, 71–75. doi: 10.21273/jashs.125.1.71

Thiessen, L. (2018a). *Root-Knot Nematode of Tobacco: Tobacco Disease Information*. Available online at: https://content.ces.ncsu.edu/root-knot-nematode-of-tobacco (accessed July 20, 2020).

Thiessen, L. (2018b). *Impact of Guava Root Knot Nematode Internal Quarantine on Tobacco and Field Crops in NC*. Available online at: https://ipm.ces.ncsu.edu/2018/10/impact-of-guava-root-knot-nematode-internalquarantine-on-tobacco-and-field-crops-in-nc-ipm/ (accessed July 20, 2020).

Tigano, M., Siqueira, K., Castagnone-Sereno, P., Mulet, K., Queiroz, P., dos Santos, M., et al. (2010). Genetic diversity of the root-knot nematode *Meloidogyne enterolobii* and development of a SCAR marker for this guava-damaging species. *Plant Pathol.* 59, 1054–1061. doi: 10.1111/j.1365-3059.2010.02350.x

Toyota, K., Shirakashi, T., Sato, E., Satoko Wada, S., and Min, Y. Y. (2008). Development of a real-time PCR method for the potato cyst nematode *Globodera rostochiensis* and the root-knot nematode *Meloidogyne incognita*. *Soil Sci. Plant Nutr.* 54, 72–76.

Urwin, P. E., Lilley, C. J., McPherson, M. J., and Atkinson, H. J. (1997). Resistance to both cyst and root-knot nematodes conferred by transgenic *Arabidopsis* expressing a modified plant cystatin. *Plant J.* 12, 455–461. doi: 10.1046/j.1365-313x.1997.12020455.x

Villar-Luna, E., Gomez-Rodriguez, O., Rojas-Martinez, R. I., and Zavaleta-Mejia, E. (2015). Presence of *Meloidogyne enterolobii* on jalapeno pepper (*Capsicum annuum* L.) in Sinaloa, Mexico. *Helminthologia* 53, 155–160. doi: 10.1515/helmin-2016-0001

Watson, T. T., and Desaeger, J. A. (2019). *Non-Fumigant Nematicides Registered for Vegetable Crop Use. ENY*-033. Gainesville, FL: University of Florida Institute of Food and Agricultural Sciences.

Williamson, V. M. (1991). "Molecular techniques for nematode species identification, in "*Manual of Agricultural Nematology*," ed. W. R. Nickle (New York, NY: Marcel Dekker), 107–115.

Williamson, V. M., and Kumar, A. (2006). Nematode resistance in plants: the battle underground. *Trends Genet.* 22, 396–403. doi: 10.1016/j.tig.2006.05.003

Williamson, V. M., and Roberts, P. A. (2009). "Mechanisms and genetics of resistance," in *Root-Knot Nematodes*, eds R. N. Perry, M. Moens, and J. Starr (Wallingford: CABI Publishing), 301–325.

Yadav, B. C., Veluthambi, K., and Subramaniam, K. (2006). Host-generated double stranded RNA induces RNAi in plant-parasitic nematodes and protects the host from infection. *Mol. Biochem. Parasitol.* 148, 219–222. doi: 10.1016/j.molbiopara.2006.03.013

Yaghoobi, J., Yates, J. L., and Williamson, V. M. (2005). Fine mapping of the nematode resistance gene *Mi-3* in *Solanum peruvianum* and construction of a *S. lycopersicum* DNA contig spanning the locus. *Mol. Genet. Genomics* 274, 60–69. doi: 10.1007/s00438-005-1149-2

Yang, B., and Eisenback, J. D. (1983). *Meloidogyne enterolobii* n. sp. (*Meloidogynidae*), a root-knot nematode parasitizing Pacara Earpod tree in China. *J. Nematol.* 15, 381–391.

Ye, W. M., Koennig, S. R., Zhuo, K., and Liao, J. L. (2013). First Report of *Meloidogyne enterolobii* on cotton and soybean in North Carolina, United States. *Plant Dis.* 97, 1262. doi: 10.1094/pdis-03-13-0228-pdn

Yenofsky, R., Bergmann, I., and Brawerman, G. (1982). Messenger RNA species partially in a repressed state in mouse sarcoma ascites cells. *Proc. Natl. Acad. Sci. U.S.A.* 79, 5876–5880. doi: 10.1073/pnas.79.19.5876

Zasada, I. A., Halbrendt, J. M., Kokalis-Burelle, N., LaMondia, J., McKenry, M. V., and Noling, J. W. (2010). Managing nematodes without methyl bromide. *Annu. Rev. Phytopathol.* 48, 311–328. doi: 10.1146/annurev-phyto-073009-114425

Zhuo, K., Chen, J., Lin, B., Wang, J., Sun, F., Hu, L., et al. (2017). A novel *Meloidogyne enterolobii* effector MeTCTP promotes parasitism by suppressing programmed cell death in host plants. *Mol. Plant Pathol.* 18, 45–54. doi: 10.1111/mpp.12374

Zijlstra, C. (2000). Identification of *Meloidogyne chitwoodi*, *M. fallax* and *M. hapla* based on SCAR-PCR: a powerful way of enabling reliable identification of populations or 57 individuals that share common traits. *Eur. J. Plant Pathol.* 106, 283–290.

Conflict of Interest: The authors declare that the research was conducted in the absence of any commercial or financial relationships that could be construed as a potential conflict of interest.

frontiers in Plant Science

ORIGINAL RESEARCH
published: 11 December 2020
doi: 10.3389/fpls.2020.597819

iTRAQ-Based Proteomic Analysis Reveals the Role of the Biological Control Agent, *Sinorhizobium fredii* Strain Sneb183, in Enhancing Soybean Resistance Against the Soybean Cyst Nematode

Yuanyuan Wang[1,2], Ruowei Yang[2], Yaxing Feng[2], Aatika Sikandar[2], Xiaofeng Zhu[2], Haiyan Fan[2], Xiaoyu Liu[2,3], Lijie Chen[2] and Yuxi Duan[2]*

[1]College of Bioscience and Biotechnology, Shenyang Agricultural University, Shenyang, China, [2]Nematology Institute of Northern China, Shenyang Agricultural University, Shenyang, China, [3]College of Sciences, Shenyang Agricultural University, Shenyang, China

OPEN ACCESS

Edited by:
Claudia S. L. Vicente, University of Évora, Portugal

Reviewed by:
Esther Menendez, University of Evora, Portugal
Ryoji Shinya, Meiji University, Japan

***Correspondence:**
Yuanyuan Wang
duanyx@syau.edu.cn

Specialty section:
This article was submitted to Plant Pathogen Interactions, a section of the journal Frontiers in Plant Science

Received: *22 August 2020*
Accepted: *20 November 2020*
Published: *11 December 2020*

Citation:
Wang Y, Yang R, Feng Y, Sikandar A, Zhu X, Fan H, Liu X, Chen L and Duan Y (2020) iTRAQ-Based Proteomic Analysis Reveals the Role of the Biological Control Agent, Sinorhizobium fredii Strain Sneb183, in Enhancing Soybean Resistance Against the Soybean Cyst Nematode. Front. Plant Sci. 11:597819. doi: 10.3389/fpls.2020.597819

The soybean cyst nematode (SCN), *Heterodera glycines* Ichinohe, poses a serious threat to soybean production worldwide. Biological control agents have become eco-friendly candidates to control pathogens. Our previous study indicated that the biocontrol agent, *Sinorhizobium fredii* strain Sneb183, may induce soybean resistance to SCN. To study the mechanisms underlying induced disease resistance in the plant by Sneb183, an iTRAQ (isobaric tag for relative and absolute quantitation)-based proteomics approach was used to identify proteomic changes in SCN-infected soybean roots derived from seeds coated with the Sneb183 fermentation broth or water. Among a total of 456 identified differentially expressed proteins, 212 and 244 proteins were upregulated and downregulated, respectively, in Sneb183 treated samples in comparison to control samples. Some identified differentially expressed proteins are likely to be involved in the biosynthesis of phenylpropanoid, flavone, flavanol, and isoflavonoid and have a role in disease resistance and adaptation to environmental stresses. We used quantitative real-time PCR (qRT-PCR) to analyze key genes, including *GmPAL* (phenylalanine ammonia-lyase), *GmCHR* (chalcone reductase), *GmCHS* (chalcone synthase), and *GmIFS* (isoflavone synthase), that are involved in isoflavonoid biosynthesis in Sneb183-treated and control samples. The results showed that these targeted genes have higher expression levels in Sneb183-treated than in control samples. High performance liquid chromatography (HPLC) analysis further showed that the contents of daidzein in Sneb183-treated samples were 7.24 times higher than those in control samples. These results suggested that the *Sinorhizobium fredii* strain Sneb183 may have a role in inducing isoflavonoid biosynthesis, thereby resulting in enhanced resistance to SCN infection in soybean.

Keywords: soybean cyst nematode, *Sinorhizobium fredii*, induced resistance, biological control, isoflavonoid biosynthesis

INTRODUCTION

Soybean [*Glycine max* (L.) Merr] is one of the most important crops for human consumption and livestock feed and has diverse applications for industrial products. The most economically damaging plant-parasitic nematode (PPN) is *Heterodera glycines* (Williamson and Gleason, 2003). In China, yield losses due to *H. glycines* have been estimated at more than 120 million USD and approximately 1.5 billion USD worldwide (Wrather et al., 2001; Moens et al., 2008; Hosseini and Matthews, 2014). Chemical nematicides, as the main management technique, are used to reduce nematode incidence. However, they are being withdrawn from use due to their toxicity to humans and their impact on the environment. Thus, there is an increased demand for eco-friendly products to manage *H. glycines*.

Rhizobia are a diverse group of nodule-forming bacteria known for inhabiting the soil and establishing functional symbiotic associations with legume plants. The symbioses between legumes and different genera of rhizobia, including *Rhizobium*, *Bradyrhizobium*, and *Mesorhizobium*, are a cheaper source of N and an effective agronomic practice that ensure an adequate supply of N compared to the N fertilizer (Subramanian et al., 2004). They not only play a major role in biological nitrogen fixation but also improve plant growth and reduce disease incidence in various crops. Some rhizobia strains have also been reported as biocontrol agents (BCAs) for the control of diseases caused by parasitic nematodes through direct and/or indirect mechanisms. Siddiqui et al. (2007) studied the biocontrol of *Meloidogyne javanica* in lentils inoculated with the selected strain of *Rhizobium* as single and co-inoculations, which significantly reduced galls per root system and population of nematodes per kg soil, in addition to causing a greater increase in the plant growth in the absence of *M. javanica*. Ashoub and Amara (2010) demonstrated the ability of a *Rhizobium* strain isolated from the broad bean (*Vicia faba*) to cause 100% juvenile mortality of *Meloidogyne incognita in vitro* for 72 h. *Rhizobium* spp. efficiently reduced the *M. javanica* infection on eggplant (*Solanum melongena*; Mohamedova et al., 2016). Even individual cellular components of the *Rhizobium* had been shown to induce ISR viz. lipopolysaccharides (LPSs), flagella, cyclic lipopeptides, homoserine lactones, acetoin, and butanediol (Lugtenberg and Kamilova, 2009).

Isoflavonoids are specialized metabolites of dual importance for plant-environment interactions. They act as signaling molecules in symbiotic nitrogen fixation by Rhizobia (Phillips and Kapulnik, 1995; Ferguson and Mathesius, 2003; Subramanian et al., 2006) and as phytoalexins with antimicrobial properties (Lozovaya et al., 2004; Lygin et al., 2013). Isoflavonoids are synthesized through a legume-specific branch of the phenylpropanoid pathway, which is regulated by the coordinated expression of several structural genes. *PAL*, *CHS*, *C4H*, *CHR*, and *IFS*, considered as markers for the isoflavonoid biosynthetic pathway, exist intrinsically in the cell but are sometimes activated under certain conditions (Dao et al., 2011; Anguraj Vadivel et al., 2019), which are induced and regulated by internal and external factors, and they regulate isoflavonoid biosynthesis at both the transcription and post-transcriptional levels (Nakatsuka et al., 2003; Arfaoui et al., 2016). Defense-induced expression of IFS and several other genes involved in isoflavonoid metabolism in alfalfa leaves was previously reported (He and Dixon, 2000). The expression pattern of IFS in soybean is consistent with the physiological roles of isoflavonoids as defense compounds against pathogens and signal molecules to symbiotic bacteria, which are related to the regulation of the expression of SA (salicylic acid) and JA (jasmonic acid) hormones in soybean (Subramanian et al., 2004). The isoflavonoids that accumulate at PPN feeding sites may affect nematode fertility and fecundity by limiting egg production or skewing the ratio of males to females, as more females are formed under abundant nutrition and vice versa (Volpiano et al., 2019), while the ratio of males to females is an important index because it determines the population size and the extent of damage (Triantaphyllou, 1973). Our previous study indicated that the BCA, *Rhizobium* strain Sneb183, originally isolated from the rhizosphere of pines in Liaoning, China, and was identified as *Sinorhizobium fredii* (Zhao et al., 2009), triggered an induced systemic resistance (ISR) to soybean cyst nematode (SCN) infection in soybean by split-root experiments (Tian et al., 2014). ISR induces the host physiological and metabolic responses, leading to the synthesis and accumulation of additional defensive chemicals in plants, which interfere with the invasion of plant pathogens.

This study was conducted to evaluate the molecular mechanisms of ISR by *S. fredii* strain Sneb183. The differentially expressed proteins (DEPs) involved in disease resistance and adaptation to environmental stresses in Sneb183 pre-treated samples were compared with those in control samples by iTRAQ (isobaric tag for relative and absolute quantitation) technology. The quantitative real-time PCR (qRT-PCR) and high performance liquid chromatography (HPLC) analyses were also conducted to evaluate the efficacy of Sneb183, which regulates the expression of isoflavonoid biosynthesis-related genes during SCN infection. The results of this analysis will serve as the theoretical framework for the production of marketable and useful BACs.

MATERIALS AND METHODS

Isolation of Cysts and J2 of SCN

Surface soil samples (0–2 cm depth) were collected from the rhizosphere of soybean (*G. max* cv. Liaodou 15, an SCN-susceptible cultivar). Cysts were collected following elutriation and hand-picking under a stereomicroscope and surface-sterilized by immersion in a 0.1% $HgCl_2$ solution for 1 min, followed by rinsing three times with the sterile distilled water. They were then placed in the Baermann funnel at 25°C. J2s were collected from the bottom of the Baermann funnel every 2 or 3 days (Liu, 1995).

Preparation of the *Sinorhizobium fredii* Sneb183 Fermentation Broth

The *S. fredii* strain Sneb183, preserved at −80°C, was suspended in the sterilized water and adjusted to 1.0×10^8 CFU/ml with a hemocytometer under a microscope, followed by the addition of 1.0 ml of this suspension to 50 ml of the sterilized TY

liquid medium (Duelli and Noel, 1997). The Sneb183 fermentation broth was maintained at 28°C and 150 rpm for 168 h for the subsequent use.

Plant Materials and Treatments

The soybean cultivars Liaodou 15, which are susceptible to SCN, were used. The seeds were surface-sterilized with 0.5% NaClO for 10 min, washed several times with sterile distilled water, and air-dried. The sterilized seeds were equally coated with fermentation broth of Sneb183 with a ratio of 70:1 (g/ml), and distilled water was used as control. For seed coating, fermentation of Sneb183 was added and properly mixed for uniform coating on all seed and left for complete drying. They were then germinated on filter paper in distilled water in Petri dishes and incubated at 28 ± l°C for a week. The seeds were sown in 18-cm plastic pots containing a sterile soil mixture (topsoil:sand:vermiculite; 3:2:1). The seedlings were separated into four treatments until the Vc stage. The treatments were (1) seed coated with the Sneb183 fermentation broth (Sneb183), (2) inoculated with 2,000 J2s of SCN (J2), (3) seed coated with the Sneb183 fermentation broth and inoculated with 2,000 J2s of SCN (Sneb183 + J2), and (4) seed coated with the distilled water (CK). After 7 days of inoculation of J2s, the soybean seedlings from the treatments (2) and (3) were transferred to new plastic containers filled with the sterile soil mixture and irrigated with 1/4 Hoagland nutrient solution in a growth chamber under normal conditions (25/20°C day/night temperature, the relative humidity of 60–80%, and 16 h light/day with the intensity of 160 μmol photons m^{-2} s^{-1}). At 3, 7, 14, 21, and 28 days after the inoculation, the treated soybean root samples were collected at proteomic and transcript levels. Three independent sets of four treatment samples were collected, and each replicate represented a pooled sample of three individual plants.

Protein Extraction and Quantification

At 7 days post-inoculation (dpi), the proteomics analysis was performed using root samples and total protein from three biological replicates was prepared from four treatments. For each sample group, the total protein was extracted from root samples using trichloroacetic acid (TCA) and acetone (Méchin et al., 2007) with the following modifications. Briefly, about 0.5 g of soybean root samples was pulverized to a fine powder in liquid nitrogen using a mortar and pestle. The root proteins were suspended in pre-cooled 10% (w/v) TCA in acetone and incubated at −20°C for 2 h. The mixture was then centrifuged at 20,000 *g* for 30 min at 4°C. The protein pellets were thoroughly washed twice with the pre-cooled acetone and dried in a SpeedVac. The dried pellets were resuspended with the lysis buffer containing 8 M urea, 30 mM HEPES, 1 mM PMSF, 2 mM EDTA, and 10 mM dithiothreitol (DTT), with the pH of 8.8, sonicated for 5 min (pulse on 2 s/off 3 s power, 180 W), and centrifuged at 20,000 *g* for 30 min. DTT was added to 10 mM in a 56°C water bath for 1 h and IAM was added to 55 mM, and they were placed in the dark for 1 h. The volume of four times greater than the volume of the sample solution was added to the pre-cooled acetone at −20°C for 3 h. The precipitate was obtained by centrifugation at 20,000 *g* at 4°C for 30 min. Around 500 μl buffer was added, sonicated for 3 min, and centrifuged at 20,000 *g* at 4°C for 30 min. The supernatants were collected and stored at −80°C for further use. Protein concentrations were determined using the Bradford assay (Bio-Rad) using BSA as the standard.

Protein Digestion and iTRAQ Labeling

Around 100 μg of protein sample was digested with trypsin at 20:1 (w/w) at 37°C for 36 h. The digest was lyophilized, and the peptide was reconstituted in 30 μl of TEAB per tube (water:TEAB = 1:1, containing 0.1% SDS). After digestion, 1 μl peptide segments were labeled using the iTRAQ Reagents 8 plex kit, according to the manufacturer's instructions (AB Sciex Inc., United States). The Sneb183, J2, Sneb183 + J2, and CK were labeled as iTRAQ tags 113, 115, 117, and 119, respectively. Three sets of iTRAQ samples were used for the three biological replicates. After labeling, samples were combined and lyophilized. The peptide mixture was dissolved in strong cation exchange (SCX) solvent A containing 2% (v/v) acetonitrile, 20 mM ammonium formate, and 25% ammonium hydroxide with the pH of 10.0, and then fractionated on the Agilent HPLC system 1100 with Phenomenex Luna C18 column (250 × 4.6 mm, 5 μm, 100 Å). Peptides were eluted with a flow rate of 200 μl min^{-1} and a gradient of 0–12% buffer B containing 85% (v/v) acetonitrile, 20 mM ammonium formate, and 25% ammonium hydroxide with the pH of 10.0 for 1 min, 12–56% buffer B for 35 min, and 56–100% buffer B for 5 min, followed by ramping up to 100% solvent B for 5 min. The absorbance was measured at 280 nm, and a total of 16 fractions were collected.

Protein Identification by Mass Spectrometry

Each SCX fraction was lyophilized, dissolved in 1 ml MilliQ water, and loaded onto a C18 nanoflow column (75 mm internal diameter, 5 μm, 300 Å). Peptides from iTRAQ samples were separated using a gradient of 65 min, ranging from 95% solvent A containing water and 0.1% formic acid/5% solvent B containing acetonitrile and 0.1% formic acid for 10 min, followed by 5–30% solvent B for 30 min, 30–60% solvent B for 5 min, and 60–80% solvent B for 3 min, holding 80% solvent B for 7 min, 80–5% solvent B for 3 min, and 5% solvent B for 7 min.

MS/MS analysis was carried out on a Q Exactive mass spectrometer (Thermo Scientific, Bremen, Germany). Briefly, a full MS survey scan was performed with a mass range of 350–2,000 m/z and a resolution of R = 17,500. HCD fragmentation was used for MS/MS analysis, and the 10 most intense signals in the survey scan were fragmented.

Analysis and Proteomic Interpretation of Data

The raw files were converted to Mascot generic format (.mgf) files using Proteome Discoverer 1.4 (Thermo Fisher Scientific, Waltham, MA, United States) with default settings for deep

proteome analysis. The following parameters were used for searching: the minimum and maximum precursor mass of 350 and 6,000 Da, respectively; minimum S/N ratio of 1.5; enzyme:trypsin; maximum missed cleavages of 1; FDR ≤ 0.01; and mass tolerance of 15 ppm for precursor ions. Mascot (Matrix Science, London, V2.3.0) was used for deep proteome and protein quantitation analyses with .mgf files as input.

In order to be identified as substantially differentially expressed, a protein should be quantified with at least three peptides in each experimental replicate, with a value of p smaller than 0.05 and a fold change of greater than 1.2. The searches were performed against the Swiss-Prot GreenPlants database (Release 2012_05, Number of sequences: 538585).

The functional annotation of proteins obtained was determined by Blast2GO[1] (Bioinformatics Department, CIPF, Valencia, Spain), and WEGO[2] was used to enrich the GO annotation results. To enrich pathways for DEP, KEGG,[3] was used to estimate the metabolic pathways involved in the defense response of soybean to the infection to optimize pathways for DEP.

RNA Extraction and Quantitative Real-Time PCR

The key enzyme genes involved in the isoflavonoid biosynthesis in different treatments were validated by qRT-PCR to verify the quality of the iTRAQ-based proteomic analysis. Total RNA was extracted from soybean roots from four treatments separately by the RNA pure Plant Kit (CWBIO, Beijing, China), according to the manufacturer's instructions. The RNA quality was tested by 1% agarose gel electrophoresis, and concentrations and purity were determined using a NanoVue plus spectrophotometer (GE, MA, United States). cDNA was reverse-transcribed from 1 μg of total RNA using the RT Reagent Kit (Takara). qRT-PCR was performed using the CFX Connect Real-Time PCR Detection System (Bio-Rad, CA, United States). Gene-specific primers (GSPs) used for *PAL*, *CHS*, *CHR*, and *IFS* were described in **Supplementary Table S1**. The soybean *actin 11* gene was used as an endogenous control for normalization. The 20-μl reaction mixture contained 10 μl 2 × TB Green premix (Takara), 1 μl cDNA template (1:5 dilution), 0.4 μl 50 × ROX Reference DyeII (Takara), 7 μl SDW, and 0.8 μl of each forward and reverse primers for selected genes. The thermal cycling conditions of qRT-PCR for all reactions were 95°C for 1 min and 50 s, followed by 40 cycles of 95°C for 10 s, 55°C for 33 s, and 68°C for 30 s. There were three biological replicates and three technical replicates per time-point for each treatment. The qRT-PCR data were analyzed using the $2^{-\Delta\Delta Ct}$ relative quantification method (Livak and Schmittgen, 2001).

Measurement of Genistein and Daidzein Contents in Soybean Roots

About 0.5 g of fresh hairy roots of soybean from four treatments were accurately weighed and extracted with 50 ml of 70% ethanol at 60°C for 2 h. The homogenates were centrifuged at 10,000 *g* for 10 min, evaporated, and resuspended in 80% methanol. Genistein and daidzein contents were determined using the A262 HPLC–UV System (Agilent 1100 series, DAD, Agilent Technologies, Palo Alto, CA, United States) on a Platisil ODS C18 column (3 μm, 250 × 4.6 mm, Dikmatech). The digests were then separated by a linear gradient ranging from 87% solvent A (0.1% acetic acid)/13% solvent B (0.1% acetonitrile acetate) to 50% solvent A/50% solvent B in 87 min at a flow rate of 1.2 ml min^{-1}. The temperature of the column and the volume of injection were 40°C and 10 μl, respectively. All measurement experiments were performed at least in triplicate.

Statistical Analysis

Statistical analysis was performed using a two-way ANOVA using Graphpad Prism v.8.0. Significant differences between group means were determined by the Tukey's multiple comparisons test at $p < 0.05$.

RESULTS

Protein Identification by iTRAQ Analysis

Changes in the proteome of soybean roots from four treatments were analyzed using iTRAQ-LC/MS-MS technology. Data from three biological replicates were analyzed, and proteins were detected by querying data using a soybean protein database. Among a total of 443,104 spectra, 25,406 could be matched to the database, resulting in a total of 4,193 peptides assembled into 1,366 protein groups with high confidence (confidence level > 95%).

According to the quantitative data of the Swiss-Prot GreenPlants library protein, DEPs were selected with more than 1.2-fold differences, the expression levels at $p < 0.05$, and a false discovery rate of less than 1%. Based on these rules, 459 DEPs were identified in soybean roots (**Figure 1**, **Supplementary Table S2**), of which 226 (49.2%) showed an increase and 233 (50.8%) showed a decrease in abundance between Sneb183 vs. CK treatment. At the same time, 456 DEPs in soybean roots, including the increased numbers of 212 (47.6%), and decreased numbers of 244 (52.4%) were identified between Sneb183 + J2 vs. J2 treatment (**Figure 1**, **Supplementary Table S3**). The further function annotations of 456 identified DEPs demonstrated that these proteins were involved in a variety of metabolisms, such as energy, carbohydrate, and amino acid. Besides, some DEPs were also enriched in pathways such as energy metabolism, systemic resistance, and adaptation to environmental stresses, including calcium signaling pathway, isoflavonoid biosynthesis, pentose phosphate pathway, glutathione metabolism, etc. The findings revealed the responses to Sneb183 inoculation at the level of protein in the soybean core. They could provide valuable tools for more research on the *S. fredii* strain Sneb183 ISR's molecular mechanism against the soybean cyst nematode. In the meanwhile, the identification of proteins from other treatments was shared (**Supplementary Tables S4**, **S5**).

[1]https://www.blast2go.com/
[2]http://wego.genomics.org.cn/
[3]http:/www.kegg.jp/

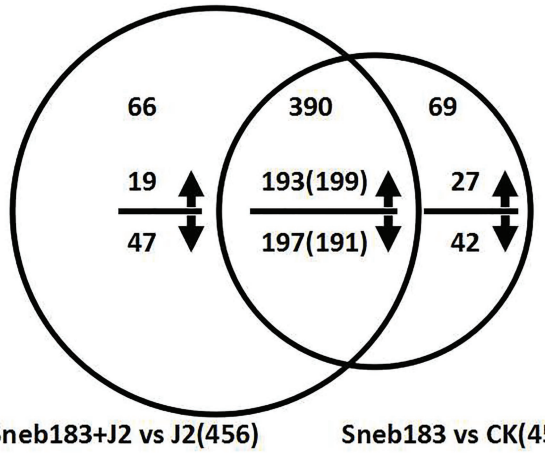

FIGURE 1 | Venn diagram of differentially expressed proteins responsive in seed-coated with Sneb183 fermentation broth then inoculated J2 of SCN (Sneb183 + J2) vs. inoculated J2 of SCN (J2) and seed-coated with Sneb183 (Sneb183) vs. CK. The number above or below the horizontal line in each portion indicated the number of upregulated or downregulated proteins. The over lapping regions indicated the number of common proteins. Among the 390 common DEPs, 193 were upregulated and 197 were downregulated in Sneb183 + J2 vs. J2; and 199 were upregulated and 191 were downregulated Sneb183 vs. CK.

Protein Annotation and Enrichment

According to the BLAST database, Gene Ontology annotation was performed based on all DEPs of Sneb183 + J2 vs. J2. A total of 2,832 GO terms, including 979 biological words, 568 cell words, and 1,285 feature terms were annotated as a result of GO annotation of the protein-coding genes. The results of the annotation showed that 578, 520, 507, 448, and 294 genes were enriched in the metabolic process, binding, catalytic activity, cell process, and cell part, respectively (**Figure 2**). This result suggests that the *S. fredii* strain Sneb183 may improve the resistance to *H. glycines* by affecting the metabolic process of soybean.

The results of the KEGG study showed that 337 out of 456 DEPs involved in more than 118 metabolic pathways were identified; some proteins are involved in multiple metabolic pathways at the same time, suggesting that these proteins have multiple biological roles. The identified DEPs are involved in some of the metabolic pathways related to plant disease resistance and adaptation to stressful environments, and the enrichment occurs in pathways (**Figure 3**), such as biosynthesis of phenylalanine, tyrosine, and tryptophan (map00400), phenylpropanoid biosynthesis (map00940), flavonoid biosynthesis (map00941), and flavone and flavanol biosynthesis (map00944). We further summarized the list of DEPs involved in flavonoids and isoflavonoid pathways associated with plant resistance (**Supplementary Table S6**). Our results also indicated that four DEPs upregulated were related to the isoflavonoid metabolism pathway (**Figure 4**). However, further studies are required to investigate the metabolic pathways associated with other DEPs.

Regulation of Some Proteins Involved in Isoflavonoid Biosynthesis at the mRNA Level

The *S. fredii* Sneb183 induced resistance against SCN in soybean, and some DEPs involved in pathways for biosynthesis of flavone and isoflavonoid were enriched. Accordingly, in our study, qRT-PCR was used to further analyze and verify the key genes, including *GmPAL*, *GmCHS*, *GmCHR*, and *GmIFS* in the isoflavonoid biosynthesis pathway (**Figure 5**).

After 7 dpi, a significantly and consistently enhanced transcription of *GmPAL* was induced in the treatments J2/Sneb183/Sneb183 + J2 compared to CK. The transcript level of *GmPAL* was not different at 3 dpi when the J2 feeding sites were established. At 7 and 14 dpi, during J2 development in roots, the expressions of *GmPAL* in Sneb183 + J2 increased by 2.7-fold and 3.6-fold, respectively, which were 1.42-fold and 1.51-fold greater than those in the J2 treatment at the same time point. As J2s developed to the adult stage, the *GmPAL* transcription was enhanced in the treatments J2, Sneb183, and Sneb183 + J2 compared to CK, with no differences between the treatments. The transcript levels of *GmCHS* and *GmCHR* showed a similar trend in four treatments. No difference was observed at 3 dpi; however, at 7 and 14 dpi, the expression of *GmCHS* in Sneb183 + J2 was significantly higher than that in CK, J2, and Sneb183 during the development of nematode in roots. In Sneb183 + J2, which was 5.89-fold higher than that in J2, the highest expression level of *GmCHS* occurred at 7 dpi. In Sneb183 + J2, *GmCHR* had the largest 2.18-fold greater expression level than in J2 at 14 dpi. However, at 28 dpi, *GmCHS* and *GmCHR* expression levels decreased slightly in both treatments.

The expression pattern of *GmIFS* was as follows: in each treatment, in the early stage (at 3 and 7 dpi) of the nematode development, the expression level was higher than that in the later stage (14, 21, and 28 dpi). On the 7th day, the expression level in Sneb183 + J2 was the highest, 1.56 times greater than in J2, which was significantly different in other treatments.

Measurement of Genistein and Daidzein Contents in Soybean Roots

The observed influence of seed coating with Sneb183 on genes encoding key enzymes in the isoflavonoid biosynthesis pathway raised the question of whether such modifications would contribute to a substantial change in isoflavonoid concentrations. Therefore, the contents of two isoflavonoids (genistein and daidzein) in soybean roots, treated with Sneb183 from four treatments, were detected by HPLC. The accumulation of genistein and daidzein in response to different treatments is shown in **Figure 6**.

Genistein contents in soybean roots increased gradually from 7 days in all treatments. The seed coating with the Sneb183 fermentation broth resulted in a significant increase in genistein contents as compared to the other treatments at 7 days. Longitudinal comparison of the genistein content in each treatment, we found it reached the peak at 21 days in the CK treatment, while in treatments of J2 and Sneb183, the

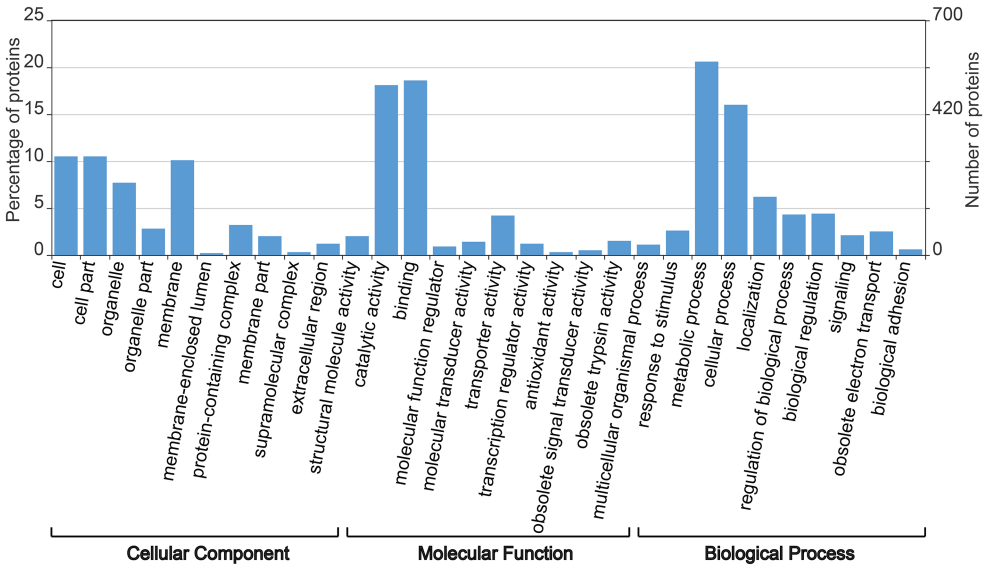

FIGURE 2 | Gene ontology annotations for all differentially expressed proteins in seed-coated with Sneb183 fermentation broth then inoculated J2 of SCN (Sneb183 + J2) vs. inoculated J2 of SCN (J2).

speed of genistein accumulation were accelerated and reached the peak at 14 and 7 days, respectively. Regarding daidzein content, it is higher than that of genistein in each treatment during the same period. Similarly to genistein, there was a significant difference in the content of daidzein compared to the other treatment at 7 days. There was a steady increase in daidzein content until 21 days in Sneb183 and Sneb183 + J2 treatments, followed by a dramatic increase. Daidzein content in all coating treatments with or without nematode inoculation significantly increased as compared to CK and J2 since 21 days. At 35 days, the contents of daidzein in Sneb183 treatment were 7.24 times higher than those in roots derived from control samples.

DISCUSSION

It is well-known that soybean [*G. max* (L.) err.] is economically the most important bean in the world (Mendoza-Suárez et al., 2020). SCN (*H. glycines* Ichinohe) is the most serious pest in soybean production, and the complete elimination of *H. glycines* from the soil is difficult due to its polyphagous nature. Plant growth-promoting bacteria (PGPB), colonize the rhizosphere of many plant species, are the most potential BCAs of plant-parasitic nematode. Numerous study indicated seed coating with PGPB, such as *Rhizobium etli*, *Bacillus firmus*, *B. subtilis*, *B. simplex*, *Klebsiella pneumoniae* (Hallmann et al., 2001; Siddiqui and Shaukat, 2003; Terefe et al., 2009; Kang et al., 2018; Liu et al., 2018) elicited systemic resistance against nematode disease. Previously studies verified that *S. fredii* Sneb183 ISR in the split-root system by seed coating and significantly reduce cysts on roots after seed coating with the Sneb183 fermentation. Admittedly, seed coating is a cost-effective and more efficient agricultural processing operation with strong operability, without altering their genome sequences, these plants obtain extensive resistance, respond more rapidly and strongly to various stresses (Mathre et al., 1999; Pathak et al., 2016; Pedrini et al., 2017).

The present study involved the comparative analysis of soybean roots by iTRAQ to investigate the plant resistance to SCN induced by the *S. fredii* strain Sneb183. Isoflavonoid, plant defense enzymes, phenolics or other phytoalexins, which are induced and accumulated in the plant in response to rhizobia, have been reported to protect plants from phytopathogens (Dakora, 2003). Flavones and isoflavonoides have usually been used as defense compounds against many plant-parasitic nematodes (Chin et al., 2018). Carpentieri-Pípolo et al. (2005) demonstrated that soybean isoflavonoids such as genistein and daidzein have many effects on host-pathogen interactions and displayed resistance against *M. incognita*. During the present study, seedlings were moved to a pot filled with sterilized soil after sampling to prevent further invasion of J2s since it typically takes 3–7 days for plant-parasitic nematodes to migrate, locate, and penetrate the preferred host root *via* root exudate signals (Duan et al., 2011). To further investigate whether J2 entirely invaded the soybean root, roots used for proteomic analysis by iTRAQ were sampled at 7 dpi. The outcomes of the annotation showed that 578, 520, 507, 448, and 294 genes were enriched in the metabolic process, binding, catalytic activity, cell process, and cell part, respectively. In order to suppress a pathogen challenge, plant has a sophisticated immune response strategy and metabolism with interactions among several metabolic pathways. According to the results of protein identification from two treatments, Sneb183 + J2 initiated a difference in types of protein in soybean root, indicated rhizobia, a refined parasite, and triggered soybeans to produce an extensive resistance. The functions of some

ID	Pathway	Richratio*	Count of DEPs in This Pathway
ko01051	Photosynthesis	0.25	4
ko00941	Tryptophan metabolism	0.25	2
ko00340	Fatty acid biosynthesis	0.25	2
ko00040	Sulfur metabolism	0.25	2
ko00100	Glycine, serine and threonine metabolism	0.26	6
ko00960	Nitrogen metabolism	0.27	7
ko00401	Purine metabolism	0.29	10
ko00945	Pyruvate metabolism	0.30	16
ko00562	Cysteine and methionine metabolism	0.30	10
ko00860	Phenylalanine, tyrosine and tryptophan biosynthesis	0.31	4
ko00650	Methane metabolism	0.31	17
ko00590	Arginine and proline metabolism	0.31	10
ko00950	Glutathione metabolism	0.32	10
ko00944	Glycolysis / Gluconeogenesis	0.33	26
ko00500	Pentose phosphate pathway	0.33	9
ko00280	alpha-Linolenic acid metabolism	0.33	3
ko00940	Cyanoamino acid metabolism	0.33	2
ko00520	Galactose metabolism	0.35	8
ko00290	Carbon fixation in photosynthetic organisms	0.35	23
ko00360	Streptomycin biosynthesis	0.36	4
ko00565	Ascorbate and aldarate metabolism	0.37	7
ko00900	Glyoxylate and dicarboxylate metabolism	0.37	10
ko00051	Pantothenate and CoA biosynthesis	0.38	3
ko00250	Glycerophospholipid metabolism	0.38	3
ko00190	Citrate cycle (TCA cycle)	0.38	15
ko00350	Oxidative phosphorylation	0.40	28
ko00410	Tyrosine metabolism	0.40	4
ko00020	beta-Alanine metabolism	0.40	2
ko00770	Alanine, aspartate and glutamate metabolism	0.41	12
ko00564	Fructose and mannose metabolism	0.42	13
ko00630	Phenylalanine metabolism	0.43	12
ko00053	Ether lipid metabolism	0.43	3
ko00521	Terpenoid backbone biosynthesis	0.43	3
ko00710	Valine, leucine and isoleucine biosynthesis	0.44	7
ko00052	Amino sugar and nucleotide sugar metabolism	0.44	15
ko00030	Phenylpropanoid biosynthesis	0.45	13
ko00592	Valine, leucine and isoleucine degradation	0.46	6
ko00460	Starch and sucrose metabolism	0.48	21
ko00010	Arachidonic acid metabolism	0.50	4
ko00480	Isoquinoline alkaloid biosynthesis	0.50	3
ko00330	Flavone and flavonol biosynthesis	0.50	3
ko00680	Porphyrin and chlorophyll metabolism	0.57	4
ko00400	Butanoate metabolism	0.57	4
ko00270	Inositol phosphate metabolism	0.58	7
ko00620	Steroid biosynthesis	0.60	3
ko00230	Tropane, piperidine and pyridine alkaloid biosynthesis	0.60	3
ko00910	Novobiocin biosynthesis	0.60	3
ko00260	Stilbenoid, diarylheptanoid and gingerol biosynthesis	0.60	3
ko00380	Pentose and glucuronate interconversions	0.63	10
ko00061	Flavonoid biosynthesis	0.67	6
ko00920	Histidine metabolism	0.67	4
ko00195	Biosynthesis of ansamycins	1.00	4

*: Richratio = count of DEPs / count of total proteins annotated in this pathway

FIGURE 3 | The count of DEPs in seed-coated with Sneb183 fermentation broth then inoculated J2 of SCN (Sneb183 + J2) vs. inoculated J2 of SCN (J2) in each metabolic pathways.

proteins are involved in flavones and isoflavonoids synthesis pathways are discussed further below (**Figure 4**).

As the initial enzyme in the phenylpropanoid pathway, PAL catalyzes the precursor of the amino acid L-phenylalanine to cinnamic acid and produces the phenylpropanoid compounds function as preformed or inducible resistance against infection of pathogens (Yadav et al., 2020). In higher plants, PAL catalytic activity affects the efficiency of the isoflavonoid biosynthesis pathway (Jiang et al., 2013). In this study, five PAL were identified to be upregulated in Sneb183 + J2 vs. J2, these proteins provide novel insights into the understanding of the induce resistance in soybean in response to Sneb183. Trans-cinnamate 4-monooxygenase that is also called as cinnamate 4-hydroxylase (C4H) participates in the synthesis of numerous polyphenoid compounds by plants when challenged by pathogens, such as flavones, isoflavonoids, and lignin (Zhu et al., 2020). The accumulation of the enzyme in our study could be related to the accumulation of flavones and isoflavonoids, increasing

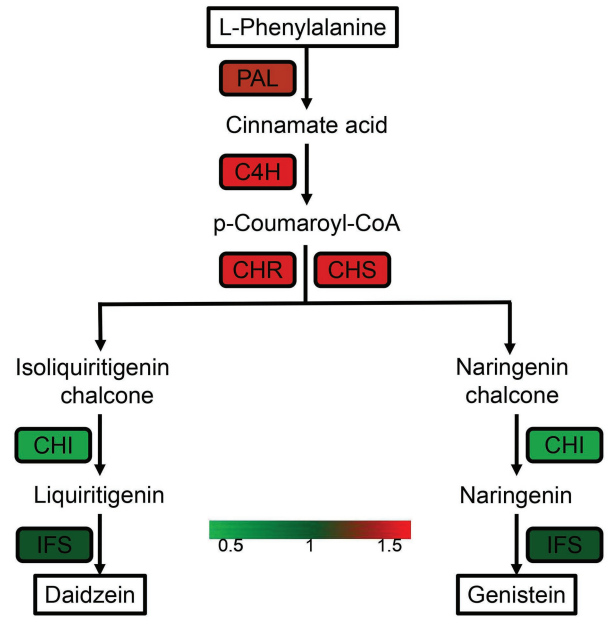

FIGURE 4 | DEPs in seed-coated with Sneb183 fermentation broth then inoculated J2 of SCN (Sneb183 + J2) vs. inoculated J2 of SCN (J2) associated with isoflavonoid biosynthesis pathway. Different colors reflect the changes in protein abundance based on the iTRAQ data.

lignification of the cell wall and then enhance soybean resistance, which is similar to the results in *Ulmus pumila* (Zuo et al., 2019). Moreover, increased expression levels of seven CHS were identified in present study. CHS is a plant-specific polypeptide synthase and the first committed enzyme in regulating biosynthesis and flux control in the isoflavonoid pathway (Schröder, 1997). The involvement of CHS in phytoalexin synthesis has also been reported (Dao et al., 2011; Cho and Lee, 2015). Parasitic nematode fine-tunes the pattern of plant cell death by stimulating host NADPH oxidases to produce reactive oxygen species to limit plant cell death and promote infection (Siddique et al., 2014). It is well-known that POD (peroxidase) is crucial antioxidant enzymes responsible for ROS scavenging (Choudhury et al., 2017), in the present study, of six POD, four were up-regulated and two were suppressed. Similar results were showed in soybean root inoculated by BCA *Bacillus simplex* Sneb545 (Kang et al., 2018). These results suggested that the biosynthesis of isoflavonoids in soybean root was associated with ISR induced by Sneb183.

Throughout this research results, the key genes (*GmPAL*, *GmCHS*, *GmCHR*, and *GmIFS*), the key enzymes in the isoflavonoids pathway (Jiao et al., 2014; Anguraj Vadivel et al., 2019), were upregulated at different stages after treatments, and the synthesis and accumulation of isoflavonoids were induced. But the induction processes and the abundance of isoflavonoids were different among four treatments. *GmIFS*, that is a relatively latter step in the general isoflavonoids biosynthesis, was the first to be upregulated expressed at 3 dpi in Sneb183-treated soybean root and synthesized genistein using the existing precursors in soybean. Until 7–21 dpi, the expression of *GmCHR* and *GmCHS* began to be upregulated in two treatments of with Sneb183 coating, thereby synthesizing the precursor in the phenylpropanoid pathway that has been consumed. Evidence showed that during the initial process, some rhizobia is recognized as possible invaders, then the plant's immune response is triggered after the active invasion (Zamioudis and Pieterse, 2012), the rhizobia triggering immunity pattern is similar to our findings, once Sneb183 invaded and successfully proliferated in soybean root, it tuned the metabolism and immune response of soybean against pathogens. Consequently, the transcription of *GmCHS* and *GmCHR* were enhanced and biosynthesis of genistein and daidzein increased rapidly as compared to the control and J2.

Both SCN and *S. fredii* Sneb183 infiltrated soybean as soybean parasite, triggering plant resistance and contributing to isoflavonoids accumulation. Interestingly, in the four treatments, we studied the accumulation of two isoflavonoids was initiated by Sneb183-treated were more advanced than that without *S. fredii* Sneb183 coating. That indicated the procedures of inoculation of *S. fredii* Sneb183 and invasion of nematodes to stimulate resistance to soybean are clearly different. Meanwhile, isoflavonoids, especially genistein and daidzein in induced resistance of soybean by *S. fredii* Sneb183 are work together to reduce nematode invasion and inhibit the development of nematodes in soybean root. Some reported genistein and daidzein, more important compounds produced in soybean, were 50 and 40%, respectively (Ren et al., 2001), but in our study, daidzein content is beyond the content of genistein after Sneb183-treated. It is the trait of induced system resistance of *S. fredii* Sneb183 by quickly stimulates the production of isoflavonoids especially daidzein after inoculation. Some researchers recorded that genistein-treated nematode parasites show alterations and deformities in their tegmental architecture (Pal and Tandon, 1998; Kar and Tandon, 2000), thus inducing muscular paralysis around the pharynx and affects stylet puncture and withdraw nutrition (Toner et al., 2009; Tandon and Lyndem, 2010). The content of daidzein increases rapidly in the latter stage of treatment as compared to genistein. While no clear evidence exists to support the essential function of daidzein in nematodes, daidzein was found in our study to significantly kill J2 and inhibit egg hatching (Guo et al., 2017). Evidence reveals that isoflavonoids impede SCN replication by influencing the sex ratio and the number of female eggs (Chin et al., 2018). We, therefore, believe that the rapid accumulation of genistein at 7 days and daidzein at 21 days was jointed to prevent the development of the juvenile of SCN, cyst formation, even subsequent death of nematodes due to unfavorable conditions of nutrients, especially in the treatment of Sneb183. This is consistent with our previous research results that inoculated with Sneb183 fermentation broth; the development of SCN in soybean root was inhibited and declined the number of cysts (Tian et al., 2014). The genistein and daidzein content reached its peak at 35 dpi and inhibited second-generation SCN infection, indicating that the resistance caused by Sneb183 is relatively long-lasting. The susceptible cultivar Liaodou 15 acquired broad resistance, responded immediately against SCN *via* seed coated with *S. fredii* Sneb183. Carter et al. (2018)

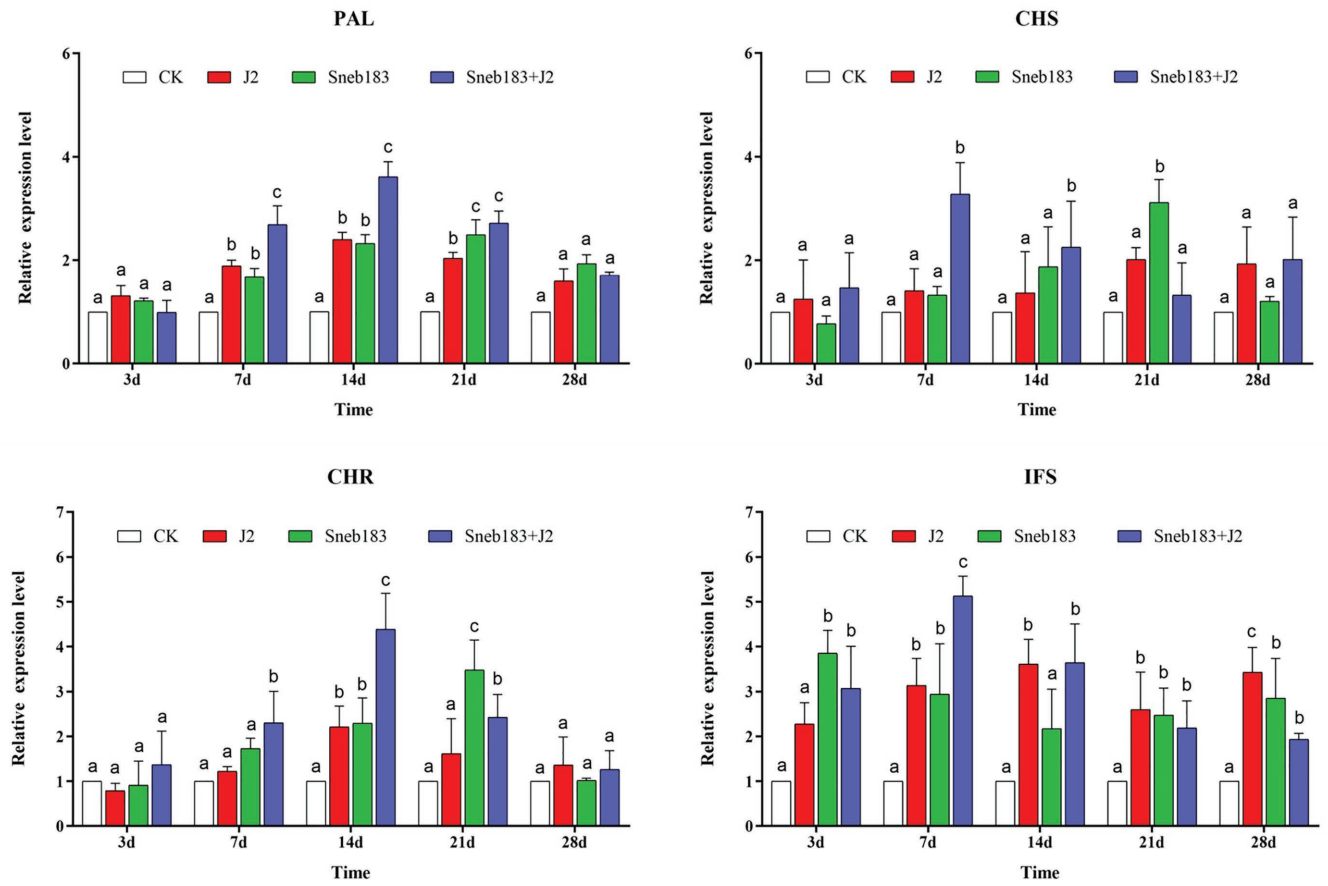

FIGURE 5 | Quantitative RT-PCR analysis of key genes involved in the isoflavonoids synthesis pathway in the root. Gene expression levels were analyzed from four treatments: CK, J2, Sneb183, and Sneb183 + J2 at 3, 7, 14, 21, and 28 days after *H. glycines* infection. Relative transcript levels were compared with those of CK for each time point. Error bars represent standard error of the mean values of three technical replicates from three biological replicates. The differences in expression levels were tested by two-way ANOVA using Graphpad Prism v.8.0. According to Tukey's multiple comparisons test at $p < 0.05$. For each gene and time point, bars with different letters indicate statistically significant differences between the treatments.

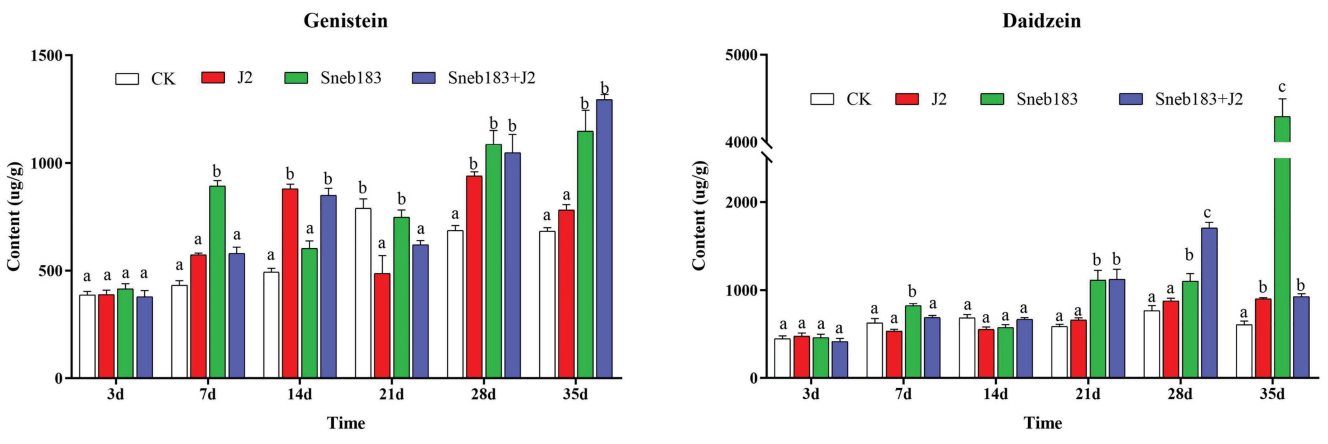

FIGURE 6 | Contents of genistein and daidzein in soybean seedling at different times intervals. The error bars illustrated the mean contents of genistein or daidzein ± standard deviation ($n = 3$). The same letters on bars are significantly similar, according to Tukey's multiple comparisons test ($p < 0.05$).

reported that the SCN resistant genotypes had significantly higher isoflavonoids content than the susceptible genotypes in SCN infested environments.

In summary, to the best of our knowledge, the *S. fredii* Sneb183 induced local and systemic resistance through seed coating with the Sneb183 fermentation. This study is the first report of Sneb183 eliciting isoflavonoids biosynthesis against *H. glycines*. Overall, 456 DEPs were identified relating to metabolic molecular mechanisms that induced the expression of key genes involved in the pathways of isoflavonoid biosynthesis. The content of isoflavonoids was analyzed by HPLC, and the results showed that the *S. fredii* Sneb183 can induce and regulate the synthesis of genistein and daidzein in soybean roots. However, *S. fredii* Sneb183 in inducing ISR against SCN is a complicated and delicate response. The overall results of the present study support *S. fredii* Sneb183 as a potential BCA inducing ISR against *H. glycines*.

DATA AVAILABILITY STATEMENT

The datasets presented in this study can be found in online repositories. The names of the repository/repositories and accession number(s) can be found in the article/ **Supplementary Material**.

AUTHOR CONTRIBUTIONS

YW: method optimization, data analysis, and drafting the manuscript. RY: protein isolation and data analysis. YF: qRT-PCR analysis and data analysis. AS: manuscript preparation and editing. XZ and HF: Sneb183 fermentation and nematodes preparation and seedlings treatment. XL: measurement of genistein and daidzein content by HPLC. LC and YD: overall design of the project and experiments. All authors contributed to the article and approved the submitted version.

FUNDING

This work was supported by the National Nature Science Fund Key Projects (313300630), Special Fund for China Agriculture Research System (CARS-04-PS13), and National Parasitic Resources Center (NPRC-2019–194–30).

SUPPLEMENTARY MATERIAL

The Supplementary Material for this article can be found online at: https://www.frontiersin.org/articles/10.3389/fpls.2020.597819/full#supplementary-material

REFERENCES

Anguraj Vadivel, A. K., Renaud, J., Kagale, S., and Dhaubhadel, S. (2019). GmMYB176 regulates multiple steps in isoflavonoid biosynthesis in soybean. *Front. Plant Sci.* 10:562. doi: 10.3389/fpls.2019.00562

Arfaoui, A., El Hadrami, A., Adam, L. R., and Daayf, F. (2016). Pre-treatment with calcium enhanced defense-related genes' expression in the soybean's isoflavones pathway in response to *Sclerotinia sclerotiorum*. *Physiol. Mol. Plant Pathol.* 93, 12–21. doi: 10.1016/j.pmpp.2015.11.004

Ashoub, A., and Amara, M. (2010). Biocontrol activity of some bacterial genera against root-knot nematode, *Meloidogyne incognita*. *J. Amer. Sci.* 6, 321–328.

Carpentieri-Pípolo, V., Mandarino, J., Carrao-Panizzi, M., Souza, A., and Kikuchi, A. (2005). Association of isoflavonoids with the incompatible response of soybean roots to *Meloidogyne incognita* race 3. *Nematropica* 35, 103–110.

Carter, A., Rajcan, I., Woodrow, L., Navabi, A., and Eskandari, M. (2018). Genotype, environment, and genotype by environment interaction for seed isoflavone concentration in soybean grown in soybean cyst nematode infested and non-infested environments. *Field Crops Res.* 216, 189–196. doi: 10.1016/j.fcr.2017.11.021

Chin, S., Behm, C. A., and Mathesius, U. (2018). Functions of flavonoids in plant-nematode interactions. *Plants* 7:85. doi: 10.3390/plants7040085

Cho, M. -H., and Lee, S. -W. (2015). Phenolic phytoalexins in rice: biological functions and biosynthesis. *Int. J. Mol. Sci.* 16, 29120–29133. doi: 10.3390/ijms161226152

Choudhury, F. K., Rivero, R. M., Blumwald, E., and Mittler, R. (2017). Reactive oxygen species, abiotic stress and stress combination. *Plant J.* 90, 856–867. doi: 10.1111/tpj.13299

Dakora, F. D. (2003). Defining new roles for plant and rhizobial molecules in sole and mixed plant cultures involving symbiotic legumes. *New Phytol.* 158, 39–49. doi: 10.1046/j.1469-8137.2003.00725.x

Dao, T., Linthorst, H., and Verpoorte, R. (2011). Chalcone synthase and its functions in plant resistance. *Phytochem. Rev.* 10, 397–412. doi: 10.1007/s11101-011-9211-7

Duan, Y., Chen, L., Liu, G., Li, H., Wang, X., and Wang, Y. (2011). *Plant pathogenic nematodes. The economic importance of plant pathogenic nematodes*. Beijing: Sinece Press, 1–2.

Duelli, D. M., and Noel, K. D. (1997). Compounds exuded by *Phaseolus vulgaris* that induce a modification of *Rhizobium etli* lipopolysaccharide. *Mol. Plant-Microbe Interact.* 10, 903–910. doi: 10.1094/MPMI.1997.10.7.903

Ferguson, B. J., and Mathesius, U. (2003). Signaling interactions during nodule development. *J. Plant Gro. Regul.* 22, 47–72. doi: 10.1007/s00344-003-0032-9

Guo, C., Zhu, X., Duan, Y., Wang, Y., and Chen, L. (2017). Suppression of different soybean isoflavones on *Heterodera glycines*. *Chin. J. Oil Crop Sci.* 39, 540–545.

Hallmann, J., Quadt-Hallmann, A., Miller, W., Sikora, R., and Lindow, S. (2001). Endophytic colonization of plants by the biocontrol agent *Rhizobium etli* G12 in relation to *Meloidogyne incognita* infection. *Phytopathology* 91, 415–422. doi: 10.1094/PHYTO.2001.91.4.415

He, X. -Z., and Dixon, R. A. (2000). Genetic manipulation of isoflavone 7-O-methyltransferase enhances biosynthesis of 4′-O-methylated isoflavonoid phytoalexins and disease resistance in alfalfa. *Plant Cell* 12, 1689–1702. doi: 10.1105/tpc.12.9.1689

Hosseini, P., and Matthews, B. F. (2014). Regulatory interplay between soybean root and soybean cyst nematode during a resistant and susceptible reaction. *BMC Plant Biol.* 14:300. doi: 10.1186/s12870-014-0300-9

Jiang, L., Johnston, E., Åberg, K. M., Nilsson, U., and Ilag, L. L. (2013). Strategy for quantifying trace levels of BMAA in cyanobacteria by LC/MS/MS. *Anal. Bioanal. Chem.* 405, 1283–1292. doi: 10.1007/s00216-012-6550-1

Jiao, C., Yang, R., and Gu, Z. (2014). Biosynthesis, metabolism and regulation of isoflavones in higher plants. *Plant Physiol. J.* 50, 1613–1620.

Kang, W., Zhu, X., Wang, Y., Chen, L., and Duan, Y. (2018). Transcriptomic and metabolomic analyses reveal that bacteria promote plant defense during infection of soybean cyst nematode in soybean. *BMC Plant Biol.* 18:86. doi: 10.1186/s12870-018-1302-9

Kar, P., and Tandon, V. (2000). Anthelmintic efficacy of *Flemingia vestita* (Fabaceae): genistein induced effect on the nervous components in two digenetic trematodes. *J. Parasit. Dis.* 24, 141–146.

Liu, W. (1995). *The research technique of plant pathogenic nematodes. Screen method of nematodes in soil and plants*. Shenyang, China: Liaoning Science and Technology Press, 47–49.

Liu, D., Chen, L., Zhu, X., Wang, Y., Xuan, Y., Liu, X., et al. (2018). *Klebsiella pneumoniae* SnebYK mediates resistance against *Heterodera glycines* and promotes soybean growth. *Front. Microbiol.* 9:1134. doi: 10.3389/fmicb.2018.01134

Livak, K. J., and Schmittgen, T. D. (2001). Analysis of relative gene expression data using real-time quantitative PCR and the $2^{-\Delta\Delta CT}$ method. *Methods* 25, 402–408. doi: 10.1006/meth.2001.1262

Lozovaya, V., Lygin, A., Li, S., Hartman, G., and Widholm, J. (2004). Biochemical response of soybean roots to *Fusarium solani* f. sp. glycines infection. *Crop Sci.* 44, 819–826. doi: 10.2135/cropsci2004.8190

Lugtenberg, B., and Kamilova, F. (2009). Plant-growth-promoting rhizobacteria. *Annu. Rev. Micobiol.* 63, 541–556. doi: 10.1146/annurev.micro.62.081307.162918

Lygin, A. V., Zernova, O. V., Hill, C. B., Kholina, N. A., Widholm, J. M., Hartman, G. L., et al. (2013). Glyceollin is an important component of soybean plant defense against *Phytophthora sojae* and *Macrophomina phaseolina*. *Phytopathology* 103, 984–994. doi: 10.1094/PHYTO-12-12-0328-R

Mathre, D., Cook, R., and Callan, N. W. (1999). From discovery to use: traversing the world of commercializing biocontrol agents for plant disease control. *Plant Dis.* 83, 972–983. doi: 10.1094/PDIS.1999.83.11.972

Méchin, V., Damerval, C., and Zivy, M. (2007). "Total protein extraction with TCA-acetone" in *Plant proteomics.* eds. H. Thiellement, M. Zivy, C. Damerval and V. Méchin (Totowa, New Jersey: Springer), 1–8.

Mendoza-Suárez, M. A., Geddes, B. A., Sánchez-Cañizares, C., Ramírez-González, R. H., Kirchhelle, C., Jorrin, B., et al. (2020). Optimizing *Rhizobium*-legume symbioses by simultaneous measurement of rhizobial competitiveness and N_2 fixation in nodules. *Proc. Natl. Acad. Sci. U. S. A.* 117, 9822–9831. doi: 10.1073/pnas.1921225117

Moens, M., Li, Y., Ou, S., Liu, X., and Peng, D. (2008). Identification of *Heterodera glycines* using PCR with sequence characterised amplified region (SCAR) primers. *Nematology* 10, 397–403. doi: 10.1163/156854108783900212

Mohamedova, M., Draganova, D., Valcheva, I., and Naydenov, M. (2016). Effects of rhizobacteria on *Meloidogyne javanica* infection on eggplants. *Afr. J. Agric. Res.* 11, 4141–4146. doi: 10.5897/AJAR2016.11446

Nakatsuka, A., Izumi, Y., and Yamagishi, M. (2003). Spatial and temporal expression of chalcone synthase and dihydroflavonol 4-reductase genes in the Asiatic hybrid lily. *Plant Sci.* 165, 759–767. doi: 10.1016/S0168-9452(03)00254-1

Pal, P., and Tandon, V. (1998). Anthelmintic efficacy of *Flemingia vestita* (Fabaceae): genistein-induced alterations in the esterase activity in the cestode, *Raillietina echinobothrida*. *J. Biosci.* 23, 25–31. doi: 10.1007/BF02728520

Pathak, R., Gehlot, P., and Singh, S. (2016). *Seed priming-mediated induced disease resistance in arid zone plants*. Singapore: Springer.

Pedrini, S., Merritt, D. J., Stevens, J., and Dixon, K. (2017). Seed coating: science or marketing spin? *Trends Plant Sci.* 22, 106–116. doi: 10.1016/j.tplants.2016.11.002

Phillips, D. A., and Kapulnik, Y. (1995). Plant isoflavonoids, pathogens and symbionts. *Trends Microbiol.* 3, 58–64. doi: 10.1016/S0966-842X(00)88876-9

Ren, M. Q., Kuhn, G., Wegner, J., and Chen, J. (2001). Isoflavones, substances with multi-biological and clinical properties. *Euro. J. Nutr.* 40, 135–146. doi: 10.1007/PL00007388

Schröder, J. (1997). A family of plant-specific polyketide synthases: facts and predictions. *Trends Plant Sci.* 2, 373–378. doi: 10.1016/S1360-1385(97)87121-X

Siddique, S., Matera, C., Radakovic, Z. S., Hasan, M. S., Gutbrod, P., Rozanska, E., et al. (2014). Parasitic worms stimulate host NADPH oxidases to produce reactive oxygen species that limit plant cell death and promote infection. *Sci. Signal.* 7:ra33. doi: 10.1126/scisignal.2004777

Siddiqui, Z. A., Baghel, G., and Akhtar, M. (2007). *Biocontrol of Meloidogyne javanica* by *Rhizobium* and plant growth-promoting rhizobacteria on lentil. *World J. Microbiol. Biotechnol.* 23, 435–441. doi: 10.1007/s11274-006-9244-z

Siddiqui, I., and Shaukat, S. (2003). Endophytic bacteria: prospects and opportunities for the biological control of plant-parasitic nematodes. *Nematol. Mediterr.* 31, 111–120.

Subramanian, S., Hu, X., Lu, G., Odelland, J. T., and Yu, O. (2004). The promoters of two isoflavone synthase genes respond differentially to nodulation and defense signals in transgenic soybean roots. *Plant Mol. Biol.* 54, 623–639. doi: 10.1023/B:PLAN.0000040814.28507.35

Subramanian, S., Stacey, G., and Yu, O. (2006). Endogenous isoflavones are essential for the establishment of symbiosis between soybean and *Bradyrhizobium japonicum*. *Plant J.* 48, 261–273. doi: 10.1111/j.1365-313X.2006.02874.x

Tandon, V., and Lyndem, L. (2010). Anthelmintic efficacy of medicinal palnts from Northeast India against hookworms: an *in vitro* study on *Ancylostoma Ceylanicum*. *Pharmacologyonline* 3, 697–707.

Terefe, M., Tefera, T., and Sakhuja, P. (2009). Effect of a formulation of *Bacillus firmus* on root-knot nematode *Meloidogyne incognita* infestation and the growth of tomato plants in the greenhouse and nursery. *J. Invertebr. Pathol.* 100, 94–99. doi: 10.1016/j.jip.2008.11.004

Tian, F., Chen, L., Wang, Y., Zhu, X., and Duan, Y. (2014). Effect of *Sinorhizobium fredii* strain Sneb183 on the biological control of soybean cyst nematode in soybean. *J. Basic Microbiol.* 54, 1258–1263. doi: 10.1002/jobm.201301014

Toner, E., McConvery, F., Brennan, G., Meaney, M., and Fairweather, I. (2009). A scanning electron microscope study on the route of entry of triclabendazole into the liver fluke, *Fasciola hepatica*. *Parasitology* 136, 523–535. doi: 10.1017/S0031182009005642

Triantaphyllou, A. (1973). Environmental sex differentiation of nematodes in relation to pest management. *Annu. Rev. Phytopathol.* 11, 441–462. doi: 10.1146/annurev.py.11.090173.002301

Volpiano, C. G., Lisboa, B. B., Granada, C. E., São José, J. F. B., de Oliveira, A. M. R., Beneduzi, A., et al. (2019). "Rhizobia for biological control of plant diseases" in *Microbiome in plant health and disease.* eds. V. Kumar, R. Prasad, M. Kumar and D. Choudhary (Singapore: Springer), 315–336.

Williamson, V. M., and Gleason, C. A. (2003). Plant-nematode interactions. *Curr. Opin. Plant Biol.* 6, 327–333. doi: 10.1016/S1369-5266(03)00059-1

Wrather, J., Anderson, T., Arsyad, D., Tan, Y., Ploper, L. D., Porta-Puglia, A., et al. (2001). Soybean disease loss estimates for the top ten soybean-producing countries in 1998. *Can. J. Plant Pathol.* 23, 115–121. doi: 10.1080/07060660109506918

Yadav, V., Wang, Z., Wei, C., Amo, A., Ahmed, B., Yang, X., et al. (2020). Phenylpropanoid pathway engineering: an emerging approach towards plant defense. *Pathogens* 9:312. doi: 10.3390/pathogens9040312

Zamioudis, C., and Pieterse, C. M. (2012). Modulation of host immunity by beneficial microbes. *Mol. Plant-Microbe Interact.* 25, 139–150. doi: 10.1094/MPMI-06-11-0179

Zhao, Y. -S., Duan, Y. -X., Wang, Y. -Y., Chen, L. -J., and YIN, L. -N. (2009). Stress resistance and biocontrol potential of soybean rhizobia resources isolated from Liaoning Province. *Soybean Sci.* 28, 114–117.

Zhu, H., Ai, H., Hu, Z., Du, D., Sun, J., Chen, K., et al. (2020). Comparative transcriptome combined with metabolome analyses revealed key factors involved in nitric oxide (NO)-regulated cadmium stress adaptation in tall fescue. *BMC Genomics* 21:601. doi: 10.1186/s12864-020-07017-8

Zuo, L., Zhang, S., Liu, Y., Huang, Y., Yang, M., and Wang, J. (2019). The reason for growth inhibition of *Ulmus pumila* 'Jinye': lower resistance and abnormal development of chloroplasts slow down the accumulation of energy. *Int. J. Mol. Sci.* 20:4227. doi: 10.3390/ijms20174227

Conflict of Interest: The authors declare that the research was conducted in the absence of any commercial or financial relationships that could be construed as a potential conflict of interest.

frontiers in Plant Science

ORIGINAL RESEARCH
published: 17 December 2020
doi: 10.3389/fpls.2020.606178

Potato Cyst Nematodes: Geographical Distribution, Phylogenetic Relationships and Integrated Pest Management Outcomes in Portugal

*Maria João Camacho[1,2], Eugénia de Andrade[1], Manuel Mota[3], Filomena Nobrega[1], Claudia Vicente[1,2], Leidy Rusinque[1] and Maria Lurdes Inácio[1,4]**

[1] INIAV – National Institute for Agriculture and Veterinary Research, Oeiras, Portugal, [2] NemaLab, MED – Mediterranean Institute for Agriculture, Environment and Development, Institute for Advanced Studies and Research, Universidade de Évora, Évora, Portugal, [3] NemaLab, Departamento de Biologia, Escola de Ciências e Tecnologia, MED – Mediterranean Institute for Agriculture, Environment and Development, Universidade de Évora, Évora, Portugal, [4] GREEN-IT Bioresources for Sustainability, ITQB NOVA, Oeiras, Portugal

The identification and phylogenetic relationships of potato cyst nematodes (PCN) were studied to assess the potential value of geographical distribution information for integrated pest management of potato production in Portugal. This research focused on PCN species, *Globodera pallida* and *Globodera rostochiensis*. From 2013 until 2019, 748 soil samples from the rhizosphere of different potato cultivars were surveyed in the Portuguese mainland to detect and identify both species and track their location. PCN are widespread invasive species throughout Portugal. In fact, during the survey period an incidence of 22.5% was estimated for the tested samples. The patterns of infestation vary among regions, increasing from south to north, where PCN were first detected. Currently, both species are present in all potato producing regions of the country, with a greater incidence of *G. pallida*. Phytosanitary control measures are influencing to the observed results. The use of potato cultivars resistant *to G. rostochiensis* led to a decrease of this species but had no influence on *G. pallida* detections, which continues its reproduction freely since there are no effective resistant cultivars for this species. The relationship between the presence, infestation rate, spread and geographical distribution of PCN is discussed in terms of behavioral responses of the potato cultivars and the implications for developing new integrated crop protection measures.

Keywords: ***Globodera pallida***, ***Globodera rostochiensis***, ***Solanum tuberosum***, **disease, Heteroderidae**

OPEN ACCESS

Edited by:
Christina Cowger, Plant Science Research Unit (USDA-ARS), United States

Reviewed by:
Aarti Bairwa, Indian Council of Agricultural Research (ICAR), India
Zafar Ahmad Handoo, United States Department of Agriculture, United States
Julio Carlos Pereira Silva, Federal University of Santa Maria, Brazil
Valdir Correia, Instituto Federal de Educação, Ciência e Tecnologia do Tocantins (IFTO), Brazil

***Correspondence:**
Maria Lurdes Inácio
lurdes.inacio@iniav.pt

Specialty section:
This article was submitted to Plant Pathogen Interactions, a section of the journal Frontiers in Plant Science

Received: *14 September 2020*
Accepted: *16 November 2020*
Published: *17 December 2020*

Citation:
Camacho MJ, de Andrade E, Mota M, Nobrega F, Vicente C, Rusinque L and Inácio ML (2020) Potato Cyst Nematodes: Geographical Distribution, Phylogenetic Relationships and Integrated Pest Management Outcomes in Portugal. Front. Plant Sci. 11:606178. doi: 10.3389/fpls.2020.606178

INTRODUCTION

Potato crop (*Solanum tuberosum*) has great social and economic importance in Portugal since it is grown throughout the country. The most representative production regions are the North and West Regions (**Figure 1**), with a total potato growing area of approximately 20,000 hectares and a total production of 430,000 tons.

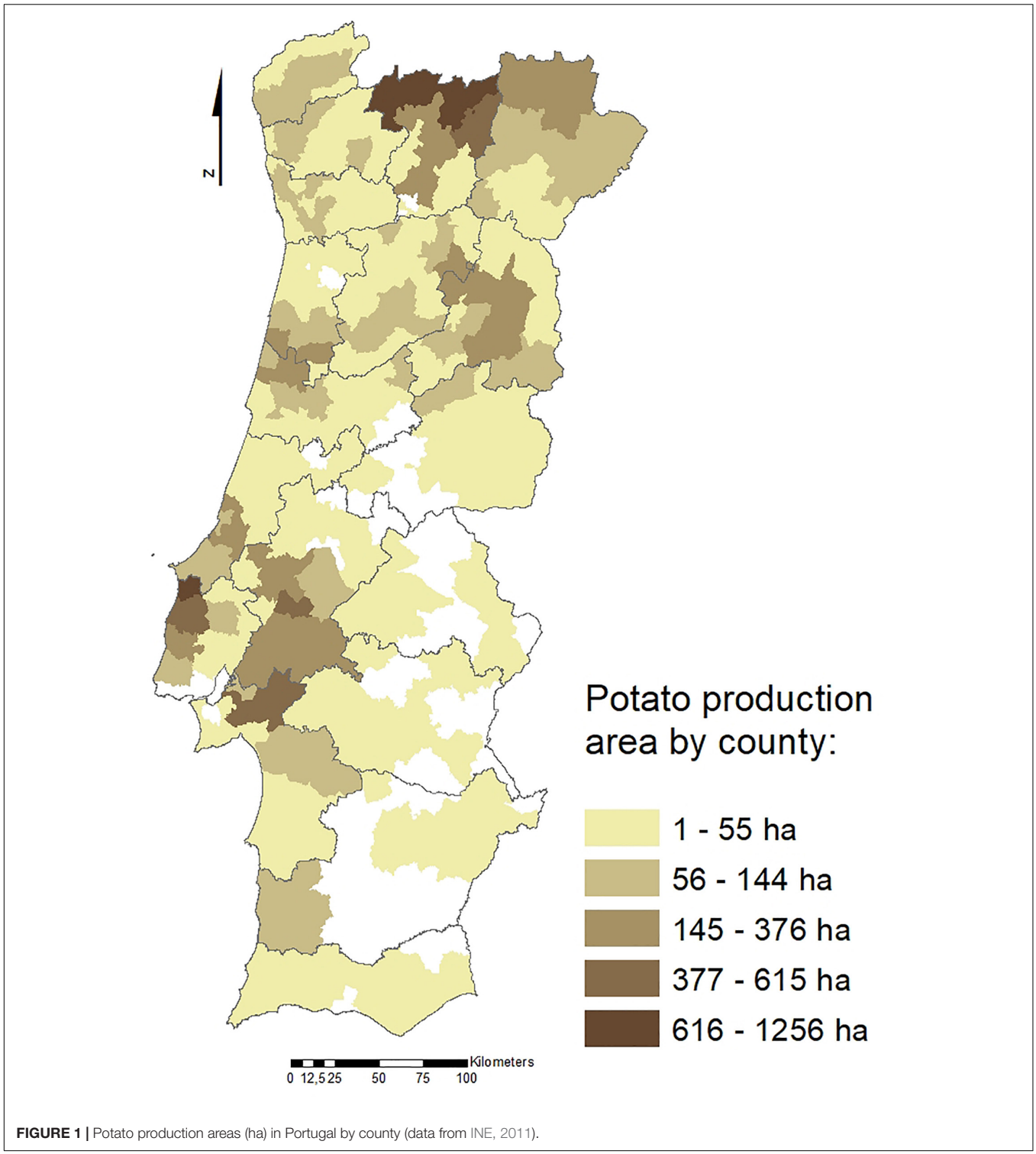

FIGURE 1 | Potato production areas (ha) in Portugal by county (data from INE, 2011).

Several nematode species have been reported associated with potato. Among those, the potato cyst nematodes (PCN), *Globodera rostochiensis* (Wollenweber, 1923; Skarbilovich, 1959) and *Globodera pallida* (Stone, 1973), are two of the major species limiting potato yield. These two species are sedentary endoparasites of the potato root system, deteriorate the quality and commercial value of tubers and contribute to infection of potatoes by other opportunistic plant pathogens, such as fungi (Lavrova et al., 2017).

Yield losses due to the presence of PCN, estimated at €220 million/year in Europe (Viaene, 2016), can vary from

slight losses to crop failure depending on the infestation level (Lima et al., 2018).

Both PCN species are considered harmful quarantine organisms and are subject to stringent regulatory measures when detected singly or in combination (EPPO, 2017).

The golden potato cyst nematode, *G. rostochiensis,* and the pale potato cyst nematode, *G. pallida,* originated from the Andes region in southern Peru and have spread as the result of anthropogenic activity into many regions of the world (Grenier et al., 2010). They are thought to have been introduced to Europe in the 16–17th century by means of potato tubers carrying infested soil and nowadays have worldwide distribution. PCN have been reported throughout Europe, South America and parts of Asia, North America, Oceania and Africa where potatoes are grown (EPPO, 2020). However, new *Globodera* sp. detections continue to be reported (Hafez et al., 2007; Mburu et al., 2018; Niragire et al., 2019; Inácio et al., 2020).

In Portugal, *G. rostochiensis* was first reported in 1956 (Macara, 1963) in a field of seed potatoes near Bragança (Trás-os-Montes district, North of Portugal) and is currently present in all potato producing regions of the country (DGAV, 2015; Camacho et al., 2017), including the Madeira and Azores islands (DGAV, 2015; Inácio et al., 2020). *Globodera pallida* was first identified in 1988 (Santos and Fernandes, 1988), also in Trás-os-Montes, but its current national distribution has not yet been reported.

The knowledge on the geographical distribution, density and spatial dynamics of pest populations is indispensable in integrated pest management (IPM) systems, as it raises considerable interest among plant breeders and plant pathologists for the need to better understand the interaction between pest or pathogen and host and to estimate the risk of crop damage. Therefore, information of PCN distribution and potato cultivars used is essential to understand the *Globodera* spp. regional range of expansion since their first report. As human activity is the most probable means of spreading PCN, there is a specific interest in the evaluation of the implemented control measures and their consequences to adopt more effective management practices.

Controlling PCN is a difficult task due to their high level of adaptation to the environment, the prolonged viability of cysts in the absence of the host plant for more than 20 years, either quiescent or diapause in the form of encysted eggs (Christoforou et al., 2014), and the risk of appearance of aggressive pathotypes in the monoculture of nematode-tolerant potato cultivars. To assess the prevalence and distribution of PCN species across the territory, a country-wide survey was established in 2010, outlining a new framework for phytosanitary protection measures against these harmful organisms to avoid dispersion in national and European Community territories and to ensure potato production of a guaranteed quality for consumers. The main potato growing regions of Portugal have been surveyed for the presence of *G. rostochiensis* and *G. pallida* since 2013.

Before the national survey started, infestations were almost entirely due to *G. rostochiensis* (Santos and Fernandes, 1988; Santos et al., 1995; Martins et al., 1996; Conceição et al., 2003, Cunha et al., 2004, 2006, 2012). The few *G. pallida* populations found in Portugal may suggest that it was introduced after *G. rostochiensis* or there were only few introductions that were kept confined by their low natural mobility. Recently, the analysis of soils sampled in Portuguese potato fields revealed a spread of *G. pallida* (Camacho et al., 2017). In case of PCN positive detection, growers have to choose one of the following options as a phytosanitary measure: (a) culture with a PCN-resistant potato cultivar for a 3-year quarantine period, (b) culture with non-host species or (c) uncultivated land for a 6-year quarantine period. The use of resistant cultivars must be done carefully, in order to prevent the increase of *G. pallida* populations, which are more difficult to control as there are only a few available resistant cultivars.

Currently, in Portugal, there is a lack of detailed information on the geographical distribution of potato cyst nematodes, the correlation between their pattern, the potato cultivars and the near future implications for potato production. Therefore, this study aims to: (i) gather all PCN detections data in Portugal; (ii) carry out a molecular characterization of Portuguese *Globodera* isolates based on sequences of the ITS-rRNA region; (iii) study the phylogenetic relationships of Globodera spp. isolates from Portugal; and (iv) correlate cyst infestations with potato cultivars used.

The research reported herein includes PCN isolates collected from Portuguese potato fields for the national PCN surveys from 2013 to 2019, which made it possible to obtain an accurate assessment of the incidence and phylogenetic relationship of the two PCN species in the territory and their spread in different PCN-resistant cultivars fields.

MATERIALS AND METHODS

Sampling

Soil was collected during the surveys between 2013 and 2019. Sampling was conducted by official inspectors of the National Plant Protection Organization (DGAV, Portugal). According to Annex II of DL 87/2010, sampling consists of a randomized collection of a soil volume with 1500 ml of soil/ha, harvested at least 100 subsamples/ha, preferably in a rectangular mesh, not less than 5 m wide and no more than 20 m long between sampling points, covering the entire field. Soil samples were stored in plastic bags and individually coded by the official services to ensure the anonymity of the samples during the analysis period. Potato field location at the county level and potato cultivars used in these fields were accessed only after analysis results.

The detection, identification and infestation rate of the PCN species were related to their sample location, given by DGAV, and species positive detection maps were made using the ArcMap 10.6 software (ESRI, United States), CAOP2017_PORTUGAL and CAOPP2017_DISTRITOS shapefiles (DGT, 2017).

Globodera spp. Molecular Identification

Cysts were extracted from soil samples using the Fenwick's can method (Fenwick, 1940), according to the EPPO PM7/40 (3) protocol, isolated and counted under a binocular microscope (Leica MZ6, Germany). Cysts (1 to 20 depending on the sample

TABLE 1 | Samples tested for *Globodera rostochiensis* and *Globodera pallida* in Portuguese regions between 2013 and 2019 (absolute values and %).

Region	Positive detections								Negative detections		Total
	G. rostochiensis		*G. pallida*		*Gr + Gp*		Total				
	Value	%	Value	%	Value	%	Value	%	Value	%	
North	30	40.5	39	52.7	5	06.8	74	42.5	100	57.5	174
Center	11	18.0	32	52.5	18	29.5	61	25.5	178	74.5	239
South	7	21.2	12	36.4	14	42.4	33	9.9	302	90.1	335
Total	48	28.6	83	49.4	37	22.0	168	22.5	580	77.5	748

infestation) containing eggs and juveniles were used for DNA extraction by means of the DNeasy Blood & Tissue Kit (Qiagen, Valencia, CA, United States) following the manufacturer's instructions. The internal transcribed spacer region (ITS) of the ribosomal DNA repeat unit was amplified by duplex PCR for species identification. PCR reactions were performed in a 25 μL final volume using the Promega GoTaq Flexi DNA Polymerase Kit (Promega, Madison, United States), containing 1 μL template DNA, 5 μL GoTaq Flexi PCR buffer (2x), 1.5 mM $MgCl_2$, 0.20 mM each dNTPs, 1.25 U GoTaq Flexi DNA Polymerase (Promega, Madison, United States) and 0.4 μM of each primer in a Biometra TGradient thermocycler (Biometra, Gottingen, Germany). The set of primers was composed of the forward primer ITS5 (5′-GGA AGT AAA AGT CGT AAC AAG G-3′) and the reverse PITSr3 (5′-AGC GCA GAC ATG CCG CAA-3′) for *G. rostochiensis* and PITSp4 (5′-ACA ACA GCA ATC GTC GAG-3′) for *G. pallida* (Bulman and Marshall, 1997). The amplification profile for ITS-rDNA consisted of an initial denaturation of 94°C for 2 min followed by 35 cycles of 94°C for 30 s, 55°C for 30 s, and 72°C for 30 s and a final extension of 72°C for 7 min (EPPO, 2017). The amplified products were loaded onto a 1.5% agarose gel containing 0.5 $\mu g.mL^{-1}$ ethidium bromide and 0.5× Tris-borate-EDTA (TBE) running buffer and electrophoresed at 5 V/cm. Amplifications were visualized using the VersaDoc Gel Imaging System (Bio-Rad, United States). The expected length of the PCR products was 265 bp for *G. pallida* and 434 bp for *G. rostochiensis*. Possible contaminations were checked by including negative controls (no template control – NTC) in all amplifications.

Globodera spp. Phylogenetic Analysis

The ITS-rDNA region of 36 samples was amplified and sequenced using the primers 5′-CGT AAC AAG GTA GCT GTA G-3′ and 5′-TCC TCC GCT AAA TGA TAT G-3′ (Ferris et al., 1993). The expected length of PCR fragments is 1040 bp and corresponds to the 3′ end of 18S rDNA-ITS1-5.8S-ITS2-5′ of 28S rDNA. The thermal cycling conditions performed consisted of an initial denaturation of 95°C for 5 min followed by 40 cycles of 94°C for 30 s, 55°C for 30 s, and 72°C for 33 s and a final extension of 72°C for 7 min. Nucleotide sequences were edited and analyzed using BioEdit v7.2.0 (Hall, 2007). The resulting ITS-rDNA sequences were used as query at BLAST from NCBI GenBank to retrieve the most similar sequences within *Globodera* species for phylogenetic reconstruction, and they were deposited in the GenBank database (NCBI). Sequences from *Globodera artemisiae*, *Globodera tabacum,* and *Globodera hypolysi* were selected as outgroup taxa. All sequences were aligned by CLUSTAW (Thompson et al., 1994) with default parameters, trimmed manually and evaluated by Maximum Likelihood phylogeny using the best AIC (Akaike Information Criteria) nucleotide substitution model determined, namely Hasegawa-Kishino-Yano with Gamma Distribution (HKY + G). A bootstrap analysis with 1000 replications was also conducted to infer robustness of the phylogenetic tree. The CLC Main Workbench software package 8.1[1] was used for phylogenetic analysis.

Statistical Analysis

The differences obtained in the detection of the two PCN species in Portugal were achieved through a *Z*-test for the equality of two proportions using the software R[2]. Only soil samples with one or more cysts were used. The hypothesis tests were performed with a significance level $\alpha = 0.05$.

[1]https://www.qiagenbioinformatics.com/

[2]https://www.r-project.org/

TABLE 2 | Potato cultivars grown in Portuguese sampled fields (2013–2019) and their resistance status toward *Globodera rostochiensis* and *Globodera pallida.*

Cultivar	Resistance status		Cultivar	Resistance status	
	G. rostochiensis	*G. pallida*		*G. rostochiensis*	*G. pallida*
Agria	R	S	Jelly	R	S
Alcander	R	R	Kenebeck	S	S
Allison	R	R	Lady rosetta	R	S
Asterix	R	S	Manitou	R	S
Aurea	R	S	Monalisa	S	S
Baraka	R	S	Monte carlo	R	R
Bellarosa	R		Olho de perdiz	R	
Camberra	R		Picasso	R	
Carlita	R		Red Lady	R	
Colomba	R	S	Red scarlet	R	
Daifla	R	S	Romano	S	S
Delila	S	S	Rudolph	S	S
Désirée	S	S	Soleny	S	S
Evolution	R	S	Stemster	R	
Evora	S	S	Taurus	R	S
Hermes	S	S	Yona	R	S

R, resistant; S, susceptible.

Subsequently, the same test was used, with the same level of significance, to infer differences between PCN detections in north, center and south producing regions and between *G. pallida* and *G. rostochiensis* detections in fields with PCN susceptible and *G. rostochiensis* resistant potato cultivars.

RESULTS AND DISCUSSION

During the survey period (2013–2019), 748 soil samples were collected throughout the country by the official services and tested in the plant health national reference laboratory (INIAV). Potato cyst nematodes were identified in 168 samples, representing 22.5% of the tested samples. Forty-eight samples tested positive for *G. rostochiensis* populations alone (28.6%) and 83 for *G. pallida* populations alone (49.4%). Mixed populations were found in 37 samples (22%) (**Table 1**). Statistics revealed that two species detections are significantly different (p-value = 0.00014, α = 0.05), *G. pallida* detection being greater than *G. rostochiensis* detection (p-value = 0.999, α = 0.05, which allows us to accept the null hypothesis that *G. pallida* detections are significantly greater to *G. rostochiensis* detections) between 2013 and 2019. These results contrast with those reported by Cunha et al. (2004) in which out of 423 tested populations (samples collected from various districts of continental Portugal), 83% were *G. rostochiensis* populations alone, 8% were *G. pallida* populations alone and 9% consisted of a mixture of the two species. This reverse situation can be explained due to the use of *G. rostochiensis* resistant potato cultivars, which has been considered the most widespread PCN species in Portugal.

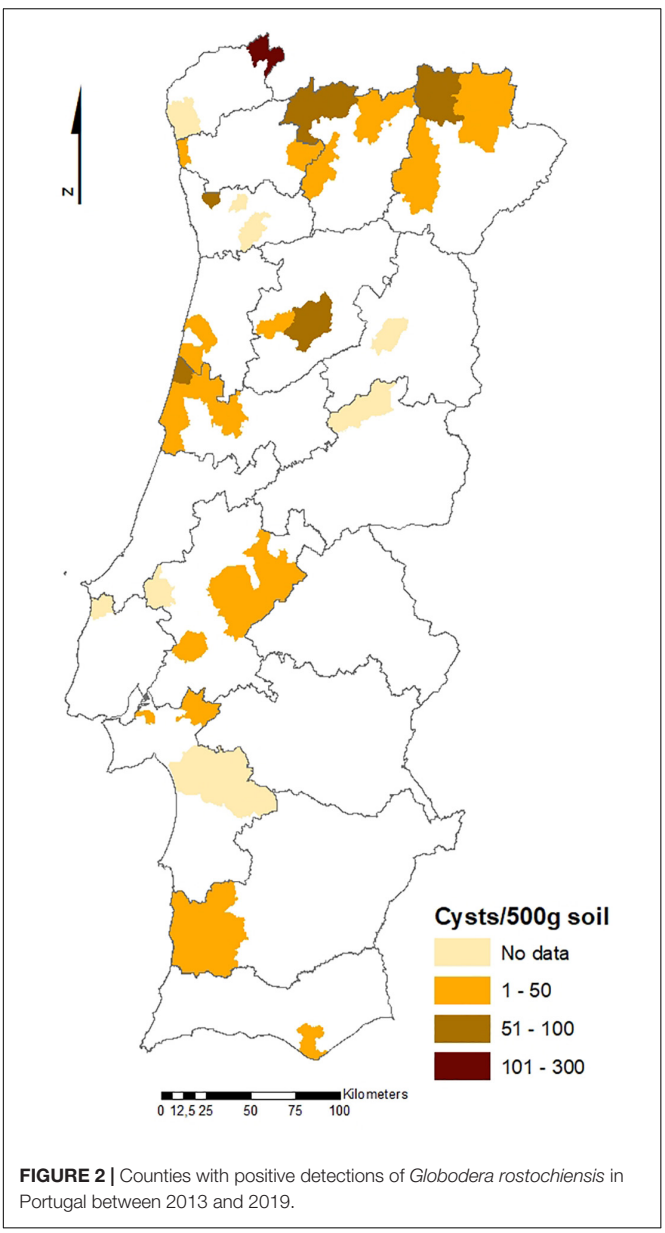

FIGURE 2 | Counties with positive detections of *Globodera rostochiensis* in Portugal between 2013 and 2019.

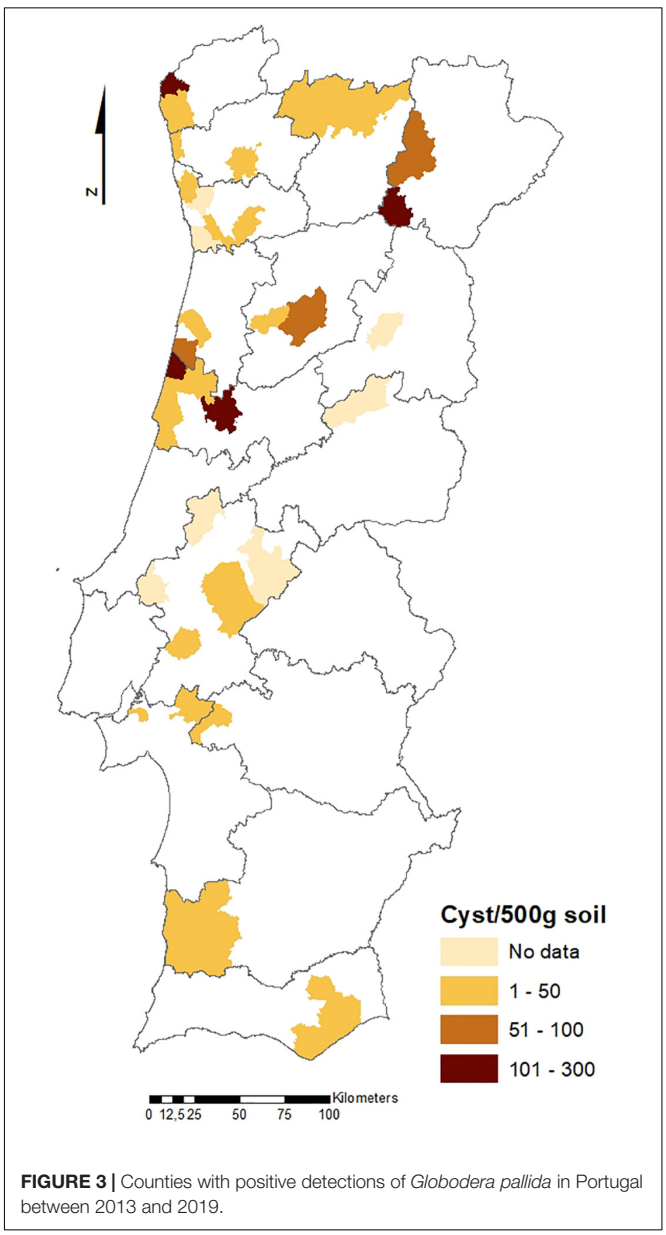

FIGURE 3 | Counties with positive detections of *Globodera pallida* in Portugal between 2013 and 2019.

The use of *G. rostochiensis* resistant potato cultivars (**Table 2**), effective only against certain races of *G. rostochiensis* and with no resistance to *G. pallida*, is leading to the predominance in Portugal of the more difficult species to control, *G. pallida*. The obtained *p*-value (*p*-value = 0.996, α = 0.05) supported the null hypothesis, confirming that *G. rostochiensis* detection in potato fields with *G. rostochiensis* resistant cultivars is significantly smaller than *G. rostochiensis* detection in potato fields with PCN susceptible cultivars. With this result it is possible to infer that resistant cultivars are more efficient in reducing cyst infestations in potato production fields compared with susceptible cultivars fields. However, *G. pallida* detection in potato fields with *G. rostochiensis* resistant cultivars is not different to *G. pallida* detection (*p*-value = 0.2048, α = 0.05, which allows us to accept the null hypothesis that *G. pallida* detections in *G. rostochiensis* resistant cultivars are significantly similar to *G. pallida* detections in PCN susceptible cultivars) and *G. rostochiensis* detection in PCN susceptible potato cultivars fields (*p*-value = 0.5415, α = 0.05, which allows us to accept the null hypothesis that *G. pallida* detections in *G. rostochiensis* resistant cultivars are significantly similar to *G. rostochiensis* detections in PCN susceptible cultivars). With this result it is possible to infer that resistant cultivars used in Portugal allow us to reduce *G. rostochiensis* cysts infestation but has no influence on *G. pallida* cysts infestations in potato production fields. Therefore, the use of *G. rostochiensis* resistant potato cultivars has led to a decrease in *G. rostochiensis* detection but has no influence on *G. pallida* detection. These results agree with the published literature (Minnis et al., 2002; Pickup et al., 2019).

There is no available data to infer about the use of *G. pallida* resistant potato cultivars. This raises the question of whether phytosanitary measures are effective or whether they are contributing to the increase of *G. pallida*, as also reported in the United Kingdom (Minnis et al., 2002). On the other hand, the market has caused potato growers to predominantly use *G. rostochiensis* resistant potato cultivars (i.e., Aurea, Agria, Lady rosetta, Taurus), and this is the main cause of *G. pallida* detections increase.

The geographical distribution of PCN infestations in Portugal is illustrated in **Figures 2**, **3**, which present the infestation rate in counties with positive detections of *G. rostochiensis* and *G. pallida* between 2013 and 2019. This information completes a picture of the PCN situation in Portugal to date.

According to these results, the incidence of PCN in Portugal is quite high, and both species are currently present in all potato producing regions of the country. PCN detections in the different regions are significantly different. Statistics revealed that the Northern PCN detection is greater than the Center PCN detection (*p*-value = 0.998, α = 0.05, which allows us to accept the null hypothesis that PCN detection in northern fields is significantly greater than PCN detection in central fields) and the Center PCN detection is greater than the Southern (Lisbon and Tagus Valley, Alentejo and Algarve regions) PCN detection (*p*-value = 1, α = 0.05, which allows us to accept the null hypothesis that PCN detection in central fields is significantly greater than the PCN detection in southern fields), meaning that PCN detection increases from south to north (see **Figures 2**, **3**), where PCN were first detected and nematode reproduction are

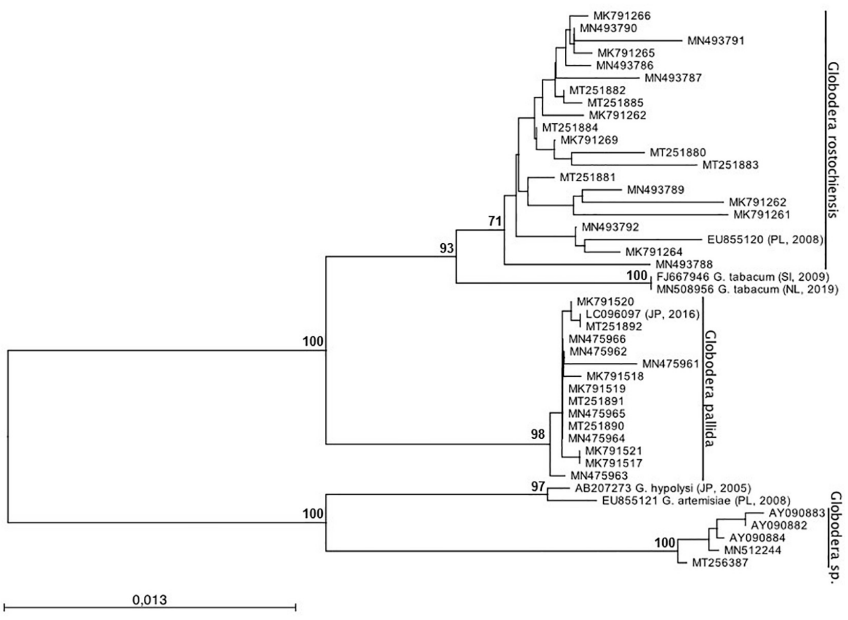

FIGURE 4 | Phylogenetic relationships of 36 *Globodera* sp. isolates collected from Portugal based on the sequence alignment of the ITS-rDNA loci. The condensed phylogenetic tree was generated using the Maximum Likelihood method based on the HKY + G model with 1,000 bootstrap replications. Bootstrap values are indicated at the nodes (bootstrap higher than 70%). The analysis involved a total of 45 nucleotide sequences. All positions containing gaps and missing data were eliminated. *Globodera tabacum*, *G. hypolysi*, and *G. artemisiae* were used as outgroup.

happening for a longer period. These results are also in line with previous reports, which state that the cysts are adapted to higher altitudes (Jones et al., 2017) since the altitude grows from south to northern regions in Portugal.

To infer the phylogenetic relationship of *Globodera* isolates, ML analyses were performed (**Figure 4**). Two major clades, highly supported, can be observed: clade (I) with sub-clades *G. rostochiensis* and *G. pallida* and clade (II) with the sub-clades *Globodera* sp. recently re-detected. Within the first clade, two sub-clades were formed with *G. rostochiensis* and the related species *G. tabacum* and *G. pallida*. The second clade groups a Portuguese *Globodera* sp., discovered in 1997 (Reis, 1997;

TABLE 3 | *Globodera* spp. isolates sequenced in the present study (*E*-value = 0.0).

Globodera species	GenBank accession number	Locality	Collection code/year		Sequence length (bp)	NCBI BLAST homology (%)
Globodera rostochiensis	EU855120	Poland	*	2008	4064	100.00
	MK791260	Coimbra	650P	2014	893	100.00
	MK791261	Montalegre	5244	2015	888	100.00
	MK791262	Montalegre	5245	2015	909	100.00
	MK791263	Viseu	9996	2018	871	98.62
	MK791264	Mirandela	14598	2018	969	99.79
	MK791265	Mirandela	14600	2018	871	99.89
	MK791266	Bragança	14601	2018	909	99.89
	MN493786	Montalegre	13486	2017	937	99.25
	MN493787	Chaves	8850	2016	937	98.50
	MN493788	Viseu	9610	2017	920	98.58
	MN493789	Viseu	5967	2016	936	98.82
	MN493790	Viseu	7047	2017	973	100.00
	MN493791	Odemira	3663	2018	915	99.13
	MN493792	Aveiro	7913	2018	897	99.78
	MT251880	Coimbra	1252	2019	929	99.14
	MT251881	Montalegre	1681-2	2019	909	99.34
	MT251882	Montalegre	1681-6	2019	924	99.89
	MT251883	Chaves	1681-7	2019	933	98.71
	MT251884	Mirandela	1681-10	2019	928	99.35
	MT251885	Melgaço	1249-1	2019	946	98.94
Globodera tabacum	FJ667946	Slovenia	*	2009	923	99.46
	MN508956	Netherlands	NL:c6876	2018	953	99.89
Globodera pallida	LC096097	Japan	*	2016	964	100.00
	MN475961	Viseu	3876	2014	898	99.33
	MN475962	S. Magos	4261	2016	970	99.90
	MN475963	S. Magos	15731	2018	933	99.03
	MN475964	Vagos	9993	2018	977	98.89
	MN475965	Montalegre	14002	2017	914	99.89
	MN475966	Esposende	5087	2016	926	99.56
	MK791517	Penafiel	4694	2015	873	100.00
	MK791518	Viseu	5961	2016	890	99.22
	MK791519	Guimarães	11309	2018	901	99.78
	MK791520	Mirandela	14593	2018	878	100.00
	MK791521	Mirandela	14599	2018	873	100.00
	MT251890	Vagos	1223-7	2019	938	100.00
	MT251891	Aveiro	1223-8	2019	915	99.89
	MT251892	Mira	1086-3	2019	913	99.67
Globodera sp.	AY090883	Bouro	*	1997	908	99.89
	AY090882	Canha	*	1997	908	99.89
	AY090884	Ladoeiro	*	1997	908	99.78
	MN512244	Montijo	12031	2018	953	99.45
	MT256387	Lagameças	1479-2	2019	913	99.67
Globodera artemisiae	EU855121	Poland	*	2008	4092	100.00
Globodera hypolysi	AB207273	Japan	*	2005	909	99.45

**Sequences available from GenBank, NCBI.*

Sabo et al., 2002) and not re-detected until recently (data not shown), and their most closely related *Globodera* species, *G. hypolysi* and *G. artemisiae*. As can be clearly seen, no spatial-temporal relation can be redrawn evidencing the co-existence between the two major species of *Globodera* in Portugal. These results are in accordance with those reported by Cunha et al. (2012), who reported that no relationship could be found between the two-dimensional electrophoresis protein patterns or virulence behavior of the isolates and their geographic origin within Portugal.

It is also worth noting that the topology differs between *G. rostochiensis* and *G. pallida* sub-clades. The first is more branched, with 96–100% of similarity, showing more genetic variability due to being present for a longer period in Portugal, while the second is flatter, with 99–100% of similarity, showing more identical sequences (**Supplementary Table 1**).

Concerning the new species *Globodera* sp. (Reis, 1997; Sabo et al., 2002), re-detected recently in Portugal, it is out of the scope of this work, but additional research is being carried out to determine its pathogenicity and impact on potato.

The nucleotide sequences obtained in this study were deposited in the GenBank database (NCBI) under the accession numbers given in **Table 3**.

Phytosanitary measures have been taken to prevent further spread of *Globodera* spp. in recent years. In the case of *G. rostochiensis*, up until now the dominant species, measures include non-host crop rotation (for 6 years), fallow (for 6 years) or growing of resistant potato cultivars (for 3 years). The use of resistant cultivars containing the H1 gene (single dominant resistance gene for *G. rostochiensis*) (Gebhardt et al., 1993), as already shown, is effective against many populations of *G. rostochiensis* and is likely to be an advantageous management tactic to reduce population densities and thereby yield losses. However, the deployment of resistance in such cultivars may have caused the predominance of *G. pallida* in Portugal, as already predicted by Cunha et al. (2004) and statistically verified in this study.

Therefore, it is urgent to follow a new approach for the management of PCN, mainly *G. pallida*. Non-infested areas need to be managed to minimize the opportunities for the introduction of *Globodera* species. On the other hand, and in infested soils, a greater use of integrated control strategies (such as crop rotation, solarization, trap cropping, biofumigation and selected nematicides) (Evans and Haydock, 2000; Alptekin, 2011; Davie et al., 2019), in addition to PCN-resistant potato cultivars, should be a priority. These interactions require careful research into the effects of one or another strategy under a specific set of environmental conditions and a specific nematode infestation level. The efficacy of the integrated program will be determined by the interaction, overlap and complementarity of the various components. Despite the difficulties associated with *G. pallida* resistance being quantitatively inherited, the breeding of more resistance with different R-genes to avoid PCN capacity to overcome the plant resistance and commercially attractive cultivars is highly important. As *G. pallida* field populations tend to show increased virulence toward a particular partially resistant cultivar each time that it is grown (Trudgill et al., 2003; Pickup et al., 2019), potato growers would need a choice of different cultivars to allow effectiveness to be maintained. Currently, there are insufficient alternatives to partially resistant cultivars for growers to meet the requirements of markets.

DATA AVAILABILITY STATEMENT

The datasets presented in this study can be found in online repositories. The names of the repository/repositories and accession number(s) can be found in the article/**Supplementary Material**.

AUTHOR CONTRIBUTIONS

MC, MI, EA, and MM: conceptualization. MC: investigation and writing – original draft. MC, MI, EA, FN, CV, and LR: methodology. MI, EA, and MM: supervision. MC, MI, EA, MM, and CV: writing – review and editing. All authors contributed to the article and approved the submitted version.

FUNDING

This work was funded by National Funds through FCT – Foundation for Science and Technology under the Ph.D. fellowships BD 138724/2018 and through the R&D Unit, UIDB/04551/2020 (GREEN-IT – Bioresources for Sustainability).

ACKNOWLEDGMENTS

Thanks to DGAV (The National Plant Protection Authority) for the information to support this study.

SUPPLEMENTARY MATERIAL

The Supplementary Material for this article can be found online at: https://www.frontiersin.org/articles/10.3389/fpls.2020.606178/full#supplementary-material

Supplementary Table 1 | Sequence percentage of similarity.

REFERENCES

Alptekin, Y. (2011). Integrated pest management of potatoes. *Agric. Sci.* 2, 297–300. doi: 10.4236/as.2011.23039

Bulman, S., and Marshall, J. (1997). Differentiation of Australasian potato cyst nematode (PCN) populations using the polymerase chain reaction (PCR). *N. Z. J. Crop Hortic. Sci.* 25, 123–129. doi: 10.1080/01140671.1997.9513998

Camacho, M. J., Nóbrega, F., Lima, A., Mota, M., and Inácio, M. L. (2017). Morphological and molecular identification of the potato cyst nematodes (*Globodera rostochiensis* and *G. pallida*) in Portuguese potato fields. *Nematology* 19, 883–889. doi: 10.1163/15685411-00003094

Christoforou, M., Pantelides, I. S., Kanetis, L., Ioannou, N., and Tsaltas, D. (2014). Rapid detection and quantification of viable potato cyst nematodes using qPCR in combination with propidium monoazide. *Plant Pathol.* 63, 1185–1192. doi: 10.1111/ppa.12193

Conceição, I., Santos, M., Abrantes, I., and Santos, S. (2003). Using RAPD markers to analyse genetic diversity in Portuguese potato cyst nematode populations. *Nematology* 5, 137–143. doi: 10.1163/156854102765216759

Cunha, M., Conceição, I., Abrantes, I., Evans, K., and Santos, S. (2004). Characterisation of potato cyst nematode populations from Portugal. *Nematology* 6, 55–58. doi: 10.1163/15685410432307 2928

Cunha, M., Conceição, I., Abrantes, I., and Santos, S. (2006). Assessment of the use of high-performance capillary gel electrophoresis to differentiate isolates of *Globodera* spp. *Nematology* 8, 139–146. doi: 10.1163/15685410677617 9980

Cunha, M., Cunha, M., Conceição, I., Abrantes, I., and Santos, S. (2012). Virulence assessment of Portuguese isolates of potato cyst nematodes (*Globodera* spp.). *Phytopathol. Mediterr.* 51, 51–68. doi: 10.14601/Phytopathol_Mediterr-9517

Davie, K., Pickup, J., Block, V., Kuhfuss, L., Kettle, H., Ewing, D., et al. (2019). Potato cyst nematodes in Scotland – management challenges and options to overcome these. *Asp. Appl. Biol.* 142, 25–31.

DGAV (2015). *Organismos de Quarentena. Acções Realizadas. Relatórios de 2014*. Lisbon: Direção-Geral de Alimentação e Veterinária.

DGT (2017). *Carta Administrativa Oficial de Portugal - CAOP2017*. Direção-Geral do Território. Available online at: https://www.dgterritorio.gov.pt/cartografia/cartografia-tematica/caop#tab-24b1t-1 (accessed December 2018).

EPPO (2017). *Globodera rostochiensis* and *Globodera pallida* PM 7/40 (4). European and mediterranean plant protection organization. *EPPO Bull.* 47, 174–197. doi: 10.1111/epp.12391

EPPO (2020). *EPPO Global Database: Globodera pallida*. European and Mediterranean Plant Protection Organization. Available online at: https://gd.eppo.int/taxon/HETDPA/distribution (accessed October 30, 2020).

Evans, K., and Haydock, P. (2000). Potato cyst nematode management – present and future. *Asp. Appl. Biol.* 59, 91–97.

Fenwick, D. (1940). Methods for the recovery and counting of cysts of *Heterodera schachtii* from soil. *J. Helminthol.* 18, 155–172. doi: 10.1017/S0022149X00031485

Ferris, V. R., Ferris, J. M., and Faghihi, J. (1993). Variation in spacer ribosomal DNA in some cyst-forming species of plant parasitic nematodes. *Fundam. Appl. Nematol.* 16, 177–184.

Gebhardt, C., Mugniery, D., Ritter, E., Salamini, F., and Bonnel, E. (1993). Identification of RFLP markers closely linked to the H1 gene conferring resistance to *Globodera rostochiensis* in potato. *Theor. Appl. Genet.* 85, 541–544. doi: 10.1007/BF00220911

Grenier, E., Fournet, S., Petit, E., and Anthoine, G. (2010). A cyst nematode 'species factory' called the Andes. *Nematology* 12, 163–169. doi: 10.1163/138855409X12573393054942

Hafez, S. L., Sundararaj, P., Handoo, Z. A., Skantar, A. M., Carta, L. K., and Chitwood, D. J. (2007). First report of the pale cyst nematode, *Globodera pallida*, in the United States. *Plant Dis.* 91:325. doi: 10.1094/PDIS-91-3-0325B

Hall, T. (2007). *BioEdit: Biological Sequence Alignment Editor for Win95/98/NT/2K/XP*. Available online at: http://www.mbio.ncsu.edu/BioEdit/bioedit.html

Inácio, M. L., Camacho, M. J., Serra, C., Cordevile, C., Cordeiro, L., and Andrade, E. (2020). First report of the potato cyst nematode, *Globodera rostochiensis*, on potato in the Azores, Portugal. *Plant Dis.* 104:1874. doi: 10.1094/PDIS-07-19-1429-PDN

INE (2011). *Superfície das Culturas Temporárias (ha) por Localização Geográfica (NUTS - 2001) e Tipo (Culturas temporárias); Decenal – INE, Recenseamento Agrícola – Séries Históricas. Instituto Nacional de Estatística*. Available online at: https://www.ine.pt/xportal/xmain?xpid=RA2009&xpgid=ine_ra2009_indicador&contexto=ind&indOcorrCod=0004356&selTab=tab10&xlang=pt (accessed November 3, 2019).

Jones, L. M., Koehler, A. K., Trnka, M., Balek, J., Challinor, A. J., Atkinson, H. J., et al. (2017). Climate change is predicted to alter the current pest status of *Globodera pallida* and *G. rostochiensis* in the United Kingdom. *Glob. Chang. Biol.* 23, 4497–4507. doi: 10.1111/gcb.13676

Lavrova, V. V., Matveeva, E. M., and Zinovieva, S. V. (2017). Expression of genes, encoded defense proteins, in potato plants infected with the cyst-forming nematode *Globodera rostochiensis* (Wollenweber, 1923) Behrens, 1975 and modulation of their activity during short-term exposure to low temperatures. *Biol. Bull. Russ. Acad. Sci.* 44, 128–136. doi: 10.1134/S1062359017020108

Lima, F. S. O., Mattos, V. S., Silva, E. S., Carvalho, M. A. S., Teixeira, R. A., Silva, J. C., et al. (2018). "Nematodes affecting potato and sustainable practices for their management," in *Potato: From Incas to All Over the World*, ed. M. Yildiz (London: IntechOpen), 107. doi: 10.5772/intechopen.73056

Macara, A. (1963). Aspectos sobre a importância dos nemátodos de interesse agrícola em Portugal e no ultramar português. *Agros* 46, 367–384.

Martins, F., Santos, S., Abreu, C., Abrantes, I., and Evans, K. (1996). "Potato cyst nematodes – the situation in the north east part of Portugal," in *Proceedings of the Abstracts Book of the 13th Triennial Conference of EAPR*, Veldhoven, 369–370.

Mburu, H., Cortada, L., Mwangi, G., Gitau, K., Kiriga, A., Kinyua, Z., et al. (2018). First report of potato cyst nematode *Globodera pallida* infecting potato (*Solanum tuberosum*) in Kenya. *Plant Dis.* 12:1671. doi: 10.1094/PDIS-11-17-1777-PDN

Minnis, S. T., Haydock, P. P., Ibrahim, S. K., and Grove, I. G. (2002). Potato cyst nematodes in England and Wales occurrence and distribution. *Ann. Appl. Biol.* 140, 187–195. doi: 10.1111/j.1744-7348.2002.tb00172.x

Niragire, I., Couvreur, M., Karssen, G., Uwumukiza, B., and Bert, W. (2019). First report of potato cyst nematode (*Globodera rostochiensis*) infecting potato (*Solanum tuberosum* L.) in Rwanda. *Plant Dis.* 104:293. doi: 10.1094/PDIS-04-19-0891-PDN

Pickup, J., Davie, K., Block, V., Kuhfuss, L., Kettle, H., Ewing, D., et al. (2019). Potato cyst nematodes in Scotland – where are we now and where are we heading. *Asp. Appl. Biol.* 142, 11–17.

Reis, L. G. (1997). Some morphological characters of a remarkable *Globodera* species (Nematoda: Heteroderidae) occurring in Portugal. *Parasitol. Port.* 4, 126–127.

Sabo, A., Reis, L. G., Krall, E., Mundo-Ocampo, M., and Ferris, V. R. (2002). Phylogenetic relationships of a distinct species of *Globodera* from Portugal and two *Punctodera* species. *J. Nematol.* 34, 263–266.

Santos, S., Evans, K., Abreu, C., Martins, F., and Abrantes, I. (1995). A review of potato cyst nematodes in Portugal. *Nematol. Mediterr.* 23, 35–42.

Santos, S., and Fernandes, M. (1988). The occurrence of *Globodera rostochiensis* and *G. pallida* in Portugal. *Nematol. Mediterr.* 16:145.

Skarbilovich, T. S. (1959). On the structure and systematics of the nematode order Tylenchida Thorne, 1949. *Acta Pol.* 7, 117–132.

Stone, A. (1973). *Heterodera pallida* n.sp. (Nematoda: Heteroderidae), a second species of potato cyst nematode. *Nematologica* 18:591. doi: 10.1163/187529272X00179

Thompson, J. D., Higgins, D. G., and Gibson, T. J. (1994). CLUSTAL W: improving the sensitivity of progressive multiple sequence alignment through sequence weighting, position-specific gap penalties and weight matrix choice. *Nucleic Acids Res.* 22, 4673–4680. doi: 10.1093/nar/22.22.4673

Trudgill, D. L., Elliott, M. J., Evans, K., and Phillips, M. S. (2003). The white potato cyst nematode (*Globodera pallida*) – a critical analysis of the threat in Britain. *Ann. Appl. Biol.* 143, 73–80. doi: 10.1111/j.1744-7348.2003.00073.x

Viaene, N. (2016). "Ring testing of diagnostic methods for the identification of potato cyst nematodes and assessing resistance of potato cultivars," in *Poster at the Report of the Joint EEC-EPPO Workshop on Euphresco*, (Moscow: Eurasian Economic Commission (EEC) and the European and Mediterranean Plant Protection Organisation (EPPO)).

Wollenweber, H. (1923). *Krankheiten und BeschSdigungen der Kartoffel*. Berlin: Arb. Forsch. Inst. Kartof, 56.

Conflict of Interest: The authors declare that the research was conducted in the absence of any commercial or financial relationships that could be construed as a potential conflict of interest.

frontiers in Plant Science

ORIGINAL RESEARCH
published: 08 January 2021
doi: 10.3389/fpls.2020.602825

Hatching Induction of Cyst Nematodes in Bare Soils Drenched With Root Exudates Under Controlled Conditions

*Bruno Ngala[1], Nicolas Mariette[2], Mélina Ianszen[1], Pauline Dewaegeneire[1], Marie-Christine Denis[2], Catherine Porte[2], Christophe Piriou[2], Emilie Robilliard[3], Antoine Couetil[3], Eric Nguema-Ona[4], Jean-Claude Yvin[4], Virginie Gobert[1], Amélie Beury[1], Anne-Claire Le Roux[5], Josselin Montarry[2] and Sylvain Fournet[2]**

[1] FN3PT/inov3PT, Rue des Champs Potez, Achicourt, France, [2] IGEPP, INRAE, Institut Agro, Univ Rennes, Le Rheu, France, [3] Société d'Investissement Légumière et maraîchère de Basse Normandie (SILEBAN), Gatteville le Phare, France, [4] Centre Mondial de l'Innovation-Roullier, Laboratoire de Nutrition Végétale, Pôle Stress Biotiques, Saint Malo, France, [5] FN3PT/inov3PT, INRAE-IGEPP, Le Rheu, France

OPEN ACCESS

Edited by:
Shahid Siddique, University of California, Davis, United States

Reviewed by:
Holger Heuer, Julius Kühn-Institut, Germany
Sebastian Kiewnick, Julius Kühn-Institut – Bundesforschungsinstitut für Kulturpflanzen, Germany

***Correspondence:**
Sylvain Fournet
sylvain.fournet@inrae.fr

Specialty section:
This article was submitted to Plant Pathogen Interactions, a section of the journal Frontiers in Plant Science

Received: *04 September 2020*
Accepted: *30 November 2020*
Published: *08 January 2021*

Citation:
Ngala B, Mariette N, Ianszen M, Dewaegeneire P, Denis M-C, Porte C, Piriou C, Robilliard E, Couetil A, Nguema-Ona E, Yvin J-C, Gobert V, Beury A, Le Roux A-C, Montarry J and Fournet S (2021) Hatching Induction of Cyst Nematodes in Bare Soils Drenched With Root Exudates Under Controlled Conditions. Front. Plant Sci. 11:602825. doi: 10.3389/fpls.2020.602825

Cyst nematodes account for substantial annual yield losses in crop production worldwide. Concerns over environmental and health issues due to the use of chemical nematicides mean alternative sustainable and integrated solutions are urgently required. Hatch induction of encysted eggs in the absence of host plants, i.e., 'suicide-hatching,' could be a sustainable alternative in reducing population densities of cyst nematodes in infested soils. Here we examined *in situ* hatching of encysted eggs of *Globodera pallida*, *Heterodera carotae,* and *Heterodera schachtii* at varying soil depths, following exogenous applications of host root exudates in repeated glasshouse experiments. Cysts were retrieved 30 or 43 days post-incubation depending on the nematode species and assessed for hatching rates relative to the initial number of viable eggs per cyst. Hatching of the potato cyst nematode *G. pallida* depended on both soil moisture and effective exposure to root exudates, and to a lesser extent on exudate concentration. The carrot cyst nematode *H. carotae* had over 75% hatched induced by root exudate irrespective of the concentration, with better hatch induction at 20 cm as compared with 10 cm soil depth. Hatching of the beet cyst nematode *H. schachtii* largely depended on the soil moisture level at constant temperature, rather than the type or concentration of root exudates applied. As a conclusion, exogenously applied host root exudates may play a major role in inducing *in situ* hatch of encysted eggs of potato and carrot cyst nematodes in the absence of host plant under favorable soil temperature/moisture conditions. To improve such strategy, the characterization of chemical profiles of the root exudate composition and field validation are currently ongoing.

Keywords: *Globodera*, *Heterodera*, *in vitro*, *in situ*, hatching, soil depth, encysted eggs, root exudates

INTRODUCTION

Cyst nematodes are sedentary root endo-parasites of many plants, causing stunted growth and wilt on their hosts. They are associated with serious damages to a broad range of crops amongst which include potatoes, carrots, beets, brassicas and cereals. These organisms represent a major threat in agriculture, especially species belonging to the genera *Globodera* and *Heterodera* which are among

the most devastating crop pests worldwide (Jones et al., 2013). The economic losses associated with cyst nematodes are difficult to estimate. An annual figure of 9% worldwide have been estimated for potato cyst nematodes (PCN) for total potato production (Turner and Subbotin, 2013). Annual excesses of US$1.5 billion have been estimated for soybean cyst nematode in the United States alone (Chen et al., 2001), while cereal cyst nematodes may sometimes exceed 90% yield lost depending on environmental conditions (Nicol et al., 2011).

Effective management of cyst nematodes at a field scale is very challenging considering their soil borne nature coupled with their high survival abilities in the absence of the host plant (Marks and Brodie, 1998). The cyst, which corresponds to the desiccated body of the dead female, can contain hundreds of eggs protected against environmental extremes. Infective juvenile (J2) in their dormant state are contained within encysted eggs and can remain viable for several years (Evans and Stone, 1977), making these pests particularly difficult to eradicate once established in the field (Bairwa et al., 2017). The requirements for more environmentally friendly control methods has led to the ban of the broad-spectrum soil fumigant, methyl bromide in 2005, which used to be a silver bullet against soil borne plant parasitic nematodes and complete phase out from use in developing countries in 2015. Hence, there is an urgent need to develop new effective management strategies.

Upon hatch, infective second stage juveniles (J2) are vulnerable and can only navigate through a limited distance, as they depends entirely on their lipid reserves to locate a suitable host to invade and start feeding (Storey, 1984). In potato cyst nematodes, Robinson et al. (1987) noticed that hatched J2 could not survive for more than 2 weeks. This vulnerability is usually offset in some groups of cyst nematode with a sophisticated synchronization of hatching with the presence of signals from the host root exudates (Masler and Perry, 2018). These host-specific compounds collectively referred to as hatching factors include glycoalkaloids or terpenes such as the Glycinoeclepins in root exudates of kidney beans, responsible for hatch induction of *Heterodera glycines* (Masamune et al., 1982; Fukuzawa et al., 1985a,b). Discrepancies in the hatching response to host root exudates exist among cyst nematodes and have been nicely categorized into four broad groups by Perry (2002). In general, this synchronization is very strict for species with a narrow host range, such as *Globodera* spp., which are restricted to members of the Solanaceae (Subbotin et al., 2010), and *Heterodera carotae* which is restricted to the genera *Daucus* and *Torilis* (Aubert, 1986). By contrast, species like *Heterodera schachtii*, which have a wide host range tend to be less dependent on host root exudates. For the latter, *in vitro* hatching of juveniles can be induced with the presence of water only, although hatching is, however, enhanced in the presence of host root exudates (Masler and Perry, 2018).

Here the idea was thus to exploit the vulnerability of hatched J2 and the specificity of hatching factors to develop a control strategy based on the artificial induction of hatching using natural extracts in the absence of the host plant. This strategy, called 'suicide hatching' will thus lead to the death of newly hatched J2 and to the reduction of population levels in the soil (Devine and Jones, 2000; Kushida et al., 2003). This is not a new idea and even less a new strategy. Indeed *in vitro* experiments have already demonstrated high levels of hatching in some cyst nematodes, induced by host root exudates produced in laboratory (Mugniéry and Bossis, 1988; Scholte, 2000). Devine and Jones (2001) also reported significant induction of 'suicide hatching' on field population of *Globodera rostochiensis* by the incorporation of tomato root exudates in the soil. Their report also indicated that successful application of the 'suicide hatching' technique was dependent on soil type, with best results achieved on sandy soils unlike clay and peaty soils. These observations demonstrated the potential of 'suicide hatching' in a sustainable management of cyst nematodes but, despite these promising results, this strategy is still not operational in natural conditions. There have been some advances in the development of tools needed for the characterization of the chemical profiles of hatching factors.

This study thus aimed at: (i) screening a large range of wild or cultivated reference host plants previously reported with satisfactory results of hatching induction, (ii) determine the optimal doses and exposure times that induce the highest hatching *in vitro* and (iii) confirm the efficiency of this control strategy in soil experiments according to the applied doses and soil depth. Three cyst nematode species, *G. pallida*, *H. carotae,* and *H. schachtii,* characterized by different ecological requirements and host ranges were tested.

MATERIALS AND METHODS

Nematode Species

Three cyst nematode species were used in these experiments and include the potato cyst nematode (PCN) *G. pallida,* the carrot cyst nematode (CCN) *H. carotae*, and the beet cyst nematode (BCN) *H. schachtii*. The cyst population for each nematode species was from the same generation produced in glasshouse between 2016 and 2018, and stored at 4°C after extraction for minimum of 3–9 months to break obligate diapause prior to use in experiments. Cyst sizes selected for the experiment ranged from 300 to 450 μm in diameter with special attention to physical damage, thus, all broken or cysts with cracks were discarded.

Root Exudates Production

The production of root exudates from non-tuberous species was performed by soil leaching according to the protocol described by Widdowson and Wiltshire (1958) with some modifications. Seeds were sawn on cell seedling trays and placed in glasshouse regulated at 21/17°C day/night temperatures, respectively, with a photoperiod of 16 h over 2 weeks to attain the four-leaf stage. Seedlings were then transplanted into individual pots filled with 1 L of sterile soil. The collection of root exudates began 2 weeks post-transplanting and continued at a weekly interval up-to week-six. At each time of root exudates collection, plant pots were allowed for 24 h without application of water before being saturated by slowly pouring tap water from the top of the pot. Following pot saturation (water holding capacity), the pots were each suspended on a 1 L beaker before 100 ml of tap water was added from the top of the pot and allowed over 30 min to leach into the beaker underneath the pot. After 30 min, an additional

100 ml of tap water was added to the pot and allowed for a further 30 min before the content of the beaker (200 ml) was retrieved. For each plant species, root exudates collected at the different times were pooled.

Unlike with seeds, to produce root exudates from tuberous species, tubers previously sprouted over 14 days at 21°C in the dark were suspended on tap water in plastic boxes such that the distance between the tubers and water was approximately 0.5 cm. The close proximity of tubers to water meant that roots produced by the tubers were immediately immersed in water. The setup was placed in the dark at 20°C (±0.5°C) and monitored over 21 days, before the water was collected and adjusted such that one tuber was equivalent to 250 ml.

Each batch of root exudates obtained for each species was homogenized and filtrated through cellulose filters of 0.2 μm pore sizes before storage at −20°C until required for the experiments.

Selection and Screening of Root Exudates

In order to select the most efficient root exudates for each nematode species, a wide range of cultivated plants or wild related members of the same family able to induce hatching of each nematode species were selected based on both their host status and phylogenetic criteria following previous reports such as the studies by Evans (1983); Mugniéry and Bossis (1988), Franco et al. (1999), or Scholte (2000). In addition, some non-host plants or plants with an unknown host status, but phylogenetically related to the host plants were also selected. Overall, 120 species/cultivars, both wild and cultivated plants, were selected for the three cyst nematode species with, respectively, 62 for *G. pallida* 26 for *H. schachtii* and 32 for *H. carotae*. Seeds were obtained from different European Biological Resource Centers and seed sailors.

The ability of root exudates to induce hatching of encysted eggs of *G. pallida*, *H. carotae,* and *H. schachtii* was evaluated *in vitro* with the aid of 24-well plastic plates. For each set of root exudates, one cyst, representing an individual replicate, was deposited on an adapted 250 μm sieve (Ngala et al., 2014) placed in individual wells. The sieve allowed active passage of hatched juveniles, while enabling the easy transfer of the cyst to new/refreshed hatching solution. One ml of the test root exudate, adjusted to 45% of the crude exudates, was then added in each well and plates were incubated in the dark at 20°C (±0.5°C), with each treatment consisting of 12 replicates (i.e., 12 cysts). The number of hatched juveniles were scored at days 1[1], 2, 4, 10, 15, and 30 days. At each time of assessment, the sieves with the cyst were rinsed and transferred into new wells containing fresh root exudates. At the end of the experiments, individual cysts were opened to count the number of unhatched viable and non-viable eggs/juveniles in a bid to compute hatching rate (as a proportion of the viable eggs).

Following the screening, two most efficient root exudates were selected for each nematode species based on their level of hatch activation and the speed of hatching when the tested nematode species were exposed to the respective root exudates. In addition to rate of hatch induction, the ease of obtaining the cultivars and the production of root exudates played a central role in the selection process.

[1] Assessments conducted on *H. schachtii* only due to it fast rate of hatching.

Dose and Exposure Time Experiments

To determine the optimum concentrations of root exudates able to activate maximum hatch of cyst nematodes, *in vitro* hatching experiments were set-up with the root exudates selected in the screening assays for *G. pallida*. The root exudates selected included *Solanum tuberosum* cv. Désirée and Iodéa each diluted to 10, 25, 45, and 70% of the crude exudates as compared with tap water (0%). The experiment was conducted following the same protocol used for the screening of the root exudates with the exception that the assessments for hatched juveniles was done at 4, 7, 9, 11, 15, and 30 days post-incubation. Each test exudate or concentration had six replicates. Preliminary experiments with *H. carotae* and *H. schachtii* revealed that exudate concentration was not an important factor, thus it was not necessary to conduct the concentration test on these cyst nematode species.

To determine the exposure time necessary between root exudates and encysted eggs of cyst nematodes to induce a maximum hatching, *in vitro* hatching experiments were set-up in 24-well plastic plates as described above for the determination of optimum concentration. The different exposure time tested included 0, 4, 7, 9, 11, 15, and 30 days for *G. pallida*, and 0, 1, 2, 4, 10, 15, and 30 days for *H. carotae* and *H. schachtii*, with the concentration of root exudates in both cases adjusted to 30% of the crude root exudates. Therefore, assessments for hatched J2 were conducted at the stated exposure times, during which, cysts were either transferred into water after their respective time of exposure with root exudates, or the solution was refreshed if the end of the exposure time of the cysts with the hatching solution had not finished. Each test exudate or concentration had six replicates.

To determine whether a continuous exposure was needed to induce a maximum hatching, cysts were periodically exposed to root exudates for 4 h every 6 days before re-deposition into tap water. A positive control consisted of a treatment with continuous exposure between root exudates and cysts, while a negative control (continuous exposure with water) were added for each nematode species. The test root exudates were diluted to 85% for *H. schachtii* and 45% for *G. pallida* and *H. carotae*. All treatments had six replicates.

Root Exudates Efficiency Under Soil Conditions

These experiments were conducted in 2018 and 2019 under controlled environmental conditions (20/16°C day/night temperatures, respectively, with a photoperiod of 16 h) at three different sites depending on the nematode species. Samples of soils used in all experiments were sent to Centre Mondial d'Innovation (CMI) Groupe-Roullier, St-Malo, France for texture and pH analysis.

All experiments except experiments with *H. schachtii* were conducted in plastic pots (35 cm height-8 cm diameter) under controlled conditions, filled with natural field soils free from any

cyst nematode species. Smaller plastic pots (8 cm*8 cm*8 cm) were used in experiments with *H. schachtii*.

In all experiments, each set of pot experiments was arranged in a randomized complete block design with each treatment having ten replicates. The soil moisture was maintained around 80% of field capacity throughout the period of test. Therefore, prior to each application of treatment or water, the moisture content of the soils was recorded to determine the amount of water loss. This lose was then compensated by the prior application of tap water to the respective pots with water deficit where applicable to attain 80% of the field capacity.

For the three nematode species, the initial number of encysted viable eggs (P_i) was estimated from 10 × 10 cysts. Therefore, 10 cysts from same population measuring between 300 and 450 μm were randomly picked and placed onto a tiny droplet of tap water on a piece of aluminum block and crushed with the aid of a glass slide. The crushed cysts/eggs mixture was rinsed into an 80 mL Pyrex beaker, vigorously homogenized to separate egg clusters and suspended into 40 mL tap water. The suspension was homogenized before aliquots of 3 mL × 1 mL were pulled with a 2 mL glass pipette onto 1 mL nematode counting slide for the quantification of viable and non-viable J2 to determine the initial viable eggs per cyst (P_i).

At the end of the experiments, to count the remaining (unhatched) viable J2 per cyst (P_f) and determine the hatching rate for each treatment, the incubated cyst sachets were retrieved and numbered according to levels, before being arranged into appropriately labeled petri-dishes according to treatment on each block. Each sachet was carefully cut open with a pair of scissors and the cysts were carefully retrieved. The number of viable and non-viable eggs/cyst was then estimated as described above for P_i assessments. The hatching percentage for each treatment was then computed as the ratio of difference between the mean P_i and P_f values to the mean P_i value ($[(P_i - P_f)/P_i]$) and expressed as percentages.

Experiments with *G. pallida* were conducted in 2018 at FN3PT/inov3PT (Achicourt, France) and INRAE (Le Rheu, France) laboratories with soils collected from Laon and La Gruche, respectively, and repeated in 2019 only in FN3PT/inov3PT. Soils were pre-moistened at 45 to 50% of field capacity prior to filling into experimental pots to the 30 cm level. In 2018, treatments included Désirée root exudates at 25% or 45% dilutions of the crude root exudates, with tap water as control. In the repeated experiments in 2019, exudates were further diluted to 5% while maintaining 25% of the crude root exudates with the addition of Iodéa root exudates to the treatment list. Each pot was inoculated with three sachets each containing 10 cysts placed at 5, 15, and 25 cm from top soil. The mesh allowed the movement of hatched J2 from the cysts to the soil. Experimental pots each received 60 ml of the test root exudates at their respective concentrations or tap water at a 4 days interval over the first 16 days (5 applications). Soil moisture was then maintained with tap water only until the end of the experiments (43 days).

Experiments with *H. carotae* were conducted at the SILEBAN laboratories (Gatteville-le-Phare, France). The soil used for the experiments was collected from a single field (Gatteville-le-Phare, France). Pots were filled with soil as describe above for *G. pallida* and inoculated with two sachets each containing 15 cysts at 10 and 20 cm depth from top soil. Treatments for these experiments included carrot cv. Touchon or cv. Pusar Kesar, as crude exudates or at 50% dilution, with tap water as a control. Each pot received 50 ml of the respective treatments or tap water at a 4-days interval for the first 20 days (six applications). We then maintained the moisture content with tap water only until the end of the experiments (40 days).

Experiments with *H. schachtii* were conducted at the INRAE laboratories (Le Rheu, France), with the same soil used in the experiments with *G. pallida*. Treatments for these experiments included undiluted root exudates of sugar beet cv. Acacia or tap water as control. Pots were inoculated with one sachet only, at 4 cm depth from top soil, containing 10 cysts for each replicated treatment. For treatment with root exudates, two application regimes (R) were employed, which included an amount of 15 or 30 ml of undiluted root exudates every 2 (R1) or 4 (R2) days, respectively, during the first 16 days. We then maintained the moisture content with 30 ml of tap water until the end of the experiments (30 days).

Statistical Analysis

All data was checked for normality of residuals with the aid of the residual and mean plots. Data for pot experiments were subjected to a general analysis of variance (ANOVA) specifically the general treatment structure in randomized blocks using GenStat® 19th Edition software pack (VSNI Products, United Kingdom). Significant differences between treatments and controls were determined using Tukey's multiple range test (5% significance level). For dose and exposure time experiments, the relationship with the percentage of hatched eggs per cyst was explored using linear and quadratic models. The model selection based on Akaike's information criteria, AIC (Johnson and Omland, 2004), was used in order to determine the model of best fit. Linear regression was therefore, performed on exposure time experiments to observe the relationship with the rate of hatch for each cyst nematode species, while quadratic models were used to explain dose effect on rate of hatching for *G. pallida*.

RESULTS

Root Exudates Screening Experiments

Root exudates collected from 66 plants and/or varieties were screened for *G. pallida* hatch induction: 62 specifically selected for this species and two root exudates each initially selected for *H. carotae* and *H. schachtii* (**Table 1A**), respectively. High levels of hatch induction was observed for root exudates of some solanaceous plants, with the top five including *Solanum tuberosum* cv. Iodéa & Magnum, *S. gourlayi*, *S. tuberosum* cv. Désirée, and *S. melongena* cv. Listada de Gandia, in this order, which accounted for 75–95% hatch induction after an incubation period of 30 days (**Table 1A**). The hatching rate was faster for root exudates of some potato varieties such as Iodéa, Magnum, Blanche as well as tomato cv. Saint-Pierre in which between 41 and 79% hatch was observed just after 10 days exposure of encysted eggs of *G. pallida* to the root

TABLE 1A | Plant species and/or cultivars screened for the ability of their root exudates to induce hatching of *Globodera pallida in vitro.*

Species	Cultivar	Family	Source	% Hatch (10-*dpe*)	% Hatch (45-*dpe*)
Solanum tuberosum	Iodéa	Solanaceae	Tubers	79.0	95
S. tuberosum	Magnum	Solanaceae	Tubers	67.0	89
S. gourlayi	88S.315.18	Solanaceae	Tubers	22.0	86.6
S. tuberosum	Désirée	Solanaceae	Tubers	50.0	80.9
S. melongena	Listada de Gandia	Solanaceae	Grains	34.0	75.1
S. demissum	69S.167.104	Solanaceae	Tubers	34.9	68.9
S. tuberosum	Blanche	Solanaceae	Tubers	43.0	62
S. tuberosum	Inovator	Solanaceae	Tubers	35.0	62
S. viarum		Solanaceae	Grains	11.1	62
S. spegazzinii	88S.334.19	Solanaceae	Tubers	26.2	61.8
S. andigena	88S.255. 2	Solanaceae	Tubers	14.8	61.6
S. tuberosum	94T146.52	Solanaceae	Tubers	16.8	61.4
S. vernei	78S.248. 4	Solanaceae	Tubers	24.8	60.3
S. phureja	78S.222. 7	Solanaceae	Tubers	18	58.5
S. lycopersicum	Saint-Pierre	Solanaceae	Grains	41	57.5
Brassica oleracea var. italica	Early purple sprouting	Brassicaceae	Grains	12.8	56.7
S. stenotomum	74S.14.1	Solanaceae	Tubers	21.1	55.7
S. tuberosum	Désirée	Solanaceae	Grains	30.7	55.4
S. sisymbriifolium		Solanaceae	Grains	24.1	54.0
S. melanocerasum		Solanaceae	Grains	20.5	52.9
S. lycopersicum	Cornue des Andes	Solanaceae	Grains	32.9	52.5
S. tuberosum	Stronga	Solanaceae	Tubers	35	50
S. berthaultii	88S.282. 36	Solanaceae	Tubers	20.2	49.1
S. schenckii	99S. 72. 6	Solanaceae	Tubers	16.8	42.8
S. mauritianum		Solanaceae	Grains	18.6	40.3
S. aethiopicum	Var. N'Goyo	Solanaceae	Grains	16.2	39.3
S. andigena	88S.249. 1	Solanaceae	Tubers	20.4	39.1
S. phureja	88S.511.7	Solanaceae	Tubers	19.6	38.2
S. pseudocapsicum		Solanaceae	Grains	15.3	32
S. trifidum	00S.100. 20	Solanaceae	Tubers	8.1	29.5
Ullucus tuberosus		Basellaceae	Tubers	11.7	28.8
Nicotiana tabacum	Xanthi	Nicotianeae	Grains	13.3	28.7
S. cardiophyllum	00S. 42. 3	Solanaceae	Tubers	8.1	28.6
Petunia inflata		Solanaceae		14.2	27.5
S. melongena	Barbentane	Solanaceae	Grains	16.7	26
Oxalis tuberosa		Oxalidaceae	Tubers	7	25.7
S. gourlayi	88S.495.5	Solanaceae	Tubers	5.3	25.5
S. tarijense	90S. 14. 11	Solanaceae	Tubers	16.2	24.6
S. nigrum		Solanaceae	Grains	9	22.2
Foeniculum vulgare	Cormo	Apiaceae	Grains	8.6	21.9
S. stoloniferum	00S. 83. 13	Solanaceae	Tubers	8.3	21.2
Lupinus sp.		Fabaceae	Grains	15.1	21
S. macrocarpon		Solanaceae	Grains	5.7	19.9
S. sparsipilum	88S.329.18	Solanaceae	Tubers	7.8	19.6
Physalis peruviana	Peruviana	Solanaceae	Grains	10.7	18.4
Brugmansia suaveolens		Solanaceae		6.4	17.2
Cestrum parqui		Solanaceae		9.9	16.4
Ipomoea purpurea	Royal Ensign	Convolvulaceae	Grains	7.8	14.4
Orge commune		Poaceae	Grains	7.4	14
Ipomée		Convolvulaceae	Grains	6.6	14
S. polytrichon	00S. 69. 8	Solanaceae	Tubers	4.4	13.6
S. hougasii	00S. 60. 1	Solanaceae	Tubers	4.8	12.7
Capsicum annuum	Yolo wonder	Solanaceae	Grains	2.9	10.8
N. tabacum	Benthamiana	Nicotianeae	Grains	5.1	9.8

(Continued)

TABLE 1A | Continued

Species	Cultivar	Family	Source	% Hatch (10-*dpe*)	% Hatch (45-*dpe*)
S. stenotomum	74S. 16. 3	Solanaceae	Tubers	3	9.2
Datura stramonium		Solanaceae	Grains	3.4	9
B. juncea	Aurea	Brassicaceae	Grains	1.9	7.3
D. carota	Western red	Apiaceae	Grains	0.6	6.2
Iochroma australe		Solanaceae		1.6	5.4
Ipomoea batatas		Convolvulaceae	Tubers	0	4.7
Petunia integrifolia		Solanaceae	Grains	1.7	4.1
C. annuum	Cayenne	Solanaceae	Grains	1.6	3.9
C. annuum	Belrubi	Solanaceae	Grains	0	1
Tropaeolum tuberosum		Tropaeolaceae	Tubers	0.3	0.7

exudates (**Table 1A**). Although the percentage hatch of *G. pallida* was generally low in root exudates of non-solanaceous plant species, (<30%), some solanaceous plants also induced very low hatch (**Table 1A**). Surprisingly, 56% hatch was observed in root exudates of *Brassica oleracea* cv. 'Early Sprouting,' a non-solanaceous plant.

Root exudates collected from 34 plants were screened for *H. carotae,* with 32 specifically selected for this species and one each initially selected for *G. pallida* and *H. schachtii,* respectively. Results (**Table 1B**) highlighted two distinct group of plants: the first group induced hatching of 20% and above, and included wild or cultivated carrot varieties and species, whereas the second group had less than 1% hatch induction, and included plants not belonging to the carrot's family. Among the exudates of the first group, three induced hatching of 70% and above, especially the carrots cv. Touchon and Pusa Kesar (**Table 1B**).

Root exudates collected from 30 plants were screened for *H. schachtii*, with 26 belonging to the Brassicaceae (host family), and two each initially selected for *G. pallida* and *H. carotae* (**Table 1C**). Plants belonging to the host range induced high hatching levels (above 80%) after 30 days exposure. Sugar beets cv. Julietta and Acacia were notably the most efficient, inducing 100% hatch *in vitro*. The rate of hatch was faster in root exudates from species such as *Brassica carinata* cv. Aurea and *B. oleracea* cv. Early sprouting (**Table 1C**).

Following results from the screening, *Solanum tuberosum* cv. Iodéa and Désirée were selected for *G. pallida*, while *Daucus carota* cv. Touchon and cv. Pusa Kesar were selected for *H. carotae* and *Beta vulgaris* cv. Acacia and was selected for *H. schachtii* (**Table 1**).

Dose and Exposure Time Experiments

For the dose effect, the quadratic model fitted best for the data, for the test root exudates (Désirée an Iodéa). Dose dependent hatch induction of *G. pallida* showed an optimum performance at 45% concentration of root exudates for potato cv. Iodéa. *Globodera pallida* hatch induction by potato cv. Désirée root exudates increase to a peak of 25%, before stabilizing from 25 to 70% concentration (**Figure 1**). Generally, hatching of *G. pallida* was positively correlated with concentration of Iodéa ($R^2 = 0.975$; $P = 0.025$) up to 45% concentrations, beyond which the rate of hatching draped. Similarly, Désirée root exudates showed positive relationship with *G. pallida* hatching ($R^2 = 0.950$; $P = 0.047$) up to a peak of 25% with further increase in dose having no additional effect on% hatch (**Figure 1**).

A periodic exposure for 4 h every 6 days induced similar hatching rates in the three species as a continuous exposure to root exudates (**Table 2**). Linear regression analysis revealed that the exposure time between root exudates and encysted eggs necessary to induce significant levels of hatch was an important factor for *G. pallida* and *H. carotae*, but not for *H. schachtii* (**Figure 2**). Generally, 11 days exposure to Désirée root exudates was necessary to induce a significant ($R^2 = 0.632$; $P < 0.001$) amount of hatching of *G. pallida*, with an optimum hatch at 15 days of incubation (**Figure 2A**). *Heterodera carotae* needed a minimum of 4 days exposure to root exudates for a significant induction ($R^2 = 0.790$; $P < 0.001$) hatch, with an optimum exposure time of 30 days (**Figure 2B**). However, *H. schachtii* had a similar level of hatching in water and root exudates, with a weak and non-significant ($R^2 = 0.325$; $P = 0.088$) relationship with exposure time under *in vitro* conditions (**Figure 2C**).

Root Exudates Efficiency Under Soil Conditions

An analysis for the particle size distribution of the soils used for the pot experiments revealed that the soil texture was more or less sandy with a fairly neutral pH (**Table 3**).

Hatching of *Globodera pallida* in Soil

Soil experiments conducted on *G. pallida* in 2018 revealed a significant increase of hatching (>70%) following potato cv. Désirée root exudate as compared with tap water applications (<40%) ($F_{2,27} = 24.49$; $P < 0.001$ at 5 cm, $F_{2,27} = 32.2$; $P < 0.001$ at 15 cm and $F_{2,27} = 29.2$; $P < 0.001$ at 25 cm; **Figure 3A**). However, there was no significant dose effect on the hatching rate with exudates diluted to 25 or 45%. There was also no significant depth effect on the rate of hatching for all concentrations of root exudates tested. Results obtained in 2018 were partially confirmed in the repeated experiments in 2019, but there were no significant differences at 25 cm soil depth ($F_{4,45} = 1.872$; $P = 0.132$; **Figure 3B**). For cysts placed at 5 and 15 cm soil depth, hatching was significantly higher than the control (tap water) for pots drenched with Désirée and Iodéa root exudates ($F_{4,45} = 9.524$; $P < 0.001$ at 5 cm and $F_{4,45} = 7.916$; $P < 0.001$

TABLE 1B | Plant species and/or cultivars screened for the ability of their root exudates to induce hatching of *Heterodera carotae in vitro.*

Species	Cultivar	Family	Source	% Hatch (10-*dpe*)	% Hatch (30-*dpe*)
D. carota	Touchon	Apiaceae	Seed	8	84.3
D. c. carota ssp. *maximus*		Apiaceae	Seed	11.7	72.8
D. carota	Puska kaesar	Apiaceae	Seed	27	69.6
D. carota	Western red	Apiaceae	Seed	14.3	63.9
D. c. carota ssp. *carota* var. *carota*		Apiaceae	Seed	3	63.3
D. c. gummifer ssp. *gummifer* var. *gummifer*		Apiaceae	Seed	20.4	58
D. c. gummifer ssp. *drepanensis*		Apiaceae	Seed	2.2	55.2
D. carota	Haian-3-sun	Apiaceae	Seed	9.6	54.3
D. carota	Nantaise	Apiaceae	Seed	5.6	52.4
D. c. intermediaire		Apiaceae	Seed	2.8	48.5
D. c. gummifer ssp. *hispidus*		Apiaceae	Seed	2	42.2
D. carotae	T16	Apiaceae	Seed	2.6	40.9
D. c. gummifer ssp. *hispanicus* 684		Apiaceae	Seed	3.7	40.9
D. carota	Muscade d'Alger	Apiaceae	Seed	8.5	36.8
D. c. gummifer ssp. *commutatus*		Apiaceae	Seed	3	33.2
D. c. carota ssp. *maritimus*		Apiaceae	Seed	2.2	33
D. carota	Violette turque	Apiaceae	Seed	14.3	31
D. *c. carota* ssp. *gadecaei*		Apiaceae	Seed	3	25.4
D. carota	Jaune du Doubs	Apiaceae	Seed	1.7	20.9
D. capillifolius		Apiaceae	Seed	0.7	20.7
Petroselinum crispum		Apiaceae	Seed	0.4	0.6
P. c. ssp. *tuberosum*		Apiaceae	Seed	0,0	0.6
Pastinaca sativa		Apiaceae	Seed	0.2	0.2
Apium graveolens var. *rapaceum*		Apiaceae	Seed	0.2	0.2
Foeniculum vulgare	"Finale"	Apiaceae	Seed	0.0	0.2
Anthriscus cerefolium		Apiaceae	Seed	0.0	0.2
F. vulgare	"Cormo"	Apiaceae	Seed	0.2	0.2
Beta vulgaris	Julietta	Amaranthaceae	Seed	0.2	0.2
Anethum graveolens		Apiaceae	Seed	0.0	0.0
Anthriscus cerefolium crispum		Apiaceae	Seed	0.0	0.0
Conium maculatum		Apiaceae	Seed	0.0	0.0
Coriandrum sativum		Apiaceae	Seed	0.0	0.0
Apium graveolens		Apiaceae	Seed	0.0	0.0
S. tuberosum	'94T146.52'	Solanaceae	Seed	0.0	0.0

at 15 cm; **Figure 3B**). Whatever the root exudate (Désirée and Iodéa), hatching was higher at 25% as compared with 5% concentration of root exudates. In line with some observations in 2018, cyst incubated within the top 15 cm soil depth in 2019 experiments had an increase in level of *in situ* hatch as compared with hatching at 25 cm soil depth for *G. pallida*.

Hatching of *Heterodera carotae* and *H. schachtii* in Soil

The general average hatch of *H. carotae* in soil drenched with root exudates of *Daucus carota* cv. Pusa Kesar or carrot Touchon was approximately 70% irrespective of the concentration of the root exudates, whereas in soil drenched with tap water, the hatching level was approximately 40% (**Figure 4**). At 20 cm soil depth, there was approximately a 15% improvement in hatching when compared with hatching of encysted eggs placed at 10 cm soil depth for all treatments with root exudates, irrespective of concentration. Significant differences between treatments and control were observed at 20 cm ($F_{4,45} = 7.363$; $P < 0.001$) but not at 10 cm ($F_{4,45} = 2.018$; $P = 0.108$) soil depth (**Figure 4**).

H. schachtii performed well in pots drenched with tap water, inducing over 60% hatch, which was further significantly enhanced in pots drenched with undiluted sugar beet root exudates ($F_{2,27} = 15.94$; $P < 0.001$; **Figure 5**).

DISCUSSION

The main objective of this study was to evaluate the feasibility of the management of the three cyst nematode species, *G. pallida*, *H. carotae,* and *H. schachtii* using naturally produced root exudates. This study has provided some new and sometime surprising insights into the hatching behavior such as induction time, hatching dynamics and soil depth effects for the three studied cyst nematode species. Under the framework of optimizing the 'suicide hatching' strategy with natural plant secretions, this study enabled the development facilities for

TABLE 1C | Plant species and/or cultivars screened for the ability of their root exudates to induce hatching of *Heterodera schachtii in vitro*.

Species	Cultivar	Family	Source	% Hatch (2-*dpe*)	% Hatch (30-*dpe*)
Beta vulgaris	Julietta	Amaranthaceae	Seed	63.8	100
Beta vulgaris	Acacia	Amaranthaceae	Seed	56.9	100
Brassica oleracea var. *botrytis*	Snowball	Brassicaceae	Seed	68.7	100
B. napus	Yudal	Brassicaceae	Seed	83.2	99.3
B. oleracea var. *italica*	Early purple sprouting	Brassicaceae	Seed	82	97.3
Amaranthus cruentus	Golden Giant	Amaranthaceae	Seed	66.7	95.1
B. juncea	Aurea	Brassicaceae	Seed	86.5	93.9
Aurinia saxatilis		Brassicaceae	Seed	72.1	93.5
Beta vulgaris	Bison	Amaranthaceae	Seed	50.9	91.9
Beta vulgaris	Sanetta	Amaranthaceae	Seed	54.1	91.4
B. rapa ssp. *pekinensis*		Brassicaceae	Seed	79.9	91.4
Beta vulgaris	Ardan	Amaranthaceae	Seed	57.6	87.2
Spinacia oleracea	Géant d'hiver	Amaranthaceae	Seed	42.4	86.8
B. napus	Alpaga	Brassicaceae	Seed	64.3	86.8
Beta vulgaris	Nemata	Amaranthaceae	Seed	64.6	86.2
B. vulgaris ssp. *maritima*		Amaranthaceae	Seed	30	85.5
Portulaca oleracea		Portulaceae	Seed	56.6	84.4
Atriplex hortensis		Amaranthaceae	Seed	43	83.6
Nasturtium officinale		Brassicaceae	Seed	57	82.9
S. tuberosum	Désirée	Solanaceae	Tuber	67	82.3
Pisum sativum	James	Fabaceae	Seed	35	82
Chenopodium quinoa		Amaranthaceae	Seed	32.3	81.9
Pastinaca sativa	Demi Long de Guernesey	Apiaceae	Seed	47.2	79.3
D. carota ssp. *sativus*	Nantaise	Apiaceae	Seed	41.1	68.5
Dianthus barbatus	Kaléïdoscope	Caryophyllaceae	Seed	42.1	66.6
A. thaliana		Brassicaceae	Seed	43.6	64.9
S. lycopersicum	"Saint-Pierre"	Solanaceae	Seed	52.3	64.6
Sinapis alba	Cador	Brassicaceae	Seed	22	61.1
Eruca vesicaria ssp. *sativa*		Brassicaceae	Seed	26	60.3
Pisum sativum	Lumina	Fabaceae	Seed	6.3	47.6

the mass production of root exudates with satisfactory levels of hatching induction attributes and the ideal conditions for application to obtain optimum levels of hatching for two of the three studied nematode species (*G. pallida* and *H. carotae*).

In vitro screening confirmed documented information about the host range of each species. *H. schachtii* exhibited high levels of hatching with the majority of root exudates. This could in part be attributed to its limited dependency on hatching stimulants as this species has a wide host range and also know to hatch readily in water (Perry, 2002). It was further demonstrated in soil experiments that favorable soil conditions (i.e., appropriate temperature and moisture) without host root exudates were sufficient to induce hatching of up to 60% in *H. schachtii*. However, hatching factors acted as accelerators in hatching dynamic as after 2 days of exposure, the core plants within its host range such as sugar beet, oil seed rape and other Brassicaceae induced hatching above 50%. With the observed levels of hatching without the presence of host root exudates, it was deemed not necessary to advice for the incorporation of the 'suicide hatching' strategy in the management of *H. schachtii*. This was because the application of root exudates would not generate substantial gains when compared with natural conditions only or the use of resistant varieties/cultivars or traps in an intercrop.

Unlike *H. schachtii*, the hatching of the carrot cyst nematode *H. carotae* was mainly induced by carrot varieties (*Daucus carota*). However, the novel findings included five wild relative species that featured within the top ten varieties, inducing high levels of hatching. Plants belonging to other genera outside *Daucus* were unable of inducing significant levels of hatching as compared with water. These observations are in line with the referenced narrow host range of this nematode species (Aubert, 1986) with a high dependence on chemical cues emitted by the host plant for hatch induction. This reinforced the hypothesis that *H. carotae* had coevolved with wild relative of carrots for a long time in its native area before being adapted to the cultivated varieties (Gautier et al., 2019).

The hatching behavior of *G. pallida* has been extensively studied (see Perry, 2002; Masler and Perry, 2018 for reviews) and not surprisingly, our screening revealed a strong induction of hatching by solanaceous cultivated plants such as potatoes, tomatoes and eggplants. The top five plants that induced the highest levels of hatching included three European cultivated varieties of potato, one cultivated variety of eggplant and

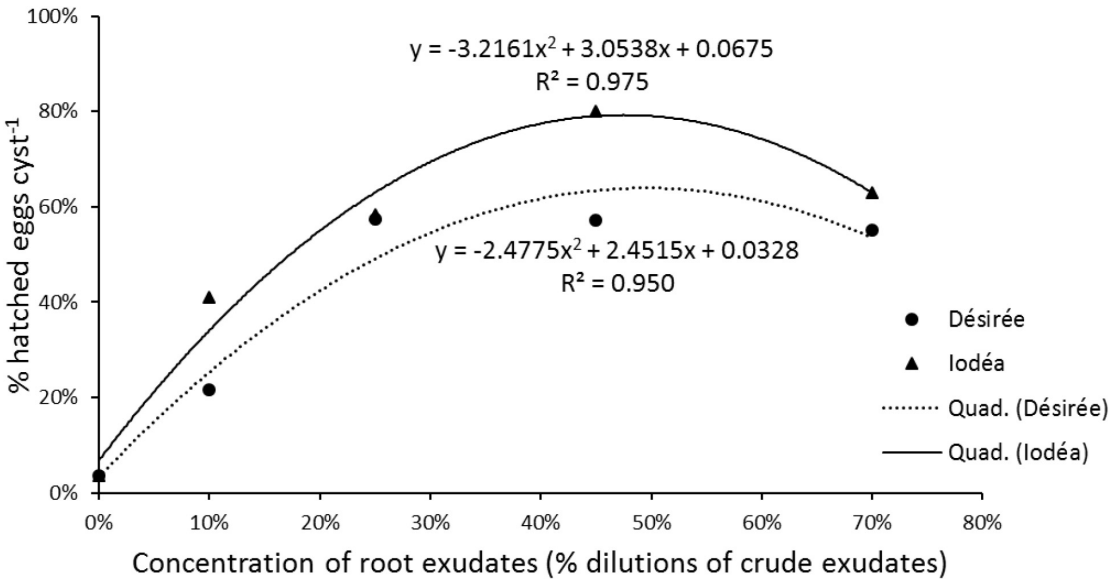

FIGURE 1 | The relationships between *in vitro* hatching of *Globodera pallida* and concentration (0, 10, 25, 45, or 70%) of the crude root exudates of *Solanum tuberosum* var. Désirée or Iodéa. The regression coefficient (R^2) and equations of the quadratic model are indicated for each potato variety. Data points represents means values of six replicates.

TABLE 2 | Percentage hatched eggs cyst^{-1} (±SE) following continuous or periodic exposure for 4 h every 6 days to root exudates over 30 days.

Nematode species	Root exudate	Dilutions (%)	Exposure time of cysts with root exudates		
			4 h every 6 days	Continuous exposure	No exposure (water)
Globodera pallida	Potato var. Désirée	30	91.9 (1.4)^a	95.7 (0.6)^a	14,1 (5.9)^b
Heterodera carotae	Carrot cv. Touchon	30	68.3 (6.8)^a	78.8 (5.9)^a	1,1 (0.9)^b
H. schachtii	Sugar beet cv. Acacia	85	98.2 (0,1)	93.2 (1.0)	93.9 (1.9)

Data across each raw with similar superscript lower case letters are not statistically different according to Tukey test (5% level of significance).

also one wild potato from South-America. Nevertheless, the distinction between host and non-host for *G. pallida* did not appear as clear as for *H. carotae,* with a stable decline from 95% in hosts to 1% hatching in non-host species (**Table 1A**). However, the screening experiment revealed some surprising results with broccoli (*Brassica oleracea* var. Italica) which induced 56.7% hatch. This was unexpected as this plant has not previously been listed in *G. pallida*'s host range, and more so, the Brassicaceae are phylogenetically far from Solanaceae. These results raised the questions whether all broccoli varieties have this ability and whether hatching is stimulated at the same level for all populations of *G. pallida* [i.e., European population and South American populations belonging to the 5 clades described by Picard et al. (2007)]. These results revealed that, it might be possible to identify non-host plants that can induce substantial hatching and that it may be interesting to screen outside the referenced host range for future use as cash and/or trap crops. The identification of specific chemical cues present in broccoli root exudates might help save time usually spent on screening assays. This would facilitate the selection for appropriate cultivated plants and varieties based on their chemical composition as well as to compare the hatching factors present in broccoli root exudates with those present in solanaceous plants.

Following the mass screening, root exudates that produced satisfactory results under *in vitro* conditions were further assessed for ideal doses and exposure times necessary to induce optimum hatching, before the confirmation of their efficiency in a more complex soil environment. The choice was driven by the ability of the root exudates to induce satisfactory levels of hatching, as well as the ease of production. Two varieties of potatoes, Désirée and Iodéa were therefore selected for potato cyst nematodes, while two varieties of carrots, Touchon and Pusa Kesar were selected for carrot cyst nematode, *H. carotae* and two sugar beet varieties, Julietta and Acacia were retained for *H. schachtii*.

In vitro experiments demonstrated that simulating the presence of the host plant by exposing *H. carotae* or *G. pallida* to their respective host root exudates at very low concentration or for very short and repeated periods induced significant hatching as compared with water control. These observations are in line with previous reports, which demonstrated that hatching factors were able to induce substantial levels of hatching in cyst nematodes at very low concentration (Masler and Perry, 2018) and that a brief exposure may as well induce similar levels of

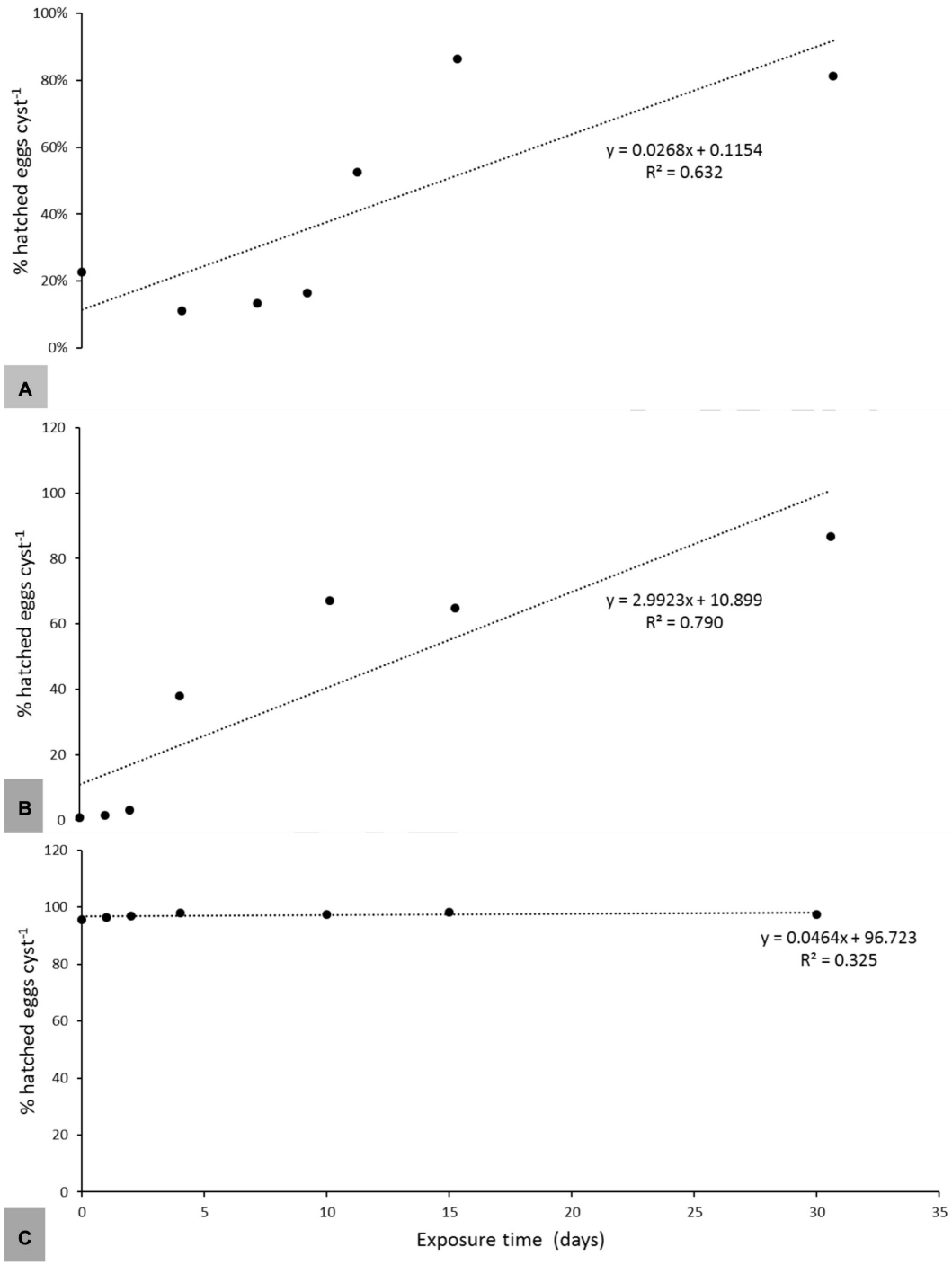

FIGURE 2 | The relationships between *in vitro* hatching of *G. pallida* **(A)**, *H. carotae* **(B)**, and *H. schachtii* **(C)** and exposure time to root exudates of *Solanum tuberosum* var. Désirée, *Daucus carota* cv. Touchon and *Beta vulgaris* cv. Acacia at 45% dilution, respectively. The regression coefficient (R^2) and equations of the linear model are indicated for each potato variety. Data points represents means values of six replicates.

hatching as a continuous exposure. There exist sufficient evidence of the hatching behavior for *G. pallida* (Perry and Beane, 1982; Perry, 2002), but little information was available on the hatching behavior of *H. carotae*. An average exposure time of 15 days to root exudates was necessary to induce satisfactory levels of hatching for both *H. carotae* and *G. pallida* with approximately over 60 and 80% hatched juveniles, respectively. For *G. pallida*, the level of hatching was comparable with hatching observed in continuous exposure to root exudates. This confirmed previous observations where 80% of encysted J2 hatched within 12 days

TABLE 3 | Characteristics of the soils used in the pot experiments with the respective sites where the soils were collected.

Soil origin	Texture	Clay (%)	Fine silt (%)	Coarse silt (%)	Fine sand (%)	Coarse sand (%)	pH
Laon, France	Sandy-soil	10,1	6,6	10,6	65,6	7,1	7,9
La Gruche, France	Silty-sand	8,5	12,8	26	8,1	44,6	6,9
Gatteville-le-Phare, France	Sandy-clay	13,4	11,9	10,5	34,3	29,9	6,8

Data across each raw with similar superscript lower case letters are not statistically different according to Tukey test (5% level of significance).

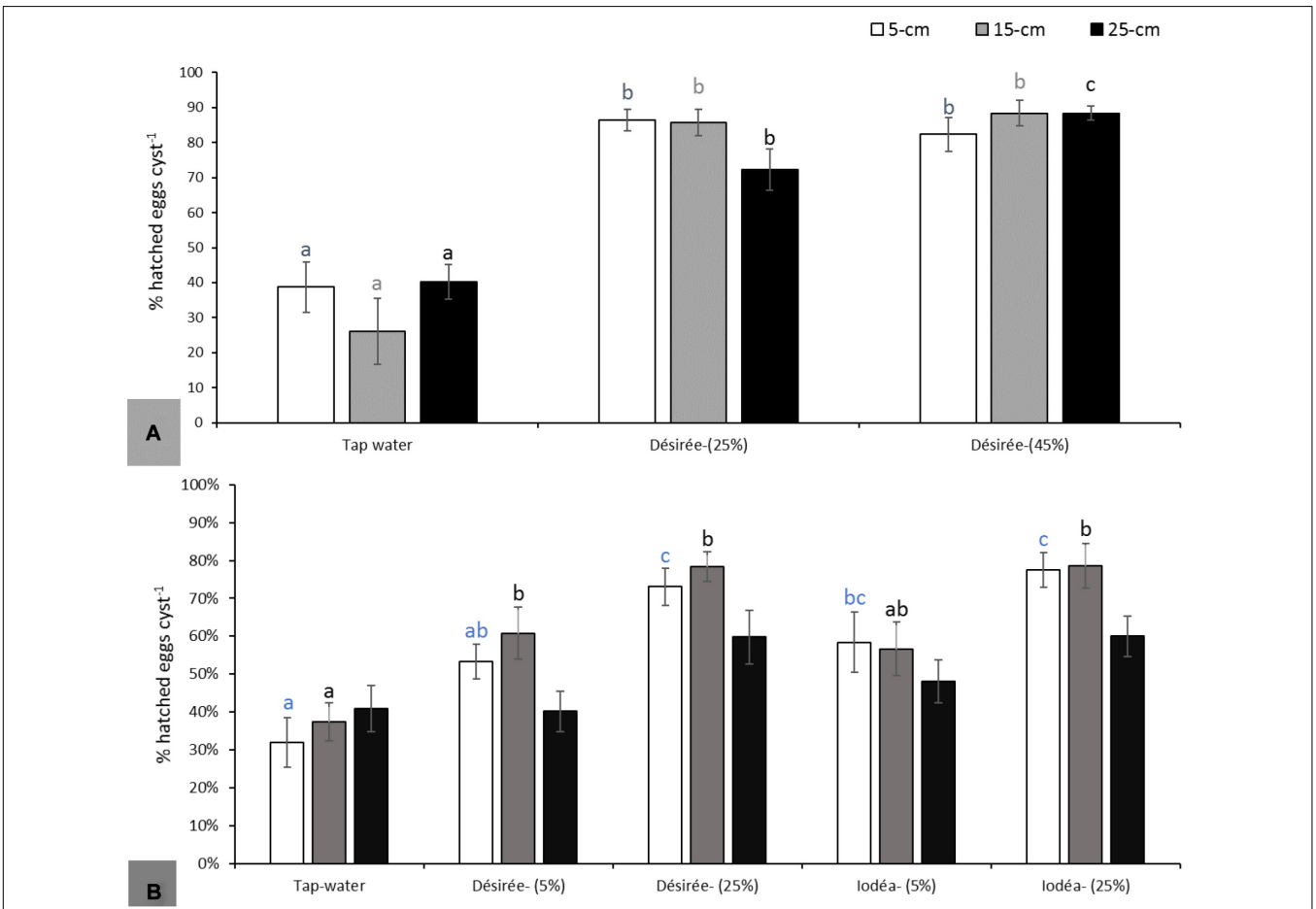

FIGURE 3 | Hatching of *Globodera pallida* at 5, 15, and 25 cm soil depth following application of Désirée or Iodéa root exudates from top soil at 5, 25, or 45% concentration of the crude root exudates as compared with tap water in 2018 **(A)** and the repeated experiments in 2019 **(B)**. Different colored lowercase letters above the error bars represent significant differences between treatments for the same soil depth according to Tukey test (5% significance level).

of exposure (Masler et al., 2008a,b), which is an adaptation by infective juveniles to maximize their chance for successful infection of young healthy roots of the host plant (LaMondia and Brodie, 1984). It was also observed that brief exposure to root exudates for 6 h every 4 days was able to stimulate similar level of hatching as in continuous exposure. The dilution of potato root exudates to concentrations as low as 10% of the crude root exudates induced satisfactory levels of hatching, which was not significantly different from hatching in root exudates diluted to 25%. Preliminary experiments conducted on *H. carotae* exhibited similar hatching behavior (data not shown), suggesting that the high sensitivity to hatching factors, coupled with the high specificity were probably shared traits between species that had a narrow host range, such as *H. carotae* and *G. pallida*.

As a follow-up from *in vitro* studies, it was necessary to assess the performance of the root exudates in a more complex soil environment, much closer to field conditions. Therefore, treatments for the pot experiments were based on observations from *in vitro* tests. Observations on *H. schachtii* revealed only a slight increase in hatching percent for treatment with root exudate as compared with water, confirming *in vitro* observations. On the contrary, *H. carotae* and *G. pallida* responded better to host root exudates as compared with water, depending on the soil depth and on the applied dose of the root exudates. Generally, hatching is optimized at soil moisture equivalent to field capacity and favorable temperatures (Masler and Perry, 2018) which matches the conditions employed in the present study (within 60–80% of field capacity, at 14–20°C).

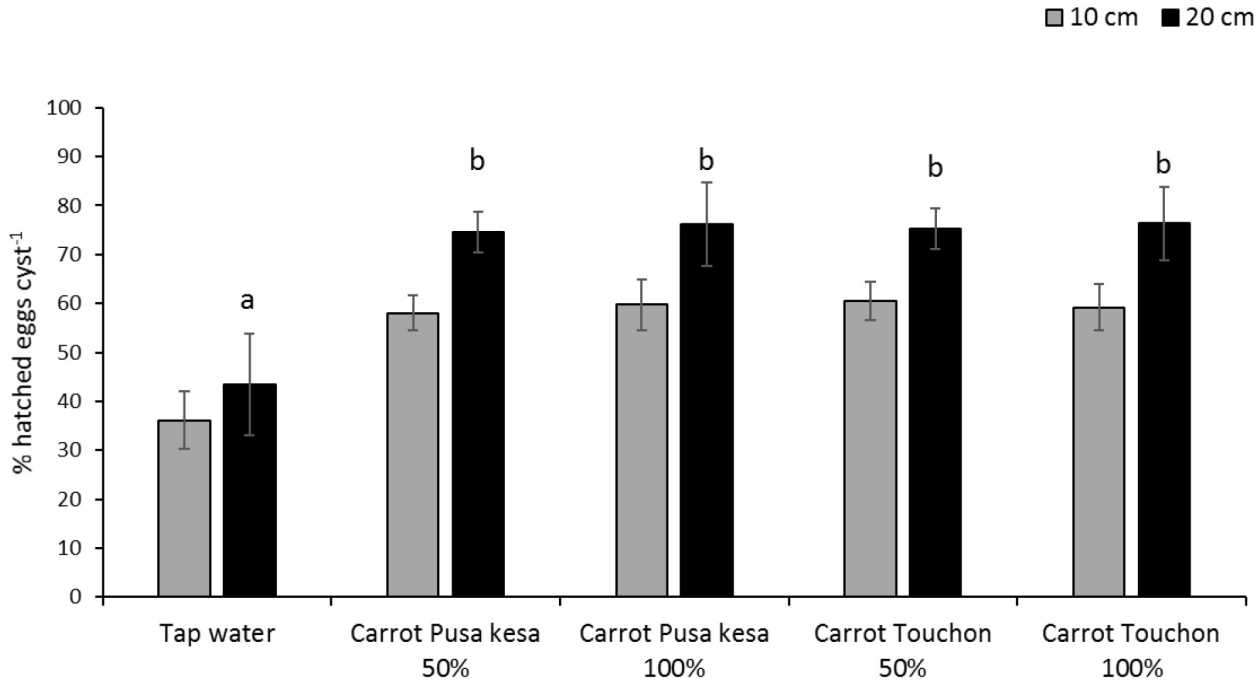

FIGURE 4 | Hatching of *Heterodera carotae* at 10 or 20 cm soil depth following application of root exudates from *Daucus carota* cv. Pusa kesa or Touchon from top soil at 50 or 100% concentration of the crude root exudates as compared with tap water. Different lowercase letters above the error bars represent significant differences between treatments at the same soil depth according to Tukey test (5% significance level).

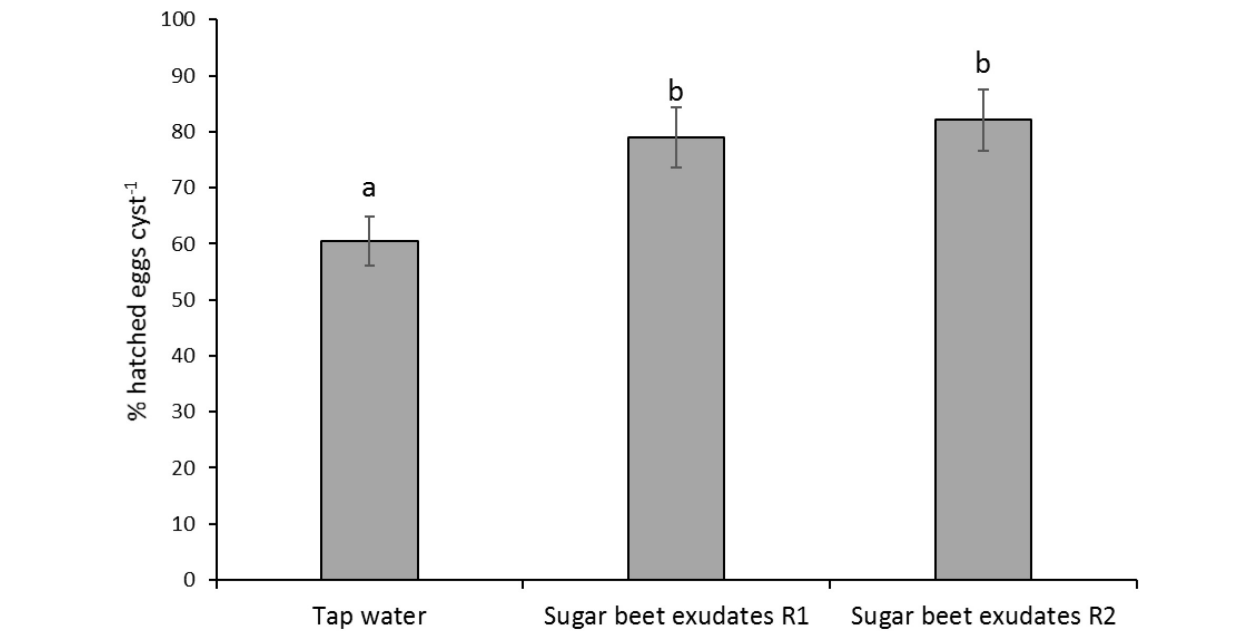

FIGURE 5 | Hatching of *Heterodera schachtii* at 4 cm soil depth following application of 15 or 30 ml root exudates of sugar beet from top soil at 100% concentration at 2 (R1) or 4 (R2) days intervals, respectively, as compared with tap water as controls. Different lowercase letters above the error bars represent significant differences between treatments according to Tukey test (5% significance level).

There was a significant dose effect for Iodéa root exudates on *G. pallida*, but not for Désirée root exudates. Likewise, concentration was not an important factor for *H. carotae* under soil conditions. For *G. pallida*, hatching was often greater within the top 15 cm of soil than at 25 cm depth, except at 45% concentration in which the level of hatching was identical

between the three soil depths investigated. The low hatch observed at 25 cm depth meant either that the root exudates did not reach the 25 cm level or that the quantity that attained this level was insufficient to stimulate the levels of hatch observed within the top 15 cm soil depth. These observations are in line with those of Ryan and Devine (2005) who demonstrated a progressive increase in PCN hatch over a period of 8 weeks post-planting, depending on the distance at which encysted eggs were incubated from the host plant. Earlier report by Rawsthorne and Brodie (1987) also demonstrated that root exudates produced near the root tip were biologically more active in hatching induction. However, unlike *G. pallida*, hatching was enhanced for *H. carotae* cysts incubated at 20 cm than for cysts incubated at 10 cm soil depth, with no observed dose effect.

From the present study, useful information could be drawn for future use of the 'suicide hatching' strategy for application on a field scale to control populations of *G. pallida* and *H. carotae*. This would involve the application of host root exudates: (i) in the absence of host crops, (ii) at a period where abiotic conditions will be favorable to hatching, (iii) at different intervals within the first 15 days or using a slow diffusion process (for granular forms) to stimulate encysted eggs to ensure optimum hatching and (iv) at a dose that allowed the induction of hatching within the vicinity of soil where cysts are usually detected (top 30 cm). These results would complement previous studies to address different challenges and select best practices. Devine and Jones (2001) investigated the effect of exogenously applied root exudates on hatching and in-egg mortality under field conditions, and although the effect of soil depth was not taken into account, the soil was rotavated following root exudates application to ensure their uniform distribution within the targeted soil profiles. Been and Schomaker (2013) reported approximately 90% of the PCN population within the upper 35 cm of soil in an infested field, while sampling at 25 cm was more uniform and represented approximately 84% of PCN population. Whitehead (1977) reported similar results for the vertical distribution of PCN, beet and pea cyst nematodes, although pea cyst nematodes were rarely found beyond 20 cm soil depth. The respective depth reported for each group of nematodes represents the vicinity within which the majority of host roots reside within the planting ridge. Under natural conditions, factors such as soil temperature, moisture, pH, organic matter content all influence the activity of hatching related compounds as well as the response of cyst nematodes to hatching chemicals (see Masler and Perry, 2018 for a review). Hatching activity induced by exogenously applied root exudates have previously been demonstrated to respond best and faster in sandy soils when compared with clay and peaty soils under field conditions (Devine and Jones, 2001). Poor results in peaty soils may in part be associated with possible sorption of hatching chemicals to organic matter, as negative correlations have previously been reported between organic matter content and hatch factors activity (Devine et al., 2001). In the present study, sandy soils were used for all groups of nematodes, and gave satisfactory results.

In addition to the influence of these parameters, major challenges will be (i) to ensure that soil biological communities have no impact on efficiency of hatching factors, or if it will have to be consider by adjusting the doses for instance, and (ii) to chemically identify hatching factors for both species for mass production and at a lower cost which would compensate for deregistered chemicals previously used in controlling these groups of cyst nematodes. Field validation of these observations are now needed.

DATA AVAILABILITY STATEMENT

The raw data supporting the conclusions of this article will be made available by the authors, without undue reservation.

AUTHOR CONTRIBUTIONS

All experimental protocols were jointly discussed and developed by the CMI, FN3PT/inov3PT, INRAE, and SILEBAN scientific and technical team. BN, MI, and PD established and assessed the laboratory and glasshouse experiments involving *Globodera pallida* conducted at FN3PT/inov3PT, and supervised by VG, AB, and A-CLR. NM, M-CD, CaP, and ChP established and assessed the laboratory and glasshouse experiments involving *Globodera pallida* and *Heterodera schachtii* conducted at IGEPP, and supervised by JM and SF. ER and AC established and assessed the laboratory and glasshouse experiments involving *Heterodera carotae* conducted at SILEBAN. Host root exudates for potato and beet cyst nematodes were produced at FN3PT/inov3PT, and IGEPP, respectively. Carrot root exudate production was jointly developed by SILEBAN and CMI, performed at SILEBAN, and supervised by ER and AC. Root exudate analyses was done at CIM Groupe-Roullier and coordinated by EN-O and J-CY, who also supervised the analysis for soil particle size distribution for the soils used in glasshouse experiments. All authors contributed to the article and approved the submitted version.

FUNDING

This work was funded by ADEME (Agence de l'Environnement et de la Maîtrise de l'Energie) through the French "Programme Investissement d'Avenir" (PIA) BIODERA Project (n°: 1682C0289) which was coordinated by the Centre Mondial de l'Innovation - Roullier.

REFERENCES

Aubert, V. (1986). "Hatching of the carrot cyst nematodes," in *Cyst Nematodes*, eds F. Lamberti and C. E. Taylor (New York, NY: Plenum Press), 347–348. doi: 10.1007/978-1-4613-2251-1_26

Bairwa, A., Venkatasalam, E. P., Umamaheswari, R., Sudha, R., and Singh, B. P. (2017). Effect of cultural practices on potato cyst nematode population dynamics and potato tuber yield. *Indian J. Hortic.* 74, 91–96. doi: 10.5958/0974-0112.2017.00021.4

Been, T. H., and Schomaker, C. H. (2013). "Distribution patterns and sampling," in *Plant Nematology*, 2nd Edn, eds R. N. Perry and M. Moens (Wallingford: CAB International), 331–358. doi: 10.1079/9781780641515.0331

Chen, S. Y., Porter, P. M., Orf, J. H., Reese, C. D., Stienstra, W. C., Young, N. D., et al. (2001). Soybean cyst nematode population development and associated soybean yields of resistant and susceptible cultivars in Minnesota. *Plant Dis.* 85, 760–766. doi: 10.1094/PDIS.2001.85.7.760

Devine, K. J., Byrne, J., and Jones, P. W. (2001). In vitro studies on the relative availability and mobility in soil of natural hatching factors for the potato cyst nematodes, *Globodera rostochiensis* and *G. pallida*. *Nematology* 3, 75–83. doi: 10.1163/156854101300106919

Devine, K. J., and Jones, P. W. (2000). Response of *Globodera rostochiensis* to exogenously applied hatching factors in soil. *Ann. Appl. Biol.* 137, 21–29. doi: 10.1111/j.1744-7348.2000.tb00053.x

Devine, K. J., and Jones, P. W. (2001). Effects of hatching factors on potato cyst nematode hatch and in-egg mortality in soil and in vitro. *Nematology* 3, 65–74. doi: 10.1163/156854101300106900

Evans, K. (1983). Hatching of potato cyst nematodes in root diffusates collected from 25 potato cultivars. *Crop Protection* 2, 97–103. doi: 10.1016/0261-2194(83)90029-7

Evans, K., and Stone, A. (1977). A review of the distribution and biology of the potato cyst-nematodes *Globodera rostochiensis* and *G. pallida*. *PANS* 23, 178–189. doi: 10.1080/09670877709412426

Franco, J., Main, G., and Oros, R. (1999). Trap crops as a component for the integrated management of *Globodera* spp. (potato cyst nematodes) in Bolivia. *Nematropica* 29, 51–60.

Fukuzawa, A., Furusaki, A., Ikura, M., and Masamune, T. (1985a). Glycinoeclepin A, a natural hatching stimulant for the soybean cyst nematode. *J. Chem. Soc.* 4, 222–224. doi: 10.1039/c39850000222

Fukuzawa, A., Matsue, H., Ikura, M., and Masamune, R. (1985b). Glycinoeclepins B and C, nortriterpenes related to glycinoeclepin A. *Tetrahedron Lett.* 26, 5539–5542. doi: 10.1016/s0040-4039(01)80882-0

Gautier, C., Esquibet, M., Fournet, S., Piriou, C., Yvin, J. C., Nguema-Ona, E., et al. (2019). Microsatellite markers reveal two genetic groups in European populations of the carrot cyst nematode *Heterodera carotae*. *Infection Genet. Evol.* 73, 81–92. doi: 10.1016/j.meegid.2019.04.011

Johnson, J. B., and Omland, K. S. (2004). Model selection in ecology and evolution. *Trends Ecol. Evol.* 19, 101–108. doi: 10.1016/j.tree.2003.10.013

Jones, T. J., Annelies, H., Etienne, G. J. D., Hari, S. G., Johannes, H., Michael, G. K. J., et al. (2013). Top 10 plant-parasitic nematodes in molecular plant pathology. *Mol. Plant Pathol.* 14, 946–961. doi: 10.1111/mpp.12057

Kushida, A., Suwa, N., Ueda, Y., and Momota, Y. (2003). Effects of *Crotalaria juncea* and *C. spectabilis* on hatching and population density of the soybean cyst nematode, *Heterodera glycines* (Tylenchida: Heteroderidae). *Appl. Entomol. Zool.* 38, 393–399. doi: 10.1303/aez.2003.393

LaMondia, J. A., and Brodie, B. B. (1984). Control of *Globodera rostochiensis* by solar heat. *Plant Dis.* 68, 474–476. doi: 10.1094/PD-69-474

Marks, R. J., and Brodie, B. B. (1998). *Potato Cyst Nematodes: Biology, Distribution and Control*. Wallingford: CAB International.

Masamune, T., Anetai, M., Takasugi, M., and Katsui, N. (1982). Isolation of a natural hatching stimulus, glycinoeclepin A, for the soybean cyst nematode. *Nature* 297, 495–496. doi: 10.1038/297495a0

Masler, E. P., Donald, P. A., and Sardanelli, S. (2008a). Stability of *Heterodera glycines* (Tylenchida: Heteroderidae) juvenile hatching from eggs obtained from different sources of soybean, Glycine max. *Nematology* 10, 271–278. doi: 10.1163/156854108783476322

Masler, E. P., and Perry, R. N. (2018). *Hatch, Survival and Sensory Perception. Cyst Nematodes*. Oxforshire: CAB International, 44–73.

Masler, E. P., Zasada, I. A., and Sardanelli, S. S. (2008b). Hatching behavior in *Heterodera glycines* in response to low temperature. *Comp. Parasitol.* 75, 76–81. doi: 10.1654/4292.1

Mugniéry, D., and Bossis, M. (1988). *Heterodera carotae* Jones, (1950). Gamme d'hôtes, vitesse de développement, cycle. *Rev. Nématol.* 11, 307–313.

Ngala, B. M., Haydock, P. J., Wood, S., and Back, M. A. (2014).). Biofumigation with *Brassica juncea*, *Raphanus sativus* and *Eruca sativa* fort the management of field populations of the potato cyst nematode *Globodera pallida*. *Pest Manage. Sci.* 71, 759–769. doi: 10.1002/ps.3849

Nicol, J. M., Turner, S. J., Coyne, D. L., den Nijs, L., Hockland, S., and Maafi, Z. T. (2011). "Current nematode threats to world agriculture," in *Genomics and Molecular Genetics of Plant–Nematode Interactions*, eds J. Jones, G. Gheysen, and C. Fenoll (Dordrecht: Springer), 21–43. doi: 10.1007/978-94-007-0434-3_2

Perry, R. (2002). "Hatching," in *The Biology of Nematodes*, ed. D. L. Lee (Abingdon: Taylor & Francis), 147–170.

Perry, R. N., and Beane, J. (1982). The effect of brief exposures to potato root difusate on the hatching of *Globodera rostochiensis*. *Rev. Nematol.* 5, 221–224.

Picard, D., Sempere, T., and Plantard, O. (2007). A northward colonisation of the Andes by the potato cyst nematode during geological times suggests multiple host-shifts from wild to cultivated potatoes. *Mol. Phylogenet. Evol.* 42, 308–316. doi: 10.1016/j.ympev.2006.06.018

Rawsthorne, D., and Brodie, B. B. (1987). Movement of potato root diffusate through the soil. *J. Nematol.* 19, 119–122.

Robinson, M., Atkinson, H., and Perry, R. (1987). The influence of temperature on the hatching activity and lipid utilization of second stage juveniles of the potato cyst nematodes *Globodera rostochiensis* and *G. pallida*. *Rev. Nematol.* 10, 349–354.

Ryan, A., and Devine, K. J. (2005). Comparison of the in-soil hatching responses of *Globodera rostochiensis* and *G. pallida* in the presence and absence of the host potato crop cv. British Queen. *Nematology* 7, 587–597. doi: 10.1163/156854105774384804

Scholte, K. (2000). Screening of non-tuber bearing Solanaceae for resistance to and induction of juvenile hatch of potato cyst nematodes and their potential for trap cropping. *Ann. Appl. Biol.* 136, 239–246. doi: 10.1111/j.1744-7348.2000.tb00030.x

Storey, R. M. J. (1984). The relationship between neutral lipid reserves and infectivity for hatched and dormant juveniles of *Globodera* spp. *Ann. Appl. Biol.* 104, 511–520. doi: 10.1111/j.1744-7348.1984.tb03034.x

Subbotin, S. A., Mundo-Ocampo, M., and Baldwin, J. G. (2010). "Systematics of cyst nematodes (Nematoda: Heteroderinae)," in *Nematology Monographs and Perspectives 8A Series*, eds D. J. Hunt and R. N. Perry (Leiden: Brill).

Turner, S. J., and Subbotin, S. A. (2013). "Cyst nematodes," in *Plant Nematology*, 2nd Edn, eds R. N. Perry and M. Moens (Wallingford: CAB International), 109–143.

Whitehead, A. G. (1977). Vertical distribution of potato, beet and pea cyst nematodes in some heavily infested soils. *Plant Pathol.* 26, 85–90. doi: 10.1111/j.1365-3059.1977.tb01029.x

Widdowson, E., and Wiltshire, G. H. (1958). The potato eelworm hatching factor. *Ann. Appl. Biol.* 46, 95–101. doi: 10.1111/j.1744-7348.1958.tb02181.x

Conflict of Interest: The authors declare that the research was conducted in the absence of any commercial or financial relationships that could be construed as a potential conflict of interest.

frontiers in Plant Science

ORIGINAL RESEARCH
published: 08 March 2021
doi: 10.3389/fpls.2021.640459

Comparative Secretome and Functional Analyses Reveal Glycoside Hydrolase Family 30 and Cysteine Peptidase as Virulence Determinants in the Pinewood Nematode *Bursaphelenchus xylophilus*

Ryoji Shinya[1]*†, Haru Kirino[1]†, Hironobu Morisaka[2], Yuko Takeuchi-Kaneko[2], Kazuyoshi Futai[2] and Mitsuyoshi Ueda[2]

[1] School of Agriculture, Meiji University, Kawasaki, Japan, [2] Graduate School of Agriculture, Kyoto University, Kyoto, Japan

Pine wilt disease, caused by the pinewood nematode, *Bursaphelenchus xylophilus*, is one of the world's most serious tree diseases. Although the *B. xylophilus* whole-genome sequence and comprehensive secretome profile have been determined over the past decade, it remains unclear what molecules are critical in pine wilt disease and govern *B. xylophilus* virulence in host pine trees. Here, a comparative secretome analysis among four isolates of *B. xylophilus* with distinct virulence levels was performed to identify virulence determinants. The four candidate virulence determinants of *B. xylophilus* highly secreted in virulent isolates included lipase (Bx-lip1), glycoside hydrolase family 30 (Bx-GH30), and two C1A family cysteine peptidases (Bx-CAT1 and Bx-CAT2). To validate the quantitative differences in the four potential virulence determinants among virulence groups at the protein level, we used real-time reverse-transcription polymerase chain reaction analysis to investigate these determinants at the transcript level at three time points: pre-inoculation, 3 days after inoculation (dai), and 7 dai into pine seedlings. The transcript levels of *Bx-CAT1*, *Bx-CAT2*, and *Bx-GH30* were significantly higher in virulent isolates than in avirulent isolates at pre-inoculation and 3 dai. A subsequent leaf-disk assay based on transient overexpression in *Nicotiana benthamiana* revealed that the GH30 candidate virulent factor caused cell death in the plant. Furthermore, we demonstrated that Bx-CAT2 was involved in nutrient uptake for fungal feeding via soaking-mediated RNA interference. These findings indicate that the secreted proteins Bx-GH30 and Bx-CAT2 contribute to *B. xylophilus* virulence in host pine trees and may be involved in pine wilt disease.

Keywords: pinewood nematode, secreted protein, virulence determinant, *Nicotiana benthamiana*, glycoside hydrolase family 30, cysteine peptidase

OPEN ACCESS

Edited by:
Juan Emilio Palomares-Rius, Consejo Superior de Investigaciones Científicas (CSIC), Spain

Reviewed by:
Lee Robertson, National Institute for Agricultural and Food Research and Technology, Spain
Margarida Espada, University of Évora, Portugal

***Correspondence:**
Ryoji Shinya
shinya@meiji.ac.jp

† *These authors have contributed equally to this work*

Specialty section:
This article was submitted to Plant Pathogen Interactions, a section of the journal Frontiers in Plant Science

Received: *11 December 2020*
Accepted: *03 February 2021*
Published: *08 March 2021*

Citation:
Shinya R, Kirino H, Morisaka H, Takeuchi-Kaneko Y, Futai K and Ueda M (2021) Comparative Secretome and Functional Analyses Reveal Glycoside Hydrolase Family 30 and Cysteine Peptidase as Virulence Determinants in the Pinewood Nematode Bursaphelenchus xylophilus. Front. Plant Sci. 12:640459. doi: 10.3389/fpls.2021.640459

INTRODUCTION

Pine wilt disease, caused by the pinewood nematode (PWN), *Bursaphelenchus xylophilus*, is one of the most serious tree diseases worldwide because pine forests are essential sources of forest products. Moreover, pine trees are used in wind-, tide-, and sand-breaks, as well as in landslide prevention and to beautify landscapes. However, pine forests face a catastrophic threat from pine wilt disease in East Asian countries. The disease was first discovered in the early 20th century in Japan, following its introduction from the United States, and *B. xylophilus* was identified as the etiologic agent of the disease in 1971 (Kiyohara and Tokushige, 1971). In the 1980s, the pathogen spread to neighboring East Asian countries (Yi et al., 1989), and was subsequently isolated in Portugal in 1999 (Mota et al., 1999) and in Spain in 2008 (Abelleira et al., 2011). Because of active international trade in forest products, the PWN poses a potentially serious problem in both the Southern and Northern Hemispheres. Thus, the PWN is currently a worldwide threat.

There is a significant variation among *B. xylophilus* isolates in terms of level of virulence in pine trees (Kiyohara and Bolla, 1990; Akiba, 2006). Virulent isolates of *B. xylophilus* can effectively kill pine seedlings when thousands of nematodes are inoculated into 2–3-year-old pine seedlings. However, avirulent isolates typically kill pine seedlings only when host pines are exposed to stresses such as low light conditions (Ikeda, 1996). In addition to differences in virulence to host pines, remarkable differences have been observed in various biological characteristics between virulent and avirulent isolates (e.g., transmission to vector beetles, reproduction in healthy pine trees and on a fungal mat, and tolerance to oxidative stress) (Kiyohara and Bolla, 1990; Aikawa et al., 2003; Aikawa and Kikuchi, 2007; Shinya et al., 2012; Vicente et al., 2015). Several reports investigated the genetic diversity and the difference in gene expression patterns to identify the factors that control these phenotypic differences between virulent and avirulent isolates (Palomares-Rius et al., 2015; Ding et al., 2016; Filipiak et al., 2020). These studies reported candidate molecules that may be related to the virulence of *B. xylophilus* and significant differences in peptidases and antioxidant enzymes between virulent and avirulent isolates. However, the mechanisms that determine the differences in these *B. xylophilus* traits remain unclear due to the lack of effective functional analysis.

Here, we focused on *B. xylophilus* secreted proteins to investigate the mechanisms underlying the differences in these *B. xylophilus* traits, especially virulence in host pines. Secreted proteins of plant-parasitic nematodes are considered important for their parasitism. Several molecules have been suggested as *B. xylophilus* pathogenic factors: cell-wall-degrading enzymes secreted by the PWN (Odani et al., 1985; Kikuchi et al., 2004, 2006), venom allergen-like proteins (Kang et al., 2012), sphingolipid activator protein (Hu et al., 2019), thaumatin-like proteins (Kirino et al., 2020), cysteine protease inhibitors (Kirino et al., 2020), and PWN-associated bacterial toxins (Han et al., 2003; Zhao and Lin, 2005). The previous proteomic and transcriptomic analyses revealed the comprehensive profile and unique characteristics of *B. xylophilus* secreted proteins (Shinya et al., 2013; Cardoso et al., 2016; Espada et al., 2016, 2018). However, the contribution of each molecule to *B. xylophilus* virulence in pines and the development of pine wilt disease remains unclear because no systematic screening of virulence factors has been performed. Moreover, there are few functional analysis tools available for *B. xylophilus* (e.g., transgenesis and CRISPR/Cas9).

In this study, a comparative secretome analysis among four isolates of *B. xylophilus* with distinct virulence levels was performed to identify virulence determinants. We presumed that different expression levels of secreted proteins among groups with disparate virulence would reflect involvement in PWN pathogenicity. Here, we demonstrated that four proteins were highly expressed in virulent isolates. A subsequent leaf-disc assay based on transient overexpression in *Nicotiana benthamiana* revealed that one of four candidate virulent factors, glycoside hydrolase family 30 (GH30), was able to cause plant cell death. Furthermore, we demonstrated that Bx-CAT2 was involved in nutrient uptake for fungal feeding via soaking-mediated RNA interference.

MATERIALS AND METHODS

Nematodes Used in Comparative Proteome Analysis

Four isolates of *B. xylophilus* were used in this study: two virulent isolates (Ka4 and S10) and two avirulent isolates (OKD-1 and C14-5) (Aikawa and Kikuchi, 2007; Zhou et al., 2007). Ka4 and S10 were originally isolated from *Pinus densiflora* in 1994 and 1982, respectively. C14-5 was originally isolated from the Japanese pine sawyer, *Monochamus alternatus*, emerged from *P. densiflora* in 1975 with low virulence (Kiyohara, 1989). OKD-1 was originally isolated from *Pinus thunbergii* in 1984, and its virulence level was decreased during subculturing on the fungus *Botrytis cinerea* (Kawazu et al., 1996). A mixed culture of the propagative forms, including second- (J2), third- (J3), and fourth-stage juveniles (J4), as well as adults and eggs, were propagated on the fungus *B. cinerea* on potato dextrose agar medium (*Nissui*-seiyaku) containing 100 units/ml penicillin and 100 μg/ml streptomycin at 25°C. After incubation for 10 days, the PWNs were extracted from the culture for 6 h using the Baermann funnel technique (Baermann, 1917), then washed 10 times in sterile water containing 100 units/ml penicillin, 100 μg/ml streptomycin, and 0.25 μg/ml amphotericin B.

Production and Preparation of Secreted Proteins for Comparative Secretome Analysis

To induce the secretion of PWN proteins, PWN populations (1×10^7 nematodes per isolate) were soaked in 5-ml pine wood extracts on a 100-mm low attachment surface plate (EZ-BindShut dish; Iwaki) at 28°C for 16 h with agitation. The pine wood extract was prepared from nematode non-inoculated 3-year-old Japanese black pine, *P. thunbergii*, seedlings that is susceptible to PWN according to the method described in Shinya et al. (2013).

The nematodes were then pelletized by centrifugation at 800 × *g* for 5 min at 25°C, and the supernatant was collected. Each resulting protein solution was desalted and buffer-exchanged in PD-10 columns (GE Healthcare) with 20 mM Tris-HCl (pH 8.0), in accordance with the manufacturer's protocol. The solution containing secreted proteins was subsequently concentrated to 800 μl using an Amicon Ultra centrifugal filter (Millipore) with a 3-kDa cutoff, then subjected to two-dimensional high-performance liquid chromatography (2D-HPLC) analysis without adjusting the protein concentration. Three biological replicates were analyzed for each isolate.

Protein Separation Using 2D-HPLC and Sodium Dodecyl Sulfate-Polyacrylamide Gel Electrophoresis

The extracted and desalted mass proteins were separated on a 2D-HPLC system using an ion-exchange column for the first dimension and a reverse-phase monolithic column for the second dimension (Morisaka et al., 2012). The 2D-HPLC system consisted of PU-712 and PU-714 pumps (GL Sciences), two trap columns (Nacalai Tesque), a 7725 injector (Rheodyne), a MU-701 UV detector (GL Sciences), and a 10-port valve MV-790 (GL Sciences). Raw chromatographic ASCII formatted data files were collected with EZChrom Elite software (GL Sciences). The secreted proteins were separated into six (F1–F6) fractions for the first-dimension extraction in ion-exchange mode. An anion-exchange column, NUCLEOSIL 4000-7 PEI (MACHEREY-NAGEL), was used with a flow rate of 0.8 ml/min for the ion-exchange mode for the first-dimension extraction. A gradient was provided by changing the mixing ratio of two eluents: A, 20 mM Tris/HCl (pH 8.2) and B, 20 mM Tris/HCl (pH 8.2) containing 1 M NaCl. The gradient involved six steps (F1–F6) with 0, 10, 20, 30, 50, or 100% B for 3 min. Each fraction was loaded into the second-dimension column through a 10-port valve and separated in reverse-phase mode. In reverse-phase mode, a wide-pore monolithic column [5 cm length, 2.3 mm inner diameter (ID)] was used with a flow rate of 1.0 or 1.5 ml/min. A gradient was provided by changing the mixing ratio of two eluents: C, 0.1% (v/v) trifluoroacetic acid and D, acetonitrile containing 0.1% (v/v) trifluoroacetic acid. The gradient initially contained 10% B, which was increased to 60% B for 5 or 3 min, then increased to 95% B to wash the column, and finally restored to the initial conditions and maintained for re-equilibration of the column. Because no protein was detected in fractions from 0 to 2 min in the preliminary test, the fractions including separated proteins were collected only from 2 min to 4.5 min at 30-s intervals for each ion-exchange mode fraction (F1–F6). In total, 30 fractions were collected during 2D-HPLC analysis. These fractions were dried by vacuum centrifugation and re-suspended in 10 μl of phosphate-buffered saline (pH 7.4). The re-suspended samples were mixed with an equal volume of 2× sodium dodecyl sulfate (SDS) sample buffer, then heated at 100°C for 3 min prior to loading onto a gel for subsequent SDS-polyacrylamide gel electrophoresis (SDS-PAGE) analysis.

Tricine SDS-PAGE and Laemmli SDS-PAGE systems were used. The fractions from 2 to 3 min (total of 12 fractions) were separated using a Tricine SDS-PAGE system with 15% Tris-tricine gels (e-PAGEL; ATTO) and a standard minislab PAGE apparatus (model AE-6500; ATTO) to separate low-molecular-weight proteins. Low-Range Rainbow Molecular Weight Markers (GE Healthcare) were used to determine the molecular masses of the proteins. In addition, the fractions from 3 to 4.5 min (total of 18 fractions) were separated using a Laemmli SDS-PAGE system with 5–20% gradient gels (e-PAGEL; ATTO). Full-Range Rainbow Molecular Weight Markers (GE Healthcare) were used to determine the molecular masses of the proteins. The proteins were silver-stained using a Sil-Best staining kit (Nacalai Tesque), in accordance with the manufacturer's instructions.

Gel Band Visualization and Relative Quantification

ImageJ software (National Institutes of Health, version 1.42) was used for relative quantitative densitometric analysis of gel band intensities. Eighty-nine selected bands with high repeatability were quantified based on their relative intensities. A relative fold change value was calculated for each gel band, compared with the expected value. The densitometry values for three independent replicates of each sample were subjected to Bartlett's test to determine whether equal variances were present. When Bartlett's test indicated that the group variances were equal, one-way analysis of variance (ANOVA) was performed, followed by Tukey's multiple comparison *post hoc* test. When the group variances were unequal, the non-parametric Kruskal–Wallis multiple comparison *post hoc* test was used. A *P*-value of <0.01 was regarded as indicating statistical significance. Furthermore, fold changes in gel band intensities were calculated among isolates. Finally, proteins with gel bands with statistically significant fold change values that constituted >5-fold greater intensities for both virulent isolates (Ka4 and S10) relative to the avirulent isolates (C14-5 and OKD-1) were regarded as potential "virulence determinants" in this study. The log-transformed expression ratios of the 89 protein bands were subjected to hierarchical analysis with CLUSTER software and visualized in a clustergram with TreeView software.

Tryptic In-Gel Digestion

In-gel digestion was performed as follows. Only the protein bands from Ka4 isolate were used for subsequent analysis. In accordance with the manufacturer's protocol, protein bands with significant differences between samples were excised and destained using the Sil-Best Destain Kit (Nacalai Tesque). The destained gels were dehydrated in 100 μl of acetonitrile and completely dried via vacuum centrifugation. The excised gel pieces were incubated in freshly prepared 10 mM dithiothreitol/25 mM ammonium hydrogen carbonate (NH_4HCO_3) at 56°C for 1 h. The proteins were then alkylated in 55 mM iodoacetamide/25 mM NH_4HCO_3 in the dark for 45 min at room temperature. The gel pieces were subsequently dehydrated twice in 200 μl of 25 mM NH_4HCO_3 in 50% acetonitrile, then dried via vacuum centrifugation for 15 min. The samples were incubated in 20 μl of 50 mM NH_4HCO_3 containing 10 μg/ml trypsin (Promega Diagnostics) for 12 h at 37°C. Following enzymatic digestion, the resultant

peptides were extracted twice with 50 μl and then 25 μl of 0.1% trifluoroacetic acid in 50% acetonitrile, and concentrated to 10–15 μl via vacuum centrifugation. Furthermore, the peptides were desalted using a MonoTip C18 (GL Sciences) and eluted with 0.1% trifluoroacetic acid in 50% acetonitrile.

Nano Liquid Chromatography-Tandem Mass Spectrometry Analysis

Protein identification was performed using a liquid chromatography (LC; EASY-nLC II, Thermo Scientific)-mass spectrometry (MS; LTQ Velos orbitrap mass spectrometer, Thermo Scientific) system. First, 10 μl of proteolysis products was injected and separated via reverse-phase chromatography using a packed tip column (NTCC-360, 100 mm × 75 μm ID, Nikkyo Technos), at a flow rate of 300 nl/min. A gradient was achieved by changing the mixing ratio of two eluents: A, 0.1% (v/v) formic acid, and B, acetonitrile containing 0.1% (v/v) formic acid. The gradient was initiated with 5% B, increased to 40% B for 45 min, further increased to 95% B to wash the column, then returned to the initial condition, and maintained for re-equilibration. The separated analytes were detected on a mass spectrometer (with a full scan range of 300–2,000 m/z). The method was designed to automatically analyze the 10 ions with the highest intensity as observed in the MS scan for data-dependent acquisition. An ESI voltage of 1.5 kV was applied directly to the LC buffer distal to the chromatography column using a microtee. The ion-transfer tube temperature in the LTQ Velos ion trap was set at 250°C. The MS data were used for protein identification with Mascot software (Matrix Science), with a protein database built from *B. xylophilus* genome data (Kikuchi et al., 2011). MS/MS spectra were collected for *B. xylophilus* secreted proteins (**Supplementary Data Sheets 1–4**). The enzyme parameter was limited to full tryptic peptides with the maximum mis-cleavage default setting (carbamidomethylation of cysteines, ±6 ppm for precursor ions, ±0.6 Da for fragment ions). A concatenated forward-reverse database was constructed to calculate the *in situ* false discovery rate (Shaffer, 1995). An identification filtering criterion—1% false discovery rate—was used at the peptide level for each search.

Gene Expression of Potential Virulence Determinants in Relation to Infection Process

Quantitative real-time polymerase chain reaction (PCR) analysis was used to quantify the gene expression levels of four potential virulence determinants: *Bx-lip1* (BUX.s00961.62), *Bx-GH30* (BUX.s00713.1066), *Bx-CAT1* (BUX.s01288.15), and *Bx-CAT2* (BUX.s00813.52).

Nematode Preparation and Inoculation Into Pine Seedlings

Four isolates of *B. xylophilus* were used in this experiment: two virulent isolates (Ka4 and S10) and two avirulent isolates (C14-5 and OKD-1). To investigate the gene expression levels of PWN target genes during *in vitro* culture and infection of pine seedlings, nematodes were propagated on the fungus *Botrytis cinerea* on potato dextrose agar at 25°C. After 10 days of incubation, nematodes were collected and 60,000 of each isolate was used to inoculate 3-year-old Japanese black pine seedlings following the method described by Shinya et al. (2010). At 3 and 7 days after inoculation (dai), the nematodes were extracted from woody pieces of inoculated seedlings using the Baermann funnel technique for 3 h, then washed five times in sterile water. The nematodes collected at three different time points (pre-inoculation, 3 dai, and 7 dai into pine seedlings) were prepared for total RNA extraction.

Preparation of Template cDNA via RNA Extraction and Reverse Transcription

For the extraction of total RNA, 5,000 nematodes of each isolate were used at each time point. Three biological replicates of each treatment were performed. Nematodes were ground to powder in liquid nitrogen using a mortar and pestle, and total RNA was extracted and purified with a RNeasy Plus Micro kit (Qiagen), in accordance with the manufacturer's protocol. Reverse transcription (RT) was performed with 500 ng of total RNA from each treatment using a ReverTra Ace qPCR RT kit (Toyobo), in accordance with the manufacturer's protocol. Transcribed cDNA was adjusted to 500 ng/μl and subjected to quantitative real-time PCR analysis.

Quantitative Real-Time PCR to Investigate Gene Expression of Potential Virulence Determinants During Host Infection

For each target gene, a primer pair was selected with Primer Express 3.0 software (Applied Biosystems) using the default settings for SYBR Green real-time PCR analyses. These primers were designed based on the genome sequence of *B. xylophilus* (Kikuchi et al., 2011). The nucleotide sequences of the primers are shown in **Supplementary Table 1**. The reaction mixture for real-time amplification included 12.5 μl of Power SYBR Green PCR Master Mix (Applied Biosystems), 1 μl of each primer (10 μM), 1 μl of template DNA, and 9.5 μl of distilled water. The real-time PCR conditions were as follows: an initial hot start at 95°C for 10 min, then 40 cycles of denaturation at 95°C for 15 s and annealing and extension at 60°C for 1 min. The reactions were performed on an Applied Biosystems 7500 real-time PCR system. The system software provided was used for standard curve analysis of the results. To correct for inter-sample variation, the β-tubulin gene (BUX.s01109.465) of the Ka4 isolate of *B. xylophilus* was used as an internal control. Three biological replicate samples were analyzed for each treatment–time combination with three technical replicates per sample. Gene expression levels were determined relative to that of the OKD-1 isolate on fungus (pre-inoculation). The statistical analysis was performed using a Tukey's HSD test.

Gateway Plasmid Construction for Leaf-Disk Assay With *N. benthamiana*

A leaf-disk assay based on transient overexpression in *N. benthamiana* was performed to allow functional screening of candidate virulence determinants of the PWN, in accordance with the method used by Kirino et al. (2020). Total RNA was

extracted from mixed-stage nematodes and purified using a RNeasy Mini kit (Qiagen) for this assay, in accordance with the manufacturer's protocol. RT was performed with 1 μg of total RNA using a PrimeScript™ II 1st strand cDNA Synthesis kit (Takara Bio Inc.), in accordance with the manufacturer's protocol. The transcribed cDNA was adjusted to a concentration of 200 ng/μl and subjected to PCR amplification. The sequences of *Bx-lip1*, *Bx-GH30*, *Bx-CAT1,* and *Bx-CAT2* were amplified from cDNA extracted from the Ka4 isolate of *B. xylophilus*. All PCR analyses were performed with Takara PrimeSTAR GXL DNA polymerase (Takara Bio Inc.), in accordance with the manufacturer's protocol. The PCR components were as follows: 10 μl of 5X Prime STAR GXL buffer, 4 μl of dNTP mixture (2.5 mM each), 1 μl of forward primer (10 μM), 1 μl of reverse primer (10 μM), 1 μl of Prime STAR GXL polymerase, 1 μl of cDNA template (200 ng/μl), and 32 μl of H_2O. The cycling conditions were as follows: 35 cycles at 98°C for 10 s, 55°C for 15 s, and 68°C for 60 s/kb. The primers were designed using Primer 3 Plus software[1]. The presence of secretory signal peptides (SPs) in the sequences of the associated genes was determined with the SignalP version 4.1 server. In this study, the constructs for each protein were prepared without a putative SP because the SPs were expected to be cleaved and discarded before secretion from the nematode stylet.

Gateway expression vectors were constructed with a BP reaction, using the Donor vector pDONR207, and with an LR reaction, using the Destination vector pUBC-GFP-dest, in accordance with the manufacturer's specifications (Invitrogen). The target genes were amplified, and the stop codon was removed via PCR using primers containing the attB1 and attB2 sites. The amplification product was cloned into the pDONR 207 entry vector, then subcloned into the pUBC-GFP-Dest vector for C-terminal GFP fusion. The primers used in this analysis are listed in **Supplementary Table 2**.

Transient Overexpression Assay of PWN Proteins in *N. benthamiana*

Nicotiana benthamiana plants were grown in a growth chamber at 20–30°C under a 16-h-light/8-h-dark cycle. For all assays, the sixth or seventh leaves of 4–6-week-old specimens were used. Expression vectors harboring each gene of the four candidates and GFP-only vector control were transformed into *Agrobacterium tumefaciens* strain C58 via electroporation. *A. tumefaciens* bacteria harboring expression vectors were grown in yeast extract beef medium containing 100 mg/l spectinomycin, 50 mg/l carbenicillin, and 25 mg/l rifampicin. Cultures of the *A. tumefaciens* suppressor strain P19 were grown at 28°C in yeast extract beef medium containing 50 mg/l kanamycin until an optical density at 600 nm of 0.5–0.7 was reached. Cells were harvested via centrifugation for 10 min at 3,500 rpm, then re-suspended to a final optical density at 600 nm of 0.3 in 10 mM MES buffer with 10 mM $MgCl_2$ and 150 μM acetosyringone. Strains of *A. tumefaciens* were mixed in roughly equimolar quantities. The P19 suppressor strain was then added at approximately 25% of the total volume. The *A. tumefaciens* suspension was manually infiltrated into *N. benthamiana* leaves using a 1-ml syringe. Symptom development was visually monitored for 10 days after infiltration and categorized visually into two classes: cell death or no cell death (Kettles et al., 2017; Kirino et al., 2020). The proportions of spots indicating cell death were analyzed using Fisher's exact test ($^{**}P < 0.01$). A total of 32 spots were examined (8 plants per gene and four spots per plant) for each candidate molecule. For the GFP control, a total of 120 spots were examined (30 plants and four spots per plant).

For co-localization analysis, an mCherry-labeled endoplasmic reticulum marker, ER-rk CD3–959, was included in a co-transformation procedure (Nelson et al., 2007). The third or fourth leaf of 3-week-old *N. benthamiana* plants was agro-infiltrated with GFP or GFP-fusion pathogenic candidate proteins with p19 and ER-rk CD3-959 in a 1:1:2 ratio. GFP or mCherry fluorescence in the epidermal cells of the abaxial leaf side was assessed at 3 days post-infiltration using an LSM 880 laser scanning microscope fitted with a 40× objective lens (Carl Zeiss). Pieces of the infiltrated leaf were sampled randomly from the infected area, and samples were mounted in 400 mM sucrose for observation via microscopy.

Western blot analysis was performed to validate the expression of Bx-GH-30-GFP fusion protein in *N. benthamiana* according to the method described in Kirino et al. (2020). Briefly, the gel was transferred to an Immun-Blot polyvinylidene fluoride membrane (Bio-Rad) using the *Trans*-Blot Turbo Transfer System (Bio-Rad) with *Trans*-Blot Turbo Midi Transfer Packs. The membrane was blocked in Tris-buffered saline with 0.05% Tween 20 with 1% skim milk powder. After the membrane had been blocked, it was incubated with a rabbit polyclonal anti-GFP antibody (MBL, diluted 1:10,000). Then, it was incubated with a polyclonal anti-IgG-HRP antibody (secondary antibody, diluted 1:10,000). After the membrane had been incubated with Western ECL Substrate (Bio-Rad), the image was visualized using an Image Quant LAS 4000 biomolecular imager (Fujifilm).

In situ Hybridization in PWNs

In situ hybridization was performed to determine the localization of *Bx-GH30* transcript expression in PWNs, generally following the procedures of Espada et al. (2016). The gene sequences of *Bx-GH30* were PCR-amplified from cDNA extracted from *B. xylophilus*. In the first round of PCR, each fragment was amplified with Takara PrimeSTAR GXL DNA polymerase, in accordance with the protocol described above. The primers were designed using Primer 3 Plus software (primers listed in **Supplementary Table 3**). The resulting product was used as a template to synthesize ssDNA probes via linear PCR in a 30-μl reaction mixture [2.25 μl of digoxigenin–DNA labeling mix (Roche Diagnostics), 6 μl each of 10 μM reverse primer, 6 μl of PCR buffer, 0.6 μl of Prime STAR GXL polymerase, 2.25 μl of template, and 12.9 μl of H_2O]. The cycling conditions were as follows: 95°C for 2 s, followed by 35 cycles of 95°C for 15 s, 55°C for 30 s, and 72°C for 90 s. The quality and yield of the reaction were assessed using electrophoresis in a 1.5% agarose gel. The remaining reaction volume was boiled for 10 min and immediately quenched on ice to denature the ssDNA probe.

[1]http://www.bioinformatics.nl/cgi-bin/primer3plus/primer3plus.cgi

Adult *B. xylophilus* nematodes cultured on the fungus *B. cinerea* were soaked in pine wood extract, in accordance with the protocol described by Shinya et al. (2013). They were then fixed for 18 h to few days at 4°C in 4 ml of 2% paraformaldehyde in M9 buffer, followed by 4 h in fixative at room temperature. The fixed nematodes were centrifuged and resuspended in 0.2% paraformaldehyde in M9 buffer, then divided into 2–5 fragments with a needle on a clean microscope slide. The nematode sections were washed twice in 1 ml of M9 buffer, then incubated at room temperature for 45 min in 0.5 mg/ml proteinase K (Life Technologies) in 500 μl of M9 buffer. After the nematodes had been washed in 1 ml of M9 buffer, they were pelleted, frozen at −20°C for 15 min, incubated for 30 s in 1 ml of cold methanol at −20°C, then incubated for 1 min in 1 ml of cold acetone. After the nematode sections had been pelleted at 13,000 rpm, they were rehydrated in distilled water.

The hybridization buffer contained 50% deionized formamide, 20% 20X SSC buffer, 1% 1X blocking reagent (10× blocking reagent: 10× maleic acid: diethyl pyrocarbonate-H_2O at a 10:9:81 ratio), 2% SDS, 1% 100× Denhardt's solution, 1 mM ethylenediaminetetraacetic acid, 0.2 mg/ml fish sperm DNA, and 0.15 mg/ml yeast tRNA. The rehydrated nematode sections were washed in 500 μl of hybridization buffer, then pre-hybridized in 150 μl of hybridization buffer at 50°C for 15 min with rotation. Pre-hybridized nematode sections were added to 20 μl of DNA-digoxigenin probe. The hybridization process was allowed to proceed for 18 h at 50°C with rotation. The nematode sections were washed three times and incubated for 15 min with 100 μl of 4× SSC (20% 20× SSC and 80% diethyl pyrocarbonate-H_2O) at 50°C with rotation, washed three more times, then incubated for 20 min with 100 μl of 0.1× SSC/0.1% SDS at 50°C with rotation. The nematode sections were washed once in 100 μl of 1× maleic acid (10× maleic acid: diethyl pyrocarbonate-H_2O at a 1:9 ratio) and incubated for 30 min with 100 μl of 1× blocking reagent at room temperature with rotation. The nematodes were then labeled for 2 h with 100 μl of alkaline phosphatase-conjugated anti-digoxigenin antibody fragments that had been diluted to 1:500 in blocking reagent. After the nematodes had been washed three more times and incubated with rotation for 15 min in 100 μl of 1× digoxigenin washing buffer (10× digoxigenin washing buffer: diethyl pyrocarbonate-H_2O at a 1:9 ratio), they were stained overnight at 4°C in 100 μl of detection buffer with 0.34 μl of nitroblue tetrazolium and 0.35 μl X-phosphatase. Staining was terminated by two washes in diethyl pyrocarbonate-H_2O with 0.1% Tween 20. The nematodes were then observed under differential interference contrast microscopy.

dsRNA Synthesis

Full-length cDNA clones encoding the *Bx-CAT1*, *Bx-CAT2*, and *Bx-GH30* genes of the Ka4 isolate were used as templates for RNA synthesis. Full-length cDNAs were synthesized from total RNA using a CapFishing full-length cDNA premix kit (Seegene), in accordance with the manufacturer's protocol. The sequences of primers used in this experiment are shown in **Supplementary Table 4**. A dsRNA negative control was included in the experiments by amplifying a fragment from a gene encoding EGFP. The plasmid pYEX-GI3 was used as a template for the preparation of the negative control. PCR amplification was performed using the following cycle profile: 94°C for 2 min, followed by 35 cycles of 98°C for 10 s, 56°C for 30 s, and 68°C for 1 min, and a final step of 68°C for 7 min. The PCR products were purified using a MiniElute PCR purification kit (Qiagen), and the quality and yield of the reactions were checked using agarose gel electrophoresis. Sense and antisense RNAs were synthesized in a single *in vitro* reaction using a MEGAscript RNAi kit (Ambion), in accordance with the manufacturer's instructions. The quality of the generated dsRNA was checked using agarose gel electrophoresis and quantified with a NanoDrop 1000 spectrophotometer. Each dsRNA product was adjusted to a final concentration of 8 μg/μl in nuclease-free water and stored at −80°C.

dsRNA Treatment

RNA interference (RNAi) soaking treatment was performed generally in accordance with the method of Cheng et al. (2010). A mixed culture of the propagative forms was prepared by culturing on the fungus *B. cinerea*, which was grown on potato dextrose agar medium at 25°C. After 10 days of incubation, eggs were collected and the development of nematodes was synchronized by allowing the J2 to hatch in the absence of food. Then, only J2 and J3 PWNs were collected as described in Shinya et al. (2009). The soaking protocol involved RNA dissolution in M9 soaking buffer (43 mM Na_2HPO_4, 22 mM KH_2P0_4, 2 mM NaCl, and 4.6 mM NH_4Cl). A 20-μl aliquot of a suspension containing 20,000 J2 and J3 nematodes was mixed with 50 μl of dsRNA solution (final concentration of 4 μg/μl) with 50 mM octopamine (Sigma). The PWN suspensions were shaken lightly (130 rpm) in a rotary shaker for 24 h at 25°C. Control treatments included 50 μl of distilled water, instead of dsRNA solution.

Transcript Analysis Using Quantitative Real-Time PCR

For each silencing assay, 5,000 nematodes were collected after soaking in dsRNA solution (4 μg/μl) or control solution. The methods of total RNA extraction and quantitative real-time PCR analysis were identical to those described above.

Effect of RNAi Treatment on *B. xylophilus* Reproduction on Gray Mold

The feed fungus *B. cinerea* was initially cultured at 25°C for approximately 6 days on potato dextrose agar medium in a 35-mm plate. A 10-μl suspension containing 100 nematodes, collected after soaking in a dsRNA solution (4 μg/μl) or control solution, was inoculated on the fungal mat and incubated at 25°C. After 10 days, nematodes were collected using the Baermann funnel method (25°C for 24 h) and counted under a stereomicroscope. All experiments were performed with eight biological replicates. The number of PWNs in the eight replicate samples was subjected to statistical analysis. Multiple comparisons were performed with one-way ANOVA. When the ANOVA revealed a significant difference ($P < 0.05$) among groups, Tukey's honestly significant difference (HSD) test was performed.

RESULTS

Quantitative Densitometric Analysis Based on Protein Band Intensity

Analyses using 2D-HPLC and SDS-PAGE revealed 89 protein bands with high repeatability. These gel bands were subjected to relative quantitative densitometric analysis using ImageJ software (**Figure 1** and **Supplementary Figure 1**). Subsequently, hierarchical clustering analysis was performed for these 89 protein bands, revealing four potential virulence determinants—bands 28B, 28C, 38C, and 56A (**Figure 2**), with molecular masses of 32.5, 59, 31.5, and 23.5 kDa, respectively. Clustering analysis also showed that the protein expression profiles differed between virulent and avirulent isolates of *B. xylophilus*.

Identification of Potential Virulence Determinants Using LC-MS/MS Analysis

To characterize the potential virulence determinants identified in the above screening, nanoLC-MS/MS analysis was performed using a *B. xylophilus* genome database. The potential virulence determinants are listed in **Table 1**. They were identified as class 3 lipase (BUX.s00961.62), glycosyl hydrolase family 30 (BUX.s00713.1066), cathepsin L (BUX.s01288.15), and cathepsin L1 (BUX.s00813.52). Henceforth, they are referred to as Bx-lip1, Bx-GH30, Bx-CAT1, and Bx-CAT2, respectively. All of these proteins were previously identified in the *B. xylophilus* secretome, and these were at least sixfold more abundant than the whole *B. xylophilus* proteins (Shinya et al., 2013).

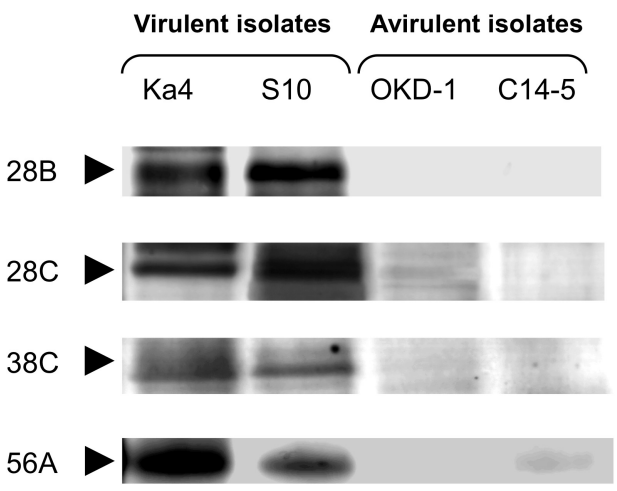

FIGURE 1 | Comparative analysis with sodium dodecyl sulfate-polyacrylamide gel electrophoresis (SDS-PAGE) of *Bursaphelenchus xylophilus* secreted proteins derived from two-dimensional high-performance liquid chromatography (2D-HPLC) fractions. Each fraction was run in a sequential manner. Four protein bands that were significantly different from the others ($P < 0.05$; Tukey's HSD test) with >5-fold greater intensities in both virulent isolates (Ka4 and S10), compared with avirulent isolates (C14-5 and OKD-1), are shown.

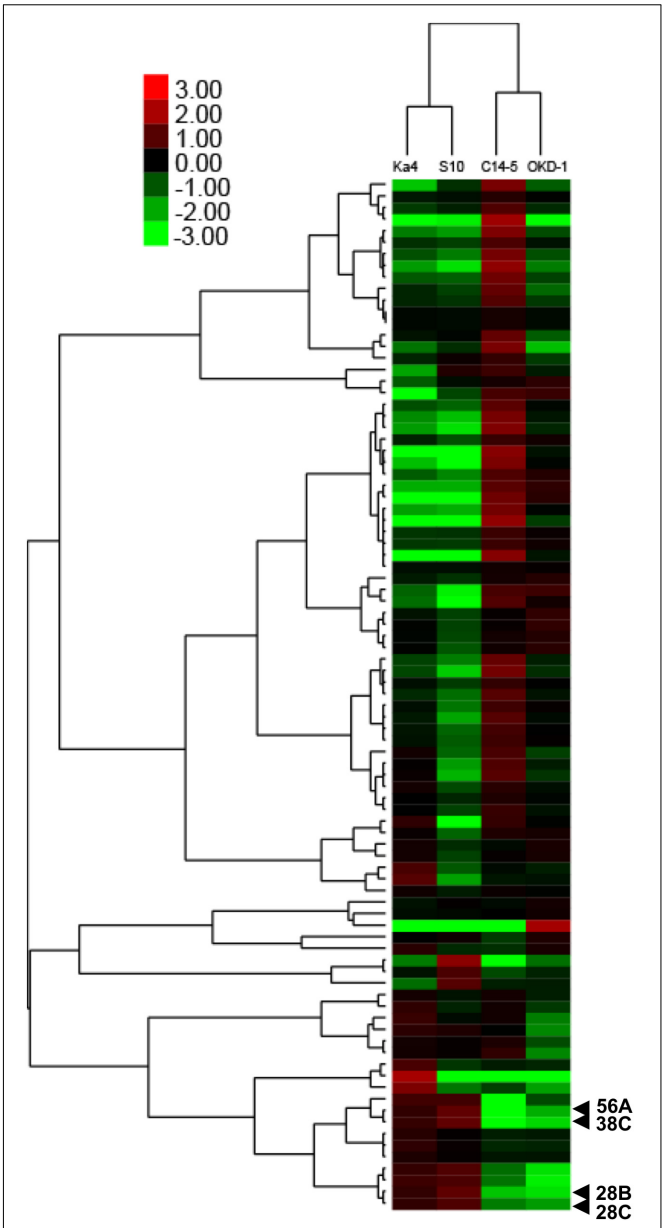

FIGURE 2 | Two-way hierarchical clustering analysis of different amounts of secreted proteins based on relative quantitative densitometric analysis of gel band intensities using ImageJ software. The *x*-axis indicates isolates of *B. xylophilus* and the *y*-axis indicates the mean values of $\log_2$ ratios of relative fold changes calculated for each gel band, compared with the expected value. Four protein bands that were significantly different from the others ($P < 0.05$; Tukey's HSD test) with >5-fold greater intensities in both virulent isolates (Ka4 and S10), compared with avirulent isolates (C14-5 and OKD-1), are indicated.

Gene Expression of Potential Virulence Determinants During Host Infection

Using real-time RT-PCR, the transcript levels of the four potential virulence determinants of *B. xylophilus* were measured at three time points: pre-inoculation (on fungus culture) and 3 and 7 dai into host pines (**Figure 3**). The transcript levels of *Bx-CAT1*,

TABLE 1 | List of potential virulence determinants identified via liquid chromatography-tandem mass spectrometry analysis.

Band no.	Protein ID	Annotation	Theo. MM (kDa)	Coverage (%)	Relative expression* (fold change)
28B	BUX.s00961.62	Class 3 lipase	32.5	21	10.2
28C	BUX.s00713.1066	Glycosyl hydrolase family 30	58.5	19	5.3
38C	BUX.s01288.15	Cathepsin L	26.5	10	15.1
56A	BUX.s00813.52	Cathepsin L	44.5	16	10.2

**Relative expression indicates mean fold change of the expression level in virulent isolates (Ka4 and S10) relative to that in avirulent isolates (C14-5 and OKD-1).*

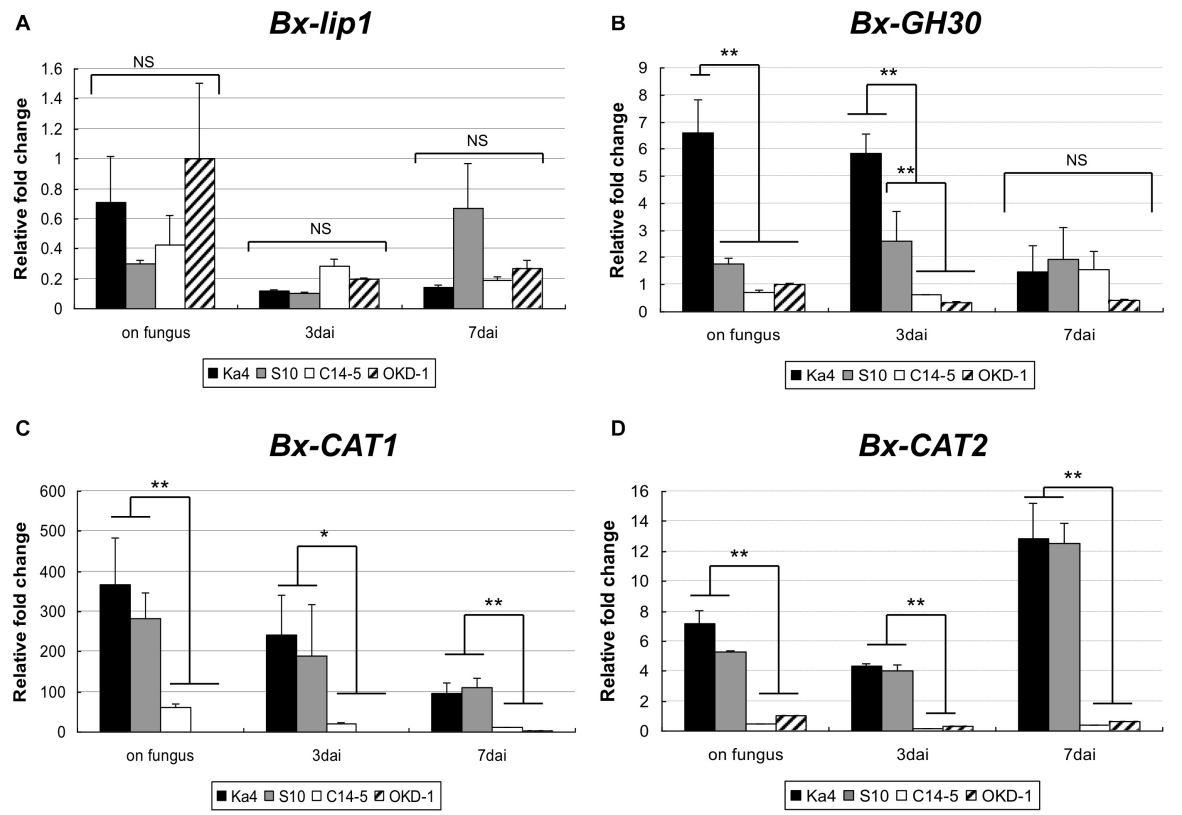

FIGURE 3 | Temporal gene expression levels of **(A)** *Bx-lip1*, **(B)** *Bx-GH30*, **(C)** *Bx-CAT1*, and **(D)** *Bx-CAT2* in four isolates of *B. xylophilus* as evaluated using real-time polymerase chain reaction (PCR). Gene expression levels were determined relative to that of the OKD-1 isolate on fungus (pre-inoculation). Each bar represents the mean ± SD of three biological replicates (**P* < 0.05, ***P* < 0.01, Tukey's HSD test).

BxCAT-2, and *Bx-GH30* were significantly higher in virulent isolates than in avirulent isolates at pre-inoculation and 3 dai. Only the *Bx-GH30* transcript level declined in virulent isolates at 7 dai, such that no significant difference was observed between virulent and avirulent isolates at 7 dai. The *Bx-CAT1* transcript level was always more than 100-fold greater in virulent isolates than in avirulent isolates. Temporal analysis showed that the transcript levels of *Bx-GH30* and *Bx-CAT1* tended to be high during the pre-infection and early infection periods (3 dai), and the transcript level of *Bx-CAT2* was higher in the later infection period (7 dai). Only the *Bx-lip1* transcript level was not consistent with the results of comparative proteome analysis, in which the amount of Bx-lip1 protein was significantly greater in virulent isolates than in avirulent isolates. At the transcript level, no significant differences were observed in the expression of *Bx-lip1* between virulent and avirulent isolates at all three time points (**Figure 3A**) ($P > 0.01$, Tukey's HSD test).

Bx-GH30 Influence on Plant Cell Death

Using a pUBQ10 promoter, transgenic *N. benthamiana* lines were generated expressing each of the four potential virulence determinant proteins, and their contributions to tobacco plant cell death were investigated (**Figure 4**). The presence of SPs within the sequences of the associated genes was determined using the SignalP server (version 4.1). Predicted SPs in the sequences of Bx-lip1, Bx-GH30, and Bx-CAT2 were excised. In the sequence of Bx-CAT1, an SP was not predicted. Bx-GH30 induced significant cell death relative to the GFP-only control

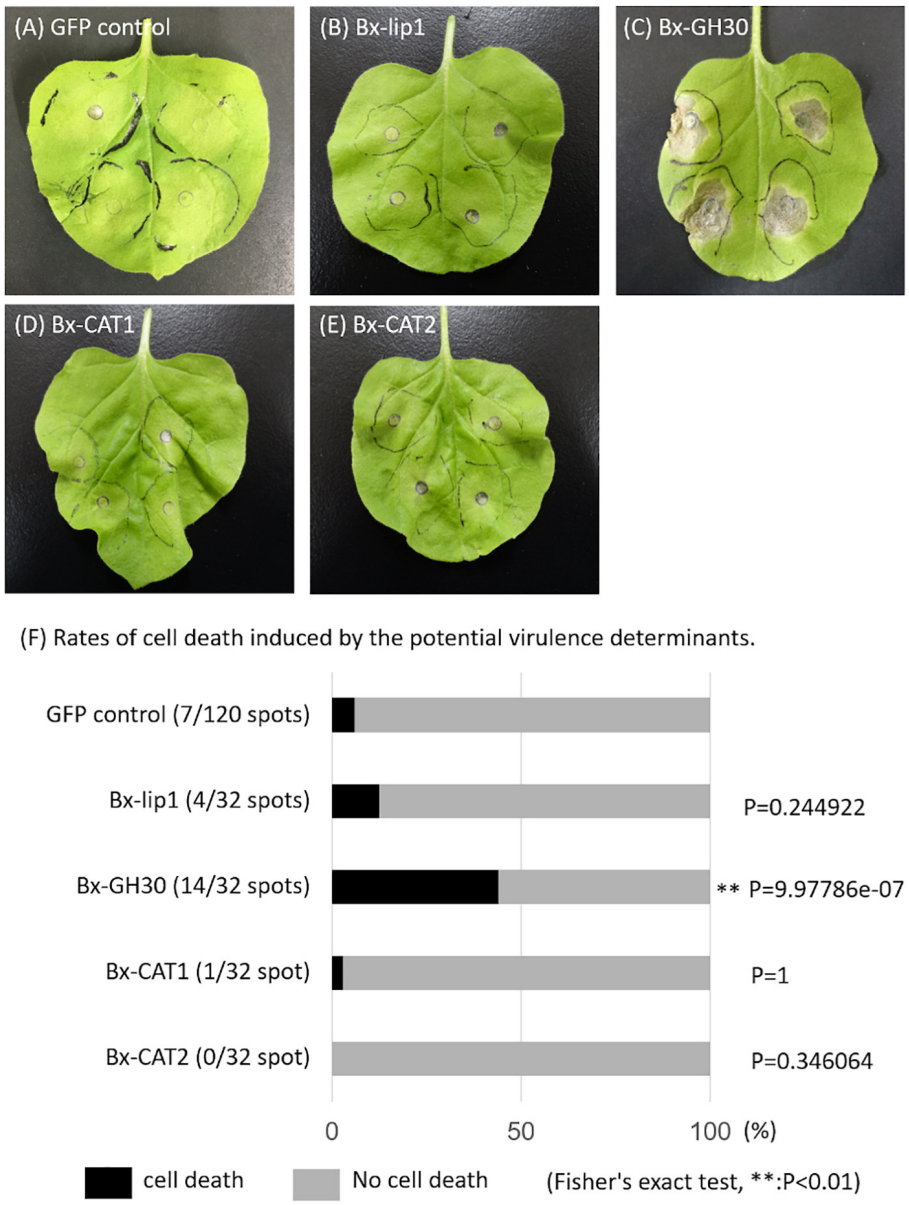

FIGURE 4 | Symptoms and rates of cell death induced by potential virulence determinants. Leaves of *Nicotiana benthamiana* were infiltrated with *Agrobacterium tumefaciens* strains to express candidate *B. xylophilus* proteins. Images were captured at 10 days after infiltration: **(A)** the GFP-only vector control, **(B)** Bx-lip1, **(C)** Bx-GH30, **(D)** Bx-CAT1, and **(E)** Bx-CAT2. **(F)** The rates of cell death induced by candidate molecules are presented graphically. The degree of symptoms after infiltration was monitored visually and categorized into two classes: cell death (black bar) and no cell death (gray bar). The proportions of cell death in parentheses were statistically analyzed using Fisher's exact test (**$P < 0.01$). Asterisks indicate a significant increase in cell death induced by one of the four candidate pathogenic proteins, compared with the GFP-only vector control.

($P < 0.01$). No significant cell death relative to the GFP-only control was observed in treatments with the other potential virulence determinants: Bx-lip1, Bx-CAT1, and Bx-CAT2.

Bx-GH30 Localization in Plants

To determine its subcellular localization, Bx-GH30 was fused to the gene encoding GFP, then transfected into *N. benthamiana* with an mCherry-labeled endoplasmic reticulum marker (ER-rk CD3–959). The transiently expressed GFP fusion protein and mCherry-labeled endoplasmic reticulum marker in tobacco leaves was visualized using confocal microscopy (**Figure 5**). The GFP signal of Bx-GH30 was co-localized with the endoplasmic reticulum marker. By contrast, the GFP signal of the vector control was present in both the plant cytoplasm and nucleus. In addition to the observation by fluorescence microscopy, the expression of Bx-GH-30-GFP fusion protein was validated by Western blot analysis using anti-GFP polyclonal antibodies. As a result, the

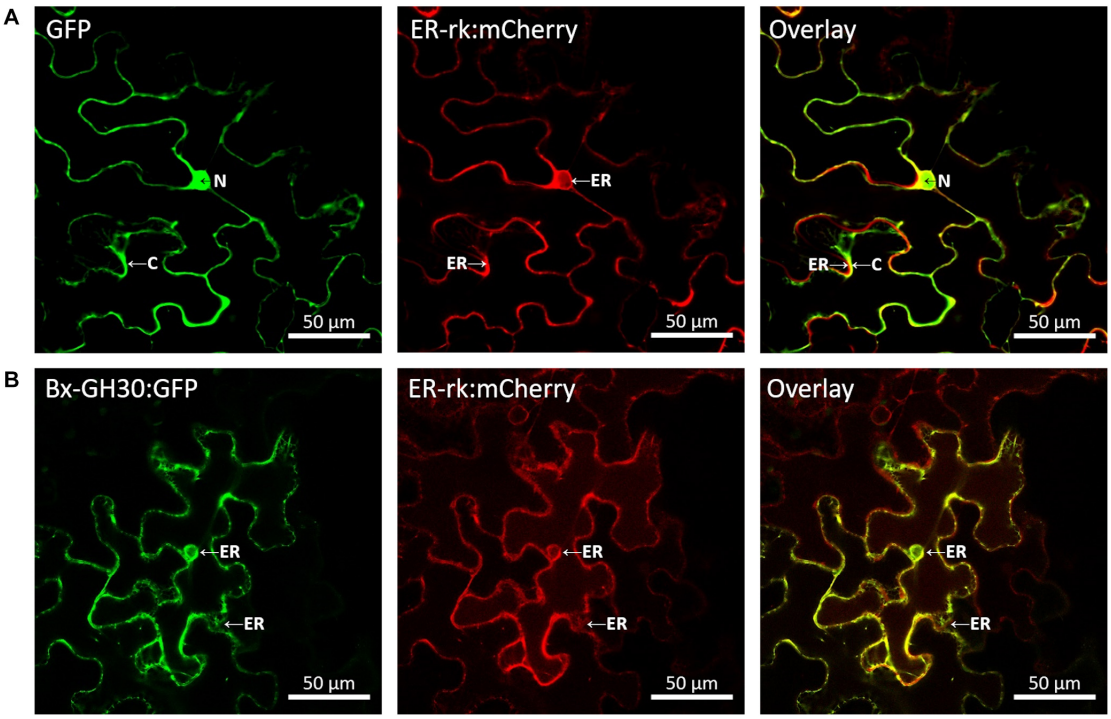

FIGURE 5 | Localization of Bx-GH30 in plant cells. Confocal images of GFP **(A)** and Bx-GH30 **(B)** infiltrated into *N. benthamiana* leaves, together with an mCherry-labeled endoplasmic reticulum marker (ER-rk CD3-959). For confocal laser scanning microscopy, samples were taken at 3 days post-inoculation, and fluorescent channels were scanned sequentially. GFP fluorescence is shown in green (left panel) and mCherry fluorescence is shown in red (middle panel). The overlay of green and red signals appears yellow (right panel). N, nucleus; C, cytoplasm; ER, endoplasmic reticulum. Scale bar = 50 µm.

83 kDa protein band was detected in the Bx-GH30 sample and was consistent with the predicted molecular mass (**Supplementary Figure 2**).

Bx-GH30 mRNA Expression in Adult *B. xylophilus*

In situ mRNA hybridization was used to investigate the spatial expression patterns of *Bx-GH30* in adult PWNs soaked in pine wood extract. Digoxigenin-labeled antisense probes generated from the cellulase gene (*Bx-ENG-1*; reportedly expressed in esophageal gland cells) were used as a positive control (Kikuchi et al., 2004). The *Bx-ENG-1* signal was detected specifically in esophageal gland cells (**Supplementary Figure 3A**). Although no clear localization was obtained in a specific area, a diffuse signal was observed for *Bx-GH30* around esophageal gland cells (**Supplementary Figure 3C**). Similar signal patterns were detected in both female and male nematodes. No hybridization with control sense cDNA probes was observed in the nematodes (**Supplementary Figures 3B,D**).

Evaluation of RNAi Efficiency Using Real-Time PCR Analyses

Quantitative real-time RT-PCR was performed to confirm the efficiency of gene silencing by RNAi. The ds*Bx-GH30* and ds*Bx-CAT2* treatments had some effects on *Bx-GH30* and *Bx-CAT2* transcript levels, respectively (**Supplementary Figure 4**). Taking the mRNA transcript level of the control (treated with non-dsRNA) as 100%, the mean transcript levels of *Bx-GH30* and *Bx-CAT2* were 66 and 49%, respectively ($P < 0.01$, Student's *t*-test). No significant effect on *Bx-CAT1* transcript levels was observed after RNAi treatment, with a mean transcript level of 82% ($P > 0.01$, Student's *t*-test). The negative control, ds*EGFP*, caused no significant changes in transcript levels of *Bx-GH30*, *Bx-CAT*, or *Bx-CAT2*, indicating that the gene-silencing effect observed in this experiment was sequence-specific.

Effects of RNAi on *B. xylophilus* Reproduction on Gray Mold

To investigate the effects of RNAi on *B. xylophilus* reproductive ability, nematodes were counted after treatment with each dsRNA or M9 buffer (control) over 10 days of culture at 25°C on gray mold (**Figure 6**). As a negative control, dsRNA for non-endogenous *EGFP* was used to assess dsRNA toxicity, revealing no toxicity. Nematodes treated with ds*Bx-CAT2* propagated significantly less than did control nematodes ($P < 0.01$, Student's *t*-test). However, no significant reductions in nematode number were observed after treatment with ds*Bx-GH30*, or ds*EGFP*, compared with the control ($P > 0.01$, Student's *t*-test). *Bx-CAT1* was omitted from this portion of the study because no significant effect on *Bx-CAT1* transcript levels was observed after RNAi treatment (**Supplementary Figure 4**).

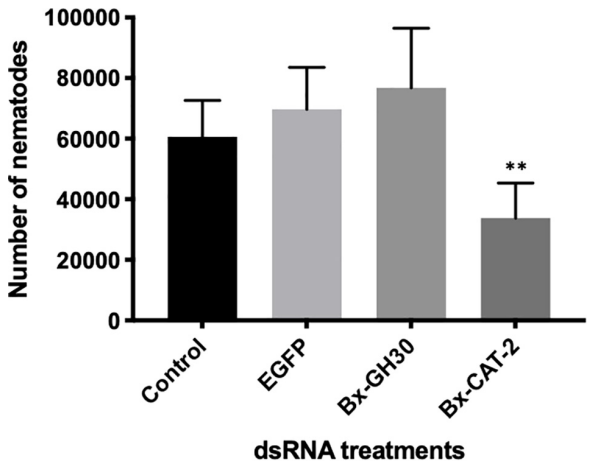

FIGURE 6 | Effects of RNA interference (RNAi) treatment on *B. xylophilus* reproductive ability. Each bar represents the mean ± SD of eight replicates (**$P < 0.01$, Student's *t*-test).

DISCUSSION

In the present study, a comparative secretome analysis of four isolates of *B. xylophilus* with distinct degrees of virulence against host pines was performed using 2D-HPLC and SDS-PAGE, combined with LC-MS/MS analysis. We initially targeted 89 protein bands with high reproducibility and quantified them on the basis of protein band intensities. We identified four proteins that were highly expressed in two virulent isolates: class 3 lipase (Bx-lip1), glycosyl hydrolase family 30 (Bx-GH30), cathepsin L (Bx-CAT1), and cathepsin L (Bx-CAT2) (**Table 1**). All of these were also identified in our previous comprehensive analysis of the *B. xylophilus* secretome (Shinya et al., 2013). In the present study, a 3D-protein separation system was used for comparative and semi-quantitative proteome analysis. In recent decades, label-based protein quantification techniques such as iTRAQ and SILAC have been used for comparative proteomics (Ong et al., 2002; Ross et al., 2004). Although these label-based methods are generally considered more sensitive and comprehensive compared to the gel-based methods used in our study, we presume that we have identified the major differentially secreted proteins between virulent and avirulent isolates. To validate quantitative differences in these four potential virulence determinants between virulence groups at the transcript level, quantitative RT-PCR was carried out at three time points (pre-inoculation, 3 dai, and 7 dai). The transcript levels of *Bx-CAT1*, *BxCAT-2*, and *Bx-GH30* were significantly higher in virulent isolates than in avirulent isolates at pre-inoculation and 3 dai, although the *Bx-GH30* transcript level in virulent isolates declined by 7 dai (**Figure 3**). These findings were consistent with the results of quantitative analysis at the protein level. The expression levels of *Bx-CAT1* and *Bx-GH30* genes were upregulated in virulent isolates during fungus feeding and the early phase of infection. Furthermore, *BxCAT-2* was upregulated during the late phase of infection. Only *Bx-lip1* exhibited a gene expression pattern that differed from the protein dynamics results. This implies that the amount of Bx-lip1 protein secreted by *B. xylophilus* was regulated in a post-transcriptional manner, and the levels of the other three proteins were mainly regulated at the transcript level. The gene expression level of *Bx-CAT1* was higher in virulent isolates than in avirulent isolates at all time points examined, but the highest expression was observed when PWNs were cultured on fungus. In *Bx-CAT2*, gene expression levels were lowest at 3 dai and higher during growth on fungus and at 7 dai in the pine seedlings. This suggests that *Bx-CAT1* and *Bx-CAT2* are enzymes that aid in fungus digestion and nutrient uptake. It remains unclear why the gene expression of *Bx-CAT2* was downregulated after PWNs entered the pine seedlings, although the PWNs might have migrated rapidly inside the tree after invasion (without a feeding phase). Ekino et al. (2020) demonstrated phenotypic plasticity in PWNs and revealed differences in ultrastructure between phytophagous and mycetophagous phases. In particular, atrophied intestinal microvilli were observed in the phytophagous phase, compared with the mycetophagous phase, suggesting that the phytophagous phase is a stage of active migration within the living pine tree, instead of feeding. Virulent isolates (e.g., Ka4 and S10) reportedly exhibited more robust reproductive ability, compared with avirulent isolates (e.g., C14-5 and OKD-1), when cultured on the fungus *B. cinerea* (Aikawa and Kikuchi, 2007; Shinya et al., 2012). It is likely that Bx-CAT1 and Bx-CAT2 are responsible for food digestion and contribute to reproductive ability. Among the four proteins differentially secreted between virulent and avirulent isolates, Bx-GH30 exhibited a unique gene expression pattern. In particular, significantly greater gene expression was observed in virulent isolates only at 3 dai.

To investigate the molecular functions of Bx-lip1, Bx-CAT1, Bx-CAT2, and Bx-GH30 during plant infection, we conducted an *in planta* functional analysis using *N. benthamiana* to screen for molecules that induced hypersensitive cell death in tobacco. Notably, Bx-GH30 induced significant cell death in *N. benthamiana*, relative to the GFP-only control (**Figure 4**). The GH30 family contains glycoside hydrolases with several known enzyme activities, such as β-glucosylceramidase and β-1,6-glucanase, and divided into largely two groups, distinguished by levels of sequence identity (St John et al., 2010). The amino acid sequence of Bx-GH30 secreted by *B. xylophilus* shows high similarity with the enzymes characterizing glucosylceramidase. β-glucosylceramidase hydrolyzes β-glucoside from the glycolipid glucosylceramide and from glucose-conjugated sphingolipids. Glucosylceramides are major components of the endomembrane system and plasma membrane in most eukaryotic cells. Although the molecular functions of glucosylceramides are not well-characterized, ceramides and sphingolipids have been identified as lipid signaling molecules (Hannun and Obeid, 2008) and are involved in programmed plant cell death associated with plant defense (Dunn et al., 2004; Saucedo-García et al., 2011; Berkey et al., 2012). GH30 also has a β-1,6-glucanase function. However, because β-1,6-glucans are major yeast cell-wall components, GH30 having a β-1,6-glucanase is unlikely to be involved in the induction of plant cell death. To verify the actual molecular function of Bx-GH30, a recombinant Bx-GH30

protein should be designed, which will allow examination of its function as an enzyme.

To determine the subcellular localization of Bx-GH30 in tobacco, its localization was observed using a GFP fusion protein and a mCherry-labeled endoplasmic reticulum marker (ER-rk CD3–959). Notably, Bx-GH30 was localized in the endoplasmic reticulum (**Figure 5**). Conversely, the GFP signal of the vector control was present in both the plant cytoplasm and nucleus. Given that an endoplasmic reticulum stress-inducible protein was upregulated in PWN-infested *Pinus pinaster* (a pine species very susceptible to PWNs), compared with PWN-infested *Pinus pinea* (a less susceptible pine species) (Santos et al., 2012), Bx-GH30 localized in the endoplasmic reticulum may induce hypersensitive cell death in pines. During the process of pine wilt disease, a hypersensitive reaction is accompanied by the leakage of abnormal oleophilic substances from parenchymal cells, resulting in blockage of the water conducting system (Futai, 2013). Bx-GH30 may play an important role in pine wilt disease as a trigger to induce a hypersensitive reaction. In addition to clarifying the enzymatic activity of Bx-GH30 as mentioned above, further studies to investigate Bx-GH30 localization in host pine trees are needed in the future. In this study, we also performed *in situ* hybridization analysis and found that Bx-GH30 was expressed around esophageal gland cells in PWNs (**Supplementary Figure 3**). The pharyngeal gland cells are the source of most nematode effectors (e.g., Haegeman et al., 2012). Therefore, Bx-GH30 may be produced in the pharyngeal gland cells and secreted from the nematode stylet into the plant apoplast or plant cells. Our findings demonstrate that Bx-GH30 causes cell death in tobacco, but its mechanisms are unclear. Further detailed studies are needed to determine how Bx-GH30 causes plant cell death and elucidate its specific role in pine wilt disease.

RNAi was used to examine the functions of potential virulence determinant genes during reproduction on gray mold. *Bx-lip1* was omitted from this portion of the study because our above results suggested that the amount of Bx-lip1 protein was regulated in a post-transcriptional manner. Furthermore, no significant effect on *Bx-CAT1* transcript levels was observed after RNAi treatment. In the analysis of *B. xylophilus* reproductive ability, silencing of the *Bx-CAT2* gene resulted in a reduction in the number of PWNs cultured on the fungal mat of *B. cinerea*. By contrast, no significant effect was observed after treatment with ds*Bx-GH30*, compared with the control. These results suggest that Bx-CAT2 is responsible for reproduction on gray mold, but that Bx-GH30 is not, indicating that only Bx-GH30 plays an important role in the induction of cell death within the plant. It has been reported that RNAi targeting of the *GH45* gene in *B. xylophilus* caused a decrease in reproductive ability (Cheng et al., 2010; Ma et al., 2011). Ma et al. (2011) also reported that silencing of the *GH45* gene resulted in reduced fungal-feeding ability. Because GH45 protein exhibits cellulose-degradation activity, silencing of the *GH45* gene may reduce the fungal cell wall degradation ability, thus impacting the reproductive ability of PWNs (Ma et al., 2011). However, in the present study, no clear difference was observed in the rate of fungal feeding among treatments (data not shown). Therefore, *Bx-CAT2* may be involved in nutrient uptake, and the silencing of this gene might have caused a substantial decrease in *B. xylophilus* reproductive ability. A clear difference in reproductive ability on the fungal mat has been reported between virulent and avirulent isolates (Aikawa and Kikuchi, 2007; Shinya et al., 2012). Palomares-Rius et al. (2015) suggested that avirulent isolates of *B. xylophilus* are likely to be the lack of activities of digestive proteases due to the loss of function mutations based on a comparative genomics between virulent and avirulent isolates. Bx-CAT2 is presumably responsible for this difference in reproductive ability on fungus because it is secreted more abundantly in virulent isolates than in avirulent isolates. In addition to differences in reproductive ability, remarkable differences have been reported between virulent and avirulent isolates in other biological traits, such as the ability to disperse in host tissues (Ichihara et al., 2000) and to tolerate oxidative stress (Vicente et al., 2015). Since it has been suggested that the ability of *B. xylophilus* to avoid and/or tolerate plant defense response is a key element in the process of pine wilt (Shinya et al., 2013; Vicente et al., 2015; Ding et al., 2016; Filipiak et al., 2020), the potential virulence determinants found in this study may have different functions involved in these traits. RNAi is a valuable tool for studying the biological function of genes because it causes sequence-specific degradation of mRNA mediated by homologous dsRNA, which inhibits gene function in a post-transcriptional manner (Hammond et al., 2001). However, the effects of RNAi are transient and weak in most nematodes other than *Caenorhabditis elegans* (Geldhof et al., 2007; Knox et al., 2007; Viney and Thompson, 2008), and the efficiency of this approach is strongly influenced by the type of target gene. In contrast to analyses of *C. elegans*, the reduction of gene expression was limited in our study. Moreover, the effect was transient and could not be inherited. Because of the limited effect of RNAi in *B. xylophilus*, a pathogenicity test using RNAi could not be conducted. Thus, the development of an alternative approach for further analysis is urgently needed to more comprehensively understand the molecular basis of *B. xylophilus* parasitism, and the functional analysis using *N. benthamiana* employed in this study will be a powerful tool in future analyses of pine wilt disease.

This study demonstrated that Bx-GH30, which is abundantly secreted by virulent isolates of *B. xylophilus*, can induce cell death in *N. benthamiana*. Bx-GH30 is a virulence-determining molecule among *B. xylophilus* isolates and is presumably an effector that causes cell death in host pines. Furthermore, Bx-CAT2 was involved in nutrient uptake during fungal feeding and contributed to differences in reproductive ability on fungus between virulent and avirulent isolates. To determine the molecular functions of two other potential virulence determinants, *Bx-lip1* and *Bx-CAT1*, a gene-knockout method must be established in *B. xylophilus*.

DATA AVAILABILITY STATEMENT

The original contributions presented in the study are included in the article/**Supplementary Material**, further inquiries can be directed to the corresponding author.

AUTHOR CONTRIBUTIONS

RS and HM designed the study. RS, HK, and HM performed the research and analyzed the data. RS, HK, HM, YT-K, KF, and MU wrote the manuscript. All authors contributed to the article and approved the submitted version.

FUNDING

This study was funded by a Japan Society for the Promotion of Science Grant-in-Aid for Early-Career Scientists (number JP19K15853 to RS) and a grant from the Japan Science and Technology Agency PRESTO (number JPMJPR17Q5 to RS).

ACKNOWLEDGMENTS

We sincerely thank Dr. Kohki Yoshimoto, Meiji University, for his assistance with the *in planta* functional analysis and Dr. Claudia S. L. Vicente, University of Évora, for her assistance with the *in situ* hybridization procedure.

SUPPLEMENTARY MATERIAL

The Supplementary Material for this article can be found online at: https://www.frontiersin.org/articles/10.3389/fpls.2021.640459/full#supplementary-material

Supplementary Figure 1 | SDS-PAGE comparative analysis of *B. xylophilus* proteins derived from 2D-HPLC fractions. Each fraction was run in a sequential manner for the four isolates of *B. xylophilus* (Ka4, S10, C14-5, and OKD-1).

Supplementary Figure 2 | Bands of Bx-GH30 on Western blot membranes. GFP-only vector control protein and Bx-GH-30-GFP fusion protein expressed in *N. benthamiana* were detected with anti-GFP antibodies. The GFP control band is approximately 27 kDa. Bx-GH30 band is approximately 83 kDa.

Supplementary Figure 3 | mRNA localization of *Bx-GH30* in nematodes. The localization of *Bx-ENG-1* **(A)** as a positive control for gene expression in pharyngeal gland cells, after *in situ* hybridization. Localization of transcripts encoding *Bx-GH30* of the pine wood nematode around pharyngeal glands, after *in situ* hybridization **(C)**. No signals were produced using the sense probes for *Bx-ENG-1* **(B)** and *Bx-GH30* **(D)**.

Supplementary Figure 4 | mRNA expression levels of *Bx-GH30* **(A)**, *Bx-CAT1* **(B)**, and *Bx-CAT2* **(C)** genes in *B. xylophilus* after soaking in target dsRNA solution and EGFP dsRNA solution (a non-endogenous gene), relative to the control level (non-dsRNA treatment). Each bar represents the mean ± SD of three biological replicates. The expression level in the control was regarded as 1.0. Different letters indicate significant differences between genes ($P < 0.01$, Student's *t*-test).

Supplementary Table 1 | Primers used in real-time PCR analyses to quantify transcript levels.

Supplementary Table 2 | List of primers used in Gateway vector construction.

Supplementary Table 3 | List of primers used in *in situ* hybridization.

Supplementary Table 4 | Primers used to prepare dsRNA for nematode soaking experiments.

Supplementary Data Sheet 1 | MS/MS spectra for the protein band 28B.

Supplementary Data Sheet 2 | MS/MS spectra for the protein band 28C.

Supplementary Data Sheet 3 | MS/MS spectra for the protein band 38C.

Supplementary Data Sheet 4 | MS/MS spectra for the protein band 56A.

REFERENCES

Abelleira, A., Picoaga, A., Mansilla, J. P., and Aguin, O. (2011). Detection of *Bursaphelenchus Xylophilus*, causal agent of pine wilt disease on *Pinus pinaster* in northwestern Spain. *Plant Dis.* 95, 776–776. doi: 10.1094/PDIS-12-10-0902

Aikawa, T., and Kikuchi, T. (2007). Estimation of virulence of *Bursaphelenchus xylophilus* (Nematoda: Aphelenchoididae) based on its reproductive ability. *Nematology* 9, 371–377. doi: 10.1163/156854107781352007

Aikawa, T., Kikuchi, T., and Kosaka, H. (2003). Demonstration of interbreeding between virulent and avirulent populations of *Bursaphelenchus xylophilus* (Nematoda: Aphelenchoididae) by PCR-RFLP method. *Appl. Entomol. Zool.* 38, 565–569. doi: 10.1303/aez.2003.565

Akiba, M. (2006). Diversity of pathogenicity and virulence in the pinewood nematode, *Bursaphelenchus xylophilus*. *J. Jpn. For. Soc.* 88, 383–391.

Baermann, G. (1917). The conditions of spread of ankylostomiasis by ground infection and its control. *Geneesk. Tijdschr. v. Nederl-Indie.* 57, 131–137.

Berkey, R., Bendigeri, D., and Xiao, S. (2012). Sphingolipids and plant defense/disease: the "death" connection and beyond. *Front. Plant Sci.* 3:68. doi: 10.3389/fpls.2012.00068

Cardoso, J., Anjo, S., Fonseca, L., Egas, C., Manadas, B., and Abrantes, I. (2016). *Bursaphelenchus xylophilus* and *B. mucronatus* secretomes: a comparative proteomic analysis. *Sci. Rep.* 6:39007. doi: 10.1038/srep39007

Cheng, X. Y., Dai, S. M., Xiao, L., and Xie, B. Y. (2010). Influence of cellulase gene knockdown by dsRNA interference on the development and reproduction of the pine wood nematode, *Bursaphelenchus xylophilus*. *Nematology* 12, 225–233. doi: 10.1163/138855409X12469541205044

Ding, X., Ye, J., Lin, S., Wu, X., Li, D., and Nian, B. (2016). Deciphering the molecular variations of pine wood nematode *Bursaphelenchus xylophilus* with different virulence. *PLoS One* 11:e0156040. doi: 10.1371/journal.pone.0156040

Dunn, T. M., Lynch, D. V., Michaelson, L. V., and Napier, J. A. (2004). A post-genomic approach to understanding sphingolipid metabolism in *Arabidopsis thaliana*. *Ann. Bot.* 93, 483–497. doi: 10.1093/aob/mch071

Ekino, T., Kirino, H., Kanzaki, N., and Shinya, R. (2020). Ultrastructural plasticity in the plant-parasitic nematode, *Bursaphelenchus xylophilus*. *Sci. Rep.* 10:11576. doi: 10.1038/s41598-020-68503-3

Espada, M., Akker, S., Maier, T., Vijayapalani, P., Baum, T., Mota, M., et al. (2018). STATAWAARS: a promoter motif associated with spatial expression in the major effector-producing tissues of the plant-parasitic nematode *Bursaphelenchus xylophilus*. *BMC Genomics* 19:553. doi: 10.1186/s12864-018-4908-2

Espada, M., Silva, A. C., Akker, S. E., van den Cock, P. J. A., Mota, M., and Jones, J. T. (2016). Identification and characterization of parasitism genes from the pinewood nematode *Bursaphelenchus xylophilus* reveals a multilayered detoxification strategy. *Mol. Plant Pathol.* 17, 286–295. doi: 10.1111/mpp.12280

Filipiak, A., Malewski, T., Matczyńska, E., and Tomalak, M. (2020). Molecular variation among virulent and avirulent strains of the quarantine nematode *Bursaphelenchus xylophilus*. *Mol. Genet. Genomics*. doi: 10.1007/s00438-020-01739-w

Futai, K. (2013). Pine wood nematode, *Bursaphelenchus xylophilus*. *Annu. Rev. Phytopathol.* 51, 61–83. doi: 10.1146/annurev-phyto-081211-172910

Geldhof, P., Visser, A., Clark, D., Saunders, G., Britton, C., Gilleard, J., et al. (2007). RNA interference in parasitic helminths: current situation, potential pitfalls and future prospects. *Parasitology* 134, 609–619. doi: 10.1017/S0031182006002071

Haegeman, A., Mantelin, S., Jones, J. T., and Gheysen, G. (2012). Functional roles of effectors of plant-parasitic nematodes. *Gene* 492, 19–31. doi: 10.1016/j.gene.2011.10.040

Hammond, S. M., Boettcher, S., Caudy, A. A., Kobayashi, R., and Hannon, G. J. (2001). Argonaute2, a link between genetic and biochemical analyses of RNAi. *Science* 293, 1146–1150. doi: 10.1126/science.1064023

Han, Z. M., Hong, Y. D., and Zhao, B .G. (2003). A study on pathogenicity of bacteria carried by pine wood nematodes. *J. Phytopathol.* 151, 683–689. doi: 10.1046/j.1439-0434.2003.00790.xİ

Hannun, Y. A., and Obeid, L. M. (2008). Principles of bioactive lipid signalling: lessons from sphingolipids. *Nat. Rev. Mol. Cell Biol.* 9, 139–150. doi: 10.1038/nrm2329

Hu, L. J., Wu, X. Q., Li, H. Y., Zhao, Q., Wang, Y. C., and Ye, J. R. (2019). An effector, BxSapB1, induces cell death and contributes to virulence in the pine wood nematode *Bursaphelenchus xylophilus*. *Mol. Plant Microbe Interact.* 32, 452–463. doi: 10.1094/MPMI-10-18-0275-R

Ichihara, Y., Fukuda, K., and Suzuki, K. (2000). Early symptom development and histological changes associated with migration of *Bursaphelenchus xylophilus* in seedling tissues of *Pinus thunbergii*. *Plant Dis.* 84, 675–680. doi: 10.1094/PDIS.2000.84.6.675

Ikeda, T. (1996). Responses of water-stressed *Pinus thunbergii* to inoculation with avirulent pine wood nematode (*Bursaphelenchus xylophilus*): water relations and xylem histology. *J. For. Res.* 1, 223–226. doi: 10.1007/BF02348329

Kang, J. S., Koh, Y. H., Moon, Y. S., and Lee, S. H. (2012). Molecular properties of a venom allergen-like protein suggest a parasitic function in the pinewood nematode *Bursaphelenchus xylophilus*. *Int. J. Parasitol.* 42, 63–70. doi: 10.1016/j.ijpara.2011.10.006

Kawazu, K., Zhang, H., Yamashita, H., and Kanzaki, H. (1996). Relationship between the pathogenicity of the pinewood nematode, *Bursaphelenchus xylophilus*, and phenylacetic acid production. *Biosci. Biotechnol. Biochem.* 60, 1413–1415. doi: 10.1271/bbb.60.1413

Kettles, G. J., Bayon, C., Canning, G., Rudd, J. J., and Kanyuka, K. (2017). Apoplastic recognition of multiple candidate effectors from the wheat pathogen *Zymoseptoria tritici* in the nonhost plant *Nicotiana benthamiana*. *New Phytol.* 213, 338–350. doi: 10.1111/nph.14215

Kikuchi, T., Cotton, J. A., Dalzell, J. J., Hasegawa, K., Kanzaki, N., McVeigh, P., et al. (2011). Genomic insights into the origin of parasitism in the emerging plant pathogen *Bursaphelenchus xylophilus*. *PLoS Pathog.* 7:e1002219. doi: 10.1371/journal.ppat.1002219

Kikuchi, T., Jones, J. T., Aikawa, T., Kosaka, H., and Ogura, N. (2004). A family of glycosyl hydrolase family 45 cellulases from the pine wood nematode *Bursaphelenchus xylophilus*. *FEBS Lett.* 572, 201–205. doi: 10.1016/j.febslet.2004.07.039

Kikuchi, T., Shibuya, H., Aikawa, T., and Jones, J. T. (2006). Cloning and characterization of pectate lyases expressed in the esophageal gland of the pine wood nematode *Bursaphelenchus xylophilus*. *Mol. Plant Microbe Interact.* 19, 280–287. doi: 10.1094/MPMI-19-0280

Kirino, H., Yoshimoto, K., and Shinya, R. (2020). Thaumatin-like proteins and a cysteine protease inhibitor secreted by the pine wood nematode *Bursaphelenchus xylophilus* induce cell death in *Nicotiana benthamiana*. *PLoS One* 15:e0241613. doi: 10.1371/journal.pone.0241613

Kiyohara, T. (1989). Etiological study of pine wilt disease. *Bull. For. For. Prod. Res. Instit.* 353, 127–176.

Kiyohara, T., and Bolla, R. I. (1990). Pathogenic variability among populations of the pinewood nematode, *Bursaphelenchus Xylophilus*. *For. Sci.* 36, 1061–1076. doi: 10.1093/forestscience/36.4.1061

Kiyohara, T., and Tokushige, Y. (1971). Inoculation experiments of a nematode, *Bursaphelenchus* sp., onto pine trees. *J. Jpn. For. Soc.* 53, 210–218. doi: 10.11519/jjfs1953.53.7_210

Knox, D. P., Geldhof, P., Visser, A., and Britton, C. (2007). RNA interference in parasitic nematodes of animals: a reality check? *Trends Parasitol.* 23, 105–107. doi: 10.1016/j.pt.2007.01.007

Ma, H. B., Lu, Q., Liang, J., and Zhang, X. (2011). Functional analysis of the cellulose gene of the pine wood nematode, *Bursaphelenchus xylophilus*, using RNA interference. *Genet. Mol. Res.? GMR* 10, 1931–1941. doi: 10.4238/vol10-3gmr1367

Morisaka, H., Kirino, A., Kobayashi, K., and Ueda, M. (2012). Two-Dimensional protein separation by the HPLC system with a monolithic column. *Biosci. Biotech. Biochem.* 76, 585–588. doi: 10.1271/bbb.110770

Mota, M. M., Braasch, H., Bravo, M. A., Penas, A. C., Burgermeister, W., Metge, K., et al. (1999). First report of *Bursaphelenchus xylophilus* in Portugal and in Europe. *Nematology* 1, 727–734. doi: 10.1163/156854199508757

Nelson, B. K., Cai, X., and Nebenführ, A. (2007). A multicolored set of *in vivo* organelle markers for co-localization studies in *Arabidopsis* and other plants. *Plant J.* 51, 1126–1136. doi: 10.1111/j.1365-313X.2007.03212.x

Odani, K., Sasaki, S., Yamamoto, N., Nishiyama, Y., and Tamura, H. (1985). Differences in dispersal and multiplication of two associated nematodes, *Bursaphelenchus xylophilus* and *Bursaphelenchus mucronatus* in pine seedlings in relation to the pine wilt disease development. *J. Jpn. For. Soc.* 67, 398–403. doi: 10.11519/jjfs1953.67.10_398

Ong, S.-E., Blagoev, B., Kratchmarova, I., Kristensen, D. B., Steen, H., Pandey, A., et al. (2002). Stable isotope labeling by amino acids in cell culture, SILAC, as a simple and accurate approach to expression proteomics. *Mol. Cell. Proteomics* 1, 376–386. doi: 10.1074/mcp.M200025-MCP200

Palomares-Rius, J. E., Tsai, I. J., Karim, N., Akiba, M., Kato, T., Maruyama, H., et al. (2015). Genome-wide variation in the pinewood nematode *Bursaphelenchus xylophilus* and its relationship with pathogenic traits. *BMC Genomics* 16:845. doi: 10.1186/s12864-015-2085-0

Ross, P. L., Huang, Y. N., Marchese, J. N., Williamson, B., Parker, K., Hattan, S., et al. (2004). Multiplexed protein quantitation in *Saccharomyces cerevisiae* using amine-reactive isobaric tagging reagents. *Mol. Cell. Proteomics MCP* 3, 1154–1169. doi: 10.1074/mcp.M400129-MCP200

Santos, C. S., Pinheiro, M., Silva, A. I., Egas, C., and Vasconcelos, M. W. (2012). Searching for resistance genes to *Bursaphelenchus xylophilus* using high throughput screening. *BMC Genomics* 13:599. doi: 10.1186/1471-2164-13-599

Saucedo-García, M., Guevara-García, A., González-Solís, A., Cruz-García, F., Vázquez-Santana, S., Markham, J. E., et al. (2011). MPK6, sphinganine and the LCB2a gene from serine palmitoyltransferase are required in the signaling pathway that mediates cell death induced by long chain bases in *Arabidopsis*. *New Phytol.* 191, 943–957. doi: 10.1111/j.1469-8137.2011.03727.x

Shaffer, J. P. (1995). Multiple Hypothesis Testing. *Annu. Rev. Psychol.* 46, 561–584.

Shinya, R., Takeuchi, Y., and Futai, K. (2009). A technique for separating the developmental stages of the propagative form of the pine wood nematode (*Bursaphelenchus xylophilus*). *Nematology* 11, 305–307. doi: 10.1163/156854108X399164

Shinya, R., Morisaka, H., Takeuchi, Y., Ueda, M., and Futai, K. (2010). Comparison of the surface coat proteins of the pine wood nematode appeared during host pine infection and *in vitro* culture by a proteomic approach. *Phytopathol.* 100, 1289–1297. doi: 10.1094/PHYTO-04-10-0109

Shinya, R., Takeuchi, Y., Ichimura, K., Takemoto, S., and Futai, K. (2012). Establishment of a set of inbred strains of the pine wood nematode, *Bursaphelenchus xylophilus* (Aphelenchida: Aphelenchoididae), and evidence of their varying levels of virulence. *Appl. Entomol. Zool.* 47, 341–350. doi: 10.1007/s13355-012-0124-8

Shinya, R., Morisaka, H., Kikuchi, T., Takeuchi, Y., Ueda, M., and Futai, K. (2013). Secretome analysis of the pine wood nematode *Bursaphelenchus xylophilus* reveals the tangled roots of parasitism and its potential for molecular mimicry. *PLoS One* 8:e67377. doi: 10.1371/journal.pone.0067377

St John, F. J., González, J. M., and Pozharski, E. (2010). Consolidation of glycosyl hydrolase family 30: a dual domain 4/7 hydrolase family consisting of two structurally distinct groups. *FEBS Lett.* 584, 4435–4441. doi: 10.1016/j.febslet.2010.09.051

Vicente, C. S. L., Ikuyo, Y., Shinya, R., Mota, M., and Hasegawa, K. (2015). Catalases induction in high virulence pinewood nematode *Bursaphelenchus xylophilus* under hydrogen peroxide-induced stress. *PLoS One* 10:e0123839. doi: 10.1371/journal.pone.0123839

Viney, M. E., and Thompson, F. J. (2008). Two hypotheses to explain why RNA interference does not work in animal parasitic nematodes. *Int. J. Parasitol.* 38, 43–47. doi: 10.1016/j.ijpara.2007.08.006

Yi, C. K., Byun, B. H., Park, J. D., Yang, S. I., and Chang, K. H. (1989). First finding of the pine wood nematode, *Bursaphelenchus xylophilus* (Steiner et Buhrer) Nickle and its insect vector in Korea. *Res. Rep. For. Res. Inst.* 38, 141–149.

Zhao, B. G., and Lin, F. (2005). Mutualistic symbiosis between *Bursaphelenchus xylophilus* and bacteria of the genus *Pseudomonas*. *For. Pathol.* 35, 339–345. doi: 10.1111/j.1439-0329.2005.00417.x

Zhou, Z., Sakaue, D., Wu, B., and Hogetsu, T. (2007). Genetic structure of populations of the pinewood nematode *Bursaphelenchus xylophilus*, the pathogen of pine wilt disease, between and within pine forests. *Phytopathology* 97, 304–310. doi: 10.1094/PHYTO-97-3-0304

Conflict of Interest: The authors declare that the research was conducted in the absence of any commercial or financial relationships that could be construed as a potential conflict of interest.

frontiers in Plant Science

REVIEW
published: 09 March 2021
doi: 10.3389/fpls.2021.641582

Molecular and Cellular Mechanisms Involved in Host-Specific Resistance to Cyst Nematodes in Crops

*Qi Zheng, Vera Putker and Aska Goverse**

Laboratory of Nematology, Department of Plant Sciences, Wageningen University, Wageningen, Netherlands

Cyst nematodes are able to infect a wide range of crop species and are regarded as a major threat in crop production. In response to invasion of cyst nematodes, plants activate their innate immune system to defend themselves by conferring basal and host-specific defense responses depending on the plant genotype. Basal defense is dependent on the detection of pathogen-associated molecular patterns (PAMPs) by pattern recognition receptors (PRRs), while host-specific defense mainly relies on the activation of canonical and non-canonical resistance (*R*) genes or quantitative trait loci (QTL). Currently, application of *R* genes and QTLs in crop species is a major approach to control cyst nematode in crop cultivation. However, emerging virulent cyst nematode field populations are threatening crop production due to host genetic selection by the application of a limited set of resistance genes in current crop cultivars. To counteract this problem, increased knowledge about the mechanisms involved in host-specific resistance mediated by *R* genes and QTLs to cyst nematodes is indispensable to improve their efficient and sustainable use in field crops. Despite the identification of an increasing number of resistance traits to cyst nematodes in various crops, the underlying genes and defense mechanisms are often unknown. In the last decade, indebt studies on the functioning of a number of cyst nematode *R* genes and QTLs have revealed novel insights in how plants respond to cyst nematode infection by the activation of host-specific defense responses. This review presents current knowledge of molecular and cellular mechanisms involved in the recognition of cyst nematodes, the activation of defense signaling and resistance response types mediated by *R* genes or QTLs. Finally, future directions for research are proposed to develop management strategies to better control cyst nematodes in crop cultivation.

Keywords: cyst nematode, host-specific resistance, resistance gene, resistance locus, effector, plant immunity, immune receptor

OPEN ACCESS

Edited by:
Juan Emilio Palomares-Rius, Consejo Superior de Investigaciones Científicas (CSIC), Spain

Reviewed by:
John Jones, The James Hutton Institute, United Kingdom
Miroslaw Sobczak, Warsaw University of Life Sciences, Poland

****Correspondence:***
Aska Goverse
aska.goverse@wur.nl

Specialty section:
This article was submitted to Plant Pathogen Interactions, a section of the journal Frontiers in Plant Science

Received: *14 December 2020*
Accepted: *16 February 2021*
Published: *09 March 2021*

Citation:
Zheng Q, Putker V and Goverse A (2021) Molecular and Cellular Mechanisms Involved in Host-Specific Resistance to Cyst Nematodes in Crops. Front. Plant Sci. 12:641582. doi: 10.3389/fpls.2021.641582

INTRODUCTION

Cyst nematodes are notorious plant parasites infecting a broad range of crops worldwide. The most damaging species include soybean cyst nematode (SCN; *Heterodera glycines*), with more than US1.5 billion of economic losses each year in the United States alone; potato cyst nematode (PCN; *Globodera pallida* and *Globodera rostochiensis*), with an estimated yield loss of 9% worldwide; and cereal cyst nematode (CCN; *Heterodera avenae*), with yield losses

up to 90% under nematode favorable environmental conditions (Jones et al., 2013). For long, the management of cyst nematode infections relied on the use of nematicides. Currently, cyst nematode control is highly dependent on crop rotation strategies and the application of a limited set of resistance genes in crop cultivars due to the ban on pesticide use in the soil since the early 00's (Hillocks, 2012). However, the application of a limited repertoire of resistance genes has resulted in host genetic selection of resistance-breaking populations in the field (Turner and Fleming, 2002; Niblack et al., 2008; McCarville et al., 2017; Mwangi et al., 2019), which threatens the lifespan of current resistant crop cultivars. These concerns demand for new resistance resources as well as increased knowledge of the genes involved for the durable application of resistant crop cultivars in the future.

Cysts can persist in the soil for decades, which make them particularly difficult to control (Lilley et al., 2005; Jones et al., 2013). One female can produce hundreds of nematode eggs. When she dies her swollen body hardens into a cyst to protect eggs, allowing them to stay viable in the soil for many years in the absence of a proper host. Upon hatching from the eggs, the pre-parasitic second-stage juveniles (pre-J2) migrate through the soil in search of a suitable host plant. Upon entering the host plant roots, they move intracellularly through the root to establish a permanent feeding site near the vascular cylinder. In a susceptible host, a large, multinucleate feeding structure is formed through cell wall dissolution and fusion of neighboring cells, a so called syncytium. Cyst nematodes are fully dependent on this feeding structure for their development and reproduction as the syncytium is the only source of nutrients for this group of sedentary endoparasitic nematodes. Parasitic J2 develop through three molting steps into adult females when nutrients are abundantly available, but into adult vermiform males when this is not the case (Grundler et al., 1991). In resistant crop plants, however, cyst nematodes are unable to establish such a successful feeding relationship. Upon recognition of the infective cyst nematode juvenile, the development of a syncytium and subsequently the formation of cysts are prevented due to a local defense response. The application of resistant crop cultivars is therefore very effective, but only a limited set of resistance traits to control cyst nematodes is currently known. In addition, the genes responsible for cyst nematode resistance are identified and characterized for only a few single dominant resistance (*R*) genes or quantitative trait loci (QTL) like *Gpa2* (van der Vossen et al., 2000) in potato and *Rhg1* in soybean (Concibido et al., 2004). However, indebt studies on the functioning of the corresponding genes revealed novel insights in host-specific defense responses to cyst nematodes. Hence, they can serve as an example for other *R* genes and QTLs conferring resistance to cyst nematodes, for which this information is still lacking.

In this review, we explore the current knowledge on the molecular and cellular mechanisms involved in host-specific resistance against cyst nematodes as conferred by either single dominant *R* genes or QTLs. We first shortly address the plant immune system, including basal immunity against cyst nematodes. Then, we focus on host-specific resistance by addressing *R* gene-mediated defense responses, including effector-triggered immunity. We highlight how these *R* genes are able to recognize cyst nematodes and activate downstream defense responses in plant cells based on a few available model systems. Then, we briefly address how cyst nematodes are able to evade or suppress this type of host defense responses. We also specify the potential mechanisms of host-specific resistance mediated by QTLs, including non-canonical resistance phenotypes. Finally, we discuss how this knowledge may contribute to a better understanding of plant defense to cyst nematodes as well as the control of cyst nematodes in crop cultivation.

BASAL DEFENSE RESPONSES TO CYST NEMATODES

During early stages in parasitism, cyst nematodes move intracellularly and cause root damage, leading to the release of Nematode-Associated Molecular Patterns (NAMPs) or Damage-Associated Molecular Patterns (DAMPs). These compounds can be perceived by extracellular Pattern Recognition Receptors (PRRs) and thereby elicit basal immunity, also named Pathogen-Associated Molecular Patterns (PAMPs)-Triggered Immunity (PTI; Choi and Klessig, 2016). To date, information about this first layer of plant immunity to cyst nematodes, including the role of NAMPs and PRRs, is limited. A conserved ascaroside (Asc#18) from *H. glycines* was identified as a NAMP as well as compounds present in cyst nematode (*Heterodera schachtii*) incubation water (NemaWater; Manosalva et al., 2015; Mendy et al., 2017). The *Arabidopsis* leucine-rich repeat (LRR) receptor-like kinase (RLK) NILR1 is yet the only classified cyst nematode PRR (Mendy et al., 2017). The activation of PTI results in a series of immune responses like reactive oxygen species (ROS)/NO production, secondary metabolite production, reinforcement of cell walls, and cell death around the migratory tract. For more details on cyst nematode-elicited PTI responses as well as the underlying molecular mechanism, we refer the reader to Sato et al. (2019).

Although PTI responses slow down nematode invasion and contribute to an effective defense in non-host plants, they are insufficient to stop the nematode from successfully infecting susceptible host plant roots. Just like other pathogens, nematodes are able to overcome PTI by the secretion of effector proteins which suppress basal immune responses (also called effector-triggered suppression or ETS; Jones and Dangl, 2006). Such cyst nematode effectors include GrVAP1, RHA1B, Ha18764, and GrCEP12 (Lozano-Torres et al., 2012; Chen et al., 2013; Kud et al., 2019; Yang et al., 2019). Most effectors are synthesized in esophageal gland cells and are secreted into the plant *via* a needle-like structure named the stylet (Hewezi and Baum, 2013; Vieira and Gleason, 2019). The suppression of basal immune responses enables cyst nematodes to establish a successful feeding relationship with a susceptible host plant for their development and reproduction (Ali et al., 2017; Vieira and Gleason, 2019).

EFFECTOR-TRIGGERED DEFENSE RESPONSES TO CYST NEMATODES

In response to ETS, plants have evolved a second layer of immunity according to the zigzag model (Jones and Dangl, 2006). Resistant plant genotypes exhibit single dominant *R* genes, encoding immune receptors that recognize specific pathogen effectors or their activities, and subsequently activate so called effector-triggered immunity (ETI). Recognition can either be direct or indirect, meaning that a host-derived co-factor is required for successful pathogen perception (Jones and Dangl, 2006; Araújo et al., 2019). Moreover, *R* genes can only recognize their matching effector which is encoded by a corresponding avirulence (*Avr*) gene. Only when an *Avr* gene containing pathotype matches an *R* gene containing plant genotype, the plant can successfully activate a host-specific resistance response. This is known as the gene-for-gene concept (Flor, 1971), which also applies to cyst nematodes as demonstrated for the single dominant *R* gene *H1* from potato that confers host-specific resistance to avirulent populations of *G. rostochiensis* (Janssen et al., 1991).

R Genes Against Cyst Nematodes Encode Different Types of Plant Immune Receptors

Effector detection by immune receptors occurs intra- and extracellularly. Extracellular immune receptors, including RLKs and receptor-like proteins (RLPs), contain a LRR domain fused to a transmembrane domain (Takken and Joosten, 2000; Kanyuka and Rudd, 2019). Extracellular immune receptors encoded by *R* genes have the same type of structure as PRRs (Boutrot and Zipfel, 2017), but they are able to activate highly specific defense responses upon the direct or indirect detection of apoplastic effectors from specific pathogen strains. In terms of resistance to cyst nematodes, so far two RLP immune receptors have been characterized (**Figure 1**). One example is the sugar beet receptor $Hs1^{pro\text{-}1}$, which was linked to resistance to the cyst nematode *H. schachtii* (Cai et al., 1997). However, the resistance phenotype cannot be inherited to the next generations by backcrossing of an $Hs1^{pro\text{-}1}$ genotype and a susceptible genotype (Sandal et al., 1997) raising questions about its contributions to cyst nematode immunity in sugar beet. Another example is the tomato immune receptor Cf-2, which confers resistance to the PCN *G. rostochiensis* (Lozano-Torres et al., 2012).

The most abundant class of *R* genes encodes intracellular Nucleotide binding (NB)-LRR proteins (NLR). NLRs contain a C-terminal LRR (LRR) domain involved in recognition and a central nucleotide-binding, Apaf-1, R-proteins, and CED-4 (NB-ARC) domain, which acts as a molecular switch and consists of three subdomains (NB, ARC1, and ARC2). The N-terminus is a signaling domain, which divides NLRs into either a subclass of Toll-interleukin receptor (TIR)-like receptors (TIR-NB-LRRs) or coiled coil (CC) receptors (CC-NB-LRRs). Both subclasses are found to be encoded by *R* genes conferring resistance against cyst nematodes (**Figure 1**). For example, the potato resistance gene *Gpa2* confers resistance to *G. pallida* and its product belongs to the CC-NB-LRR (CNL) type (van der Vossen et al., 2000), whereas a typical example of a TIR-NB-LRR (TNL) is encoded by *Gro1-4* from potato conferring resistance to *G. rostochiensis* (Paal et al., 2004). In addition, some CNLs exhibit an extended Solanaceae Domain (SD) at the N terminus of the CC domain, which is uniquely found in Solanaceous plant species. For example, the tomato resistance gene *Hero A* is a typical example that belongs to the SD-CNL type, which confers broadspectrum resistance to PCN populations from *G. pallida* and *G. rostochiensis* (Ernst et al., 2002).

Molecular Mechanisms of Different Types of Cyst Nematode *R* Genes

A major bottleneck in our understanding of *R* gene-mediated cyst nematode resistance is that the matching effector for most nematode *R* genes is unknown. Currently, only two *R* gene-effector pairs are identified. These are the extracellular immune receptor Cf-2, which elicits an immune response upon recognition of the effector GrVAP1 from *G. rostochiensis* (Lozano-Torres et al., 2012) and the intracellular immune receptor Gpa2, which recognizes the effector GpRBP-1 from *G. pallida* (Sacco et al., 2009). Over the last decade, several indebt studies have revealed novel insights in their functioning and role in conferring host-specific resistance to cyst nematodes. Therefore, *Cf-2* and *Gpa2* can serve as examples for other cyst nematode resistance genes, for which information on the molecular mechanisms underlying recognition and downstream signaling activation of immune responses against cyst nematodes is still lacking.

Cf2-Mediated Apoplastic Immunity to Cyst Nematodes

The extracellular immune receptor Cf-2 belongs to the RLP type of immune receptors and confers apoplastic immunity to the PCN *G. rostochiensis* upon detection of the effector GrVAP1, which is produced in the subventral glands during the onset of parasitism (Lozano-Torres et al., 2012). The detection of GrVAP1 by Cf-2 is indirect through the detection of perturbations of the apoplastic papain-like cysteine protease (PLCP) Rcr3. Cf-2 detection of GrVAP1 through Rcr3 results in the activation of cyst nematode resistance, which induces a local programmed cell death response in cells directly around the nematodes as well as in most of the nematode-induced feeding structures (Lozano-Torres et al., 2012). A recent study shows the underlying mechanism of how Rcr3 in tomato participates in the activation of defense responses. Rcr3 is present in its inactive form ProRcr3, and a group of proteases called subtilases cleave off the prodomain of Rcr3. This results in a mature mRcr3, thereby creating a binding site for the effector (Paulus et al., 2020). Since distantly related subtilases can also activate Rcr3 in *Nicotiana benthamiana*, this suggests that there might be a network of proteolytic cascades in Solanaceous plants to provide robust apoplastic immunity (Kourelis et al., 2020; Paulus et al., 2020), which may also apply to cyst nematodes in Cf-2 resistant tomato plants.

Interestingly, GrVAP1 is not the only pathogen effector that targets Rcr3. Avr2, from the fungus *Cladosporium fulvum*,

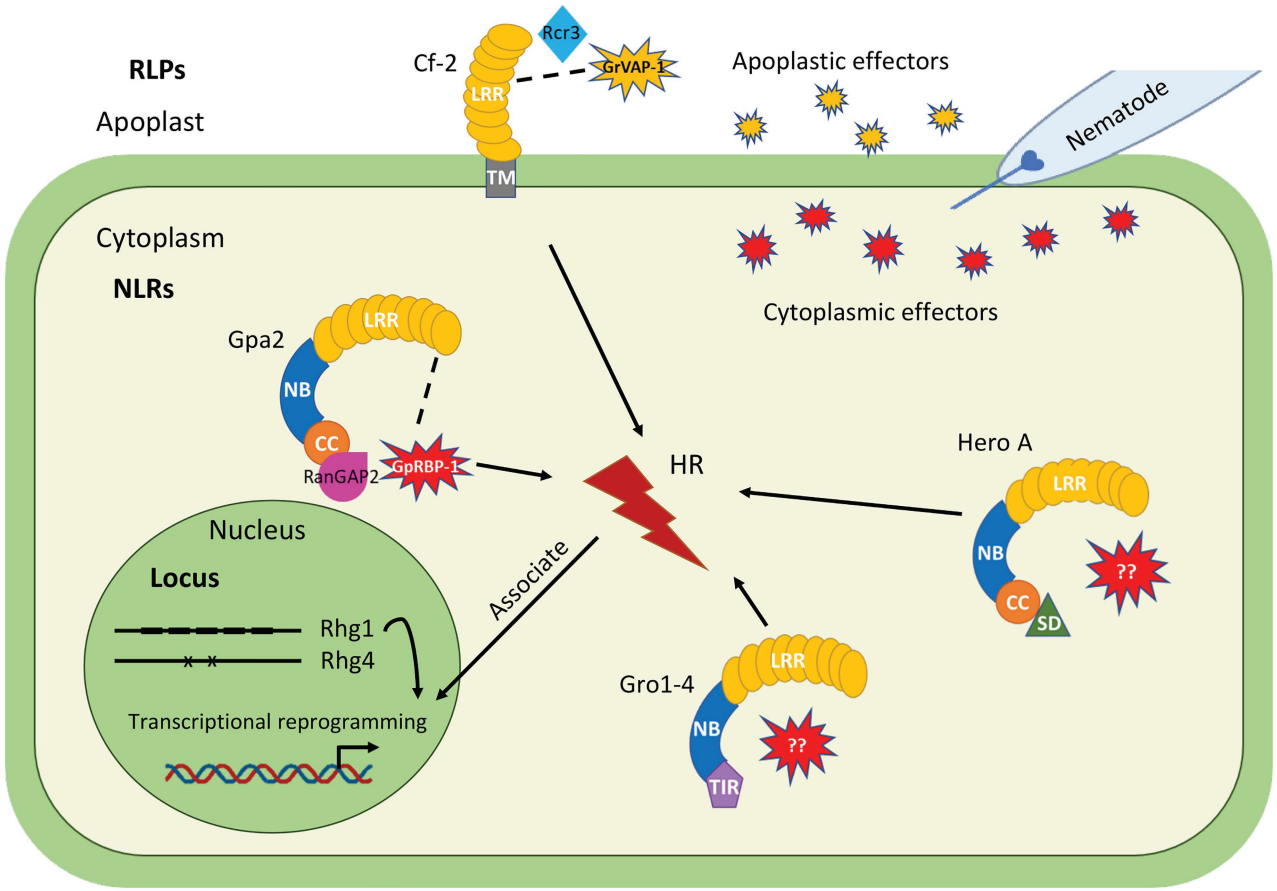

FIGURE 1 | Overview of major cyst nematode resistance (*R*) genes and loci (QTLs) identified in crop species, for which knowledge is available on the molecular and cellular mechanisms underlying cyst nematode resistance. Extracellular immune receptors: *Cf-2* from tomato encodes a RLP and confers resistance to the potato cyst nematode (PCN) *Globodera rostochiensis*, respectively. Cf-2 detects the nematode effector GrVAP-1 *via* the host factor Rcr3, which is activated by apoplastic serine proteases named subtilases to induce apoplastic immunity. Intracellular Nucleotide binding (NB)-Leucine-rich Repeat (LRR; NLR) immune receptors: *Gro1-4* from potato encodes a toll-interleukin receptor-nucleotide binding-LRR (TIR-NB-LRR) protein, whereas *Gpa2* from potato encodes a coiled coil-NB-LRR (CC-NB-LRR) protein. *Hero A* from tomato encodes a Solanaceae Domain-CC-NB-LRR (SD-CC-NB-LRR) protein. These intracellular immune receptors all confer resistance to specific PCN populations from *G. rostochiensis*, *Globodera pallida*, or both. Only for Gpa2, the matching nematode effector GpRBP-1 is known which is able to activate a local HR response. Detection of nematode effector GpRBP-1 by Gpa2 requires a host factor RanGAP2. Resistance loci: the *Rhg1* and *Rhg4* loci from soybean confer resistance to field populations from the cyst nematode *Heterodera glycines*. *Rhg1*-mediated resistance depends on copy number variation, as the high copy number *Rhg1* type confers resistance on its own while the low copy number *Rhg1* type requires the *Rhg4* locus to confer resistance. Two polymoriphisms determine *Rhg4*-mediated resistance.

Cip1 from the bacteria *Pseudomonas syringae*, and several EPIC effectors from the oomycete *Phytophthora infestans* target Rcr3 as well with a variable prosperity in Cf-2-mediated defense responses (Rooney et al., 2005; Ilyas et al., 2015; Misas Villamil et al., 2019). However, these effectors also inhibit a paralog of Rcr3: Pip1 which is present more abundantly compared to Rcr3. Findings by knockdown studies (Ilyas et al., 2015) suggested that Pip1 is the actual operative target of the effectors, while Rcr3 acts as a decoy to trap the pathogen into a recognition event. This guard/decoy-recognition model allows plants to respond faster and more efficient to multiple and unrelated pathogens present in the environment *via* a common host target (van der Hoorn and Kamoun, 2008). Moreover, it indicates that different pathogens including cyst nematodes have evolved effectors that are able to inhibit plant proteases during co-evolution (Kourelis et al., 2020).

Gpa2-Mediated Intracellular Immunity to Cyst Nematodes

In contrast to Cf-2, the intracellular CNL immune receptor Gpa2 activates a specific defense response upon detection of the dorsal gland effector GpRBP-1 from *G. pallida* inside the cell, resulting in a hypersensitive response (HR) in *N. benthamiana* leaves in agroinfiltration assays (Sacco et al., 2009). GpRBP-1 recognition by Gpa2 is determined by a single amino acid polymorphism at position 187 in the SPRY domain of GpRBP-1 (Sacco et al., 2009). However, no physical interaction between Gpa2 and GpRBP-1 was detected which may point at an

indirect interaction. It is hypothesized that Gpa2 senses the presence of GpRBP-1 *via* a host factor RanGAP2, due to a physical interaction between the CC domain of Gpa2 and RanGAP2 (Sacco et al., 2007, 2009). Silencing of RanGAP2 compromises Gpa2-mediated HR, but artificial tethering of RanGAP2 and GpRBP-1 enhances Gpa2-mediated defense responses (Sacco et al., 2009). These data suggest that RanGAP2 potentially works as a recognition co-factor for Gpa2 and may play an important role in downstream signaling regulation.

Remarkably, RanGAP2 is also required for Rx1-mediated resistance responses. The CNL Rx1 is a close homolog of Gpa2 that resides in the same *R* gene cluster on ChrXII of potato and confers resistance to *Potato virus X* (van der Vossen et al., 2000). The CC domain of Rx1 interacts with the N-terminal WPP domain of RanGAP2 and is present in plant cells as a heteromeric complex when in its inactive state (Sacco et al., 2007; Hao et al., 2013). Moreover, Rx1 locates in both the nucleus and the cytoplasm of plant cells, and RanGAP2 acts as a cytoplasmic retention factor of Rx1, thereby facilitating Rx1 functioning (Tameling et al., 2010). The nuclear hyperaccumulation of Rx1 mediated by nuclear targeted RanGAP2 WPP domain blocks Rx1 auto-activity. As the Gpa2, CC domain also interacts with RanGAP2, it is speculated that hyperaccumulation of Gpa2 in the nucleus may also block its defense signaling initiation. Nonetheless, whether RanGAP2 also regulates Gpa2 functioning by mediating its subcellular partitioning remains to be demonstrated.

Structure-informed studies revealed the contribution of intra- and interdomain interactions in Gpa2 functioning as a molecular switch in plant immunity to cyst nematodes. Extensive sequence exchange between Gpa2 and Rx1 showed that a minimal region of the ARC2 together with the N-terminal repeats of the LRR domain is sufficient to initiate activation of the immune receptors (Slootweg et al., 2013). Additionally, domain swaps between regions of the LRR of Gpa2 and Rx1 resulted in the conversion of virus resistance into nematode resistance and vice versa (Slootweg et al., 2017), demonstrating that the CC-NB-ARC domain operates independently of the pathogen that is recognized whereas the LRR domain determines recognition specificity. Furthermore, comparative sequence analysis and computational structure analysis revealed that Rx1/Gpa2 polymorphisms in the LRR domain are under positive selection and surface exposed consistent with a possible role in pathogen detection (Slootweg et al., 2013). However, the dynamic process of how *R* genes like Gpa2 switch from an inactive to an active state upon cyst nematode detection remains elusive. Breakthrough discoveries on the 3D modeling and cryoEM-structure analyses as reported for the *Arabidopsis* CNL immune receptor ZAR1 in its inactive, primed, and activated state (Wang et al., 2019a,b) are expected to provide novel insights in the functional dynamics of NLR immune receptors in the near future. Moreover, it underscores the importance of structural approaches in plant resistance research to increase our understanding about the molecular warfare between cyst nematodes and their host plants.

Recently, both Rx1 and Gpa2 have been identified as so called sensor NLRs (Wu et al., 2017; Adachi et al., 2019a). In Solanaceous plants, a major class of CNLs, have been identified to form an immunoreceptor network in which sensor NLRs can directly or indirectly perceive molecules derived from pathogens, but require paired so called helper NLRs to activate immune responses. As a helper, NRCs (NLR required for cell death) are thought to translate upstream signaling from sensor NLRs to downstream signaling components for the activation of immune responses (Wu et al., 2018; Adachi et al., 2019b). Rx1 requires NRC2, NRC3, or NRC4 to activate a resistance response. The triple silencing of NRC2, NRC3, and NRC4 compromises Rx1-mediated resistance to PVX while the individual silencing remains Rx1 functional, indicating that these NRC proteins redundantly contribute to Rx1-mediated resistance. It remains to be seen which helper NRCs are required for the activation of downstream defense response to cyst nematodes mediated by sensor NLRs like Gpa2 as well as Hero A (Wu et al., 2017). NRCs including NRC4 carry a MADA motif at the N-terminus, which is sufficient for triggering cell death (Adachi et al., 2019a). Interestingly, the MADA motif does not exist in NRC-dependent sensor NLRs like Rx1 and Gpa2, suggesting this motif might be degenerated during evolution. It is therefore likely that Rx1 and Gpa2 rely on the MADA motif of their helper NRCs to activate defense responses upon virus and nematode recognition, respectively.

Downstream Signaling Pathways Involved in Host-Specific Resistance to Cyst Nematodes

Activation of R proteins leads to the transcriptional reprogramming of cells leading to the activation of local and systemic defense responses. Transcriptome studies revealed insights in downstream signaling pathways involved in host-specific resistance to cyst nematodes (Uehara et al., 2010; Walter et al., 2018). For instance, in resistant tomato harboring the *Hero A* gene, the salicylic acid (SA)-dependent pathogenesis-related protein 1 (PR-1) shows a markable increase in expression at 3 dpi upon *G. rostochiensis* infection compared to susceptible plants (Uehara et al., 2010). This was not the case in resistant plants with an extra inserted *NahG* gene, which can prevent SA accumulation, indicating that SA plays a key role in Hero A-mediated resistance to cyst nematodes. Another transcriptome study performed on resistant potato containing the *H1* gene shows upregulation of many genes after *G. rostochiensis* infection, including the tomato stress-responsive factor TSRF1 and a cysteine protease (Walter et al., 2018). TSRF1 is an ethylene responsive factor, which can be upregulated by ethylene or SA treatment (Zhang et al., 2004). The same study also shows that TSRF1 can interact with the GCC box located in the promoter of *PR* genes. Taken together, H1-induced TSRF1 upregulation possibly triggers PR proteins accumulation, which is consistent with the finding of systemic PR protein accumulation in leaves in *G. rostochiensis* infected H1 resistant potato plants (Hammond-Kosack et al., 1989). From this, a picture emerges in which ethylene- and/or SA-dependent pathways might be involved in H1-triggered resistance to cyst nematodes similar to what has been reported for other *R* gene-mediated

resistance responses to other pathogens (Denancé et al., 2013; Broekgaarden et al., 2015; Islam et al., 2019).

Transcriptome analysis on the resistant wheat genotype VP1620 shows that jasmonic acid (JA) regulated PR4 and PR10 are significantly induced upon infection by CCN *H. avenae*, suggesting that the JA pathway is involved in resistance against CCN in this monocot crop (Kong et al., 2015). Moreover, the abundant presence of phospholipase D1/2 in the KEGG pathways suggests a role for ROS in conferring resistance to CCN (Kong et al., 2015), since phospholipase positively regulates defense responses *via* the ROS pathway (Wang, 2005; Pinosa et al., 2013). In another transcriptome study, transcription factor WRKY40 and WRKY70 are upregulated in resistant soybean genotype PI533561 upon infection by a *H. glycines* virulent type named HG type 0 (Jain et al., 2016). WRKY70 has been shown to be involved in the regulation of the ROS pathway in defense, suggesting that the ROS pathway might be involved in resistance to SCN as well. Moreover, the PR-5 like receptor kinase shows an upregulation in the resistant genotype, indicating that a similar SA pathway may be involved in response to SCN infection. Interestingly, WRKY40/70 and one PR family protein (Phvul.005G081500) also show an upregulation in susceptible genotype GTS-900 (Jain et al., 2016); implying ROS and SA pathways may also be involved in basal defense.

R Gene-Mediated Resistance Response Types to Cyst Nematodes

In resistant plants, cyst nematodes are blocked in their life cycle and reproduction due to host-specific defense responses induced by R proteins. During normal cyst nematode development and reproduction, the syncytium is crucial since it functions as the only nutrient source for this obligatory biotrophic endoparasite. Host-specific resistance by *R* genes often associates with an HR, which causes necrosis around the nematode-induced syncytia. According to the timing in the ontogeny of feeding structures and characteristic cytological features, host-specific resistance to cyst nematodes can be roughly divided into two types (Goverse and Smant, 2014; Smant et al., 2018). The first type allows the initiation of a syncytium, but the expansion of the syncytium is restricted by the formation of a layer of necrotic cells around the young feeding structure (**Figure 2**). The initiated syncytium still allows the development of males, but does not support the development of females due to the poorly developed feeding structure. This type of "male-biased" resistance is observed for *R* genes like *H1* and *Hero A* (Rice et al., 1985; Sobczak et al., 2005). The second type of resistance occurs in a later stage of the plant-nematode interaction and allows syncytium formation and expansion (**Figure 2**). These young syncytia are functional and support the initiation of female development. However, a layer of necrosis around the syncytium is formed soon thereafter to disconnect the syncytium from the vascular cylinder. In this way, the transfer cell function of the syncytium is compromised and female development is arrested due to starvation. A typical example of this delayed resistance responses are induced by the potato R protein Gpa2, which confers host-specific resistance to PCN *G. pallida* (van der Vossen et al., 2000; Mwangi et al., 2019).

EVASION OR SUPPRESSION OF *R* GENE-MEDIATED IMMUNITY BY CYST NEMATODE EFFECTORS

To evade recognition by R proteins, cyst nematodes have evolved effector variants which are not recognized or able to suppress the activation of host-specific defense responses. Examples of such effectors were recently identified, such as SPRYSEC effectors (Diaz-Granados et al., 2016), an E3 ubiquitin ligase RHA1B (Kud et al., 2019), and an expansin-like protein GrEXPB2 (Ali et al., 2015a). The SPRYSEC effector family is characterized as a single SPRY domain-containing protein, secreted from the dorsal esophageal gland of PCNs (Diaz-Granados et al., 2016). SPRYSEC effectors from *G. rostochiensis*, including SPRYSEC-4/5/8/18/19, function as suppressors of HR and disease resistance mediated by CNL immune receptors like Rx1 (Postma et al., 2012; Ali et al., 2015b). A typical example is *G. rostochiensis* effector SPRYSEC-19, which can physically interact with the tomato intracellular CNL immune receptor homolog Sw5F both *in vitro* and *in planta* as show by Y2H; GST-pull down and Co-IP (Rehman et al., 2009; Postma et al., 2012). The minimal domain for this interaction is the C-terminal end of the LRR domain. Although this is in line with a possible role for the LRR in cyst nematode detection, co-expression of Sw5F and SPRYSEC-19 did not trigger an HR or resistance response to nematodes. Therefore, the function of Sw5F in plant immunity to cyst nematode still remains elusive (Postma et al., 2012).

Another example is the effector from *G. pallida* named RHA1B, which is characterized as an E3 ubiquitin ligase that functions in ubiquitin-proteasome pathway-mediated protein degradation (Kud et al., 2019). RHA1B applies two distinct ways to suppress plant immunity during nematode parasitism: it suppresses PTI signaling *via* a yet unknown E3-independent manner, and it suppresses HR mediated by several R proteins *via* E3-dependent degradation of R proteins. In addition, an apoplastic effector from *G. rostochiensis*, an expansin-like protein GrEXPB2, could inhibit a set of NLR immune receptors, including Rx1 and N mediated defense responses in the cytoplasm (Ali et al., 2015a). As GrEXPB2 is highly accumulating in pre-parasitic stages and decreases quickly during plant infection, it is speculated that GrEXPB2 might be involved in suppression of early PTI or ETI upon root invasion by cyst nematodes. However, GrEXPB2 also triggers necrosis in tomato and potato but not tobacco (Ali et al., 2015a). The activation of defense in a plant species-dependent manner suggests the specific recognition of the effector by the plant immune system, indicating that GrEXPB2 retains its dual role in suppressing and triggering plant defense responses.

QUANTITATIVE TRAIT LOCI CONFERRING HOST-SPECIFIC RESISTANCE TO CYST NEMATODES

In addition to single dominant *R* genes that encode for immune receptors, host-specific resistance to cyst nematodes can also

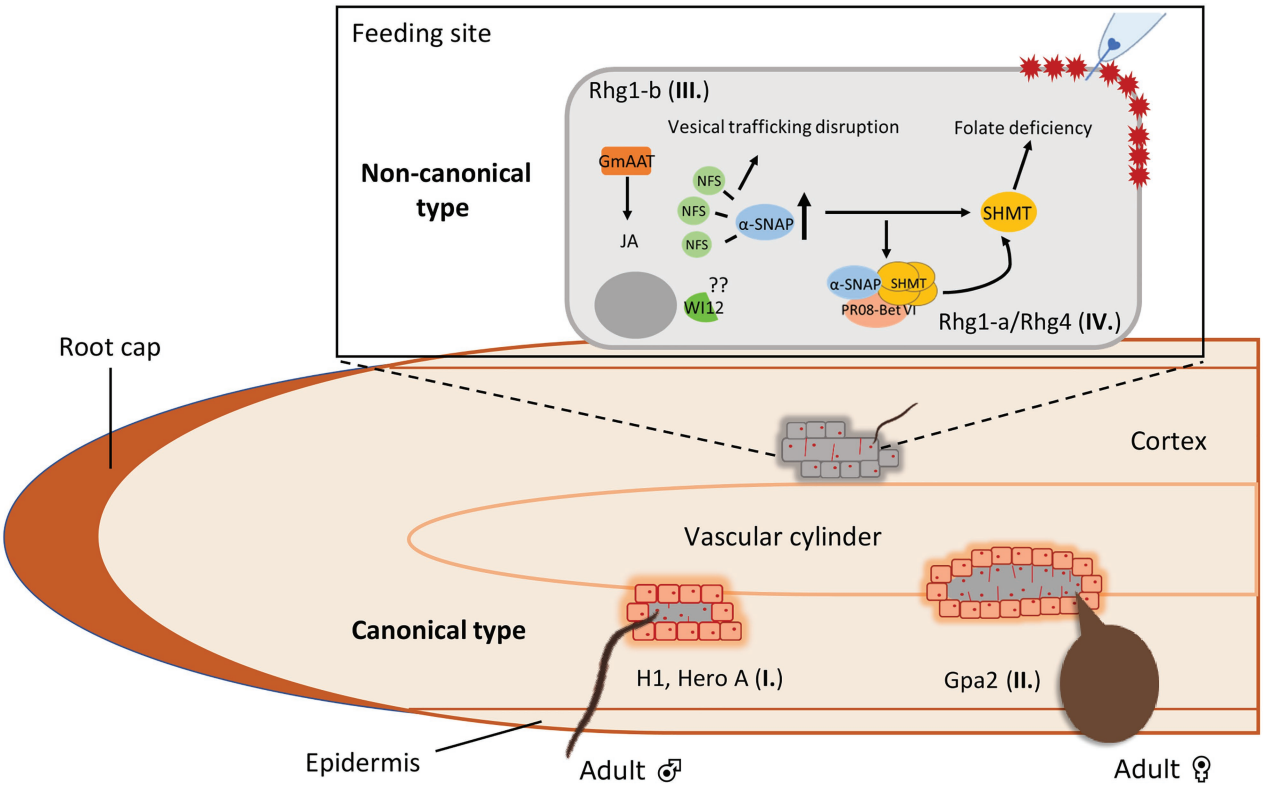

FIGURE 2 | Host-specific defense responses against cyst nematodes in plant roots harboring major *R* genes or resistance loci (QTLs). Type I. A subset of *R* genes mediate early defense responses to cyst nematodes that allows syncytium initiation but restricts further expansion by forming a layer of necrotic cells around the young feeding structures. As a result, these encapsulated syncytia allow the development of males but not females. This "male-biased" resistance is seen for *R* genes like *H1* in potato and *Hero A* in tomato. Type II. Another subset of *R* genes mediates a late defense response that allows syncytium formation and expansion, supporting the development of females. In this case, a layer of necrotic cells is formed around the expanded syncytium which disrupts the connection between the syncytium and the vascular cylinder. Thereby, female development is restricted due to the lack of nutrition. This "female-biased" resistance is observed for *R* genes like *Gpa2* from potato. Whereas the type I and II responses are typical for cyst nematode *R* genes encoding NB-LRR immune receptors, the resistance loci *Rhg1* and *Rhg4* trigger non-canonical resistance responses to cyst nematodes in soybean roots. Type III. The high copy number *Rhg1-b* type encodes a α-SNAP protein that poorly interacts with the protein NSF to disrupt vesical trafficking. Meanwhile, the hyperaccumulation of α-SNAP is thought to promote the collapse of the plant-nematode biotrophic interface leading to nematode resistance. Type IV. *Rhg4*-mediated resistance is determined by two polymorphisms in the encoded protein serine hydroxymethyltransferase (SHMT). SHMT regulates folate homeostasis leading to folate deficiency, causing the poor development and difficult maintenance of syncytia. Interestingly, cross-talk occurs in low copy number *Rhg1-a*, which requires *Rhg-4* to activate SCN resistance. It is thought that the elevated levels of *Rhg1-a* encoded α-SNAP induces *Rhg-4* encoded SHMT, which then physically interact with each other to form a complex with the pathogenesis-related protein PR08-Bet. This multiprotein complex regulates the activity of SHMT which leads to syncytium collapse and thus cyst nematode resistance.

be conferred by QTLs. In the last decades, many QTLs to different cyst nematode species in various major food crops have been identified such as *Rhg1* and Rhg4 to SCN in soybean (Cook et al., 2012; Liu et al., 2012), *Rha2* from barley conferring resistance to CCN (Kretschmer et al., 1997), and *Gpa*, *Grp1*, and *Gpa5* among others in potato conferring resistance to PCN (Kreike et al., 1994; van der Voort et al., 1998, 2000). QTLs may involve multiple or polymorphic genes present at different loci or even a particular locus, including essential genes that are required for achieving nematode resistance. Often, QTLs co-localize with NLR gene clusters as observed in potato suggesting that classical resistance gene homologs may contribute to host-specific resistance mediated by these QTLs (Bakker et al., 2011). However, an alternative explanation for the quantitative behavior of these QTLs loci could be the result of the heterogeneous composition of cyst nematode field populations used in the resistance tests. Interestingly, in case of *Rhg1* and *Rhg4*, host-specific resistance is not linked to NLR-mediated immunity and was shown to be mediated by non-canonical resistance genes (Cook et al., 2012; Liu et al., 2012).

Recently, several studies have revealed first insights in the molecular mechanisms underlying this novel type of resistance to cyst nematodes (**Figure 1**). For *Rhg1*, copy number variation plays an important role in determining SCN resistance since a higher copy number of genes at the *Rhg1* locus relates to an increased resistance phenotype (Cook et al., 2012, 2014; Yu et al., 2016). A copy of a 31-kilobase segment carrying three genes that contribute to resistance leads to an increased resistance to SCN, but only when the expression of this set of genes increases at the same time. Based on the copy number, at least two classes of

Rhg1 haplotypes are identified: low-copy *rhg1* (*rhg1-a*, Peking-type) and high-copy *rhg1* (*rhg1-b*, PI 88788-type). Three genes located in the 31-kilobase segment are required for resistance, which encode for an amino acid transporter, an alpha-soluble NSF (N-ethylmaleimide–sensitive factor) attachment protein (α-SNAP) protein and a wound-inducible domain (WI12) protein (Cook et al., 2012; Guo et al., 2019). The *rhg1-a* and *rhg1-b* haplotypes encode two different α-SNAP variants (Liu et al., 2017; Bayless et al., 2019), but both variants hyperaccumulate at SCN infection sites (Bayless et al., 2016, 2019; Lakhssassi et al., 2020a). The *rhg1-a* encoded α-SNAP carries a copia retrotransposon in its structure named RAC (*Rhg1* α-SNAP copia), which harbors intrinsic transcriptional activity (Bayless et al., 2019). However, the exact role of RAC in SCN resistance is not clear yet as no direct effect of RAC in regulating Peking-type *GmSNAP18* mRNA and protein level is detected. Different from the Peking-type GmSNAP18, *rhg1-b* encoded α-SNAP lacks the RAC element in its structure (Bayless et al., 2019). Interestingly, PI 88788-type GmSNAP18 poorly interacts with the NSF protein and disrupts vesical trafficking (Bayless et al., 2016). As such, the hyperaccumulation of PI 88788-type GmSNAP18 is thought to promote the collapse of the plant-nematode biotrophic interface leading to nematode resistance (**Figure 2**). The role of the amino acid transporter *Rhg1*-GmAAT in SCN resistance may be *via* the JA pathway, as overexpression of *Rhg1*-GmAAT induces JA accumulation and glutamic acid tolerance (Guo et al., 2019). The role of WI12 in *rhg1* mediated SCN resistance is not understood yet.

Rhg4 is another non-canonical resistance locus and *Rhg4*-mediated resistance to SCN is determined by two genetic polymorphisms residing near the ligand-binding sites of a serine hydroxymethyltransferase (SHMT; Liu et al., 2012). Mutation analysis showed that these polymorphisms affect the enzymatic activity of SHMT, which ubiquitously exists in nature and exhibits a key role in one-carbon folate metabolism (Cossins and Chen, 1997). The change of folate homeostasis can lead to folate deficiency, which may cause the poor development and difficult maintenance of syncytia. Alternatively, folate deficiency may trigger HR-like programmed cell death of the syncytium and lead to the death of nematodes as nematodes get insufficient folate from the host plant. The findings of *Rhg4*-mediated resistance reveal that plants may disrupt developmental or metabolic processes of the feeding structure itself to achieve resistance (**Figure 2**). The functional study of mutations on the SHMT protein structure revealed key residues that affect resistance to SCN (Kandoth et al., 2017; Shaibu et al., 2020). Meanwhile, the SHMT mutant still exhibits other functions in addition to its main enzymatic role in SCN resistance.

Rhg4 is required for Peking-type *rhg1-a* to confer resistance to SCN successfully (Liu et al., 2012) and this involves both Peking-type *rhg1-a* GmSNAP18 and *Rhg4-a* GmSHMT08 (Liu et al., 2017). Interestingly, two recent studies have revealed novel insights in the mechanisms underlying the crosstalk between Peking-type *rhg1-a* GmSNAP18 and *Rhg4-a* GmSHMT08. Peking-type GmSNAP18 physically interacts with the *Rhg4-a* GmSHMT08 tetramer and this interaction is strengthened by the pathogenesis-related protein GmPR08-Bet VI (Lakhssassi et al., 2020a,b). Mutational analysis shows that GmSHMT08 tetrameric structure is essential for GmSNAP18/GmSHMT08/GmPR08-Bet VI multi-protein complex formation (Lakhssassi et al., 2020b). GmPR08-Bet VI is suggested to contribute in SCN resistance as overexpression of the gene leads to an enhanced resistance to SCN while mutation of cytokinin-binding sites of the gene product abolishes its effect on SCN resistance (Lakhssassi et al., 2020a). Furthermore, these studies indicate that SA, cytokinin, and ROS pathways are involved in SCN resistance. Under SA and cytokinin treatments, GmSNAP18 and GmPR08-Bet VI are induced while GmSHMT08 is only induced in the presence of GmSNAP18, implying GmSHMT08 functions downstream of GmSNAP18 (Lakhssassi et al., 2020a). Collectively, a picture emerges in which SCN infection induces increased expression of GmSNAP18 which leads to a subsequent induction of GmSHMT08. Next, a GmSNAP18/GmSHMT08/GmPR08-Bet VI multi-protein complex is formed to regulate activity of GmSHMT08, including one-carbon folate metabolism and redox metabolism maintenance. Also, the trafficking of GmPR08-Bet VI toward infected cells increases the cytotoxicity in the cells. Consequently, necrosis and disruption of the syncytium occurs (**Figure 2**). Interestingly, for PI 88788-type of resistance, GmSNAP18 also interacts with GmSHMT08 and GmPR08-Bet VI is able to strengthen this interaction in the cells as in Peking-type (Lakhssassi et al., 2020b). However, PI 88788-type GmSNAP18 shows the incompatibility with Peking-type GmSHMT08 and this may explain the current difficulty in applying soybean lines that combine PI 88788-type and Peking-type in breeding strategies.

CONCLUSION AND FUTURE PERSPECTIVES

In this review, we have highlighted the current knowledge on the molecular and cellular mechanisms involved in host-specific resistance against cyst nematodes based on a few well-studied examples. In addition, information from other studies on the activation of host-specific downstream defense responses were addressed as well and integrated in this review to provide a comprehensive picture of the molecular mechanisms underlying different types of cyst nematode resistance known to date. From this, it can be concluded that host-specific defense to cyst nematodes in most cases is conferred by classical *R* genes encoding extra- and intracellular immune receptors upon specific recognition of cyst nematode effectors or their activities in the plant cell. Interestingly, host-specific defense to cyst nematodes is also conferred by non-canonical resistance loci directly interfering in the biotrophic interface between nematodes and their host plants. To counteract host-specific defense responses, either mediated by typical single dominant *R* genes as well as non-canonical QTLs, cyst nematodes have evolved molecular mechanisms to evade recognition by the plant immune system or by active suppression of defense responses. This co-evolutionary arms race explains both the diversity and copy number variation observed in *R* gene homologs as well as effector variants similar to what is reported for other pathosystems.

For cyst nematode *R* genes, only two model systems (e.g., Gpa2/GpRBP-1 and Cf2/GrVAP-1) are currently available for

which the matching immune receptor-effector pair is known. Such pairs allow the performance of biochemical, cellular, molecular, and functional studies to resolve the mechanisms underlying plant immunity to cyst nematodes. For example, agroinfiltration assays on leaves of *N. benthamiana* can be used instead of time consuming and highly variable nematode infection assays on crop plants, for which often effective genetic tools are lacking. However, only a few cyst nematode *R* genes and resistance loci are identified and characterized to date, which hampers advances in the field. It is anticipated though that this number will increase in the near future as the result of sequencing efforts of genomic regions combined with refined genetic mapping approaches in various crops linked to cyst nematode resistance (Concibido et al., 2004; Banu et al., 2017) For example, cyst nematode *R* gene loci are known in crops for years, such as the *H1* and *H2* gene in potato (Ellenby, 1952; Blok and Phillips, 2012), but the genes responsible for the resistance are still unknown. However, with the tools currently available for genetical and functional genomics studies, it is possible to identify the causal genes. Fine mapping in combination with genome sequencing revealed that the *H1* locus harbors a cluster of NLR candidate genes, suggesting that the *H1* gene is a classical single dominant *R* gene (Finkers-Tomczak et al., 2011). Similarly, the recent mapping of the *H2* gene in combination with NLR-specific enrichment sequencing (RenSeq), Diagnostic resistance gene enrichment (dRenSeq), and Generic-mapping enrichment sequencing of single/low-copy number genes (GenSeq) also revealed candidate *R* genes encoding NLR immune receptors (Strachan et al., 2019). So, the next step is to show their contribution to cyst nematode resistance, which can be examined by for example RNA interference (RNAi) or CRISPR-Cas9 gene editing techniques in a resistant background followed by infection of plants with a matching avirulent cyst nematode population to see if *R* gene mediated resistance is compromised (Shaibu et al., 2020).

The application of these advanced sequencing techniques combined with molecular mapping approaches will not only enhance the identification of novel *R* genes to cyst nematodes in major crops like potato, but also provides the accurate positioning of these genes on the chromosomes of crop genomes. Together, this knowledge and knowhow will facilitate the improvement of crop resistance to cyst nematodes by marker assisted selection and molecular breeding. Functional characterization of the (novel) responsible genes or QTLs as well as detailed insights about the underlying molecular and cellular mechanisms can contribute to the rational design of novel *R* genes (loci) with different recognition spectra, either through gene editing or targeted selection of resistance gene homologs in natural or breeding populations. In this way, broad spectrum resistance could be achieved in crop species to different cyst nematode populations. Also the stacking of *R* genes with different recognition spectra provides a promising strategy to obtain broad spectrum and durable resistance to cyst nematodes.

Another major bottleneck in this research area is the lack of knowledge on the corresponding effectors recognized by known cyst nematode *R* genes like *Hero A* or *GroV1*. Over the last decades, an increasing number of cyst nematode effectors have been identified and characterized, including several suppressors of plant immunity. However, whether certain effector variants are recognized by the plant immune system remains to be demonstrated. Gland-specific sequencing coupled with available nematode transcriptomics and genomics data allows identification of novel effectors, thereby expanding the current effector cyst nematode repertoire (Vieira and Gleason, 2019). Also, the prediction of dorsal gland promoter elements or specific motifs such as the dorsal gland box (DOG box; Eves-van den Akker and Birch, 2016; Eves-van den Akker et al., 2016) will contribute to the identification of pioneer cyst nematode effectors. Effector libraries can be subsequently used in screening approaches on resistant plant backgrounds with known *R* genes to find the corresponding Avirulence factors. In addition, such so called effectoromics approaches can also enable the identification of novel *R* genes based on the activation of a specific hypersensitive response upon screening of natural or breeding populations. So in conclusion, expanding the repertoire of R and Avr proteins in future research is a key step to obtain novel insights on the different molecular and cellular mechanisms underlying cyst nematode resistance and virulence. Moreover, it will contribute to a better understanding on how cyst nematodes are detection by the plant's immune system, but also how cyst nematodes have evolved mechanisms to evade host-specific defense mechanisms to increase their virulence. Ultimately, this knowledge can be exploited to develop improved control strategies to counteract cyst nematodes in crops.

AUTHOR CONTRIBUTIONS

QZ and AG contributed to the outline of the study. All authors contributed to manuscript writing, revision, reading, and approved the submitted version.

FUNDING

This work was supported by the China Scholarship Council (QZ) and the Dutch Technology Foundation STW and Earth and Life Sciences ALW (STW-GG 14529), which are part of the Netherlands Organization for Scientific Research (NWO).

REFERENCES

Adachi, H., Contreras, M., Harant, A., Wu, C. H., Derevnina, L., Sakai, T., et al. (2019a). An N-terminal motif in NLR immune receptors is functionally conserved across distantly related plant species. *eLife* 8:e49956. doi: 10.7554/eLife.49956

Adachi, H., Derevnina, L., and Kamoun, S. (2019b). NLR singletons, pairs, and networks: evolution, assembly, and regulation of the intracellular immunoreceptor circuitry of plants. *Curr. Opin. Plant Biol.* 50, 121–131. doi: 10.1016/j.pbi.2019.04.007

Ali, M. A., Azeem, F., Li, H., and Bohlmann, H. (2017). Smart parasitic nematodes use multifaceted strategies to parasitize plants. *Front. Plant Sci.* 8:1699. doi: 10.3389/fpls.2017.01699

Ali, S., Magne, M., Chen, S., Côté, O., Stare, B. G., Obradovic, N., et al. (2015a). Analysis of putative apoplastic effectors from the nematode, *Globodera*

rostochiensis, and identification of an expansin-like protein that can induce and suppress host defenses. *PLoS One* 10:e0115042. doi: 10.1371/journal.pone.0115042

Ali, S., Magne, M., Chen, S., Obradovic, N., Jamshaid, L., Wang, X., et al. (2015b). Analysis of *Globodera rostochiensis* effectors reveals conserved functions of SPRYSEC proteins in suppressing and eliciting plant immune responses. *Front. Plant Sci.* 6:623. doi: 10.3389/fpls.2015.00623

Araújo, A. C., de Fonseca, F. C. D. A., Cotta, M. G., Alves, G. S. C., and Miller, R. N. G. (2019). Plant NLR receptor proteins and their potential in the development of durable genetic resistance to biotic stresses. *Biotechnol. Res. Innov.* 3, 80–94. doi: 10.1016/j.biori.2020.01.002

Bakker, E., Borm, T., Prins, P., van der Vossen, E., Uenk, G., Arens, M., et al. (2011). A genome-wide genetic map of NB-LRR disease resistance loci in potato. *Theor. Appl. Genet.* 123, 493–508. doi: 10.1007/s00122-011-1602-z

Banu, J. G., Meena, K. S., Selvi, C., and Manickam, S. (2017). Molecular marker-assisted selection for nematode resistance in crop plants. *J. Entomol. Zool. Stud.* 5, 1307–1311.

Bayless, A. M., Smith, J. M., Song, J., McMinn, P. H., Teillet, A., August, B. K., et al. (2016). Disease resistance through impairment of α-SNAP-NSF interaction and vesicular trafficking by soybean Rhg1. *Proc. Natl. Acad. Sci. U. S. A.* 113, E7375–E7382. doi: 10.1073/pnas.1610150113

Bayless, A. M., Zapotocny, R. W., Han, S., Grunwald, D. J., Amundson, K. K., and Bent, A. F. (2019). The rhg1-a (Rhg1 low-copy) nematode resistance source harbors a copia-family retrotransposon within the Rhg1-encoded α-SNAP gene. *Plant Direct* 3:e00164. doi: 10.1002/pld3.164

Blok, V. C., and Phillips, M. S. (2012). Biological characterisation of Globodera pallida from Idaho. *Nematology* 14, 817–826. doi: 10.1163/156854112X627336

Boutrot, F., and Zipfel, C. (2017). Function, discovery, and exploitation of plant pattern recognition receptors for broad-spectrum disease resistance. *Annu. Rev. Phytopathol.* 55, 257–286. doi: 10.1146/annurev-phyto-080614-120106

Broekgaarden, C., Caarls, L., Vos, I. A., Pieterse, C. M. J., and Van Wees, S. C. M. (2015). Ethylene: traffic controller on hormonal crossroads to defense. *Plant Physiol.* 169, 2371–2379. doi: 10.1104/pp.15.01020

Cai, D., Kleine, M., Kifle, S., Harloff, H. J., Sandal, N. N., Marcker, K. A., et al. (1997). Positional cloning of a gene for nematode resistance in sugar beet. *Science* 275, 832–834. doi: 10.1126/science.275.5301.832

Chen, S., Chronis, D., and Wang, X. (2013). The novel GrCEP12 peptide from the plant-parasitic nematode *Globodera rostochiensis* suppresses flg22-mediated PTI. *Plant Signal. Behav.* 8:e25359. doi: 10.4161/psb.25359

Choi, H. W., and Klessig, D. F. (2016). DAMPs, MAMPs, and NAMPs in plant innate immunity. *BMC Plant Biol.* 16:232. doi: 10.1186/s12870-016-0921-2

Concibido, V. C., Diers, B. W., and Arelli, P. R. (2004). A decade of QTL mapping for cyst nematode resistance in soybean. *Crop Sci.* 44, 1121–1131. doi: 10.2135/cropsci2004.1121

Cook, D. E., Bayless, A. M., Wang, K., Guo, X., Song, Q., Jiang, J., et al. (2014). Distinct copy number, coding sequence, and locus methylation patterns underlie Rhg1-mediated soybean resistance to soybean cyst nematode. *Plant Physiol.* 165, 630–647. doi: 10.1104/pp.114.235952

Cook, D. E., Lee, T. G., Guo, X., Melito, S., Wang, K., Bayless, A. M., et al. (2012). Copy number variation of multiple genes at Rhg1 mediates nematode resistance in soybean. *Science* 338, 1206–1209. doi: 10.1126/science.1228746

Cossins, E. A., and Chen, L. (1997). Folates and one-carbon metabolism in plants and fungi. *Phytochemistry* 45, 437–452. doi: 10.1016/S0031-9422(96)00833-3

Denancé, N., Sánchez-Vallet, A., Goffner, D., and Molina, A. (2013). Disease resistance or growth: the role of plant hormones in balancing immune responses and fitness costs. *Front. Plant Sci.* 4:155. doi: 10.3389/fpls.2013.00155

Diaz-Granados, A., Petrescu, A. -J., Goverse, A., and Smant, G. (2016). SPRYSEC effectors: a versatile protein-binding platform to disrupt plant innate immunity. *Front. Plant Sci.* 7:1575. doi: 10.3389/fpls.2016.01575

Ellenby, C. (1952). Resistance to the potato root eelworm, *Heterodera rostochiensis* Wollenweber. *Nature* 170:1016. doi: 10.1038/1701016a0

Ernst, K., Kumar, A., Kriseleit, D., Kloos, D. U., Phillips, M. S., and Ganal, M. W. (2002). The broad-spectrum potato cyst nematode resistance gene (Hero) from tomato is the only member of a large gene family of NBS-LRR genes with an unusual amino acid repeat in the LRR region. *Plant J.* 31, 127–136. doi: 10.1046/j.1365-313X.2002.01341.x

Eves-van den Akker, S., and Birch, P. R. J. (2016). Opening the effector protein toolbox for plant–parasitic cyst nematode interactions. *Mol. Plant* 9, 1451–1453. doi: 10.1016/j.molp.2016.09.008

Eves-van den Akker, S., Laetsch, D. R., Thorpe, P., Lilley, C. J., Danchin, E. G. J., Da Rocha, M., et al. (2016). The genome of the yellow potato cyst nematode, *Globodera rostochiensis*, reveals insights into the basis of parasitism and virulence. *Genome Biol.* 17:124. doi: 10.1186/s13059-016-0985-1

Finkers-Tomczak, A., Bakker, E., de Boer, J., van der Vossen, E., Achenbach, U., Golas, T., et al. (2011). Comparative sequence analysis of the potato cyst nematode resistance locus H1 reveals a major lack of co-linearity between three haplotypes in potato (*Solanum tuberosum ssp.*). *Theor. Appl. Genet.* 122, 595–608. doi: 10.1007/s00122-010-1472-9

Flor, H. H. (1971). Current status of the gene-for-gene concept. *Annu. Rev. Phytopathol.* 9, 275–296. doi: 10.1146/annurev.py.09.090171.001423

Goverse, A., and Smant, G. (2014). The activation and suppression of plant innate immunity by parasitic nematodes. *Annu. Rev. Phytopathol.* 52, 243–265. doi: 10.1146/annurev-phyto-102313-050118

Grundler, F., Betka, M., and Wyss, U. (1991). Influence of changes in the nurse cell system (syncytium) on sex determination and development of the cyst nematode *Heterodera schachtii*: total amounts of proteins and amino acids. *Phytopathology* 81, 70–74. doi: 10.1094/Phyto-81-70

Guo, W., Zhang, F., Bao, A., You, Q., Li, Z., Chen, J., et al. (2019). The soybean Rhg1 amino acid transporter gene alters glutamate homeostasis and jasmonic acid-induced resistance to soybean cyst nematode. *Mol. Plant Pathol.* 20, 270–286. doi: 10.1111/mpp.12753

Hammond-Kosack, K. E., Atkinson, H. J., and Bowles, D. J. (1989). Systemic accumulation of novel proteins in the apoplast of the leaves of potato plants following root invasion by the cyst-nematode *Globodera rostochiensis*. *Physiol. Mol. Plant Pathol.* 35, 495–506. doi: 10.1016/0885-5765(89)90091-X

Hao, W., Collier, S. M., Moffett, P., and Chai, J. (2013). Structural basis for the interaction between the potato virus X resistance protein (Rx) and its cofactor ran GTPase-activating protein 2 (RanGAP2). *J. Biol. Chem.* 288, 35868–35876. doi: 10.1074/jbc.M113.517417

Hewezi, T., and Baum, T. J. (2013). Manipulation of plant cells by cyst and root-knot nematode effectors. *Mol. Plant-Microbe Interact.* 26, 9–16. doi: 10.1094/MPMI-05-12-0106-FI

Hillocks, R. J. (2012). Farming with fewer pesticides: EU pesticide review and resulting challenges for UK agriculture. *Crop Prot.* 31, 85–93. doi: 10.1016/j.cropro.2011.08.008

Ilyas, M., Hörger, A. C., Bozkurt, T. O., van den Burg, H. A., Kaschani, F., Kaiser, M., et al. (2015). Functional divergence of two secreted immune proteases of tomato. *Curr. Biol.* 25, 2300–2306. doi: 10.1016/j.cub.2015.07.030

Islam, W., Naveed, H., Zaynab, M., Huang, Z., and Chen, H. Y. H. (2019). Plant defense against virus diseases; growth hormones in highlights. *Plant Signal. Behav.* 14:1596719. doi: 10.1080/15592324.2019.1596719

Jain, S., Chittem, K., Brueggeman, R., Osorno, J. M., Richards, J., and Nelson, B. D. (2016). Comparative transcriptome analysis of resistant and susceptible common bean genotypes in response to soybean cyst nematode infection. *PLoS One* 11:e0159338. doi: 10.1371/journal.pone.0159338

Janssen, R., Bakker, J., and Gommers, F. (1991). Mendelian proof for a gene-for-gene relationship between virulence of *Globodera rostochiensis* and the H. *Rev. nématologie* 14, 207–211.

Jones, J. D. G., and Dangl, J. L. (2006). The plant immune system. *Nature* 444, 323–329. doi: 10.1038/nature05286

Jones, J. T., Haegeman, A., Danchin, E. G. J., Gaur, H. S., Helder, J., Jones, M. G. K., et al. (2013). Top 10 plant-parasitic nematodes in molecular plant pathology. *Mol. Plant Pathol.* 14, 946–961. doi: 10.1111/mpp.12057

Kandoth, P. K., Liu, S., Prenger, E., Ludwig, A., Lakhssassi, N., Heinz, R., et al. (2017). Systematic mutagenesis of serine hydroxymethyltransferase reveals an essential role in nematode resistance. *Plant Physiol.* 175, 1370–1380. doi: 10.1104/pp.17.00553

Kanyuka, K., and Rudd, J. J. (2019). Cell surface immune receptors: the guardians of the plant's extracellular spaces. *Curr. Opin. Plant Biol.* 50, 1–8. doi: 10.1016/j.pbi.2019.02.005

Kong, L. A., Wu, D. Q., Huang, W. K., Peng, H., Wang, G. F., Cui, J. K., et al. (2015). Large-scale identification of wheat genes resistant to cereal cyst nematode *Heterodera avenae* using comparative transcriptomic analysis. *BMC Genomics* 16:801. doi: 10.1186/s12864-015-2037-8

Kourelis, J., Malik, S., Mattinson, O., Krauter, S., Kahlon, P. S., Paulus, J. K., et al. (2020). Evolution of a guarded decoy protease and its receptor in solanaceous plants. *Nat. Commun.* 11:4393. doi: 10.1038/s41467-020-18069-5

Kreike, C. M., de Koning, J. R. A., Vinke, J. H., van Ooijen, J. W., and Stiekema, W. J. (1994). Quantitatively-inherited resistance to Globodera pallida is dominated by one major locus in Solanum spegazzinii. *Theor. Appl. Genet.* 88, 764–769. doi: 10.1007/BF01253983

Kretschmer, J. M., Chalmers, K. J., Manning, S., Karakousis, A., Barr, A. R., Islam, A. K. M. R., et al. (1997). RFLP mapping of the Ha2 cereal cyst nematode resistance gene in barley. *Theor. Appl. Genet.* 94, 1060–1064. doi: 10.1007/s001220050515

Kud, J., Wang, W., Gross, R., Fan, Y., Huang, L., Yuan, Y., et al. (2019). The potato cyst nematode effector RHA1B is a ubiquitin ligase and uses two distinct mechanisms to suppress plant immune signaling. *PLoS Pathog.* 15:e1007720. doi: 10.1371/journal.ppat.1007720

Lakhssassi, N., Piya, S., Bekal, S., Liu, S., Zhou, Z., Bergounioux, C., et al. (2020a). A pathogenesis-related protein GmPR08-bet VI promotes a molecular interaction between the GmSHMT08 and GmSNAP18 in resistance to *Heterodera glycines*. *Plant Biotechnol. J.* 18, 1810–1829. doi: 10.1111/pbi.13343

Lakhssassi, N., Piya, S., Knizia, D., El Baze, A., Cullen, M. A., Meksem, J., et al. (2020b). Mutations at the serine hydroxymethyltransferase impact its interaction with a soluble nsf attachment protein and a pathogenesis-related protein in soybean. *Vaccine* 8:349. doi: 10.3390/vaccines8030349

Lilley, C. J., Atkinson, H. J., and Urwin, P. E. (2005). Molecular aspects of cyst nematodes. *Mol. Plant Pathol.* 6, 577–588. doi: 10.1111/j.1364-3703.2005.00306.x

Liu, S., Kandoth, P. K., Lakhssassi, N., Kang, J., Colantonio, V., Heinz, R., et al. (2017). The soybean GmSNAP18 gene underlies two types of resistance to soybean cyst nematode. *Nat. Commun.* 8:14822. doi: 10.1038/s41467-017-02320-7

Liu, S., Kandoth, P. K., Warren, S. D., Yeckel, G., Heinz, R., Alden, J., et al. (2012). A soybean cyst nematode resistance gene points to a new mechanism of plant resistance to pathogens. *Nature* 492, 256–260. doi: 10.1038/nature11651

Lozano-Torres, J. L., Wilbers, R. H. P., Gawronski, P., Boshoven, J. C., Finkers-Tomczak, A., Cordewener, J. H. G., et al. (2012). Dual disease resistance mediated by the immune receptor Cf-2 in tomato requires a common virulence target of a fungus and a nematode. *Proc. Natl. Acad. Sci. U. S. A.* 109, 10119–10124. doi: 10.1073/pnas.1202867109

Manosalva, P., Manohar, M., Von Reuss, S. H., Chen, S., Koch, A., Kaplan, F., et al. (2015). Conserved nematode signalling molecules elicit plant defenses and pathogen resistance. *Nat. Commun.* 6:7795. doi: 10.1038/ncomms8795

McCarville, M. T., Marett, C. C., Mullaney, P. M., Gebhart, G. D., and Tylka, G. L. (2017). Increase in soybean cyst nematode virulence and reproduction on resistant soybean varieties in Iowa from 2001 to 2015 and the effects on soybean yields. *Plant Health Prog.* 18, 146–155. doi: 10.1094/PHP-RS-16-0062

Mendy, B., Wang'ombe, M. W., Radakovic, Z. S., Holbein, J., Ilyas, M., Chopra, D., et al. (2017). *Arabidopsis* leucine-rich repeat receptor–like kinase NILR1 is required for induction of innate immunity to parasitic nematodes. *PLoS Pathog.* 13:e1006284. doi: 10.1371/journal.ppat.1006284

Misas Villamil, J. C., Mueller, A. N., Demir, F., Meyer, U., Ökmen, B., Schulze Hüynck, J., et al. (2019). A fungal substrate mimicking molecule suppresses plant immunity via an inter-kingdom conserved motif. *Nat. Commun.* 10:1576. doi: 10.1038/s41467-019-09472-8

Mwangi, J. M., Niere, B., Finckh, M. R., Krüssel, S., and Kiewnick, S. (2019). Reproduction and life history traits of a resistance breaking Globodera pallida population. *J. Nematol.* 51, 1–13. doi: 10.21307/jofnem-2019-079

Niblack, T. L., Colgrove, A. L., Colgrove, K., and Bond, J. P. (2008). Shift in virulence of soybean cyst ematode is associated with use of resistance from PI 88788. *Plant Health Prog.* 9:29. doi: 10.1094/PHP-2008-0118-01-RS

Paal, J., Henselewski, H., Muth, J., Meksem, K., Menéndez, C. M., Salamini, F., et al. (2004). Molecular cloning of the potato Gro1-4 gene conferring resistance to pathotype Ro1 of the root cyst nematode *Globodera rostochiensis*, based on a candidate gene approach. *Plant J.* 38, 285–297. doi: 10.1111/j.1365-313X.2004.02047.x

Paulus, J. K., Kourelis, J., Ramasubramanian, S., Homma, F., Godson, A., Hörger, A. C., et al. (2020). Extracellular proteolytic cascade in tomato activates immune protease Rcr3. *Proc. Natl. Acad. Sci.* 117, 17409–17417. doi: 10.1073/pnas.1921101117

Pinosa, F., Buhot, N., Kwaaitaal, M., Fahlberg, P., Thordal-Christensen, H., Ellerström, M., et al. (2013). *Arabidopsis* phospholipase Dδ is involved in basal defense and nonhost resistance to powdery mildew fungi. *Plant Physiol.* 163, 896–906. doi: 10.1104/pp.113.223503

Postma, W. J., Slootweg, E. J., Rehman, S., Finkers-Tomczak, A., Tytgat, T. O. G. G., van Gelderen, K., et al. (2012). The effector SPRYSEC-19 of *Globodera rostochiensis* suppresses CC-NB-LRR-mediated disease resistance in plants. *Plant Physiol.* 160, 944–954. doi: 10.1104/pp.112.200188

Rehman, S., Postma, W., Tytgat, T., Prins, P., Qin, L., Overmars, H., et al. (2009). A secreted SPRY domain-containing protein (SPRYSEC) from the plant-parasitic nematode *Globodera rostochiensis* interacts with a CC-NB-LRR protein from a susceptible tomato. *Mol. Plant-Microbe Interact.* 22, 330–340. doi: 10.1094/MPMI-22-3-0330

Rice, S. L., Leadbeater, B. S. C., and Stone, A. R. (1985). Changes in cell structure in roots of resistant potatoes parasitized by potato cyst-nematodes. I. Potatoes with resistance gene H1 derived from *Solanum tuberosum ssp. andigena*. *Physiol. Plant Pathol.* 27, 219–234. doi: 10.1016/0048-4059(85)90069-4

Rooney, H. C. E., van't Klooster, J. W., van der Hoorn, R. A. L., Joosten, M. H. A. J., Jones, J. D. G., and de Wit, P. J. G. M. (2005). Cladosporium Avr2 inhibits tomato Rcr3 protease required for Cf-2-dependent disease resistance. *Science* 308, 1783–1786. doi: 10.1126/science.1111404

Sacco, M. A. A., Koropacka, K., Grenier, E., Jaubert, M. J. J., Blanchard, A., Goverse, A., et al. (2009). The cyst nematode SPRYSEC protein RBP-1 elicits Gpa2- and RanGAP2-dependent plant cell death. *PLoS Pathog.* 5:e1000564. doi: 10.1371/journal.ppat.1000564

Sacco, M. A., Mansoor, S., and Moffett, P. (2007). A RanGAP protein physically interacts with the NB-LRR protein Rx, and is required for Rx-mediated viral resistance. *Plant J.* 52, 82–93. doi: 10.1111/j.1365-313X.2007.03213.x

Sandal, N. N., Salentijn, E. M. J., Kleine, M., Cai, D., Arens-De Reuver, M., Van Druten, M., et al. (1997). Backcrossing of nematode-resistant sugar beet: a second nematode resistance gene at the locus containing Hslpro-1? *Mol. Breed.* 3, 471–480. doi: 10.1023/A:1009697119097

Sato, K., Kadota, Y., and Shirasu, K. (2019). Plant immune responses to parasitic nematodes. *Front. Plant Sci.* 10:1165. doi: 10.3389/fpls.2019.01165

Shaibu, A. S., Li, B., Zhang, S., and Sun, J. (2020). Soybean cyst nematode-resistance: gene identification and breeding strategies. *Crop J.* 8, 892–904. doi: 10.1016/j.cj.2020.03.001

Slootweg, E. J., Helder, J., van Schaik, C., Goverse, A., Dees, R., Smant, G., et al. (2017). Sequence exchange between homologous NB-LRR genes converts virus resistance into nematode resistance, and vice versa. *Plant Physiol.* 175, 498–510. doi: 10.1104/pp.17.00485

Slootweg, E. E. J. E. J., Spiridon, L. N. N., Roosien, J., Butterbach, P., Pomp, R., Westerhof, L., et al. (2013). Structural determinants at the interface of the ARC2 and leucine-rich repeat domains control the activation of the plant immune receptors Rx1 and Gpa2. *Plant Physiol.* 162, 1510–1528. doi: 10.1104/pp.113.218842

Smant, G., Helder, J., and Goverse, A. (2018). Parallel adaptations and common host cell responses enabling feeding of obligate and facultative plant parasitic nematodes. *Plant J.* 93, 686–702. doi: 10.1111/tpj.13811

Sobczak, M., Avrova, A., Jupowicz, J., Phillips, M. S., Ernst, K., and Kumar, A. (2005). Characterization of susceptibility and resistance responses to potato cyst nematode (Globodera spp.) infection of tomato lines in the absence and presence of the broad-spectrum nematode resistance Hero gene. *Mol. Plant-Microbe Interact.* 18, 158–168. doi: 10.1094/MPMI-18-0158

Strachan, S. M., Armstrong, M. R., Kaur, A., Wright, K. M., Lim, T. Y., Baker, K., et al. (2019). Mapping the H2 resistance effective against Globodera pallida pathotype Pa1 in tetraploid potato. *Theor. Appl. Genet.* 132, 1283–1294. doi: 10.1007/s00122-019-03278-4

Takken, F. L. W., and Joosten, M. H. A. J. (2000). Plant resistance genes: their structure, function and evolution. *Eur. J. Plant Pathol.* 106, 699–713. doi: 10.1023/A:1026571130477

Tameling, W. I. L., Nooijen, C., Ludwig, N., Boter, M., Slootweg, E., Goverse, A., et al. (2010). RanGAP2 mediates nucleocytoplasmic partitioning of the NB-LRR immune receptor Rx in the Solanaceae, thereby dictating Rx function. *Plant Cell* 22, 4176–4194. doi: 10.1105/tpc.110.077461

Turner, S. J., and Fleming, C. C. (2002). Multiple selection of potato cyst nematode Globodera pallida virulence on a range of potato species. I. Serial selection on Solanum-hybrids. *Eur. J. Plant Pathol.* 108, 461–467. doi: 10.1023/A:1016018002152

Uehara, T., Sugiyama, S., Matsuura, H., Arie, T., and Masuta, C. (2010). Resistant and susceptible responses in tomato to cyst nematode are differentially regulated by salicylic acid. *Plant Cell Physiol.* 51, 1524–1536. doi: 10.1093/pcp/pcq109

van der Hoorn, R. A. L., and Kamoun, S. (2008). From guard to decoy: a new model for perception of plant pathogen effectors. *Plant Cell* 20, 2009–2017. doi: 10.1105/tpc.108.060194

van der Voort, J. R., Lindeman, W., Folkertsma, R., Hutten, R., Overmars, H., van der Vossen, E., et al. (1998). A QTL for broad-spectrum resistance to cyst nematode species (Globodera spp.) maps to a resistance to gene cluster in potato. *Theor. Appl. Genet.* 96, 654–661. doi: 10.1007/s001220050785

van der Voort, J. R., van der Vossen, E., Bakker, E., Overmars, H., van Zandvoort, P., Hutten, R., et al. (2000). Two additive QTLs conferring broad-spectrum resistance in potato to Globodera pallida are localized on resistance gene clusters. *Theor. Appl. Genet.* 101, 1122–1130. doi: 10.1007/s001220051588

van der Vossen, E. A. G., van der Voort, J. N. A. M. R., Kanyuka, K., Bendahmane, A., Sandbrink, H., Baulcombe, D. C., et al. (2000). Homologues of a single resistance-gene cluster in potato confer resistance to distinct pathogens: a virus and a nematode. *Plant J.* 23, 567–576. doi: 10.1046/j.1365-313x.2000.00814.x

Vieira, P., and Gleason, C. (2019). Plant-parasitic nematode effectors—insights into their diversity and new tools for their identification. *Curr. Opin. Plant Biol.* 50, 37–43. doi: 10.1016/j.pbi.2019.02.007

Walter, A. J., Willforss, J., Lenman, M., Alexandersson, E., and Andreasson, E. (2018). RNA seq analysis of potato cyst nematode interactions with resistant and susceptible potato roots. *Eur. J. Plant Pathol.* 152, 531–539. doi: 10.1007/s10658-018-1474-z

Wang, X. (2005). Regulatory functions of phospholipase D and phosphatidic acid in plant growth, development and stress responses. *Plant Physiol.* 139, 566–573. doi: 10.1104/pp.105.068809

Wang, J. J., Hu, M., Wang, J. J., Qi, J., Han, Z., Wang, G., et al. (2019a). Reconstitution and structure of a plant NLR resistosome conferring immunity. *Science* 364:eaav5870. doi: 10.1126/science.aav5870

Wang, J. J., Wang, J. J., Hu, M., Wu, S., Qi, J., Wang, G., et al. (2019b). Ligand-triggered allosteric ADP release primes a plant NLR complex. *Science* 364, eaav5868. doi: 10.1126/science.aav5868

Wu, C. -H., Abd-El-Haliem, A., Bozkurt, T. O., Belhaj, K., Terauchi, R., Vossen, J. H., et al. (2017). NLR network mediates immunity to diverse plant pathogens. *Proc. Natl. Acad. Sci.* 114, 8113–8118. doi: 10.1073/pnas.1702041114

Wu, C. -H., Derevnina, L., and Kamoun, S. (2018). Receptor networks underpin plant immunity. *Science* 360, 1300–1301. doi: 10.1126/science.aat2623

Yang, S., Dai, Y., Chen, Y., Yang, J., Yang, D., Liu, Q., et al. (2019). A novel G16B09-like effector from *Heterodera avenae* suppresses plant defenses and promotes parasitism. *Front. Plant Sci.* 10:66. doi: 10.3389/fpls.2019.00066

Yu, N., Lee, T. G., Rosa, D. P., Hudson, M., and Diers, B. W. (2016). Impact of Rhg1 copy number, type, and interaction with Rhg4 on resistance to *Heterodera glycines* in soybean. *Theor. Appl. Genet.* 129, 2403–2412. doi: 10.1007/s00122-016-2779-y

Zhang, H., Zhang, D., Chen, J., Yang, Y., Huang, Z., Huang, D., et al. (2004). Tomato stress-responsive factor TSRF1 interacts with ethylene responsive element GCC box and regulates pathogen resistance to Ralstonia solanacearum. *Plant Mol. Biol.* 55, 825–834. doi: 10.1007/s11103-005-2140-3

Conflict of Interest: The reviewer JJ declared a past co-authorship with one of the authors AG to the handling editor.

The remaining authors declare that the research was conducted in the absence of any commercial or financial relationships that could be construed as a potential conflict of interest.

frontiers in Plant Science

REVIEW
published: 25 March 2021
doi: 10.3389/fpls.2021.661194

Resisting Potato Cyst Nematodes With Resistance

*Ulrike Gartner[1,2], Ingo Hein[1,3], Lynn H. Brown[1,3], Xinwei Chen[1], Sophie Mantelin[4], Sanjeev K. Sharma[1], Louise-Marie Dandurand[5], Joseph C. Kuhl[6], John T. Jones[1,2], Glenn J. Bryan[1] and Vivian C. Blok[1]**

[1] Cell and Molecular Sciences, The James Hutton Institute, Dundee, United Kingdom, [2] School of Biology, University of St Andrews, St Andrews, United Kingdom, [3] School of Life Sciences, University of Dundee, Dundee, United Kingdom, [4] INRAE UMR Institut Sophia Agrobiotech, Sophia Antipolis, France, [5] Entomology, Plant Pathology and Nematology Department, University of Idaho, Moscow, ID, United States, [6] Department of Plant Sciences, University of Idaho, Moscow, ID, United States

Potato cyst nematodes (PCN) are economically important pests with a worldwide distribution in all temperate regions where potatoes are grown. Because above ground symptoms are non-specific, and detection of cysts in the soil is determined by the intensity of sampling, infestations are frequently spread before they are recognised. PCN cysts are resilient and persistent; their cargo of eggs can remain viable for over two decades, and thus once introduced PCN are very difficult to eradicate. Various control methods have been proposed, with resistant varieties being a key environmentally friendly and effective component of an integrated management programme. Wild and landrace relatives of cultivated potato have provided a source of PCN resistance genes that have been used in breeding programmes with varying levels of success. Producing a PCN resistant variety requires concerted effort over many years before it reaches what can be the biggest hurdle—commercial acceptance. Recent advances in potato genomics have provided tools to rapidly map resistance genes and to develop molecular markers to aid selection during breeding. This review will focus on the translation of these opportunities into durably PCN resistant varieties.

Keywords: nematodes, *Globodera*, resistance, virulence, molecular markers, genomics, potato breeding, integrated pest management

OPEN ACCESS

Edited by:
Juan Emilio Palomares-Rius, Consejo Superior de Investigaciones Científicas (CSIC), Spain

Reviewed by:
Maria Lurdes Inacio, Instituto Nacional Investigaciao Agraria e Veterinaria (INIAV), Portugal
Aurelio Ciancio, Istituto per la Protezione Sostenibile delle Piante, Italy
Isabel Luci Conceição, University of Coimbra, Portugal

***Correspondence:**
Vivian C. Blok
Vivian.Blok@hutton.ac.uk

Specialty section:
This article was submitted to Plant Pathogen Interactions, a section of the journal Frontiers in Plant Science

Received: *30 January 2021*
Accepted: *03 March 2021*
Published: *25 March 2021*

Citation:
Gartner U, Hein I, Brown LH, Chen X, Mantelin S, Sharma SK, Dandurand L-M, Kuhl JC, Jones JT, Bryan GJ and Blok VC (2021) Resisting Potato Cyst Nematodes With Resistance. Front. Plant Sci. 12:661194. doi: 10.3389/fpls.2021.661194

INTRODUCTION

Potato is now the third most important food crop after rice and wheat for human consumption (CIP, 2020). Being an important source of carbohydrates, potato provides more protein and minerals than any other staple crop (Birch et al., 2012). With the increasing demand from a growing world population, optimised pest and disease management are of increasing importance for the sustainability of this crop. Potato cyst nematodes (PCN) are the most economically important parasitic nematodes of potato. They are soil inhabiting biotrophic sedentary endoparasites (Wyss, 1997) and are specialised pathogens of solanaceous species (Sabeh et al., 2019). The global economic impact of PCN has not been fully quantified, however, even a small infestation can incur considerable costs, including loss of income to growers, closure of local and international markets as well as expenses for regulatory activities such as surveys and monitoring systems (Hodda and Cook, 2009). There are estimates that the two species, *Globodera rostochiensis* and *G. pallida,* are responsible for the loss of 9% of the crop worldwide (Turner and Subbotin, 2013). A potential

third PCN species was reported by Skantar et al. (2011) and has subsequently been described as *G. ellingtonae* (Handoo et al., 2012). It has been detected in Oregon and Idaho in the United States, and in the Andean region of South America (Lax et al., 2014). However, its pathogenicity to potato is inconsistent (Zasada et al., 2019).

PCN co-evolved with their hosts from the genus *Solanum* in South America (Canto Saenz and Mayer de Scurrah, 1977; Stone, 1985). For *G. pallida*, this co-evolution is estimated to have taken place over 20 million years, with a northward expansion from the south of Peru around Lake Titicaca (Picard et al., 2004, 2007). Both nematode species were probably introduced and became established in Europe in the 1850s as a consequence of the Irish potato famine (Evans et al., 1975), when tubers, with contaminated soil attached, were collected and brought to Europe as breeding material for late blight resistant potatoes. In the 1880s, damage to potato crops from nematodes was noted in Germany, and from the early 1900s in the United Kingdom (Evans et al., 1975). PCN have subsequently been spread, mainly via contaminated seed potatoes, to almost all countries where potato is grown. To date, they have been detected in 126 countries (79 for *G. rostochiensis* and 55 for *G. pallida*) (CABI, 2020a,b). PCN are quarantine pathogens, which means that phytosanitary regulations are applied to prevent the introduction or spread within a country, and once detected, eradication or containment measures are applied (reviewed in Pickup et al., 2018). Protection of seed land from infestations is vital to prevent spread into non-infested land within the EU, and testing of seed land prior to planting is required by the EU Council Directive 2007/33/EC. The regulations that apply to PCN provide a framework for the potato industry, but despite these regulations PCN continues to spread. The long delay between introduction and detection, which may require several crop cycles, confounds interpretation of how effective these regulations may be. The widespread presence of these nematodes in East Africa provides a contemporary example of the failure to prevent spread and the devastating consequences incurred by subsistence farmers who have become dependent on potato for their livelihoods (Mburu et al., 2020). Both species of PCN are also widespread in Algeria, the largest potato producer in Africa (Djebroune et al., 2021).

Disease symptoms caused by PCN are initially minimal, due to low infection levels in localised patches. Such symptoms are frequently interpreted as the effects of abiotic stress, and infestations frequently remain unidentified for many years until reduced yields or premature plant senescence are observed. PCN population dynamics has been studied since the 1950s, in order to predict yield losses by modelling different parameters such as level of field infestation at the start of the season, use of nematicides, soil type, rotation length and use of resistant/susceptible potato cultivars (e.g., Seinhorst, 1982; Been and Schomaker, 1998; Trudgill et al., 2014). Online tools such as NemaDecide[1] and PCN Calculator[2] were developed in an attempt to allow potato growers to simulate expected tuber yields and PCN population development when different conditions are applied. **Figure 1A** shows the time that passes between introduction of PCN to a field and reaching the detection/damage thresholds under different rotation schedules of susceptible crops in a very simplified model, only considering a constant multiplication rate, set at 15-fold per annum, and a fixed rate of natural decline, set at 25% per annum. In **Figure 1B**, an example of the predictions for population levels and yield trends is shown. The parameters used such as initial population level, decline rate, soil type, nematicide treatment, rotation length, cultivar resistance and tolerance can be adjusted with the PCN Calculator for *G. pallida*[2].

The fact that PCN cysts are highly durable, and viable eggs can survive for decades in the absence of a host (Turner, 1996), together with difficulty in detection of new infestations, makes preventing the spread of PCN very challenging. An example of a successful eradication is from Western Australia, where in the late 1980s a total area of 35 ha was found to contain *G. rostochiensis*. This area was declared PCN free in 2010. However, at least part of this land has been converted to housing estates, precluding further sampling (Collins et al., 2010; IPPC, 2010). In Idaho, a containment and eradication programme is in progress following the detection in 2006 of two potato fields infested with *G. pallida* (Skantar et al., 2007; USDA, 2007). Preventing spread and eradication with soil fumigants is the focus of the regulatory programme in Idaho[3]. When PCN is well established but not widespread, preventing spread to uninfected fields becomes paramount. With widespread infestations, management involves various strategies (Back et al., 2018), including crop rotation, chemical and biological control, bio-fumigation and trap cropping. This review focuses on the use of host resistance to manage PCN.

HOST NEMATODE INTERACTIONS

Potato cyst nematodes have long lasting biotrophic interactions with their hosts. Cysts, located in the soil after detaching from host roots, contain several hundred eggs, each of which contains a juvenile nematode (J). The moult from J1 to J2 takes place within the egg once embryogenesis is complete. The unhatched J2 is protected by a chitinous eggshell which is an impermeable barrier and provides physical protection against potential bacterial or fungal pathogens. Furthermore, the unhatched J2 is dehydrated and suspended in a perivitelline fluid that contains a high concentration of trehalose, which provides protection against low winter temperatures (Perry, 2002). Hatching of PCN eggs is triggered by exposure to chemicals released from the host roots, termed host root hatching factors. The requirement for hatching factors in root exudates to stimulate hatching of the J2s provides a means for synchronisation of the PCN life cycle with the presence of a host plant (Masler and Perry, 2018). The presence of hatching factors triggers a calcium dependent change in eggshell permeability, allowing water to enter the egg, reactivating the metabolic activity of the unhatched J2 (Clarke and Perry, 1985).

[1]http://www.nemadecide.com

[2]https://pcncalculator.ahdb.org.uk

[3]https://www.aphis.usda.gov/aphis/ourfocus/planthealth/plant-pest-and-disease-programs/pests-and-diseases/nematode/pcn/pcn-home

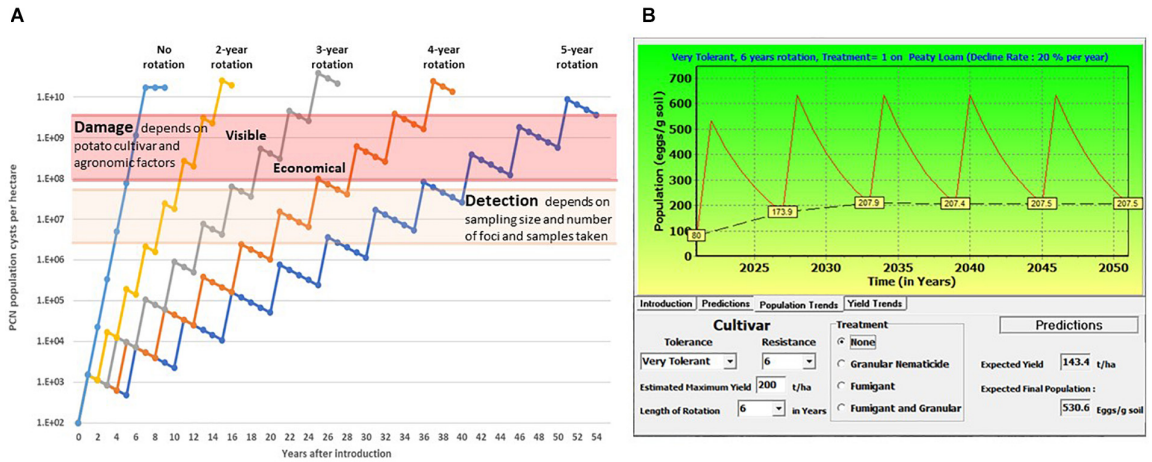

FIGURE 1 | (A) Schematic illustration of the increase of potato cyst nematodes (PCN) cysts with different rotation intervals, and the time until detection and damage thresholds are reached. This simplified sketch shows a natural decrease of viable cysts of 25% per year, and a 15-fold multiplication rate per year, no other factors are considered. **(B)** This illustrates the predictions of a model in which different factors including initial population level (in this example 80 eggs/g soil) soil type, nematicide treatment and rotation length, and cultivar characters including tolerance and resistance, can be altered to predict population and yield trends using a specified decline rate of 20% (https://pcncalculator.ahdb.org.uk).

The J2 nematode subsequently cuts its way out of the eggshell using its stylet (Doncaster and Seymour, 1973). Host resistance is not associated with the ability to reduce hatch of PCN—root exudates of resistant plants induce similar levels of hatch as those from susceptible plants (Turner and Stone, 1981). After hatching, the J2 moves through the soil, locating, and invading the host root. Physiologically active roots exude an array of molecules that form chemical gradients in soil that are perceived by the nematodes, allowing their orientation and migration toward the host. Despite the importance of the chemical signalling that governs the nematode chemotaxis, advances in nematode chemical ecology are relatively recent (Torto et al., 2018). To date, there is no evidence that host resistance affects PCN chemotaxis.

After penetrating the host, the nematodes migrate destructively through the root cells until reaching the inner cortical layer. Migration is facilitated by the production of a cocktail of plant cell wall degrading enzymes and modifying proteins including cellulases (Smant et al., 1998), pectate lyases (Popeijus et al., 2000), and expansins (Qin et al., 2004). The genes encoding these proteins are likely to have been acquired as a result of horizontal gene transfer from bacteria (Kikuchi et al., 2017). After reaching the inner cortical layer, the behaviour of the J2 changes and the nematode probes cells with its stylet to select an initial syncytial cell (ISC) that does not respond adversely by producing callose (Sobczak and Golinowski, 2011). Effectors are introduced into this ISC which then undergoes a transformation into a syncytium. Within the ISC the central vacuole degrades, the cytoplasm becomes enriched in subcellular organelles, and the nucleus becomes enlarged and ameboid in shape (Golinowski et al., 1996). The syncytium develops into a multinucleate structure through controlled breakdown of the cell walls separating the ISC from its neighbours, initially at the sites of plasmodesmata, with the subsequent fusion of protoplasts of adjoining cells (Grundler et al., 1998; **Figure 2**). Up to 300 cells can be included in the final structure. The syncytium provides a rich food source for the developing nematode but needs to be kept alive for the duration of the nematode life cycle as the nematode is not able to induce more than one such structure. The nematode produces a feeding tube during each cycle of feeding (Eves-van den Akker et al., 2015a). The precise nature of this structure remains unknown, but it likely acts as a molecular sieve and prevents damage to the syncytium when feeding.

The interactions between PCN and its host are mediated by effectors. These proteins are secreted from the nematode into the host to manipulate its metabolism to the benefit of the nematode. PCN effectors, like those of other plant-parasitic nematodes, are produced in two subventral and one dorsal gland cell. Ultrastructural studies (Hussey and Mims, 1990), as well as transcriptome analysis (Thorpe et al., 2014) indicate that effectors important in the early stages of the host-parasite interaction (including migration) tend to be produced in the subventral gland cells, while those that are important at later stages are produced in the dorsal gland cell. In terms of the interaction between PCN and its host, effectors have been characterised that assist in the migration of the nematode through the root (e.g., Smant et al., 1998), in the induction of the syncytium and suppression of host defence responses (e.g., Mei et al., 2015).

The precise details of how the syncytium is formed remain unclear. However, it is known that nematode control of several plant hormone pathways is key to this process (Gheysen and Mitchum, 2019). Manipulation of these pathways can be achieved through effectors and plant peptide hormone mimics produced by the nematode (Ali et al., 2017). In particular, the role of auxin, which is a central regulator of plant organogenesis, has been investigated during the feeding site formation. Studies of auxin synthesis and perception mutants showed that manipulation of the auxin signalling pathway plays a critical role in the development of syncytia. For example, auxin insensitive mutants

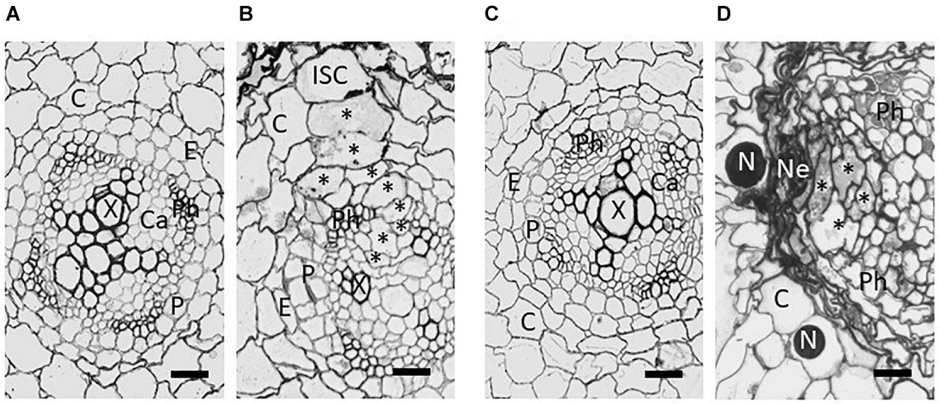

FIGURE 2 | Brightfield images from tangential sections of potato roots showing development of syncytia induced by *Globodera pallida* in the roots of susceptible *Solanum tuberosum* cv. Pentland Ivory **(A,B)** and resistant reaction of Sa_12601 [*S. tuberosum* ssp. *andigena* CPC 2802 (*H3*)] **(C,D)**. **(A)** Uninfected root and **(B)** syncytium at 4 dpi of susceptible cv Pentland Ivory, **(C)** uninfected and **(D)** necrosis and collapse of syncytium at 7 dpi of Sa_12601. C, cortex; Ca, pro-/cambium; E, endodermis; ISC, initial syncytial cell; N, nematode; Ne, necrosis; P, pericycle; Ph, phloem; X, xylem. Asterisks (*) indicate selected syncytial elements. Scale bars: 20 μm (from Varypatakis et al., 2020).

are unable to support normal syncytium development, while disruption of polar auxin transport gives rise to abnormally large syncytia (Goverse et al., 2000). In addition, the rearrangement of PIN and AUX/LAX auxin transporters in developing syncytial cells, where auxin responsive promoters are also activated, indicates that changes in local auxin concentration are important during syncytium formation (Grunewald et al., 2009).

As in other pathosystems, resistance against PCN is triggered by recognition of its effectors by *R*-genes, either directly or indirectly (Sacco et al., 2009). The effector gene *RBP-1* was identified as the *Gpa2* resistance cognate avirulence (*Avr)* factor (Sacco et al., 2009). It belongs to the SPRYSEC effector gene family (secreted SP1a and ryanodine receptor domain-containing effector), which is unique to cyst nematodes. Recently, a list of *G. pallida* candidate *Avr* genes, implicated in the interaction with plants containing the *H3* or *GpaV* resistance sources, has been proposed by Varypatakis et al. (2020). The most common candidates belong to the SPRYSEC family. Other putative *Avr* candidate genes included cellulases, glutathione synthase and an orthologue of *Heterodera glycines* GLAND3, with unknown function.

Ultrastructural studies comparing the development of the syncytium in susceptible and resistant hosts showed structural differences evident within 2 days post infection (dpi) (Rice et al., 1985; Varypatakis et al., 2020). By 4 dpi susceptible plants showed incorporation of many additional cells into the syncytium and expansion into the vascular cylinder. However, no expansion was found in the resistant host apart from some degradation of cytoplasm. By 7 dpi most syncytia were degraded and compressed in a host with the *H3* resistance derived from *S. tuberosum* ssp. *andigena* CPC 2802, and extensive necrosis of neighbouring cells was also observed (**Figure 2**; Varypatakis et al., 2020). Failure to incorporate cells within the vascular cylinder prevents development of a viable syncytium, which is needed by the feeding nematode to progress through moults to the adult stages. Some variation in the degree of syncytial degradation has been observed and this may account for the increased number of males observed in some hosts that are "partially resistant" and have syncytia which are compromised in their nutritional capabilities. Males do not require a sustained viable syncytium to reach maturity as they do not produce eggs, and hence a shift in the sex ratio toward males has been observed with some sources of resistance (Rice et al., 1985; Sobczak et al., 2005). Modification of the host root's functions, caused by the initiation of the feeding sites and the establishment of the resistance response with extensive necrotic area can greatly affect plant growth and lead to crop failure at high nematode densities. The destructive root penetration during PCN invasion that occurs irrespective of the resistance, can also lead to colonisation by other root pathogens, exacerbating damage to the crop.

VIRULENCE, PATHOTYPES, AND DURABILITY OF RESISTANCE

Nematode virulence is defined as the ability to reproduce on a host plant that contains specific genes, otherwise conferring resistance. Nematodes which cannot reproduce on the same resistant plant are called avirulent (Vanderplank, 1978; Turner et al., 1983; Blok et al., 2018). Virulence traits represent a characteristic of individual nematodes. Nematode populations can consist of a mixture of virulent and avirulent individuals. This proportion can change over time, depending on environmental conditions, such as use of resistant or susceptible hosts. The reproduction rate of virulent nematodes on resistant plants is typically lower than on a fully susceptible plant. Nematodes, like other pathogens, usually conform to the so-called trade-off concept, stating that resistance-breaking populations of pathogens pay a price by losing fitness on susceptible hosts compared to avirulent populations (Stearns, 1989; Laine and Barres, 2013). Nevertheless, a recent experimental evolution study (Fournet et al., 2016) found that this might not always be

the case for *G. pallida*, for which virulent populations became fitter on resistant hosts, producing bigger cysts with more juveniles that hatched earlier. However, these experiments were conducted in petri-dishes with nutrient enriched agar, and thus might not represent the behaviour in the field.

In Europe, over 40 years ago, a pathotype scheme was developed (Kort et al., 1977), in order to identify which sources of resistance were most effective against European populations of *G. rostochiensis* and *G. pallid*a. *Globodera rostochiensis* was subdivided into five pathotypes, Ro1–Ro5. Ro1 and Ro4 were differentiated by their low multiplication rate on *S. tuberosum* ssp. *andigena* CPC 1673, compared to Ro2, Ro3, and Ro5. *Solanum kurtzianum* hybrid 60.21.19 differentiated Ro2 from Ro3 and Ro5, and Ro1 from Ro4. Ro3 multiplied poorly on *S. vernei 58.16/12/4,* compared to Ro5. All *G. rostochiensis* pathotypes were unable to multiply on *S. vernei* hybrid 65.346/19. *Globodera pallida* was categorised into three European pathotypes, Pa1, Pa2, and Pa3; *S. multidissectum* hybrid P55/7 differentiated Pa1 from Pa2 and Pa3, and *S. vernei (VTn)2 62.33.3* differentiated Pa2 from Pa3.

The Kort pathotype scheme provided a panel of PCN populations representing the phenotypic spectrum in Europe and identified several sources of resistance and their specificities for use by potato breeders. For *G. rostochiensi*s, Ro1 is the dominant pathotype outside South America, and breeding efforts have focused on this pathotype. The occurrence of *G. rostochiensis* in the United Kingdom is probably the result of a single introduction (Evans et al., 1975; Bendezu et al., 1998), and resistance to *G. rostochiensis* Ro1 has proven to be remarkably durable. For *G. pallida*, the situation has been more complicated and the progress from breeding has been much slower. The differentiation of the pathotypes Pa2 and Pa3 on *S. vernei (VTn)2 62.33.3* was not found to be robust, and this has led to questions about the validity of the pathotype scheme. Trudgill (1985) demonstrated that the reproduction factor of <1 used in the Kort scheme to indicate resistance was environmentally sensitive and proposed that the Pa2 and Pa3 pathotypes were a continuum (Pa2/3) that could not be distinguished reliably. Most European populations of *G. pallida* belong to the Pa2/3 pathotype, though genetic evidence supports a distinct introduction which includes the populations Chavornay and Luffness, classified as Pa3 in the Kort scheme (Hockland et al., 2012). At least three independent introductions of *G. pallida* from South America have occurred in Europe (Plantard et al., 2008; Hockland et al., 2012). In Scotland, mixtures of these three genotypes can be present in the same field (Eves-van den Akker et al., 2015b). Since this scheme was introduced, other sources of resistance to *G. pallida* have been found that are being used in breeding programmes and resistance-breaking populations of *G. pallida* have been detected. Taken together, these facts have confounded the issue of pathotype designation.

The PCN populations outside South America represent a small portion of the total genetic diversity of these species (Plantard et al., 2008; Grenier et al., 2010). This restricted genetic variation makes it possible to consider a potato breeding approach using host resistance for their control. While the *H1* resistance to *G. rostochiensis* has shown to be highly durable, the resistance sources available for *G. pallida* are not expected to be as long-lasting due the greater genetic diversity of *G. pallida* populations. Also, in general, the resistances that have been identified for this species have not been as effective. It is possible that the combination of the more heterogenous nature of *G. pallida* populations with the more genetically complex nature of the quantitative resistances involved, will require the action of two genes for very high levels of durable resistance.

The use of resistant hosts exerts a selection pressure on nematode populations that can lead to an increase in the proportion of virulent vs. avirulent individuals (Whitehead, 1991; Hockland et al., 2012). Varypatakis et al. (2019) observed this effect when using different potato cultivars challenged with *G. pallida* populations previously grown repeatedly on potato cultivars with partial resistance to *G. pallida*. Beniers et al. (2019) also used partially resistant potato cultivars to show an increase of virulence in a population when the same source of resistance was applied over generations as have others (Turner, 1990; Phillips and Blok, 2008). Ultimately, this shift could lead to resistance-breaking PCN populations. This effect has already been reported for the resistant potato cultivar Innovator in some regions in Germany (Niere et al., 2014). Pyramiding different sources of resistance to *G. pallida* is likely to be needed to produce potato cultivars with durable, broad spectrum resistance. Indeed, Dalton et al. (2013) demonstrated a synergistic effect of increased resistance when combining two different PCN resistance loci in potato and Rigney et al. (2017) showed that this effect could be replicated with several *G. pallida* populations, though the durability of this material has not yet been assessed.

RESISTANCE AND TOLERANCE TO PCN AND THEIR ASSESSMENT

Resistance and tolerance to pests and pathogens are two different strategies that plants and animals use to cope with biotic threats. Resistance to PCN is defined as the host plant's ability to inhibit or limit reproduction, relative to a susceptible plant (Evans and Haydock, 1990; Blok et al., 2018; Pagán and García-Arenal, 2020). In contrast, tolerance toward PCN is defined as the ability of the potato to tolerate PCN infection without a reduction in yield. Unlike resistance, tolerance does not significantly affect the nematodes' ability to infect the host and reproduce (Starr et al., 2002; Pagán and García-Arenal, 2020), and the two traits are independent of each other (Evans and Haydock, 1990; Trudgill, 1991). When confronted with high PCN population densities, resistant cultivars that are intolerant do not perform well (in terms of yield) although they will restrict reproduction of PCN, whereas susceptible tolerant cultivars allow PCN populations levels to rise and produce adequate yields (Trudgill, 1991). Combining resistance and tolerance is now regarded as essential by potato breeders in areas where PCN is widespread.

Resistance

The cultivated tetraploid species *S. tuberosum* ssp. *tuberosum* does not show any resistance to PCN (Rousselle-Bourgeois and Mugniery, 1995). However, related wild potato species and

landraces are a genetic resource for resistance to pests such as PCN, resilience to abiotic stresses and tuber quality characters. Many of them have been systematically tested for PCN resistance (e.g., Rousselle-Bourgeois and Mugniery, 1995; Castelli et al., 2003). To date, more than 50 potato species have been identified that show resistance to *G. rostochiensis* and/or *G. pallida* for at least one pathotype, in at least one accession. Wild potato species can be found in their natural habitats from the southwestern US to Argentina, with most species being native to Mexico and the Andean Highlands (Bethke et al., 2017). Initial approaches for identifying sources of resistance to PCN in potato involved the screening of over 1,200 accessions of wild species from the Commonwealth Potato Collection and led to the first identified PCN resistance locus (*H1*) from *S. tuberosum* ssp. *andigena*, which offers nearly complete resistance to *G. rostochiensis* pathotypes Ro1 and Ro4 (Ellenby, 1952). More recently, it was reported that *G. ellingtonae* does not reproduce on potato genotypes which carry the *H1* resistance locus (Whitworth et al., 2018; Zasada et al., 2019).

Based on the "gene-for-gene" concept (Flor, 1971), quantitative resistance to PCN may be conferred by products of dominant resistance (*R*) genes. These genes recognise pathogen-produced effector proteins in infected cells, encoded by *Avr* genes, and trigger defence responses, which may include a hypersensitive reaction (Van der Biezen and Jones, 1998; Davies and Elling, 2015). The latter involves cells that are committed to cell death, depriving the nematodes of an adequate food source, and thus leading to resistance. While all known genomic loci conferring resistance to *G. rostochiensis* or *G. pallida* belong to the nucleotide-binding site and leucine-rich repeat (NB-LRR) family of R genes, it is notable that other gene classes may be important in providing resistance to PCN and other cyst nematodes. For example, the *Cf-2* gene, which confers resistance against the fungal pathogen *Cladosporium fulvum*, encodes an extracellular receptor-like protein with a LRR domain, also provides resistance against *G. rostochiensis* (Lozano-Torres et al., 2012). For both *C. fulvum* and PCN, Cf-2 is activated by pathogen attempts to interfere with the apoplastic cysteine proteinase Rcr3. In addition, resistance against the soybean cyst nematode, *H. glycines*, can be underpinned by completely different molecular mechanisms that cause a toxic response specifically targeted at the syncytium. Resistance derived from the *Rhg1* locus is based on a copy number variation of multiple genes, with three of these genes contributing to full resistance in soybean: a putative amino acid transporter, an α-SNAP [soluble NSF (N-ethylmaleimide sensitive fusion)-associated protein] and a protein containing a wound-inducible domain (Cook et al., 2012). Only the function of the α-SNAP has been elucidated to some extent. The defective resistance-type α-SNAP protein accumulates preferentially in the nematode feeding site relative to its wild type counterpart, causing cytotoxicity (Bayless et al., 2016). Similarly, the resistance conferred by *Rhg4* is mediated through a defective variant form of a serine hydroxymethyl transferase expressed in the syncytium. This enzyme is otherwise essential for cellular one-carbon metabolism, causing a failure of nutrients reaching the nematode (Liu et al., 2012). No similar mechanisms against PCN have been identified to date but, interestingly, the proteins encoded by the soybean *Rhg1* gene can function in different plant families and confers resistance to PCN in potato (Butler et al., 2019).

Tolerance

Factors that enhance tolerance of potato to PCN are not necessarily specific to PCN. Tolerance factors may involve enhanced root growth, the activation of general plant stress responses or combinations thereof, and can provide additional tolerance to e.g., drought or other pathogens (Trudgill, 1991; Blok et al., 2018). Environmental conditions have a major impact on tuber yield (Evans and Haydock, 1990), and tolerance is therefore environmentally sensitive and difficult to reliably assess.

The damage caused by PCN depends on the initial nematode density in the soil. Intolerant (sensitive) and susceptible cultivars show damage at even low rates of infestation (10 eggs/g soil). If damage is extensive, this can lead to low reproduction of the nematodes even though the plants are susceptible. Tolerant and susceptible cultivars, planted in infested land, can lead to a very high prevalence of PCN by increasing nematode population levels, while still giving acceptable yields, which thwarts PCN management programmes. But even a tolerant plant will suffer damage at high nematode densities, mostly due to reduced uptake of nutrients (Trudgill, 1987). When PCN is well-managed and populations have a low density, intolerant resistant potatoes may be grown, however, the best way to manage PCN would be the use of potato cultivars which are highly resistant and tolerant. Resistance ensures the reduction of nematode population levels and tolerance ensures reliable crop yields, even when the initial PCN levels are high (Blok et al., 2018). Tolerance to pathogens is usually not selected for in breeding programmes, therefore this trait is often lost, unless it is linked to another commercially useful trait (Trudgill, 1991). Very few quantitative trait loci (QTLs) for tolerance to cyst nematodes have been described so far (Williams et al., 2003, 2006; Ravelombola et al., 2020).

Assessment of Resistance

Any breeding programme that aims to include PCN resistance in a new cultivar requires a reliable, and ideally rapid, method for resistance screening. Screening methods to determine the level of resistance in potatoes are usually performed in a greenhouse in pots or rootrainer, or in a dark incubation chamber when using canisters (**Figure 3**). The choice of which test to use depends on the accuracy required, resources available and time constraints. PCN cysts, eggs or the J2 stage juveniles can be used as inoculum. For good practice, each assessment should include at least one susceptible and resistant control cultivar, be performed at least twice with a minimum of four biological replicates of each genotype grown, in a randomised planting design.

Canister tests can be used with relatively large numbers of progeny and therefore provide an efficient method to separate susceptible and resistant clones in a breeding programme. Potatoes are grown in the dark in transparent canisters with a lid, filled with moist soil and inoculated with PCN. After 8 weeks the number of female nematodes that are visible on the surface of the roots through the transparent canisters are counted (Phillips et al., 1980). The test in rootrainers is an

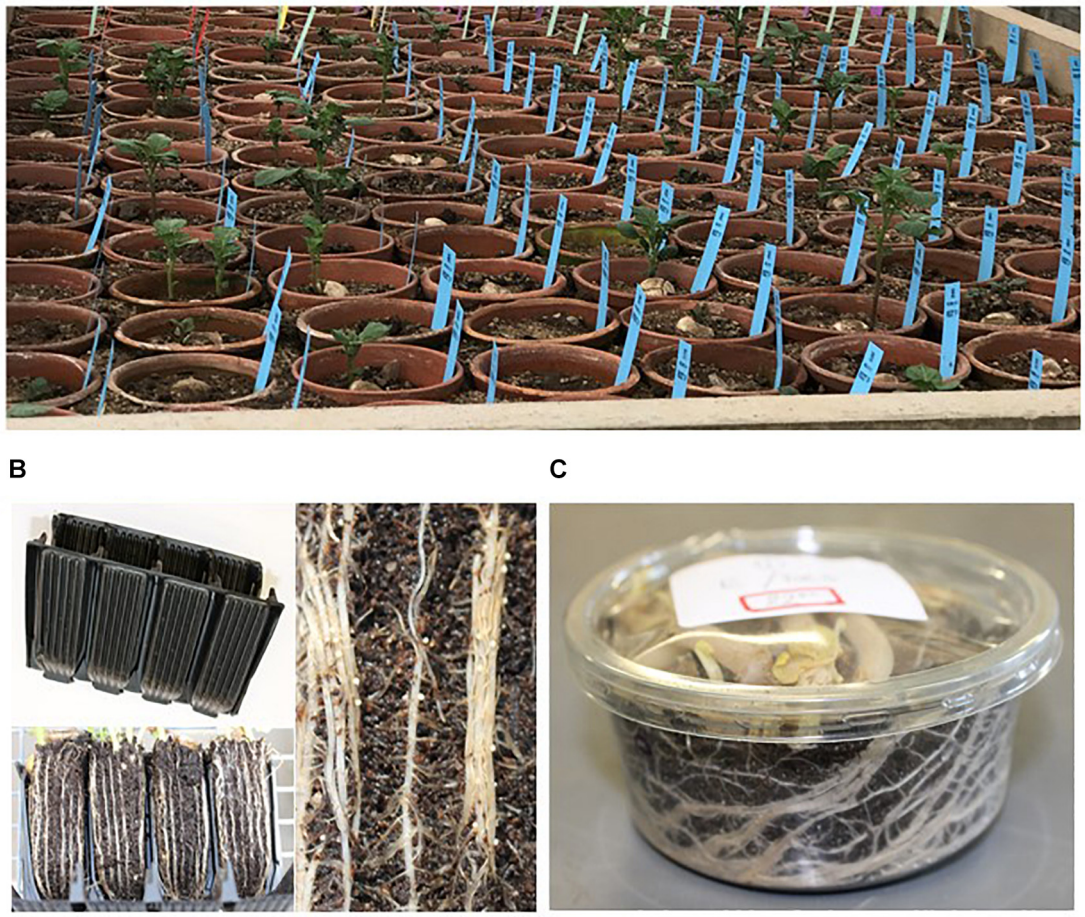

FIGURE 3 | Methods for assessing PCN resistance in potatoes: **(A)** clay pots with potato plants growing in a sand/loam mixture which has been inoculated with cysts, **(B)** empty rootrainer cassette, 4 root systems in rootrainer with roots growing on surface of compost and female nematodes on root surface, **(C)** transparent canister with potato roots visible for counting female nematodes.

alternative to the canister test. It is performed in a temperature-controlled greenhouse and is more labour intensive, as the plants require regular maintenance. Potato plants are grown in PCN infested soil in rootrainers for 7–8 weeks, then the number of female nematodes on the roots visible on the surface of the "root-ball" are counted after carefully removing them from the rootrainers (Strachan et al., 2019; Varypatakis et al., 2019). The most accurate assay for phenotyping potatoes is a pot test, where plants are grown for 12 weeks in a sand/loam 1:1 mixture that has been inoculated with PCN. When using cysts as inoculum, these need to be bagged to ensure that they are not counted as new cysts after the experiment is completed. The cysts are then washed out of the sand/loam mixture and counted (Fenwick, 1940; Reid et al., 2015).

The nematode reproduction rate P_f/P_i (multiplication factor with P_f and P_i being the final and initial female/cyst numbers, respectively) is a measurement used to assess the relative resistance of a potato genotype. If there are very few cysts, the eggs are extracted from the cysts and counted instead to assess reproduction. The current resistance evaluation system for PCN used in Europe was introduced in 2006 (EPPO, 2006). The reproduction rate of the *G. pallida* population Chavornay on the susceptible potato cultivar Desirée is assessed, and the susceptibility is divided into 9 susceptibility groups, with 1–3 being susceptible (>100–5%), 4–6 partially resistant (<25–3%) and 7–9 resistant (<3%). This system uses an agreed set of protocols and means that resistance ratings can be applied consistently to new cultivars.

All these bioassays require specialised materials and trained staff. They are time consuming and therefore expensive. Using genetically linked molecular markers to determine the presence or absence of resistance loci is faster and allows more progeny to be screened. However, bioassays ultimately need to be performed to confirm resistance. The accuracy of molecular markers is not always absolute, as homologous recombination can separate the marker and the resistance locus in each generation, the likelihood of recombination increasing with distance between marker and resistant locus on the genetic map. This problem

may be overcome when the marker resides in the resistance gene itself, or if two markers flanking the resistance are used, as two recombination events in one generation are extremely rare.

Assessment of Tolerance

Tolerance to PCN is a complex trait and to date no molecular markers are available. Bioassays are therefore the only option to assess tolerance. To assess tolerance, the performance of different infected and non-infected potato genotypes is compared with that of genotypes with known tolerances (Cook and Evans, 1987; Trudgill, 1991). Field tests for the evaluation of tolerance are described in Trudgill (1991), whereas Arntzen and Wouters (1994) described a high correlation between pot and field evaluations of tolerance against PCN during early growth. The use of resistant and susceptible control potato cultivars with known levels of tolerance is advised in those assays, as the results are highly variable, both in replicates and in different experiments (Dale et al., 1988). If the assay is performed with and without nematicides, tolerant potatoes are expected to have the least increase of yield in conjunction with nematicide use (Trudgill and Cotes, 1983a). Tolerant cultivars often grow larger roots in heavily infested soil compared to nematicide treated or only lightly infested soil (Trudgill and Cotes, 1983b).

BREEDING FOR PCN RESISTANCE AND THE DEVELOPMENT OF MOLECULAR MARKERS FOR MARKER ASSISTED BREEDING

History of Breeding for PCN Resistant Potatoes

The modern cultivated potato derives mainly from a relatively small number of introductions into Europe from South America in the 16th, 17th, and 18th centuries centuries. By the end of the 18th century the crop had quite rapidly been adapted to tuberise in the long-day conditions found in Northern Europe through selection for early-tuberisation and higher tuber yields. However, early cultivars lacked sufficient genetic variation to provide resistance to major pests and diseases. This became a problem once the crop became widely grown as the predominant staple food crop in many countries in the 19th century. The most notable pathogens have been late blight (*Phytophthora infestans*) and latterly, PCN. This has led to the need to introgress genes for disease and pest resistance into potato varieties from the many wild and cultivated species of Central and South America, some of which can be crossed directly with cultivated potato.

Commercial potato breeding is still performed mainly at the tetraploid level, whereas many of the wild and primitive cultivated species containing disease resistance are diploid. The highly heterozygous nature of tetraploid potato breeding germplasm greatly compromises potato improvement. Potato breeding remains largely empirical and genetically unsophisticated, and most economically important traits are genetically complex, displaying continuous variation. Resistance to pest and disease threats are largely an exception, being generally controlled by the action of one or two dominant genes. This property has led to a focus on developing genetic markers for use in breeding for pest and disease resistance. Development of molecular genetic tools facilitating the mapping and cloning of genes that confer resistance has significantly accelerated the process of PCN-resistant cultivar development through marker-assisted selection (MAS) in recent years.

Efforts to breed resistance to PCN have been ongoing since the middle of the 20th century (**Figure 4**). The first cross to introgress the *H1* resistance source, which confers resistance to Ro1 and Ro4 pathotypes of *G. rostochiensis*, was between *S. tuberosum* ssp. *andigena* CPC 1673 and the variety Kerr's Pink in 1952. The resistance was found to be simply inherited, and after backcrossing and selection for commercially important traits as well as resistance, the varieties Maris Piper (England) and Pentland Javelin (Scotland) were released in 1966 and 1967, respectively. Maris Piper remains one of the dominant commercial cultivars in the United Kingdom. The *H1* resistance has been widely deployed in breeding and is the most frequently used source of resistance to *G. rostochiensis* (Przetakiewicz and Milczarek, 2017) in current European and North American potato varieties. This resistance source has proven to be extremely durable to date.

Breeding for resistance to *G. pallida* has been complicated by the more complex nature of most resistance sources to this species and the higher genetic variability of *G. pallida* populations outwith South America, compared to *G. rostochiensis*. A resistance source, denoted *H2*, found in the diploid wild species *S. multidissectum* was shown to confer resistance to some *G. pallida* populations. This resistance was transferred to cultivated potato by interploidy crosses (Bradshaw et al., 1996). However, this gene has not been widely deployed as it does not provide strong resistance to the Pa2/3 populations of *G. pallida* that are the most prevalent in Europe. Breeding efforts in the United Kingdom and mainland Europe focused on the South American diploid species *S. vernei*, which includes accessions with quantitative resistance to both PCN species. Resistance derived from *S. vernei* has been introgressed independently in United Kingdom and mainland European breeding programmes, but it took many years to develop cultivars showing high levels of resistance. Chromosome doubling of *S. vernei* was performed by chemical means. The resulting tetraploid plants were crossed for several generations to cultivars and breeding lines over 30 years, leading to the eventual release of varieties (e.g., Innovator, Arsenal, Eurostar), which contain high levels of resistance to *G. pallida* Pa1, 2/3 populations. The *Grp1* resistance has also been used by breeders in Europe to produce cultivars such as Iledher, Seresta, and Aveka. However, *G. pallida* populations are already able to overcome this resistance (Grenier et al., 2020).

A third source of resistance for *G. pallida* to be successfully targeted in United Kingdom breeding programmes is the so called *H3* source, originating from the landrace *S. tuberosum* spp. *andigena* (CPC 2775 and CPC 2802). It was originally thought to be determined by a single gene, but subsequent analysis has shown that *H3* is genetically controlled by QTLs on chromosomes IV (locus subsequently known as *GpaIV*)

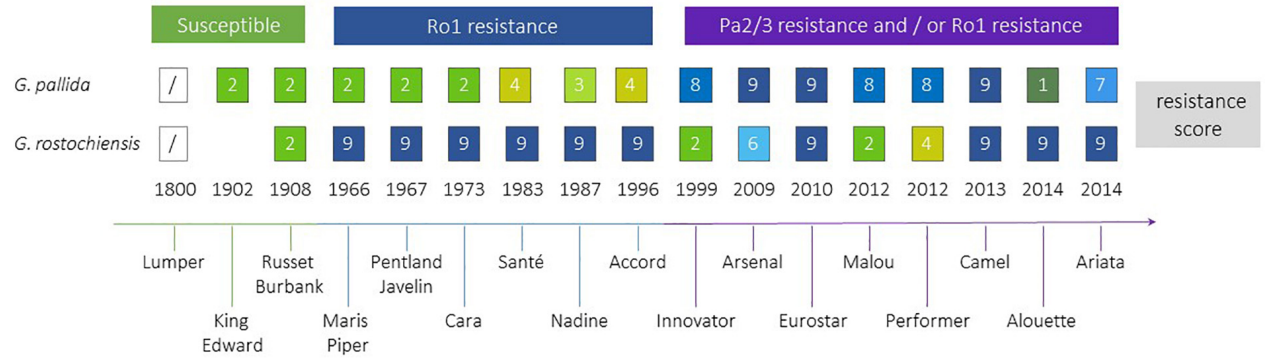

FIGURE 4 | Selected potato cultivars, approximate time when they became commercially available, the introduction of resistances to *Globodera rostochiensis* and *G. pallida*. *H1* resistance is used in all above cultivars against *G. rostochiensis*, whereas for *G. pallida* several sources of resistance have been introgressed. PCN resistance scores from 1 to 9 indicate increasing resistance levels from susceptible (1) to highly resistant (9) (EPPO, 2006).

and XI (Bryan et al., 2002, 2004). It took over 20 years (but only 2 breeding generations) to produce the partially resistant cultivar Eden and breeding line 12601ab1, which has a higher level of resistance than Eden to pathotypes Pa2/3. The latter also has excellent processing traits, leading to its heavy use in United Kingdom breeding programmes. Several cultivars carrying *GpaIV* have been released with moderate levels of resistance to Pa2/3, such as Vales Everest, Midas, Olympus and Rocket.

Ongoing efforts in potato breeding are aimed at "pyramiding" various sources of PCN resistance into single genotypes. Most of the known sources of resistance to *G. pallida* provide only partial resistance, and moreover are genetically complex, involving the action of more than one gene. The value of pyramiding different loci conferring *G. pallida* resistance has been shown in previous studies, notably that of Caromel et al. (2005) who showed that "stacking" two separate QTLs from the wild species *S. sparsipilum* into individual genotypes resulted in a stronger resistance phenotype than either QTL deployed individually. The ideal scenario would be to combine *H1* with at least two of the major effect QTLs conferring *G. pallida* resistance (e.g., *H2, GpaIV, GpaV*). The successful accomplishment of this goal would be facilitated by the existence of breeding lines with high "dosages" of the relevant functional alleles, as well as genetic markers diagnostic for both the presence and dosage of the functional alleles of these genes.

Diagnostic Molecular Markers Linked to PCN Resistance and Their Applications

Progress in the genetic analysis of PCN resistance sources led to the mapping of these sources, and in some cases the functional alleles have been isolated (**Table 1**). This also allowed the development of molecular markers tightly linked to the resistance phenotypes that can be deployed in potato breeding. These markers enable more informed breeding approaches that do not rely solely on time-consuming and progress-limiting phenotypic assessments. The use of MAS in breeding for PCN resistance has been well adopted in most breeding programmes. A brief history of the main resistance mapping efforts and marker development is presented below.

The *H1* gene was first localised on chromosome V using restriction fragment length polymorphism (RFLP) mapping technology (Gebhardt et al., 1993). Further attempts to clone *H1* have led to the development of several tightly linked markers (Finkers-Tomczak et al., 2011). The RFLP marker CP113, linked in coupling to *H1*, was deployed to test for the presence of the marker in 53 tetraploid German potato varieties with unknown sources of resistance. This was perhaps the earliest attempt of using molecular markers to survey PCN resistance in potato. Unfortunately, this marker failed to detect the presence of *H1* in resistant varieties, highlighting the need for validating the "transferability" of markers to populations other than those in which the marker was developed. This is a common problem in outbreeding crop species showing low levels of linkage disequilibrium. Two further markers, TG689 and 57R have been reported and deployed for *H1* PCN resistance screening, showing more than 90% congruence between the marker assay and the PCN-resistance phenotype (Biryukova et al., 2008; Milczarek et al., 2011; Schultz et al., 2012). The marker TG689 has been used successfully in a breeding programme which led to the potato cultivar Missaukee, a processing cultivar with resistance to late blight, verticillium wilt and *G. rostochiensis* (Douches et al., 2010). The presence or absence of a 452 bp amplicon for the marker 57R proved to be the most effective diagnostic marker for the prediction of PCN resistance conferred by *H1* (Park et al., 2018). This marker successfully identified *H1* in 90 resistant potato cultivars and in 299 out of 300 from potato breeding programmes, and correctly categorised all susceptible potato cultivars (Schultz et al., 2012). Further development of single nucleotide polymorphisms (SNP) markers diagnostic for *H1* has been reported by Meade et al. (2020) who deployed a highly effective pooled "whole-genome resequencing" approach using previously deployed markers (in this case 57R) to identify novel sequence polymorphisms that could be converted into a more generic competitive allele-specific PCR format than the gel-based system used for 57R.

TABLE 1 | List of described genes and QTLs involved in PCN resistance and their references.

Species of origin	Name	Chromosome	Species	Pathotype	References
Genes					
S. spegazzinii	*Gro1–4*	VII	*G. rostochiensis*	Ro1	Paal et al., 2004
S. tuberosum ssp. *andigena*	*Gpa2*	XII	*G. pallida*	Pa2/3	Rouppe van der Voort et al., 1997; van der Vossen et al., 2000
S. pimpinellifolium	*Hero*	IV	*G. rostochiensis*, *G. pallida*	Ro1 Pa2/3	Ernst et al., 2002
QTLs					
S. multidissectum	*H2*	V	*G. pallida*	Pa1 Pa2/3	Phillips et al., 1994; Strachan et al., 2019
S. sparsipilum	$Gpa^{V}{}_{spl}$	V	*G pallida*	Pa2/3	Caromel et al., 2005
	$Gpa^{XI}{}_{spl}$	XI	*G pallida*	Pa2/3	Caromel et al., 2005
S. spegazzinii	*Gpa*	V	*G. pallida*	Pa2/3	Kreike et al., 1994; Caromel et al., 2005
	GpaM1	V	*G. pallida*	Pa2/3	Caromel et al., 2003
	GpaM2	VI	*G. pallida*	Pa2/3	Caromel et al., 2003
	GpaM3	XII	*G. pallida*	Pa2/3	Caromel et al., 2003
	Gro 1.2	X	*G. rostochiensis*	Ro1	Kreike et al., 1993; Park et al., 2019
	Gro 1.3	XI	*G. rostochiensis*	Ro1	Kreike et al., 1993
	Gro 1.4	III	*G. rostochiensis*	Ro1	Kreike et al., 1996
S. tarijense	$Gpa^{XII}{}_{tar}$	XI	*G. pallida*	Pa3	Tan et al., 2009
S. tuberosum ssp. *andigena*	*H1*	V	*G. rostochiensis*	Ro1 Ro4	Bakker et al., 2004; Finkers-Tomczak et al., 2011
	H3	IV	*G pallida*	Pa2/3	Bryan et al. (2004)
S. vernei	*GpaV*	V	*G. pallida*	Pa2/3	Rouppe van der Voort et al., 2000; van Eck et al., 2017
	Gpa VI	IX	*G. pallida*	Pa2/3	Rouppe van der Voort et al., 2000; Bryan et al., 2002
	GroVI	*V*	*G. rostochiensis*	Ro1, Ro4	Jacobs et al., 1996
S.tuberosum, S. oplocense, S. vernei (3 different) and *S. tuberosum* ssp. *andigena*	*Grp1*	V	*G. rostochinesis*, *G. pallida*	Ro5 Pa2/3	Rouppe van der Voort et al., 1998; Finkers-Tomczak et al., 2009
S. tuberosum ssp. *andigena* and S. *vernei*	*Ro2_A*	V	*G. rostochiensis*	Ro2	Park et al., 2019
	Ro2_B	V	*G. rostochiensis*	Ro2	Park et al., 2019
	Pa2/3_A	V	*G. pallida*	Pa2/3	Park et al., 2019
	Pa2/3_B	X	*G. pallida*	Pa2/3	Park et al., 2019
S. tuberosum ssp. *andigena* and *S. vernei*	*Gpa IV*	IV	*G. pallida*	Pa2/3	Bradshaw et al., 1998

Attempts to develop diagnostic molecular markers for *GpaIV* and *GpaV* major QTLs have been only partially successful, progress being hampered by the quantitative nature of these resistances. A PCR-based marker, SPUD 1636, was reported for the *GpaV* QTL which was developed by converting a closely linked amplified fragment length polymorphism (AFLP) marker (Bryan et al., 2002). This presence/absence marker generates a 226 bp amplicon from resistant sources, and the diagnostic value of the SPUD1636 marker to identify sources of resistance was demonstrated for some accessions of *S. vernei* as well as varieties and breeding lines (Bryan et al., 2002). The marker has also been adapted for MAS in a Spanish resistance breeding programme (Ortega and Lopez-Vizcon, 2012) and used for resistance screening by Sudha et al. (2016). However, it has turned out to be inefficient in selecting breeding lines (Milczarek et al., 2011). Subsequently, Sattarzadeh et al. (2006) reported the development of the PCR marker "HC" to tag the same resistance QTL from *S. vernei*. Rather than developing markers based on single polymorphic sites linked to the QTL, the authors performed "haplotype" analysis on a set of seven closely linked SNPs, all located at the QTL region spanning over several hundred kilobases (kb) and each showed significant associations with resistance phenotypes. Of the three haplotypes identified, haplotype "c" stood out as the one associated in coupling with the resistance. Two SNPs that were specific to the haplotype "c" were targeted to develop the PCR marker HC. Tests of the HC marker on 56 potato varieties beyond the experimental population indicated that HC was highly diagnostic for the presence of the *S. vernei*-derived resistance to *G. pallida* pathotype Pa2/3. The HC marker, since its development, has been used widely to screen for resistance (Sharma et al., 2014; Bhardwaj et al., 2019; Sudha et al., 2019). It generally shows good agreement with phenotypic tests although discrepancies occasionally occur. Schwarzfischer et al. (2010) showed that HC is an appropriate diagnostic tool to identify resistance in diverse German potato varieties. It has also been discovered that many European breeding lines contain the

HC marker, indicating that this marker has been widely used in resistance breeding (Sattarzadeh et al., 2006).

For the "*H3*" source, the first marker to be used in breeding was the microsatellite STM3016, for which a particular allele (STM3016-122/177) was diagnostic for the *GpaIV* gene on chromosome IV (Moloney et al., 2010). Further work, based on the targeted resequencing of bacterial-artificial chromosome (BAC) clones from the region, led to the development of the PCR marker contig237, as well as three others (Moloney et al., 2010), which were highly predictive for *GpaIV* in a breeding population.

Other resistance sources to PCN targeted for marker development, are the gene *Gro1–4*, for which a sequence characterised amplified region (SCAR) marker was developed following efforts to isolate the gene (Paal et al., 2004). Additional primer pairs were developed (Asano et al., 2012) but neither has been reliable for screening purposes. A further source of resistance to *G. rostochiensis* is the gene *GroVI*, identified in *S. vernei* (Jacobs et al., 1996) and mapped to chromosome V at the same region as *H1*. Its allelic relation to *H1* remains unclear. Two reported SCAR markers were developed by converting two RAPD markers, U14 and X02 that flank *GroVI*, which generate amplicons of 366 and 854 bp, respectively. The two markers mapped 19 cM distal and 4 cM proximal to *GroVI* (Jacobs et al., 1996). Milczarek et al. (2011) used the two markers to screen a collection of 72 cultivars for resistances and generated the expected bands but found them to be undiagnostic as they were observed in both resistant and susceptible cultivars. Like *Gro1–4*, the *GroVI* resistance has not been deployed as widely as *H1*, probably due to overlapping with *H1* in its resistance specificity to the most common pathotype Ro1.

The majority of described resistance genes or QTLs for PCN are located within resistance "gene clusters" within the potato genome. Almost half of the described QTLs from different potato wild species map to the same region on chromosome V, where resistances for other potato pathogens are also described. This region, defined by RFLP markers GP21 and GP179 is called a "hotspot" for resistances (Gebhardt and Valkonen, 2001). Therefore, some of these resistances might share a common origin and possibly developed in ancestors and later evolved by diversification in wild potato species (Finkers-Tomczak et al., 2009). The resistances *Grp1* and *GpaV* have been mapped to the same chromosomal region, raising the possibility that they might be conferred by the same genetic factors (Finkers-Tomczak et al., 2009). **Figure 5** illustrates these findings, showing the alignment and clustering of known nematode *R*-gene loci to higher numbers of predicted NB-LRRs, or hotspots of resistance, in the doubled monoploid *S. tuberosum* group *Phureja* clone DM 1-3 516 R44 (DM), which was developed as the first potato reference genome.

Potato Genomics Tools Applied to the Analysis of PCN Resistance

The first nematode *R* gene, $Hs1^{pro-1}$, was identified in sugar beet against the beet cyst nematode, *Heterodera schachtii,* in 1997 and relied on analysing chromosomal breakage points alongside a "satellite" marker (Cai et al., 1997). However, subsequent genetic analysis showed that resistance does not co-segregate with the presence of this gene (Sandal et al., 1997). Other plant resistances were studied with the aid of bulked segregant analysis (BSA) using molecular markers such as RFLPs; cleaved amplified polymorphic sequences (CAPS) and AFLPs (Michelmore et al., 1991). In 1998, the tomato gene *Mi-1* was cloned, which provides resistance to both root knot nematodes (*Meloidogyne incognita*, *M. javanica*, *M. arenaria*) and several phloem-feeding insects, through the use of yeast-artificial chromosome libraries (Vos et al., 1998). Similarly, *Gpa2* from potato was mapped to a 115kb region linked to a sequence-related NB-LRR gene, which provides resistance to potato virus X (Rouppe van der Voort et al., 2000; van der Vossen et al., 2000). *Gro1–4* was isolated in a similar way (Paal et al., 2004). The identification of the *Hero* locus from tomato, although initially defined with RFLP markers in a segregating population, was more complex than *Gpa2* or *Gro1–4* (Ganal et al., 1995). A total of 14 potential candidate NB-LRRs were identified by sequencing 19 cosmids spanning the 180kb locus. Based on cosmid sequence information, these gene candidates were narrowed down by analysis of open reading frames, and the use of specific PCR markers. This allowed the functional analysis of just three potential candidate genes to identify the *Hero* gene conferring broad spectrum resistance to *G. rostochiensis* and some *G. pallida* pathotypes (Ernst et al., 2002). For other resistance genes, a map-based BSA approach has proven to be unsuitable. The *H1* gene for example, mapped to the distal end of chromosome V that contains numerous NB-LRR homologues, has very limited recombination and a lack of co-linearity between different haplotypes (Bakker et al., 2004; Finkers-Tomczak et al., 2011). While this gene has not yet been isolated, despite great efforts to do so, newer approaches and technologies may allow this and other genes to be isolated from such complex loci.

The three PCN resistance genes cloned so far belong to the NB-LRR family of *R*-genes. *Gro1–4* encodes an NB-LRR protein with a Toll-interleukin receptor domain at the N-terminus (Paal et al., 2004), while *Hero* (Ernst et al., 2002) and *Gpa2* (van der Vossen et al., 2000) encode CC-NB-LRR proteins, which have a coiled-coil domain at the N-terminus. *Gro1–4* and *Gpa2* originate from *S. spegazzinii* and *S. tuberosum* ssp. *andigena,* respectively, while the *Hero* resistance gene is derived from the wild tomato species *S. pimpinellifolium*. None of the other important PCN resistances have yet been isolated, despite significant efforts to do so. Nevertheless, mapping work has led to the development of several genetic markers for resistance that are used in potato breeding programmes, as described above.

With the availability of a reference potato genome (The Potato Genome Sequencing Consortium, 2011) followed by rapid advancements and cost reductions in next-generation sequencing (NGS), modern genotyping methods, for example genotyping-by-sequencing (GBS) (Elshire et al., 2011) with novel genetic approaches, such as genome-wide association studies (GWAS) (Visscher et al., 2012) for QTL discovery and marker-trait analyses, have emerged and have been applied to potato (e.g., Sharma et al., 2018). These approaches provide much higher genetic resolution than the previously used "low density" approaches. They also allow for high throughput analyses and larger populations to be rapidly

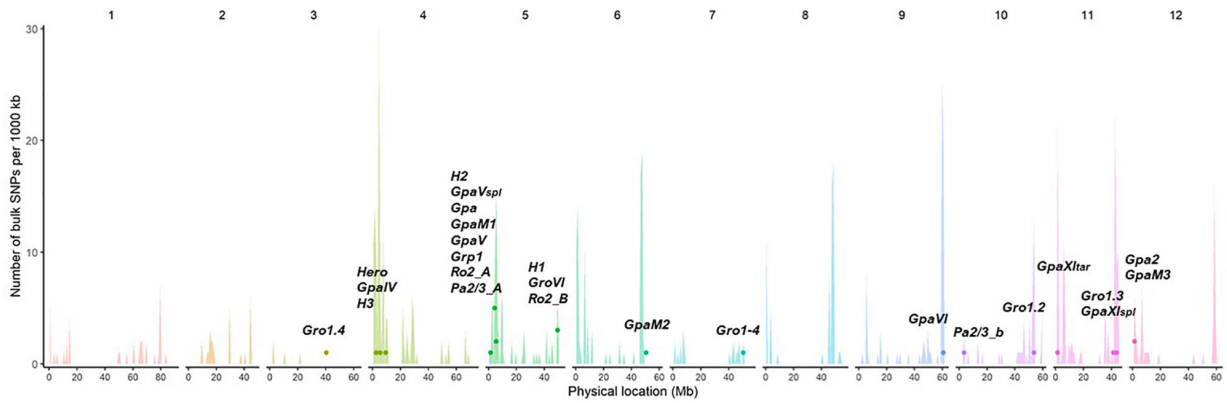

FIGURE 5 | Potato cyst nematodes (PCN) resistance loci align with known R gene clusters. The unequal distribution and position of predicted NB-LRR genes in the genome of DM is illustrated in the histogram, with spikes indicating clusters of resistance. The approximate relative location in the reference genome DM (PGSC v4.03) of known nematode resistance genes and QTLs are displayed as dots. The histogram spikes indicate numbers of predicted NB-LRR genes per 1,000 kb across the potato genome.

screened (Deschamps et al., 2012). The release of the potato reference genome aimed to provide a resource for identifying important genes (Sharma et al., 2013) including NB-LRRs. Although this reference has been invaluable in genetic studies, it only offers an incomplete picture, particularly in highly repetitive regions or in the case of NB-LRR genes where the reference is from a largely susceptible background. Thus, more recently, potato genomes have been sequenced from the homozygous diploid inbred potato clone M6 of *S. chacoense*, which is used as a breeding line and in genetics analysis (Jansky et al., 2014). A heterozygous clone, RH, has also solved haplotype blocks with third generation sequencing technology (Leisner et al., 2018; Zhou et al., 2020). These additional genomes will allow a greater resolution and understanding of NB-LRR loci and aid in the isolation and cloning of target genes.

An alternative to conventional "genome-wide" mapping approaches that overcomes some of the limitations of the potato reference genomes is provided by targeted enrichment sequencing. This process reduces the genome complexity to the most likely candidates with the help of specific "baits" designed to a subset of all potato genes. For potato, the following enrichment strategies have been adopted to date and comprise whole exome capture (WEC), generic-mapping enrichment sequencing (GenSeq) which targets single copy, conserved genes dispersed throughout the potato genome, two defence gene related capture approaches, resistance gene enrichment sequencing (RenSeq), and receptor-like protein enrichment sequencing (Jupe et al., 2013; Giolai et al., 2016; Chen et al., 2018; Lin et al., 2020). RenSeq was developed to allow high resolution SNP markers to be obtained for the detection and mapping of NB-LRRs (Jupe et al., 2013). RenSeq has also proven important to identify full length candidate NB-LRRs in combination with long-read sequencing (Witek et al., 2016). Furthermore, when used as a diagnostic tool (dRenSeq), the application informs resistance breeders, providing a full and detailed picture of the known NB-LRRs present in wild species and parental material (Van Weymers et al., 2016; Armstrong et al., 2019).

The most recent approach to isolate and map resistance genes is independent of a reference genome and takes advantage of *K*-mers in conjunction with association studies. *K*-mers are subreads of a length = *K* and, unlike SNPs, can inform on small haplotypes. The genetic mapping processes of *K*-mers are similar to GWAS by analysing diverse accessions for association between sequence polymorphisms and traits, but this can be conducted independently of a reference genome. *K*-mer studies based on RenSeq derived reads are referred to as AgRenSeq and have been used, for example, to isolate four resistance genes in wheat (Arora et al., 2019). Other, non-RenSeq-based *K*-mer approaches have also recently been used to map resistance against wart disease in potatoes (Prodhomme et al., 2019).

As sequencing methods continue to improve, so will the outputs for the *de novo* assembly of genomes or loci of interest, particularly in highly repetitive regions and for the many potato species with high levels of heterozygosity. Indeed, newly emerging and rapidly improving long-read sequencing technologies such as Oxford Nanopore and PacBio, are already starting to provide potential solutions for potato genomics and new potato genomes are being released (van Lieshout et al., 2020; Zhou et al., 2020). With these technological advances and the computational tools that facilitate ever more complex analyses, mapping and cloning of resistance genes should become more routine in the future.

DISCUSSION

While host resistance deployment remains a preferred strategy to control pests and pathogens of potato, introgression of resistance genes from wild and landrace species into commercially successful cultivars remains a considerable challenge. On the one hand, adaptation of pests and pathogens to overcome resistance can negate all of the efforts of breeders. On the other hand, meeting commercial requirements in which resistance

is only one of many characters the breeder must deliver, can also negate their efforts. Education, incentives and interventions may all be required in order for PCN resistant cultivars to be more widely grown by the potato industry and for consumer acceptance. More options in cultivars are urgently needed that meet different requirements of the potato markets. Rapid advances in genomics improving transferability of markers for specific traits, such as PCN resistance, but also for a wide range of other agronomically important characters, should revolutionise potato breeding in the future.

One reason for the relative lack of success in breeding for *G. pallida* resistance is that efforts have tended to focus on the larger QTL and neglect the smaller effect loci (chromosomes IX and XI for *S. vernei* and *H3*, respectively). Caromel et al. (2005) demonstrated the potential of MAS for introgression of *G. pallida* resistance genes derived from *S. sparsipilum* in a potato breeding programme by "stacking" two separate QTLs into individual genotypes. This resulted in a more-robust resistance phenotype than was obtained by the presence of a single QTL. This study and those of Dalton et al. (2013) and Rigney et al. (2017) underpin the basis for current efforts to "pyramid" resistance genes and QTLs into the same genetic background. Combined with the implementation of genomic selection (GS), which takes advantage of the availability of genome-wide high density markers to estimate the breeding value and the analysis of more complex traits, molecular markers are gaining significant traction in the breeding of potatoes (Slater et al., 2016).

Resistance genes that act to protect potatoes from PCN are a precious commodity. There are limited numbers of resistance genes that are amenable to introgression that will likely make a significant impact in the foreseeable future for the management of *G. pallida*. While there is an urgent need for new cultivars with *G. pallida* resistance that meet commercial requirements, more effort will be needed to ensure that resistance remains effective and durable.

AUTHOR CONTRIBUTIONS

UG and VB coordinated the manuscript. All authors listed have made direct intellectual contributions to the article and its underpinning research and have approved it for publication.

FUNDING

This work was funded by the Scottish Government Rural and Environment Science and Analytical Services Division and the USDA NIFA 2015-69004-23634 project GLOBAL.

REFERENCES

Ali, M. A., Azeem, F., Li, H., and Bohlmann, H. (2017). Smart parasitic nematodes use multifaceted strategies to parasitize plants. *Front. Plant Sci.* 8:1699. doi: 10.3389/fpls.2017.01699

Armstrong, M. R., Vossen, J., Lim, T. Y., Hutten, R. C. B., Xu, J. F., Strachan, S. M., et al. (2019). Tracking disease resistance deployment in potato breeding by enrichment sequencing. *Plant Biotechnol. J.* 17, 540–549. doi: 10.1111/pbi.12997

Arntzen, F. K., and Wouters, T. C. A. E. (1994). Assessing the tolerance to *Globodera pallida* of resistant potato genotypes by means of field and pot tests. *Potato Res.* 37, 51–63. doi: 10.1007/BF02360432

Arora, S., Steuernagel, B., Gaurav, K., Chandramohan, S., Long, Y. M., Matny, O., et al. (2019). Resistance gene cloning from a wild crop relative by sequence capture and association genetics. *Nat. Biotechnol.* 37, 139–143. doi: 10.1038/s41587-018-0007-9

Asano, K., Kobayashi, A., Tsuda, S., Nishinaka, M., and Tamiya, S. (2012). DNA marker-assisted evaluation of potato genotypes for potential resistance to potato cyst nematode pathotypes not yet invading into Japan. *Breed. Sci.* 62, 142–150. doi: 10.1270/jsbbs.62.142

Back, M. A., Cortada, L., Grove, I. G., and Taylor, V. (2018). "Field management and control strategies," in *Cyst Nematodes*, eds R. N. Perry, M. Moens, and J. T. Jones (Wallingford: CAB International), 305–336. doi: 10.1079/9781786390837.0305

Bakker, E., Achenbach, U., Bakker, J., van Vliet, J., Peleman, J., Segers, B., et al. (2004). A high-resolution map of the *H1* locus harbouring resistance to the potato cyst nematode *Globodera rostochiensis*. *Theor. Appl. Genet.* 109, 146–152. doi: 10.1007/s00122-004-1606-z

Bayless, A. M., Smith, J. M., Song, J., McMinn, P. H., Teillet, A., August, B. K., et al. (2016). Disease resistance through impairment of alpha-SNAP-NSF interaction and vesicular trafficking by soybean *Rhg1*. *Proc. Natl. Acad. Sci. U.S.A.* 113, E7375–E7382. doi: 10.1073/pnas.1610150113

Been, T. H., and Schomaker, C. H. (1998). *Quantitative Studies on the Management of Potato cyst Nematodes (Globodera* spp.) in the Netherlands. Ph.D. Thesis, University Wageningen, Wageningen.

Bendezu, I. F., Russell, M. D., and Evans, K. (1998). Virulence of populations of potato cyst nematodes (*Globodera* spp.) from Europe and Bolivia towards differential potato clones frequently used for pathotype classification. *Nematologica* 44, 667–681. doi: 10.1163/005725998x00078

Beniers, J. E., Nollen, Y., van Eck, H. J., and Schouten, H. J. (2019). Increased virulence of *Globodera pallida* during repeated rearing on different resistant potato cultivars explained by a simple model. *Plant Pathol.* 68, 445–453. doi: 10.1111/ppa.12969

Bethke, P. C., Halterman, D. A., and Jansky, S. (2017). Are we getting better at using wild potato species in light of new tools? *Crop Sci.* 57, 1241–1258. doi: 10.2135/cropsci2016.10.0889

Bhardwaj, V., Salej, S., Ashwani, K., Vanishree, G., Sanjeev, S., Sundaresha, S., et al. (2019). Efficiency and reliability of marker assisted selection for resistance to major biotic stresses in potato. *Potato J.* 46, 56–66.

Birch, P. R. J., Bryan, G., Fenton, B., Gilroy, E. M., Hein, I., Jones, J. T., et al. (2012). Crops that feed the world 8: potato: are the trends of increased global production sustainable? *Food Secur.* 4, 477–508. doi: 10.1007/s12571-012-0220-1

Biryukova, V. A., Zhuravlev, A. A., Abrosimova, S. B., Kostina, L. I., Khromova, L. M., Shmyglya, I. V., et al. (2008). Use of molecular markers of potato golden nematode resistance genes *H1* and *GRO1*. *Russ. Agric. Sci.* 34, 365–368. doi: 10.3103/s1068367408060013

Blok, V., Tylka, G., Smiley, R., deJong, W., and Taub, M. (2018). "Resistance breeding," in *Cyst Nematodes*, eds R. N. Perry, M. Moens, and J. T. Jones (Wallingford: CAB International), 174–214.

Bradshaw, J., Dale, M., and Phillips, M. (1996). Breeding potatoes at SCRI for resistance to potato cyst nematodes. *SCRI, Annu. Rep.* 1995, 30–34.

Bradshaw, J. E., Meyer, R. C., Milbourne, D., McNicol, J. W., Phillips, M. S., and Waugh, R. (1998). Identification of AFLP and SSR markers associated with quantitative resistance to *Globodera pallida* (Stone) in tetraploid potato (*Solanum tuberosum* subsp. *tuberosum*) with a view to marker-assisted selection. *Theor. Appl. Genet.* 97, 202–210. doi: 10.1007/s001220050886

Bryan, G. J., McLean, K., Bradshaw, J. E., De Jong, W. S., Phillips, M., Castelli, L., et al. (2002). Mapping QTLs for resistance to the cyst nematode *Globodera pallida* derived from the wild potato species *Solanum vernei*. *Theor. Appl. Genet.* 105, 68–77. doi: 10.1007/s00122-002-0873-9

Bryan, G. J., McLean, K., Pande, B., Purvis, A., Hackett, C. A., Bradshaw, J. E., et al. (2004). Genetical dissection of *H3*-mediated polygenic PCN resistance in a heterozygous autotetraploid potato population. *Mol. Breed.* 14, 105–116. doi: 10.1023/b:molb.0000037999.13581.9c

Butler, K. J., Chen, S., Smith, J. M., Wang, X., and Bent, A. F. (2019). Soybean resistance locus *Rhg*1 confers resistance to multiple cyst nematodes in diverse plant species. *Phytopathology* 109, 2107–2115. doi: 10.1094/phyto-07-19-0225-r

CABI (2020a). *Invasive Species Compendium Datasheet Globodera Pallida*. Available Online at: https://www.cabi.org/isc/datasheet/27033 (accessed September 10, 2020).

CABI (2020b). *Invasive species compendium datasheet Globodera rostochiensis*. Available Online at: https://www.cabi.org/isc/datasheet/27034 (accessed September 10, 2020).

Cai, D. G., Kleine, M., Kifle, S., Harloff, H. J., Sandal, N. N., Marcker, K. A., et al. (1997). Positional cloning of a gene for nematode resistance in sugar beet. *Science* 275, 832–834. doi: 10.1126/science.275.5301.832

Canto Saenz, M., and Mayer de Scurrah, M. (1977). Races of the potato cyst nematode in the Andean region and a new system of classification. *Nematologica* 23, 340–349. doi: 10.1163/187529277x00066

Caromel, B., Mugniery, D., Kerlan, M. C., Andrzejewski, S., Palloix, A., Ellisseche, D., et al. (2005). Resistance quantitative trait loci originating from *Solanum sparsipilum* act independently on the sex ratio of *Globodera pallida* and together for developing a necrotic reaction. *Mol. Plant Microbe Interact.* 18, 1186–1194. doi: 10.1094/mpmi-18-1186

Caromel, B., Mugniery, D., Lefebvre, V., Andrzejewski, S., Ellisseche, D., Kerlan, M. C., et al. (2003). Mapping QTLs for resistance against *Globodera pallida* (Stone) Pa2/3 in a diploid potato progeny originating from *Solanum spegazzinii*. *Theor. Appl. Genet.* 106, 1517–1523. doi: 10.1007/s00122-003-1211-6

Castelli, L., Ramsay, G., Bryan, G., Neilson, S. J., and Phillips, M. S. (2003). New sources of resistance to the potato cyst nematodes *Globodera pallida* and *G. rostochiensis* in the Commonwealth Potato Collection. *Euphytica* 129, 377–386. doi: 10.1023/A:1022264111096

Chen, X. W., Lewandowska, D., Armstrong, M. R., Baker, K., Lim, T. Y., Bayer, M., et al. (2018). Identification and rapid mapping of a gene conferring broad-spectrum late blight resistance in the diploid potato species *Solanum verrucosum* through DNA capture technologies. *Theor. Appl. Genet.* 131, 1287–1297. doi: 10.1007/s00122-018-3078-6

CIP (2020). *Potato facts and figures*. Available online at: https://cipotato.org/potato/potato-facts-and-figures/ (accessed september 10, 2020).

Clarke, A. J., and Perry, R. N. (1985). Eggshell calcium and the hatching of *Globodera rostochiensis*. *Int. J. Parasitol.* 15, 511–516. doi: 10.1016/0020-7519(85)90046-3

Collins, S., Vanstone, V., and Zhang, X. (2010). *PCN "Area Freedom" for WA: Evaluation of the Current Status of Potato Cyst Nematode (Globodera rostochiensis) in Western Australia*". Final Report for Project PT04004 and MT04000. Sydney, NSW: Horticulture Australia Limited.

Cook, D. E., Lee, T. G., Guo, X., Melito, S., Wang, K., Bayless, A. M., et al. (2012). Copy number variation of multiple genes at *Rhg1* mediates nematode resistance in soybean. *Science* 338, 1206–1209. doi: 10.1126/science.1228746

Cook, R., and Evans, K. (1987). "Resistance and tolerance," in *Principles and Practice of Nematode Control in Crops*, eds R. H. Brown and B. R. Kerry (Marrickville, NSW: Academic Press), 179–231.

Dale, M. F. B., Phillips, M. S., Ayres, R. M., Hancock, M., Holliday, M., Mackay, G. R., et al. (1988). The assessment of the tolerance of partially resistant potato clones to damage by the potato cyst nematode *Globodera pallida* at different sites and in different years. *Ann. Appl. Biol.* 113, 79–88. doi: 10.1111/j.1744-7348.1988.tb03284.x

Dalton, E., Griffin, D., Gallagher, T. F., de Vetten, N., and Milbourne, D. (2013). The effect of pyramiding two potato cyst nematode resistance loci to *Globodera pallida* Pa2/3 in potato. *Mol. Breed.* 31, 921–930. doi: 10.1007/s11032-013-9845-9

Davies, L. J., and Elling, A. A. (2015). Resistance genes against plant-parasitic nematodes: a durable control strategy? *Nematology* 17, 249–263. doi: 10.1163/15685411-00002877

Deschamps, S., Llaca, V., and May, G. D. (2012). Genotyping-by-sequencing in plants. *Biology* 1, 460–483. doi: 10.3390/biology1030460

Djebroune, A., Chakali, G., de Andrade, E., Camacho, M. J., Rusinque, L., and Inácio, M. L. (2021). Integrative morphometric and molecular approach to update the impact and distribution of potato cyst nematodes *Globodera rostochiensis* and *Globodera pallida* (Tylenchida: *Heteroderidae*) in Algeria. *Pathogens* 10:216. doi: 10.3390/pathogens10020216

Doncaster, C. C., and Seymour, M. K. (1973). Exploration and selection of penetration sites by tylenchida. *Nematologica* 19, 137–145. doi: 10.1163/187529273x00277

Douches, D. S., Coombs, J., Felcher, K., Kirk, W. W., Long, C., and Bird, G. (2010). Missaukee: A round white potato variety combining chip-processing with resistance to late blight, verticillium wilt and golden cyst nematode. *Am. J. Potato Res.* 87, 10–18. doi: 10.1007/s12230-009-9111-1

Ellenby, C. (1952). Resistance to the potato root eelworm. *Heterodera rostochiensis* Wollenweber. *Nature* 170:1016. doi: 10.1038/1701016a0

Elshire, R. J., Glaubitz, J. C., Sun, Q., Poland, J. A., Kawamoto, K., Buckler, E. S., et al. (2011). A robust, simple genotyping-by-sequencing (GBS) approach for high diversity species. *PLoS One* 6:e19379. doi: 10.1371/journal.pone.0019379

EPPO (2006). Testing of potato varieties to assess resistance to *Globodera rostochiensis* and *Globodera pallida*. *Bull. OEPP* 36, 419–420. doi: 10.1111/j.1365-2338.2006.01032.x

Ernst, K., Kumar, A., Kriseleit, D., Kloos, D. U., Phillips, M. S., and Ganal, M. W. (2002). The broad-spectrum potato cyst nematode resistance gene (*Hero*) from tomato is the only member of a large gene family of NBS-LRR genes with an unusual amino acid repeat in the LRR region. *Plant J.* 31, 127–136. doi: 10.1046/j.1365-313X.2002.01341.x

Evans, K., Franco, J., and Descurrah, M. M. (1975). Distribution of species of potato cyst nematodes in South America. *Nematologica* 21, 365–369. doi: 10.1163/187529275x00103

Evans, K., and Haydock, P. P. J. (1990). A review of tolerance by potato plants of cyst nematode attack, with consideration of what factors may confer tolerancce and methods of assaying and improving it in crops. *Ann. Appl. Biol.* 117, 703–740. doi: 10.1111/j.1744-7348.1990.tb04836.x

Eves-van den Akker, S., Lilley, C. J., Jones, J. T., and Urwin, P. E. (2015a). Plant-parasitic nematode feeding tubes and plugs: new perspectives on function. *Nematology* 17, 1–9. doi: 10.1163/15685411-00002832

Eves-van den Akker, S., Lilley, C. J., Reid, A., Pickup, J., Anderson, E., Cock, P. J. A., et al. (2015b). A metagenetic approach to determine the diversity and distribution of cyst nematodes at the level of the country, the field and the individual. *Mol. Ecol.* 24, 5842–5851. doi: 10.1111/mec.13434

Fenwick, D. W. (1940). Methods for the recovery and counting of cysts of *Heterodera schachtii* from soil. *J. Helminthol.* 18, 155–172. doi: 10.1017/S0022149X00031485

Finkers-Tomczak, A., Bakker, E., de Boer, J., van der Vossen, E., Achenbach, U., Golas, T., et al. (2011). Comparative sequence analysis of the potato cyst nematode resistance locus *H1* reveals a major lack of co-linearity between three haplotypes in potato (*Solanum tuberosum* ssp.). *Theor. Appl. Genet.* 122, 595–608. doi: 10.1007/s00122-010-1472-9

Finkers-Tomczak, A., Danan, S., van Dijk, T., Beyene, A., Bouwman, L., Overmars, H., et al. (2009). A high-resolution map of the *Grp1* locus on chromosome V of potato harbouring broad-spectrum resistance to the cyst nematode species *Globodera pallida* and *Globodera rostochiensis*. *Theor. Appl. Genet.* 119, 165–173. doi: 10.1007/s00122-009-1026-1

Flor, H. H. (1971). Current status of gene-for-gene concept. *Ann. Rev. Phytopathol.* 9, 275–296. doi: 10.1146/annurev.py.09.090171.001423

Fournet, S., Eoche-Bosy, D., Renault, L., Hamelin, F. M., and Montarry, J. (2016). Adaptation to resistant hosts increases fitness on susceptible hosts in the plant parasitic nematode *Globodera pallida*. *Ecol. Evol.* 6, 2559–2568. doi: 10.1002/ece3.2079

Ganal, M. W., Simon, R., Brommonschenkel, S., Arndt, M., Phillips, M. S., Tanksley, S. D., et al. (1995). Genetic mapping of a wide spectrum nematode resistance gene (*Hero*) against *Globodera rostochiensis* in tomato. *Mol. Plant Microbe Interact.* 8, 886–891. doi: 10.1094/mpmi-8-0886

Gebhardt, C., Mugniery, D., Ritter, E., Salamini, F., and Bonnel, E. (1993). Identification of RFLP markers closely linked to the *H1* gene conferring resistance to *Globodera rostochiensis* in potato. *Theor. Appl. Genet.* 85, 541–544. doi: 10.1007/bf00220911

Gebhardt, C., and Valkonen, J. P. T. (2001). Organization of genes controlling disease resistance in the potato genome. *Annu. Rev. Phytopathol.* 39, 79–102. doi: 10.1146/annurev.phyto.39.1.79

Gheysen, G., and Mitchum, M. G. (2019). Phytoparasitic nematode control of plant hormone pathways. *Plant Physiol.* 179, 1212–1226. doi: 10.1104/pp.18.01067

Giolai, M., Paajanen, P., Verweij, W., Percival-Alwyn, L., Baker, D., Witek, K., et al. (2016). Targeted capture and sequencing of gene-sized DNA molecules. *Biotechniques* 61, 315–322. doi: 10.2144/000114484

Golinowski, W., Grundler, F. M. W., and Sobczak, M. (1996). Changes in the structure of *Arabidopsis thaliana* during female development of the plant-parasitic nematode *Heterodera schachtii*. *Protoplasma* 194, 103–116. doi: 10.1007/bf01273172

Goverse, A., Overmars, H., Engelbertink, J., Schots, A., Bakker, J., and Helder, J. (2000). Both induction and morphogenesis of cyst nematode feeding cells are mediated by auxin. *Mol. Plant Microbe Interact.* 13, 1121–1129. doi: 10.1094/mpmi.2000.13.10.1121

Grenier, E., Fournet, S., Petit, E., and Anthoine, G. (2010). A cyst nematode 'species factory' called the andes. *Nematology* 12, 163–169. doi: 10.1163/138855409x12573393054942

Grenier, E., Kiewnick, S., Smant, G., Fournet, S., Montarry, J., Holterman, M., et al. (2020). Monitoring and tackling genetic selection in the potato cyst nematode *Globodera pallida*. *EFSA Supp. Publ* 17:1874E. doi: 10.2903/sp.efsa.2020.EN-1874

Grundler, F. M. W., Sobczak, M., and Golinowski, W. (1998). Formation of wall openings in root cells of *Arabidopsis thaliana* following infection by the plant-parasitic nematode *Heterodera schachtii*. *Eur. J. Plant Pathol.* 104, 545–551. doi: 10.1023/a:1008692022279

Grunewald, W., Cannoot, B., Friml, J., and Gheysen, G. (2009). Parasitic nematodes modulate pin-mediated auxin transport to facilitate infection. *PLos Pathog.* 5:e1000266. doi: 10.1371/journal.ppat.1000266

Handoo, Z. A., Carta, L. K., Skantar, A. M., and Chitwood, D. J. (2012). Description of *Globodera ellingtonae* n. sp. (Nematoda: *Heteroderidae*) from oregon. *J. Nematol.* 44, 40–57.

Hockland, S., Niere, B., Grenier, E., Blok, V., Phillips, M., Den Nijs, L., et al. (2012). An evaluation of the implications of virulence in non-European populations of *Globodera pallida* and *G. rostochiensis* for potato cultivation in Europe. *Nematology* 14, 1–13. doi: 10.1163/138855411x587112

Hodda, M., and Cook, D. C. (2009). Economic impact from unrestricted spread of potato cyst nematodes in Australia. *Phytopathology* 99, 1387–1393. doi: 10.1094/phyto-99-12-1387

Hussey, R. S., and Mims, C. W. (1990). Ultrastructure of esophageal glands and their secretory granules in the root-knot nematode *Meloidogyne incognita*. *Protoplasma* 156, 9–18. doi: 10.1007/bf01666501

IPPC (2010). *Eradication of Potato Cyst Nematode (PCN) from Western Australia*. Available Online at: https://www.ippc.int/en/countries/Australia/pestreports/2010/09/eradication-of-potato-cyst-nematode-pcn-from-western-australia/ (accessed September 10, 2020)

Jacobs, J. M. E., van Eck, H. J., Horsman, K., Arens, P. F. P., Verkerk-Bakker, B., Jacobsen, E., et al. (1996). Mapping of resistance to the potato cyst nematode *Globodera rostochiensis* from the wild potato species *Solanum vernei*. *Mol. Breed.* 2, 51–60. doi: 10.1007/bf00171351

Jansky, S. H., Chung, Y. S., and Kittipadukal, P. (2014). M6: a diploid potato inbred line for use in breeding and genetics research. *J. Plant Regist.* 8, 195–199. doi: 10.3198/jpr2013.05.0024crg

Jupe, F., Witek, K., Verweij, W., Sliwka, J., Pritchard, L., Etherington, G. J., et al. (2013). Resistance gene enrichment sequencing (RenSeq) enables reannotation of the NB-LRR gene family from sequenced plant genomes and rapid mapping of resistance loci in segregating populations. *Plant J.* 76, 530–544. doi: 10.1111/tpj.12307

Kikuchi, T., Eves-van den Akker, S., and Jones, J. T. (2017). Genome evolution of plant-parasitic nematodes. *Annu. Rev. Phytopathol.* 55, 333–354. doi: 10.1146/annurev-phyto-080516-035434

Kort, J., Ross, H., Rumpenhorst, H. J., and Stone, A. R. (1977). International scheme for identifying and classifying pathotypes of potato cyst nematodes *Globodera rostochiensis* and *G. pallida*. *Nematologica* 23, 333–339. doi: 10.1163/187529277x00057

Kreike, C. M., Dekoning, J. R. A., Vinke, J. H., Vanooijen, J. W., Gebhardt, C., and Stiekema, W. J. (1993). Mapping of loci involved in quantitatively inherited resistance to the potato cyst nematode *Globodera rostochiensis* pathotype Ro1. *Theor. Appl. Genet.* 87, 464–470. doi: 10.1007/bf00215092

Kreike, C. M., Dekoning, J. R. A., Vinke, J. H., Vanooijen, J. W., and Stiekema, W. J. (1994). Quantitatively-inherited resistance to *Globodera pallida* is dominated by one major locus in *Solanum spegazzinii*. *Theor. Appl. Genet.* 88, 764–769. doi: 10.1007/bf01253983

Kreike, C. M., Kok-Westeneng, A. A., Vinke, J. H., and Stiekema, W. J. (1996). Mapping of QTLs involved in nematode resistance, tuber yield and root development in *Solanum* sp. *Theor. Appl. Genet.* 92, 463–470. doi: 10.1007/bf00223694

Laine, A. L., and Barres, B. (2013). Epidemiological and evolutionary consequences of life-history trade-offs in pathogens. *Plant Pathol.* 62, 96–105. doi: 10.1111/ppa.12129

Lax, P., Dueñas, J. C. R., Franco-Ponce, J., Gardenal, C. N., Doucet, M. E., and Arntzen, J. W. (2014). Morphology and DNA sequence data reveal the presence of *Globodera ellingtonae* in the andean region. *Contrib. Zool.* 83:227. doi: 10.1163/18759866-08304002

Leisner, C. P., Hamilton, J. P., Crisovan, E., Manrique-Carpintero, N. C., Marand, A. P., Newton, L., et al. (2018). Genome sequence of M6, a diploid inbred clone of the high-glycoalkaloid-producing tuber-bearing potato species *Solanum chacoense*, reveals residual heterozygosity. *Plant J.* 96, 482–482. doi: 10.1111/tpj.14075

Lin, X., Armstrong, M., Baker, K., Wouters, D., Visser, R. G. F., Wolters, P. J., et al. (2020). RLP/K enrichment sequencing; a novel method to identify receptor-like protein (RLP) and receptor-like kinase (RLK) genes. *New Phytol.* 227, 1264–1276. doi: 10.1111/nph.16608

Liu, S. M., Kandoth, P. K., Warren, S. D., Yeckel, G., Heinz, R., Alden, J., et al. (2012). A soybean cyst nematode resistance gene points to a new mechanism of plant resistance to pathogens. *Nature* 492, 256–260. doi: 10.1038/nature11651

Lozano-Torres, J. L., Wilbers, R. H. P., Gawronski, P., Boshoven, J. C., Finkers-Tomczak, A., Cordewener, J. H. G., et al. (2012). Dual disease resistance mediated by the immune receptor Cf-2 in tomato requires a common virulence target of a fungus and a nematode. *Proc. Natl. Acad. Sci. U.S.A* 109, 10119–10124. doi: 10.1073/pnas.1202867109

Masler, E. P., and Perry, R. N. (2018). "Hatch, survival and sensory perception," in *Cyst nematodes*, eds R. N. Perry, M. Moens, and J. T. Jones (Wallingford: CAB International), 44–73. doi: 10.1079/9781786390837.0044

Mburu, H., Cortada, L., Haukeland, S., Ronno, W., Nyongesa, M., Kinyua, Z., et al. (2020). Potato cyst nematodes: a new threat to potato production in East Africa. *Front. Plant Sci.* 11:670. doi: 10.3389/fpls.2020.00670

Meade, F., Byrne, S., Griffin, D., Kennedy, C., Mesiti, F., and Milbourne, D. (2020). Rapid development of KASP markers for disease resistance genes using pooled whole-genome resequencing. *Potato Res.* 63, 57–73. doi: 10.1007/s11540-019-09428-x

Mei, Y., Thorpe, P., Guzha, A., Haegeman, A., Blok, V. C., MacKenzie, K., et al. (2015). Only a small subset of the SPRY domain gene family in *Globodera pallida* is likely to encode effectors, two of which suppress host defences induced by the potato resistance gene *Gpa2*. *Nematology* 17, 409–424. doi: 10.1163/15685411-00002875

Michelmore, R. W., Paran, I., and Kesseli, R. V. (1991). Identification of markers linked to disease-resistances genes by bulked segregant analysis - a rapid method to detect markers in specific genomic regions by using segregating populations. *Proc. Natl. Acad. Sci. U.S.A.* 88, 9828–9832. doi: 10.1073/pnas.88.21.9828

Milczarek, D., Flis, B., and Przetakiewicz, A. (2011). Suitability of molecular markers for selection of potatoes tesistant to *Globodera* spp. *Am. J. Potato Res.* 88, 245–255. doi: 10.1007/s12230-011-9189-0

Moloney, C., Griffin, D., Jones, P. W., Bryan, G. J., McLean, K., Bradshaw, J. E., et al. (2010). Development of diagnostic markers for use in breeding potatoes resistant to *Globodera pallida* pathotype Pa2/3 using germplasm derived from *Solanum tuberosum* ssp. *andigena* CPC 2802. *Theor. Appl. Genet.* 120, 679–689. doi: 10.1007/s00122-009-1185-0

Niere, B., Krüssel, S., and Osmers, K. (2014). Auftreten einer außergewöhnlich virulenten Population der Kartoffelzystennematoden. *J. Kulturpflanzen* 66, 426–427.

Ortega, F., and Lopez-Vizcon, C. (2012). Application of molecular marker-assisted selection (MAS) for disease resistance in a practical potato breeding programme. *Potato Res.* 55, 1–13. doi: 10.1007/s11540-011-9202-5

Paal, J., Henselewski, H., Muth, J., Meksem, K., Menendez, C. M., Salamini, F., et al. (2004). Molecular cloning of the potato *Gro1-4* gene conferring resistance to pathotype Ro1 of the root cyst nematode *Globodera rostochiensis*, based on a candidate gene approach. *Plant J.* 38, 285–297. doi: 10.1111/j.1365-313X.2004.02047.x

Pagán, I., and García-Arenal, F. (2020). Tolerance of plants to pathogens: a unifying view. *Annu. Rev. Phytopathol* 58, 77–96. doi: 10.1146/annurev-phyto-010820-012749

Park, J., Hackett, C., Dandurand, L., Wang, X., and Jong, W. D. D. (2019). QTL for resistance to *Globodera rostochiensis* pathotype Ro2 and *G. pallida* pathotype Pa2/3 in autotetraploid potato. *Am. J. Potato Res.* 96, 552–563. doi: 10.1007/s12230-019-09745-4

Park, J., Yang, H., De Jong, W. S., and Wang, X. (2018). An evaluation of two *H1*-linked markers and their suitability for selecting *Globodera rostochiensis* resistant potatoes in the New York breeding program. *Am. J. Potato Res.* 95, 170–177. doi: 10.1007/s12230-017-9623-z

Perry, R. N. (2002). "Hatching," in *The Biology of Nematodes*, ed. D. L. Lee (London: Taylor and Francis), 147–169.

Phillips, M. S., and Blok, V. C. (2008). Selection for reproductive ability in *Globodera pallida* populations in relation to quantitative resistance from *Solanum vernei* and *S. tuberosum* ssp. *andigena* CPC2802. *Plant Pathol.* 57, 573–580. doi: 10.1111/j.1365-3059.2007.01771.x

Phillips, M. S., Blok, V. C., Dale, M. F. B., and Trudgill, D. L. (1994). Virulence to plant resistance in potato cyst nematodes. *Asp. Appl. Biol.* 39, 139–143.

Phillips, M. S., Forrest, J. M. S., and Wilson, L. A. (1980). Screening for resistance to potato cyst nematode using closed containers. *Ann. Appl. Biol.* 96, 317–322. doi: 10.1111/j.1744-7348.1980.tb04782.x

Picard, D., Plantard, O., Scurrah, M., and Mugniery, D. (2004). Inbreeding and population structure of the potato cyst nematode (*Globodera pallida*) in its native area (Peru). *Mol. Ecol.* 13, 2899–2908. doi: 10.1111/j.1365-294X.2004.02275.x

Picard, D., Sempere, T., and Plantard, O. (2007). A northward colonisation of the andes by the potato cyst nematode during geological times suggests multiple host-shifts from wild to cultivated potatoes. *Mol. Phylogenet. Evol.* 42, 308–316. doi: 10.1016/j.ympev.2006.06.018

Pickup, J., Roberts, A. M. I, and Nijs, L. J. M. F. D. (2018). "Quarantine, distribution patterns and sampling," in *Cyst Nematodes*, eds R. N. Perry, M. Moens, and J. T. Jones (Wallingford: CAB International), 128–153. doi: 10.1079/9781786390837.0128

Plantard, O., Picard, D., Valette, S., Scurrah, M., Grenier, E., and Mugniery, D. (2008). Origin and genetic diversity of Western European populations of the potato cyst nematode (*Globodera pallida*) inferred from mitochondrial sequences and microsatellite loci. *Mol. Ecol.* 17, 2208–2218. doi: 10.1111/j.1365-294X.2008.03718.x

Popeijus, H., Overmars, H., Jones, J., Blok, V., Goverse, A., Helder, J., et al. (2000). Degradation of plant cell walls by a nematode. *Nature* 406, 36–37. doi: 10.1038/35017641

Prodhomme, C., Esselink, D., Borm, T., Visser, R. G. F., van Eck, H. J., and Vossen, J. H. (2019). Comparative subsequence sets analysis (CoSSA) is a robust approach to identify haplotype specific SNPs; mapping and pedigree analysis of a potato wart disease resistance gene *Sen3*. *Plant Methods* 15:60. doi: 10.1186/s13007-019-0445-5

Przetakiewicz, A., and Milczarek, D. (2017). Evaluation of potato cultivars and breeding lines for resistance to *Globodera rostochiensis* and *Globodera pallida*. *Plant Breed. Seed. Sci.* 76, 3–8. doi: 10.1515/plass-2017-0014

Qin, L., Kudla, U., Roze, E. H. A., Goverse, A., Popeijus, H., Nieuwland, J., et al. (2004). A nematode expansin acting on plants. *Nature* 427, 30–30. doi: 10.1038/427030a

Ravelombola, W. S., Qin, J., Shi, A., Nice, L., Bao, Y., Lorenz, A., et al. (2020). Genome-wide association study and genomic selection for tolerance of soybean biomass to soybean cyst nematode infestation. *PLoS One* 15:e0235089. doi: 10.1371/journal.pone.0235089

Reid, A., Evans, F., Mulholland, V., Cole, Y., and Pickup, J. (2015). High-throughput diagnosis of potato cyst nematodes in soil samples. *Methods Mol. Biol.* 1302, 137–148. doi: 10.1007/978-1-4939-2620-6_11

Rice, S. L., Leadbeater, B. S. C., and Stone, A. R. (1985). Changes in cell structure in roots of resistant potatoes parasitized by potato cyst-nematodes. I. Potatoes with resistance gene *H1* derived from *Solanum tuberosum* spp. *andigena*. *Physiol. Plant Pathol.* 27, 219–234. doi: 10.1016/0048-4059(85)90069-4

Rigney, B., Blok, V., Griffin, D., Dalton, E., and Milbourne, D. (2017). Consistent action of two partially effective loci conferring resistance to *Globodera pallida* Pa2/3 across multiple nematode field populations. *Plant Pathol.* 66, 1031–1040. doi: 10.1111/ppa.12640

Rouppe van der Voort, J., Lindeman, W., Folkertsma, R., Hutten, R., Overmars, H., van der Vossen, E., et al. (1998). A QTL for broad-spectrum resistance to cyst nematode species (*Globodera* spp.) maps to a resistance gene cluster in potato. *Theor. Appl. Genet.* 96, 654–661. doi: 10.1007/s001220050785

Rouppe van der Voort, J., van der Vossen, E., Bakker, E., Overmars, H., van Zandvoort, P., Hutten, R., et al. (2000). Two additive QTLs conferring broad-spectrum resistance in potato to *Globodera pallida* are localized on resistance gene clusters. *Theor. Appl. Genet.* 101, 1122–1130. doi: 10.1007/s001220051588

Rouppe van der Voort, J. R., Wolters, P., Folkertsma, R., Hutten, R., van Zandvoort, P., Vinke, H., et al. (1997). Mapping of the cyst nematode resistance locus *Gpa2* in potato using a strategy based on comigrating AFLP markers. *Theor. Appl. Genet.* 95, 874–880. doi: 10.1007/s001220050638

Rousselle-Bourgeois, F., and Mugniery, D. (1995). Screening tuber-bearing *Solanum* spp. for resistance to *Globodera rostochiensis* Ro1 Woll. and *G. pallida* Pa2/3 stone. *Potato Res.* 38, 241–249. doi: 10.1007/BF02359906

Sabeh, M., Lord, E., Grenier, E., St-Arnaud, M., and Mimee, B. (2019). What determines host specificity in hyperspecialized plant parasitic nematodes? *BMC Genom.* 20:457. doi: 10.1186/s12864-019-5853-4

Sacco, M. A., Koropacka, K., Grenier, E., Jaubert, M. J., Blanchard, A., Goverse, A., et al. (2009). The cyst nematode SPRYSEC Protein RBP-1 elicits Gpa2-and RanGAP2-dependent plant cell death. *PLoS Pathog.* 5:14. doi: 10.1371/journal.ppat.1000564

Sandal, N. N., Salentijn, E. M. J., Kleine, M., Cai, D. G., Arens-de Reuver, M., Van Druten, M., et al. (1997). Backcrossing of nematode-resistant sugar beet: a second nematode resistance gene at the locus containing Hs1(pro-1)? *Mol. Breed.* 3, 471–480. doi: 10.1023/a:1009697119097

Sattarzadeh, A., Achenbach, U., Lubeck, J., Strahwald, J., Tacke, E., Hofferbert, H. R., et al. (2006). Single nucleotide polymorphism (SNP) genotyping as basis for developing a PCR-based marker highly diagnostic for potato varieties with high resistance to *Globodera pallida* pathotype Pa2/3. *Mol. Breed.* 18, 301–312. doi: 10.1007/s11032-006-9026-1

Schultz, L., Cogan, N. O. I., McLean, K., Dale, M. F. B., Bryan, G. J., Forster, J. W., et al. (2012). Evaluation and implementation of a potential diagnostic molecular marker for *H1*-conferred potato cyst nematode resistance in potato (*Solanum tuberosum* L.). *Plant Breed.* 131, 315–321. doi: 10.1111/j.1439-0523.2012.01949.x

Schwarzfischer, A., Behn, A., Groth, J., Reichmann, M., Kellermann, A., and Songe, Y. (2010). "Marker-assisted selection in practical potato breeding - experience and outlook," in *Proceedings of the 60. Jahrestagung der Vereinigung der Pflanzenzuchter Und Saatgutkaufleute Osterreichs, 24-26 November 2009*, (Irdning: Raumberg-Gumpenstein), 81–85.

Seinhorst, J. W. (1982). The relationship in field experiments between population density of *Globodera rostochiensis* before planting potatoes and yield of potato tubers. *Nematologica* 28, 277–284. doi: 10.1163/187529282X00312

Sharma, R., Bhardwaj, V., Dalamu, D., Kaushik, S. K., Singh, B. P., Sharma, S., et al. (2014). Identification of elite potato genotypes possessing multiple disease resistance genes through molecular approaches. *Sci. Hortic.* 179, 204–211. doi: 10.1016/j.scienta.2014.09.018

Sharma, S. K., Bolser, D., de Boer, J., Sonderkaer, M., Amoros, W., Carboni, M. F., et al. (2013). Construction of reference chromosome-scale pseudomolecules for potato: integrating the potato genome with genetic and physical maps. *G3 (Bethesda)* 3, 2031–2047. doi: 10.1534/g3.113.007153

Sharma, S. K., MacKenzie, K., McLean, K., Dale, F., Daniels, S., and Bryan, G. J. (2018). Linkage disequilibrium and evaluation of genome-wide association mapping models in tetraploid potato. *G3 (Bethesda)* 8, 3185–3202. doi: 10.1534/g3.118.200377

Skantar, A., Handoo, Z., Carta, L., and Chitwood, D. (2007). Morphological and molecular identification of *Globodera pallida* associated with potato in Idaho. *J. Nematol.* 39, 133–144.

Skantar, A. M., Handoo, Z. A., Zasada, I. A., Ingham, R. E., Carta, L. K., and Chitwood, D. J. (2011). Morphological and molecular characterization of

Globodera populations from Oregon and Idaho. *Phytopathology* 101, 480–491. doi: 10.1094/phyto-01-10-0010

Slater, A. T., Cogan, N. O. I., Forster, J. W., Hayes, B. J., and Daetwyler, H. D. (2016). Improving genetic gain with genomic selection in autotetraploid potato. *Plant Genome* 9:15. doi: 10.3835/plantgenome2016.02.0021

Smant, G., Stokkermans, J., Yan, Y. T., de Boer, J. M., Baum, T. J., Wang, X. H., et al. (1998). Endogenous cellulases in animals: isolation of beta-1,4-endoglucanase genes from two species of plant-parasitic cyst nematodes. *Proc. Natl. Acad. Sci. U.S.A* 95, 4906–4911. doi: 10.1073/pnas.95.9.4906

Sobczak, M., Avrova, A., Jupowicz, J., Phillips, M. S., Ernst, K., and Kumar, A. (2005). Characterization of susceptibility and resistance responses to potato cyst nematode (*Globodera* spp.) infection of tomato lines in the absence and presence of the broad-spectrum nematode resistance *Hero* gene. *Mol. Plant Microbe Interact.* 18, 158–168. doi: 10.1094/mpmi-18-0158

Sobczak, M., and Golinowski, W. (2011). "Cyst nematodes and syncytia," in *Genomics and Molecular Genetics of Plant-Nematode Interactions*, eds J. Jones, G. Gheysen, and C. Fenoll (Dordrecht: Springer Academic Publisher), 61–82. doi: 10.1007/978-94-007-0434-3_4

Starr, J. L., Bridge, J., and Cook, R. (2002). "Resistance to plant-parasitic nematodes: history, current use and future potential," in *Plant Resistance to Parasitic Nematodes*, eds J. L. Starr, R. Cook, and J. Bridge (Wallingford: CABI Publishing), 1–22. doi: 10.1079/9780851994666.0001

Stearns, S. C. (1989). Trade-offs in life-history evolution *Funct. Ecol* 3, 259–268. doi: 10.2307/2389364

Stone, A. R. (1985). Co-evolution of potato cyst nematodes and their host: implication for pathotypes and resistance. *Bull. OEPP* 15, 131–137. doi: 10.1111/j.1365-2338.1985.tb00212.x

Strachan, S. M., Armstrong, M. R., Kaur, A., Wright, K. M., Lim, T. Y., Baker, K., et al. (2019). Mapping the *H2* resistance effective against *Globodera pallida* pathotype Pa1 in tetraploid potato. *Theor. Appl. Genet.* 132, 1283–1294. doi: 10.1007/s00122-019-03278-4

Sudha, R., Mhatre, P. H., Lekshmanan, D. K., Venkatasalam, E. P., Bairwa, A., Bhardwaj, V., et al. (2019). Phenotypic and molecular characterization of potato germplasm for potato cyst nematode resistance. *Indian J. Genet. Plant. Breed.* 79, 394–403. doi: 10.31742/ijgpb.79.2.2

Sudha, R., Venkatasalam, E. P., Bairwa, A., Bhardwaj, V., Dalamu, and Sharma, R. (2016). Identification of potato cyst nematode resistant genotypes using molecular markers. *Sci. Hortic.* 198, 21–26. doi: 10.1016/j.scienta.2015.11.029

Tan, A. M. Y., Park, T. H., Alles, R., Hutten, R. C., Visser, R. G., and van Eck, H. J. (2009). *GpaXI*$^{I}_{tar}$ originating from *Solanum tarijense* is a major resistance locus to *Globodera pallida* and is localised on chromosome 11 of potato. *Theor. Appl. Genet.* 119, 1477–1487. doi: 10.1007/s00122-009-1149-4

The Potato Genome Sequencing Consortium (2011). Genome sequence and analysis of the tuber crop potato. *Nature* 475, 189–195. doi: 10.1038/nature10158

Thorpe, P., Mantelin, S., Cock, P. J., Blok, V. C., Coke, M. C., Eves-van den Akker, S., et al. (2014). Genomic characterisation of the effector complement of the potato cyst nematode *Globodera pallida*. *BMC Genom.* 15:923. doi: 10.1186/1471-2164-15-923

Torto, B., Cortada, L., Murungi, L. K., Haukeland, S., and Coyne, D. L. (2018). Management of cyst and root knot nematodes: a chemical ecology perspective. *J. Agric. Food Chem.* 66, 8672–8678. doi: 10.1021/acs.jafc.8b01940

Trudgill, D. L. (1985). Potato cyst nematodes: a critical review of the current pathotyping scheme. *Bull. OEPP* 15, 273–279. doi: 10.1111/j.1365-2338.1985.tb00228.x

Trudgill, D. L. (1987). Effects of rates of a nematicide and of fertiliser on the growth and yield of cultivars of potato which differ in their tolerance of damage by potato cyst nematodes (*Globodera rostochiensis* and *G. pallida*). *Plant Soil* 104, 235–243. doi: 10.1007/BF02372537

Trudgill, D. L. (1991). Resistance to and tolerance of plant parasitic nematodes in plants. *Annu. Rev. Phytopathol.* 29, 167–192. doi: 10.1146/annurev.py.29.090191.001123

Trudgill, D. L., and Cotes, L. M. (1983a). Differences in the tolerance of potato cultivars to potato cyst nematodes (*Globodera rostochiensis* and *Globodera pallida*) in field trials with and without nemticides. *Ann. Appl. Biol.* 102, 373–384. doi: 10.1111/j.1744-7348.1983.tb02707.x

Trudgill, D. L., and Cotes, L. M. (1983b). Tolerance of potato to potato cyst nematodes (*Globodera rostochiensis* and *G. pallida*) in relation to the growth and efficiency of the root system. *Ann. Appl. Biol.* 102, 385–397. doi: 10.1111/j.1744-7348.1983.tb02708.x

Trudgill, D. L., Phillips, M. S., and Elliott, M. J. (2014). Dynamics and management of the white potato cyst nematode *Globodera pallida* in commercial potato crops. *Ann. Appl. Biol.* 164, 18–34. doi: 10.1111/aab.12085

Turner, S. J. (1990). The identification and fitness of virulent potato cyst nematode populations (*Globodera pallida*) selected on resistant *Solarium vernei* hybrids for up to eleven generations. *Ann. Appl. Biol.* 117, 385–397. doi: 10.1111/j.1744-7348.1990.tb04225.x

Turner, S. J. (1996). Population decline of potato cyst nematodes (*Globodera rostochiensis, G. pallida*) in field soils in Northern Ireland. *Ann. Appl. Biol.* 129, 315–322. doi: 10.1111/j.1744-7348.1996.tb05754.x

Turner, S. J., and Stone, A. R. (1981). Hatching of potato cyst nematodes (*Globodera rostochiensis, G. pallida*) in root exudates of Solanum vernei hybrids. *Nematologica* 27, 315–318. doi: 10.1163/187529281x00548

Turner, S. J., Stone, A. R., and Perry, J. N. (1983). Selection of potato cyst-nematodes on resistant *Solanum vernei* hybrids. *Euphytica* 32, 911–917. doi: 10.1007/BF00042173

Turner, S. J., and Subbotin, S. A. (2013). "Cyst nematodes," in *Plant Nematology*, eds R. N. Perry and M. Moens (Wallingford: CAB International), 109–143.

USDA (2007). *Potato Cyst Nematode Eradication in Idaho*. Available Online at: https://www.aphis.usda.gov/plant_health/ea/downloads/pcn-ameded-ea.pdf (accessed 10.09.2020)

Van der Biezen, E. A., and Jones, J. D. (1998). Plant disease-resistance proteins and the gene-for-gene concept. *Trends Biochem. Sci.* 23, 454–456. doi: 10.1016/s0968-0004(98)01311-5

van der Vossen, E. A., van der Voort, J. N., Kanyuka, K., Bendahmane, A., Sandbrink, H., Baulcombe, D. C., et al. (2000). Homologues of a single resistance-gene cluster in potato confer resistance to distinct pathogens: a virus and a nematode. *Plant J.* 23, 567–576. doi: 10.1046/j.1365-313x.2000.00814.x

van Eck, H. J., Vos, P. G., Valkonen, J. P. T., Uitdewilligen, J. G. A. M. L., Lensing, H., de Vetten, N., et al. (2017). Graphical genotyping as a method to map $Ny_{(o,n)sto}$ and *Gpa5* using a reference panel of tetraploid potato cultivars. *Theor. Appl. Genet.* 130, 515–528. doi: 10.1007/s00122-016-2831-y

van Lieshout, N., van der Burgt, A., de Vries, M. E., ter Maat, M., Eickholt, D., Esselink, D., et al. (2020). Solyntus, the new highly contiguous reference genome for potato (*Solanum tuberosum*). *G3 (Bethesda)* 10, 3489–3495. doi: 10.1534/g3.120.401550

Van Weymers, P. S. M., Baker, K., Chen, X. W., Harrower, B., Cooke, D. E. L., Gilroy, E. M., et al. (2016). Utilizing "Omic" technologies to identify and prioritize novel sources of resistance to the oomycete pathogen phytophthora infestans in potato germplasm collections. *Front. Plant Sci.* 7:11. doi: 10.3389/fpls.2016.00672

Vanderplank, J. E. (1978). "Genetic and molecular basis of plant pathogenesis," in *Part of Advanced Series in Agricultural Sciences*, (Berlin: Springer-Verlag).

Varypatakis, K., Jones, J. T., and Blok, V. C. (2019). Susceptibility of potato varieties to populations of *Globodera pallida* selected for increased virulence. *Nematology* 21, 995–998. doi: 10.1163/15685411-00003283

Varypatakis, K., Veronneau, P.-Y., Thorpe, P., Cock, P. J. A., Lim, J. T.-Y., Armstrong, M. R., et al. (2020). The genomic impact of selection for virulence against resistance in the potato cyst nematode. *Globodera pallida*. *Genes* 11:1429. doi: 10.3390/genes11121429

Visscher, P. M., Brown, M. A., McCarthy, M. I., and Yang, J. (2012). Five Years of GWAS Discovery. *Am. J. Hum. Genet.* 90, 7–24. doi: 10.1016/j.ajhg.2011.11.029

Vos, P., Simons, G., Jesse, T., Wijbrandi, J., Heinen, L., Hogers, R., et al. (1998). The tomato *Mi-1* gene confers resistance to both root-knot nematodes and potato aphids. *Nat. Biotechnol.* 16, 1365–1369. doi: 10.1038/4350

Whitehead, A. G. (1991). Selection for virulence in the potato cyst-nematode. *Globodera pallida*. *Ann. Appl. Biol.* 118, 395–402. doi: 10.1111/j.1744-7348.1991.tb05639.x

Whitworth, J. L., Novy, R. G., Zasada, I. A., Wang, X., Dandurand, L.-M., and Kuhl, J. C. (2018). Resistance of potato breeding clones and cultivars to three species of potato cyst nematode. *Plant Dis.* 102, 2120–2128. doi: 10.1094/pdis-12-17-1978-re

Williams, K. J., Lewis, J. G., Bogacki, P., Pallotta, M. A., Willsmore, K. L., Kuchel, H., et al. (2003). Mapping of a QTL contributing to cereal cyst nematode tolerance and resistance in wheat. *Aust. J. Agric. Res.* 54, 731–737. doi: 10.1071/AR02225

Williams, K. J., Willsmore, K. L., Olson, S., Matic, M., and Kuchel, H. (2006). Mapping of a novel QTL for resistance to cereal cyst nematode in wheat. *Theor. Appl. Genet.* 112, 1480–1486. doi: 10.1007/s00122-006-0251-0

Witek, K., Jupe, F., Witek, A. I., Baker, D., Clark, M. D., and Jones, J. D. G. (2016). Accelerated cloning of a potato late blight-resistance gene using RenSeq and SMRT sequencing. *Nat. Biotechnol.* 34, 656–660. doi: 10.1038/nbt.3540

Wyss, U. (1997). "Root parasitic nematodes: an overview," in *Cellular and Molecular Aspects of Plant-Nematode Interactions*, eds C. Fenoll, F. M. W. Grundler, and S. A. Ohl (Netherlands: Springer), 5–22. . doi: 10.1007/978-94-011-5596-0_2

Zasada, I. A., Ingham, R. E., Baker, H., and Phillips, W. S. (2019). Impact of *Globodera ellingtonae* on yield of potato (*Solanum tuberosum*). *J. Nematol.* 51, 1–10. doi: 10.21307/jofnem-2019-073

Zhou, Q., Tang, D., Huang, W., Yang, Z. M., Zhang, Y., Hamilton, J. P., et al. (2020). Haplotype-resolved genome analyses of a heterozygous diploid potato. *Nat. Genet.* 52, 1018–1023. doi: 10.1038/s41588-020-0699-x

Conflict of Interest: The authors declare that the research was conducted in the absence of any commercial or financial relationships that could be construed as a potential conflict of interest.

frontiers in Plant Science

ORIGINAL RESEARCH
published: 09 April 2021
doi: 10.3389/fpls.2021.641480

The *Meloidogyne incognita* Nuclear Effector MiEFF1 Interacts With *Arabidopsis* Cytosolic Glyceraldehyde-3-Phosphate Dehydrogenases to Promote Parasitism

Nhat My Truong[1,2], Yongpan Chen[1,3], Joffrey Mejias[1], Salomé Soulé[1], Karine Mulet[1], Maëlle Jaouannet[1], Stéphanie Jaubert-Possamai[1], Shinichiro Sawa[2], Pierre Abad[1], Bruno Favery[1] and Michaël Quentin[1]**

[1]Institut Sophia Agrobiotech, INRAE, CNRS, Université Côte d'Azur, Sophia Antipolis, France, [2]Graduate School of Science and Technology, Kumamoto University, Kumamoto, Japan, [3]Department of Plant Pathology and Key Laboratory of Pest Monitoring and Green Management of the Ministry of Agriculture, China Agricultural University, Beijing, China

OPEN ACCESS

Edited by:
Shahid Siddique, University of California, Davis, United States

Reviewed by:
Paulo Vieira, Virginia Tech, United States
Henok Yimer, University of California, Davis, United States

***Correspondence:**
Michaël Quentin
michael.quentin@inrae.fr
Bruno Favery
bruno.favery@inrae.fr

Specialty section:
This article was submitted to Plant Pathogen Interactions, a section of the journal Frontiers in Plant Science

Received: *14 December 2020*
Accepted: *22 March 2021*
Published: *09 April 2021*

Citation:
Truong NM, Chen Y, Mejias J, Soulé S, Mulet K, Jaouannet M, Jaubert-Possamai S, Sawa S, Abad P, Favery B and Quentin M (2021) The Meloidogyne incognita Nuclear Effector MiEFF1 Interacts With Arabidopsis Cytosolic Glyceraldehyde-3-Phosphate Dehydrogenases to Promote Parasitism. Front. Plant Sci. 12:641480. doi: 10.3389/fpls.2021.641480

Root-knot nematodes are obligate endoparasites that maintain a biotrophic relationship with their hosts over a period of several weeks. They induce the differentiation of root cells into specialized multinucleate hypertrophied feeding cells known as giant cells. Nematode effectors synthesized in the esophageal glands and injected into the plant tissue through the syringe-like stylet play a key role in giant cell ontogenesis. The *Meloidogyne incognita* MiEFF1 is one of the rare effectors of phytopathogenic nematodes to have been located *in vivo* in feeding cells. This effector specifically targets the giant cell nuclei. We investigated the *Arabidopsis* functions modulated by this effector, by using a yeast two-hybrid approach to identify its host targets. We characterized a universal stress protein (USP) and cytosolic glyceraldehyde-3-phosphate dehydrogenases (GAPCs) as the targets of MiEFF1. We validated the interaction of MiEFF1 with these host targets in the plant cell nucleus, by bimolecular fluorescence complementation (BiFC). A functional analysis with *Arabidopsis* GUS reporter lines and knockout mutant lines showed that GAPCs were induced in giant cells and that their non-metabolic functions were required for root-knot nematode infection. These susceptibility factors are potentially interesting targets for the development of new root-knot nematode control strategies.

Keywords: root-knot nematode (*Meloidogyne incognita*), effector, giant cell, cytosolic glyceraldehyde-3-phosphate dehydrogenases, susceptibility gene

INTRODUCTION

Root-knot nematodes (RKNs), *Meloidogyne* spp., are extremely polyphagous biotrophic plant parasites with a worldwide distribution. These microscopic worms cause dramatic root deformations, known as galls or root knots, which decrease crop yields, resulting in considerable economic losses (Abad et al., 2008; Jones et al., 2013). RKN are obligate parasites with a life cycle of

3–8 weeks, depending on the nematode species and environmental conditions. They spend most of their active life within plant roots. Four juvenile stages in addition to egg-laying adult female line the success of their life cycle. The hatching second-stage juvenile (J2) in the soil are attracted by the plant root, burrow into the host root close to the growing tip, and migrate intercellular to reach the vascular cylinder. They establish and maintain permanent feeding cells in the host root to supply them with nutrients. Feeding cell formation requires a reprograming of the selected root vascular cells into specialized hypertrophied and hypermetabolic feeding cells. Successive nuclear divisions without cell division and isotropic growth lead to multinucleate feeding "giant cells" containing up to 100 endoreduplicated and hypertrophied nuclei (Favery et al., 2016). The induction of these giant cells, which are found only in RKN parasitism, is mediated by effector proteins secreted into the host tissues by the nematode (Truong et al., 2015; Nguyen et al., 2018; Vieira and Gleason, 2019). These effectors are produced principally in the nematode esophageal glands (one dorsal and two subventral glands) and are delivered to the plant *via* a syringe-like stylet. Some effectors may also be produced by other secretory organs such as the chemosensory amphids or the hypodermis (Zhao et al., 2019). Effectors may be secreted into the apoplast (i.e., the intercellular space) to facilitate root penetration, intracellular migration, and the suppression of host defenses or into the cytoplasm of the 5–7 vascular cells destined to become the giant cells. The effectors involved in giant cells neo-organogenesis and functioning may target different subcellular compartments and cellular host functions. Indeed, transcriptomic studies of the plant response to RKN infection have revealed that RKN can hijack several key host cellular processes, such as the cell cycle, phytohormone signaling, intercellular transport, and metabolism to favor parasitism (Caillaud et al., 2008; Gheysen and Mitchum, 2019; Favery et al., 2020).

Meloidogyne incognita secretes hundreds of effectors into host plants (Bellafiore et al., 2008; Wang et al., 2012). A role in parasitism has been demonstrated for very few of these effectors, and the target in the plant has been identified for only 10 of these proteins (Mejias et al., 2019, 2020; Zhao et al., 2020). RKN effectors often target multifunctional proteins regulating key biological processes and conserved in all eukaryotes. The known target proteins include annexins, which are involved in development and responses to the biotic and abiotic environment in plants (Baucher et al., 2012) and have been shown to interact with the *M. incognita* MiMIF-2 effector (Zhao et al., 2019). The *M. chitwoodi* Mc1194 effector targets a papain-like cysteine protease (PLCP; Davies et al., 2015). In plants, PCLPs are involved in physiological processes as diverse as seed germination, leaf senescence, abiotic stress responses, and immunity (Liu et al., 2018). Another example is provided by the PASSE-MURAILLE effector (MiPM), which has been shown to interact with the *Arabidopsis thaliana* CSN5 protein (Bournaud et al., 2018), a subunit of the COP9 signalosome (CSN), a multifunctional eukaryotic protein complex (Cope and Deshaies, 2003). Finally, the nuclear MiEFF18 targets the *Arabidopsis* core spliceosomal protein SmD1 (Mejias et al., 2020), which regulates pre-mRNA splicing and alternative splicing, thereby increasing the diversity of the giant cell proteome (Elvira-Matelot et al., 2016; Mejias et al., 2020).

We describe here the identification and functional analysis of the direct targets of *M. incognita* EFFECTOR 1 (MiEFF1), the first RKN effector shown to be secreted *in planta* and to target the nuclei of the feeding cells within the host giant cells (Jaouannet et al., 2012). *MiEFF1* (*Minc17998*) is specifically expressed in the dorsal esophageal gland of parasitic juveniles. However, MiEFF1 displays no similarity to any of the sequences present in database and has no domain of known function other than a predicted nuclear localization signal (NLS). Using the yeast two-hybrid (Y2H) approach and *in planta* bimolecular fluorescence complementation (BiFC), we demonstrated that, in *A. thaliana*, MiEFF1 interacts with multifunctional cytoplasmic proteins, a universal stress protein (AtUSP) and cytosolic glyceraldehyde-3-phosphate dehydrogenases (AtGAPCs) displaying moonlighting or having alternative nuclear functions required for plant responses to abiotic and/or biotic stress (Zaffagnini et al., 2013; Chi et al., 2019). We also showed that the *AtUSP* and *AtGAPC* genes are induced upon RKN parasitism. Finally, we demonstrated that *AtGAPCs* are required for *Arabidopsis* susceptibility to *M. incognita*.

MATERIALS AND METHODS

Plant Material and Growth Conditions

The *Arabidopsis* lines used for the experiments were from the Wassilewskija (WS-4) and Columbia (Col-0) genetic backgrounds. The *usp* mutants, the SALK_146059 mutant line, referred to here as *usp.1*, previously described by Jung et al. (2015) and SALK_071209, referred to here as *usp.2*, were purchased from the *Arabidopsis* Biological Resource Center (United States). The *gapc1* (SALK_010839) and *gapc2* (SALK_016539) mutant lines and the *AtGAPC1* transcriptional reporter GUS line have been described elsewhere (Vescovi et al., 2013). The *abp39* and *abx27* mutants, harboring T-DNA insertions in *AtGAPC1* and *AtGAPC2*, respectively, were obtained from the INRAE Versailles T-DNA insertion collection (Bechtold et al., 1993). Homozygous mutants were identified by PCR-based genotyping, and new lines were further analyzed by RT-PCR and RT-qPCR, with the primers listed in **Supplementary Table 1**. Seeds of wild-type *A. thaliana*, mutants, and transgenic lines were surface-sterilized and sown on Murashige and Skoog (Duchefa) agar plates (0.5 × MS salts, 1% sucrose, 0.8% agar, and pH 6.4) or on a mixture of soil and sand. Seeds were incubated at 4°C for 2 days, and the plates were then transferred to a growth chamber with an 8 h photoperiod at 21°C. For propagation and transformation, seedlings were transferred to a growth chamber with a 16 h photoperiod at 21°C. *Nicotiana benthamiana* plants were grown in soil, under a 16 h photoperiod, at 24°C.

Sequence Analysis and Alignment

The sequences of EFF1 orthologs were obtained from NCBI and Wormbase parasite. Protein sequences were aligned with the MAFFT tool on the EBI server.[1]

[1]https://www.ebi.ac.uk/Tools/msa/mafft/

Plasmid Constructs

The *M. incognita MiEFF1* (*Minc17998*; GenBank MW345915) and *MiEFF18* (*Minc18636*; GenBank KX907770) coding sequences (CDS) lacking the signal peptide, the *A. thaliana AtUSP* (*At3g53990*), *AtGAPC1* (*At3g04120*), *AtGAPC2* (*At1g13440*), and *AtSmD1b* (*At4g02840*), the *AtUSP* and *AtGAPC2* promoters, the SV40 T antigen and the murin P53 sequences were amplified by PCR with specific primers (**Supplementary Table 1**) and inserted into the pDON207 donor vector. The entry clones were recombined with pK7WGF2 (p35S:eGFP-GW), pK7WGR2 (p35S:RFP-GW), pKGWFS7 (GWpromoter:eGFP-GUS), BiFC vectors (pAM-35SS:GW-YFPc, pAM-35SS:GW-YFPn, pAM-35SS:YFPc-GW, and pAM-35SS:YFPn-GW) or Y2H vectors, pGBK-GW, pB27-GW, or pP6-GW (Karimi et al., 2002; Caillaud et al., 2009; Zhao et al., 2020), with Gateway technology (Invitrogen). All constructs were sequenced (GATC Biotech) and used to transform *Agrobacterium tumefaciens* strain GV3101 or *Saccharomyces cerevisiae* strains AH109, L40ΔGal4, or Y187.

Y2H Assay

The yeast-two hybrid (Y2H) screen was performed according to the instructions supplied with the BD Matchmaker Library Construction and Screening Kit (Clontech). The coding sequence of MiEFF1 was inserted into the bait vector pGBKT7, which was used to transform *S. cerevisiae* strain AH109. For screening, cells carrying the bait construct were cotransformed with the commercial "normalized *A. thaliana* universal P02403 cDNA library" constructed by Dualsystems Biotech (Switzerland), using RNAs extracted from different *Arabidopsis* tissues, mixed in equal quantities and covering >95% of *Arabidopsis* genes. Yeasts displaying an interaction were recovered on selective SD medium without leucine, tryptophan, histidine, and adenine (SD/−Leu-Trp-His-Ade). To further validate the interactions, the *MiEFF1* CDS lacking the peptide signal was cloned into the bait pB27 vector and used to transform yeast strain L40ΔGal4. The whole sequences encoding the AtUSP, AtGAPC1, and AtGAPC2 were cloned into the pP6 prey vectors, which were used to transform yeast strain Y187. The pairwise mating experiments with Y187 (matα) and L40ΔGal4 (mata) yeast strains were performed as previously described (Zhao et al., 2020).

In planta Subcellular Localization and BiFC

Leaves from 3–4-week-old *N. benthamiana* plants were subjected to agroinfiltration with recombinant strains of *A. tumefaciens* containing GFP, RFP, or BiFC vectors, as described by Caillaud et al. (2009). Images were captured, 48 h after agroinfiltration, with an inverted confocal microscope (Zeiss LSM880) equipped with an argon and HeNe laser as the excitation source. Samples were excited at 488 nm for GFP/YFP and 543 nm for RFP. GFP or YFP emission was detected selectively with a 505–530 nm band-pass emission filter. We detected RFP fluorescence with a 560–615 nm band-pass emission filter.

RNA Methods

Total RNA was extracted from *A. thaliana* seedlings or hand-dissected root segments and galls 7 and 14 days post-infection (dpi) with TRIzol reagent (Invitrogen), according to the manufacturer's instructions. We reverse-transcribed 1 µg DNAse-treated (Ambion) RNA with the Superscript IV reverse transcriptase (Invitrogen). Semi quantitative RT-PCR was performed to analyze transcript abundancy in wild-type *Arabidopsis* and in the various newly generated mutant lines, with the primers described in **Supplementary Table 1**. Transcripts of the constitutively expressed *OXA1* gene (*At5g62050*) were amplified to check that the amounts of intact cDNA used were similar in RT-PCR experiments. RT-qPCR analyses were performed and analyzed as described by Mejias et al. (2020), with the primers described in **Supplementary Table 1**. *OXA1* and *UBP22* (*AT5G10790*) were used for the normalization of RT-qPCR data. Data were analyzed using the $2^{-\Delta\Delta Ct}$ method and were presented as Log2 fold change or as Normalized Relative Quantity generated using qBase software (Hellemans et al., 2007). Three technical replicates for 2–3 independent biological experiments were performed.

Nematode Infection Assays

Meloidogyne incognita strain "Morelos" was multiplied in tomato (*Solanum lycopersicum* cv. "Saint Pierre") grown in a growth chamber (25°C and 16 h photoperiod). Freshly hatched J2s were collected as previously described (Caillaud and Favery, 2016). Three-week-old *Arabidopsis* plants grown individually in small pots of soil/sand were inoculated with 150 *M. incognita* J2 larvae per plant. Roots were collected and weighted 6 weeks after infection, and the females laying egg masses stained with 4.5% eosin under a binocular microscope were counted. For each experiment, we used n = 17–25 plants per line. Four independent infection experiments were performed for each *gapc* mutant line, and one infection experiment was performed for each *usp* mutant line.

Transgenic GUS Reporter Lines and Histochemical Analysis

The *AtGAPC1promoter::GUS* construct was previously described (Vescovi et al., 2013), and the *Arabidopsis* line was a kind gift from Prof. Alex Costa. The *AtGAPC2promoter::GUS* and *AtUSPpromoter::GUS* constructs were generated and introduced in *A. tumefaciens* as described above. *Arabidopsis thaliana* plants were transformed with those constructs by the floral dip method (Clough and Bent, 1998). Homozygous T3 transformants were used for further analysis. Plants were inoculated with *M. incognita* as described above, and GUS activity was analyzed histochemically 7 and 21 days after inoculation with *M. incognita*, as previously described (Caillaud et al., 2009). Reporter *GUS* expression in galls was revealed following 2–16 h staining. Two to four independent biological experiments were performed.

RESULTS

MiEFF1 Interacts With a Universal Stress Protein and Cytosolic GAPDHs in *Arabidopsis*

MiEFF1 is a pioneer protein of unknown function. Orthologs can be identified in the eight available RKNs genome sequences:

M. incognita, *M. javanica*, *M. arenaria* (Blanc-Mathieu et al., 2017), *M. hapla* (Opperman et al., 2008), *M. enterolobii* (Koutsovoulos et al., 2020), *M. floridensis* (Lunt et al., 2014), *M. luci* (Susič et al., 2020), and *M. graminicola* (Phan et al., 2020; **Supplementary Figure 1**). EFF1 is, however, absent from other plant parasitic nematodes and other organisms. We searched for possible host targets of the MiEFF1 effector, by screening a normalized *Arabidopsis* prey Y2H library. Approximately 1.2×10^5 yeast cells transformed with the prey and bait vectors were obtained, and 48 clones carrying a potential target were selected on SD/−Leu-Trp-His-Ade. Bait vector sequencing identified 30 sequences in frame with the transcriptional activation domain of GAL4 (**Figure 1A**). These sequences include that for the universal stress protein AtUSP (AT3G53990), which was captured eight times. All the clones isolated carried the complete sequence of *AtUSP* encoding a 160-amino acid (aa) protein containing the USPA domain (PF00582). In addition, five sequences encoding a cytosolic glyceraldehyde 3-phosphate dehydrogenase (AtGAPC2, AT1G13440) were identified. AtGAPC2 is 338 aa protein containing a NADP binding domain (aa 6–156, PF00044) and a catalytic domain (aa 161–318, PF02800). Two proteins were captured twice: a Glycine Rich Protein (AtGRP19, AT5G07550) and the Fragile Histidine Triad (AT5G58240) that are not nuclear proteins, and thus are not expected to interact with the MiEFF1 *in vivo* (**Figure 1A**). Finally, 13 proteins were captured once, that were not retained for further analysis (**Figure 1A**). Thus, only AtUSP and AtGAPC2 proteins were considered as potential targets of MiEFF1 in *A. thaliana*. We were also interested in analyzing whether AtGAPC1 (encoded by *At3g04120*), which is 97.9% identical to AtGAPC2 (Vescovi et al., 2013), could also interact with MiEFF1. For the confirmation of interactions, full-length sequences of *AtGAPC1*, *AtGAPC2*, and *AtUSP* were inserted into prey vectors to test the interactions with MiEFF1 in a LexA-based Y2H assay. The growth of diploids on selective SD/−Leu-Trp-His medium confirmed that the interactions between MiEFF1 and the full-length AtUSP, AtGAPC2, and AtGAPC1 proteins occurred in yeast (**Figure 1B**). These results demonstrate that MiEFF1 interacts with AtUSP, AtGAPC1, and AtGAPC2 in yeast.

MiEFF1 Interacts With AtUSP, AtGAPC1, and AtGAPC2 in the Plant Cell Nucleus

We investigated whether MiEFF1 would be able to interact physically with AtUSP and AtGAPCs in plant cells, by determining the subcellular distributions of these proteins *in planta*. We expressed the AtUSP, AtGAPC1, and AtGAPC2 proteins, fused to GFP or RFP, in *N. benthamiana* epidermal leaf cells, by agroinfiltration. AtGAPC1, AtGAPC2, and AtUSP were localized to the cytoplasm and the nucleus of agroinfiltrated *N. benthamiana* epidermal leaf cells (**Figure 2A**), consistent with the results obtained in *Arabidopsis* stable transgenic lines or protoplasts (Vescovi et al., 2013; Schneider et al., 2018), and in *Nicotiana tabacum* agro-infiltrated leaves (Melencion et al., 2017). These results suggest that the nuclear MiEFF1 (**Figure 2A**), and its identified targets would easily be able to interact in the nucleus of plant cells. We then performed BiFC to check the interactions between Mi-EFF1 and the AtGAPCs and AtUSP *in planta*. The co-expression of MiEFF1-YFPc and YFPn-GAPCs or YFPn-USP fusion proteins reconstituted YFP fluorescence signals in the nucleus of agro-infiltrated *N. benthamiana* epidermal cells (**Figure 2B**). Analogous combinations with the nuclear effector MiEFF18 (Mejias et al., 2020) as negative controls resulted in no interaction with any of the identified targets of MiEFF1 (**Figure 2B**). Similarly, no interaction was observed between MiEFF1-YFPc and the previously described nuclear protein AtSmD1b (Mejias et al., 2020), fused to an N-terminal YFPn (**Figure 2B**). Various other constructs, resulting in fusions with YFPc or YFPn at the C- or N-terminus of the encoded protein, were used to check the interactions between MiEFF1

A

Protein AGI accession	Description	Time captured
AT3G53990	**Universal stress protein (USP); Adenine nucleotide alpha hydrolases-like superfamily protein**	**8**
AT1G13440	**Cytosolic glyceraldehyde 3-phosphate dehydrogenase (GAPC2)**	**5**
AT5G07550	Glycine-rich protein 19 (GRP19)	2
AT5G58240	Fragile Histidine Triad; Bis(5'-adenosyl)-triphosphatase-like	2
AT1G22610	PRT-C superfamily protein; Phosphoribosyltransferase	1
AT1G27450	Adenine phosphoribosyltransferase 1	1
AT1G29920	Chlorophyll a/b-binding protein	1
AT1G60950	Ferredoxine 2	1
AT1G79260	Unknown	1
AT2G16070	Plastid division protein PDV2-like	1
AT2G36430	Plant protein of unknown function (DUF247)	1
AT3G52930	Fructose-bisphosphate aldolase	1
AT4G01150	Unknown	1
AT4G17085	Putative membrane lipoprotein	1
AT5G54270	Light-harvesting chlorophyll B-binding protein 3	1
AT5G64180	Unknown	1
AT5G67240	SDN3 small RNA degrading nuclease 3	1

B

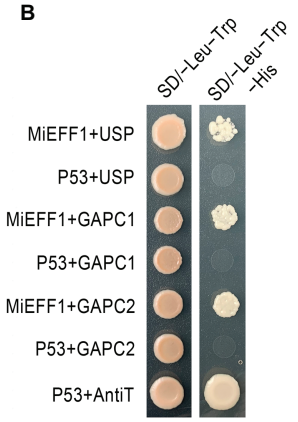

FIGURE 1 | MiEFF1 interacts with AtUSP, AtGAPC1, and AtGAPC2 in yeast. **(A)** List of putative MiEFF1-interacting proteins from *Arabidopsis* obtained in our Y2H screen. **(B)** Yeasts containing the bait and prey plasmids carrying MiEFF1 and AtUSP, AtGAPC1, or AtGAPC2 and controls were spotted onto plates. SD/−Leu-Trp (Leu, leucine; Trp, tryptophane) is the non-selective medium without leucine and tryptophan. Only yeasts carrying a protein-protein interaction can survive on SD/−Leu-Trp-His (His, histidine) selective medium. Murine p53 and SV40 T antigen (anti T) were used as a positive control. Murine P53 and AtUSP, AtGAPC1, or AtGAPC2 were used as a negative control.

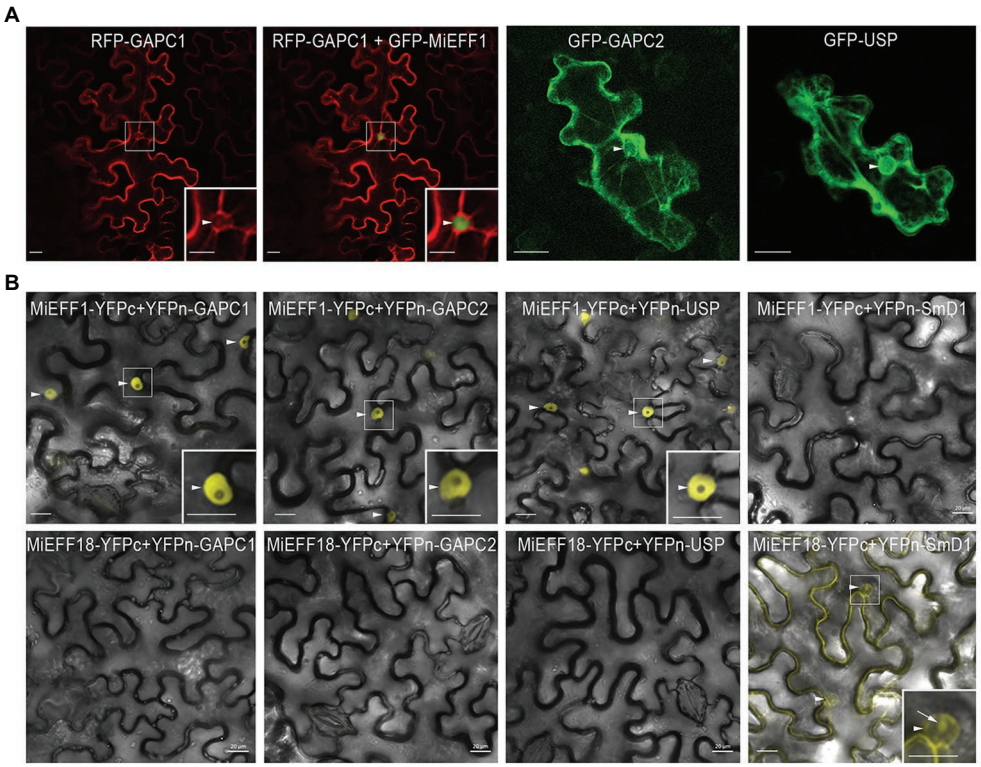

FIGURE 2 | MiEFF1 interacts with AtUSP, AtGAPC1, and AtGAPC2 *in planta*. **(A)** Localization of GFP-AtUSP, -AtGAPC1, and -AtGAPC2 in *Nicotiana benthamiana* epidermal leaf cells. Enlargements of the area framed are shown. Arrowheads indicate nuclei. **(B)** MiEFF1 interacts with AtUSP, AtGAPC1, and AtGAPC2 in the nucleus in *Nicotiana benthamiana* cells. Confocal images of YFP fluorescence in bimolecular fluorescence complementation (BiFC) experiments with MiEFF1-YFPc and YFPn-GAPCs/USP fusion proteins expressed in *Nicotiana benthamiana* epidermal cells. MiEFF18 and AtSmD1b were used as controls. Three independent experiments were performed with similar results. Enlargements of the area framed are shown. Arrowheads indicate nuclei, arrow indicates nucleolus. Bars = 20 μm.

and the three interacting proteins identified; all gave results similar to those presented in **Figure 2B** (**Supplementary Figure 2**). These results confirm that a specific interaction occurs between MiEFF1 and AtUSP, AtGAPC1, and AtGAPC2 in plant cells.

AtGAPC and AtUSP Accumulate in RKN-Induced Feeding Sites

We then investigated the expression of *AtUSP*, *AtGAPC2*, and *AtGAPC1* in giant cells and galls, using published transcriptomic data (Yamaguchi et al., 2017). These RNAseq data showed induction of *AtGAPC1* gene in galls at 3, 5, and 7 dpi (**Figure 3A**), suggesting a possible role for *AtGAPC1* in the plant response to nematode infection. No accumulation of AtGAPC2 and AtUSP was observed in galls according to those RNAseq data (**Figure 3A**). The expression pattern of *AtGAPC1*, *AtGAPC2* and *AtUSP* in galls, at 7 and 14 dpi, was further investigated using RT-qPCR. As shown in **Figure 3A**, *AtGAPC1* and *AtGAPC2* transcripts accumulated significantly in galls at 7 dpi. *AtUSP* expression increased slightly only at 14 dpi.

Arabidopsis transgenic lines carrying *promoter::GUS* constructs were used to analyze *AtGAPC1*, *AtGAPC2*, and *AtUSP* spatio-temporal expression upon *M. incognita* infection. As previously described (Vescovi et al., 2013), *AtGAPC1* is expressed in roots of non-infected plants (**Figure 3B**; **Supplementary Figures 3, 4**). Consistent with our RT-qPCR data, the transgenic plants carrying the *AtGAPC1promoter::GUS* construct (Vescovi et al., 2013) displayed strong promoter activity in galls at 7 dpi and to a lesser extent at 21 dpi (**Figure 3B**). The *AtGAPC2promoter::GUS* construct was generated by cloning a 1,200 bp sequence immediately upstream from the translation initiation codon. Transgenic plants carrying the *AtGAPC2promoter::GUS* construct displayed promoter activity in non-inoculated root tips (**Figure 3B**; **Supplementary Figures 3, 4**). Induction of *AtGAPC2* was observed in galls only at 7 dpi (**Figure 3B**), validating the transcriptomic data. No activity of the *AtGAPC2* promoter was detected at 21 dpi. Moreover, an *AtUSPpromoter::GUS* construct was generated, harboring the 1,070 bp sequence immediately upstream from the translation initiation codon. The *AtUSP* promoter displayed activity in vascular tissues of non-inoculated root tips (**Supplementary Figure 5**). No GUS signal was detected in galls at 7 dpi, but a signal was observed in galls at 21 dpi (**Figure 3B**; **Supplementary Figures 3, 4**). Thus, these results showed that *AtGAPC1* and *AtGAPC2* transcripts accumulated significantly in galls at 7 dpi, while *AtUSP* is expressed at a later stage of the interaction. Altogether, these data support the hypothesis that MiEFF1-interacting proteins may be involved in plant responses to RKN parasitism.

A

		RKN-induced galls				
		RNAseq (Yamaguchi et al., 2017)			qRT-PCR	
		3 dpi	5 dpi	7 dpi	7 dpi	14 dpi
AtGAPC1	*At3g04120*	0.39 ± 0.12	0.56 ± 0.12	0.85 ± 0.12	2.0 ± 0.7	-1.2 ± 0.2
AtGAPC2	*At1g13440*	-0.23 ± 0.10	0.0018 ± 0.10	-0.012 ± 0.10	2.9 ± 0.3	0.36 ± 0.4
AtUSP	*At3g53990*	0.05 ± 0.14	-0.38 ± 0.14	-0.25 ± 0.14	0.56 ± 0.7	0.64 ± 0.3

B

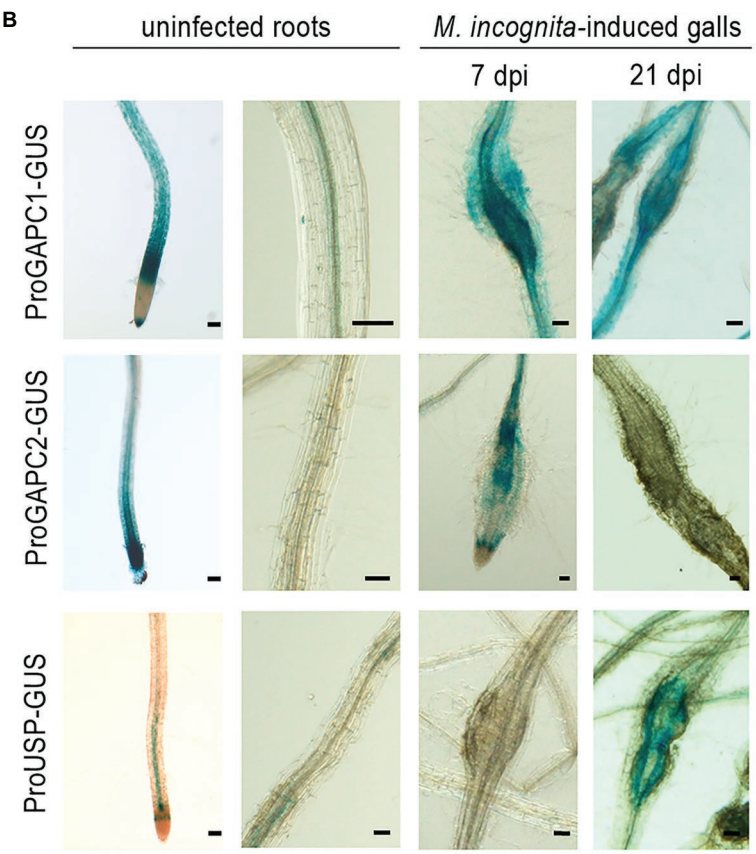

FIGURE 3 | MiEFF1-interacting proteins accumulate in RKN-induced feeding sites. **(A)** Expression ratios of the *AtUSP*, *AtGAPC1*, and *AtGAPC2* genes in galls vs. uninfected roots (log2) were obtained from RNAseq (Yamaguchi et al., 2017) data. Data presented are log2 fold changes ± standard deviation (SD) from three biological replicates. The mRNA expression level of these genes was further measured by quantitative real-time PCR (RT-qPCR) in galls at 7 and 14 days post *M. incognita* infection (dpi) and uninfected roots. Data were normalized against *OXA1* and *UBP22* as constitutive genes. Data presented are log2 fold changes ± SD from two biological replicates. dpi, days post-infection. Gray coloring indicates an absence of differential expression, a magenta coloring indicates an upregulation and a blue coloring a downregulation. **(B)** GUS expression in galls at 7 and 21 dpi, and uninfected roots, of plants transformed with *AtGAPC1*, *AtGAPC2*, and *AtUSP* promoter –GUS fusions. Reporter *GUS* expression in galls was revealed following 2 h (*AtGAPC1promoter::GUS*) or 16 h (*AtGAPC2promoter::GUS* and *AtUSPpromoter::GUS*) staining. Two to three independent experiments were performed with similar results. NI, not infected. Bars = 50 μm.

AtGAPC1 and AtGAPC2 Are Involved in Plant Susceptibility to Root-Knot Nematodes

We further investigated the possible involvement of the proteins encoded by the *AtUSP*, *AtGAPC1*, and *AtGAPC2* genes in the development and/or physiology of the giant cells induced by RKN, by performing infection tests with *M. incognita* in *Arabidopsis* loss-of-function mutant lines. A previously characterized *usp.1* knockout (KO) line (SALK_146059; Jung et al., 2015) and a new *usp.2* KO mutant line (SALK_071209; **Supplementary Figure 5**) carrying a T-DNA insertion in the third exon were challenged with *M. incognita*. We scored the number of females producing egg masses 6 weeks after infection. The test of these two alleles indicated no significant difference in the number of females producing egg masses between the *usp* mutants and Col-0 wild-type plants (**Supplementary Figure 5**). The two previously described *gapc1* and *gapc2* KO lines in the Col-0 genetic background (Vescovi et al., 2013; **Figure 4A**) were used here to investigate the role of *AtGAPC* genes in the plant-RKN interaction. We also selected two new mutant alleles in the WS genetic background, KO *abp39* and knockdown *abx27*, carrying T-DNA insertions in the sixth exon of *AtGAPC1*, and in the *AtGAPC2* promoter, respectively (**Figures 4A,B**; **Supplementary Figure 6**). These lines were inoculated with *M. incognita* juveniles. For all the lines tested, the number of females producing egg masses was smaller in

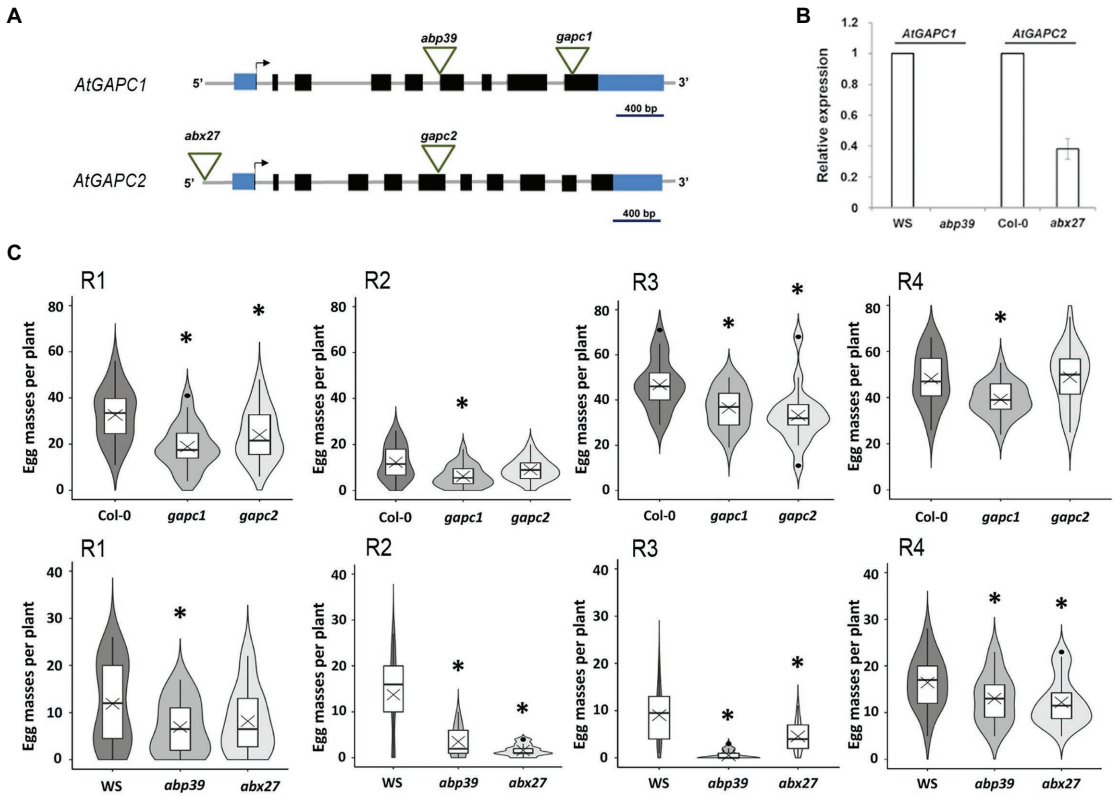

FIGURE 4 | *AtGAPC1* and *AtGAPC2* are involved in *Arabidopsis* susceptibility to *M. incognita*. **(A)** Schematic illustration of the genomic organization of *AtGAPC1* and *AtGAPC2* and T-DNA insertion sites. Black boxes represent exons, gray lines correspond to introns, blue boxes represent untranslated sequences and the arrows represent START codons. **(B)** RT-qPCR analysis of *AtGAPC1* and *AtGAPC2* expression in *abp39* and *abx27* mutants. Data were normalized against *OXA1* and *UBP22* constitutive genes. **(C)** Results of four independent nematode infection assays, performed on *Arabidopsis* mutants *AtGAPC1* (*gapc1* and *abp39*) and *AtGAPC2* (*gapc2* and *abx27*), relative to wild-type plants (Col-0 and WS). Number of egg masses (*y*-axis), at 6 weeks post infection, in independent nematode infection assays, is shown as violin-plot diagrams. Box indicates interquartile range (25–75th percentile). The horizontal bar in the box indicates the median of the reported values. The crosses show the mean value. Whiskers mark the lowest and highest values within 1.5 times the interquartile range, and black dots indicate outliers. The box plot is included in a kernel density plot (shade of grays) showing the entire distribution of the data. R1–R4 indicate independent replicates. n = 17–25 plants per line. Asterisks indicate a significant difference between the wild-type and the mutant lines, as shown by Student's t test ($p < 0.05$).

the mutants than in wild-type plants: 19.4–94.0% fewer egg masses were found in *atgapc1* mutants and 25.7–88.3% fewer in *atgapc2* mutants (**Figure 4C**). A slight root developmental phenotype was observed in the *gapc2* mutant, but not in the *abx27* (**Supplementary Figure 6**), and both these *gapc2* mutant lines exhibited a rather similar decreased susceptibility to RKN. For the two *atgapc1* mutants, a significant and reproducible reductions in the egg mass number were observed over four independent experiments (**Figure 4C**), and this phenotype is not associated to a defect in root development (**Supplementary Figure 6**). Overall, these results demonstrate that *AtGAPC* genes play a role in *Arabidopsis* susceptibility to RKN.

AtGAPC1 and AtGAPC2 Regulate Expression of Defense-Associated Genes

To investigate whether AtGAPC1 and AtGAPC2 manipulation by MiEFF1 could affect *Arabidopsis* immunity, we measured, using RT-qPCR, the expression of genes involved in antioxidative functions (*AtCDS2*) and abiotic (*AtADH1* and *AtSAP12*) or biotic (*AtPR1a*, *AtPDF1.2a*, and *AtPR4*) stress responses (Zhao et al., 2020) in *abp39* and *abx27* mutants. In both mutants, *AtPR1a* and *AtPDF1.2a*, regulators of salicylic acid (SA)- and ethylene- and jasmonate (JA)-mediated defense responses, respectively, showed a strong constitutive expression, while *AtPR4*, encoding an ethylene-responsive PR protein, was repressed in both lines (**Figure 5**). The *AtCDS2* gene encoding a Cu/Zn superoxide dismutase was also significantly induced in both mutants while the *AtADH1*, *AtSAP12* encoding an alcohol dehydrogenase and a stress-associated protein, respectively, were not differentially expressed (**Figure 5**). These results indicate that targets of MiEFF1 are involved in regulating the expression of SA and JA defense-related genes in *Arabidopsis*.

DISCUSSION

Plant parasitic nematodes of the genus *Meloidogyne* have developed original and complex mechanisms of parasitism.

By injecting proteins called as "effectors" into the host plant, they induce cellular reprograming and the transformation of root cells into hypertrophied polynucleate feeding cells known as "giant cells." The development and maintenance of giant cells induced by RKN requires the manipulation of several host cellular processes (Favery et al., 2016). The nucleus is a key cellular compartment that must be targeted by the parasite (Quentin et al., 2013), and effectors, such as Mi16D10 and MiEFF18, have already been shown to target host transcription factors and the splicing machinery, respectively (Huang et al., 2006; Mejias et al., 2020). MiEFF1, a protein carrying a NLS, is produced in the parasitic RKN dorsal gland, secreted *in planta* and has been shown to accumulate in host giant cell nuclei during parasitism (Jaouannet et al., 2012). However, the function of MiEFF1 remained unknown. The identification of pathogen effector targets is now widely used as an approach to elucidating the molecular functions of these effectors (Khan et al., 2018; Mejias et al., 2019). Our yeast two-hybrid experiments identified three potential targets of the MiEFF1 nuclear effector in *Arabidopsis*: AtUSP, and two cytosolic GAPDHs, AtGAPC1 and AtGAPC2.

USPs were originally discovered in *Escherichia coli* and have been implicated in responses to various stress conditions in bacteria, archaea, plants, and some invertebrate animals (Vollmer and Bark, 2018). Plant USPs are multifunctional proteins involved in the development in addition to their role in responses to biotic and abiotic stresses (Chi et al., 2019). USPs proteins containing the *E. coli* universal stress protein A (USPA) domain and are encoded by members of a multigene family in *Arabidopsis* (Kerk et al., 2003; Chi et al., 2019). AtUSP (AT3G53990) has been implicated in plant responses to drought (Isokpehi et al., 2011), oxidative stress (Jung et al., 2015), and heat and cold stress (Jung et al., 2015; Melencion et al., 2017). A role in plant defense against pathogens was recently documented, with AtUSP accumulating in plants exposed to *Pseudomonas syringae* and displaying antimicrobial activity against various fungi (Park et al., 2017). We confirmed the presence of AtUSP in both the cytoplasm and the nucleus (Melencion et al., 2017), consistent with a possible dual function for this protein. In the cytoplasm, AtUSP acts as a protein chaperone in response to heat shock (Jung et al., 2015; Chi et al., 2019), whereas, in the nucleus, it may bind and protect nucleic acids, particularly RNA, enabling the plant to tolerate cold stress (Melencion et al., 2017; Chi et al., 2019). The induction of *AtUSP* upon RKN attack, at the end of giant cell formation, and its interaction with MiEFF1 within the plant cell nucleus suggest that it is the nuclear function of AtUSP in nucleic acid protection that is targeted by MiEFF1. Further investigation will be required, using multiple KO lines because of the redundancy of *USPs* in *A. thaliana* (Kerk et al., 2003), to conclude on AtUSP function in plant-RKN interaction.

Interestingly, we also found that nuclear MiEFF1 interacted with two cytosolic GAPDHs. Not only these proteins act as key enzymes in glycolysis, but are also well-known "moonlighting" (multifunctional) proteins with functions in several processes unrelated to metabolism in animal and plant cells, such as apoptosis, autophagy, gene expression regulation, and responses to abiotic or biotic stress (Sirover, 2011; Zaffagnini et al., 2013). This functional versatility is regulated, in part, by redox-based post-translational modifications that alter GAPDH catalytic activity and influence the subcellular distribution of the enzyme. Animals have a single isoform of GAPDH, with well-established moonlighting properties, whereas plants have multiple isoforms, the

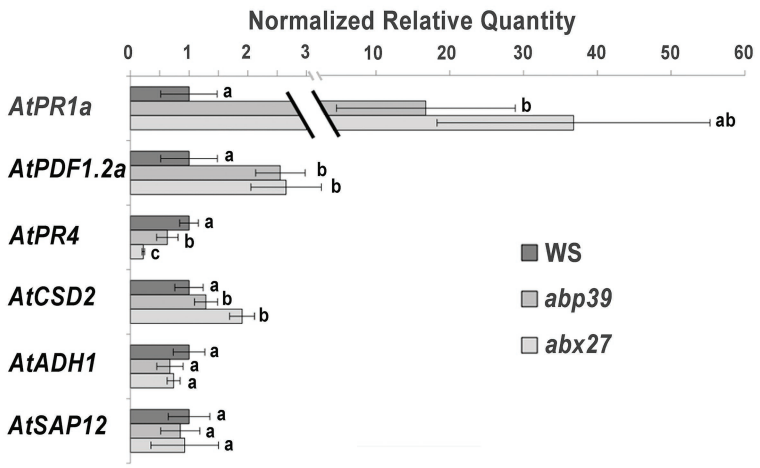

FIGURE 5 | AtGAPC1 and AtGAPC2 regulate expression of defense-associated genes in Arabidopsis. RT-qPCR was used to investigate expression of defense- and stress-associates genes in *abp39* and *abx27* mutant seedlings. The genes considered were *AtPR1a* (*At2g14610*; salicylic acid (SA)-mediated defense response marker gene), *AtPDF1.2a* (*At5g44420*; encoding ethylene- and jasmonate-responsive plant defenses), *AtPR4* (*At3g04720*; ethylene-responsive pathogenesis-related protein), *AtCSD2* (*At2g28190*; chloroplastic Cu/Zn superoxide dismutase), *AtADH1* (*At1g77120*; catalyzing the reduction of acetaldehyde with NADH as reductant), and *AtSAP12* (*At3g28210*; stress-associated protein). *AtOXA1* (*AT5G62050*) and *AtUBP22* (*AT5G10790*) were used as internal controls. Data are presented as means ± standard deviation (SD) from three biological replicates. Different letters indicate statistically significant differences, $^*p < 0.05$, Wilcoxon sign-rank test.

non-metabolic roles of which have yet to be discovered (Zaffagnini et al., 2013). *Arabidopsis* has four gene families encoding seven phosphorylating GAPDH isoenzymes and one non-phosphorylating GAPDH isoenzyme. Only AtGAPC1 and AtGAPC2 and the non-phosphorylating GAPDH (NP-GAPDH) are cytosolic. The other GAPDHs are located in other cellular compartments such as chloroplasts (Zaffagnini et al., 2013). Interestingly, the two cytoplasmic GAPCs have been shown to relocalize to the plant cell nucleus upon exposure to oxidative stresses, such as H_2O_2 (Schneider et al., 2018) or nitric oxide (Testard et al., 2016; Schneider et al., 2018), and following exposure to cadmium (Vescovi et al., 2013), salt stress (Wawer et al., 2010), or heat stress (Kim et al., 2020). Similarly, a strong accumulation of AtGAPC1 has been shown in the nucleus following the perception of flagellin during infection with *P. syringae*, and a mutation of *AtGAPC1* renders *Arabidopsis* less susceptible to these pathogenic bacteria (Henry et al., 2015). The function of GAPCs in the nucleus remains unclear. They have been shown to interact with plant nucleic acids, suggesting a potential role of GAPCs in protecting nucleic acids during stress responses (Testard et al., 2016). GAPCs were recently shown to interact with the NF-YC10 transcription factor to promote the expression of heat-inducible genes and heat tolerance in *Arabidopsis* (Kim et al., 2020). We show here that *AtGAPC1* and *AtGAPC2* were induced during giant cell formation and that the corresponding proteins were targeted by the nuclear effector MiEFF1, suggesting that one of the moonlighting nuclear functions of these proteins is targeted by RKN. A stronger and faster response of *AtGAPC1* was observed in response to *M. incognita*, in line with the response to biotic and abiotic stress previously described (Vescovi et al., 2013; Henry et al., 2015). We also found that GAPCs were important for parasitic success in RKNs, as shown for several bacterium-host and virus-host interactions (Han et al., 2015; Henry et al., 2015; Zeng et al., 2018). Finally, *N. benthamiana* GAPCs have been shown to be targeted by the citrus tristeza virus (CTV), *via* interaction with the viral p23, to facilitate the infectious cycle of the virus (Ruiz-Ruiz et al., 2018). Thus, GAPCs appear to be common targets of evolutionarily diverse plant-pathogens. Considering *AtGAPC1* induction in galls, and susceptibility of *gapc1* mutants to *M. incognita*, we postulate that AtGAPC1 assume most of GAPCs function required for disease establishment. GAPC2 would reinforce the action of GAPC1 at a key moment of giant cell formation. Previous studies showed GAPCs have multiple functions in the regulation of autophagy, hypersensitive response, and plant innate immunity, and described a role of GAPCs as negative regulators of plant defense in *Arabidopsis* (Henry et al., 2015), *N. benthamiana* (Han et al., 2015), or *Manihot esculenta* (Zeng et al., 2018). Microarray analysis on *Arabidopsis gapc* mutants showed that several genes encoding for enzymes regulating reactive oxygen species (ROS) homeostasis, such as peroxidases, catalases, or superoxide dismutases, had altered expression (Rius et al., 2008), and here, using a RT-qPCR approach, we demonstrated a differential expression of defense- and stress-associated genes in *abp39* and *abx27* mutants, both mutant lines showing strong constitutive expression of *AtPR1a* and *AtPDF1.2a* genes.

While several RKN effectors were shown to be responsible for host defense suppression (Quentin et al., 2013; Vieira and Gleason, 2019), very few have had their host target identified, i.e., MiMIF2 (Zhao et al., 2019), MiPDI1 (Zhao et al., 2020), Mg16820 (Naalden et al., 2018), MgMO237 (Chen et al., 2018), and MjTTL5 (Lin et al., 2016). This work adds MiEFF1 to the list of RKN effectors modulating host immunity and confirms that defense- and stress-related proteins are key targets of effectors, particularly those of nematodes, during disease establishment. These genes, particularly those encoding GAPCs, constitute attractive conserved candidates for targeting to reduce susceptibility in novel breeding strategies aiming to develop durable and broad-spectrum resistance (van Schie and Takken, 2014; Zaidi et al., 2018).

DATA AVAILABILITY STATEMENT

The original contributions presented in the study are included in the article/**Supplementary Material**, further inquiries can be directed to the corresponding authors.

AUTHOR CONTRIBUTIONS

NT designed and performed the experiments and interpreted the results. YC contributed to BiFC and Y2H experiments. JM contributed to subcellular localizations. SSo and KM performed the qRT-PCR analysis. MJ contributed to material and data analysis. NT, PA, BF, and MQ wrote the article. SJ-P, SSa, PA, BF, and MQ obtained the funding, designed the work, supervised the experiments, and data analyses. All authors contributed to the article and approved the submitted version.

FUNDING

NT was supported by a USTH fellowship, 911-USTH program, from the Ministry of Education and Training of The Socialist Republic of Vietnam, and received a Short Term Scientific Mission grant (STSM) from the COST action FA1208 (Pathogen-informed strategies for sustainable broad-spectrum crop resistance). YC got scholarships from China Scholarship Council (No. 201806350108) for studying at INRAE, France. JM benefited from a doctoral fellowship of the Ministère de l'Enseignement Supérieur, de la Recherche et de l'Innovation (MENRT grant). SSo was supported by a doctoral fellowship from INRAE SPE department and IDEX UCAJedi ANR-15-IDEX-01. This work was supported by the INRAE, the French Government (National Research Agency, ANR) through the programs LABEX SIGNALIFE ANR-11-LABX-0028 and IDEX UCAJedi ANR-15-IDEX-01, the French-Japanese bilateral collaboration programs (PHC SAKURA 2016 #35891VD and 2019 #43006VJ), and the French-Chinese bilateral collaboration program PHC XU GUANGQI 2020 #45478PF.

ACKNOWLEDGMENTS

We thank Prof. Alex Costa (Università di Milano, Italy) for the generous gift of the *gapc1* and *gapc2* mutants and the *AtGAPC1promoter::GUS* reporter line, Dr. Olivier Pierre for technical support, and Nathalie Marteu for producing nematodes. We also thank Hybrigenics Services (France) for providing the pB27 and pP6 vectors and the L40ΔGal4 and Y187 yeast strains. Microscopy work was performed at the PlantBIOs imaging facility of the Institut Sophia Agrobiotech.

SUPPLEMENTARY MATERIAL

The Supplementary Material for this article can be found online at: https://www.frontiersin.org/articles/10.3389/fpls.2021.641480/full#supplementary-material

REFERENCES

Abad, P., Gouzy, J., Aury, J.-M., Castagnone-Sereno, P., Danchin, E. G. J., Deleury, E., et al. (2008). Genome sequence of the metazoan plant-parasitic nematode Meloidogyne incognita. *Nat. Biotechnol.* 26, 909–915. doi: 10.1038/nbt.1482

Baucher, M., Pérez-Morga, D., and El Jaziri, M. (2012). Insight into plant annexin function. From shoot to root signaling. *Plant Signal. Behav.* 7, 524–528. doi: 10.4161/psb.19647

Bechtold, N., Elis, J., and Pelletier, G. (1993). In planta agrobacterium mediated gene transfer by infiltration of adult *Arabidopsis thaliana*. *C.R. Acad. Sci.* 316, 1194–1199.

Bellafiore, S., Shen, Z., Rosso, M.-N., Abad, P., Shih, P., and Briggs, S. P. (2008). Direct identification of the Meloidogyne incognita secretome reveals proteins with host cell reprogramming potential. *PLoS Pathog.* 4:e1000192. doi: 10.1371/journal.ppat.1000192

Blanc-Mathieu, R., Perfus-Barbeoch, L., Aury, J.-M. M., Da Rocha, M., Gouzy, J., Sallet, E., et al. (2017). Hybridization and polyploidy enable genomic plasticity without sex in the most devastating plant-parasitic nematodes. *PLoS Genet.* 13:e1006777. doi: 10.1371/journal.pgen.1006777

Bournaud, C., Gillet, F.-X., Murad, A. M., Bresso, E., Albuquerque, E. V. S., and Grossi-de-Sá, M. F. (2018). *Meloidogyne incognita* PASSE-MURAILLE (MiPM) gene encodes a cell-penetrating protein that interacts with the CSN5 subunit of the COP9 signalosome. *Front. Plant Sci.* 9:904. doi: 10.3389/fpls.2018.00904

Caillaud, M.-C., Dubreuil, G., Quentin, M., and Favery, B. (2008). Root-knot nematodes manipulate plant cell functions during a compatible interaction. *J. Plant Physiol.* 165, 104–113. doi: 10.1016/j.jplph.2007.05.007

Caillaud, M. C., and Favery, B. (2016). In vivo imaging of microtubule organization in dividing giant cell. *Methods Mol. Biol.* 1370, 137–144. doi: 10.1007/978-1-4939-3142-2_11

Caillaud, M.-C., Paganelli, L., Lecomte, P., Deslandes, L., Quentin, M., Pecrix, Y., et al. (2009). Spindle assembly checkpoint protein dynamics reveal conserved and unsuspected roles in plant cell division. *PLoS One* 4:e6757. doi: 10.1371/journal.pone.0006757

Chen, J., Hu, L., Sun, L., Lin, B., Huang, K., Zhuo, K., et al. (2018). A novel Meloidogyne graminicola effector, MgMO237, interacts with multiple host defence-related proteins to manipulate plant basal immunity and promote parasitism. *Mol. Plant Pathol.* 19, 1942–1955. doi: 10.1111/mpp.12671

Chi, Y. H., Koo, S. S., Oh, H. T., Lee, E. S., Park, J. H., Phan, K. A. T., et al. (2019). The physiological functions of universal stress proteins and their molecular mechanism to protect plants from environmental stresses. *Front. Plant Sci.* 10:750. doi: 10.3389/fpls.2019.00750

Clough, S. J., and Bent, A. F. (1998). Floral dip: a simplified method for agrobacterium-mediated transformation of *Arabidopsis thaliana*. *Plant J.* 16, 735–743. doi: 10.1046/j.1365-313x.1998.00343.x

Cope, G. A., and Deshaies, R. J. (2003). COP9 signalosome: a multifunctional regulator of SCF and other cullin-based ubiquitin ligases. *Cell* 14, 663–671. doi: 10.1016/s0092-8674(03)00722-0

Davies, L. J., Zhang, L., and Elling, A. A. (2015). The *Arabidopsis thaliana* papain like cysteine protease RD21 interacts with a root-knot nematode effector protein. *Nematology* 17, 655–666. doi: 10.1163/15685411-00002897

Elvira-Matelot, E., Bardou, F., Ariel, F., Jauvion, V., Bouteiller, N., Le Masson, I., et al. (2016). The nuclear ribonucleoprotein SmD1 interplays with splicing, RNA quality control, and posttranscriptional gene silencing in *Arabidopsis*. *Plant Cell* 28, 426–438. doi: 10.1105/tpc.15.01045

Favery, B., Dubreuil, G., Chen, M.-S., Giron, D., and Abad, P. (2020). Gall-inducing parasites: convergent and conserved strategies of plant manipulation by insects and nematodes. *Annu. Rev. Phytopathol.* 58, 1–22. doi: 10.1146/annurev-phyto-010820-012722

Favery, B., Quentin, M., Jaubert-Possamai, S., and Abad, P. (2016). Gall-forming root-knot nematodes hijack key plant cellular functions to induce multinucleate and hypertrophied feeding cells. *J. Insect Physiol.* 84, 60–69. doi: 10.1016/j.jinsphys.2015.07.013

Gheysen, G., and Mitchum, M. G. (2019). Phytoparasitic nematode control of plant hormone pathways. *Plant Physiol.* 179, 1212–1226. doi: 10.1104/pp.18.01067

Han, S., Wang, Y., Zheng, X., Jia, Q., Zhao, J., Bai, F., et al. (2015). Cytoplastic glyceraldehyde-3-phosphate dehydrogenases interact with ATG3 to negatively regulate autophagy and immunity in *Nicotiana benthamiana*. *Plant Cell* 27, 1316–1331. doi: 10.1105/tpc.114.134692

Hellemans, J., Mortier, G., De Paepe, A., Speleman, F., and Vandesompele, J. (2007). qBase relative quantification framework and software for management and automated analysis of real-time quantitative PCR data. *Genome Biol.* 8, 1–14. doi: 10.1186/gb-2007-8-2-r19

Henry, E., Fung, N., Liu, J., Drakakaki, G., and Coaker, G. (2015). Beyond glycolysis: GAPDHs are multi-functional enzymes involved in regulation of ROS, autophagy, and plant immune responses. *PLoS Genet.* 11:e1005199. doi: 10.1371/journal.pgen.1005199

Huang, G., Dong, R., Allen, R., Davis, E. L., Baum, T. J., and Hussey, R. S. (2006). A root-knot nematode secretory peptide functions as a ligand for a plant transcription factor. *Mol. Plant-Microbe Interact.* 19, 463–470. doi: 10.1094/MPMI-19-0463

Isokpehi, R. D., Simmons, S. S., Cohly, H. H. P., Ekunwe, S. I. N., Begonia, G. B., and Ayensu, W. K. (2011). Identification of drought-responsive universal stress proteins in viridiplantae. *Bioinform. Biol. Insights* 5, 41–58. doi: 10.4137/BBI.S6061

Jaouannet, M., Perfus-Barbeoch, L., Deleury, E., Magliano, M., Engler, G., Vieira, P., et al. (2012). A root-knot nematode-secreted protein is injected into giant cells and targeted to the nuclei. *New Phytol.* 194, 924–931. doi: 10.1111/j.1469-8137.2012.04164.x

Jones, J. T., Haegeman, A., Danchin, E. G. J., Gaur, H. S., Helder, J., Jones, M. G. K., et al. (2013). Top 10 plant-parasitic nematodes in molecular plant pathology. *Mol. Plant Pathol.* 14, 946–961. doi: 10.1111/mpp.12057

Jung, Y. J., Melencion, S. M. B., Lee, E. S., Park, J. H., Alinapon, C. V., Oh, H. T., et al. (2015). Universal stress protein exhibits a redox-dependent chaperone function in arabidopsis and enhances plant tolerance to heat shock and oxidative stress. *Front. Plant Sci.* 6:1141. doi: 10.3389/fpls.2015.01141

Karimi, M., Inzé, D., and Depicker, A. (2002). GATEWAY® vectors for agrobacterium-mediated plant transformation. *Trends Plant Sci.* 7, 193–195. doi: 10.1016/S1360-1385(02)02251-3

Kerk, D., Bulgrien, J., Smith, D. W., and Gribskov, M. (2003). Arabidopsis proteins containing similarity to the universal stress protein domain of bacteria. *Plant Physiol.* 131, 1209–1219. doi: 10.1104/pp.102.016006

Khan, M., Seto, D., Subramaniam, R., and Desveaux, D. (2018). Oh, the places they'll go ! A survey of phytopathogen effectors and their host targets. *Plant J.* 93, 651–663. doi: 10.1111/tpj.13780

Kim, S.-C., Guo, L., and Wang, X. (2020). Nuclear moonlighting of cytosolic glyceraldehyde-3-phosphate dehydrogenase regulates *Arabidopsis* response to heat stress. *Nat. Commun.* 11:3439. doi: 10.1038/s41467-020-17311-4

Koutsovoulos, G. D., Poullet, M., Elashry, A., Kozlowski, D. K. L., Sallet, E., Da Rocha, M., et al. (2020). Genome assembly and annotation of *Meloidogyne*

enterolobii, an emerging parthenogenetic root-knot nematode. *Sci. Data.* 7:324. doi: 10.1038/s41597-020-00666-0

Lin, B., Zhuo, K., Chen, S., Hu, L., Sun, L., Wang, X., et al. (2016). A novel nematode effector suppresses plant immunity by activating host reactive oxygen species-scavenging system. *New Phytol.* 209, 1159–1173. doi: 10.1111/nph.13701

Liu, H., Hu, M., Wang, Q., Lin Cheng, L., and Zhang, Z. (2018). Role of papain-like cysteine proteases in plant development. *Front. Plant Sci.* 9:1717. doi: 10.3389/fpls.2018.01717

Lunt, D. H., Kumar, S., Koutsovoulos, G., and Blaxter, M. L. (2014). The complex hybrid origins of the root knot nematodes revealed through comparative genomics. *PeerJ* 2:e356. doi: 10.7717/peerj.356

Mejias, J., Bazin, J., Truong, N.-M., Chen, Y., Marteu, N., Bouteiller, N., et al. (2020). The root-knot nematode effector MiEFF18 interacts with the plant core spliceosomal protein SmD1 required for giant cell formation. *New Phytol.* 229, 3408–3423. doi: 10.1111/nph.17089

Mejias, J., Truong, N. M., Abad, P., Favery, B., and Quentin, M. (2019). Plant proteins and processes targeted by parasitic nematode effectors. *Front. Plant Sci.* 10:970. doi: 10.3389/fpls.2019.00970

Melencion, S. M. B., Chi, Y. H., Pham, T. T., Paeng, S. K., Wi, S. D., Lee, C., et al. (2017). RNA chaperone function of a universal stress protein in arabidopsis confers enhanced cold stress tolerance in plants. *Int. J. Mol. Sci.* 18:2546. doi: 10.3390/ijms18122546

Naalden, D., Haegeman, A., de Almeida-Engler, J., Birhane Eshetu, F., Bauters, L., and Gheysen, G. (2018). The Meloidogyne graminicola effector Mg16820 is secreted in the apoplast and cytoplasm to suppress plant host defense responses. *Mol. Plant Pathol.* 19, 2416–2430. doi: 10.1111/mpp.12719

Nguyen, C.-N., Perfus-Barbeoch, L., Quentin, M., Zhao, J., Magliano, M., Marteu, N., et al. (2018). A root-knot nematode small glycine and cysteine-rich secreted effector, MiSGCR1, is involved in plant parasitism. *New Phytol.* 217, 687–699. doi: 10.1111/nph.14837

Opperman, C. H., Bird, D. M., Williamson, V. M., Rokhsar, D. S., Burke, M., Cohn, J., et al. (2008). Sequence and genetic map of *Meloidogyne hapla*: a compact nematode genome for plant parasitism. *Proc. Natl. Acad. Sci. U. S. A.* 105, 14802–14807. doi: 10.1073/pnas.0805946105

Park, S. C., Jung, Y. J., Lee, Y., Kim, I. R., Seol, M. A., Kim, E. J., et al. (2017). Functional characterization of the *Arabidopsis* universal stress protein AtUSP with an antifungal activity. *Biochem. Biophys. Res. Commun.* 486, 923–929. doi: 10.1016/j.bbrc.2017.03.126

Phan, N. T., Orjuela, J., Danchin, E. G. J., Klopp, C., Perfus-Barbeoch, L., Kozlowski, D. K., et al. (2020). Genome structure and content of the rice root-knot nematode (*Meloidogyne graminicola*). *Ecol. Evol.* 10, 11006–11021. doi: 10.1002/ece3.6680

Quentin, M., Abad, P., and Favery, B. (2013). Plant parasitic nematode effectors target host defense and nuclear functionsto establish feeding cells. *Front. Plant Sci.* 4:53. doi: 10.3389/fpls.2013.00053

Rius, S. P., Casati, P., Iglesias, A. A., and Gomez-Casati, D. F. (2008). Characterization of *Arabidopsis* lines deficient in GAPC-1, a cytosolic NAD-dependent glyceraldehyde-3-phosphate dehydrogenase. *Plant Physiol.* 148, 1655–1667. doi: 10.1104/pp.108.128769

Ruiz-Ruiz, S., Spanò, R., Navarro, L., Moreno, P., Peña, L., and Flores, R. (2018). Citrus tristeza virus co-opts glyceraldehyde 3-phosphate dehydrogenase for its infectious cycle by interacting with the viral-encoded protein p23. *Plant Mol. Biol.* 98, 363–373. doi: 10.1007/s11103-018-0783-0

Schneider, M., Knuesting, J., Birkholz, O., Heinisch, J. J., and Scheibe, R. (2018). Cytosolic GAPDH as a redox-dependent regulator of energy metabolism. *BMC Plant Biol.* 18:184. doi: 10.1186/s12870-018-1390-6

Sirover, M. A. (2011). On the functional diversity of glyceraldehyde-3-phosphate dehydrogenase: biochemical mechanisms and regulatory control. *Biochim. Biophys. Acta* 1810, 741–751. doi: 10.1016/j.bbagen.2011.05.010

Susič, N., Koutsovoulos, G. D., Riccio, C., Danchin, E. G. J., Blaxter, M. L., Lunt, D. H., et al. (2020). Genome sequence of the root-knot nematode *Meloidogyne luci*. *J. Nematol.* 52, 1–5. doi: 10.21307/jofnem-2020-025

Testard, A., da Silva, D., Ormancey, M., Pichereaux, C., Pouzet, C., Jauneau, A., et al. (2016). Calcium and nitric oxide-dependent nuclear accumulation of cytosolic glyceraldehyde-3-phosphate dehydrogenase in response to long chain bases in tobacco BY-2 cells. *Plant Cell Physiol.* 57, 2221–2231. doi: 10.1093/pcp/pcw137

Truong, N. M., Nguyen, C.-N., Abad, P., Quentin, M., and Favery, B. (2015). Function of root-knot nematode effectors and their targets in plant parasitism. *Adv. Bot. Res.* 75, 293–324. doi: 10.1016/bs.abr.2014.12.010

van Schie, C. C. N., and Takken, F. L. W. (2014). Susceptibility genes 101: how to be a good host. *Annu. Rev. Phytopathol.* 52, 551–581. doi: 10.1146/annurev-phyto-102313-045854

Vescovi, M., Zaffagnini, M., Festa, M., Trost, P., Lo Schiavo, F., and Costa, A. (2013). Nuclear accumulation of cytosolic glyceraldehyde-3-phosphate dehydrogenase in cadmium-stressed arabidopsis roots. *Plant Physiol.* 162, 333–346. doi: 10.1104/pp.113.215194

Vieira, P., and Gleason, C. (2019). Plant-parasitic nematode effectors—insights into their diversity and new tools for their identification. *Curr. Opin. Plant Biol.* 50, 37–43. doi: 10.1016/j.pbi.2019.02.007

Vollmer, A. C., and Bark, S. J. (2018). Twenty-five years of investigating the universal stress protein: function, structure, and applications. *Adv. Appl. Microbiol.* 102, 1–36. doi: 10.1016/bs.aambs.2017.10.001

Wang, X. R., Moreno, Y. A., Wu, H. R., Ma, C., Li, Y. F., Zhang, J. A., et al. (2012). Proteomic profiles of soluble proteins from the esophageal gland in female Meloidogyne incognita. *Int. J. Parasitol.* 42, 1177–1183. doi: 10.1016/j.ijpara.2012.10.008

Wawer, I., Bucholc, M., Astier, J., Anielsaa-Mazur, A., Dahan, J., Kulik, A., et al. (2010). Regulation of *Nicotiana tabacum* osmotic stress-activated protein kinase and its cellular partner GAPDH by nitric oxide in response to salinity. *Biochem. J.* 429, 73–83. doi: 10.1042/BJ20100492

Yamaguchi, Y. L., Suzuki, R., Cabrera, J., Nakagami, S., Sagara, T., Ejima, C., et al. (2017). Root-knot and cyst nematodes activate procambium-associated genes in Arabidopsis roots. *Front. Plant Sci.* 8:1195. doi: 10.3389/fpls.2017.01195

Zaffagnini, M., Fermani, S., Costa, A., Lemaire, S. D., and Trost, P. (2013). Plant cytoplasmic GAPDH: redox post-translational modifications and moonlighting properties. *Front. Plant Sci.* 4:450. doi: 10.3389/fpls.2013.00450

Zaidi, S. S., Mukhtar, M. S., and Mansoor, S. (2018). Genome editing: targeting susceptibility genes for plant disease resistance. *Trends Biotechnol.* 36, 898–906. doi: 10.1016/j.tibtech.2018.04.005

Zeng, H., Xie, Y., Liu, G., Lin, D., He, C., and Shi, H. (2018). Molecular identification of GAPDHs in cassava highlights the antagonism of MeGAPCs and MeATG8s in plant disease resistance against cassava bacterial blight. *Plant Mol. Biol.* 97, 201–214. doi: 10.1007/s11103-018-0733-x

Zhao, J., Li, L., Liu, Q., Liu, P., Li, S., Yang, D., et al. (2019). A MIF-like effector suppresses plant immunity and facilitates nematode parasitism by interacting with plant annexins. *J. Exp. Bot.* 70, 5943–5958. doi: 10.1093/jxb/erz348

Zhao, J., Mejias, J., Quentin, M., Chen, Y., de Almeida-Engler, J., Mao, Z., et al. (2020). The root-knot nematode effector MiPDI1 targets a stress-associated protein (SAP) to establish disease in Solanaceae and Arabidopsis. *New Phytol.* 228, 1417–1430. doi: 10.1111/nph.16745

Conflict of Interest: The authors declare that the research was conducted in the absence of any commercial or financial relationships that could be construed as a potential conflict of interest.

The handling editor declared a past co-authorship with one of the authors PA.

frontiers in Plant Science

ORIGINAL RESEARCH
published: 16 April 2021
doi: 10.3389/fpls.2021.659322

A Pilot Approach Investigating the Potential of Crop Rotation With Sainfoin to Reduce *Meloidogyne enterolobii* Infection of Maize Under Greenhouse Conditions

Milad Rashidifard[1], Samad Ashrafi[2], Sarina Claassens[1], Torsten Thünen[3†] and Hendrika Fourie[1†]*

[1] Unit for Environmental Sciences and Management, North-West University, Potchefstroom, South Africa, [2] Julius Kühn-Institut, Federal Research Centre for Cultivated Plants, Institute for Epidemiology and Pathogen Diagnostics, Braunschweig, Germany, [3] Julius Kühn-Institut, Federal Research Centre for Cultivated Plants, Institute for Crop and Soil Science, Braunschweig, Germany

OPEN ACCESS

Edited by:
Juan Emilio Palomares-Rius, Institute for Sustainable Agriculture, Consejo Superior de Investigaciones Científicas (CSIC), Spain

Reviewed by:
Pablo Castillo, Institute for Sustainable Agriculture, Spanish National Research Council, Spain
Johan Desaeger, University of Florida, United States
José Castro, Embrapa Semiárido, Brazil

***Correspondence:**
Milad Rashidifard
milad.rashidifard@nwu.ac.za

† These authors share last authorship

Specialty section:
This article was submitted to Plant Pathogen Interactions, a section of the journal Frontiers in Plant Science

Received: 27 January 2021
Accepted: 25 March 2021
Published: 16 April 2021

Citation:
Rashidifard M, Ashrafi S, Claassens S, Thünen T and Fourie H (2021) A Pilot Approach Investigating the Potential of Crop Rotation With Sainfoin to Reduce Meloidogyne enterolobii Infection of Maize Under Greenhouse Conditions. Front. Plant Sci. 12:659322. doi: 10.3389/fpls.2021.659322

Root-knot nematodes (RKNs) are one of the most important plant-parasitic nematodes of cereal crops in sub-Saharan Africa. This study was designed to evaluate the rotation effects of different cultivars of sainfoin (Esparsette, Perly, Taja and Visnovsky), soybean (DM-5953-RSF) and alfalfa (BAR 7) with maize (P-2432-R), on a *Meloidogyne enterolobii* population, compared to monoculture maize. The results showed that sainfoin (Perly and Esparsette) and alfalfa had significantly ($P \leq 0.05$) lower numbers of *M. enterolobii* eggs and second stage juveniles (J2) compared to the monoculture maize in the first experiment. However, in the repeat experiment all treatments had significantly ($P \leq 0.05$) lower numbers of eggs and J2 compared to monoculture maize. Rotation of sainfoin Esparsette/maize resulted in the lowest numbers of eggs and J2 (91 and 202, respectively) in the first and repeat experiments. Rotation of sainfoin Esparsette/maize reduced *M. enterolobii* population density by 81 and 60% in the first and repeat experiments, respectively, followed by alfalfa (54 and 43%, respectively). Ultimately, substantial variation was evident in terms of the efficacy of different sainfoin cultivars with regards to their effect on nematode reduction when used in rotation with maize.

Keywords: crop rotation, maize, management, *Meloidogyne*, *Onobrychis viciifolia*, plant-parasitic nematodes, sainfoin

INTRODUCTION

Due to an increasing human population, more food has to be produced with cereal crops representing the staple food source for human and livestock consumption worldwide (FAO, 2017). Production of cereal crops in Africa, however, declined by 4.6% in 2019 in comparison to 2018 (FAO, 2020) and is a risk to food security in Africa. In South Africa, maize (*Zea mays*) is the most important cereal crop, but production of the crop is adversely affected due to various diseases and pests. Among others, plant-parasitic nematodes (PPNs) represent one of the major limiting biotic factors in maize cropping systems (Fourie et al., 2017; Mc Donald et al., 2017). The most

economically important PPNs in maize production areas in South Africa are root-knot nematodes (*Meloidogyne* spp.) and root lesion nematodes (*Pratylenchus* spp.) (Degenkolb and Vilcinskas, 2016; Mc Donald et al., 2017). High population densities of *Meloidogyne* and/or *Pratylenchus* spp. have been reported recently for maize and other rotation crops (Fourie et al., 2017; Mc Donald et al., 2017). Earlier studies demonstrated that root-knot nematodes parasitism caused up to 60% yield losses to South African maize crops (Riekert and Henshaw, 1998). While *M. incognita* and *M. javanica*, followed by *M. arenaria*, are considered the predominant root-knot nematode species parasitizing local maize crops, *M. enterolobii* has also been discovered in a major maize producing area of the country (Pretorius, 2018). The latter species is known for its higher pathogenicity toward agricultural crops and especially for its virulence since it overcomes resistance in crops that are effective to its counterpart thermophilic species (Kiewnick et al., 2009).

To minimize damages caused by PPNs and increase crop production, combating destructive nematode pests should be considered a priority. Use of chemical nematicides was one of the most effective approaches in nematode management in the last decades (Fernández et al., 2001). Nevertheless, increasing awareness of the toxicity of pesticides (to animals, humans and the environment) and the emergence of resistance against synthetic nematicides (Kishi et al., 1995; Kaplan, 2004) are some of the reasons for the use of more environmentally friendly nematode management strategies. Therefore, to maintain PPN populations under a certain threshold, biological and cultural management strategies would play a major role in the future. In this context, the well-planned use of crop rotation is one of the possible management practices that can reduce the PPN populations in maize-based agriculture systems. However, most of the crops, especially legumes, which are used in rotation with maize in sub-Saharan Africa (SSA) and other parts of the world are parasitized by the same nematode pests of maize (Fourie et al., 2017; Coyne et al., 2018; Dababat and Fourie, 2018). Ultimately, it is crucial to find suitable crops that can be used as a rotation or cover crop in maize-based cropping systems, and that can suppress PPN densities. Sainfoin (*Onobrychis viciifolia*) can be an appropriate alternative, particularly due to its chemical properties, which amongst others include the production of condensed tannins with anthelmintic properties (Novobilský et al., 2013). Sainfoin was used for animal feeding in the past but after the green revolution it was replaced by alfalfa (*Medicago sativa*) especially because of alfalfa's potential to produce higher yields. The yield range of sainfoin is 20–30% lower than that of alfalfa in the long-term, however, in the first cut, sainfoin yields are higher than that of alfalfa (Baldridge and Lohmiller, 1990). Sainfoin is a perennial, non-bloating forage legume, which grows up to 20–90 cm tall. It is highly palatable as a fodder source to ruminants when compared to alfalfa (Hume and Withers, 1985). Sainfoin is tolerant to drought and harsh environmental conditions due to the large and deep root system. A major trait, especially in regard to the topic of this study is that this plant is not subjected to major pests of alfalfa (Kaldy et al., 1979; Lance, 1980). The nematicidal activity of condensed tannins of sainfoin on the gastrointestinal parasitic nematodes of ruminants has been well documented (Novobilský et al., 2013; Mueller-Harvey et al., 2019). Consumption of low or moderate concentrations of condensed tannins is also associated with positive effects e.g., the increase in milk, growth and wool production in herbivore animals (Hoste et al., 2006) and a decrease in greenhouse gas emissions (Mueller-Harvey, 2006).

Both root-knot (*Meloidogyne* spp.) and stem nematodes (*Ditylenchus dipsaci*) have been reported to parasitize sainfoin in the US (Mathre, 1968). Most sainfoin cultivars used in the US, for example, showed high susceptibility when evaluated against *M. hapla* populations (Wofford and Gray, 1987; Wofford et al., 1989). By contrast, another study showed tolerance of sainfoin "Shoshone" to *M. hapla* (Gray et al., 2006b). In the last decades, research on sainfoin from a plant nematology point of view has ceased. Currently no information about the effect of sainfoin on PPN populations when grown in rotation with maize is available. This research aimed to elucidate the effect of four different sainfoin cultivars to *Meloidogyne enterolobii* population densities when used in a glasshouse set-up in a maize-based rotation system and compared the nematode susceptibility of one maize, one soybean (*Glycine max*) (a common rotation crop for maize) and one alfalfa cultivar (a closely-related plant to sainfoin).

MATERIALS AND METHODS

Nematode Material

An original population of *M. enterolobii* was obtained from the Mbombela area where it infected roots of tomato (*Solanum lycopersicon*). A pure population was derived from single egg masses, and used for the experiments after confirmation of its identity using the SCAR-PCR method (Rashidifard et al., 2019b). The nematode was reared on roots of seedlings of the nematode susceptible tomato cultivar of "Moneymaker" (Fourie et al., 2012) and kept in a glasshouse at an ambient temperature range of 19–28°C and a photoperiod of 14L:10D. The main reason why *M. enterolobii* was selected for this study was the concerns raised regarding the widespread occurrence and pathogenicity of this species on various crops in SSA (Collett et al., 2021). Nematode infected tomato plants were uprooted 30 days after egg mass inoculation, and processed for nematode extraction using an adapted NaOCl extraction method (Riekert, 1995). The total numbers of eggs and second-stage juveniles (J2) for inoculation purposes were counted in a water suspension using a De Grisse counting dish (De Grisse, 1963) and Nikon SMZ 1 500 dissection microscope. Aliquots of ±500 eggs and J2 per pot were used to inoculate the plant roots.

Plant Material and Nematode Infection

This experiment was designed to evaluate the rotation of crops in a maize-based cultivation system with the inclusion of sainfoin as a cover crop. The seven treatments (sequences) consisted of the following: monoculture maize (maize/maize), soybean/maize, sainfoin (Visnovsky)/maize, sainfoin (Perly)/maize, sainfoin (Taja)/maize, sainfoin (Esparsette)/maize, alfalfa/maize, and tomato/tomato (positive control). Seeds of these cultivars were obtained from the respective owner companies. The effect of

each plant rotation in terms of the reduction of the population densities of *M. enterolobii* was compared to the treatment of monoculture maize.

One week before the experiment commenced, 0.5-L capacity, white plastic pots were filled with a sandy loamy soil [5.3% clay, 93.6% sand, 1.1% silt, 0.47% organic matter; pH (H_2O) of 7.47)] that has been fumigated with Telone II (a.s. 1,3 dichloropropene @ a dosage rate of 120 l/ha) on June 16, 2020 and was kept under plastic cover in the sun for 3 weeks until 07 July when the first experiment started. The second experiment was conducted on October 07, 2020 using the same batch of soil. For all treatments, pots were sown with four seeds of the respective crop cultivars and maintained in a glasshouse at the temperature range of 20–28 ± 1.6°C and a photoperiod of 14L:10D. Two weeks after germination when the seedlings were at the two-leave stage, they were thinned to contain one seedling per pot and each plant root system was inoculated with ± 500 eggs and J2 of the *in vivo* reared *M. enterolobii* population (1 egg/J2 per cc) as this was reported as damage threshold for *Meloidogyne* (Bowen et al., 2008; Tiwari et al., 2019). Five weeks after nematode inoculation –required time for *M. enterolobii* to have at least one generation (Collett, 2020), all plants were uprooted, the aerial parts and roots cut off into small pieces (2 cm) and incorporated into the soil (4–8 cm deep). One week after the incorporation of the roots and aerial plant parts, all pots were sown with one maize seed, except for those designated to contain tomato, to which seedlings of Moneymaker were replanted. The pots were maintained in the greenhouse for 5 weeks under the same conditions described above for the preceding trial. The plants were watered four times a week or as necessary and each plant was also provided with 50 ml (2 g/L) Starke Ayres Nutrifeed (nitrogen 6.5%; phosphorous 2.7%; potassium 13.0%; calcium 7.0%; magnesium 2.2%; sulfur 7.5%) every second week.

At termination of the experiments, maize plants were removed from the pots and the areal parts discarded after measuring shoot lengths. The root system of each plant was weighed and then rinsed with running tap water. Eggs and J2 of *M. enterolobii* were extracted using the adapted NaOCl method of Riekert (1995) and counted as explained above. The reproduction factor (Rf) [final population (Pf) / initial population (Pi)] of the nematode population was determined for each treatment according to Oostenbrink's reproduction factor (Windham and Williams, 1987). The experiment was repeated once (at a different time interval) using the same protocols (for nematodes, plant material, inoculation, maintenance) and glasshouse conditions as described above for the first study.

Data Analysis

A randomized complete block design (RCBD) with six replicates (one plant per pot; six pots for each treatment) was chosen for the experimental layout for both experiments. Nematode data (eggs and J2 numbers per root system), were log(x) transformed, this also was applied for plant height in the repeat experiment. Data from each experiment was first subjected to an ANOVA (Statistica, Version 13.3) individually. Subsequently, Tukey's HSD Test ($P \leq 0.05$) was conducted to separate the means of the eight treatments of the two experiments. Combined data of both experiments was then subjected to a Factorial Analysis of Variance (ANOVA) (Statistica, Version 13.3) with time (representing the two experiments) as the main factor and treatments as the sub-factor. The effect of different treatments on control of nematode was calculated based on the following formula:

$$\left(\frac{X \times 100}{Y}\right) - 100$$

where "X" is the final number of eggs and J2 and "Y" is the initial nematode population (*ca*. 500 eggs and J2). The graphs showing the results of both experiments independently were generated using GraphPad Prism version 8.02[1].

RESULTS

Plant height, as well as the number of nematode eggs and J2 and the Rf values per root system of each crop cultivar were significantly different ($P \leq 0.05$) among the treatments for both experiments. There were no significant differences for the root mass among the treatments of each experiment. Significant interaction was observed for all parameters for experiment x treatments, showing that the maize plants (treatments) reacted differently with regard to the *M. enterolobii* population densities representing the different crop treatments during the two experiments.

Numbers of Eggs and J2s per Plant

A significant interaction ($P = 0.000$; $F = 21.9$) was observed for the numbers of eggs and J2 of *M. enterolobii* per root system for experiment × treatments (**Supplementary Table 1**) being significantly different ($P \leq 0.05$) for the sainfoin (Taja)/maize rotation and the tomato standard for the two experiments.

The rotation of sainfoin (Esparsette)/maize and soil amendment with the roots and aerial parts of this cultivar resulted in the lowest numbers of *M. enterolobii* eggs and J2 per root system (91 and 202, respectively) in the first and repeat experiments. Among the treatments (excluding tomato), soil amendment and rotation of the sainfoin Taja/maize had the highest number (2581) of eggs and J2 in the first experiment, whilst the monoculture maize showed the highest number of eggs and J2 (1541) in the repeat experiment. In the first experiment two cultivars of sainfoin (Perly and Esparsette), and alfalfa had significantly ($P \leq 0.05$) lower number of eggs and J2 compared to monoculture maize (**Figure 1**). However, in this experiment the results showed that soil amendment and rotation of sainfoin (Taja) with maize increased the nematode population significantly ($P \leq 0.05$). No significant differences ($P \leq 0.05$) were observed when soybean used for soil amendment and rotated with maize compared to monoculture maize in the first experiment. However, the repeat experiment indicated

[1]http://www.graphpad.com

that rotation and amendment of all treatments resulted in significantly ($P \leq 0.05$) lower number of eggs and J2 per root system compared to monoculture maize.

Effect of Rotation on Nematode Population Densities

Results from the first experiment showed that monoculture maize, soybean/maize and sainfoin (Visnovsky and Taja)/maize treatments increased *M. enterolobii* population densities, with Taja/maize having the highest (470%) and monoculture maize the second highest (146%) values (**Figure 2**). Sainfoin Perly, alfalfa and sainfoin Esparsette used for soil amendment and rotated with maize reduced nematode population densities by 7, 54, and 81%, respectively (**Figure 2**). In the repeat experiment monoculture maize had the highest increase (208%) in the *M. enterolobii* density, followed by soybean/maize (27%). Similar to the first experiment, soil amendment and rotation of sainfoin (Esparsette)/maize had the highest reduction (60%) in the nematode population density followed by the alfalfa/maize (43%). In contrast to the first experiment, sainfoin Taja/maize this time increased the nematode population by 19% (**Figure 2**).

Rf Value

There was a significant interaction ($P = 0.00$; $F = 156.8$) for Rf value for experiment x treatment, which was the result of a significant difference ($P \leq 0.05$) for tomato as the positive control in the first (8.7) and repeat (58.8) experiments (**Supplementary Table 1**).

In the first experiment Rf values (excluding for tomato) ranged between 0.1 (sainfoin Esparsette/maize) and 2.4 (monoculture maize) with the former being significantly ($P \leq 0.05$) lower, and sainfoin (Taja)/maize (5.7) significantly ($P \leq 0.05$) higher than monoculture maize (**Figure 3**). In the repeat experiment Rf values ranged between 0.4 (sainfoin Esparsette/maize) and 3 (monoculture maize). In this experiment, all treatments had significantly ($P \leq 0.05$) lower Rf values in comparison with monoculture maize (**Figure 3**).

Plant Height

A significant interaction ($P = 0.004$; $F = 3.53$) for plant height for experiment x treatments was observed that can be ascribed by the significant difference ($P \leq 0.05$) recorded for

FIGURE 1 | Population densities of *Meloidogyne enterolobii* in roots of maize, 12 weeks post-inoculation with ± 500 eggs and second-stage juveniles and incorporation of aerial material of previously grown maize (P-2432-R), soybean (DM-5953-RSF), sainfoin (Esparsette, Taja, Perly, Visnovsky), and alfalfa (BAR 7) into the soiland rotation thereof. The *y*-axis shows the log(x) transformed data. Different letters indicate significant differences at $P \leq 0.05$ based on Tukey's test for each experiment separately.

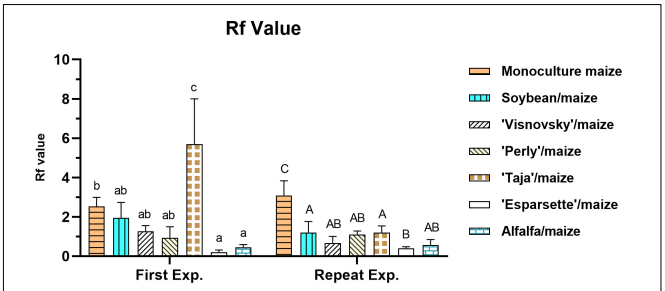

FIGURE 3 | Reproduction factor (Rf) value of a *Meloidogyne enterolobii* population on maize, 12 weeks post-inoculation with ± 500 eggs and second-stage juveniles, and incorporation of aerial material of maize (P-2432-R), soybean (DM-5953-RSF), sainfoin (Esparsette, Taja, Perly, Visnovsky), and alfalfa (BAR 7) into the soil and rotation thereof. The *y*-axis shows Rf value. Different letters indicate significant differences at $P \leq 0.05$ based on Tukey's test for each experiment separately.

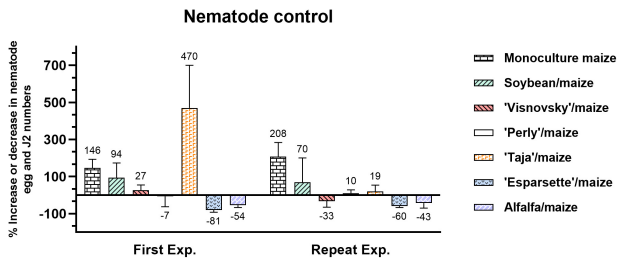

FIGURE 2 | Variable *Meloidogyne enterolobii* density levels in roots of maize 12 weeks post-inoculation with ± 500 eggs and second-stage juveniles, and incorporation of aerial material of previously grown maize (P-2432-R), soybean (DM-5953-RSF), sainfoin (Esparsette, Taja, Perly, Visnovsky), and alfalfa (BAR 7) into the soil and rotation thereof of. The *y*-axis shows the percentage among which positive numbers show increase and negative numbers indicate reduction in nematode population.

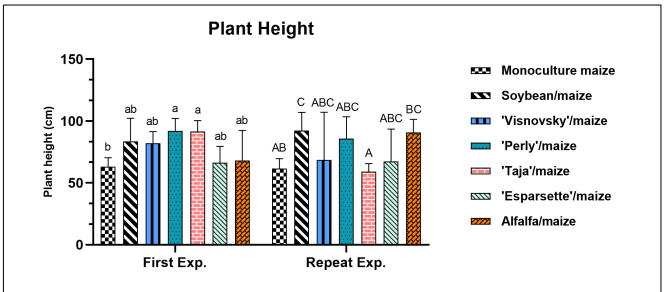

FIGURE 4 | Plant height (cm) of maize plants, 12 weeks post-inoculation with ± 500 eggs and second-stage juveniles of *Meloidogyne enterolobii*, and incorporation of aerial material of maize (P-2432-R), soybean (DM-5953-RSF), sainfoin (Esparsette, Taja, Perly, Visnovsky), and alfalfa (BAR 7) into the soil and rotation thereof. The *y*-axis shows plant height value (cm). Different letters indicate significant differences at $P \leq 0.05$ based on Tukey's test for each experiment separately.

sainfoin (Taja)/maize 91.5 and 59 cm during the first and repeat experiments, respectively (**Supplementary Table 2**).

In the first experiment the plant height ranged from 63 cm (monoculture maize) to 92.1 cm (sainfoin Perly/maize). There were significant differences ($P \leq 0.05$) between treatments in the first experiment, with soil amendment and rotation of sainfoin (Perly and Taja)/maize being significantly ($P \leq 0.05$) taller than monoculture maize (**Figure 4**). Plant height values ranged between 56.1 cm (sainfoin Esparsette/maize) to 92.2 cm (soybean/maize) in the repeat experiment, with soybean/maize being significantly higher ($P \leq 0.05$) than monoculture maize (**Figure 4**).

Root Mass

A significant interaction ($P = 0.16$; $F = 6.045$) for root weight for experiment × treatments was observed due to the significant differences ($P \leq 0.05$) in root weight of the sainfoin: Taja/maize for the two experiments (**Supplementary Table 2**). No significant differences, however, existed among the treatments for the root weight in the first or repeat experiment (**Supplementary Table 2**). The root mass weight ranged between 16.8 g (sainfoin Taja/maize) to 21 g (soybean/maize and sainfoin (Esparsette)/maize) in the first experiment. In the repeat experiment, it ranged between 14.6 g (sainfoin Perly/maize) and 21.3 g (monoculture maize) and there was no significant difference ($P \leq 0.05$) between different treatments (**Figure 5**).

DISCUSSION

In this study we observed significant reductions (compared to the initial/inoculated nematode population) of 81 and 60% of *M. enterolobii* population densities in the first and repeat experiments, respectively, when sainfoin cultivar Esparsette was rotated with maize and incorporated into the soil. This result highlights the positive role sainfoin can potentially play in grain-based sequences to minimize damage caused by *M. enterolobii*. Substantial reductions of 54 and 43% of *M. enterolobii* population densities (in the first and repeat experiments, respectively) when using the nematode resistant alfalfa cultivar BAR 7 in rotation with maize, further emphasizes the beneficial impact of using sainfoin for nematode control in cropping sequences. For sainfoin cultivar Taja contradicting results were observed with regard to the final *M. enterolobii* densities between the first and repeat experiment. Possible explanations that compromised these results could be that the inoculation effectivity in terms of numbers (although the same inoculation protocol was followed and the same *M. enterolobii* population was used) and/or hatching rate of J2 varied between the two experiments, and/or that potential differences in root growth of Taja existed in the respective experiments. These results, however, accentuated that growing Taja may lead to increased population densities of *M. enterolobii*. Similar experiences were recorded by Rashidifard et al. (2019a) and Agenbag (2016) in terms of differences recorded for root-knot final nematode population densities for initial and repeat experiments conducted with tomato.

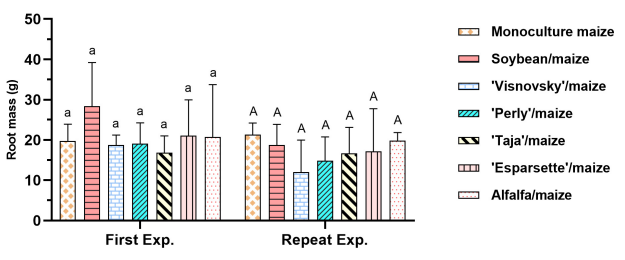

FIGURE 5 | Root mass (g) of maize plants, 12 weeks post-inoculation with ± 500 eggs and second-stage juveniles of *Meloidogyne enterolobii*, and incorporation of aerial material of maize (P-2432-R), soybean (DM-5953-RSF), sainfoin (Esparsette, Taja, Perly, Visnovsky), and alfalfa (BAR 7) into the soil and rotation thereof. The *y*-axis shows plant weight (g). Different letters indicate significant differences at $P \leq 0.05$ based on Tukey's test for each experiment separately.

The significant inhibiting effects of sainfoin cultivar Esparsette on *M. enterolobii* population densities suggests that it can be a potential alternative for alfalfa cultivar BAR 7 (reported as resistant to pest and disease)[2] in areas where alfalfa pests, such as *Sitona* weevils, are a serious concern. In addition, it is important to take other advantages of sainfoin into consideration. Sainfoin was reported to be resistant to various pests that feed on alfalfa (Wallace, 1969; Lance, 1980). The condensed tannin present in sainfoin were reported to have non-bloating and anthelmintic effects (Novobilský et al., 2013).

The significantly lower numbers of *M. enterolobii* eggs and J2s on maize rotated with sainfoin cultivars Perly and Esparsette, and alfalfa (BAR 7) in the first experiment (compared to monoculture maize) opposed to similar population densities on maize rotated with soybean, demonstrate the potential use of these fodders as an alternative in traditional grain-based cropping systems. The high susceptibility of soybean to the same nematode pests that parasitize maize poses problems in SSA (Fourie et al., 2017) and other regions (Coyne et al., 2018; Dababat and Fourie, 2018) and could compromise the sustainable production of grain crops (Riekert and Henshaw, 1998; Miller et al., 2006).

The low Rf data obtained in both experiments, revealed that sequences with sainfoin cultivar Esparsette and alfalfa cultivar BAR 7 may be resistant to *M. enterolobii*. This should, however, be verified in host status experiments since this study was only investigating cropping sequences of the selected crops.

The current study showed high variation among sainfoin cultivars in terms of their effectiveness in reducing root-knot nematode population density levels when used in a crop rotation system. Additionally, the inhibiting effects of sainfoin on *M. enterolobii* recorded in our study were in contrast with previous reports that showed high susceptibility of sainfoin to *M. hapla* (Griffin, 1971; Wofford and Gray, 1987; Shigaki et al., 2008). This could be attributed to the high genetic diversity that was reported among different sainfoin cultivars (Mohajer et al., 2013; Zarrabian et al., 2013). It is speculated that the incorporation of leaves of sainfoin into soil substrate would result

[2]https://www.barenbrug.co.za/forage/products/lucerne/bar-7.htm

in the release of condensed tannins. The released tannins might then play a role in suppression of *M. enterolobii* in soil or in the plant tissues where this nematode pest feeds. Further studies will be needed to analyze the impact of condensed tannins in control of PPNs.

The value of a crop rotation and soil amendment with soybean, sainfoin and alfalfa reflected by maize height data was greater than monoculture maize in both experiments. This is a common phenomenon when crop rotation with legumes is practiced and it is in agreement with previous reports (Tanimu et al., 2007). High numbers of *M. enterolobii* population densities did not show a negative effect on plant height, showing that this cannot be used as an indication for nematode damage in these kind of experiments.

The root mass value for both experiments showed no significant differences among the treatments which is agreed with the results reported from a local study (Rashidifard et al., 2019a) and warrants no further discussion.

Besides this study, there has been only one report regarding a tolerant cultivar of sainfoin (Gray et al., 2006a), "Shoshone," identified as tolerant to *M. hapla*. Other sainfoin cultivars that have been tested for their host status against *M. hapla* and *Ditylenchus destructor*, showed high susceptibility to these nematodes (Wofford and Gray, 1987; Wofford et al., 1989; Shigaki et al., 2008). Reporting the beneficial effects of sainfoin cultivar Esparsette, which is the only available cultivar in South Africa, is a novel addition to the limited, existing research on this crop. The fact that this cultivar was tested against *M. enterolobii*, known as an emerging threat for agriculture production and food security in SSA (Coyne et al., 2018; Visagie et al., 2018; Rashidifard et al., 2019b; Bello et al., 2020; Collett et al., 2021) could be an advantage for producers and crop industries.

CONCLUSION

In this paper, we showed that introducing sainfoin in a crop rotation system is a novel nematode management strategy with potential to be used by producers across the globe. Especially, sainfoin cultivar Esparsette showed a high efficacy in nematode reduction, making it a promising candidate to be used in rotation with maize and as cover crop for soil amendment in SSA where PPNs are a serious concern. More studies need to be conducted to elucidate the host status of different sainfoin cultivars against *Meloidogyne* and other economically important PPNs such as *Pratylenchus* species, with the role that condensed tannins play in this regard to be emphasized.

DATA AVAILABILITY STATEMENT

The original contributions presented in the study are included in the article/**Supplementary Material**, further inquiries can be directed to the corresponding author/s.

AUTHOR CONTRIBUTIONS

MR and SA developed the project and designed the experiments and drafted the manuscript. MR executed the experiments, collected, analyzed, and interpreted the data. SC, TT, and HF contributed to the design of the work. All authors reviewed and edited the manuscript.

FUNDING

Partial funding by the North-West University of South Africa and open access publication fees from the Julius Kühn-Institut, Federal Research Centre for Cultivated Plants, Germany are acknowledged.

SUPPLEMENTARY MATERIAL

The Supplementary Material for this article can be found online at: https://www.frontiersin.org/articles/10.3389/fpls.2021.659322/full#supplementary-material

REFERENCES

Agenbag, M. (2016). *Identification and Reproduction Potential of South African Meloidogyne species*. Master thesis, North-West Universit, Potchefstroom.

Baldridge, D. E., and Lohmiller, R. (1990). *Montana interagency Plant maTerials Handbook for Forage Production, Conservation, Reclamation, and Wildlife*. Bozeman: Montana State University, Extension Service.

Bello, T. T., Coyne, D. L., Rashidifard, M., and Fourie, H. (2020). Abundance and diversity of plant-parasitic nematodes associated with watermelon in Nigeria, with focus on *Meloidogyne* spp. *Nematology* 22, 781–797. doi: 10.1163/15685411-00003340

Bowen, K. L., Hagan, A. K., Campbell, H. L., and Nightengale, S. (2008). Effect of southern Root-knot nematode (*Meloidogyne incognita* race 3) on corn yield in Alabama. *Plant Health Prog.* 9, 1–9. doi: 10.1094/PHP-2008-0910-01-RS

Collett, R. L. (2020). *A comparative Study of the Development and Reproduction of 388 Meloidogyne Enterolobii and Other Thermophilic South African Meloidogyne species*. Master thesis, North-West University, Potchefstroom, 389.

Collett, R. L., Marais, M., Daneel, M. S., Rashidifard, M., and Fourie, H. (2021). *Meloidogyne enterolobii*, a threat to crop production with particular reference to sub-Saharan Africa: a critical and updated review. *Nematology* 23, 247–285. doi: 10.1163/15685411-bja10076

Coyne, D. L., Cortada, L., Dalzell, J. J., Claudius-Cole, A. O., Haukeland, S., Luambano, N., et al. (2018). Plant-parasitic nematodes and food security in Sub-Saharan Africa. *Annu. Rev. Phytopathol.* 56, 381–403. doi: 10.1146/annurev-phyto-080417-045833

Dababat, A. A., and Fourie, H. (2018). "Nematode parasites of cereals," in *Plant Parasitic Nematodes in Subtropical and Tropical Agriculture*, 3rd Edn, eds R. Sikora, D. Coyne, and J. Hallmann (Wallingford: CAB International), 163–221. doi: 10.1079/9781786391247.0163

De Grisse, A. (1963). A counting dish for nematodes excluding border effect. *Nematologica* 9, 162–162. doi: 10.1163/187529263x00313

Degenkolb, T., and Vilcinskas, A. (2016). Metabolites from nematophagous fungi and nematicidal natural products from fungi as an alternative for biological control. Part I: metabolites from nematophagous ascomycetes. *Appl. Microbiol. Biotechnol.* 100, 3799–3812. doi: 10.1007/s00253-015-7233-6

FAO (2017). *The Future of Food and Agriculture – Trends and Challenges*. Rome: FAO.

FAO (2020). *Crop Prospects and Food Situation* – Quarterly Global Report No. 1. Rome: FAO.

Fernández, C., Rodrıguez-Kábana, R., Warrior, P., and Kloepper, J. W. (2001). Induced soil suppressiveness to a root-knot nematode species by a nematicide. *Biol. Control* 22, 103–114. doi: 10.1006/bcon.2001.0961

Fourie, H., Mc Donald, A. H., Steenkamp, S., and De Waele, D. (2017). "Nematode pests of leguminous and oilseed crops," in *Nematology in South Africa: a view from the 21st Century*, eds H. Fourie, V. W. Spaull, R. K. Jones, M. S. Daneel, and D. De Waele (Cham: Springer International Publishing), 201–230. doi: 10.1007/978-3-319-44210-5_9

Fourie, H., Mothata, T., Ntidi, K. N., Mc Donald, A. H., and De Waele, D. G. M. A. (2012). Indications of variation in host suitability to root knot nematode populations in commercial tomato varieties. *Afr. J. Agric. Res.* 7, 2344–2355. doi: 10.5897/AJAR11.706

Gray, F. A., Koch, D. W., Delaney, R. H., and Gray, A. M. (2006b). Development and release of shoshone sainfoin (*Onobrychus viciifolia*) with some tolerance to the northern root knot nematode. *Phytopathology* 96:168.

Gray, F., Shigaki, T., Koch, D., Delaney, R., Hruby, F., Gray, A., et al. (2006a). Registration of 'Shoshone'sainfoin. *Crop Sci.* 46, 988–988. doi: 10.2135/cropsci2005.07-0190

Griffin, G. (1971). Susceptibility of common sainfoin to *Meloidogyne hapla*. *Plant Dis. Rep.* 55, 1069–1072.

Hoste, H., Jackson, F., Athanasiadou, S., Thamsborg, S. M., and Hoskin, S. O. (2006). The effects of tannin-rich plants on parasitic nematodes in ruminants. *Trends Parasitol.* 22, 253–261. doi: 10.1016/j.pt.2006.04.004

Hume, L., and Withers, N. (1985). Nitrogen fixation in sainfoin (*Onobrychis viciifolia*) 1. Responses to changes in nitrogen nutrition. *New Zeal. J. Agric. Res.* 28, 325–335. doi: 10.1080/00288233.1985.10430435

Kaldy, M., Hanna, M., and Smoliak, S. (1979). Amino acid composition of sainfoin forage. *Grass Forage Sci.* 34, 145–148. doi: 10.1111/j.1365-2494.1979.tb01459.x

Kaplan, R. M. (2004). Drug resistance in nematodes of veterinary importance: a status report. *Trends Parasitol.* 20, 477–481. doi: 10.1016/j.pt.2004.08.001

Kiewnick, S., Dessimoz, M., and Franck, L. (2009). Effects of the Mi-1 and the N root-knot nematode-resistance gene on infection and reproduction of *Meloidogyne enterolobii* on tomato and pepper cultivars. *J. Nematol.* 41, 134–139.

Kishi, M., Hirschhorn, N., Djajadisastra, M., Satterlee, L. N., Strowman, S., and Dilts, R. (1995). Relationship of pesticide spraying to signs and symptoms in Indonesian farmers. *Scand. J. Work Environ. Health* 21, 124–133. doi: 10.5271/sjweh.19

Lance, R. (1980). Breeding lucernes that resist aphids. *Rural Res. CSIRO* 106, 22–27.

Mathre, D. (1968). "Disease in sainfoin," in *Proceedings of the Sainfoin Symposium*, eds C. S. Cooper and A. E. Carleton (Montana: Montana Agricultural Experiment Station Publications), 65–66.

Mc Donald, A. H., De Waele, D., and Fourie, H. (2017). "Nematode pests of maize and other cereal crops," in *Nematology in South Africa: a View from the 21st Century*, eds H. Fourie, V. W. Spaull, R. K. Jones, M. S. Daneel, and D. De Waele (Cham: Springer International Publishing), 183–199. doi: 10.1007/978-3-319-44210-5_8

Miller, D., Chen, S., Porter, P., Johnson, G., Wyse, D., Stetina, S., et al. (2006). Rotation crop evaluation for management of the soybean cyst nematode in Minnesota. *Agron. J.* 98, 569–578. doi: 10.2134/agronj2005.0185

Mohajer, S., Jafari, A. A., Taha, R. M., Yaacob, J. S., and Saleh, A. (2013). Genetic diversity analysis of agro-morphological and quality traits in populations of sainfoin (*Onobrychis sativa*). *Austr. J. Crop Sci.* 7, 1024–1031.

Mueller-Harvey, I. (2006). Unravelling the conundrum of tannins in animal nutrition and health. *J. Sci. Food Agric.* 86, 2010–2037. doi: 10.1002/jsfa.2577

Mueller-Harvey, I., Bee, G., Dohme-Meier, F., Hoste, H., Karonen, M., Kölliker, R., et al. (2019). Benefits of condensed tannins in forage legumes fed to ruminants: importance of structure, concentration, and diet composition. *Crop Sci.* 59, 861–885. doi: 10.2135/cropsci2017.06.0369

Novobilský, A., Stringano, E., Carbonero, C. H., Smith, L., Enemark, H. L., Mueller-Harvey, I., et al. (2013). In vitro effects of extracts and purified tannins of sainfoin (Onobrychis viciifolia) against two cattle nematodes. *Veter. Parasitol.* 196, 532–537. doi: 10.1016/j.vetpar.2013.03.024

Pretorius, M. (2018). *The Abundance, Identity and Population Dynamics of Meloidogyne spp. Associated with Maize in South Africa*. Master thesis, North-West University, Potchefstroom.

Rashidifard, M., Marais, M., Daneel, M. S., and Fourie, H. (2019a). Reproductive potential of South African thermophilic *Meloidogyne* populations, with special reference to *Meloidogyne enterolobii*. *Nematology* 21, 913–921. doi: 10.1163/15685411-00003263

Rashidifard, M., Marais, M., Daneel, M. S., Mienie, C. M. S., and Fourie, H. (2019b). Molecular characterisation of *Meloidogyne enterolobii* and other *Meloidogyne* spp. from South Africa. *Trop. Plant Pathol.* 44, 213–224. doi: 10.1007/s40858-019-00281-4

Riekert, H. (1995). A modified sodium hypochlorite technique for the extraction of root-knot nematode eggs and larvae from maize root samples. *Afr. Plant Protect.* 1, 41–43.

Riekert, H., and Henshaw, G. (1998). Effect of soybean, cowpea and groundnut rotations on root-knot nematode build-up and infestation of dryland maize. *Afr. Crop Sci. J.* 6, 377–383.

Shigaki, T., Gray, F. A., Delaney, R. H., and Koch, D. W. (2008). Evaluation of host resistance and intercropping for management of the northern root-knot nematode in sainfoin, *Onobrychis viciifolia*. *J. Sustain. Agric.* 12, 23–39. doi: 10.1300/J064v12n01_04

Tanimu, J., Iwuafor, E., Odunze, A., and Tian, G. (2007). Effect of incorporation of leguminous cover crops on yield and yield components of maize. *World J. Agric. Sci.* 3, 243–249.

Tiwari, S., Eisenback, J. D., and Youngman, R. R. (2019). *Root-knot Nematode in Field Corn*. Petersburg, VA: Virginia Cooperative Extension, Virginia Tech, Virginia State University.

Visagie, M., Mienie, C. M., Marais, M., Daneel, M., Karssen, G., and Fourie, H. (2018). Identification of *Meloidogyne* spp. associated with agri-and horticultural crops in South Africa. *Nematology* 20, 397–401. doi: 10.1163/15685411-00003160

Wallace, L. (1969). "Current and potential insect problems of sainfoin in America," in *Proceedings of the Sainfoin Symposium*, eds C. S. Cooper and A. E. Carleton (Bozeman: Montana State University).

Windham, G. L., and Williams, W. P. (1987). Host suitability of commercial corn hybrids to *Meloidogyne arenaria* and *M. incognita*. *J. Nematol.* 19, 13–16.

Wofford, D., and Gray, F. (1987). Evaluation of cultivars, experimental lines and plant introduction collection of Sainfoin for resistance to *Meloidogyne hapla* Chitwood. *J. Nematol.* 19, 30–37.

Wofford, D., Gray, F., and Eckert, J. (1989). Pathogenicity of two populations of *Meloidogyne hapla* Chitwood on alfalfa and sainfoin. *J. Nematol.* 21, 87–91.

Zarrabian, M., Majidi, M. M., and Ehtemam, M. H. (2013). Genetic diversity in a worldwide collection of sainfoin using morphological, anatomical, and molecular markers. *Crop Sci.* 53, 2483–2496. doi: 10.2135/cropsci2013.03.0130

Conflict of Interest: The authors declare that the research was conducted in the absence of any commercial or financial relationships that could be construed as a potential conflict of interest.

frontiers in Plant Science

ORIGINAL RESEARCH
published: 30 April 2021
doi: 10.3389/fpls.2021.636663

The Armadillo BTB Protein ABAP1 Is a Crucial Player in DNA Replication and Transcription of Nematode-Induced Galls

*Danila Cabral[1], Helkin Forero Ballesteros[1,2], Bruno Paes de Melo[1,3†], Isabela Tristan Lourenço-Tessutti[1,4†], Kércya Maria Simões de Siqueira[1], Luciana Obicci[1], Maria Fatima Grossi-de-Sa[4], Adriana S. Hemerly[2] and Janice de Almeida Engler[1]**

[1] INRAE, Université Côte d'Azur, CNRS, ISA, Sophia Antipolis, France, [2] Instituto de Bioquímica Médica Leopoldo de Meis, Universidade Federal do Rio de Janeiro, Rio de Janeiro, Brazil, [3] Departamento de Bioquímica e Biologia Molecular, Universidade Federal de Viçosa, Viçosa, Brazil, [4] Laboratório de Interação Molecular Planta-Praga, Embrapa Recursos Genéticos e Biotecnologia, Brasília, Brazil

OPEN ACCESS

Edited by:
Juan Emilio Palomares-Rius, Consejo Superior de Investigaciones Científicas (CSIC), Spain

Reviewed by:
Lucy N. Moleleki, University of Pretoria, South Africa
Francesca De Luca, National Research Council (CNR), Italy

***Correspondence:**
Janice de Almeida Engler
janice.de-almeida@inrae.fr

† These authors have contributed equally to this work

Specialty section:
This article was submitted to Plant Pathogen Interactions, a section of the journal Frontiers in Plant Science

Received: *01 December 2020*
Accepted: *16 February 2021*
Published: *30 April 2021*

Citation:
Cabral D, Forero Ballesteros H, de Melo BP, Lourenço-Tessutti IT, Simões de Siqueira KM, Obicci L, Grossi-de-Sa MF, Hemerly AS and de Almeida Engler J (2021) The Armadillo BTB Protein ABAP1 Is a Crucial Player in DNA Replication and Transcription of Nematode-Induced Galls. Front. Plant Sci. 12:636663. doi: 10.3389/fpls.2021.636663

The biogenesis of root-knot nematode (*Meloidogyne* spp.)-induced galls requires the hyperactivation of the cell cycle with controlled balance of mitotic and endocycle programs to keep its homeostasis. To better understand gall functioning and to develop new control strategies for this pest, it is essential to find out how the plant host cell cycle programs are responding and integrated during the nematode-induced gall formation. This work investigated the spatial localization of a number of gene transcripts involved in the pre-replication complex during DNA replication in galls and report their akin colocation with the cell cycle S-phase regulator Armadillo BTB Arabidopsis Protein 1 (ABAP1). ABAP1 is a negative regulator of pre-replication complex controlling DNA replication of genes involved in control of cell division and proliferation; therefore, its function has been investigated during gall ontogenesis. Functional analysis was performed upon *ABAP1* knockdown and overexpression in *Arabidopsis thaliana*. We detected *ABAP1* promoter activity and localized ABAP1 protein in galls during development, and its overexpression displayed significantly reduced gall sizes containing atypical giant cells. Profuse *ABAP1* expression also impaired gall induction and hindered nematode reproduction. Remarkably, *ABAP1* knockdown likewise negatively affected gall and nematode development, suggesting its involvement in the feeding site homeostasis. Microscopy analysis of cleared and nuclei-stained whole galls revealed that ABAP1 accumulation resulted in aberrant giant cells displaying interconnected nuclei filled with enlarged heterochromatic regions. Also, imbalanced *ABAP1* expression caused changes in expression patterns of genes involved in the cell division control as demonstrated by qRT-PCR. *CDT1a*, *CDT1b*, *CDKA;1*, and *CYCB1;1* mRNA levels were significantly increased in galls upon *ABAP1* overexpression, possibly contributing to the structural changes in galls during nematode infection. Overall, data obtained in galls reinforced the role of *ABAP1* controlling DNA replication and mitosis and, consequently, cell proliferation. *ABAP1* expression might

likely take part of a highly ordered mechanism balancing of cell cycle control to prevent gall expansion. *ABAP1* expression might prevent galls to further expand, limiting excessive mitotic activity. Our data strongly suggest that *ABAP1* as a unique plant gene is an essential component for cell cycle regulation throughout gall development during nematode infection and is required for feeding site homeostasis.

Keywords: ABAP1, *Arabidopsis thaliana,* cell cycle, galls, origin of replication, ROOT-KNOT nematode

INTRODUCTION

Nematode-induced galls in plant roots are unusual tumor-like structures formed as a consequence of vascular tissue cell dedifferentiation and proliferation strongly engaging cell cycle reprogramming. The root-knot nematode (RKN) *Meloidogyne incognita* is an economically important species that must exploit and disturb the plant cell cycle to establish a successful parasitism (de Almeida-Engler et al., 1999). Several functional studies employing the model host *Arabidopsis thaliana* have shown that a number of cell cycle components are required for an effectual nematode infection (reviewed by de Almeida-Engler et al., 2011, 2015; Kyndt et al., 2016; Vieira and de Almeida Engler, 2017). Nematode feeding sites (NFS) are likely induced by nematode secretions and hold giant cells (GCs) used as the only nourishing source for the nematode (Vieira and Gleason, 2019). These giant-feeding cells are surrounded by neighboring cells (NCs) undergoing cycles of asymmetric cell divisions during initial gall genesis and require the activation and balance of mitotic and endocycle phases (de Almeida-Engler et al., 1999; de Almeida Engler and Gheysen, 2013; Vieira et al., 2013).

The eukaryotic cell cycle consists of four sequential phases (G1, S, G2, and M), when DNA is replicated at S phase and equally distributed into two daughter cells at mitosis (M phase) (Van't Hof, 1985). The endocycle is an alternative cell cycle comprising recurrent S phases interceded by a G phase, resulting in an increase in cellular ploidy levels (Breuer et al., 2014). The passage across successive cell cycle phases is controlled by cyclin-dependent kinases (*CDKA;1* in Arabidopsis) that are activated upon binding to regulatory proteins such as mitotic cyclins, and by phosphorylation (Jeffrey et al., 1995; Nigg, 1995; Russo et al., 1996).

DNA replication is a cellular process regulated by the coordinated expression and action of numerous genes and proteins (Bell and Dutta, 2002; Shultz et al., 2007). During S phase, cells are licensed for DNA replication by the activation of the pre-replication complex (pre-RC) (Blow and Dutta, 2005; Brasil et al., 2017). The formation of the pre-RC starts with the sequential binding of ORC (Origin Recognition Complex) proteins to DNA replication origins, followed by the recruitment of additional DNA replication factors, like CDC6, CDT1a, CDT1b, and the minichromosome maintenance complex (MCM) (Bell and Dutta, 2002), culminating with the licensing of DNA for replication (Gutierrez et al., 2002; De Veylder et al., 2003; Machida and Dutta, 2004; Brasil et al., 2017). Plant cells exit the mitotic cycle and switch to the endocycle during differentiation, possibly using a similar DNA replication machinery, but the precise controls are still not clear. Cycles of DNA endoreduplication are likely essential for a number of plant cells to undergo differentiation routes and for proper organ development (Gutierrez, 2005), and this may include organ-like structures such as nematode-induced galls. Functional analyses of Arabidopsis mutant plants demonstrated that lack of pre-RC elements, like the *AtCDT1* homologs, *AtCDC6* and *AtORC2*, and two *AtMCM*s, may affect plant development by disturbing DNA replication, and consequently cell division, as well as the endocycle and heterochromatin structure (Springer et al., 2000; Holding and Springer, 2002; Castellano et al., 2004; Collinge et al., 2004; Dresselhaus et al., 2006).

The Armadillo BTB Arabidopsis Protein 1 (ABAP1) is a negative regulator of DNA replication and transcription that is specifically expressed in G1 and early S phase (Masuda et al., 2008). ABAP1 has been reported to be implicated in balancing cell division rates in leaves by negatively regulating pre-RC activity and DNA replication (Masuda et al., 2008). ABAP1 mechanism of action involves direct binding to members of the pre-RC and also association to transcription factors to negatively regulate the transcription of essential pre-RC genes (Masuda et al., 2008; Brasil et al., 2017). Plants overexpressing *ABAP1* present an overall decrease in cell numbers in leaves, and an opposite effect is observed in plants with downregulated levels of *ABAP1* (Masuda et al., 2008).

Thus, herein, we report for the first time the localization of a number of gall-expressed genes involved in DNA replication and report their akin colocation with the DNA replication inhibitor *ABAP1*. This study permitted us to decipher the function of a unique cell cycle inhibitor gene, *ABAP1*, in nematode-induced galls. Our tailored morphological and nuclear analysis shows that *ABAP1* knockdown resulted in increased mitotic activity in gall cells. Not surprisingly, overexpression of *ABAP1* inhibited gall development leading to less nematode reproduction. Cleared galls under markedly *ABAP1* expression confirmed decreased mitosis in galls brought by the excess of the inhibitory effect of the G1/S phase of the cell cycle. Finally, fluctuations upon down- and upregulation of *ABAP1* affected the expression of pre-RC and cell cycle control genes like *CDT1a*, *CDT1b*, *CYCB1;1*, and *CDKA;1*. *ABAP1* not only might regulate cell divisions in galls by repressing transcription of pre-RC genes or by associating to pre-RC complex apparatus but also might be remarkably affecting the endocycle. Our data further suggest that this unique ABAP1 protein might be an essential component of the cell cycle machinery controlling RKN-induced gall expansion, development and homeostasis.

MATERIALS AND METHODS

Plant Material, Growth Conditions and Nematode Infection

Transgenic *ABAP1pro:GUS, ABAP1* over-expressor line (*ABAP1*^{OE}), and a single T-DNA insertion mutant line with *ABAP1* knocked down expression (*ABAP1/abap1)* have been previously described by Masuda et al. (2008). *A. thaliana* Col-0 and genotype *Landsberg erecta* (LER) were used as the wild-type control of *ABAP1* knockdown (*ABAP1/abap1)* and *ABAP1* over-expressor line (*ABAP1*^{OE}), respectively. Complete *ABAP1* knockout is lethal (Masuda et al., 2008); thus, we used single insertion heterozygote mutant lines (*ABAP1/abap1*). Seeds of Arabidopsis wild-type and transgenic lines were surface sterilized for 10 min in 5% NaOCl, followed by four washes with 95% ethanol and dried overnight. *ABAP1/abap1* line was selected in 50 mg/L kanamycin in germination medium. Plated seeds were kept in a growth chamber with 8-h light/16-h dark photoperiod at 21°C/18°C, respectively. After 4 weeks, Arabidopsis seedlings wild-type and healthy green plantlets of transgenic lines were placed in soil containing 30% of sand and were kept in a growth chamber in with 8-h light/16-h dark photoperiod at 21°C/18°C for growth for approximately 20 days. Each plant was then infected with 300 freshly hatched pre-parasitic stage 2 juvenile nematodes according to de Almeida-Engler et al. (2016).

In situ Hybridization Analyses on Arabidopsis Galls

Galls undergoing high cell cycle activity (7–14 days after nematode inoculation-DAI) of Arabidopsis wild-type (Col-0) were dissected from infected seedlings, fixed in 2% glutaraldehyde, paraffin embedded, and sectioned to 10 μm with a microtome. All *in situ* hybridization stages have been executed essentially as explained by de Almeida Engler et al. (2009). Gene-specific sense and antisense radioactive probes of *CDC6, MCM5, ORC1, ORC2, ORC4, ORC5*, and *ORC6* were generated and hybridized with sectioned galls. *ORC1* AS probe will localize *ORC1a* and *ORC1b* homologs sharing 90% sequence similarity. Also, *CDC6* AS probe will localize *CDC6a* and *CDC6b* homologs. Microscopy slides filled with gall sections were developed, stained with 0.05% toluidine blue, and examined by dark-field optics. For transcript localization of *CDT1a* and *CDT1b* genes, all *in situ* hybridization steps have been executed essentially as explained by de Almeida Engler et al. (2009). Non-radioactive gene-specific sense and antisense probes were also generated for *CDT1a, CDT1b* localization. Hybridization procedure and probe synthesis for both *CDT1* probes was performed as described by de Almeida Engler et al. (2001).

Microcopy Analysis of Promoter Activity and Protein Localization of *ABAP1*

Arabidopsis ABAP1 promoter activity was observed in uninfected roots (UR) and during nematode infection (3, 5, 7, 10, 14, and 21 DAI), and GUS activity was measured as previously described by de Almeida-Engler et al. (1999). GUS assays were performed overnight (12 h). Uninfected roots (UR) and galls of the *ABAP1pro:GUS* line (3, 5, and 10 DAI) were fixed in 2% glutaraldehyde and transferred to the chloral-lactophenol clearing solution (Beeckman and Engler, 1994). Remaining UR and gall samples were embedded in Technovit 7100 (Heraeus Kulzer) as described by the manufacturer and sectioned (3 μm) using standard microtomy. Whole mount and section images were taken with a digital Axiocam (Zeiss) with standard bright-field or dark-field optics.

Immunocytochemical Assay

Galls 14 DAI of Arabidopsis wild-type cv. LER and *ABAP1*^{OE} transgenic line were fixed in 4% formaldehyde in 50 mM Pipes buffer (pH 6.9). Galls and uninfected roots were dehydrated and embedded in butyl-methylmethacrylate essentially as described by Kronenberger et al. (1993) and Vieira et al. (2012). Primary anti-ABAP1 antibody and secondary antibody Alexa 488 goat anti-rabbit IgG (Molecular Probes, Eugene, OR, United States) were diluted 100- and 300-fold, respectively, in blocking solution (1% bovine serum albumin in 50 mM Pipes buffer, pH 6.9, and 0.2% DMSO). As control, primary antibody was omitted in some slides. Samples were then washed twice 15 min in Pipes buffer. A 2-h incubation at 37°C was performed with the secondary antibody. DNA was stained with 1 μg ml^{-1} 4′,6-diamidino-2-phenylindole (Sigma-Aldrich) in water, briefly rinsed, and mounted in glycerol 90%. Samples were observed under a microscope (Axioskop, Zeiss, Jena, Germany) equipped for epifluorescence microscopy, and images were acquired with a digital camera (Axiocam, Zeiss).

Histological Analysis and Nematode Infection Assays

For nematode infection tests and histological analysis, plantlets from Arabidopsis wild-type (cv. Col-0 and LER) and transgenic lines (*ABAP1/abap1* and *ABAP1*^{OE}) germinated in soil were infected with 300 juvenile nematodes (J2) of *M. incognita* per plant (de Almeida-Engler et al., 2016). Plantlets were then kept in a growth chamber (8-h light/16-h darkness) during 6–7 weeks after nematode inoculation. The numbers of galls and egg masses for the two biological repetitions of transgenic lines were recorded and compared to wild-type plants. For morphological analyses of each line, galls were dissected at different time points after inoculation (3, 7, 14, and 21 DAI), were fixed in 2% glutaraldehyde in 50 mM Pipes buffer, pH 6,9, and then dehydrated and embedded in Technovit 7100 (Heraeus Kulzer) as depicted by the manufacturer. Embedded roots and galls were sectioned (3 μm), stained in 0.05% toluidine blue, and mounted in DPX (Sigma-Aldrich). Microscopic examinations were performed under bright-field optics and images were taken with a digital camera (Axiocam, Zeiss). In addition, subsequent gall tissue sections used for histological analysis were stained with 1 μg/ml 4,6-Diamidino-2-phenylindole (DAPI) and mounted in 90% glycerol on a microscope slide and cover-slipped. Nuclear staining was then observed by fluorescence microscopy (Axioplan 2, Zeiss) equipped for epifluorescence.

Measurements of GC Area and Gall Diameter of *ABAP1* Transgenic Lines

Two of the largest GCs per gall section (21 DAI) of the *ABAP1/abap1* and *ABAP1*^{OE} at different time points after nematode infection (7, 14, 21, and 40 DAI) were surface measured using the Axioplan 2 (Zeiss) software. A minimum of 30 GCs and diameter of galls per transgenic line were measured at each time point. Measurements were analyzed by two-way analysis of variance (ANOVA), and significant differences between average values were identified by Tukey–Kramer test using PROC GLM in SAS (version 9.1.3, SAS Institute Inc., Cary, North Carolina).

Nuclei Morphology Analysis of *ABAP1* Lines

ABAP1/abap1, *ABAP1*^{OE}, and wild-type mature galls (21 DAI) were dissected, mounted in 3% agarose (Thermo-Fischer, United States), and sectioned with a vibratome (Microm HM650V) to 80–100 μm. Nuclei of cleared galls were DAPI stained as described by Antonino de Souza Junior et al. (2017) and analyzed by confocal microscopy (Zeiss LSM 880). Samples were mounted in 90% glycerol between two coverslips in order to be able to observe both sides. Stacks were generated from approximately 50 images per sample with approximately 1 μm optical slice thickness. Dye excitation was done with a diode 405-nm laser and fluorescence was collected between 431 and 532 nm.

Ploidy Level Analyses of *ABAP1* Transgenic Lines

Flow cytometry analysis was performed on uninfected roots and galls (21 DAI) of *ABAP1/abap1, ABAP1*^{OE}, and wild-type (cv. Col-0 and LER). Samples were chopped for 2 min with a razor blade in a buffer solution containing 300 μl of 45 mM $MgCl_2$, 30 mM sodium citrate, 20 mM MOPS, pH 7.0, and 0.1% Triton X-100, as previously described by Vieira et al. (2013). Harvested plant material was filtered in a 70-μl mesh and stained in 1 μg/ml of DAPI. The previous steps were performed twice. The ploidy levels were measured with the LSRII Fortessa (BD Biosciences) flow cytometer and the BD FACS Diva software (BD Biosciences). An average of 100,000 nuclei per run was collected for uninfected roots, the fraction of nuclei with ploidy levels from 2C to 16C was expressed as a percentage of the total number of nuclei measured. For gall tissues, a minimum of 30 galls (40 DAI) were extracted and pooled for each independent trial, composed of two technical and two biological repetitions for each line. For galls, ±30,000–100,000 events/run nuclei per run were collected. The mean values of repetitions of independent trials were calculated, and the fraction of nuclei at ploidy levels from 2C to 64C was expressed as a percentage of the total number of nuclei recorded.

Acid Fuchsin Staining of *ABAP1* Transgenic Lines Infected Roots

Acid fuchsin staining was performed in infected roots of *ABAP1/abap1*, *ABAP1*^{OE}, and wild-type seedlings as described by de Almeida-Engler et al. (2016), to track nematode development within the roots. The whole infected roots (40 DAI) were fixed and stained for 5 h in a solution of equal parts of 95% ethanol and glacial acetic acid, containing 17.5 mg/L acid fuchsin. The root tissue and galls were distained by incubating in a solution of chloral hydrate (0.2 g/ml in water) for 16 h. After rinsing the roots several times with tap water, roots containing nematodes were stored in acidified glycerol (five drops of 1.0 M HCl were added to 50 ml of glycerol). Nematode-infected roots were observed with a digital camera (Axiocam; Zeiss).

Quantitative Real-Time PCR (qRT-PCR)

The expression profile of genes involved in DNA replication and cell cycle progression, as well as genes directly regulated by ABAP1, was investigated by qRT-PCR. Total RNA was extracted from isolated galls 14 DAI, using Trizol reagent (Thermo Fisher Scientific) according to the manufacturer's guidelines. The RNA was then treated with RNase-free DNase I (Thermo Fisher Scientific) before reverse transcription. One microgram of treated RNA was used to synthetize the cDNA using a SuperScript III Reverse Transcriptase (Thermo Fisher Scientific) synthesis kit using oligo DT primers. This cDNA (1/20) was then amplified using SYBR Green I PCR Master No Rox (Eurogentec, Angers, France), and amplification of *PCNA1, CDT1a, CDT1b, CYCB1;1, CDKA;1, SOG1, E2Fa*, and *TCP24* genes was performed with each specific primer pair (**Supplementary Table 1**). Relative expression was calculated using the 2-ΔΔCT method with Oxaloacetate and NADPH as constitutive genes. qRT-PCR values are means from three biological replicates.

RESULTS

Transcripts of Representative Pre-RC Genes Are Expressed in Galls

To investigate the replication licensing system in galls, we performed *in situ* hybridization with a number of partners of the pre-RC involved in DNA replication during different phases of feeding site development. At 7 DAI, galls are ongoing intense mitotic activity, whereas at 14 DAI, they entered the endocycle phase. All genes analyzed were expressed in gall cells at varying intensities (*CDC6, MCM5, ORC1, ORC2, ORC3, ORC4, ORC5, ORC6, CDT1a*, and *CDT1b*) (**Figure 1** and **Supplementary Figure 1**). Illustrated images of *MCM5*, *ORC1, ORC4*, and *ORC5* shows apparently stronger hybridization signal at 7 DAI, whereas *ORC2* and *ORC6* showed similar intensities at 7 and 14 DAI in feeding cells. *CDC6* and *ORC4* expression was high in dividing NCs (**Figure 1**). Only *ORC6* showed a quite strong hybridization signal at 14 DAI. Overall results are illustrated in the table in **Figure 1B**, which may slightly differ from images since it reflects observations performed on at least 50 galls. Both *CDT1a* and *CDT1b* were later analyzed by non-radioactive *in situ* hybridization and revealed that both genes were expressed in uninfected root vascular tissue and in galls 7 and 14 DAI. For all experiments, control hybridizations resulted in no signal. Results of hybridizations in uninfected roots have been previously reported and illustrated in de Almeida Engler et al. (2012).

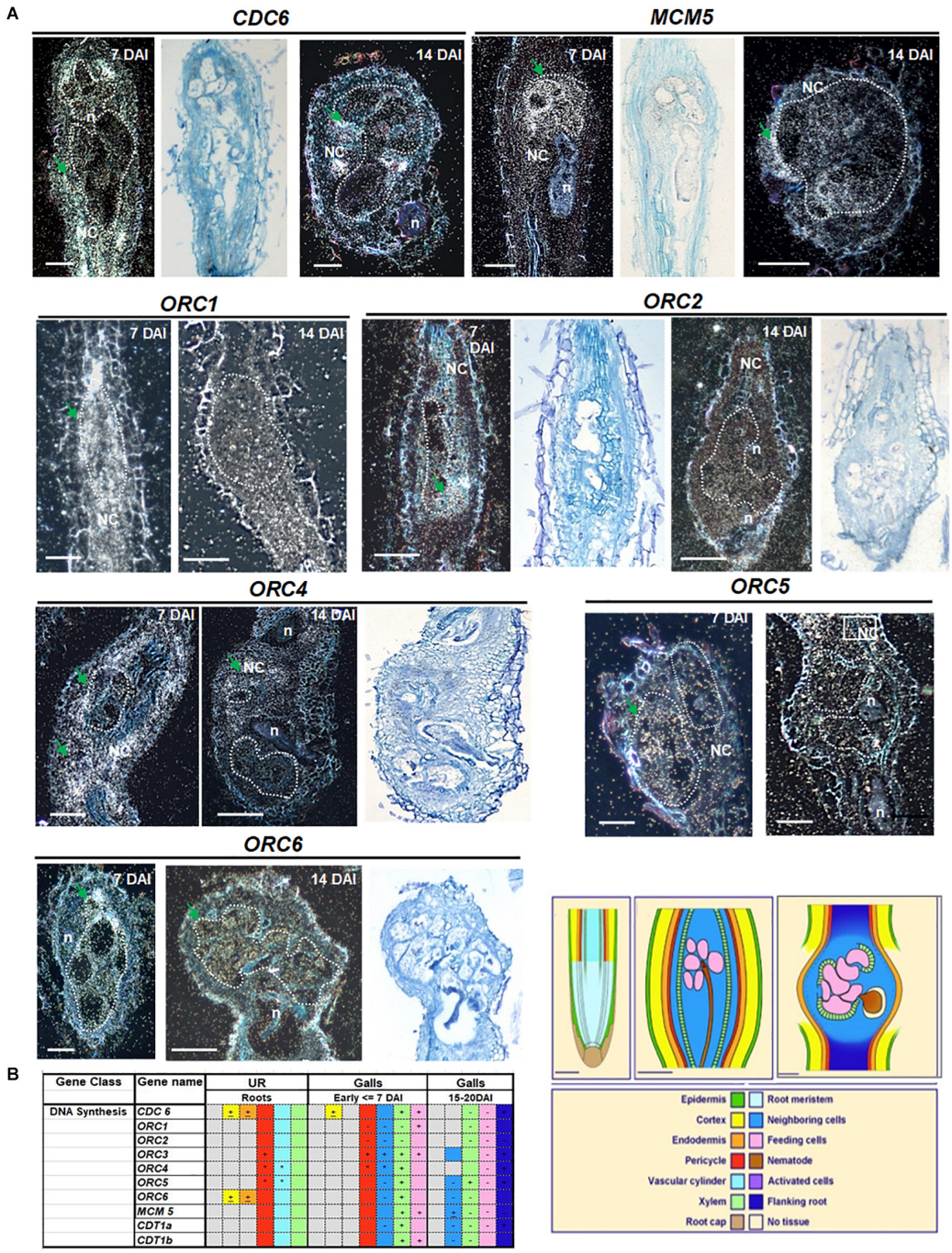

FIGURE 1 | Cell cycle pre-replication complex members: *CDC6, MCM5, ORC1, ORC2, ORC3, ORC4, ORC5*, and *ORC6* localization in *Meloidogyne incognita*-induced galls of Arabidopsis. mRNA *in situ* localization illustrating transcripts of *CDC6, MCM5, ORC1, ORC2, ORC3, ORC4, ORC5*, and *ORC6* in *Meloidogyne incognita*-induced galls in Arabidopsis roots and summarized data in tissue color table. **(A)** Dark- and bright-field images of *CDC6, MCM5, ORC1, ORC2, ORC4, ORC5,* and *ORC6* showing mRNA *in situ* localization in 7 and 14 days after inoculation galls. Sections were hybridized with 35S-labeled antisense (AS) RNA probes and the hybridization signal is shown as white dots under dark-field optics and black dots under bright-field optics. Regions with high silver grain concentrations are depicted with green arrows. Feeding cells are surrounded by dotted lines. **(B)** Table summarizing transcript localization and hybridization intensities of genes analyzed involved in DNA synthesis. Colors in the table and drawings illustrate different tissues of an uninfected root and of young (<7 DAI) and mature galls (15–21 DAI). Patterns described in the table are based on at least 30 sections of each time point. Signs within colored squares represent intensity of signal: +, strong; -, weak; ±, sometimes expressed and *, patchy expression, based on visual recording of silver grain concentration. Colored squares with no sign mean intermediate levels of expression. Gray colors mean no signal, often observed for epidermis and cortical tissues. DAI, days after inoculation; n, nematode; NC, neighboring cells; UR, uninfected root. Scale bars drawings and images = 50 μm.

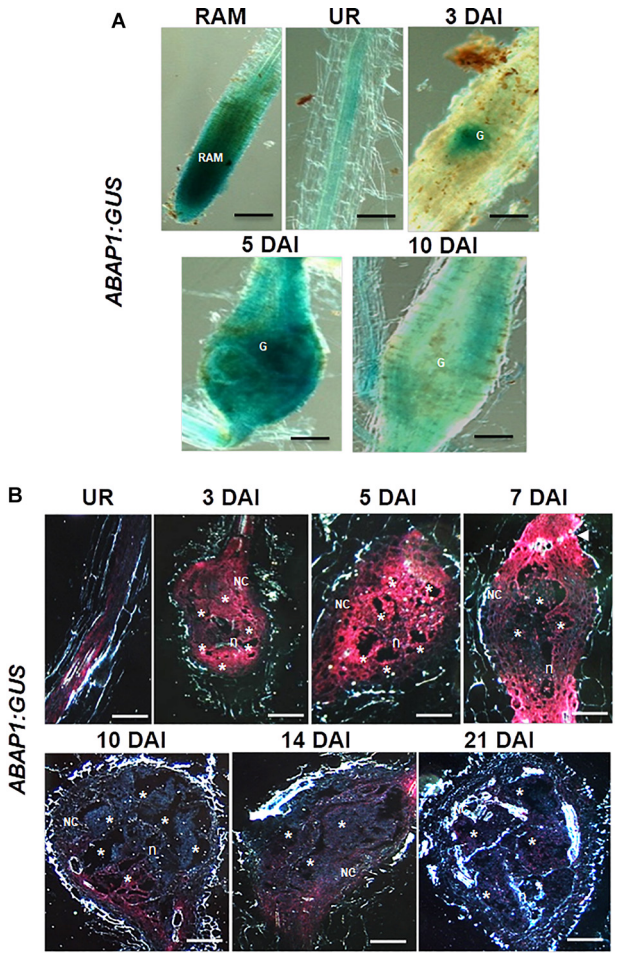

FIGURE 2 | Expression pattern of the *Arabidopsis ABAP1pro:GUS* line in uninfected roots and in *M. incognita*-induced galls. **(A,B)** Illustrate *ABAP1* promoter activity in the root apical meristem (RAM), in an uninfected root (UR) and during gall development (3, 5, 7, 10, 14, and 21 days after inoculation). Bright-field images of whole roots and galls illustrate the GUS staining in blue **(A)** and dark-field images show GUS staining in red **(B)**. G, gall; Asterisk, giant cell; NC, neighboring cells; n, nematode. Scale bars = 50 μm.

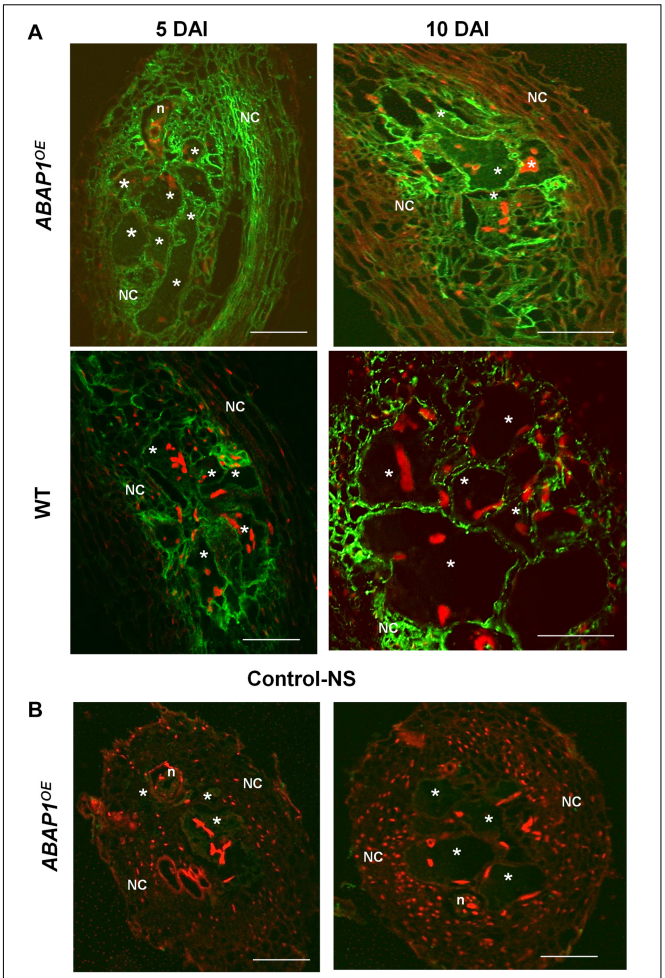

FIGURE 3 | ABAP1 localization in *M. incognita*-induced galls. **(A)** Immunofluorescence of ABAP1 (green) in wild-type and ABAP1^{OE} galls 5 DAI and 10 DAI. **(B)** Images show galls 5 and 10 DAI treated with the normal serum (NS). DAPI-stained nuclei are visualized in red. Asterisk, giant cell; n, nematode, NC, neighboring cells. Scale bars = 50 μm.

ABAP1 Is Expressed in Root-Knot Nematode-Induced Galls

The promoter activity of *ABAP1* was examined by carrying out GUS assays in uninfected roots and in Arabidopsis galls at different stages of development (3, 5, 7, 10, 14, and 21 DAI). *ABAP1* was expressed in the root apical meristem (RAM) and weakly in vascular root tissue of uninfected roots (**Figure 2A**). GUS staining performed on entire galls illustrated an early (3 DAI) and localized induction of *ABAP1* promoter activity, which then spread along all gall cells (5 DAI), correlating with the increased cell cycle activity in galls. Sectioned galls revealed intense GUS staining in GCs and in NCs at 3 and 5 DAI decreasing at 7 DAI as gall matured (**Figures 2A,B**). Expression was then significantly decreased at 10–14 DAI and nearly disappeared at later stages of gall expansion (21 DAI). It was notable that at 10 and 14 DAI, GUS staining was stronger in NCs, which are still proliferating close to the endoreduplicating GCs. The lowered but still present promoter activity in GCs at 7–14 DAI suggests the involvement of ABAP1 expression in the GC endocycle phase. In addition, lowered *ABAP1* expression in NCs after 7 DAI coincides with the decreased mitotic activity in galls at later stages. Interestingly, GUS staining remained strong only in root zones flanking the gall (**Figure 2B** illustrated in gall at 7 DAI). This observation suggests that *ABAP1* expression might be somehow linked to the presence of a neighboring gall.

Immunocytochemical analysis of ABAP1 protein confirmed promoter GUS analysis in galls and revealed a visible fluorescence localized in GCs and NCs within galls during the mitotic stage (5 DAI) decreasing but still present during the endocycle stage (10 DAI; **Figure 3A**). No clear fluorescence was detected in the differentiated cortex or epidermis tissues bordering the galls, which normally do not undergo mitotic activity since later these cells will flop off (**Figure 3A**). Strongest fluorescence was detected

in *ABAP1*^{OE} galls and a weaker pattern was seen in wild-type galls. No fluorescence was detected in *ABAP1*^{OE} galls treated with the normal serum used as a control (**Figure 3B**).

ABAP1 Knockdown Expression in Arabidopsis Reduced the Gall Size and Affected Nematode Development

To address whether *ABAP1* downregulation could disturb gall induction as well as nematode development, we used a single insertion mutant line (*ABAP1/abap1*), considering that full *ABAP1* knockout is lethal (Masuda et al., 2008). A detailed morphological analysis of *ABAP1/abap1* galls illustrated small vacuolated GCs with cell wall stubs during the mitotic phase (7 DAI) and increased NCs proliferation compared to wild-type galls (**Figure 4A**). As galls developed, these remained smaller than wild-type even when the visible increased density of xylem elements was remarked (**Figure 4A**). Gall measurements in infected *ABAP1/abap1* line confirmed their reduced sizes in diameter as well as decreased GC area compared to wild-type (**Figures 4C,D**). Thus, even when a plethora of NCs and xylem divisions are visible, galls are still apparently smaller than in wild-type. To examine whether *ABAP1* knockdown had an influence on nematode development and reproductive ability, infection tests were performed. Although no significant changes in gall numbers was observed among *ABAP1/abap1* and wild-type plants, a significant reduction in egg mass production was observed (**Figure 4E**). Also, nematode development in *ABAP1/abap1* plants showed a clear delay or arrest in maturation (**Figure 4F**). DAPI-stained gall sections 14 DAI in *ABAP1/abap1* revealed small grouped nuclei and extra NCs compared to a wild-type gall (**Figure 4B** and **Supplementary Movies 1, 2**). 3D reconstruction of *ABAP1/abap1* galls cleared and DAPI stained revealed that nuclei were small, clumped, and more circuitous compared to the wild-type and GCs were apparently smaller than wild-type (**Figure 4B**, **Supplementary Movies 1, 2**).

ABAP1 Overexpression Had a Noteworthy Negative Impact in Gall and Nematode Development

The effects on cell proliferation and tissue defects of increased *ABAP1* concentration were obvious during gall ontogeny (5, 7, 10, 14, 21 DAI) as visualized by histological analysis. Seen in longitudinal gall sections, GCs presented irregular forms, were more vacuolated, and illustrated severely reduced division of NCs (**Figure 5A**). Cell wall stubs present in GCs suggested additional mitotic defects than normally observed in wild-type galls. Reduced gall diameter measurements confirmed decreased mitotic activity in ABAP1^{OE} galls. Statistical decrease in gall size was seen mainly during expansion around 21 DAI and remained visibly small until gall fully matured (40 DAI) (**Figure 5B**). The average of GC area in the *ABAP1*^{OE} (after 21 DAI) was also statistically significantly smaller than in wild-type (**Figure 5C**). No statistical differences of GCs of mature galls (40 DAI) were due to the regularly observed two populations of GC sizes within the same galls, named small (*ABAP1*^{OE}*-S)* and large (*ABAP1*^{OE}*-L*) (**Figure 5C**). Two types of GC morphologies were observed in a same feeding site: GCs with smaller areas containing a dense cytoplasm and others containing large vacuoles with increased area (**Figures 5A**, **6**). Acid fuchsin stain allowed us to remark the delayed nematode development in *ABAP1*^{OE} galls in contrast to wild-type infected roots at 7, 14, 21, and 40 DAI (**Figure 5D**). A large fraction of nematodes remained as parasitic second-stage juveniles and were associated with reduced size feeding sites within these transgenic roots (**Figure 5D**). Infection tests revealed an approximately 50% reduction in gall number in the *ABAP1*^{OE} line, followed by a statistically significant reduction in egg mass number compared with infected wild-type control roots (**Figure 5E**).

Increased *ABAP1* Expression Led to Aberrant Nuclear Pattern in GCs

The effect of surplus *ABAP1* expression in the nuclear structure and to a certain level gall morphology was observed in detail by DAPI-stained semi-thin sections and in thick slices by confocal microscopy (**Figures 6**, **7A** and **Supplementary Movie 4**). DAPI-stained gall slices 7, 14, and 21 DAI revealed GCs with variable sizes quite vacuolated and the frequent presence of cell wall stubs, flanked by nuclei in enlarged GCs suggestive of aberrant mitotic activity. Remarkably, nuclei were clustered, apparently displaying irregular shapes, and presented a large number of bright fluorescing condensed chromatin dots. We then performed 3D nuclei reconstruction generating thick slices of *ABAP1*^{OE} galls cleared and DAPI stained to better picture nuclear defects that undeniably became more pronounced as galls matured (**Figure 7A** and **Supplementary Movie 4**). Interconnected nuclei were correlated with the presence of the *ABAP1* overexpression, and this phenotype was not present in wild-type GC nuclei (**Figure 7A**, **Supplementary Movies 3, 4**). Nuclear ploidy levels in uninfected roots did not show significant differences among *ABAP1/abap1*, *ABAP1*^{OE}, and wild-type (**Figure 7B**). The decreased 4C DNA ploidy levels in *ABAP1*^{OE} galls most probably derived from the hindered NC division (**Figure 7C**). Comparable lessened 8C–64C levels in *ABAP1*^{OE} galls, challenged to *ABAP1/abap1* and control wild-type (**Figure 7C**), might be derived from the inhibited mitotic activity ensuing in aberrant apparently connected nuclear phenotypes.

Increased or Decreased Levels of *ABAP1* Affect the Regulation of Cell Cycle Genes Expression in Galls

To extend our knowledge of *ABAP1* function during gall development, mRNA levels of genes involved in DNA replication and cell cycle progression, as well as genes directly regulated by ABAP1, were investigated by qRT-PCR. The following described genes were chosen to be investigated in galls 14 DAI in *ABAP1*^{OE}, *ABAP1/abap1*, and wild-type plants. The TCP24, a class-II TCP transcription factor family, negatively regulates plant cell proliferation and leaf morphogenesis when associated with ABAP1 (Cubas et al., 1999; Nath et al., 2003; Palatnik et al., 2003). *PCNA1* (Proliferating Cell Nuclear Antigen) is an auxiliary protein for DNA polymerase that is highly expressed during the S phase of the cell cycle and is

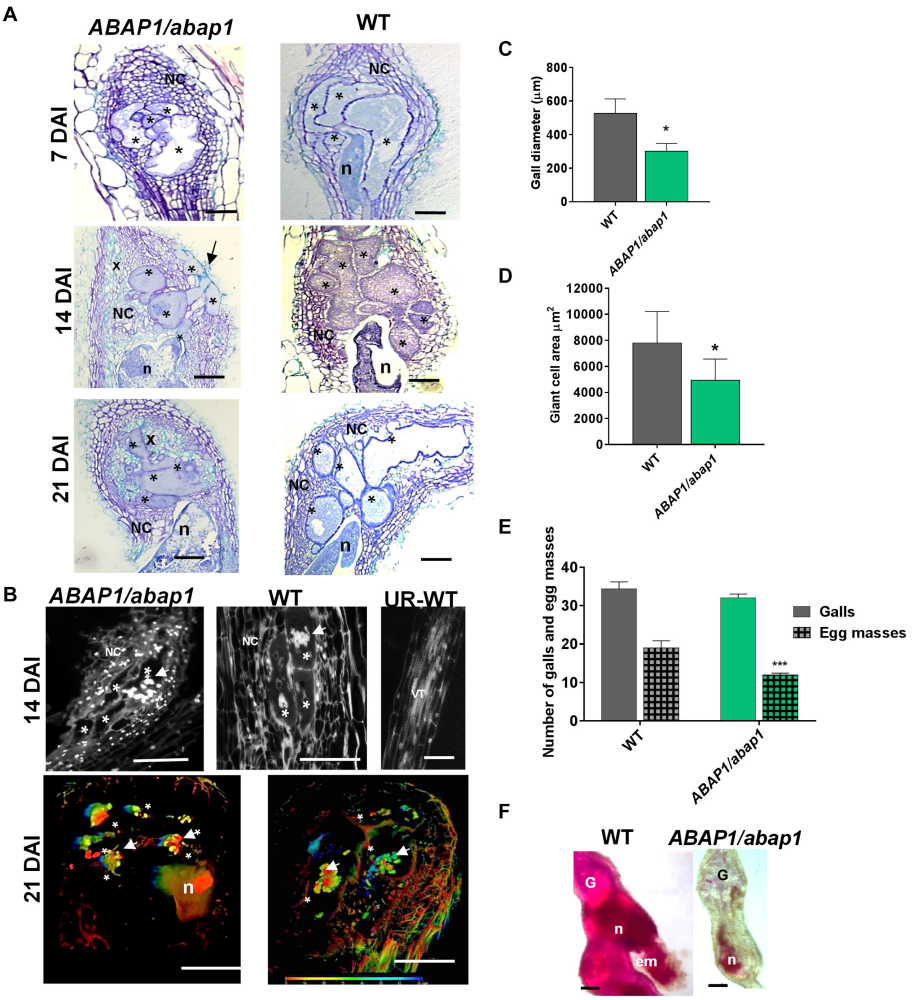

FIGURE 4 | Histological analysis and nuclei morphology of galls, and resistance tests of *ABAP1* knockdown plants infected with *M. incognita*. **(A)** Bright-field images of gall sections of *ABAP1/abap1* and wild-type (7, 14, and 21 DAI) stained with toluidine blue. Note abnormally convoluted giant cells extended to the gall border (arrow 14 DAI) and xylem (x) proliferation (14 and 21 DAI) upon *ABAP1* knockdown. **(B)** Gall 21 DAI and uninfected root sections of *ABAP1/abap1* and wild-type stained with 4,6-diamidino-2-phenylindole (DAPI); and 3D confocal projections of serial optical sections of wild-type (WT) and *ABAP1/abap1* galls 21 DAI nuclei (white arrows), cleared and DAPI stained. Colored bars represent the depth of nuclei within the gall. DAI, days after inoculation; asterisk, giant cell. Bars = 50 µm. **(C)** Gall diameter measurements revealed that *ABAP1/abap1* plants have smaller galls than wild-type. **(D)** Giant cell measurements showed smaller giant cell area in the *ABAP1* knockdown line compared to the wild-type. **(E)** Resistance test of *ABAP1/abap1* line showed a significant reduction of eggs mass number. **(F)** Galls (40 DAI) from these resistance tests were acid fuchsin stained and showed a delay in nematode development under low *ABAP1* levels. Statistical analysis was performed $^{*}P < 0.05$) or $^{***}P < 0.01$ based on Student's *t* -est. Asterisk, giant cell; NC, neighboring cells; n, nematode; x, xylem; G, gall; em, egg mass. Scale bars = 50 µm.

widely used as an index of the proliferative cell activity in cancer tissues and plant cells (Strzalka and Ziemienowicz, 2011; Yokoyama et al., 2016). *CDT1* (Chromatin Licensing and DNA Replication Factor 1) is required for both DNA replication and chromosome segregation, and in mammalian cells, small changes in *CDT1* control can lead to catastrophic consequences for genome stability (Brasil et al., 2017). Moreover, *CDT1a* and *CDT1b* are direct targets of ABAP1 transcription repression in Arabidopsis, being used as a marker of ABAP1 levels and activity (Masuda et al., 2008; Brasil et al., 2017). *CYCB1;1* (Cyclin-B1-1) and *CDKA;1* (Cyclin-dependent kinase A-1) are core proteins driving cell cycle control (De Veylder et al., 1997, 2003; Coudreuse and Nurse, 2010). The transcription factor E2Fa is implicated in cellular proliferation and endocycle stimulation (De Veylder et al., 2002; Magyar et al., 2012). Ultimately, *SOG1* (suppressor of gamma-response 1) is a cell cycle checkpoint control transcription factor that functions downstream of the ATR and ATM pathway and is required for both cell cycle arrest and the induction of DNA repair genes (Yoshiyama et al., 2009). In our qRT-PCR analyses, no significant difference was seen on the mRNA levels of *TCP24* and *PCNA1* among *ABAP1*^{OE}, *ABAP1/abap1*, and wild-type galls, suggesting that minimal concentrations might be enough for replication progression. However, *CDKA;1* expression was significantly repressed in *ABAP1*^{OE} galls, and *CDKA;1* and *CYCB1;1* were induced in *ABAP1/abap1* galls compared to

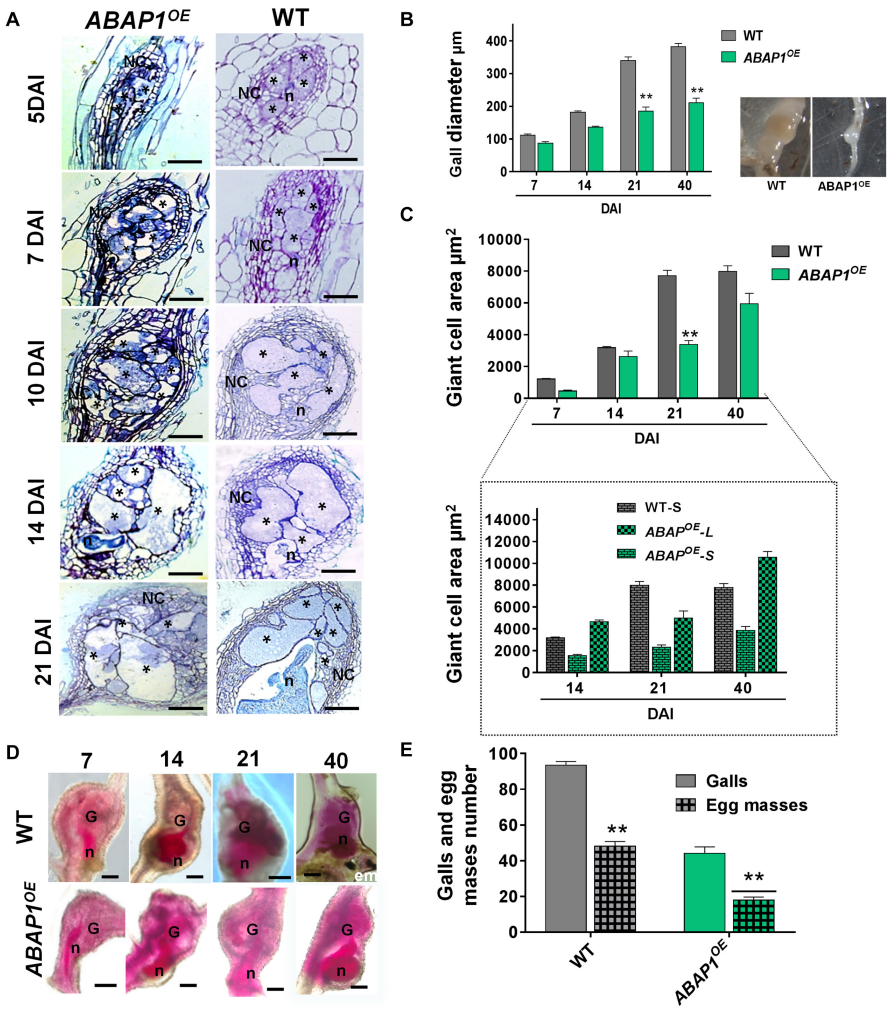

FIGURE 5 | Ectopic *ABAP1* expression affects gall morphology and revealed feeding sites with reduced sizes leading to decreased nematode reproduction. **(A)** Histological analysis of galls overexpressing *ABAP1*^{OE} compared to wild-type (WT) at different stages of nematode infection (5, 7, 10, 14, and 21 DAI). Bright-field micrographs show longitudinal gall sections stained with toluidine blue. **(B,C)** Gall diameter and giant cell area of *ABAP1*^{OE} galls compared with WT. Note that galls from *ABAP1*^{OE} are smaller than WT galls and two sizes categories of giant cells in *ABAP1*^{OE} were observed: small and cytoplasm filled giant cells (*ABAP1*^{OE}-*S*) and large containing large vacuoles (*ABAP1*^{OE}-*L*). **(D)** Acid fuchsin staining of *ABAP1*^{OE} and WT galls at different developmental stages (7, 14, 21, 40 DAI) of nematode development. A visible delay or arrest in nematode development is seen in the *ABAP1*^{OE} line consequently inhibiting and delaying egg mass laying. **(E)** Nematode infection tests of *ABAP1*^{OE} showed a significant decrease in galls and egg masses numbers compared to the WT. Data shown represent means ± SD from two experiments with $n = 20$ plants per line. Statistical differences are marked with $^{*}P < 0.05$) or $^{**}P < 0.01$ based on Student's *t*-test analysis. Asterisk, giant cell; NC, neighboring cells; n, nematode; G, gall; em, egg mass. Scale bars = 50 µm.

wild-type (**Figures 8**, **9**). These data corroborate with a negative regulation of cell divisions in *ABAP1*^{OE} galls and an increase in cell division rates in *ABAP1/abap1* galls. Also, the repression of *CDT1a* expression in *ABAP1*^{OE} galls and higher *CDT1a* and *CDT1b* expression in *ABAP1/abap1* galls illustrated their induced gene expression regulation in galls as targets of *ABAP1* transcription repression (**Figures 8**, **9**). Curiously, *E2Fa* expression levels were repressed in both *ABAP1*^{OE} and *ABAP1/abap1* galls compared to wild-type ones, suggesting that a committed *ABAP1* expression is needed for gall development. In addition, the *SOG1* gene was less expressed in *ABAP1/abap1* galls and did not show difference in *ABAP1*^{OE} galls compared to wild-type galls, suggesting that *ABAP1* fluctuation in gene expression did not induce check point control activation in galls.

DISCUSSION

Throughout development, gall cells hyperactivate and regulate their mitotic cell cycle, later undergoing endoreduplication to allow increased ploidy levels (de Almeida-Engler et al., 2015) as described for plant cells (Sugimoto-Shirasu and Roberts, 2003). Aiming to understand DNA replication control through the gall cell cycle, we primarily investigated the expression of representative pre-RC genes that license DNA for replication.

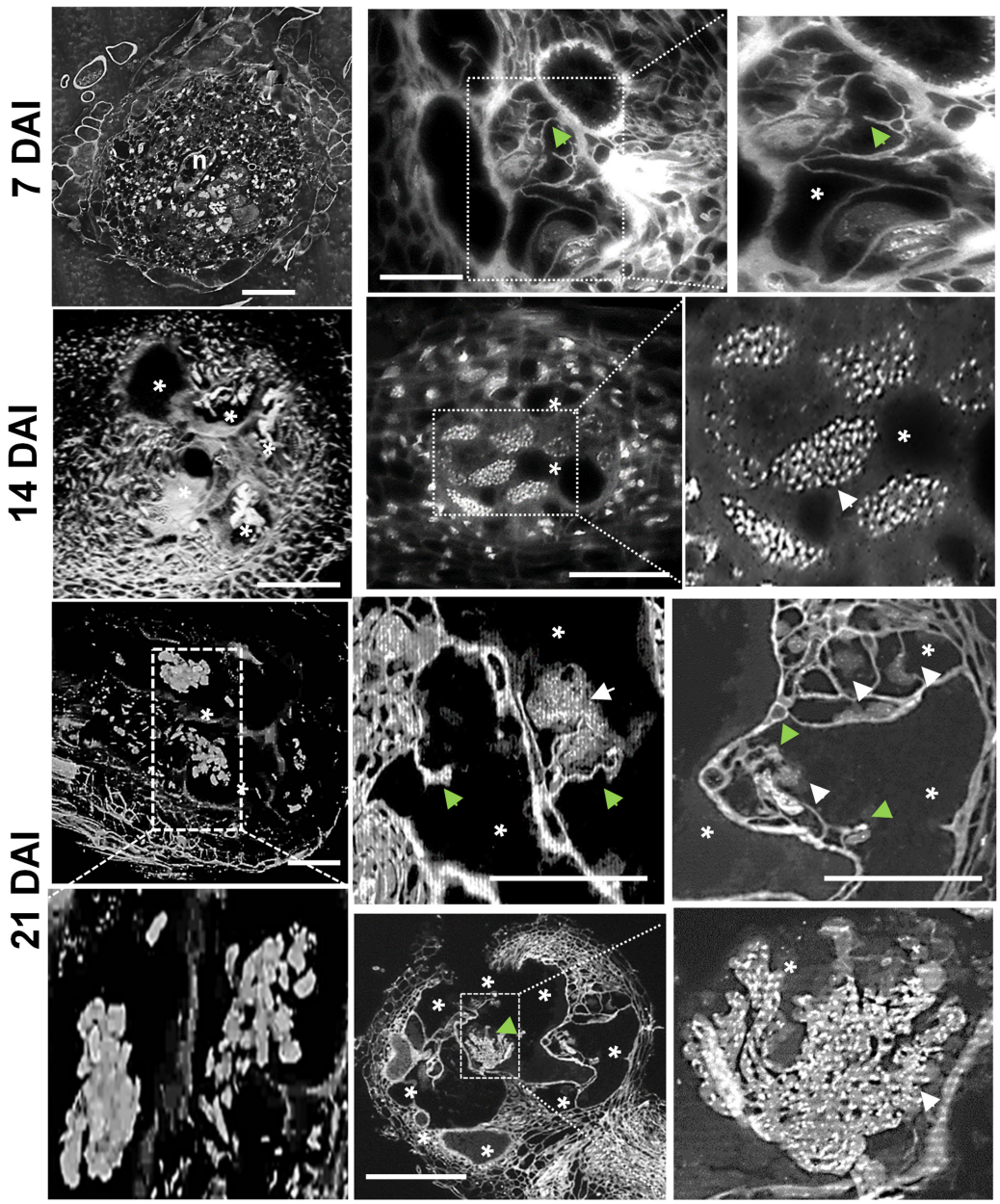

FIGURE 6 | *ABAP1* overexpression induces nuclear morphology changes in root-knot nematode-induced giant cells. Gall nuclei from *ABAP1*^{OE} and wild-type (WT) plants, stained with 4,6-Diamidino-2-phenylindole (DAPI), were observed under dark-field optics. Numerous large stained nuclear dots (white arrows) likely illustrate condensed chromatin at different stages of gall development (7, 14, and 21 DAI). Abnormal cell wall stubs (green arrows) were also seen in *ABAP1*^{OE} galls. Strong cellular and nuclei phenotypes in mature galls suggest cumulative mitotic defects upon ABAP1 overexpression. DAI, days after inoculation; asterisk, giant cell; n, nematode. Scale bars = 50μm.

The activation of origins of replication results from multisource signaling pathways where positive and negative signals will control the pre-RC machiner (Brasil et al., 2017). Along these lines, we subsequently assessed the function of the ABAP1, a negative G1/S cell cycle regulator, in RKN-induced galls. ABAP1 is a repressor of the DNA replication-licensing machinery for replication, and it regulates the G1 to S phase progression cell rate. Also, ABAP1 acts as a possible sensor of internal and external conditions through its dual role in the regulation of DNA replication and transcription (Masuda et al., 2008). Herein, we show that the right balance of ABAP1 is needed for proper gall development as the knockdown or overexpression of

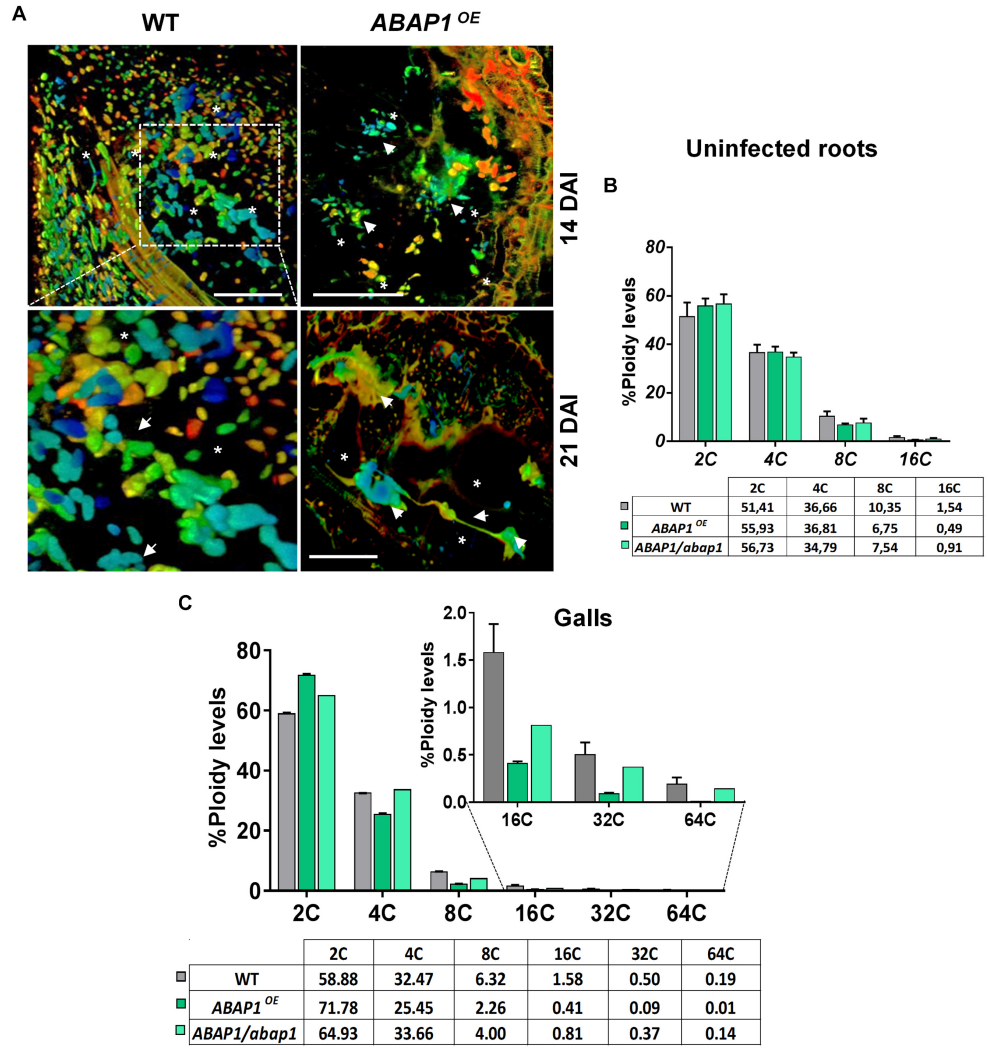

	2C	4C	8C	16C
WT	51,41	36,66	10,35	1,54
ABAP1 ^{OE}	55,93	36,81	6,75	0,49
ABAP1/abap1	56,73	34,79	7,54	0,91

	2C	4C	8C	16C	32C	64C
WT	58.88	32.47	6.32	1.58	0.50	0.19
ABAP1 ^{OE}	71.78	25.45	2.26	0.41	0.09	0.01
ABAP1/abap1	64.93	33.66	4.00	0.81	0.37	0.14

FIGURE 7 | *ABAP1* overexpression affects nuclei morphology and ploidy levels in *M. incognita-induced* galls. **(A)** 3D confocal projections of serial optical sections of wild-type (WT) and *ABAP1*^{OE} galls 14 and 21 DAI nuclei (white arrows), cleared and stained with 4,6-diamidino-2-phenylindole (DAPI). Elongated and apparently connected nuclei are observed in giant cells in *ABAP1*^{OE} galls 21 DAI. DAI, days after inoculation; asterisk, giant cell. Bars = 50 μm. **(B,C)** Flow cytometry analysis and ploidy levels (percentage) of uninfected roots **(B)**, and galls of *ABAP1*^{OE} and *ABAP1/abap1* lines compared to WT **(C)**. The ploidy levels were kept high for GCs in *ABAP1/abap1* as in WT and decreased progressively from 8C to 64C in *ABAP1*^{OE}, when compared to *ABAP1/abap1* and WT galls. For each line and experiment, three independent biological repetitions (± 30 galls) were performed. Scale bars = 50μm.

ABAP1 disturbed gall expansion, as a result affecting nematode development and reproduction. Data on the functional study of ABAP1 in galls as well as transcriptional analysis are summarized in **Figure 9**.

Expression of Pre-RC Genes Are Temporally and Spatially Coordinated for Proper Cell Cycle Progression During Gall Development

Licensing DNA for replication involves the activation of origins of replication and the sequential recruitment of proteins to DNA replication origins, establishing the pre-RC, which is the key process in controlling chromosome duplication. Permission to replicate depends on internal and external features so cells can decide when entering the S phase (Brasil et al., 2017). Here, nematodes, by secreting proteins in the root host, hyperactivate the cell cycle, increasing DNA replication levels in a new tumor-like organ, named galls. To find out if similar pre-RC components of uninfected plant cells regulate replication origins in gall cells, the spatial and temporal expression of the pre-RC-members was performed. Assembly and accurate control of pre-RC are crucial prerequisites for cell cycle progression, and we demonstrated here that several elements of the pre-RC are expressed in root-knot nematode-induced galls. We also showed that gall cells expressed several Arabidopsis pre-RC assembly components like *CDC6, MCM5, ORC1, ORC2, ORC3, ORC4, ORC5, ORC6, CDT1a*, and *CDT1b* during the gall mitotic phase (7 DAI) and also during

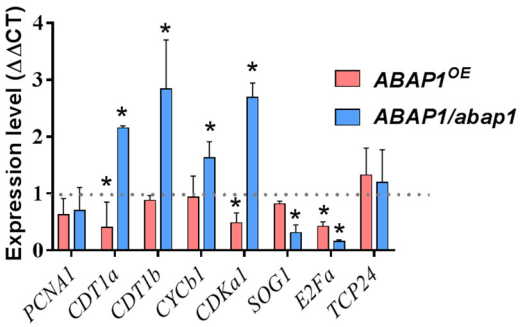

FIGURE 8 | qRT-PCR assays revealed a regulation of cell cycle genes in galls induced by *M. incognita* in *ABAP1*^{OE} and *ABAP1/abap1* plants. *PCNA*, *CDT1a*, *CDT1b*, *CYCB1;1*, *CDKA;1, SOG1*, and *E2Fa* were up- or downregulated upon knockdown or overexpression of *ABAP1* in galls. The analysis was performed in galls 14 days after inoculation, when cell cycle activity is high. *AtOxaloacetate* and *AtNAPDH* genes were used as endogenous reference genes. Data represent mean ± SEM of three independent experiments. The values were normalized according to mRNA levels of wild-type controls (WT-Col-0 for *ABAP1/abap1* and WT-Ler for *ABAP1*^{OE}) (dashed black line). Asterisks indicate values statistically different from the wild-type (Student's *t*-test, $P = 0.05$).

the gall endocycle phase (14 DAI). Gall growth and development is dependent on the mitotic as well as the endoreduplication cycles (de Almeida-Engler et al., 2015). Thus, several of these pre-RC components are likely recruited for the mitotic cycle as well as during the endocycle in developing galls as seen by the presence of transcripts in GCs and NCs including vascular cells. The foremost event in the assembly of the pre-RC is association of ORCs in a complex of six subunits (ORC1–ORC6) to the replication origins containing chromatin marks recognized by ORCs (Bell, 2002; Cunningham and Berger, 2005). All six *ORC*s as well as *CDC6* were shown here to be expressed in galls. Successively, other members of the pre-RC use ORC as a landing platform for CDC6, followed by the recruitment of CDT1s (Bell and Dutta, 2002; Masuda et al., 2004). Besides the ORCs, CDC6 is part of the minimum licensing factor assembling in late G1 during mitosis and the ORCs recruit CDC6 to chromatin further interacting with CDT1s as the cell cycle progresses (Dorn and Cook, 2011; Leonard and Mechali, 2013; MacAlpine and Almouzni, 2013; Pozo and Cook, 2017). In addition, CDC6 and CDT1 proteins act synergistically loading the six DNA helicase MCMs (MCM2–7) opening the replication forks (DePamphilis, 2003; Masai et al., 2005). Also, Bryant (2010) has shown that the *CDC6* gene is expressed during the endoreduplication and, when overexpressed, induced extra endocycles, suggestive of having a similar function in GCs. *MCM5* transcript was detected during gall development with initially higher expression in GCs corroborating with its ubiquitous expression throughout the cell cycle (Springer et al., 2000). MCM5 is a member of the MCM gene family, and MCM5 and MCM7 topologically load onto DNA in plants (Shultz et al., 2009). All through the replicative phase, MCM is shown as the core component of the DNA helicase and, once recruited onto DNA replication origins, leads to replication licensing (Cunningham and Berger, 2005). Thus, the presence of *CDC6*, *MCM5*, and *CDT1a* and *CDT1b* transcripts during the gall mitotic as well as the endocycle phases suggests that nematode-induced galls make use of members of the plant pre-RC machinery in order to activate DNA replication in the host root cell cycle. Possibly, plant–nematode interaction signals driving the cell cycle in galls could engage changes in architecture of pre-RC; thus, other forms of the complex could be altering and hyperactivating the cell cycle in giant-feeding cells. Previous work on plants reported that the cell cycle inhibitor ABAP1 might associate with ORC1a and ORC1b and with pre-RC subunits, or with the fully assembled complex (Masuda et al., 2008). We then investigated ABAP1, a negative cell cycle regulator that controls the assembly of pre-RC in plants (Masuda et al., 2008), to find out if gall ontogeny somewhat underwent this level of cell cycle control.

ABAP1 Expression Might Control Mitotic Activity in Galls and Its Overexpansion

Promoter activity of *ABAP1* observed during gall development suggested its function as a key regulator of the cell cycle and cell division in galls, as for plants. *ABAP1* expression was formerly observed in the Arabidopsis' shoot apex, young leaves, flower buds, and dividing root cells, being weakly expressed in lateral roots (Masuda et al., 2008). Higher *ABAP1* promoter activity was reported during early stages of gall development (3 DAI), suggesting that ABAP1 might be regulating entry into S phase, balancing mitosis rates in galls. As galls matured (7–14 DAI), mitotic activity decreased and *ABAP1* expression became weak but still detected. The strong signal observed in flanking roots suggests that nematode infection might control the proliferative state of these bordering root vascular cells. Thus, *ABAP1* expression might prevent galls to expand limiting further mitotic activity. Fainter ABAP1 expression in GCs at later stages of infection (14 DAI) suggests, to a certain level, its involvement during the gall endocycle phase. Endorsement of promoter activity analysis was given by ABAP1 protein localization in galls, where its high expression was obvious in *ABAP1*^{OE} galls up to 10 DAI (gall endocycle phase) differently from the wild-type where expression decreased. Results of both approaches strongly suggest that *ABAP1* is a candidate to be involved in gall proliferation control. Thus, without a proper cell cycle control, cell cycle hyperactivation occurring in galls might promote uncontrolled growth, leading to a level of root damage that might cause the host death. Thus, gall proliferation must be somewhat controlled by genes regulating the cell cycle such as *ABAP1*. Decreased *ABAP1* expression in maturing galls (10 DAI) corresponds with the entry into the endocycle phase. Overall, ABAP1 expression might likely take part of a highly ordered mechanism of cell cycle control balance preventing gall overexpansion.

Gall Mitotic Phase Is Prolonged and Endocycle Phase Is Delayed in ABAP1 Knockdown Plants

To assess the role of ABAP1 in galls, as a protein interacting with the pre-RC and directly regulating DNA replication and

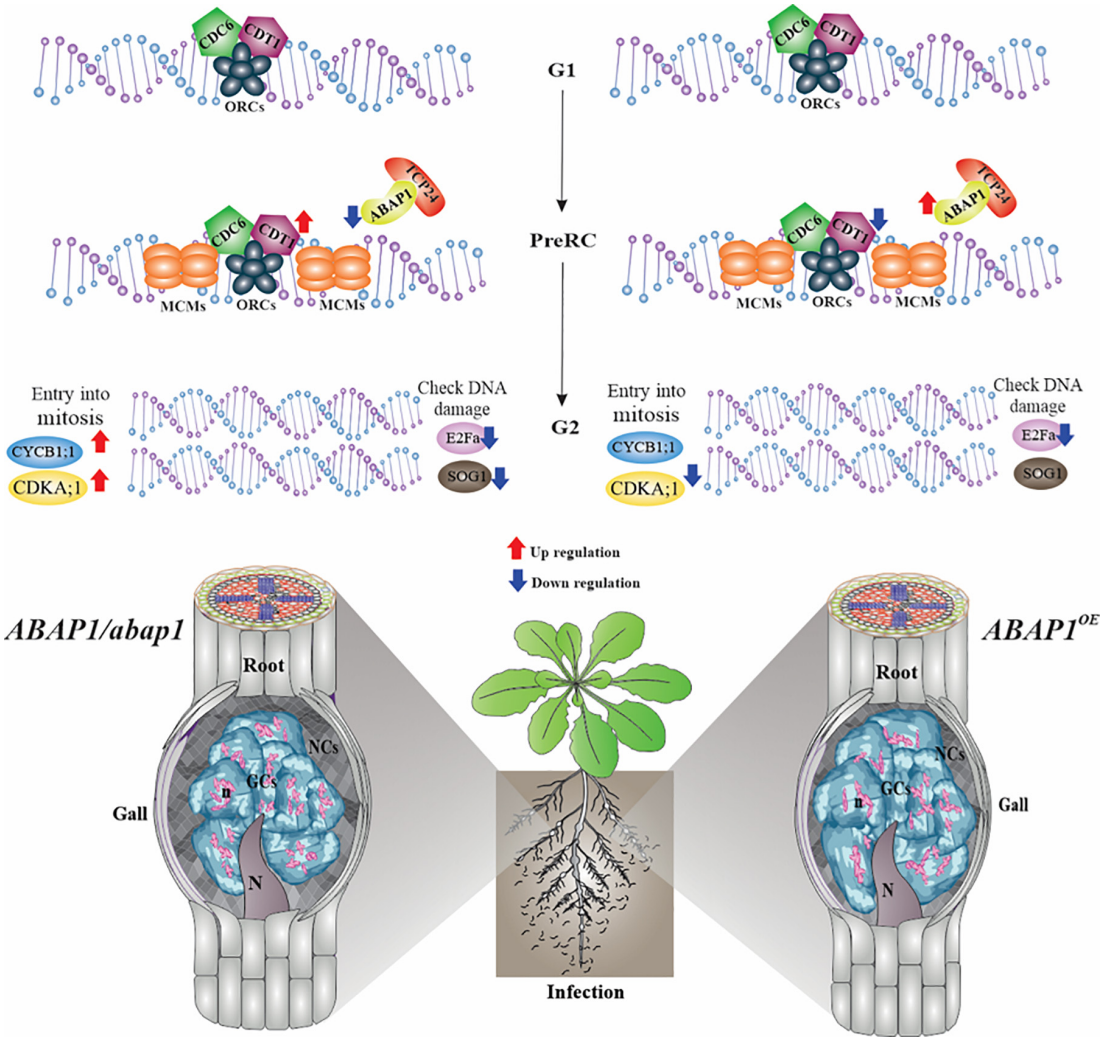

FIGURE 9 | Schematic view and proposed model for *ABAP1* control in galls during DNA replication and S-phase progression. *ABAP1* expression senses and responds to intra- and extracellular signals like nematode infection, leading to changes in the expression pattern of gene members of the pre-replication complex and other S-phase genes. Genes analyzed by *in situ* hybridization are illustrated on the upper DNA drawing, and genes analyzed by qRT-PCR are shown with arrows of up- and downregulation upon increased (red arrows) or decreased (blue arrows) *ABAP1* expression. When *ABAP1* is downregulated (left side), genes like *CDT1*, *CDKA;1*, and *CYCB1;1* increased their expression levels and galls showed more mitotic activity also illustrated in the drawing on the left side. On the other hand, when the *ABAP1* is overexpressed (right side), decreased activity of the pre-RC can possibly regulate negativity of other partakers of the cell cycle such as *CDT1* and CDK1 decreasing mitotic events and inhibiting DNA replication in galls. These might lead to aberrant forms of the nuclei in giant cells illustrated at the right side. Overall, these changes might drastically affect the nematode development and reproduction.

cell proliferation (Masuda et al., 2008), a mutant T-DNA insertion line having reduced expression levels of *ABAP1* was investigated. Downregulation of *ABAP1* in Arabidopsis did not influence gall induction as gall numbers remained close to the wild-type. However, the impending increased cell cycle activity caused by *ABAP1* knockdown was revealed on the visible changes in gall structure and size and was marked by boosted NC and xylem cell proliferation surrounding GCs. In these GCs, the presence of cell wall stubs indicated an early cytokinesis stimulation. GCs with low *ABAP1* expression levels likewise presented asymmetric and convoluted expansion patterns (14–21 DAI) up to the gall borders but remained apparently smaller compared to the wild-type. Thus, overall, this boosted proliferative state likely caused by the reduced cell cycle inhibition by *ABAP1* led to the increased NCs and xylem division around GCs and their distorted expansion. Nuclear stain of galls with decreased ABAP1 levels shows that as galls matured, the multiple GC nuclei were often clumped and apparently small, likely illustrating the fact that galls remained longer in a proliferative state, delaying progression into the endocycle. Although *ABAP1* knockdown did not affect gall induction, the observed failure in proper gall expansion and reduced GC area resulted in the decreased production of egg masses due to an inhibition on nematode maturation. Thus, these analyses

suggest that decreased *ABAP1* expression caused an imbalance of the cell cycle regulation in the feeding site and confirm our previous theory that the mitosis and endocycle offset is needed for a proper gall expansion (de Almeida Engler et al., 2012; de Almeida-Engler et al., 2015; Vieira et al., 2013). The somewhat decreased ploidy levels in GCs of *ABAP1/abap1* line compared to wild-type suggested that activation of nuclei division might delay the endocycle or even that low ABAP1 concentrations might be enough to control the endocycle in galls. Thus, it is reasonable to hypothesize that ABAP1 could participate in a mechanism that control the timing of the switch between the gall mitotic phase to the gall endocycle phase, balancing gall expansion.

ABAP1 Might Be Participating in a Mechanism That Coordinates the Balance of the Mitotic Cycle and Endocycle During Gall Induction and Expansion

The effect of *ABAP1* upregulation in RKN-induced galls was also accessed here, and its overexpression noticeably exerted a negative function in gall cell proliferation resulting in smaller galls than the ones in wild-type plants. Mitotic activity decreased in NCs and in GCs, possibly by the hindered DNA replication, likewise affecting GC expansion. Furthermore, overexpression of *ABAP1* also hampered gall induction, resulting in lower gall numbers and a decrease in overall nematode reproduction. This inhibitory effect of high ABAP1 levels on gall initiation suggests that an early cell cycle stimulation is primordial for gall induction. Highly vacuolated GCs in $ABAP1^{OE}$ galls and reduced ploidy levels may well illustrate a prompt differentiation and decrease in the high metabolic activity, consequently repressing the mitotic cycle and the endocycle. Also, lower GC ploidy suggests that the ABAP1 might function in mitotic as well as in DNA replication during the endocycle progression in galls. DAPI-stained galls overexpressing *ABAP1* illustrated nuclear but also structural changes in GCs like the presence of cell wall stubs, with aberrant expanded patterns with a poor cytoplasm and grouped nuclei filled with spots of condensed chromatin. These densely stained nuclear spots suggest an increase in heterochromatic regions that might be associated to the decreased endocycle. Components of the pre-RC have been described as players into the heterochromatin assembly, sister chromatin cohesion, chromosome segregation, and cytokinesis in yeast and metazoans, as well as in the epigenetic regulation of transcriptionally repressed regions in yeasts, flies, and mammals (reviewed in Sasaki and Gilbert, 2007; Hemerly et al., 2009). Thus, the interconnected nuclei and compacted chromatin regions remarked upon *ABAP1* overexpression are likely the result of the direct effect of the negative control exerted by ABAP1 on pre-RC in these feeding cells. Overall, the observations suggest that ABAP1 might be participating in a mechanism that coordinates the balance of the mitotic cycle and endocycle during gall induction and expansion, regulating cell proliferation and feeding site homeostasis.

Genes of Pre-RC Assembly Are Downregulated in $ABAP1^{OE}$ and *ABAP1/abap1* Galls

Expression levels of candidate genes interacting, or directly and indirectly affected by *ABAP1* levels, were examined upon its up- or downregulation, to validate that cell cycle hyperactivation in galls usurps the plant cells' replication machinery. The expression of the *TCP24* (a class I member of the TCP family) in galls suggests that TCP24 is a potential interactor of ABAP1, and its expression seems not to depend on *ABAP1* expression levels. Alternatively, ABAP1 might regulate cell cycle activity in galls with another partner than TCP24, the ABAP1 interactor in leaves (Masuda et al., 2008). The expression profile of *CDT1a* and *CDT1b* in $ABAP1^{OE}$ and *ABAP1/abap1* galls indicates that an ABAP1–TCP complex might bind *CDT1a* and *CDT1b* promoters in galls, repressing its transcription and regulating cell cycle progression at G1/S in galls and DNA replication.

In galls overexpressing *ABAP1,* the downregulated expression of *CDT1a,* a DNA replication marker, supported the observed phenotype in GCs and their NCs showing inhibited mitotic activity, reinforcing ABAP1 function during the cell cycle in galls. Downregulation of *CDT1a* in $ABAP1^{OE}$ and upregulation of both *CDT1a* and *CDT1b* in *ABAP1* knockdown galls agreed with similar previous observations in leaves of inhibition and stimulation of cell division, respectively (Masuda et al., 2008; Brasil et al., 2017). Thus, low *CDT1a* expression in $ABAP1^{OE}$ galls might be related to the abnormal nuclei phenotype observed in GCs. Also, high *CDT1* levels have been associated with increased endoreduplication (Castellano et al., 2004). Thus, both *CDT1a* and *CDT1b* are likely targets of *ABAP1* in galls and in the control of their expression during DNA replication licensing. Along these lines, *CDT1* might be involved in both DNA replication and also possibly in chromosome segregation; thus, ABAP1 might repress *CDT1a* and *CDT1b* expression, consequently negatively regulating mitotic cell divisions. When downregulated upon high ABAP1 concentration, low *CDT1a* and *CDT1b* levels delay cell cycle progression, driving plants into endoreduplication (Raynaud et al., 2005), similar to what is observed in galls showing increased ploidy levels.

In eukaryotes, members of the pre-RC are regulated by CDK phosphorylation and phosphorylation sites were demonstrated in CDC6 and MCMs from Arabidopsis (Brasil et al., 2017). CDC6 phosphorylation targets the protein for degradation and CDC6 overexpression induces endocycles in Arabidopsis (Bryant and Aves, 2011). Therefore, decreased expression of *CDKA;1* in $ABAP1^{OE}$ galls could contribute to inhibit DNA replication and could participate in the switch to the endocycle phase. In parallel, CDKA;1-CYCB1 complexes are core cell cycle regulators that can be used as markers of active dividing cells (Barrôco et al., 2005). *CYCB1;1* is also a marker of cells at G2 to M phase, being mostly expressed in dividing cells of uninfected roots (Ferreira et al., 1994) and in young galls undergoing the mitotic cycle (Niebel et al., 1996; de Almeida-Engler et al., 1999). Thus, decreased *CDKA;1* expression in $ABAP1^{OE}$ galls could reflect decreased mitotic activity due to *ABAP1* inhibition of DNA replication. No significant changes in *CYCB1;1* level suggests

not to be *ABAP1* concentration dependent in *ABAP1*^{OE} galls. Increased *ABAP1* expression might negatively affect cell cycle progression in galls by targeting genes that regulate phase-to-phase progression, such as *CDT1* and *CDKA;1*, affecting mitotic events and likely contributing to the aberrant nuclei observed in GCs. On the other hand, the upregulation of *CDKA1;1* and *CYCB1;1* seen upon *ABAP1* knockdown is likely associated with the high mitotic activity in galls. No variation in the *PCNA1* mRNA levels in galls suggests that its expression is independent of *ABAP1* levels and that minimum concentration might be enough to hold polymerase activity. Also, in plants, *PCNA1* and its paralogous *PCNA2* are highly conserved genes, with similar sequences, structures, and pattern of protein–protein interaction (Qian et al., 2019), suggesting a redundant function that might overcome some imbalances in their expression as for in galls. PCNA1 is an auxiliary protein of DNA polymerase involved in the control of eukaryotic DNA replication and is the major coordinator of DNA repair at replication forks (Kosugi and Ohashi, 2002; Stevens et al., 2002). Stress-induced effects on the cell cycle has been shown to occur in galls by induction of check point control, likely as a DNA damage response (Cabral et al., 2020). The transcription factor *SOG1* was not activated in galls of both *ABAP1*^{OE} and *ABAP1/abap1* lines, and its expression was significantly decreased upon *ABAP1* downregulation. Therefore, DNA repair mechanism seems not to be activated upon changed *ABAP1* levels. No increase in *SOG1* expression in galls could also be associated with the reduced stress caused in the host root seen by the smaller galls in both *ABAP1*^{OE} and *ABAP1/abap1* lines. Finally, we monitored the expression of *E2Fa*, a member of E2F transcription factors involved in the mitotic as well as the endocycle in plants. Transcription of *E2Fa* promotes the expression of pre-RC genes that bind to DNA replication origins at G1 phase (Castellano et al., 2001, 2004; Diaz-Trivino et al., 2005). *E2Fa* levels in galls in both *ABAP1*^{OE} and *ABAP1/abap1* lines were reduced likely due to the decreased cell cycle activity observed in both transgenic lines.

CONCLUDING REMARKS

Our results provide strong evidences that galls induced by parasitic root-knot nematodes usurp the pre-RC of plant hosts in order to hyperactivate their cell cycle (**Figure 9**). Even when mitotic activity ceases in galls, transcription of pre-RC components here studied remained during DNA replication through the endocycle, suggesting the use of a common regulation of the DNA replication machinery in both phases. Divergences between pre-RC control in galls compared to uninfected roots might occur, given that variations in expression levels were observed, likely reflecting slight differences in strategies of cell cycle regulation. Our functional data indicate that in RKN-induced galls, *ABAP1* can play a novel role during the G1/S phase progression on the course of the endocycle. *ABAP1* upregulation arrested gall development and knockdown perturbed gall homeostasis, suggesting that the accurate cell cycle regulation in GCs is of utmost importance to avoid the accumulation of mitotic defects leading to aberrant nuclear phenotypes. ABAP1 might also be mainly necessary to slow down gall expansion and development, controlling proliferative cell divisions leading to size control during this unique nematode-induced organ growth. Thus, we hypothesize that ABAP1 operates as a negative regulator of the S phase in the mitotic cell cycle and endocycle in galls, possibly participating on NFS induction and development. Most likely, ABAP1 has TCP24 as a partner negatively regulating *CDT1a* expression and then disturbing the pre-RC assembly impeding proper DNA replication and gall mitotic activity. In addition, signaling controls coming from nematode infection might be involved in regulating steps during DNA replication. Finally, understanding the function of cell cycle control genes directing gall homeostasis may well be useful to generate tools enhancing plant resistance to cell cycle-dependent pathogens like nematodes.

DATA AVAILABILITY STATEMENT

The original contributions presented in the study are included in the article/**Supplementary Material**, further inquiries can be directed to the corresponding author/s.

AUTHOR CONTRIBUTIONS

JA, DC, and HF conceived and designed the experiments. DC, JA, HF, IL-T, BM, KS, and LO performed the experiments. JA, DC, HF, and AH analyzed the data. AH and MG contributed reagents, materials, and analysis tools. JA, DC, and BM wrote the manuscript. JA and AH amended the manuscript. All authors contributed to the article and approved the submitted version.

FUNDING

DC was supported by a CAPES-doctoral grant (99999.002114/2015-01). HF and IL-T were supported by a post-doctoral grant and BM was supported a doctoral grant from the CAPES-COFECUB Sv.622/18. LO was supported by a doctoral CAPES grant and KS was supported a post-doctoral CNPq grant. We are grateful to the technical help of G. Martinez, A. Gaïtanaros, B. Carol.

ACKNOWLEDGMENTS

We thank R. De Groodt and J. Cazareth for technical assistance for the *in situ* hybridization experiments and flow cytometry analysis, respectively, N. Marteau for supplying us with pre-parasitic nematodes; and M. Karimi for color drawings in **Figure 1**.

SUPPLEMENTARY MATERIAL

The Supplementary Material for this article can be found online at: https://www.frontiersin.org/articles/10.3389/fpls.2021.636663/full#supplementary-material

Supplementary Figure 1 | Spatial localization of *CDT1a* and *CDT1b* transcripts by non-radioactive *in situ* hybridization in *Meloidogyne incognita*-induced galls of Arabidopsis. Bright-field images of mRNA *in situ* hybridization in nematode feeding sites (orange dotted lines) 7 and 14 DAI. Sections were hybridized with DIG-labeled antisense (AS) probes. *CDT1a* and *CDT1b* hybridization signal is shown as purple color under bright-field optics. UR, uninfected root; DAI, days after inoculation; VT, vascular tissue; DAI, days after inoculation; n, nematodes. Bars = 50 μ m.

Supplementary Table 1 | List of primer sequences used for qRT-PCRPCR analysis.

Supplementary Movie 1 | Confocal projections of serial optical sections of a gall 30 DAI induced by *M. incognita* in Arabidopsis- Wild-type.

Supplementary Movie 2 | Confocal projections of serial optical sections of a gall 30 DAI induced by *M. incognita* in Arabidopsis-*ABAP1/abap1*.

Supplementary Movie 3 | Confocal projections of serial optical sections of a gall 30 DAI induced by *M. incognita* in Arabidopsis-Wild-type.

Supplementary Movie 4 | Confocal projections of serial optical sections of a gall 30 DAI induced by *M. incognita* in Arabidopsis-*ABAP1*^{OE}.

REFERENCES

Antonino de Souza Junior, J. D., Pierre, O., Coelho, R. R., Grossi-de-Sa, M. F., Engler, G., et al. (2017). Application of nuclear volume measurements to comprehend the cell cycle in root-knot nematode-induced giant cells. *Front. Plant Sci.* 8:961. doi: 10.3389/fpls.2017.00961

Barrôco, R. M., Van Poucke, K., Bergervoet, J. H., De Veylder, L., Groot, S. P., Inzé, D., et al. (2005). The role of the cell cycle machinery in resumption of postembryonic development. *Plant Physiol.* 137, 127–140. doi: 10.1104/pp.104.049361

Beeckman, T., and Engler, G. (1994). An easy technique for the clearing of histochemically stained plant tissue. *Plant Mol. Biol. Rep.* 12, 37–42. doi: 10.1007/BF02668662

Bell, S. P. (2002). The origin recognition complex: from simple origins to complex functions. *Genes Dev.* 16, 659–672. doi: 10.1101/gad.969602

Bell, S. P., and Dutta, A. (2002). DNA replication in eukaryotic cells. *Annu. Rev. Biochem.* 71, 333–374. doi: 10.1146/annurev.biochem.71.110601.135425

Blow, J. J., and Dutta, A. (2005). Preventing re-replication of chromosomal DNA. *Nat. Rev. Mol. Cell Biol.* 6, 476–486. doi: 10.1038/nrm1663

Brasil, J. N., Costa, C. N. M., Cabral, L. M., Ferreira, P. C., and Hemerly, A. S. (2017). The plant cell cycle: pre-replication complex formation and controls. *Genet. Mol. Biol.* 40, 276–291. doi: 10.1590/1678-4685-gmb-2016-0118

Breuer, C., Braidwood, L., and Sugimoto, K. (2014). Endocycling in the path of plant development. *Curr. Opin. Plant Biol.* 17, 78–85. doi: 10.1016/j.pbi.2013.11.007

Bryant, J. A. (2010). Replication of nuclear DNA. *Prog. Botany* 71, 25–60.

Bryant, J. A., and Aves, S. J. (2011). Initiation of DNA replication: functional and evolutionary aspects. *Annals Botany* 107, 1119–1126. doi: 10.1093/aob/mcr075

Cabral, D., Banora, M. Y., Antonino, J. D., Rodiuc, N., Vieira, P., Coelho, R. R., et al. (2020). The plant WEE1 kinase is involved in checkpoint control activation in nematode-induced galls. *New Phytol.* 225, 430–447. doi: 10.1111/nph.16185

Castellano, M. M., Boniotti, M. B., Caro, E., Schnittger, A., and Gutierrez, C. (2004). DNA replication licensing affects cell proliferation or endoreplication in a cell type-specific manner. *Plant Cell* 16, 2380–2393. doi: 10.1105/tpc.104.022400

Castellano, M. M., Carlos, J., Ramirez-Parra, E., Brown, S., and Gutierrez, C. (2001). Expression and stability of *Arabidopsis* CDC6 are associated with endoreplication. *Plant Cell* 13, 2671–2686. doi: 10.1105/tpc.010329

Collinge, M. A., Spillane, C., Kohler, C., Gheyselinck, J., and Grossniklaus, U. (2004). Genetic interaction of an origin recognition complex subunit and the polycomb group gene MEDEA during seed development. *Plant Cell* 16, 1035–1046. doi: 10.1105/tpc.019059

Coudreuse, D., and Nurse, P. (2010). Driving the cell cycle with a minimal CDK control network. *Nature* 468, 1074–1079. doi: 10.1038/nature09543

Cubas, P., Lauter, N., Doebley, J., and Coen, E. (1999). The TCP domain: a motif found in proteins regulating plant growth and development. *Plant J.* 18, 215–222. doi: 10.1046/j.1365-313X.1999.00444.x

Cunningham, E. L., and Berger, J. M. (2005). Unraveling the early steps of prokaryotic replication. *Curr. Opin. Struct. Biol.* 15, 68–76. doi: 10.1016/j.sbi.2005.01.003

de Almeida Engler, J., De Groodt, R., Van Montagu, M., and Engler, G. (2001). In situ hybridization to mRNA of Arabidopsis tissue sections. *Methods* 23, 325–334. doi: 10.1006/meth.2000.1144

de Almeida Engler, J., De Veylder, L., De Groodt, R., Rombauts, S., Boudolf, V., De Meyer, B., et al. (2009). Systematic analysis of cell cycle gene expression during *Arabidopsis* development. *Plant J.* 59, 645–660. doi: 10.1111/j.1365-313X.2009.03893.x

de Almeida Engler, J., and Gheysen, G. (2013). Nematode-induced endoreduplication in plant host cells: why and how? *Mol. Plant-Microbe Interact.* 26, 17–24. doi: 10.1094/mpmi-05-12-0128-cr

de Almeida-Engler, J., Engler, G., and Gheysen, G. (2011). "Unravelling the plant cell cycle in nematode induced feeding sites," in *Genomics and Molecular Genetics of Plant-nematode Interactions*, eds J. Jones, G. Gheysen and C. Fenoll (Dordrecht: Springer), 349–368. doi: 10.1007/978-94-007-0434-3_17

de Almeida-Engler, J., De Vleesschauwer, V., Burssens, S., Celenza, J. L. Jr., Inzé, D., Van Montagu, M., et al. (1999). Molecular markers and cell cycle inhibitors show the importance of cell cycle progression in nematode-induced galls and syncytia. *Plant Cell* 11, 793–807. doi: 10.1105/tpc.11.5.793

de Almeida Engler, J., Kyndt, T., Vieira, P., Van Cappelle, E., Boudolf, V., Sanchez, V., et al. (2012). CCS52 and DEL1 genes are key components of the endocycle in nematode-induced feeding sites. *Plant J.* 72, 185–198. doi: 10.1111/j.1365-313X.2012.05054.x

de Almeida-Engler, J., Siqueira, K. M. S., Nascimento, D. C., Costa, T. G., and Engler, G. (2016). A cellular outlook of galls induced by root-knot nematodes in the model host *Arabidopsis thaliana*. *Nematoda* 1:e062016. doi: 10.4322/nematoda.00616

de Almeida-Engler, J., Vieira, P., Rodiuc, N., Grossi-de-sa, M. F., and Engler, G. (2015). "The Plant cell cycle machinery: usurped and modulated by plant-parasitic nematodes," in *Plant Nematode Interactions: A View on Compatible Interrelationships*, eds C. Escobar and C. Fenoll (Amsterdam: Elsevier), 91–118. doi: 10.1016/bs.abr.2014.12.003

De Veylder, L., Beeckman, T., Beemster, G. T., de Almeida Engler, J., Ormenese, S., Maes, S., et al. (2002). Control of proliferation, endoreduplication and differentiation by the *Arabidopsis* E2Fa–DPa transcription factor. *EMBO J.* 21, 1360–1368. doi: 10.1093/emboj/21.6.1360

De Veylder, L., Joubès, J., and Inzé, D. (2003). Plant cell cycle transitions. *Curr. Opin. Plant Biol.* 6, 536–543. doi: 10.1016/j.pbi.2003.09.001

De Veylder, L., Segers, G., Glab, N., Casteels, P., Van Montagu, M., and Inzé, D. (1997). The *Arabidopsis* Cks1At protein binds the cyclin-dependent kinases Cdc2aAt and Cdc2bAt. *FEBS Lett.* 412, 446–452. doi: 10.1016/S0014-5793(97)00822-3

DePamphilis, M. L. (2003). Eukaryotic DNA replication origins: reconciling disparate data. *Cell* 114, 274–275. doi: 10.1016/S0092-8674(03)00604-4

Diaz-Trivino, S., del Mar, Castellano, M., Sanchez, M., de, P., Ramirez-Parra, E., et al. (2005). The genes encoding *Arabidopsis* ORC subunits are E2F targets and the two ORC1 genes are differently expressed in proliferating and endoreplicating cells. *Nucleic Acids Res.* 33, 5404–5414. doi: 10.1093/nar/gki854

Dorn, E. S., and Cook, J. G. (2011). Nucleosomes in the neighborhood: new roles for chromatin modifications in replication origin control. *Epigenetics* 6, 552–559. doi: 10.4161/epi.6.5.15082

Dresselhaus, T., Srilunchang, K. O., Jak-Levaniæ, D., Schreiber, D. N., and Garg, P. (2006). The fertilization-induced DNA replication factor MCM6 of maize shuttles between cytoplasm and nucleus and is essential for plant growth and development. *Plant Physiol.* 140, 512–527. doi: 10.1104/pp.105.074294

Ferreira, P. C., Hemerly, A. S., Engler, J. D., van Montagu, M., Engler, G., and Inzé, D. (1994). Developmental expression of the *Arabidopsis cyclin* gene cyc1At. *Plant Cell* 6, 1763–1774. doi: 10.1105/tpc.6.12.1763

Gutierrez, C. (2005). Coupling cell proliferation and development in plants. *Nat. Cell Biol.* 7, 535–541. doi: 10.1038/ncb0605-535

Gutierrez, C., Ramirez-Parra, E., Castellano, M. M., and del Pozo, J. C. (2002). G(1) to S transition: more than a cell cycle engine switch. *Curr. Opin. Plant Biol.* 5, 480–486. doi: 10.1016/S1369-5266(02)00301-1

Hemerly, A. S., Prasanth, S. G., Siddiqui, K., and Stillman, B. (2009). Orc1 controls centriole and centrosome copy number in human cells. *Science* 323, 789–793. doi: 10.1126/science.1166745

Holding, D. R., and Springer, P. S. (2002). The *Arabidopsis* gene prolifera is required for proper cytokinesis during seed development. *Planta* 214, 373–382. doi: 10.1007/s00425-001-0686-0

Jeffrey, P. D., Russo, A. A., Polyak, K., Gibbs, E., Hurwitz, J., Massagué, J., et al. (1995). Mechanism of cdk activation revealed by the structure of a cyclinA-CDK2 complex. *Nature* 376, 313–320. doi: 10.1038/376313a0

Kosugi, S., and Ohashi, Y. (2002). Interaction of the *Arabidopsis* E2F and DP proteins confers their concomitant nuclear translocation and transactivation. *Plant Physiol.* 128, 833–843. doi: 10.1104/pp.010642

Kronenberger, J., Desprez, T., Höfte, H., Caboche, M., and Traas, J. (1993). A methacrylate embedding procedure developed for immunolocalization on plant tissues is also compatible with in situ hybridization. *Cell Biol. Int.* 17, 1013–1022. doi: 10.1006/cbir.1993.1031

Kyndt, T., Goverse, A., Haegeman, A., Warmerdam, S., Wanjau, C., Jahani, M., et al. (2016). Redirection of auxin flow in *Arabidopsis thaliana* roots after infection by root-knot nematodes. *J. Exp. Bot.* 67, 4559–4570. doi: 10.1093/jxb/erw230

Leonard, A. C., and Mechali, M. (2013). DNA replication origins. *Cold Spring Harb. Perspect. Biol.* 5:a010116. doi: 10.1101/cshperspect.a010116

MacAlpine, D. M., and Almouzni, G. (2013). Chromatin and DNA replication. *Cold Spring Harb. Perspect. Biol.* 5:a010207. doi: 10.1101/cshperspect.a010207

Machida, Y. J., and Dutta, A. (2004). Cellular checkpoint mechanisms monitoring proper initiation of DNA replication. *J. Biol. Chem.* 280, 6253–6256. doi: 10.1074/jbc.R400037200

Magyar, Z., Horvath, B., Khan, S., Mohammed, B., Henriques, R., De Veylder, L., et al. (2012). Arabidopsis E2FA stimulates proliferation and endocycle separately through RBRbound and RBR-free complexes. *EMBO J.* 31, 1480–1493. doi: 10.1038/emboj.2012.13

Masai, H., You, Z., and Arai, K. (2005). Control of DNA replication: regulation and activation of eukaryotic replicative helicase. MCM. *IUBMB Life* 57, 323–335. doi: 10.1080/15216540500092419

Masuda, H. P., Cabral, L. M., De Veylder, L., Tanurdzic, M., de Almeida Engler, J., Geelen, D., et al. (2008). ABAP1 is a novel plant Armadillo BTB protein involved in DNA replication and transcription. *EMBO J.* 27, 2746–2756. doi: 10.1038/emboj.2008.191

Masuda, H. P., Ramos, G. B. A., de Almeida-Engler, J., Cabral, L. M., Coqueiro, V. M., Macrini, C. M. T., et al. (2004). Genome based identification and analysis of the pre-replicative complex of *Arabidopsis thaliana*. *FEBS Lett.* 574, 192–202. doi: 10.1016/j.febslet.2004.07.088

Nath, U., Crawford, B. C. W., Carpenter, R., and Coen, E. (2003). Genetic control of surface curvature. *Science* 299, 1404–1407. doi: 10.1126/science.1079354

Niebel, A., de Almeida Engler, J., Hemerly, A., Ferreira, P., Inzé, D., Van Montagu, M., et al. (1996). Induction of cdc2a and cyc1At expression in *Arabidopsis thaliana* during early phases of nematode-induced feeding cell formation. *Plant J.* 10, 1037–1043. doi: 10.1046/j.1365-313X.1996.10061037.x

Nigg, E. A. (1995). Cyclin-dependent protein kinases: key regulators of the eukaryotic cell cycle. *Bioessays* 17, 471–480. doi: 10.1002/bies.950170603

Palatnik, J. F., Allen, E., Wu, X., Schommer, C., Schwab, R., Carrington, J. C., et al. (2003). Control of leaf morphogenesis by microRNAs. *Nature* 425, 257–263. doi: 10.1038/nature01958

Pozo, P. N., and Cook, J. G. (2017). Regulation and function of Cdt1; a key factor in cell proliferation and genome stability. *Genes* 8:2. doi: 10.3390/genes8010002

Qian, J., Chen, Y., Xu, Y., Zhang, X., Kang, Z., Jiao, J., et al. (2019). Interactional similarities and differences in the protein complex of PCNA and DNA replication factor C between rice and *Arabidopsis*. *BMC Plant Biol.* 19:257. doi: 10.1186/s12870-019-1874-z

Raynaud, C., Perennes, C., Reuzeau, C., Catrice, O., Brown, S., and Bergounioux, C. (2005). Cell and plastid division are coordinated through the prereplication factor AtCDT1. *Proc. Natl. Acad. Sci. U S A.* 102, 8216–8221. doi: 10.1073/pnas.0502564102

Russo, A., Jeffrey, P., and Pavletich, N. (1996). Structural basis of cyclin-dependent kinase activation by phosphorylation. *Nat. Struct. Mol. Biol.* 3, 696–700. doi: 10.1038/nsb0896-696

Sasaki, T., and Gilbert, D. M. (2007). The many faces of the origin recognition complex. *Curr. Opin. Cell Biol.* 19, 337–343. doi: 10.1016/j.ceb.2007.04.007

Shultz, R. W., Lee, T. J., Allen, G. C., Thompson, W. F., and Hanley-Bowdoin, L. (2009). Dynamic localization of the DNA replication proteins MCM5 and MCM7 in plants. *Plant Physiol.* 150, 658–669. doi: 10.1104/pp.109.136614

Shultz, R. W., Tatineni, V. M., Hanley-Bowdoin, L., and Thompson, W. F. (2007). Genome-wide analysis of the core DNA replication machinery in the higher plants *Arabidopsis* and rice. *Plant Physiol.* 144, 1697–1714. doi: 10.1104/pp.107.10110

Springer, P. S., Holding, D. R., Groover, A., Yordan, C., and Martienssen, R. A. (2000). The essential Mcm7 protein PROLIFERA is localized to the nucleus of dividing cells during the G1 phase and is required maternally for early *Arabidopsis* development. *Development* 127, 1815–1822.

Stevens, R., Mariconti, L., Rossignol, P., Perennes, C., Cella, R., and Bergounioux, C. (2002). Two E2F sites in the ArabidopsisMCM3 promoter have different roles in cell cycle activation and meristematic expression. *J. Biol. Chem.* 277, 32978–32984. doi: 10.1074/jbc.M205125200

Strzalka, W., and Ziemienowicz, A. (2011). Proliferating cell nuclear antigen (PCNA): a key factor in DNA replication and cell cycle regulation. *Ann. Bot.* 107, 1127–1140. doi: 10.1093/aob/mcq243

Sugimoto-Shirasu, K., and Roberts, K. (2003). "Big it up": endoreduplication and cell-size control in plants. *Curr. Opin. Plant Biol.* 6, 544–553. doi: 10.1016/j.pbi.2003.09.009

Van't Hof, J. (1985). *Control Points Within the Cell Cycle. The cell Division Cycle in Plants*. Cambridge: Cambridge University Press, 1–13.

Vieira, P., and de Almeida Engler, J. (2017). Plant cyclin-dependent kinase inhibitors of the KRP family: potent inhibitors of root-knot nematode feeding sites in plant roots. *Front. Plant Sci.* 8:1514. doi: 10.3389/fpls.2017.01514

Vieira, P., Engler, G., and de Almeida Engler, J. (2012). Whole-mount confocal imaging of nuclei in giant feeding cells induced by root-knot nematodes in *Arabidopsis*. *New Phytol.* 195, 488–496. doi: 10.1111/j.1469-8137.2012.04175.x

Vieira, P., Escudero, C., Rodiuc, N., Boruc, J., Russinova, E., Glab, N., et al. (2013). Ectopic expression of Kip-related proteins restrains root-knot nematode-feeding site expansion. *New Phytol.* 199, 505–519. doi: 10.1111/nph.12255

Vieira, P., and Gleason, C. (2019). Plant-parasitic nematode effectors—insights into their diversity and new tools for their identification. *Curr. Opin. Plant Biol.* 50, 37–43. doi: 10.1016/j.pbi.2019.02.007

Yokoyama, R., Hirakawa, T., Hayashi, S., Sakamoto, T., and Matsunaga, S. (2016). Dynamics of plant DNA replication based on PCNA visualization. *Sci. Rep.* 6:29657. doi: 10.1038/srep29657

Yoshiyama, K., Conklin, P. A., Huefner, N. D., and Britt, A. B. (2009). Suppressor of gamma response 1 (SOG1) encodes a putative transcription factor governing multiple responses to DNA damage. *Proc. Natl. Acad. Sci. U S A.* 106, 12843–12848. doi: 10.1073/pnas.0810304106

Conflict of Interest: The authors declare that the research was conducted in the absence of any commercial or financial relationships that could be construed as a potential conflict of interest.

frontiers in Plant Science

ORIGINAL RESEARCH
published: 05 May 2021
doi: 10.3389/fpls.2021.671677

The Defense Response Involved in Sweetpotato Resistance to Root-Knot Nematode *Meloidogyne incognita*: Comparison of Root Transcriptomes of Resistant and Susceptible Sweetpotato Cultivars With Respect to Induced and Constitutive Defense Responses

Il-Hwan Lee[1†], Ho Soo Kim[2†], Ki Jung Nam[3], Kang-Lok Lee[3], Jung-Wook Yang[4], Sang-Soo Kwak[2], Jeung Joo Lee[5], Donghwan Shim[6] and Yun-Hee Kim[3]**

[1] Department of Forest Bio-Resources, National Institute of Forest Science, Suwon, South Korea, [2] Plant Systems Engineering Research Center, Korea Research Institute of Bioscience and Biotechnology (KRIBB), Daejeon, South Korea, [3] Department of Biology Education, IALS, Gyeongsang National University, Jinju, South Korea, [4] Department of Crop Cultivation & Environment, Research National Institute of Crop Science, Rural Development Administration, Suwon, South Korea, [5] Department of Plant Medicine, IALS, Gyeongsang National University, Jinju, South Korea, [6] Department of Biological Sciences, Chungnam National University, Daejeon, South Korea

Sweetpotato (*Ipomoea batatas* [L.] Lam) is an economically important, nutrient- and pigment-rich root vegetable used as both food and feed. Root-knot nematode (RKN), *Meloidogyne incognita,* causes major yield losses in sweetpotato and other crops worldwide. The identification of genes and mechanisms responsible for resistance to RKN will facilitate the development of RKN resistant cultivars not only in sweetpotato but also in other crops. In this study, we performed RNA-seq analysis of RKN resistant cultivars (RCs; Danjami, Pungwonmi and Juhwangmi) and susceptible cultivars (SCs; Dahomi, Shinhwangmi and Yulmi) of sweetpotato infected with *M. incognita* to examine the induced and constitutive defense response-related transcriptional changes. During induced defense, genes related to defense and secondary metabolites were induced in SCs, whereas those related to receptor protein kinase signaling and protein phosphorylation were induced in RCs. In the uninfected control, genes involved in proteolysis and biotic stimuli showed differential expression levels between RCs and SCs during constitutive defense. Additionally, genes related to redox regulation, lipid and cell wall metabolism, protease inhibitor and proteases were putatively identified as RKN defense-related genes. The root transcriptome of SCs was also analyzed under uninfected conditions, and several potential candidate genes were identified. Overall, our data provide key insights into the transcriptional changes in sweetpotato genes that occur during induced and constitutive defense responses against RKN infection.

Keywords: constitutive defense, induced defense response, resistant cultivars, root-knot nematodes, susceptible cultivar, sweetpotato, transcriptome

OPEN ACCESS

Edited by:
Claudia S. L. Vicente, University of Évora, Portugal

Reviewed by:
Juan Emilio Palomares-Rius, Consejo Superior de Investigaciones Científicas (CSIC), Spain
Tushar Kanti Dutta, Indian Agricultural Research Institute (ICAR), India

****Correspondence:***
Donghwan Shim
dshim104@cnu.ac.kr
Yun-Hee Kim
cefle@gnu.ac.kr

[†] These authors have contributed equally to this work

Specialty section:
This article was submitted to Plant Pathogen Interactions, a section of the journal Frontiers in Plant Science

Received: *24 February 2021*
Accepted: *13 April 2021*
Published: *05 May 2021*

Citation:
Lee I-H, Kim HS, Nam KJ, Lee K-L, Yang J-W, Kwak S-S, Lee JJ, Shim D and Kim Y-H (2021) The Defense Response Involved in Sweetpotato Resistance to Root-Knot Nematode Meloidogyne incognita: Comparison of Root Transcriptomes of Resistant and Susceptible Sweetpotato Cultivars With Respect to Induced and Constitutive Defense Responses. Front. Plant Sci. 12:671677. doi: 10.3389/fpls.2021.671677

INTRODUCTION

Sweetpotato (*Ipomoea batatas* [L.] Lam) is the fifth most important food crop in the world and a representative root vegetable, with a total production of 91.8 million tons worldwide and an annual harvest area of 7.7 million ha. Sweetpotato is cultivated primarily in Asia and Africa (Afuape et al., 2014; Heider et al., 2021), where it plays an important role in sustainable agriculture, as it serves as a valuable source of nutrients, including minerals, vitamins and pigments, as well as processed foods, animal feeds and alcohol (Diaz et al., 2014; Grace et al., 2014). However, given the narrow genetic base of cultivated sweetpotato, together with its complex hexaploid genome, the development of sweetpotato cultivars with pathogen resistance, high yield, high quality and other desirable traits remains challenging.

Sweetpotato production around the world is affected by various pathogens, including viruses, fungi and parasitic nematodes (Clark and Moyer, 1998; Kreuze, 2002; Palomares-Rius and Kikuchi, 2013). Among the plant parasitic nematodes, root-knot nematodes (RKNs), members of the genus *Meloidogyne*, represent a major threat to many agricultural crops including sweetpotato (Castagnone-Sereno et al., 2013; Kim and Yang, 2019). *Meloidogyne incognita* is a destructive RKN and the most common nematode species found in agricultural regions worldwide. Sweetpotato is highly susceptible to RKN, especially *M. incognita*, which occurs in tropical regions throughout the world and causes severe damage to plant roots (Bridge and Starr, 2010; Kim and Yang, 2019). However, studies on the mechanism of resistance to RKN in sweetpotato are still lacking.

To respond to pathogen infection, including plant parasitic nematode infestation, host plants employ both constitutive and induced defense mechanisms (Boots and Best, 2018). Constitutive defense prevents infection in the first place, while induced defense typically shortens the infectious period. Therefore, these two defense routes have very different implications, not only in individuals but also in terms of the epidemiology of the disease. Moreover, the cost of constitutive defense mechanisms is likely to be paid even in the absence of the pathogen, while induced defense is likely to incur the most substantial cost when used in response to pathogen infection (Lam et al., 2001; Wittstock and Gershenzon, 2002). However, there has been no research on the inducible and constitutive defense mechanisms of host plants under nematode attack.

Sweetpotato cultivars show differences in their susceptibility and resistance to RKNs, which can be exploited to reveal the genes and mechanisms responsible for resistance to RKN. We previously conducted proteome and transcriptome profiling of two sweetpotato cultivars, Yulmi and Juhwangmi, with contrasting responses to infection with *M. incognita* (Ha et al., 2017; Lee et al., 2019). Recently, we identified and studied the responses of candidate genes to RKN infection in these two cultivars (Sung et al., 2019; Lee et al., 2020). However, these studies were limited in their ability to elucidate the mechanism of RKN resistance in sweetpotato because the analysis was limited to only two cultivars, and the late response to RKN (generation of number of galls) was confirmed after 2 months in the growth chamber and 3 months in the greenhouse. In the experimental conditions of this study, transcriptome analysis was performed at 1 week after RKN egg inoculation to confirm the early response, and the numbers of galls produced by RKN were counted at 4 weeks from the eggs of nematodes. Therefore, in the present study, considering that RKN infection is a major limiting factor affecting sweetpotato production, we aimed to decipher the RKN resistance mechanism of sweetpotato by performing RNA-seq analysis of three susceptible cultivars (SCs; Dahomi, Shinhwangmi and Yulmi) and three resistant cultivars (RCs; Danjami, Pungwonmi and Juhwangmi) of sweetpotato infected with *M. incognita*, and examined the induced and constitutive defense response-related transcriptional changes in these cultivars. The results revealed transcriptional changes in genes involved in defense response, secondary metabolites, cellular response and macromolecule metabolism during induced defense response. During constitutive defense, genes related to redox regulation, lipid and cell wall metabolism, protease inhibitor and proteases were putatively identified as RKN resistance genes in RCs. Several downregulated potential candidate genes involved in regulations of metabolism, signal and cell wall were also identified in SCs, based on their transcriptome analysis under uninfected root conditions.

MATERIALS AND METHODS

Plant Materials and *M. incognita* Treatment

Six sweetpotato (*Ipomoea batatas* [L.] Lam) cultivars obtained from the Bioenergy Crop Research Center, National Crop Research Institute (RDA, Muan, Jeonnam, Korea) were used in this study; these included RKN sensitive cultivars (SCs), namely Dahomi (DHM), Shinhwangmi (SHM) and Yulmi (YM), and RKN resistant cultivars (RCs), including Danjami (DJM), Pungwonmi (PWM), and Juhwangmi (JHM). The six cultivars used in this study had different origins. Among RCs, DJM was the result of a cross between Yeonjami and Yeonhwangmi. PWM was the result of a cross between benisazma and Luby3074, and JHM was the result of a cross between SQ27 and BB95024-2. Among SCs, DHM was the result of a cross between Muan-4 and Jinhongmi. SHM was the result of a cross between MI874-1 and Ddosabeni, and YM was the result of a cross between Jinmi and MI78001-15. Fifteen plants per sweetpotato variety were planted in sterilized sand: soil mixture (50:50) in perforated 500-cm^3 clay pots arranged in a completely randomized design. The pots were placed in a greenhouse maintained at 25 ± 3°C, and plants were watered as required. Two weeks after planting, approximately 3,000 *M. incognita* eggs were applied to the soil in each pot and covered with a moist layer of sand. Inoculated and uninoculated plants were harvested 1 week, and the number of galls was visually rated by staining with 0.015% Phloxin B solution for 15 min in roots harvested at 4 weeks after inoculation, as described previously (Fassuliotis, 1985). For each cultivar, seven root samples were ground to a fine powder in liquid nitrogen

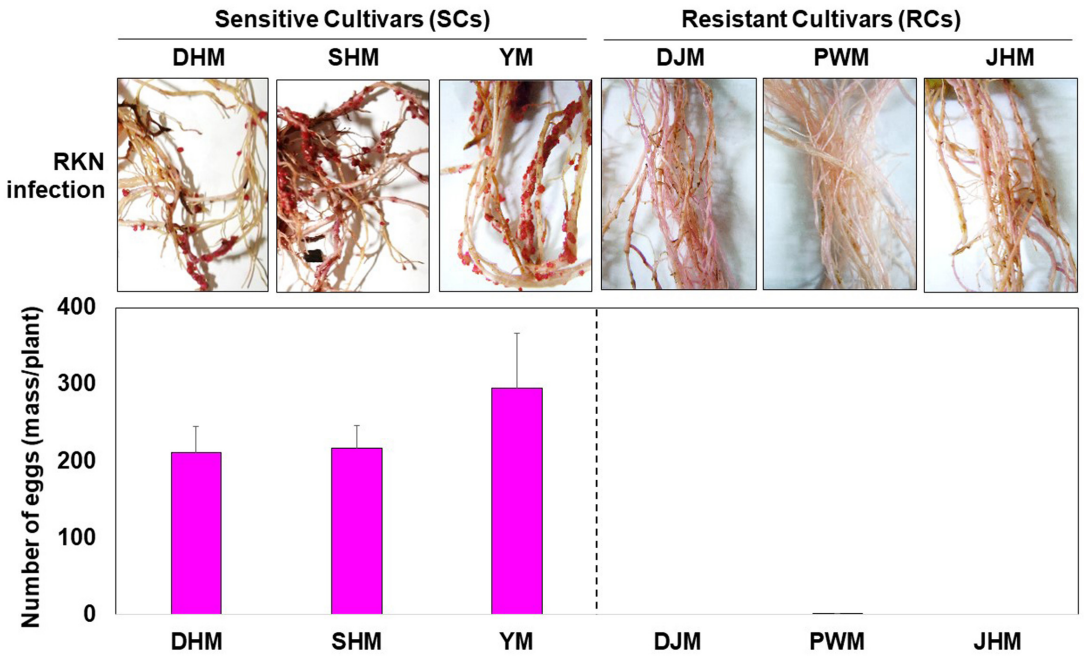

FIGURE 1 | Effect of the root-knot nematode (RKN) *Meloidogyne incognita* on susceptible cultivars (SCs; DHM, SHM, and YM) and resistant cultivars (RCs; DJM, PWM, and JHM) of sweetpotato. Plants were grown under greenhouse conditions for 1 month. Egg masses were formed in non-sterilized sand containing *M. incognita* but not in sweetpotato plants cultured in sterilized soil. Data represent mean ± standard deviation (SD) of 10 replicates. DHM, Dahomi; SHM, Shinhwangmi; YM, Yulmi; DJM, Danjami; PWM, Pungwonmi; JHM, Juhwangmi.

using a pestle and mortar, and stored at −70°C until needed for further analysis.

RNA Extraction, cDNA Library Construction, and Sequencing

Total RNA was isolated from fibrous sweetpotato roots using TRIzol RNA Isolation Kit (Invitrogen, United States). Samples with an RNA integrity number (RIN) > 8 were used for library construction. Each paired-end cDNA library was prepared according to the TruSeq RNA Sample Preparation Guide (Illumina, San Diego, CA, United States) and then sequenced on the HiSeq 2500 platform. Three independent replications were performed for each sample.

RNA-Seq Data Analysis

Paired-end reads were cleaned using prinseq-lite version 0.20.4, with the following parameters: min_len 50; min_qual_score 5; min_qual_mean 20; derep 14; trim_qual_left 20; trim_qual_right 20. Clean paired-end reads of each sample were aligned to the sweetpotato reference genome sequence[1] using Bowtie2. The RSEM 1.3.0 software was used to obtain read counts and TMM-normalized TPM (trimmed mean of M value-normalized transcripts per million) values for each transcript. EdgeR version 3.16.5 was used to calculate the negative binomial dispersion across conditions for differential gene expression analysis. Genes were determined to be significantly differentially expressed if they showed >4-fold change in expression, with a false discovery rate (FDR)-adjusted $P < 0.001$. Principal component analysis (PCA) plot and heatmap analysis was utilized to visualize and assess the clustering of the data using programs of Mev and PtR of Trinity package (Howe et al., 2011; Haas et al., 2013; Braich et al., 2019).

Functional Annotation

Functional annotation of differentially expressed genes (DEGs) was performed via sequence similarity searches using the BLAST program against the *Arabidopsis thaliana* protein database, with an *e*-value threshold of 1E-5. Gene Ontology (GO) term and Kyoto Encyclopedia of Genes and Genomes (KEGG) pathway enrichment analyses were performed using DAVID[2]. To conduct MapMan analysis, *Arabidopsis* homolog gene IDs and fold changes of DEGs in the six sweetpotato cultivars were mapped to biotic stress pathways. Pictorial representations of the biotic stress pathways were uploaded from the MapMan website[3].

Quantitative Real-Time PCR (qRT-PCR)

Gene expression was verified by qRT-PCR analysis in a fluorometric thermal cycler (DNA Engine Opticon 2; MJ Research, Waltham, MA, United States) using gene-specific primers (**Supplementary Table 1**) and EvaGreen fluorescent dye, according to the manufacturer's instructions. Data were normalized relative to the mean CT value of the stable reference

[1]https://ipomoea-genome.org/

[2]https://david.ncifcrf.gov/

[3]https://mapman.gabipd.org/home

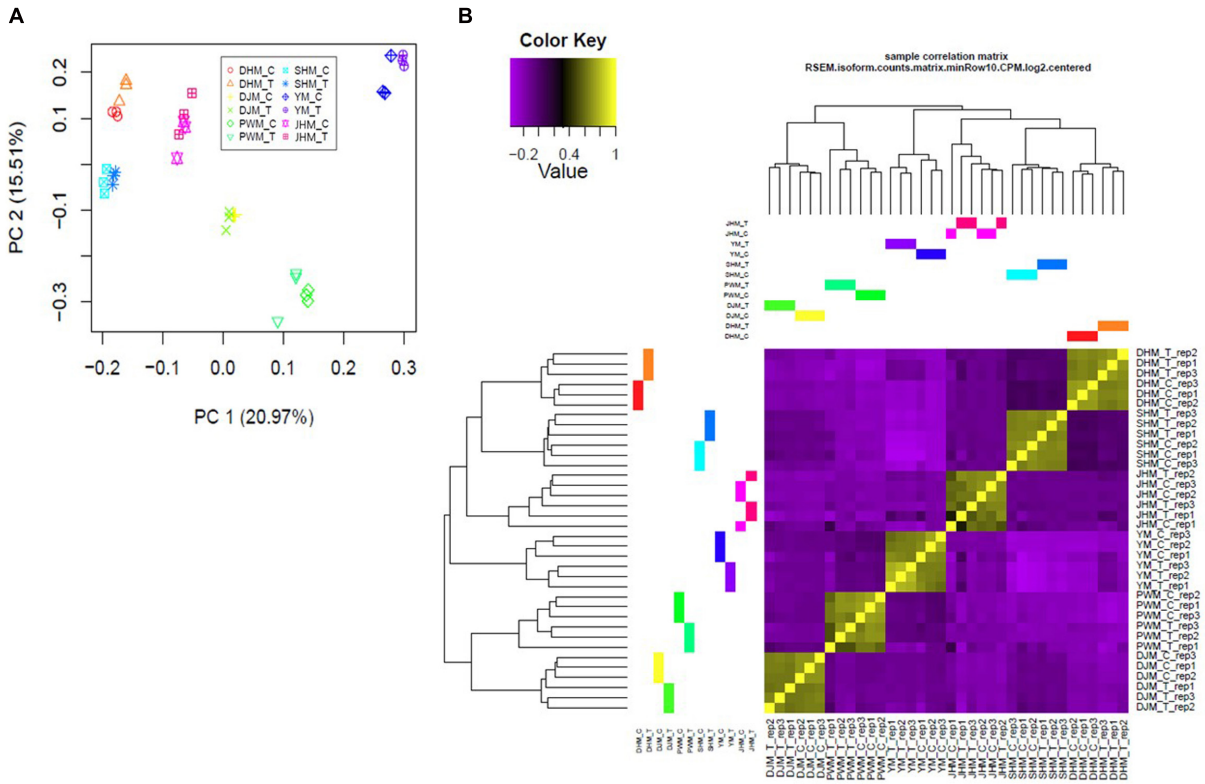

FIGURE 2 | Statistical analysis of differentially expressed genes (DEGs) across samples. **(A)** Principal component analysis (PCA) of all samples by treatment shows general clustering of samples with a few outliers. Colors denote different cultivars and treatment conditions. **(B)** Clustered heatmap showing the Pearson correlation matrix of pairwise sample comparisons. The color key was adjusted based on the log2-centered values for optimal visual detection of differences, and the dendrogram illustrates the relationship among samples. DHM, Dahomi; DJM, Danjami; PWM, Pungwonmi; SHM, Shinhwangmi; JHM, Juhwangmi; YM, Yulmi; RCs, resistant cultivars; SCs, sensitive cultivars; C, control; T, treatment.

gene, *ADP-ribosylation factor* (*ARF*) (Livak and Schmittgen, 2001; Park et al., 2012).

Statistical Analyses

Data were analyzed by one-way analysis of variance (ANOVA). Statistical significance levels were set at $P < 0.05$. The subsequent multiple comparisons were examined based on Dunnett's multiple range test. All statistical analyses were performed using Statistical Package for the Social Sciences software (SPSS 12).

RESULTS

RKN Resistance Differs Between Sweetpotato Cultivars

According to the Bioenergy Crop Research Center and our previous study on Korean sweetpotato accessions maintained in South Korea (Choi et al., 2006; Lee et al., 2012; Ha et al., 2017), cultivars DHM, SHM and YM are highly sensitive to RKNs, specifically *M. incognita*, whereas DJM, PWM and JHM are highly resistant. Therefore, we compared the resistance of SCs and RCs to *M. incognita* by measuring nematode egg mass formation after infestation under greenhouse conditions. The experiment was conducted by checking the roots at 1 week (7 days) and 4 weeks (28 days) after infection with RKN eggs. At 1 week after infection, the state of the roots was not significantly changed by RKN infection irrespective of the cultivar. Interestingly, at 4 weeks after infection, galls were found only in susceptible cultivars. *M. incognita* formed 210, 216, and 295 egg masses in DHM, SHM and YM plants, respectively, but only 0–0.6 egg masses in RCs, such as DJM, PWM, and JHM (**Figure 1**). Thus, these data confirm the differences in *M. incognita* resistance levels between SCs and RCs.

Transcriptome Sequencing of Sweetpotato Fibrous Roots in Response to RKN

In order to confirm the mechanism of resistance during the early response to RKN infection, transcriptome analysis was performed on roots at 7 days after infection. To analyze the effect of *M. incognita* infection on the transcriptome of fibrous roots of SCs and RCs, we performed RNA-seq analysis of *M. incognita*-infected and uninfected (control) plants using the Illumina HiSeq2500 platform. A total of 693,206,233 raw paired-end reads (140,027,659,066 bp) were generated from the six cultivars. After

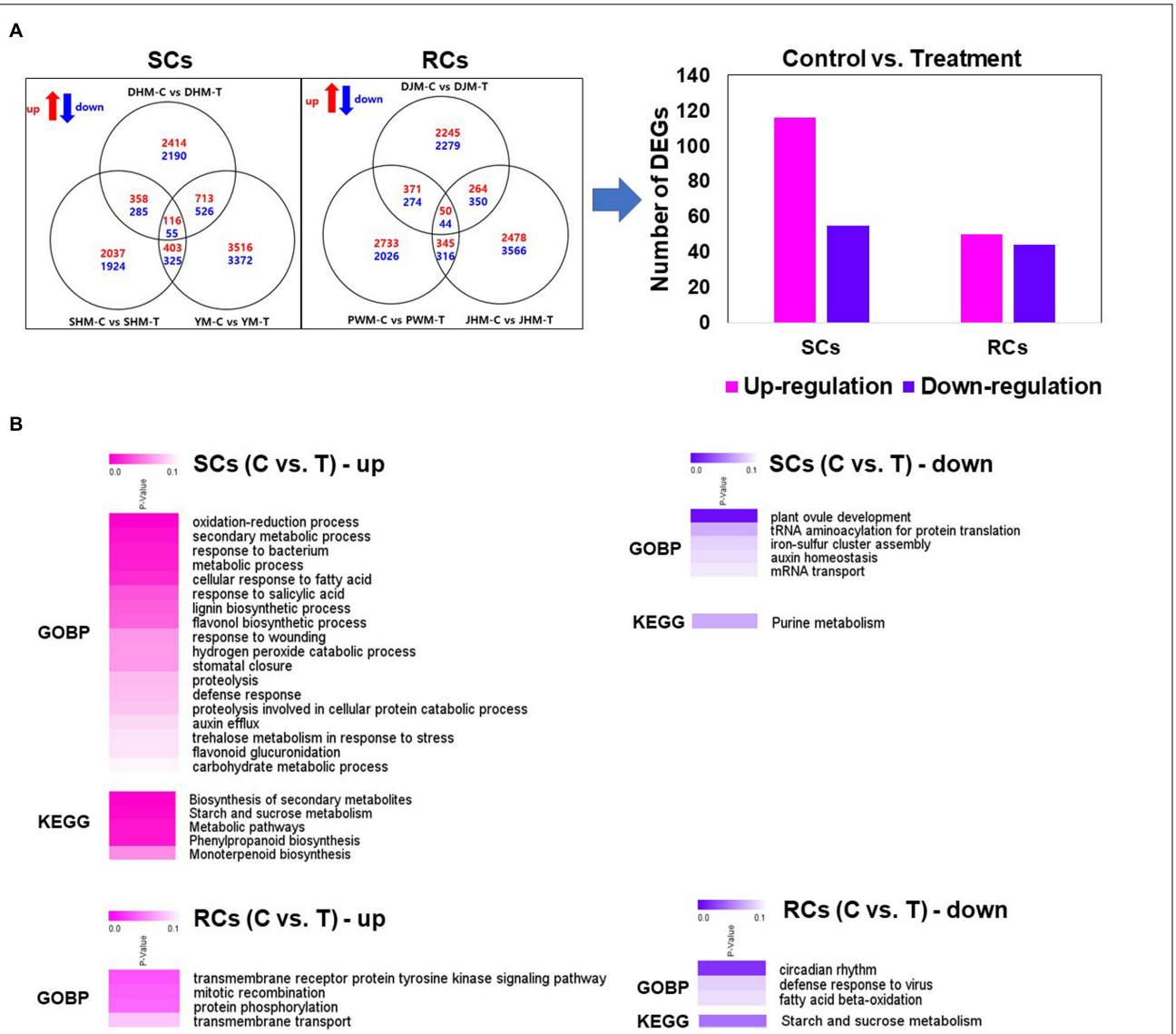

FIGURE 3 | Identification of DEGs in pairwise comparisons across samples, and heatmap of Gene Ontology (GO) biological process category and Kyoto Encyclopedia of Genes and Genomes (KEGG) pathways enriched in the induced defense response. **(A)** Venn diagrams showing the number of DEGs with up- or downregulated expression in the pairwise sample comparisons. **(B)** Heatmap of GO biological process category and KEGG pathway of DEGs in pairwise sample comparisons between control (C) and treatment (T). The heatmap shows Benjamini–Hochberg-adjusted ($P < 0.05$) for DEGs enriched in specific GO terms in the biological process category. DHM, Dahomi; DJM, Danjami; PWM, Pungwonmi; SHM, Shinhwangmi; JHM, Juhwangmi; YM, Yulmi; RCs, resistant cultivars; SCs, sensitive cultivars; C, control; T, treatment.

filtering out low-quality and unpaired reads using the prinseq-lite software, we obtained 612,064,327 high-quality paired-end reads (**Supplementary Table 2**). All raw read data were deposited at the National Center for Biotechnology Information (NCBI) Sequence Read Archive (SRA) database under the accession number SRP128609 (PRJNA429283).

Global Statistical Evaluation of Samples Used for Comparative Transcriptomics

To perform a statistical evaluation of samples used for comparative transcriptome analyses, we mapped high-quality reads to the reported transcriptome[4], and calculated transcript abundance. Next, we performed principal component analysis (PCA) to evaluate the transcriptomic differences among the six sweetpotato cultivars under *M. incognita* treated (T) and control conditions (C) (**Figure 2A**). In pairwise comparisons, independent biological replicates were more highly correlated within samples than between samples, and biological replicates of a given cultivar clustered with each other than with other cultivars, regardless of the treatment (*M. incognita*-infected or control) (**Figure 2B**). We also identified DEGs based

[4]https://ipomoea-genome.org/

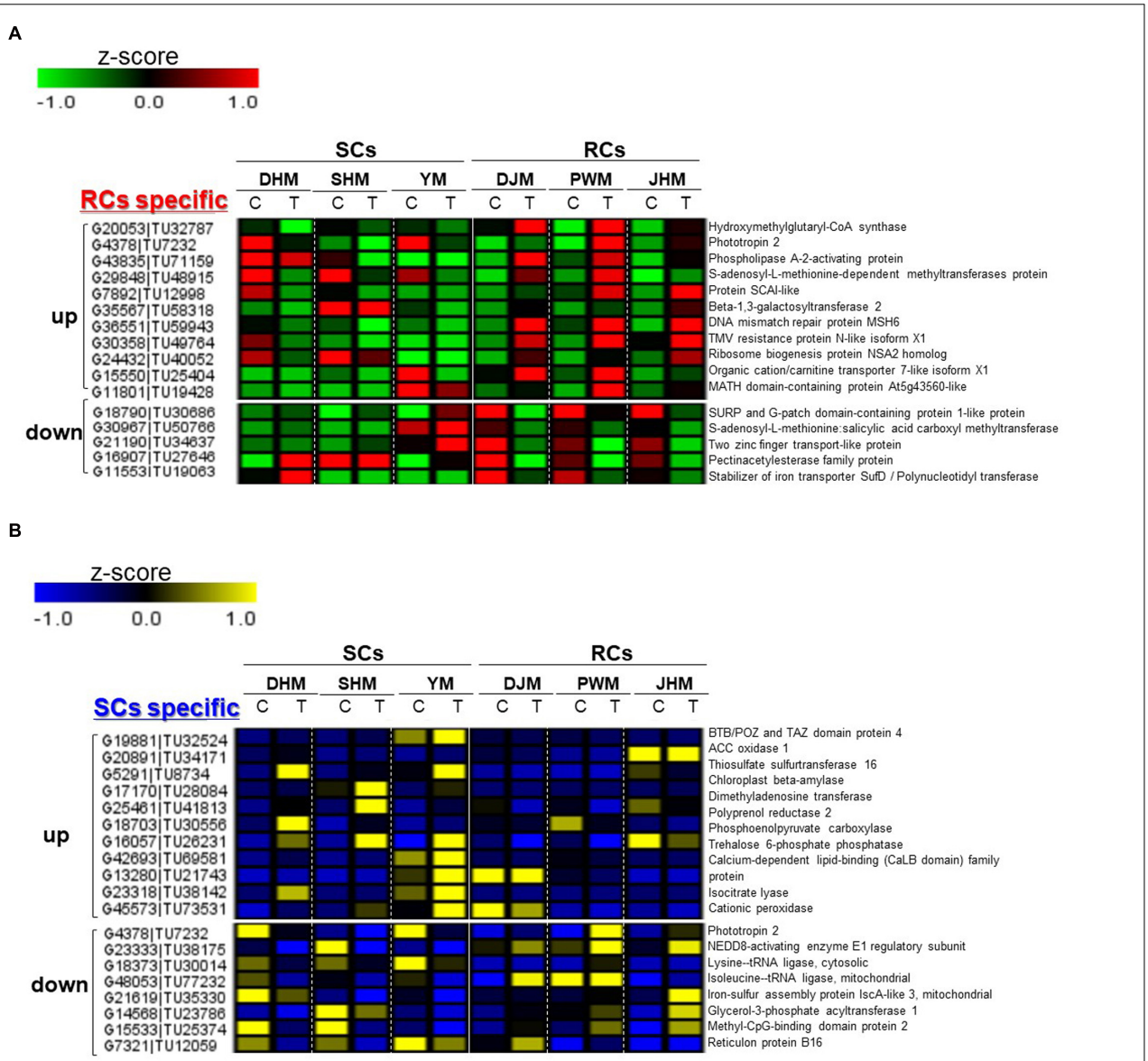

FIGURE 4 | Comparison of the expression levels of induced defense response-related specific candidate genes in six sweetpotato cultivars under RKN-infected and control conditions. DEGs include **(A)** RC-specific and **(B)** SC-specific up- and downregulated genes. DHM, Dahomi; DJM, Danjami; PWM, Pungwonmi; SHM, Shinhwangmi; JHM, Juhwangmi; YM, Yulmi; RCs, resistant cultivars; SCs, sensitive cultivars; C, control; T, treatment. The heatmap was constructed using Multi Experiment Viewer (MeV).

on pairwise sample comparisons. Each SC and RC showed different patterns of DEG distribution between the control and *M. incognita* infection treatments, as shown by the volcano plots (**Supplementary Figure 1**). Thus, each of RCs and SCs showed different patterns between untreated and RKN-treated conditions.

Identification and Characterization of DEGs of the Induced Defense Response

To analyze the induced defense response of sweetpotato during *M. incognita* infection via RNA-seq, we identified putative unique transcripts as reliable DEGs (fold change $>$ 2; Kal's *z*-test FDR $P < 0.005$) in pairwise sample comparisons (**Figure 3A**). First, we examined the transcriptional responses of both SC and RC groups against *M. incognita*. Among the identified DEGs, 116 and 55 were significantly up- and downregulated in SCs, respectively, after *M. incognita* infection compared with the control, consistent with the three cultivars DHM, SHM and YM (**Figure 3A** and **Supplementary Table 3**). Fifty upregulated and 44 downregulated DEGs were identified in RCs infected with *M. incognita* compared with the control (**Figure 3A** and **Supplementary Table 4**). To functionally characterize the DEGs, we identified their encoded products

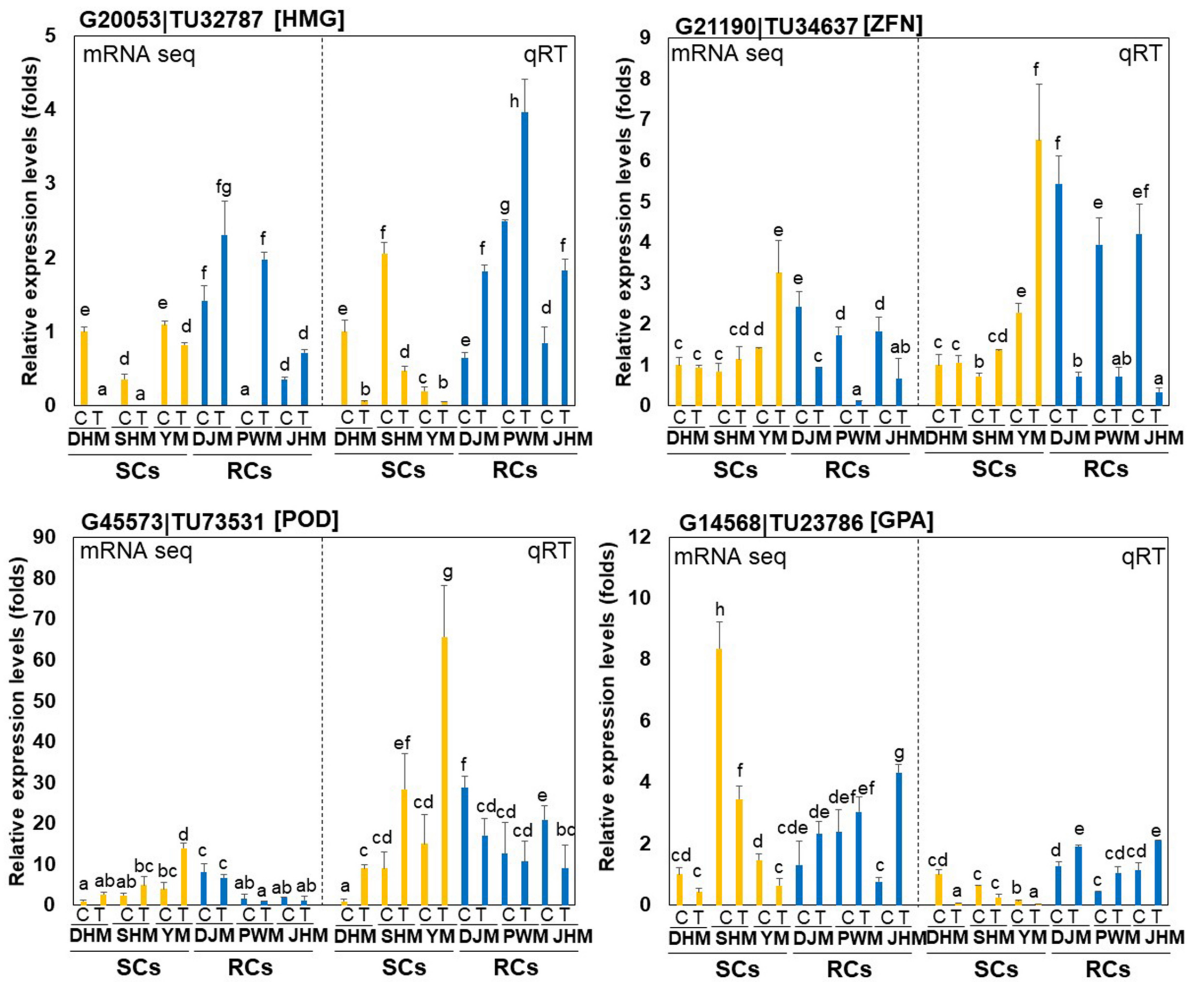

FIGURE 5 | Comparison of quantitative real-time PCR (qRT-PCR) results and RNA-seq data. The graphs show relative transcript levels of two RC-specific genes, hydroxymethylglutaryl-CoA synthase (HMG; G20053| TU32787) and zinc finger protein (ZFN; G21190| TU34637), and two SC-specific genes, cationic peroxidase (POD; G45573| TU73531) and glycerol-3-phosphate acyltransferase (GPA; G14568| TU23786), which were differentially expressed between SCs (yellow bars) and RCs (blue bars) infected with *M. incognita*, as determined by RNA-seq (left *Y*-axis) and qRT-PCR (right *Y*-axis). DHM, Dahomi; DJM, Danjami; PWM, Pungwonmi; SHM, Shinhwangmi; JHM, Juhwangmi; YM, Yulmi; RCs, resistant cultivars; SCs, sensitive cultivars; C, control; T, treatment. Bars denoted with the same letter are not significantly different ($P = 0.05$) according to Dunnett's test.

via comparisons with *A. thaliana* protein database, and then performed GO and KEGG pathway enrichment analyses of the annotated genes (with Benjamini–Hochberg-adjusted $P < 0.05$; **Figure 3B**). In SCs, several genes differentially expressed between *M. incognita*-infected and control treatments were enriched in the biological process category under various GO terms, including process of oxidation-reduction, secondary metabolic process, response to bacterium, cellular response to fatty acid and response to salicylic acid, and in KEGG pathways including biosynthetic secondary metabolites, starch and sucrose metabolism, phenylpropanoid biosynthesis and monoterpenoid biosynthesis. In RCs, GO terms enriched in the biological process category included transmembrane receptor protein tyrosine kinase signaling pathway, mitotic recombination, and protein phosphorylation with untreated control and RKN infection.

Differential Regulation of RKN Resistance-Related Candidate Genes Involved in Induced Defense Response

We identified RC- and SC-specific DEGs involved in induced defense response (**Figure 4**). Among the RC-specific induced defense response-related DEGs (**Figure 4A**), genes encoding hydroxymethylglutaryl-CoA synthase (G20053| TU32787), phototropin 2 (G4378| TU7232), phospholipase A-2-activating protein (G43835| TU71159) and beta-1,3-galactosyltransferase 2 (G35567| TU58318) were upregulated, whereas those encoding a S-adenosyl-L-methionine: salicylic acid carboxyl methyltransferase (G30967| TU50766), two zinc finger transport-like proteins (G21190| TU34637) and a pectinacetylesterase family protein (G16907| TU27646) were downregulated RKN infection. Among the SC-specific DEGs (**Figure 4B**), genes

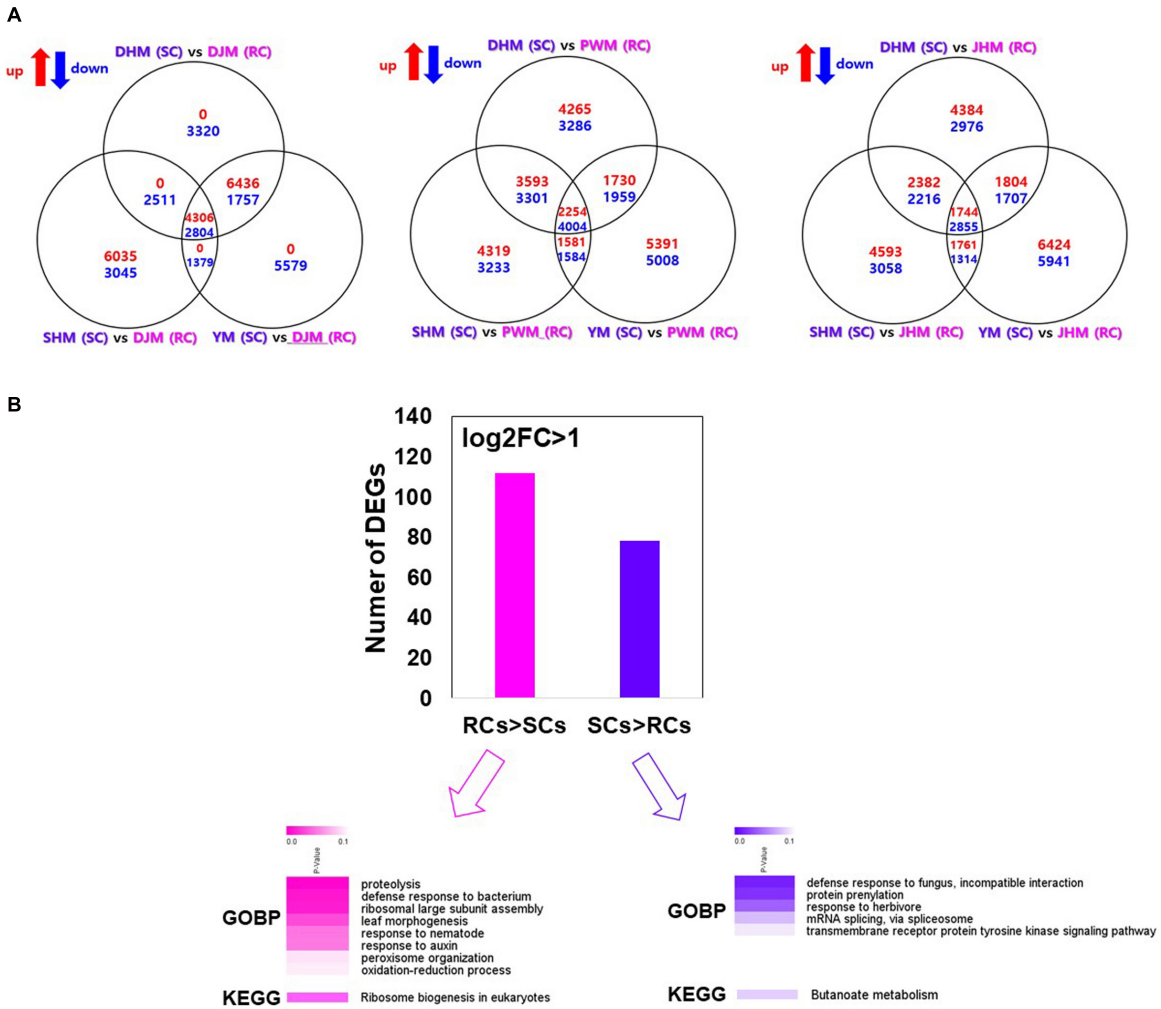

FIGURE 6 | Identification and GO enrichment analysis of sweetpotato genes involved in constitutive defense response against M. incognita infection. **(A)** Venn diagrams showing the number of genes differentially up- or downregulated in pairwise sample comparisons. **(B)** Heatmap of the GO and KEGG enrichment analyses of genes differentially expressed between RCs and SCs. The heatmap shows Benjamini–Hochberg-adjusted ($P < 0.05$) for the biological process GO terms and KEGG pathways associated with DEGs. DHM, Dahomi; DJM, Danjami; PWM, Pungwonmi; SHM, Shinhwangmi; JHM, Juhwangmi; YM, Yulmi.

encoding ACC oxidase 1 (G20891| TU34171), thiosulfate sulfurtransferase 16 (G5291| TU8734), chloroplast beta-amylase (G17170| TU28084), polyprenol reductase 2 (G18703| TU30556), phosphoenolpyruvate carboxylase (G16057| TU26231), trehalose 6-phosphate phosphatase (G42693| TU69581) and cationic peroxidase (G45573| TU73531) were upregulated, whereas those encoding phototropin 2 (G4378| TU7232), isoleucine–tRNA ligase (G48053| TU77232) and glycerol-3-phosphate acyltransferase 1 (G14568| TU23786) were downregulated.

Expression Profiling of RKN-Responsive Candidate Genes by qRT-PCR

We performed qRT-PCR to analyze the expression patterns of four candidate RKN-responsive genes, including two RC-specific genes, hydroxymethylglutaryl-CoA synthase (HMG; G20053| TU32787) and zinc finger protein (ZFN; G21190| TU34637), and two SC-specific genes, cationic peroxidase (POD; G45573| TU73531) and glycerol-3-phosphate acyltransferase (GPA; G14568| TU23786), in the root tissues all six cultivars infected with *M. incognita* (**Figure 5**). Both qRT-PCR and RNA-seq analysis revealed significant DEGs between the two groups (SCs and RCs). The HMG gene was specifically induced, whereas the ZFN gene specifically downregulated in RCs during RKN infection. On the other hand, the POD gene was specifically induced in SCs during RKN infection, whereas the GPA gene was downregulated.

Identification and Characterization of DEGs of the Constitutive Defense Response

In RKN-resistant plants, defense related systems are active not only during infection but also under uninfected (normal)

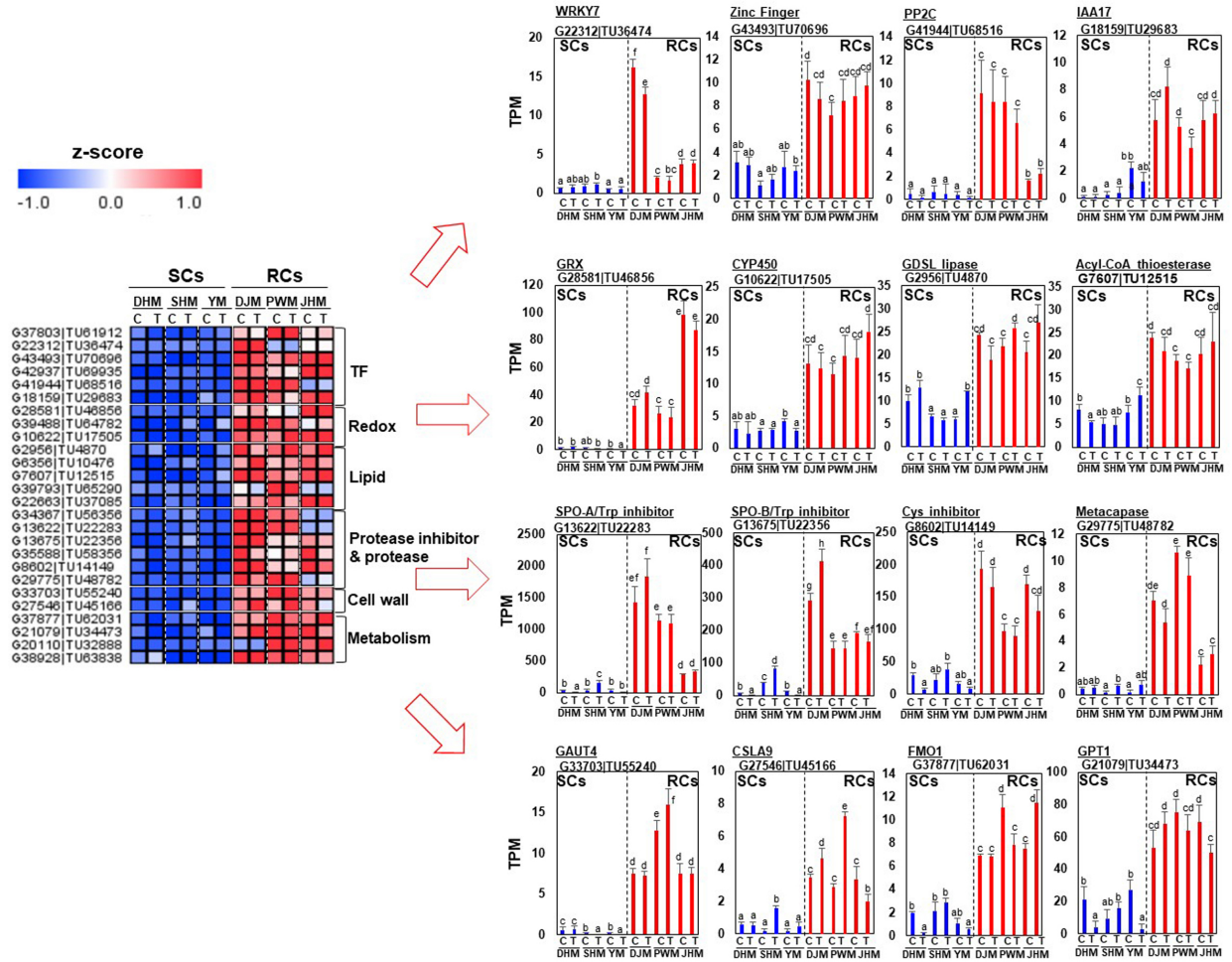

FIGURE 7 | Comparison of the expression levels of RC-specific candidate genes in six sweetpotato cultivars under control and RKN-infected conditions. DEGs related to transcription factors, redox regulation, lipid, cell wall, metabolism, protease and protease inhibitors were identified. The heatmap was constructed using Multi Experiment Viewer (MeV). DHM, Dahomi; DJM, Danjami; PWM, Pungwonmi; SHM, Shinhwangmi; JHM, Juhwangmi; YM, Yulmi; RCs, resistant cultivars; SCs, sensitive cultivars; C, control; T, treatment. Bars denoted with the same letter are not significantly different ($P = 0.05$) according to Dunnett's test.

conditions (Boots and Best, 2018). Therefore, to confirm the constitutive defense-mediated resistance mechanism in RCs, we compared the transcriptional responses of RCs and SCs under the untreated (control) condition (**Figure 6**), and identified putative unique transcripts as reliable DEGs (fold change > 2; Kal's *z*-test FDR $P < 0.005$) in pairwise sample comparisons (**Figure 6A**). Among the identified DEGs, 4,360 and 2,804 were upregulated and downregulated, respectively, in DJM (an RC) compared with SCs (DHM, SHM, and YM). In addition, 2,254 and 4,004 were significantly up- and downregulated in PWM, while 1,744 and 2,855 were significantly up- and downregulated in JHM compared with SCs. Finally, 112 genes were significantly upregulated in RCs compared with SCs, whereas 78 genes were significantly upregulated in SCs compared with RCs (**Figure 6B** and **Supplementary Tables 5, 6**). To functionally characterize the DEGs, we also identified their encoded products via comparisons with *A. thaliana* protein database, and then performed GO and KEGG pathway enrichment analyses of the annotated genes (with Benjamini–Hochberg-adjusted $P < 0.05$). Several biotic stress related GO terms were enriched in the biological process category, including proteolysis, defense response to bacterium, response to nematode, and response to auxin, in RCs compared with SCs under control conditions. GO terms including defense response to fungus, incompatible interaction, protein prenylation and response to herbivore were enriched in SCs compared with RCs under control conditions.

Differential Regulation of RKN Resistance-Related Candidate Genes Involved in Constitutive Defense Response

First, we identified RC-specific DEGs as candidates for constitutive defense response-related genes (**Figure 7**). Genes encoding various transcription factors, including putative jasmonic acid (JA)-dependent WRKY7 (G22312| TU36474),

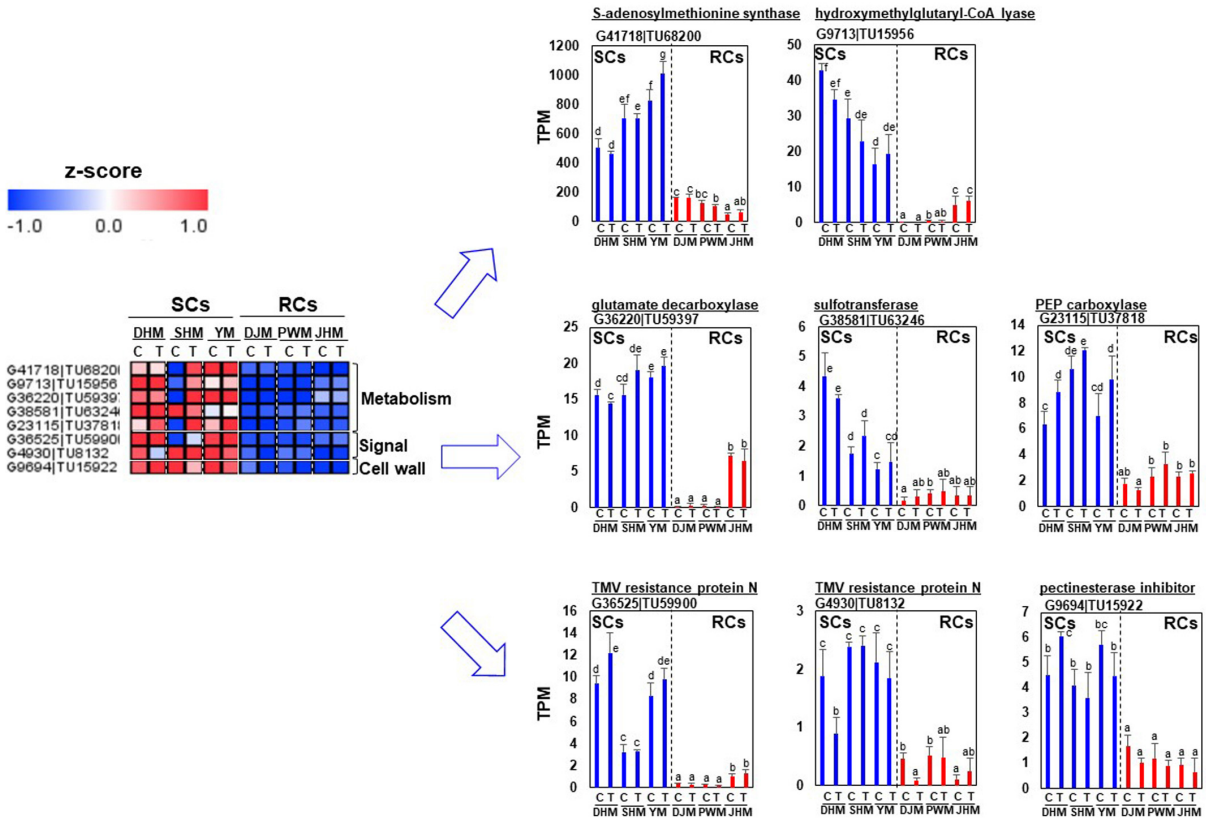

FIGURE 8 | Comparison of the expression levels of SC-specific candidate genes in six sweetpotato cultivars under control and RKN-infected conditions. DEGs related to metabolism, signals and cell wall were identified. The heatmap was constructed using Multi Experiment Viewer (MeV). DHM, Dahomi; DJM, Danjami; PWM, Pungwonmi; SHM, Shinhwangmi; JHM, Juhwangmi; YM, Yulmi; RCs, resistant cultivars; SCs, sensitive cultivars; C, control; T, treatment. Bars denoted with the same letter are not significantly different (P = 0.05) according to Dunnett's test.

a zinc finger protein (G43493| TU70696), auxin repressor IAA17 (G18159| TU29683) and ABA signaling related PP2C (G41944| TU68516), were specifically expressed in RCs under *M. incognita*-infected and control conditions. Genes encoding redox-related GRX (G28581| TU46856), CYP450 (G10622| TU17505), lipid-related GDSL lipase (G2956| TU4870) and acyl-CoA thioesterase (G7607| TU12515) were highly and specifically expressed in RCs. Cell wall and metabolism related genes were also highly expressed in RCs. Interestingly, genes encoding protease inhibitors, including sporamin (G13622| TU22283, G13675| TU22356), which exhibits trypsin inhibitor activity (Cai et al., 2003), and cysteine inhibitor (G8602| TU14149), showed extremely high expression levels in RCs under infected and control conditions. Next, we identified DEGs showing SC-specific expression (**Figure 8**). Metabolism, signal and cell wall related genes were specifically expressed in SCs under infected and control conditions.

Temporal Profiling of RKN Resistance Related Genes

In order to confirm the responses of genes that are specifically regulated in RCs via the constitutive defense response, we investigated for changes in expression at the early (day 7) and late period (day 28) of RKN infection using qRT-PCR (**Figure 9**). In general, the expression of RC-specific genes, such as those encoding sporamin A (G13675| TU22356), GDSL esterase/lipase (G2956| TU4870), flavin-containing monooxygenase 1 (G37877| TU62031) and metacapase 1 (G29775| TU48782), was upregulated in RCs upon *M. incognita* infection but was downregulated in SCs. Even within RCs, there were changes in the expression of each gene. The expression of sporamin A was lower in all RCs on day 28 after infection than on day 7. By contrast, the expression of GDSL esterase/lipase, flavin-containing monooxygenase 1, and metacapase 1 was higher on day 7 than on day 28 after infection. Interestingly, their levels were the highest in the resistant cultivar DJM. However, the expression of these four genes was higher in RCs than in SCs on both days 7 and 28. Detailed examination of the qRT-PCR data revealed that *M. incognita* infection triggered changes in the expression of RC-specific genes, and the defense mechanism was different between RCs and SCs.

Differential Regulation of ROS-Related Candidate Genes in Response to RKN

During RKN infection, resistance is often associated with hypersensitive response (HR)-mediated programmed cell death

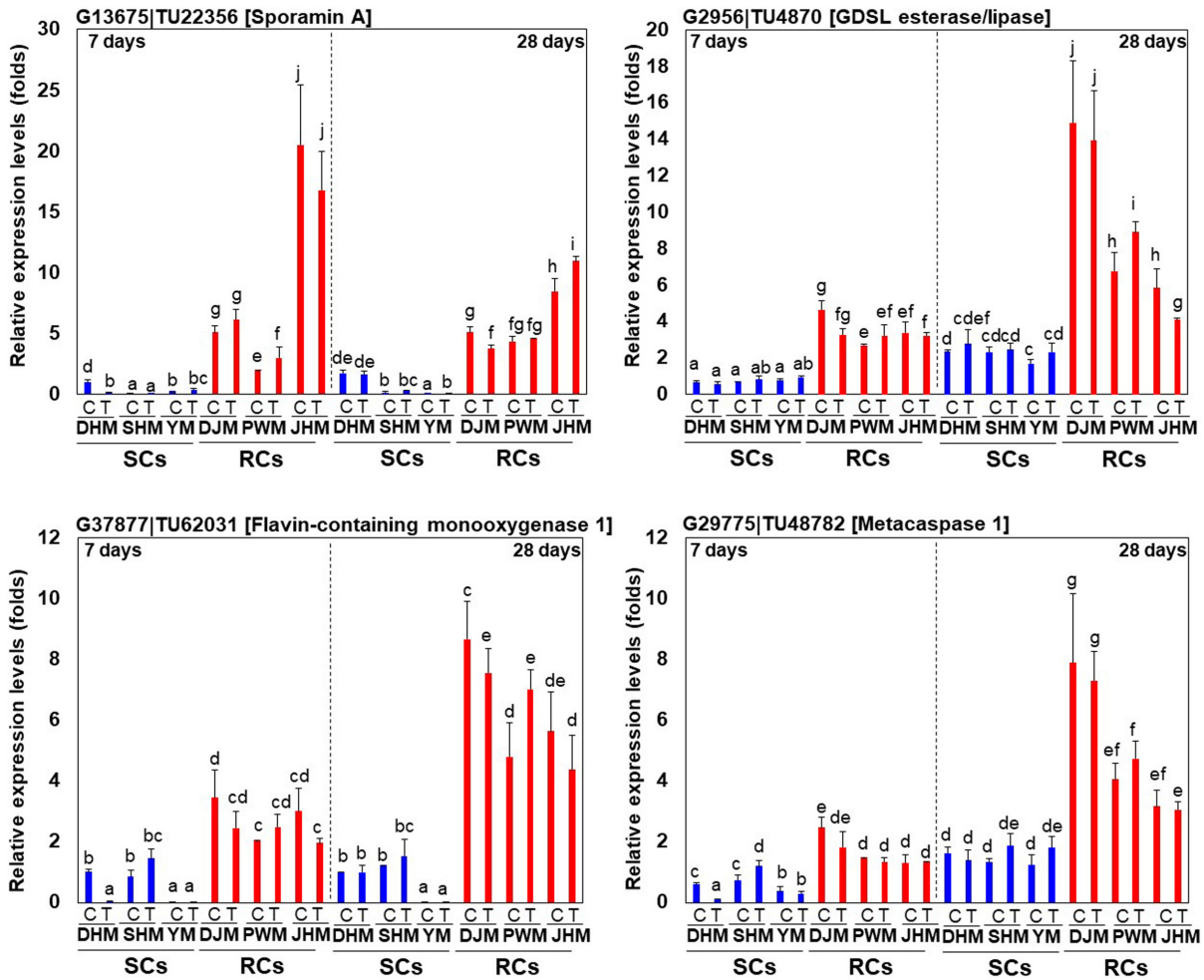

FIGURE 9 | Expression profiling of RC-specific RKN resistance marker genes. Relative transcript levels of DEGs encoding protease inhibitor sporamin A (G13675| TU22356), lipid-related GDSL lipase (G2956| TU4870), secondary metabolism-related flavin-containing monooxygenase G37877| TU62031) and protease metacaspase (G29775| TU48782) in RKN-infected sweetpotato cultivars are shown. DHM, Dahomi; DJM, Danjami; PWM, Pungwonmi; SHM, Shinhwangmi; JHM, Juhwangmi; YM, Yulmi; RCs, resistant cultivars; SCs, sensitive cultivars; C, control; T, treatment. Bars denoted with the same letter are not significantly different ($P = 0.05$) according to Dunnett's test.

(PCD), in which rapid localized cell death in root tissue around the nematode prevents the formation of a developed feeding site. This has been reported for many plant species such as tomato (Williamson, 1999; Melillo et al., 2006), pepper (Pegard et al., 2005), and coffee (Anthony et al., 2005), which show typical HR-mediated PCD during incompatible plant-RKN interactions. At the biochemical level, the rapid generation of reactive oxygen species (ROS), such as superoxide anionic radicals (O_2^-) and hydrogen peroxide (H_2O_2), is the first reaction in response to attack by avirulent and virulent pathogens. In incompatible interactions between avirulent pathogens and resistant plants, transient ROS production is followed by massive and prolonged ROS accumulation, and the latter is intimately associated with the HR response (De Gara et al., 2003). These two-phase kinetics of ROS production are typical of the incompatible defense mechanism of HR-mediated PCD. ROS play an important role in plant defense, and during pathogen attack ROS, such as H_2O_2, are generated by the enzyme superoxide dismutases (SODs), and H_2O_2 detoxifying enzymes such as ascorbate peroxidase (APX) and catalase (CAT) are often suppressed in pathogen resistant plants (Klessig et al., 2000). As a result, plants produce more ROS and interactions with these components lead to a HR-mediated defense response in plant cells. Particularly, the H_2O_2 plays a major role in triggering HR-mediated defense mechanisms in incompatible interactions between plants and pathogens including RKN (Dangl and Jones, 2001; Melillo et al., 2006). In this study, we identified DEGs that are specifically involved in the regulation of ROS (H_2O_2) generation during the defense response in RCs and SCs (**Figure 10**). In RCs, genes encoding H_2O_2 generating SODs were expressed at higher levels than in SCs, whereas genes encoding H_2O_2 scavenging cytosolic APXs (cAPXs) and CATs were expressed at lower levels in RCs than in SCs, which could indicate that RCs generate more H_2O_2 than SCs.

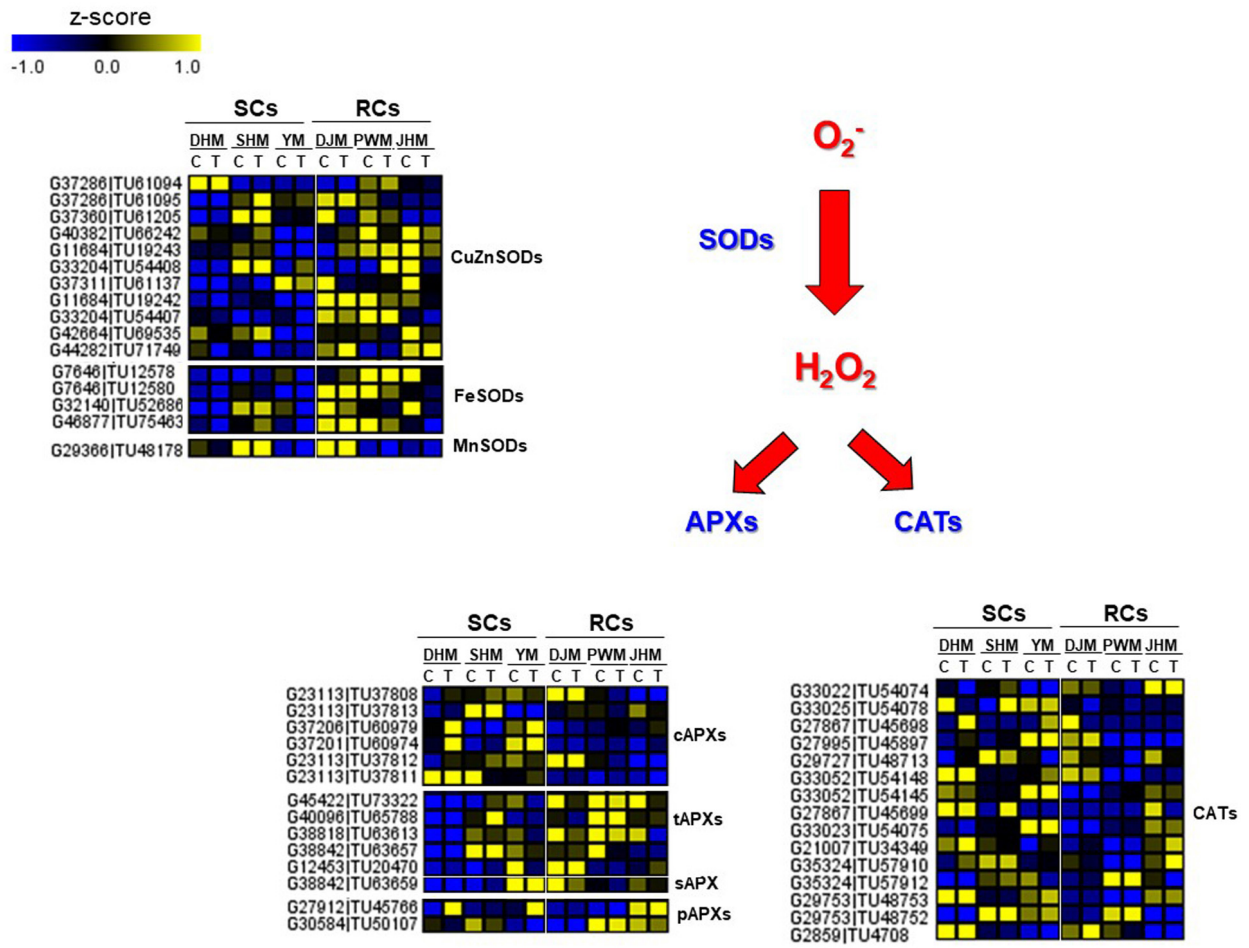

FIGURE 10 | Comparison of the relative expression levels of ROS-related genes in six sweetpotato cultivars under control and RKN-infected conditions. DEGs included the following ROS-related genes. SOD, superoxide dismutase; CuZnSOD, copper zinc SOD; FeSOD, iron SOD; MnSOD, manganese SOD; APX, ascorbate peroxidase; CAT, catalase; cAPX, cytosolic APXs; tAPX, thylakoid APX; sAPX, stroma APX; pAPX, peroxisomal APX. Cultivars were DHM, Dahomi; DJM, Danjami; PWM, Pungwonmi; SHM, Shinhwangmi; JHM, Juhwangmi; YM, Yulmi. Abbreviations are RCs, resistant cultivars; SCs, sensitive cultivars; C, control; T, treatment. The heatmap was constructed using Multi Experiment Viewer (MeV).

These DEG patterns correlated with phenotypic responses in sweetpotato (**Figure 1**).

DISCUSSION

Defense against pathogens, including plant parasitic nematodes, results from a complex set of interdependent mechanisms, ranging from mechanical and chemical barriers to the complex array of initial effector molecules in the plant immune system (Boots and Best, 2018). Preformed elements of defense, such as cell wall modification, toxic metabolites and phytochemicals, represent the first barrier for any kind of pathogenic invader. The complicated induced defense response system, which is activated upon infection, is based on the capability of plants to recognize and identify pathogenic invaders including plant parasitic nematodes. During pathogen infection, plants exhibit resistance by altering the global transcriptional responses to activate induced and/or constitutive defense. Plant parasitic nematodes induce a wide range of resistance responses in plants, with some interactions resulting in a qualitative response, which involves induced and/or constitutive defense. However, the molecular mechanisms of nematode resistance in sweetpotato are poorly understood. Although multiple resistance genes involved in qualitative response to nematode infection have been discovered in sweetpotato through transcriptome, proteome and transgenic analyses, the exact function and mode of action of these genes remain unknown (Fan et al., 2015; Zhai et al., 2016; Ha et al., 2017; Lee et al., 2019). Here, we performed a comprehensive analysis of gene expression in three RCs and three SCs of sweetpotato before and after infection with *M. incognita* infection to characterize induced and constitutive defense responses.

During the induced defense response, different resistance related genes can function in different ways in the contrasting sweetpotato cultivars. When examining gene expression data, the

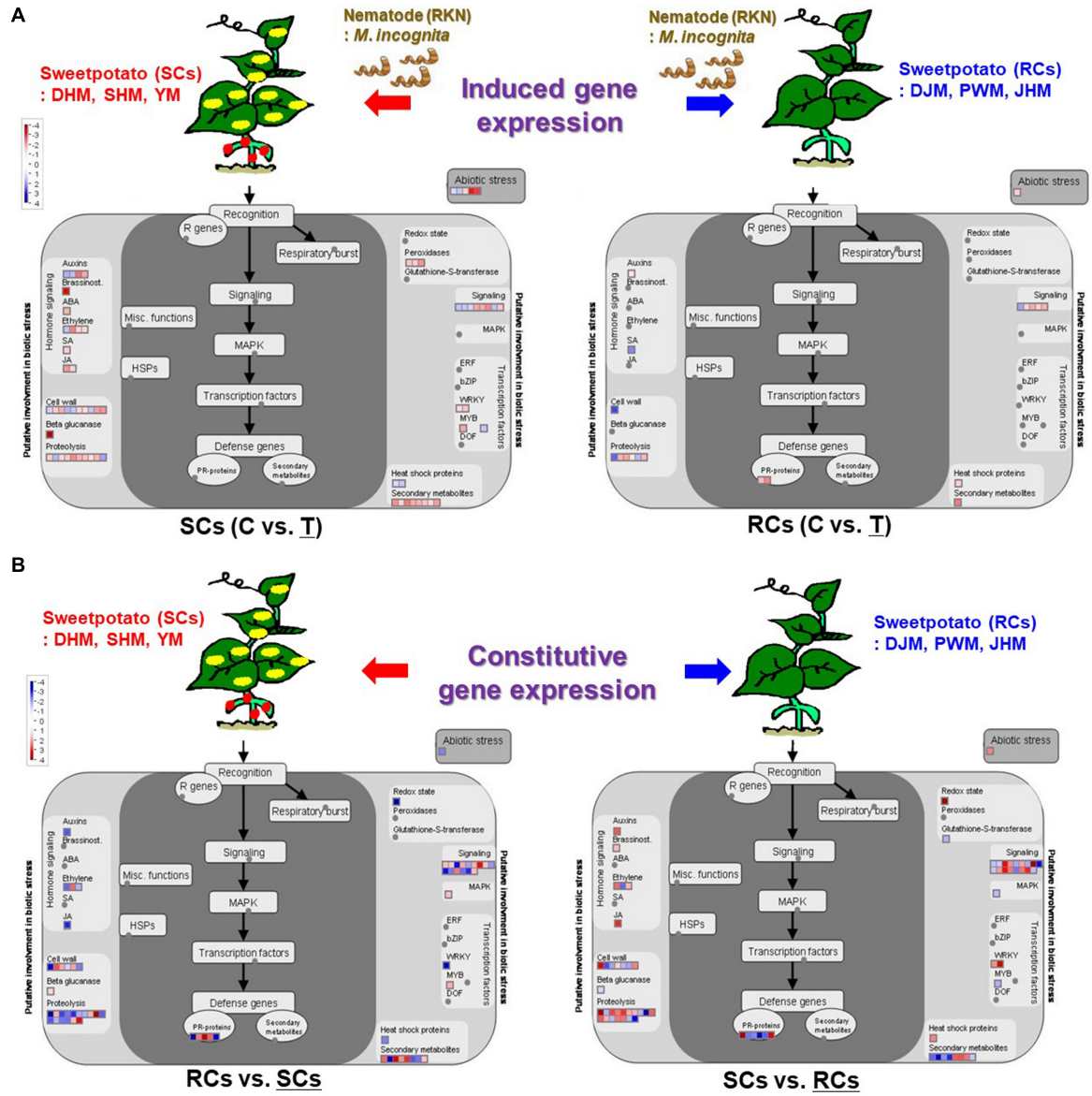

FIGURE 11 | MapMan diagram of sweetpotato genes involved in induced defense and constitutive defense response to *M. incognita* infection in SCs (left) and RCs (right). **(A)** Induced defense response to *M. incognita* infection in sweetpoato. **(B)** Constitutive defense response to *M. incognita* infection in sweetpoato. An overview of gene expression patterns (log_2FC) in infected plants relative to the untreated control is shown. Dots indicate the different paralogous genes encoding proteins related to a certain step in the defense response. Red dots indicate upregulation, blue dots indicate downregulation and gray dots indicate no response. DHM, Dahomi; DJM, Danjami; PWM, Pungwonmi; SHM, Shinhwangmi; JHM, Juhwangmi; YM, Yulmi; RCs, resistant cultivars; SCs, sensitive cultivars; C, control; T, treatment.

majority of the known resistance genes, such as those encoding ethylene biosynthesis-related ACC oxidases (G2553| TU4254, G3204| TU5260, and G20891| TU34171), polyprenol reductase (G18703| TU30556), trehalose 6-phosphate phosphatases (G42399| TU69169 and G42693| TU69581) and cationic peroxidases (G41119| TU67300 and G45573| TU73531), which are upregulated, especially in SCs, upon nematode infection, are often the central focus, as pathogen resistance pathways are expected to be induced (**Figure 4** and **Supplementary Table 3**; Bajda et al., 2009; Melillo et al., 2014; Zhang et al., 2016; Leonetti et al., 2017; Sung et al., 2019). There can also be considerable value in genes downregulated upon RKN infection, especially in SCs, which may explain RKN success (**Figure 4** and **Supplementary Table 4**) as noted in other studies (Guimaraes et al., 2015; Shukla et al., 2018).

With respect to the constitutive defense response, we identified 177 genes uniquely upregulated in RCs compared with SCs under untreated control conditions (**Figure 6** and **Supplementary Table 5**). Notably, we identified JA- or ethylene-dependent genes encoding WRKY7 (G22312| TU36474), CYP450

(G19945| TU32621, G39488| TU64782, and G10622| TU17505), GDSL lipase (G6356| TU10476 and G2956| TU4870), sporamin (G13622| TU22283, G13675| TU22356, and G34367| TU56356) and metacaspase (G29775| TU48782), indicating that the pathways involving these genes might be important for nematode defense (Wang et al., 2000, 2002; Kim et al., 2006; Kandel et al., 2007; Kwon et al., 2009; Rajendran et al., 2014; Liu et al., 2016). Interestingly, these genes were upregulated in RCs but downregulated in SCs during *M. incognita* infection (**Figures 7**, **9**). However, the involvement of these genes in nematode resistance is not verified and needs further investigation.

Figure 11 show genes involved in the response to nematode infection including those related to pathogen recognition, defense response signaling, phytohormones, cell wall metabolism, proteolysis, redox state, transcription factors and secondary metabolism. Overall, the MapMan ontology analysis enabled us to construct a genome-wide outline of the expression of sweetpotato genes that respond to *M. incognita* infection by identifying pathways involved in the main steps leading to induced and constitutive defense responses. During the induced defense response, genes related to phytohormones, cell wall and proteolysis-mediated response were upregulated in SCs during *M. incognita* infection (**Figure 11A**). Additionally, genes related to beta-glucanase, peroxidase and secondary metabolites were also upregulated. However, in RCs, genes related to phytohormones, cell wall, proteolysis, redox regulation and abiotic stress were downregulated upon *M. incognita* infection. These data suggest that SCs respond to RKN infection, whereas RCs do not exhibit induced defense response upon RKN infection. In the case of constitutive defense response, interestingly, genes involved in phytohormones (auxin, ethylene, and JA) and proteolysis-related defense signaling pathways (such as protease inhibitor and protease), which are directly or indirectly related to resistance responses and play a role in plant immunity, were upregulated in RCs under control conditions (**Figure 11B**).

Previously, we reported the proteome and transcriptome profiling of two sweetpotato cultivars, namely JHM and YM, at different temporal points after infection with the RKN *M. incognita* (Ha et al., 2017; Lee et al., 2019). The results showed that JHM was more resistant to RKN infection than YM when plants were cultivated for 50 days in a growth chamber and 90 days under greenhouse conditions. A proteomic study of 50-day cultivated sweetpotato, confirmed differences in the intensities of 64 protein spots on 2-D gel electrophoresis gels between the two cultivars during RKN infection (Ha et al., 2017). Of these 64 protein spots, 20 were identified as belonging to widely different functional categories, such as the defense response, cell structure, and energy metabolism. In a transcriptomic study of 90-day cultivated sweetpotato, 74,733 transcripts were assembled and a number of unique genes were found to be differentially expressed upon RKN infection (Lee et al., 2019). DEGs encoding transcription factors involved in various hormonal signaling-related pathways were identified as being associated with RKN infection. SA-dependent WRKY genes were not expressed or were slightly induced upon RKN infection in both cultivars. By contrast, the expression of ET-dependent ERF and JA-dependent MYC genes was more upregulated in JHM than in YM during RKN infection. Various pathogenesis-related (PR) genes activated through transcription factor dependent pathways were also regulated during RKN infection. Previous transcriptome and proteomic analysis were limited in their ability to elucidate the mechanism of RKN resistance in sweet potato because the analysis was limited to only two representative cultivars, YM and JHM. In this study, six cultivars from different origins were used and the study was conducted by dividing the cultivars into two groups according to susceptibility to RKN, namely RCs (DHM, PWM, and JHM) and SCs (DJM, SHM, and YM). Transcriptomics examined induced and constitutive defense response-related transcriptional changes in these cultivars 7 days after inoculation with RKN, which revealed transcriptional changes in genes involved in the induced defense response and constitutive defense during RKN infection. This study is the first to study to examine the common resistance and susceptibility mechanisms of sweetpotato using cultivars of different origins.

CONCLUSION

In conclusion, we identified changes in the expression of defense response-related genes in a total of six sweetpotato cultivars sensitive or resistant to *M. incognita* infection, thus characterizing the induced and constitutive defense response mechanisms. We identified many candidate genes that might trigger changes in specific induced and constitutive defense responses involved in phytohormone regulation, defense related metabolism and RKN signaling in sweetpotato. The identification of RKN resistance-related genes by marker-assisted selection could offer several advantages for nematode control in an integrated management system. Further investigation is needed to elucidate the exact role of each candidate gene in the regulation of the signaling pathway involved in the induced and/or constitutive defense response of sweetpotato during infection with RKN. Transgenic plants overexpressing or underexpressing each candidate gene will be generated to determine their roles in RKN-resistant mechanisms. Overall, our results provide valuable information for the development of crops with enhanced resistance to RKNs.

DATA AVAILABILITY STATEMENT

The original contributions presented in the study are publicly available. This data can be found here: The RNA-seq data has been uploaded to NCBI (https://www.ncbi.nlm.nih.gov/). The BioProject ID is PRJNA429283.

AUTHOR CONTRIBUTIONS

Y-HK, I-HL, DS, and HK conceived and designed the experiments. I-HL, HK, and J-WY performed the experiments. KN and K-LL analyzed the data. S-SK and JL contributed to the analyses and provided materials and reagents. Y-HK, I-HL, DS,

and HK wrote the manuscript. All authors contributed to the article and approved the submitted version.

FUNDING

This research was supported by the Basic Science Research Program through the National Research Foundation of Korea (NRF) funded by the Ministry of Science, ICT, and Future Planning (2021R1A2C400188711) and the Korea Research Institute of Bioscience and Biotechnology (KRIBB) Research Initiative Program (KGM5372113).

SUPPLEMENTARY MATERIAL

The Supplementary Material for this article can be found online at: https://www.frontiersin.org/articles/10.3389/fpls.2021.671677/full#supplementary-material

Supplementary Figure 1 | Volcano plots showing pairwise comparisons of transcript levels across samples. Log_2 fold change (logFC) between two samples is plotted on the *Y*-axis, and log_2 average of the counts normalized by size factor is shown on the *X*-axis. Red dots indicate transcripts with logFC significantly >2 or lower than –2. Black dots indicate transcripts with logFC was between –2 and 2. DHM, Dahomi; DJM, Danjami; PWM, Pungwonmi; SHM, Shinhwangmi; JHM, Juhwangmi; YM, Yulmi; RCs, resistant cultivars; SCs, sensitive cultivars; C, control; T, treatment.

REFERENCES

Afuape, S. O., Nwankwo, I. I. M., Omodamiro, R. M., Echendu, T. N. C., and Toure, A. (2014). Studies on some important consumer and processing traits for breeding sweet potato for varied end-uses. *Am. J. Exp. Agri.* 4, 114–124. doi: 10.9734/ajea/2014/5827

Anthony, F., Topart, P., Martinez, A., Silva, M., and Nicole, M. (2005). Hypersensitive-like reaction conferred by the Mex-1 resistance gene against Meloidogyne exigua in coffee. *Plant Pathol.* 54, 476–482. doi: 10.1111/j.1365-3059.2005.01239.x

Bajda, A., Postupolska, D. K., Krzymowska, M., Hennig, J., Tudek, K. S., Surmacz, L., et al. (2009). Role of polyisoprenoids in tobacco resistance against biotic stresses. *Physiol. Plant* 135, 351–364. doi: 10.1111/j.1399-3054.2009.01204.x

Boots, M., and Best, A. (2018). The evolution of constitutive and induced defences to infectious disease. *Proc. R. Soc. B* 285:20180658. doi: 10.1098/rspb.2018.0658

Braich, S., Baillie, R. C., Jewell, L. S., Spangenberg, G. C., and Cogan, N. O. I. (2019). Generation of a comprehensive transcriptome atlas and transcriptome dynamics in medicinal cannabis. *Sci. Rep.* 9:16583.

Bridge, J., and Starr, J. L. (2010). *Plant Nematodes of Agricultural Importance A Color Handbook*. San Diego, CA: Academic Press, 77–78.

Cai, D., Thurau, T., Tian, Y., Lange, T., Yeh, K. W., and Jung, C. (2003). Sporamin-mediated resistance to beet cyst nematodes (*Heterodera schachtii Schm.*) is dependent on trypsin inhibitory activity in sugar beet (*Beta vulgaris* L.) hairy roots. *Plant Mol. Biol.* 51, 839–849.

Castagnone-Sereno, P., Danchin, E. G., Perfus-Barbeoch, L., and Abad, P. (2013). Diversity and evolution of root knot nematodes, genus Meloidogyne: new insights from the genomic era. *Annu. Rev. Phytopathol.* 51, 203–220. doi: 10.1146/annurev-phyto-082712-102300

Choi, D. R., Lee, J. K., Park, B. Y., and Chung, M. N. (2006). Occutrrence of rootknot nematodes in sweet potato fields and resistance screening of sweet potato cultivars. *Kor. J. Appl. Entomol.* 45, 211–216.

Clark, C. A., and Moyer, J. W. (1998). *Compendium of Sweetpotato Diseases*. Saint Paul, MN: APS Press.

Dangl, J. L., and Jones, J. D. G. (2001). Plant pathogens and integrated defence response to infection. *Nature* 418, 203–206.

De Gara, L., de Pinto, M. C., and Tommasi, F. (2003). The antioxidant systems vis-a'-vis reactive oxygen species during plant–pathogen interactions. *Plant Physiol. Biochem.* 41, 863–870. doi: 10.1016/s0981-9428(03)00135-9

Diaz, J. T., Chinn, M. S., and Truong, V. D. (2014). Simultaneous saccharification and fermentation of industrial sweetpotatoes for ethanol production and anthocyanins extraction. *Indust. Crops Prod.* 62, 53–60. doi: 10.1016/j.indcrop.2014.07.032

Fan, W. J., Wei, Z. R., Zhang, M., Ma, P. Y., Liu, G. L., Zheng, J. L., et al. (2015). Resistance to Ditylenchus destructor infection in sweetpotato by the expression of small interfering RNAs targeting unc-15, a movement-related gene. *Phytopathology* 105, 1458–1465. doi: 10.1094/phyto-04-15-0087-r

Fassuliotis, G. (1985). "The role of nematologist in the development of resistance cultivars," in *An Advanced Treatise on Meloidogyne: Biology and Control*, Vol. I, eds J. N. Sasser and C. C. Carter (Raleigh, NC: North Carolina State University), 234–240.

Grace, M. H., Yousef, G. G., Gustafson, S. J., Truong, V. D., Yencho, G. C., and Lila, M. A. (2014). Phytochemical changes in phenolics, anthocyanins, ascorbic acid, and carotenoids associated with sweetpotato storage and impacts on bioactive properties. *Food Chem.* 145, 717–724. doi: 10.1016/j.foodchem.2013.08.107

Guimaraes, P. M., Guimaraes, L. A., Morgante, C. V., Silva, O. B. Jr., Araujo, A. C. G., Martins, A. C. Q., et al. (2015). Root transcriptome analysis of wild peanut reveals candidate genes for nematode resistance. *PLoS One* 10:e0140937. doi: 10.1371/journal.pone.0140937

Ha, J., Won, J. C., Jung, Y. H., Yang, J. W., Lee, H. U., Nam, K. J., et al. (2017). Comparative proteomic analysis of the response of fibrous roots of nematode-resistant and -sensitive sweet potato cultivars to root-knot nematode Meloidogyne incognita. *Acta Physiol. Plant.* 39:262.

Haas, B. J., Papanicolaou, A., Yassour, M., Grabherr, M., Blood, P. D., Bowden, J., et al. (2013). De novo transcript sequence reconstruction from RNA-seq using the Trinity platform for reference generation and analysis. *Nat. Prot.* 8, 1494–1512. doi: 10.1038/nprot.2013.084

Heider, B., Struelens, Q., Raye, É, Flores, C., Palacios, J., Eyzaguirre, R., et al. (2021). Intraspecific diversity as a reservoir for heat-stress tolerance in sweet potato. *Nat. Clim. Change* 11, 64–69. doi: 10.1038/s41558-020-00924-4

Howe, E. A., Sinha, R., Schlauch, D., and Quackenbush, J. (2011). RNA-Seq analysis in MeV. *Bioinformatics* 27, 3209–3210. doi: 10.1093/bioinformatics/btr490

Kandel, S., Sauveplane, V., Compagnon, V., Franke, R., Millet, Y., Schreiber, L., et al. (2007). Characterization of a methyl jasmonate and wounding-responsive cytochrome P450 of *Arabidopsis thaliana* catalyzing dicarboxylic fatty acid formation *in vitro*. *FEBS J.* 274, 5116–5127. doi: 10.1111/j.1742-4658.2007.06032.x

Kim, K. C., Fan, B., and Chen, Z. (2006). Pathogen-Induced *Arabidopsis* WRKY7 is a transcriptional repressor and enhances plant susceptibility to *Pseudomonas* syringae. *Plant Physiol.* 142, 1180–1192. doi: 10.1104/pp.106.082487

Kim, Y. H., and Yang, J. W. (2019). Recent research on enhanced resistance to parasitic nematodes in sweetpotato. *Plant Biotechnol. Rep.* 13, 559–566. doi: 10.1007/s11816-019-00557-w

Klessig, D. F., Durner, J., Noad, R., Navarre, D. A., Wendehenne, D., Kumar, D., et al. (2000). Nitric oxide and salicylic acid signaling in plant defence. *Proc. Nat. Acad. Sci. U.S.A.* 97, 8849–8855.

Kreuze, J. (2002). "Molecular studies on the sweetpotato virus disease and its two causal agents," in *Acta Universitatis Agriculturae Sueciae Agraria 335*. Dept. of Plant Biology, Sveriges lantbrukuniversitet, Uppsala.

Kwon, S. J., Jin, H. C., Lee, S., Nam, M. H., Chung, J. H., Kwon, S. I., et al. (2009). GDSL lipase-like 1 regulates systemic resistance associated with ethylene signaling in *Arabidopsis*. *Plant J.* 58, 235–245. doi: 10.1111/j.1365-313x.2008.03772.x

Lam, E., Kato, N., and Lawton, M. (2001). Programmed cell death, mitochondria and the plant hypersensitive response. *Nature* 411, 848–853. doi: 10.1038/35081184

Lee, I. H., Shim, D., Jeong, J. C., Sung, Y. W., Nam, K. J., Yang, J. W., et al. (2019). Transcriptome analysis of root-knot nematode (Meloidogyne incognita)-resistant and susceptible sweetpotato cultivars. *Planta* 249, 431–444. doi: 10.1007/s00425-018-3001-z

Lee, J. J., Park, K. W., Kwak, Y. S., Ahn, J. Y., Jung, Y. H., Lee, B. H., et al. (2012). Comparative proteomic study between tuberous roots of light orange- and purple-fleshed sweetpotato cultivars. *Plant Sci.* 19, 120–129. doi: 10.1016/j.plantsci.2012.06.003

Lee, S. H., Shim, D., Lee, K. L., Nam, K. J., Yang, J. W., Lee, J. J., et al. (2020). Expression analysis of sweetpotato NADPH oxidase-encoding Rboh genes in response to infection with the root knot nematode Meloidogyne incognita. *Plant Biotechnol. Rep.* 14, 635–642. doi: 10.1007/s11816-020-00631-8

Leonetti, P., Zonno, M. C., Molinari, S., and Altomare, C. (2017). Induction of SA-signaling pathway and ethylene biosynthesis in Trichoderma harzianum-treated tomato plants after infection of the root-knot nematode Meloidogyne incognita. *Plant Cell Rep.* 36, 621–631. doi: 10.1007/s00299-017-2109-0

Liu, H., Deng, Z., Chen, J., Wang, S., Hao, L., and Li, D. (2016). Genome-wide identification and expression analysis of the metacaspase gene family in Hevea brasiliensis. *Plant Physiol. Biochem.* 105, 90–101. doi: 10.1016/j.plaphy.2016.04.011

Livak, K. J., and Schmittgen, T. D. (2001). Analysis of relative gene expression data using realtime quantitative PCR and the 2-ΔΔCT method. *Methods* 25, 402–408. doi: 10.1006/meth.2001.1262

Melillo, M. T., Leonetti, P., Bongiovanni, M., Castagnone-Sereno, P., and Bleve-Zacheo, T. (2006). Modulation of reactive oxygen species activities and H2O2 accumulation during compatible and incompatible tomato–root-knot nematode interactions. *New Phytol.* 170, 501–512. doi: 10.1111/j.1469-8137.2006.01724.x

Melillo, M. T., Leonetti, P., and Veronico, P. (2014). Benzothiadiazole effect in the compatible tomato-Meloidogyne incognita interaction: changes in giant cell development and priming of two root anionic peroxidases. *Planta* 240, 841–854. doi: 10.1007/s00425-014-2138-7

Palomares-Rius, J. E., and Kikuchi, T. (2013). -Omics fields of study related to plant-parasitic nematodes. *J. Integ. Omic.* 3, 1–10. doi: 10.1080/03235408.2021.1890912

Park, S. C., Kim, Y. H., Ji, C. Y., Park, S., Jeong, J. C., Lee, H. S., et al. (2012). Stable internal reference genes for the normalization of real-time PCR in different sweetpotato cultivars subjected to abiotic stress conditions. *PLoS One* 7:e51502. doi: 10.1371/journal.pone.0051502

Pegard, A., Brizzard, G., Fazari, A., Soucaze, O., Abad, P., and Djian Caporalino, C. (2005). Histological characterization of resistance to different root-knot nematode species related to phenolics accumulation in Capsicum annuum. *Phytopathology* 95, 158–165. doi: 10.1094/phyto-95-0158

Rajendran, S., Lin, I. W., Chen, M. J., Chen, C. Y., and Yeh, K. W. (2014). Differential activation of sporamin expression in response to abiotic mechanical wounding and biotic herbivore attack in the sweet potato. *BMC Plant Biol.* 14:112. doi: 10.1186/1471-2229-14-112

Shukla, N., Yadav, R., Kaur, P., Rasmussen, S., Goel, S., Agarwal, M., et al. (2018). Transcriptome analysis of root-knot nematode (Meloidogyne incognita)-infected tomato (*Solanum lycopersicum*) roots reveals complex gene expression profiles and metabolic networks of both host and nematode during susceptible and resistance responses. *Mol. Plant Pathol.* 19, 615–633. doi: 10.1111/mpp.12547

Sung, Y. W., Lee, I. H., Shim, D., Lee, K. L., Nam, K. J., Yang, J. W., et al. (2019). Transcriptomic changes in sweetpotato peroxidases in response to infection with the root-knot nematode Meloidogyne incognita. *Mol. Biol. Rep.* 46, 4555–4564. doi: 10.1007/s11033-019-04911-7

Wang, C., Zien, C. A., Afitlhile, M., Welti, R., Hildebrand, D. F., and Wang, X. (2000). Involvement of phospholipase D in wound-induced accumulation of jasmonic acid in *Arabidopsis*. *Plant Cell* 12, 2237–2246. doi: 10.2307/3871117

Wang, S. J., Lan, Y. C., Chen, S. F., Chen, Y. M., and Yeh, K. W. (2002). Wound-response regulation of the sweet potato sporamin gene promoter region. *Plant Mol. Biol.* 48, 223–231.

Williamson, V. M. (1999). Plant nematode resistance genes. *Curr. Opin. Plant Biol.* 2, 327–331. doi: 10.1016/s1369-5266(99)80057-0

Wittstock, U., and Gershenzon, J. (2002). Constitutive plant toxins and their role in defense against herbivores and pathogens. *Curr. Opin. Plant Biol.* 5, 300–307. doi: 10.1016/s1369-5266(02)00264-9

Zhai, H., Wang, F., Si, Z., Huo, J., Xing, L., An, Y., et al. (2016). A myo-inositol-1-phosphate synthase gene, IbMIPS1, enhances salt and drought tolerance and stem nematode resistance in transgenic sweetpotato. *Plant Biotechnol. J.* 14, 592–602. doi: 10.1111/pbi.12402

Zhang, H., Hong, Y., Huang, L., Liu, S., Tian, L., Dai, Y., et al. (2016). Virus-induced gene silencing-based functional analyses revealed the involvement of several putative trehalose-6-phosphate synthase/phosphatase genes in disease resistance against Botrytis cinerea and *Pseudomonas* syringae pv. tomato DC3000 in tomato. *Front. Plant Sci.* 7:1176. doi: 10.3389/fpls.2016.01176

Conflict of Interest: The authors declare that the research was conducted in the absence of any commercial or financial relationships that could be construed as a potential conflict of interest.

frontiers in Plant Science

ORIGINAL RESEARCH
published: 10 May 2021
doi: 10.3389/fpls.2021.640714

Impact of Wheat on Soybean Cyst Nematode Population Density in Double-Cropping Soybean Production

Leonardo F. Rocha[1], Mirian F. Pimentel[1], John Bailey[2], Terry Wyciskalla[3], Dan Davidson[4], Ahmad M. Fakhoury[1] and Jason P. Bond[1]**

[1] School of Agricultural Sciences, Southern Illinois University, Carbondale, IL, United States, [2] JCB Ag Research, Effingham, IL, United States, [3] Wyciskalla Consulting, Nashville, IL, United States, [4] Davidson Consulting, Stanton, NE, United States

OPEN ACCESS

Edited by:
Shahid Siddique, University of California, Davis, United States

Reviewed by:
Johannes Hallmann, Julius Kühn-Institut - Braunschweig, Germany
Shree Pariyar, Helmholtz-Verband Deutscher Forschungszentren (HZ), Germany

***Correspondence:**
Leonardo F. Rocha
leonardo.rocha@siu.edu
Jason P. Bond
jbond@siu.edu

Specialty section:
This article was submitted to Plant Pathogen Interactions, a section of the journal Frontiers in Plant Science

Received: *11 December 2020*
Accepted: *29 March 2021*
Published: *10 May 2021*

Citation:
Rocha LF, Pimentel MF, Bailey J, Wyciskalla T, Davidson D, Fakhoury AM and Bond JP (2021) Impact of Wheat on Soybean Cyst Nematode Population Density in Double-Cropping Soybean Production. Front. Plant Sci. 12:640714. doi: 10.3389/fpls.2021.640714

Double-cropping is defined as producing more than one crop on the same parcel of land in a single growing season. It is reported to have many benefits when incorporated in cropping systems, including improving soil health. In some double-cropping systems, soybean is planted following winter wheat. The soybean cyst nematode (SCN) (*Heterodera glycines* Ichinohe) is a major soybean pathogen, and several reports suggest suppressive effects of wheat on SCN populations. Field trials were conducted from 2017 to 2018 to investigate the effect of wheat on SCN populations in double-cropping soybean. Nine fields with three levels of initial SCN populations (low, moderate, and high) were selected in Illinois. Wheat was planted in strips alternating with strips-maintained weed-free and under fallow over winter and early spring. Soybean was planted in all strips after wheat harvest. SCN egg densities were acquired at four time points: wheat establishment, post-wheat/pre-soybean, mid-soybean (R1 growth stage or beginning of flowering), and post-soybean harvest. Wheat strips reduced SCN egg densities compared with fallow strips at the R1 stage (−31.8%) and after soybean harvest (−32.7%). Double-cropping soybean with wheat has the potential to suppress SCN field populations and is a system with the potential to provide additional farm income. This study is meant to be a first step toward a better understanding of the mechanisms that govern the suppression of SCN by wheat.

Keywords: SCN, *Heterodera glycines*, soybean diseases, crop rotation, plant-parasitic nematodes, integrated pest management, nematode suppression, suppressive soils

INTRODUCTION

Many modern cropping systems are based on the cultivation of single crops in yearly rotations. However, fall-planted crops have been increasingly incorporated due to resulting weed suppression and enhanced environmental stewardship (Leslie et al., 2017). Double-cropping is defined as producing more than one crop on the same parcel of land in a single growing season. This system is being adopted as one of the multiple strategies used to increase biomass productivity in agricultural lands and to help supply the increasing demand for food and feed (Caviglia and Andrade, 2010). Compared with monocropping, double-cropping systems stand out in capturing radiation and

rainfall and more effectively using inputs, thus allowing to optimize the exploitation of the potential productivity of fields (Caviglia et al., 2004; Heggenstaller et al., 2009). In the United States, crops established in the fall are harvested in late spring and followed directly by a second warm-season crop (Heggenstaller et al., 2009). Due to the shorter growing season and fewer winter crop options, this practice is less adopted in the Midwest compared with southern and mid-southern areas of the United States (Heggenstaller et al., 2009).

Double-cropped soybeans are commonly planted in fields following the harvest of winter wheat in mid to late June (Nafziger, 2009). Although two distinct crops are grown in one season, farmers are still recommended to rotate summer crops, as double-cropping is not considered a crop rotation. In Illinois, double-cropping has been more successful in the southern portion of the state, where favorable weather conditions allow earlier wheat harvest and soybean planting, while warmer weather in the fall season allows winter crops to grow for an extended window before being exposed to freezing temperatures (Nafziger, 2009). Shorter soybean growing windows due to late wheat harvest may lead to reduced vegetative development before flowering and consequential yield reduction (Nafziger, 2009). Therefore, the main factors reducing yield in double-cropping soybean are later planting dates, water deficit, reduced radiation/photoperiod, the effect of winter crop residues, nutrient deficits, and susceptibility to early frost (Hansel et al., 2019). Nevertheless, the benefits of double-cropping include improvement of soil chemical and physical properties, control of erosion, reduction in tillage requirements, economic value of two crops in the same season, and improved soil microbial and faunal activity (Peralta et al., 2018).

The soybean cyst nematode (SCN) (*Heterodera glycines* Ichinohe) is a major plant-parasitic nematode on soybean, and it is widely distributed in all major soybean production areas of the United States (Niblack and Tylka, 2008). In Illinois, SCN is present in more than 80% of the fields (Niblack et al., 2009) and in every county (Tylka and Marett, 2017). SCN causes losses of up to 60% in susceptible cultivars (Hershman, 2014), and often losses of up to 30% occur without showing noticeable aboveground symptoms (Mueller et al., 2016; Tylka and Marett, 2017). In a survey from 2010 to 2014, soybean yield losses caused by SCN nationwide were estimated to be twice those caused by other diseases combined (Allen et al., 2017). In order to reduce losses, several management practices are recommended, including using resistant and tolerant cultivars, crop rotation with non-hosts, weed management, seed-applied nematicides, and biological control products (Niblack and Tylka, 2008; Niblack et al., 2009; Wight et al., 2011; Mueller et al., 2016). Currently, most commercial cultivars available within Illinois share a common source of resistance, the plant introduction (PI) 88788. Over the years, the lack of rotation among sources of resistance led to the selection of SCN populations able to reproduce on available resistant soybean cultivars (Niblack and Tylka, 2008). This has resulted in the reduction of management options available for farmers.

Several research reports show significant suppression effects of wheat on SCN populations, but many do not separate effects of tillage from cover crops or assess the effect of the initial SCN population on the system (Baird and Bernard, 1984; Koenning, 1991; Hershman and Bachi, 1995; Long and Todd, 2001; Warnke et al., 2006; Wight et al., 2011; Bernard, 2018). In addition, most wheat/SCN research was conducted in the midsouth and southern United States and in small plot trials. Farmers commonly use wheat in double-cropping soybean systems in Illinois, and this cropping system has the potential to be expanded to soybean farming areas in higher latitudes of the United States (Zabel et al., 2014; Seifert and Lobell, 2015). Therefore, the objective of this work was to assess the effect of wheat on SCN population densities in double-cropping soybean in farming conditions in Illinois.

MATERIALS AND METHODS

Field Establishment

This study was conducted in row crop fields provided by farmers, located in commercial farms in Illinois. The fields were selected based on the results from an initial SCN field survey performed in 2017 (**Supplementary Table 1**). The SCN population densities were determined in 22 fields in seven counties. From this survey, nine fields were identified for use in this study, including three locations each for low, moderate, and high initial SCN population densities (**Figure 1**). Fields with >6,500 eggs/100 cm^3 of soil were classified as high SCN. Those with 2,000–6,500 eggs/100 cm^3 were classified as moderate, and fields with <2,000 eggs/100 cm^3 were classified as low SCN (adapted from the University of Illinois Extension, 2014). The SCN HG (*H. glycines*) type was determined for field populations as described by Niblack et al. (2002). HG type testing is a greenhouse assay that quantifies how much SCN populations reproduce on sources of resistance available in soybean cultivars, replacing the race classification system. All field populations were HG type 2.5.7 with the exception of field 8, which was HG type 7 (**Supplementary Table 1**). HG type 2.5.7 has reproduction greater than or equal to 10% of that observed on the susceptible (Lee 74) on the soybean indicator lines PI88788, PI209332, and PI548316 (Cloud). HG type 7 indicates reproduction greater than or equal to 10% of the susceptible g only for PI548316 (Cloud) (Tylka, 2016). Location descriptions including initial SCN populations, rainfall, and soil chemical analysis are listed in **Table 1**.

All fields were planted using commercial soybean cultivars with resistance to SCN (PI88788) in the previous summer (2017). In each location, the experimental design consisted of two treatments (WT: winter wheat and FL: fallow) with three replications. Each treatment was in strips (9.14 m wide × 182.9 m long), with three strips assigned for winter wheat and three strips that remained for fallow. Strips were subdivided into three subplots (9.14 m wide × 61.0 m long for soil sampling). Thus, the study consisted of a total of 18 subplots with a total of 1.1 hectares per location (**Figure 2**). Wheat was planted in fall 2017, and 2 weeks after emergence, wheat was terminated with herbicides to establish and maintain fallow strips. Herbicides were applied over winter to keep plots weed-free and prevent any potential SCN reproduction on volunteer soybeans and weeds,

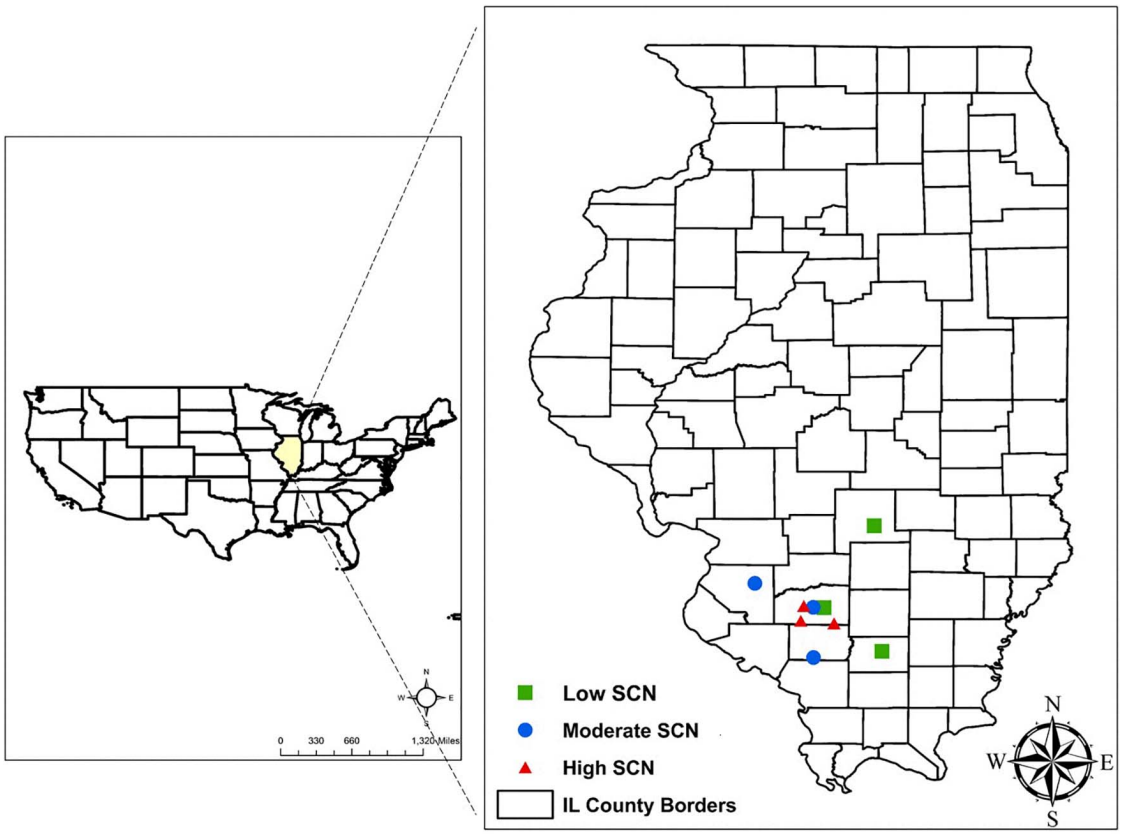

FIGURE 1 | Field locations selected in Illinois to study the impact of wheat on soybean cyst nematode (SCN) in double-cropping soybean. SCN population densities were defined as high SCN when having >6,500 eggs/100 cm^3 of soil, moderate for 2,000–6,500 eggs/100 cm^3, and low when <2,000 eggs/100 cm^3.

TABLE 1 | Field locations, initial SCN population densities, soil chemical properties, and cumulative rainfall.

Field	IL county	Soybean cyst nematode		Rainfall (mm)[4]	pH[1]	OM (%)	P[2]	K[2]	Mg[2]	Ca[2]	[3]CEC
		Egg density[5]	Level[6]				mg kg^{-1}				
1	Perry	3,902	Moderate	680.72	6.3	2.7	27	85	65	1,134	7.6
2	St. Clair	2,140	Moderate	643.34	6.4	2.6	33	124	143	1,624	10.8
3	Washington	667	Low	790.45	5.7	2.7	16	85	77	1,161	9.1
4	Fayette	600	Low	710.69	5.3	2.1	33	76	68	826	8.1
5	Franklin	940	Low	670.56	6.8	2.8	32	101	195	1,350	9.4
6	Washington	7,700	High	790.45	7.0	2.1	50	85	90	1,526	8.6
7	Washington	8,858	High	790.45	6.1	2.0	57	91	71	994	7.0
8	Washington	8,626	High	790.45	6.5	2.3	32	116	86	1,239	8.4
9	Washington	3,909	Moderate	790.45	6.3	3.6	46	138	100	1,753	11.5

[1] *(1:1 H_2O).*
[2] *Mehlich-3 (M3).*
[3] *Total cation exchange capacity meq/100 g.*
[4] *Average county rainfall during field trials (November 17 to October 18).*
[5] *Expressed in eggs/100 cm^3.*
[6] *SCN population densities were defined as high SCN when having >6,500 eggs/100 cm^3 of soil, moderate for 2,000–6,500 eggs/100 cm^3, and low when <2,000 eggs/100 cm^3.*

since more than a 100 weed species are reported to be potential hosts of SCN (Rocha et al., 2021). Soybean was planted in all subplots following wheat harvest in June 2018 using cultivars with resistance to SCN (PI88788), as this is a widely available resistance source in commercial cultivars, allowing thus to better simulate conditions experienced by soybean producers. Soybean was harvested in September 2018 and yield was assessed. All field operations from planting to harvest were conducted by producer

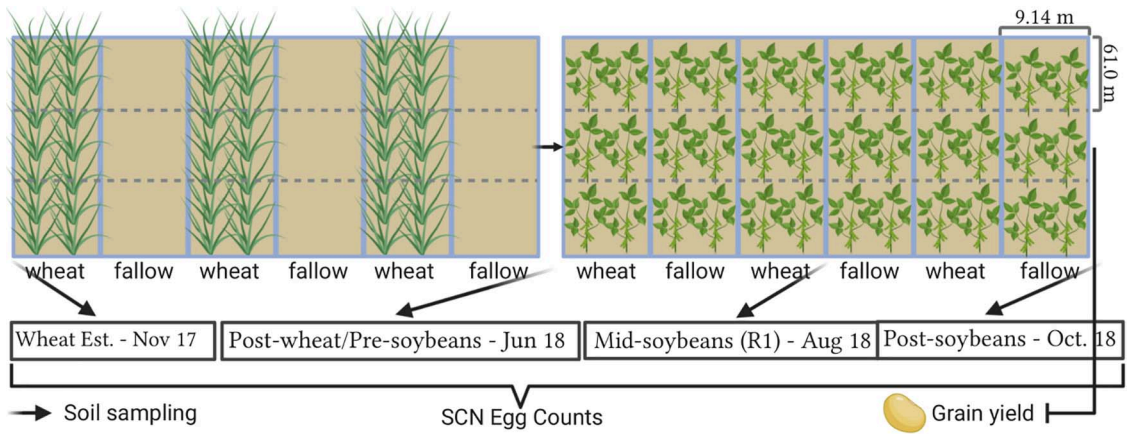

FIGURE 2 | Field trial layout and sampling intervals. Plot representations are not in scale. Created with BioRender® (Biorender.com).

collaborators across the entire study area at each location, with the exception of herbicide applications in fallow plots. A list of all soybean and wheat cultivars, planting dates, and fertilizers and herbicides used, as well as soil descriptions, is available in **Supplementary Table 3**.

Soil Sampling and SCN Egg Density

The population densities of SCN were assessed at four intervals in this study. Soil samples were collected at wheat establishment (1: November 2017—2 weeks after wheat emergence or Feekes 2); in the window after wheat harvest and soybean planting (2: June 2018); at soybean growth stage R1, which denotes beginning of flowering (3: August 2018); and after soybean harvest (4: October 2018). From each location, a total of 18 soil samples were collected (2 treatments × 3 replicates × 3 subsamples per replicate) for each of the four sampling intervals. A total of 648 samples were collected and processed for this study.

Soil samples were collected from subplots at each of the four intervals using a cylindrical soil probe. Each sample was a composite of 20 soil cores (2.5 cm diam. × 20 cm deep) collected in a zigzag pattern, bulked in a bucket, sieved through a 6,350-μm pore mesh, and stored in a cooler for transport. Subsequent soil samples were collected approximately in the same area at each time point, as points were georeferenced, maintaining a 0.30-m foot distance from the previous sampling spot to avoid effects of disturbed soil on surrounding SCN egg densities. SCN cysts were extracted from 100 cm^3 of soil by wet-sieving through nested 707- and 250-μm pore sieves. Eggs were extracted from the cysts and stained with acid fuchsin to facilitate visualization, and density was assessed using a counting slide (Chalex Corporation, Grasonville, MD, United States) under a Nikon SMZ-645 stereoscope. SCN population densities were expressed in eggs/100 cm^3 of soil.

Data Analysis

Statistical analyses were performed using SAS version 9.4 (SAS Institute Inc., Cary, NC, United States). Population densities of SCN were analyzed at each sampling interval using a generalized linear mixed model applying the GLIMMIX procedure with Poisson distribution and a log link function. Initial SCN population densities, winter rotation, and their interaction were considered fixed effects, whereas initial SCN population densities within field location, replications and treatments within subplots, and subplots within field location were considered random effects. When the main effects were significant ($P < 0.05$), the means were separated using Tukey's HSD test ($P = 0.05$).

RESULTS

Soybean cyst nematode population densities were enumerated at four sampling intervals to assess the effect of the winter option—wheat or fallow—on SCN egg densities and to monitor subsequent fluctuations in SCN population densities over time. The effects of initial SCN population densities (I), winter rotation (W), and the interaction between these two factors (I * W) on egg densities are presented in **Table 2**. Fluctuations in field population densities over time are displayed in **Figure 3**.

At wheat establishment, an initial SCN population density was determined to create a baseline for this study (**Table 2**). In the sampling interval following the wheat growing season and prior to soybean planting, the main factor driving SCN egg densities at wheat harvest was the field initial SCN population density ($F = 41.465$; $P < 0.0001$). Since wheat is a non-host of SCN, neither winter option ($F = 0.540$; $P = 0.4638$) nor factorial interaction (I * W) ($F = 0.062$; $P = 0.9399$) affected SCN egg densities (**Table 2**).

At R1 soybeans (beginning of flowering), the initial SCN population density was a driver of SCN egg densities at mid-soybean ($F = 8.142$; $P = 0.0004$). The SCN egg density was also significantly affected by winter option ($F = 9.390$; $P = 0.0026$) (**Table 2**). In fact, SCN egg densities were reduced by 31.8% in wheat strips compared with fallow strips (**Table 3**). It is to be noted that the factorial interaction (I * W) was non-significant ($F = 1.582$; $P = 0.2093$) on SCN egg densities (**Table 2**). At this interval, SCN population densities significantly dropped

TABLE 2 | ANOVA table indicating the effect of SCN initial population density (I—low, moderate, or high[1]) and winter rotation (W—fallow or wheat) on the number of SCN eggs (eggs/100 cm^3 of soil) at four time points throughout the soybean season.

SCN egg densities			
Source	***DF***	***F* ratio**	***P* > *F***
1: Wheat establishment			
SCN initial pop. (I)	2	21.167	<0.0001*
Winter rotation (W)	1	0.749	0.3882
I * W	2	1.207	0.3020
2: Post-wheat/pre-soybean			
SCN initial pop. (I)	2	41.465	<0.0001*
Winter rotation (W)	1	0.540	0.4638
I * W	2	0.062	0.9399
3: Mid-soybean (R1)			
SCN initial pop. (I)	2	8.143	0.0004*
Winter rotation (W)	1	9.390	0.0026*
I * W	2	1.582	0.2093
4: Post-soybean			
SCN initial pop. (I)	2	16.387	<0.0001*
Winter rotation (W)	1	9.769	0.0021*
I * W	2	2.6416	0.0747
Soybean yield			
SCN initial pop. (I)	2	1.008	0.4288
Winter rotation (W)	1	59.898	<0.0001*
I * W	2	2.166	0.1192

**Indicates a significant effect of the factor on the tested variable ($P < 0.05$).*
[1]SCN population densities were defined as high SCN when having >6,500 eggs/100 cm^3 of soil, moderate for 2,000–6,500 eggs/100 cm^3, and low when <2,000 eggs/100 cm^3.

across fields and treatments, demonstrating an attrition of SCN populations throughout time (**Figure 3**).

After soybean harvest, the results follow a trend similar to what was observed at the mid-soybean sampling interval (R1). Both initial SCN population density ($F = 16.387$; $P < 0.0001$) and winter option ($F = 9.769$; $P = 0.0021$) impacted SCN egg densities (**Table 3**). SCN egg densities in wheat strips were reduced by 32.7% compared with those in fallow strips. In addition, there was an overall upsurge in SCN population densities across fields and treatments, demonstrating an increase in SCN egg densities in later soybean reproductive stages. At this sampling interval, the factorial interaction (I * W) was non-significant ($F = 2.6416$; $P = 0.0747$) on the SCN egg densities.

An overall increase in SCN egg densities was observed at harvest, but the SCN population recovery rate was slower in wheat strips in comparison with that in fallow strips (**Figure 3**). These results are confirmed when analyzing population ratios comparing end of soybean season egg counts to soybean planting (October 2018/June 2018). Such ratios allow to observe population dynamics throughout the soybean growing season. Fields with low initial SCN population experienced higher population increase rates (9.441) compared with fields with moderate (1.1183) and high (1.015) ($F = 19.166$; $P < 0.001$) initial SCN populations (**Supplementary Table 2** and **Figure 3**). In fallow plots, the average population ratio was 4.999, whereas in double-cropping plots, those ratios were statistically lower and equal to 1.811 ($F = 12.263$; $P = 0.0006$) (**Supplementary Table 2**). These results support the conclusions drawn from the time point analysis, highlighting a reduction in SCN reproduction in double-cropping fields. A pattern of increase in SCN population density under fallow is especially observed in fields with high and low initial SCN population densities. In fields with a moderate population level, initial population densities were slightly higher in wheat plots at the beginning of the experiment, even though not statistically significant, and this was probably due to patchiness (non-homogeneity) in the distribution of SCN. In those fields, although final egg densities were similar, SCN population densities were reduced over time in wheat strips (**Figure 3**).

The winter option significantly impacted soybean yield ($F = 59.89$; $P < 0.0001$). Soybean yield was reduced by 300 kg per hectare (4.45 bushel/acre or 7.5%) on average in wheat strips compared with that in fallow strips (**Table 4**). There was no detected effect of the initial SCN population level ($F = 1.01$; $P < 0.4288$) nor of the factorial interaction (I * W) on soybean yield ($F = 2.17$; $P = 0.1192$) (**Table 2**).

DISCUSSION

Field trials were conducted with normal production practices in Illinois to assess the effect of wheat on SCN populations in double-cropping soybean. This study was conducted at locations further north than prior research. In addition, by expanding plot sizes and conducting trials in production fields, this study more closely simulates conditions experienced by producers. In soybean, SCN management is predominantly based on the use of resistant cultivars, crop rotation, and the application of nematicides *via* seed treatment. Management practices such as crop rotation and cover crops may reduce SCN populations, although SCN demonstrates the ability to survive in fields for years in the absence of growing soybean (Francl and Dropkin, 1986). This indicates that even a long-term rotation with non-hosts may not be sufficient to eliminate SCN from fields (Wight et al., 2011).

In this study, SCN egg densities were similar in wheat strips compared with fallow strips at wheat harvest. At that sampling interval, the main driver of SCN egg density was the initial SCN population densities. Furthermore, SCN egg densities did not fluctuate significantly during the wheat growing season, since wheat is a non-host of SCN, with comparable SCN population densities post-wheat harvest and at wheat establishment. Spring temperatures in Illinois were below average in 2018, especially in April, marking the second coldest record for this month for the state (Kerschner, 2018), possibly delaying SCN hatching and early development. Winter survival rates of SCN in the Midwest may attain 100%, which adds additional pressure on management practices aimed at maintaining or increasing soybean yield, since fields may be harboring high initial SCN inoculum at planting (Riggs et al., 2001). Data from double-cropping studies in the literature indicate that SCN population densities at soybean planting were not affected following wheat, yet plots with wheat

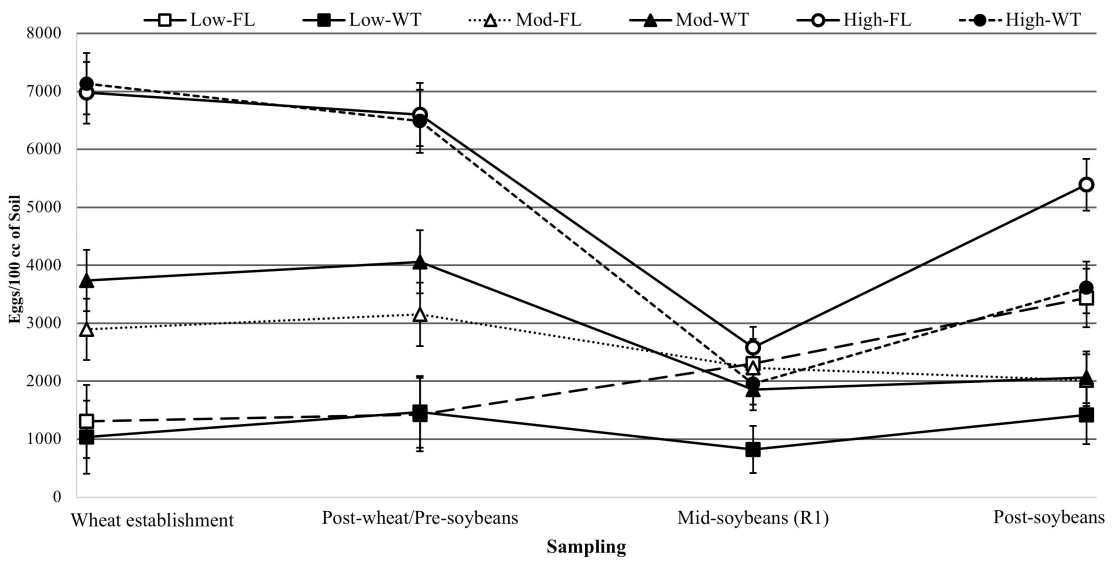

FIGURE 3 | Egg densities (eggs/100 cm^3 of soil) over time in soybean fields with low, high, or moderate initial SCN populations following winter wheat (WT) or fallow (FL). * Denotes significant differences in egg densities between winter options for all initial populations at that time point ($P < 0.05$).

TABLE 3 | Effects of initial SCN population density (I—low, moderate, or high) and winter rotation (W—fallow or wheat) on SCN egg densities (eggs/100 cm^3 of soil).

Factor	Level[1]	Wheat establishment			Post-wheat/Pre-soy			Mid-soybean (R1)			Post-soybean		
		Mean	Group	SE[2]	Mean	Group	SE	Mean	Group	SE	Mean	Group	SE
Initial pop.	Low	1,166.8	C	446.9	1,448.3	C	442.3	1,488.8	B	290.1	2,427.1	B	357.9
	Moderate	3,317.0	B	374.9	3,605.9	B	385.3	2,041.5	A	252.7	2,040.4	B	315.6
	High	7,056.3	A	374.9	6,543.0	A	385.3	2,268.5	A	252.7	4,504.0	A	315.6
Winter rotation	Fallow	3,726.2	A	326.9	3,944.3	A	332.4	2,347.3	A	218.0	3,628.8	A	269.7
	Wheat	3,969.5	A	326.9	4,207.2	A	329.2	1,601.1	B	215.9	2,442.3	B	269.7

Means followed by the same letter in the columns at each time of sampling are not different following Tukey's HSD Test (P = 0.05).
[1]SCN population densities were defined as high SCN when having >6,500 eggs/100 cm^3 of soil, moderate for 2,000–6,500 eggs/100 cm^3, and low with <2,000 eggs/100 cm^3.
[2]Standard error.
*Factorial interaction (I * W) was non-significant.*

residue were reported to show reduced SCN population densities at soybean harvest (Hershman and Bachi, 1995). Results from Rothrock and Kirkpatrick (2018) denoted no differences in SCN population densities in early season, late season, or postharvest among winter cover crops, including wheat. Others have shown potential suppressive effects of cover crops on SCN population densities at soybean planting. However, these studies allude to high initial SCN populations and exponential reproduction driving population densities at later stages, with yield losses being observed especially when susceptible cultivars are used (Long and Todd, 2001; McSorley, 2011).

At the R1 growth stage of soybean (beginning of flowering), our data reflected a reduction in SCN egg densities in wheat strips compared with fallow. At this sampling interval, the SCN egg density was affected by the initial SCN population densities. The literature suggests environmental factors, influence of wheat stubble and wheat root exudates, and mechanical interference with host recognition by SCN as possible factors leading to reduced SCN population densities where wheat preceded soybean. However, results from this field trial and from the literature demonstrate that the suppressive effects of wheat on SCN are not fully expressed at soybean planting, suggesting that wheat production alone may not explain all SCN suppression (Baird and Bernard, 1984; Jennings and Bernard, 1987; Hershman and Bachi, 1995). Wheat crop residues may as well lower soil temperatures at soybean planting and during the initial stages of development of the crop (Hansel et al., 2019). Even though SCN egg hatch, root penetration, and development can occur at a widespread temperature range, the rate of SCN growth, development, and reproduction is strongly influenced by temperature (Alston and Schmitt, 1988; Bernard, 2018). Although planting dates were similar in the current study, early maturity cultivars are often used in double-cropping fields, which could limit SCN reproduction due to reduced period with a host available.

TABLE 4 | Effect of initial SCN population level (low, moderate, or high) and winter option (winter wheat or fallow) on soybean yield (kg ha^{-1}).

Factor (winter option)	Level[a]	Yield (kg ha^{-1}[b,c])	SE[d]
Initial SCN population	Low	3,763.3 A	336.5
	Moderate	3,384.0 A	336.5
	High	3,944.4 A	412.1
Winter option	Wheat	3,688.0 B	211.6
	Fallow	3,987.3 A	211.6

[a]*SCN population densities were defined as high SCN when having >6,500 eggs/100 cm^3 of soil, moderate for 2,000–6,500 eggs/100 cm^3, and low when <2,000 eggs/100 cm^3.*
[b]*One bushel/acre = 67.25 kg ha^{-1}.*
[c]*Means followed by the same letter in the columns for each factor do not differ by Tukey's HSD test (P = 0.05).*
[d]*Standard error.*

Furthermore, egg density data at R1 growth stage of soybean indicate an attrition in SCN populations, since both fallow and wheat strips exhibited reduction in egg density at the R1 stage compared with the time of planting. Nematode attrition is commonly observed in field trials (McSorley and Dickson, 1989; Chen et al., 2006; Walthall et al., 2013), and it is characterized by a decrease in field population densities over time. Attrition is especially reported high during summer and is attributed to multiple biotic and abiotic factors. Fluctuations in populations of phytoparasitic nematodes are often driven by the availability and growth stage of susceptible hosts, environmental conditions, parasitism, and the production of harmful metabolites by competitors (Acedo et al., 1984).

Similar trends were observed at the soybean harvest sampling interval compared with those at R1 growth stage of soybean; SCN egg densities were reduced in wheat strips than in fallow strips. Likewise, in previous studies, fall-planted Italian ryegrass, rye, and oat led to reduced SCN populations at soybean harvest in the following year and were reported to have potential in helping farmers practicing continuous soybean production (Ackley, 2013). In this study, SCN field populations at soybean harvest interval increased compared with those at soybean R1 growth stage. Research indicates a peak in egg hatching and second-stage juvenile (J2) infectivity rates near August and with the expansion of the root system during the last vegetative growth stages. This can result in an exponential growth in field SCN populations (Yen et al., 1995). It is to be noted that, in this study, the population recovery rate was slower in wheat strips compared with that noted in fallow strips, resulting in reduced egg densities in double-cropping fields at harvest.

The diversification of cropping systems increases the richness of soil microbial communities and results in shifts in the core groups of fungi and bacteria (Peralta et al., 2018). Moreover, SCN can be parasitized by different nematophagous microorganisms, and research suggests an effect of changes in soil microbial communities on suppressing nematode populations in production fields (Tyler et al., 1987; Nour et al., 2003; Song et al., 2016). In a study conducted in Jackson, Tennessee, Bernard et al. (1997) reported a threefold increase in SCN female parasitism by fungi in September compared with that in July and August. Interestingly, in our study, this coincides with a similar time window where slower recovery rates of SCN populations were detected following wheat strips, suggesting that microbial antagonists might contribute to the suppressive effects of wheat. In similar studies, the effect of wheat suppressing SCN became more pronounced after multiple seasons. In fact, studies report that several years is needed before the impact of crop rotation or the use of cover crops was no longer impacting soil nematode communities. Long and Todd (2001) reported reductions in an SCN population 3–4 years after the establishment of a double-cropping system. Similarly, Tyler et al. (1987) reported that long-term tillage reduced SCN populations in the first 3 or 4 years after the establishment of their cropping system.

Soybean yield was reduced in fields with wheat as winter option. Results from the literature report both reduced and unaffected soybean yield following winter wheat, but overall, full season tends to yield more than double-cropping soybean, especially in high-yielding environments, where the prospect of maximized soybean yield decreases with increased wheat yield and delayed soybean planting date (Nelson et al., 2010; Hansel et al., 2019). Double-cropped soybean generally has higher total return compared to the full-season crop, but many producers also adopt this system to increase cash flow and as a risk diversification strategy, reducing the dependency on a single commodity market (Holshouser, 2015). While maximized wheat production may lead to reduced soybean yield, high-yielding wheat is a prerequisite for a profitable double-cropping system (Holshouser, 2015). In summary, there is a balance on how double-cropping could spread fixed inputs over a large volume of output (wheat + soybean yield) while taking into account increasing production costs and augmenting income by having a second crop (Farno et al., 2002; Kelley, 2003; Holshouser, 2015). The yield gap between full-season and double-cropping soybeans becomes more evident as latitudes increase, due to reduced growing season, which may as well affect seed quality (Koenning, 1991; Caviglia et al., 2011). Reduction in yield in double-cropping soybean may be linked to different factors, including shorter growing seasons, reduced water and nutrient availability, and the presence of undecomposed and undistributed wheat residue (Caviglia et al., 2011; Holshouser, 2015).

Looking to the future, climate change and increasing temperatures may allow farmers to practice double-cropping at even higher latitudes, which may alleviate some of the predicted negative impacts of climate change on soybean and corn (Seifert and Lobell, 2015). Several simulations predict an increase in areas suitable for double-cropping by 0.35 million km^2 (Zabel et al., 2014; Seifert and Lobell, 2015). Zabel et al. (2014), using predictive models, estimated that rises in prevailing temperatures of 2, 3, and 4°C will expand areas with potential for double-cropping by 8,370 (55.1%), 11,630 (89.5%), and 13,580 (89.5%) km^2, respectively (% value of current double-cropping total area: 15,180 km^2). A large part of these areas with the potential for wheat–soybean acreage increase is in Illinois, Indiana, and Eastern Ohio. In the current study, winter wheat led to a reduction in SCN egg densities compared with fallow at R1 growth stage of soybean and after soybean harvest. Farmers growing full-season soybeans in South/Central Illinois and similar regions may benefit from introducing wheat as a winter crop. Incorporating wheat into double-cropping systems can help growers to maintain SCN field populations under

damage threshold and reduce costs and losses caused by SCN, the main yield-limiting biotic factor in U.S. soybean production. This study is meant to be a first step toward a better understanding of the mechanisms that govern the effect of wheat on SCN populations. Future research will explore the potential effects of wheat and related plant exudates on soil microbial communities and associated impacts on SCN populations.

DATA AVAILABILITY STATEMENT

The raw data supporting the conclusions of this article will be made available by the authors, without undue reservation.

AUTHOR CONTRIBUTIONS

JB, TW, and DD planned, conducted, and supervised field trials. JB and TW applied pesticides and collected the soil samples. LR wrote the manuscript with editing assistance from MP, AF, and JPB. LR designed the figures and formatted and submitted the manuscript. All authors read and agreed to the published version of the manuscript.

FUNDING

This project was funded by the Illinois Soybean Association Checkoff Program.

ACKNOWLEDGMENTS

This work is part of the LR's dissertation. We are thankful for the assistance from SIU researchers and from the undergraduate and graduate students.

SUPPLEMENTARY MATERIAL

The Supplementary Material for this article can be found online at: https://www.frontiersin.org/articles/10.3389/fpls.2021.640714/full#supplementary-material

REFERENCES

Acedo, J., Dropkin, V., and Luedders, V. (1984). Nematode population attrition and histopathology of *Heterodera glycines*-soybean associations. *J. Nematol.* 16, 48–56.

Ackley, B. A. (2013). *Interactions of Purple Deadnettle, Lamium Purpureum, Soybean Cyst Nematode, Heterodera Glycines and Italian Ryegrass, Lolium Multiflorum*. Thesis. Columbus, OH: The Ohio State University.

Allen, T. W., Bradley, C. A., Sisson, A. J., Byamukama, E., Chilvers, M. I., Corker, C. M., et al. (2017). Soybean yield loss estimates due to diseases in the United States and Ontario, Canada from 2010 to 2014. *Plant Health Prog.* 18, 19–27. doi: 10.1094/PHP-RS-16-0066

Alston, D., and Schmitt, D. (1988). Development of *Heterodera glycines* life stages as influenced by temperature. *J. Nematol.* 20, 366–372.

Baird, S. M., and Bernard, E. C. (1984). Nematode population and community dynamics in soybean-wheat cropping and tillage regimes. *J. Nematol.* 16:379.

Bernard, E. C. (2018). "Plant parasitic nematodes of tennessee and kentucky," in *Plant Parasitic Nematodes in Sustainable Agriculture of North America*, eds S. A. Subbotin and J. J. Chitambar (Cham: Springer), 305–325. doi: 10.1007/978-3-319-99588-5_12

Bernard, E. C., Self, L. H., and Tyler, D. D. (1997). Fungal parasitism of soybean cyst nematode, Heterodera glycines (Nemata: Heteroderidae), in differing cropping-tillage regimes. *Appl. Soil Ecol.* 5, 57–70. doi: 10.1016/S0929-1393(96)00125-4

Caviglia, O. P., and Andrade, F. H. (2010). Sustainable intensification of agriculture in the argentinean pampas: capture and use efficiency of environmental resources. *Am. J. Plant Sci. Biotechnol.* 3, 1–8. doi: 10.1007/978-981-33-4203-3_1

Caviglia, O. P., Sadras, V. O., and Andrade, F. H. (2004). Intensification of agriculture in the south-eastern pampas: I. capture and efficiency in the use of water and radiation in double-cropped wheat–soybean. *Field Crops Res.* 87, 117–129. doi: 10.1016/j.fcr.2003.10.002

Caviglia, O. P., Sadras, V. O., and Andrade, F. H. (2011). Yield and quality of wheat and soybean in sole-and double-cropping. *Agron. J.* 103, 1081–1089. doi: 10.2134/agronj2011.0019

Chen, S., Wyse, D. L., Johnson, G. A., Porter, P. M., Stetina, S. R., Miller, D. R., et al. (2006). Effect of cover crops alfalfa, red clover, and perennial ryegrass on soybean cyst nematode population and soybean and corn yields in Minnesota. *Crop Sci.* 46, 1890–1897. doi: 10.2135/cropsci2005.09-0296

Farno, L. A., Edwards, L. H., Keim, K., and Epplin, F. M. (2002). Economic analysis of soybean-wheat cropping systems. *Crop Manag.* 1, 1–6. doi: 10.1094/cm-2002-0816-01-rs

Francl, L., and Dropkin, V. (1986). *Heterodera glycines* population dynamics and relation of initial population to soybean yield. *Plant Dis.* 70, 791–795. doi: 10.1094/pd-70-791

Hansel, S., Sulzbach, D., Schwalbert, R. A., Shoup, D. E., Holshouser, D. L., Parvej, R., et al. (2019). A review of soybean yield when double-cropped after wheat. *Agron. J.* 111, 677–685. doi: 10.2134/agronj2018.06.0371

Heggenstaller, A. H., Liebman, M., and Anex, R. P. (2009). Growth analysis of biomass production in sole-crop and double-crop corn systems. *Crop Sci.* 49, 2215–2224. doi: 10.2135/cropsci2008.12.0709

Hershman, D. E. (2014). *2015 Soybean Cyst Nematode (SCN) Management Recommendations for Kentucky*. Lexington, KY: University of Kentucky Extension.

Hershman, D., and Bachi, P. (1995). Effect of wheat residue and tillage on *Heterodera glycines* and yield of double crop soybean in Kentucky. *Plant Dis.* 79, 631–633. doi: 10.1094/pd-79-0631

Holshouser, D. L. (2015). *Double Cropping Soybeans in Virginia*. Blacksburg, VA: Virginia Cooperative Extension.

Jennings, P. L., and Bernard, E. C. (1987). Effect of wheat on *Heterodera glycines* under greenhouse conditions. *J. Nematol.* 19, 1. doi: 10.1016/j.apsoil.2017.07.018

Kelley, K. W. (2003). Double-cropping winter wheat and soybean improves net returns in the eastern Great Plains. *Crop Manag.* 2, 1–7. doi: 10.1094/CM-2003-1112-01-RS

Kerschner, B. (2018). *2018 Illinois Climate Recap*. Available online at: https://stateclimatologist.web.illinois.edu/2018/12/24/2018-illinois-climate-recap/. (Accessed October 6th, 2020).

Koenning, S. R. (1991). Effects of wheat and soybean planting date on *Heterodera glycines* population dynamics and soybean yield with conventional tillage. *Plant Dis.* 75, 301–304. doi: 10.1094/pd-75-0301

Leslie, A. W., Wang, K.-H., Meyer, S. L., Marahatta, S., and Hooks, C. R. (2017). Influence of cover crops on arthropods, free-living nematodes, and yield in a succeeding no-till soybean crop. *Appl. Soil Ecol.* 117, 21–31. doi: 10.1016/j.apsoil.2017.04.003

Long, J., and Todd, T. (2001). Effect of crop rotation and cultivar resistance on seed yield and the soybean cyst nematode in full-season and double-cropped soybean. *Crop Sci.* 41, 1137–1143. doi: 10.2135/cropsci2001.4141137x

McSorley, R. (2011). Assessment of rotation crops and cover crops for management of root-knot nematodes (Meloidogyne spp.) in the southeastern United States. *Nematropica* 41, 200–214.

McSorley, R., and Dickson, D. (1989). Effects and dynamics of a nematode community on soybean. *J. Nematol.* 21:490.

Mueller, D., Wise, K., Sisson, A., Smith, D., Sikora, E., Bradley, C., et al. (2016). *A Farmer's Guide to Soybean Diseases*. Saint Paul, MN: APS Press, 99–101.

Nafziger, E. (2009). "Soybean," in *Illinois Agronomy Handbook*, ed University of Illinois Extension (Urbana, IL: University of Illinois Cooperative Extension Service), 27–36.

Nelson, K. A., Meinhardt, C. G., and Smoot, R. L. (2010). Wheat (*Triticum aestivum* L.) cultivar selection affects double-crop and relay-intercrop soybean (*Glycine max* L.) response on claypan soils. *Int. J. Agron.* 2010:543261 . doi: 10.1155/2010/543261

Niblack, T. L., and Tylka, G. L. (2008). *Soybean Cyst Nematode Management Guide*. Urbandale, IA: North Central Soybean Research Program.

Niblack, T., Arelli, P., Noel, G., Opperman, C., Orf, J. H., Schmitt, D., et al. (2002). A revised classification scheme for genetically diverse populations of *Heterodera glycines*. *J. Nematol.* 34, 279–288.

Niblack, T., Tylka, G. L., Arelli, P., Bond, J., Diers, B., Donald, P., et al. (2009). A standard greenhouse method for assessing soybean cyst nematode resistance in soybean: SCE08 (standardized cyst evaluation 2008). *Plant Health Prog.* 10, 1–9. doi: 10.1094/PHP-2009-0513-01-RV

Nour, S. M., Lawrence, J. R., Zhu, H., Swerhone, G. D., Welsh, M., Welacky, T. W., et al. (2003). Bacteria associated with cysts of the soybean cyst nematode (*Heterodera glycines*). *Appl. Environ. Microbiol.* 69, 607–615. doi: 10.1128/AEM.69.1.607-615.2003

Peralta, A. L., Sun, Y., McDaniel, M. D., and Lennon, J. T. (2018). Crop rotational diversity increases disease suppressive capacity of soil microbiomes. *Ecosphere* 9:e02235. doi: 10.1002/ecs2.2235

Riggs, R., Niblack, T., Kinloch, R., MacGuidwin, A., Mauromoustakos, A., and Rakes, L. (2001). Overwinter population dynamics of *Heterodera glycines*. *J. Nematol.* 33:219.

Rocha, L. F., Gage, K. L., Pimentel, M. F., Bond, J. P., and Fakhoury, A. M. (2021). Weeds hosting the soybean cyst nematode (*Heterodera glycines* Ichinohe): management implications in agroecological systems. *Agronomy* 11:146. doi: 10.3390/agronomy11010146

Rothrock, C., and Kirkpatrick, T. (2018). *Potential for the Integration of Brassica Winter Cover Crops into Soybean Production Systems for the Suppression of Nematodes*. Fayetteville, AK: University of Arkansas System Division of Agriculture.

Seifert, C. A., and Lobell, D. B. (2015). Response of double-cropping suitability to climate change in the United States. *Env. Res. Lett.* 10:024002. doi: 10.1088/1748-9326/10/2/024002

Song, J., Li, S., Xu, Y., Wei, W., Yao, Q., and Pan, F. (2016). Diversity of parasitic fungi from soybean cyst nematode associated with long-term continuous cropping of soybean in black soil. *Acta Agric. Scand. B. Soil. Plant Sci.* 66, 432–442. doi: 10.1080/09064710.2016.1158862

Tyler, D., Chambers, A., and Young, L. (1987). No-tillage effects on population dynamics of soybean cyst nematode. *Agron. J.* 79, 799–802. doi: 10.2134/agronj1987.00021962007900050008x

Tylka, G. L. (2016). Understanding soybean cyst nematode HG types and races. *Plant Health Progr.* 17, 149–151. doi: 10.1094/PHP-PS-16-0615

Tylka, G. L., and Marett, C. C. (2017). Known distribution of the soybean cyst nematode, *Heterodera glycines*, in the United States and Canada, 1954 to 2017. *Plant Health Prog.* 18, 167–168. doi: 10.1094/PHP-05-17-0031-BR

University of Illinois Extension (2014). *The Soybean Cyst Nematode Problem. Report on Plant Disease, RPD 501*. Urbana-Champaign, IL: University of Illinois Plant Clinic.

Walthall, C. L., Anderson, C. J., Baumgard, L. H., Takle, E., and Wright-Morton, L. (2013). *Climate Change and Agriculture in the United States: Effects and Adaptation (USDA Technical Bulletin 1935)*. Washington, DC: USDA.

Warnke, S., Chen, S., Wyse, D. L., Johnson, G., and Porter, P. M. (2006). Effect of rotation crops on *Heterodera glycines* population density in a greenhouse screening study. *J. Nematol.* 38:391.

Wight, J. P., Allen, F. L., Donald, P. A., Tyler, D. D., and Saxton, A. M. (2011). Impact of crop rotation and bio-covers on soybean cyst nematode. *Plant Health Prog.* 12, 1–9. doi: 10.1094/PHP-2010-0930-04-RS

Yen, J., Niblack, T., and Wiebold, W. (1995). Dormancy of *Heterodera glycines* in Missouri. *J. Nematol.* 27:153.

Zabel, F., Putzenlechner, B., and Mauser, W. (2014). Global agricultural land resources–a high resolution suitability evaluation and its perspectives until 2100 under climate change conditions. *PLoS One* 9:e114980. doi: 10.1371/journal.pone.0107522

Conflict of Interest: TW was employed by the company Wyciskalla Consulting. JB was employed by JCB Ag Research. DD was employed by Davidson Consulting.

The remaining authors declare that the research was conducted in the absence of any commercial or financial relationships that could be construed as a potential conflict of interest.

frontiers in Plant Science

ORIGINAL RESEARCH
published: 11 May 2021
doi: 10.3389/fpls.2021.668064

Comparative Analysis of *Bursaphelenchus xylophilus* Secretome Under *Pinus pinaster* and *P. pinea* Stimuli

*Hugo Silva[1], Sandra I. Anjo[2], Bruno Manadas[2], Isabel Abrantes[1], Luís Fonseca[1] and Joana M. S. Cardoso[1]**

[1] University of Coimbra, Centre for Functional Ecology, Department of Life Sciences, Coimbra, Portugal, [2] CNC – Center for Neuroscience and Cell Biology, University of Coimbra, Coimbra, Portugal

The pinewood nematode (PWN), *Bursaphelenchus xylophilus*, the pine wilt disease's (PWD) causal agent, is a migratory endoparasitic nematode skilled to feed on pine tissues and on fungi that colonize the trees. In order to study *B. xylophilus* secretomes under the stimulus of pine species with different susceptibilities to disease, nematodes were exposed to aqueous pine extracts from *Pinus pinaster* (high-susceptible host) and *P. pinea* (low-susceptible host). Sequential windowed acquisition of all theoretical mass spectra (SWATH-MS) was used to determine relative changes in protein amounts between *B. xylophilus* secretions, and a total of 776 secreted proteins were quantified in both secretomes. From these, 22 proteins were found increased in the *B. xylophilus* secretome under the *P. pinaster* stimulus and 501 proteins increased under the *P. pinea* stimulus. Functional analyses of the 22 proteins found increased in the *P. pinaster* stimulus showed that proteins with peptidase, hydrolase, and antioxidant activities were the most represented. On the other hand, gene ontology (GO) enrichment analysis of the 501 proteins increased under the *P. pinea* stimulus revealed an enrichment of proteins with binding activity. The differences detected in the secretomes highlighted the diverse responses from the nematode to overcome host defenses with different susceptibilities and provide new clues on the mechanism behind the pathogenicity of this plant-parasitic nematode. Proteomic data are available *via* ProteomeXchange with identifier PXD024011.

Keywords: pinewood nematode, pine trees, pine wilt disease, plant–nematode interactions, proteomics, SWATH-MS

OPEN ACCESS

Edited by:
Koichi Hasegawa, Chubu University, Japan

Reviewed by:
Margarida Espada, University of Evora, Portugal
Lee Robertson, National Institute of Agricultural and Food Research and Technology, Spain

***Correspondence:**
Joana M. S. Cardoso
joana.cardoso@uc.pt

Specialty section:
This article was submitted to Plant Pathogen Interactions, a section of the journal Frontiers in Plant Science

Received: *15 February 2021*
Accepted: *29 March 2021*
Published: *11 May 2021*

Citation:
Silva H, Anjo SI, Manadas B, Abrantes I, Fonseca L and Cardoso JMS (2021) Comparative Analysis of Bursaphelenchus xylophilus Secretome Under Pinus pinaster and P. pinea Stimuli. Front. Plant Sci. 12:668064. doi: 10.3389/fpls.2021.668064

INTRODUCTION

The pinewood nematode (PWN), *Bursaphelenchus xylophilus*, is the causal agent of the pine wilt disease (PWD). It is present in its native region, North America, and also in Japan, China, South Korea, Taiwan, Portugal, and Spain. In non-native regions, this nematode has caused heavy economic losses and dramatic and irreparable changes to the native forest ecosystems

(Akbulut et al., 2015). Its main hosts belong to the genus *Pinus* and it is known that there is a variation in the susceptibility of several pine species to PWN infection. The maritime pine, *Pinus pinaster*, is considered one of the most susceptible hosts, and on the other hand, the stone pine, *P. pinea*, is a low-susceptible host (Evans et al., 1996). These two species are the most representative and economically important pine species in Portugal. Differences in the host susceptibility have been validated by pathogenicity studies with artificial nematode inoculation using pine seedlings, under laboratory conditions (Kanzaki et al., 2011; Nunes Da Silva et al., 2015; Menéndez-Gutiérrez et al., 2017). Intermediate and resistant host trees can control the PWN invasion more successfully, avoiding the nematode migration through the tree or the destruction of the tissues (cortex, phloem, cambium, and resin canals) (Fukuda, 1997). On susceptible trees, the PWN begins to feed on parenchymal cells, using the resin canals to spread quickly from the entry point throughout the tree. This leads to tracheid cavitation and disruption of water transportation, which causes the appearance of wilting symptoms and tree death within a few months after the infection. The PWN can also feed on fungi that colonize dying or dead trees (Jones et al., 2008). When feeding on plants and fungi, the PWN uses the stylet to pierce the cell wall, secrete proteins, and ingest the nutrients. Additionally, PWN proteins are also secreted from other nematode natural openings. Secreted proteins are known to have important roles on nematode–plant interaction as they are involved in cell wall degradation, cellular metabolism, cellular regulation, and host-defense evasion (Shinya et al., 2013b).

Despite the great importance that PWD denotes, due to enormous economic and ecological losses, the pathogenicity mechanism of PWN is not completed understood. Advances have been made on this mainly supported by *B. xylophilus* transcriptomic and genomic studies (Kikuchi et al., 2011; Kang et al., 2012; Espada et al., 2016; Tsai et al., 2016; Tanaka et al., 2019). All these molecular data were very useful and provided the basis for the development of proteomic studies. Few studies focus principally on the nematode secretome and have been reported and allowed the identification of proteins that are actually produced and secreted. Essentially, groups of secreted proteins such as cell-wall-degrading enzymes and peptidases were identified in *B. xylophilus* secretome and associated with the plant cell wall degradation and nematode migration through host tissues. Additionally, proteins related to tolerance against host defenses such as proteins with antioxidant and detoxifying activity, proteases, and protease inhibitors were also identified (Shinya et al., 2013a; Cardoso et al., 2016). In the comparative proteomic analysis of *B. xylophilus* secretome with the secretome of the closest phylogenetic related but non-pathogenic species, *B. mucronatus*, differences in the amount of some of these secreted proteins were found, mostly with an increase of proteins with peptidase, glycoside hydrolase, and peptidase inhibitor activities in *B. xylophilus* secretome (Cardoso et al., 2016).

In the present study, the *B. xylophilus* secretome under the stimulus of a highly susceptible host, *P. pinaster*, and a low-susceptible host, *P. pinea*, was obtained and compared to gain new insights into the molecular basis of *B. xylophilus* interaction with hosts with different susceptibilities.

MATERIALS AND METHODS

Pine Extracts and Nematodes

Pine wood extracts were prepared from 2-year-old *P. pinaster* and *P. pinea* seedlings as previously described (Cardoso et al., 2016), and the obtained solution was used to simulate pine stimulus of high-susceptible and low-susceptible trees, respectively. Briefly, 15 g of small wood pieces from pine seedling stems were soaked in 75 ml of distilled water for 24 h at 4°C. The supernatant solution was passed through a filter paper and then centrifuged through a Vivaspin 5-kDa cutoff membrane (Sartorius Stedim). The pass-through solution containing proteins and metabolites <5 kDa was collected, refiltered in a Minisart 0.2-μm cellulose acetate membrane, and used to stimulate the nematode protein secretion, simulating, *in vitro*, the natural pine stimulus. Nematodes from a Portuguese isolate (BxPt17AS) maintained in cultures of *Botrytis cinerea* grown on malt extract agar medium at 25°C for approximately 2 weeks were used. Mixed developmental nematode stages were collected with water from fungal cultures using a 20-μm sieve and washed at least three times with sterile water.

Pine Extract Stimuli Assay

About 1×10^6 nematodes were resuspended with 5 ml of pine extract previously prepared and incubated overnight at 25°C in 10 cm Petri dishes. Six biological replicates for each stimulus were performed. Nematodes were then sedimented by centrifugation and separated from the supernatant containing the secreted proteins (±5 ml). Samples containing the secreted proteins were stored at −80°C until the proteomic analysis.

Sample Preparation for Proteomic Analysis

For the preparation of secreted proteins, an internal standard [(IS—the recombinant protein maltose-binding protein fused with green fluorescent protein (MBP-GFP)] was added in equal amounts (1 μg of recombinant protein) to each sample (Anjo et al., 2019), and the supernatants with the secreted proteins were completely dried under vacuum using a Speedvac Concentrator Plus (Eppendorf). The resulting pellets were resuspended in SDS-sample buffer, aided by steps of ultrasonication (using a 750-W Ultrasonic processor) and denaturation at 95°C. In addition to the individual replicates (in a total of six replicates per condition), two pooled samples were created for protein identification and library creation by combining one-sixth of each replicate. To improve the protein identification and create a more comprehensive library of proteins from nematodes, pooled samples of the stimulated nematodes were also digested and analyzed. Afterward, samples were alkylated with acrylamide

addiction, and gel digestion was accomplished by the short-GeLC approach (Anjo et al., 2015).

Protein Quantification by Sequential Windowed Acquisition of All Theoretical Mass Spectra

All samples were analyzed using the Triple TOF^{TM} 6600 System (ABSciex®) using two acquisition modes: (i) the pooled samples were analyzed by information-dependent acquisition (IDA) and (ii) the individual samples by the sequential windowed acquisition of all theoretical mass spectra (SWATH-MS) mode. Peptides were resolved by liquid chromatography (nanoLC Ultra 2D, Eksigent®) on a MicroLC column ChromXP^{TM} C18CL [300 μm internal diameter (ID) × 15 cm length, 3 μm particles, 120 Å pore size, Eksigent®] at 5 μl/min with a multistep gradient: 0–3 min 2% mobile phase B and 3–46 min linear gradient from 2 to 30% of mobile phase B. Mobile phase A corresponds to 0.1% FA with 5% DMSO, and mobile phase B to 0.1% FA and 5% DMSO in ACN. Peptides were eluted into the mass spectrometer using an electrospray ionization source (DuoSpray^{TM} Source, ABSciex®) with a 25-μm ID hybrid PEEKsil/stainless steel emitter (ABSciex®).

For the protein identification by IDA experiments, the mass spectrometer was set to scan full spectra (350–1,250 m/z) for 250 ms, followed by up to 80 MS/MS scans (100–1,500 m/z from a dynamic accumulation time—minimum 40 ms for precursor above the intensity threshold of 1,000—in order to maintain a cycle time of 3.499 s). Candidate ions with a charge state between +2 and +5 and counts above a minimum threshold of 10 counts per second were isolated for fragmentation, and one MS/MS spectrum was collected before adding those ions to the exclusion list for 25 s (mass spectrometer operated by Analyst®TF 1.7, ABSciex®). The rolling collision was used with a collision energy spread (CES) of 5.

For SWATH-MS-based experiments, the mass spectrometer was operated in a looped product ion mode (Gillet et al., 2012), and the same chromatographic conditions were used as in the IDA run described above. A set of 168 windows (**Supplementary Table 1**) of variable width (containing 1 m/z for the window overlap) was constructed, covering the precursor mass range of 350–1,250 m/z. A 50-ms survey scan (350–1,500 m/z) was acquired at the beginning of each cycle for instrument calibration, and SWATH-MS/MS spectra were collected from 100 to 1,500 m/z for 19 ms resulting in a cycle time of 3.291 s from the precursors ranging from 350 to 1,250 m/z. The collision energy for each window was determined according to the calculation for a charge +2 ion centered upon the window with variable CES, according to the window.

Peptide identification and library generation were performed with Protein Pilot software (v5.1, ABSciex®) with the following parameters: (i) search against the annotated *B. xylophilus* protein database obtained from Wormbase Parasite derived from BioProject PRJEA64437 (Kikuchi et al., 2011) and MBP-GFP (IS), (ii) acrylamide alkylated cysteines as fixed modification, and (iii) trypsin as digestion type. An independent false discovery rate (FDR) analysis using the target-decoy approach provided with Protein Pilot software was used to assess the quality of the identifications, and positive identifications were considered when identified proteins and peptides reached a 5% local FDR (Tang et al., 2008; Sennels et al., 2009).

Quantitative data processing was conducted using SWATH^{TM} processing plug-in for PeakView^{TM} (v2.0.01, ABSciex®) (Lambert et al., 2013). After retention time adjustment using the MBP-GFP peptides, up to 15 peptides, with up to five fragments each, were chosen per protein, and quantitation was attempted for all proteins in library file that were identified from the ProteinPilot^{TM} search.

Only proteins with at least one confidence peptide (FDR < 0.01) in no less than three of the six replicates per condition and with at least three transitions were considered. Peak areas of the target fragment ions (transitions) of the retained peptides were extracted across the experiments using an extracted-ion chromatogram (XIC) window of 3 min with 100 ppm XIC width.

The proteins' levels were estimated by summing all the transitions from all the peptides for a given protein that met the criteria described above (an adaptation of Collins et al., 2013) and normalized to the levels of the internal standard of each sample. Statistical analysis was carried out to identify the differentially regulated proteins using a Mann–Whitney *U* test to the proteins that fulfill these criteria, with a *q* value of 0.05 as cutoff performed in InfernoRDN (version 1.1.5581.33355) (Polpitiya et al., 2008). Pairwise comparisons were done using the normalized protein levels.

Mass spectrometry proteomics data have been deposited to the ProteomeXchange Consortium through the PRIDE (Perez-Riverol et al., 2019) partner repository with the data set identifier PXD024011.

Functional Annotation

Gene ontology (GO) annotations were performed using the Blast2GO 5.2.5 software (Conesa and Gotz, 2008), based on the BLAST against the non-redundant protein database NCBI and InterPro database using default settings in each step. The GO analysis was done in three different categories: the molecular function that describes the gene products' molecular activities, the cellular component that describes where gene products are active, and the biological process describing the pathways and larger processes made up of multiple gene products' activities. GO enrichment analysis was carried out for the proteins increased in *B. xylophilus* secretome under the *P. pinea* stimulus comparing samples against all quantified proteins, using the Blast2GO software with the statistical Fisher's exact test associated and a *P* value of 0.05 as a cutoff.

RESULTS

Bursaphelenchus xylophilus Secretome Profile

From the SWATH-MS analysis, 776 proteins were quantified and compared between *B. xylophilus* secretomes under the *P. pinaster* and *P. pinea* stimuli. GO analysis of the overall secretome profile

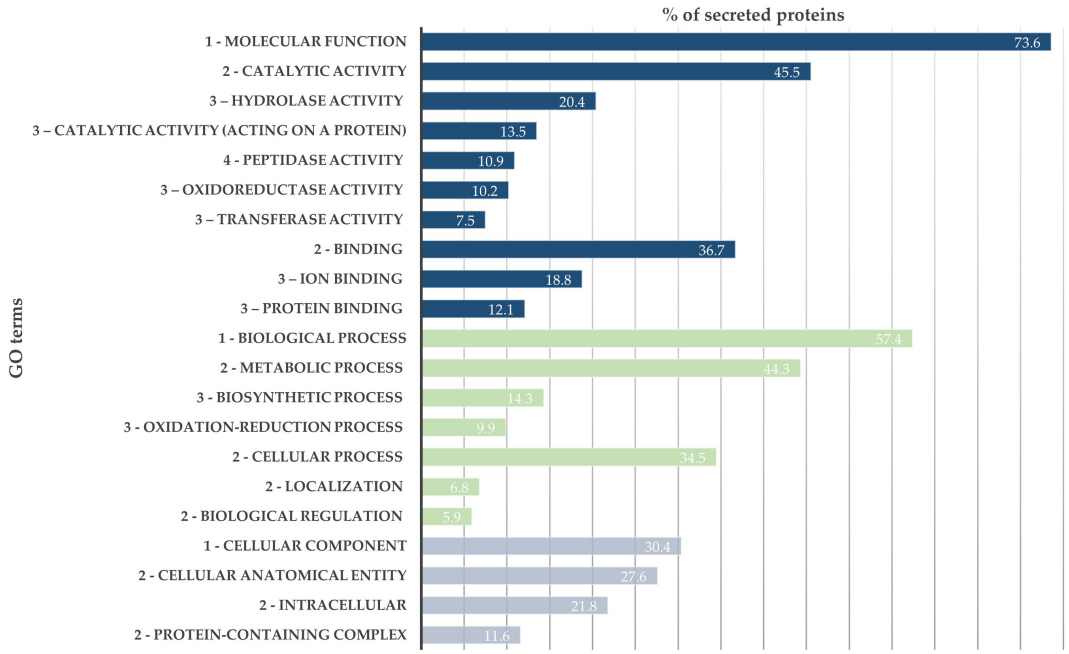

FIGURE 1 | *Bursaphelenchus xylophilus* secretome profile. Distribution of 776 secreted proteins according to gene ontology (GO) terms: molecular function (blue), biological process (green), and cellular component (gray).

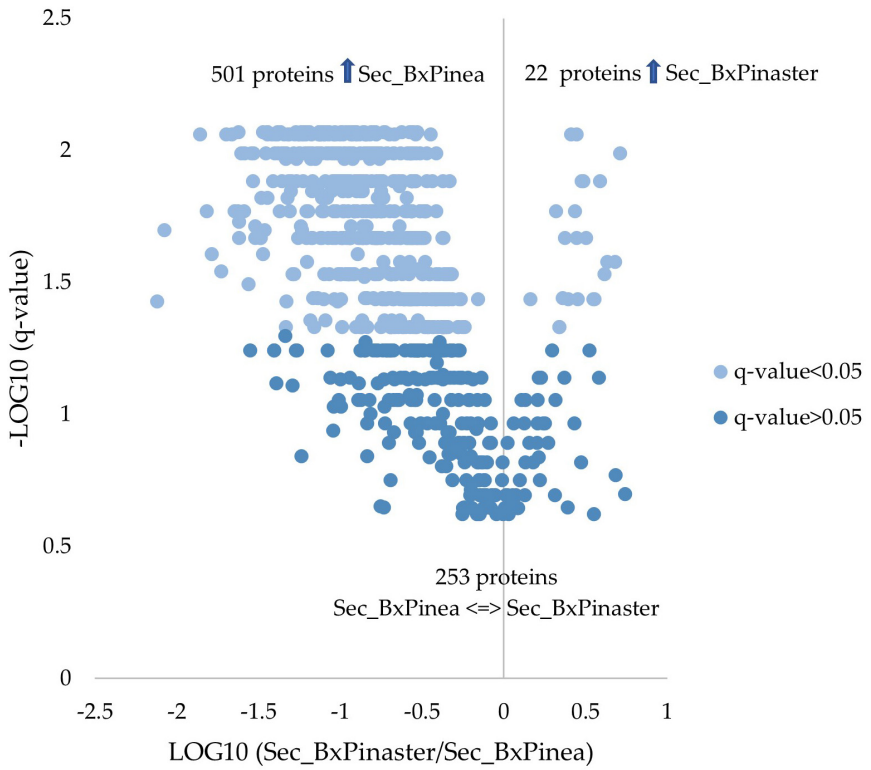

FIGURE 2 | Quantitative proteomic analysis. Volcano plot with the results from the statistical analysis of the 776 proteins quantified among the secretomes of *Bursaphelenchus xylophilus* under *Pinus pinaster* (Sec_BxPinaster) and *P. pinea* (Sec_BxPinea) stimuli. Statistical analysis was performed by the Mann–Whitney *U* test, and statistical significance was considered for *q* values < 0.05.

showed that 73.6% of the quantified proteins were associated with a molecular function GO term, and from these, a higher percentage of proteins is associated with catalytic activity (45.5%), such as peptidase, hydrolase, or oxidoreductase activity, and binding activity (36.7%). The 57.4% of proteins associated with a biological process were mainly associated with metabolic and cellular processes. About 21.8% of identified proteins associated with cellular component GO term are intracellular proteins (**Figure 1**).

Differential Quantitative Analysis of Secreted Proteins Under Different Stimuli

From the 776 proteins quantified and compared between the two secretomes, 523 proteins were found differentially secreted according to the different stimuli. Twenty-two proteins were increased in *B. xylophilus* secretome under the *P. pinaster* stimulus, and 501 increased in *B. xylophilus* secretome under the *P. pinea* stimulus. The number of proteins secreted by the nematode in a higher amount was much higher when the nematode was exposed to *P. pinea* stimulus than when exposed to *P. pinaster* (**Supplementary Table 2** and **Figure 2**). A similar tendency was also observed considering a conventional protein identification analysis of the representative pooled samples of each secretome, created to obtain the SWATH library (list of all the proteins identified in the assay) (**Supplementary Figure 1**).

From the 22 proteins found increased in *B. xylophilus* secretome under the *P. pinaster* stimulus, five were associated with peptidase activity, belonging to two different groups of peptidases, aspartic and serine peptidases. Proteins with hydrolase activity were also found increased: two phosphatases; a lysozyme-like protein belonging to glycoside hydrolase family 18 (GH18); a lipase EstA/esterase EstB; and a trehalase, belonging to GH37. With oxidoreductase activity, a short-chain dehydrogenase/reductase (SDR) was found increased. Six proteins are very diverse and have several different functions assigned. One of them is described as a signal recognition particle involved in binding processes. An intermediate filament protein, component of the cytoskeleton, and an integral component of the membrane were also identified. The other three proteins increased are a C-type lectin, a degenerin, and a protein involved in chromosomes' structural maintenance. Five of them could not be annotated (**Table 1**).

In order to find which group of proteins are overrepresented in increased proteins in *B. xylophilus* secretome under the *P. pinea* stimulus, a GO enrichment analysis (Fisher's exact test and a *P* value of 0.05 as a cutoff) was done against the 776 quantified proteins. This analysis revealed a strong enrichment of proteins associated with binding activity, and from these, the most represented proteins are related to protein binding. On lower GO levels, cytoskeletal protein binding and actin binding are also terms overrepresented in increased proteins (**Table 2**). On the biological process category, the most represented GO term is the regulation of biological process. Many of these proteins are related to cellular catabolic processes. Proteins associated with cellular component were also found enriched, related to cytoskeleton and cell periphery (**Table 2**).

TABLE 1 | Description of increased proteins in *Bursaphelenchus xylophilus* secretome under the *Pinus pinaster* stimulus, based on molecular function gene ontology terms.

Activity	Annotation	No. of proteins	Protein ID
Peptidase	Aspartic peptidase	4	BXY_0035000.1 BXY_0555800.1 BXY_0820600.1 BXY_0821000.1
	Serine peptidase	1	BXY_0959000.1
Hydrolase	Acid sphingomyelinase	1	BXY_0542900.1
	Histidine acid phosphatase	1	BXY_1236200.1
	Lysozyme-like protein (GH18)	1	BXY_0522000.1
	Lipase EstA/esterase EstB	1	BXY_1125700.1
	Trehalase (GH37)	1	BXY_1306200.1
Oxido reductase	Short-chain dehydrogenase/ reductase	1	BXY_0328000.1
Diverse	Signal recognition particle	1	BXY_1012800.1
	Intermediate filament tail domain protein	1	BXY_1639600.1
	Integral component of membrane	1	BXY_0888500.1
	C-type lectin	1	BXY_0360300.1
	Degenerin unc-8	1	BXY_1546700.1
	Structural maintenance of chromosomes protein	1	BXY_1747100.1
	Putative proteins with no description	5	BXY_0073000.1 BXY_1760900.1 BXY_0799700.1 BXY_0583800.1 BXY_0463500.1

DISCUSSION

The proteomic analysis carried out in this study allowed the quantification of 776 secreted proteins by *B. xylophilus* when exposed to stimuli of a highly susceptible host, *P. pinaster*, and a low-susceptible host, *P. pinea*. The functional analysis of these proteins displayed a GO distribution with a higher percentage of proteins associated with binding and catalytic activities in molecular function GO term and cellular and metabolic processes in biological process GO category, similar to the distribution previously described for *B. xylophilus* secretomes (Shinya et al., 2013a; Cardoso et al., 2016).

Interestingly, some differences were found in the distribution of proteins associated with catalytic activity compared with that previously reported for the *B. xylophilus* secretome under *P. pinaster* extract (Cardoso et al., 2016), with a higher percentage

of proteins associated with hydrolase activity than with peptidase activity. Moreover, a higher percentage of proteins associated with transferase activity was found. These may reflect the *P. pinea* stimulus influence on *B. xylophilus* secretome profile obtained in this study.

The comparative quantitative data on *B. xylophilus* secretome under the different stimuli showed that 22 proteins mostly associated with nematode feeding and migration during its phytophagous phase were increased under the *P. pinaster* stimulus. From these, proteins with peptidase and hydrolase activities were the most represented. Aspartic peptidases are described predominantly in functions associated with the digestion of nutrients (Malagón et al., 2013), and several aspartic peptidases have been found on *B. xylophilus*, including on the nematode secretome. Shinya et al. (2013a) mentioned that a large number of aspartic peptidases are expressed in *B. xylophilus*, and Cardoso et al. (2016) reported that five aspartic peptidases have an increased expression when compared with *B. mucronatus*, a related but not pathogenic nematode species. Recently, Cardoso et al. (2019) studied the transcript levels of three aspartic peptidases when stimulated with *P. pinaster* extract and when stimulated with *P. pinea* extract, the same species used in this work, obtaining higher levels of transcripts of these proteins when exposed to *P. pinaster* extract. These discoveries are in line with our findings, where the family of peptidases was found increased in the secretome under the stimulus of the high-susceptible host, *P. pinaster*. In addition to the aspartic peptidases, a serine peptidase was also found increased in the *P. pinaster* stimulus. This family of peptidases is believed to be related to the invasion of host tissues, being very important for that process to occur (Sakanari and Mckerrow, 1990).

From the five proteins identified with hydrolase activity, two are phosphatases, one is a histidine acid phosphatase, and the other an acid sphingomyelinase. To date, *in vivo* functions of the phosphatases are not well defined, and the histidine acid phosphatase is the one with more information available for nematodes. The histidine acid phosphatase belongs to a wide class of high molecular weight phosphatases with an acid ideal pH that usually cleaves phosphomonoester substrates (Fukushige et al., 2005). The remaining three proteins with hydrolase activity are a trehalase, a lipase EstA/esterase EstB family protein, and a lysozyme-like protein. The protein identified as a trehalase belongs to the GH37 family and is an enzyme that hydrolyses the disaccharide trehalose into two molecules of D-glucose (Łopieńska-Biernat et al., 2019). Trehalose is important in nematode physiology as an energy source and as a protection agent against environmental stress (Pellerone et al., 2003). The influence of trehalose against environmental stresses like desiccation and freezing is known in nematodes. Trehalose interacts with lipid membranes and proteins to protect them from damage caused by those stresses (Behm, 1997). The increased amount of trehalase can be the nematode's response to a less aggressive environment that allows the nematode to dismiss trehalose as a protective agent and use it as an energy source. Lysozymes are enzymes that cleave peptidoglycan, a vital constituent of the bacteria cell wall, and may have

TABLE 2 | Gene ontology (GO) enrichment analysis of the 501 proteins increased in *Bursaphelenchus xylophilus* secretome under the *Pinus pinea* stimulus.

GO ID	GO level	GO name	GO category	*P* value	No. of proteins
GO:0005488	2	Binding	MF	2.77E-02	202
GO:0005515	3	Protein binding	MF	4.15E-02	70
GO:0008092	4	Cytoskeletal protein binding	MF	5.00E-03	12
GO:0003779	5	Actin binding	MF	5.00E-03	12
GO:0050789	2	Regulation of biological process	BP	4.24E-02	32
GO:0050794	3	Regulation of cellular process	BP	4.38E-02	27
GO:0044248	4	Cellular catabolic process	BP	4.38E-02	27
GO:0016043	4	Cellular component organization	BP	4.33E-02	22
GO:0009057	5	Macromolecule catabolic process	BP	4.81E-02	19
GO:0006996	5	Organelle organization	BP	2.86E-02	18
GO:0044265	5	Cellular macromolecule catabolic process	BP	3.89E-02	17
GO:0051603	6	Proteolysis involved in cellular protein catabolic process	BP	3.89E-02	17
GO:0044257	6	Cellular protein catabolic process	BP	3.89E-02	17
GO:0051186	4	Cofactor metabolic process	BP	1.82E-02	13
GO:0006732	5	Coenzyme metabolic process	BP	1.22E-02	10
GO:0051188	5	Cofactor biosynthetic process	BP	1.90E-02	9
GO:0007010	6	Cytoskeleton organization	BP	1.90E-02	9
GO:0009108	6	Coenzyme biosynthetic process	BP	1.90E-02	9
GO:0030029	3	Actin filament-based process	BP	2.96E-02	8
GO:0030036	4	Actin cytoskeleton organization	BP	2.96E-02	8
GO:0005856	5	Cytoskeleton	CC	7.82E-03	22
GO:0071944	3	Cell periphery	CC	2.96E-02	8

MF, molecular function; BP, biological process; CC, cellular component. Enrichment analysis was performed against the 776 quantified proteins using the statistical Fisher's exact test and the P value of 0.05 as a cutoff.

a role in nematode protection against pathogenic bacteria (Boehnisch et al., 2011). Moreover, alongside with *B. xylophilus*, several bacterial species are associated with the nematode (Vicente et al., 2012), and the lysozyme enzymes secreted by the nematode may be involved in the restriction of bacterial growth in order to reduce the competition for food resources, as previously suggested (Espada et al., 2016). Possibly also related to PWN–bacteria interaction, a C-type lectin was found increased in the secretome under the *P. pinaster* stimulus. The C-type lectin domain has been proposed to contribute to the immune system of nematodes. Experimental evidence suggests that upon a bacterial invasion in *Caenorhabditis elegans*, this protein is involved in the immune response. They participate in cell adhesion, glycoprotein clearance, and binding of pathogen molecules. This group of proteins participates on binding of carbohydrates, namely peptidoglycan molecules (Schulenburg et al., 2008; Bauters et al., 2017), suggesting that this protein can be involved in nematode protection against pathogens, such as bacteria. These two upregulated secreted proteins can be working together, one as a binding protein capable to interact with bacteria carbohydrates and the other capable to degrade these carbohydrates, to protect the nematode and reduce the competition for food resources.

From the remaining increased secreted proteins under the *P. pinaster* stimulus, one is a SDR associated with oxidoreductase activity. This family of proteins is involved in the detoxification and excretion of compounds that are harmful to the organisms (Lindblom and Dodd, 2006), and 25 transcripts encoding SDR were found on *B. xylophilus* transcriptome (Yan et al., 2012). In order to understand the response mechanisms of *B. xylophilus* to defensive compounds produced by plants when infected by the nematode, Li et al. (2019) studied the response of the nematode when exposed to α-pinene and found that, when the nematode is exposed to this compound, some genes of several families of proteins related with detoxification process are upregulated. Among those upregulated genes, some are related to the SDR family, showing that this type of proteins is important for the nematode detoxification process.

A degenerin unc-8 protein was also found increased in *B. xylophilus* secretome under *P. pinaster*. Degenerins are known to be involved in ion channel activity and have been proposed as important for the modulation of nematode locomotion (García-Añoveros et al., 1998; Kellenberger and Schild, 2002).

Remarkably, the number of proteins secreted by the nematode in a higher amount was much higher when the nematode was exposed to a low-susceptible tree stimulus than when exposed to a highly susceptible tree. GO enrichment analysis of the increased proteins in the secretome under the *P. pinea* stimulus revealed an enrichment of proteins with binding activity, particularly the actin-binding proteins. In agreement with the actin-binding activity, several GO terms associated with the cytoskeleton and actin function were found enriched considering the biological process category. Terms like cytoskeleton organization, actin filament-based process, or actin cytoskeleton organization represent a great number of proteins more expressed under the *P. pinea* stimulus. Actin is a component of the cytoskeleton, with various functions on eukaryotic cells, and is involved in cell morphology, endocytosis and intracellular trafficking, motility, and cell division, among others. Actin activity is controlled by actin-binding proteins (Winder and Ayscough, 2005). In plant-parasitic nematodes, an actin-binding protein was described as an effector for the root knot nematode *Meloidogyne incognita*, being secreted by the nematode to the host plant, interfering in actin functions and promoting the parasitism (Leelarasamee et al., 2018).

The differences found in *B. xylophilus* secretome under the *P. pinaster* and *P. pinea* stimuli revealed a clear different response of the nematode to these two hosts with different susceptibilities. A much higher number and type of proteins were found increased in the nematode secretome when stimulated with the less susceptible host stimulus representing a clear response to a more challenging environment, *P. pinea*. This could be a consequence of that difficult environment, leading to a more intense production and secretion of proteins to overcome the plant host defenses.

DATA AVAILABILITY STATEMENT

The datasets presented in this study can be found in online repositories. The names of the repository/repositories and accession number(s) can be found below: https://www.ebi.ac.uk/pride/archive/projects/PXD024011.

AUTHOR CONTRIBUTIONS

SA, BM, IA, LF, and JC conceived and designed the experiments and revised and edited the manuscript. HS, SA, and JC performed the experiments and analyzed the data. HS wrote the original draft. All authors have read and approved the final version of the manuscript.

FUNDING

This research was supported by the Portuguese Foundation for Science and Technology (FCT) through national funds and the co-funding by FEDER, PT2020, and COMPETE 2020 under the projects POINTERS—PTDC/ASP-SIL/31999/2017 (POCI-01-145-FEDER-031999), UIDB/04004/2020, and UIDB/04539/2020, Project ReNATURE—Valorization of the Natural Endogenous Resources of the Centro Region (Centro 2020, Centro-01-0145-FEDER-000007), Instituto do Ambiente, Tecnologia e Vida, and the National Mass Spectrometry Network (RNEM) under contract POCI-01-0145-FEDER-402-022125 (Ref. ROTEIRO/0028/2013).

ACKNOWLEDGMENTS

The authors would like to thank Joana Duarte for her technical assistance on *Bursaphelenchus xylophilus* culture maintenance.

SUPPLEMENTARY MATERIAL

The Supplementary Material for this article can be found online at: https://www.frontiersin.org/articles/10.3389/fpls.2021.668064/full#supplementary-material

Supplementary Figure 1 | Venn diagram comparing the proteins identified in each pooled sample used to obtain the SWATH-MS library. Each pool was created by combining one-sixth of each individual biological replicate and was analyzed in data dependent acquisition mode for protein identification and library generation. A total of 324 proteins (22% of all the identified proteins) were common to the secretomes of *Bursaphelenchus xylophilus* under *Pinus pinaster* (Sec_BxPinaster) and *P. pinea* (Sec_BxPinea) stimuli.

Supplementary Table 1 | SWATH-MS method.

Supplementary Table 2 | Secretome analysis by SWATH-MS. Statistical analysis was performed by Mann–Whitney *U* test and statistical significance was considered for q-values <0.05. Pairwise comparisons were performed using the normalized protein levels subjected to Log10 transformation. The levels of the proteins were estimated by summing all the filtered transitions from all the filtered peptides for a given protein and normalized to the total intensity within the same experimental condition.

REFERENCES

Akbulut, S., Yüksel, B., Serin, M., and Erdem, M. (2015). Comparison of pathogenic potential of *Bursaphelenchus* species on conifer seedlings between greenhouse and outdoor conditions. *Phytoparasitica* 43, 209–214. doi: 10.1007/s12600-014-0433-2

Anjo, S. I., Santa, C., and Manadas, B. (2015). Short GeLC-SWATH: a fast and reliable quantitative approach for proteomic screenings. *Proteomics* 15, 757–762. doi: 10.1002/pmic.201400221

Anjo, S. I., Simões, I., Castanheira, P., Grãos, M., and Manadas, B. (2019). Use of recombinant proteins as a simple and robust normalization method for untargeted proteomics screening: exhaustive performance assessment. *Talanta* 205:120163. doi: 10.1016/j.talanta.2019.120163

Bauters, L., Naalden, D., and Gheysen, G. (2017). The distribution of lectins across the phylum Nematoda: a genome-wide search. *Int. J. Mol. Sci.* 18:91. doi: 10.3390/ijms18010091

Behm, C. A. (1997). The role of trehalose in the physiology of nematodes. *Int. J. Parasitol.* 27, 215–229. doi: 10.1016/s0020-7519(96)00151-8

Boehnisch, C., Wong, D., Habig, M., Isermann, K., Michiels, N. K., Roeder, T., et al. (2011). Protist-type lysozymes of the nematode *Caenorhabditis elegans* contribute to resistance against pathogenic *Bacillus thuringiensis*. *PLoS One* 6:e24619. doi: 10.1371/journal.pone.0024619

Cardoso, J. M., Anjo, S. I., Fonseca, L., Egas, C., Manadas, B., and Abrantes, I. (2016). *Bursaphelenchus xylophilus* and *B. mucronatus* secretomes: a comparative proteomic analysis. *Sci Rep* 6:39007.

Cardoso, J. M. S., Fonseca, L., and Abrantes, I. (2019). Aspartic peptidases of the pinewood nematode *Bursaphelenchus xylophilus*: molecular characterization and in silico structural analysis. *For. Pathol.* 49:e12545. doi: 10.1111/efp.12545

Collins, B. C., Gillet, L. C., Rosenberger, G., Röst, H. L., Vichalkovski, A., Gstaiger, M., et al. (2013). Quantifying protein interaction dynamics by SWATH mass spectrometry: application to the 14-3-3 system. *Nat. Methods* 10, 1246–1253. doi: 10.1038/nmeth.2703

Conesa, A., and Gotz, S. (2008). Blast2GO: a comprehensive suite for functional analysis in plant genomics. *Int. J. Plant Genomics* 2008:619832.

Espada, M., Silva, A. C., Eves Van Den Akker, S., Cock, P. J., Mota, M., and Jones, J. T. (2016). Identification and characterization of parasitism genes from the pinewood nematode *Bursaphelenchus xylophilus* reveals a multilayered detoxification strategy. *Mol. Plant Pathol.* 17, 286–295. doi: 10.1111/mpp.12280

Evans, H. F., Mcnamara, D. G., Braasch, H., Chadoeuf, J., and Magnusson, C. (1996). Pest Risk Analysis (PRA) for the territories of the European Union (as PRA area) on *Bursaphelenchus xylophilus* and its vectors in the genus *Monochamus*. *EPPO Bull.* 26, 199–249. doi: 10.1111/j.1365-2338.1996.tb00594.x

Fukuda, K. (1997). Physiological process of the symptom development and resistance mechanism in Pine wilt disease. *J. For. Res.* 2, 171–181. doi: 10.1007/bf02348216

Fukushige, T., Goszczynski, B., Yan, J., and Mcghee, J. D. (2005). Transcriptional control and patterning of the pho-1 gene, an essential acid phosphatase expressed in the *C. elegans* intestine. *Dev. Biol.* 279, 446–461. doi: 10.1016/j.ydbio.2004.12.012

García-Añoveros, J., García, J. A., Liu, J.-D., and Corey, D. P. (1998). The nematode degenerin UNC-105 forms ion channels that are activated by degeneration or hypercontraction causing mutations. *Neuron* 20, 1231–1241. doi: 10.1016/s0896-6273(00)80503-6

Gillet, L. C., Navarro, P., Tate, S., Rost, H., Selevsek, N., Reiter, L., et al. (2012). Targeted data extraction of the MS/MS spectra generated by data-independent acquisition: a new concept for consistent and accurate proteome analysis. *Mol. Cell. Proteomics* 11:O111016717.

Jones, J. T., Moens, M., Mota, M., Li, H., and Kikuchi, T. (2008). *Bursaphelenchus xylophilus*: opportunities in comparative genomics and molecular host-parasite interactions. *Mol. Plant Pathol.* 9, 357–368. doi: 10.1111/j.1364-3703.2007.00461.x

Kang, J. S., Koh, Y. H., Moon, Y. S., and Lee, S. H. (2012). Molecular properties of a venom allergen-like protein suggest a parasitic function in the pinewood nematode *Bursaphelenchus xylophilus*. *Int. J. Parasitol.* 42, 63–70. doi: 10.1016/j.ijpara.2011.10.006

Kanzaki, N., Aikawa, T., Maehara, N., and Ichihara, Y. (2011). An inoculation experiment of Japanese *Bursaphelenchus* nematodes on Japanese black and red pine, *Pinus thunbergi*i and *P. densiflora*. *J. For. Res.* 16, 325–330. doi: 10.1007/s10310-010-0225-6

Kellenberger, S., and Schild, L. (2002). Epithelial sodium channel/degenerin family of ion channels: a variety of functions for a shared structure. *Physiol. Rev.* 82, 735–767. doi: 10.1152/physrev.00007.2002

Kikuchi, T., Cotton, J. A., Dalzell, J. J., Hasegawa, K., Kanzaki, N., Mcveigh, P., et al. (2011). Genomic insights into the origin of parasitism in the emerging plant pathogen *Bursaphelenchus xylophilus*. *PLoS Pathog.* 7:e1002219. doi: 10.1371/journal.ppat.1002219

Lambert, J. P., Ivosev, G., Couzens, A. L., Larsen, B., Taipale, M., Lin, Z. Y., et al. (2013). Mapping differential interactomes by affinity purification coupled with data-independent mass spectrometry acquisition. *Nat. Methods* 10, 1239–1245. doi: 10.1038/nmeth.2702

Leelarasamee, N., Zhang, L., and Gleason, C. (2018). The root-knot nematode effector MiPFN3 disrupts plant actin filaments and promotes parasitism. *PLoS Pathog.* 14:e1006947. doi: 10.1371/journal.ppat.1006947

Li, Y., Meng, F., Deng, X., Wang, X., Feng, Y., Zhang, W., et al. (2019). Comparative transcriptome analysis of the pinewood nematode *Bursaphelenchus xylophilus* reveals the molecular mechanism underlying its defense response to host-derived α-pinene. *Int. J. Mol. Sci.* 20:911. doi: 10.3390/ijms20040911

Lindblom, T. H., and Dodd, A. K. (2006). Xenobiotic detoxification in the nematode *Caenorhabditis elegans*. *J. Exp. Zool.* 305A, 720–730.

Łopieńska-Biernat, E., Paukszto, Ł, Jastrzębski, J. P., Makowczenko, K., and Stryiński, R. (2019). Genes expression and *in silico* studies of functions of trehalases, a highly dispersed Anisakis simplex s. l. specific gene family. *Int. J. Biol. Macromol.* 129, 957–964. doi: 10.1016/j.ijbiomac.2019.02.042

Malagón, D., Benítez, R., Kašný, M., and Adroher, F. J. (2013). "Peptidases in parasitic nematodes: A review," in *Parasites*, ed. I. G. S. Erzinger (Hauppauge, NY: Nova Science Publishers, Inc), 61–102.

Menéndez-Gutiérrez, M., Alonso, M., Toval, G., and Díaz, R. (2017). Variation in pinewood nematode susceptibility among Pinus pinaster Ait. Provenances from the Iberian Peninsula and France. *Ann. For. Sci.* 74:76.

Nunes Da Silva, M., Solla, A., Sampedro, L., Zas, R., and Vasconcelos, M. W. (2015). Susceptibility to the pinewood nematode (PWN) of four pine species involved in potential range expansion across Europe. *Tree Physiol.* 35, 987–999. doi: 10.1093/treephys/tpv046

Pellerone, F. I., Archer, S. K., Behm, C. A., Grant, W. N., Lacey, M. J., and Somerville, A. C. (2003). Trehalose metabolism genes in *Caenorhabditis elegans* and filarial nematodes. *Int. J. Parasitol.* 33, 1195–1206. doi: 10.1016/s0020-7519(03)00173-5

Perez-Riverol, Y., Csordas, A., Bai, J., Bernal-Llinares, M., Hewapathirana, S., Kundu, D. J., et al. (2019). The PRIDE database and related tools and resources in 2019: improving support for quantification data. *Nucleic Acids Res.* 47, D442–D450.

Polpitiya, A. D., Qian, W.-J., Jaitly, N., Petyuk, V. A., Adkins, J. N., Camp, D. G., et al. (2008). DAnTE: a statistical tool for quantitative analysis of -omics data. *Bioinformatics* 24, 1556–1558. doi: 10.1093/bioinformatics/btn217

Sakanari, J. A., and Mckerrow, J. H. (1990). Identification of the secreted neutral proteases from *Anisakis simplex*. *J Parasitol*. 76, 625–630. doi: 10.2307/3282971

Schulenburg, H., Hoeppner, M. P., Weiner, J., and Bornberg-Bauer, E. (2008). Specificity of the innate immune system and diversity of C-type lectin domain (CTLD) proteins in the nematode *Caenorhabditis elegans*. *Immunobiology* 213, 237–250. doi: 10.1016/j.imbio.2007.12.004

Sennels, L., Bukowski-Wills, J. C., and Rappsilber, J. (2009). Improved results in proteomics by use of local and peptide-class specific false discovery rates. *BMC Bioinformatics* 10:179. doi: 10.1186/1471-2105-10-179

Shinya, R., Morisaka, H., Kikuchi, T., Takeuchi, Y., Ueda, M., and Futai, K. (2013a). Secretome analysis of the pine wood nematode *Bursaphelenchus xylophilus* reveals the tangled roots of parasitism and its potential for molecular mimicry. *PLoS One* 8:e67377. doi: 10.1371/journal.pone.0067377

Shinya, R., Morisaka, H., Takeuchi, Y., Futai, K., and Ueda, M. (2013b). Making headway in understanding pine wilt disease: what do we perceive in the postgenomic era? *J. Biosci. Bioeng.* 116, 1–8. doi: 10.1016/j.jbiosc.2013.01.003

Tanaka, S. E., Dayi, M., Maeda, Y., Tsai, I. J., Tanaka, R., Bligh, M., et al. (2019). Stage-specific transcriptome of *Bursaphelenchus xylophilus* reveals temporal regulation of effector genes and roles of the dauer-like stages in the lifecycle. *Sci. Rep.* 9:6080.

Tang, W. H., Shilov, I. V., and Seymour, S. L. (2008). Nonlinear fitting nethod for determining local false discovery rates from decoy database searches. *J. Proteome Res.* 7, 3661–3667. doi: 10.1021/pr070492f

Tsai, I. J., Tanaka, R., Kanzaki, N., Akiba, M., Yokoi, T., Espada, M., et al. (2016). Transcriptional and morphological changes in the transition from mycetophagous to phytophagous phase in the plant-parasitic nematode *Bursaphelenchus xylophilus*. *Mol. Plant Pathol.* 17, 77–83. doi: 10.1111/mpp.12261

Vicente, C., Espada, M., Vieira, P., and Mota, M. (2012). Pine Wilt Disease: a threat to European forestry. *Eur. J. Plant Pathol.* 133, 89–99. doi: 10.1007/s10658-011-9924-x

Winder, S. J., and Ayscough, K. R. (2005). Actin-binding proteins. *J. Cell Sci.* 118:651.

Yan, X., Cheng, X. Y., Wang, Y. S., Luo, J., Mao, Z. C., Ferris, V. R., et al. (2012). Comparative transcriptomics of two pathogenic pinewood nematodes yields insights into parasitic adaptation to life on pine hosts. *Gene* 505, 81–90. doi: 10.1016/j.gene.2012.05.041

Conflict of Interest: The authors declare that the research was conducted in the absence of any commercial or financial relationships that could be construed as a potential conflict of interest.

frontiers in Plant Science

ORIGINAL RESEARCH
published: 12 May 2021
doi: 10.3389/fpls.2021.651943

Priming Soybean cv. Primus Leads to Successful Systemic Defense Against the Root-Lesion Nematode, *Pratylenchus penetrans*

*Shimaa Adss[1], Benye Liu[2], Ludger Beerhues[2], Volker Hahn[3], Holger Heuer[1] and Ahmed Elhady[1,4]**

[1] Institute for Epidemiology and Pathogen Diagnostics, Julius Kühn-Institute, Federal Research Centre for Cultivated Plants, Braunschweig, Germany, [2] Institute of Pharmaceutical Biology, Technische Universität Braunschweig, Braunschweig, Germany, [3] State Plant Breeding Institute, Universität Hohenheim, Stuttgart, Germany, [4] Department of Plant Protection, Faculty of Agriculture, Benha University, Benha, Egypt

OPEN ACCESS

Edited by:
Claudia S. L. Vicente,
University of Évora, Portugal

Reviewed by:
Paulo Vieira,
Virginia Tech, United States
Maria Lurdes Inacio,
Instituto Nacional Investigaciao Agraria e Veterinaria (INIAV), Portugal
Esther Menendez,
University of Evora, Portugal

***Correspondence:**
Ahmed Elhady
ahmed.gomaa@julius-kuehn.de

Specialty section:
This article was submitted to Plant Pathogen Interactions, a section of the journal Frontiers in Plant Science

Received: 11 January 2021
Accepted: 19 April 2021
Published: 12 May 2021

Citation:
Adss S, Liu B, Beerhues L, Hahn V, Heuer H and Elhady A (2021) Priming Soybean cv. Primus Leads to Successful Systemic Defense Against the Root-Lesion Nematode, Pratylenchus penetrans. Front. Plant Sci. 12:651943. doi: 10.3389/fpls.2021.651943

Root lesion nematodes, *Pratylenchus penetrans*, are major pests of legumes with little options for their control. We aimed to prime soybean cv. Primus seedlings to improve basic defense against these nematodes by root application of *N*-3-oxo-tetradecanoyl-*L*-homoserine lactone (oxo-C14-HSL). The invasion of soybean roots by *P. penetrans* was significantly reduced in plants that were pre-treated with the oxo-C14-HSL producing rhizobacterium *Ensifer meliloti* strain ExpR+, compared to non-inoculated plants or plants inoculated with the nearly isogenic strain *E. meliloti* AttM with plasmid-mediated oxo-C14-HSL degradation. The nematodes were more clustered in the root tissues of plants treated with the AttM strain or the control compared to roots treated with the ExpR+ strain. In split-root systems primed on one side with strain ExpR+, root invasion was reduced on the opposite side compared to non-primed plants indicating a systemic plant response to oxo-C14-HSL. No additional local effect was detected, when inoculating nematodes on the ExpR+ primed side. Removal of oxo-C14-HSL after root exposure resulted in reduced root invasion compared to non-primed plants when the nematodes were added 3, 7, or 15 days later. Thus, probably the plant memorized the priming stimulus. Similarly, the plants were primed by compounds released from the surface of the nematodes. HPLC analysis of the root extracts of oxo-C14-HSL treated and untreated plants revealed that priming resulted in enhanced phytoalexin synthesis upon *P. penetrans* challenge. Without root invading nematodes, the phytoalexin concentrations of primed and non-primed plants did not significantly differ, indicating that priming did not lead to a persistently increased stress level of the plants. Upon nematode invasion, the phytoalexins coumestrol, genistein, and glyceollin

increased in concentration in the roots compared to control plants without nematodes. Glyceollin synthesis was significantly more triggered by nematodes in primed plants compared to non-primed plants. The results indicated that the priming of soybean plants led to a more rapid and strong defense induction upon root invasion of nematodes.

Keywords: induced systemic resistance, defense priming, plant-parasitic nematode, *Pratylenchus*, *N*-acyl-homoserine lactone, phytoalexin, *Ensifer meliloti*, *Glycine max*

INTRODUCTION

In their natural environment, plants are continuously exposed to a wide range of biotic stresses and evolved defense strategies that presumably harness associated microbes (Liu et al., 2020). In agriculture, pathogens and pests severely lower crop productivity and influence food security. Plant-parasitic nematodes are among the major limiting factors of crop production worldwide (Jones et al., 2013). The root lesion nematodes, *Pratylenchus* spp., invade roots, cause lesions by migrating through root tissues, only feed on living root cells, and lay eggs within the root or in soil. The root lesion nematodes are a major problem for legumes due to high reproduction rates on these hosts. They are abundant in soybean fields (Elhady et al., 2018, 2019, 2020).

Priming crop plants for enhanced defense against pathogens could become an environmentally friendly strategy for plant protection (Borges et al., 2014; Conrath et al., 2015; Wehner et al., 2019). Priming of plants by an inducer results in a faster and stronger response of the plant defense upon pathogen attack. Such a fast defense response is crucial for the plant to resist nematode attack because effectors of these pathogens suppress plant defenses during establishment in the root (Vieira et al., 2018). The priming state is preserved for a period after removal of the priming stimulus, and sometimes it is even transgenerationally transmitted (Ramírez-Carrasco et al., 2017). Ideally, it is not associated with a cost for the plant after the initial phase of priming because the stimulus does not trigger an ongoing defense reaction (Martínez-Medina et al., 2016).

Defense priming can be induced by different chemical compounds such as β-aminobutyric acid, salicylic acid, pipecolic acid, jasmonic acid, or volatile organic compounds (Navarova et al., 2012; Zhong et al., 2014; Ji et al., 2015; Hu et al., 2017; Thevenet et al., 2017). Plants may also be primed by beneficial soil organisms such as rhizobacteria or fungi (Jung et al., 2012; Molinari and Leonetti, 2019). Pathogen-associated molecules have been used to induce defense priming, among them are peptides, polysaccharides, and lipids that are perceived by plants through pattern recognition receptors (Dodds and Rathjen, 2010). For nematodes, ascarosides were reported to be perceived by plants and were shown to trigger plant defense responses (Klessig et al., 2019), but were not tested for priming of plant defense.

Recently, several reports suggested that bacterial quorum sensing signaling molecules like the *N*-acyl-homoserine lactones induce plant defense responses like callose deposition in the cell wall, accumulation of oxylipins, and stomata closure (Zarkani et al., 2013; Schenk and Schikora, 2014; Shrestha et al., 2019). The induction of defense against powdery mildew in barley by *N*-3-oxo-tetradecanoyl-*L*-homoserine lactone (oxo-C14-HSL), produced by *Ensifer meliloti*, was genotype-dependent (Shrestha et al., 2019). However, it was not investigated whether enhanced defense of the plant persisted over longer periods after removal of the inducer oxo-C14-HSL or the bacterial strain that produced it, or whether it enhances defense of roots against soilborne diseases. Investigations to prime plants for defense against plant-parasitic nematodes are rare. Rice plants treated with β-aminobutyric acid (Ji et al., 2015) or silicon (Zhan et al., 2018) reduced the invasion of *Meloidogyne graminicola* by activation of basal defenses as indicated by callose deposition and accumulation of reactive oxygen species (ROS), but defense priming of rice was not investigated.

In this study, we tested whether soybean cv. Primus plants are primed by root exposure to oxo-C14-HSL to better defend against a later attack of the plant-parasitic nematode *Pratylenchus penetrans*. We investigated whether and for how long an enhanced defense persisted after removal of the stimulus. The effect by the rhizobacterial inducer oxo-C14-HSL was compared to that of surface-released compounds of the nematode as priming agent. We hypothesized that the priming effect of oxo-C14-HSL on plant defense against nematode invasion is mediated by a systemic plant response rather than by a local response of the tissue exposed to oxo-C14-HSL, or by a direct effect of oxo-C14-HSL on the nematodes. This was investigated in split-root systems. Furthermore, we analyzed the accumulation of phytoalexins as a measure of plant defense induction after root exposure to oxo-C14-HSL, and after invasion of nematodes into roots of either primed or non-primed plants. The study provided a proof of concept for primability of soybean plants for defense against plant-parasitic nematodes to pave the way for further investigations on how to enhance the effect with respect to responsiveness of plant genotypes and the efficiency of different priming agents or microbes.

MATERIALS AND METHODS

Plants, Bacteria, and Nematodes

Soybean (*Glycine max*) cv. Primus seeds were thoroughly washed with water. Each washed seed was surface disinfected with 1.5% sodium hypochlorite for 5 min and then washed with sterile water three times for 1 min and once for 10 min. The seeds were placed on moist sterilized paper towels in Petri dishes for germination. After 5 days, equally developed seedlings were selected and three of them were grown in a jar containing 60 ml of $\frac{1}{2}$ MS medium. Plants were allowed to grow for additional 3 days in controlled

conditions: day/night 16/8 h and 18/16°C, the light intensity of 150 μmol/m^2 s, and 60% humidity, in a growing chamber.

Mixed stages of *P. penetrans* were extracted from 2-month-old axenic cultures on carrot discs through a Baermann funnel (European and Mediterranean Plant Protection Organization, 2013). Nematodes were surface disinfected on 5-μm sieves (CellTrics, Sysmex, Norderstedt, Germany) by soaking in 0.02% $HgCl_2$ for 3 min, 4,000 ppm streptomycin sulfate for 3 min, and CellCultureGuard (PanReac AppliChem, Darmstadt, Germany) for 4 h. Finally, the nematodes were washed on the sieve and incubated overnight in sterilized tap water. The concentration of nematode suspension was calibrated using a counting chamber to have a final suspension containing 500 nematodes per ml. Inoculation of plants with 1,000 *P. penetrans* was done by digging four 5 cm deep half an-inch-wide holes in 2 cm distance around the shoot, and equally distributing the nematode suspension.

Ensifer meliloti Rm2011 ExpR+ (strain ExpR+) and *E. meliloti* Rm2011 pBBR2-attM (strain AttM) carrying the lactonase gene *attM* from *Agrobacterium tumefaciens* on the plasmid vector pBBR1MCS-2 (Pellock et al., 2002; Zarkani et al., 2013) were grown in TY medium (Beringer, 1974) until the $OD_{600\ nm}$ reached 0.6–0.8. Bacterial cultures were centrifuged at 4,000 × *g* for 10 min and resuspended in 10 mM $MgCl_2$. The roots of soybean plants were inoculated three times over 2 weeks with 10 ml suspensions of strain ExpR+ or strain AttM in 10 mM $MgCl_2$ ($OD_{600\ nm}$ 0.1), or 10 mM $MgCl_2$ as control.

Priming of Soybean With oxo-C14-HSL for Defense Against *P. penetrans*

To explore and confirm the effect of oxo-C14-HSL (Sigma-Aldrich, Munich, Germany) on the priming of soybean cv. Primus defense toward *P. penetrans,* both the oxo-C14-HSL producing rhizobacterium *E. meliloti* strain ExpR + and the pure compound oxo-C14-HSL were used. Five-day-old soybean seedlings were planted in 8 cm × 6.2 cm pots filled with 200 ml autoclaved sand as an artificial growth substrate. The roots of the soybean plants were drenched three times over 2 weeks with a 10 ml suspension of *E. meliloti* strain ExpR+ in 10 mM $MgCl_2$. The same density and volume of strain AttM was used as bacterial control, and 10 mM $MgCl_2$ as solvent control. This resulted in three treatments including control, *E. meliloti* AttM, and *E. meliloti* ExpR+. Each treatment represented 20 biological replicates from two independent experiments.

As for synthetic oxo-C14-HSL, soybean seedlings of cv. Primus were first induced *in vitro*. A 60 mM stock solution of oxo-C14-HSL was prepared in acetone and diluted with sterile deionized water to a 6 μM working solution. For priming of soybean plants, roots were treated *in vitro* for 5 days with 6 μM oxo-C14-HSL. Plants were transplanted to pots in the greenhouse and left for 3 days to adapt to the conditions. Mixed stages of *P. penetrans* were prepared as described to inoculate 1,000 to each pot. One week later, plants were sampled. Shoot and root fresh weights were measured. Nematodes were stained in cleared roots with 1% acid fuchsin and microscopically counted (Bybd et al., 1983). In order to analyze the spatial dispersion of nematodes within primed and non-primed plants, roots were stained, sectioned into 1.2 cm pieces, and 25 pieces from each plant were randomly selected to determine the index of dispersion I_D = (n–1) * variance/mean (Iwao, 1968), with n = number of analyzed root sections per plant. I_D was used to calculate the coefficient Z = sqrt (2 *I_D) − sqrt (2 * (n − 1) − 1) (Ghaderi et al., 2018) and to statistically compare among the three treatments including control, *E. meliloti* AttM, and *E. meliloti* ExpR+. Each treatment represented 10 biological replicates. The nematodes were quantified and visualized using a stereomicroscope (Olympus Microscope SZX12) and photographed with a Jenoptik ProgRes® digital camera. Images were recorded using CapturePro 2.8 software (Jenoptic, Jena, Germany).

Priming by oxo-C14-HSL Compared to DL-β-Aminobutyric Acid (BABA) and Surface-Released Compounds of *P. penetrans* (PpNemawater)

We investigated to what extent oxo-C14-HSL can prime the defense of soybean cv. Primus compared to the known priming agent BABA, or PpNemawater. The surface released compounds were derived from *P. penetrans* according to Mendy et al. (2017) with slight modifications: Approximately 300,000 freshly hatched juveniles of *P. penetrans* were incubated in 10 ml sterile water for 48 h at room temperature with continuous rotation. After centrifugation at 800 × *g* for 3 min, the supernatant was filtered through a 20-μm filter and referred as PpNemawater. Plants were treated *in vitro* for 5 days with 6 μM oxo-C14-HSL, 25 mM BABA, or 5 ml PpNemawater. Sterile water was used as a control. Plants were transplanted to a pot system in the greenhouse and infected with 1,000 *P. penetrans* after 3 days. Nematodes were counted 10 days post-infection. This resulted in four treatments with 10 replicates per treatment.

Direct and Plant Mediated Effect of oxo-C14-HSL on *P. penetrans*

To investigate whether the effect of oxo-C14-HSL on nematode invasion is a local effect or mediated by a systemic response, a split-root experiment (Dababat and Sikora, 2007) was done in the greenhouse. Three square pots of 7 cm × 7 cm × 8 cm were arranged as follows: Two pots were attached to each other and one pot was placed in the center above those two pots. Two-week-old seedlings of soybean were transplanted in the center of the upper pot, which was half filled with sterile sand. Roots were divided into two halves. One-half of each split-root was inoculated three times with *E. meliloti* ExpR+. Infective stages of *P. penetrans* were inoculated either to the side of the roots colonized by strain ExpR+ or to the opposite side, with 700 nematodes of mixed stages per pot. In controls, only nematodes and no bacteria were inoculated to one of the split-roots. After 7 days, the shoot of each plant and the roots from both sides were harvested and weighed. Roots from the side of nematode inoculation were stained with acid fuchsin to microscopically count invaded nematodes (Bybd et al., 1983). This resulted in three treatments including control, local, and systemic response. Each treatment was represented by 10 biological replicates.

To further explore any direct effect of oxo-C14-HSL on *P. penetrans*, we used *in vitro* assays to analyze the mortality of the nematodes induced by the bacterial strain ExpR+, strain AttM, or oxo-C14-HSL. Cultures of the bacterial strains as mentioned previously in Section "Plants, Bacteria, and Nematodes" and a 6 μM solution of oxo-C14-HSL were prepared. As controls, 10 mM $MgCl_2$ (to explore the effect of bacterial strains), and a solution of sterile water containing 25 μl acetone (to explore the effect of molecules) were used. In a 96-well plate, 200 freshly extracted *P. penetrans* were added to 250 μl of the up-mentioned solutions and incubated at room temperature. Total and dead nematodes were counted after 48 h using a stereomicroscope (Olympus Microscope SZX12) to calculate the mortality as a percentage. This resulted in five treatments including ExpR+, AttM strains, oxo-C14-HSL, 10 mM $MgCl_2$, and diluted acetone as controls. Each treatment was represented by 24 replicates.

Persistence of Plant Defense After Removal of Inducers

Soybean seedlings of cv. Primus growing on $^1/_2$ MS medium under sterile conditions were treated with oxo-C14-HSL for 5 days at a final concentration of 10 μM for priming induction. The oxo-C14-HSL solution was added in a reservoir in the middle of a jar with three plants around it with their roots in the reservoir. In controls, the reservoir was filled with the solvent control. Other samples were treated with 5 ml of PpNemawater. Plants were allowed to grow for an additional 5 days at the same conditions: light/dark 16/8 h, 18/16°C, light intensity 150 μmol/m^2 s, 60% humidity. Plant roots were exposed to oxo-C14-HSL or PpNemawater for 5 days. Plants were taken from the jars, roots were gently washed with water to remove the inducer, and plants were transplanted into sterile sand and kept for 3, 7, or 15 days before inoculation of 750 *P. penetrans*. Roots were harvested 7 days after inoculation to quantify invaded nematodes by staining with 1% acid fuchsin and microscopic counting (Bybd et al., 1983). This experiment was done with 9–14 biological replicates.

Analysis of Phytoalexins by HPLC

Soybean roots were harvested 5 days after the treatment with oxo-C14-HSL and inoculation of nematodes. Roots (0.25 g) were kept at −20°C and homogenized using a TissueLyser II (Qiagen, Germany) with a 3 mm glass bead at 30 Hz for 5 min. Phytoalexins were extracted with five volumes of 80% methanol at 20°C for 12 h. After centrifugation at 12,000 *g* for 10 min, the supernatants were filtered through a 0.45-μm membrane before HPLC analysis. A Waters 2795 Seperatons Module coupled with Waters 2996 Photodiode Array Detector was operated with Software Empower Pro 2002. A Water symmetry C8 column (4.6 × 150 mm) was used for separation. The mobile phase was water with 0.1% formic acid (A) and acetonitrile (B). The separation program was as follows: starting with 5% B for 2 min with a flow rate of 0.5 ml/min, then a linear gradient of acetonitrile from 5 to 60% in 30 min. The injection volume was 20 μL. Glyceollin and coumestrol were detected at 285 or 343 nm, respectively.

Quantification of Total Phenolics

To quantify the total phenolic compounds in roots of primed and non-primed soybean plants in response to nematode attack, roots of soybean plants were collected 3 days after nematode inoculation. Plants without nematode infection were used as control. Roots were frozen with liquid nitrogen, pulverized in a TissueLyser II (Qiagen) with a 3 mm glass bead at 30 Hz for 5 min. The total phenolic compounds in 1 g were quantified by a colorimetric assay using the Folin-Ciocalteu method (Ainsworth and Gillespie, 2007). Gallic acid (Sigma-Aldrich, Darmstadt, Germany) was used as a reference for the quantification by spectrophotometry at 765 nm.

Statistical Analysis

Analysis of variance was done using the procedure GLIMMIX of the statistical software SAS 9.4 (SAS Institute Inc., Cary, NC, United States) to fit generalized linear models. For count data and the dispersion coefficient *Z*, the procedure was used with the assumption of a Poisson distribution with a log link function, and the Kenward–Roger's procedure was used to estimate degrees of freedom. For multiple comparisons, the *p*-value was adjusted by the method of Tukey. Graphs were generated using Prism 7 (GraphPad Software, La Jolla, CA, United States).

RESULTS

Rhizosphere Inoculation of Soybean Plants With *E. meliloti* ExpR+ Producing oxo-C14-HSL Reduced Root Invasion of *P. penetrans*

We investigated the potential of bacteria producing oxo-C14-HSL in the rhizosphere to enhance the defense of soybean plants toward *P. penetrans*. Significantly fewer nematodes invaded the roots of plants that were exposed to the oxo-C14-HSL-producing strain *E. meliloti* ExpR+ compared to control plants, or compared to plants inoculated with the lactonase-expressing strain *E. meliloti* AttM that does not accumulate oxo-C14-HSL (**Figure 1**). This suggested that oxo-C14-HSL induced plant defense and thereby reduced nematode invasion into roots. A less pronounced reduction of the invasion of *P. penetrans* was observed in soybean roots that have been treated with the AttM strain compared to the control (**Figure 1**). This can be attributed to a slight defense induction by bacteria associated molecular patterns to which plants usually respond. Moreover, we tested the commercially available form of oxo-C14-HSL to confirm that the priming effect is due to this signaling molecule. Plants were treated either with oxo-C14-HSL *in vitro* or with the acetone control. The invasion of *P. penetrans* was significantly reduced in the oxo-C14-HSL treated roots compared to the control (**Figure 2**). Plant growth was not significantly changed by oxo-C14-HSL compared to control plants within the period of the experiment (**Supplementary Figure 1**).

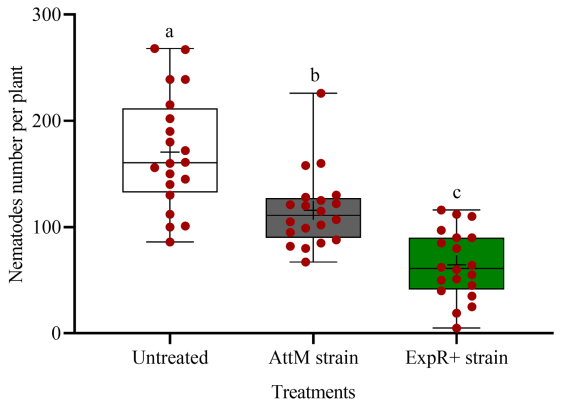

FIGURE 1 | Effect of previous plant priming with the oxo-C14-HSL-producing *Ensifer meliloti* ExpR + strain on the invasion of *Pratylenchus penetrans* into soybean roots. The lactonase-expressing strain *E. meliloti* AttM and $MgCl_2$ were used as controls without oxo-C14-HSL priming. Invaded nematodes were stained and counted 10 days post-infection. Different letters indicate significant differences among treatments (GLM, Poisson distribution and log link, Tukey adjustment, $n = 20$).

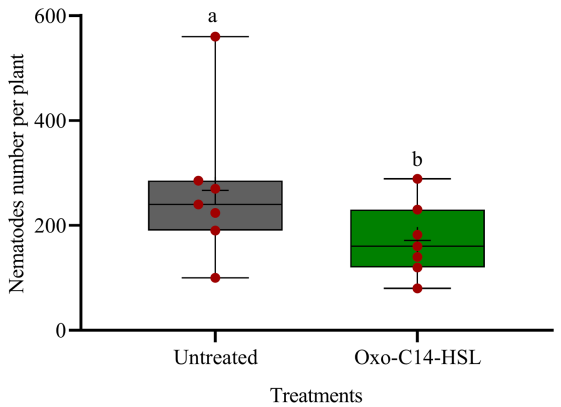

FIGURE 2 | Effect of synthetic oxo-C14-HSL as priming agent on *Pratylenchus penetrans* invasion into soybean roots. Different letters indicate significant differences among treatments (GLM, Poisson distribution and log link, Tukey adjustment, $n = 7$).

The spatial dispersion of *P. penetrans* inside the roots was changed by strain ExpR+ (**Figure 3**). The nematodes were significantly more aggregated in the roots of untreated or AttM treated plants compared to roots of ExpR+ primed plants (P-value < 0.0001). This suggested that primed plants responded more strongly to the early invasion of nematodes compared to non-primed plants, where nematodes easily established in the roots.

Similar Effect of oxo-C14-HSL and BABA in Reducing *P. penetrans* Invasion Into Roots

We tested the efficacy of synthesic oxo-C14-HSL for defense priming, compared to the known priming inducer BABA and

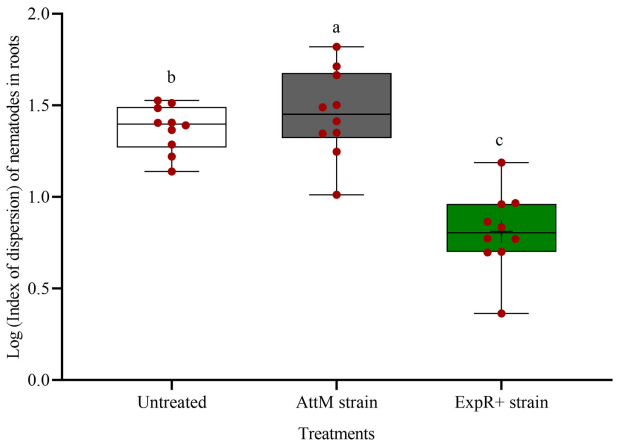

FIGURE 3 | Spatial dispersion of invaded *Pratylenchus penetrans* inside the roots of soybean plants primed with *Ensifer meliloti* ExpR + producing oxo-C14-HSL compared to roots of non-primed soybean inoculated with the lactonase-expressing strain *E. meliloti* AttM, or $MgCl_2$ as control. The coefficient of dispersion Z of *P. penetrans* was compared to a random (Poisson) distribution using the GLIMMIX procedure. (Tukey adjustment, log link, $n = 10$). Different letters indicate significant differences among treatments.

nematode associated molecules (PpNemawater). Stimulating soybean cv. Primus with oxo-C14-HSL or BABA led to a significant reduction of nematode invasion when compared to the control (GLM with Dunnet adjustment for multiple comparisons to the control, P-value < 0.005; **Figure 4**). Both compounds did not significantly differ in their reduction effect on nematode invasion into soybean roots. The nematode number in soybean roots stimulated with PpNemawater did not significantly differ from the control (P-value $= 0.487$). No significant effect on root fresh weight was observed within the experimental period, although a trend for a slightly better growth was observed for roots treated with oxo-C14-HSL (**Supplementary Figure 2**).

Oxo-C14-HSL Systemically Induced Plant Defense Against *P. penetrans*

In split-root systems, we investigated whether the observed effect of oxo-C14-HSL on nematode invasion is a local effect or mediated by a systemic plant response. When strain ExpR+ is inoculated on the same side of the split-root system as the nematodes, then it may affect the nematodes by both, systemic induction of plant defense and local interactions. Locally, there may be a direct antagonism against the nematodes or local plant responses like production of ROS or cell wall thickening in the affected root tissue. When strain ExpR+ is inoculated on the opposite side of the split-root system as the nematodes, then only one of both mechanisms can reduce the invasion of the nematode on the other side. Thus, a similar effect in both situations indicated a systemic plant-mediated mechanism and a negligible local interaction. The oxo-C14-HSL-producing *E. meliloti* strain ExpR+ was inoculated to the rhizosphere in one-half of the split-root system. Infective stages of *P. penetrans* were inoculated either to the side of

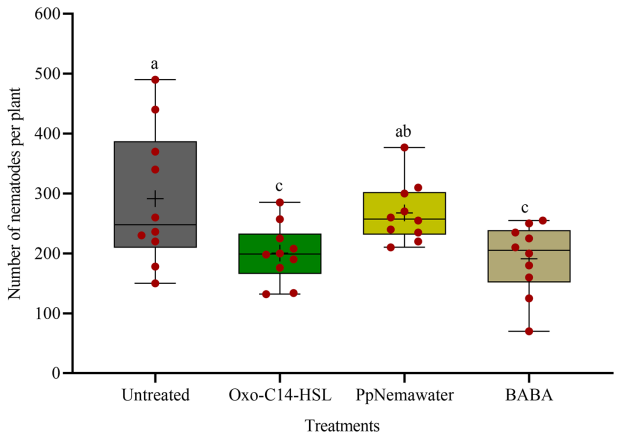

FIGURE 4 | Effect of synthetic oxo-C14-HSL compared to DL-β-aminobutyric acid (BABA) and PpNemawater on the invasion of *Pratylenchus penetrans* into soybean roots. Different letters indicate significant differences among treatments (SAS proc GLIMMIX, Tukey adjustment, $n = 10$).

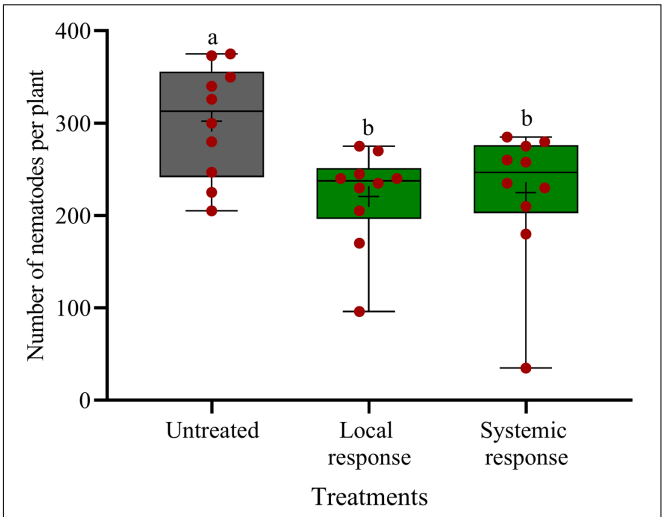

FIGURE 5 | Systemic and local effects of the oxo-C14-HSL-producing *Ensifer meliloti* ExpR + strain on the invasion of *Pratylechus penetrans* into soybean roots. Different letters indicate significant differences among treatments in Tukey's test ($n = 10$). Mean numbers of invaded nematodes in roots are shown as (+) for each treatment, while the medians are shown as (–).

the roots colonized by strain ExpR+ or to the opposite side, and counted in roots after 7 days. *P. penetrans* invasion into the roots was equally reduced on both sides of the roots of primed plants compared to the control without strain ExpR+ (**Figure 5**). Compared to the bacteria-free control, the total number of nematodes was significantly lower on both sides, with strain ExpR+ (223 ± 53, P-value < 0.0001) and on the opposite side without ExpR+ (225 ± 75, P-value = 0.0092). The additional reduction in median numbers of nematodes in the root due to co-localization of ExpR+ and *P. penetrans* compared to localization on opposite roots was minor and not significant (P-value = 0.88). This suggested that *E. meliloti* ExpR + systemically induced plant defense against *P. penetrans*, and that direct antagonism of strain ExpR + against *P. penetrans* or an induction of local root defense by strain ExpR+ did not significantly contribute to the suppression of the nematode. Roots infected with nematodes did not significantly differ among treatments after the experimental period. A trend of higher root mass was observed for roots that were locally inoculated with strain ExpR+. Overall, drenching soybean roots with *E. meliloti* strain ExpR + slightly increased the plant growth (**Supplementary Table 1**).

When testing direct toxic effects of the bacterial strains or synthetic oxo-C14-HSL against *P. penetrans*, only 3.0% of the tested nematodes were affected. This did not significantly differ from the $MgCl_2$ control or the acetone control, respectively (**Supplementary Table 2**).

Enhanced Defense of Plants Against *P. penetrans* Persisted After Removal of Priming Agents

We tested whether a temporary exposure of the root to oxo-C14-HSL was sufficient to result in reduced root invasion of the nematodes 3, 7, or 15 days after removal of the trigger. In parallel, we tested whether such a priming of plant defense was triggered by signaling compounds released from the surface of the nematode that simulated biotic stress. Soybean plants inoculated with oxo-C14-HSL were significantly less invaded by *P. penetrans* compared to control plants that were not exposed to oxo-C14-HSL (**Figure 6**). This priming effect stayed significant 3, 7, and 15 days after removal of oxo-C14-HSL. Similarly, the invasion of nematodes into soybean roots that have been exposed to surface-released compounds of *P. penetrans* was significantly lower compared to control plants, 3 and 7 days after removal of the inducer. After 15 days, the reduction compared to the control was statistically not significant.

Priming Was Associated With Enhanced Synthesis of Phytoalexins and Phenolic Compounds in Roots Upon *P. penetrans* Challenge

The phytoalexins in roots after exposure to oxo-C14-HSL and after invasion of *P. penetrans* into primed and non-primed roots were monitored by HPLC. Glyceollin I and coumestrol-like isoflavonoids were detected and quantified (**Supplementary Figure 3**). Without nematode invasion, the concentration of coumestrol-like compounds in primed and non-primed roots did not significantly differ, indicating that priming did not lead to an increased stress level to the plants (**Figure 7**). After nematode invasion, the phytoalexins coumestrol and glyceollin increased in concentration in the roots compared to control plants without nematodes. Most interestingly, upon nematode challenge, glyceollin synthesis was significantly enhanced in oxo-C14-HSL primed roots compared to non-primed roots (**Figure 8**). This suggested that the priming of soybean plants led to a more rapid and strong defense when inoculated with

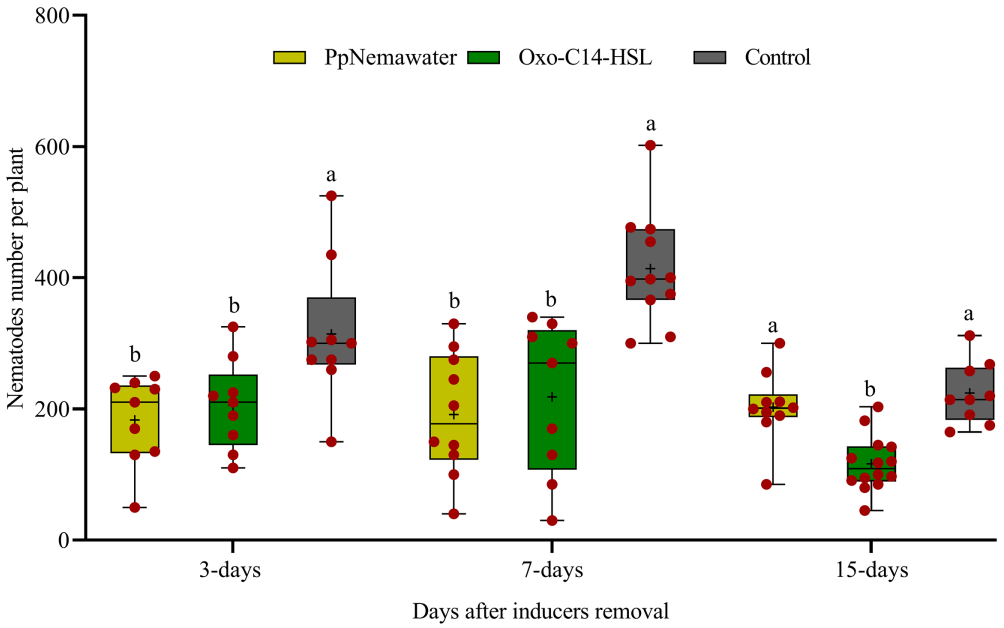

FIGURE 6 | Persistence of enhanced defense of plants against root invasion of *Pratylenchus penetrans* after removal of inducing agents (oxo-C14-HSL or PpNemawater). Different letters indicate significant differences among treatments in Tukey's test (n = 10).

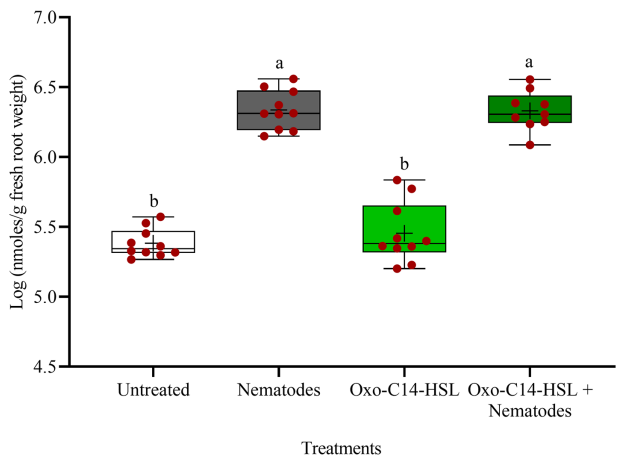

FIGURE 7 | Quantification of coumestrol-like phytoalexins in roots of oxo-C14-HSL primed and non-primed plants of soybean cv. Primus by high-performance liquid chromatography. The mean of phytoalexin content in roots in soybean roots is shown as (+) for each treatment, while the medians are shown as (–). Different letters indicate significant differences among treatments in Tukey's test (n = 10).

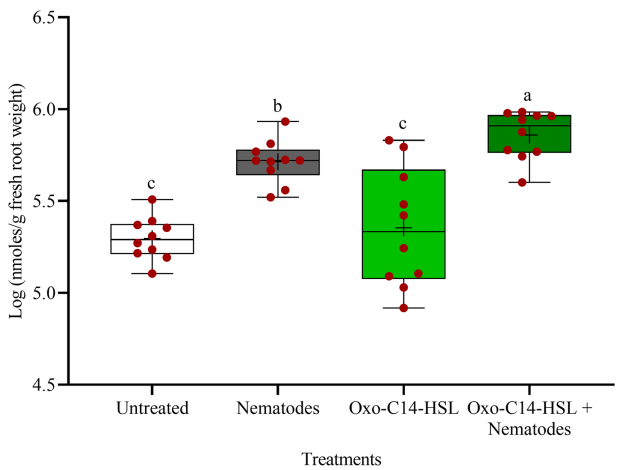

FIGURE 8 | Quantification of glyceollin I content in roots of oxo-C14-HSL primed and non-primed plants of soybean cv. Primus by high-performance liquid chromatography. The mean of glyceollin content in roots is shown as (+) for each treatment, while the medians are shown as (–). Different letters indicate significant differences among treatments in Tukey's test (n = 10).

nematodes. In accordance, the oxo-C14-HSL primed roots showed a trend for a higher accumulation of total phenolic compounds compared to the acetone control after challenge with nematodes (**Figure 9**). However, measurement of total phenolic compounds was not sensitive enough to reveal significant differences between primed and non-primed roots before or after nematode invasion.

DISCUSSION

Rhizosphere inoculation of soybean cv. Primus with the *N*-acyl homoserine lactone oxo-C14-HSL producing strain ExpR+ reduced invasion of *P. penetrans* into roots. In contrast, rhizosphere inoculation of the nearly isogenic strain AttM, which expressed a lactonase to remove any synthesized oxo-C14-HSL, led to significantly more nematodes in the root. The pure

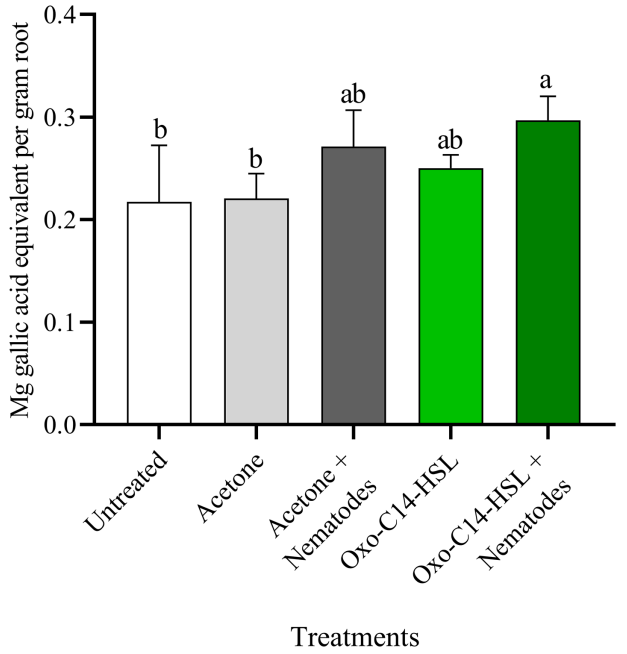

FIGURE 9 | Quantification of total phenolic compounds in roots of oxo-C14-HSL primed and non-primed plants of soybean cv. Primus. Total phenolic compounds were quantified according to the Folin-Ciocalteu method by spectrophotometry at an absorbance of 765 nm and normalized to gallic acid. Different letters indicate significant differences among treatments in Tukey's test (n = 5).

compound oxo-C14-HSL also enhanced the plant defense; thus, other strain-related factors like exopolysaccharide production could not explain the observed effect. When the compound and nematodes were added to opposite parts of a split-root system, priming of plant defense was also achieved. This showed that the nematodes were not directly affected by oxo-C14-HSL or by local root responses to the compound. Thus, oxo-C14-HSL acted as a signaling molecule that systemically induced priming of the plant defense against *P. penetrans*. In a study by Zarkani et al. (2013), oxo-C14-HSL but not a short chain *N*-acyl homoserine lactone systemically induced resistance against leaf infection by the bacterium *Pseudomonas syringe* in *Arabidopsis thaliana*. In other studies on airborne diseases, oxo-C14-HSL induced systemic resistance of barley against the powdery mildew fungus *Blumeria graminis* f. sp. *hordei* (Shrestha et al., 2019) or the leaf rust causing fungus *Puccinia hordei* (Wehner et al., 2019) in a barley-genotype-dependent manner. Induction of barley by oxo-C14-HSL resulted in activation of MAP kinases, up-regulation of defense-related genes, and accumulation of lignin. Such basic defense reactions and strengthening of cell walls are likely to affect root penetration of *P. penetrans* as well.

Earlier studies used leaves from plants, which were exposed to oxo-C14-HSL, to test for a primed state of the plant in defense against the respective pathogen or pest (Zarkani et al., 2013; Shrestha et al., 2019; Wehner et al., 2019, 2021), without a time lag between oxo-C14-HSL exposure and biotic challenge. Our study showed that enhanced defense of the plants against root invasion of *P. penetrans* persisted after removal of the inducing compound for at least 2 weeks. This priming of the plant's defense system was equally achieved by compounds released by the nematodes and the bacterial signaling compound oxo-C14-HSL. While perception of the nematode by the root and the following preparation of the plant for a nematode attack make sense ecologically, the priming by the bacterial inducer is less perspicuous and implies a cooperation among plants and rhizobacteria. Mostly, studies to chemically induce plant resistance or priming used compounds that mimic plant metabolites like β-aminobutyric acid, salicylic acid, pipecolic acid, or jasmonic acid (Navarova et al., 2012; Zhong et al., 2014; Ji et al., 2015; Hu et al., 2017; Thevenet et al., 2017). Depending on the concentration, such compounds may significantly stress the plant by activation of basal defense mechanisms like ROS accumulation, lignin formation, and callose deposition (Ji et al., 2015). In contrast, priming involves a memory of the plant and avoids ongoing stress and waste of resources. Priming of soybean plants was associated with enhanced synthesis of the isoflavonoid phytoalexin glyceollin upon *P. penetrans* challenge. Rapid production of glyceollin in soybean roots was shown to protect the roots from attack of the fungus *Fusarium solani* f. sp. *glycines* that causes sudden death syndrome (Lozovaya et al., 2004). The importance of rapid glyceollin synthesis was also shown for the defense of soybean plants against the pathogens *Macrophomina phaseolina* and *Phytophthora sojae* by comparing the susceptibility of transgenic plants with suppressed glyceollin synthesis to the wildtype (Lygin et al., 2013). Upon penetration of soybean roots by the soybean cyst nematode *Heterodera glycines*, glyceollin accumulated locally in roots of resistant but not in susceptible soybean cultivars (Huang and Barker, 1991). These plants were not primed and accumulation of glyceollin in roots of the resistant cultivar took 24 h. In our study, upregulation of the defense marker glyceollin by oxo-C14-HSL was not observed directly after the priming phase, but reached higher concentrations in primed plants than in non-primed plants after root invasion of the nematode. This observation corresponded to the model of defense priming in the narrow sense, where the priming stimulus is not causing a strong defense response of the plant but activates a memory mechanism that leads to a faster and stronger defense response upon subsequent challenge by a pathogen (Mauch-Mani et al., 2017). The primed state of the plant allows for a fast defense response, which is crucial for a successful defense against plant-parasitic nematodes. During root invasion, these nematodes start to suppress immune responses of the host locally. However, when the plant is faster in activating defense responses than the nematode can suppress innate immunity, then it may boost basal defenses using systemic signaling pathways and subsequently stop the attack (Topalović et al., 2020). The mechanism of defense priming in this study remains to be investigated. In isogenic soybean lines differing in susceptibility to soybean cyst nematodes, significant differences in DNA methylation between resistant and susceptible lines were observed that regulated miRNA functions during nematode–soybean interaction (Rambani et al., 2020). Studies showing dynamic epigenetic changes that play a role in plant-nematode interaction have recently been reviewed (Hewezi, 2020), but

evidence for epigenetic changes of the plant to prime its innate immunity for enhanced resistance to plant-parasitic nematodes is lacking. The molecular mechanisms on how the plant memorized the priming event and activated defense still need to be investigated.

Interestingly, the dispersion pattern of invaded nematodes varied between primed and non-primed plants. Dense clusters of nematodes were observed in the root tissue of non-primed plants, in contrast to a significantly more even distribution of the nematodes in ExpR+ primed roots. Root-lesion nematodes explore the local physiological state of the root tissue by thrusting the stylet several times into a cell before entering the root (Kurppa and Vrain, 1985; Karakas, 2009). In non-primed roots, many nematodes may enter at a favorable root area or even the same entry site, thus leading to aggregated clusters of parasitic nematodes in the root. In primed plants, the fast local induction of plant defense may distract followers from entering at the same side, which resulted in a more even dispersion of the nematodes in the root.

Defense priming of barley cultivars against two airborne fungal pathogens was proposed to be genotype-specific and thus amenable to exploitation in breeding programs (Shrestha et al., 2019; Wehner et al., 2019). Differences in primability of soybean cultivars for induced defense against the soilborne root lesion nematodes still need to be investigated.

In conclusion, we showed that chemical signals in the rhizosphere can be harnessed to prime immunity of the soybean cultivar Primus against the root lesion nematode *P. penetrans*. The defense priming was systemically induced in the plant, did not lead to accumulation of defense markers prior to nematode attack, and persisted after removal of the priming agent. These results may have implications for future sustainable crop production, in which microbes could replace or complement chemical plant protection. Strengthening the primability of soybean varieties by marker-assisted breeding could become an environmentally friendly strategy of plant protection. As a vision, future cultivars may sensitively perceive signals from associated rhizobacteria that help to anticipate nematode attack, and rhizodeposits of the cultivar together with agricultural soil biome management may help to strengthen the bacterial priming inducers within the rhizosphere community of such a cultivar.

DATA AVAILABILITY STATEMENT

The original contributions presented in the study are included in the article/**Supplementary Material**, further inquiries can be directed to the corresponding author/s.

AUTHOR CONTRIBUTIONS

HH, AE, and LB designed the research plan. VH contributed with his expertise on soybean, chose and provided plant material, and discussed the experimental design and results. SA and AE performed the experiments. SA and BL analyzed phytoalexins. HH and AE did the statistical analyses. AE prepared the figures. SA wrote the manuscript. All authors revised the manuscript, contributed to the article, and approved the submitted version.

FUNDING

The study was funded by the German Research Foundation DFG EL 1038/2-1. AE's participation in conferences was funded by the "Gisela und Hermann Stegemann Foundation" and "Gemeinschaft der Förderer und Freunde des Julius Kühn-Instituts."

ACKNOWLEDGMENTS

We thank Adam Schikora for providing the stains ExpR+ and AttM, and Kristina Bachteler and the Sojaförderring for support with advice and provision of soybean seeds.

SUPPLEMENTARY MATERIAL

The Supplementary Material for this article can be found online at: https://www.frontiersin.org/articles/10.3389/fpls.2021.651943/full#supplementary-material

REFERENCES

Ainsworth, E. A., and Gillespie, K. M. (2007). Estimation of total phenolic content and other oxidation substrates in plant tissues using Folin-Ciocalteu reagent. *Nat. Protoc.* 2, 875–877. doi: 10.1038/nprot.2007.102

Beringer, J. E. (1974). R factor transfer in *Rhizobium leguminosarum*. *J. Gen. Microbiol.* 84, 188–198. doi: 10.1099/00221287-84-1-188

Borges, A. A., Jimenez-Arias, D., Exposito-Rodriguez, M., Sandalio, L. M., and Perez, J. A. (2014). Priming crops against biotic and abiotic stresses: MSB as a tool for studying mechanisms. *Front. Plant Sci.* 5:642. doi: 10.3389/fpls.2014.00642

Bybd, D. W. Jr., Kirkpatrick, T., and Barker, K. R. (1983). An improved technique for clearing and staining plant tissues for detection of nematodes. *J. Nematol.* 15, 142–143.

Conrath, U., Beckers, G. J. M., Langenbach, C. J. G., and Jaskiewicz, M. R. (2015). Priming for enhanced defense. *Annu. Rev. Phytopathol.* 53, 97–119. doi: 10.1146/annurev-phyto-080614-120132

Dababat, A. A., and Sikora, R. A. (2007). Induced resistance by the mutualistic endophyte, *Fusarium oxysporum* strain 162, toward *Meloidogyne incognita* on tomato. *Biocontrol Sci. Technol.* 17, 969–975. doi: 10.1080/09583150701582057

Dodds, P. N., and Rathjen, J. P. (2010). Plant immunity: towards an integrated view of plant-pathogen interactions. *ıNat. Rev. Genet.* 11, 539–548. doi: 10.1038/nrg2812

Elhady, A., Hallmann, J., and Heuer, H. (2020). Symbiosis of soybean with nitrogen fixing bacteria affected by root lesion nematodes in a density-dependent manner. *Sci. Rep.* 10, 1619. doi: 10.1038/s41598-020-58546-x

Elhady, A., Heuer, H., and Hallmann, J. (2018). Plant parasitic nematodes on soybean in expanding production areas of temperate regions. *J. Plant Dis. Prot.* 125, 642. doi: 10.1007/s41348-018-0188-y

Elhady, A., Thünen, T., Höppner, F., Balko, C., Heuer, H., and Hallmann, J. (2019). Evaluation of soybean cultivars for their susceptibility to root-lesion nematodes under temperate conditions. *Nematology* 21, 523–531. doi: 10.1163/15685411-00003232

European and Mediterranean Plant Protection Organization. (2013). PM 7/119 (1) Nematode extraction. *EPPO Bull.* 43, 471–495. doi: 10.1111/epp.12077

Ghaderi, S., Fathipour, Y., and Asgari, S. (2018). Population Density and Spatial Distribution Pattern of *Tuta absoluta* (Lepidoptera: Gelechiidae) on Different Tomato Cultivars. *J. Agr. Sci. Tech.* 20, 543–556.

Hewezi, T. (2020). Epigenetic mechanisms in nematode-plant interactions. *Annu. Rev. Phytopathol.* 58, 119–138. doi: 10.1146/annurev-phyto-010820-012805

Hu, Y., You, J., Li, C., Hua, C., and Wang, C. (2017). Exogenous application of methyl jasmonate induces defence against *Meloidogyne hapla* in soybean. *Nematology* 19, 293–304. doi: 10.1163/15685411-00003049

Huang, J.-S., and Barker, K. R. (1991). Glyceollin I in soybean-cyst nematode interactions: spatial and temporal distribution in roots of resistant and susceptible soybeans. *Plant Physiol.* 96, 1302–1307.

Iwao, S. (1968). A new regression method for analyzing the aggregation pattern of animal populations. *Res. Popul. Ecol.* 10, 1–20.

Ji, H., Kyndt, T., He, W., Vanholme, B., and Gheysen, G. (2015). ß-Aminobutyric acid-induced resistance against root-knot nematodes in rice is based on increased basal defense. *Mol. Plant Microbe Interact.* 28, 519–533. doi: 10.1094/MPMI-09-14-0260-R

Jones, J. T., Haegeman, A., Danchin, E. G. J., Gaur, H. S., Helder, J., Jones, M. G. K., et al. (2013). Top 10 plant-parasitic nematodes in molecular plant pathology. *Mol. Plant Pathol.* 14, 946–961. doi: 10.1111/mpp.12057

Jung, S. C., Martínez-Medina, A., López-Ráez, J. A., and Pozo, M. J. (2012). Mycorrhiza-induced resistance and priming of plant defenses. *J. Chem. Ecol.* 38, 651–664. doi: 10.1007/s10886-012-0134-6

Karakas, M. (2009). Penetration and feeding behavior of *Pratylenchus penetrans* (Nematoda Pratylenchidae) in red radish roots. *Kafkas Üniv. Fen Bil. Enst. Derg.* 1, 31–36.

Klessig, D. F., Manohar, M., Baby, S., Koch, A., Danquah, W. B., Luna, E., et al. (2019). Nematode ascaroside enhances resistance in a broad spectrum of plant–pathogen systems. *J. Phytopathol.* 167, 265–272. doi: 10.1111/jph.12795

Kurppa, S., and Vrain, T. C. (1985). Penetration and feeding behavior of Pratylenchus penetrans in strawberry roots. *Revue Nématol.* 8, 273–276.

Liu, H., Brettell, L. E., Qiu, Z., and Singh, B. K. (2020). Microbiome-mediated stress resistance in plants. *Trends Plant Sci.* 25, 733–743. doi: 10.1016/j.tplants.2020.03.014

Lozovaya, V. V., Lygin, A. V., Zernova, O. V., Li, S., Hartman, G. L., and Widholm, J. M. (2004). Isoflavonoid accumulation in soybean hairy roots upon treatment with *Fusarium solani*. *Plant Physiol. Biochem.* 42, 671–679. doi: 10.1016/j.plaphy.2004.06.007

Lygin, A. V., Zernova, O. V., Hill, C. B., Kholina, N. A., Widholm, J. M., Hartman, G. L., et al. (2013). Glyceollin is an important component of soybean plant defense against *Phytophthora sojae* and *Macrophomina phaseolina*. *Phytopathology* 103, 984–994. doi: 10.1094/PHYTO-12-12-0328-R

Martínez-Medina, A., Flors, V., Heil, M., Mauch-Mani, B., Pieterse, C. M. J., Pozo, M. J., et al. (2016). Recognizing plant defense priming. *Trends Plant Sci.* 21, 818–822. doi: 10.1016/j.tplants.2016.07.009

Mauch-Mani, B., Baccelli, I., Luna, E., and Flors, V. (2017). Defense priming: an adaptive part of induced resistance. *Annu. Rev. Plant Biol.* 68, 485–512. doi: 10.1146/annurev-arplant-042916-041132

Mendy, B., Wang'ombe, M. W., Radakovic, Z. S., Holbein, J., Ilyas, M., Chopra, D., et al. (2017). Arabidopsis leucine-rich repeat receptor-like kinase NILR1 is required for induction of innate immunity to parasitic nematodes. *PLoS Pathog.* 13:e1006284. doi: 10.1371/journal.ppat.1006284

Molinari, S., and Leonetti, P. (2019). Bio-control agents activate plant immune response and prime susceptible tomato against root-knot nematodes. *PLoS One*. 14:e0213230. doi: 10.1371/journal.pone.0213230

Navarova, H., Bernsdorff, F., Doring, A.-C., and Zeier, J. (2012). Pipecolic acid, an endogenous mediator of defense amplification and priming, is a critical regulator of inducible plant immunity. *Plant Cell* 24, 5123–5141. doi: 10.1105/tpc.112.103564

Pellock, B. J., Teplitski, M., Boinay, R. P., Bauer, W. D., and Walker, G. C. (2002). A LuxR homolog controls production of symbiotically active extracellular polysaccharide II by *Sinorhizobium meliloti*. *J. Bacteriol.* 184, 5067–5076. doi: 10.1128/JB.184.18.5067-5076.2002

Rambani, A., Hu, Y., Piya, S., Long, M., Rice, J. H., Pantalone, V., et al. (2020). Identification of differentially methylated miRNA genes during compatible and incompatible interactions between soybean and soybean cyst nematode. *Mol. Plant Microbe Interact.* 33, 1340–1352. doi: 10.1094/MPMI-07-20-0196-R

Ramírez-Carrasco, G., Martínez-Aguilar, K., and Alvarez-Venegas, R. (2017). Transgenerational defense priming for crop protection against plant pathogens: a hypothesis. *Front. Plant Sci.* 8:696. doi: 10.3389/fpls.2017.00696

Schenk, S. T., and Schikora, A. (2014). AHL-priming functions via oxylipin and salicylic acid. *Front. Plant Sci.* 5:784. doi: 10.3389/fpls.2014.00784

Shrestha, A., Elhady, A., Adss, S., Wehner, G., Böttcher, C., Heuer, H., et al. (2019). Genetic differences in barley govern the responsiveness to *N*-acyl homoserine lactone. *Phytobiomes J.* 3, 191–202. doi: 10.1094/PBIOMES-03-19-0015-R

Thevenet, D., Pastor, V., Baccelli, I., Balmer, A., Vallat, A., Neier, R., et al. (2017). The priming molecule beta-aminobutyric acid is naturally present in plants and is induced by stress. *New Phytol.* 213, 552–559. doi: 10.1111/nph.14298

Topalović, O., Bredenbruch, S., Schleker, A. S. S., and Heuer, H. (2020). Microbes attaching to endoparasitic phytonematodes in soil trigger plant defense upon root penetration by the nematode. *Front. Plant Sci.* 11:138. doi: 10.3389/fpls.2020.00138

Vieira, P., Mayer, T., Eves-van den Akker, S., Howe, D. K., Zasada, I., Baum, T., et al. (2018). Identification of candidate effector genes of *Pratylenchus penetrans*. *Mol. Plant Pathol.* 19, 1887–1907. doi: 10.1111/mpp.12666

Wehner, G., Kopahnke, D., Richter, K., Kecke, S., Schikora, A., and Ordon, F. (2019). Priming is a suitable strategy to enhance resistance towards leaf rust in barley. *Phytobiomes J.* 3, 46–51. doi: 10.1094/PBIOMES-09-18-0041-R

Wehner, G., Schikora, A., Ordon, F., and Will, T. (2021). Priming negatively affects feeding behaviour and aphid biomass of *Rhopalosiphum padi* on barley. *J. Pest Sci* doi: 10.1007/s10340-021-01329-8 **VPQ,

Zarkani, A. A., Stein, E., Rohrich, C. R., Schikora, M., Evguenieva-Hackenberg, E., Degenkolb, T., et al. (2013). Homoserine lactones influence the reaction of plants to rhizobia. *Int. J. Mol. Sci.* 14, 17122–17146. doi: 10.3390/ijms140817122

Zhan, L.-P., Peng, D.-L., Wang, X.-L., Kong, L.-A., Peng, H., Liu, S.-M., et al. (2018). Priming effect of root-applied silicon on the enhancement of induced resistance to the root-knot nematode *Meloidogyne graminicola* in rice. *BMC Plant Biol.* 18:50. doi: 10.1186/s12870-018-1266-9

Zhong, Y., Wang, B., Yan, J., Cheng, L., Yao, L., Xiao, L., et al. (2014). DL-ß-aminobutyric acid-induced resistance in soybean against *Aphis glycines* Matsumura (Hemiptera: Aphididae). *PLoS One*. 9:e85142. doi: 10.1371/journal.pone.0085142

Conflict of Interest: The authors declare that the research was conducted in the absence of any commercial or financial relationships that could be construed as a potential conflict of interest.

frontiers in Plant Science

ORIGINAL RESEARCH
published: 25 May 2021
doi: 10.3389/fpls.2021.680151

Transcriptomic Analysis of Resistant and Susceptible Responses in a New Model Root-Knot Nematode Infection System Using *Solanum torvum* and *Meloidogyne arenaria*

Kazuki Sato[1], Taketo Uehara[2], Julia Holbein[3], Yuko Sasaki-Sekimoto[4], Pamela Gan[1], Takahiro Bino[5], Katsushi Yamaguchi[5], Yasunori Ichihashi[6], Noriko Maki[1], Shuji Shigenobu[5], Hiroyuki Ohta[4], Rochus B. Franke[7], Shahid Siddique[3,8], Florian M. W. Grundler[3], Takamasa Suzuki[9], Yasuhiro Kadota[1] and Ken Shirasu[1,10]**

[1] RIKEN Center for Sustainable Resource Science, Yokohama, Japan, [2] Central Region Agricultural Research Center, National Agriculture and Food Research Organization, Tsukuba, Japan, [3] INRES – Molecular Phytomedicine, Rheinische Friedrich-Wilhelms-University of Bonn, Bonn, Germany, [4] School of Life Science and Technology, Tokyo Institute of Technology, Yokohama, Japan, [5] NIBB Core Research Facilities, National Institute for Basic Biology, Okazaki, Japan, [6] RIKEN BioResource Research Center, Tsukuba, Japan, [7] Institute of Cellular and Molecular Botany, Rheinische Friedrich-Wilhelms-University of Bonn, Bonn, Germany, [8] Department of Entomology and Nematology, University of California, Davis, Davis, CA, United States, [9] Department of Biological Chemistry, College of Bioscience and Biotechnology, Chubu University, Kasugai, Japan, [10] Graduate School of Science, The University of Tokyo, Bunkyo, Japan

OPEN ACCESS

Edited by:
Daguang Cai,
University of Kiel, Germany

Reviewed by:
Mihir Kumar Mandal,
Claflin University, United States
Yunliang Peng,
Sichuan Academy of Agricultural Sciences, China

***Correspondence:**
Yasuhiro Kadota
yasuhiro.kadota@riken.jp
Ken Shirasu
ken.shirasu@riken.jp

Specialty section:
This article was submitted to Plant Pathogen Interactions, a section of the journal Frontiers in Plant Science

Received: 13 March 2021
Accepted: 30 April 2021
Published: 25 May 2021

Citation:
Sato K, Uehara T, Holbein J, Sasaki-Sekimoto Y, Gan P, Bino T, Yamaguchi K, Ichihashi Y, Maki N, Shigenobu S, Ohta H, Franke RB, Siddique S, Grundler FMW, Suzuki T, Kadota Y and Shirasu K (2021) Transcriptomic Analysis of Resistant and Susceptible Responses in a New Model Root-Knot Nematode Infection System Using Solanum torvum and Meloidogyne arenaria. Front. Plant Sci. 12:680151. doi: 10.3389/fpls.2021.680151

Root-knot nematodes (RKNs) are among the most devastating pests in agriculture. *Solanum torvum* Sw. (Turkey berry) has been used as a rootstock for eggplant (aubergine) cultivation because of its resistance to RKNs, including *Meloidogyne incognita* and *M. arenaria*. We previously found that a pathotype of *M. arenaria*, A2-J, is able to infect and propagate in *S. torvum*. *In vitro* infection assays showed that *S. torvum* induced the accumulation of brown pigments during avirulent pathotype A2-O infection, but not during virulent A2-J infection. This experimental system is advantageous because resistant and susceptible responses can be distinguished within a few days, and because a single plant genome can yield information about both resistant and susceptible responses. Comparative RNA-sequencing analysis of *S. torvum* inoculated with A2-J and A2-O at early stages of infection was used to parse the specific resistance and susceptible responses. Infection with A2-J did not induce statistically significant changes in gene expression within one day post-inoculation (DPI), but afterward, A2-J specifically induced the expression of chalcone synthase, spermidine synthase, and genes related to cell wall modification and transmembrane transport. Infection with A2-O rapidly induced the expression of genes encoding class III peroxidases, sesquiterpene synthases, and fatty acid desaturases at 1 DPI, followed by genes involved in defense, hormone signaling, and the biosynthesis of lignin at 3 DPI. Both isolates induced the expression of suberin biosynthetic genes, which may be triggered by wounding during

nematode infection. Histochemical analysis revealed that A2-O, but not A2-J, induced lignin accumulation at the root tip, suggesting that physical reinforcement of cell walls with lignin is an important defense response against nematodes. The *S. torvum*-RKN system can provide a molecular basis for understanding plant-nematode interactions.

Keywords: Turkey berry, plant immunity, plant-parasitic nematode, lignin deposition, comparative transcriptomics

INTRODUCTION

Plant-parasitic nematodes (PPNs) infect a broad range of commercially important crop families such as the Solanaceae (tomato, potato, pepper), Fabaceae (soybean, lucerne, lentils), Malvaceae (cotton), Amaranthaceae (sugar beet), and Poaceae (syn. Gramineae; rice, wheat, maize), causing an estimated annual loss of $80 billion USD (Jones et al., 2013; Sato et al., 2019). The most economically important group of PPNs are sedentary endoparasites, including root-knot nematodes (RKNs) and cyst nematodes (CNs) (Palomares-Rius et al., 2017). Sedentary endoparasites induce the formation of permanent feeding cells that provide specialized nutrient sources for nematodes (Bartlem et al., 2014; Siddique and Grundler, 2018; Smant et al., 2018). Infective second-stage juveniles (J2s) of RKNs (*Meloidogyne* spp.) predominantly invade near the root tip and then migrate intercellularly toward the apical meristematic region without crossing the endodermis, making a U-turn to enter the vascular cylinder where they induce several giant cells as a feeding site by stimulating the redifferentiation of root cells into multinucleate giant cells by repeated nuclear divisions without cytoplasmic division. After maturation, adult RKN females lay eggs in a gelatinous egg mass on or below the surface of the root (Sijmons et al., 1991; Abad et al., 2009; Escobar et al., 2015). In contrast, CNs move destructively through cells into the vascular cylinder, select a single cell, and form a syncytium as a feeding site by local dissolution of cell walls and protoplast fusion of neighboring cells. A CN female produces hundreds of eggs and its body forms a cyst that can protect the eggs for many years in the soil (Wyss and Zunke, 1986; Bohlmann and Sobczak, 2014; Bohlmann, 2015).

Nematicides have been commonly used to control PPNs in agriculture, but some nematicides such as methyl bromide and aldicarb are currently banned from use in many countries due to their negative effects on the environment and human health (Zasada et al., 2010; Brennan et al., 2020; Oka, 2020). It has therefore become important to understand the molecular mechanisms of plant immunity against PPNs to provide a foundation for the development of new environmentally friendly and effective control methods.

In general, the plant immune system is represented by two inter-related tiers (Jones and Dangl, 2006; Dodds and Rathjen, 2010). The first is governed by cell surface-localized pattern recognition receptors (PRRs) that perceive pathogen-associated molecular patterns (PAMPs), leading to pattern-triggered immunity (PTI) (Boutrot and Zipfel, 2017). Successful pathogens secrete effector molecules into the apoplast or directly into plant cells, which interfere with PTI, resulting in successful infection. Resistant plants recognize cell-invading effectors through recognition by intracellular nucleotide-binding domain leucine-rich repeat (NLR)-type immune receptors, which are encoded by resistance (*R*) genes. Similar mechanisms are also conserved in plant-PPN interactions. For example, the well-conserved nematode pheromone ascaroside has been identified as a PAMP (Manosalva et al., 2015), but the corresponding PRR has not yet been found. PPN genome sequence analyses identified a number of candidate virulence effectors (summarized in Mejias et al., 2019), and a handful of NLR protein-encoding *R* genes involved in PPN recognition have been well-studied and characterized, including tomato *Mi-1.2*, *Mi-9,* and *Hero-A*; potato *Gpa2* and *Gro1-4*; pepper *CaMi*; and prune *Ma* (Milligan et al., 1998; van der Vossen et al., 2000; Ernst et al., 2002; Paal et al., 2004; Chen et al., 2007; Jablonska et al., 2007; Claverie et al., 2011; Kaloshian et al., 2011). *Mi-1.2*, *Mi-9*, *CaMi*, and *Ma* confer resistance against RKNs, whereas *Hero-A*, *Gpa2*, and *Gro1-4* provide resistance against CNs.

Although the PPN perception mechanism is somewhat clearer at the molecular level, it is still largely unknown what kind of downstream responses are induced after the recognition of avirulent PPNs. It is also unclear what kind of host responses are induced after infection with virulent PPNs, leading to susceptibility and infestation. There are several difficulties in working on plant responses against PPNs. First and foremost, most model plants, such as Arabidopsis, are susceptible to PPNs and therefore cannot be used to study the cascade of responses leading to resistance. Second, PPNs migrate long-distances inside roots, inducing complicated responses as they go, triggered by mechanical stress and wounding, among others, making it difficult to pinpoint the key genes involved in resistance or susceptibility by transcriptome analyses. Some studies have used comparative transcriptomics using susceptible and resistant plants infected with a single genotype of nematode (Postnikova et al., 2015; Xing et al., 2017; Ye et al., 2017; Zhang H. et al., 2017). However, it is difficult to rule out the possibility that differences in gene expression were due to resistance or susceptibility rather than to differences in the genetic backgrounds of host plants. Lastly, susceptible responses such as the formation of feeding sites are induced in specific cells targeted by PPNs, and defense responses are likely to be induced in the cells directly impacted by PPN activity. Thus, cells responding to PPNs are rather limited, making the analysis technically challenging.

Here we have introduced *Solanum torvum* Sw "Torvum Vigor" to overcome these problems. *S. torvum* has been widely used as a rootstock of eggplant (aubergine) to prevent disease caused by PPNs, as well as the soil-borne pathogens *Ralstonia*

Abbreviations: CN, cyst nematode; DPI, day-post inoculation; RKN, root-knot nematode; PPN, plant-parasitic nematode.

solanacearum, *Verticillium dahliae*, and *Fusarium oxysporum* f. *melongenae* n. f. (Gousset et al., 2005; Yamaguchi et al., 2010; Bagnaresi et al., 2013; Yang et al., 2014; Uehara et al., 2017; García-Mendívil and Sorribas, 2019; García-Mendívil et al., 2019; Murata and Uesugi, 2021). *S. torvum* Sw "Torvum Vigor" is resistant to *Meloidogyne arenaria* pathotype A2-O (A2-O), but susceptible to *M. arenaria* pathotype A2-J (A2-J) (Uehara et al., 2017). By using *S. torvum* and avirulent or virulent isolates, we established an *in vitro* infection system and performed comparative transcriptome analyses to identify genes whose expressions were associated with either resistance or susceptibility by carefully collecting only root tips attacked by RKNs, which allowed us to detect gene expression only in cells directly affected by nematodes. In addition, observation of infected root tip morphology suggests that the success or failure of the immune system against PPNs is determined within a few days of invasion. Thus, we decided to focus on the transcriptional changes that occurred in the very early stages of infection, which has not been studied in previous transcriptomic analyses (Bagnaresi et al., 2013; Postnikova et al., 2015; Xing et al., 2017).

Comparative clustering analyses of gene expression identified a large number of novel genes, especially those involved in susceptibility through cell wall modification and transmembrane transport; resistance through lignin and isoprenoid biosynthesis and fatty acid metabolism; and suberin biosynthesis in mechanical wounding. Consistent with the transcriptional up-regulation of lignin biosynthetic genes from A2-O invasion, lignin is accumulated at the root tip of *S. torvu*m infected with avirulent A2-O but not with virulent A2-J, suggesting that *S. torvum* reinforces the cell wall as a defense response against the avirulent RKN.

MATERIALS AND METHODS

Plant Materials and Growth Conditions

Seeds of *S. torvum* cultivar "Torvum Vigor" were sown on half-strength Murashige-Skoog (MS) medium containing 1% sucrose and 0.5% Gelrite (Wako, Japan). Plants were grown in a controlled growth chamber under long-day photoperiods (16 hours light/8 hours dark) at 25°C.

Nematode Infection Assay

M. arenaria pathotypes A2-J and A2-O were propagated on *Solanum lycopersicum* cultivar "Micro-Tom" in a greenhouse. Nematode eggs were isolated from infected roots and then hatched at 25 °C. Freshly hatched J2s were collected and transferred to a Kimwipe filter (a folded Kimwipe tissue) placed on the top of a glass beaker filled with sterilized distilled water (SDW) containing 100 μg/ml streptomycin and 10 μg/ml nystatin. Only active J2s pass through the filter. Filtered J2s were surface sterilized with 0.002 % mercuric chloride, 0.002 % sodium azide, and 0.001 % Triton X-100 for 10 min, and then rinsed three times with SDW (Mitchum et al., 2004). Eleven-day-old *S. torvum* seedlings grown on the MS-Gelrite in 6-well plates were inoculated with 200–300 J2s resuspended in SDW. The plates were wrapped in aluminum foil for 2–3 days after inoculation to promote nematode infection. When mature giant cells were observed 18 days post-inoculation (DPI), we used the MS-Gelrite media without sucrose to prevent the formation of callus-like structures. The difference in the number of normal galls formed by A2-J or A2-O at 4 DPI was statistically tested using the Mann-Whitney *U* test with R software (v3.6.3). Nematodes resident in root tissues were stained with acid fuchsin 2–4 DPI (Bybd et al., 1983), photographed by light microscopy (Olympus BX51, Olympus, Japan), and the photomicrographs were processed using cellSens (Olympus, Japan). For the observation of giant cells and developing nematodes at 18 DPI, infection sites were fixed with glutaraldehyde and cleaned with benzyl-alcohol/benzyl-benzoate (BABB) (Cabrera et al., 2018). We observed BABB-cleaned samples by confocal laser scanning microscopy (TCS SP5, Leica Microsystems GmbH, Germany). Photomicrographs were processed using LAS X software (version 3.7.0.20979, Leica Microsystems GmbH, Germany).

RNA-Sequencing and *de novo* Assembly

S. torvum seedlings were grown on half-strength MS-Gelrite medium containing 1% sucrose. Eleven-day-old seedlings were treated with SDW as a mock infection or with 200–300 J2s of *M. arenaria* A2-J for susceptible infection or A2-O for resistant infection. Root tips attacked by the nematodes were checked under microscopy, and more than 50 root tips were cut (approximately 3–5 mm from the tip) and collected for each treatment (**Figure 2A**). Root tip samples were collected at 1, 2, and 3 DPI with four biological replicates. Whole shoot and root samples were collected at 1, 3, 6, and 9 DPI with four biological replicates. Root tip samples were used for *de novo* assembly and differential gene expression analyses, and whole shoot and root samples were used only for *de novo* assembly.

RNA-seq libraries were prepared from the collected samples using a high-throughput RNA-seq method (Kumar et al., 2012). The 85-bp paired-end reads for the root tip samples, and the 85-bp single-end reads for the whole shoot and root samples were sequenced on an Illumina NextSeq 500 platform (Illumina, CA, United States). The FASTX toolkit 0.0.13.2 (Hannonlab) was used for quality filtering. Low-quality nucleotides (Phred scores of <30) were removed from the 3′ ends, and short reads (<76bp) were excluded. Reads with at least 95% of nucleotides with Phred scores > 20 were kept and used for the downstream analyses (**Supplementary Table 1A**). Adaptor sequences were removed using custom scripts written in Perl (Kumar et al., 2012). Filtered reads were mapped to the genome assembly of *M. arenaria* A2-J (GenBank accession number JAEEAS010000000) or A2-O (GenBank accession number QEUI01000000) (Sato et al., 2018) using HISAT2 (version 2.1.0) (Kim et al., 2019) to exclude reads of nematode origin. Unmapped reads were used for *de novo* transcriptome assembly (**Supplementary Figure 1A**).

Three different transcriptome assemblers were used for *de novo* assembly: SOAPdenovo-Trans v1.03 (Xie et al., 2014), Velvet v1.2.10 (Zerbino and Birney, 2008)/Oases v0.2.09 (Schulz et al., 2012) and Trinity package v2.4.0 (Grabherr et al., 2011; Haas et al., 2013). Unmapped paired-end and single-end reads were normalized using Trinity and assembled independently (Mamrot et al., 2017). For assemblies of each dataset, SOAPdenovo-Trans was set at *k*-mer sizes: 21, 23, 25, 27, 29, 31, 35, 41, 51, 61, Velvet/Oases was set at *k*-mer sizes: 21, 23,

25, 27, 29, 31, 35, 41, 51, 61, and Trinity was set at *k*-mer size 25 (**Supplementary Table 1B**).

Assemblies were merged into a non-redundant dataset using the EvidentialGene pipeline[1] as previously described (Nakasugi et al., 2014). Oases assembled scaffolds were split at gaps into contigs before merging with contigs from the other assemblies with the EvidentialGene tr2aacds pipeline. The tr2aacds pipeline produces 'primary' and 'alternate' sequences of non-redundant transcripts with 'primary' transcripts being the longest coding sequence for a predicted locus. Next, we used the evgmrna2tsa program from EvidentialGene to generate mRNA, coding, and protein sequences. BUSCO v3.0.2 (Simão et al., 2015) was applied for quantitative assessment of assembly completeness. This assembly and one previously reported for *S. torvum* by Yang et al. (2014) (GenBank accession number GBEG01000000) were compared to the Embryophyta odb9 dataset, which contains 1,440 BUSCO groups. The homology of the contigs from the final assembly was searched against the NCBI non-redundant database using BLASTX (BLAST+ v2.7.1) with an e-value threshold of 1E-05. We also compared the contigs with Arabidopsis genome annotation (TAIR10) (Berardini et al., 2015) using BLASTX at the e-value cutoff of 10. Results of the annotation are summarized in **Supplementary Table 2**.

Differential Expression Analysis

Quantification of *S. torvum* transcripts was performed with the mapping-based mode of Salmon v0.10.2 (Patro et al., 2017) by using reads that did not map to nematode genome assemblies. Quantified transcript-level abundance data were imported to R (v3.6.3) using tximport v.1.14.2 (Soneson et al., 2015) package, and differential gene expression analysis was carried out with the edgeR package (v3.28.1) (Robinson et al., 2010). Transcripts with very low expression values were filtered out with the "filterByExpr" function. Counts per million are shown in **Supplementary Table 3**. Differentially expressed genes (DEGs) (false discovery rate (FDR) ≤ 0.01, log-transformed fold change (logFC) ≥ 1 or logFC ≤ -1) were identified using the quasi-likelihood F-test by comparing expression levels during infection with A2-J or A2-O to SDW (mock) treatment at the same time point (**Supplementary Table 4**). We also compared gene expression levels between *S. torvum* infected with A2-J and A2-O, and all analyzed genes were listed in **Supplementary Table 5**.

Principal Component Analysis With Self-Organizing Map Clustering

To group genes by expression pattern, we applied the self-organizing map (SOM) clustering method on genes within the top 25 % of the coefficient of variation for expression across samples as previously described (Chitwood et al., 2013; Ranjan et al., 2014; Goto et al., 2020). Scaled expression values, representing the average principal component (PC) values among each gene in a cluster were used for multilevel three-by-three hexagonal SOM (Wehrens and Buydens, 2007). One hundred training iterations were used during the clustering, over which the α learning rate decreased from 0.0071 to 0.0061. The final assignment of genes to winning units formed the basis of the gene clusters. The results of SOM clustering were visualized in a principal component analysis (PCA) space where PC values were calculated based on gene expression across samples (**Figure 4A**).

Functional Annotation of Transcriptome and Gene Ontology Enrichment Analysis

We compared the contigs of our assembly with the NCBI non-redundant database using BLASTX (BLAST+ v2.7.1) with an *e*-value threshold of 1E-05. In addition, predicted amino acid sequences that begin with methionine were also annotated using InterProScan (v5.32-71.0) (Jones et al., 2014). BLASTX and InterProScan outputs were used for Blast2GO (v5.2.5) analysis to annotate the contigs with Gene Ontology (GO) terms (Gotz et al., 2008). GO enrichment analyses of the sets of genes induced by A2-O infection at 1 DPI or that were assigned to each cluster generated by SOM was performed by comparison with all genes using GO terms generated by Blast2GO at the FDR cutoff of 1E-04 (Gotz et al., 2008). We further used the "Reduce to most specific terms" option in Blast2GO to remove general GO terms and obtain only the most specific GO terms.

Histochemistry of Lignin Deposition

Lignin deposition during infection with A2-J or A2-O was visualized by phloroglucinol-HCl staining as previously described (Jensen, 1962). Eleven-day-old *S. torvum* seedlings were inoculated with nematodes or treated with SDW (mock) as described above. We collected root tips 3 DPI for lignin staining with phloroglucinol-HCl. Microphotographs were taken and processed as described above and combined manually.

Aliphatic Suberin Monomer Analysis

Quantification of aliphatic suberin was performed as described previously (Holbein et al., 2019). Eleven-day-old plants were treated with SDW (mock) or infected with A2-J or A2-O. At 4 DPI, root tips inoculated with nematodes were microscopically checked for infection, and more than 50 infected root tips were cut (approximately 3–5 mm from the tip) and collected for each treatment. To remove unbound lipids, samples were extracted in methanol for 24 h then in chloroform for 24 h, dried, and weighed. Samples were depolymerized and analyzed by gas chromatography-mass spectrometry (GC-MS) (Agilent 6890N-Agilent 5973N quadrupole mass-selective detector, Agilent Technologies, Germany) for monomer identification and for quantitative analysis based on an internal standard using an identical gas chromatography system coupled with a flame ionization detector as described previously (Franke et al., 2005).

RESULTS

A2-O Induces a Browning Response, and A2-J Induces Gall Formation in *S. torvum*

To understand the differential responses of *S. torvum* to *M. arenaria* A2-J and A2-O, we first established an *in vitro*

[1]http://arthropods.eugenes.org/genes2/about/EvidentialGene_trassembly_pipe.html (version 2017.12.21).

infection system. Seedlings of *S. torvum* were grown in MS-Gelrite plates for 11 days and then inoculated with 200–300 J2s of A2-J or A2-O. At 4 DPI, more than 90 % of root tips infected with A2-J induced the formation of gall-like structures ranging in size. These galls are classified here as "normal" galls, while the rest produced brown pigments. Normal galls lacked obvious brown pigment accumulation and were further classified based on the width of the gall into small (shorter than 0.5 mm), medium (0.5–0.8 mm), and large (wider than 0.8 mm) (**Figure 1A**). In contrast, about 60 % of A2-O-infected root tips accumulated at least some brown pigment. Some of these brownish root tips also had an abnormal appearance due to the formation of balloon-like structures, and others had many localized and highly pigmented spots. There were a very few small gall-like structures formed after infection with A2-O, but far fewer and smaller than in root tips infected with A2-J (**Figure 1B**). RKN staining by acid fuchsin revealed that both A2-J and A2-O successfully invaded the roots (**Figure 1C**). Interestingly, host cells invaded by A2-O uniformly accumulated brownish pigments, suggesting that the surrounding tissue is strongly responding to, and highly correlated with A2-O infection, a response that was absent from A2-J infected roots. It is generally known that browning of plant tissue is related to enzymatic or non-enzymatic oxidation of phenolic substances (Mesquita and Queiroz, 2013), but the identity of the brown pigments synthesized upon infection with A2-O is unknown. By 18 DPI, A2-J had induced the formation of mature multinucleate giant cells and developed into fourth stage juveniles (**Figure 1D**). In contrast, A2-O did not induce the formation of giant cells nor develop past second stage juveniles. These results suggest that *S. torvum* rapidly induces defense responses against A2-O, which inhibits the maturation of A2-O and gall formation. In contrast, A2-J inhibits or evades the induction of defense responses, continues development, and induces gall formation.

RNA-Seq Analysis of *S. torvum* Root Tips Infected With A2-O or A2-J

RNA-seq analysis was performed to understand the differences in transcriptional regulation of the *S. torvum* response to

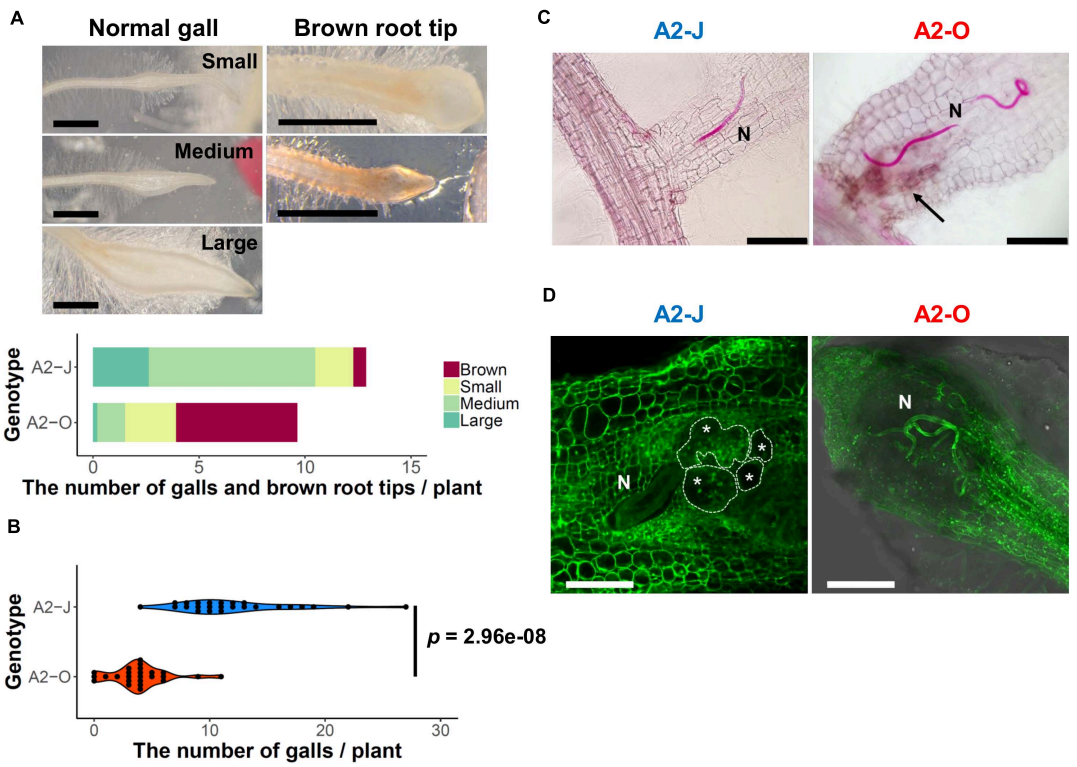

FIGURE 1 | *M. arenaria* A2-J induced gall formation in *S. torvum* upon infection, while *M. arenaria* A2-O infection resulted in the accumulation of brown pigment at root tips. **(A)** Microscopic examination of *S. torvum* root tips infected with A2-J or A2-O. Seedlings of *S. torvum* were infected with 200–300 *M. arenaria* A2-J or A2-O juveniles. The number of galls and brown root tips per plant were counted at 4 DPI. Normal galls without accumulation of brown pigment were binned by gall length into small (shorter than 0.5 mm), medium (0.5–0.8 mm), or large (wider than 0.8 mm). Scale bars indicate 1 mm. The average number of galls per plant (n = 25) is shown as a bar chart. Experiments were performed four times with similar results. **(B)** A2-J induced the formation of more galls than A2-O. The violin plot indicates variation in the number of galls per plant at 4 DPI. A p-value was calculated by the Mann-Whitney U test from the mean number of galls per plant. Similar results were obtained from four independent experiments. **(C)** Both A2-J and A2-O entered roots. Nematodes (N) in the roots were stained with acid fuchsin 2–4 DPI. The arrow indicates the accumulation of brown pigment. Scale bars indicate 200 μm. **(D)** *S. torvum* inhibited the growth of A2-O, but not A2-J. Nematodes and giant cells in the *S. torvum* roots 18 DPI were visualized by a method described previously (Cabrera et al., 2018). Nematodes and giant cells are indicated by N and asterisks, respectively. Scale bars indicate 200 μm.

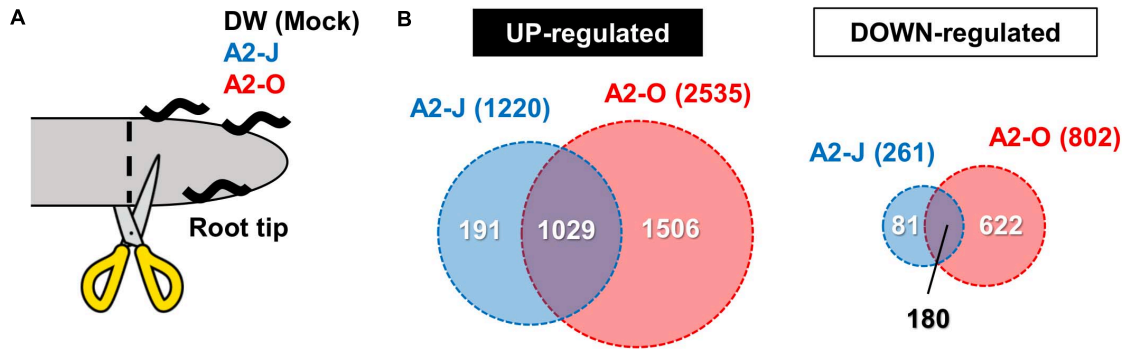

C

logFC

-0.5 0 12.5

Function	Annotation	Accession	A2-J 1 DPI	A2-J 2 DPI	A2-J 3 DPI	A2-O 1 DPI	A2-O 2 DPI	A2-O 3 DPI
SA marker genes	*PR1*	*Storvum022076t1*	2.4	4.8	5.9	4.0	7.8	9.3
	PR2	*Storvum012010t1*	5.4	8.0	8.7	5.3	10.7	12.4
JA marker genes	*LoxD*	*Storvum001432t1*	0.1	-0.2	0.6	1.7	1.8	3.0
	PI-II	*Storvum018700t1*	-0.4	3.9	2.6	3.9	8.5	7.2
ET marker genes	*ACO*	*Storvum007005t1*	2.5	4.5	6.1	5.3	6.3	9.1
	ACS	*Storvum011673t5*	0.8	1.2	0.3	1.8	1.7	1.3

D

logFC

0 4.0

Function	Annotation	Accession	A2-J 1 DPI	A2-J 2 DPI	A2-J 3 DPI	A2-O 1 DPI	A2-O 2 DPI	A2-O 3 DPI
Positive regulation of immunity	*WRKY31*	*Storvum005679t1*	0.5	0.4	0.5	1.2	1.5	1.8
	WRKY33	*Storvum005757t1*	0.4	0.0	0.3	1.2	1.1	1.6
	WRKY39	*Storvum011736t1*	0.8	1.1	1.1	3.0	2.5	2.2
	WRKY80	*Storvum014692t1*	0.8	1.0	1.9	2.5	2.7	3.9

FIGURE 2 | Transcriptome analysis of DEGs in *S. torvum* infected with *M. arenaria* A2-J or A2-O. **(A)** Sampling of *S. torvum* root tips infected by A2-J or A2-O for RNA-seq analysis. Root tips (approximately 3–5 mm from the tip) were cut (scissors not to scale) and collected at 1, 2, and 3 DPI for RNA-seq. **(B)** Venn diagrams show the overlap of up-regulated genes (logFC $\geq$ 1, FDR $\leq$ 0.01) and down-regulated genes (logFC ≤ -1, FDR $\leq$ 0.01) for at least one time point after infection with A2-J or A2-O. **(C,D)** Infection with A2-O induced the expression of phytohormone marker genes and WRKY transcription factors. *PR1* and *PR2* are marker genes of salicylic acid (SA), *LoxD* and *PI-II* are marker genes for jasmonic acid (JA), and *ACS* and *ACO* are marker genes for ethylene (ET). The homologs of tomato WRKY genes *WRKY31*, *WRKY33*, *WRKY39*, and *WRKY80* positively regulate immunity. The logFC values of the genes (compared to mock treatment) at 1, 2, and 3 DPI are shown. Heatmaps indicate relative gene expression levels. Gray color indicates values with no statistically significant differences at | logFC| $\geq$ 1 and FDR $\leq$ 0.01.

infection by nematodes that induce an immune response or that are successful parasites. Eleven-day-old *S. torvum* seedlings grown on MS-Gelrite plates were inoculated with 200–300 surface-sterilized J2s of A2-J or A2-O, or treated with SDW (mock treatment) *in vitro*. Since there were clear morphological differences between the root tips infected with A2-J and A2-O after four days (**Figure 1A**), it should follow that the success or failure of infection is determined within a few days post-inoculation. We therefore decided to analyze the transcriptome at 1–3 DPI, corresponding to the early stages of infection. In addition, to detect gene expression in cells directly affected by the nematodes, we carefully collected infected root tips under a stereomicroscope (**Figure 2A**). Root tips were cut with precision forceps and flash-frozen with liquid nitrogen to preclude the induction of wound responses. More than 50 root tips were pooled for each treatment, and four biological replicates were used for the RNA-seq based transcriptome analyses. We also carried out RNA-seq of whole roots and shoots of *S. torvum* infected with A2-J or A2-O, or mock treatment (1, 3, 6, and 9 DPI) to improve the completeness of *de novo* transcriptome assembly. As a result, we obtained 218,024,788 paired-end reads from root tips and 341,297,551 single-end reads from whole shoots and roots after quality filtering (**Supplementary Table 1A**). After removing the reads derived from nematodes, we performed *de novo* assembly using multiple assemblers with a variety of *k*-mer sizes (**Supplementary Figure 1A** and

Supplementary Table 1B). A set of non-redundant transcripts was generated by merging these multiple assemblies. The final assembly had 88,596 contigs with an N50 of 1,298 bp, an average size of 800.62 bp, and a total length of 70,931,593 bp (**Table 1**). We assessed the accuracy and completeness of the final assembly using BUSCO. The assembly included an estimated > 95 % of the assessed dataset, improving the current status of the transcriptome assembly of *S. torvum* (Yang et al., 2014; **Supplementary Figure 1B**) and provided a high-quality transcriptome assembly of *S. torvum* for further analyses.

Infection With A2-O, but Not A2-J, Induces the Expression of Defense-Related Genes

Differential expression analysis showed that 1,220 genes were significantly up-regulated and 261 genes were down-regulated upon infection with A2-J, while 2,535 genes were up-regulated and 802 genes were down-regulated by infection with A2-O at at least one-time point during root tip infection, compared to the mock treatment (logFC ≥ 1 for up-regulation and logFC ≤ -1 for down-regulation, FDR ≤ 0.01, **Figure 2B**; **Supplementary Figure 2**; **Supplementary Table 4**). 1,029 genes were up-regulated, and 180 genes were down-regulated at at least one-time point in both A2-J and A2-O infected plants (**Figure 2B**). Previous studies showed that the expression of genes associated with the salicylic acid (SA), jasmonic acid (JA), and ethylene (ET) signaling pathways are induced in resistant plants infected with PPNs (Ye et al., 2017; Zhang H. et al., 2017; Bali et al., 2019; Du et al., 2020; Ghaemi et al., 2020), so we investigated the expression of marker genes for hormone biosynthesis, hormone signaling (**Figure 2C**), and defense responses (**Figure 2D**). Infection with A2-O significantly induced the expression of SA-regulated genes that encode basic pathogenesis-related protein 1 (*PR1*) and β-1,3-glucanase (*PR2*), as well as a JA biosynthesis gene (lipoxygenase D (*LoxD*)), the JA-regulated gene protease inhibitor II (*PI-II*), and two ET biosynthesis genes (1-aminocyclopropane-1-carboxylate synthase (*ACS*) and 1-aminocyclopropane-1-carboxylate oxidase (*ACO*)) (Farmer et al., 1992; Yan et al., 2013; Booker and DeLong, 2015; Zhang et al., 2018; Marhavý et al., 2019; **Figure 2C**). Infection with A2-J induced the expression of *PR1* and *PR2* to a lesser extent, but did not induce the expression of *LoxD*, *PI-II*, *ACS*, or *ACO*.

Tomato (*S. lycopersicum*) WRKY transcription factors are induced by pathogen infection and positively regulate defense responses against pathogens (Liu et al., 2014; Li et al., 2015a,b; Zhou et al., 2015). For example, SlWRKY31 and SlWRKY33 play important roles in resistance against fungal and oomycete pathogens, while SlWRKY39 is involved in resistance against bacterial pathogens (Huang et al., 2012; Sun et al., 2015). SlWRKY80 is required for *Mi-1.2*-mediated resistance against RKN *Meloidogyne javanica* (Atamian et al., 2012). We found that the *S. torvum* homologs of tomato WRKY31, 33, and 39 were specifically up-regulated upon infection with A2-O, but not with A2-J (**Figure 2D**). In the case of WRKY80, A2-J induced its expression at a later time point (3 DPI), while A2-O induced the WRKY80 homolog to much higher levels. These results suggest that A2-O, but not A2-J, strongly and specifically induces the expression of defense-related genes in *S. torvum*.

TABLE 1 | *De novo* assembly of the *S. torvum* transcriptome.

Parameter	
Number of contigs	88,596
Total size of contigs	70,931,593 bp
Average length	800.62 bp
Median length	469.00 bp
N50 contig length	1,298 bp
Minimum length	96 bp
Maximum length	16,903 bp

Infection With A2-O Rapidly Induces the Expression of Sesquiterpene Synthases and Class III Peroxidases

Infection with A2-O caused an increase in expression of more genes and to a greater extent than A2-J (**Figures 2B**, **3A** and **Supplementary Figure 2**). Importantly, at 1 DPI, A2-J did not induce any statistically significant changes in the expression of any genes, whereas A2-O induced 204 genes, suggesting that infection with A2-O rapidly induces the expression of early responsive genes, which is prevented or avoided in A2-J infection. Since the speed of a defense response is one of the most important factors for successful immunity against pathogens, we hypothesized there must be important defense components among the 204 up-regulated genes. We therefore performed a GO enrichment analysis to identify significantly represented GO terms amongst the 204 up-regulated genes (FDR $\leq$ 1E-04, **Supplementary Table 6**). The list of enriched GO terms was further reduced using "Reduce to most specific terms" option in Blast2GO to remove general GO terms and obtain only the most specific terms (**Table 2**). Some GO terms that were significantly enriched among the 204 genes were related to the biosynthesis of isoprenoids ("farnesyl diphosphate catabolic process (GO:0045339)", "sesquiterpene biosynthetic process (GO:0051762)", and "terpenoid biosynthetic process (GO:0016114)"). To follow up on this result, we checked the expression of all the genes up-regulated by A2-O that are related to isoprenoid biosynthesis and found that A2-O infection induced the expression of genes encoding sesquiterpene synthases, such as viridiflorene synthase, vetispiradiene synthase, germacrene C synthase-like protein, and 5-epiaristolochene synthase. Several other enzymes involved in isoprenoid biosynthesis, such as xanthoxin dehydrogenase-like protein and UDP-glycosyltransferase 91C1 were also up-regulated (**Figure 3B**). Sesquiterpene synthases convert farnesyl diphosphate to sesquiterpenes such as germacrene C, 5-epiaristolochene, viridiflorene, and vetispiradiene. Because some isoprenoids have nematicidal activity (Ohri and Pannu, 2009), it is possible that the sesquiterpenes produced by *S. torvum* in response to infection with A2-O are nematicidal and contribute to suppressing A2-O infection. Other GO terms significantly enriched among the 204 up-regulated genes were related to oxidative stress ("hydrogen peroxide catabolic process (GO:0042744)" and "response to oxidative stress (GO:0006979)"). The most up-regulated genes by A2-O

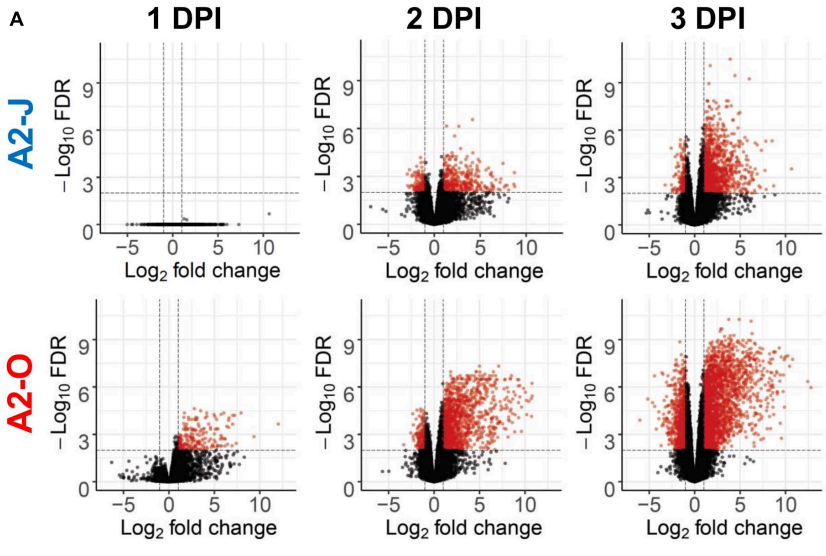

Annotation	Accession	A2-J 1 DPI	A2-J 2 DPI	A2-J 3 DPI	A2-O 1 DPI	A2-O 2 DPI	A2-O 3 DPI
viridiflorene synthase	*Storvum021327t1*	-0.6	4.8	3.3	5.1	7.8	6.4
	Storvum005152t1	2.1	3.2	3.4	5.0	5.4	6.0
vetispiradiene synthase	*Storvum016407t1*	0.9	2.8	3.3	3.4	5.0	5.7
	Storvum005195t1	1.1	2.9	2.5	3.8	5.2	5.2
vetispiradiene synthase-like	*Storvum052918t1*	0.0	5.1	5.3	5.8	8.6	8.2
	Storvum053117t1	3.2	4.7	4.0	6.6	7.1	6.7
germacrene C synthase-like	*Storvum005388t1*	2.2	5.6	4.8	5.7	8.4	8.2
5-epiaristolochene synthase	*Storvum005271t1*	-1.6	4.6	4.3	1.3	6.6	7.9
xanthoxin dehydrogenase-like	*Storvum014467t1*	0.0	2.8	0.0	1.6	6.8	6.3
UDP-glycosyltransferase 91C1	*Storvum007555t1*	-0.1	2.8	2.1	0.7	4.4	4.6
UDP-glycosyltransferase 73D1-like	*Storvum006700t1*	0.9	1.2	1.8	3.4	2.8	3.2

FIGURE 3 | Infection with A2-O, but not with A2-J induced rapid expression of genes involved in *S. torvum* isoprenoid biosynthesis. **(A)** Volcano plots showing the distribution of DEGs in *S. torvum* infected with *M. arenaria* A2-J or A2-O compared to mock treatment. The logarithms of the fold change of individual genes are plotted against the negative logarithms of their FDR. Red dots represent genes up-regulated (logFC ≥ 1) or down-regulated (logFC ≤ -1) with an FDR ≤ 0.01. **(B)** Infection with A2-O rapidly induced the expression of the genes involved in isoprenoid biosynthesis listed as "farnesyl diphosphate catabolic process (GO:0045339)", "sesquiterpene biosynthetic process (GO:0051762)", and "terpenoid biosynthetic process (GO:0016114)". LogFC values of the genes (compared to mock treatment) at 1, 2, and 3 DPI are shown. In the heatmap, gray boxes indicate no statistically significant difference at | logFC| ≥ 1 and FDR ≤ 0.01.

in the GO term group were class III peroxidases, which are involved in lignification, cell elongation, seed germination, and response to abiotic and biotic stresses (Cosio and Dunand, 2009; Shigeto and Tsutsumi, 2016; **Supplementary Figure 3**). The transcriptional up-regulation of the class III peroxidases is consistent with the fact that resistant tomato lines more strongly elevate peroxidase activity during RKN infection than susceptible lines (Zacheo et al., 1993).

Infection With A2-J Induces Genes Related to Cell Wall Modification and Transmembrane Transport

To identify the expression pattern of genes that are specific to A2-J or A2-O infection and common in both pathotypes, we clustered genes according to their transcript profiles by PCA with SOM clustering. SOM clustering grouped 6,502 genes into nine clusters based on their differential gene expression profiles after mock treatment or infection with either A2-J or A2-O (**Figure 4** and **Supplementary Table 7**). 429 genes in Cluster 2 and 554 genes in Cluster 4 were specifically up-regulated after infection with A2-J. In contrast, 1,769 and 600 genes in Cluster 8 and 9, respectively, were specifically up-regulated after infection with A2-O. 1,000 genes in Cluster 7 were up-regulated after infection with either A2-J or A2-O (**Figure 4B**).

We once again used GO enrichment to identify functional terms enriched in the genes in each cluster (FDR ≤ 1E-04, **Supplementary Table 8**) by further filtering enriched GO terms using the "Reduce to most specific terms" option in Blast2GO. In Cluster 4 (specifically A2-J up-regulated genes), significantly enriched GO terms were related to cell wall remodeling, including "cell wall modification (GO:0042545)",

TABLE 2 | GO enrichment analysis of genes up-regulated by infection with *M. arenaria* A2-O at 1 DPI[a].

GO term	Fold	FDR
farnesyl diphosphate catabolic process (GO:0045339)	347.4	7.9E-08
sesquiterpene biosynthetic process (GO:0051762)	248.2	4.0E-07
hydrogen peroxide catabolic process (GO:0042744)	23.6	6.6E-06
response to oxidative stress (GO:0006979)	11.8	2.2E-05
terpenoid biosynthetic process (GO:0016114)	21.9	7.1E-05

[a] *The most specific GO terms enriched in 204 genes up-regulated by infection with A2-O at 1 DPI (FDR ≤ 1E-04) are listed with fold enrichment (Fold) and FDR values. "Reduce to most specific" option in Blast2GO was used to remove general GO terms. All of the significantly enriched GO terms are shown in* ***Supplementary Table 6*** *(FDR ≤ 1E-04). Only GO category "Biological Process" is shown.*

"cell wall organization or biogenesis (GO:0071554)", and "pectin catabolic process (GO:0045490)" (**Table 3** and **Supplementary Table 8**). This is consistent with the observation that the expansion of giant cells is associated with an increase in cell wall thickness (Bartlem et al., 2014; Bozbuga et al., 2018). GO terms associated with the significantly A2-J up-regulated genes include enzymes such as cellulose synthase-like protein, xyloglucan endotransglucosylase/hydrolase protein, and a non-catalytic subunit of a polygalacturonase isozyme (**Supplementary Figure 4A**). The transcriptional up-regulation of these enzymes is consistent with the presence of the common polysaccharides pectic homogalacturonan, xyloglucan, and pectic arabinan in the cell walls of giant cells (Bozbuga et al., 2018). Similarly, A2-J infection also activated the expression of COBRA-like protein, expansin, and LRR-RLK PXC1, which play important roles in cellulose deposition, loosening of cell walls, and secondary wall formation (Cosgrove, 2000; Brown et al., 2005; Wang et al., 2013; Kumar et al., 2016; **Supplementary Figure 4A**). Another GO term significantly enriched in Cluster 4 was "transmembrane transport (GO:0055085)" (**Supplementary Table 8**). Other significantly up-regulated genes encode sugar transporter ERD6-like protein (Hammes et al., 2005) and amino acid transporter family protein (Elashry et al., 2013). These transporters may promote the uptake of nutrients into giant cells or alter transportation through cells surrounding giant cells (**Supplementary Figure 4B**). We also performed GO enrichment analyses for Cluster 2, but no GO terms were enriched.

In addition to GO enrichment analyses, we looked for interesting genes whose expression were dramatically up-regulated in Clusters 2 and 4. These clusters included genes encoding chalcone synthase and a spermidine synthase that were specifically and highly expressed after infection with A2-J (**Figure 5A**). Chalcone synthase is the first enzyme of the flavonoid biosynthetic pathway (Dao et al., 2011), and spermidine synthase is a key enzyme involved in polyamine biosynthesis (Liu et al., 2007). In summary, A2-J infection significantly and specifically up-regulates genes related to cell wall modification and membrane transport, chalcone synthase, and spermidine synthase at an early phase of gall formation.

Infection With A2-O Induces Genes Related to Defense Responses

In Cluster 8 (genes specifically up-regulated by A2-O), GO terms that were significantly enriched were related to defense responses, including "defense response to fungus (GO: 0050832)", "defense response to bacterium (GO: 0042742)", "killing of cells of other organism (GO:0031640)", and "regulation of salicylic acid biosynthetic process (GO: 0080142)". In addition, GO terms involved in lignin biosynthesis, including "lignin biosynthetic process (GO:0009809)" was also overrepresented in Cluster 8 (**Table 4** and **Supplementary Table 8**). In Cluster 9, the significantly enriched GO terms were related to biosynthesis of isoprenoids ("sesquiterpene biosynthetic process (GO: 0051762)", "terpenoid biosynthetic process (GO: 0016114)", and "farnesyl diphosphate catabolic process (GO:0045339)") (**Table 4** and **Supplementary Table 8**).

We also found that the genes that are highly expressed after infection with A2-O in Cluster 8 and 9 include (1) defense-related genes encoding chitinase, β-1,3-glucanase, and serine protease inhibitor, (2) sesquiterpene synthase, (3) fatty acid desaturase 2 (FAD2), (4) ferulic acid 5-hydroxylase (F5H) which is involved in lignin biosynthesis, (5) berberine bridge enzyme (BBE)-like protein, which is involved in oxidation of cinnamyl alcohol (**Figure 5B**). Fatty acids are major and essential components of all plant cells and are also precursors for a variety of plant metabolites, including signaling molecules and phytoalexins (Ohlrogge and Browse, 1995; Lim et al., 2017). *FAD2* encodes Δ12-desaturase that catalyzes the conversion of oleic acid (C18:1) to linoleic acid (C18:2) (Ohlrogge and Browse, 1995). The Arabidopsis genome has only a single *FAD2* gene (AT3G12120), but most other plant species carry multiple *FAD2* homologs (Cao et al., 2013; Lee et al., 2020). The duplication of *FAD2* genes in plants would have enabled the functional diversification of these enzymes, leading to divergent catalytic activities and the synthesis of novel metabolites. For example, recent studies have shown that tomato has non-canonical FAD2 family proteins that lack Δ12-desaturase activity (Jeon et al., 2020; Lee et al., 2020). In particular, ACET1a/b (Solyc12g100240 and Solyc12g100260) and FAD2-9 (Solyc12g100250) are non-canonical FAD2 involved in the biosynthesis pathway from linoleic acid to a phytoalexin, falcarindiol (Jeon et al., 2020). Falcarindiol has not only anti-bacterial and anti-fungal activities but also nematicidal activity to *M. incognita* and pinewood nematode *Bursaphelenchus xylophilus* (Liu et al., 2016). Infection with A2-O rapidly induced the expression of *ACET1a/b* and *FAD2-9* (**Figure 5B**), suggesting that infection with A2-O rapidly activates a biosynthesis pathway similar to the falcarindiol pathway, but the production of falcarindiol by *S. torvum* needs to be experimentally confirmed in the future.

Infection With A2-O Induces Lignin Accumulation in *S. torvum*

The GO enrichment analysis of Cluster 8 revealed that "lignin biosynthetic process (GO:0009809)" was significantly enriched (**Table 4** and **Supplementary Table 8**), and that the expression of *F5H* in Cluster 8 was very high and

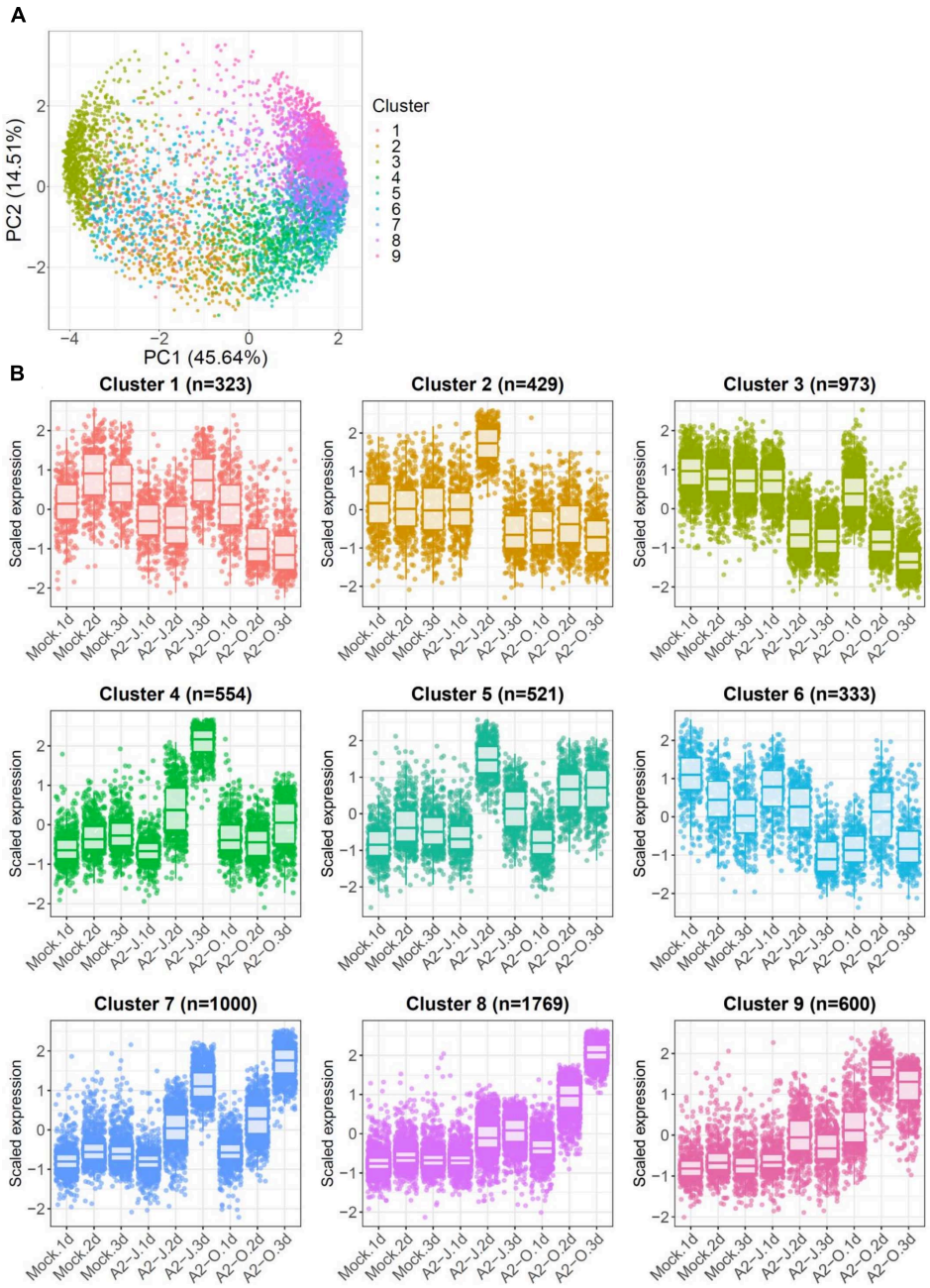

FIGURE 4 | PCA and SOM clustering of gene expression in *S. torvum*. **(A)** Clustering of gene expression patterns in *S. torvum* treated with SDW (mock) or infected with A2-J or A2-O at 1, 2, and 3 DPI. The expression profiles of each gene were represented in a PCA space separated by PC1 and PC2, with SOM node memberships (cluster) represented by different colors and numbers. The percentage shown along the x or y-axis represents the percentage of variance explained by each component. A total of nine clusters with different expression patterns were defined. **(B)** Scaled expression profiles of genes by SOM clustering. The number of genes assigned to each SOM cluster is shown in parentheses. Each dot represents the value of the scaled expression of the gene. The upper and lower horizontal lines of the box correspond to the 25th and 75th percentiles. The horizontal bar in the box indicates the median. The upper and lower end of horizontal bars outside the box indicate 90th and 10th percentiles.

specifically induced after infection with A2-O (**Figure 5B**). These results suggest that the infection with A2-O transcriptionally activates lignin biosynthesis. Lignin is a phenylpropanoid polymer that is deposited predominantly in the secondary cell wall, making the cell wall rigid and impervious to water (Vanholme et al., 2010). Lignin polymer is synthesized via oxidative combinational coupling of lignin monomers (or monolignols), namely *p*-coumaryl alcohol, sinapyl alcohol, and coniferyl alcohol. The lignin subunits constituted by these monolignols are *p*-hydroxyphenyl (H), syringyl (S),

TABLE 3 | GO enrichment analysis of Cluster 4 genes up-regulated specifically by infection with *M. arenaria* A2-J[a].

Cluster	GO term	Fold	FDR
Cluster 4	pectin catabolic process (GO:0045490)	16.9	8.1E-07
	cell wall modification (GO:0042545)	14.7	8.1E-05
	negative regulation of catalytic activity (GO:0043086)	7.0	9.8E-05

[a] *The most specific GO terms enriched in Cluster 4 (FDR ≤ 1E-04) are listed with fold enrichment (Fold) and FDR values. "Reduce to most specific" option in Blast2GO was used to remove general GO terms. All of the significantly enriched GO terms in each cluster are shown in* ***Supplementary Table 8*** *(FDR ≤ 1E-04). Only GO category "Biological Process" is shown.*

and guaiacyl (G) groups, respectively. All of the monolignols are synthesized from phenylalanine through the general phenylpropanoid and monolignol-specific pathways (Vanholme et al., 2012; **Figure 6A**). Normally, lignin deposition occurs in the root endodermis of the differentiation zone and constitutes the Casparian strip, which functions as a physical barrier that prevents free diffusion of solutes and ions between the xylem and the soil (Robbins et al., 2014). However, biosynthesis and deposition of lignin can be induced in response to biotic stresses (Miedes et al., 2014; Mutuku et al., 2019), which prompted a closer examination of the expression patterns of genes involved in the lignin biosynthetic pathway whose expression was up-regulated by infection with either A2-J or A2-O (logFC $\geq$ 1, FDR $\leq$ 0.01) (**Figure 6B**). Infection with A2-O induced the expression of genes encoding phenylalanine ammonia-lyase (PAL), cinnamate 4-hydroxylase (C4H), 4-coumaroyl-CoA ligase (4CL), *p*-hydroxycinnamoyl-CoA:shikimate *p*-hydroxycinnamoyl transferase (HCT), caffeoyl-CoA O-methyltransferase (CCoAOMT), cinnamoyl-CoA reductase (CCR), F5H, caffeic acid O-methyltransferase (COMT), and cinnamyl alcohol dehydrogenase (CAD). Infection with A2-J also induced the expression of some of these genes, but to a much lesser extent than A2-O (**Figure 6B**). Phloroglucinol staining of infected roots allowed us to visualize the intensity and location of lignin accumulation (**Figure 7**). Infection with A2-O, but not with mock treatment, induced ectopic accumulation of lignin in root tips. With A2-J infection, the area of the root proximal to gall tissue was very slightly stained with phloroglucinol, but the gall itself had little or no detectable phloroglucinol staining. These differences in lignin staining intensity may reflect differences in the expression of lignin biosynthetic genes after infection with A2-J and A2-O (**Figure 5B**).

Infection With A2-O or A2-J Induces the Expression of Genes Related to Suberin Biosynthesis

There was no enrichment of specific GO terms in Cluster 7 (up-regulated by the infection with A2-J or A2-O) (**Supplementary Table 8**). However, we found that both A2-J and A2-O strongly activate the expression of suberin biosynthetic genes, including *aliphatic suberin feruloyl transferase* (*ASFT*), *cytochrome P450 86A1* (*CYP86A1*), *cytochrome P450 86B1* (*CYP86B1*), *glycerol-3-phosphate acyltransferase 5* (*GPAT5*), and β−*ketoacyl*−*CoA synthase* (*KCS*) (**Figure 5C**), but A2-O induced slightly higher expression of these genes than A2-J. Suberin is a cell wall component that restricts water loss, nutrient elution, and pathogen infection (Dean and Kolattukudy, 1976; Lulai et al., 2008; Leide et al., 2012; Froschel et al., 2020). It is normally deposited in the cell walls of endodermal cells, but not in the root tip (Barberon, 2017), and several reports showed that suberin synthesis is induced in wounded tissues (Dean and Kolattukudy, 1976; Bernards and Lewis, 1998). Considering that both A2-J and A2-O induced the expression of suberin biosynthetic genes, the expression of these genes was possibly up-regulated by a generalized wounding signal during nematode infection. We therefore investigated the expression levels of the wound-responsive genes *Arabidopsis thaliana activation factor 2 (ATAF2)*, which encodes a wound-responsive NAC transcription factor (Collinge and Boller, 2001; Wang and Culver, 2012), and *pathogen-related 4* (Stanford et al., 1989; Marhavý et al., 2019; **Supplementary Figure 5**). Not surprisingly, the expression patterns of wound-responsive genes were similar to those of the suberin biosynthetic genes. These results suggest that infection with A2-O may cause more wounding and damage than A2-J, but that the wounding signal generated during the earliest events in nematode infection, whether a resistant or susceptible reaction occurs later, may induce the expression of suberin biosynthetic genes.

Considering the suberin biosynthetic gene transcription data, we predicted that infection with A2-O or A2-J would induce the accumulation of suberin. To test our prediction, we examined and measured the chemical composition of aliphatic suberin at the nematode infection site, but total aliphatic suberin content did not increase after A2-J or A2-O infection (Welch' s *t*-test with Bonferroni correction, $p \leq 0.05$) (**Figure 8A**). However, the abundance of single monomers, ω-hydroxy acid (ω-OH-acid) C16 and α,ω-diacid C16, were significantly higher after infection with A2-O than mock treatment ($p \leq 0.05$, Welch's *t*-test followed by Bonferroni correction) (**Figure 8B**).

DISCUSSION

Comparative Transcriptome Analyses for Host Defense and Susceptible Responses at the Early Stages of Nematode Infection

In this study we established an experimental system using a single cultivar of *S. torvum* and two pathotypes of RKNs *M. arenaria* A2-J, which is able to infect and establish a parasitic relationship with the plant, and A2-O, which induces a resistance response. To the best of our knowledge, this is the first comparative RNA-seq analyses in a single cultivar with virulent or avirulent nematodes. Using this experimental system, we were able to catalog changes in gene expression

A **Genes up-regulated specifically by A2-J (Cluster 4)**

color scale: -3.1 0 6.1

Function	Annotation	Accession / Cluster	logFC A2-J 1 DPI	A2-J 2 DPI	A2-J 3 DPI	A2-O 1 DPI	A2-O 2 DPI	A2-O 3 DPI
flavonoid biosynthesis	chalcone synthase	*Storvum009968t1* / 4	-0.8	1.7	4.1	1.8	-0.1	-0.2
polyamine biosynthesis	spermidine synthase	*Storvum011691t8* / 4	-3.0	3.2	6.0	0.6	1.5	2.1

B **Genes up-regulated specifically by A2-O (Cluster 8 or Cluster 9)**

color scale: -1.6 0 12.5

Function	Annotation	Accession / Cluster	logFC A2-J 1 DPI	A2-J 2 DPI	A2-J 3 DPI	A2-O 1 DPI	A2-O 2 DPI	A2-O 3 DPI
defense-related	chitinase	*Storvum015519t1* / 8	1.7	4.7	6.6	4.1	8.2	10.8
		Storvum015469t1 / 8	2.1	3.4	3.9	4.1	5.0	6.2
	β-1,3-glucanase	*Storvum012010t1* / 8	5.4	8.0	8.7	5.3	10.7	12.4
		Storvum011888t2 / 8	0.9	5.0	6.6	1.9	6.9	10.4
	serine protease inhibitor	*Storvum029584t1* / 8	-0.5	0.5	1.9	0.4	4.7	6.0
sesquiterpene synthase	5-epiaristolochene synthase	*Storvum005271t1* / 8	-1.6	4.6	4.3	1.3	6.6	7.9
	germacrene C synthase-like	*Storvum005388t1* / 8	2.2	5.6	4.8	5.7	8.4	8.2
	viridiflorene synthase	*Storvum005152t1* / 9	2.1	3.2	3.4	5.0	5.4	6.0
		Storvum021327t1 / 9	-0.6	4.8	3.3	5.1	7.8	6.4
	vetispiradiene synthase	*Storvum005195t1* / 9	1.1	2.9	2.5	3.8	5.2	5.2
		Storvum016407t1 / 9	0.9	2.8	3.3	3.4	5.0	5.7
	vetispiradiene synthase-like	*Storvum052918t1* / 9	0.0	5.1	5.3	5.8	8.6	8.2
		Storvum053117t1 / 9	3.2	4.7	4.0	6.6	7.1	6.7
	premnaspirodiene oxygenase	*Storvum006295t1* / 9	4.3	4.4	3.7	7.2	6.8	6.6
	CYP71D7-like	*Storvum005560t1* / 8	2.4	4.3	5.8	2.3	8.1	10.0
fatty acid metabolism	FAD2-7 in tomato	*Storvum010279t1* / 9	2.7	4.0	2.9	5.7	6.1	5.5
	FAD2-9 in tomato	*Storvum010044t1* / 9	2.4	6.0	2.2	7.5	8.8	5.4
	ACETYLENASE1a/b in tomato	*Storvum010307t1* / 9	1.7	3.2	3.2	5.1	5.7	5.7
		Storvum010327t1 / 9	3.9	4.5	4.0	7.0	6.6	6.2
	non canonical FAD2 family	*Storvum010536t1* / 8	2.1	3.9	5.2	5.8	6.5	8.2
		Storvum008080t1 / 9	1.6	2.7	2.4	4.2	4.8	4.9
lignin biosynthesis	ferulic acid 5-hydroxylase	*Storvum004425t1* / 8	0.2	2.9	2.8	1.3	6.7	6.9
oxidation of cinnamyl alcohol	berberine bridge enzyme-like protein	*Storvum005117t1* / 8	0.0	1.6	3.8	3.7	6.3	8.6

C **Genes up-regulated commonly by A2-J and A2-O (Cluster 7)**

color scale: -4.1 0 5.5

Function	Annotation	Accession / Cluster	logFC A2-J 1 DPI	A2-J 2 DPI	A2-J 3 DPI	A2-O 1 DPI	A2-O 2 DPI	A2-O 3 DPI
suberin biosynthesis	fatty acid reductase	*Storvum006447t1* / 7	-1.2	4.1	3.5	-2.0	3.9	4.6
	3-ketoacyl-CoA synthase	*Storvum006003t1* / 7	-1.1	3.3	3.3	-4.0	1.7	4.0
	aliphatic suberin feruloyl transferase	*Storvum008595t1* / 7	-0.4	2.0	3.9	-1.8	1.4	4.9
	cytochrome P450 86A1	*Storvum006001t1* / 7	0.5	2.7	3.3	-1.5	3.0	4.8
	cytochrome P450 86B1	*Storvum005197t1* / 7	-0.6	1.6	3.1	-1.5	0.1	4.0
	glycerol-3-phosphate acyltransferase 5	*Storvum006696t1* / 7	-1.5	3.5	4.1	-1.5	3.6	5.4

FIGURE 5 | Up-regulated genes in Clusters 4, 7, 8, and 9. Highly up-regulated genes (logFC ≥ 4, FDR ≤ 0.01) in each cluster are listed. **(A)** Infection with A2-J specifically up-regulated the expression of chalcone synthase and spermidine synthase (Cluster 4). **(B)** Infection with A2-O dramatically up-regulated defense-related proteins, sesquiterpene synthase, fatty acid desaturase 2 (FAD2), ferulic acid 5-hydroxylase, and berberine bridge enzyme-like protein (Cluster 8 and 9). **(C)** Both A2-J and A2-O induced the expression of suberin biosynthetic enzymes (Cluster 7). LogFC values of the genes compared to mock treatment at 1, 2, and 3 DPI are shown. The heatmap gray to indicate values with no statistically significant differences at | logFC| ≥ 1 and FDR ≤ 0.01.

at the very early stage of infection (1–3 DPI) with a high degree of sensitivity compared to previous studies (Bagnaresi et al., 2013; Postnikova et al., 2015; Xing et al., 2017; Shukla et al., 2018). Because there are clear morphological differences in root tips infected with A2-J and A2-O within 4 DPI, the sum of host responses by this stage of infection likely has determined the outcome of infection. Interestingly, at 1 DPI, A2-O induced the expression of genes encoding class III peroxidases, fatty acid desaturases, and enzymes involved in isoprenoid biosynthesis (**Figures 3B, 5B** and **Supplementary Figure 3**), whereas A2-J had not induced any statistically significant changes in the expression of defense response genes (**Figure 3A**). These results suggest that A2-J initially evades recognition by *S. torvum* and/or actively suppresses the induction of transcriptional changes in the host. Our results also show that A2-J induces the expression of genes associated with susceptible

responses that are related to gall formation at around 2–3 DPI (**Supplementary Figure 4**). The delay in expression of susceptibility-associated genes is consistent with the length of time it takes for nematodes to migrate through the plant's vascular system to their target cells.

Sampling only infected root tips reduced background plant transcripts and enabled us to detect dynamic changes in gene expression that are directly associated with the establishment of a parasitic relationship or with active host defense. The range of calculated logFC values of root tip genes expressed at 3 DPI with A2-O was from −8 to 12.8 (that is, from 1/256 to 7131 times), which is quite broad for very early stages of infection. For example, in previous transcriptome analyses using *S. torvum* during infection with an avirulent isolate of *M. incognita*, chitinase expression in whole roots was only 2–4 times higher upon infection than in uninfected roots (Bagnaresi et al., 2013). In contrast, our analyses showed that the expression of chitinases in the root tips infected with A2-O at 3 DPI was several hundred times higher than in the mock treatment, clearly demonstrating the high sensitivity of this method for host-parasite transcriptomics (**Figure 5B**). This level of sensitivity allowed us to identify genes that had not previously been connected with resistance or susceptibility in this system. In addition, comparative transcriptome analyses of *S. torvum* combined with SOM clustering can be used to pinpoint genes that are associated with susceptibility or resistance.

TABLE 4 | GO enrichment analysis of Cluster 8 and 9 genes up-regulated specifically by infection with *M. arenaria* A2-O[a].

Cluster	GO term	Fold	FDR
Cluster 8	glutathione metabolic process (GO:0006749)	18.1	1.8E-27
	recognition of pollen (GO:0048544)	8.9	1.2E-13
	protein ubiquitination (GO:0016567)	3.5	1.2E-11
	defense response to fungus (GO:0050832)	8.2	5.4E-10
	cellular oxidant detoxification (GO:0098869)	4.9	6.1E-09
	defense response to bacterium (GO:0042742)	6.3	1.2E-08
	hydrogen peroxide catabolic process (GO:0042744)	6.6	5.6E-08
	lignin biosynthetic process (GO:0009809)	11.7	9.4E-08
	protein autophosphorylation (GO:0046777)	4.1	1.0E-07
	chitin catabolic process (GO:0006032)	18.2	3.1E-07
	response to oxidative stress (GO:0006979)	3.6	3.5E-06
	mRNA transcription (GO:0009299)	21.5	7.1E-06
	killing of cells of other organism (GO:0031640)	18.8	1.7E-05
	regulation of salicylic acid biosynthetic process (GO:0080142)	15.8	5.3E-05
	response to abscisic acid (GO:0009737)	3.7	9.1E-05
Cluster 9	negative regulation of endopeptidase activity (GO:0010951)	17.7	5.9E-07
	farnesyl diphosphate catabolic process (GO:0045339)	118.1	2.0E-06
	sesquiterpene biosynthetic process (GO:0051762)	84.4	1.1E-05
	terpenoid biosynthetic process (GO:0016114)	11.2	1.9E-05

[a] *The most specific GO terms enriched in Cluster 8 and 9 (FDR ≤ 1E-04) are listed with fold enrichment (Fold) and FDR values. "Reduce to most specific" option in Blast2GO was used to remove general GO terms. All of the significantly enriched GO terms in each cluster are shown in* ***Supplementary Table 8*** *(FDR ≤ 1E-04). Only GO category "Biological Process" is shown.*

Infection With A2-J Induces the Expression of Genes Related to Cell Wall Modification and Spermidine Synthase

A2-J specifically induced the expression of cell wall modification enzymes such as cellulose synthase-like protein, xyloglucan endotransglucosylase/hydrolase protein, and a non-catalytic subunit of the polygalacturonase isozyme (**Table 3** and **Supplementary Figure 3A**). The cell walls of giant cells require thickening and loosening to allow cell expansion that increases the surface area of the plasma membrane, and to support nutrient uptake by the nematodes (Bartlem et al., 2014; Bozbuga et al., 2018; Meidani et al., 2019). The cell walls of giant cells and syncytial feeding sites induced by CNs contain high-ester pectic homogalacturonan, xyloglucan, and pectic arabinan (Davies et al., 2012; Zhang L. et al., 2017), suggesting that these polysaccharides are responsible for the flexible properties of feeding site cell walls. Our transcriptome results confirm the importance of cell wall modification enzymes during gall formation.

In addition to cell wall modification enzymes, infection with A2-J specifically induced the expression of spermidine synthase (**Figure 5A**). Interestingly, a virulence effector protein secreted from CNs, 10A06, functions through its interaction with Arabidopsis spermidine synthase 2 (Hewezi et al., 2010) by increasing spermidine concentrations, subsequently increasing polyamine oxidase activities. An increase in polyamine oxidase activity results in the induction of cellular antioxidant machinery in syncytia and disruption of SA-mediated defense signaling. Although there is no clear homolog of 10A06 in RKNs such as *M. incognita*, it is possible that there is a functional ortholog of 10A06 that up-regulates the expression of spermidine synthase. Potentially, transcriptional activation of the spermidine synthase gene by PPNs may turn out to be a common strategy for suppressing plant immunity.

Infection With A2-O Up-Regulates Genes Related to Sesquiterpene Biosynthesis and Fatty Acid Metabolism

Infection with A2-O, but not with A2-J, strongly induced genes encoding sesquiterpene synthases (**Table 4** and **Figure 5B**). High levels of expression of these genes occurs at the very early stages of infection (1 DPI), which sets these genes apart from the other genes induced by A2-O infection (**Figures 3B**, 5B), suggesting the importance of sesquiterpenes as an early line of defense against PPNs. Capsidiol, a sesquiterpene, is the major phytoalexin produced in the Solanaceae plants *Nicotiana* spp. and *Capsicum* spp. in response to fungal and bacterial infection (Grosskinsky et al., 2011; Song et al., 2019). Capsidiol is toxic to many oospore and fungal pathogens, such as *Phytophthora capsici* and *Botrytis cinerea* (Stoessl et al., 1972; Ward et al., 1974), and suppresses the mobility of false root-knot nematode *Nacobbus aberrans* (Godinez-Vidal et al., 2010). We found that A2-O induces the expression of CYP71D7-like

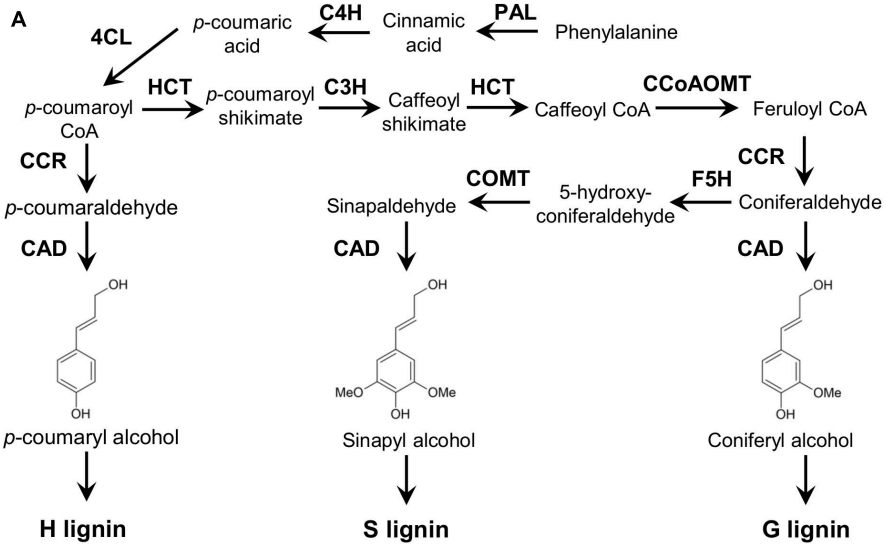

B

logFC

-0.4 0 7.0

Annotation	Accession	A2-J 1 DPI	A2-J 2 DPI	A2-J 3 DPI	A2-O 1 DPI	A2-O 2 DPI	A2-O 3 DPI
PAL	*Storvum016056t1*	0.1	0.6	1.3	0.7	1.2	1.9
	Storvum002660t1	0.2	0.6	1.0	1.2	1.5	1.6
C4H	*Storvum005843t1*	-0.1	1.0	2.8	0.8	1.8	3.8
4CL	*Storvum004995t1*	0.0	-0.2	1.5	0.3	0.8	2.8
	Storvum004904t1	-0.4	-0.2	0.7	0.5	0.9	1.1
HCT	*Storvum008424t1*	0.2	0.2	1.2	0.7	0.1	1.1
	Storvum008380t1	0.1	0.8	0.9	0.8	1.2	1.1
CCoAOMT	*Storvum016481t1*	0.5	0.1	0.8	1.2	1.1	1.7
	Storvum016905t1	0.0	0.6	0.9	0.2	1.1	1.6
CCR	*Storvum012499t1*	0.6	1.4	2.0	1.4	2.0	3.2
F5H	*Storvum004425t1*	0.2	2.9	2.8	1.3	6.7	6.9
COMT	*Storvum010436t1*	0.1	0.5	1.7	1.0	1.7	3.0
CAD	*Storvum011430t1*	-0.4	-0.3	0.4	0.8	0.9	1.3
	Storvum009854t1	0.3	1.2	0.9	1.3	1.8	2.3
	Storvum010887t1	0.2	-0.3	0.7	0.5	1.6	2.2
	Storvum011275t1	4.2	4.6	3.4	5.9	6.2	5.6
	Storvum011337t1	0.7	1.1	1.9	1.9	2.6	3.2
	Storvum011654t1	0.7	1.4	1.0	1.4	2.8	3.0
	Storvum011209t1	0.3	0.3	1.3	1.3	1.6	2.3

FIGURE 6 | Infection with A2-O induced the expression of lignin biosynthetic genes. **(A)** Overview of the lignin biosynthesis pathway. PAL, phenylalanine ammonia-lyase; C4H, cinnamate 4-hydroxylase; 4CL, 4-coumaroyl-CoA ligase; HCT, p-hydroxycinnamoyl-CoA:shikimate p-hydroxycinnamoyl transferase; C3H, p-coumarate 3-hydroxylase; CCoAOMT, caffeoyl-CoA O-methyltransferase; CCR, cinnamoyl-CoA reductase; F5H, ferulate 5-hydroxylase; COMT, caffeic acid O-methyltransferase; CAD, cinnamyl alcohol dehydrogenase. **(B)** Expression patterns of genes involved in the lignin biosynthetic pathway whose expression was significantly up-regulated by infection with A2-J or A2-O (logFC $\geq$ 1, FDR $\leq$ 0.01). LogFC values of the genes compared to mock treatment at 1, 2, and 3 DPI are shown. The heatmap uses gray to indicate values with no statistically significant differences at | logFC| $\geq$ 1 and FDR $\leq$ 0.01.

protein, the closest homologue to CYP71D20 from *Nicotiana benthamiana*, which converts 5-epiaristolochene to capsidiol (Ralston et al., 2001). A2-O also induces the expression of genes encoding 5-epiaristolochene synthase, which converts farnesyl diphosphate to 5-epiaristolochene (Vogeli and Chappell, 1988; Facchini and Chappell, 1992). Although capsidiol production is not common in *Solanum* spp., *S. torvum* may produce similar sesquiterpene derivatives that are toxic to PPNs. Another sesquiterpene that may be involved in resistance is the phytoalexin solavetivone, because A2-O induces the expression of genes encoding vetispiradiene synthase and premnaspirodiene oxygenase, which sequentially convert farnesyl diphosphate to solavetivone via vetispiradiene (Takahashi et al., 2007). Although the nematicidal activity of solavetivone has not yet been reported,

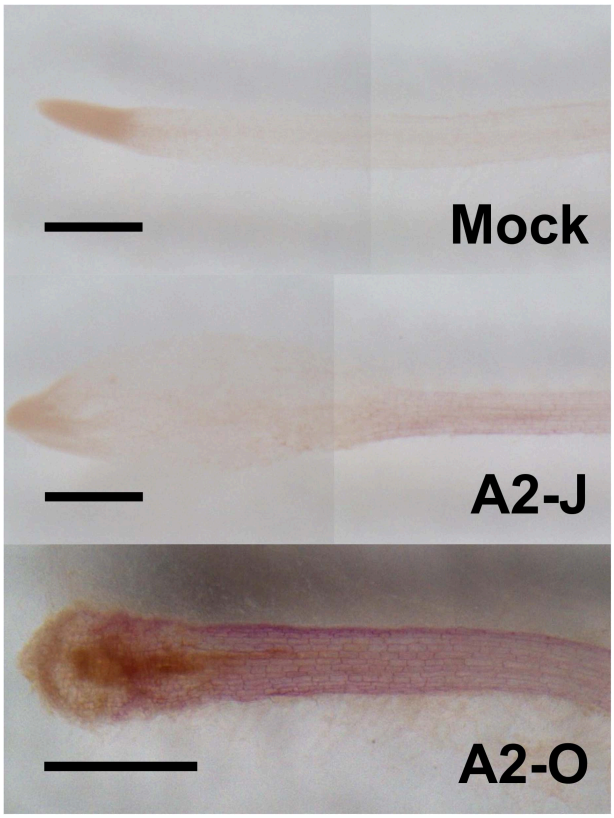

FIGURE 7 | Infection with A2-O but not with A2-J induced lignin deposition. Phloroglucinol staining of lignin (red) in *S. torvum* root tips treated with SDW (mock) or infected with A2-J or A2-O for three days. Scale bars indicate 0.5 mm. This experiment was performed four times with the same results.

genetic analyses indicate that the production of solavetivone is associated with resistance in potato against CN *Globodera rostochiensis* (Desjardins et al., 1997). It would be interesting to test the nematicidal activity of these sesquiterpenes and their production after A2-O infection in *S. torvum*.

We also found that infection with A2-O induces the expression of genes encoding the non-canonical FAD2 proteins ACET1a/b (Solyc12g100240 and Solyc12g100260) and FAD2-9 (Solyc12g100250), which are involved in the biosynthesis of falcarindiol, a modified fatty acid found in a variety of plants, including Solanaceae. It is toxic to RKNs and pinewood nematodes (Liu et al., 2016), but it is not known if falcarindiol is produced by *S. torvum*. In any case, the higher expression of FAD2 after A2-O infection suggests the importance of fatty acid metabolism in plant immunity against PPNs. We consistently found that A2-O infection results in the accumulation of linoleic acid (C18:2), while infection with A2-J reduced linoleic acid (C18:2) and palmitic acid (C16:0) (**Supplementary Figure 6**). Increases in linoleic acid elicits resistance to the fungal pathogen *Colletotrichum gloeosporioides* in avocado (Madi et al., 2003), and to *B. cinerea* in bean plants (Ongena et al., 2004). The importance of fatty acids in resistance is further supported by the fact that PPNs secrete fatty-acid- and retinol-binding family proteins as a mechanism to increase susceptibility (Prior et al., 2001; Iberkleid et al., 2013, 2015). Thus, the battle over fatty acid synthesis is likely to be important in *S. torvum*-PPN interactions.

Lignin Accumulation as a Defense Against PPNs

Because PPNs penetrate the cell wall and migrate within roots, reinforcement of cell walls by lignin accumulation has been implicated as an effective defense response to PPNs (Holbein et al., 2016; Sato et al., 2019). In fact, several studies showed that PPN infection induces more extensive lignin accumulation in resistant plants than in susceptible plants. For example, Veronico et al. (2018) performed a histochemical analysis of lignin in the roots of susceptible and resistant tomatoes infected with *M. incognita*, and found that accumulation of higher lignin levels in the root tissues (e.g., cortical cells) of resistant tomato than in susceptible varieties. Similarly, upon infection with the cereal CN *Heterodera avenae*, a resistant wheat cultivar gives a strong lignin accumulation response in the walls of cells affected by nematode infection, but a susceptible cultivar responded with only minor additional lignification, and only in cell walls mechanically damaged during nematode penetration (Andres et al., 2001). Since these studies used resistant and susceptible lines, it is certainly possible that differences in lignin accumulation are due to multiple differences in genetic background, and thus there would not necessarily be a direct relationship to resistance. In the present study, by using a single host cultivar with virulent and avirulent nematodes, we showed that susceptible and resistant responses are correlated with the levels of lignin. Infection with A2-O significantly up-regulated genes involved in lignin biosynthesis, and induced lignin accumulation near the root tip (**Figures 6B**, 7). In contrast, infection with A2-J induced lignin biosynthetic genes to some limited extent that did not result in additional lignin accumulation. We also found that infection with A2-O significantly up-regulated the expression of class III peroxidases, some of which are thought to be involved in the polymerization of lignin (Zacheo et al., 1993, 1997; Marjamaa et al., 2009). The importance of lignin accumulation in PPN resistance is also supported by the fact that plant defense inducers such as β-aminobutyric acid, thiamine, sclareol, and benzothiadiazole induce lignin biosynthesis and enhance resistance against PPNs (Fujimoto et al., 2015; Ji et al., 2015; Huang et al., 2016; Veronico et al., 2018). Thus, ectopic lignification may result in cell wall reinforcement that restricts RKN invasion and migration.

In contrast to the resistance interaction with A2-O, infection with A2-J did not induce lignin accumulation. One potential mechanism to explain this is that A2-J may alter the metabolic flux of lignin biosynthesis by specifically inducing the expression of the gene encoding chalcone synthase, which converts *p*-coumaroyl-CoA into naringenin chalcone (**Figure 5A**). The biosynthetic pathways leading to lignin and flavonoids diverge at the common intermediate *p*-coumaroyl CoA, so higher chalcone synthase expression should decrease lignin content. Indeed, silencing of the chalcone synthase gene increases lignin deposition in wheat (Eloy et al., 2017).

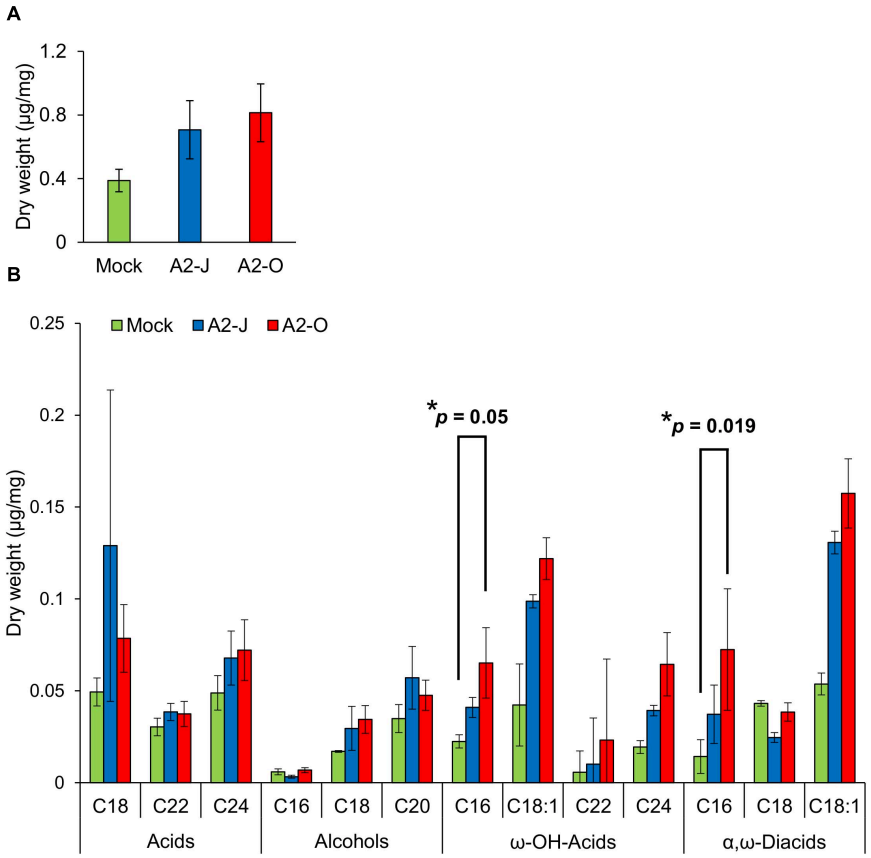

FIGURE 8 | Infection with A2-O changed suberin monomer composition in the root tips. **(A)** Total aliphatic suberin and **(B)** suberin monomer composition in root tips treated with SDW (mock) or infected with A2-J or A2-O for four days. GC-MS was performed to measure the content of aliphatic suberin monomers in root tips. Bars indicate means ± SE of four biological replicates. Asterisks indicate significant differences compared with mock treatment (Welch's *t*-test with Bonferroni correction, * $p \leq 0.05$). There was no statistically significant difference at $p \leq 0.05$ in the total amount of aliphatic suberin between samples (Welch's *t*-test with Bonferroni correction).

Activation of the phenylpropanoid biosynthesis pathway may also be involved in the production of anti-PPN secondary metabolites (Khanam et al., 2018). For example, *trans*-cinnamaldehyde is a phenylpropanoid compound that is highly toxic to RKNs and pinewood nematodes (Oka, 2001; Kong et al., 2007). Cinnamaldehyde can be synthesized from L-phenylalanine, and its biosynthesis requires enzymatic reactions mediated by PAL, 4CL, and CCR (Bang et al., 2016). Expression of genes encoding these enzymes was specifically induced in A2-O-infected *S. torvum* (**Figure 6B**). We also observed a drastic induction of a BBE-like protein homologous to AtBBE-like 13 and AtBBE-like 15 (**Figure 5B**), which can convert cinnamyl alcohol to cinnamaldehyde in Arabidopsis (Daniel et al., 2015). Thus, *S. torvum* may activate the production of cinnamaldehyde to suppress PPN infection.

Both A2-J and A2-O Induce the Expression of Suberin Synthetic Genes

Suberin is a lipid-phenolic biopolyester deposited in the cell walls of the root endodermis. Suberin lamellae and the lignin-based Casparian strip in the endodermis form the apoplastic diffusion barrier between vascular tissues and outer ground tissues to enforce selective absorption of water and nutrients (Alassimone et al., 2012; Vishwanath et al., 2015). The suberized endodermis may also play a role in defense against pathogens as the last line of defense before pathogens invade the vasculature (Thomas et al., 2007). Moreover, several reports showed that fungal or viral attack induces the deposition of suberin in the walls of cells in and around the site of penetration (Tippett and Hill, 1984; Kolattukudy and Espelie, 1989). In contrast, the virulent vascular pathogen, *Verticillium longisporum* reduces suberin deposition by suppressing the translation of genes involved in suberin biosynthesis (Froschel et al., 2020). These results may indicate the general importance of suberin in plant immunity. Infection with A2-J or A2-O induced the expression of genes involved in suberin biosynthesis at the root tip, with A2-O induction being slightly higher (**Figure 5C**). The total aliphatic suberin content tended to increase upon infection with A2-J and A2-O, but there was no statistically significant difference due to the large variation of the data (**Figure 8A**). The large variation in the data may be due to variation in the number of

infected root tips, nematode aggressiveness, and/or the severity of wounding, which can vary by experiment and cause disparity in the proportions of suberized areas among the fragile root tips. Because infection with RKN *M. incognita* induces the expression of suberin biosynthetic genes and a patchy suberin accumulation pattern within the cell layer surrounding the infection site in later stages of infection (10 DPI) in susceptible Arabidopsis plants (Holbein et al., 2019), it is possible that the synthesis of large amounts of suberin takes longer in *S. torvum* that what was allowed for in this assay. Although there was no statistical difference in total aliphatic suberin content, infection with A2-O increased the accumulation of suberin monomers such as ω-OH-acid C16 and α, ω-diacid C16 (**Figure 8**). These results suggest that *de novo* suberin synthesis is induced at the site of infection. Considering that A2-J also induces the expression of suberin biosynthesis genes (**Figure 5C**), it is possible that *de novo* suberin synthesis is induced in both incompatible and compatible interactions between plants and RKNs. This would be consistent with the fact that infection with RKN *M. incognita* induces the expression of *GPAT5*, a suberin biosynthetic gene, as well as the patchy suberin accumulation pattern within the cell layer surrounding infection sites in susceptible Arabidopsis plants (Holbein et al., 2019). Because the expression pattern of the suberin biosynthetic genes was similar to that of wound-inducible genes (**Supplementary Figure 5**), the induction of suberin biosynthesis could be triggered by wounding during nematode infection, but this need to be confirmed experimentally. In addition, it is important to clarify the biological relevance of ectopic suberin accumulation at the site of infection in the resistance response against PPNs in the future. We may be able to assess the individual contribution of ectopic suberin accumulation to the resistance response by selectively expressing a suberin-degrading enzyme CDEF1 (cuticle destructing factor 1) only at the site of infection (Takahashi et al., 2010). However, transformation of *S. torvum* is technically challenging at the moment.

A Model for Resistant and Susceptible Responses to RKN Infection

In this study, we were able to examine detail the transcriptional reprogramming of *S. torvum* in response to infection with virulent and avirulent RKNs at early infection stages by comparative transcriptome analyses (**Figure 9**). Shortly after infection with A2-O, *S. torvum* rapidly induces the expression of genes encoding fatty acid desaturases and sesquiterpene synthases, which may act as the first, or at least an early line of defense. Infection with A2-O also induces the expression

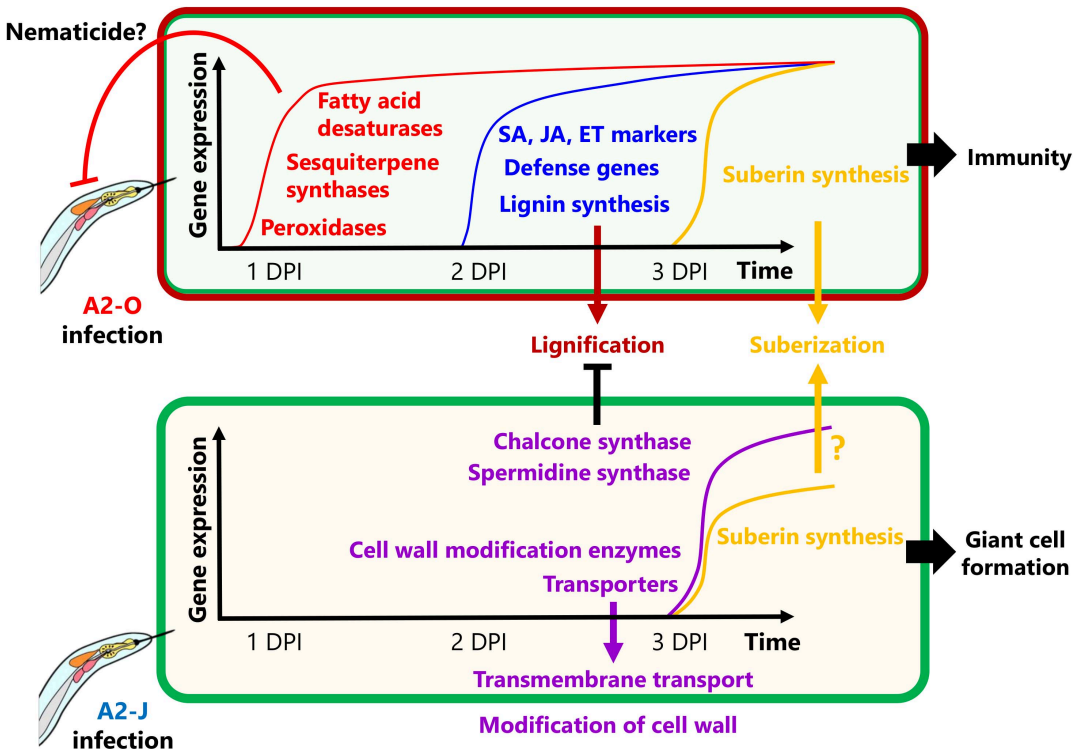

FIGURE 9 | Schematic model of *S. torvum* responses to *M. arenaria* A2-O and A2-J. In the *S. torvum*/*M. arenaria* model, shortly after infection with avirulent RKN, plant genes encoding fatty acid desaturases and sesquiterpene synthases are induced to act as an early line of defense. Avirulent RKN infection also induces lignin accumulation in root tip, which may result in cell wall reinforcement that restricts RKN invasion and migration. Infection with virulent RKN results in a delayed gene expression response by specifically inducing chalcone synthase and spermidine synthase, which suppress multiple defense responses. Virulent RKN infection also results in induced expression of cell wall modification and transmembrane transport genes whose products contribute to giant cell formation for nematode feeding and completion of the life cycle.

of SA, JA, and ET marker genes, and defense-related genes (WRKY transcription factors, chitinases, and β-1,3-glucanases), as well as the expression of lignin biosynthetic genes, leading to lignin accumulation in root tips. In contrast, infection with A2-J fails to alter gene expression at 1 DPI, but it does specifically induce the expression of genes encoding chalcone synthase and spermidine synthase, which might suppress lignin synthesis and the SA-mediated defense response (Hewezi et al., 2010). A2-J infection also induces the expression of genes related to cell wall modification and transmembrane transport, which may be important for the development and maturation of giant cells, and which in turn support nematode feeding, and are necessary to complete the parasitic life cycle. Interestingly, nematode invasion generally induces the expression of suberin synthetic genes, suggesting that the wounds caused by nematode entry and movement trigger suberin gene transcriptional activation. In the future, it will be important to independently assess the contribution of these genes to immunity and susceptibility against RKNs. It is also important to understand the molecular mechanisms and signal transduction pathways that decide the fate of infected plants and their nematode parasites, but will likely include whether or not plants have receptors that can recognize PPNs, and can transduce those signals to trigger defense responses, and/or whether or not PPNs produce virulence effectors that inhibit recognition, disrupt signal transduction, or suppress the defense response. As the next step, it is important to identify the specific effectors of A2-J and A2-O by comparative genomics, transcriptomics, and effectoromics, and to characterize their functions at the molecular level.

DATA AVAILABILITY STATEMENT

The datasets presented in this study can be found in online repositories. The names of the repository/repositories and accession number(s) are as follows: NCBI (https://www.ncbi.nlm.nih.gov), PRJNA681478; Figshare (https://figshare.com), https://doi.org/10.6084/m9.figshare.14054354.

AUTHOR CONTRIBUTIONS

YK and KSh supervised the research. YK designed the experiments. YK and KSa carried out histopathological observation. YK and TU propagate the nematodes and YK collected samples for RNA-seq, lipid, and suberin analyses. NM generated RNA-seq libraries. TS carried out RNA-seq. YI performed quality filtering of raw RNA-seq reads. KSa carried out bioinformatic analyses, including assembly, annotation, gene expression analyses, and GO enrichment tests. PG helped in bioinformatic analyses. TB, KY, and SSh provided RKN genome assemblies. YK and KSa performed lignin staining. YS-S and HO performed lipid quantification. JH, RF, SSi, and FG carried out suberin monomer quantification. KSa, YK, and KSh wrote the manuscript. All authors read and approved the final manuscript.

FUNDING

This research was financially supported by Cabinet Office, Government of Japan, cross-ministerial Strategic Innovation Promotion Program (SIP), "Technologies for Creating Next-Generation Agriculture, Forestry and Fisheries" (funding agency, Bio-oriented Technology Research Advancement Institution, NARO) (to TU and YK), an NIBB Collaborative Research Program (20–421) (to YK), MEXT/JSPS KAKENHI Grant Number, JP16H06186 (to YK), JP16KT0037, JP19H02962, and JP20H02994 (to TU and YK), JP17H06172 and JP20H05909 (to KSh), and Grant-in-Aid for JSPS Fellows Grant Number JP19J00655 (to KSa).

ACKNOWLEDGMENTS

We thank all members of the Shirasu lab for intensive and helpful discussions. We thank Akiko Ueno, Naomi Watanabe, Mamiko Kouzai, Yoko Nagai, and Kanako Hori for their support of this project. Hideaki Iwahori at Ryukoku University for sharing *M arenaria* A2-O. We thank Mitsuyasu Hasebe, Shoko Ohi, Miwako Matsumoto (NIBB), and Tomoko Shibata for the PacBio sequencing and the Data Integration and Analysis Facility at NIBB for computer resources. We also thank B. Favery for sharing the BABB cleaning protocols.

SUPPLEMENTARY MATERIAL

The Supplementary Material for this article can be found online at: https://www.frontiersin.org/articles/10.3389/fpls.2021.680151/full#supplementary-material

REFERENCES

Abad, P., Castagnone-Sereno, P., Rosso, M. N., Engler, J. D. A., and Favery, B. (2009). "Invasion, Feeding and Development," in *Root-knot nematodes*, eds R. N. Perry, M. Moens, and J. L. Starr, (Cambridge: CABI International Press), 163–181.

Alassimone, J., Roppolo, D., Geldner, N., and Vermeer, J. E. (2012). The endodermis — development and differentiation of the plant's inner skin. *Protoplasma* 249, 433–443. doi: 10.1007/s00709-011-0302-5

Andres, M. F., Melillo, M. T., Delibes, A., Romero, M. D., and Bleve-Zacheo, T. (2001). Changes in wheat root enzymes correlated with resistance to cereal cyst nematodes. *New Phytol.* 152, 343–354.

Atamian, H. S., Eulgem, T., and Kaloshian, I. (2012). *SlWRKY70* is required for *Mi-1*-mediated resistance to aphids and nematodes in tomato. *Planta* 235, 299–309. doi: 10.1007/s00425-011-1509-6

Bagnaresi, P., Sala, T., Irdani, T., Scotto, C., Lamontanara, A., Beretta, M., et al. (2013). responses to the root-knot nematode *Meloidogyne incognita*. *BMC Genomics* 14:540. doi: 10.1186/1471-2164-14-540

Bali, S., Vining, K., Gleason, C., Majtahedi, H., Brown, C. R., and Sathuvalli, V. (2019). Transcriptome profiling of resistance response to *Meloidogyne chitwoodi* introgressed from wild species *Solanum bulbocastanum* into cultivated potato. *BMC Genomics* 20:907. doi: 10.1186/s12864-019-6257-1

Bang, H. B., Lee, Y. H., Kim, S. C., Sung, C. K., and Jeong, K. J. (2016). Metabolic engineering of *Escherichia coli*. *Microb Cell Fact* 16:415. doi: 10.1186/s12934-016-0415-9

Barberon, M. (2017). The endodermis as a checkpoint for nutrients. *New Phytol.* 213, 1604–1610. doi: 10.1111/nph.14140

Bartlem, D. G., Jones, M. G., and Hammes, U. Z. (2014). Vascularization and nutrient delivery at root-knot nematode feeding sites in host roots. *J. Exp. Bot.* 65, 1789–1798. doi: 10.1093/jxb/ert415

Berardini, T. Z., Reiser, L., Li, D., Mezheritsky, Y., Muller, R., Strait, E., et al. (2015). The Arabidopsis information resource: Making and mining the "gold standard" annotated reference plant genome. *Genesis* 53, 474–485. doi: 10.1002/dvg.22877

Bernards, M. A., and Lewis, N. G. (1998). The macromolecular aromatic domain in suberized tissue: A changing paradigm. *Phytochemistry* 47, 915–933. doi: 10.1016/S0031-9422(98)80052-6

Bohlmann, H. (2015). "Chapter Two - Introductory Chapter on the Basic Biology of Cyst Nematodes," in *Plant nematode interactions: a view on compatible interrelationships, vol 73, Advances in Botanical Research*, eds C. Escobar, and C. Fenoll, (Oxford, UK: Elsevier), 33–60.

Bohlmann, H., and Sobczak, M. (2014). The plant cell wall in the feeding sites of cyst nematodes. *Front. Plant. Sci.* 5:89. doi: 10.3389/fpls.2014.00089

Booker, M. A., and DeLong, A. (2015). Producing the ethylene signal: regulation and diversification of ethylene biosynthetic enzymes. *Plant Physiol.* 169, 42–50. doi: 10.1104/pp.15.00672

Boutrot, F., and Zipfel, C. (2017). Function, discovery, and exploitation of plant pattern recognition receptors for broad-spectrum disease resistance. *Annu. Rev. Phytopathol.* 55, 257–286. doi: 10.1146/annurev-phyto-080614-120106

Bozbuga, R., Lilley, C. J., Knox, J. P., and Urwin, P. E. (2018). Host-specific signatures of the cell wall changes induced by the plant parasitic nematode. *Meloid. Incognita*. *Sci. Rep.* 8:17302. doi: 10.1038/s41598-018-35529-7

Brennan, R. J. B., Glaze-Corcoran, S., Wick, R., and Hashemi, M. (2020). Biofumigation: An alternative strategy for the control of plant parasitic nematodes. *J. Integr. Agric.* 19, 1680–1690. doi: 10.1016/S2095-3119(19)62817-0

Brown, D. M., Zeef, L. A., Ellis, J., Goodacre, R., and Turner, S. R. (2005). Identification of novel genes in Arabidopsis involved in secondary cell wall formation using expression profiling and reverse genetics. *Plant Cell* 17, 2281–2295. doi: 10.1105/tpc.105.031542

Bybd, D. W., Kirkpatrick, T., and Barker, K. R. (1983). An improved technique for clearing and staining plant tissues for detection of nematodes. *J. Nematol.* 15, 142–143.

Cabrera, J., Olmo, R., Ruiz-Ferrer, V., Abreu, I., Hermans, C., Martinez-Argudo, I., et al. (2018). A Phenotyping Method of Giant Cells from Root-Knot Nematode Feeding Sites by Confocal Microscopy Highlights a Role for CHITINASE-LIKE 1 in Arabidopsis. *Int. J. Mol. Sci.* 19:429. doi: 10.3390/ijms19020429

Cao, S., Zhou, X. R., Wood, C. C., Green, A. G., Singh, S. P., Liu, L., et al. (2013). A large and functionally diverse family of *Fad2* genes in safflower (*Carthamus tinctorius* L.). *BMC Plant Biol.* 13:5. doi: 10.1186/1471-2229-13-5

Chen, R., Li, H., Zhang, L., Zhang, J., Xiao, J., and Ye, Z. (2007). *CaMi*, a root-knot nematode resistance gene from hot pepper (*Capsium annuum* L.) confers nematode resistance in tomato. *Plant Cell Rep.* 26, 895–905. doi: 10.1007/s00299-007-0304-0

Chitwood, D. H., Maloof, J. N., and Sinha, N. R. (2013). Dynamic transcriptomic profiles between tomato and a wild relative reflect distinct developmental architectures. *Plant Physiol.* 162, 537–552. doi: 10.1104/pp.112.213546

Claverie, M., Dirlewanger, E., Bosselut, N., Van Ghelder, C., Voisin, R., Kleinhentz, M., et al. (2011). The *Ma* gene for complete-spectrum resistance to *Meloidogyne* species in *Prunus* is a TNL with a huge repeated C-terminal post-LRR region. *Plant Physiol.* 156, 779–792. doi: 10.1104/pp.111.176230

Collinge, M., and Boller, T. (2001). Differential induction of two potato genes, *Stprx2* and *StNAC*, in response to infection by *Phytophthora infestans* and to wounding. *Plant Mol. Biol.* 46, 521–529. doi: 10.1023/a:1010639225091

Cosgrove, D. J. (2000). Loosening of plant cell walls by expansins. *Nature* 407, 321–326. doi: 10.1038/35030000

Cosio, C., and Dunand, C. (2009). Specific functions of individual class III peroxidase genes. *J. Exp. Bot.* 60, 391–408. doi: 10.1093/jxb/ern318

Daniel, B., Pavkov-Keller, T., Steiner, B., Dordic, A., Gutmann, A., Nidetzky, B., et al. (2015). Oxidation of Monolignols by Members of the Berberine Bridge Enzyme Family Suggests a Role in Plant Cell Wall Metabolism. *J. Biol. Chem.* 290, 18770–18781. doi: 10.1074/jbc.M115.659631

Dao, T. T., Linthorst, H. J., and Verpoorte, R. (2011). Chalcone synthase and its functions in plant resistance. *Phytochem. Rev.* 10, 397–412. doi: 10.1007/s11101-011-9211-7

Davies, L. J., Lilley, C. J., Paul Knox, J., and Urwin, P. E. (2012). Syncytia formed by adult female *Heterodera schachtii* in *Arabidopsis thaliana* roots have a distinct cell wall molecular architecture. *New Phytol.* 196, 238–246. doi: 10.1111/j.1469-8137.2012.04238.x

Dean, B. B., and Kolattukudy, P. E. (1976). Synthesis of Suberin during Wound-healing in Jade Leaves, Tomato Fruit, and Bean Pods. *Plant Physiol.* 58, 411–416. doi: 10.1104/pp.58.3.411

Desjardins, A. E., McCormick, S. P., Plaisted, R. L., and Brodie, B. B. (1997). Association between solavetivone production and resistance to *Globodera rostochiensis* in potato. *J. Agric. Food. Chem.* 45, 2322–2326.

Dodds, P. N., and Rathjen, J. P. (2010). Plant immunity: towards an integrated view of plant-pathogen interactions. *Nat. Rev. Genet.* 11, 539–548. doi: 10.1038/nrg2812

Du, C., Jiang, J., Zhang, H., Zhao, T., Yang, H., Zhang, D., et al. (2020). Transcriptomic profiling of *Solanum peruvianum* LA3858 revealed a *Mi-3*-mediated hypersensitive response to *Meloidogyne incognita*. *BMC Genomics* 21:250. doi: 10.1186/s12864-020-6654-5

Elashry, A., Okumoto, S., Siddique, S., Koch, W., Kreil, D. P., and Bohlmann, H. (2013). The *AAP* gene family for amino acid permeases contributes to development of the cyst nematode *Heterodera schachtii* in roots of Arabidopsis. *Plant Physiol. Biochem.* 70, 379–386. doi: 10.1016/j.plaphy.2013.05.016

Eloy, N. B., Voorend, W., Lan, W., Saleme, M. L., Cesarino, I., Vanholme, R., et al. (2017). Silencing *CHALCONE SYNTHASE* in Maize Impedes the Incorporation of Tricin into Lignin and Increases Lignin Content. *Plant Physiol.* 173, 998–1016. doi: 10.1104/pp.16.01108

Ernst, K., Kumar, A., Kriseleit, D., Kloos, D. U., Phillips, M. S., and Ganal, M. W. (2002). The broad-spectrum potato cyst nematode resistance gene (*Hero*) from tomato is the only member of a large gene family of NBS-LRR genes with an unusual amino acid repeat in the LRR region. *Plant J.* 31, 127–136.

Escobar, C., Barcala, M., Cabrera, J., and Fenoll, C. (2015). "Chapter One - Overview of Root-Knot Nematodes and Giant Cells," in *Plant nematode interactions: a view on compatible interrelationships, vol 73, Advances in Botanical Research*, eds C. Escobar, and C. Fenoll, (Oxford, UK: Elsevier), 1–32.

Facchini, P. J., and Chappell, J. (1992). Gene family for an elicitor-induced sesquiterpene cyclase in tobacco. *Proc. Natl. Acad. Sci. U. S. A.* 89, 11088–11092. doi: 10.1073/pnas.89.22.11088

Farmer, E. E., Johnson, R. R., and Ryan, C. A. (1992). Regulation of expression of proteinase inhibitor genes by methyl jasmonate and jasmonic Acid. *Plant Physiol.* 98, 995–1002. doi: 10.1104/pp.98.3.995

Franke, R., Briesen, I., Wojciechowski, T., Faust, A., Yephremov, A., Nawrath, C., et al. (2005). Apoplastic polyesters in *Arabidopsis* surface tissues – A typical suberin and a particular cutin. *Phytochemistry* 66, 2643–2658. doi: 10.1016/j.phytochem.2005.09.027

Froschel, C., Komorek, J., Attard, A., Marsell, A., Lopez-Arboleda, W. A., Le Berre, J., et al. (2020). Plant roots employ cell-layer-specific programs to respond to pathogenic and beneficial microbes. *Cell Host. Microbe.* 11:14. doi: 10.1016/j.chom.2020.11.014

Fujimoto, T., Mizukubo, T., Abe, H., and Seo, S. (2015). Sclareol induces plant resistance to root-knot nematode partially through ethylene-dependent enhancement of lignin accumulation. *Mol. Plant Microbe Interact* 28, 398–407. doi: 10.1094/MPMI-10-14-0320-R

García-Mendívil, H. A., Escudero, N., and Sorribas, F. J. (2019). Host suitability of *Solanum torvum*. *Plant Pathol.* 36, 1215–1224. doi: 10.1111/ppa.13036

García-Mendívil, H. A., and Sorribas, F. J. (2019). Fitness cost but no selection for virulence in *Meloidogyne incognita* after two consecutive crops of eggplant grafted onto *Solanum torvum*. *Meloidogyne Incognita*. 11:13092. doi: 10.1111/ppa.13092

Ghaemi, R., Pourjam, E., Safaie, N., Verstraeten, B., Mahmoudi, S. B., Mehrabi, R. (2020). Molecular insights into the compatible and incompatible interactions between sugar beet and the beet cyst nematode. *BMC Plant Biol.* 20:483. doi: 10.1186/s12870-020-02706-8

Godinez-Vidal, D., Soto-Hernández, M., Rocha Sosa, M., Lozoya-Gloria, E., Rojas-Martínez, R. I., Guevara Olvera, L., et al. (2010). Capsidiol content in CM-334

pepper roots infected with *Nacobbus aberrans* and its effect on second stage juveniles. *Nematropica* 40, 227–237.

Goto, Y., Maki, N., Ichihashi, Y., Kitazawa, D., Igarashi, D., Kadota, Y., et al. (2020). Exogenous Treatment with Glutamate Induces Immune Responses in *Arabidopsis*. *Mol. Plant Microbe Interact.* 33, 474–487. doi: 10.1094/MPMI-09-19-0262-R

Gotz, S., Garcia-Gomez, J. M., Terol, J., Williams, T. D., Nagaraj, S. H., Nueda, M. J., et al. (2008). High-throughput functional annotation and data mining with the Blast2GO suite. *Nucleic Acids Res.* 36, 3420–3435. doi: 10.1093/nar/gkn176

Gousset, C., Collonnier, C., Mulya, K., Mariska, I., Rotino, G. L., Besse, P., et al. (2005). , as a useful source of resistance against bacterial and fungal diseases for improvement of eggplant (*S. melongena* L.).Solanum torvum. *Plant Sci.* 7, 319–327. doi: 10.1016/j.plantsci.2004.07.034

Grabherr, M. G., Haas, B. J., Yassour, M., Levin, J. Z., Thompson, D. A., Amit, I. (2011). Full-length transcriptome assembly from RNA-Seq data without a reference genome. *Nat. Biotechnol.* 29, 644–652. doi: 10.1038/nbt.1883

Grosskinsky, D. K., Naseem, M., Abdelmohsen, U. R., Plickert, N., Engelke, T., Griebel, T., et al. (2011). Cytokinins mediate resistance against *Pseudomonas*. *Plant Physiol.* 11, 815–830. doi: 10.1104/pp.111.182931

Haas, B. J., Papanicolaou, A., Yassour, M., Grabherr, M., Blood, P. D., Bowden, J., et al. (2013). *De novo* transcript sequence reconstruction from RNA-seq using the Trinity platform for reference generation and analysis. *Nat. Protoc.* 8, 1494–1512. doi: 10.1038/nprot.2013.084

Hammes, U. Z., Schachtman, D. P., Berg, R. H., Nielsen, E., Koch, W., McIntyre, L. M., et al. (2005). Nematode-induced changes of transporter gene expression in *Arabidopsis* roots. *Mol. Plant Microbe Interact.* 18, 1247–1257. doi: 10.1094/MPMI-18-1247

Hewezi, T., Howe, P. J., Maier, T. R., Hussey, R. S., Mitchum, M. G., Davis, E. L., et al. (2010). Arabidopsis spermidine synthase is targeted by an effector protein of the cyst nematode *Heterodera schachtii*. *Plant Physiol.* 152, 968–984. doi: 10.1104/pp.109.150557

Holbein, J., Franke, R. B., Marhavý, P., Fujita, S., Gorecka, M., Sobczak, M., et al. (2019). Root endodermal barrier system contributes to defence against plant-parasitic cyst and root-knot nematodes. *Plant J.* 100, 221–236. doi: 10.1111/tpj.14459

Holbein, J., Grundler, F. M., and Siddique, S. (2016). Plant basal resistance to nematodes: an update. *J. Exp. Bot.* 67, 2049–2061. doi: 10.1093/jxb/erw005

Huang, S., Gao, Y., Liu, J., Peng, X., Niu, X., Fei, Z., et al. (2012). Genome-wide analysis of WRKY transcription factors in *Solanum lycopersicum*. *Mol. Genet Genom.* 287, 495–513. doi: 10.1007/s00438-012-0696-6

Huang, W. K., Ji, H. L., Gheysen, G., and Kyndt, T. (2016). Thiamine-induced priming against root-knot nematode infection in rice involves lignification and hydrogen peroxide generation. *Mol. Plant Pathol.* 17, 614–624. doi: 10.1111/mpp.12316

Iberkleid, I., Sela, N., and Brown Miyara, S. (2015). *Meloidogyne javanica* fatty acid- and retinol-binding protein (Mj-FAR-1) regulates expression of lipid-, cell wall-, stress- and phenylpropanoid-related genes during nematode infection of tomato. *BMC Genomics* 16:272. doi: 10.1186/s12864-015-1426-3

Iberkleid, I., Vieira, P., de Almeida Engler, J., Firester, K., Spiegel, Y., and Horowitz, S. B. (2013). Fatty acid-and retinol-binding protein, Mj-FAR-1 induces tomato host susceptibility to root-knot nematodes. *PLoS One* 8:e64586. doi: 10.1371/journal.pone.0064586

Jablonska, B., Ammiraju, J. S., Bhattarai, K. K., Mantelin, S., Martinez, de Ilarduya, O., et al. (2007). The *Mi-9* gene from *Solanum arcanum* conferring heat-stable resistance to root-knot nematodes is a homolog of *Mi-1*. *Plant Physiol.* 143, 1044–1054. doi: 10.1104/pp.106.089615

Jensen, W. A. (1962). *Botanical Histochemistry*. London: W.H. Freeman & Co.

Jeon, J. E., Kim, J. G., Fischer, C. R., Mehta, N., Dufour-Schroif, C., Wemmer, K., et al. (2020). A Pathogen-Responsive Gene Cluster for Highly Modified Fatty Acids in Tomato. *Cell* 180, 176–187e119. doi: 10.1016/j.cell.2019.11.037

Ji, H., Kyndt, T., He, W., Vanholme, B., and Gheysen, G. (2015). β-aminobutyric acid-induced resistance against root-knot nematodes in rice is based on increased basal defense. *Mol. Plant Microbe Interact.* 28, 519–533. doi: 10.1094/MPMI-09-14-0260-R

Jones, J. D., and Dangl, J. L. (2006). The plant immune system. *Nature* 444, 323–329. doi: 10.1038/nature05286

Jones, J. T., Haegeman, A., Danchin, E. G., Gaur, H. S., Helder, J., Jones, M. G., et al. (2013). Top 10 plant-parasitic nematodes in molecular plant pathology. *Mol. Plant Pathol.* 14, 946–961. doi: 10.1111/mpp.12057

Jones, P., Binns, D., Chang, H. Y., Fraser, M., Li, W., McAnulla, C., et al. (2014). InterProScan 5: genome-scale protein function classification. *Bioinformatics* 30, 1236–1240. doi: 10.1093/bioinformatics/btu031

Kaloshian, I., Desmond, O. J., and Atamian, H. S. (2011). "Disease Resistance-Genes and Defense Responses During Incompatible Interactions," in *Genomics and Molecular Genetics of Plant-Nematode Interactions*, eds J. Jones, G. Gheysen, and C. Fenoll, (Netherlands: Springer), 309–324.

Khanam, S., Bauters, L., Singh, R. R., Verbeek, R., Haeck, A., Sultan, S. M. D., et al. (2018). Mechanisms of resistance in the rice cultivar Manikpukha to the rice stem nematode *Ditylenchus angustus*. *Mol. Plant Pathol.* 19, 1391–1402. doi: 10.1111/mpp.12622

Kim, D., Paggi, J. M., Park, C., Bennett, C., and Salzberg, S. L. (2019). Graph-based genome alignment and genotyping with HISAT2 and HISAT-genotype. *Nat. Biotechnol.* 37, 907–915. doi: 10.1038/s41587-019-0201-4

Kolattukudy, P. E., and Espelie, K. E. (1989). "Chemistry, Biochemistry, and Function of Suberin and Associated Waxes," in *Natural Products of Woody Plants*, ed. J. W. Rowe, (Heidelberg: Springer).

Kong, J. O., Lee, S. M., Moon, Y. S., Lee, S. G., and Ahn, Y. J. (2007). Nematicidal Activity of Cassia and Cinnamon Oil Compounds and Related Compounds toward *Bursaphelenchus xylophilus* (Nematoda: Parasitaphelenchidae). *J. Nematol.* 39, 31–36.

Kumar, M., Campbell, L., and Turner, S. (2016). Secondary cell walls: biosynthesis and manipulation. *J. Exp. Bot.* 67, 515–531. doi: 10.1093/jxb/erv533

Kumar, R., Ichihashi, Y., Kimura, S., Chitwood, D. H., Headland, L. R., Peng, J., et al. (2012). A High-Throughput Method for Illumina RNA-Seq Library Preparation. *Front. Plant Sci.* 3:202. doi: 10.3389/fpls.2012.00202

Lee, M. W., Padilla, C. S., Gupta, C., Galla, A., Pereira, A., Li, J., et al. (2020). The *FATTY ACID DESATURASE2* Family in Tomato Contributes to Primary Metabolism and Stress Responses. *Plant Physiol.* 182, 1083–1099. doi: 10.1104/pp.19.00487

Leide, J., Hildebrandt, U., Hartung, W., Riederer, M., and Vogg, G. (2012). Abscisic acid mediates the formation of a suberized stem scar tissue in tomato fruits. *New Phytol.* 194, 402–415. doi: 10.1111/j.1469-8137.2011.04047.x

Li, J. B., Luan, Y. S., and Liu, Z. (2015a). Overexpression of *SpWRKY1* promotes resistance to *Phytophthora nicotianae* and tolerance to salt and drought stress in transgenic tobacco. *Physiol. Plant.* 155, 248–266. doi: 10.1111/ppl.12315

Li, J. B., Luan, Y. S., and Liu, Z. (2015b). *SpWRKY1* mediates resistance to *Phytophthora infestans* and tolerance to salt and drought stress by modulating reactive oxygen species homeostasis and expression of defense-related genes in tomato. *Plant Cell Tiss. Organ. Cult.* 123, 67–81. doi: 10.1007/s11240-015-0815-2

Lim, G. H., Singhal, R., Kachroo, A., and Kachroo, P. (2017). Fatty Acid- and Lipid-Mediated Signaling in Plant Defense. *Annu. Rev. Phytopathol.* 55, 505–536. doi: 10.1146/annurev-phyto-080516-035406

Liu, B., Hong, Y. B., Zhang, Y. F., Li, X. H., Huang, L., Zhang, H. J., et al. (2014). Tomato WRKY transcriptional factor SlDRW1 is required for disease resistance against *Botrytis cinerea* and tolerance to oxidative stress. *Plant Sci.* 227, 145–156. doi: 10.1016/j.plantsci.2014.08.001

Liu, G., Lai, D., Liu, Q. Z., Zhou, L., and Liu, Z. L. (2016). Identification of Nematicidal Constituents of *Notopterygium incisum* Rhizomes against *Bursaphelenchus xylophilus* and *Meloidogyne incognita*. *Molecules* 21:276. doi: 10.3390/molecules21101276

Liu, J.-H., Kitashiba, H., Wang, J., Ban, Y., and Moriguchi, T. (2007). Polyamines and their ability to provide environmental stress tolerance to plants. *Plant Biotechnol.* 24, 117–126. doi: 10.5511/plantbiotechnology.24.117

Lulai, E. C., Suttle, J. C., and Pederson, S. M. (2008). Regulatory involvement of abscisic acid in potato tuber wound-healing. *J. Exp. Bot.* 59, 1175–1186. doi: 10.1093/jxb/ern019

Madi, L., Wang, X., Kobiler, I., Lichter, A., and Prusky, D. (2003). Stress on avocado fruits regulates Δ9-stearoyl ACP desaturase expression, fatty acid composition, antifungal diene level and resistance to *Colletotrichum gloeosporioides* attack. *Physiol. Mol. Plant Pathol.* 62, 277–283. doi: 10.1016/S0885-5765(03)00076-6

Mamrot, J., Legaie, R., Ellery, S. J., Wilson, T., Seemann, T., Powell, D. R., et al. (2017). *De novo* transcriptome assembly for the spiny mouse (*Acomys cahirinus*). *Sci. Rep.* 7:8996. doi: 10.1038/s41598-017-09334-7

Manosalva, P., Manohar, M., von Reuss, S. H., Chen, S., Koch, A., Kaplan, F., et al. (2015). Conserved nematode signalling molecules elicit plant defenses and pathogen resistance. *Nat. Commun.* 6:7795. doi: 10.1038/ncomms8795

Marhavý, P., Kurenda, A., Siddique, S., Denervaud Tendon, V., Zhou, F., Holbein, J., et al. (2019). Single-cell damage elicits regional, nematode-restricting ethylene responses in roots. *EMBO J.* 38:972. doi: 10.15252/embj.2018100972

Marjamaa, K., Kukkola, E. M., and Fagerstedt, K. V. (2009). The role of xylem class III peroxidases in lignification. *J. Exp. Bot.* 60, 367–376. doi: 10.1093/jxb/ern278

Meidani, C., Ntalli, N. G., Giannoutsou, E., and Adamakis, I. S. (2019). Cell Wall Modifications in Giant Cells Induced by the Plant Parasitic Nematode *Meloidogyne incognita* in Wild-Type (Col-0) and the *fra2 Arabidopsis thaliana* Katanin Mutant. *Int. J. Mol. Sci.* 20:21. doi: 10.3390/ijms20215465

Mejias, J., Truong, N. M., Abad, P., Favery, B., and Quentin, M. (2019). Plant Proteins and Processes Targeted by Parasitic Nematode Effectors. *Front. Plant Sci.* 10:970. doi: 10.3389/fpls.2019.00970

Mesquita, V. L. V., and Queiroz, C. (2013). "Enzymatic Browning," in *Biochemistry of Foods (Third Edition)*, eds N. A. M. Eskin, and F. Shahidi, (New York: Academic Press), 387–418.

Miedes, E., Vanholme, R., Boerjan, W., and Molina, A. (2014). The role of the secondary cell wall in plant resistance to pathogens. *Front. Plant Sci.* 5:358. doi: 10.3389/fpls.2014.00358

Milligan, S. B., Bodeau, J., Yaghoobi, J., Kaloshian, I., Zabel, P., and Williamson, V. M. (1998). The root knot nematode resistance gene *Mi* from tomato is a member of the leucine zipper, nucleotide binding, leucine-rich repeat family of plant genes. *Plant Cell* 10, 1307–1319. doi: 10.1105/tpc.10.8.1307

Mitchum, M. G., Sukno, S., Wang, X., Shani, Z., Tsabary, G., Shoseyov, O., et al. (2004). The promoter of the *Arabidopsis thaliana Cel1* endo-1,4-beta glucanase gene is differentially expressed in plant feeding cells induced by root-knot and cyst nematodes. *Mol. Plant Pathol.* 5, 175–181. doi: 10.1111/j.1364-3703.2004.00216.x

Murata, G., and Uesugi, K. (2021). Parasitism of *Solanum torvum*. *J. Phytopathol.* 122–128. doi: 10.1111/jph.12966

Mutuku, J. M., Cui, S., Hori, C., Takeda, Y., Tobimatsu, Y., Nakabayashi, R., et al. (2019). The Structural Integrity of Lignin Is Crucial for Resistance against *Striga hermonthica* Parasitism in Rice. *Plant Physiol.* 179, 1796–1809. doi: 10.1104/pp.18.01133

Nakasugi, K., Crowhurst, R., Bally, J., and Waterhouse, P. (2014). Combining transcriptome assemblies from multiple *de novo* assemblers in the allo-tetraploid plant *Nicotiana benthamiana*. *PLoS One* 9:e91776. doi: 10.1371/journal.pone.0091776

Ohlrogge, J., and Browse, J. (1995). Lipid biosynthesis. *Plant Cell* 7, 957–970. doi: 10.1105/tpc.7.7.957

Ohri, P., and Pannu, S. K. (2009). Effect of terpenoids on nematodes: a review. *J. Environ. Res. Dev.* 4, 171–177.

Oka, Y. (2001). Nematicidal activity of essential oil components against the root-knot nematode *Meloidogyne javanica*. *Nematology* 3, 159–164. doi: 10.1163/156854101750236286

Oka, Y. (2020). From Old-Generation to Next-Generation Nematicides. *Agronomy* 10:1387. doi: 10.3390/agronomy10091387

Ongena, M., Duby, F., Rossignol, F., Fauconnier, M. L., Dommes, J., and Thonart, P. (2004). Stimulation of the lipoxygenase pathway is associated with systemic resistance induced in bean by a nonpathogenic *Pseudomonas*. *Mol. Plant Microbe Interact.* 9, 1009–1018. doi: 10.1094/MPMI.2004.17.9.1009

Paal, J., Henselewski, H., Muth, J., Meksem, K., Menendez, C. M., Salamini, F., et al. (2004). Molecular cloning of the potato *Gro1-4* gene conferring resistance to pathotype Ro1 of the root cyst nematode *Globodera rostochiensis*, based on a candidate gene approach. *Plant J.* 38, 285–297. doi: 10.1111/j.1365-313X.2004.02047.x

Palomares-Rius, J. E., Escobar, C., Cabrera, J., Vovlas, A., and Castillo, P. (2017). Anatomical alterations in plant tissues induced by plant-parasitic nematodes. *Front. Plant Sci.* 8:1987. doi: 10.3389/fpls.2017.01987

Patro, R., Duggal, G., Love, M. I., Irizarry, R. A., and Kingsford, C. (2017). Salmon provides fast and bias-aware quantification of transcript expression. *Nat. Methods* 14, 417–419. doi: 10.1038/nmeth.4197

Postnikova, O. A., Hult, M., Shao, J., Skantar, A., and Nemchinov, L. G. (2015). Transcriptome analysis of resistant and susceptible alfalfa cultivars infected with root-knot nematode *Meloidogyne incognita*. *PLoS One* 10:e0118269. doi: 10.1371/journal.pone.0118269

Prior, A., Jones, J. T., Blok, V. C., Beauchamp, J., McDermott, L., Cooper, A., et al. (2001). A surface-associated retinol- and fatty acid-binding protein (Gp-FAR-1) from the potato cyst nematode *Globodera pallida*: lipid binding activities, structural analysis and expression pattern. *Biochem. J.* 356, 387–394. doi: 10.1042/0264-6021:3560387

Ralston, L., Kwon, S. T., Schoenbeck, M., Ralston, J., Schenk, D. J., Coates, R. M., et al. (2001). Cloning, heterologous expression, and functional characterization of 5-*epi*-aristolochene-1,3-dihydroxylase from tobacco (*Nicotiana tabacum*). *Arch. Biochem. Biophys.* 393, 222–235. doi: 10.1006/abbi.2001.2483

Ranjan, A., Ichihashi, Y., Farhi, M., Zumstein, K., Townsley, B., David-Schwartz, R., et al. (2014). De novo assembly and characterization of the transcriptome of the parasitic weed dodder identifies genes associated with plant parasitism. *Plant Physiol.* 166, 1186–1199. doi: 10.1104/pp.113.234864

Robbins, N. E., Trontin, C., Duan, L., and Dinneny, J. R. (2014). Beyond the barrier: communication in the root through the endodermis. *Plant Physiol.* 166, 551–559. doi: 10.1104/pp.114.244871

Robinson, M. D., McCarthy, D. J., and Smyth, G. K. (2010). edgeR: a Bioconductor package for differential expression analysis of digital gene expression data. *Bioinformatics* 26, 139–140. doi: 10.1093/bioinformatics/btp616

Sato, K., Kadota, Y., Gan, P., Bino, T., Uehara, T., Yamaguchi, K., et al. (2018). High-Quality Genome Sequence of the Root-Knot Nematode *Meloidogyne arenaria* Genotype A2-O. *Genome Announc.* 6:26. doi: 10.1128/genomeA.00519-18

Sato, K., Kadota, Y., and Shirasu, K. (2019). Plant Immune Responses to Parasitic Nematodes. *Front. Plant Sci.* 10:1165. doi: 10.3389/fpls.2019.01165

Schulz, M. H., Zerbino, D. R., Vingron, M., and Birney, E. (2012). *Oases*: robust *de novo* RNA-seq assembly across the dynamic range of expression levels. *Bioinformatics* 28, 1086–1092. doi: 10.1093/bioinformatics/bts094

Shigeto, J., and Tsutsumi, Y. (2016). Diverse functions and reactions of class III peroxidases. *N. Phytol.* 209, 1395–1402. doi: 10.1111/nph.13738

Shukla, N., Yadav, R., Kaur, P., Rasmussen, S., Goel, S., Agarwal, M., et al. (2018). Transcriptome analysis of root-knot nematode (*Meloidogyne incognita*)-infected tomato (*Solanum lycopersicum*) roots reveals complex gene expression profiles and metabolic networks of both host and nematode during susceptible and resistance responses. *Mol. Plant Pathol.* 19, 615–633. doi: 10.1111/mpp.12547

Siddique, S., and Grundler, F. M. (2018). Parasitic nematodes manipulate plant development to establish feeding sites. *Curr. Opin. Microbiol.* 46, 102–108. doi: 10.1016/j.mib.2018.09.004

Sijmons, P. C., Grundler, F. M. W., von Mende, N., Burrows, P. R., and Wyss, U. (1991). *Arabidopsis thaliana* as a new model host for plant-parasitic nematodes. *Plant J.* 1, 245–254. doi: 10.1111/j.1365-313X.1991.00245.x

Simão, F. A., Waterhouse, R. M., Ioannidis, P., Kriventseva, E. V., and Zdobnov, E. M. (2015). BUSCO: assessing genome assembly and annotation completeness with single-copy orthologs. *Bioinformatics* 31, 3210–3212. doi: 10.1093/bioinformatics/btv351

Smant, G., Helder, J., and Goverse, A. (2018). Parallel adaptations and common host cell responses enabling feeding of obligate and facultative plant parasitic nematodes. *Plant J.* 93, 686–702. doi: 10.1111/tpj.13811

Soneson, C., Love, M. I., and Robinson, M. D. (2015). Differential analyses for RNA-seq: transcript-level estimates improve gene-level inferences. *F1000Res* 4:1521. doi: 10.12688/f1000research.7563.2

Song, N., Ma, L., Wang, W., Sun, H., Wang, L., Baldwin, I. T., et al. (2019). An ERF2-like transcription factor regulates production of the defense sesquiterpene capsidiol upon *Alternaria alternata* infection. *J. Exp. Bot.* 70, 5895–5908. doi: 10.1093/jxb/erz327

Stanford, A., Bevan, M., and Northcote, D. (1989). Differential expression within a family of novel wound-induced genes in potato. *Mol. Gen. Genet.* 215, 200–208. doi: 10.1007/BF00339718

Stoessl, A., Unwin, C. H., and Ward, E. W. B. (1972). Postinfectional inhibitors from plants I. Capsidiol, an antifungal compound from *Capsicum frutescens*. *J. Phytopathol.* 74, 141–152.

Sun, X. C., Gao, Y. F., Li, H. R., Yang, S. Z., and Liu, Y. S. (2015). Over-expression of *SlWRKY39* leads to enhanced resistance to multiple stress factors in tomato. *J. Plant Biol.* 58, 52–60. doi: 10.1007/s12374-014-0407-4

Takahashi, K., Shimada, T., Kondo, M., Tamai, A., Mori, M., Nishimura, M., et al. (2010). Ectopic expression of an esterase, which is a candidate for the

unidentified plant cutinase, causes cuticular defects in Arabidopsis thaliana. *Plant Cell Physiol.* 51, 123–131. doi: 10.1093/pcp/pcp173

Takahashi, S., Yeo, Y. S., Zhao, Y., O'Maille, P. E., Greenhagen, B. T., Noel, J. P., et al. (2007). Functional characterization of premnaspirodiene oxygenase, a cytochrome P450 catalyzing regio- and stereo-specific hydroxylations of diverse sesquiterpene substrates. *J. Biol. Chem.* 282, 31744–31754. doi: 10.1074/jbc.M703378200

Thomas, R., Fang, X., Ranathunge, K., Anderson, T. R., Peterson, C. A., and Bernards, M. A. (2007). Soybean root suberin: anatomical distribution, chemical composition, and relationship to partial resistance to *Phytophthora sojae*. *Plant Physiol.* 144, 299–311. doi: 10.1104/pp.106.091090

Tippett, J. T., and Hill, T. C. (1984). Role of periderm in resistance of *Eucalyptus marginata* roots against *Phytophthora cinnamomi*. *Eur. J. Pathol.* 14, 431–439.

Uehara, T., Tateishi, Y., Kadota, Y., and Iwahori, H. (2017). Differences in parasitism of *Meloidogyne incognita* and two genotypes of *M. arenaria* on. *J. Phytopathol.* 94, 575–579. doi: 10.1111/jph.12594

van der Vossen, E. A., van der Voort, J. N., Kanyuka, K., Bendahmane, A., Sandbrink, H., Baulcombe, D. C., et al. (2000). Homologues of a single resistance-gene cluster in potato confer resistance to distinct pathogens: a virus and a nematode. *Plant J.* 23, 567–576.

Vanholme, R., Demedts, B., Morreel, K., Ralph, J., and Boerjan, W. (2010). Lignin biosynthesis and structure. *Plant Physiol.* 153, 895–905. doi: 10.1104/pp.110.155119

Vanholme, R., Storme, V., Vanholme, B., Sundin, L., Christensen, J. H., Goeminne, G., et al. (2012). A systems biology view of responses to lignin biosynthesis perturbations in *Arabidopsis*. *Plant Cell* 24, 3506–3529. doi: 10.1105/tpc.112.102574

Veronico, P., Paciolla, C., Pomar, F., De Leonardis, S., Garcia-Ulloa, A., and Melillo, M. T. (2018). Changes in lignin biosynthesis and monomer composition in response to benzothiadiazole and root-knot nematode *Meloidogyne incognita* infection in tomato. *J. Plant Physiol.* 230, 40–50. doi: 10.1016/j.jplph.2018.07.013

Vishwanath, S. J., Delude, C., Domergue, F., and Rowland, O. (2015). Suberin: biosynthesis, regulation, and polymer assembly of a protective extracellular barrier. *Plant Cell Rep.* 34, 573–586. doi: 10.1007/s00299-014-1727-z

Vogeli, U., and Chappell, J. (1988). Induction of sesquiterpene cyclase and suppression of squalene synthetase activities in plant cell cultures treated with fungal elicitor. *Plant Physiol.* 88, 1291–1296. doi: 10.1104/pp.88.4.1291

Wang, J., Kucukoglu, M., Zhang, L., Chen, P., Decker, D., Nilsson, O., et al. (2013). The Arabidopsis LRR-RLK, *PXC1*, is a regulator of secondary wall formation correlated with the TDIF-PXY/TDR-WOX4 signaling pathway. *BMC Plant Biol.* 13:94. doi: 10.1186/1471-2229-13-94

Wang, X., and Culver, J. N. (2012). DNA binding specificity of ATAF2, a NAC domain transcription factor targeted for degradation by Tobacco mosaic virus. *BMC Plant Biol.* 12:157. doi: 10.1186/1471-2229-12-157

Ward, E. W. B., Unwin, C. H., and Stoessl, A. (1974). Postinfectional inhibitors from plants. XIII. Fungitoxicity of the phytoalexin, capsidiol, and related sesquiterpenes. *Can. J. Bot.* 52, 2481–2488. doi: 10.1139/b74-324

Wehrens, R., and Buydens, L. M. C. (2007). Self- and Super-organizing Maps in R: The kohonen Package. *J. Stat. Softw.* 21, 1–19. doi: 10.18637/jss.v021.i05

Wyss, U., and Zunke, U. (1986). Observations on the behavior of second stage juveniles of *Heterodera schachtii* inside host roots. *Rev. Nématol.* 9, 153–165.

Xie, Y., Wu, G., Tang, J., Luo, R., Patterson, J., Liu, S., et al. (2014). SOAPdenovo-Trans: *de novo* transcriptome assembly with short RNA-Seq reads. *Bioinformatics* 30, 1660–1666. doi: 10.1093/bioinformatics/btu077

Xing, X., Li, X., Zhang, M., Wang, Y., Liu, B., Xi, Q., et al. (2017). Transcriptome analysis of resistant and susceptible tobacco (*Nicotiana tabacum*) in response to root-knot nematode *Meloidogyne incognita* infection. *Biochem. Biophys. Res. Commun.* 482, 1114–1121. doi: 10.1016/j.bbrc.2016.11.167

Yamaguchi, H., Fukuoka, H., Arao, T., Ohyama, A., Nunome, T., Miyatake, K., et al. (2010). Gene expression analysis in cadmium-stressed roots of a low cadmium-accumulating solanaceous plant. *J. Exp. Bot.* 131, 423–437. doi: 10.1093/jxb/erp313

Yan, L., Zhai, Q., Wei, J., Li, S., Wang, B., Huang, T. (2013). Role of tomato lipoxygenase D in wound-induced jasmonate biosynthesis and plant immunity to insect herbivores. *PLoS Genet* 9:e1003964. doi: 10.1371/journal.pgen.1003964

Yang, X., Cheng, Y. F., Deng, C., Ma, Y., Wang, Z. W., Chen, X. H., et al. (2014). Comparative transcriptome analysis of eggplant (*Solanum melongena* L.) and turkey berry (*Solanum torvum*). *BMC Genomics* 15:412. doi: 10.1186/1471-2164-15-412

Ye, D. Y., Qi, Y. H., Cao, S. F., Wei, B. Q., and Zhang, H. S. (2017). Histopathology combined with transcriptome analyses reveals the mechanism of resistance to *Meloidogyne incognita* in *Cucumis metuliferus*. *J. Plant Physiol.* 212, 115–124. doi: 10.1016/j.jplph.2017.02.002

Zacheo, G., Bleve-Zacheo, T., and Melillo, M. T. (1997). "Biochemistry of Plant Defence Responses to Nematode Infection," in *Cellular and Molecular Aspects of Plant-Nematode Interactions. Developments in Plant Pathology*, Vol. 10, eds C. Fenoll, F. M. W. Grundler, and S. A. Ohl, (Dordrecht: Springer).

Zacheo, G., Orlando, C., and Bleve-Zacheo, T. (1993). Characterization of Anionic Peroxidases in Tomato Isolines Infected by Meloidogyne incognita. *J. Nematol.* 25, 249–256.

Zasada, I. A., Halbrendt, J. M., Kokalis-Burelle, N., LaMondia, J., McKenry, M. V., and Noling, J. W. (2010). Managing nematodes without methyl bromide. *Annu. Rev. Phytopathol.* 48, 311–328. doi: 10.1146/annurev-phyto-073009-114425

Zerbino, D. R., and Birney, E. (2008). Velvet: algorithms for de novo short read assembly using de Bruijn graphs. *Genome Res.* 18, 821–829. doi: 10.1101/gr.074492.107

Zhang, H., Kjemtrup-Lovelace, S., Li, C., Luo, Y., Chen, L. P., and Song, B. H. (2017). Comparative RNA-Seq Analysis Uncovers a Complex Regulatory Network for Soybean Cyst Nematode Resistance in Wild Soybean (*Glycine soja*). *Sci. Rep.* 7:9699. doi: 10.1038/s41598-017-09945-0

Zhang, L., Lilley, C. J., Imren, M., Knox, J. P., and Urwin, P. E. (2017). The Complex Cell Wall Composition of Syncytia Induced by Plant Parasitic Cyst Nematodes Reflects Both Function and Host Plant. *Front. Plant Sci.* 8:1087. doi: 10.3389/fpls.2017.01087

Zhang, P. J., He, Y. C., Zhao, C., Ye, Z. H., and Yu, X. P. (2018). Jasmonic Acid-Dependent Defenses Play a Key Role in Defending Tomato Against *Bemisia tabaci* Nymphs, but Not Adults. *Front. Plant Sci.* 9:1065. doi: 10.3389/fpls.2018.01065

Zhou, J., Wang, J., Zheng, Z., Fan, B., Yu, J. Q., and Chen, Z. (2015). Characterization of the promoter and extended C-terminal domain of Arabidopsis WRKY33 and functional analysis of tomato WRKY33 homologues in plant stress responses. *J. Exp. Bot.* 66, 4567–4583. doi: 10.1093/jxb/erv221

Conflict of Interest: The authors declare that the research was conducted in the absence of any commercial or financial relationships that could be construed as a potential conflict of interest.

frontiers in Plant Science

ORIGINAL RESEARCH
published: 14 June 2021
doi: 10.3389/fpls.2021.675429

Transcriptomic and Histological Analysis of the Response of Susceptible and Resistant Cucumber to *Meloidogyne incognita* Infection Revealing Complex Resistance *via* Multiple Signaling Pathways

Xvzhen Li[1], Yinhui Sun[1], Yuting Yang[1], Xiaopei Yang[1], Wanyu Xue[1], Meiqian Wu[1], Panpan Chen[1], Yiqun Weng[2] and Shuxia Chen[1]**

[1] College of Horticulture, Northwest A&F University/Shaanxi Engineering Research Center for Vegetables, Yangling, China, [2] United States Department of Agriculture, Agriculture Research Service, Vegetable Crops Research Unit, Horticulture Department, University of Wisconsin, Madison, WI, United States

OPEN ACCESS

Edited by:
Claudia S. L. Vicente, University of Évora, Portugal

Reviewed by:
Joana M. S. Cardoso, University of Coimbra, Portugal
Tariq Mukhtar, Pir Mehr Ali Shah Arid Agriculture University, Pakistan

***Correspondence:**
Yiqun Weng
yiqun.weng@wisc.edu
Shuxia Chen
shuxiachen@nwsuaf.edu.cn

Specialty section:
This article was submitted to Plant Pathogen Interactions, a section of the journal Frontiers in Plant Science

Received: *03 March 2021*
Accepted: *18 May 2021*
Published: *14 June 2021*

Citation:
Li X, Sun Y, Yang Y, Yang X, Xue W, Wu M, Chen P, Weng Y and Chen S (2021) Transcriptomic and Histological Analysis of the Response of Susceptible and Resistant Cucumber to Meloidogyne incognita Infection Revealing Complex Resistance via Multiple Signaling Pathways. Front. Plant Sci. 12:675429. doi: 10.3389/fpls.2021.675429

The root-knot nematode (RKN), *Meloidogyne incognita*, is a devastating pathogen for cucumber (*Cucumis sativus* L.) specially in production under protected environments or continuous cropping. High level RKN resistance has been identified in African horned melon *Cucumis metuliferus* (CM). However, the resistance mechanism remains unclear. In this study, the comparative analysis on phenotypic and transcriptomic responses in the susceptible cucumber inbred line Q24 and the resistant CM, after *M. incognita* infection, was performed. The results showed that, in comparison with Q24, the CM was able to significantly reduce penetration numbers of second stage juveniles (J2), slow its development in the roots resulting in fewer galls and smaller giant cells suggesting the presence of host resistance in CM. Comparative transcriptomes analysis of Q24 and CM before and after *M. incognita* infection was conducted and differentially expressed genes (DEGs) associated with host resistance were identified in CM. Enrichment analyses revealed most enriched DEGs in Ca^{2+} signaling, salicylic acid (SA)/jamonate signaling (JA), as well as auxin (IAA) signaling pathways. In particular, in CM, DEGs in the Ca^{2+} signaling pathway such as those for the calmodulin and calcium-binding proteins were upregulated at the early stage of *M. incognita* infection; genes for SA/JA synthesis/signal transduction were markedly activated, whereas the IAA signaling pathway genes were inhibited upon infection suggesting the importance of SA/JA signaling pathways in mediating *M. incognita* resistance in CM. A model was established to explain the different molecular mechanisms on *M. incognita* susceptibility in cucumber and resistance to *M. incognita* infection in CM.

Keywords: cucumber, transcriptome analysis, defense responses, *Cucumis sativus*, *Cucumis metuliferus*, *Meloidogyne incognita*

INTRODUCTION

The root-knot nematode (RKN), *Meloidogyne incognita*, is among the most destructive pathogens of many crop plants. Nematodes use a hollow protrusible stylet to break into the cells of host roots to induce highly specialized nematode feeding sites (NFS), withdraw nutrients, and inhibit the plant immune system (Abad and Williamson, 2010; Siddique and Grundler, 2018). A large number of galls are formed on the host roots, the nutrition balance in the host plant is disrupted resulting in significant yield reduction (Kayani et al., 2017). Globally, annual losses caused by the RKNs are estimated to be over $118 billion (Atkinson et al., 2012).

As a warm-season vegetable, cucumber (*Cucumis sativus* L.) is mainly cultivated in greenhouses or plastic tunnels in China. In recent years, RKN and other soil-borne diseases have become a serious constraint in cucumber production (Gine et al., 2014; Mao et al., 2016). Host resistance against *M. incognita* has been identified in some wild relatives in *Cucumis* like *C. metuliferus* Naud, *C. hystrix* Chakr, and *C. melo* var. *texanus* (Faske, 2013; Expósito et al., 2018; Cheng et al., 2019). Among them, upon infection of *M. incognita* on the resistant *C. metuliferus*, fewer J2 (second-stage juveniles) nematodes were able to penetrate in the roots, form smaller giant cells (GCs); the nematodes grow slower and produce fewer eggs than on susceptible plants (Faske, 2013; Ye et al., 2017).

The defense responses induced by plant-parasitic nematodes are associated with both pattern-triggered immunity (PTI) and effector-triggered immunity (ETI) (Teixeira et al., 2016). The tomato resistance gene *Mi-1.2* (*R* gene) is involved in PTI, which is associated with the nematode recognition and signal transduction pathway, and ETI is also related to defense responses and mitogen-activated protein kinase (*MAPK*) signaling cascades (Liu et al., 2016); the defense responses induced by nematodes are associated with Ca^{2+} signaling and *WRKY,* which both consists of positive regulators of plant defense transcriptional networks (Davies et al., 2015; Manosalva et al., 2015).

Researchers also believe that phytohormones might play an important role in the plant defense against nematode infection, such as salicylic acid (SA), jasmonic acid (JA), auxin (IAA) and the responsive signaling pathway (Gheysen and Mitchum, 2019). SA and JA pathway are activated when plants are infected by RKNs, leading to a hypersensitive response (HR) and systemic acquired resistance (SAR) (Nahar et al., 2011; Molinari et al., 2014). During the parasitic stage of RKN, the initiation and maturation of NFS are associated with the local accumulation of IAA (Siddique and Grundler, 2018). The expression network of defense-related genes functioning in nematode resistance currently includes IAA and cell cycle-related genes in cucumber (Wang et al., 2018), phenylpropanoid biosynthesis in cucumber (Ye et al., 2017), metabolite defense signaling pathways and hormones in tomato (Shukla et al., 2018), transcription factors and hormones in sweet potato (Lee et al., 2019), and defense-related genes in tobacco (Li et al., 2018). Therefore, the resistance mechanism of host to RKN involves in complex and multiple metabolic pathways.

While no cucumber cultivars with high resistance to root knot nematodes in China, the identification of host resistance in *C. metuliferus* presents us an opportunity to understand the phenotypic and molecular mechanisms of host resistance against this pest. Thus, in this study, we conducted microscopic and histological investigation in the susceptible cucumber inbred line Q24 and a resistant CM upon *M. incognita* infection. We also conducted transcriptome profiling in the two lines before and after infection, and identified differentially expressed genes (DEGs) and defense responsive pathways associated with host resistance.

MATERIALS AND METHODS

Plant Materials and *M. incognita* Inoculum Preparation

The cultivated cucumber inbred line Q24 (Chinese Long, north China fresh market type) and an inbred of cucumber wild relative, *Cucumis metuliferus* (CM) were used in this study. CM was a derivative of PI 482443 through self-pollination for at least three generations. The germinated seeds were sown in 8 × 8 cm plastic pots with autoclaved sands. All pots were arranged in an illumination incubator (RXZ-5COB-LED, Ningbo, Zhejiang, China) under conditions of 26°C, 14 h-light/18°C, 10 h-dark, and RH 85–90%. The seedlings were watered with 1/2 Hoagland's nutrient solution twice weekly.

M. incognita were maintained on the susceptible tomato cultivar "Dongfen No. 3" in a glasshouse at 22–26°C. The roots of plants were cut and sterilized with 0.5% NaOCl, and then rinsed with distilled water (dH_2O). The eggs were collected using a 25-μm sieve and kept for hatching in double layered paper tissues in a Petri dish with dH_2O at 28°C for 24 h (Fudali et al., 2013). J2s were re-suspended in dH_2O, and the concentration was adjusted to 1,000 J2's per mL for inoculation.

Comparative Analysis of *M. incognita* Development in Resistant and Susceptible Lines

Q24 and CM seedlings with two fully expanded true leaves were inoculated by dropping 1 mL J2s suspension into a 2 cm deep hole that was 1 cm away from the seedling. The control plants were watered with 1 mL dH_2O.

The roots at 3 days post inoculation (dpi) were isolated from Q24, CM and stained with acid fuchsin according to Zhang et al. (2017) to count the number of J2s under a stereoscopic fluorescence microscope (MZ10F-Leica, Germany). For the developmental stages of the *M. incognita* within the galls were observed at 25 dpi, the numbers of nematodes at J3, J4, female and male were recorded in the roots of CM Q24 and CM. For each sample, there were four biological replicates (3 seedlings per replicates) and three technical replicates.

The number of galls on roots was counted at 25 dpi. The galls were also photographed using a stereoscopic fluorescence microscope (MZ10F-Leica, Germany) to measure the gall size under the microscope using the SPOT software

(SPOT Imaging, United States). Twenty-four seedlings were used for every biological replicate, and the experiment was repeated in three times.

To observe the cellular changes induced by *M. incognita* infection, paraffin sections of Q24 and CM roots were prepared according to Wang et al. (2018). Root samples at both 3 and 15 dpi were fixed in FAA, transferred into a graded ethanol series (10–100%) and chloroform series (10–100%), and followed by embedding in paraffin. The samples were cut into 8-μm-thick sections, stained with hematoxylin eosin, sealed with gum, and observed under a fully automatic upright fluorescence microscope (OLYMPUS BX63).

Expression Analysis by qRT-PCR

The expression patterns of 4 genes related to hormone metabolism were analysis with quantitative real-time PCR (qPCR). The qPCR primers of the four genes are provided in **Supplementary Table 1**. Total RNAs were extracted from the roots of Q24 and CM at 2, 3, 4, 5 dpi using the RNA plus kit (TaKaRa Biotechnology, Dalian, China). cDNA synthesis was performed with the RevertAid First Strand cDNA Synthesis Kit (Roche Diagnostics, Indianapolis, United States). qPCR was performed with SYBR green (TaKaRa Biotechnology, Dalian, China) on a QuantStudio5 real time-PCR machine (Life Technologies, United States). Expression values were normalized to the *CsUBQ5* (Csa2G301530) gene. Reactions were carried out using two biological, and three technical replicates for each sample.

Transcriptome Profiling and Enrichment Analysis

For RNA-Seq, roots of *M. incognita*-inoculated (T, 3 dpi) and control (CK) plants of Q24 and CM were selected and collected, gently washed, flash frozen in liquid nitrogen and stored at −80°C. The roots of three plants were used as one replicate and three replicates are included (total 12 samples). Total RNA isolation, cDNA synthesis/library construction, and sequencing were all conducted through commercial service at the Novogene Inc. (Beijing, China). The cDNA samples were further enriched by PCR to construct the final cDNA libraries that were sequenced using the Hiseq 2500 (150 bp paired-ends) sequencing platform.

High quality, clean reads were aligned to the 9930 cucumber reference genome (v2.0)[1] using HISAT2 (v2.0.5). Differentially expressed genes (DEGs) in CM-T, CM-CK, Q24-T, and Q24-CK pairs were identified using the DESeq2 R package (1.16.1). A DEG in a particular comparison was defined as the adjusted $P < 0.05$ and|log2FoldChange|>0.0. All DEGs were subjected to enrichment analysis including Gene Ontology (GO) and Kyoto Encyclopedia of Genes and Genomes (KEGG), which were conducted in the ClusterProfiler R package (V.3.4.4). Additional analysis was performed for DEGs involving in plant-pathogen interactions (PPI), hormone signaling, and signal transduction in host defense responses. RNA-seq raw data are available under the website of NCBI[2] with the Bioproject ID PRJNA707668.

[1]http://cucurbitgenomics.org/organism/2/

[2]https://www.ncbi.nlm.nih.gov/

Statistical Analysis of Data

All numerical data collected from this study were subjected to statistical analysis and significance tests. Specifically, physiological data measured upon nematode infection were analyzed by one-way analysis of variance (ANOVA), and statistical significance was determined by pairwise comparisons ($P < 0.05$), which was implemented in SPSS 22.0 (Statistical Package for the Social Sciences, Chicago, IL, United States). The expression patterns of DEGs were showed the value of the log2FoldChange and presented as a heat map by using MeV software (MultiExperiment Viewer 4.7.4).

RESULTS

Comparison of Symptom and Gall Development in the Roots of Q24 and CM in Response to *M. incognita* Inoculation

The galls formed on the roots of the susceptible Q24 and resistant CM were counted and measured. In the susceptible Q24, there were significantly more and larger galls that were observed throughout the root system than in CM, where the small galls were clustered mainly on some lateral roots (**Figure 1A**). At 25 dpi, on average, 63 and 17 galls on roots of Q24 and CM, which were 1.73 and 1.03 mm in size, respectively (**Figure 1B**).

The microscopic root structures in the two lines were comparing by histological examination before and after *M. incognita* infection. In roots of control, there were no visible differences in root tip cell structure between Q24 and CM; the root crown was intact with regular arrangement of root tip cells. At 3 dpi, loose cells and void tissue in the apical meristem zone of Q24 were observed, whereas those in CM remained compact (**Figure 1C**). At 15 dpi, much larger GCs and more nuclei in GCs were observed in Q24 roots than that in CM, and GCs connected with parenchyma cells were observed in Q24, which may facilitate supply of nutrients to GCs from the surrounding parenchyma cells. In contrast, fewer GCs were observed in CM; there were also few nuclei in the GCs. Hollow cells around the GCs in the roots of CM were observed, which separated GCs from parenchymal cells. This may result in difficulty for GCs to obtain nutrients from the surrounding parenchyma cells (**Figure 1D**). The GC size in CM was significantly smaller than that in Q24 (**Figure 1B**). Taken together, these results suggested host resistance in CM plant plays an important role in reducing the severity of symptom development although the CM plant is not immune to *M. incognita infection.*

Number Invasion and Development Difference of *M. incognita* in Roots of Resistant and Susceptible Plants

The number and development of nematodes were compared in the roots of CM and Q24. The significant difference in nematode invasion was observed between Q24 and CM at 3 dpi, on average, 36 and 10 J2s, respectively. The J2s invaded into the roots of CM was hindered to some extent. In Q24 at 25 dpi, after J2s invasion, 33.6% of J2s developed to adult females and 11.9% developed

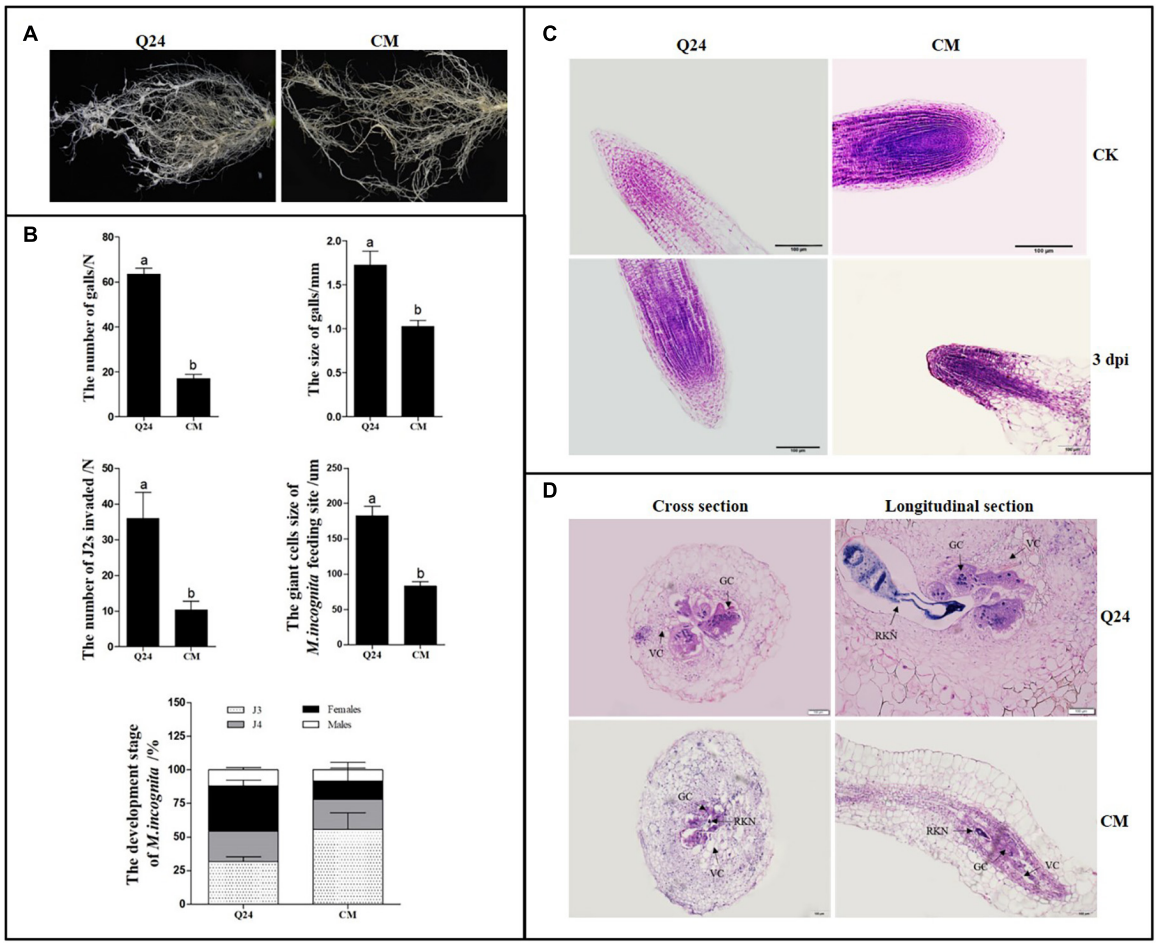

FIGURE 1 | Symptom development and growth on susceptible Q24 and resistant CM plants. **(A)** The roots of Q24 and CM at 25 dpi; **(B)** comparison of disease indexes of Q24 and CM at 25 dpi. Error bars indicate the standard error of the means. Different letters on the bars "a, b, c" indicate statistically significant means between Q24 and CM at 25 dpi at $P < 0.05$ based on Duncan's *t*-tests; **(C)** root tips of Q24 and CM at 3 dpi and the corresponding controls; **(D)** cross and longitudinal sections of nematode feeding sites (NFS) inside the galls at 15 dpi. GC, giant cell; VC, vacant cell; V, vacuole.

to adult males. The J2s development in CM roots was obviously different from J2s in roots of Q24, which were only 13.7% females and 8.4% males at 25 dpi. The development of most J2s in CM was blocked to J3 and J4 stages. These observations indicated that, few J2s were able to penetrate into roots of CM at the stage of infection and J2s were developing poorly in roots of CM at the parasitic stage (**Figure 1B**).

Relative Expression of Selected Genes Related to Defense Response and Hormone Metabolism

In order to determine the expression time of genes induced by *M. incognita* infection, the expression patterns of several genes were validated in the roots of Q24 and CM at 2, 3, 4, 5 dpi. Among them, *MAPK9* (Csa2G361890) was known to be involved in plant-pathogen interaction, phenylalanine ammonia-lyase genes (*PAL*, Csa6G445760), *bZIP* transcription factor *TGA7* (Csa2G403160) were related to SA and indole-3-acetic acid-amido synthetase GH3 (*GH3.6*, Csa6G125240) were related to IAA. It showed that *MAPK9*, *TGA7* was significantly downregulated after *M. incognita* infection and *GH3.6* and *PAL* were upregulated significantly at 3 dpi in Q24. In CM after infection, the *TGA7*, *PAL* were significantly upregulated at 3 dpi and then *TGA7* downregulated at 4, 5 dpi. The *MAPK9* was significantly downregulated at 3 dpi and gradually return to expression at 5 dpi. The expression of *GH3.6* in CM was low and changed little after *M. incognita* infection (**Supplementary Figure 1**).

Transcriptional Sequencing of Cucumber Plants in Response to *M. incognita*

Based on the expression pattern of genes selected in qPCR in Q24 and CM after infection, 3 dpi and the CK were selected for transcriptome analysis. Approximately 47.47–67.57 million 150 bp paired-end clean reads per sample were obtained after cleaning and checking. Approximately 97% of clean reads were aligned uniquely to the cucumber genome using the software

HISAT2 v2.0.5 (**Supplementary Table 2**). The correlation clustering among the three biological replicates of each sample was conducted based on the expression level of all genes. All biological replicates showed correlation coefficients above 0.9 indicating good reproducibility between biological replicates (**Supplementary Figure 2**).

Differential Gene Expression Analysis and Functional Categorization

A total of 17,612 and 17,966 genes were identified by the DESeq2 R package among inoculated samples compared with respective non-inoculated controls of Q24 and CM, respectively (false discovery rate < 0.03, DESeq2 padj < 0.05 and | log2FoldChange| > 0.0). There were 4,556 significantly differentially expressed genes (DEGs) between Q24 and the control, and 5,258 DEGs were identified between CM and the control. From these, there were 1,586 DEGs identified in both genotypes (**Figure 2A**). Among the identified DEGs, 2,386 DEGs and 2,700 DEGs were significantly upregulated in Q24 and CM, respectively, and 793 were upregulated in both genotypes (**Figure 2B**). There were 2,170 DEGs significantly downregulated in Q24 and 2,558 DEGs significantly downregulated in CM. 365 DEGs were downregulated in both Q24 and CM after *M. incognita* infection (**Figure 2C**). Among these DEGs, *MAPK9* (Csa2G361890), *PAL* (Csa6G445760), *TGA7* (Csa2G403160), and *GH3.6* (Csa6G125240) were all identified among inoculated samples compared with respective controls of Q24 and CM. The expression of these four genes in transcriptomic were in accordance with the results of qRT-PCR (**Supplementary Figure 3**).

Based on GO enrichment analysis, the categories of total DEGs were enriched significantly in biological terms in both phenotypes in response to *M. incognita* (adjusted $P < 0.05$). In comparison of 3 dpi with the control of Q24, GO biological enriched significantly in the categories of response to stimulus and signaling, secondary metabolites metabolic processes and biosynthetic processes, protein related with cell wall and membrane synthesis process, transcription factor activity, reduction and scavenging of reactive oxygen species (ROS) products, and more genes showing upregulation than downregulation in these terms (**Figure 2D**). In resistant plants of CM, more GO biological terms were enriched than that in Q24, including translation process, organonitrogen compound metabolic process, peptide biosynthetic process and metabolic process, transmembrane transport, transporter activity and so on. Comparing the DEGs in each biological term, more DEGs were identified in CM than that in Q24, and most of them were downregulated in each term, all of them indicating that a large number of genes played a vital role in CM responding to *M. incognita* (**Figure 2E**).

On the basis of the KEGG Pathway database, the DEGs enrichment were analyzed using clusterProfiler R package to identify the metabolic pathways in which they function

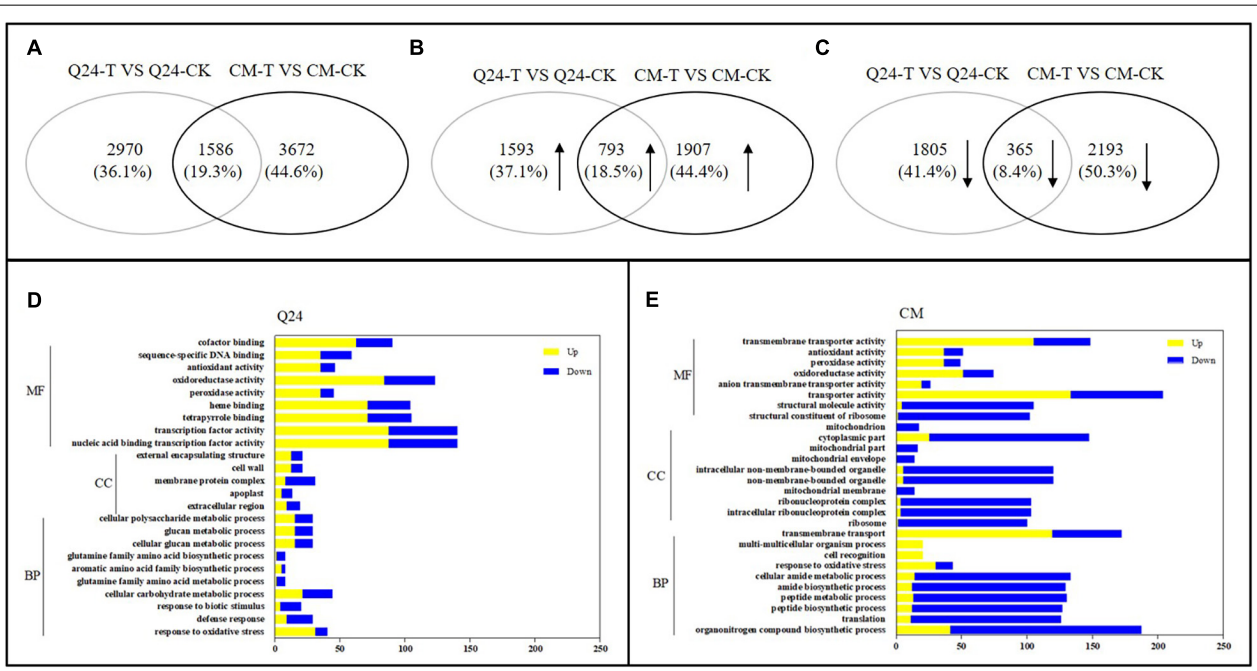

FIGURE 2 | The number of differentially expressed genes (DEGs) and Gene Ontology (GO) enrichment analysis in responding to the infection of *M. incognita* in Q24, CM. **(A)** All DEGs mapped in Q24 and CM (adjusted $P < 0.05$); **(B)** the upregulated DEGs mapped in Q24 and CM (adjusted $P < 0.05$); **(C)** the downregulated DEGs mapped in Q24 and CM (adjusted $P < 0.05$). The percentage in **(A–C)** was the number of DEGs related to the total of identified DEGs in all DEGs, in all upregulated DEGs or in all downregulated DEGs in Q24, CM; **(D)** GO terms of DEGs in Q24; **(E)** GO terms of DEGs in CM. Yellow indicated upregulation and blue indicated downregulation. DEGs were classified into specific biological process categories with high classification stringency (adjusted $P < 0.05$). The horizontal ordinate represents the number of genes in the category. MF, molecular function; CC, cellular component; BP, biological process.

(adjusted $P < 0.05$). In comparison of infection with the control of Q24, the enrichment of upregulated biological process was involving PPI, phenylpropanoid biosynthesis, MAPK signaling pathway and protein processing in endoplasmic reticulum. Furthermore, a small part of genes was enriched in downregulated process including photosynthesis, nitrogen metabolism and carbon fixation in photosynthetic organisms (**Figure 3A**). Comparing with the biological process of Q24 enrichment, more biological process and more DEGs were involved in the response of resistant plant CM to *M. incognita*, such as upregulated biological process MAPK signaling pathway, PPI, Carbon metabolism, Biosynthesis of amino acids and downregulated process Ribosome (**Figure 3B**). The difference in metabolic pathways between Q24 and CM indicated that the mechanisms were different in two genotypes facing to *M. incognita* infection.

Most researchers believed that genes related to nematode recognition and phytohormones metabolism might play an important role in the plant defense against RKN infection. So multiple DEGs were related to PPI, MAPK signaling cascades, hormone biosynthesis and signal transduction were analysis in this study. The number of DEGs related to PPI was greatest between the treatment and its control; 35 DEGs were identified in Q24, and 40 were identified in CM. The second largest number of DEGs were related to MAPK signaling cascades, which was consisting of 21 DEGs in Q24 and 33 in CM (**Figure 3C**). Between the two genotypes and their controls, more than half of the DEGs related to PPI, MAPK signaling cascades, JA pathway were upregulated, while most of the DEGs related to IAA were downregulated. DEGs related to MAPK signaling cascades and SA showed a significant difference between the two genotypes and their controls. Most DEGs related to SA were downregulated in Q24 and upregulated in CM (**Figures 3D,E**).

Differentially Expressed Genes Related to Ca^{2+} and MAPK Signaling

Some DEGs were involved in the plant defense were identified in the cucumber plant after *M. incognita* infection (**Figure 4A**). Most of them were involved in the Ca^{2+} and MAPK signaling pathways and were significantly upregulated at the early stage of *M. incognita* infection, and there was a notable difference between Q24 and CM. The calcium-binding protein genes (*CML*, Csa5G067670, Csa4G639730, Csa3G823060), calmodulin gene (*CaM*, Csa3G727960), *MAPK* (Csa1G479630), serine/threonine protein kinase (*OXI1*), respiratory burst oxidase (*Rboh*) were

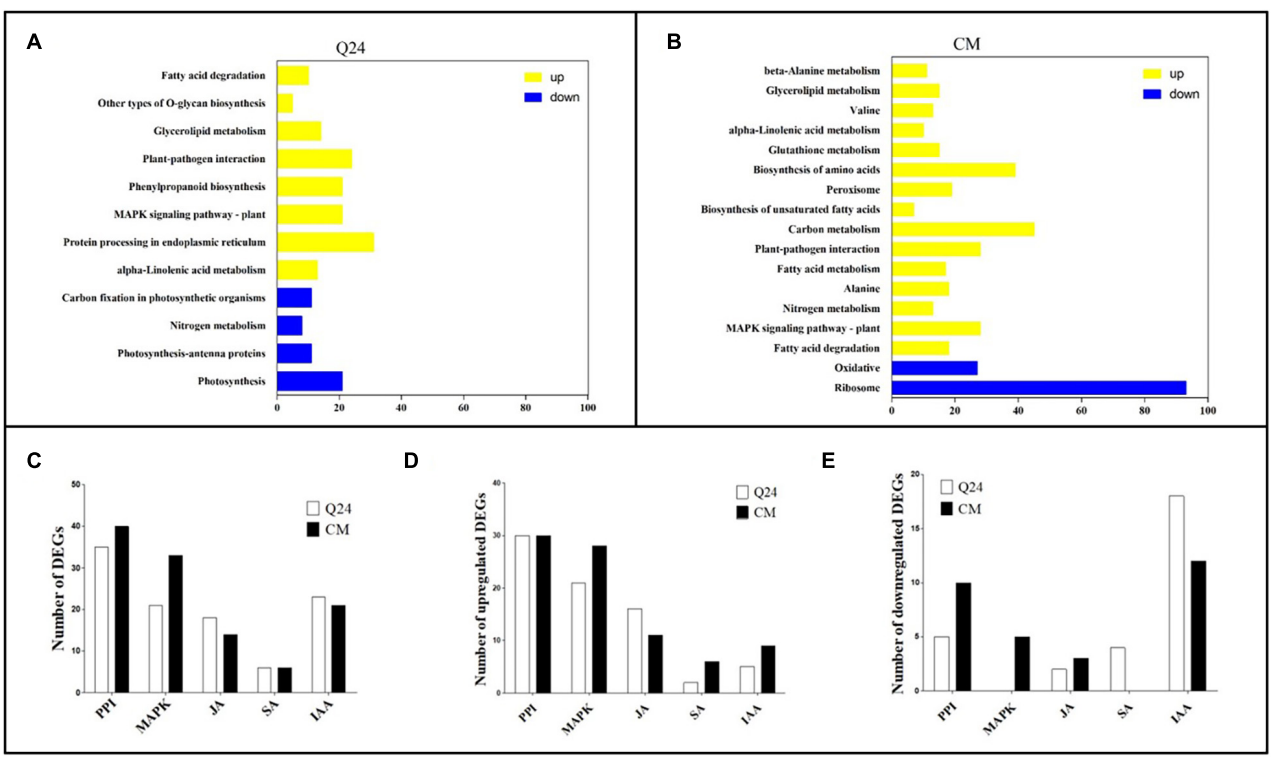

FIGURE 3 | Kyoto Encyclopedia of Genes and Genomes (KEGG) enrichment analysis in responding to the *M. incognita* infection of Q24, CM. DEGs were classified into pathway categories with high classification stringency (adjusted $P < 0.05$). The horizontal ordinate represents the number of genes in the category. **(A)** KEGG terms of DEGs in Q24; **(B)** KEGG terms of DEGs in CM. Yellow indicated upregulation and blue indicated downregulation; **(C)** the DEGs mapped to hormone metabolism and plant pathogen interactions of Q24 and CM responding to infection (adjusted $P < 0.05$); **(D)** the number of upregulated DEGs and downregulated DEGs mapped to hormone metabolism and plant pathogen interactions of Q24 (adjusted $P < 0.05$); **(E)** the upregulated DEGs and downregulated DEGs mapped to hormone metabolism and plant pathogen interactions of CM (adjusted $P < 0.05$). PPI, plant-pathogen interactions; MAPK, mitogen-activated protein kinase signaling cascades.

identified clearly upregulated in Q24, which indicating that the defense response of Q24 to *M. incognita* mainly referred to signal transduction upon CaM/CML, later the activation of defense response genes and the outbreak of ROS. While the defense response of CM to *M. incognita* referred to signal transduction upon pathogen perception through not only CaM/CML, but also cyclic nucleotide gated channel (CNGCs)/calcium-dependent protein kinase (CDPK), such as *CNGC* (Csa3G835850, Csa5G638350) and *CDPK* (Csa6g052030) were upregulated in CM. Additionally, more genes involved in the defense response genes, HR and cell wall reinforcement were also induced in CM than in Q24, such as WRKY transcription factor 23 (*WRKY23*, Csa3G121580), chitin elicitor receptor kinase 1(*CERK1*, Csa7G041930), Serine/threonine-protein kinase (*PBS1*, Csa6G092530), SGT1 suppressor of G2 allele of SKP1(*SGT1*, Csa3G184080). All of them indicated that the activation of defense response genes, HR, cell wall reinforcement, ROS and programmed cell death in CM were induced after *M. incognita* infection (**Figure 4B**).

Differentially Expressed Genes Related to the SA Biosynthesis and Signaling Pathway

Three gene families associated with the SA pathway were identified both in Q24 and CM in response to *M. incognita* infection (**Figure 5A**), including *PAL*, regulatory protein gene NPR (*NPR1-1*), and bZIP transcription factor (*bZIP/TGA*).

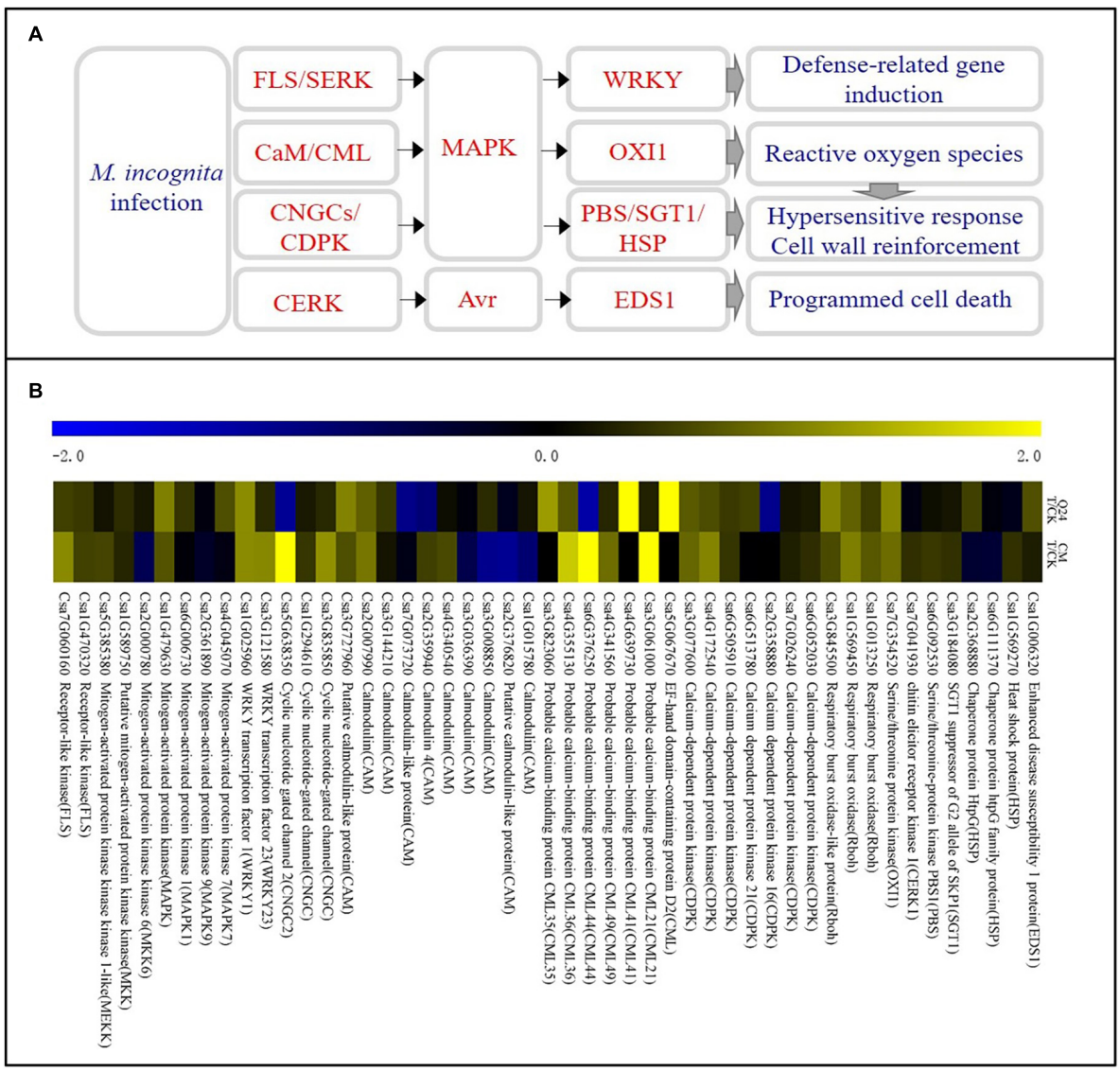

FIGURE 4 | Ca^{2+} signaling pathway and heat map of differentially expressed genes in Q24 and CM responding to infection. **(A)** All differentially expressed genes mapped to Ca^{2+} signaling of Q24 and CM responding to infection; **(B)** the heat map showed the value of the log2FoldChange of genes compared with that of the control in plant defense in Q24 and CM. Yellow indicated up expression and blue indicated down expression.

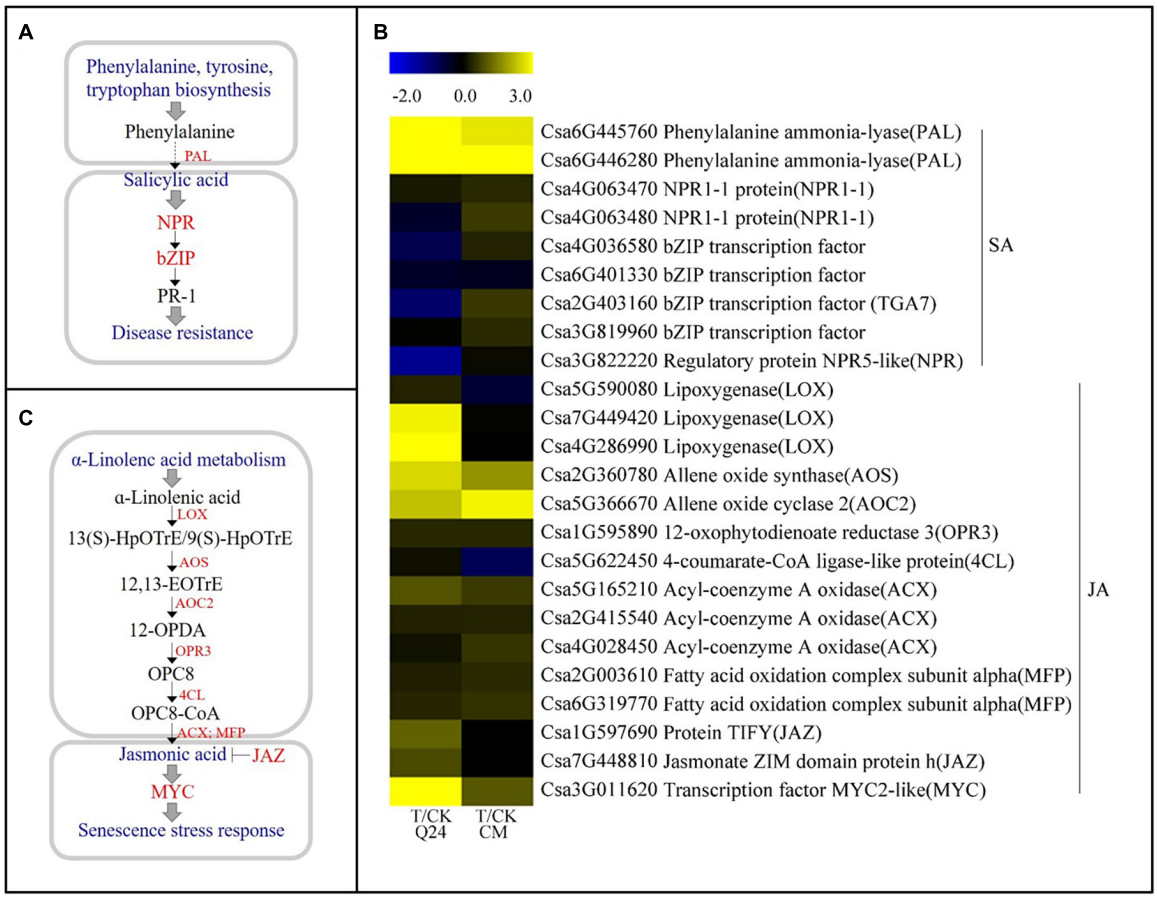

FIGURE 5 | SA and JA biosynthesis and signal transduction pathways and heat map of differentially expressed genes in Q24 and CM responding to infection. **(A)** SA biosynthesis and signal transduction; **(B)** JA biosynthesis and signal transduction; **(C)** the heat map showed the value of the log2FoldChange of genes compared with that of the control in SA and JA pathway in Q24 and CM. Yellow indicated up expression and blue indicated down expression.

The *PAL* genes (Csa6G445760, Csa6G446280), which encode a critical enzyme in the SA biosynthesis pathway, were significantly upregulated both in Q24 and CM. On the other hand, the *NPR1-1* (Csa4G063470), which is a key regulator of the SA signaling pathway, and the bZIP transcription factors (Csa4G036580, Csa2G403160, Csa3G819960) were not induced or significantly downregulated in Q24 and they were highly induced in CM after infection (**Figure 5B**). The SA biosynthesis and signaling pathways were markedly activated in CM.

Differentially Expressed Genes Related to the JA Biosynthesis and Signaling Pathway

Some molecules associated with the JA biosynthesis and signaling pathway were identified after *M. incognita* infection (**Figure 5C**). Most genes upstream of JA biosynthesis were highly induced after infection, particularly in Q24, such as the lipoxygenase gene (*LOX*, Csa7G449420, Csa4G286990), allene oxide synthase (*AOS*, Csa2G360780), and allene oxide cyclase 2 (*AOC2*, Csa5G366670). While some key genes participated in both JA biosynthesis and JA-dependent SAR, maintaining a low level of expression in Q24 and induction in CM during *M. incognita* infection, such as the acyl-coenzyme a oxidase *(ACX*, Csa4G028450) encoding key enzymes for acyl-CoA oxidase, and the fatty acid oxidation complex subunit alpha genes (*MFP*, Csa2G003610, Csa6G319770) encoding a multifunctional protein in JA biosynthesis. Additionally, the negative regulatory factors in the JA signaling pathway, *JAZs* (Csa1G597690, Csa7G448810), were significantly induced in Q24 and not changed in CM at 3 dpi (**Figure 5B**).

Differentially Expressed Genes Related to the IAA Biosynthesis and Signaling Pathway

IAA has been reported to be involved in the formation of GCs. In this study, IAA-related DEGs showed significant differences between Q24 and CM (**Figure 6A**). Many major auxin-related genes were significantly downregulated in CM at 3 dpi, including the indole-3-pyruvate monooxygenase (*YUCCA*, Csa2G379350, Csa3G133910), auxin signaling F-box 2 (*TIR,* Csa7G393970),

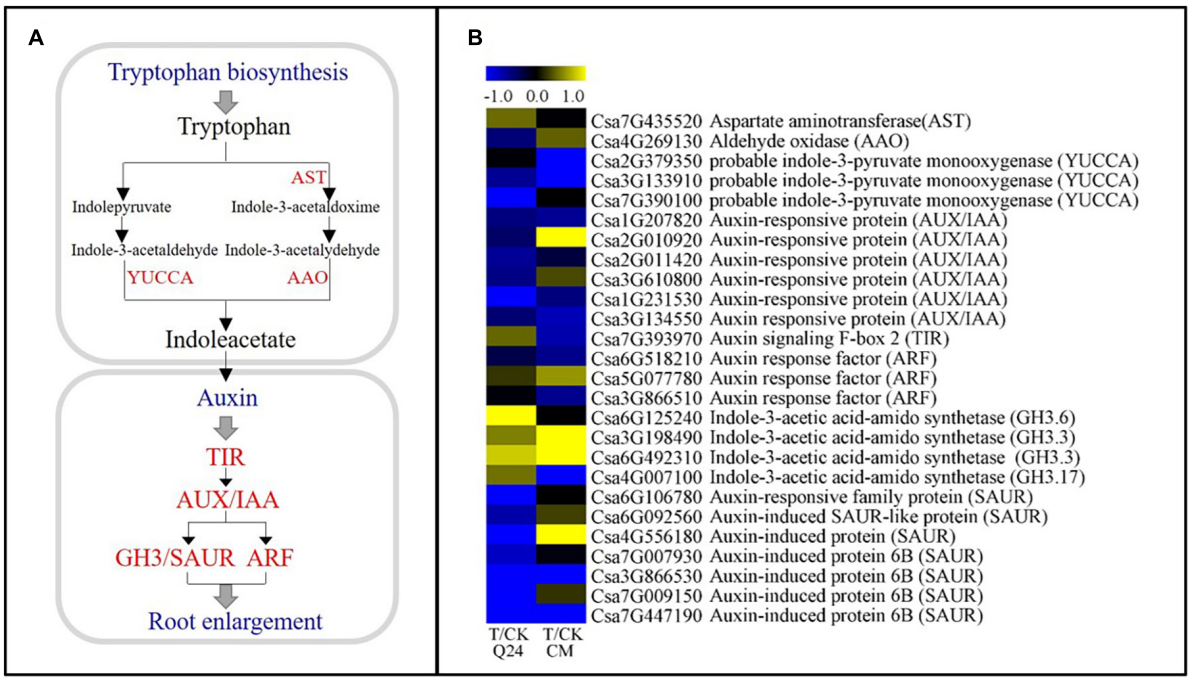

FIGURE 6 | IAA biosynthesis and signal transduction pathways and heat map of differentially expressed genes in Q24 and CM. **(A)** IAA biosynthesis and signal transduction pathway; **(B)** the heat map showed the value of the log2FoldChange of genes compared with that of the control in IAA pathway. Yellow indicated up expression and blue indicated down expression.

auxin response factor (*ARF,* Csa6G518210, Csa3G866510), *GH3* (*GH.3.17*, Csa4G007100), which were the key gene in the TAA-YUC pathway of auxin biosynthesis and auxin signaling pathways. While the genes of *TIR* (Csa7G393970) and *GH3* (Csa6G125240, Csa3G198490, Csa6G492310, Csa4G007100) were upregulation in Q24 after nematode infection, indicating that the IAA signal was transduced and affected the GC formation in Q24. Several genes related to IAA signal transduction were also found upregulated in CM, such as auxin-responsive protein genes *AUX/IAA* (Csa2G0010920) and *GH3* (Csa3G198490, Csa6G492310), auxin-induced protein gene (*SAUR,* Csa2G010920), which indicated that the invasive J2s interfered with signal transmission in the NFS of CM (**Figure 6B**). These results indicated that auxin biosynthesis and signaling pathways were inhibited more strongly in CM than in Q24.

DISCUSSION

The Plant Defense Response Was Activated by *M. incognita* Infection Upon Ca^{2+} Signaling

Ca^{2+}/calmodulin has long been considered a crucial component in the mediating plant defense against various biotic attackers, and cellular Ca^{2+} fluxes are among the earliest detectable biochemical features upon pathogen recognition (Reddy et al., 2011). It was proved that Ca^{2+} signaling is then triggered and translated by CaM, CMLs, calcineurin-like proteins (CBLs), and CDPKs in order to interact with effector proteins of plant-parasitic nematodes (Perochon et al., 2011; Haegeman et al., 2012). Ca^{2+} signaling mediators that also induced PTI, ETI and participated in SA- or JA-mediated long-term resistance to pathogens. In addition, the sequential activation of the MAPK cascade eventually leads to activation of the expression of specific genes and, subsequently, the induction of HR, ROS, cell wall reinforcement and defense-related gene expression (Bigeard et al., 2015). Other studies have shown that the resistance of gene $R_{Mc1(blb)}$ in potato to *Meloidogyne chitwoodi* were dependent on a hypersensitive response and involves calcium, indicating that Ca^{2+} plays a role in the $R_{Mc1(blb)}$-mediated resistance against *M. chitwoodi* in potato (Davies et al., 2015). Calcium/calmodulin-mediated signaling might coordinate various regulatory pathways in response to *Heterodera glycine* infection in soybeans (Zhang et al., 2017). We speculate that Ca^{2+} mediated regulation might function as a dispatcher between MAPK cascade, PTI, ETI, SA-, and JA-mediated resistance to response to *M. incognita* infection. Therefore, the differences in DEGs of Ca^{2+} signals between Q24 and CM may mediate different regulatory pathways to respond to *M. incognita* infestation, which requires further research.

SA and JA Signal Pathway Activation Was Involved in the Basal Defense of CM Against *M. incognita* Infestation

At the early stage of J2 infection, chorismate mutase was secreted and suppressed plant immunity by regulating the

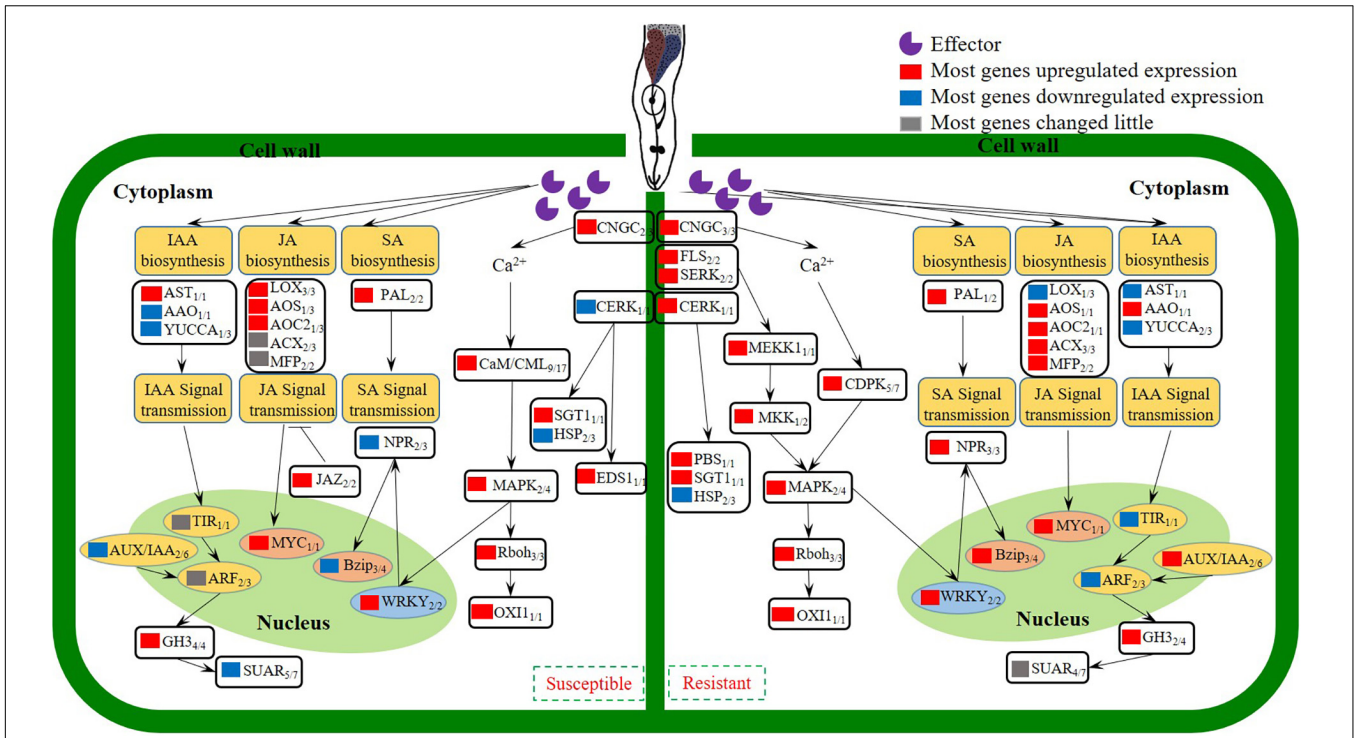

FIGURE 7 | Model depicting how the coordinated signaling network in cucumber leads to the induction of local and systemic defense against *M. incognita* invasion.

SA pathway (Wang et al., 2018). Studies have shown that increasing SA levels enhance the resistance of host plant against RKN infection (Priya et al., 2011). The bZIP transcription factor is a transcriptional co-activator of NPR1 in the transduction of SA, and loss-of-function studies have shown that class II TGA factors (bZIP transcription factor) in particular play important roles in SA-mediated gene expression. The tga2/tga5/tga6 triple mutant shows compromised PR-1 expression (Zhang et al., 2003), indicating that the SA transduction signal was activated in CM during the early infection stage. Therefore, we assumed that the basic defense mechanisms of CM were activated by the upregulated expression of *bZIP* and *NPR* related to SA signal transduction during *M. incognita* infection.

The functions of the genes in the JA metabolic pathway were more complex during the process of nematode infection. Many studies have shown that JA acts as a defense factor against nematode in plants (Nahar et al., 2011; Zhou et al., 2015), and overexpression of *OsAOS* in rice enhances resistance to *M. graminicola* (Mei et al., 2006). The *Arabidopsis* mutant *lox3-1*, *lox4-1*, and *aoc* are all more susceptible to RKN infection (Ozalvo et al., 2014; Naor et al., 2018). It has also been reported that JA-related genes in GCs are suppressed, as verified by transcriptome analyses (Ji et al., 2013). Our results showed that the expression of most genes related to JA biosynthesis were not significantly induced in the susceptible Q24 compared with the resistant CM. In addition, two alleles of *JAZ*, a negative regulator of the JA signaling pathway, were significantly induced in Q24 but suppressed in CM after *M. incognita* infection, indicating that JA played a positive role in the defense of the resistant germplasm against *M. incognita*.

Suppression of the Expression of Genes Related to IAA Limited the Development of GCs in CM

GCs formation is a key factor for a successful plant-nematode interaction after the nematode arrive into the cortical cylinder. If GCs appear as degenerated, the nematode development or reproduction will be suppressed (Expósito et al., 2018). Studies have shown that the GCs in feeding site of *C. metuliferus* were smaller and less voluminous, with fewer nuclei than susceptible plants and some of them were empty of cytoplasm along with a slow nematode development (Ye et al., 2017; Expósito et al., 2018, 2020). In our study, smaller galls and GCs and fewer nuclei in the GCs of CM than Q24 were observed, and the J2s development in CM roots was significantly slower in comparison to that in Q24, which was consistent with previous reports (Wang et al., 2018).

IAA is the key factor for NFS formation (Perrot-Rechenmann, 2010). The cell wall growth and cell cycle activation of GCs was promoted by IAA biosynthesis and response genes in the host cell after nematode infection (Hwang and Williamson, 2003). GH3, an auxin-responsive promoter, was rapidly and transiently activated during root gall initiation by *Meloidogyne* (Hutangura et al., 1999). Other studies showed that the nematode development was impaired in auxin insensitive mutants because of the arrest in early feeding cell formation

(Goverse et al., 2000; Gheysen and Mitchum, 2009). Moreover, the expression of most homologous genes of auxin-responsive promoter *GH3* were inhibited in the resistance material cucumber introgression line "IL10–1" (Wang et al., 2018). In the present study, fewer members of the *GH3* gene family were found upregulated in resistant CM than in susceptible Q24, which was consistent with previously published reports. In addition, the upregulation of *AUX/IAA*, the auxin/indole-3-acetic acid transcriptional repressor gene, and the downregulation of *TIR* in resistant CM after *M. incognita* infection, indicating that the IAA concentration was significantly lower in resistant CM than that in the control. Thus, we conjectured that the lack of auxin contributed greatly to the abnormal development of GCs in CM, which was consistent with the in resistant line "IL10–1" (Wang et al., 2018).

CONCLUSION

In conclusion, studies on an inbred of cucumber wild relative CM identified with *M. incognita* resistance, indicated that reducing J2s invasion, suppressing the development of J2s and the GCs of *M. incognita* were the resistance characteristics. Comparison of transcriptomes revealed that Ca^{2+} signaling, SA/JA genes were activated, which triggered an active defense response that leading to the resistance of CM against *M. incognita*. Transcriptomes also revealed that IAA genes were inhibited in CM, which caused the abnormal development of GCs, and finally resulted in the blocking of *M. incognita* development. According to our data, a model was established to probe the changes of gene expression involved in the biological processes of *M. incognita* recognition, signal transduction, hormone biosynthesis and signal transmission in different resistant species (**Figure 7**). A number of genes involved in the recognition and signaling of nematode infestation in CM were identified, thus providing a basis for research examining the interaction between cucumber plants and *M. incognita*.

DATA AVAILABILITY STATEMENT

The original contributions presented in the study are publicly available. This data can be found here: NCBI repository, accession: PRJNA707668.

AUTHOR CONTRIBUTIONS

SC designed the experiment and revised the manuscript. YW participated in the data analysis and preparation of the manuscript. XL performed the experiments and wrote the manuscript. YS conducted the RNA-Seq. YY performed the sampling for transcriptome analyze. XY carried out the qRT-PCR. WX, MW, and PC contributed to the reagents and materials. All authors have read and approved the final manuscript.

FUNDING

This work was supported by grants from the Key Research and Development Program of Shaanxi Province (2019ZDLNY03-02, 2021ZDLNY03-04), Commercialization of Scientific and Research Findings Program of Northwest A&F University (TGZX2020-20) and the Agricultural Sci-Tech and Innovation Achievements into the project in Shaanxi (NYKJ-2019-YL04).

SUPPLEMENTARY MATERIAL

The Supplementary Material for this article can be found online at: https://www.frontiersin.org/articles/10.3389/fpls.2021.675429/full#supplementary-material

Supplementary Figure 1 | Relative expression level of selected hormone metabolism related genes in roots of Q24 and CM at 2, 3, 4, 5 dpi by qPCR. *MAPK9*, mitogen-activated protein kinase 9; *PAL*, phenylalanine ammonia-lyase genes; *TGA7*, bZIP transcription factor; *GH3.6*, indole-3-acetic acid-amido synthetase GH3.6.

Supplementary Figure 2 | The heat map showing the correlation between all root samples of CM and Q24 at 3 dpi and the control. The color represents the correlation coefficient between every two samples. The deeper the color, the greater the correlation coefficient.

Supplementary Figure 3 | The FPKM of 4 genes related hormone metabolism in transcriptomic data. *MAPK9*, mitogen-activated protein kinase 9; *PAL*, phenylalanine ammonia-lyase genes; *TGA7*, bZIP transcription factor; *GH3.6*, indole-3-acetic acid-amido synthetase GH3.6.

Supplementary Table 1 | Primers used in this study.

Supplementary Table 2 | The statistics of RNA-seq sequencing data in this study. CM-ck, Q24-ck and CM-T, Q24-T represent the control and the treatment of CM and Q24. 1, 2, 3 represent three biological replicates.

REFERENCES

Abad, P., and Williamson, V. M. (2010). Plant nematode interaction: a sophisticated dialogue. *Adv. Bot. Res.* 53, 147–192. doi: 10.1016/S0065-2296(10)53005-2

Atkinson, H. J., Lilley, C. J., and Urwin, P. E. (2012). Strategies for transgenic nematode control in developed and developing world crops. *Curr. Opin. Biotechnol.* 23, 251–256. doi: 10.1016/j.copbio.2011.09.004

Bigeard, J., Colcombet, J., and Hirt, H. (2015). Signaling mechanisms in pattern-triggered immunity (PTI). *Mol. Plant.* 8, 521–539. doi: 10.1016/j.molp.2014.12.022

Cheng, C., Wang, X., Liu, X., Yang, S., Yu, X., Qian, C., et al. (2019). Candidate genes underlying the quantitative trait loci for root-knot nematode resistance in a *Cucumis hystrix* introgression line of cucumber based on population sequencing. *J. Plant Res.* 132, 813–823. doi: 10.1007/s10265-019-01147-1

Davies, L. J., Brown, C. R., and Elling, A. A. (2015). Calcium is involved in the $R_{Mc1(blb)}$-mediated hypersensitive response against *Meloidogyne chitwoodi* in potato. *Plant Cell Rep.* 34, 167–177. doi: 10.1007/s00299-014-1697-1

Expósito, A., Munera, M., Giné, A., López-Gómez, M., Cáceres, A., Picó, B., et al. (2018). *Cucumis metuliferus* is resistant to root-knot nematode *Mi1.2* gene (a) virulent isolates and a promising melon rootstock. *Plant Pathol.* 67, 1161–1167. doi: 10.1111/ppa.12815

Expósito, A., Pujolà, M., Achaerandio, I., Giné, A., Escudero, N., Fullana Aïda, M., et al. (2020). Tomato and melon *Meloidogyne* resistant rootstocks improve crop yield but melon fruit quality is influenced by the cropping season. *Front Plant Sci.* 11:560024. doi: 10.3389/fpls.2020.560024

Faske, T. R. (2013). Penetration, post-penetration development, and reproduction of *Meloidogyne incognita* on *Cucumis melo* var. *texanus*. *J. Nematol.* 45:58.

Fudali, S. L., Wang, C., and Williamson, V. M. (2013). Ethylene signaling pathway modulates attractiveness of host roots to the root-knot nematode *Meloidogyne hapla*. *Mol. Plant Microbe Interact.* 26, 75–86. doi: 10.1094/MPMI-05-12-0107-R

Gheysen, G., and Mitchum, M. G. (2009). "Molecular insights in the susceptible plant response to nematode infection," in *Cell Biology of Plant Nematode Parasitism*, eds R. H. Berg and C. G. Taylor (Berlin: Springer), doi: 10.1007/978-3-540-85215-5_3

Gheysen, G., and Mitchum, M. G. (2019). Phytoparasitic nematode control of plant hormone pathways. *Plant Physiol.* 179:1212. doi: 10.1104/pp.18.01067

Gine, A., Lopezgomez, M., Vela, M. D., Ornat, C., Talavera, M., Verdejolucas, S., et al. (2014). Thermal requirements and population dynamics of root-knot nematodes on cucumber and yield losses under protected cultivation. *Plant Pathol.* 63, 1446–1453. doi: 10.1111/ppa.12217

Goverse, A., Overmars, H., Engelbertink, J., Schots, A., Bakker, J., and Helder, J. (2000). Both induction and morphogenesis of cyst nematode feeding cells are mediated by auxin. *Mol. Plant Microbe Interact.* 13, 1121–1129. doi: 10.1094/MPMI.2000.13.10.1121

Haegeman, A., Mantelin, S., Jones, J. T., and Gheysen, G. (2012). Functional roles of effectors of plant-parasitic nematodes. *Gene* 492, 19–31. doi: 10.1016/j.gene.2011.10.040

Hutangura, P., Mathesius, U., Jones, M. G. K., and Rolfe, B. G. (1999). Auxin induction is a trigger for root gall formation caused by root-knot nematodes in white clover and is associated with the activation of the flavonoid pathway. *Funct. Plant Biol.* 26, 221–231. doi: 10.1071/PP98157

Hwang, C. F., and Williamson, V. M. (2003). Leucine-rich repeat-mediated intramolecular interactions in nematode recognition and cell death signaling by the tomato resistance protein *Mi*. *Plant J.* 34, 585–593. doi: 10.1046/j.1365-313X.2003.01749.x

Ji, H., Gheysen, G., Denil, S., Lindsey, K., Topping, J. F., Nahar, K., et al. (2013). Transcriptional analysis through RNA sequencing of giant cells induced by *Meloidogyne graminicola* in rice roots. *J. Exp. Bot.* 64, 3885–3898. doi: 10.1093/jxb/ert219

Kayani, M. Z., Mukhtar, T., and Hussain, M. A. (2017). Effects of southern root knot nematode population densities and plant age on growth and yield parameters of cucumber. *Crop Prot.* 92, 207–212. doi: 10.1016/j.cropro.2016.09.007

Lee, I. H., Shim, D., Jeong, J. C., Sung, Y. W., Nam, K. J., Yang, J., et al. (2019). Transcriptome analysis of root-knot nematode (*Meloidogyne incognita*)-resistant and susceptible sweetpotato cultivars. *Planta* 249, 431–444. doi: 10.1007/s00425-018-3001-z

Li, X., Xing, X., Tian, P., Zhang, M., Huo, Z., Zhao, K., et al. (2018). Comparative transcriptome profiling reveals defense-related genes against *Meloidogyne incognita* invasion in *Tobacco*. *Molecules* 23:2081. doi: 10.3390/molecules23082081

Liu, L., Sonbol, F. M., Huot, B., Gu, Y., Withers, J., Mwimba, M., et al. (2016). Salicylic acid receptors activate jasmonic acid signalling through a non-canonical pathway to promote effector-triggered immunity. *Nat. Commun.* 7:13099. doi: 10.1038/ncomms13099

Manosalva, P., Manohar, M., von Reuss, S. H., Chen, S., Koch, A., Kaplan, F., et al. (2015). Conserved nematode signalling molecules elicit plant defenses and pathogen resistance. *Nat. Commun.* 6:7795. doi: 10.1038/ncomms8795

Mao, L., Wang, Q., Yan, D., Liu, P., Shen, J., Fang, W., et al. (2016). Application of the combination of 1, 3-dichloropropene and dimethyl disulfide by soil injection or chemigation: effects against soil borne pests in cucumber in China. *J. Integr. Agric.* 15, 145–152. doi: 10.1016/S2095-3119(15)61065-6

Mei, C. S., Qi, M., Sheng, G. Y., and Yang, Y. N. (2006). Inducible overexpression of a rice allene oxide synthase gene increases the endogenous jasmonic acid level, *PR* gene expression, and host resistance to fungal infection. *Mol. Plant Microbe Interact.* 19, 1127–1137. doi: 10.1094/MPMI-19-1127

Molinari, S., Fanelli, E., and Leonetti, P. (2014). Expression of tomato salicylic acid (SA)-responsive pathogenesis-related genes in *Mi*-1-mediated and SA-induced resistance to root-knot nematodes. *Mol. Plant Pathol.* 15, 255–264. doi: 10.1111/mpp.12085

Nahar, K., Kyndt, T., De Vleesschauwer, D., Höfte, M., and Gheysen, G. (2011). The jasmonate pathway is a key player in systemically induced defense against root knot nematodes in rice. *Plant Physiol.* 157, 305–316. doi: 10.1104/pp.111.177576

Naor, N., Gurung, F. B., Ozalvo, R., Bucki, P., Sanadhya, P., and Miyara, S. B. (2018). Tight regulation of allene oxide synthase (*AOS*) and allene oxide cyclase-3 (*AOC3*) promote Arabidopsis susceptibility to the root-knot nematode *Meloidogyne javanica*. *Eur. J. Plant Pathol.* 150, 149–165. doi: 10.1007/s10658-017-1261-2

Ozalvo, R., Cabrera, J., Escobar, C., Christensen, S. A., Borrego, E. J., Kolomiets, M. V., et al. (2014). Two closely related members of *Arabidopsis* 13-lipoxygenases (*13-LOXs*), *LOX3* and *LOX4*, reveal distinct functions in response to plant-parasitic nematode infection. *Mol. Plant Pathol.* 15, 319–332. doi: 10.1111/mpp.12094

Perochon, A., Aldon, D., Galaud, J. P., and Ranty, B. (2011). Calmodulin and calmodulin-like proteins in plant calcium signaling. *Biochimie* 93, 2048–2053. doi: 10.1016/j.biochi.2011.07.012

Perrot-Rechenmann, C. (2010). Cellular responses to auxin: division versus expansion. *Cold Spring Harb. Perspect. Biol.* 2:a001446. doi: 10.1101/cshperspect.a001446

Priya, D. B., Somasekhar, N., Prasad, J. S., and Kirti, P. B. (2011). Transgenic tobacco plants constitutively expressing *Arabidopsis NPR1* show enhanced resistance to root-knot nematode, *Meloidogyne incognita*. *BMC Res. Notes* 4:231. doi: 10.1186/1756-0500-4-231

Reddy, A. S., Ali, G. S., Celesnik, H., and Day, I. S. (2011). Coping with stresses: roles of calcium-and calcium/calmodulin-regulated gene expression. *Plant Cell.* 23, 2010–2032. doi: 10.1105/tpc.111.084988

Shukla, N., Yadav, R., Kaur, P., Rasmussen, S., Goel, S., Agarwal, M., et al. (2018). Transcriptome analysis of root-knot nematode (*Meloidogyne incognita*)-infected tomato (*Solanum lycopersicum*) roots reveals complex gene expression profiles and metabolic networks of both host and nematode during susceptible and resistance responses. *Mol. Plant Pathol.* 19, 615–633. doi: 10.1111/mpp.12547

Siddique, S., and Grundler, F. M. (2018). Parasitic nematodes manipulate plant development to establish feeding sites. *Curr. Opin. Microbiol.* 46, 102–108. doi: 10.1016/j.mib.2018.09.004

Teixeira, M. A., Wei, L., and Kaloshian, I. (2016). Root-knot nematodes induce pattern-triggered immunity in *Arabidopsis thaliana* roots. *N. Phytol.* 211, 276–287. doi: 10.1111/nph.13893

Wang, X., Cheng, C., Zhang, K., Tian, Z., Xu, J., Yang, S., et al. (2018). Comparative transcriptomics reveals suppressed expression of genes related to auxin and the cell cycle contributes to the resistance of cucumber against *Meloidogyne incognita*. *BMC genomics* 19:583. doi: 10.1186/s12864-018-4979-0

Ye, D., Qi, Y., Cao, S., Wei, B., and Zhang, H. (2017). Histopathology combined with transcriptome analyses reveals the mechanism of resistance to *Meloidogyne incognita* in *Cucumis metuliferus*. *J. Plant Physiol.* 2017, 115–124. doi: 10.1016/j.jplph.2017.02.002

Zhang, H. Y., Kjemtrup-Lovelace, S., Li, C. B., Luo, Y., Chen, L. P., and Song, B. H. (2017). Comparative RNA-Seq analysis uncovers a complex regulatory network for soybean cyst nematode resistance in wild soybean (*Glycine soja*). *Sci. Rep.* 7:9699. doi: 10.1038/s41598-017-09945-0

Zhang, Y., Tessaro, M. J., Lassner, M., and Li, X. (2003). Knockout analysis of *Arabidopsis* transcription factors *TGA2*, *TGA5*, and *TGA6* reveals their redundant and essential roles in systemic acquired resistance. *Plant Cell.* 15, 2647–2653. doi: 10.1105/tpc.014894

Zhou, J., Jia, F., Shao, S., Zhang, H., Li, G., Xia, X., et al. (2015). Involvement of nitric oxide in the jasmonate-dependent basal defense against root-knot nematode in tomato plants. *Front. Plant Sci.* 6:193. doi: 10.3389/fpls.2015.00193

Conflict of Interest: The authors declare that the research was conducted in the absence of any commercial or financial relationships that could be construed as a potential conflict of interest.

Advantages of publishing in Frontiers

OPEN ACCESS
Articles are free to read for greatest visibility and readership

FAST PUBLICATION
Around 90 days from submission to decision

HIGH QUALITY PEER-REVIEW
Rigorous, collaborative, and constructive peer-review

TRANSPARENT PEER-REVIEW
Editors and reviewers acknowledged by name on published articles

Frontiers
Avenue du Tribunal-Fédéral 34
1005 Lausanne | Switzerland

Visit us: www.frontiersin.org
Contact us: frontiersin.org/about/contact

REPRODUCIBILITY OF RESEARCH
Support open data and methods to enhance research reproducibility

DIGITAL PUBLISHING
Articles designed for optimal readership across devices

FOLLOW US
@frontiersin

IMPACT METRICS
Advanced article metrics track visibility across digital media

EXTENSIVE PROMOTION
Marketing and promotion of impactful research

LOOP RESEARCH NETWORK
Our network increases your article's readership